Scientific and Technical Aerospace Reports

STAR

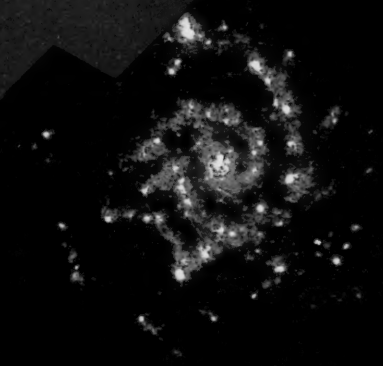

An Abstract Journal

Volume 30, Number 2
January 23, 1992
N92-10972 to N92-11965

Scientific and Technical Aerospace Reports

Scientific and Technical Aerospace Reports (STAR) is an abstract journal that provides comprehensive coverage of worldwide aerospace-related reports. It is a major product of the International Aerospace Database managed by the NASA Scientific and Technical Information (STI) Program. The coverage includes reports on aeronautics, space, and supporting disciplines. *STAR* lists current, publicly available reports entered into the NASA STI Database during the 2-week period preceding publication. A typical citation and abstract appear on page viii. They explain how to read the items that are announced in this journal.

NASA sponsors a companion journal, *International Aerospace Abstracts (IAA)* (*NOVA* for internal NASA use) that lists abstracts of the open literature on aerospace subjects available worldwide. *IAA* is available for sale through the AIAA.

Entries found in *STAR* and *IAA* are available through NASA's online service, RECON, as the International Aerospace Database and through DIALOG as the Aerospace Database.

Information on aerospace and related subjects is gathered by the NASA STI Program through national and international agreements and exchanges and is made available to the NASA community as well as to the public in many forms through various outlets. The section on NASA STI Program Products and Services contains additional information.

For further information please contact:
NASA Center for AeroSpace Information (CASI)
P.O. Box 8757
Baltimore, Maryland 21240-0757
(301) 621-0390

US ISSN 0036-8741

Volume 30 Number 2 / January 23, 1992

TABLE OF CONTENTS

AERONAUTICS For related information see also *Astronautics.*

01 AERONAUTICS (GENERAL) **181**

02 AERODYNAMICS **181**
Includes aerodynamics of bodies, combinations, wings, rotors, and control surfaces; and internal flow in ducts and turbomachinery. For related information see also *34 Fluid Mechanics and Heat Transfer.*

03 AIR TRANSPORTATION AND SAFETY **184**
Includes passenger and cargo air transport operations; and aircraft accidents. For related information see also *16 Space Transportation* and *85 Urban Technology and Transportation.*

04 AIRCRAFT COMMUNICATIONS AND NAVIGATION **184**
Includes digital and voice communication with aircraft; air navigation systems (satellite and ground based); and air traffic control. For related information see also *17 Space Communications, Spacecraft Communications, Command and Tracking* and *32 Communications and Radar.*

05 AIRCRAFT DESIGN, TESTING AND PERFORMANCE **185**
Includes aircraft simulation technology. For related information see also *18 Spacecraft Design, Testing and Performance* and *39 Structural Mechanics.* For land transportation vehicles see *85 Urban Technology and Transportation.*

06 AIRCRAFT INSTRUMENTATION **187**
Includes cockpit and cabin display devices; and flight instruments. For related information see also *19 Space craft Instrumentation* and *35 Instrumentation and Photography.*

07 AIRCRAFT PROPULSION AND POWER **187**
Includes prime propulsion systems and systems components, e.g., gas turbine engines and compressors; and onboard auxiliary power plants for aircraft. For related information see also *20 Spacecraft Propulsion and Power, 28 Propellants and Fuels,* and *44 Energy Production and Conversion.*

08 AIRCRAFT STABILITY AND CONTROL **188**
Includes aircraft handling qualities; piloting; flight controls; and autopilots. For related information see also *05 Aircraft Design, Testing and Performance.*

09 RESEARCH AND SUPPORT FACILITIES (AIR) **189**
Includes airports, hangars and runways; aircraft repair and overhaul facilities; wind tunnels; shock tubes; and aircraft engine test stands. For related information see also *14 Ground Support Systems and Facilities (Space).*

ASTRONAUTICS For related information see also *Aeronautics.*

12 ASTRONAUTICS (GENERAL) **190**
For extraterrestrial exploration see *91 Lunar and Planetary Exploration.*

13 ASTRODYNAMICS ..... **N.A.**
Includes powered and free-flight trajectories; and orbital and launching dynamics.

14 GROUND SUPPORT SYSTEMS AND FACILITIES (SPACE) **191**
Includes launch complexes, research and production facilities; ground support equipment, e.g., mobile transporters; and simulators. For related information see also *09 Research and Support Facilities (Air).*

15 LAUNCH VEHICLES AND SPACE VEHICLES **191**
Includes boosters; operating problems of launch/space vehicle systems; and reusable vehicles. For related information see also *20 Spacecraft Propulsion and Power.*

16 SPACE TRANSPORTATION **192**
Includes passenger and cargo space transportation, e.g., shuttle operations; and space rescue techniques. For related information see also *03 Air Transportation and Safety* and *18 Spacecraft Design, Testing and Performance.* For space suits see *54 Man/System Technology and Life Support.*

17 SPACE COMMUNICATIONS, SPACECRAFT COMMUNICATIONS, COMMAND AND TRACKING . **192**
Includes telemetry; space communications networks; astronavigation and guidance; and radio blackout. For related information see also *04 Aircraft Communications and Navigation* and *32 Communications and Radar.*

N.A.—no abstracts were assigned to this category for this issue.

18 SPACECRAFT DESIGN, TESTING AND PERFORMANCE **196**
Includes satellites; space platforms; space stations; spacecraft systems and components such as thermal and environmental controls; and attitude controls. For life support systems see *54 Man/System Technology and Life Support.* For related information see also *05 Aircraft Design, Testing and Performance, 39 Structural Mechanics,* and *16 Space Transportation.*

19 SPACECRAFT INSTRUMENTATION ..... **N.A.**
For related information see also *06 Aircraft Instrumentation* and *35 Instrumentation and Photography.*

20 SPACECRAFT PROPULSION AND POWER **200**
Includes main propulsion systems and components, e.g., rocket engines; and spacecraft auxiliary power sources. For related information see also *07 Aircraft Propulsion and Power, 28 Propellants and Fuels, 44 Energy Production and Conversion,* and *15 Launch Vehicles and Space Vehicles.*

CHEMISTRY AND MATERIALS

23 CHEMISTRY AND MATERIALS (GENERAL) **208**

24 COMPOSITE MATERIALS **208**
Includes physical, chemical, and mechanical properties of laminates and other composite materials. For ceramic materials see *27 Nonmetallic Materials.*

25 INORGANIC AND PHYSICAL CHEMISTRY **209**
Includes chemical analysis, e.g., chromatography; combustion theory; electrochemistry; and photochemistry. For related information see also *77 Thermodynamics and Statistical Physics.*

26 METALLIC MATERIALS **213**
Includes physical, chemical, and mechanical properties of metals, e.g., corrosion; and metallurgy.

27 NONMETALLIC MATERIALS **216**
Includes physical, chemical, and mechanical properties of plastics, elastomers, lubricants, polymers, textiles, adhesives, and ceramic materials. For composite materials see *24 Composite Materials.*

28 PROPELLANTS AND FUELS **220**
Includes rocket propellants, igniters and oxidizers; their storage and handling procedures; and aircraft fuels. For related information see also *07 Aircraft Propulsion and Power, 20 Spacecraft Propulsion and Power,* and *44 Energy Production and Conversion.*

29 MATERIALS PROCESSING **221**
Includes space-based development of products and processes for commercial application. For biological materials see *55 Space Biology.*

ENGINEERING For related information see also *Physics.*

31 ENGINEERING (GENERAL) **221**
Includes vacuum technology; control engineering; display engineering; cryogenics; and fire prevention.

32 COMMUNICATIONS AND RADAR **222**
Includes radar; land and global communications; communications theory; and optical communications. For related information see also *04 Aircraft Communications and Navigation* and *17 Space Communications, Spacecraft Communications, Command and Tracking.* For search and rescue see *03 Air Transportation and Safety,* and *16 Space Transportation.*

33 ELECTRONICS AND ELECTRICAL ENGINEERING **227**
Includes test equipment and maintainability; components, e.g., tunnel diodes and transistors; microminiaturization; and integrated circuitry. For related information see also *60 Computer Operations and Hardware* and *76 Solid-State Physics.*

34 FLUID MECHANICS AND HEAT TRANSFER **232**
Includes boundary layers; hydrodynamics; fluidics; mass transfer and ablation cooling. For related information see also *02 Aerodynamics* and *77 Thermodynamics and Statistical Physics.*

35 INSTRUMENTATION AND PHOTOGRAPHY **239**
Includes remote sensors; measuring instruments and gauges; detectors; cameras and photographic supplies; and holography. For aerial photography see *43 Earth Resources and Remote Sensing.* For related information see also *06 Aircraft Instrumentation* and *19 Spacecraft Instrumentation.*

36 LASERS AND MASERS **241**
Includes parametric amplifiers. For related information see also *76 Solid-State Physics.*

37 MECHANICAL ENGINEERING 243
Includes auxiliary systems (nonpower); machine elements and processes; and mechanical equipment.

38 QUALITY ASSURANCE AND RELIABILITY 245
Includes product sampling procedures and techniques; and quality control.

39 STRUCTURAL MECHANICS 246
Includes structural element design and weight analysis; fatigue; and thermal stress. For applications see *05 Aircraft Design, Testing and Performance* and *18 Spacecraft Design, Testing and Performance.*

GEOSCIENCES For related information see also *Space Sciences.*

42 GEOSCIENCES (GENERAL) ..... N.A.

43 EARTH RESOURCES AND REMOTE SENSING 250
Includes remote sensing of earth resources by aircraft and spacecraft; photogrammetry; and aerial photography. For instrumentation see *35 Instrumentation and Photography.*

44 ENERGY PRODUCTION AND CONVERSION 279
Includes specific energy conversion systems, e.g., fuel cells; global sources of energy; geophysical conversion; and windpower. For related information see also *07 Aircraft Propulsion and Power, 20 Spacecraft Propulsion and Power,* and *28 Propellants and Fuels.*

45 ENVIRONMENT POLLUTION 280
Includes atmospheric, noise, thermal, and water pollution.

46 GEOPHYSICS 282
Includes aeronomy; upper and lower atmosphere studies; ionospheric and magnetospheric physics; and geomagnetism. For space radiation see *93 Space Radiation.*

47 METEOROLOGY AND CLIMATOLOGY 283
Includes weather forecasting and modification.

48 OCEANOGRAPHY 285
Includes biological, dynamic, and physical oceanography; and marine resources. For related information see also *43 Earth Resources and Remote Sensing.*

LIFE SCIENCES

51 LIFE SCIENCES (GENERAL) 287

52 AEROSPACE MEDICINE 288
Includes physiological factors; biological effects of radiation; and effects of weightlessness on man and animals.

53 BEHAVIORAL SCIENCES 290
Includes psychological factors; individual and group behavior; crew training and evaluation; and psychiatric research.

54 MAN/SYSTEM TECHNOLOGY AND LIFE SUPPORT 291
Includes human engineering; biotechnology; and space suits and protective clothing. For related information see also *16 Space Transportation.*

55 SPACE BIOLOGY ..... N.A.
Includes exobiology; planetary biology; and extraterrestrial life.

MATHEMATICAL AND COMPUTER SCIENCES

59 MATHEMATICAL AND COMPUTER SCIENCES (GENERAL) 292

60 COMPUTER OPERATIONS AND HARDWARE 293
Includes hardware for computer graphics, firmware, and data processing. For components see *33 Electronics and Electrical Engineering.*

61 COMPUTER PROGRAMMING AND SOFTWARE 293
Includes computer programs, routines, algorithms, and specific applications, e.g., CAD/CAM.

62 COMPUTER SYSTEMS 301
Includes computer networks and special application computer systems.

63 CYBERNETICS **304**
Includes feedback and control theory, artificial intelligence, robotics and expert systems. For related information see also *54 Man/System Technology and Life Support.*

64 NUMERICAL ANALYSIS **304**
Includes iteration, difference equations, and numerical approximation.

65 STATISTICS AND PROBABILITY **308**
Includes data sampling and smoothing; Monte Carlo method; and stochastic processes.

66 SYSTEMS ANALYSIS **310**
Includes mathematical modeling; network analysis; and operations research.

67 THEORETICAL MATHEMATICS ..... **N.A.**
Includes topology and number theory.

PHYSICS For related information see also *Engineering.*

70 PHYSICS (GENERAL) **310**
For precision time and time interval (PTTI) see *35 Instrumentation and Photography;* for geophysics, astrophysics or solar physics see *46 Geophysics, 90 Astrophysics,* or *92 Solar Physics.*

71 ACOUSTICS **311**
Includes sound generation, transmission, and attenuation. For noise pollution see *45 Environment Pollution.*

72 ATOMIC AND MOLECULAR PHYSICS **313**
Includes atomic structure, electron properties, and molecular spectra.

73 NUCLEAR AND HIGH-ENERGY PHYSICS **315**
Includes elementary and nuclear particles; and reactor theory. For space radiation see *93 Space Radiation.*

74 OPTICS **316**
Includes light phenomena and optical devices. For lasers see *36 Lasers and Masers.*

75 PLASMA PHYSICS **318**
Includes magnetohydrodynamics and plasma fusion. For ionospheric plasmas see *46 Geophysics.* For space plasmas see *90 Astrophysics.*

76 SOLID-STATE PHYSICS **333**
Includes superconductivity. For related information see also *33 Electronics and Electrical Engineering* and *36 Lasers and Masers.*

77 THERMODYNAMICS AND STATISTICAL PHYSICS ..... **N.A.**
Includes quantum mechanics; theoretical physics; and Bose and Fermi statistics. For related information see also *25 Inorganic and Physical Chemistry* and *34 Fluid Mechanics and Heat Transfer.*

SOCIAL SCIENCES

80 SOCIAL SCIENCES (GENERAL) ..... **N.A.**
Includes educational matters.

81 ADMINISTRATION AND MANAGEMENT **336**
Includes management planning and research.

82 DOCUMENTATION AND INFORMATION SCIENCE **337**
Includes information management; information storage and retrieval technology; technical writing; graphic arts; and micrography. For computer documentation see *61 Computer Programming and Software.*

83 ECONOMICS AND COST ANALYSIS ..... **N.A.**
Includes cost effectiveness studies.

84 LAW, POLITICAL SCIENCE AND SPACE POLICY ..... **N.A.**
Includes NASA appropriation hearings; aviation law; space law and policy; international law; international cooperation; and patent policy.

85 URBAN TECHNOLOGY AND TRANSPORTATION ..... **N.A.**
Includes applications of space technology to urban problems; technology transfer; technology assessment; and surface and mass transportation. For related information see *03 Air Transportation and Safety, 16 Space Transportation,* and *44 Energy Production and Conversion.*

SPACE SCIENCES For related information see also *Geosciences.*

88 SPACE SCIENCES (GENERAL) **339**

89 ASTRONOMY **340**
Includes radio, gamma-ray, and infrared astronomy; and astrometry.

90 ASTROPHYSICS **340**
Includes cosmology; celestial mechanics; space plasmas; and interstellar and interplanetary gases and dust. For related information see also *75 Plasma Physics.*

91 LUNAR AND PLANETARY EXPLORATION **342**
Includes planetology; and manned and unmanned flights. For spacecraft design or space stations see *18 Spacecraft Design, Testing and Performance.*

92 SOLAR PHYSICS **343**
Includes solar activity, solar flares, solar radiation and sunspots. For related information see *93 Space Radiation.*

93 SPACE RADIATION **344**
Includes cosmic radiation; and inner and outer earth's radiation belts. For biological effects of radiation see *52 Aerospace Medicine.* For theory see *73 Nuclear and High-Energy Physics.*

GENERAL

Includes aeronautical, astronautical, and space science related histories, biographies, and pertinent reports too broad for categorization; histories or broad overviews of NASA programs.

99 GENERAL **345**

SUBJECT INDEX **I-1**

PERSONAL AUTHOR INDEX **I-67**

CORPORATE SOURCE INDEX **I-77**

CONTRACT NUMBER INDEX **I-89**

REPORT/ACCESSION NUMBER INDEX **I-93**

APPENDIX **A-1**

TYPICAL CITATION AND ABSTRACT

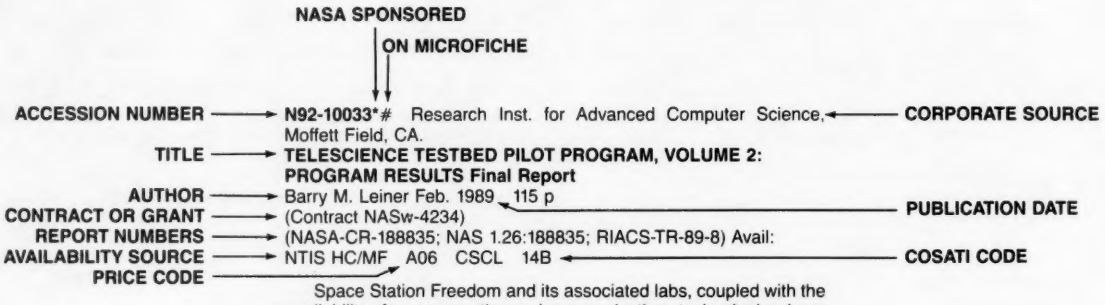

Space Station Freedom and its associated labs, coupled with the availability of new computing and communications technologies, have the potential for significantly enhancing scientific research. A Telescience Testbed Pilot Program (TTPP), aimed at developing the experience base to deal with issues in the design of the future information system of the Space Station era. The testbeds represented four scientific disciplines (astronomy and astrophysics, earth sciences, life sciences, and microgravity sciences) and studied issues in payload design, operation, and data analysis. This volume, of a 3 volume set, which all contain the results of the TTPP, contains the integrated results. Background is provided of the program and highlights of the program results. The various testbed experiments and the programmatic approach is summarized. The results are summarized on a discipline by discipline basis, highlighting the lessons learned for each discipline. Then the results are integrated across each discipline, summarizing the lessons learned overall.

Author

VOLUME 30 NUMBER 2 / JANUARY 23, 1992

Scientific and Technical Aerospace Reports

A Semimonthly Publication of the National Aeronautics and Space Administration

01 AERONAUTICS (GENERAL)

N92-10972# National Park Service, Washington, DC.
STUDY OF ALTERNATIVES: DAYTON'S AVIATION HERITAGE, OHIO
1991 67 p
(PB91-202275) Avail: NTIS HC/MF A04 CSCL 01B

Three conceptual alternatives for the preservation, development, and interpretation of aviation-related resources of national, state, and local significance are presented. These alternatives include: (1) West Dayton-- home of a legend; (2) the Wrights as inventors-- catalyst for a world change; and (3) innovation and aviation-- Dayton as a major technological center. A brief preliminary analysis of impacts is also included within each alternative description to aid decision makers in evaluating the study alternatives as to their suitability, feasibility, and environmental consequences. Seven different approaches to implement these alternatives are examined. Focus is on the three nationally significant resources in Dayton, Ohio (the Wright Cycle Company Building, Huffman Prairie Flying Field, and Wright Flyer 3). A limited discussion of the Hoover Block and Hawthorn Hill is presented. The study includes the following information: (1) a general description of resources, including the surrounding urban environment and specific sites and structures designated as National Historical Landmarks; (2) present ownership; (3) existing and proposed uses and their effects on the resources; (4) a range of feasible alternatives (without a preferred alternative) for the preservation, interpretation, and use of resources; (5) a preliminary analysis of the economic, social, cultural, and environmental impacts of the alternatives; (6) an analysis of feasible implementation and management strategies; and (7) preliminary costs for possible National Park Service involvement if mandated by Congress. Author

N92-10973* National Aeronautics and Space Administration, Washington, DC.
AERONAUTICAL ENGINEERING: A CONTINUING BIBLIOGRAPHY WITH INDEXES (SUPPLEMENT 270)
Oct. 1991 176 p
(NASA-SP-7037(270); NAS 1.21:7037(270)) Avail: NTIS HC A09; NTIS standing order as PB91-914100, $17.00 domestic, $34.00 foreign CSCL 01B

This bibliography lists 600 reports, articles, and other documents introduced into the NASA scientific and technical information system in September, 1991. Subject coverage includes: design, construction and testing of aircraft and aircraft engines; aircraft components, equipment and systems; ground support systems; and theoretical and applied aspects of aerodynamics and general fluid dynamics. Author

N92-10974* National Aeronautics and Space Administration, Washington, DC.
AERONAUTICAL ENGINEERING: A CONTINUING BIBLIOGRAPHY WITH INDEXES (SUPPLEMENT 269)
Sep. 1991 153 p
(NASA-SP-7037(269); NAS 1.21:7037(269)) Avail: NTIS HC A08; NTIS standing order as PB91-914100, $17.00 domestic, $34.00 foreign CSCL 01B

This bibliography lists 539 reports, articles, and other documents introduced into the NASA scientific and technical information system in August, 1991. Subject coverage includes: design, construction and testing of aircraft and aircraft engines; aircraft components, equipment and systems; ground support systems; and theoretical and applied aspects of aerodynamics and general fluid dynamics. Author

02 AERODYNAMICS

Includes aerodynamics of bodies, combinations, wings, rotors, and control surfaces; and internal flow in ducts and turbomachinery.

For related information see also *34 Fluid Mechanics and Heat Transfer.*

N92-10975*# National Aeronautics and Space Administration. Langley Research Center, Hampton, VA.
STATIC INTERNAL PERFORMANCE OF VENTRAL AND REAR NOZZLE CONCEPTS FOR SHORT-TAKEOFF AND VERTICAL-LANDING AIRCRAFT
Richard J. Re and George T. Carson, Jr. Washington Sep. 1991 71 p
(NASA-TP-3103; L-16902; NAS 1.60:3103) Avail: NTIS HC/MF A04 CSCL 01A

The internal performance of two exhaust system concepts applicable to single-engine short-take-off and vertical-landing tactical fighter configurations was investigated. These concepts involved blocking (or partially blocking) tailpipe flow to the rear (cruise) nozzle and diverting it through an opening to a ventral nozzle exit for vertical thrust. A set of variable angle vanes at the ventral nozzle exit were used to vary ventral nozzle thrust angle between 45 and 110 deg relative to the positive axial force direction. In the vertical flight mode the rear nozzle (or tailpipe flow to it) was completely blocked. In the transition flight mode flow in the tailpipe was split between the rear and ventral nozzles and the flow was vectored at both exits for aircraft control purposes through this flight regime. In the cruise flight mode the ventral nozzle was sealed and all flow exited through the rear nozzle. Author

N92-10976*# National Aeronautics and Space Administration. Lewis Research Center, Cleveland, OH.
RESULTS FROM COMPUTATIONAL ANALYSIS OF A MIXED COMPRESSION SUPERSONIC INLET
J. D. Saunders and T. G. Keith (Ohio Aerospace Inst., Brook Park.) 1991 18 p Presented at the 27th Joint Propulsion Conference, Sacramento, CA, 24-27 Jun. 1991; sponsored by AIAA, SAE, ASME, and ASEE Previously announced in IAA as A91-45818 Original contains color illustrations
(NASA-TM-104475; E-6322; NAS 1.15:104475; AIAA-91-2581) Copyright Avail: NTIS HC/MF A03; 5 functional color pages CSCL 01A

A numerical study was performed to simulate the critical flow through a supersonic inlet. This flow field has many phenomena such as shock waves, strong viscous effects, turbulent boundary layer development, boundary layer separations, and mass flow suction through the walls, (bleed). The computational tools used were two full Navier-Stokes (FNS) codes. The supersonic inlet that was analyzed is the Variable Diameter Centerbody, (VDC),

inlet. This inlet is a candidate concept for the next generation supersonic involved effort in generating an efficient grid geometry and specifying boundary conditions, particularly in the bleed region and at the outflow boundary. Results for a critical inlet operation compare favorably to Method of Characteristics predictions and experimental data. Author

N92-10977*# Research Inst. for Advanced Computer Science, Moffett Field, CA.
A FAST SORTING ALGORITHM FOR A HYPERSONIC RAREFIED FLOW PARTICLE SIMULATION ON THE CONNECTION MACHINE
Leonardo Dagum (Stanford Univ., CA.) Nov. 1989 20 p
(Contract NCC2-387; NAGw-965; AF-AFOSR-0139-88)
(NASA-CR-188903; NAS 1.26:188903; RIACS-TR-89-44) Avail: NTIS HC/MF A03 CSCL 01A

The data parallel implementation of a particle simulation for hypersonic rarefied flow described by Dagum associates a single parallel data element with each particle in the simulation. The simulated space is divided into discrete regions called cells containing a variable and constantly changing number of particles. The implementation requires a global sort of the parallel data elements so as to arrange them in an order that allows immediate access to the information associated with cells in the simulation. Described here is a very fast algorithm for performing the necessary ranking of the parallel data elements. The performance of the new algorithm is compared with that of the microcoded instruction for ranking on the Connection Machine. Author

N92-10978*# Georgia Inst. of Tech., Atlanta. Signature Technology Lab.
LV SOFTWARE SUPPORT FOR SUPERSONIC FLOW ANALYSIS Final Technical Report, Oct. 1990 - Oct. 1991
William A. Bell 9 Oct. 1991 77 p
(Grant NAG3-1215)
(NASA-CR-188914; NAS 1.26:188914) Avail: NTIS HC/MF A05 CSCL 01A

During 1991, the software developed allowed an operator to configure and checkout the TSI, Inc. laser velocimeter (LV) system prior to a run. This setup procedure established the operating conditions for the TSI MI-990 multichannel interface and the RMR-1989 rotating machinery resolver. In addition to initializing the instruments, the software package provides a means of specifying LV calibration constants, controlling the sampling process, and identifying the test parameters. Author

N92-10979*# United Technologies Research Center, East Hartford, CT.
DEVELOPMENT OF UNSTEADY AERODYNAMIC ANALYSES FOR TURBOMACHINERY AEROELASTIC AND AEROACOUSTIC APPLICATIONS
Joseph M. Verdon, Mark Barnett, Kenneth C. Hall, and Timothy C. Ayer Washington NASA Oct. 1991 112 p
(Contract NAS3-25425)
(NASA-CR-4405; E-6528; NAS 1.26:4405; R91-957907-3) Avail: NTIS HC/MF A06 CSCL 01A

Theoretical analyses and computer codes are being developed for predicting compressible unsteady inviscid and viscous flows through blade rows. Such analyses are needed to determine the impact of unsteady flow phenomena on the structural durability and noise generation characteristics of turbomachinery blading. Emphasis is being placed on developing analyses based on asymptotic representations of unsteady flow phenomena. Thus, flow driven by small-amplitude unsteady excitations in which viscous effects are concentrated in thin layers are being considered. The resulting analyses should apply in many practical situations, lead to a better understanding of the relevent physics, and they will be efficient computationally, and therefore, appropriate for aeroelastic and aeroacoustic design applications. Under the present phase (Task 3), the effort was focused on providing inviscid and viscid prediction capabilities for subsonic unsteady cascade flows. Author

N92-10980# National Aerospace Lab., Tokyo (Japan). Airframe Div.
UNSTEADY AERODYNAMIC CALCULATIONS FOR GENERAL CONFIGURATIONS BY THE DOUBLE-POINT METHOD
Tetsuhiko Ueda Apr. 1991 31 p In JAPANESE; ENGLISH summary
(NAL-TR-1101T; ISSN-0389-4010) Avail: NTIS HC/MF A03

A method for predicting unsteady aerodynamic loadings on general configurations is presented. The procedures are based on the lifting surface theory, with the time variable being transformed to the Laplace domain so that the calculation is valid in the region of off axis from the frequency domain. The results are subsequently compared with those from other methods and experiments in both the subsonic and supersonic frequency domains. In addition, a generalized force is calculated in the Laplace domain for a rectangular wing in supersonic flow. Author

N92-10981*# National Aeronautics and Space Administration. Ames Research Center, Moffett Field, CA.
NACA 0015 WING PRESSURE AND TRAILING VORTEX MEASUREMENTS
K. W. McAlister and R. K. Takahashi Washington Nov. 1991 141 p
(NASA-TP-3151; A-91056; NAS 1.60:3151;
AVSCOM-TR-91-A-003) Avail: NTIS HC/MF A07 CSCL 01A

A NACA 0015 semispan wing was placed in a low-speed wind tunnel, and measurements were made of the pressure on the upper and lower surface of the wing and of velocity across the vortex trailing downstream from the tip of the wing. Pressure data were obtained for both 2-D and 3-D configurations. These data feature a detailed comparison between wing tips with square and round lateral edges. A two-component laser velocimeter was used to measure velocity profiles across the vortex at numerous stations behind the wing and for various combinations of conditions. These conditions include three aspect ratios, three chord lengths, a square- and a round lateral-tip, presence or absence of a boundary-layer trip, and three image plane positions located opposite the wing tip. Both pressure and velocity measurements were made for the angles of attack 4 deg less than or equal to alpha less than or equal to 12 deg and for Reynolds numbers 1 x 10(exp 6) less than or equal to Re less than or equal to 3 x 10(exp 6). Author

N92-10982*# Old Dominion Univ., Norfolk, VA. Dept. of Mechanical Engineering and Mechanics.
VISCOUS COMPUTATIONS OF COLD AIR/AIR FLOW AROUND SCRAMJET NOZZLE AFTERBODY
Oktay Baysal and Walter C. Engelund Washington NASA Oct. 1991 73 p
(Grant NAG1-811)
(NASA-CR-4406; NAS 1.26:4406) Avail: NTIS HC/MF A04 CSCL 01A

The flow field in and around the nozzle afterbody section of a hypersonic vehicle was computationally simulated. The compressible, Reynolds averaged, Navier Stokes equations were solved by an implicit, finite volume, characteristic based method. The computational grids were adapted to the flow as the solutions were developing in order to improve the accuracy. The exhaust gases were assumed to be cold. The computational results were obtained for the two dimensional longitudinal plane located at the half span of the internal portion of the nozzle for over expanded and under expanded conditions. Another set of results were obtained, where the three dimensional simulations were performed for a half span nozzle. The surface pressures were successfully compared with the data obtained from the wind tunnel tests. The results help in understanding this complex flow field and, in turn, should help the design of the nozzle afterbody section. Author

N92-10983*# National Aeronautics and Space Administration. Ames Research Center, Moffett Field, CA.
EXPERIMENTAL STUDY OF AN INDEPENDENTLY DEFLECTED WINGTIP MOUNTED ON A SEMISPAN WING
D. M. Martin (Kansas Univ. Center for Research, Inc., Lawrence.)

and L. A. Young Sep. 1991 58 p
(NASA-TM-102842; A-90210; NAS 1.15:102842) Avail: NTIS HC/MF A04 CSCL 01A

The results of a subsonic wind tunnel test of a semispan wing with an independently deflected tip surface are presented and analyzed. The tip surface was deflected about the quarter chord of the rectangular wing and accounted for 17 percent of the wing semispan. The test was conducted to measure the loads on the tip surface and to investigate the nature of aerodynamic interference effects between the wing and the deflected tip. Results are presented for two swept tip surfaces of similar planform but different airfoil distributions. The report contains plots of tip lift, drag, and pitching moment for various Reynolds numbers and tip deflection angles with respect to the inboard wing. Oil flow visualization photographs for a typical Reynolds number are also included. Important aerodynamic parameters such as lift and pitching moment slopes and tip aerodynamic center location are tabulated. A discussion is presented on the relationship between tip experimental data acquired in a steady flow and the prediction of unsteady tip motion at fixed wing angles of attack. Author

N92-10984# Tulane Univ., New Orleans, LA. Dept. of Mathematics.
A GRID-FREE METHOD FOR HIGH REYNOLDS NUMBER FLOW AROUND AN IMMERSED ELASTIC STRUCTURE Final Report, 1 Apr. 1989 - 31 Jul. 1990
Lisa J. Fauci 31 Jul. 1990 29 p
(Grant AF-AFOSR-0295-89; AF Proj. 6177)
(AD-A240048; AFOSR-91-0730TR) Avail: NTIS HC/MF A03 CSCL 01/1

Finite difference schemes do not perform well in simulations of high Reynolds number flow because a restrictive number of grid points must be used to resolve boundary layers. In this report we present a grid-free numerical method which may be used to calculate flows around an immersed elastic structure. Numerical results are presented in two simple cases: flow past a circular cylinder and flow past a flat past a flat plate. Here the boundary motion is specified and is not time dependent. However, this algorithm can be used to simulate more complicated, time dependent problems in biological fluid mechanics. GRA

N92-10985# West Virginia Univ., Morgantown. Dept. of Mechanical and Aerospace Engineering.
EXPERIMENTAL INVESTIGATION OF THE EFFECTS OF BLOWING ON BURSTING OF STRAKE VORTICES Final Technical Report, 12 Jul. 1989 - 22 Apr. 1991
Robert Allen Roach and John M. Kulhman Jul. 1991 177 p
(Contract F33615-89-C-3001)
(AD-A240256; WL-TR-91-3065) Avail: NTIS HC/MF A09 CSCL 01/1

Laser light sheet flow visualization and laser Doppler Anemometry (LDA) have been utilized to study the effects of pneumatic jet blowing on the breakdown and coupling locations of the strake and wing vortices generated over a generic fighter aircraft model with 55 degree sweep cropped delta wing planform fitted with forebody strakes. Experiments were conducted at low speed (15 m/sec), corresponding to a chord Reynolds number of 270,000, over an angle of attack range of 20 to 36 degrees. Flow visualization has been used to determine jet blowing locations and nozzle configurations which have the maximum beneficial effects of delaying both vortex breakdown and coupling of the strake and wing vortices. Significant reductions were observed both in vortex coupling interaction and in strake vortex breakdown at a blowing coefficient referenced to the wing area of 0.016. The LDA data indicated increases in the mean axial velocity above the vortices and increased turbulent velocities due to jet blowing. GRA

N92-10986# Wright Lab., Wright-Patterson AFB, OH.
SUBSONIC WIND TUNNEL TESTING HANDBOOK Interim Report, 1 May 1990 - 1 May 1991
Michael G. Alexander May 1991 296 p
(AF Proj. 2404)
(AD-A240263; WL-TR-91-3073) Avail: NTIS HC/MF A13 CSCL 14/2

This handbook is predominantly structured for subsonic (noncompressible flow), force and moment wind tunnel testing. Its purpose is to provide to the aerodynamic testing engineer equations, concepts, illustrations, and definitions that would aid him or her in wind tunnel testing. The information in this handbook is a living document readily expandable to include personal notes and additional sections. This handbook has not and cannot encompass every wind tunnel testing technique or principle. GRA

N92-10987# New Mexico State Univ., Las Cruces. Physical Science Lab.
ENGINEERING AND INSTRUMENTATION SUPPORT OF GL RESEARCH BALLOON PROGRAM Final Report, 1 Dec. 1987 - 10 Dec. 1989
Squire B. Seagraves 26 Jul. 1991 15 p
(Contract F19628-88-C-0009)
(AD-A240616; GL-TR-90-0340) Avail: NTIS HC/MF A03 CSCL 01/3

The activity during this report period was primarily concerned with command and instrumentation preflight support for the command and data acquisition systems, batteries, control room and launch systems support, balloon and parachute rigging support, payload support, aircraft observer and recovery crew support, design and fabrication support for balloon payload systems, including gondola systems, pointing controls, navigational systems, scientific instrumentation, and ground support instrumentation and services. GRA

N92-10988# Centre d'Etudes et de Recherches, Toulouse (France). Groupe d'Analyse Numerique.
NUMERICAL RESOLUTION OF THREE DIMENSIONAL EULER EQUATIONS IN TOTALLY UNSTRUCTURED MESH Final Report [RESOLUTION NUMERIQUE DES EQUATIONS D'EULER TRIDIMENSIONNELLES EN MAILLAGE TOTALEMENT DESTRUCTURE. RAPPORT FINAL]
Philippe Delorme Dec. 1990 33 p In FRENCH
(Contract DRET-89-002-29)
(CERT-RF-1/3369-00/DERI-GAN; ETN-91-90075) Avail: NTIS HC/MF A03

Numerical attempts relating to the method of kinetic description of fluxes are reported. Problems at high Mach number were resolved over a preconditioning. Automatic mesh refining techniques were applied to implicit two dimensional stationary flow on the test case of the Hermes workshop. Three dimensional utilities were developed. A method already applied to chemically nonequilibrium gas mixtures was extended to real gas (quantic perfect gas) and to thermally nonequilibrium gas mixtures. ESA

N92-10989# Office National d'Etudes et de Recherches Aerospatiales, Paris (France). Direction Scientifique de la Resistance des Structures.
THREE DIMENSIONAL NUMERICAL METHOD FOR RESOLVING SMALL TRANSONIC PERTURBATIONS IN UNSTRUCTURED MESH Final Report [METHODE NUMERIQUE 3D DE RESOLUTION DES PETITES PERTURBATIONS TRANSSONIQUES EN MAILLAGE NON STRUCTURE. RAPPORT FINAL]
F. Bangui Feb. 1991 63 p In FRENCH
(Contract DRET-89-34-001)
(ONERA-RT-56/3064-RY-006-R; ETN-91-90096) Avail: NTIS HC/MF A04

A resolution method for Euler equations in small transonic perturbations is presented. Theoretical developments to substitute to the hyperbolic type problem a discretized elliptic type problem by finite element method are reviewed. The algebra of boundary conditions on the moving parts is presented. Steady and unsteady numerical applications are given. ESA

N92-10990*# Stanford Univ., CA. Dept. of Aeronautics and Astronautics.
COMPUTATIONAL STUDY OF THE AERODYNAMICS AND CONTROL BY BLOWING OF ASYMMETRIC VORTICAL FLOWS OVER DELTA WINGS
Ken Craig Sep. 1991 38 p Sponsored by NASA. Ames Research Center
(NASA-CR-187979; NAS 1.26:187979; JIAA-TR-104) Avail: NTIS HC/MF A03 CSCL 01A

Some of the work is described which was done in a study of the flow field produced by tangential leading edge blowing on a 60 deg. delta wing. The flow is studied computationally by solving the Thin Layer Navier-Stokes equations. Steady state flow fields are calculated for various angles of attack and yaw, with and without the presence of tangential leading edge blowing. The effectiveness of blowing as a rolling moment control mechanism to extend the envelope of controllability is illustrated at pre- and post-stall angles of attack. The numerical grid is generated using algebraic grid generation and various interpolation and blending techniques. The jet emanates from a slot with linearly varying thickness and is introduced into the flow field using the concept of an actuator plane, thereby not requiring resolution of the jet slot geometry. The Baldwin-Lomax algebraic turbulence model is used to provide turbulent closure. The computational results are compared with those of experiments. Author

03 AIR TRANSPORTATION AND SAFETY

Includes passenger and cargo air transport operations; and aircraft accidents.

For related information see also *16 Space Transportation* and *85 Urban Technology and Transportation.*

N92-10991# California Univ., Berkeley. Air Transportation Technology Center.
PERSONAL AIR TRANSPORT: STATE OF THE ART Final Report
David D. Little Apr. 1991 25 p Sponsored by California State Dept. of Transportation
(PB91-204768; CA/TL-91-03) Avail: NTIS HC/MF A03 CSCL 01C

As congestion on roadways and at airports continues to increase and the cost of capacity expansion becomes prohibitive, new ways of addressing personal transportation needs have to be considered. Addressed here is the state of the art in Personal Air Transport (PAT), commonly referred to as the flying automobile. It is concluded that the PAT technology faces a number of technical, mechanical, regulatory, cost, and perception obstacles in its attempt to become economically feasible. No one of the obstacles appears to be insurmountable, but the combination of obstacles could keep PAT from significantly impacting the personal transportation market. Author

N92-10992# Federal Aviation Administration, Atlantic City, NJ.
PROGRAM PLAN: NATIONAL AGING AIRCRAFT RESEARCH PROGRAM
Sep. 1991 54 p
(DOT/FAA/CT-88/32-1) Avail: NTIS HC/MF A04

The inevitable effects of aircraft aging are progressive increases in the probability of damage from fatigue corrosion. The continued safe operation of the U.S. commercial fleet will depend on the ability to anticipate required adjustments in the inspection and maintenance activities to compensate for the aging process. Increasing numbers of aircraft are exceeding their economic design life. Presumably, commercial aircraft are designed for infinite life with proper maintenance, but public confidence in operators' abilities to properly maintain older aircraft significantly diminished following the widely publicized failure of the Aloha Airlines 737 fuselage in 1988. The FAA established the National Aging Aircraft Research Program (NAARP) to address this diminished public confidence in the airlines' ability to properly maintain their older aircraft. The goal is to assure continued airworthiness of the U.S. commercial fleet of in-service and future aircraft beyond their economic design life. This will be achieved through improvements in equipment, techniques, practices, and procedures in aircraft and engine design, repair, maintenance, and inspection. The FAA will identify and direct the research to reach this goal. The results of the program will include a technical information data base that will be used by the FAA and/or industry to update or develop new rules, standards, advisories, and facilities. Author

N92-10993# Systems Control Technology, Inc., Arlington, VA.
GUIDELINES FOR INTEGRATING HELICOPTER ASSETS INTO EMERGENCY PLANNING Final Report
Sandra Henninger, Jack Thompson, and Catherine Adams (Advanced Aviation Concepts, Jupiter, FL.) Jul. 1991 66 p (Contract DTFA01-87-C-00014)
(SCT-91RR-18; DOT/FAA/RD-90/11) Avail: NTIS HC/MF A04

The guidelines are presented which contain recommendations on how to best integrate helicopters into existing emergency planning in order to provide maximum protection and life saving services in the community. Further information is provided on developing an inventory of helicopter resources; surveying helicopter operators capabilities; determining communication capabilities and requirements; designating, establishing, and controlling landing zones; and implementing a planned helicopter response. Author

N92-10994*# National Aeronautics and Space Administration. Langley Research Center, Hampton, VA.
A COMPARISON OF AIRBORNE WAKE VORTEX DETECTION MEASUREMENTS WITH VALUES PREDICTED FROM POTENTIAL THEORY
Eric C. Stewart Washington Nov. 1991 38 p
(NASA-TP-3125; L-16899; NAS 1.60:3125) Avail: NTIS HC/MF A03 CSCL 01C

An analysis of flight measurements made near a wake vortex was conducted to explore the feasibility of providing a pilot with useful wake avoidance information. The measurements were made with relatively low cost flow and motion sensors on a light airplane flying near the wake vortex of a turboprop airplane weighing approximately 90000 lbs. Algorithms were developed which removed the response of the airplane to control inputs from the total airplane response and produced parameters which were due solely to the flow field of the vortex. These parameters were compared with values predicted by potential theory. The results indicated that the presence of the vortex could be detected by a combination of parameters derived from the simple sensors. However, the location and strength of the vortex cannot be determined without additional and more accurate sensors. Author

04 AIRCRAFT COMMUNICATIONS AND NAVIGATION

Includes digital and voice communication with aircraft; air navigation systems (satellite and ground based); and air traffic control.

For related information see also *17 Space Communications, Spacecraft Communications, Command and Tracking* and *Communications and Radar.*

N92-10995# Electronics Research Lab., Adelaide (Australia).
USING A DISCRETE FOURIER TRANSFORM TO ESTIMATE PHASE IN INTERFEROMETRIC DIRECTION FINDING
Gareth J. Parker Dec. 1990 35 p
(AD-A231414; ERL-0530-RN; DODA-006-443) Avail: NTIS HC/MF A03 CSCL 17/11

This document discusses the use of the Discrete Fourier Transform to estimate the phase of particular frequency components of a sampled signal. Attention is paid to the limitations of the Discrete Fourier Transform in general. Particular emphasis

is placed on estimating phase for use in Interferometric Direction Finding. GRA

N92-10996# Messerschmitt-Boelkow-Blohm G.m.b.H., Munich (Germany, F.R.).
A SYSTEMATIC FORMULATION, AS AN APPROACH TO AIR TRAFFIC [DER LOESUNGSWEG FUER DEN LUDVERKEHR HEISST SYSTEMISCHER ANSATZ]
H. Fleckenstein 1991 27 p In GERMAN Presented at the Lufthansa DS-Symposium, Frankfurt, Fed. Republic of Germany, 6 Mar. 1991
(MBB-Z-0371-91-PUB; OTN-033124; ETN-91-90199) Avail: NTIS HC/MF A03

A proposal for a new Lufthansa air traffic information system is presented. It is shown that the global formulation system air traffic is to be considered as a system between airport, aircraft and flight safety subsystems. The basic pattern of the system takes into account the following determining functions which are to be optimized in an iterative process: project management, project planning, reliability/quality safety, configuration management, and system engineering. The functional streams of an air traffic system are defined. The position determination process is the key of general traffic control processes. The tasks of a safety/security management are defined. The execution of operative workshops is recommended. ESA

N92-10997# Technische Univ., Berlin (Germany, F.R.). Inst. fuer Luft- und Raumfahrt.
THE ELECTRONIC AERONAUTICAL CHART FOR GENERAL AERONAUTICS: A SYSTEM SPECIFICATION [DIE ELEKTRONISCHE LUFTFAHRTKARTE FUER DIE ALLGEMEINE LUFTFAHRT: EIN SYSTEMENTWURF]
Marius Schlingelhof and Detlef Stolze 17 May 1991 54 p In GERMAN; ENGLISH summary
(ILR-Mitt-263(1991); ETN-91-90209) Avail: NTIS HC/MF A04

A new concept for a low cost navigational computer, which would provide new possibilities of increasing safety and reducing workload for pilots, is presented. An interface between computer and pilot can be provided by a moving map display making it unnecessary to trace flight paths with a finger on a paper map. A design of such a moving map display system is described. The aspects of software and hardware development, and the data acquisition problems are mentioned. ESA

N92-10998# Technical Research Centre of Finland, Espoo.
NAVIGATION AND POSITIONING OF MOBILE ROBOTS
H. Maekelae, K. Koskinen, J. Annanpalo, and A. Penttinen Jan. 1991 93 p In FINNISH; ENGLISH summary
(DE92-704014; VTT-TIED-1210) Avail: NTIS HC/MF A05

Dead reckoning was studied by combining the direction and distance measurements. Travelled distance was measured by using a microwave based Doppler radar and an odometer. Both these methods were quite accurate. The direction of the vehicle was measured by a magnetic compass. Its performance was degraded by the acceleration of the vehicle. Feasibility of ultrasonic sensors was tested for obstacle detection and contour following. The sensors tested were able to detect obstacles but they could not distinguish between various types of obstacles. Infrared switches were tested for detecting reflecting landmarks. Their operation proved to be very reliable for the application. An infrared distance sensor was used to obtain distance to nearby objects. The reflection properties of the object had a great effect on the reliability of the measurement. Artificial landmarks can be used for marking the route of a mobile robot. These landmarks can be detected by computer vision. The experiments for testing this principle gave promising results. The accelerations and tilts of the machine were monitored by accelerometers and inclinometers. A properly dampened inclinometer can be used for detecting dangerous tilts of a mobile robot. The natural frequency of the accelerometer has to be adjusted according to the vibrations of the vehicle body. Microwave techiques for measuring the vehicle position was studied in cooperation with Swedish Institute of Microelectronics. Laser techniques was also studied for accurate positioning. DOE

05 AIRCRAFT DESIGN, TESTING AND PERFORMANCE

Includes aircraft simulation technology.

For related information see also *18 Spacecraft Design, Testing and Performance* and *39 Structural Mechanics*.For land transportation vehicles see *85 Urban Technology and Transportation.*

N92-10999*# Textron Bell Helicopter, Fort Worth, TX.
TECHNOLOGY NEEDS FOR HIGH SPEED ROTORCRAFT (3) Final Report
Jack DeTore and Scott Conway 10 Sep. 1991 109 p
(Contract NAS2-13072)
(NASA-CR-186433; NAS 1.26:186433; BHTI-699-099-329) Avail: NTIS HC/MF A06 CSCL 01C

The objectives of this high speed rotorcraft technology evaluation are threefold: (1) to identify technologies needed to extend the cruise speed capability of rotorcraft; (2) to identify technology issues which must be resolved to obtain technical goals; and (3) to propose a technology plan that takes the technical disciplines to a state of readiness enabling applications with reasonably low risk. The spectrum of rotorcraft is examined with the intent of selecting two or more configurations for a more detailed analysis. The results of this investigation are presented. Author

N92-11000*# National Aeronautics and Space Administration. Ames Research Center, Moffett Field, CA.
ANALYSIS OF OPEN LOOP HIGHER HARMONIC CONTROL AT HIGH AIRSPEEDS ON A MODERN FOUR-BLADED ARTICULATED ROTOR
Sesi Kottapalli and Jane Leyland Aug. 1991 17 p
(NASA-TM-103876; A-91190; NAS 1.15:103876) Avail: NTIS HC/MF A03 CSCL 01C

The effects of open loop higher harmonic control (HHC) on rotor hub loads, performance, and push rod loads of a Sikorsky S-76 helicopter rotor at high airspeeds (up to 200 knots) and moderate lift (10,000 lbs) were studied analytically. The analysis was performed as part of a wind tunnel pre-test prediction and preparation procedure, as well as to provide analytical results for post-test correlation efforts. The test associated with this study is to be concluded in the 40- by 80-Foot Wind Tunnel of the National Full-Scale Aerodynamics Complex (NFAC) at the NASA Ames Research Center. The results from this analytical study show that benefits from HHC can be achieved at high airspeeds. These results clear the way for conducting (with the requirement of safe pushrod loads) an open loop HHC test a high airspeeds in the 40- by 80-Foot Wind Tunnel using an S-76 rotor as the test article. Author

N92-11001# Advisory Group for Aerospace Research and Development, Neuilly-Sur-Seine (France). Flight Mechanic's Panel.
ROTORCRAFT SYSTEM IDENTIFICATION
Sep. 1991 291 p
(AGARD-AR-280; ISBN-92-835-0632-4) Copyright Avail: NTIS HC/MF A13; Non-NATO Nationals requests available only from AGARD/Scientific Publications Executive

For fixed wing aircraft, system identification methods to determine stability and control derivatives from flight test data are used with confidence. The application of the same techniques to rotorcraft is not so far advanced mainly because of the helicopter aeromechanical complexity. Only a few specialists have concentrated on this field and the application in industry is still sporadic. To coordinate these activities within the AGARD nations, a working group was constituted to focus on the applicational aspects of the various individual approaches and to evaluate the strengths and weaknesses of the different methods. The findings are presented of the Working Group including a documentation of the data bases, the applied identification methodologies, and major application areas. For each of the three helicopters, comparisons

of the obtained results are discussed in the format of case studies, covering data quality evaluations, identification, and the verification of the obtained models. Author

N92-11002# Naval Postgraduate School, Monterey, CA.
DEVELOPMENTAL FLIGHT TESTING OF A HALF SCALE UNMANNED AIR VEHICLE M.S. Thesis
James D. Salmons Sep. 1990 61 p
(AD-A240347) Avail: NTIS HC/MF A04 CSCL 01/3

This thesis sought to perform developmental flight testing of a half-scale unmanned air vehicle. To do this the half scale version of the Pioneer (used by the U.S. Marine Corps for training) was chosen as the airframe to instrument because of problems that the Unmanned Air Vehicle Office at the Pacific Missile Test Center had identified in the full scale version of the Pioneer. Problems included: (1) discrepancies in the predicted and flight tested rate-of-climb, time-to-climb and fuel flow at altitude; (2) apparent autopilot related pitch instability; (3) tail boom structural failure; (4) severely limited lateral control; (5) slow pitch response causing degraded maneuverability at high gross weights; and (6) insufficient testing to determine the effects of the new wing on flight endurance. A developmental flight test was conducted for the purpose of predicting the longitudinal and lateral directional behavior of the full scale vehicle. Instrumentation, developed and installed in the radio controlled aircraft, allowed for measurement and recording of control surface movement, indicated airspeed, sideslip angle and angle of attack. The measurement system operated successfully; the data recording system suffered limitations due to vibration introduced into the airframe by the propeller and engine. Lateral directional data were obtained from steady sideslip maneuvers, but longitudinal data taken for trimmed flights with varied center-of-gravity positions were unusable. GRA

N92-11003# Strategic Air Command, Offutt AFB, NE. Directorate of Weather.
STRATEGIC AIR COMMAND CONTRAIL FORMATION STUDY
Jeffrey L. Peters Aug. 1991 7 p
(AD-A240467; SAC/DOW/CP-91/001) Avail: NTIS HC/MF A02 CSCL 04/2

To investigate trends in contrail formation, military aircraft reports of contrail occurrence and non occurrence were collected from 1 May 1990 to 30 April 1991. Over 4,800 contrail reports were collected and analyzed. Below 40,000 feet, 64 percent were occurrences. The data confirms the dependence of contrail formation on ambient temperature and moisture. Results suggest previous formation theory is limited in scope and requires review. Data indicated the presence of warm contrails. Results also suggest the potential for an improved forecast capability by incorporating synoptic-scale vertical motion into the contrail forecast algorithm. Between -46 C and -49 C, the verification rate for occurrences using current contrail forecast techniques was 21 percent. However, analysis indicates contrails formed in this temperature range 69 percent of the time when synoptic-scale upward motion was present. This study focuses on contrail formation below 40,000 feet; additional study is required to understand formation and optical properties of contrails above 40,000 feet. Author

N92-11004# Army Aeromedical Research Lab., Fort Rucker, AL.
CONCEPT EVALUATION OF THE UH-60 EXTERNALLY MOUNTED RESCUE HOIST Final Report
Joseph R. Licina, Larry C. Woodrum, and Douglas P. Pritts Jan. 1991 73 p
(DA Proj. 3M4-63807-D-836)
(AD-A240545) Avail: NTIS HC/MF A04 CSCL 01/3

The concept evaluation of an Externally Mounted Rescue Hoist (EMRH) was performed with the Breeze Eastern EMRH installed on a U.S. Army UH-60 helicopter. A comparative analysis was conducted between the EMRH and the Internally Mounted Rescue Hoist (IMRH) which assessed initial inspection, physical characteristics, installation, and compatibility with the aircraft, performance, and safety. The EMRH showed a significant improvement over the IMRH currently used in U.S. Army MEDEVAC aircraft. GRA

N92-11005# Naval War Coll., Newport, RI. Dept. of Operations.
THE ROLE OF STEALTH IN NAVAL AVIATION AND JOINT/COMBINED OPERATIONS Final Report
Mark P. Grissom 20 May 1991 27 p
(AD-A240595) Avail: NTIS HC/MF A03 CSCL 15/6

The low observable (stealth) technology holds great promise in increasing the effectiveness of naval aviation in support of the maritime strategy and joint/combined operations. Although at first it may seem that stealth is a panacea for nearly all tactical missions, its use needs scrutiny, particularly in strategic implications. This paper looks at stealth and its applicability in each of the four naval missions of power projection, presence, deterrence and sea control, as well as several supporting warfare areas such as anti-air warfare and anti-surface warfare. Lastly, the operational and strategic implications of its use in representative joint/combined operations is addressed. It is found that stealth reduces the risk of many power projection missions and needs less tactical support than conventional strike aircraft. The technology is not required in all missions, however, since the risk level of the mission may not justify the cost of stealth or the mission requires high power electromagnetic energy emissions which are counter to the reason for having stealth. Low observable aircraft can support joint operations such as the AirLand Battle Doctrine of the Army, although there are limitations. Combined operations are supported tactically for the same reasons naval warfare missions are but the risk of loss of allied aircraft and crews must be properly managed to avoid dissension among the haves and have nots of stealth technology. GRA

N92-11006# McDonnell-Douglas Corp., Saint Louis, MO.
NEW INSULATION CONSTRUCTIONS FOR AEROSPACE WIRING APPLICATIONS. VOLUME 1: TESTING AND EVALUATION Final Report, Feb. 1989 - Jan. 1991
Ron Soloman, Lynn Woodford, and Steve Domalewski Jun. 1991 853 p
(Contract F33615-89-C-5605)
(AD-A240638; WL-TR-91-4066-Vol-1) Avail: NTIS HC/MF A99 CSCL 09/1

This test program evaluated existing and new wire insulation constructions in a round wire configuration for aerospace applications. The goal of the program was to identify insulation candidates with balanced electrical, thermal, and mechanical properties. A comprehensive test program was developed to evaluate and statistically rank each wire construction. Testing was conducted using existing military and industry test methods. Forty-three tests were conducted on the wire samples evaluated. Initially, ten insulation candidates and two baseline constructions MIL-W-81381 and MIL-W-22759 (cross-linked ETEE) were evaluated using the 15 most important tests. The majority of candidates consisted of composite constructions of polyimide film and a fluoropolymer layer(s). Four of the best performing candidates and the baseline constructions were further evaluated for overall performance by evaluating properties such as abrasion and cut-through resistance, chemical and fluid resistance, dry and wet arc tracking, and flammability and smoke generation. GRA

N92-11007# McDonnell-Douglas Corp., Saint Louis, MO.
NEW INSULATION CONSTRUCTIONS FOR AEROSPACE WIRING APPLICATIONS. VOLUME 2: THE 270 VDC ARC TRACKING TESTING WITH POWER CONTROLLERS Final Report, Feb. 1989 - Jan. 1991
Ron Soloman, Lynn Woodford, and Steve Domalewski Jun. 1991 218 p
(Contract F33615-89-C-5605)
(AD-A240639; WL-TR-91-4066-Vol-2) Avail: NTIS HC/MF A10 CSCL 09/1

The objective of Amendment 2 testing was to further evaluate the ability of insulations to inhibit arc propagation during short circuit conditions in 270 volt dc power distribution systems.

Evaluations were performed using dry arc propagation tests on three inorganic insulations in unprotected harnesses and on four candidate and two baseline insulation constructions protected by power controllers. Six different power controllers were tested. Evaluations showed that the three unprotected inorganic insulations were not able to inhibit arc propagation in a 270 volt dc power distribution system. The three solid state power controllers demonstrated good to excellent performance in inhibiting arc propagation in 270 volt dc power distribution systems, and two of the three electromechanical controllers demonstrated moderate abilities. The third electromechanical controller was not able to inhibit arc propagation. The insulation constructions played no part in inhibiting arc propagation. GRA

N92-11008# Naval Postgraduate School, Monterey, CA.
DEVELOPMENT OF A 1/7TH SCALE FIGHTER UAV FOR FLIGHT RESEARCH M.S. Thesis
Daniel M. Lee Sep. 1990 82 p
(AD-A240703) Avail: NTIS HC/MF A05 CSCL 01/3

A program was initiated to develop a radio-controlled fighter aircraft to be used for supermaneuverability and agility flight research. High angle-of-attack flight testing a high-risk and very expensive endeavor in manned aircraft, and wind tunnel testing to duplicate dynamic maneuvers is extremely difficult. Another means to conduct agility flight research in a low-cost, low-risk environment has been sought. Construction of a scaled generic Navy fighter model, to be powered by ducted-fan engines and controlled by radio command, was begun. Also, it was deemed essential to incorporate an emergency recovery system in the aircraft, should control be lost due to radio component failure, primary flight system malfunction, or departure from controlled flight. A parachute recovery system was designed, constructed, and tested for structural integrity, opening shock dampening, rapid deployment, and desired rate of descent. Work will continue, leading to flight testing of forebody modifications for enhanced control at high angles of attack. GRA

N92-11009# Office National d'Etudes et de Recherches Aerospatiales, Paris (France). Direction de l'Aerodynamique.
WING TIP TURBINE: ANALYSIS OF THE RESULTS OF S2MA SOUNDING OF MARGINAL VORTEX OF THE A320, TECHNICAL SUMMARY [TURBINE DE BOUT D'AILE: ANALYSE DES RESULTATS DES SONDAGES A S2MA DU TOURBILLON MARGINAL DE L'A320. RAPPORT TECHNIQUE DE SYNTHESE]
F. Manie Nov. 1990 34 p In FRENCH
(Contract STPA-85-95-009)
(ONERA-RTS-21/4365-AY-056A; ETN-91-90082) Avail: NTIS HC/MF A03

Tests (force, pressure, sounding) were carried out at the S2MA wind tunnel for flight conditions of A320 transonic crossing on the 4A.2 model at 1:16.5. The device has six degrees of freedom equipped with a pressure sensor of five holes. Six lower airfoils of free wing extremity were investigated to define the flow structure neighboring the marginal vortex. The results were analyzed to determine the entry conditions for defining the vanes and the positioning of a wing tip turbine, a device intended to reduce the induced drag or to produce a power injection for transport aircraft. ESA

N92-11010*# National Aeronautics and Space Administration. Langley Research Center, Hampton, VA.
MAXIMIZED GUST LOADS FOR A NONLINEAR AIRPLANE USING MATCHED FILTER THEORY AND CONSTRAINED OPTIMIZATION
Robert C. Scott, Anthony S. Pototzky (Lockheed Engineering and Sciences Co., Hampton, VA.), and Boyd Perry, III Sep. 1991 10 p Presented at the 1991 AIAA Atmospheric Flight Mechanics Conference, New Orleans, LA, 19-21 Aug. 1991 Previously announced in IAA as A91-47155
(NASA-TM-104138; NAS 1.15:104138) Avail: NTIS HC/MF A02 CSCL 01C

Two matched filter theory based schemes are described and illustrated for obtaining maximized and time correlated gust loads for a nonlinear aircraft. The first scheme is computationally fast because it uses a simple 1-D search procedure to obtain its answers. The second scheme is computationally slow because it uses a more complex multi-dimensional search procedure to obtain its answers, but it consistently provides slightly higher maximum loads than the first scheme. Both schemes are illustrated with numerical examples involving a nonlinear control system. Author

06 AIRCRAFT INSTRUMENTATION

Includes cockpit and cabin display devices; and flight instruments.

For related information see also *19 Spacecraft Instrumentation* and *35 Instrumentation and Photography.*

N92-11011# Air Force Environmental Technical Applications Center, Scott AFB, IL.
C-29A AIRCRAFT ALTIMETER ERRORS
William R. Schaub, Jr. Jun. 1991 38 p
(AD-A240486; USAFETAC/PR-91/011) Avail: NTIS HC/MF A03 CSCL 01/4

This report documents the results of a study initiated to solve problems with pressure altimeter errors (differences between indicated and true altitude) aboard Air Force C-29A flight inspection aircraft. A basic review of altimetry is provided, along with an explanation of how atmospheric changes affect barometric pressure and pressure altimeters. A method for in-flight correction of altimeter errors is provided, along with an appendix that gives monthly error statistics for the three C-29A working flight levels (1,000, 1,500, and 2,000 feet above ground level). Although the results of this study are applicable only to Scott Air Force Base, Illinois, they can be considered generally representative of other stations with similar field elevations in the midwestern United States. USAFETAC has the ability to produce climatological altimeter error data for any location from which representative upper-air and surface observations are available. GRA

07 AIRCRAFT PROPULSION AND POWER

Includes prime propulsion systems and systems components, e.g., gas turbine engines and compressors; and onboard auxilliary power plants for aircraft.

For related information see also *20 Spacecraft Propulsion and Power, 28 Propellants and Fuels,* and *44 Energy Production and Conversion.*

N92-11012 University Coll. of North Wales, Bangor.
PARALLEL PROCESSING APPLICATIONS FOR GAS TURBINE ENGINE CONTROL Ph.D. Thesis
Haydn Ashley Thompson 1990 275 p
Avail: Univ. Microfilms Order No. BRDX92129

The application of parallel processing to gas turbine control is described. A 3-spool high-bypass gas turbine engine and a controller simulation are written in Occam and mapped onto transputer arrays. These simulations are further complicated with the addition of reheat. A comparison of the same simulations written in C is then performed using the Helios operating system for transputers and the Uniform system upon the Butterfly Plus Computer. These two systems use radically different approaches for interprocessor communication: the transputer using point-to-point serial links and the Butterfly using shared memory. The problems of applying formal methods to parallel asynchronous systems are addressed and the current design specifications are reviewed for their applicability to transputers. Using these specifications, three fault tolerant systems are implemented which address permanent, transient, persistent intermittent and Byzantine failures. A generalized solution to the problem of handling communication failures between the asynchronous transputers using a masking technique is also presented. The fault tolerant

systems that are described use a variety of fault tolerant techniques and attempt to exploit the parallelism within the multiprocessor array for a reduction in execution time while simultaneously exploiting the inherent redundancy for fault tolerance. These implementations highlight the current limitations of present transputers and the advantages of the Occam language.
Dissert. Abstr.

N92-11013*# Sverdrup Technology, Inc., Brook Park, OH.
MACH 6.5 AIR INDUCTION SYSTEM DESIGN FOR THE BETA 2 TWO-STAGE-TO-ORBIT BOOSTER VEHICLE
Anthony C. Midea Oct. 1991 14 p Presented at the Aircraft Design Systems and Operations Meeting, Baltimore, MD, 23-25 Sep. 1991; sponsored by AIAA, AHS, and ASEE Previously announced in IAA as A91-54099
(Contract NAS3-25266)
(NASA-CR-187233; E-6602; NAS 1.26:187233; AIAA-91-3196) Avail: NTIS HC/MF A03 CSCL 21E

A preliminary, two-dimensional, mixed compression air induction system is designed for the Beta II Two Stage to Orbit booster vehicle to minimize installation losses and efficiently deliver the required airflow. Design concepts, such as an external isentropic compression ramp and a bypass system were developed and evaluated for performance benefits. The design was optimized by maximizing installed propulsion/vehicle system performance. The resulting system design operating characteristics and performance are presented. The air induction system design has significantly lower transonic drag than similar designs and only requires about 1/3 of the bleed extraction. In addition, the design efficiently provides the integrated system required airflow, while maintaining adequate levels of total pressure recovery. The excellent performance of this highly integrated air induction system is essential for the successful completion of the Beta II booster vehicle mission. Author

N92-11014*# Maine Univ., Orono.
NUMERICAL SIMULATION OF THE REACTIVE FLOW IN ADVANCED (HSR) COMBUSTORS USING KIVA-2 Final Report, 1 Feb. 1990 - 31 Aug. 1991
Nicholas S. Winowich 1991 113 p
(Grant NAG3-1115)
(NASA-CR-188996; NAS 1.26:188996) Avail: NTIS HC/MF A06 CSCL 21E

Recent work has been done with the goal of establishing ultralow emission aircraft gas turbine combustors. A significant portion of the effort is the development of three dimensional computational combustor models. The KIVA-II computer code which is based on the Implicit Continuous Eulerian Difference mesh Arbitrary Lagrangian Eulerian (ICED-ALE) numerical scheme is one of the codes selected by NASA to achieve these goals. This report involves a simulation of jet injection through slanted slots within the Rich burn/Quick quench/Lean burn (RQL) baseline experimental rig. The RQL combustor distinguishes three regions of combustion. This work specifically focuses on modeling the quick quench mixer region in which secondary injection air is introduced radially through 12 equally spaced slots around the mixer circumference. Steady state solutions are achieved with modifications to the KIVA-II program. Work currently underway will evaluate thermal mixing as a function of injection air velocity and angle of inclination of the slots. Author

N92-11015# Cranfield Inst. of Tech., Bedford (England). Dept. of Turbomachinery and Engineering Mechanics.
RADIAL INFLOW TURBINE STUDY Interim Report No. 5, 21 Jan. - 30 Jun. 1991
S. Hamid and R. L. Elder Jun. 1991 17 p
(Contract DAJA45-89-C-0006)
(AD-A240169; CIT-REF-06/769E(5); R/D-5824-AN-01) Avail: NTIS HC/MF A03 CSCL 21/5

The radial inflow turbine is a primary component used both in small gas turbines and turbochargers. Better understanding of the flow processes occurring within the small passages of the machine could well result in the improved design of units. As most of the detailed aerodynamics is still ill-defined, a joint research project with the objective of improving our understanding has been instigated by Cranfield, the U.S. Army and Turbomach (San Diego). This document describes the early attempts at obtaining measurements downstream of the rotor and provides some results. GRA

N92-11016*# United Technologies Corp., East Hartford, CT.
STRUCTURAL TAILORING OF ADVANCED TURBOPROPS (STAT): USER'S MANUAL
K. W. Brown Nov. 1991 124 p
(Contract NAS3-23941)
(NASA-CR-187101; NAS 1.26:187101; PWA-5967-43) Avail: NTIS HC/MF A06 CSCL 21E

This user's manual describes the Structural Tailoring of Advanced Turboprops program. It contains instructions to prepare the input for optimization, blade geometry and analysis, geometry generation, and finite element program control. In addition, a sample input file is provided as well as a section describing special applications (i.e., non-standard input). Author

N92-11017*# National Aeronautics and Space Administration. Lewis Research Center, Cleveland, OH.
REAL-TIME FAULT DIAGNOSIS FOR PROPULSION SYSTEMS
Walter C. Merrill, Ten-Huei Guo, John C. DeLaat, and Ahmet Duyar (Florida Atlantic Univ., Boca Raton.) 1991 8 p Presented at the International Federation of Automatic Control Symposium on Fault Detection, Supervision and Safety for Technical Processes-SAFEPROCESS 1991, Baden-Baden, Germany, 10-13 Sep. 1991
(NASA-TM-105303; E-6650; NAS 1.15:105303) Avail: NTIS HC/MF A02 CSCL 21E

Current research toward real time fault diagnosis for propulsion systems at NASA-Lewis is described. The research is being applied to both air breathing and rocket propulsion systems. Topics include fault detection methods including neural networks, system modeling, and real time implementations. Author

08 AIRCRAFT STABILITY AND CONTROL

Includes aircraft handling qualities; piloting; flight controls; and autopilots.

For related information see also *05 Aircraft Design, Testing and Performance.*

N92-11018# Honeywell, Inc., Minneapolis, MN. Systems and Research Center.
NEW METHODS IN ROBUST CONTROL Final Draft Technical Report, Mar. 1988 - Aug. 1991
John Doyle, Blaise Morton, and Mike Elgersma 14 Aug. 1991 86 p
(Contract F49620-88-C-0077)
(AD-A240221; HSRC-C910684; AFOSR-91-0740TR) Avail: NTIS HC/MF A05 CSCL 01/4

This report describes advances in robust control in three areas: Optimal H infinity control, singular values, and dynamic inversion. The H infinity results are a thorough treatment of the theory as it has been developed over the last three years. The structured singular value section describes an application of the technique to represent inertia parametric variations in the Space Station. The dynamic inversion section addresses global stability of aircraft pitch axis dynamics using a dynamic inversion control approach. This document is the first draft of the final report for the program New Methods in Robust Control. The emphasis of this program was to develop mathematical theory to help control system designers faced with challenging control problems associated with advanced aerospace vehicles. Relevant applications include flight control systems for new Air force fighter/bomber aircraft, the F-18 HARV research vehicle, the NASP vehicle, the next generation launch system (ALS or NLS), and the Space Station. GRA

N92-11019# Naval Postgraduate School, Monterey, CA.
INITIAL DESIGN STUDY OF EXISTING FLIGHT CONTROL SYSTEM OF RPH AND FEASIBILITY STUDY OF IMPLEMENTING HHC ON THE SH-60B M.S. Thesis
Charles D. Webb Sep. 1990 52 p
(AD-A240522) Avail: NTIS HC/MF A04 CSCL 01/4

The paper reports on two subjects, first the initial design study of a Remotely Piloted Helicopter's flight control system and secondly a feasibility study of implementing Higher Harmonic Control on the SH-60B aircraft. Described for the former is a complete study of stiffness constants, system freeplays and power requirements needed to provide Higher Harmonic Control to the Remotely Piloted Helicopter. The later gives practical design considerations for four alternate mechanical/hydraulic designs. The Remotely Piloted Helicopter Higher Harmonic Control work is an ongoing project at the Naval Postgraduate School and the SH-60B work is an initial study which is currently being evaluated at the Naval Air Test Center. GRA

09 RESEARCH AND SUPPORT FACILITIES (AIR)

Includes airports, hangars and runways; aircraft repair and overhaul facilities; wind tunnels; shock tubes; and aircraft engine test stands.

For related information see also *14 Ground Support Systems and Facilities (Space).*

N92-11020# Association Aeronautique et Astronautique de France, Paris.
APPLICATION OF INFRARED THERMOGRAPHY TO THERMAL FLUX MEASUREMENT IN WIND TUNNELS [APPLICATION DE LA THERMOGRAPHIE INFRAROUGE A LA MESURE DES FLUX THERMIQUES EN SOUFFLERIE]
D. Balageas, D. Boscher, P. Delpech, A. Deom, J. Fournier, G. Gardette, C. Lempereur, P. Berthoumieux, and J. M. Mathe (Centre d'Etudes et de Recherches, Toulouse, France) 1989 21 p In FRENCH Presented at the 26th Colloque d'Aerodynamique Appliquee, Toulouse, France, 23-25 Oct. 1990 Previously announced in IAA as A90-21051 Sponsored by Direction des Recherches, Etudes et Techniques; Service Technique des Programmes Aeronautiques; CEA; and Societe Matra
(AAAF-NT-89-12; ISBN-2-7170-0945-0; ISSN-0243-0177; ETN-91-99953) Avail: NTIS HC/MF A03; CEDOCAR, Section des Diffusions, 26 Blvd Victor, 75996 Paris Armees, France, HC 15 francs

Different thermographic measuring methods are presented: passive thermography, in which the model is heated only by convection; stimulated thermography, in which a short radiative flux is superimposed. Practical examples of wind tunnel measurements are presented. A variety of technical problems to be resolved are addressed, related in particular to the three dimensionality of models, the control of their emissivity, to the presence of porthole windows, and to the quite limited spatial resolution of thermographic images obtained with current industrial imagers. ESA

N92-11021# Federal Aviation Administration, Atlantic City, NJ.
EVALUATION OF TWO HIGH-SPEED RUNWAY EXITS
Rick Marinelli Sep. 1991 23 p
(DOT/FAA/CT-TN91/36) Avail: NTIS HC/MF A03

The effect of proposed changes in runway exit geometry and lighting on runway occupancy time was evaluated. Testing was conducted using a Boeing 727-200 simulator and a Boeing 727-100 aircraft. Subject pilots performed landings to runways equipped with the standard-design and the alternative-design exits. Exit speed was found to be affected most by pilot technique, with no advantage offered by the alternative design. Subjective evaluations by 12 pilots indicated a general preference for the standard-design exit. Author

N92-11022*# National Aeronautics and Space Administration. Langley Research Center, Hampton, VA.
MODEL REPRESENTATION IN THE PANCOR WALL INTERFERENCE ASSESSMENT CODE
Jassim A. Al-Saadi Aug. 1991 26 p
(NASA-TM-104152; NAS 1.15:104152) Avail: NTIS HC/MF A03 CSCL 14B

An investigation into the aircraft model description requirements of a wall interference assessment and correction code known as PANCOR was conducted. The accuracy necessary in specifying various elements of the model description were defined. It was found that the specified lift coefficient is the most important model parameter in the wind tunnel simulation. An accurate specification of the model volume was also found to be important. Also developed was a partially automated technique for generating wing lift distributions that are required as input to PANCOR. An existing three dimensional transonic small disturbance code was modified to provide the necessary information. A group of auxiliary computer programs and procedures was developed to help generate the required input for PANCOR. Author

N92-11023*# Old Dominion Univ., Norfolk, VA. Dept. of Mechanical Engineering and Mechanics.
FURTHER DEVELOPMENTS RELATING TO THE NASA LANGLEY RESEARCH CENTER 13-INCH MAGNETIC SUSPENSION AND BALANCE SYSTEM Final Report, period ending 31 Jul. 1991
Colin P. Britcher Nov. 1991 28 p
(Grant NAG1-1142)
(NASA-CR-188995; NAS 1.26:188995) Avail: NTIS HC/MF A03 CSCL 14B

A few specific developments that were undertaken recently to the magnetic suspension and balance system (MSBS) are detailed. The improvements are as follows: modifications to the digital control system to accommodate a modified position sensing system; development of pressure telemetry systems; and revisions to the wind tunnel test section. Author

N92-11024*# Naval Postgraduate School, Monterey, CA.
PARAMETER IDENTIFICATION STUDIES ON THE NASA/AMES RESEARCH CENTER ADVANCED CONCEPTS FLIGHT SIMULATOR M.S. Thesis
Thomas P. McKavitt, Jr. Sep. 1990 73 p Sponsored by NASA. Ames Research Center
(NASA-TM-105126; NAS 1.15:105126; AD-A240587) Avail: NTIS HC/MF A04 CSCL 14/2

The results of an aircraft parameters identification study conducted on the National Aeronautics and Space Administration/Ames Research Center Advanced Concepts Flight Simulator (ACFS) in conjunction with the Navy-NASA Joint Institute of Aeronautics are given. The ACFS is a commercial airline simulator with a design based on future technology. The simulator is used as a laboratory for human factors research and engineering as applied to the commercial airline industry. Parametric areas examined were engine pressure ratio (EPR), optimum long range cruise Mach number, flap reference speed, and critical take-off speeds. Results were compared with corresponding parameters of the Boeing 757 and 767 aircraft. This comparison identified two areas where improvements can be made: (1) low maximum lift coefficients (on the order of 20-25 percent less than those of a 757); and (2) low optimum cruise Mach numbers. Recommendations were made to those anticipated with the application of future technologies. GRA

N92-11025# Naval Postgraduate School, Monterey, CA.
CALIBRATION OF THE NAVAL POSTGRADUATE SCHOOL 3.5' X 5.0' ACADEMIC WIND TUNNEL M.S. Thesis
Duane E. Nestor Sep. 1990 83 p
(AD-A240614) Avail: NTIS HC/MF A05 CSCL 14/2

The purpose of this thesis was to revitalize the Naval Postgraduate School's 3.5' x 5.0' academic wind tunnel. The wind tunnel had sustained previous damage to one of two sets of counter-rotating blades. Because of this change in configuration,

a wind tunnel calibration was deemed necessary. Along with the calibration a digital data acquisition system was designed and implemented to aid in the data collection, storage and analysis for this project and future projects, using this wind tunnel. The test section airspeed calibration data contained a substantial amount of scatter indicating flow straighteners may be required. The wind tunnel turbulence intensity was found to be relatively low considering the configuration change and is expected to reach an acceptable level (less than 0.3 percent) with the planned installation of turbulence screens in the settling chamber. GRA

N92-11026# Range Commanders Council, White Sands Missile Range, NM.
WORLD GEODETIC SYSTEM 1984 (WGS-84) CONSOLIDATED DATABASE FOR TEST RANGES
Aug. 1991 40 p
(AD-A240621; RCC-750-91) Avail: NTIS HC/MF A03 CSCL 08/5

In an effort to encourage all test ranges to implement WGS-84 as the standard geodetic coordinate system, a test range consolidated database was established using approximately 200 key points from the ranges. Because of concerns over data origin, transformation procedures, and other possible errors, the database is a starting point to provide all ranges with a listing containing identical coordinates for selected sites. GRA

N92-11027# Range Commanders Council, White Sands Missile Range, NM. Documentation Group.
A BRIEF INTRODUCTION TO THE UNIVERSAL DOCUMENTATION SYSTEM. UNIVERSAL DOCUMENTATION SYSTEM HANDBOOK
Aug. 1991 17 p
(AD-A240622; RCC/DG-501-90) Avail: NTIS HC/MF A03 CSCL 05/2

The UDS endeavors to standardize the efforts of all agencies who seek support in conducting operations on the various ranges. The illustrations in this introduction have been prepared to familiarize potential range user with the UDS which has been published as RCC documents in the 501-90 series. An overview of the system, including descriptions of the documentation levels, options with the system, and guidelines for the user have been included. GRA

N92-11028# Federal Aviation Administration, Atlantic City, NJ.
PROTOTYPE RUNWAY HOLD-SHORT LIGHTING SYSTEM
Eric S. Katz and Thomas H. Paprocki (MiTech, Inc., Washington, DC.) Sep. 1991 16 p
(DOT/FAA/CT-TN91/43) Avail: NTIS HC/MF A03

A prototype runway hold-short lighting system was developed at the FAA Technical Center. The purpose of this lighting system is to provide identification to a pilot, while landing during intersecting runway landing and takeoff operations, of the point at which he must hold short when so instructed by Air Traffic Control. During an in-service evaluation at Boston Logan Airport, user airline pilots were asked to comment on the effectiveness of the hold-short lighting system. Results of the evaluation indicate that the hold-short lighting system provides a landing pilot with a positive indication of the point at which he must hold short during the rollout after landing. Author

N92-11029# Federal Aviation Administration, Atlantic City, NJ.
SURFACE PAINTED TAXIWAY MARKINGS AT SEATTLE-TACOMA INTERNATIONAL AIRPORT
Keith W. Bagot and Thomas H. Paprocki (MiTech, Inc., Washington, DC.) Oct. 1991 20 p
(DOT/FAA/CT-TN91/49) Avail: NTIS HC/MF A03

A prototype system of surface painted taxiway markings was evaluated at Seattle-Tacoma International Airport (SEATAC). The purpose of this evaluation was to determine the usefulness, from the pilot's and controller's viewpoint, of the surface painted markings to provide controllers with location of queued aircraft under conditions of low visibility. User pilots from Alaska Airlines as well as user controllers from SEATAC Tower were asked to comment on the effectiveness of the markings. Results of the evaluation indicate this system of painted taxiway surface markings does not provide the aircraft location information essential for supporting low visibility (400-ft runway visual range) taxi operations. Author

N92-11030*# National Aeronautics and Space Administration. Langley Research Center, Hampton, VA.
MAGNETIC SUSPENSION AND BALANCE SYSTEMS: A COMPREHENSIVE, ANNOTATED BIBLIOGRAPHY
Marie H. Tuttle, Deborah L. Moore (Vigyan Research Associates, Inc., Hampton, VA.), and Robert A. Kilgore Washington Aug. 1991 68 p Supersedes NASA-TM-80225 and NASA-TM-84661 (NASA-TM-4318; L-16974; NAS 1.15:4318; NASA-TM-80225; NASA-TM-84661) Avail: NTIS HC/MF A04 CSCL 14B

This bibliography contains 301 entries. Results are reported of recent studies aimed at increasing the research capabilities of magnetic suspension and balance systems; e.g., increasing force and torque capability, increasing angle of attack capability, and increasing overall system reliability. The problem is addressed of scaling from the relatively small size of existing systems to much larger sizes. The purpose of the bibliography is to provide an up-to-date list of publications that might be helpful to persons interested in magnetic suspension and balance systems for use in wind tunnels. The arrangement is generally chronological by date of presentation. However, papers presented at conferences or meetings are placed under dates of presentation. The numbers assigned to many of the citations have been changed from those used in the previous bibliography. This has been done in order to allow outdated citations to be removed and some recently discovered older works to be included in their proper chronological order. Author, source, and subject indexes are included in order to increase the usefulness of this compilation. Author

12 ASTRONAUTICS (GENERAL)

For extraterrestrial exploration see *91 Lunar and Planetary Exploration.*

N92-11031 Motorbooks International Publishers and Wholesalers, Osceola, WI.
SPACE YEAR 1991: THE COMPLETE RECORD OF THE YEAR'S SPACE EVENTS
Nigel Macknight, ed. 1991 178 p LIMITED REPRODUCIBILITY: More than 20% of this document may be affected by color photographs Original contains color illustrations
(ISBN-0-87938-482-4) Copyright Avail: Issuing Activity

A record and appraisal is presented of all the major space events which took place over the period 1 July 1989 to 30 June 1990. The manned space flights are reviewed of Columbia, Atlantis, and Discovery for the time frame. An accounting is given of the progress of the fourth space shuttle, Endeavour. The two Soviet manned missions are also reviewed, Soyuz TM-8 and TM-9. U.S. planetary missions are also reviewed. An introduction is given which is made up of a review of the entire year. Author

N92-11032# Joint Publications Research Service, Arlington, VA.
JPRS REPORT: SCIENCE AND TECHNOLOGY. USSR: SPACE. FEOKTISTOV'S VIEWS ON FUTURE DIRECTIONS FOR SPACE PROGRAM
K. P. Feoktistov 1 Oct. 1991 27 p Transl. into ENGLISH of Novoye v Zhizni, Nauke, Tekhnike: Seriya Kosmonavtika, Astronomiya (Moscow, USSR, Izdatelstvo Znaniye), no. 4, Apr. 1991 p 1-63
(JPRS-USP-91-005) Avail: NTIS HC/MF A03

What has been done so far and what may lie ahead according to the thoughts of Feoktistov is presented. This is something of a summary of the development of the U.S.S.R. space program. An attempt is made to predict how it will develop. The author is one of the first Russian cosmonauts. Author

13 ASTRODYNAMICS

Includes powered and free-flight trajectories; and orbital and launching dynamics.

No abstracts in this category.

14 GROUND SUPPORT SYSTEMS AND FACILITIES (SPACE)

Includes launch complexes, research and production facilities; ground support equipment, e.g., mobile transporters; and simulators.

For related information see also *09 Research and Support Facilities (Air).*

N92-11033*# Research Inst. for Advanced Computer Science, Moffett Field, CA.

TELESCIENCE WORKSTATION Final Report

Robert L. Brown, Dee Doyle, Richard F. Haines, and Michael Slocum 1989 14 p

(NASA-CR-188878; NAS 1.26:188878; RIACS-TR-89-1) Avail: NTIS HC/MF A03 CSCL 14B

As part of the Telescience Testbed Pilot Program, the Universities Space Research Association/ Research Institute for Advanced Computer Science (USRA/RIACS) proposed to support remote communication by providing a network of human/machine interfaces, computer resources, and experimental equipment which allows: remote science, collaboration, technical exchange, and multimedia communication. The telescience workstation is intended to provide a local computing environment for telescience. The purpose of the program are as follows: (1) to provide a suitable environment to integrate existing and new software for a telescience workstation; (2) to provide a suitable environment to develop new software in support of telescience activities; (3) to provide an interoperable environment so that a wide variety of workstations may be used in the telescience program; (4) to provide a supportive infrastructure and a common software base; and (5) to advance, apply, and evaluate the telescience technolgy base. A prototype telescience computing environment designed to bring practicing scientists in domains other than their computer science into a modern style of doing their computing was created and deployed. This environment, the Telescience Windowing Environment, Phase 1 (TeleWEn-1), met some, but not all of the goals stated above. The TeleWEn-1 provided a window-based workstation environment and a set of tools for text editing, document preparation, electronic mail, multimedia mail, raster manipulation, and system management. Author

15 LAUNCH VEHICLES AND SPACE VEHICLES

Includes boosters; operating problems of launch/space vehicle systems; and reusable vehicles.

For related information see also *20 Spacecraft Propulsion and Power.*

N92-11034*# National Aeronautics and Space Administration. Lewis Research Center, Cleveland, OH.

OVERVIEW OF THE BETA II TWO-STAGE-TO-ORBIT VEHICLE DESIGN

Robert M. Plencner Oct. 1991 12 p Presented at the Aircraft Design Systems and Operations Meeting, Baltimore, MD, 23-25 Sep. 1991; sponsored by AIAA, AHS, and ASEE Previously announced in IAA as A91-54088

(NASA-TM-105298; E-6641; NAS 1.15:105298; AIAA-91-3175) Copyright Avail: NTIS HC/MF A03 CSCL 22B

A study of a near-term, low risk two-stage-to-orbit (TSTO) vehicle was undertaken. The goal of the study was to assess a fully reusable TSTO vehicle with horizontal takeoff and landing capability that could deliver 10,000 pounds to a 120 nm polar orbit. The configuration analysis was based on the Beta vehicle design. A cooperative study was performed to redesign and refine the Beta concept to meet the mission requirements. The vehicle resulting from this study was named Beta II. It has an all-airbreathing first stage and a staging Mach number of 6.5. The second stage is a conventional wing-body configuration with a single SSME. Author

N92-11035*# National Aeronautics and Space Administration. Langley Research Center, Hampton, VA.

USER MODELING TECHNIQUES FOR ENHANCED USABILITY OF OPSMODEL OPERATIONS SIMULATION SOFTWARE

William T. Davis Washington Nov. 1991 13 p

(NASA-TM-4306; L-16915; NAS 1.15:4306) Avail: NTIS HC/MF A03 CSCL 09B

The PC based OPSMODEL operations software for modeling and simulation of space station crew activities supports engineering and cost analyses and operations planning. Using top-down modeling, the level of detail required in the data base can be limited to being commensurate with the results required of any particular analysis. To perform a simulation, a resource environment consisting of locations, crew definition, equipment, and consumables is first defined. Activities to be simulated are then defined as operations and scheduled as desired. These operations are defined within a 1000 level priority structure. The simulation on OPSMODEL, then, consists of the following: user defined, user scheduled operations executing within an environment of user defined resource and priority constraints. Techniques for prioritizing operations to realistically model a representative daily scenario of on-orbit space station crew activities are discussed. The large number of priority levels allows priorities to be assigned commensurate with the detail necessary for a given simulation. Several techniques for realistic modeling of day-to-day work carryover are also addressed. Author

N92-11036*# Virginia Polytechnic Inst. and State Univ., Blacksburg.

LARGE DEPLOYABLE ANTENNA PROGRAM. PHASE 1: TECHNOLOGY ASSESSMENT AND MISSION ARCHITECTURE

Craig A. Rogers and Warren L. Stutzman Washington NASA Oct. 1991 87 p

(Contract NAS1-18471)

(NASA-CR-4410; NAS 1.26:4410) Avail: NTIS HC/MF A05 CSCL 20N

The program was initiated to investigate the availability of critical large deployable antenna technologies which would enable microwave remote sensing missions from geostationary orbits as required for Mission to Planet Earth. Program goals for the large antenna were: 40-meter diameter, offset-fed paraboloid, and surface precision of 0.1 mm rms. Phase 1 goals were: to review the state-of-the-art for large, precise, wide-scanning radiometers up to 60 GHz; to assess critical technologies necessary for selected concepts; to develop mission architecture for these concepts; and to evaluate generic technologies to support the large deployable reflectors necessary for these missions. Selected results of the study show that deployable reflectors using furlable segments are limited by surface precision goals to 12 meters in diameter, current launch vehicles can place in geostationary only a 20-meter class antenna, and conceptual designs using stiff reflectors are possible with areal densities of 2.4 deg/sq m. Author

16 SPACE TRANSPORTATION

Includes passenger and cargo space transportation, e.g., shuttle operations; and space rescue techniques.

For related information see also *03 Air Transportation and Safety* and *18 Spacecraft Design, Testing and Performance.* For space suits see *54 Man/System Technology and Life Support.*

N92-11037# Naval Postgraduate School, Monterey, CA.
THE SPACE SHUTTLE: AN ATTEMPT AT LOW-COST, ROUTINE ACCESS TO SPACE M.S. Thesis
Jeffery D. Wonch Sep. 1990 114 p
(AD-A240589) Avail: NTIS HC/MF A06 CSCL 22/1

This thesis examines the Space Shuttle's purpose of low-cost, routine access to space and how the lessons learned during the Space Shuttle program have affected the thinking on new heavy-fit launch systems. The thesis objective is to show the Space Shuttle was an attempt at developing a routine, low-cost access to space but, because of Shuttle-unique capabilities, cost-effective operations may never be realized with the Shuttle system. The Space Shuttle concept definition is addressed and the impact on design by DOD influence. The Space Shuttle developmental history is presented, and how budgetary constraints, coupled with NASA's desire to build a low-cost system resulted in over-runs in schedule and costs. The thesis looks at the operational period of the Space Shuttle, the use of Government subsidies to keep the price of a Shuttle launch artificially low, and the difficulties experienced by NASA in maintaining planned launch schedule. The Challenger accident resulted in restructure of U.S. space policy as well as how the Shuttle will be used in the future. In conclusion, lessons learned from the Space Shuttle program are presented that the next generation of space transportation systems can build upon.
GRA

N92-11038*# National Aeronautics and Space Administration. John F. Kennedy Space Center, Cocoa Beach, FL.
DEBRIS/ICE/TPS ASSESSMENT AND PHOTOGRAPHIC ANALYSIS FOR SHUTTLE MISSION STS-43
Gregory N. Katnik, Scott A. Higginbotham, and James Bradley Davis Sep. 1991 152 p Original contains color illustrations
(NASA-TM-103823; NAS 1.15:103823) Avail: NTIS HC/MF A08; 76 functional color pages CSCL 22B

A debris/ice Thermal Protection System (TPS) assessment and photographic analysis was conducted for Space Station Mission STS-43. Debris inspections of the flight elements and launch pad were performed before and after launch. Ice/frost conditions on the External Tank (ET) were assessed by the use of computer programs, nomographs, and infrared scanner data during cryogenic loading of the vehicle followed by on-pad visual inspection. High speed photography was analyzed after launch to identify ice/debris sources and to evaluate potential vehicle damage and/or in-flight anomalies.
Author

17 SPACE COMM., SPACECRAFT COMM., COMMAND & TRACKING

Includes telemetry; space communications networks; astronavigation and guidance; and radio blackout.

For related information see also *04 Aircraft Communications and Navigation* and *32 Communications and Radar.*

N92-11039*# National Aeronautics and Space Administration. Goddard Space Flight Center, Greenbelt, MD.
SPACE NETWORK CONTROL CONFERENCE ON RESOURCE ALLOCATION CONCEPTS AND APPROACHES
Karen L. Moe, ed. Sep. 1991 298 p Conference held in Greenbelt, MD, 12-13 Dec. 1990
(NASA-CP-3124; Rept-91B00130; NAS 1.55:3124) Avail: NTIS HC/MF A13 CSCL 22A

The results are presented of the Space Network Control (SNC) Conference. In the late 1990s, when the Advanced Tracking and Data Relay Satellite System is operational, Space Network communication services will be supported and controlled by the SNC. The goals of the conference were to survey existing resource allocation concepts and approaches, to identify solutions applicable to the Space Network, and to identify avenues of study in support of the SNC development. The conference was divided into three sessions: (1) Concepts for Space Network Allocation; (2) SNC and User Payload Operations Control Center (POCC) Human-Computer Interface Concepts; and (3) Resource Allocation Tools, Technology, and Algorithms. Key recommendations addressed approaches to achieving higher levels of automation in the scheduling process. For individual titles, see N92-11040 through N92-11064.

N92-11040*# National Aeronautics and Space Administration. Goddard Space Flight Center, Greenbelt, MD.
SPACE NETWORK CONTROL (SNC) CONFERENCE ON RESOURCE ALLOCATION CONCEPTS AND APPROACHES. OVERVIEW
In its Space Network Control Conference on Resource Allocation Concepts and Approaches Sep. 1991 p 45-60 (For primary document see N92-11039 02-17)
Avail: NTIS HC/MF A13 CSCL 22A

In session 1 of the conference, Concepts for space network resource allocation was the main topic. In session 2, Space Network Control and user payload operations and control center human-computer interface, was the topic of discussion. The topic of session 3 was Resource allocation tools, technology, and algorithms. Some of the stated goals for the conference are as follows: to survey existing resource allocation concepts and approaches; to identify solutions applicable to the SN problem; to identify fruitful avenues of study in support of SNC development; and to capture knowledge in proceedings and make available to bidders on the SNC concept definition procurement.
Author

N92-11041*# Computer Technology Associates, Inc., Rockville, MD. NASA Programs Office.
WHAT WE WERE ASKED TO DO
In NASA. Goddard Space Flight Center, Space Network Control Conference on Resource Allocation Concepts and Approaches Sep. 1991 p 61-68 (For primary document see N92-11039 02-17)
Avail: NTIS HC/MF A13 CSCL 22A

Recommendations are made after 32 interviews, lesson identification, lesson analysis, and mission characteristics identification. The major recommendations are as follows: (1) to develop end-to-end planning and scheduling operations concepts by mission class and to ensure their consideration in system life cycle documentation; (2) to create an organizational infrastructure at the Code 500 level, supported by a Directorate level steering committee with project representation, responsible for systems engineering of end-to-end planning and scheduling systems; (3) to develop and refine mission capabilities to assess impacts of early mission design decisions on planning and scheduling; and (4) to emphasize operational flexibility in the development of the Advanced Space Network, other institutional resources, external (e.g., project) capabilities and resources, operational software and support tools.
Author

N92-11042*# National Aeronautics and Space Administration, Washington, DC.
CONCEPTS, REQUIREMENTS, AND DESIGN APPROACHES FOR BUILDING SUCCESSFUL PLANNING AND SCHEDULING SYSTEMS **c81**
Rhoda Shaller Hornstein and John K. Willoughby (Information Sciences, Inc., Englewood, CO.) *In* NASA. Goddard Space Flight Center, Space Network Control Conference on Resource Allocation Concepts and Approaches Sep. 1991 p 69-84 (For primary document see N92-11039 02-17)
Avail: NTIS HC/MF A13 CSCL 05A

Traditional practice of systems engineering management assumes requirements can be precisely determined and unambiguously defined prior to system design and implementation;

practice further assumes requirements are held static during implementation. Human-computer decision support systems for service planning and scheduling applications do not conform well to these assumptions. Adaptation to the traditional practice of systems engineering management are required. Basic technology exists to support these adaptations. Additional innovations must be encouraged and nutured. Continued partnership between the programmatic and technical perspective assures proper balance of the impossible with the possible. Past problems have the following origins: not recognizing the unusual and perverse nature of the requirements for planning and scheduling; not recognizing the best starting point assumptions for the design; not understanding the type of system that being built; and not understanding the design consequences of the operations concept selected. Author

N92-11043*# National Aeronautics and Space Administration. Goddard Space Flight Center, Greenbelt, MD.
PROPOSED PLANNING AND SCHEDULING SERVICES FOR THE SNC IN THE CDOS ERA c81
Todd Welden *In its* Space Network Control Conference on Resource Allocation Concepts and Approaches Sep. 1991 p 85-91 (For primary document see N92-11039 02-17)
Avail: NTIS HC/MF A13 CSCL 05A

Studies indicate that the current NCC mode of operation needs to be enhanced to meet the needs of the mid to late 19990's. There is a need to simplify the request interface for Space Network services. This is because there are more complex missions, more flexible spacecraft operations, more scheduling data volume, and more events per spacecraft and scheduling period. Author

N92-11044*# National Aeronautics and Space Administration. Goddard Space Flight Center, Greenbelt, MD.
AN RF INTERFERENCE MITIGATION METHODOLOGY WITH POTENTIAL APPLICATIONS IN SCHEDULING c81
Yen F. Wong and James L. Rash *In its* Space Network Control Conference on Resource Allocation Concepts and Approaches Sep. 1991 p 93-106 (For primary document see N92-11039 02-17)
Avail: NTIS HC/MF A13 CSCL 05A

Software tools for interference analysis and mitigation were developed in the Communications Link Analysis and Simulation System (CLASS) environment for: communications performance evaluation; and mission planning. Potential applications are seen in analysis, evaluation, and optimization of user schedules. Tools producing required separation angles and potential interference intervals can be used as an aid to mutual interference mitigation within a scheduling system. Author

N92-11045*# TRW Systems Group, Redondo Beach, CA. Systems Development Div.
AUTOMATED CONFLICT RESOLUTION ISSUES c81
Jeffrey S. Wike *In* NASA. Goddard Space Flight Center, Space Network Control Conference on Resource Allocation Concepts and Approaches Sep. 1991 p 107-113 (For primary document see N92-11039 02-17)
Avail: NTIS HC/MF A13 CSCL 05A

A discussion is presented of how conflicts for Space Network resources should be resolved in the ATDRSS era. The following topics are presented: a description of how resource conflicts are currently resolved; a description of issues associated with automated conflict resolution; present conflict resolution strategies; and topics for further discussion. Author

N92-11046*# Martin Marietta Corp., Bethesda, MD. Information and Communication Systems
EFFECT OF LOCUS OF RESOURCE CONTROL ON OPERATIONAL EFFICIENCY IN DISTRIBUTED OPERATIONS
A. L. Geoffroy *In* NASA. Goddard Space Flight Center, Space Network Control Conference on Resource Allocation Concepts and Approaches Sep. 1991 p 115-120 (For primary document see N92-11039 02-17)
Avail: NTIS HC/MF A13 CSCL 22A

The following topics are presented in view graph form: space network control (SNC) usage in the Advanced Tracking and Data Relay Satellite (ATDRSS) era; an acronym and icon list; demands of the SNC; tightness of resources coupling; sharing information and sharing control; potential ways of distributing control; efficiency problems unrelated to distribution of control; efficiency problems related to distribution of control; and recommendations. Author

N92-11047*# Jet Propulsion Lab., California Inst. of Tech., Pasadena.
RESOURCE ALLOCATION PLANNING HELPER (RALPH)
David G. Werntz *In* NASA. Goddard Space Flight Center, Space Network Control Conference on Resource Allocation Concepts and Approaches Sep. 1991 p 121-124 (For primary document see N92-11039 02-17)
Avail: NTIS HC/MF A13 CSCL 22A

The following topics are presented in view graph form: the background of the Resource Allocation Planning Helper (RALPH); RALPH schedule lifecycle; scheduling approach; technology layering; details; and RALPH directions. Author

N92-11048*# Jet Propulsion Lab., California Inst. of Tech., Pasadena.
USER INTERFACE ISSUES IN SUPPORTING HUMAN-COMPUTER INTEGRATED SCHEDULING
Lynne P. Cooper and Eric W. Biefeld *In* NASA. Goddard Space Flight Center, Space Network Control Conference on Resource Allocation Concepts and Approaches Sep. 1991 p 125-133 (For primary document see N92-11039 02-17)
Avail: NTIS HC/MF A13 CSCL 22A

The topics are presented in view graph form and include the following: characteristics of Operations Mission Planner (OMP) schedule domain; OMP architecture; definition of a schedule; user interface dimensions; functional distribution; types of users; interpreting user interaction; dynamic overlays; reactive scheduling; and transitioning the interface. Author

N92-11049*# Computer Technology Associates, Inc., Rockville, MD.
HUMAN FACTORS ISSUES IN THE DESIGN OF USER INTERFACES FOR PLANNING AND SCHEDULING c54
Elizabeth D. Murphy *In* NASA. Goddard Space Flight Center, Space Network Control Conference on Resource Allocation Concepts and Approaches Sep. 1991 p 135-144 (For primary document see N92-11039 02-17)
Avail: NTIS HC/MF A13 CSCL 05H

The purpose is to provide and overview of human factors issues that impact the effectiveness of user interfaces to automated scheduling tools. The following methods are employed: (1) a survey of planning and scheduling tools; (2) the identification and analysis of human factors issues; (3) the development of design guidelines based on human factors literature; and (4) the generation of display concepts to illustrate guidelines. Author

N92-11050*# Ford Aerospace and Communications Corp., Seabrook, MD. Systems, Engineering, and Analysis Support.
FLEXIBLE ENVELOPE REQUEST NOTATION (FERN)
David R. Zoch, David LaVallee, and Stuart Weinstein *In* NASA. Goddard Space Flight Center, Space Network Control Conference on Resource Allocation Concepts and Approaches Sep. 1991 p 145-157 (For primary document see N92-11039 02-17)
Avail: NTIS HC/MF A13 CSCL 22A

The following topics are presented in view graph form and include the following: scheduling application; the motivation for the Flexible Envelope Request Notation (FERN); characteristics of FERN; types of information needed in requests; where information is stored in requests; FERN structures; generic requests; resource availability for pooled resources; expressive notation; temporal constraints; time formats; changes to FERN; sample FERN requests; the temporal relationship between two steps; maximum activity length to limit step delays; alternative requests; the temporal relationship between two activities; and idle resource usage between steps. Author

N92-11051*# Computer Technology Associates, Inc., Rockville, MD.
CHIMES-2: A TOOL FOR AUTOMATED HCI ANALYSIS c54
William J. Weiland *In* NASA. Goddard Space Flight Center, Space Network Control Conference on Resource Allocation Concepts and Approaches Sep. 1991 p 159-166 (For primary document see N92-11039 02-17)
Avail: NTIS HC/MF A13 CSCL 05H

The topics are presented in view graph form and include the following: Computer Human Interaction Models (CHIMES) methodology; the CHIMES-2 prototype; and CHIMES future development. Author

N92-11052*# Colorado Univ., Boulder. Lab. for Atmospheric and Space Physics.
TRUST: TDRSS RESOURCE USER SUPPORT TOOL
Thomas P. Sparn and R. Daniel Gablehouse *In* NASA. Goddard Space Flight Center, Space Network Control Conference on Resource Allocation Concepts and Approaches Sep. 1991 p 167-171 (For primary document see N92-11039 02-17)
Avail: NTIS HC/MF A13 CSCL 22A

TRUST-TDRSS (Tracking Data and Relay Satellite System) Resource User Support Tool is presented in the form of the viewgraphs. The following subject areas are covered: TRUST development cycle; the TRUST system; scheduling window; ODM/GCMR window; TRUST architecture; surpass; and summary. Author

N92-11053*# Computer Sciences Corp., Greenbelt, MD.
NETWORK CONTROL CENTER USER PLANNING SYSTEM (NCC UPS)
Brian Dealy *In* NASA. Goddard Space Flight Center, Space Network Control Conference on Resource Allocation Concepts and Approaches Sep. 1991 p 173-182 (For primary document see N92-11039 02-17)
Avail: NTIS HC/MF A13 CSCL 22A

NCC UPS is presented in the form of the viewgraphs. The following subject areas are covered: UPS overview; NCC UPS role; major NCC UPS functional requirements; interactive user access levels; UPS interfaces; interactive user subsystem; interface navigation; scheduling screen hierarchy; interactive scheduling input panels; autogenerated schedule request panel; schedule data tabular display panel; schedule data graphic display panel; graphic scheduling aid design; and schedule data graphic display.
Author

N92-11054*# Space Telescope Science Inst., Baltimore, MD. Advance Planning Systems Branch.
SPIKE: AI SCHEDULING TECHNIQUES FOR HUBBLE SPACE TELESCOPE c89
Mark D. Johnston *In* NASA. Goddard Space Flight Center, Space Network Control Conference on Resource Allocation Concepts and Approaches Sep. 1991 p 183-192 (For primary document see N92-11039 02-17)
Avail: NTIS HC/MF A13 CSCL 03A

AI (Artificial Intelligence) scheduling techniques for HST are presented in the form of the viewgraphs. The following subject areas are covered: domain; HST constraint timescales; HTS scheduling; SPIKE overview; SPIKE architecture; constraint representation and reasoning; use of suitability functions by scheduling agent; SPIKE screen example; advantages of suitability function framework; limiting search and constraint propagation; scheduling search; stochastic search; repair methods; implementation; and status. Author

N92-11055*# Space Industries, Inc., Webster, TX. Intelligent Systems.
INTELLIGENT PERTURBATION ALGORITHMS FOR SPACE SCHEDULING OPTIMIZATION c81
Clifford R. Kurtzman *In* NASA. Goddard Space Flight Center, Space Network Control Conference on Resource Allocation Concepts and Approaches Sep. 1991 p 193-205 (For primary document see N92-11039 02-17)
Avail: NTIS HC/MF A13 CSCL 05A

Intelligent perturbation algorithms for space scheduling optimization are presented in the form of the viewgraphs. The following subject areas are covered: optimization of planning, scheduling, and manifesting; searching a discrete configuration space; heuristic algorithms used for optimization; use of heuristic methods on a sample scheduling problem; intelligent perturbation algorithms are iterative refinement techniques; properties of a good iterative search operator; dispatching examples of intelligent perturbation algorithm and perturbation operator attributes; scheduling implementations using intelligent perturbation algorithms; major advances in scheduling capabilities; the prototype ISF (industrial Space Facility) experiment scheduler; optimized schedule (max revenue); multi-variable optimization; Space Station design reference mission scheduling; ISF-TDRSS command scheduling demonstration; and example task - communications check. Author

N92-11056*# Computer Sciences Corp., Greenbelt, MD.
POLYNOMIAL OPTIMIZATION TECHNIQUES FOR ACTIVITY SCHEDULING. OPTIMIZATION BASED PROTOTYPE SCHEDULER c61
Surender Reddy *In* NASA. Goddard Space Flight Center, Space Network Control Conference on Resource Allocation Concepts and Approaches Sep. 1991 p 207-215 (For primary document see N92-11039 02-17)
Avail: NTIS HC/MF A13 CSCL 09B

Polynomial optimization techniques for activity scheduling (optimization based prototype scheduler) are presented in the form of the viewgraphs. The following subject areas are covered: agenda; need and viability of polynomial time techniques for SNC (Space Network Control); an intrinsic characteristic of SN scheduling problem; expected characteristics of the schedule; optimization based scheduling approach; single resource algorithms; decomposition of multiple resource problems; prototype capabilities, characteristics, and test results; computational characteristics; some features of prototyped algorithms; and some related GSFC references. Author

N92-11057*# Mitre Corp., McLean, VA.
RANGE SCHEDULING AID (RSA) c81
J. R. Logan and M. K. Pulvermacher *In* NASA. Goddard Space Flight Center, Space Network Control Conference on Resource Allocation Concepts and Approaches Sep. 1991 p 217-223 (For primary document see N92-11039 02-17)
Avail: NTIS HC/MF A13 CSCL 05A

Range Scheduling Aid (RSA) is presented in the form of the viewgraphs. The following subject areas are covered: satellite control network; current and new approaches to range scheduling; MITRE tasking; RSA features; RSA display; constraint based analytic capability; RSA architecture; and RSA benefits. Author

N92-11058*# Ford Aerospace and Communications Corp., Seabrook, MD. Systems, Engineering, and Analysis Support.
SCHEDULING TECHNIQUES IN THE REQUEST ORIENTED SCHEDULING ENGINE (ROSE) c81
David R. Zoch *In* NASA. Goddard Space Flight Center, Space Network Control Conference on Resource Allocation Concepts and Approaches Sep. 1991 p 225-232 (For primary document see N92-11039 02-17)
Avail: NTIS HC/MF A13 CSCL 05A

Scheduling techniques in the ROSE are presented in the form of the viewgraphs. The following subject areas are covered: agenda; ROSE summary and history; NCC-ROSE task goals; accomplishments; ROSE timeline manager; scheduling concerns; current and ROSE approaches; initial scheduling; BFSSE overview and example; and summary. Author

N92-11059*# Martin Marietta Aerospace, Denver, CO. Information Systems Group.
MANAGING TEMPORAL RELATIONS IN THE MAESTRO SCHEDULING SYSTEM c81

Daniel L. Britt *In* NASA. Goddard Space Flight Center, Space Network Control Conference on Resource Allocation Concepts and Approaches Sep. 1991 p 233-240 Submitted for publication (For primary document see N92-11039 02-17)
Avail: NTIS HC/MF A13 CSCL 05A

A set of viewgraphs on managing temporal relations in the MAESTRO scheduling system are given. The viewgraphs present information on such topics as why scheduling is hard, managing temporal relations, constraints on the placement of a single activity, constraints between activities, soft constraints (such as preferences), and contingency handling. Author

N92-11060*# McDonnell-Douglas Space Systems Co., Houston, TX.
RESOURCE REPRESENTATION IN COMPASS c61
Barry R. Fox *In* NASA. Goddard Space Flight Center, Space Network Control Conference on Resource Allocation Concepts and Approaches Sep. 1991 p 241-256 (For primary document see N92-11039 02-17)
Avail: NTIS HC/MF A13 CSCL 09B

A set of viewgraphs on resource representation in COMPASS is given. COMPASS is an incremental, interactive, non-chronological scheduler written in Ada with an X-windows user interface. Beginning with an empty schedule, activities are added to the schedule one at a time, taking into consideration the placement of the activities already on the timeline and the resources that have been reserved for them. The order that the activities are added to the timeline and their location on the timeline are controlled by selection and placement commands invoked by the user. The order that activities are added to the timeline and their location are independent. The COMPASS code library is a cost effective platform for the development of new scheduling applications. It can be effectively used off the shelf for compatible scheduling applications or it can be used as a parts library for the development of custom scheduling systems. Author

N92-11061*# TRW, Inc., Redondo Beach, CA.
AUTOMATING THE CONFLICT RESOLUTION PROCESS c81
Jeffrey S. Wike *In* NASA. Goddard Space Flight Center, Space Network Control Conference on Resource Allocation Concepts and Approaches Sep. 1991 p 265-269 (For primary document see N92-11039 02-17)
Avail: NTIS HC/MF A13 CSCL 05A

The purpose is to initiate a discussion of how the conflict resolution process at the Network Control Center can be made more efficient. Described here are how resource conflicts are currently resolved as well as the impacts of automating conflict resolution in the ATDRSS era. A variety of conflict resolution strategies are presented. Author

N92-11062*# National Aeronautics and Space Administration. Goddard Space Flight Center, Greenbelt, MD.
A METHOD FOR INTERFERENCE MITIGATION IN SPACE COMMUNICATIONS SCHEDULING
Yen F. Wong and James L. Rash *In its* Space Network Control Conference on Resource Allocation Concepts and Approaches Sep. 1991 p 270-284 (For primary document see N92-11039 02-17)
Avail: NTIS HC/MF A13 CSCL 22A

Increases in the number of user spacecraft and data rates supported by NASA's Tracking and Data Relay Satellite System (TDRSS) in the S and Ku bands could result in communications conflicts due to mutual interference. A method to mitigate interference while minimizing unnecessary scheduling restrictions on both TDRSS network and user resources, based on consideration of all relevant communications parameters, was developed. The steps of this method calculate required separation angles at TDRS and produce interference intervals, which can be used in the production of schedules free of unacceptable interference. The method can also be used as a basis for analysis, evaluation, and optimization of user schedules with respect to communications performance. Described here are the proposed method and its potential application to scheduling in space communications. Test cases relative to planned missions, including the Earth Observing System, the Space Station Manned Base, and the Space Shuttle are discussed. Author

N92-11063*# National Aeronautics and Space Administration. Goddard Space Flight Center, Greenbelt, MD.
A PLANNING LANGUAGE FOR ACTIVITY SCHEDULING c61
David R. Zoch, David LaVallee, Stuart Weinstein (Ford Aerospace and Communications Corp., Seabrook, MD.), and G. Michael Tong *In its* Space Network Control Conference on Resource Allocation Concepts and Approaches Sep. 1991 p 285-294 (For primary document see N92-11039 02-17)
Avail: NTIS HC/MF A13 CSCL 09B

Mission planning and scheduling of spacecraft operations are becoming more complex at NASA. Described here are a mission planning process; a robust, flexible planning language for spacecraft and payload operations; and a software scheduling system that generates schedules based on planning language inputs. The mission planning process often involves many people and organizations. Consequently, a planning language is needed to facilitate communication, to provide a standard interface, and to represent flexible requirements. The software scheduling system interprets the planning language and uses the resource, time duration, constraint, and alternative plan flexibilities to resolve scheduling conflicts. Author

N92-11064*# Space Industries, Inc., Webster, TX. Intelligent Systems.
INTELLIGENT PERTURBATION ALGORITHMS TO SPACE SCHEDULING OPTIMIZATION c81
Clifford R. Kurtzman *In* NASA. Goddard Space Flight Center, Space Network Control Conference on Resource Allocation Concepts and Approaches Sep. 1991 p 295-298 (For primary document see N92-11039 02-17)
Avail: NTIS HC/MF A13 CSCL 05A

The limited availability and high cost of crew time and scarce resources make optimization of space operations critical. Advances in computer technology coupled with new iterative search techniques permit the near optimization of complex scheduling problems that were previously considered computationally intractable. Described here is a class of search techniques called Intelligent Perturbation Algorithms. Several scheduling systems which use these algorithms to optimize the scheduling of space crew, payload, and resource operations are also discussed. Author

N92-11065*# Ohio State Univ., Columbus. ElectroScience Lab.
PREDICTION OF THE PATTERN PERFORMANCE FOR THE AEROASSIST FLIGHT EXPERIMENT (AFE) SPACECRAFT Final Report
C. Yang, R. Rudduck, and R. Torres Washington NASA Oct. 1991 58 p
(Contract NAS1-17450)
(NASA-CR-4409; NAS 1.26:4409; OSU-715559-7) Avail: NTIS HC/MF A04 CSCL 22B

In order to provide a set of benchmark flight data for a reusable Aeroassisted Orbit Transfer Vehicle (AOTV) application, NASA undertook the development of an Aeroassisted Flight Experiment (AFE) which will be launched from the Space Shuttle. A representative aeroassist trajectory will be flown and sensor measurements of aerodynamic performance, thermal protection response, and plasma ionization reentry effects will be obtained. Discussed here is the spacecraft antenna. Estimates of signal transmissions from the AFE to the Tracking and Data Relay Satellites (TDRS) during the reentry period are given. The computer modeling of the antennas is presented with and without the reentry plasma. Author

18 SPACECRAFT DESIGN, TESTING AND PERFORMANCE

Includes satellites; space platforms; space stations; spacecraft systems and components such as thermal and environmental controls; and attitude controls.

For life support systems see *54 Man/System Technology and Life Support.* For related information see also *05 Aircraft Design, Testing and Performance, 39 Structural Mechanics,* and *16 Space Transportation.*

N92-11066*# National Aeronautics and Space Administration, Washington, DC.
THE GREAT OBSERVATORIES FOR SPACE ASTROPHYSICS
1991 57 p LIMITED REPRODUCIBILITY: More than 20% of this document may be affected by color photographs Original contains color illustrations
(NASA-NP-128; NAS 1.83:128) Avail: NTIS HC/MF A04; 38 functional color pages CSCL 22B

The nation's strategy for astrophysics research during the rest of this century and into the next is a coordinated, multispectral examination of the universe. NASA plans to launch a family of large orbital observatories, each tuned to a different part of the electromagnetic spectrum. They are as follows: the Gamma Ray Observatory (GRO); the Advanced X Ray Astrophysics Facility (AXAF); the Hubble Space Telescope (HST); and the Space Infrared Telescope Facility (SIRTF). To complement these sensitive space telescopes, a powerful new radio observatory system is envisioned: the Very Long Baseline Array (VLBA), an intercontinental network of radio telescopes, working with radio observatories in space to perform orbiting very long baseline interferometry (OVLBI). Observing the universe across the spectrum requires different kinds of telescopes based on quite different techniques of detection. An optical telescope has little in common with a gamma ray detector; they do not look alike, nor do they operate on the same principles. No single telescope can answer all the questions or make all the discoveries that await. Author

N92-11067*# National Aeronautics and Space Administration, Washington, DC.
UPPER ATMOSPHERE RESEARCH SATELLITE (UARS): A PROGRAM TO STUDY GLOBAL OZONE CHANGE
1991 32 p LIMITED REPRODUCIBILITY: More than 20% of this document may be affected by color photographs Original contains color illustrations
(NASA-TM-105100; NAS 1.15:105100) Avail: NTIS HC/MF A03; 32 functional color pages CSCL 22B

A general overview of NASA's Upper Atmosphere Research Satellite (UARS) program is presented in a broad based informational publication. The UARS will be responsible for carrying out the first systematic, comprehensive study of the stratosphere and will furnish important new data on the mesosphere and thermosphere. The UARS mission objectives are to provide an increased understanding of energy input into the upper atmosphere; global photochemistry of the upper atmosphere; dynamics of the upper atmosphere; coupling among these processes; and coupling between the upper and lower atmosphere. These mission objectives are briefly described along with the UARS on-board instrumentation and related data management systems. M.G.

N92-11068 Stanford Univ., CA.
PRECISION POINTING CONTROL OF THE SPINNING GRAVITY PROBE B SPACECRAFT Ph.D. Thesis
N. Jeremy Kasdin 1991 270 p
Avail: Univ. Microfilms Order No. DA9122549

The design and analysis is described of a precise satellite pointing control system. Attitude control for the Gravity Probe B (GP-B) spacecraft is considered. An on-board telescope is used to point the satellite at a guide star to better than 20 milliarcsec rms. This should be a most precisely pointed spinning satellite. Also, sensor noise and acceleration constraints unique to GP-B make the design particularly challenging. In addition to the pointing requirement, constraints are placed on satellite acceleration. Because the rotors must be supported against residual forces by an electrostatic suspension, large satellite acceleration couple into the rotor's out-of-roundness to produce torques and Newtonian drifts. This effect is synthesized and limits are determined on allowable accelerations induced by the pointing controller. A new digital LQR/LQG controller is designed for attitude control. This controller uses a penalty function to handle the acceleration requirements and a notch to reduce errors at the spin frequency due to inertially fixed disturbances. A digital algorithm is presented for designing discrete estimators with disturbance rejection. Dissert. Abstr.

N92-11069 Aston Univ., Birmingham (England).
DRAG COEFFICIENTS WITH APPLICATIONS TO SATELLITE ORBITS Ph.D. Thesis
Andrew Sowter 1989 134 p
Avail: Univ. Microfilms Order No. BRDX92778

In the last twenty or so years, the results of theory and experiment have produced much information on the characteristics of gas-surface interactions relevant to a satellite in hyperthermal free-molecular flow. Reviews of the rarefied gas dynamics that are applicable to satellites are presented, and an attempt to compare existing models of gas-surface interaction with contemporary knowledge of such systems is made. It is shown that a more natural approach would be to characterize the gas-surface interaction using the normal and tangential momentum accommodation coefficients (simga' and sigma, respectively) specifically in the form sigma = constant, sigma' = sigma'(sub 0)- sigma'(sub 1)sec xi(sub i) where xi(sub i) is the angle subtended between the incident flow and the surface normal and sigma, sigma'(sub 0) and sigma'(sub 1) are constants. Adopting these relationships, the effects of atmospheric lift on inclination and the effects of atmospheric drag on the semi-major axis and eccentricity were investigated. Applications to ANS-1 (1974-70A) show that the observed perturbations in inclination can be ascribed primarily to nonzero sigma'(sub 1) while perturbations in the semi-major axis and eccentricity produce constraint equations between the three parameters. The numerical results seem to imply that a good theoretical orbit is achieved despite a much lower drag coefficient than anticipated by earlier theories. Dissert. Abstr.

N92-11070*# Pennsylvania State Univ., University Park. Dept. of Aerospace Engineering.
PREDICTION OF FORCES AND MOMENTS FOR HYPERSONIC FLIGHT VEHICLE CONTROL EFFECTORS Semiannual Report
Mark D. Maughmer, Lyle N. Long, and Peter J. Pagano 1991 48 p
(Grant NAG1-849)
(NASA-CR-188954; NAS 1.26:188954) Avail: NTIS HC/MF A03 CSCL 22B

Developing methods of predicting flight control forces and moments for hypersonic vehicles, included a preliminary assessment of subsonic/supersonic panel methods and hypersonic local flow inclination methods for such predictions. While these findings clearly indicate the usefulness of such methods for conceptual design activities, deficiencies exist in some areas. Thus, a second phase of research was proposed in which a better understanding is sought for the reasons of the successes and failures of the methods considered, particularly for the cases at hypersonic Mach numbers. To obtain this additional understanding, a more careful study of the results obtained relative to the methods used was undertaken. In addition, where appropriate and necessary, a more complete modeling of the flow was performed using well proven methods of computational fluid dynamics. As a result, assessments will be made which are more quantitative than those of phase 1 regarding the uncertainty involved in the prediction of the aerodynamic derivatives. In addition, with improved understanding, it is anticipated that improvements resulting in better accuracy will be made to the simple force and moment prediction. Author

N92-11071*# Vanderbilt Univ., Nashville, TN. School of Engineering.
AERODYNAMIC CALCULATIONS RELATED TO TETHERED SUB-SATELLITE EXPERIMENTS Final Report, 1 Jun. 1988 - 31 Jul. 1991
J. Leith Potter and J. Kent Rockaway 1 Aug. 1991 35 p
(Grant NAG1-878)
(NASA-CR-188964; NAS 1.26:188964) Avail: NTIS HC/MF A03 CSCL 22B

The results are presented of four aerodynamic studies that were in support of a broader, preliminary inquiry concerning the potential use of downward-deployed tethered sub-satellites for in-flight aerothermodynamic research. There are a multitude of questions regarding the general tethered satellite concept and the present report addresses only a few of these. A method for estimating drag and local surface pressure and shear on orbiting or re-entereing bodies is described, and examples based on the planned TSS-2 (Tethered Satellite System) are given. The problem of pressure measurement are explored, taking into account thermal transpiration, lag time, and the disturbed flow field created by the satellite body. The performance of an aerodynamic stabilizer, a ring-tail design, is calculated and its influence on satellite motion is illustrated. A method for optimizing future satellite shapes for desired aerodynamic properties is transitional rarefied flow with given geometric constraints is proposed and examples are shown. Author

N92-11072 Deutsche Geodaetische Kommission, Munich (Germany, F.R.).
THE NOTION OF ARTIFICIAL SATELLITES IN THE ANISOTROPIC GRAVITATIONAL FIELD OF A UNIFORMLY ROTATING SOLID EARTH MODEL. A SECOND ORDER ANALYTICAL SOLUTION Thesis - Technische Univ. [DIE BEWEGUNG KUENSTLICHER SATELLITEN IM ANISOTROPEN GRAVITATIONSFELD EINER GLEICHMAESSIG ROTIERENDEN STARREN MODELLERDE: EINE ANALYTISCHE LOESUNG 2. ORDNUNG]
Chun-Fang Cui 1990 108 p In GERMAN; ENGLISH summary
(Ser-C-357; ISBN-3-7696-9405-8; ISSN-0065-5325;
ETN-91-90012) Copyright Avail: Deutsche Geodaetische Kommission, Bayerischen Akademie der Wissenschaften, Marstallplatz 8, D-8000 Munich 22, Fed. Republic of Germany

It is shown that the solution is consistent in the linear terms with solutions by Brower and Kaula. The numerical tests show an accuracy of the solution of the order 10(exp -10) for the zonal perturbations and of the order 10(exp -8) for the tesseral perturbations. An intermediate orbit is developed to derive the analytical solution. A quasi mean value method and an iterative method are used to solve the Lie Hori equation. The inclination function by Kaula and the eccentricity function by Lelgemann are investigated in detail. A set of recurrence formulas and symmetrical properties of both functions are derived. ESA

N92-11073*# National Aeronautics and Space Administration. Langley Research Center, Hampton, VA.
ACTIVE VIBRATION DAMPING OF THE SPACE SHUTTLE REMOTE MANIPULATOR SYSTEM
Michael A. Scott, Michael G. Gilbert, and Martha E. Demeo (Draper, Charles Stark Lab., Inc., Cambridge, MA) Aug. 1991 13 p Presented at the AIAA Guidance, Navigation, and Control Conference, New Orleans, LA, 12-14 Aug. 1991 Previously announced in IAA as A91-49597
(NASA-TM-104149; NAS 1.15:104149) Avail: NTIS HC/MF A03 CSCL 22B

The feasibility of providing active damping augmentation of the Space Shuttle Remote Manipulator System (RMS) following normal payload handling operations is investigated. The approach used in the analysis is described, and the results for both linear and nonlinear performance analysis of candidate laws are presented, demonstrating that significant improvement in the RMS dynamic response can be achieved through active control using measured RMS tip acceleration data for feedback. Author

N92-11074*# Alabama Univ., Huntsville. Dept. of Chemistry.
ANALYSIS OF SURFACES FROM THE LDEF A0114, PHASE 4 Semiannual Progress Report, 1 Mar. - 31 Aug. 1991
John C. Gregory 31 Aug. 1991 46 p
(Grant NAG1-1228)
(NASA-CR-188990; NAS 1.26:188990) Avail: NTIS HC/MF A03 CSCL 22B

Progress made from 1 Mar. to 31 Aug. 1991 is presented. The work concentrated on profilometry measurements of eroded and corroded sample surfaces, optical transmission measurements, analysis of the pinhole camera, and x-ray photoelectron spectroscopic (XPS) analysis of some samples. The following papers are presented: (1) observation of Be-7 on the surface of the Long Duration Exposure Facility (LDEF) Spacecraft; (2) measurement of the passive attitude control performance of a recovered spacecraft; (3) effects on LDEF exposed copper flim and bulk; (4) measurements of erosion characteristics for metal and polymer surfaces using profilometry; (5) the interactions of atmospheric cosmogenic radionuclides with spacecraft surfaces; (6) pinhole cameras as sensors for atomic oxygen in orbit; and (7) interaction of atomic oxygen with solid surfaces in low earth orbit- results from LDEF experiment A0114. For individual titles, see N92-11075 through N92-11078.

N92-11075*# Alabama Univ., Huntsville.
THE INTERACTIONS OF ATMOSPHERIC COSMOGENIC RADIONUCLIDES WITH SPACECRAFT SURFACES
John C. Gregory, G. J. Fishman, B. A. Harmon, and T. A. Parnell (National Aeronautics and Space Administration. Marshall Space Flight Center, Huntsville, AL.) *In its* Analysis of Surfaces from the LDEF A0114, Phase 4 31 Aug. 1991 15 p (For primary document see N92-11074 02-18)
Avail: NTIS HC/MF A03 CSCL 22B

The discovery of the cosmogenic radionuclide Be-7 on the front surface (and the front surface only) of the Long Duration Exposure Facility (LDEF) spacecraft has opened opportunities to investigate new phenomena in several disciplines of space science. The experiments performed for this work show that the Be-7 results only if the source of the isotope is the atmosphere through which the spacecraft passed. We should expect that the uptake of beryllium in such circumstances will depend on the chemical form of the Be and the chemical nature of the substrate. It was found that the observed concentration of Be-7 does, in fact, differ between metal surfaces and organic surfaces such as PTFE (teflon). It is noted, however, that: (1) organic surfaces, even PTFE, are etched by the atomic oxygen found under these orbital conditions, and (2) the relative velocity of the species is 8 km(exp -1)s relative to the surface and the interaction chemistry and physics may differ from the norm. The Be-7 is formed by spallation of O and N nuclei under cosmic ray proton bombardment. The principal source region is at altitudes of 12-15 km. While very small quantities are produced above 300 km, the amount measured on the LDEF was 3 to 4 orders of magnitude higher than expected from production at orbital attitude. The most reasonable explanation is that Be-7 is rapidly transported from low altitudes by some unknown mechanism. The process must take place on a time scale similar to the half-life of the isotope (53 days). Many other isotopes are produced by cosmic ray reactions, and some of these are suited to measurement by the extremely sensitive methods of accelerator mass spectrometry. A program was initiated to search for these isotopes and it is hoped that such studies will provide new methods for studying mixing in the upper atmosphere. Author

N92-11076*# Alabama Univ., Huntsville.
EFFECTS ON LDEF EXPOSED COPPER FILM AND BULK
Palmer N. Peters (National Aeronautics and Space Administration. Marshall Space Flight Center, Huntsville, AL.), John C. Gregory, Ligia C. Christl, and Ganesh N. Raikar *In its* Analysis of Surfaces from the LDEF A0114, Phase 4 31 Aug. 1991 8 p (For primary document see N92-11074 02-18)
(Contract NAS8-36645; NAGw-812)
Avail: NTIS HC/MF A03 CSCL 22B

Two forms of copper were exposed to the Long Duration

Exposure Facility (LDEF) Mission 1 environment: a copper film, initially 74.2 plus or minus 1.1 nm thick sputter coated on a fused silica flat and a bulk piece of oxygen-free, high conductivity (OFHC) copper. The optical density of the copper film changed from 1.33 to 0.70 where exposed, and the film thickness increased to 106.7 plus or minus 0.5 nm where exposed. The exposed area appears purple by reflection and green by transmission for the thin film and maroon color for the bulk copper piece. The exposed areas increased in thickness, but only increase in the thickness of the thin film sample could be readily measured. The increase in film thickness is consistent with the density changes occurring during conversion of copper to an oxide. However, we have not been able to confirm appreciable conversion to an oxide by x-ray diffraction studies. We have not yet subjected the sample to e-beams or more abusive investigations out of concern that the film might be modified. Author

N92-11077*# Alabama Univ., Huntsville.
MEASUREMENTS OF EROSION CHARACTERISTICS FOR METAL AND POLYMER SURFACES USING PROFILOMETRY
Ligia C. Christl, John C. Gregory, and Palmer N. Peters (National Aeronautics and Space Administration. Marshall Space Flight Center, Huntsville, AL.) *In its* Analysis of Surfaces from the LDEF A0114, Phase 4 31 Aug. 1991 12 p (For primary document see N92-11074 02-18)
(Contract NAS8-36645; NAGw-812)
Avail: NTIS HC/MF A03 CSCL 22B

The surfaces of many materials exposed in low earth orbit are modified due to interaction with atomic oxygen. Chemical changes and surface roughening effects can occur which alter optical and other properties. The experiment A0114 contained 128 solid surface samples, half of which were exposed on the front and half on the rear of Long Duration Exposure Facility. Each sample was subjected to many analyses, but only the methods and techniques are described which were used to measure the changes in roughness, erosion depths, and material growth using profilometry. Author

N92-11078*# Alabama Univ., Huntsville.
PINHOLE CAMERAS AS SENSORS FOR ATOMIC OXYGEN IN ORBIT; APPLICATION TO ATTITUDE DETERMINATION OF THE LDEF
Palmer N. Peters (National Aeronautics and Space Administration. Marshall Space Flight Center, Huntsville, AL.) and John C. Gregory *In its* Analysis of Surfaces from the LDEF A0114, Phase 4 31 Aug. 1991 9 p (For primary document see N92-11074 02-18)
(Contract NAS8-36645; NAGw-812)
Avail: NTIS HC/MF A03 CSCL 22B

Images produced by pinhole cameras using film sensitive to atomic oxygen provide information on the ratio of spacecraft orbital velocity to the most probable thermal speed of oxygen atoms, provided the spacecraft orientation is maintained stable relative to the orbital direction. Alternatively, as it is described, information on the spacecraft attitude relative to the orbital velocity can be obtained, provided that corrections are properly made for thermal spreading and a co-rotating atmosphere. The LDEF orientation, uncorrected for a co-rotating atmosphere, was determined to be yawed 8.0 minus/plus 0.4 deg from its nominal attitude, with an estimated minus/plus 0.35 deg oscillation in yaw. The integrated effect of inclined orbit and co-rotating atmosphere produces an apparent oscillation in the observed yaw direction, suggesting that the LDEF attitude measurement will indicate even better stability when corrected for a co-rotating atmosphere. The measured thermal spreading is consistent with major exposure occurring during high solar activity, which occurred late during the LDEF mission. Author

N92-11079*# Alabama Univ., Tuscaloosa. Dept. of Engineering Mechanics.
MLITemp: A COMPUTER PROGRAM TO PREDICT THE THERMAL EFFECTS ASSOCIATED WITH HYPERVELOCITY IMPACT DAMAGE TO SPACE STATION MLI
W. K. Rule and V. Giridharan Sep. 1991 79 p
(Contract NAS8-38555)
(NASA-CR-184245; NAS 1.26:184245) Avail: NTIS HC/MF A05 CSCL 22B

A family of user-friendly, DOS PC based, Microsoft BASIC programs written to provide spacecraft designers with empirical predictions of space debris damage to orbiting spacecraft are described. Spacecraft wall temperatures and condensate formation is also predicted. The spacecraft wall configuration is assumed to consist of multilayered insulation (MLI) placed between a Whipple style bumper and the pressure wall. Impact damage predictions are based on data sets of experimental results obtained from simulating debris impacts on spacecraft using light gas guns on earth. A module of the program facilitates the creation of the database of experimental results that is used by the damage prediction modules to predict damage to the bumper, the MLI, and the pressure wall. A finite difference technique is used to predict temperature distributions in the pressure wall, the MLI, and the bumper. Condensate layer thickness is predicted for the case where the pressure wall temperature drops below the dew point temperature of the spacecraft atmosphere. Author

N92-11080# Harris Corp., Melbourne, FL. Government Aerospace Systems Div.
OPUS: OPTIMAL PROJECTION FOR UNCERTAIN SYSTEMS. VOLUME 1 Final Report, 15 Oct. 1988 - 30 Sep. 1991
Dennis S. Bernstein and Wassim M. Haddad 1 Sep. 1991 368 p
(Contract F49620-89-C-0011)
(AD-A240372; AFOSR-91-0754TR) Avail: NTIS HC/MF A16 CSCL 12/4

The optimal projection for uncertain systems (OPUS) is a unified approach to control-system design and analysis for high-performance, multivariable applications such as large flexible space structures. The OPUS yields low-order, robust controllers that meet both time- and frequency-domain objectives. This final report discusses progress achieved during the previous three years in the areas of robust control, fixed-structure control, sampled-data control, tracking control, and nonlinear control. The appendices in this volume include reprints on the following topics: Optimal projection approach to robust fixed-structure control design; Combined L sub 2 H sub infinity model reduction; Robust stability and performance analysis for linear dynamic systems; Robust stability and performance via fixed-order dynamic compensation; Finite-dimensional approximation for optimal fixed-order compensation of distributed parameter systems; Minimal complexity control law synthesis; Singular linear-quadratic regulator problem; and the Goh-Riccati equation. GRA

N92-11081# Harris Corp., Melbourne, FL. Government Aerospace Systems Div.
OPUS: OPTIMAL PROJECTION FOR UNCERTAIN SYSTEMS, VOLUME 2 Final Report, 15 Oct. 1988 - 30 Sep. 1991
Dennis S. Bernstein and Wassim M. Haddad 1 Sep. 1991 425 p
(Contract F49620-89-C-0011)
(AD-A240373; AFOSR-91-0755TR) Avail: NTIS HC/MF A18 CSCL 12/4

The optimal projection for uncertain systems (OPUS) is a unified approach to control-system design and analysis for high-performance, multivariable applications such as large flexible space structures. The OPUS yields low-order, robust controllers that meet both time- and frequency-domain objectives. This final report discusses progress achieved during the previous three years in the areas of robust control, fixed-structure control, sampled-data control, tracking control, and nonlinear control. The appendices in this volume include reprints on the following topics: Controller design with regional pole constraints; Optimal output feedback for nonzero set point regulation; Inequalities for the trace of matrix exponentials; Reduced-order multirate estimation for stable and unstable plants; Nonquadratic cost and nonlinear feedback control; Some open problems in matrix theory arising in linear systems and controls; Small gain vs. positive real modeling of real parameter

uncertainty; and Compartmental modeling and power flow analysis for state space systems. GRA

N92-11082# Naval Postgraduate School, Monterey, CA.
ATTITUDE CONTROL OF FLEXIBLE STRUCTURES M.S. Thesis
Christina C. Ward Sep. 1990 59 p
(AD-A240520) Avail: NTIS HC/MF A04 CSCL 22/2

The experimental set-up for laboratory study of spacecraft control/structural interaction have been designed. Design specifications have been derived, and all the actuators and sensors have been selected except the end-point displacement sensing of the arm. The mainbody and the flexible arm have been fabricated to meet design criteria. The equations of motion for the experimental model have been derived and natural frequencies determined. The natural frequencies of the flexible arm has been determined experimentally and compared with analytical predictions obtained by using the GIFTS finite element analysis program. The experimental and analytical results are in good agreement except the first mode. GRA

N92-11083# Flight Mechanics and Control, Inc., Hampton, VA.
A METHODOLOGY TO ASSESS THE BEST ESTIMATE TRAJECTORY (BET) RESULTS GENERATED FOR THE KWAJALEIN MISSILE RANGE Final Report, 13 Mar. - 13 Sep. 1991
John T. Findlay 13 Sep. 1991 48 p
(Contract DASG60-91-C-0024)
(AD-A240770) Avail: NTIS HC/MF A03 CSCL 16/2

The primary objective of this study is the creation of a methodology whereby more realistic assessments of the aerodynamic forces acting upon reentry vehicles flown from the U.S. West Coast to the Kwajalein Missile Range (KMR) are obtained. This proposed methodology is based on a compilation of various sources of information into a knowledge base. These data would include trajectory estimates via all available post-flight Best Estimate Trajectory (BET) sources, associated data from radar and optical tracking sites, and information from atmospheric models and measurements. Additionally, this database will incorporate telemetered on-board sensor measurements when available. As a result, a knowledge base would exist including historical and future-generated data to be utilized for detailed statistical assessments of the aerodynamic and atmospheric issues effecting reentry vehicles. These findings could then be implemented in the various trajectory fitting processes by enhancing the subsequent modeling of these critical forces. Also, this report discusses, and recommends the use of, a BET methodology to support a limited set of reentry vehicle tests which utilize on-board instrumentation. These results would provide another set of valuable data to be included in the database analyses implied above. Moreover, this BET generation process is proposed herein as the primary contributor for a KMR tracking sensor study. GRA

N92-11084*# Axiomatix, Los Angeles, CA.
SPACE STATION TRACKING REQUIREMENTS FEASIBILITY STUDY, VOLUME 2 Final Report
Sergei Udalov and James Dodds 27 Jul. 1988 364 p
(Contract NAS9-17414)
(NASA-CR-185641-Vol-2; NAS 1.26:185641-Vol-2; R8807-3-Vol-2)
Avail: NTIS HC/MF A16 CSCL 22B

The objective of this feasibility study is to determine analytically the accuracies of various sensors being considered as candidates for Space Station use. Specifically, the studies were performed whether or not the candidate sensors are capable of providing the required accuracy, or if alternate sensor approaches should be investigated. Other topics related to operation in the Space Station environment were considered as directed by NASA-JSC. The following topics are addressed: (1) Space Station GPS; (2) Space Station Radar; (3) Docking Sensors; (4) Space Station Link Analysis; (5) Antenna Switching, Power Control, and AGC Functions for Multiple Access; (6) Multichannel Modems; (7) FTS/EVA Emergency Shutdown; (8) Space Station Information Systems Coding; (9) Wanderer Study; and (10) Optical Communications System Analysis. Brief overviews of the abovementioned topics are given. Wherever applicable, the appropriate appendices provide detailed technical analysis. The report is presented in two volumes. This is Volume 2, containing Appendices K through U. Author

N92-11085*# Axiomatix, Los Angeles, CA.
SPACE STATION TRACKING REQUIREMENTS FEASIBILITY STUDY, VOLUME 1 Final Report
Sergei Udalov and James Dodds 27 Jul. 1988 381 p
(Contract NAS9-17414)
(NASA-CR-185641-Vol-1; NAS 1.26:185641-Vol-1; R8807-3-Vol-1)
Avail: NTIS HC/MF A17 CSCL 22B

The objective of this feasibility study is to determine analytically the accuracies of various sensors being considered as candidates for Space Station use. Specifically, the studies were performed whether or not the candidate sensors are capable of providing the required accuracy, or if alternate sensor approaches be investigated. Other topics related to operation in the Space Station environment were considered as directed by NASA-JCS. The following topics are addressed: (1) Space Station GPS; (2) Space Station Radar; (3) Docking Sensors; (4) Space Station Link Analysis; (5) Antenna Switching, Power Control, and AGC Functions for Multiple Access; (6) Multichannel Modems; (7) FTS/EVA Emergency Shutdown; (8) Space Station Information Systems Coding; (9) Wanderer Study; and (10) Optical Communications System Analysis. Brief overviews of the abovementioned topics are given. Wherever applicable, the appropriate appendices provide detailed technical analysis. The report is presented in two volumes. This is Volume 1, containing the main body and Appendices A through J. Author

N92-11086*# National Aeronautics and Space Administration. Lewis Research Center, Cleveland, OH.
DEVELOPMENT OF A NINETY STRING SOLAR ARRAY SIMULATOR
Thomas E. Vasek and Arthur G. Birchenough Oct. 1991 11 p
(NASA-TM-105278; E-6601; NAS 1.15:105278) Avail: NTIS HC/MF A03 CSCL 22B

A power source was developed to support testing for the Space Station Freedom Power Management and Distribution (PMAD) DC Testbed. The intent was to simulate as closely as possible the steady-state and transient responses of a solar array. Several breadboards and one thermal prototype were built and tested. Responses were successfully verified and improved upon during successive breadboards. The completed 90-string simulator consists of four power MOSFETs, four 25 watt source resistors, and four 250 watt drain source bypass resistors per string, in addition to the control circuitry. Author

N92-11087*# National Aeronautics and Space Administration. Langley Research Center, Hampton, VA.
MULTIDISCIPLINARY OPTIMIZATION OF CONTROLLED SPACE STRUCTURES WITH GLOBAL SENSITIVITY EQUATIONS
Sharon L. Padula, Benjamin B. James, Philip C. Graves (Vigyan Research Associates, Inc., Hampton, VA.), and Stanley E. Woodard Nov. 1991 39 p
(NASA-TP-3130; NAS 1.60:3130) Avail: NTIS HC/MF A03 CSCL 22B

A new method for the preliminary design of controlled space structures is presented. The method coordinates standard finite element structural analysis, multivariable controls, and nonlinear programming codes and allows simultaneous optimization of the structures and control systems of a spacecraft. Global sensitivity equations are a key feature of this method. The preliminary design of a generic geostationary platform is used to demonstrate the multidisciplinary optimization method. Fifteen design variables are used to optimize truss member sizes and feedback gain values. The goal is to reduce the total mass of the structure and the vibration control system while satisfying constraints on vibration decay rate. Incorporating the nonnegligible mass of actuators causes an essential coupling between structural design variables and control design variables. The solution of the demonstration

problem is an important step toward a comprehensive preliminary design capability for structures and control systems. Use of global sensitivity equations helps solve optimization problems that have a large number of design variables and a high degree of coupling between disciplines. Author

N92-11620# Joint Publications Research Service, Arlington, VA.
TECHNICAL REQUIREMENTS OF SICK BAYS ABOARD SPACE SHIPS Abstract Only
A. V. Perkovskiy *In its* JPRS Report: Science and Technology. USSR: Life Sciences 7 Oct. 1991 p 5 Transl. into ENGLISH from Kosmicheskaya Biologiya i Aviakosmicheskaya Meditsina (Moscow, USSR), v. 24, no. 6, Nov. - Dec. 1990 p 62-64 (For primary document see N92-11616 02-52)
Avail: NTIS HC/MF A04

19 SPACECRAFT INSTRUMENTATION

For related information see also *06 Aircraft Instrumentation* and *35 Instrumentation and Photography.*

No abstracts in this category.

20 SPACECRAFT PROPULSION AND POWER

Includes main propulsion systems and components, e.g., rocket engines; and spacecraft auxilliary power sources.

For related information see also *07 Aircraft Propulsion and Power, 28 Propellants and Fuels, 44 Energy Production and Conversion,* and *15 Launch Vehicles and Space Vehicles.*

N92-11088*# National Aeronautics and Space Administration. Lewis Research Center, Cleveland, OH.
NUCLEAR THERMAL PROPULSION: A JOINT NASA/DOE/DOD WORKSHOP
John S. Clark, ed. 1991 500 p Workshop held in Cleveland, OH, 10-12 Jul. 1990
(NASA-CP-10079; E-6456; NAS 1.55:10079) Avail: NTIS HC/MF A21 CSCL 21F

Papers presented at the joint NASA/DOE/DOD workshop on nuclear thermal propulsion are compiled. The following subject areas are covered: nuclear thermal propulsion programs; Rover/NERVA and NERVA systems; Low Pressure Nuclear Thermal Rocket (LPNTR); particle bed reactor nuclear rocket; hybrid propulsion systems; wire core reactor; pellet bed reactor; foil reactor; Droplet Core Nuclear Rocket (DCNR); open cycle gas core nuclear rockets; vapor core propulsion reactors; nuclear light bulb; Nuclear rocket using Indigenous Martian Fuel (NIMF); mission analysis; propulsion and reactor technology; development plans; and safety issues. For individual titles, see N92-11089 through N92-11116.

N92-11089*# National Aeronautics and Space Administration, Washington, DC.
NUCLEAR THERMAL PROPULSION PROGRAM OVERVIEW
Gary L. Bennett *In* NASA. Lewis Research Center, Nuclear Thermal Propulsion: A Joint NASA/DOE/DOD Workshop 1991 p 3-33 (For primary document see N92-11088 02-20)
Avail: NTIS HC/MF A21 CSCL 21F

Nuclear thermal propulsion program is described. The following subject areas are covered: lunar and Mars missions; national space policy; international cooperation in space exploration; propulsion technology; nuclear rocket program; and budgeting. Author

N92-11090*# National Aeronautics and Space Administration. Lewis Research Center, Cleveland, OH.
NUCLEAR THERMAL PROPULSION WORKSHOP OVERVIEW
John S. Clark *In its* Nuclear Thermal Propulsion: A Joint NASA/DOE/DOD Workshop 1991 p 37-52 (For primary document see N92-11088 02-20)
Avail: NTIS HC/MF A21 CSCL 21F

NASA is planning an Exploration Technology Program as part of the Space Exploration Initiative to return U.S. astronauts to the moon, conduct intensive robotic exploration of the moon and Mars, and to conduct a piloted mission to Mars by 2019. Nuclear Propulsion is one of the key technology thrust for the human mission to Mars. The workshop addresses NTP (Nuclear Thermal Rocket) technologies with purpose to: assess the state-of-the-art of nuclear propulsion concepts; assess the potential benefits of the concepts for the mission to Mars; identify critical, enabling technologies; lay-out (first order) technology development plans including facility requirements; and estimate the cost of developing these technologies to flight-ready status. The output from the workshop will serve as a data base for nuclear propulsion project planning. Author

N92-11091*# National Aeronautics and Space Administration. Lewis Research Center, Cleveland, OH.
NUCLEAR THERMAL ROCKET WORKSHOP REFERENCE SYSTEM ROVER/NERVA
Stanley K. Borowski *In its* Nuclear Thermal Propulsion: A Joint NASA/DOE/DOD Workshop 1991 p 53-92 (For primary document see N92-11088 02-20)
Avail: NTIS HC/MF A21 CSCL 21F

The Rover/NERVA engine system is to be used as a reference, against which each of the other concepts presented in the workshop will be compared. The following topics are reviewed: the operational characteristics of the nuclear thermal rocket (NTR); the accomplishments of the Rover/NERVA programs; and performance characteristics of the NERVA-type systems for both Mars and lunar mission applications. Also, the issues of ground testing, NTR safety, NASA's nuclear propulsion project plans, and NTR development cost estimates are briefly discussed. Author

N92-11092*# Rockwell International Corp., Canoga Park, CA. Rocketdyne Div.
NERVA UPGRADE: NON-NUCLEAR COMPONENTS
Stanley Gunn *In* NASA. Lewis Research Center, Nuclear Thermal Propulsion: A Joint NASA/DOE/DOD Workshop 1991 p 93-104 (For primary document see N92-11088 02-20)
Avail: NTIS HC/MF A21 CSCL 21F

The design of engine based upon the original accomplishmentns of the ROVER/NERVA program (but with the use of advanced technologies) is discussed. Some hypothetical requirements for a typical manned Mars mission are outlined. The following subject areas are covered: typical mission NTR propulsion requirements; performance of NTR operating with high pressure hydrogen; NTR expander cycles; ROVER/NERVA core reactor; Mars propulsion 100 K NTR thrust chamber thermal design parameters; 100 K NTR nozzle assembly; NTR integrated pneumatic-fluidics control system; and 100 K flight thrust module/feed system module assembly. Author

N92-11093*# Westinghouse Electric Corp., Madison, PA.
UPGRADED NERVA SYSTEMS: ENABLER NUCLEAR SYSTEM
Gerry Farbman *In* NASA. Lewis Research Center, Nuclear Thermal Propulsion: A Joint NASA/DOE/DOD Workshop 1991 p 105-126 (For primary document see N92-11088 02-20)
Avail: NTIS HC/MF A21 CSCL 21F

The NERVA/Rover Enabler technology enables to go on a low risk, short-term program to meet the requirements of the Mars mission and maybe some lunar missions. The following subject areas are covered: NERVA technology - the foundation for tomorrow's space missions; NERVA/Rover reactor system test sequence; NERVA engine development program; nuclear thermal reactor capability based on many related Westinghouse technology programs; investment in Rover/Nerva technology; synergistic applications of NERVA technology; flow schematic of the NDR engine; the NERVA nuclear subsystem; and technology evolution. Author

N92-11094*# Idaho National Engineering Lab., Idaho Falls.
LOW PRESSURE NUCLEAR THERMAL ROCKET (LPNTR) CONCEPT
J. H. Ramsthaler *In* NASA. Lewis Research Center, Nuclear Thermal Propulsion: A Joint NASA/DOE/DOD Workshop 1991 p 127-150 (For primary document see N92-11088 02-20)
Avail: NTIS HC/MF A21 CSCL 21F

A background and a description of the low pressure nuclear thermal system are presented. Performance, mission analysis, development, critical issues, and some conclusions are discussed. The following subject areas are covered: LPNTR's inherent advantages in critical NTR requirement; reactor trade studies; reference LPNTR; internal configuration and flow of preliminary LPNTR; particle bed fuel assembly; preliminary LPNTR neutronic study results; multiple LPNTR engine concept; tank and engine configuration for mission analysis; LPNTR reliability potential; LPNTR development program; and LPNTR program costs.
Author

N92-11095*# Brookhaven National Lab., Upton, NY.
PARTICLE BED REACTOR NUCLEAR ROCKET CONCEPT
Hans Ludewig *In* NASA. Lewis Research Center, Nuclear Thermal Propulsion: A Joint NASA/DOE/DOD Workshop 1991 p 151-164 (For primary document see N92-11088 02-20)
Avail: NTIS HC/MF A21 CSCL 21F

The particle bed reactor nuclear rocket concept consists of fuel particles (in this case (U,Zr)C with an outer coat of zirconium carbide). These particles are packed in an annular bed surrounded by two frits (porous tubes) forming a fuel element; the outer one being a cold frit, the inner one being a hot frit. The fuel element are cooled by hydrogen passing in through the moderator. These elements are assembled in a reactor assembly in a hexagonal pattern. The reactor can be either reflected or not, depending on the design, and either 19 or 37 elements, are used. Propellant enters in the top, passes through the moderator fuel element and out through the nozzle. Beryllium used for the moderator in this particular design to withstand the high radiation exposure implied by the long run times.
Author

N92-11096*# General Electric Co., San Jose, CA.
A CERMET FUEL REACTOR FOR NUCLEAR THERMAL PROPULSION
Gordon Kruger *In* NASA. Lewis Research Center, Nuclear Thermal Propulsion: A Joint NASA/DOE/DOD Workshop 1991 p 165-183 (For primary document see N92-11088 02-20)
Avail: NTIS HC/MF A21 CSCL 21F

Work on the cermet fuel reactor done in the 1960's by General Electric (GE) and the Argonne National Laboratory (ANL) that had as its goal the development of systems that could be used for nuclear rocket propulsion as well as closed cycle propulsion system designs for ship propulsion, space nuclear propulsion, and other propulsion systems is reviewed. It is concluded that the work done in the 1960's has demonstrated that we can have excellent thermal and mechanical performance with cermet fuel. Thousands of hours of testing were performed on the cermet fuel at both GE and AGL, including very rapid transients and some radiation performance history. We conclude that there are no feasibility issues with cermet fuel. What is needed is reactivation of existing technology and qualification testing of a specific fuel form. We believe this can be done with a minimum development risk.
Author

N92-11097*# General Electric Co., Philadelphia, PA. Astro Space Div.
HYBRID PROPULSION SYSTEMS FOR SPACE EXPLORATION MISSIONS
D. K. Darooka *In* NASA. Lewis Research Center, Nuclear Thermal Propulsion: A Joint NASA/DOE/DOD Workshop 1991 p 185-196 (For primary document see N92-11088 02-20)
Avail: NTIS HC/MF A21 CSCL 21F

Combinations of nuclear thermal propulsion (NTP), nuclear electric propulsion (NEP), and chemical propulsion are discussed. Technical details are given in viewgraph form. The characteristics of each configuration are discussed, particularly thrust characteristics.
Author

N92-11098*# Martin Marietta Aerospace, Denver, CO.
NUCLEAR ROCKET USING INDIGENOUS MARTIAN FUEL NIMF
Robert Zubrin *In* NASA. Lewis Research Center, Nuclear Thermal Propulsion: A Joint NASA/DOE/DOD Workshop 1991 p 197-216 (For primary document see N92-11088 02-20)
Avail: NTIS HC/MF A21 CSCL 21F

In the 1960's, Nuclear Thermal Rocket (NTR) engines were developed and ground tested capable of yielding isp of up to 900 s at thrusts up to 250 klb. Numerous trade studies have shown that such traditional hydrogen fueled NTR engines can reduce the inertial mass low earth orbit (IMLEO) of lunar missions by 35 percent and Mars missions by 50 to 65 percent. The same personnel and facilities used to revive the hydrogen NTR can also be used to develop NTR engines capable of using indigenous Martian volatiles as propellant. By putting this capacity of the NTR to work in a Mars descent/acent vehicle, the Nuclear rocket using Indigenous Martian Fuel (NIMF) can greatly reduce the IMLEO of a manned Mars mission, while giving the mission unlimited planetwide mobility.
Author

N92-11099*# Rockwell International Corp., Canoga Park, CA. Rocketdyne Div.
WIRE CORE REACTOR FOR NTP
R. B. Harty *In* NASA. Lewis Research Center, Nuclear Thermal Propulsion: A Joint NASA/DOE/DOD Workshop 1991 p 217-224 (For primary document see N92-11088 02-20)
Avail: NTIS HC/MF A21 CSCL 21F

The development of the wire core system for Nuclear Thermal Propulsion (NTP) that took place from 1963 to 1965 is discussed. A wire core consists of a fuel wire with spacer wires. It's an annular flow core having a central control rod. There are actually four of these, with beryllium solid reflectors on both ends and all the way around. Much of the information on the concept is given in viewgraph form. Viewgraphs are presented on design details of the wire core, the engine design, engine weight vs. thrust, a technique used to fabricate the wire fuel element, and axial temperature distribution.
Author

N92-11100*# Los Alamos National Lab., NM.
DUMBO: A PACHYDERMAL ROCKET MOTOR
Bill Kirk *In* NASA. Lewis Research Center, Nuclear Thermal Propulsion: A Joint NASA/DOE/DOD Workshop 1991 p 225-236 (For primary document see N92-11088 02-20)
Avail: NTIS HC/MF A21 CSCL 21F

A brief historical account is given of the Dumbo nuclear reactor, a type of folded flow reactor that could be used for rocket propulsion. Much of the information is given in viewgraph form. Viewgraphs show details of the reactor system, fuel geometry, and key characteristics of the system (folded flow, use of fuel washers, large flow area, small fuel volume, hybrid modulator, and cermet fuel).
Author

N92-11101*# New Mexico Univ., Albuquerque. Inst. for Space Nuclear Power.
PELLET BED REACTOR FOR NUCLEAR PROPELLED VEHICLES: PART 1: REACTOR TECHNOLOGY
Mohamed S. El-Genk *In* NASA. Lewis Research Center, Nuclear Thermal Propulsion: A Joint NASA/DOE/DOD Workshop 1991 p 237-253 (For primary document see N92-11088 02-20)
Avail: NTIS HC/MF A21 CSCL 21F

The pellet bed reactor (PBR) for nuclear propelled vehicles is briefly discussed. Much of the information is given in viewgraph form. Viewgraphs include information on the layout for a Mars mission using a PBR nuclear thermal rocket, the rocket reactor layout, the fuel pellet design, materials compatibility, fuel microspheres, microsphere coating, melting points in quasibinary systems, stress analysis of microspheres, safety features, and advantages of the PBR concept.
Author

N92-11102*# McDonnell-Douglas Astronautics Co., Huntington Beach, CA.
PELLET BED REACTOR FOR NUCLEAR PROPELLED VEHICLES: PART 2: MISSIONS AND VEHICLE INTEGRATION TRADES
V. E. Haloulakos *In* NASA. Lewis Research Center, Nuclear Thermal Propulsion: A Joint NASA/DOE/DOD Workshop 1991 p 255-264 (For primary document see N92-11088 02-20)
Avail: NTIS HC/MF A21 CSCL 21F

Mission and vehicle integration tradeoffs involving the use of the pellet bed reactor (PBR) for nuclear powered vehicles is discussed, with much of the information being given in viewgraph form. Information is given on propellant tank geometries, shield weight requirements for conventional tank configurations, effective specific impulse, radiation mapping, radiation dose rate after shutdown, space transfer vehicle design data, a Mars mission summary, sample pellet bed nuclear orbit transfer vehicle mass breakdown, and payload fraction vs. velocity increment. Author

N92-11103*# Sandia National Labs., Albuquerque, NM.
FISSION FRAGMENT ASSISTED REACTOR CONCEPT FOR SPACE PROPULSION: FOIL REACTOR
Steven A. Wright *In* NASA. Lewis Research Center, Nuclear Thermal Propulsion: A Joint NASA/DOE/DOD Workshop 1991 p 265-284 (For primary document see N92-11088 02-20)
Avail: NTIS HC/MF A21 CSCL 21F

The concept is to fabricate a reactor using thin films or foils of uranium, uranium oxide and then to coat them on substrates. These coatings would be made so thin as to allow the escaping fission fragments to directly heat a hydrogen propellant. The idea was studied of direct gas heating and direct gas pumping in a nuclear pumped laser program. Fission fragments were used to pump lasers. In this concept two substrates are placed opposite each other. The internal faces are coated with thin foil of uranium oxide. A few of the advantages of this technology are listed. In general, however, it is felt that if one look at all solid core nuclear thermal rockets or nuclear thermal propulsion methods, one is going to find that they all pretty much look the same. It is felt that this reactor has higher potential reliability. It has low structural operating temperatures, very short burn times, with graceful failure modes, and it has reduced potential for energetic accidents. Going to a design like this would take the NTP community part way to some of the very advanced engine designs, such as the gas core reactor, but with reduced risk because of the much lower temperatures. Author

N92-11104*# Brookhaven National Lab., Upton, NY.
LIQUID ANNULUS
Hans Ludewig *In* NASA. Lewis Research Center, Nuclear Thermal Propulsion: A Joint NASA/DOE/DOD Workshop 1991 p 285-296 (For primary document see N92-11088 02-20)
Avail: NTIS HC/MF A21 CSCL 21F

It is shown that the specific impulse varies with the square root of the temperature and inversely with the square root of the molecular weight of the propellant. Typical values for specific impulse corresponding to various rocket concepts are shown. The Liquid Annulus core concept consists of a fuel element which will be arranged in a moderator block. The advantages as seen for the system are: high specific impulse; structural material will all run at low temperature; and lower fission product inventory because of evaporation. It is felt that this concept is worth at least a first look because of the promise of very high specific impulse. Because of the low thrust, one would probably need a cluster of engines. This is not necessarily bad because there would be some redundancy, but because of the low thrust one might have to refuel while running. Depending on the fuel vaporization, material can be included in the uranium that is injected as one is running along. Author

N92-11105*# Florida Univ., Gainesville.
DROPLET CORE NUCLEAR ROCKET (DLNR)
Samim Anghaie *In* NASA. Lewis Research Center, Nuclear Thermal Propulsion: A Joint NASA/DOE/DOD Workshop 1991 p 297-321 (For primary document see N92-11088 02-20)
Avail: NTIS HC/MF A21 CSCL 21F

The most basic design feature of the droplet core nuclear reactor is to spray liquid uranium into the core in the form of droplets on the order of five to ten microns in size, to bring the reactor to critical conditions. The liquid uranium fuel ejector is driven by hydrogen, and more hydrogen is injected from the side of the reactor to about one and a half meters from the top. High temperature hydrogen is expanded through a nozzle to produce thrust. The hydrogen pressure in the system can be somewhere between 50 and 500 atmospheres; the higher pressure is more desirable. In the lower core region, hydrogen is tangentially injected to serve two purposes: (1) to provide a swirling flow to protect the wall from impingement of hot uranium droplets: (2) to generate a vortex flow that can be used for fuel separation. The reactor is designed to maximize the energy generation in the upper region of the core. The system can result in and Isp of 2000 per second, and a thrust-to-weight ratio of 1.6 for the shielded reactor. The nuclear engine system can reduce the Mars mission duration to less than 200 days. It can reduce the hydrogen consumption by a factor of 2 to 3, which reduces the hydrogen load by about 130 to 150 metric tons. Author

N92-11106*# Layton (J. Preston), Princeton Junction, NJ.
COMMENTS ON DUAL-MODE NUCLEAR SPACE POWER AND PROPULSION SYSTEM CONCEPTS
J. Preston Layton and Jerry Grey *In* NASA. Lewis Research Center, Nuclear Thermal Propulsion: A Joint NASA/DOE/DOD Workshop 1991 p 323-329 (For primary document see N92-11088 02-20)
Avail: NTIS HC/MF A21 CSCL 21F

Some form of Dual-Mode Nuclear Space Power & Propulsion System (D-MNSP&PS) will be essential to spacefaring throughout teh solar system and that such systems must evolve as mankind moves into outer space. The initial D-MNPSP&PS Reference System should be based on (1) present (1990), and (2) advanced (1995) technology for use on comparable mission in the 2000 and 2005 time period respectively. D-MNSP&PS can be broken down into a number of subsystems: Nuclear subsystems including the energy source and controls for the release of thermal power at elevated temperatures; power conversion subsystems; waste heat rejection subsystems; and control and safety subsystems. These systems are briefly detailed. Author

N92-11107*# Pacific Northwest Lab., Richland, WA. Reactor Technology Center.
NUCLEAR THERMAL/NUCLEAR ELECTRIC HYBRIDS
B. D. Reid *In* NASA. Lewis Research Center, Nuclear Thermal Propulsion: A Joint NASA/DOE/DOD Workshop 1991 p 331-341 (For primary document see N92-11088 02-20)
Avail: NTIS HC/MF A21 CSCL 21F

A description is given of the nuclear thermal and nuclear electric hybrid. The specifications are described along with its mission performance. Next, the technical status, development requirements, and some cost estimates are provided. Author

N92-11108*# Sverdrup Technology, Inc., Brook Park, OH.
OPEN CYCLE GAS CORE NUCLEAR ROCKETS
Robert Ragsdale *In* NASA. Lewis Research Center, Nuclear Thermal Propulsion: A Joint NASA/DOE/DOD Workshop 1991 p 343-357 (For primary document see N92-11088 02-20)
Avail: NTIS HC/MF A21 CSCL 21F

The open cycle gas core engine is a nuclear propulsion device. Propulsion is provided by hot hydrogen which is heated directly by thermal radiation from the nuclear fuel. Critical mass is sustained in the uranium plasma in the center. It has typically 30 to 50 kg of fuel. It is a thermal reactor in the sense that fissions are caused by absorption of thermal neutrons. The fast neutrons go out to an external moderator/reflector material and, by collision, slow down to thermal energy levels, and then come back in and cause fission. The hydrogen propellant is stored in a tank. The advantage of the concept is very high specific impulse because you can take

the plasma to any temperature desired by increasing the fission level by withdrawing or turning control rods or control drums.
Author

N92-11109*# Florida Univ., Gainesville. Innovative Nuclear Space and Propulsion Inst.
VAPOR CORE PROPULSION REACTORS
Nils J. Diaz *In* NASA. Lewis Research Center, Nuclear Thermal Propulsion: A Joint NASA/DOE/DOD Workshop 1991 p 389-371 (For primary document see N92-11088 02-20)
Avail: NTIS HC/MF A21 CSCL 21F

Many research issues were addressed. For example, it became obvious that uranium tetrafluoride (UF4) is a most preferred fuel over uranium hexafluoride (UF6). UF4 has a very attractive vaporization point (1 atm at 1800 K). Materials compatible with UF4 were looked at, like tungsten, molybdenum, rhenium, carbon. It was found that in the molten state, UF4 and uranium attacked most everything, but in the vapor state they are not that bad. Compatible materials were identified for both the liquid and vapor states. A series of analyses were established to determine how the cavity should be designed. A series of experiments were performed to determine the properties of the fluid, including enhancement of the electrical conductivity of the system. CFD's and experimental programs are available that deal with most of the major issues. Author

N92-11110*# United Technologies Research Center, East Hartford, CT.
NUCLEAR LIGHT BULB
Tom Latham *In* NASA. Lewis Research Center, Nuclear Thermal Propulsion: A Joint NASA/DOE/DOD Workshop 1991 p 373-384 (For primary document see N92-11088 02-20)
Avail: NTIS HC/MF A21 CSCL 21F

The nuclear light bulb engine is a closed cycle concept. The nuclear light bulb concept provides containment by keeping the nuclear fuel fluid mechanically suspended in a cylindrical geometry. Thermal heat passes through an internally cooled, fused-silica, transparent wall and heats hydrogen propellant. The seeded hydrogen propellant absorbs radiant energy and is expanded through a nozzle. Internal moderation was used in the configuration which resulted in a reduced critical density requirement. This result was supported by criticality experiments. A reference engine was designed that had seven cells and was sized to fit in what was then predicted to be the shuttle bay mass and volume limitations. There were studies done of nozzle throat cooling schemes to remove the radiant heat. Elements of the nuclear light bulb program included closed loop critical assembly tests done at Los Alamos with UF6 confined by argon buffer gas. It was shown that the fuel region could be seeded with constituents that would block UV radiation from the uranium plasma. A combination of calculations and experiments showed that internal moderation produced a critical mass reduction. Other aspects of the research are presented. Author

N92-11111*# Boeing Aerospace Co., Seattle, WA.
QUICK TRIPS TO MARS
R. Hornung *In* NASA. Lewis Research Center, Nuclear Thermal Propulsion: A Joint NASA/DOE/DOD Workshop 1991 p 385-397 (For primary document see N92-11088 02-20)
Avail: NTIS HC/MF A21 CSCL 21F

The design of a Mars Mission Vehicle that would have to be launched by two very heavy lift launch vehicles is described along with plans for a mission to Mars. The vehicle has three nuclear engine for rocket vehicle application (NERVA) boosters with a fourth in the center that acts as a dual mode system. The fourth generates electrical power while in route, but it also helps lift the vehicle out of earth orbit. A Mars Ascent Vehicle (MAV), a Mars transfer vehicle stage, and a Mars Excursion Vehicle (MEV) are located on the front end of this vehicle. Other aspects of this research including aerobraking, heat shielding, nuclear thermal rocket engines, a mars mission summary, closed Brayton cycle with and without regeneration, liquid hydrogen propellant storage, etc. are addressed. Author

N92-11112*# Rockwell International Corp., Canoga Park, CA. Rocketdyne Div.
PROPULSION SYSTEM NEEDS
Stanley Gunn *In* NASA. Lewis Research Center, Nuclear Thermal Propulsion: A Joint NASA/DOE/DOD Workshop 1991 p 399-411 (For primary document see N92-11088 02-20)
Avail: NTIS HC/MF A21 CSCL 21F

The needs of the designer of a solid core nuclear rocket engine are discussed. Some of the topics covered include: (1) a flight thrust module/feed system module assembly; (2) a nuclear thermal rocket (NTR), expander cycle, dual T/P; (3) turbopump operating conditions; (4) typical system parameters; (5) growth capability composite fuel elements; (6) a NTR radiation cooled nozzle extension; (7) a NFS-3B Feed System; and (8) a NTR Integrated Pneumatic-Fluidics Control System. Author

N92-11113*# Oak Ridge National Lab., TN.
NUCLEAR FUELS STATUS
Michael Kania *In* NASA. Lewis Research Center, Nuclear Thermal Propulsion: A Joint NASA/DOE/DOD Workshop 1991 p 413-422 (For primary document see N92-11088 02-20)
Avail: NTIS HC/MF A21 CSCL 21F

A discussion on coated particle fuel performance from a modular High Temperature Gas Reactor (HTGR) is presented along with experimental results. The following topics are covered: (1) the coated particle fuel concept; (2) the functional requirements; (3) performance limiting mechanisms; (4) fuel performance; and (5) methods/techniques for characterizing performance. Author

N92-11114*# Edgerton, Germeshausen and Grier, Inc., Idaho Falls, ID.
NUCLEAR SAFETY
D. Buden *In* NASA. Lewis Research Center, Nuclear Thermal Propulsion: A Joint NASA/DOE/DOD Workshop 1991 p 423-439 (For primary document see N92-11088 02-20)
Avail: NTIS HC/MF A21 CSCL 21F

Topics dealing with nuclear safety are addressed which include the following: general safety requirements; safety design requirements; terrestrial safety; SP-100 Flight System key safety requirements; potential mission accidents and hazards; key safety features; ground operations; launch operations; flight operations; disposal; safety concerns; licensing; the nuclear engine for rocket vehicle application (NERVA) design philosophy; the NERVA flight safety program; and the NERVA safety plan. Author

N92-11115*# National Aeronautics and Space Administration. Lewis Research Center, Cleveland, OH.
SAFETY ISSUES
R. Rohal *In its* Nuclear Thermal Propulsion: A Joint NASA/DOE/DOD Workshop 1991 p 441-444 (For primary document see N92-11088 02-20)
Avail: NTIS HC/MF A21 CSCL 21F

The purpose of the NASA safety review process is to make sure that any system hazards that can endanger the manned flight system are precluded. The systems that address manned flight in a payload safety review process are discussed. The types of basic hazards that are normally addressed on any of the payloads are: contamination, electrical shock, explosions, radiation, and temperature extremes. Author

N92-11116*# Science Applications International Corp., La Jolla, CA.
DISPOSAL METHODS
Alan Friedlander *In* NASA. Lewis Research Center, Nuclear Thermal Propulsion: A Joint NASA/DOE/DOD Workshop 1991 p 445-456 (For primary document see N92-11088 02-20)
Avail: NTIS HC/MF A21 CSCL 21F

A number of disposal options for space nuclear reactors and the associated risks, mostly in the long term, based on probabilities of Earth reentry are discussed. The results are based on a five year study that was conducted between 1978 and 1983 on the space disposal of high level nuclear waste. The study provided

assessment of disposal options, stability of disposal or storage orbits, and assessment of the long term risks of Earth reentry of the nuclear waste. Author

N92-11117# Johns Hopkins Univ., Columbia, MD. Chemical Propulsion Information Agency.
THE 27TH JANNAF COMBUSTION SUBCOMMITTEE MEETING, VOLUME 3
Mary T. Gannaway, ed. Nov. 1990 693 p Meeting held in Cheyenne, WY, 5-9 Nov. 1990
(Contract N00014-91-C-0001)
(CPIA-Publ-557-Vol-3) Avail: NTIS HC/MF A99

This volume, the third of four, is a collection of 49 papers which were presented at the conference. Specific subjects discussed include advanced propellants, ramjets, liquid and solid rocket performance, and underwater propulsion. For individual titles, see N92-11118 through N92-11125.

N92-11118*# National Aeronautics and Space Administration. Langley Research Center, Hampton, VA.
A DETAILED INVESTIGATION OF STAGED NORMAL INJECTION INTO A MACH 2 FLOW **c34**
Dean R. Eklund, G. Burton Northam, and Roy J. Hartfield, Jr. (Virginia Univ., Charlottesville.) *In* JHU, The 27th JANNAF Combustion Subcommittee Meeting, Volume 3 Nov. 1990 p 115-129 (For primary document see N92-11117 02-20)
Avail: NTIS HC/MF A99 CSCL 20D

A study of the staged injection of two jets of air behind a rearward facing step into a Mach 2 flow was performed using the SPARK 3-D Navier-Stokes code. Calculated mole fraction distributions were compared with an extensive set of planar mole fraction measurements made with a laser induced iodine fluorescence technique. A statistical measure, the standard deviation, was used to help assess agreement between calculation and experiment. Overall, good agreement was found between calculated and measured values. Generally, agreement was better in the far field of the injectors. The effect of grid resolution was investigated by calculating solutions on grids of 60,000, 200,000, and 450,000 points. Differences in the solutions on the two finer grids were small. However, the mole fraction distributions were distinguishable. The effect of turbulence modeling was investigated by employing three different algebraic models for the jet turbulence: the Baldwin-Lomax model, the Prandtl mixing length model, and the Eggers mixing length model. Overall, the Eggers mixing length model was found to be superior for this case. Finally, the effect of the jet exit conditions was examined. A recently proposed Mach number distribution at the jet exit was found to slightly improve agreement between measurement and calculation. Author

N92-11119*# National Aeronautics and Space Administration. Marshall Space Flight Center, Huntsville, AL.
CFD CODE SURVEY FOR THRUST CHAMBER APPLICATION
Klaus W. Gross *In* JHU, The 27th JANNAF Combustion Subcommittee Meeting, Volume 3 Nov. 1990 p 143-157 (For primary document see N92-11117 02-20)
Avail: NTIS HC/MF A99 CSCL 21H

In the quest fo find analytical reference codes, responses from a questionnaire are presented which portray the current computational fluid dynamics (CFD) program status and capability at various organizations, characterizing liquid rocket thrust chamber flow fields. Sample cases are identified to examine the ability, operational condition, and accuracy of the codes. To select the best suited programs for accelerated improvements, evaluation criteria are being proposed. Author

N92-11120*# National Aeronautics and Space Administration. Lewis Research Center, Cleveland, OH.
DEVELOPMENTS IN REDES: THE ROCKET ENGINE DESIGN EXPERT SYSTEM
Kenneth O. Davidian *In* JHU, The 27th JANNAF Combustion Subcommittee Meeting, Volume 3 Nov. 1990 p 185-193 Previously announced as N91-10119 (For primary document see N92-11117 02-20)
Avail: NTIS HC/MF A99 CSCL 21H

The Rocket Engine Design Expert System (REDES) was developed at NASA-Lewis to collect, automate, and perpetuate the existing expertise of performing a comprehensive rocket engine analysis and design. Currently, REDES uses the rigorous JANNAF methodology to analyze the performance of the thrust chamber and perform computational studies of liquid rocket engine problems. The following computer codes were included in REDES: a gas properties program named GASP; a nozzle design program named RAO; a regenerative cooling channel performance evaluation code named RTE; and the JANNAF standard liquid rocket engine performance prediction code TDK (including performance evaluation modules ODE, ODK, TDE, TDK, and BLM). Computational analyses are being conducted by REDES to provide solutions to liquid rocket engine thrust chamber problems. REDES was built in the Knowledge Engineering Environment (KEE) expert system shell and runs on a Sun 4/110 computer. Author

N92-11121*# Sverdrup Technology, Inc., Brook Park, OH.
LOX/HYDROGEN COAXIAL INJECTOR ATOMIZATION TEST PROGRAM
M. Zaller *In* JHU, The 27th JANNAF Combustion Subcommittee Meeting, Volume 3 Nov. 1990 p 229-237 Previously announced as N91-19117 (For primary document see N92-11117 02-20)
(Contract NAS3-25266)
Avail: NTIS HC/MF A99 CSCL 21H

Quantitative information about the atomization of injector sprays is needed to improve the accuracy of computational models that predict the performance and stability margin of liquid propellant rocket engines. To obtain this data, a facility for the study of spray atomization is being established at NASA-Lewis to determine the drop size and velocity distributions occurring in vaporizing liquid sprays at supercritical pressures. Hardware configuration and test conditions are selected to make the cold flow simulant testing correspond as closely as possible to conditions in liquid oxygen (LOX)/gaseous H2 rocket engines. Drop size correlations from the literature, developed for liquid/gas coaxial injector geometries, are used to make drop size predictions for LOX/H2 coaxial injectors. The mean drop size predictions for a single element coaxial injector range from 0.1 to 2000 microns, emphasizing the need for additional studies of the atomization process in LOX/H2 engines. Selection of cold flow simulants, measured techniques, and hardware for LOX/H2 atomization simulations are discussed. Author

N92-11122*# Alabama Univ., Huntsville. Dept. of Mechanical Engineering.
NAVIER-STOKES ENTROPY CONTROLLED COMBUSTION INSTABILITY ANALYSIS FOR LIQUID PROPELLANTS **c28**
T. J. Chung and W. S. Yoon *In* JHU, The 27th JANNAF Combustion Subcommittee Meeting, Volume 3 Nov. 1990 p 275-306 (For primary document see N92-11117 02-20)
(Contracts NAS8-36955; DAAH01-87-D-0021)
Avail: NTIS HC/MF A99 CSCL 21I

Navier-Stokes solutions are used to calculate oscillatory components of pressure, velocity, and density, which in turn provide necessary data to compute energy growth factors to determine combustion instability. It is shown that wave instabilities are associated with changes in entropy and the space and time averages of oscillatory components of pressure, velocity and density, together with the mean flow field in the energy equation. Compressible laminar and turbulent flows and reacting flows with hydrogen/oxygen combustion are considered. The SSME combustion/thrust chamber is used for illustration of the theory. The analysis shows that the increase of mean pressure and disturbances consistently results in the increase of instability. It is shown that adequate combustion instability analysis requires at least third order nonlinearity in energy growth or decay. Author

N92-11123# Pratt and Whitney Aircraft, West Palm Beach, FL. Group Engineering Technology.
JANNAF COMBUSTION INSTABILITY PANEL WORKSHOP REPORT: NUMERICAL METHODS IN COMBUSTION INSTABILITY **c25**
George B. Cox, Jr. *In* JHU, The 27th JANNAF Combustion Subcommittee Meeting, Volume 3 Nov. 1990 p 307-315 (For primary document see N92-11117 02-20)
Avail: NTIS HC/MF A99

Combustion instability in liquid propellant rocket engines was a major concern in engine development programs. The imminence of a new round of liquid rocket engine development programs focused attention on avoiding combustion instability. The advent of large supercomputer systems and CFD modeling capabilities introduces a potential new approach to combustion instability modeling through first-principals prediction of acoustic wave behavior and combustion process response. The accumulation and proliferation of combustion instability and combustion response phenomenological models and procedures, and the absence of standardization leave design, analysis, and evaluation of combustion systems in a somewhat chaotic state. Statistical methods in parametric design and process control offer the potential for rationalizing stability design, analysis, and test procedures. The conjunction of new requirements and new capabilities makes it desirable to review current numerical modeling capabilities and to determine future efforts in improved modeling and in methods standardization. The results and conclusions of the Workshop on Numerical Methods in Combustion Stability are described. Author

N92-11124*# National Aeronautics and Space Administration. Lewis Research Center, Cleveland, OH.
JANNAF LIQUID ROCKET COMBUSTION INSTABILITY PANEL RESEARCH RECOMMENDATIONS **c25**
Mark D. Klem *In* JHU, The 27th JANNAF Combustion Subcommittee Meeting, Volume 3 Nov. 1990 p 345-351 Previously announced as N91-13491 (For primary document see N92-11117 02-20)
Avail: NTIS HC/MF A99 CSCL 21B

The Joint Army, Navy, NASA, Air Force (JANNAF) Liquid Rocket Combustion Instability Panel was formed in 1988, drawing its members from industry, academia, and government experts. The panel was chartered to address the needs of near-term engine development programs and to make recommendations whose implementation would provide not only sufficient data but also the analysis capabilities to design stable and efficient engines. The panel was also chartered to make long-term recommendations toward developing mechanistic analysis models that would not be limited by design geometry or operating regime. These models would accurately predict stability and thereby minimize the amount of subscale testing for anchoring. The panel has held workshops on acoustic absorbing devices and combustion instability computational methods. At these workshops, research projects that would meet the panel's charter were suggested. The panel's conclusions about the work that needs to be done and recommendations on how to approach it, based on evaluation of the suggested research projects, are presented. Author

N92-11125*# Jet Propulsion Lab., California Inst. of Tech., Pasadena.
EROSIVE AUGMENTATION OF SOLID PROPELLANT BURNING RATE: MOTOR SIZE SCALING EFFECT **c25**
L. D. Strand and Norman S. Cohen (Cohen, Norman S. Professional Services, Inc., Redlands, CA) *In* JHU, The 27th JANNAF Combustion Subcommittee Meeting, Volume 3 Nov. 1990 p 379-391 (For primary document see N92-11117 02-20)
Avail: NTIS HC/MF A99 CSCL 21B

Two different independent variable forms, a difference form and a ratio form, were investigated for correlating the normalized magnitude of the measured erosive burning rate augmentation above the threshold in terms of the amount that the driving parameter (mass flux or Reynolds number) exceeds the threshold value for erosive augmentation at the test condition. The latter was calculated from the previously determined threshold correlation. Either variable form provided a correlation for each of the two motor size data bases individually. However, the data showed a motor size effect, supporting the general observation that the magnitude of erosive burning rate augmentation is reduced for larger rocket motors. For both independent variable forms, the required motor size scaling was attained by including the motor port radius raised to a power in the independent parameter. A boundary layer theory analysis confirmed the experimental finding, but showed that the magnitude of the scale effect is itself dependent upon scale, tending to diminish with increasing motor size. Author

N92-11126*# National Aeronautics and Space Administration. Lewis Research Center, Cleveland, OH.
ANALYTICAL STUDY OF NOZZLE PERFORMANCE FOR NUCLEAR THERMAL ROCKETS
Kenneth O. Davidian and Kenneth J. Kacynski 1991 29 p Presented at the Conference on Advanced Space Exploration Initiative Technologies, Cleveland, OH, 4-6 Sep. 1991; sponsored in part by NASA, AIAA, and OAI Previously announced in IAA as A91-52451
(NASA-TM-105251; E-6580; NAS 1.15:105251; AIAA-91-3578)
Avail: NTIS HC/MF A03 CSCL 21H

Nuclear propulsion has been identified as one of the key technologies needed for human exploration of the Moon and Mars. The Nuclear Thermal Rocket (NTR) uses a nuclear reactor to heat hydrogen to a high temperature followed by expansion through a conventional convergent-divergent nozzle. A parametric study of NTR nozzles was performed using the Rocket Engine Design Expert System (REDES) at the NASA Lewis Research Center. The REDES used the JANNAF standard rigorous methodology to determine nozzle performance over a range of chamber temperatures, chamber pressures, thrust levels, and different nozzle configurations. A design condition was set by fixing the propulsion system exit radius at five meters and throat radius was varied to achieve a target thrust level. An adiabatic wall was assumed for the nozzle, and its length was assumed to be 80 percent of a 15 degree cone. The results conclude that although the performance of the NTR, based on infinite reaction rates, looks promising at low chamber pressures, finite rate chemical reactions will cause the actual performance to be considerably lower. Parameters which have a major influence on the delivered specific impulse value include the chamber temperature and the chamber pressures in the high thrust domain. Other parameters, such as 2-D and boundary layer effects, kinetic rates, and number of nozzles, affect the deliverable performance of an NTR nozzle to a lesser degree. For a single nozzle, maximum performance of 930 seconds and 1030 seconds occur at chamber temperatures of 2700 and 3100 K, respectively. Dissert. Abstr.

N92-11127# National Aerospace Lab., Tokyo (Japan).
CALIBRATION OF TURBINE FLOWMETERS FOR STORABLE BIPROPELLANT ENGINES
Yukio Kuroda, Makoto Tadano, Masahiro Sato, Kazuo Kasaka, Hiroshi Miyajima, Ryuichi Nagashima, and Masakazu Sato Jan. 1991 22 p In JAPANESE; ENGLISH summary
(NAL-TR-1091; ISSN-0389-4010) Avail: NTIS HC/MF A03

Propellant flow rate measurement is one of the most important factors in rocket engine evaluations. In the development of the apogee engine for the engineering test satellite- IV(ETS-IV), the mass flow rate measurement uncertainty requirement for the propellants is less than +/- 0.25 percent, thus ensuring that the overall uncertainty of the measured specific impulse is less that 1 second. The engine's propulsion system design adopted a complete blowdown system, thus it is important to ensure that the measurement accuracy for a wide range of flow rates, i.e., from about 30-120 percent of the minimum flow rate. To achieve this uncertainty level, an in-place/end-to-end turbine flowmeter calibration system was developed. The calibrations were conducted with actual propellants under pressures and temperatures similar to those in firing tests, thereby reducing errors caused by variations in fluid physical properties and densities. The characteristics and

accuracies of the flow calibration system are described, as well as the method and results of the flow calibration using both hydrazine N2H4 and nitrogen tetroxide (NTO). The uncertainty of the calibration factors, K-factors (pulse per unit volume), was generally estimated to be within +/- 0.25 percent of the nominal flow rate (185 cc/sec for NTO and 265 cc/sec for N2H4).
Author

N92-11128*# National Aeronautics and Space Administration. Lewis Research Center, Cleveland, OH.
LINEAR QUADRATIC SERVO CONTROL OF A REUSABLE ROCKET ENGINE
Jeffrey L. Musgrave 1991 12 p Presented at the 27th Joint Propulsion Conference, Sacramento, CA, 24-27 Jun. 1991; cosponsored by AIAA, SAE, ASME, and ASEE
(NASA-TM-105291; E-6628; NAS 1.15:105291; AIAA-91-1999)
Avail: NTIS HC/MF A03 CSCL 21H

A design method for a servo compensator is developed in the frequency domain using singular values. The method is applied to a reusable rocket engine. An intelligent control system for reusable rocket engines was proposed which includes a diagnostic system, a control system, and an intelligent coordinator which determines engine control strategies based on the identified failure modes. The method provides a means of generating various linear multivariable controllers capable of meeting performance and robustness specifications and accommodating failure modes identified by the diagnostic system. Command following with set point control is necessary for engine operation. A Kalman filter reconstructs the state while loop transfer recovery recovers the required degree of robustness while maintaining satisfactory rejection of sensor noise from the command error. The approach is applied to the design of a controller for a rocket engine satisfying performance constraints in the frequency domain. Simulation results demonstrate the performance of the linear design on a nonlinear engine model over all power levels during mainstage operation.
Author

N92-11129*# National Aeronautics and Space Administration. Lewis Research Center, Cleveland, OH.
IMPROVED THERMODYNAMIC MODELING OF THE NO-VENT FILL PROCESS AND CORRELATION WITH EXPERIMENTAL DATA
William J. Taylor and David J. Chato 1991 18 p Presented at the 26th Thermophysics Conference, Honolulu, HI, 24-26 Jun. 1991; sponsored by AIAA Previously announced in IAA as A91-43444
(NASA-TM-104492; E-6350; NAS 1.15:104492; AIAA-91-1379)
Avail: NTIS HC/MF A03 CSCL 21H

The United States' plans to establish a permanent manned presence in space and to explore the Solar System created the need to efficiently handle large quantities of subcritical cryogenic fluids, particularly propellants such as liquid hydrogen and liquid oxygen, in low- to zero-gravity environments. One of the key technologies to be developed for fluid handling is the ability to transfer the cryogens between storage and spacecraft tanks. The no-vent fill method was identified as one way to perform this transfer. In order to understand how to apply this method, a model of the no-vent fill process is being developed and correlated with experimental data. The verified models then can be used to design and analyze configurations for tankage and subcritical fluid depots. The development of an improved macroscopic thermodynamic model is discussed of the no-vent fill process and the analytical results from the computer program implementation of the model are correlated with experimental results for two different test tanks.
Author

N92-11130*# National Aeronautics and Space Administration. Lewis Research Center, Cleveland, OH.
TECHNOLOGY READINESS ASSESSMENT OF ADVANCED SPACE ENGINE INTEGRATED CONTROLS AND HEALTH MONITORING
Marc G. Millis 1991 17 p Presented at the Conference on Advanced Space Exploration Initiative Technologies, Cleveland, OH, 4-6 Sep. 1991; cosponsored by AIAA, NASA, and OAI Previously announced in IAA as A91-52467
(NASA-TM-105255; E-6584; NAS 1.15:105255; AIAA-91-3601)
Copyright Avail: NTIS HC/MF A03 CSCL 21H

An evaluation is given for an integrated control and health monitoring system (ICHM) system that is designed to be used with hydrogen-oxygen rocket engines. The minimum required ICHM functions, system elements, technology readiness, and system cost are assessed for a system which permits the operation of H-O engines that are space-based, reusable, and descent throttleable. Based on the evaluation of the H-O ICHM, it is estimated that the minimum system requirements for demonstration on an engine system testbed will require an investment of 30 to 45 million dollars over six years.
Author

N92-11131*# National Aeronautics and Space Administration, Washington, DC.
ENABLING THE SPACE EXPLORATION INITIATIVE: NASA'S EXPLORATION TECHNOLOGY PROGRAM IN SPACE POWER
Gary L. Bennett and Ronald C. Cull Oct. 1991 27 p Previously announced in IAA as A91-52372
(NASA-TM-4325; NAS 1.15:4325) Avail: NTIS HC/MF A03 CSCL 10B

Space power requirements for Space Exploration Initiative (SEI) are reviewed, including the results of a NASA 90-day study and reports by the National Research Council, the American Institute of Aeronautics and Astronautics (AIAA), NASA, the Advisory Committee on the Future of the U.S. Space Program, and the Synthesis Group. The space power requirements for the SEI robotic missions, lunar spacecraft, Mars spacecraft, and human missions are summarized. Planning for exploration technology is addressed, including photovoltaic, chemical and thermal energy conversion; high-capacity power; power and thermal management for the surface, Earth-orbiting platform and spacecraft; laser power beaming; and mobile surface systems.
Author

N92-11132*# Rockwell International Corp., Canoga Park, CA. Rocketdyne Div.
DEFINITION, TECHNOLOGY READINESS, AND DEVELOPMENT COST OF THE ORBIT TRANSFER VEHICLE ENGINE INTEGRATED CONTROL AND HEALTH MONITORING SYSTEM ELEMENTS Final Report, Mar. - Oct. 1990
I. Cannon, S. Balcer, M. Cochran, J. Klop, and S. Peterson Oct. 1991 72 p
(Contract NAS3-23773)
(NASA-CR-187123; NAS 1.26:187123; RI/RD91-150) Avail: NTIS HC/MF A04 CSCL 21H

An Integrated Control and Health Monitoring (ICHM) system was conceived for use on a 20 Klb thrust baseline Orbit Transfer Vehicle (OTV) engine. Considered for space used, the ICHM was defined for reusability requirements for an OTV engine service free life of 20 missions, with 100 starts and a total engine operational time of 4 hours. Functions were derived by flowing down requirements from NASA guidelines, previous OTV engine or ICHM documents, and related contracts. The elements of an ICHM were identified and listed, and these elements were described in sufficient detail to allow estimation of their technology readiness levels. These elements were assessed in terms of technology readiness level, and supporting rationale for these assessments presented. The remaining cost for development of a minimal ICHM system to technology readiness level 6 was estimated. The estimates are within an accuracy range of minus/plus 20 percent. The cost estimates cover what is needed to prepare an ICHM system for use on a focussed testbed for an expander cycle engine, excluding support to the actual test firings.
Author

N92-11133*# National Aeronautics and Space Administration. Lewis Research Center, Cleveland, OH.
EFFECT OF PARTICLE SIZE OF MARTIAN DUST ON THE DEGRADATION OF PHOTOVOLTAIC CELL PERFORMANCE
James R. Gaier and Marla E. Perez-Davis 1991 17 p Proposed for presentation at the International Solar Energy Conference, Maui,

HI, 4-8 Apr. 1992; sponsored by ASME
(NASA-TM-105232; E-6556; NAS 1.15:105232) Avail: NTIS HC/MF A03 CSCL 10A

Glass coverglass and SiO2 covered and uncovered silicon photovoltaic (PV) cells were subjected to conditions simulating a Mars dust storm, using the Martian Surface Wind Tunnel, to assess the effect of particle size on the performance of PV cells in the Martian environment. The dust used was an artificial mineral of the approximate elemental composition of Martian soil, which was sorted into four different size ranges. Samples were tested both initially clean and initially dusted. The samples were exposed to clear and dust laden winds, wind velocities varying from 23 to 116 m/s, and attack angles from 0 to 90 deg. It was found that transmittance through the coverglass approximates the power produced by a dusty PV cell. Occultation by the dust was found to dominate the performance degradation for wind velocities below 50 m/s, whereas abrasion dominates the degradation at wind velocities above 85 m/s. Occultation is most severe at 0 deg (parallel to the wind), is less pronounced from 22.5 to 67.5 deg, and is somewhat larger at 90 deg (perpendicular to the wind). Abrasion is negligible at 0 deg, and increases to a maximum at 90 deg. Occultation is more of a problem with small particles, whereas large particles (unless they are agglomerates) cause more abrasion. Author

N92-11134# NSI Technology Services Corp., Dayton, OH.
PHYSICOCHEMICAL PROPERTIES AND DISSOLUTION IN SIMULATED BIOLOGICAL FLUIDS OF PARTICLES OF BERYLLIUM-POWERED ROCKET MOTOR EXHAUST AND PURE BERYLLIUM OXIDES CALCINED AT LOW AND HIGH TEMPERATURE Final Report, Aug. 1987 - Jul. 1990
E. C. Kimmel, S. A. Howe, and W. T. Brashear Dec. 1990 25 p
(AF Proj. 6302)
(AD-A240288; AAMRL-TR-90-062) Avail: NTIS HC/MF A03 CSCL 21/2

Certain physicochemical characteristics and dissolution properties, in simulated biological fluids, of Beryllium-powered rocket motor exhaust (RME) particles were compared to those of pure Beryllium oxide (BeO-the major component of RME) calcined at either 550 or 1600 C. The purpose of these comparisons was to determine which of the forms of BeO had physical and dissolution characteristics most similar to RME, thereby providing a preliminary basis for estimation of the potential toxicity of RME and to determine which form of BeO might be best suited as a surrogate for RME in future studies. RME is very scarce and difficult, as well as costly, to obtain. Though not definitive, this investigation suggests that the physical structure and dissolution properties of RME particles may be most similar to those of BeO calcined at the lower temperatures, which is widely held to be the most toxic of the BeO species. GRA

N92-11135*# National Aeronautics and Space Administration. Lewis Research Center, Cleveland, OH.
PLANS FOR THE DEVELOPMENT OF CRYOGENIC ENGINES FOR SPACE EXPLORATION
James R. Stone, Loretta M. Shaw, and Carl A. Aukerman (Sverdrup Technology, Inc., Brook Park, OH.) Sep. 1991 21 p Presented at the Conference on Advanced Space Exploration Initiative Technologies, Cleveland, OH, 4-6 Sep. 1991; cosponsored by AIAA, NASA, and OAI Previously announced in IAA as A91-52351
(NASA-TM-105250; E-6579; NAS 1.15:105250; AIAA-91-3438)
Copyright Avail: NTIS HC/MF A03 CSCL 21H

The NASA Lewis Research Center (LeRC) is conducting a broad range of basic research and focused technology development activities in both aeronautical and space propulsion. By virtue of the successful conduct of these programs, LeRC is strongly qualified to lead Advanced Development and subsequent development programs on cryogenic space propulsion systems on support of the Space Exploration Initiative. A review is provided of technology status, including recent progress in the ongoing activities, and a top level description of the proposed program. Author

N92-11136*# National Aeronautics and Space Administration. Lewis Research Center, Cleveland, OH.
TEST FACILITIES FOR HIGH POWER ELECTRIC PROPULSION
James S. Sovey, Robert H. Vetrone, Stanley P. Grisnik, Roger M. Myers, and James E. Parkes (Sverdrup Technology, Inc., Brook Park, OH.) 1991 23 p Presented at the Conference on Advanced Space Exploration Initiative Technologies, Cleveland, OH, 4-6 Sep. 1991; cosponsored by AIAA, NASA, and OAI Previously announced in IAA as A91-52396
(NASA-TM-105247; E-6576; NAS 1.15:105247; AIAA-91-3499)
Avail: NTIS HC/MF A03 CSCL 21H

Electric propulsion has applications for orbit raising, maneuvering of large space systems, and interplanetary missions. These missions involve propulsion power levels from tenths to tens of megawatts, depending upon the application. General facility requirements for testing high power electric propulsion at the component and thrust systems level are defined. The characteristics and pumping capabilities of many large vacuum chambers in the United States are reviewed and compared with the requirements for high power electric propulsion testing. Author

N92-11137*# National Aeronautics and Space Administration. Lewis Research Center, Cleveland, OH.
AN OVERVIEW OF TESTED AND ANALYZED NTP CONCEPTS
James T. Walton 1991 25 p Presented at the Conference on Advanced Space Exploration Initiative Technologies, Cleveland, OH, 4-6 Sep. 1991; cosponsored by AIAA, NASA, and OAI Previously announced in IAA as A91-52400
(NASA-TM-105252; E-6581; NAS 1.15:105252; AIAA-91-3503)
Copyright Avail: NTIS HC/MF A03 CSCL 21H

If we buy into the goals of the Space Exploration Initiative (SEI) and accept that they are worthy of the hefty investment of our tax dollars, then we must begin to evaluate the technologies which enable their attainment. The main driving technology is the propulsion systems; for interplanetary missions, the safest and most affordable is a Nuclear Thermal Propulsion (NTP) system. An overview is presented of the NTP systems which received detailed conceptual design and, for several, testing. Author

N92-11138*# National Aeronautics and Space Administration. Lewis Research Center, Cleveland, OH.
EFFECTS OF ANISOTROPIC CONDUCTION AND HEAT PIPE INTERACTION ON MINIMUM MASS SPACE RADIATORS
Karl W. Baker and Kurt O. Lund (California Univ., San Diego.) 1991 10 p Proposed for presentation at the International Solar Energy Conference, Maui, HI, 4-8 Apr. 1992; sponsored by ASME
(NASA-TM-105297; E-6636; NAS 1.15:105297) Avail: NTIS HC/MF A02 CSCL 21H

Equations are formulated for the two dimensional, anisotropic conduction of heat in space radiator fins. The transverse temperature field was obtained by the integral method, and the axial field by numerical integration. A shape factor, defined for the axial boundary condition, simplifies the analysis and renders the results applicable to general heat pipe/conduction fin interface designs. The thermal results are summarized in terms of the fin efficiency, a radiation/axial conductance number, and a transverse conductance surface Biot number. These relations, together with those for mass distribution between fins and heat pipes, were used in predicting the minimum radiator mass for fixed thermal properties and fin efficiency. This mass is found to decrease monotonically with increasing fin conductivity. Sensitivities of the minimum mass designs to the problem parameters are determined. Author

23 CHEMISTRY AND MATERIALS (GENERAL)

N92-11139*# Sverdrup Technology, Inc., Brook Park, OH.
EVALUATION OF KAPTON PYROLYSIS, ARC TRACKING, AND ARC PROPAGATION ON THE SPACE STATION FREEDOM (SSF) SOLAR ARRAY FLEXIBLE CURRENT CARRIER (FCC) Final Report
Thomas J. Stueber Nov. 1991 8 p Presented at the 22nd Photovoltaic Specialists Conference, Las Vegas, NV, 7-11 Oct. 1991; sponsored by IEEE
(Contract NAS3-25266)
(NASA-CR-189056; E-6655; NAS 1.26:189056) Avail: NTIS HC/MF A02 CSCL 07A

Recent studies involving the use of polyimide Kapton coated wires indicate that if a momentary electrical short circuit occurs between two wires, sufficient heating of the Kapton can occur to thermally char (pyrolyze) the Kapton. Such charred Kapton has sufficient electrical conductivity to create an arc which tracks down the wires and possibly propagates to adjoining wires. These studies prompted an investigation to ascertain the likelihood of the Kapton pyrolysis, arc tracking and propagation phenomena, and the magnitude of destruction conceivably inflicted on Space Station Freedom's (SSF) Flexible Current Carrier (FCC) for the photovoltaic array. The geometric layout of the FCC, having a planar-type orientation as opposed to bundles, may reduce the probability of sustaining an arc. An experimental investigation was conducted to simulate conditions under which an arc can occur on the FCC of SSF, and the consequences of arc initiation. Author

24 COMPOSITE MATERIALS

Includes physical, chemical, and mechanical properties of laminates and other composite materials.

For ceramic materials see *27 Nonmetallic Materials*.

N92-11140*# Michigan Univ., Ann Arbor. Radiation Lab.
A NEW TECHNIQUE FOR SIMULATING COMPOSITE MATERIAL Final Report, Sep. 1988 - Sep. 1991
John L. Volakis Sep. 1991 78 p
(Grant NAG2-541)
(NASA-CR-188792; NAS 1.26:188792; UMICH-025921-23-T)
Avail: NTIS HC/MF A05 CSCL 11D

This project dealt with the development on new methodologies and algorithms for the multi-spectrum electromagnetic characterization of large scale nonmetallic airborne vehicles and structures. A robust, low memory, and accurate methodology was developed which is particularly suited for modern machine architectures. This is a hybrid finite element method that combines two well known numerical solution approaches. That of the finite element method for modeling volumes and the boundary integral method which yields exact boundary conditions for terminating the finite element mesh. In addition, a variety of high frequency results were generated (such as diffraction coefficients for impedance surfaces and material layers) and a class of boundary conditions were developed which hold promise for more efficient simulations. During the course of this project, nearly 25 detailed research reports were generated along with an equal number of journal papers. The reports, papers, and journal articles are listed in the appendices along with their abstracts. Author

N92-11141 Stanford Univ., CA.
COMPRESSION RESPONSE OF LAMINATED COMPOSITE PANELS CONTAINING MULTIPLE DELAMINATIONS Ph.D. Thesis
Zafer Sukru Kutlu 1991 166 p
Avail: Univ. Microfilms Order No. DA9122556

An analytical and experimental study was made to examine the compression response of laminated composite panels containing multiple delaminations. Both flat and cylindrical panels were considered. An analytical model was developed for simulating the deformations, from initial loading to final collapse, of the laminated composite panels containing one or more through the width delaminations. The model consists of three parts: stress analysis, contact analysis, and failure analysis. These three analyses were incorporated into a nonlinear finite element program designated as PDELAM. The model and PDELAM were first verified by comparing the results from the computer code with existing analytical and numerical solutions, and experimental data. Experiments on T300/976 graphite epoxy composite panels (flat and cylindrical) were also performed to substantiate the model further. Numerical simulations were also performed using the computer code to show the effects of delamination size, location, and distribution on the compression response of delaminated composite panels. Dissert. Abstr.

N92-11142*# National Aeronautics and Space Administration. Marshall Space Flight Center, Huntsville, AL.
AN EXAMINATION OF THE DAMAGE TOLERANCE ENHANCEMENT OF CARBON/EPOXY USING AN OUTER LAMINA OF SPECTRA (R) Final Report
D. G. Lance and A. T. Nettles Washington Oct. 1991 33 p
(Proj. 90-17)
(NASA-TP-3160; M-671; NAS 1.60:3160) Avail: NTIS HC/MF A03 CSCL 11D

Low velocity instrumented impact testing was utilized to examine the effects of an outer lamina of ultra-high molecular weight polyethylene (Spectra) on the damage tolerance of carbon epoxy composites. Four types of 16-ply quasi-isotropic panels (0, +45, 90, -45) were tested. Some panels contained no Spectra, while others had a lamina of Spectra bonded to the top (impacted side), bottom, or both sides of the composite plates. The specimens were impacted with energies up to 8.5 J. Force time plots and maximum force versus impact energy graphs were generated for comparison purposes. Specimens were also subjected to cross-sectional analysis and compression after impact tests. The results show that while the Spectra improved the maximum load that the panels could withstand before fiber breakage, the Spectra seemingly reduced the residual strength of the composites.
Author

N92-11143# Case Western Reserve Univ., Cleveland, OH. Dept. of Macromolecular Science.
FRACTURE TOUGHNESS OF CARBON/CARBON COMPOSITES Final Report, 1 Apr. 1989 - 30 Jun. 1991
A. Moet and J. Minick 27 Jul. 1991 140 p
(Contract N00014-89-J-1421)
(AD-A240200) Avail: NTIS HC/MF A07 CSCL 11/4

The fracture toughness parameter, K sub max, was used to measure the resistance of 2-D and 3-D carbon/carbon composites to crack initiation. K sub max as a function of geometry and thickness was measured for two 2-D composites differing in fiber and matrix precursors, weave pattern and microdefect field. One composite, KKarb C was independent of geometry and thickness. The second, T300 HT had an average value of 16 MPa*m to the 1/2 power for the four point bend and compact-tension geometries and a value of 26 MPa*to the 1/2 power for the single edge notch configuration. The latter result occurs due to the composite strength and the interaction of the stress and microflaw fields. Also, the SEN samples had larger active zones leading to greater crack initiation resistance. Effects of notch orientation and depth were analyzed for the 3-D material. Circumferential testing direction showed the highest K sub max values for all three notch depths because the crack front encountered the highest cross-sectional area of yarns. A PASCAL program was written to compute the crack diffusion model parameters gamma *, gamma sub min, and alpha. A higher value of gamma * for the 2-D materials reflected the type, distribution, and size of defects for the 2-D materials. The alpha parameter was lower for materials showing a high degree of fluctuation in their maximum load. GRA

N92-11144 Department of the Navy, Washington, DC.
CENTRIFUGAL CASTING OF COMPOSITES Patent

Subhash D. Karmarkar, inventor (to Navy) and Amarnath P. Divecha, inventor (to Navy) 25 Jun. 1991 6 p Filed 15 Nov. 1989
(AD-D014981; US-Patent-5,025,849; US-Patent-Appl-SN-436847) Avail: US Patent and Trademark Office CSCL 11/6

This patent discloses tubes or other symmetrical shapes are formed of composite materials, such as silicon carbide and aluminum, by spin casting. The reinforcing material can be precast into a billet or bar of the matrix metal, remelted and introduced into a spinning mold. Tubes can be produced with walls having differing amounts of reinforcing materials in the tube wall. Castings can be obtained having a uniform distribution of a reinforcement in a matrix metal. GRA

N92-11145# Office National d'Etudes et de Recherches Aerospatiales, Paris (France). Direction Scientifique de la Resistance des Structures.
NUMERICAL SIMULATION OF THE DEGRADATION OF THE FOLDS OF A LAMINATED COMPOSITE STRUCTURE. STUDY OF THE IMPORTANCE OF RESIDUAL FIRING CONSTRAINTS [SIMULATION NUMERIQUE DE LA DEGRADATION DES PLIS D'UNE STRUCTURE COMPOSITE STRATIFIEE. ETUDE DE L'IMPORTANCE DES CONTRAINTES RESIDUELLES EN CUISSON]
J. Renard, F. Roudolff, and T. Jeggy Jun. 1990 50 p In FRENCH
(Contract DRET-89-34-001)
(ONERA-RT-8/7256-RY-094-R; ETN-91-90090) Avail: NTIS HC/MF A03

Applications of the model of laminated structure layer degradation are presented. Experiments, numerical simulation of traction model tests, are compared. The numerical simulation of biaxial test on holed plates is addressed. The importance of residual firing constraints and their influences on energy dissipation value computation are considered. ESA

N92-11146# Office National d'Etudes et de Recherches Aerospatiales, Paris (France). Direction Scientifique de la Resistance des Structures.
DELAMINATION PROPAGATION IN A COMPOSITE PANEL UNDER COMPRESSIVE STRESS [PROPAGATION D'UN DELAMINAGE DANS UN PANNEAU COMPOSITE SOLLICITE EN COMPRESSION]
R. Girard and D. Louis Sep. 1990 31 p In FRENCH
(ONERA-RT-23/3542-RY-093-R; ETN-91-90093) Avail: NTIS HC/MF A03

The propagation of delamination introduced artificially into a composite panel submitted to compression is considered. The analysis of this problem is carried out taking into account nonlinear geometrics (buckling and postbuckling) and physics (damaging of the composite materials), while the prediction of the delamination progression is based on the idea of the critical value of the energy restoration. Corresponding numerical tools were developed and embedded in a nonlinear computation code using the finite element method. This code is applied to a concrete problem and analyzed experimentally. ESA

N92-11147# Technische Univ., Eindhoven (Netherlands).
THE BEHAVIOUR OF FIRE-EXPOSED COMPOSITE STEEL/CONCRETE SLABS Ph.D. Thesis
Alphonse Florentinus Hamerlinck 1991 243 p Sponsored by CS and CUR
(Grant ECSC-7210-SA/509)
(ISBN-90-386-0031-3; ETN-91-90131) Copyright Avail: NTIS HC/MF A11

The development of a mathematical model for analysis of the thermal and mechanical behavior of composite steel/concrete slabs during fire exposure, with the aim of improving European recommendations and increasing knowledge, is addressed. Focus is on composite slabs with additional reinforcement as a fire resistant measure. A thermal model based on finite difference theory which takes temperature dependent thermal properties of concrete and steel, the evaporation of moisture and arbitrary fire exposure conditions into account, is used to analyze the two dimensional, transient heat transfer in the fire exposed slabs. Heat balance equations are formulated by means of heat resistances and capacities and are solved using an explicit method (forward difference). A mechanical model is subdivided into two submodels for analyzing the cross sectional behavior and the structural behavior respectively. ESA

N92-11148# Technische Univ., Berlin (Germany, F.R.). Inst. fuer Luft- und Raumfahrt.
BUCKLING VALUES AND OPTIMIZATION OF CARBON FIBER REINFORCED COMPRESSION CHORD PLATES WITH RECTANGULAR STRINGERS [BEULWERTE UND OPTIMIERUNG VON CFK-DRUCKGURTPLATTEN MIT RECHTECK-STRINGERN]
Thomas Doerfler 1991 45 p In GERMAN
(ILR-Mitt-259(1991); ETN-91-90206) Avail: NTIS HC/MF A03

The optimization of fiber coating is examined with regard to buckling and column load increasing. Local buckling is calculated with an extended transition matrix process, buckling behavior is discussed, and design indications are given. A global buckling optimization leads to a design which allows a distinct load increase, with regard to similar stringer plates made of isotropic materials. ESA

N92-11149*# National Aeronautics and Space Administration. Langley Research Center, Hampton, VA.
EFFECTS OF ELEVATED TEMPERATURE ON THE VISCOPLASTIC MODELING OF GRAPHITE/POLYMERIC COMPOSITES
Thomas S. Gates Oct. 1991 31 p Presented at ASTM Symposium on High Temperature and Environmental Effects on Polymetric Composites, San Diego, CA, 15 Oct. 1991
(NASA-TM-104160; NAS 1.15:104160) Avail: NTIS HC/MF A03 CSCL 11D

To support the development of new materials for the design of next generation supersonic transports, a research program is underway at NASA to assess the long term durability of advanced polymer matrix composites (PMC's). One of main objectives of the program was to explore the effects of elevated temperature (23 to 200 C) on the constitutive model's material parameters. To achieve this goal, test data on the observed nonlinear, stress-strain behavior of IM7/5260 and IM7/8320 composites under tension and compression loading were collected and correlated against temperature. These tests, conducted under isothermal conditions using variable strain rates, included such phenomena as stress relaxation and short term creep. The second major goal was the verification of the model by comparison of analytical predictions and test results for off axis and angle ply laminates. Correlation between test and predicted behavior was performed for specimens of both material systems over a range of temperatures. Results indicated that the model provided reasonable predictions of material behavior in load or strain controlled tests. Periods of loading, unloading, stress relaxation, and creep were accounted for. Author

25 INORGANIC AND PHYSICAL CHEMISTRY

Includes chemical analysis, e.g., chromatography; combustion theory; electrochemistry; and photochemistry.

For related information see also *77 Thermodynamics and Statistical Physics.*.

N92-11150# Helsinki Univ. of Technology, Espoo (Finland). Lab. of Paper Technology.
THE ROLE OF FIBER FLOCCULATION IN CHEMICAL PULP REFINING Ph.D. Thesis
Soili Hietanen (Metsa-Serla Paper Mill, Aanekoski, Finland) 1991 106 p Sponsored by Academy of Finland
(ETN-91-90025) Avail: NTIS HC/MF A06

The role of fiber flocculation in chemical pulp refining is

addressed. The combinations of paper properties that can be obtained if fiber treatment is homogenous, and whether or not a non homogenous fiber treatment would reduce energy consumption in refining are considered. Eight papers are annexed concerned with: the fundamental aspects of the refining process; a new hypothesis for the mechanics of refining; the development of a fundamentally new refining method; the effect of control variables and length of refining zone on the refining result with a new pilot refiner; the comparison of a new refiner with a conventional refiner; the effects of the homogeneity of the refining action on fiber and paper structure; control of the heterogeneity of the refining action. For individual titles, see N92-11151 through N92-11158.

N92-11151# Helsinki Univ. of Technology, Espoo (Finland).
FUNDAMENTAL ASPECTS OF THE REFINING PROCESS
Soili Hietanen and Kari Ebeling (Kymmene Corp., Helsinki, Finland) *In its* The Role of Fiber Flocculation in Chemical Pulp Refining 1991 p 21-33 Repr. from Paper and Timber, v. 72, no. 2, 1990 (For primary document see N92-11150 02-25)
Avail: NTIS HC/MF A06

Current theories of Low Consistency (LC) refining are addressed. In some cases, reference is also made to High Consistency (HC) refining and to the refining of mechanical pulps. In today's refiners, fibers undergo refining in a narrow gap. The most widely used refining theory (based on a narrow gap treatment of fibers) is the specific edge load theory. This theory and its shortcomings are discussed. How the different refining forces act on fibers and what kind of structural changes these forces create in the fibers is examined. The effect on the refining result of factors such as consistency temperature, pH, electrolyte concentration and refining zone parameters is described. Some nonconventional refining methods are proposed in order to show that fibers can be refined in other ways than by means of LC refiners equipped with bars. The aim of novel refining techniques is to tailor make such structural changes in the fibers that render them better to the production of a particular grade of paper.
ESA

N92-11152# Helsinki Univ. of Technology, Espoo (Finland).
A NEW HYPOTHESIS FOR THE MECHANICS OF REFINING
Soili Hietanen and Kari Ebeling (Kymmene Corp., Helsinki, Finland) *In its* The Role of Fiber Flocculation in Chemical Pulp Refining 1991 p 37-44 Repr. from Paper and Timber, v. 72, no. 2, 1990 (For primary document see N92-11150 02-25)
Avail: NTIS HC/MF A06

The energy inefficiency of the Low Consistency (LC) refining process, the heterogenous nature of refining and the role of flocs in refining are addressed. There is much evidence in the literature that only a portion of the fibers undergo refining between the refiner bars. Whether a homogeneous or heteorogeneous treatment is preferred depends on the paper grade being manufactured. Factors affecting the extent of heterogeneity in refining and how heterogeneity affects various properties are discussed. Energy inefficiency in refining is attributed partly to the heterogenous treatment of fibers during refining. Because of fiber flocculation and the large dimensions of the refining zone, a high proportion of fibers can pass through the refining zone in the grooves. The factors favoring fiber flocculation are listed. Those aspects of refiner that affect design are mentioned. Future development work of refiners should be guided by an understanding of the deficiencies of the present refining process. A hypothesis that fibers are treated as flocs rather than as individual fibers in modern refiners is proposed.
ESA

N92-11153# Helsinki Univ. of Technology, Espoo (Finland).
DEVELOPMENT OF A FUNDAMENTALLY NEW REFINING METHOD. PART 1: BASIC DESIGN CONSIDERATIONS
Soili Hietanen (Metsa-Serla Paper Mill, Aanekoski, Finland) *In its* The Role of Fiber Flocculation in Chemical Pulp Refining 1991 p 47-55 Repr. from Paper and Timber, v. 72, no. 9, 1990 (For primary document see N92-11150 02-25)
Avail: NTIS HC/MF A06

The dispersion of fiber flocs in a new pilot refiner is addressed. The refiner utilizes a fundamentally new refining principle where new refiner flocs are dispersed before the refining zone and refining treatment is directed at a thin, evenly spread fiber film in between the disks. The aim of the new refining principle is to achieve a more uniform fiber treatment and in this way improve paper properties and reduce energy consumption in refining. The operating principle of the refiner is described together with the variables governing the effectiveness of fiber bloc dispersion unit and in the refiner. The dispersion unit required considerable development before its operation was satisfactory. The structural factors critical to the operating efficiency of the dispersion unit are mentioned. The operating efficiency of the dispersion unit was evaluated using the following refiner criteria: inlet pressure; disk gap; and a combination of inlet pressure and disk gap. These criteria were chosen because the maximum inlet pressure was greatly dependent on the operating efficiency of the dispersion unit and because the refiner gap can be used as a measure of the of the dispersion state of the fibers.
ESA

N92-11154# Helsinki Univ. of Technology, Espoo (Finland).
DEVELOPMENT OF A FUNDAMENTALLY NEW REFINING METHOD. PART 2: OPERATING CONDITIONS OF THE NEW REFINER
Soili Hietanen (Metsa-Serla Paper Mill, Aanekoski, Finland) *In its* The Role of Fiber Flocculation in Chemical Pulp Refining 1991 p 59-67 (For primary document see N92-11150 02-25)
Avail: NTIS HC/MF A06

A pilot refiner operating on a new refining principle was compared with conventional Low Consistency (LC) refiners in terms of power/gap behavior. The gap behavior, the pressure and temperature in the refining zone, the idling power of the refiner and the transfer of energy is discussed. Among other conclusions, it was found that with the new refining principle, the pilot refiner operates with a small gap, and a constant, low noise level, indicating the presence of a fiber mat between the disks. The idling power of the pilot refiner operating with the new principle proved to be strongly dependent on the fiber dispersion and is thus also dependent on the gap size. The coefficient of friction of the pulp between the rotor and the stator disks was dependent on the disk geometry.
ESA

N92-11155# Helsinki Univ. of Technology, Espoo (Finland).
EFFECT OF CONTROL VARIABLES AND LENGTH OF REFINING ZONE ON THE REFINING RESULT WITH A NEW PILOT REFINER
Soili Hietanen (Metsa-Serla Paper Mill, Aanekoski, Finland) *In its* The Role of Fiber Flocculation in Chemical Pulp Refining 1991 p 71-80 Repr. from Paper and Timber, v. 73, no. 1, 1991 Sponsored by Academy of Finland and Walter Ahlstroem Foundation (For primary document see N92-11150 02-25)
Avail: NTIS HC/MF A06

How the control variables (specific edge load, volume flow, consistency, rotor speed and length of the refining zone (design parameter)) affect the refiner operation, paper properties, and energy consumption is discussed. The experiments were performed using bleached softwood kraft pulp.
ESA

N92-11156# Helsinki Univ. of Technology, Espoo (Finland).
COMPARISON OF A NEW REFINER WITH A CONVENTIONAL REFINER
Soili Hietanen (Metsa-Serla Paper Mill, Aanekoski, Finland) *In its* The Role of Fiber Flocculation in Chemical Pulp Refining 1991 p 83-94 Repr. from Paper and Timber, v. 73, no. 2, 1991 (For primary document see N92-11150 02-25)
Avail: NTIS HC/MF A06

The potential of the pilot refiner operating with the new operating principle, in which fibers are dispersed just before the refining zone and treatment in the refining zone is directed at a thin fiber film in a small gap, is evaluated by judging the refining result in terms of the requirements set by certain paper grades. A wide variety of paper grades was chosen as the basis of the evaluation. The application potential tests for various paper grades were based on the refining of dried softwood kraft pulp. The suitability of the

pilot refiner for refining other pulp grades was also assessed. The amount of refining energy needed to develop the desired properties is presented. ESA

N92-11157# Helsinki Univ. of Technology, Espoo (Finland).
HOMOGENEITY OF REFINING ACTION; EFFECTS ON FIBER AND PAPER STRUCTURE
Soili Hietanen and Kari Ebeling (Kymmene Corp., Helsinki, Finland) *In its* The Role of Fiber Flocculation in Chemical Pulp Refining 1991 p 97-107 Presented at the Tappi 1983 International Paper Physics Conference Sponsored in part by Academy of Finland (For primary document see N92-11150 02-25)
Avail: NTIS HC/MF A06

In present low consistency refiners, fibers are treated as flocs and not as individual fibers. It was hypothesized that a reduction in the consumption of refining energy and at the same time a more homogeneous refining result would be obtained if fibers could be treated individually. A research program was formulated to test the hypothesis dealing with the refining of flocs instead of individual fibers while a new refiner was constructed. This new refiner included a dispersion unit before the refining. The refining zone itself was designed so that the fibers would not be able to reflocculate inside the refiner. The next part of the research program was formulated so that the effect of refining on the structure and properties of fiber and paper could be analyzed for both refining principles. Results and conclusions of the research are given. ESA

N92-11158# Helsinki Univ. of Technology, Espoo (Finland).
CONTROL OF THE HETEROGENEITY OF THE REFINING ACTION
Soili Hietanen and Kari Ebeling (Kymmene Corp., Helsinki, Finland) *In its* The Role of Fiber Flocculation in Chemical Pulp Refining 1991 p 111-118 Presented at the PIRA International Conference on New Technologies in Refining, Birmingham, England, 1986 (For primary document see N92-11150 02-25)
Avail: NTIS HC/MF A06

Research into the verification of the floc hypothesis is discussed. A bleached pine kraft pulp was used in this verification. The effect of the design of the dispersion unit of the experimental refiner was studied. The refiner is described. The performance of the refiner was evaluated using the inlet pressure of the refiner and the refining power versus disk gap relationship. The refining result and the energy consumption of the experimental refiner is evaluated and compared with an Escher-Wyss refiner and other disk refiners. ESA

N92-11159 Vanderbilt Univ., Nashville, TN.
LASER RAMAN DIAGNOSTICS IN SUBSONIC AND SUPERSONIC TURBULENT JET DIFFUSION FLAMES Ph.D. Thesis
Tsarng-Sheng Cheng 1991 190 p
Avail: Univ. Microfilms Order No. DA9125260

Ultraviolet (UV) spontaneous vibrational Raman scattering combined with laser induced predissociative fluorescence (LIPF) is developed for temperature and multi-species concentration measurements. Simultaneous measurements of temperature, major species (H2, O2, N2, H2O), and minor species (OH) concentrations are made with a single narrow band KrF excimer laser in subsonic and supersonic lifted turbulent hydrogen-air diffusion flames. The UV Raman system is calibrated with a flat-flame diffusion burner operated at several known equivalence ratios from fuel lean to fuel rich. Temperature measurements made by the ratio of Stokes/anti-Stokes signal and by the ideal gas law are compared. Single shot uncertainties for temperature and concentration measurements are analyzed with photon statistics. Calibration constants and bandwidth factors are used in the data reduction program to arrive at temperature and species concentration measurements. The results of these measurements are presented, and these simultaneous measurements allow a better understanding of the complex turbulence-chemistry interactions and provide information for the input and validation of CFD models. Dissert. Abstr.

N92-11160# California Univ., Berkeley. Lawrence Berkeley Lab.
CONVERSION OF ETHANE AND OF PROPANE TO HIGHER OLEFIN HYDROCARBONS
H. Heinemann and G. A. Somorjai Jun. 1991 9 p
(Contract DE-AC03-76SF-00098)
(DE91-016896; LBL-30784) Avail: NTIS HC/MF A02

It is the purpose of this work to extend recent findings of oxidative methane coupling to the coupling of paraffinic hydrocarbons such as ethane and propane to produce C4 respectively C6 and higher hydrocarbons. Variables which have been shown to influence the olefin/paraffin ratio of the product will be investigated to optimize olefinic products. A study of the reaction mechanisms is to be undertaken on the basis of which improved catalysts will be synthesized. Results from work this quarter are as follows: (1) Ethane was charged together with oxygen and steam to a Ca-Ni-K oxide catalyst at three temperatures (300, 450, and 600 C) and atmospheric pressure. (2) At 300 C conversion was very low (less that 1 percent. Only hydrocarbons were found in the product. The major hydrocarbon was methane, the yield of which decreased with time on stream with a corresponding increase in propylene and ethylene. (3) At 450 C conversion reached 60-70 percent, selectivity to hydrocarbons was 50 percent or less (mostly CH4) with the remainder being carbon oxides. (4) At 600 C there was almost complete conversion of ethane to methane and carbon oxides with only very small amounts of ethylene. There appeared to be substantial coke deposition on the catalyst. (5) It is apparent from these results that temperatures of 600 C are too high and other process variables have to be explored. (6) A single run with propane feed at 600 C showed continuous catalyst deactivation and gave methane and CO(x) as major products with propylene being the largest constituent of C2-C6 hydrocarbons. DOE

N92-11161*# Maine Univ., Orono.
NUMERICAL PREDICTION OF TURBULENT FLAME STABILITY IN PREMIXED/PREVAPORIZED (HSCT) COMBUSTORS Final Report, 1 Apr. 1989 - 31 Dec. 1990
Nicholas S. Winowich 1990 75 p
(Grant NAG3-1033)
(NASA-CR-188991; NAS 1.26:188991) Avail: NTIS HC/MF A04 CSCL 21B

A numerical analysis of combustion instabilities that induce flashback in a lean, premixed, prevaporized dump combustor is performed. KIVA-II, a finite volume CFD code for the modeling of transient, multidimensional, chemically reactive flows, serves as the principal analytical tool. The experiment of Proctor and T'ien is used as a reference for developing the computational model. An experimentally derived combustion instability mechanism is presented on the basis of the observations of Proctor and T'ien and other investigators of instabilities in low speed (M less than 0.1) dump combustors. The analysis comprises two independent procedures that begin from a calculated stable flame: The first is a linear increase of the equivalence ratio and the second is the linear decrease of the inflow velocity. The objective is to observe changes in the aerothermochemical features of the flow field prior to flashback. It was found that only the linear increase of the equivalence ratio elicits a calculated flashback result. Though this result did not exhibit large scale coherent vortices in the turbulent shear layer coincident with a flame flickering mode as was observed experimentally, there were interesting acoustic effects which were resolved quite well in the calculation. A discussion of the k-e turbulence model used by KIVA-II is prompted by the absence of combustion instabilities in the model as the inflow velocity is linearly decreased. Finally, recommendations are made for further numerical analysis that may improve correlation with experimentally observed combustion instabilities. Author

N92-11162*# Institute for Computer Applications in Science and Engineering, Hampton, VA.
IGNITION AND STRUCTURE OF A LAMINAR DIFFUSION FLAME IN THE FIELD OF A VORTEX Final Report
Michele G. Macaraeg, T. L. Jackson (Old Dominion Univ., Norfolk, VA.), and M. Y. Hussaini Sep. 1991 35 p Submitted for publication
(Contract NAS1-18605)
(NASA-CR-189042; NAS 1.26:189042; ICASE-91-69) Avail: NTIS HC/MF A03 CSCL 21B

The distortion of flames in flows with vortical motion is examined via asymptotic analysis and numerical simulation. The model consists of a constant density, one step, irreversible Arrhenius reaction between initially unmixed species occupying adjacent half-planes which are then allowed to mix and react in the presence of a vortex. The evolution in time of the temperature and mass fraction fields is followed. Emphasis is placed on the ignition time and location as a function of vortex Reynolds number and initial temperature differences of the reacting species. The study brings out the influence of the vortex on the chemical reaction. In all phases, good agreement is observed between asymptotic analysis and the full numerical solution of the model equations. Author

N92-11163# Argonne National Lab., IL.
POLARIZED X RAY ABSORPTION SPECTROSCOPY FOR THE STUDY OF SUPERCONDUCTORS AND MAGNETIC MATERIALS
M. Ramanathan, E. E. Alp, S. M. Mini, S. Salem-Sugui, Jr., and A. S. Bommannavar (City Univ. of New York, Brooklyn.) Jul. 1991 13 p Presented at the Society of Photo-Optical Instrumentation Engineers (SPIE) Meeting, San Diego, CA, 21-26 Jul. 1991
(Contract W-31-109-eng-38)
(DE91-017990; ANL/CP-72758; CONF-9107115-42) Avail: NTIS HC/MF A03

Synchrotron radiation is a good source of polarized radiation in the x-ray regime. The radiation obtained from a bending magnet source is linearly polarized in the bending plane and has a varying degree of circular polarization away from the bending plane. This feature of the synchrotron radiation can be taken advantage of with proper optics to selectively use the type of polarized radiation required for the experiment in question. Linear polarized radiation is used to study the anisotropic nature of electronic and atomic structure by x-ray absorption techniques from single crystal and oriented powder samples. We will give a specific example of the use of linearly polarized X-ray Absorption Spectroscopy measurements for the study of the magnetically oriented layered copper oxide superconductors. While such linear dichroism measurements help identify the symmetry of the empty electronic states, circular dichroism measurements in magnetic systems help in determining the spin contribution to the absorption process. We will discuss magnetic circular dichroism measurements of the ordered-disordered invar alloy Fe3Pt. DOE

N92-11164# Princeton Univ., NJ.
A SYSTEMATIC APPROACH TO COMBUSTION MODEL REDUCTION AND LUMPING Final Technical Report, Dec. 1988 - Dec. 1990
Herschel Rabitz and Fredrick Dryer 1 Aug. 1991 461 p
(Grant AF-AFOSR-0070-89; AF Proj. 2308)
(AD-A240195; AFOSR-91-0714TR) Avail: NTIS HC/MF A20 CSCL 12/2

This report summarizes research activities completed over the past two years in the general area of combustion model reduction and lumping. The purpose of the research was for the further development of practical techniques capable of rendering complex combustion-transport models to their physical essence for realistic computational execution. The research followed three avenues of approach: (1) sensitivity analysis, (2) linear projective transformations; and (3) Lie algebraic techniques. The diversity of approach was necessitated by the complexity of the problem and significant progress was made in each area. Specific conclusions were made concerning the likely next level of research developments needed to advance these tools to practical fruition. GRA

N92-11165# Pennsylvania State Univ., University Park. Dept. of Mineral Engineering.
EXPLICIT DETERMINATION OF THE VAPOR FRACTION IN FLASH CALCULATIONS M.S. Thesis
John H. Warren Dec. 1991 98 p
(AD-A240376) Avail: NTIS HC/MF A05 CSCL 07/4

Flash calculations are used extensively in the oil and gas industry for process design in the separation, storage, and transportation of hydrocarbon mixtures. Inherent to flash calculations is determination of the vapor fraction. A mathematical investigation is conducted to determine if an explicit form of the Rachford-Rice equation can be developed to solve for the vapor fraction in multicomponent fluid systems containing up to 4 components. This is done by expanding the objective function in terms of the number of components being investigated and then reducing the derived equation to its simplest polynomial form. This is done for 2-, 3-, and 4-component fluid systems. The 4-component equation is then checked to ensure that it is general by reducing it to the form of the 3- and 2-component system equations. Use of the equation for the 2-component system is the easiest to implement since this system has only one root and can thus be solved for the vapor fraction without using any root-choosing techniques. For systems greater than 2 components, a root-choosing scheme must be established to choose the actual vapor fraction. To keep the method explicit in nature, the trigonometric solver for cubic equations is used on the 4-component system equation. Empirical studies of the relationship by the Newton-Raphson technique are used to establish a root-choosing scheme. The equation is evaluated by determining equilibrium ratios for a methane-ethane system and comparing the computed data against established experimental data. A practical application of the proposed equation is presented in the form of bubblepoint and dewpoint calculations for the methane-ethane system of varying compositions. A method for determining the bubblepoint and dew point is presented. GRA

N92-11166# California Univ., Berkeley. Sponsored Projects Office.
DECOMPOSITION PATHWAYS OF TETRAHYDROGEN Final Report, Jul. 1987 - Dec. 1990
William A. Lester, Jr. Aug. 1991 48 p
(Contract F04611-87-K-0030)
(AD-A240623; PL-TR-91-3059) Avail: NTIS HC/MF A03 CSCL 07/4

Bound excited states of small molecules are of both practical and theoretical interest. Stabilized and vacuum-stored excited-state molecules have been postulated as a new energy source. In their multireference single and double excitation configuration interaction (MR-SDCI) study, a species researchers labeled a maximum ionicity excited state (MIES) of pyramidal geometry with equilateral triangle base was found for which the Coulomb attraction between the ionic fragments hydrogen ion governed stability. In experiments by Moore and collaborators, however, large quenching cross sections have been measured for the interaction of excited-state hydrogen molecule with ground-state molecules. GRA

N92-11167# Chemical Research and Development Center, Aberdeen Proving Ground, MD.
TIME-RESOLVED ANALYTICAL PYROLYSIS MASS SPECTROMETRY OF BIOMATERIALS Final Report, Mar. - Oct. 1990
A. P. Snyder, Michael B. Wasserman, and Shirley A. Liebman Jul. 1991 44 p
(AD-A240624; CRDEC-TR-290) Avail: NTIS HC/MF A03 CSCL 06/5

This report documents method development for time-resolved analytical pyrolysis applied to microorganisms and biomaterials. A direct insertion probe (DIP) was the biological sample processor and was inserted into an electron ionization source of a quadrupole mass spectrometer (MS). E. coli, B. subtilis and various biochemical

compounds were investigated for biomarker information content. The DIP-MS approach provides an additional dimension toward solving the difficult problems of generation and trace descriptor fragments from complex biomaterials. GRA

N92-11168# Oak Ridge National Lab., TN.
MIXING EFFECTS IN AQUEOUS SOLUTIONS AT ELEVATED TEMPERATURES
H. F. Holmes and R. E. Mesmer 1991 21 p Presented at the 2nd International Symposium on Chemistry in High Temperature Water, Provo, UT, 19-22 Aug. 1991
(Contract DE-AC05-84OR-21400)
(DE91-017695; CONF-9108114-2) Avail: NTIS HC/MF A03

With few exceptions, the systematics and predictions of mixing effects in the thermodynamics of aqueous electrolyte solutions are not well established, particularly at high temperatures. The most useful general method for studying the excess Gibbs energy of mixed electrolyte solutions is the isopiestic technique but some calorimetric methods have desirable advantages provided suitable reference data are available. Currently, the most useful description of mixed electrolyte systems is the ion-interaction treatment of Pitzer. Relationships between various models used for mixtures and their advantages and disadvantages are discussed. Mixing contributions have their largest effect for equimolar mixtures in the case of the osmotic coefficient and for trace components in the case of activity coefficients. Various types of behavior are illustrated with examples primarily from high-temperature isopiestic studies at ORNL. DOE

N92-11169# Delaware Univ., Newark. Dept. of Chemistry and Biochemistry.
DEVELOPMENT OF AN EXPERIMENTAL DATABASE AND THEORIES FOR PREDICTION OF THERMODYNAMIC PROPERTIES OF AQUEOUS ELECTROLYTES AND NONELECTROLYTES OF GEOCHEMICAL SIGNIFICANCE AT SUPERCRITICAL TEMPERATURES AND PRESSURES
R. H. Wood 2 May 1991 6 p
(Contract DE-FG02-89ER-14080)
(DE91-018493; DOE/ER-14080/2) Avail: NTIS HC/MF A02

Volumetric measurements have been completed for CH4, CO2, and H2S at temperatures from 25 to 380 C and 2 or 3 pressures at each temperature. The H2S and CO2 solutions are stored in aluminized mylar bags in PVC pipes with water surrounding the bags at a pressure of several atmospheres. The methane is stored in a one liter autoclave with a sliding teflon piston engaging the sides of the autoclave which separates the standard methane solution from the pressurizing fluid. The solutions are prepared at 100 to 200 atmospheres and do not need to be re-standardized after each experiment. We also have some measurements on aqueous ammonia, boric acid, and acetic acid. Preliminary calculations of the free energy of methane in water at room temperature as a function of the model parameters for the methane have been finished. In preparation for these calculations, the theory and practice of the free energy perturbation calculations was reviewed. In molecular dynamics and Monte Carlo calculations a system does not immediately equilibrate to a change in the Hamiltonian, so that there is a time lag or a configuration number lag in the response of the system. These lags cause errors in free energy calculations. DOE

N92-11170# Gosudarstvennyi Komitet po Ispolzovaniyu Atomnoi Energii, Obninsk (USSR). Fiziko-Ehnergeticheskij Inst.
BOSE-CONDENSATION IN LIQUID HELIUM UNDER PRESSURE
A. V. Puchkov 1989 10 p In RUSSIAN
(DE91-634504; FEI-1974) Avail: NTIS HC/MF A02

Results of experimental investigations into Bose-condensate density (relative quantity of atoms with the pulse equal to zero) in liquid helium under pressure performed using neutron technique are discussed. Data testifying to the Bose-condensate absence in liquid helium at T = 1.82 K and 25.5 bar pressure, i.e., under such conditions when the superfluid component density is equal to zero (lambda point) are obtained using a time-of-flight spectrometer. A phenomenologic approach well-known in investigations into Bose-condensate temperature dependence is used when processing the neutron spectra. DOE

N92-11123# Pratt and Whitney Aircraft, West Palm Beach, FL. Group Engineering Technology.
JANNAF COMBUSTION INSTABILITY PANEL WORKSHOP REPORT: NUMERICAL METHODS IN COMBUSTION INSTABILITY
George B. Cox, Jr. *In* JHU, The 27th JANNAF Combustion Subcommittee Meeting, Volume 3 Nov. 1990 p 307-315 (For primary document see N92-11117 02-20)
Avail: NTIS HC/MF A99

N92-11124*# National Aeronautics and Space Administration. Lewis Research Center, Cleveland, OH.
JANNAF LIQUID ROCKET COMBUSTION INSTABILITY PANEL RESEARCH RECOMMENDATIONS
Mark D. Klem *In* JHU, The 27th JANNAF Combustion Subcommittee Meeting, Volume 3 Nov. 1990 p 345-351 Previously announced as N91-13491 (For primary document see N92-11117 02-20)
Avail: NTIS HC/MF A99 CSCL 21B

N92-11125*# Jet Propulsion Lab., California Inst. of Tech., Pasadena.
EROSIVE AUGMENTATION OF SOLID PROPELLANT BURNING RATE: MOTOR SIZE SCALING EFFECT
L. D. Strand and Norman S. Cohen (Cohen, Norman S. Professional Services, Inc., Redlands, CA) *In* JHU, The 27th JANNAF Combustion Subcommittee Meeting, Volume 3 Nov. 1990 p 379-391 (For primary document see N92-11117 02-20)
Avail: NTIS HC/MF A99 CSCL 21B

26 METALLIC MATERIALS

Includes physical, chemical, and mechanical properties of metals, e.g., corrosion; and metallurgy.

N92-11171 National Physical Lab., Teddington (England). Div. of Materials Metrology.
CONTACT ANGLE AND WORK OF ADHESION BETWEEN Ni-BASED MELTS AND NON-METALLIC SOLIDS
B. J. Keene Mar. 1991 125 p
(NPL-DMM(A)-23; ISSN-0143-7313; ETN-91-99877) Copyright
Avail: National Physical Lab., Teddington, Middelsex TW11 OLW, England

A collation of the literature data for the wetting and adhesionai behavior between molten Ni/Ni based alloys and nonmetallic solids is presented. The following are considered: new techniques to assess metal cleanness; surface tension and surface energy; contact angle, work of adhesion and their relation to interfacial energy; surface energy criteria from emergence of a solid at a gas/liquid interface; surface energy criteria for formation of inclusion agglomerates; effect of surface topography on contact angle; effect of temperatures; physical and chemical factors affecting wettability and adhesion; composition of nickel alloys. A summary of the data is given. ESA

N92-11172# Mount Holyoke Coll., South Hadley, MA.
NUCLEAR TRANSPARENCY AND DOUBLE BETA DECAY OF MOLYBDENUM 100
H. W. Nicholson Jul. 1991 13 p
(Contract DE-FG02-90ER-40553)
(DE91-016963; DOE/ER-40553/2) Avail: NTIS HC/MF A03

Work is continuing on two collaborative experiments. One, a search for double beta decay in molybdenum 100 is being carried out in the Consil silver mine in Osburn, Idaho with collaborators from the Lawrence Berkeley Laboratory, the University of New Mexico, and the Idaho National Engineering Laboratory. At this time the experiment is running with 62 foils, each with a mass of about .98 grams of isotopically enriched molybdenum 100. In approximately 1870 hours of data taking which began during the

spring 1991, we have obtained a preliminary 1(sigma) lower limit of .12 x 10(exp 23) years for the lifetime for O(+) yields O(+) neutrionoless double beta decay in molybdenum 100 based on an estimate for the event detection efficiency of the upgraded detector. This lifetime limit is 3 times greater that the one we published previously in Physical Review Letters in 1989. Monte Carlo Efforts are currently underway to determine the event detector efficiency more precisely. The second experiment involves the construction of a cylindrically symmetrical detector at the Brookhaven National Laboratory AGS to study color transparency in nuclei from 6 to 20 GeV/c. This detector consists of a large superconducting solenoidal magnet, a cylinder of scintillating fibers, several cylinders of straw tubes, and an array of trigger plastic scintillator hodoscopes. Mount Holyoke has been principally involved in the design of phototube bases for the trigger hodoscopes for the EVA detector and in the design and construction of the scintillating fiber detector tracking detector. A prototype fiber detector consisting of 2 Hamamatsu multianode photomultiplier tubes with 256 channels each and approximately 650 1.5 meter long 1 mm diameter scintillating fibers broken up into two layers and supported by a 10 centimeter diameter carbon fiber tube was constructed for the spring high energy physics run at the AGS. Data from this run obtained from the detector is included in this report. DOE

N92-11173# Sandia National Labs., Albuquerque, NM.
A PROBABILISTIC MODEL OF INTERGRANULAR STRESS CORROSION CRACKING
R. J. Bourcier, W. B. Jones, and J. R. Scully (Virginia Univ., Charlottesville.) 1991 13 p Presented at the Life Prediction of Corrodible Structures, Kauai, HI, 5-8 Nov. 1991
(Contract DE-AC04-76DP-00789)
(DE91-017986; SAND-90-2530C; CONF-911179-1) Avail: NTIS HC/MF A03

We have developed a model which utilizes a probabilistic failure criterion to describe intergranular stress corrosion cracking (IGSCC). A two-dimensional array of elements representing a section of a pipe wall is analyzed, with each element in the array representing a segment of grain boundary. The failure criterion is applied repetitively to each element of the array that is exposed to the interior of the pipe (i.e., the corrosive fluid) until that element dissolves, thereby exposing the next element. A number of environmental, mechanical, and materials factors have been incorporated into the model, including: (1) the macroscopic applied stress profile; (2) the stress history; (3) the extent and grain-to-grain distribution of carbide sensitization levels, which can be applied to a subset of elements comprising a grain boundary; and (4) a data set containing IGSCC crack growth rates as function of applied stress intensity and sensitization level averaged over a large population of grains. The latter information was obtained from the literature for AISI 304 stainless steel under light water nuclear reactor primary coolant environmental conditions. The resulting crack growth simulations are presented and discussed. DOE

N92-11174# Lawrence Livermore National Lab., CA.
NON-EQUILIBRIUM MICROSTRUCTURES PRODUCED DURING ELECTRON-BEAM AND LASER-BEAM SURFACE MODIFICATION OF METALLIC ALLOYS
J. W. Elmer 12 Aug. 1991 13 p Presented at the Fall Meeting of the Minerals, Metals and Materials Society of AIME and Materials Week of the American Society of Metals, Cincinnati, OH, 20-24 Oct. 1991
(Contract W-7405-eng-48)
(DE91-018466; UCRL-JC-107698; CONF-911003-13) Avail: NTIS HC/MF A03

Rapid solidification that occurs during electron- and laser-beam surface modification results in: (1) a refinement of the solidification features, (2) a reduction in solute segregation, (3) a reduction in the formation of interdendritic secondary phases, and (4) the formation of non-equilibrium microstructures. Solidification modeling of these microstructures will be reviewed in light of conventional dendritic-growth theory. While these models are applicable to most solidification conditions, recent observations have revealed that some alloy systems solidify under non-steady-state, non-dendritic conditions at high solidification rates. These non-steady-state microstructures consist of periodically-spaced arrays of solute-rich ultrafine particles or periodically-spaced alternating solidification modes that form bands parallel to the solidification front. The formation of these unique microstructures is discussed in the context of their distinct differences from the microstructures predicted by conventional dendritic growth theory. DOE

N92-11175# General Electric Co., Cincinnati, OH.
ALLOY MODELING AND EXPERIMENTAL CORRELATION FOR DUCTILITY ENHANCEMENT IN NEAR STOICHIOMETRIC SINGLE CRYSTAL NICKEL ALUMINIDE Final Report, 1 Mar. 1988 - 28 Feb. 1991
R. Darolia, R. D. Field, D. F. Lahrman, and A. J. Freemen 31 Jul. 1991 88 p
(Contract F49620-88-C-0052)
(AD-A240151; AFOSR-91-0743TR) Avail: NTIS HC/MF A05 CSCL 07/4

The objective of this research was to evaluate the applicability of theoretical approaches based on first principles to understand the ductility problem in intermetallic compounds. The predictive approach is based on all electron total energy band structure calculations. Predictions were evaluated on single crystals of nickel aluminum alloys. Calculations of anti-phase boundary (APB) energy in binary NiAl and the effects of ternary alloying additions on APB energy were performed. Experimental work on the effects of Cr and V additions, predicted by the calculations to reduce APB energy, was conducted. Studies aimed at exploiting the stress induced martensite transformation in NiAl to increase low temperature toughness were also conducted. Results from the calculations were found to be in good agreement with known stoichiometric effects on the transformation in binary alloys and suggested potentially beneficial ternary and quaternary alloying additions. The investigation of the role of Chromium in promoting slip in NiAl was continued. Experiments to more fully understand this effect were performed. Additional calculations were conducted to clarify the stress induced martensite effect. Calculations aimed at understanding the role of charge density distributions and bond directionality in NiAl were also initiated. Work to determine the role of microalloying in promoting ductility in NiAl was initiated, through calculations of their effect on local charge distribution and experimental work to determine their effect on slip and fracture behavior. GRA

N92-11176# Minnesota Univ., Minneapolis.
ULTRA HIGH VACUUM SPUTTERING SYSTEM Final Report, 1 Dec. 1989 - 15 Jun. 1991
E. D. Dahlberg 25 Jul. 1991 8 p
(Grant AF-AFOSR-0138-89; AF Proj. 3484)
(AD-A240157; AFOSR-91-0745TR) Avail: NTIS HC/MF A02 CSCL 11/6

This grant provided for the purchase of an ultrahigh vacuum sputtering system for the preparation of high quality multilayered magnetic films and thin films. The system allows the preparation of continuous alloys with the use of three magnetron clusters and epitaxial multilayer films using ion beam sputtering. Initial tests of the quality of the films indicate that the films prepared in this system are comparable to those prepared by other workers using similar and different techniques in this area of research. The structural quality of the samples prepared with the system has been measured with low angle x-ray scattering whereas the magnetic properties have been characterized with electrical transport, magnetization, and magneto-optic measurements. GRA

N92-11177# Naval Air Development Center, Warminster, PA. Air Vehicle and Crew Systems Technology Dept.
OXIDATION OF TITANIUM ALUMINIDE AND ITS XD COMPOSITE Final Report, 1988 - 1989
Eun U. Lee, Thomas Kircher, and Jeffrey Waldman 20 Dec. 1990 28 p

(AD-A240401; NADC-90122-60) Avail: NTIS HC/MF A03 CSCL 11/6

Martin Marietta Lab. recently developed a unique technology, whereby reinforcement dispersoids can be introduced exothermically into a metal matrix. This special alloying approach, known as Exothermic Dispersion (XD) processing, produces a metal matrix composite with a fine dispersion of a high-modulus, high-strength compound, such as titanium boride, in titanium aluminide. This study was undertaken to characterize the oxidation behavior of a Ti-45 at percent Al alloy and its XD composite with TiB2 reinforcement particles. These materials were found to oxidize in air at temperatures ranging from 400 to 1500 C. Oxidation was evidenced by surface discoloration, formation of an oxide scale and an interfacial zone, internal oxide precipitation, internal cracking, and weight gain. The oxide scale consisted of two layers; an inner TiO2 and Al2O3 mixture; and an outer TiO2 and Al2TiO5 mixture. A narrow zone along the oxide scale/base metal interface was depleted in Al, but enriched with O. In the Ti-45 at percent Al alloy, an Al-rich oxide, presumably Al2O3, was precipitated in the TiAl plate and a Ti-rich oxide, presumably TiO2, was precipitated in the Ti3Al plate. In the XD composite, an Al-rich oxide was precipitated along the lamellar structure colony boundary, and a Ti-rich oxide was precipitated in the interior of the colony. During oxidation, internal cracking occurred along the boundary and in the interior of the TiAl and Ti3Al plates. GRA

N92-11178# Illinois Univ., Urbana. Dept. of Materials Science and Engineering.

EFFECTS OF HYDROGEN AND CARBON ON THERMALLY ACTIVATED DEFORMATION IN NICKEL

E. Sirois and H. K. Birnham Aug. 1991 38 p

(Contract N00014-90-J-1769)

(AD-A240496) Avail: NTIS HC/MF A03 CSCL 07/4

Deformation experiments were performed to determine the effects of hydrogen and carbon on the activation parameters for dislocation slip in nickel. The techniques used were isothermal stress relaxation and differential temperature measurements. These methods allowed determination of the activation enthalpy and activation area for dislocation motion in nickel and the effects of hydrogen and carbon on these parameters. The results show that hydrogen increases the dislocation mobility in Ni and Ni-C alloys by reducing the activation enthalpy for dislocation motion, while carbon reduces the dislocation mobility by increasing the activation enthalpy. Hydrogen solutes decrease the activation area for dislocation motion in both pure Ni and in Ni-C alloys. GRA

N92-11179# Dayton Univ., OH.

A COMPARISON OF SINGLE CYCLE OVERLOAD EFFECT ON Al-Li 2091-T81 PLATE AND 2091-T83 SHEET Interim Report, Nov. 1990 - Jan. 1991

Russell R. Cervay and Kumar V. Jata Aug. 1991 31 p

(Contract F33615-90-C-5915)

(AD-A240627; UDR-TR-91-16; WL-TR-91-4050) Avail: NTIS HC/MF A03 CSCL 11/6

Previous researchers have established that for identical fatigue test conditions fatigue crack growth rate in aluminum-lithium alloy 2091 plate is far slower than in sheet, due to the development of a coarser fracture surface in the plate producing crack tip shielding resulting in a reduced effective crack driving parameter. Based on these results one would anticipate the plate material to exhibit a greater number of post-overload delay cycles than the sheet. This study was undertaken to quantify the effect of a single tensile overload fatigue cycle on the crack velocity of both product forms. The test procedure consisted of shedding the dynamic loads to a stress intensity range where a single 60 percent overload fatigue cycle was applied, followed by resumption of the pre-overload loading conditions. GRA

N92-11180# Naval Research Lab., Washington, DC.

HIGH PRESSURE TURBINE BLADE LIFE EXTENSION Final Memorandum Report

H. H. Smith and D. J. Michel 28 Aug. 1991 47 p

(AD-A240654; NRL-MR-6861) Avail: NTIS HC/MF A03 CSCL 21/5

The metallurgical basis for an extension of the service lifetime of directionally solidified Rene 80H HPT blades beyond the rated lifetime of 30,000 EFTC was studied. The study considered the effects of HIP processing and blade tip replacement via welding with MERL 72 on the microstructure of directionally-solidified Rene 80H (DS-R80H) superalloy blades. Elevated temperature tensile and creep rupture studies were conducted with DS-R80H specimens prepared from directionally solidified alloy test bars to ascertain the stress strain and strain time relationships and to evaluate microstructural characteristics at elevated temperatures under applied stresses. Included in the creep tests were DS-R80H specimens into which center sections of MERL 72 were inserted to evaluate the effects of stress at elevated temperature on the DS-R80H/MERL 72 interfacial integrity. In addition, the investigation considered the microstructure of MERL 72 re-tipped HPT blades following exposure of the blades in an ASMET (Accelerated Service Maintenance Engine Test) engine. GRA

N92-11181# Oak Ridge National Lab., TN.

CREEP RESPONSE OF A 9Cr-1Mo-V-Nb STEEL TO VARYING STRESSES AND TEMPERATURES

R. W. Swindeman 1991 18 p Presented at the 7th International Conference on Pressure Vessel Technology (ICPVT), Dusseldorf (Germany), 31 May - 5 Jun. 1991

(Contract DE-AC05-84OR-21400)

(DE91-017871; CONF-9105254-1) Avail: NTIS HC/MF A03

Deformation data were collected on specimens from a plate of a 9Cr-1Mo-V-Nb steel (SA 387 Grade 91) tested under constant and variable load conditions to 10,000 h. Data included results from relaxation, step-stress creep, cyclic creep, and a few nonisothermal tests. Ignoring short time transient effects, the use of a simple creep law in combination with the strain-hardening rule produced a reasonable correlation between observed and calculated creep rates for a variety of non-steady conditions in the primary and secondary creep regimes. DOE

N92-11182# Edgerton, Germeshausen and Grier, Inc., Idaho Falls, ID.

STRENGTHENING OF AN AISI 1020 STEEL BY ALUMINUM-MICROALLOYING DURING LIQUID DYNAMIC COMPACTION

S. Matsuo, T. Ando, M. C. Zody, and N. J. Grant (Massachusetts Inst. of Tech., Cambridge.) 1991 7 p Presented at the 1991 Powder Metallurgy Conference, Pittsburgh, PA, 24-26 Jun. 1991

(Contract DE-FG07-89ID-12855)

(DE91-018745; EGG-M-91290; CONF-9106277-1) Avail: NTIS HC/MF A02

Grain size refinement was achieved in an AISI 1020 steel alloyed with 0.06 wt. percent aluminum by liquid dynamic compaction (LDC), a rapid solidification spray deposition process. Atomization was done with nitrogen which resulted in incorporation of about 0.05 wt. percent nitrogen in the spray deposited steel. The spray deposit showed a fine (10 to 40 microns) equiaxed ferrite plus pearlite structure and a high as-deposited density of about 95 percent of theoretical. Minor reductions up to 70 percent in hot rolling plus annealing, both at low austenitic temperatures (850 to 900 C), fully densified the deposit and produced significantly finer (3 to 4 micron) ferritic grains with uniformly distributed fine pearlite colonies. The grain size refinement resulted from pinning of prior austenitic grain boundaries by fine AlN particles which precipitated during the thermomechanical treatments (TMT). Room temperature yield and ultimate tensile strength values exceeding 80 and 90 ksi (550 and 620 MPa), respectively, were achieved at high ductility levels. The fine microstructures were stabilized by AlN precipitates even on reheating to temperatures up to 1100 C. DOE

N92-11183# Oak Ridge National Lab., TN.

MOISTURE-INDUCED ENVIRONMENTAL EMBRITTLEMENT OF ORDERED INTERMETALLIC ALLOYS AT AMBIENT TEMPERATURES

C. T. Liu 30 Aug. 1991 14 p Presented at the NATO Advanced Research Workshop, Irsee (Germany), 23-29 Jun. 1991 (Contract DE-AC05-84OR-21400)
(DE91-018852; CONF-9106275-1) Avail: NTIS HC/MF A03

Recent studies have demonstrated that moisture-induced environmental embrittlement is a major cause of low ductility and brittle fracture in ordered intermetallics with high crystal symmetries (e.g., L1(sub 2) and B2). The embrittlement involves the reaction of reactive elements in intermetallics with moisture in air and the generation of atomic hydrogen at crack tips. The loss in ductility at ambient temperatures is generally accompanied by a change in fracture mode from ductile appearance to brittle grain-boundary fracture in many L1(sub 2) intermetallics, and to brittle cleavage in body-centered cubic (bcc)-ordered intermetallics. In a number of cases, the embrittlement was alleviated by alloy design through control of microstructure and alloy composition. DOE

27 NONMETALLIC MATERIALS

Includes physical, chemical, and mechanical properties of plastics, elastomers, lubricants, polymers, textiles, adhesives, and ceramic materials.

For composite materials see *24 Composite Materials*.

N92-11184 National Physical Lab., Teddington (England). Div. of Quantum Metrology.
INVESTIGATION OF THE STABILITY OF THE SPECTRAL RESPONSITIVITY OF SILICON PHOTODIODES
J. Bastie, N. P. Fox, T. C. E. Jones, K. Moestl, D. H. Nettleton, M. L. Rastello, and K. D. Stock (Physikalisch-Technische Bundesanstalt, Brunswick, Germany, F.R.) Nov. 1990 69 p Sponsored by Commission of the European Communities
(NPL-QU-87; ISSN-0309-3050; ETN-91-99864) Copyright Avail: National Physical Lab., Teddington, Middlesex TW11 OLW, England

An investigation of the long term stability of the spectral responsivity of silicon photodiodes, in the spectral range 250 to 1000 nm is described. Results from four laboratories are presented for the ageing rates of photodiodes manufactured by five different companies. The possible causes of ageing are briefly discussed. ESA

N92-11185 National Physical Lab., Teddington (England). Div. of Materials Metrology.
PHYSICAL AGEING AND CREEP IN PVC
B. E. Read, G. D. Dean, P. E. Tomlins, and J. L. Lesniarek-Hamid Feb. 1991 32 p
(NPL-DMM(A)-21; ISSN-0959-2423; ETN-91-99876) Copyright Avail: National Physical Lab., Teddington, Middlesex TW11 OLW, England

Tensile creep compliances were determined for Polyvinyl/Chloride (PVC) over a wide range of time at 23 C. Results were obtained on samples of different age characterized by the elapsed time between quenching from 85 C and the instant of load application. Various empirical functions were employed to model the data from both short term and long term tests in terms of compliance contributions from secondary (beta) and glass rubber (alpha) retardation regions. Results of these analyses suggest that physical ageing produces a decrease in the magnitude of the beta process, an increase in average retardation time for the alpha process and negligible changes in the widths of the respective retardation time distributions. Comments are made on the structural significance of the results for the beta process and on the validity of functions used to describe the creep curves. ESA

N92-11186*# National Aeronautics and Space Administration. Lewis Research Center, Cleveland, OH.
SOLID LUBRICANTS ON PRETREATED SURFACES Patent Application
Robert L. Fusaro, inventor (to NASA) 16 Sep. 1991 12 p
(NASA-Case-LEW-14474-2; NAS 1.71:LEW-14474-2; US-Patent-Appl-SN-760670) Avail: NTIS HC/MF A03 CSCL 11C

A solid lubricant film on a pretreated surface is described. The surface topography of the material to be lubricated is first selectively altered. Photochemical etching is employed to selectively determine contact area and shape to maximize the proper ratio of reservoir area to sliding contact area. Cadmium oxide is then sputtered onto the altered surface. The cadmium oxide acts as an intermediate layer to more tightly bond the solid lubricant, such as graphite, onto the material surface. NASA

N92-11187*# National Aeronautics and Space Administration. Goddard Space Flight Center, Greenbelt, MD.
MECHANICAL PROPERTIES OF A POROUS MULLITE MATERIAL
Michael J. Viens Sep. 1991 28 p
(NASA-TM-104547; Rept-91B00143; NAS 1.15:104547) Avail: NTIS HC/MF A03 CSCL 11C

Modulus of rupture specimens were used to determine crack growth parameters of a porous mullite material. Strength testing was performed in ambient and moist environments. The power law crack growth rate parameters n and 1n B in 50 percent relative humidity were found to be 44.98 and 0.94, respectively. The inert strength, fracture toughness, and elastic modulus were also determined and found to be 19 MPa, 055 MPa(m) exp 1/2, and 11.6 GPa, respectively. Author

N92-11188*# National Aeronautics and Space Administration. Lewis Research Center, Cleveland, OH.
HIGH-T SUB c FLUORINE-DOPED YBa2Cu3O(y) FILMS ON CERAMIC SUBSTRATES BY SCREEN PRINTING
Narottam P. Bansal Oct. 1991 18 p
(NASA-TM-105296; E-6635; NAS 1.15:105296) Avail: NTIS HC/MF A03 CSCL 11C

Thick films of fluorine-doped YBa2Cu3O(y) were screen printed on highly polished alumina, magnesia spinel, strontium titanate, and yttria-stabilized zirconia (YSZ) substrates. They were annealed at 1000 C and soaked in oxygen at 450 C, followed by slow cooling to room temperature. The films were characterized by electrical resistivity measurements as a function of temperature and x-ray diffraction. The film on YSZ showed the best characteristics with a T sub c (onset) of 91 K, T sub c (R equals 0) of 88.2 K, and a transition width, delta T sub c (10-90 percent), of approximately 1.7 K. The film adhesion, probably controlled by interdiffusion of cations between the film and the substrate, was good in all cases except on strontium titanate where the film completely detached from the substrate. Author

N92-11189# Army Lab. Command, Watertown, MA. Material Technology Lab.
DEFORMATION OF ISODAMP (A POLYVINYL CHLORIDE-BASED ELASTOMER) AT VARIOUS LOADING RATES Final Report
D. P. Dandekar, J. L. Green, M. Hankin, A. G. Martin, and W. Weisgerber May 1991 30 p
(AD-A240393; MTL-TR-91-16) Avail: NTIS HC/MF A03 CSCL 07/6

Elastomers are widely used for mitigating and blocking small amplitude and low frequency vibrations. There is an interest in utilizing this material in dynamic loading environments where it would be subjected to high strain rates and high pressures. Since a paucity of information about elastomers exists in this environment, a study was initiated. The objective of the study was to determine how the shock absorbing property of Isodamp C-1002 is modified under high strain rates of deformation and high stresses. In this investigation measurements of elastic wave velocity and attenuation to 10 MHz were obtained using ultrasonic techniques. GRA

N92-11190# Rensselaer Polytechnic Inst., Troy, NY. Dept. of Chemistry.
NEW POLYMER ELECTROLYTE HOSTS AND THEIR TETRABUTYLAMMONIUM CHLORIDE COMPLEXES. RELATIONSHIPS AMONG CONCENTRATION OF POLAR GROUPS, ESR SPIN PROBE RESPONSE, AND IONIC CONDUCTIVITY Technical Report No. 45, May 1989 - May 1991
Chia-Yu Yang and Gary E. Wnek 12 Jun. 1991 23 p
(Contract N00014-88-K-0732)
(AD-A240497) Avail: NTIS HC/MF A03 CSCL 07/4

A new polymer electrolyte host was synthesized by hydrosilation of a poly(hydromethyl siloxane) with terminal olefin bearing a silyl ketene acetal. The derivatized siloxane was subsequently reacted with 4-nitrobenzenesulfenyl chloride, affording polymers having highly polar pendants. Complexes of these polymers with tetrabutylammonium chloride were prepared. The ionic conductivities of these materials are a function of concentration of polar pendent groups and, as a result, the glass transition temperature. The weak dependence of polymer host Tg on tetrabutylammonium chloride concentration makes these ideal model systems to explore the factors which ultimately limit ionic conductivity. GRA

N92-11191# Texas A&M Univ., College Station. Mechanics and Materials Research Center.
DAMAGE EVOLUTION IN FILLED ELASTOMERS Final Report, Jun. 1989 - Sep. 1990
R. A. Schapery 9 Aug. 1991 6 p
(Contract N00014-89-J-3012)
(AD-A240532; MM-27010-91-1) Avail: NTIS HC/MF A02 CSCL 20/11

This report summarizes accomplishments on the development of mathematical models of distributed microcracking in filled elastomers, such as solid propellant, and in other linear and nonlinear viscoelastic composite materials. The work is divided into two parts. The first part is concerned with elastic composites while the second part extends the theory to viscoelastic behavior. Experimental results and the theory for axially stretched and pressurized specimens are combined to derive three material functions of damage. The theory is then used to predict behavior under pressures not used in the development of the material functions. Good agreement between theory and experiment is shown for the strain from zero to the zero pressure failure strain of approx. 55 pct. GRA

N92-11192# Massachusetts Univ., Amherst. Dept. of Polymer Science and Engineering.
DIRECT IMAGING OF DEFORMATION AND DISORDER IN EXTENDED-CHAIN POLYMER FIBERS Final Report, Jul. 1986 - Jun. 1990
David C. Martin Mar. 1991 374 p
(Contract F49620-89-C-0073; AF-AFOSR-0275-85)
(AD-A240651; WL-TR-91-4011) Avail: NTIS HC/MF A16 CSCL 07/6

The rigid rod polymers poly (paraphenylene benzo bisthiazole) (PBZT) and poly (paraphenylene benzo bisoxazole) (PBZO) can be spun from lyotropic liquid crystalline solutions into solid fibers with extraordinary mechanical properties. However, these fibers are comparatively weak in compression, with deformation occurring by strain localization into kink bands. This report examines the ultrastructure of PBZT and PBZO fibers as a function of processing condition. In particular, High Resolution Electron Microscopy (HREM)is used to directly image structural features such as grain boundaries, dislocations, and the molecular level details of deformation processes. HREM images of PBZT and PBZO enable the quantitative determination of crystallite size, shape, orientation, and internal perfection as a function of processing condition. The nature of the disorder present within and between PBZT and PBZO crystallites is analyzed, modeled, and compared to experimental Wide Angle X-ray Scattering (WAXS) and Selected Area Electron Diffraction (SAED) data. Both PBZT and PBZO exhibit high degrees of orientation on a local scale, yet measurable misorientation does exist. GRA

N92-11193# Naval Research Lab., Washington, DC.
DISCHARGE SYSTEM TESTS OF HALON 1301 TEST GAS SIMULANTS Memorandum Report, Jun. - Sep. 1988
H. W. Carhart, J. T. Leonard, P. J. DiNenno, E. W. Forssell, and M. D. Starchville 19 Sep. 1991 114 p Prepared in cooperation with Hughes Associates, Inc., Wheaton, MD
(NR Proj. S15-65)
(AD-A240679; NRL-MR-6898) Avail: NTIS HC/MF A06 CSCL 07/2

All new and retrofit installations of Halon 1301 total flooding systems in shipboard machinery spaces require an acceptance discharge test. It is desirable to use a simulant instead of Halon 1301 in view of current and future restrictions regarding the discharge of Halons into the atmosphere. Two candidate simulants; sulfur hexafluoride (SF6) and chlorodifluoromethane (R-22) were evaluated on the basis of flow through the piping networks of both modular and banked systems. A modular system with two different fill densities and six banked systems were used in this evaluation. Sulfur hexafluoride was found to discharge at a similar rate to Halon 1301, while R-22 discharged faster in all tests. The flow splits for both candidate simulants in banked systems were similar to those of Halon 1301. Together with work on leakage from an enclosure and initial mixing, these tests have shown that sulfur hexafluoride is an excellent simulant for Halon 1301. These conclusions will be confirmed in full scale tests. GRA

N92-11194# Pennsylvania Univ., Philadelphia. Dept. of Materials Science and Engineering.
SYNTHESIS OF NOVEL POLYSILOXANES BEARING POLAR GROUPS Technical Report, May 1989 - May 1991
C. Y. Yang and G. E. Wnek 12 Jun. 1991 3 p
(Contract N00014-88-K-0732)
(AD-A240722; TR-43) Avail: NTIS HC/MF A01 CSCL 07/3

Silicones having pendant silyl ketene acetals were synthesized through hydrosilation of polymethyl hydrosiloxane with a terminal olefin-ester which can be subsequently coverted to the silyl ketene acetal. The silicones can be reacted with the electrophiles such as p-nitrobenzene sulfenyl chloride, affording derivatives having highly polar pendants. These materials have dielectric constants as high as 9 at room temperature. GRA

N92-11195# California Univ., Santa Barbara. Inst. for Polymers and Organic Solids.
NONLINEAR OPTICAL PROPERTIES OF SEMICONDUCTING POLYMERS Final Report
Alan J. Heeger 1990 87 p
(Contract N00014-86-K-0514)
(AD-A240753) Avail: NTIS HC/MF A05 CSCL 20/6

This program focused on the nonlinear optical (MLO) properties of semiconducting conjugated polymers. Specific emphasis was on fast time (picosecond regime) measurements of the photoconductivity of semiconducting polymers and on NLO measurements related to the mechanism and origin of the nonlinearity, on attempts to optimize the magnitude of the nonlinear response, and on developing novel methods for measurement. In the NLO area, we succeeded in demonstrating that for conjugated polymers the nonlinear response is highly anisotropic with substantial nonlinearity only when the pump is polarized along the direction parallel to the polymer backbone. In attempting to sort out the NLO mechanism we carried out comparative studies on cis and transpolyacetylene. The larger NLO response from the trans-isomer (larger by at least a factor of 20) shows the importance of the degerate ground state. GRA

N92-11196# Pennsylvania Univ., Philadelphia. Dept. of Materials Science and Engineering.
SYNTHESIS AND REACTIVITY OF SILYL-KETENE ACETAL-MODIFIED POLYSILOXANES PREPARATION OF POLYSILOXANES WITH HIGH DIELECTRIC CONSTRAINTS Technical Report, May 1989 - May 1991

C. Y. Yang and G. E. Wnek 12 Jun. 1991 23 p
(Contract N00014-88-K-0732)
(AD-A240754; TR-44) Avail: NTIS HC/MF A03 CSCL 07/4

Silicones having pendant silyl ketene acetals were synthesized through hydrosilation of polymethylhydrosiloxane with a terminal olefin bearing a silyl ketene acetal or, alternatively, a terminal olefin-ester which can be subsequently converted to the silyl ketene acetal. The silicones can be reacted with the elecytrophiles such as p-nitrobenzenesulfenyl chloride, affording derivatives having highly polar pendants. These materials have dielectric constants as high as 9 and loss factors of 0.02-0.06 at 100 kHz at room temperature. The temperature dependencies of the dielectric constants are a function of polar pendant group concentration and the glass transition temperature. GRA

N92-11197# Rensselaer Polytechnic Inst., Troy, NY. Dept. of Chemistry.
STUDY OF SILANIZATION OF SILICA AND FIBERGLASS USING ESR SPECTROSCOPY AND SPIN LABELLING Technical Report No. 47
R. Malik and Gary E. Wnek May 1991 20 p
(Contract N00014-88-K-0732)
(AD-A240767) Avail: NTIS HC/MF A03 CSCL 07/3

In this paper we report a study performed on silane coupling agents using ESR spectroscopy and spin label synthesized from 4-hydroxy-TEMPO and 3-isocyanatopropoyl trimethoxy silane. The coupling agents used in the study were 3-aminopropyl triethoxy silane (APS), 3-methacrylopropyl trimethoxy silane (MPS), 3-aminopropyl trimethoxy silane (APMS), N methyl-3-aminopropyl trimethoxy silane (DPS). Silanization of silica and fiber glass with the above coupling agents were performed in the presence of the spin label and the supernatant as well as the silica was examined by ESR spectroscopy. The disappearance of the label in the supernatant affords data on the kinetics of surface derivatization. We find deposition kinetics to be highly dependent on the nature of the organofunctional group on the silane and on the deposition medium (e.g., 95 percent aqueous ethanol or water). The labels on the silica surfaces are sensitive to their surroundings. For example, the labels are rather immobile in the dry state but become mobile upon immersion of the silica in organic solvents such as benzene. The prospects of using spin-labeled silica to explore interfacial adhesion in silica/polymer composites are discussed. GRA

N92-11198*# National Aeronautics and Space Administration. Langley Research Center, Hampton, VA.
POLYIMIDES WITH IMPROVED COMPRESSION MOLDABILITY Patent Application
Paul M. Hergenrother, inventor (to NASA), Stephen J. Havens, inventor (to NASA), and Mark W. Beltz, inventor (to NASA) (Akron Univ., OH.) 5 May 1990 18 p
(NASA-Case-LAR-14457-1-CU; NAS 1.71:LAR-14457-1-CU; US-Patent-Appl-SN-520472) Avail: NTIS HC/MF A03 CSCL 11C

The semicrystalline polyimide prepared by reaction of 3,3',4,4' benzophenonetetracarboxylic (BTDA) and 1,3-bis(4-aminophenoxy 4' benzoyl) benzene (1,3-BABB) is modified so that it can be more readily processed to form adhesive bonds, moldings, and composites. The stoichiometric ratio of the two monomers, BTDA and 1,3-BABB is controlled so that the intermediate polyamide acid is of a calculated molecular weight. A polyimide acid with excess anhydride groups is then reacted with the stoichiometrically required amount of monofunctional aromatic or aliphatic amine required for complete endcapping. The stoichiometrically offset, encapped polimide is processed at lower temperatures and pressures than the unmodified high molecular weight polyimide with the same repeat unit, and exhibits an improved melt stability. NASA

N92-11199*# National Aeronautics and Space Administration. Langley Research Center, Hampton, VA.
LOW TOXICITY HIGH TEMPERATURE PMR POLYIMIDES Patent Application
Ruth H. Pater, inventor (to NASA) 5 Feb. 1991 39 p
(NASA-Case-LAR-14639-1; NAS 1.71:LAR-14639-1; US-Patent-Appl-SN-651062) Avail: NTIS HC/MF A03 CSCL 11C

In-situ polymerization of monomer reactants (PMR) type polyimides constitute an important class of ultra high performance composite matrix resins. PMR-15 is the best known and most widely used PMR polyimide. An object of the present invention is to provide a substantially improved high temperature PMR-15 system that exhibits better processability, toughness, and thermo-oxidative stability than PMR-15, as well as having a low toxicity. Another object is to provide new PMR polyimides that are useful as adhesives, moldings, and composite matrices. By the present invention, a new PMR polyimide comprises a mixture of the following compounds: 3,4'-oxydianiline (3,4'-ODA), NE, and BTDE which are then treated with heat. This PMR was designated LaRC-RP46 and has a broader processing window, better reproducibility of high quality composite parts, better elevated temperature mechanical properties, and higher retention of mechanical properties at an elevated temperature, particularly, at 371 C. NASA

N92-11200*# National Aeronautics and Space Administration. Langley Research Center, Hampton, VA.
DIPHENYLMETHANE-CONTAINING DIANHYDRIDE AND POLYIMIDES PREPARED THEREFROM Patent Application
Anne K. St.Clair, inventor (to NASA), Harold G. Boston, inventor (to NASA), and J. Richard Pratt, inventor (to NASA) (Lockheed Engineering and Sciences Co., Hampton, VA.) 26 Aug. 1991 22 p
(NASA-Case-LAR-14487-1; NAS 1.71:LAR-14487-1; US-Patent-Appl-SN-750158) Avail: NTIS HC/MF A03 CSCL 11C

A high temperature stable, highly optically transparent to colorless, low dielectic linear aromatic polyimide is prepared by reacting an aromatic diamine with 3,3'bis (3,4-dicarboxyphenoxy) diphenylmethane dianhydride in an amide solvent to form a linear aromatic polyamic acid. This polyamic acid is then cyclized to form the corresponding polyimide. The general structural formula is given. NASA

N92-11201*# National Aeronautics and Space Administration. Langley Research Center, Hampton, VA.
A PROCESS FOR PREPARING AN ASSEMBLY OF AN ARTICLE AND A POLYIMIDE WHICH RESISTS DIMENSIONAL CHANGE, DELAMINATION, AND DEBONDING WHEN EXPOSED TO CHANGES IN TEMPERATURE Patent Application
Diane M. Stoakley, inventor (to NASA) and Anne K. St.Clair, inventor (to NASA) 26 Jul. 1991 20 p
(NASA-Case-LAR-14538-1; NAS 1.71:LAR-14538-1; US-Patent-Appl-SN-736880) Avail: NTIS HC/MF A01 CSCL 11C

An assembly of an article and a polyimide composition is prepared. The assembly resists dimensional change, delamination, or debonding when exposed to changes to temperature. An article is provided. A polyamic acid solution which yields a polyimide having a low coefficient of thermal expansion (CTE) was prepared. Equimolar quantities of an aromatic diamine and an aromatic dianhydride were reacted in a solvent medium to form a polyamic acid solution. A metal ion containing additive was added to the solution. Examples of this additive are: TbCl3, DyCl3, ErCl3, TmCl3, Al(C5H7O2)3, and Er2S3. The polyamic acid solution was imidized and is combined with the article to form the assembly. NASA

N92-11202*# National Aeronautics and Space Administration. Lewis Research Center, Cleveland, OH.
GLASS FORMATION, PROPERTIES, AND STRUCTURE OF SODA-YTTRIA-SILICATE GLASSES
Paul W. Angel and Raiford E. Hann Oct. 1991 14 p
(NASA-TM-104488; E-6336; NAS 1.15:104488) Avail: NTIS HC/MF A03 CSCL 11C

The glass formation region of the soda yttria silicate system

was determined. The glasses within this region were measured to have a density of 2.4 to 3.1 g/cu cm, a refractive index of 1.50 to 1.60, a coefficient of thermal expansion of 7 x 10(exp -6)/C, softening temperatures between 500 and 780 C, and Vickers hardness values of 3.7 to 5.8 GPa. Aqueous chemical durability measurements were made on select glass compositions while infrared transmission spectra were used to study the glass structure and its effect on glass properties. A compositional region was identified which exhibited high thermal expansion, high softening temperatures, and good chemical durability. Author

N92-11203# Sandia National Labs., Albuquerque, NM.
LOW VOLATILE ORGANIC COMPOUND PAINTS
F. E. Martinez 1991 7 p Presented at the ECM 1991 Congress, Santa Fe, NM, 18-20 Sep. 1991
(Contract DE-AC04-76DP-00789)
(DE91-017984; SAND-91-1894C; CONF-9109274-1) Avail: NTIS HC/MF A02

Increasingly stringent air emission standards in various states has dictated the elimination of engineering finishes which are derived from high volatile organic compound (VOC) paint chemistries. In July 1989, Allied-Signal, Inc., Kansas City Division, Kansas City, Missouri, voluntarily closed its paint facility, due to non-compliance with local air emission standards. The details of the materials selection and evaluations which led to current processing using low VOC paints, which permitted the Allied Signal, Inc., paint facility to achieve compliance and resume operations. DOE

N92-11204# Sandia National Labs., Albuquerque, NM.
PHOTOTHERMAL DEFLECTION SPECTROSCOPY OF CONJUGATED POLYMERS
C. H. Seager, M. Sinclair, D. McBranch, Alan J. Heeger, and G. L. Baker (Bell Communications Research, Inc., Red Bank, NJ.) 1991 16 p Presented at the American Chemical Society (ACS) Meeting, Salt Lake City, UT, 19-22 Aug. 1991
(Contract DE-AC04-76DP-00789)
(DE91-018318; SAND-91-1883C; CONF-9108156-1) Avail: NTIS HC/MF A03

Along with the third order, non-linear susceptibility, X(exp 3), the magnitude of the optical absorption in the transparent window below the principal absorption edge is an important parameter for conjugated polymers used in active integrated optical devices. Photothermal Deflection Spectroscopy (PDS) is an ideal technique for determining the absorption coefficients of thin films of transparent materials. We have used PDS to measure the optical absorption spectra of the conjugated polymers poly (1,4-phenylene-vinylene) (and derivatives) and polydiacetylene-4BCMU in the spectral region from 0.55 to 3 eV. We find that the shape of the absorption edge varies considerably from polymer to polymer, with polydiacetylene-4BCMU having the steepest absorption edge. The minimum absorption coefficients measured varied somewhat with sample age and quality, but were typically in the range 1 to 10/cm. In the region below 1 eV, overtones of C-H stretching modes dominate the absorption behavior. We also observe that irradiation of all of these polymers with light above approx. 2.5 eV produces enhanced absorption below the fundamental edge. In the absence of light, these excitations decay with characteristic times of 10 to 1000 sec., and in some cases they may determine the effective IR transparency in the 1.0 to 1.8 eV energy range. DOE

N92-11205# Oak Ridge National Lab., TN.
THE EFFECTS OF SPECIMEN GEOMETRY AND SIZE ON THE FRACTURE TOUGHNESS OF NUCLEAR GRAPHITES
G. R. Romanoski and T. D. Burchell 1991 14 p Presented at the International Atomic Energy Agency (IAEA) Specialists Meeting on Status of Graphite Development for Gas-Cooled Reactors, Tokai (Japan), 9-12 Sep. 1991
(Contract DE-AC05-84OR-21400)
(DE92-000056; CONF-9109266-1) Avail: NTIS HC/MF A03

In a joint Oak Ridge National Laboratory (ORNL)/Japan Atomic Energy Research Institute (JAERI) study, various fracture toughness techniques were applied to Toyo Tanso grade IG-110 graphite to establish if specimen geometry influences on fracture toughness. The test geometries investigated were: compact tension (CT), disc compact tension (DCT), short rod (SR), chevron-notched short-red (CNSR), cylindrical bend specimen (BS), and centrally slotted disc (CSD). Specimen geometries which allow slow crack propagation, such as the CNSR and CT, yielded higher fracture toughness values than those where fracture is very rapid, e.g., the CSD. In a further ORNL study, the CNSR specimen geometry was selected to investigate the effect of specimen size on fracture toughness. Three specimen sizes and three grades of graphite were examined: Great Lakes Carbon grade H-451, Stackpole grade 2020, and Toyo Tanso grade IG-110. Grade H-451 was the toughest graphite, while Stackpole 2020 was the least tough. Fracture toughness increased with increasing specimen size for all graphites tested. This result was attributed to rising R-curve behavior. DOE

N92-11206# Columbia Univ., New York, NY. School of Mines.
ON THE NATURE OF BULK ELECTRICAL RELAXATION IN SILICATE GLASSES
W. K. Lee, S. Aronson-Unger, J. F. Liu, A. S. Nowick, and H. Jain (Lehigh Univ., Bethlehem, PA.) 1991 5 p Presented at the 7th International Conference on the Physics of Non-Crystalline Solids, Cambridge, MA, 4-9 Aug. 1991
(Contract DE-FG02-88ER-45341)
(DE92-000077; CONF-910874-2) Avail: NTIS HC/MF A01

Three sodium and mixed-alkali silicate glasses were studied to separate bulk relaxation processes from those due to electrode blocking. Conductance, G, and capacitance, C, were measured as a function of frequency over a wide range of temperature. Electrode effects were separated by their dependence on the type of electrode and sample thickness. We found no evidence for a bulk relaxation loss peak but the residual bulk process took the form of the well-known universal behavior involving power-law dependence of both G and C, with a fractional exponent, s, close to 0.6. The corresponding relaxation time has precisely the same activation energy as the dc conductivity. By extending the measurements to low temperatures, we find that s becomes equal to unity at the lower temperatures. DOE

N92-11207*# National Aeronautics and Space Administration. Langley Research Center, Hampton, VA.
IMPROVED COMPRESSION MOLDING TECHNOLOGY FOR CONTINUOUS FIBER REINFORCED COMPOSITE LAMINATES. PART 2: AS-4/POLYIMIDESULFONE PREPREG SYSTEM
Robert M. Baucom, Tan-Hung Hou, Paul W. Kidder, and Rakasi M. Reddy (Old Dominion Univ., Norfolk, VA.) Oct. 1991 69 p
(Contract NAS1-19000; NAG1-569)
(NASA-TM-104133; NAS 1.15:104133) Avail: NTIS HC/MF A04 CSCL 11D

AS-4/polyimidesulfone (PISO2) composite prepreg was utilized for the improved compression molding technology investigation. This improved technique employed molding stops which advantageously facilitate the escape of volatile by-products during the B-stage curing step, and effectively minimize the neutralization of the consolidating pressure by intimate interply fiber-fiber contact within the laminate in the subsequent molding cycle. Without the modifying the resin matrix properties, composite panels with both unidirectional and angled plies with outstanding C-scans and mechanical properties were successfully molded using moderate molding conditions, i.e., 660 F and 500 psi, using this technique. The size of the panels molded were up to 6.00 x 6.00 x 0.07 in. A consolidation theory was proposed for the understanding and advancement of the processing science. Processing parameters such as vacuum, pressure cycle design, prepreg quality, etc. were explored. Author

28 PROPELLANTS AND FUELS

Includes rocket propellants, igniters, and oxidizers; their storage and handling procedures; and aircraft fuels.

For related information see also *07 Aircraft Propulsion and Power, 20 Spacecraft Propulsion and Power,* and *44 Energy Production and Conversion.*

N92-11208*# National Aeronautics and Space Administration. Lewis Research Center, Cleveland, OH.

DESCRIPTION OF LIQUID NITROGEN EXPERIMENTAL TEST FACILITY

John M. Jurns, Richard E. Jacobs (Analex Corp., Brook Park, OH.), and Naseem H. Saiyed Sep. 1991 14 p

(NASA-TM-105215; E-6530; NAS 1.15:105215) Avail: NTIS HC/MF A03 CSCL 20I

The Liquid Nitrogen Test Facility is a unique test facility for ground-based liquid nitrogen experimentation. The test rig consists of an insulated tank of approximately 12.5 cubic ft in volume, which is supplied with liquid nitrogen from a 300 gal dewar via a vacuum jacketed piping system. The test tank is fitted with pressure and temperature measuring instrumentation, and with two view ports which allow visual observation of test conditions. To demonstrate the capabilities of the facility, the initial test program is briefly described. The objective of the test program is to measure the condensation rate by injecting liquid nitrogen as a subcooled spray into the ullage of a tank 50 percent full of liquid nitrogen at saturated conditions. The condensation rate of the nitrogen vapor on the subcooled spray can be analytically modeled, and results validated and corrected by experimentally measuring the vapor condensation on liquid sprays. Author

N92-11209# Materials Research Labs., Melbourne (Australia).

AN INVESTIGATION OF THE MATERIAL HAZARD OF SOME INSENSITIVE HIGH EXPLOSIVES

Robert J. Spear and Luciana Montelli 1991 24 p

(MRL-TR-91-22; AR-006-375) Copyright Avail: NTIS HC/MF A03

The number of insensitive high explosives (IHE) and formulations which were determined to have unexpectedly high sensitivness by Rotter impact testing were further assessed by Rotter powder explosiveness testing. Analysis shows that the hazard, as reflected by the ability to propagate following ignition, was low. Risk, defined as the product of hazard and frequency, was similar to assessments based on US impact test data for these materials. An assessment of both the usefulness and quantitative nature of powder explosiveness testing is made. Guidelines for using Rotter data for deciding relative risk from handling small quantities of IHEs in research and development are given. The desirability of carrying out charge hazard testing to support these risk assessments is stressed. Author

N92-11210# Sypher-Mueller International, Inc., Ottawa (Ontario).

ALTERNATIVE FUELS FOR HEAVY DUTY ENGINES: STATUS OF FLEET TRIALS

Aug. 1991 55 p

(Contract DE-GI01-87CE-50182)

(DE91-018474; DOE/CE-50182/T3) Avail: NTIS HC/MF A04

The overall objectives of Annex 3 are to collect, assess, and disseminate data on the use of methanol and natural gas in heavy duty compression ignition engines. Originally, the objective was directed at methanol, but in 1990 the mandate of Annex 3 was broadened to include natural gas. This is the latest update on field trials using these two fuels. The report outlines progress being made and identifies major trends. The more important events since the last progress report include: the U.S. Environmental Protection Agency (EPA) Certification of Detroit Diesel Corporation's 6V-92 methanol engine; the introduction of transit buses in Windsor, Ontario, Canada, using DDC methanol engines; an introduction of two DDC engined ethanol fueled transit buses at Regina, Saskatchewan, Canada; the testing of catalytic converters, by Detroit Diesel Corporation, with alcohol powered engines; the discontinuance of methanol in MAN engines/buses at Seattle Metro; a tender for over 100 methanol powered transit buses for South Coast Rapid Transit District (SCRTD), Los Angeles, California; the potential purchase of an additional 150 methanol powered buses for SCRTD, in addition to 10 buses for Sacramento Regional Transit District; and, the expanded interest of transit properties in using natural gas in both compressed natural gas (CNG) and liquefied natural gas (LNG) engines. DOE

N92-11211# Army Engineer Waterways Experiment Station, Vicksburg, MS. Structures Lab.

KA-111, PHASE C, M-1 PROPELLANT TESTS: DEFLAGRATION IN PARTIAL CONFINEMENT Final Report

Charles E. Joachim Jul. 1991 141 p

(AD-A240185; WES/TR/SL-91-11) Avail: NTIS HC/MF A07 CSCL 19/1

When a propellant material is stored under confined condition, US and NATO explosives safety regulations require that the safety hazard quantity-distance (Q-D's) used for Hazard Class 1.1 (mass detonating) explosives be applied, rather than the less restrictive Q-D's normally used for propellants and other Class 1.3 materials. This is based on the assumption that high gas pressures produced by an accidental burning of propellant in a confined volume will cause the burning (deflagration) to transition to a detonation. To test this assumption, a series of experiments were conducted in which increasing amounts of propellants were ignited and burned inside a heavy concrete structure with an internal chamber volume of 5 cu m. Pressure and temperatures were measured inside the chamber, in a connecting exhaust vent, and in the free field beyond the exhaust vent pipe. Although there was no evidence that a detonation occurred, the high gas pressures produced by burning of the largest propellant charge (250 kg) were sufficient to fail the structure. GRA

N92-11212# Department of the Navy, Washington, DC.

HIGH DENSITY ENERGETIC MATERIALS Patent Application

Michael E. Sitzmann, inventor (to Navy) 30 Apr. 1991 22 p

(AD-D014959; US-Patent-Appl-SN-695144; Navy-Case-73298) Avail: NTIS HC/MF A03 CSCL 19/1

This invention relates to explosives and more particularly high energy organic explosives. The synthesis of 2-fluoro- 2,2-dinitro ethylchloro formate, (NO2)2FCCH2OC(O)Cl, for use as an intermediate in preparation of energetic compounds is reported. A limitation of 2-fluoro- 2,2-dinitro ethylchloro formate is that energetic derivatives from this intermediate do not generally have unusually high densities or oxidant balances. For energetic materials, density is a critical property since the performance of the material is proportional to the square of its density. The oxidant balance of an energetic material is also an important property since energetic plasticizers and explosives with high oxidant balance are preferable for use in explosive formulations. Objectives are to provide new explosives, new high density, energetic explosives, and new high energy explosives having high oxidant balances. GRA

N92-11213# Pratt and Whitney Aircraft, West Palm Beach, FL.

PROPERTIES OF AIRCRAFT FUELS AND RELATED MATERIALS Final Report, 8 Jul. 1985 - 30 Nov. 1990

Tedd B. Biddle 29 Jul. 1991 515 p

(Contract F33615-85-C-2508)

(AD-A240650; PWA-FR-21509; WL-TR-91-2036) Avail: NTIS HC/MF A22 CSCL 21/4

Topics of this technical study include: general analysis and characterization of conventional and experimental fuel properties which are unique and/or critical to engine performance and durability; special investigations; development and evaluation of new test methods; refinement of existing test methods; additive evaluation and quantification; investigation of fuel and material related field problems; advanced fuel requirements; and fuel system parameters for current and advanced engines. Specific topics include: lubricity, thermal stability, vapor pressure, thermal conductivity, high density fuels, corrosion inhibitors, and combustion. GRA

N92-11214*# National Aeronautics and Space Administration. Lewis Research Center, Cleveland, OH.
BENEFITS OF SLUSH HYDROGEN FOR SPACE MISSIONS
Alan Friedlander, Robert Zubrin (Martin Marietta Corp., Littleton, CO.), and Terry L. Hardy Oct. 1991 18 p
(NASA-TM-104503; E-6364; NAS 1.15:104503) Avail: NTIS HC/MF A03 CSCL 21I

A study was performed to quantify the benefits of using slush hydrogen instead of normal boiling point liquid hydrogen as a fuel for several space missions. Vehicles considered in the study included the Space Shuttle/Shuttle-C, LEO to GEO transfer vehicles, Lunar and Mars transfer vehicles, and cryogenic depots in low Earth orbit. The advantages of using slush hydrogen were expressed in terms of initial mass differences at a constant payload, payload differences at a constant tank volume, and increases in fuel storage time for cryogenic depots. Both chemical oxygen/hydrogen and hydrogen nuclear thermal rocket propulsion were considered in the study. The results indicated that slush hydrogen offers the potential for significant decreases in initial mass and increases in payload for most missions studied. These advantages increase as the mission difficulty, or energy, increases. Author

N92-11122*# Alabama Univ., Huntsville. Dept. of Mechanical Engineering.
NAVIER-STOKES ENTROPY CONTROLLED COMBUSTION INSTABILITY ANALYSIS FOR LIQUID PROPELLANTS
T. J. Chung and W. S. Yoon *In* JHU, The 27th JANNAF Combustion Subcommittee Meeting, Volume 3 Nov. 1990 p 275-306 (For primary document see N92-11117 02-20)
(Contracts NAS8-36955; DAAH01-87-D-0021)
Avail: NTIS HC/MF A99 CSCL 21I

29 MATERIALS PROCESSING

Includes space-based development of products and processes for commercial applications.
For biological materials see *55 Space Biology.*

N92-11215*# Massachusetts Inst. of Tech., Cambridge.
SPACE ENGINEERING Final Report, 1 Nov. 1979 - 31 Mar. 1991
Harold L. Alexander 29 Oct. 1991 22 p
(Grant NAGw-21)
(NASA-CR-187820; NAS 1.26:187820) Avail: NTIS HC/MF A03 CSCL 22A

Human productivity was studied for extravehicular tasks performed in microgravity, particularly including in-space assembly of truss structures and other large objects. Human factors research probed the anthropometric constraints imposed on microgravity task performance and the associated workstation design requirements. Anthropometric experiments included reach envelope tests conducted using the 3-D Acoustic Positioning System (3DAPS), which permitted measuring the range of reach possible for persons using foot restraints in neutral buoyancy, both with and without space suits. Much neutral buoyancy research was conducted using the support of water to simulate the weightlessness environment of space. It became clear over time that the anticipated EVA requirement associated with the Space Station and with in-space construction of interplanetary probes would heavily burden astronauts, and remotely operated robots (teleoperators) were increasingly considered to absorb the workload. Experience in human EVA productivity led naturally to teleoperation research into the remote performance of tasks through human controlled robots. Author

31 ENGINEERING (GENERAL)

Includes vacuum technology; control engineering; display engineering; cryogenics; and fire prevention.

N92-11216# Oak Ridge National Lab., TN.
HEAT EXCHANGER THERMAL PERFORMANCE FOR TWO NONAZEOTROPIC REFRIGERANT MIXTURES
J. C. Conklin and E. A. Vineyard 15 Aug. 1991 11 p Presented at the International Congress on Refrigeration: New Challenges in Refrigeration, Montreal (Canada), 10-17 Aug. 1991
(Contract DE-AC05-84OR-21400)
(DE91-017250; CONF-910803-3) Avail: NTIS HC/MF A03

Two nonazeotropic refrigerant mixtures (NARMs), the first consisting of 71 percent R22 and 29 percent R114 and the second consisting of 75 percent R143a and 25 percent R124 (approximate percentages by mass), were studied at various mass flow rates and heat loads in an experimental apparatus at Oak Ridge National Laboratory. The measured thermal performance of the evaporator and the condenser are presented in terms of the number of transfer units (NTU) and effectiveness epsilon. Because the phase-change process of the NARMs is nonisothermal, a specific heat for the two-phase region can be defined. This two-phase specific heat for the NARMs varies with respect to enthalpy. Because the standard NTU-(epsilon) analysis is valid only for constant specific heat fluids, an analysis that considers variable specific heat fluids is used to compare analytical predictions of the thermal performance with the observed thermal performance. The predicted and measured results show very good agreement when the pressure drop is low. DOE

N92-11217*# National Aeronautics and Space Administration. Lewis Research Center, Cleveland, OH.
MICROGRAVITY VIBRATION ISOLATION: AN OPTIMAL CONTROL LAW FOR THE ONE-DIMENSIONAL CASE
R. D. Hampton, C. M. Grodsinsky, P. E. Allaire, D. W. Lewis, and C. R. Knospe (Virginia Univ., Charlottesville.) Oct. 1991 23 p
(NASA-TM-105146; E-6422; NAS 1.15:105146) Avail: NTIS HC/MF A03 CSCL 22A

Certain experiments contemplated for space platforms must be isolated from the accelerations of the platforms. An optimal active control is developed for microgravity vibration isolation, using constant state feedback gains (identical to those obtained from the Linear Quadratic Regulator (LQR) approach) along with constant feedforward (preview) gains. The quadratic cost function for this control algorithm effectively weights external accelerations of the platform disturbances by a factor proportional to (1/omega)(exp 4). Low frequency accelerations (less than 50 Hz) are attenuated by greater than two orders of magnitude. The control relies on the absolute position and velocity feedback of the experiment and the absolute position and velocity feedforward of the platform, and generally derives the stability robustness characteristics guaranteed by the LQR approach to optimality. The method as derived is extendable to the case in which only the relative positions and velocities and the absolute accelerations of the experiment and space platform are available. Author

N92-11218*# National Aeronautics and Space Administration. Marshall Space Flight Center, Huntsville, AL.
A GENERALIZED METHOD FOR MULTIPLE ROBOTIC MANIPULATOR PROGRAMMING APPLIED TO VERTICAL-UP WELDING
Kenneth R. Fernandez, George E. Cook, Kristinn Andersen, Robert Joel Barnett, and Saleh Zein-Sabattou (Vanderbilt Univ., Nashville, TN.) Washington Oct. 1991 30 p
(NASA-TP-3163; M-672; NAS 1.60:3163) Avail: NTIS HC/MF A03 CSCL 13I

The application is described of a weld programming algorithm for vertical-up welding, which is frequently desired for variable polarity plasma arc welding (VPPAW). The Basic algorithm performs three tasks simultaneously: control of the robotic mechanism so that proper torch motion is achieved while minimizing the sum-of-squares of joint displacement; control of the torch while the part is maintained in a desirable orientation; and control of

the wire feed mechanism location with respect to the moving welding torch. Also presented is a modification of this algorithm which permits it to be used for vertical-up welding. The details of this modification are discussed and simulation examples are provided for illustration and verification. Author

N92-11219*# National Aeronautics and Space Administration. Langley Research Center, Hampton, VA.
INTEGRAL FILL YARN INSERTION AND BEATUP METHOD Patent Application
Gary L. Farley, inventor (to NASA) 26 Sep. 1991 14 p
(NASA-Case-LAR-14046-1; NAS 1.71:LAR-14046-1; US-Patent-Appl-SN-766597) Avail: NTIS HC/MF A03 CSCL 13H

An apparatus and method for integral fill yarn insertion and beatup are disclosed. A modified rapier contains a channel for holding fill yarn. The channel is covered with a flexible and inflatable boot, and an inflating apparatus for this boot is also attached. Fill yarn is inserted into the channel, and the rapier is extended into a shed formed by warp yarn. Next, the rapier is pushed into the fell of the fabric, and the flexible and inflatable cover inflated, which both pushes the yarn into the fell of the fabric and performs beatup. The rapier is withdrawn and the shed closed to complete one step of the weaving process. NASA

N92-11220*# National Aeronautics and Space Administration. Langley Research Center, Hampton, VA.
WOVEN ANGLE PLY FABRIC AND APPARATUS AND METHOD FOR PRODUCING SUCH FABRICS Patent Application
Gary L. Farley, inventor (to NASA) 26 Sep. 1991 20 p
(NASA-Case-LAR-14048-1; NAS 1.71:LAR-14048-1; US-Patent-Appl-SN-766609) Avail: NTIS HC/MF A03 CSCL 13H

Planar or multilayer structural preforms are made having yarns extending in a bias direction of the preform. Angularly directed yarns can be inserted in planar and multilayer fabrics to increase shear strength of structural preforms made from the fabrics. In multilayer fabrics, the angle yarns can extend between layers to provide through-the-thickness reinforcement. Fabrics are formed by carrying yarns transversely across the fabric as the fabric advances. Fill yarns may be inserted by an insertion technique employing a pneumatic beating element. Angle yarn feeding arrangements are made readily removable to provide for the use of other weaving assemblies. NASA

N92-11221*# National Aeronautics and Space Administration. Lewis Research Center, Cleveland, OH.
THERMAL VERIFICATION TESTING OF COMMERCIAL PRINTED-CIRCUIT BOARDS FOR SPACEFLIGHT
William M. Foster, II 1991 9 p Proposed for presentation at the 1992 Annual Reliability and Maintainability Symposium, Las Vegas, NV, 21-23 Jan. 1991; sponsored by IEEE
(NASA-TM-105261; E-6593; NAS 1.15:105261) Avail: NTIS HC/MF A02 CSCL 13B

A method is discussed developed to verify commercial printed-circuit boards for a shuttle orbital flight. The Space Acceleration Measurement System Project used this method first with great success. The test sequence is based on early fault detection, desire to test the final assembly, and integration with other verification testing. A component thermal screening test is performed first to force flaws in design, workmanship, parts, processes, and materials into observable failures. Then temperature definition tests are performed that consist of infrared scanning, thermal vacuum testing, and preliminary thermal operational testing. Only the engineering unit is used for temperature definition testing, but the preliminary thermal operational testing is performed on the flight unit after the temperature range has been defined. In the sequence of testing, vibration testing is performed next, but most vibration failures cannot be detected without subsequent temperature cycling. Finally, final assembly testing is performed to simulate the shuttle flight. An abbreviated thermal screening test is performed as a check after the vibration test, and then a complete thermal operational test is performed. The final assembly test finishes up with a burn-in of 100 hours of trouble-free operation. Verification is successful when all components and final assemblies have passed each test satisfactory. This method was very successful in verifying that commercial printed-circuit boards will survive in the shuttle environment. Author

32 COMMUNICATIONS AND RADAR

Includes radar; land and global communications; communications theory; and optical communications.

For related information see also *04 Aircraft Communications and Navigation* and *17 Space Communications, Spacecraft Communications, Command and Tracking.* For search and rescue see *03 Air Transportation and Safety,* and *16 Space Transportation.*

N92-11222# Loughborough Univ. of Technology (England). Dept. of Electrical and Electronic Engineering.
AN EXAMINATION OF THE FACTORS AFFECTING THE USE OF INFRA-RED SEARCH AND TRACK SYSTEMS IN THE AIR-TO-AIR ROLE M.S. Thesis
J. L. Pilkington 1989 279 p
(ETN-91-99987) Copyright Avail: NTIS HC/MF A13

The employment of an IRSTS (Infrared Search and Track System) on a fighter aircraft is considered and the disadvantages of using radar to detect targets are explained. Atmospheric attenuation and scattering are investigated and optical terms and definitions are given. Thermal and photon detectors are examined. Problems associated with visual detection of targets on television type displays are discussed and the need for an automatic target detection process is highlighted. The performance of an imaging IRSTS is illustrated by simplified calculations and the future of IRSTS in the air to air role is discussed. ESA

N92-11223*# Research Inst. for Advanced Computer Science, Moffett Field, CA.
TELEVISION IMAGE COMPRESSION AND SMALL ANIMAL REMOTE MONITORING
Richard F. Haines and Robert W. Jackson Apr. 1990 20 p
(Contract NCC2-387)
(NASA-CR-186614; NAS 1.26:186614; RIACS-TR-90-19) Avail: NTIS HC/MF A03 CSCL 17B

It was shown that a subject can reliably discriminate a difference in video image quality (using a specific commercial product) for image compression levels ranging from 384 kbits per second to 1536 kbits per second. However, their discriminations are significantly influenced by whether or not the TV camera is stable or moving and whether or not the animals are quiescent or active, which is correlated with illumination level (daylight versus night illumination, respectively). The highest video rate used here was 1.54 megabits per second, which is about 18 percent of the so-called normal TV resolution of 8.4MHz. Since this video rate was judged to be acceptable by 27 of the 34 subjects (79 percent), for monitoring the general health and status of small animals within their illuminated (lights on) cages (regardless of whether the camera was stable or moved), it suggests that an immediate Space Station Freedom to ground bandwidth reduction of about 80 percent can be tolerated without a significant loss in general monitoring capability. Another general conclusion is that the present methodology appears to be effective in quantifying visual judgments of video image quality. Author

N92-11224*# Research Inst. for Advanced Computer Science, Moffett Field, CA.
EFFICIENT DETECTION OF A CW SIGNAL WITH A LINEAR FREQUENCY DRIFT
Paul N. Swarztrauber (National Center for Atmospheric Research, Boulder, CO.) and David H. Bailey Dec. 1989 16 p
(Contract NCC2-387)
(NASA-CR-188900; NAS 1.26:188900; RIACS-TR-89-51) Avail: NTIS HC/MF A03 CSCL 17B

An efficient method is presented for the detection of a continuous wave (CW) signal with a frequency drift that is linear in time. Signals of this type occur in transmissions between any two locations that are accelerating relative to one another, e.g., transmissions from the Voyager spacecraft. We assume that both the frequency and the drift are unknown. We also assume that the signal is weak compared to the Gaussian noise. The signal is partitioned into subsequences whose discrete Fourier transforms provide a sequence of instantaneous spectra at equal time intervals. These spectra are then accumulated with a shift that is proportional to time. When the shift is equal to the frequency drift, the signal to noise ratio increases and detection occurs. Here, we show how to compute these accumulations for many shifts in an efficient manner using a variety of Fast Fourier Transformations (FFT). Computing time is proportional to L log L where L is the length of the time series. Author

N92-11225*# Loyola Coll., Baltimore, MD. Japanese Technology Evaluation Center.
HIGH DEFINITION SYSTEMS IN JAPAN
Richard J. Elkus, Jr., Robert B. Cohen, Birney D. Dayton, David G. Messerschmitt, William F. Schreiber, Lawrence E. Tannas, Jr., and Duane Shelton Feb. 1991 224 p Sponsored in part by NASA, NSF, DARPA, DOC, and DOE
(Grant NSF ECS-89-02528)
(NASA-TM-105108; NAS 1.15:105108; PB91-100032) Avail: NTIS HC/MF A10 CSCL 17B

The successful implementation of a strategy to produce high-definition systems within the Japanese economy will favorably affect the fundamental competitiveness of Japan relative to the rest of the world. The development of an infrastructure necessary to support high-definition products and systems in that country involves major commitments of engineering resources, plants and equipment, educational programs and funding. The results of these efforts appear to affect virtually every aspect of the Japanese industrial complex. The results of assessments of the current progress of Japan toward the development of high-definition products and systems are presented. The assessments are based on the findings of a panel of U.S. experts made up of individuals from U.S. academia and industry, and derived from a study of the Japanese literature combined with visits to the primary relevant industrial laboratories and development agencies in Japan. Specific coverage includes an evaluation of progress in R&D for high-definition television (HDTV) displays that are evolving in Japan; high-definition standards and equipment development; Japanese intentions for the use of HDTV; economic evaluation of Japan's public policy initiatives in support of high-definition systems; management analysis of Japan's strategy of leverage with respect to high-definition products and systems. Author

N92-11226# National Inst. of Standards and Technology, Gaithersburg, MD. Office of Standards Services.
CONFORMITY ASSESSMENT WORKSHOP ON ELECTROMAGNETIC COMPATIBILITY
Bert G. Simson Jun. 1991 111 p Workshop held in Washington, DC, 4 Apr. 1991; cosponsored by American Council of Independent Laboratories and American Electronics Association
(PB91-192989; NISTIR-4611) Avail: NTIS HC/MF A06 CSCL 20N

The purpose of the workshop, which focused on information technology equipment (ITE), was to explore how the U.S. Government can assist EMC labs. in gaining acceptance of their test results in such other markets as the European Community (EC). The following consensus recommendations were reached by the private sector panelists: (1) establishing an EMC advisory committee; (2) harmonizing the National Voluntary Lab Accreditation Program (NVLAP) and Federal Communications Commission (FCC) programs; (3) negotiating an agreement with the EC to permit establishing notified bodies in the U.S.; (4) establishing a formal U.S. Government role in accrediting conformity assessment programs; and (5) establishing a proactive role for NIST in disseminating information to affected interests in the EMC area. Author

N92-11227# Lawrence Livermore National Lab., CA.
DISPERSION AND STABILITY OF TWO ELECTROMAGNETIC SOLVERS FOR TRIANGULAR MESHES
P. W. Rambo Jun. 1991 4 p Presented at the 14th Conference on Numerical Simultion of Plasmas, Annapolis, MD, 4-6 Sep. 1991
(Contract W-7405-eng-48)
(DE91-016607; UCRL-JC-107685; CONF-9109108-7) Avail: NTIS HC/MF A01

Time domain electromagnetic solvers on nonorthogonal grids is an area of current research interest. This interest stems from the need to simulate complex geometries in the fields of both plasma physics and electromagnetic scattering. Some of the approaches being investigated include curvilinear coordinates, finite volumes, and finite elements on meshes of quadrilaterals or triangles, both structured and unstructured. Most workers have concentrated on algorithm development, with test problems serving as benchmarks. Very little analytic work has been reported concerning stability and accuracy of these methods, even on regular meshes. This paper summarizes an investigation of a limited set of schemes for solving Maxwell's equations for TE polarization on a two dimensional mesh of triangles. Two particular realizations are the weighted residual finite element algorithm of Ambrosiano et al., and differencing based on Delaunay-Voronoi meshes. A dispersion relation is derived for the case of a regular skewed mesh, which includes equilaterals as a special case. As a complement, numerical dispersions tests have been performed for grids generated by randomly perturbing a regular grid. DOE

N92-11228*# Notre Dame Univ., IN. Dept. of Electrical Engineering.
ERROR CONTROL TECHNIQUES FOR SATELLITE AND SPACE COMMUNICATIONS Annual Status Report
Daniel J. Costello, Jr. Oct. 1991 107 p Original contains color illustrations
(Grant NAG5-557)
(NASA-CR-188997; NAS 1.26:188997) Avail: NTIS HC/MF A06; 1 functional color page CSCL 17B

Research activities related to error control techniques for satellite and space communication are reported. Specific areas of research include: coding gains for bandwidth efficient codes, hardware implementation of a bandwidth efficient coding scheme for the Hubble Space Telescope, construction of long trellis codes for use with sequential decoding, performance analysis of multilevel trellis codes, and M-algorithm decoding of trellis codes. Each topic is discussed in a corresponding paper that appears in the appendices. M.G.

N92-11229# Department of the Navy, Washington, DC.
IMPULSE TRANSMITTER AND QUANTUM DETECTION RADAR SYSTEM Patent Application
Robert E. Jehle, inventor (to Navy) and David F. Hudson, inventor (to Navy) 12 Apr. 1991 13 p
(AD-D014958; US-Patent-Appl-SN-687602; Navy-Case-72700)
Avail: NTIS HC/MF A03 CSCL 17/9

Pulses of short duration are radiated by an impulse radar transmitter within time domain intervals under control of a clock to monitor a moving target from which echo pulses are reflected. The received echo pulses are measured by a quantum detector in terms of photon energy levels to supply signal data processed during periods between said time domain intervals.
Author (GRA)

N92-11230 Department of the Navy, Washington, DC.
PROGRAMMABLE BEAM TRANSFORM AND BEAM STEERING CONTROL SYSTEM FOR A PHASED ARRAY RADAR ANTENNA Patent
Jefferson M. Willey, inventor (to Navy), James J. Alter, inventor (to Navy), and Jules P. Letellier, inventor (to Navy) 16 Apr. 1991 18 p Filed 29 Apr. 1988 Supersedes AD-D013864
(AD-D014970; US-Patent-5,008,680; US-Patent-Appl-SN-187804)
Avail: US Patent and Trademark Office CSCL 17/9

A programmable beam transform system is disclosed for

performing both beam steering and beam shaping operations in a phased array antenna. A programmable beam transform control circuit is responsive to a plurality of input signals for selectively generating and applying a plurality of control signals to each intelligent phase shift control circuit in an array of phase shift control circuits/phase shifters/antenna elements. Each phase shift control circuit simultaneously modifies the plurality of control signals applied thereto as a function of its internally-stored data to develop its own phase shift command signal which is used by its associated phase shifter to phase shift that portion of the total energy applied. On transmit, the phase-shifted energy outputs from the phase shifters in the array are then respectively transmitted by the associated antenna elements in the array to form the desired beam pattern at the desired beam position; when on receive, the complementary function occurs. GRA

N92-11231# Photometrics, Inc., Woburn, MA.
DESIGN AND OPERATION OF THE GL/OPA MOBILE DOPPLER LIDAR Scientific Report No. 3, 1 Sep. 1987 - 30 Sep. 1990
Patrick J. McNicholl 15 Mar. 1991 73 p
(Contract F19628-86-C-0102)
(AD-A240257; PL-TR-91-2057) Avail: NTIS HC/MF A04 CSCL 17/9

This report covers the theory, design, and operation of the GL/OPA mobile pulsed Doppler lidar facility. This system was constructed for the measurement of atmospheric scattering properties at 10.6 micron as well as eventual measurement of wind velocity. The lidar transmits pulses from a CO2 TEA laser and uses optical heterodyne techniques to measure both the frequency and amplitude of radiation backscattered by wind-borne aerosols. Detailed discussions are given of the optical layout, alignment procedures, detector performance, design and operation of the receiver electronics, and calibration procedures. A preliminary system performance evaluation is made based on the data collected during the GABLE field measurement program.
Author (GRA)

N92-11232# Naval Postgraduate School, Monterey, CA.
SPECIFICATION OF DIFFICULT TO TEST RADAR PERFORMANCE M.S. Thesis
Chen-Kuo Yu Sep. 1990 87 p
(AD-A240398) Avail: NTIS HC/MF A05 CSCL 17/9

In order to obtain detection range requirement of a new radar system, a computer simulation model is developed to evaluate the capability of the radar in an anti-air defense operation. Since the anti-ship missile is not available for test and evaluation, a technique to specify the performance requirement and design the test and evaluation plane using an airplane is developed. The effects of the propagation environment are also discussed. GRA

N92-11233# Aerospace Corp., Los Angeles, CA.
A FAST ALGORITHM FOR PLOTTING ANTENNA AND SCATTERING PATTERNS IN THREE DIMENSIONS Final Report
T. J. Peters 31 Aug. 1991 62 p
(Contract F04701-88-C-0089)
(AD-A240410; TR-009(6925-05)-6; SSD-TR-91-28) Avail: NTIS HC/MF A04 CSCL 20/12

An algorithm is presented for plotting antenna and scattering patterns in three dimensions on video displays or laser printers. The algorithm exploits the property of single-valued surfaces to allow the implicit removal of hidden lines with virtually no extra computation. This reduces the computation time significantly over that required by more general surface-representation methods. The algorithm is flexible enough to implement on most graphic systems. Simple language-independent pseudo-code is presented and tested for functions in rectangular, cylindrical, and spherical coordinates.
Author (GRA)

N92-11234# Carnegie-Mellon Univ., Pittsburgh, PA. Robotics Inst.
THREE DIMENSIONAL MIGRATION AND FORWARD MODELLING OF GROUND PENETRATING RADAR DATA
Robert Beck and Jim Osborn Jun. 1991 26 p Sponsored by EPA
(AD-A240505; CMU-RI-TR-91-12) Avail: NTIS HC/MF A03 CSCL 17/9

Carnegie Mellon University is automating the use of Ground Penetrating Radar (GPR) for the cleanup of hazardous waste sites. The current focus is on the development of an automated subsurface mapping system to locate buried objects and geological structures so that sources and migratory pathways of contaminants can be be identified and catalogued. The subsurface maps are produced using the non-invasive sensing capabilities of GPR. GPR operates similar to conventional radar, but the data acquired is more difficult to process due to the nonhomogeneous nature of the subsurface medium. Though sometimes used in waste site characterization, GPR deployment, data acquisition, and interpretation are human driven processes. The potential of GPR to generate accurate three dimensional subsurface maps has not been fully realized previously. The Site Investigation Robot uses robots to position a GPR transducer to exploit the accurate, repeatable positioning available from automated equipment. By combining the use of a position cognizant, all terrain mobile robot and a linear scanning mechanism, GPR records are acquired in a two dimensional grid on the ground surface. This method of collection simplifies processing and the positional location of features of interest in the data. To achieve accurate positional accuracy of the located subsurface objects, correct modeling of the subsurface medium and the antenna is crucial. The subsurface medium can be modelled as a composition of multiple subvolumes, each one being characterized by its own electrical parameters.
GRA

N92-11235# Naval Postgraduate School, Monterey, CA.
THE DESIGN OF BROADBAND RADAR ABSORBING SURFACES M.S. Thesis
Go H. Suk Sep. 1990 70 p
(AD-A240521) Avail: NTIS HC/MF A04 CSCL 17/4

There has been a growing and widespread interest in radar absorbing material technology. As the name implies, radar absorbing materials or RAM's are coatings whose electric and magnetic properties have been selected to allow the absorption of microwave energy at discrete or broadband frequencies. In military applications low radar cross section (RCS) of a vehicle may be required in order to escape detection while a covert mission is being carried on. These requirements have led to the very low observable or stealth technology that reduces the probability of detection of an aircraft. The design of radar absorbing materials is limited by constraints on the allowable volume and weight of the surface coating, and it is difficult to design a broadband radar absorbing structure in limited volume. This thesis investigates the use of lossy dielectric materials of high dielectric permittivity in multilayer composites for the production of low radar cross section (RCS). The analysis is done by computing the plane wave reflection coefficient at the exterior surface of the composite coating by means of a computer program which selects layer parameters which determine low reflection coefficients for electromagnetic radiation under constraint of limited layer thickness as well as maximum frequency bandwidth. Author (GRA)

N92-11236# Naval Ocean Systems Center, San Diego, CA.
SHIPBOARD ANTENNA CONCEPTS: STRUCTURALLY INDEPENDENT 2- TO 6-MHz TRANSMIT ANTENNA DESIGN Final Technical Report
R. S. Abramo Jun. 1991 42 p
(AD-A240544; NOSC-TD-2127) Avail: NTIS HC/MF A03 CSCL 09/1

This report presents the results of an investigation of various techniques to design a 2- to 6-MHz transmit antenna having reduced dependence on the ship mast and superstructure. Such an antenna is needed as a replacement for the existing fan antenna

for future ships constructed extensively of composite materials. Additional benefits of such an antenna are improved survivability and less obstruction of other ship systems than currently used designs. GRA

N92-11237# Visidyne, Inc., Burlington, MA.
AIRCRAFT LIDAR SENSITIVITY STUDY FOR MEASURING WATER VAPOR
R. J. Rieder and O. Shepherd 1 Apr. 1991 32 p
(Contract F19628-88-C-0013)
(AD-A240549; PL-TR-91-2074; SR-1) Avail: NTIS HC/MF A03 CSCL 04/2

The amount of water in the optical path between an airborne measurement platform and a target is responsible for the difference between the actual and the measurement target spectral radiance. In situ measurements of water vapor can be limited by outgassing from the sensor and/or its environment. A study was performed to investigate the use of lidar remote sensing techniques for the remote measurement of water vapor from a measurement aircraft such as the FISTA NKC-135A. GRA

N92-11238# Naval Research Lab., Washington, DC.
PULSE COMPRESSION DEGRADATION DUE TO OPEN LOOP ADAPTIVE CANCELLATION, PART 1
Karl Gerlach 31 Jul. 1991 30 p
(AD-A240552; NRL-9107-Pt-1) Avail: NTIS HC/MF A03 CSCL 17/9

Performance results for the sidelobe level of a compressed pulse that has been preprocessed through an adaptive canceller are obtained. The adaptive canceller is implemented using the Sampled Matrix Inversion (SMI) algorithm. Because of finite sampling, the quiescent compressed pulse sidelobe levels are degraded because of the preprocessing of the main channel input data stream (the uncompressed pulse) through an adaptive canceller. If N is the number of input canceller channels (main and auxiliaries) and K is the number of independent samples per channel, then it is shown that K/N can be significantly greater than one in order to retain sidelobes that are close to the original quiescent sidelobe level (with no adaptive canceller). Also, it is shown that the maximum level of degradation is independent of whether pulse compression occurs before or after the adaptive canceller if the uncompressed pulse is completely contained within the K samples that are used to calculate the canceller weights. Furthermore, this same analysis can be used to predict the canceller noise power level that is induced by having the desired signal present in the canceller weight calculation. Author (GRA)

N92-11239# Naval Research Lab., Washington, DC.
PULSE COMPRESSION DEGRADATION DUE TO OPEN LOOP ADAPTIVE CANCELLATION, PART 3 Interim Report
Karl Gerlach 23 Aug. 1991 25 p
(AD-A240553; NRL-9310-Pt-3) Avail: NTIS HC/MF A03 CSCL 17/4

An exact expression for the perturbed range sidelobe level of a compressed pulse that has been preprocessed through an adaptive canceller is derived. This result is a generalization of past research (parts 1 and 2, NRL Reports 9107 and 9309) where the signal was assumed to be completely contained within the canceller's processing batch. In this report, we allow the signal to extend over an arbitrary number of canceller processing batches. A good approximate expression is also obtained for evaluating the perturbed range sidelobe level. This report derives the number of independent samples per channel (main and auxiliaries) necessary so that the average adaptive range sidelobe level is within 3 dB of the quiescent range sidelobe level. Furthermore, the same analysis is used to predict the canceller noise power level that is induced by the desired signal's presence in the canceller weight calculation. Placement of the pulse compressor before or after the canceller is also considered. It is shown that if the desired waveform's code length L is less than or equal to the canceller's processing batch width K, it is desirable to place the pulse compression after the adaptive canceller. If L greater than K, then the issue is not so clear-cut, and a trade-off study is necessary. Author (GRA)

N92-11240# Naval Research Lab., Washington, DC.
THE PROBABILITY OF MULTIPLE CORRECT PACKET RECEPTIONS IN A MULTIRECEIVER FREQUENCY-HOPPED SPREAD-SPECTRUM SYSTEM Interim Report, May 1990 - Mar. 1991
Evaggelos Geraniotis 3 Sep. 1991 49 p Prepared in cooperation with Locus, Inc., Alexandria, VA and Maryland Univ., College Park
(AD-A240655; NRL-MR-6882) Avail: NTIS HC/MF A03 CSCL 25/5

In this report we develop exact expressions and approximations for the probability of exactly l correct packet receptions in a group of m receivers, given that k packets are transmitted simultaneously from users employing frequency-hopping spread-spectrum (FH/SS) and Reed-Solomon (RS) coding. This quantity is essential for the design and performance evaluation of multiple-access protocols in spread-spectrum packet radio networks. The evaluations are carried out for MFSK modulation with noncoherent demodulation and various types of RS minimum-distance decoding with erasures and/or errors decoding. Packet synchronous FH/SSMA systems that are hop-synchronous or hop-asynchronous are considered. The exact expressions developed have computational complexity that grows exponentially with m, thus making their evaluation for large m prohibitive. In light of such difficulties, two approximations are considered: one based on Gaussian multivariate distributions with linear computational requirements in m and k, and another based on the assumption of independent receiver operation (IROA), which has minimum computational complexity. Extensive comparisons of the approximations with the exact results establish their validity over different ranges of the system parameters. Author (GRA)

N92-11241# Naval Postgraduate School, Monterey, CA.
DISCRETE ARMA MODEL FOR NATURAL RESONANCES IN ELECTROMAGNETIC AND ACOUSTIC SCATTERING M.S. Thesis
Yuval Cohen Sep. 1990 94 p
(AD-A240656) Avail: NTIS HC/MF A05 CSCL 17/9

Investigations of scattered transient waveforms from conducting bodies have shown that it is possible to classify electromagnetic scatterers. The concept is based upon the natural resonance modes which are part of the scatterer response to an incident excitation. A new approach for describing natural resonance modes using recursive systems is introduced. A discrete auto-regressive moving-average (ARMA) type model for the case of the space-time wave equation is presented. This model results from a finite-difference approximation to the wave-equation. The ARMA model has spatially-independent coefficients for the temporal recursive terms. Computed results showing aspect- and spatial-independence of natural resonance modes, with verification of the ARMA model, are also included. Applications to target identification, using the natural resonant frequencies of the target's echo signature, are considered. Author (GRA)

N92-11242# Aerospace Corp., El Segundo, CA.
A CONJUGATE GRADIENT BASED ALGORITHM TO MINIMIZE THE SIDELOBE LEVEL OF PLANAR ARRAYS WITH ELEMENT FAILURES
T. J. Peters 31 Aug. 1991 86 p
(Contract F04701-88-C-0089)
(AD-A240667; TR-0091(6925-05)-3; SSD-TR-91-27) Avail: NTIS HC/MF A05 CSCL 09/1

Element failures increase the sidelobe power level of an array. Reconfiguring the amplitude and phase of the remaining elements can partially compensate for the failed elements and thus reduce the sidelobe level. The result of this investigation is an algorithm that yields the reconfigured distribution by minimizing the ratio of the average peak sidelobe power level to the power in the mainbeam, taking into account the defective elements. The minimization of this nonlinear function is carried out via a conjugate

gradient method. The algorithm is applied to the synthesis of sum and difference patterns of planar arrays. GRA

N92-11243# Rome Air Development Center, Griffiss AFB, NY.
A THINNED HIGH FREQUENCY LINEAR ANTENNA ARRAY TO STUDY IONOSPHERIC STRUCTURE Technical Report, Mar. 1989 - Mar. 1990
Anthony J. Gould Jul. 1991 38 p
(AF Proj. 4600)
(AD-A240764; RADC-TR-90-186) Avail: NTIS HC/MF A03
CSCL 17/9

The design, modeling, and performance measurements of a high frequency (HF) linear antenna array with 36 sensors is reported. The array was designed to achieve a narrow azimuthal beamwidth while maintaining grating lobes 10 dB below the main beam during a minus/plus 30 deg scan in azimuth. The configuration chosen utilizes two active vertical monopole elements and two parasitic backpoles to form a subarray. The subarrays, or sensors, are spaced at distances greater than half a wavelength to provide a large effective array aperture while the elemental radiation pattern, provided by the subarrays, suppresses the grating lobe as the array is scanned. Radiation patterns for the array were determined using three independent techniques: theoretical calculation, computer modeling using the Numerical Electromagnetics Code (NEC), and measurement of the fielded antenna. Results showed close agreement in antenna performance among the three methods of pattern determination. The three step process of theory, numerical modeling and measurement appears to be an optimum approach to antenna design. GRA

N92-11244# Carnegie-Mellon Univ., Pittsburgh, PA. Robotics Inst.
GROUND PENETRATING RADAR DATA ACQUISITION SYSTEM
Robert Beck, Jay Cosentino, David W. Collier, and Jim Osborn Jun. 1991 16 p
(AD-A240765; CMU-RI-TR-91-11) Avail: NTIS HC/MF A03
CSCL 17/9

Carnegie Mellon University is automating the use of Ground Penetrating Radar (GPR) for cleanup of hazardous waste sites. The Site Investigation Robot (SIR) project at the Field Robotics Center is applying robotics and image processing technologies to the investigatory phase of these waste site cleanups. The current focus is on the development of an automated subsurface mapping system to locate buried objects and geological structures so that sources and migratory pathways of contaminants can be identified and cataloged. The subsurface maps are produced using the non-invasive sensing abilities of Ground Penetrating Radar. GPR operates on principles similar to conventional radar, but the data acquired is more difficult to process due to the heterogeneous nature of the subsurface medium. GPR deployment, data acquisition, and interpretation are traditionally human-driven processes which expose operators to potentially dangerous environments. Automating the GPR data collection process eliminates this undesirable situation. Accurate three dimensional subsurface maps of GPR data have not yet been generated in the field. However, the SIR project uses robots to position GPR transducers to exploit the accurate, repeatable positioning available from automated equipment. By combining the use of a position-cognizant, all-terrain mobile robot and a linear scanning mechanism, it is possible to acquire GPR records in a two-dimensional grid on the ground surface. Author (GRA)

N92-11245 Department of the Navy, Washington, DC.
COMMUNICATIONS INTERFACE AND SYSTEM FOR RADIATION RECOVERY OF A MICROPROCESSOR PORTION THEREOF Patent
Jesus A. Rosario, inventor (to Navy) 4 Jun. 1991 6 p Filed 27 May 1982
(AD-D014977; US-Patent-5,022,027; US-Patent-Appl-SN-382977; US-Patent-Class-3T1-12) Avail: US Patent and Trademark Office
CSCL 12/7

A communications interface and system is configured to allow circumvention (recovery of control after radiation) of a microprocessor portion thereof. The communications interface portion, including a hard memory interface device serves as a communications link to the microprocessor. The system is configured so that a transient upset from prompt gamma radiation is detected and a circuit freeze of the stored information in the system is carried out until the transient subsides. The system then restores the microprocessor to the pre-irradiation condition and resumes operation. Accordingly, the hard memory interface device of the communication interface, controls a READ, CLEAR, and WRITE operations in addition to generating signals to control the handshaking between the hard memory of the communications interface and the aforementioned microprocessor. GRA

N92-11246 Department of the Navy, Washington, DC.
ACTIVE RADAR STEALTH DEVICE Patent
R. N. Cain, inventor (to Navy) and Albert J. Corda, inventor (to Navy) 30 Jul. 1991 5 p Filed 17 Sep. 1990
(AD-D014980; US-Patent-5,036,323; US-Patent-Appl-SN-583624; US-Patent-Class-342-6) Avail: US Patent and Trademark Office
CSCL 17/4

This patent discloses an active radar stealth device mounted on a host platform for minimizing the radar cross-section of the host platform. A coating which is essentially microwave transparent is attached to the surface of a host platform and is exposed to an incident microwave field. A plurality of detector/emitter pairs contained within the coating detect and actively cancel, respectively, the microwave field at each respective detector/emitter pair. GRA

N92-11247 Department of the Navy, Washington, DC.
ENHANCED CLUTTER SUPPRESSION APPARATUS FOR USE WITH AN INFRARED SEARCH AND SURVEILLANCE SYSTEM Patent
Edward S. Dayhoff, inventor (to Navy) 18 Jun. 1991 7 p Filed 6 Jul. 1982
(AD-D014984; US-Patent-5,025,143; US-Patent-Appl-SN-395223; US-Patent-Class-250-203.3) Avail: US Patent and Trademark Office CSCL 17/5

A clutter suppressor/target locator apparatus is configured to manipulate target video data on a particular channel according to a predetermined algorithm, so as to selectively emphasize those areas of a scene containing targets of appreciable contrast to the background and de-emphasize those areas where the brightness levels change gradually from point to point. The algorithm takes into account points ahead and behind the point or picture element being tested, and also equal points or adjacent channels. The apparatus is substantially free of false alarms, and the unique configuration thereof allows detection of the presence of a target on an extremely rapid basis. GRA

N92-11248# Ecole Nationale Superieure des Telecommunications, Paris (France). Groupe d'Etudes et de Recherches en Telecommunications et Systemes Aerospatiaux.
BASIC CONCEPTS OF LOW EARTH ORBIT SATELLITE SYSTEMS FOR COMMUNICATIONS
Gerard Maral and Jean-Jacques DeRidder 1991 39 p
(TELECOM-Paris-91-D-001; ISSN-0751-1345; ETN-91-90114)
Copyright Avail: NTIS HC/MF A03

The key features of Low Earth Orbit (LEO) satellite systems for communications including orbital, networking, and communication links, are described. The potential applications and the different services that can be offered by LEO communication systems are displayed. The key service requirements of LEO communication systems are enhanced. The different orbital configurations with a distinction between phased and random constellations are examined. The different network concepts for real time and delayed LEO communication systems, including network topologies and routing considerations are presented. The system multiple access possibilities are presented and communication links performance are dealt with. ESA

N92-11249# Oak Ridge National Lab., TN.
RESULTS OF FOLDED WAVEGUIDE TESTS ON RFTF
F. W. Baity, T. S. Bigelow, M. D. Carter, W. L. Gardner, R. H. Goulding, G. R. Haste, D. J. Hoffman, and D. O. Sparks 1991 4 p Presented at the 9th Topical Conference on Radio Frequency Power in Plasmas, Charleston, SC, 12-14 Aug. 1991
(Contract DE-AC05-84OR-21400)
(DE91-018930; CONF-910869-7) Avail: NTIS HC/MF A01

Experiments with the 80 MHz prototype folded waveguide on the Radio Frequency Test Facility (RFTF) at Oak Ridge National Laboratory have achieved substantially higher power levels than any previous tests on comparably sized loop antennas. This result, combined with a superior wave spectrum, suggests that the folded waveguide should be capable of several times the power flux of a loop antenna into a tokamak plasma. DOE

N92-11250# Oak Ridge National Lab., TN.
THREE-DIMENSIONAL CALCULATIONS OF FIELDS AND LOADING FOR LOOP AND FOLDED WAVEGUIDE ICRF ANTENNAS
M. D. Carter, F. W. Baity, D. B. Batchelor, D. J. Hoffman, E. F. Jaeger, D. W. Swain, and G. R. Haste 1991 6 p Presented at the 9th Topical Conference on Radio Frequency Power in Plasmas, Charleston, SC, 12-14 Aug. 1991
(Contract DE-AC05-84OR-21400)
(DE92-000065; CONF-910869-11) Avail: NTIS HC/MF A02

The ANT and ORION codes have been combined and used to study the loading of various antenna geometries with simple three-dimensional (3-D) effects. Both codes use a slab model with periodic Fourier analysis for modeling the toroidal and poloidal directions. The ANT code is used to prescribe current sets in a vacuum region where the field solutions are obtained analytically of each Fourier mode and matching conditions are used at poloidal/toroidal current sheet locations. Multiple current sheets are permitted and various feeder options are available to model the radial antenna currents. Current elements may be oriented at arbitrary angles to the static magnetic field and may be independently phased in time. The fields at the plasma surface are prescribed by an impedance matrix for each Fourier mode. The ORION code solves for the fields in the plasma region using finite difference techniques, a plasma dispersion relation that retains the lowest-order finite gyroradius effects, and all three electric field components. Results are presented for a folded waveguide mock-up and for a loop antenna design under identical plasma conditions. DOE

33 ELECTRONICS AND ELECTRICAL ENGINEERING

Includes test equipment and maintainability; components, e.g., tunnel diodes and transistors; microminiaturization; and integrated circuitry.

For related information see also *60 Computer Operations and Hardware* and *76 Solid-State Physics.*

N92-11251*# Ford Aerospace and Communications Corp., Palo Alto, CA. Space Systems Div.
MULTIPLE BEAM ANTENNA/SWITCH SYSTEM STUDY Final Report
12 May 1989 557 p
(Contract NAS5-30297)
(NASA-CR-183496; NAS 1.26:183496; SSD-TR00608) Avail: NTIS HC/MF A24 CSCL 09A

In the study of the Multiple Beam Antenna/Switch for the space to ground link (SGL) uplink and downlink services, several issues related to system engineering, antenna, transmit/receive, and switch systems were addressed and the results are provided. Bandwidth allocation at Ku band is inadequate to serve the data rate requirements for the forward and return services. Rain and depolarization effects at EHF, especially at Ka band, pose a significant threat to the link availabilities at heavy rain areas. Hardware induced effects such as the nonlinear characteristics of the power amplifier may necessitate the use of linearizers and limiters. It is also important to identify the components that are susceptible to the space radiation effects and shield or redesign them with rad-hard technologies for meeting the requirements of the space environment. Author

N92-11252*# National Aeronautics and Space Administration. Lewis Research Center, Cleveland, OH.
THE 23 TO 300 C DEMAGNETIZATION RESISTANCE OF SAMARIUM-COBALT PERMANENT MAGNETS
Janis M. Niedra (Sverdrup Technology, Inc., Brook Park, OH.) and Eric Overton Washington Nov. 1991 11 p
(NASA-TP-3119; E-6123; NAS 1.60:3119) Avail: NTIS HC/MF A03 CSCL 09A

The influence of temperature on knee point and squareness of the M-H demagnetization characteristic of permanent magnets is important information for the full utilization of the capabilities of samarium-cobalt magnets at high temperature in demagnetization resistent permanent magnet devices. Composite plots of the knee field and the demagnetizing field required to produce a given magnetic induction swing below remanence were obtained for several commercial Sm2Co17 type magnet samples in the temperature range of 23 to 300 C. Using the knee point to define the limits of operation safe against irreversible demagnetization, such plots are shown to provide an effective overview of the useable regions in the space of temperature-induction swing parameters. The observed second quadrant M-H characteristic squareness is shown, by two measures, to increase gradually with temperature, reaching a peak in the interval 200 to 300 C. Author

N92-11253# Institut National Polytechnique, Grenoble (France).
TEST AND DIAGNOSIS OF PROGRAMMABLE INTEGRATED CIRCUITS Ph.D. Thesis [TEST ET DIAGNOSTIC DE CIRCUITS INTEGRES PROGRAMMABLES]
Raoul Velazco 1990 212 p In ENGLISH and FRENCH
(ETN-91-99483) Avail: NTIS HC/MF A10

The functional test problem for programmable circuits is studied globally. A test method which is not based on error hypotheses is proposed. It consists of verifying in detail the circuit control part and activating the different blocks of the operative part with random operands. The application of this method to the test of representative circuits required two specific tools: an automatic generator for test programs, the GAPT software, and the FUTE 8 (Functional Tester), FUTE 16, and TEMAC functional testers. The experiments realized validated the approach and the tools, while outlining two of the main applications: design validation and failure analysis aid. The efficiency of GAPT programs was evaluated by injecting physical faults on circuit samples. For individual titles, see N92-11254 through N92-11268.

N92-11254# Grenoble-1 Univ. (France). Lab. de Genie Informatique.
ANALYSIS OF EXPERIMENTAL RESULTS ON FUNCTIONAL TESTING AND DIAGNOSIS OF COMPLEX CIRCUITS
Catherine Bellon, Raoul Velazco, and Haissam Ziade (Tripoli Univ., Libya) *In* Institut National Polytechnique, Test and Diagnosis of Programmable Integrated Circuits 1990 p 79-87 Presented at the IEEE International Test Conference, Washington, DC, 1988
(For primary document see N92-11253 02-33)
Avail: NTIS HC/MF A10

A number of functional level test approaches were proposed for microprocessors. The pragmatic GAPT (French acronym for automatic generation of test programs) approach is supported by a set of tools and experimental results. The GAPT test program generator and the TEMAC test environment are described. The original features of the TEMAC tester makes it a unique tool for the functional test and diagnosis of programmable circuits. The experiments performed, their goals, the test environments used, and the results obtained for each test area, are presented. The failed circuit analysis is reported. Conclusions are tentatively drawn, with respect to the efficiency and scope of the functional test generation methods. ESA

N92-11255# Grenoble-1 Univ. (France). Lab. de Genie Informatique.
FAILURE COVERAGE OF FUNCTIONAL TEST METHODS: A COMPARATIVE EXPERIMENTAL EVALUATION
Raoul Velazco, Catherine Bellon, and Bernard Martinet *In* Institut National Polytechnique, Test and Diagnosis of Programmable Integrated Circuits 1990 p 91-97 Presented at the IEEE International Test Conference, Washington, DC, Sep. 1990 (For primary document see N92-11253 02-33)
Avail: NTIS HC/MF A10

A comparative study between a structural test and three functional test methods is presented. The three functional test methods are a tailored test, a systematic pseudo exhaustive test, and a random test. Test equipment is described. The results of the performed experiments are given. It is shown that the structural test, which takes advantage of all the knowledge acquired during microprocessor 68000 life is efficient. The random test method achieves a hundred percent boolean defect coverage at the cost of a very long test length. Random tests seem to achieve an impressive fault coverage and must be the subject of further studies. ESA

N92-11256# Grenoble-1 Univ. (France). Lab. Inst. de Mathematiques Appliquees de Grenoble.
AUTOMATIC GENERATION OF MICROPROCESSOR TEST PROGRAMS
Catherine Bellon, A. Liothin, S. Sadier, Gabrielle Saucier, Raoul Velazco, Francois Grillot, and M. Issenman (Electronique Marcel Dassault, Saint Cloud, France) *In* Institut National Polytechnique, Test and Diagnosis of Programmable Integrated Circuits 1990 p 105-11 Presented at the 19th Design Automation Conference, Las Vegas, NV, 1982 Sponsored in part by Agence de l'Informatique (For primary document see N92-11253 02-33)
Avail: NTIS HC/MF A10

An automatic generation system for behavioral test programs of microprocessors is presented. The test environment which has a decisive influence on the test method and on the automatic generation is described. The test memory is composed of the program memory containing value configurations of input signals. Test principles are given. Three stages of test are applied to the microprocessor: conformity test, a scanning test, and a signal test. The automatic generation system generates the modules of the test program in assembler language, using the microprocessor description, and pedetermined test operands. ESA

N92-11257# Grenoble-1 Univ., Saint Martin d'Heres (France). Lab. Circuits et Systemes.
HARDWARE AND SOFTWARE TOOLS FOR MICROPROCESSOR FUNCTIONAL TEST
Catherine Bellon and Raoul Velazco (Grenoble-1 Univ., France) *In* Institut National Polytechnique, Test and Diagnosis of Programmable Integrated Circuits 1990 p 115-12 Presented at the International Test Conference, Philadelphia, PA, Oct. 1989 (For primary document see N92-11253 02-33)
Avail: NTIS HC/MF A10

The final phase of the GAPT (French acronym for automatic generation of test programs) project is presented. The method, software tools and hardware environments are described. A strategy to locate failures at a functional level is reported and illustrated on an actual faulty circuit. The GAPT project is to be extended in the direction of the test of peripheral circuits through a compatible microprocessor. ESA

N92-11258# Grenoble-1 Univ. (France). Lab. Circuits et Systemes.
THE GAPT SYSTEM: A CHAIN OF TEST FOR MICROPROCESSORS [LE SYSTEME GAPT: UNE CHAINE DE TEST POUR MICROPROCESSEURS]
Catherine Bellon, Erasmia Kolokithas, and Raoul Velazco *In* Institut National Polytechnique, Test and Diagnosis of Programmable Integrated Circuits 1990 p 125-13 Repr. from L'Onde Electrique, v. 65, no. 6, Nov. 1989 In FRENCH; ENGLISH summary (For primary document see N92-11253 02-33)
Avail: NTIS HC/MF A10

The functional test of microprocessors by the GAPT (French acronym for automatic generation of test programs system) is presented. An original method, the behavioral test is proposed. It allows the automatic generation of the test programs. The TEMAC tester which can be used either for a detection test or for a functional diagnosis is presented. Experimental results are given. Fault localization experiments are reported. The GAPT test chain is currently operational. ESA

N92-11259# Grenoble-1 Univ., Saint Martin d'Heres (France). Lab. Circuits et Systemes.
TAKING INTO ACCOUNT ASYNCHRONOUS SIGNALS IN FUNCTIONAL TEST OF COMPLEX CIRCUITS
Catherine Bellon and Raoul Velazco (Grenoble-1 Univ., France) *In* Institut National Polytechnique, Test and Diagnosis of Programmable Integrated Circuits 1990 p 139-14 Presented at the 21st Design Automation Conference, Albuquerque, NM, Jun. 1984 (For primary document see N92-11253 02-33)
Avail: NTIS HC/MF A10

A test method, a test environment and an automated test program generation are proposed. The tester is monitored by a computer which manages the test sequencing. It loads the test memory from a fast secondary memory, starts the test program execution and compares the results obtained with reference results. A synopsis of the signal memory is given. The basic formalism describes timing diagrams for a set of signals. Emphasis is put on signal test. A description language for signal timing diagrams is proposed. ESA

N92-11260# Grenoble-1 Univ., Saint Martin d'Heres (France). Lab. Circuits et Systemes.
FAULT LOCALIZATION WHEN TESTING COMPLEX CIRCUITS
Raoul Velazco (Grenoble-1 Univ., France) *In* Institut National Polytechnique, Test and Diagnosis of Programmable Integrated Circuits 1990 p 153-15 Repr. from IEE Proceedings, v. 132, no. 5, Oct. 1985 (For primary document see N92-11253 02-33)
Avail: NTIS HC/MF A10

An approach to state functional diagnoses when testing complex integrated circuits is presented. The test environment is described. The tester is monitored by a computer which manages test sequencing. The test programs produced by the GAPT (French acronym for automatic generation of test programs) generators may be used to state a functional diagnosis, when testing microprocessors. In some cases, it may help in finding design or manufacturing faults. The test programs generated by GAPT are used as go/no go test programs. Significant experiments, using the so called a posteriori approach were carried out, with regard to simple testing and design validation of a second source 68000, with a view to comparing the second source circuit with the original one. The test system is currently used to test a sample of Intel 8086 microprocessors, which will be implemented in a space environment. ESA

N92-11261# Grenoble-1 Univ. (France). Lab. Circuits et Systemes.
A MICROPROCESSOR TEST APPROACH ALLOWING FAULT LOCALISATION
Raoul Velazco, Haissam Ziade, and Erasmia Kolokithas *In* Institut National Polytechnique, Test and Diagnosis of Programmable Integrated Circuits 1990 p 161-16 Presented at the IEEE International Test Conference, Philidelphia, PA, Nov. 1985 (For primary document see N92-11253 02-33)
Avail: NTIS HC/MF A10

An approach allowing functional diagnoses to be stated when testing microprocessors is presented. The approach is implemented on a behavioral test dedicated system, the GAPT (French acronym for automatic generation of test programs) system, which is composed of a software tool for test program generation and a functional test environment, the TEMAC tester. Fault localization using the GAPT system is described. Experimental results are

given which were obtained during the test of samples of a second source of the 8086 microprocessors. Further experiments are reported. ESA

N92-11262# Grenoble-1 Univ. (France). Lab. Circuits et Systemes.
TOWARDS AN AUTOMATED SYSTEM FOR THE VERIFICATION AND DIAGNOSIS OF INTELLIGENT VLSI CIRCUITS
Raoul Velazco and Haissam Ziade (Tripoli Univ., Libya) *In* Institut National Polytechnique, Test and Diagnosis of Programmable Integrated Circuits 1990 p 171-17 Presented at the International Symposium on Electronic Devices, Circuits and Systems, Kharagpur, India, Dec. 1987 (For primary document see N92-11253 02-33)
Avail: NTIS HC/MF A10

The main features of a system designed to cope with both the verification and diagnosis of Very Large Scale Integration (VLSI) intelligent circuits are detailed. The system is composed of a validation program generator, the GAPT (French Acronym for automatic generation of test programs) software and a microprocessor dedicated verification system, the TEMAC functional tester. GAPT/TEMAC tools allow an easy implementation of a top down diagnosis procedure. Each diagnosis action is composed of symptom analysis, malfunction hypothesis statement, sequence generation, execution, and result evaluation. It was successfully used in various microprocessor qualification/validation experiments. The system capabilities and the diagnosis procedure are illustrated by an actual 68000 microprocessor diagnosis experiment. ESA

N92-11263# Grenoble-1 Univ. (France). Lab. Circuits et Systemes.
A METHOD AND TOOLS FOR MICROPROCESSOR VALIDATION: HIGH SAFETY FUNCTION APPLICATIONS
Raoul Velazco and Haissam Ziade (Tripoli Univ., Libya) *In* Institut National Polytechnique, Test and Diagnosis of Programmable Integrated Circuits 1990 p 177-18 In FRENCH; ENGLISH summary Presented at the Colloque International de Fiabilite et Maintenabilite, Biarritz, France, Oct. 1986 (For primary document see N92-11253 02-33)
Avail: NTIS HC/MF A10

An approach to state functional diagnosis when testing complex circuits is presented. This approach can lead in some cases, to low level fault localization. A priori and a posteriori hypotheses are developed. Experimental results are given. The 80C86 microprocessor characteristics are described, as well as test programs characteristics for 80C86 microprocessor, as generated by GAPT (French acronym for automatic generation of programs). The approach may be used to validate circuits for highly secure or highly reliable applications. ESA

N92-11264# Grenoble-1 Univ. (France). Lab. de Genie Informatique.
TOP DOWN IC FAILURE ANALYSIS USING AN E-BEAM SYSTEM COUPLED TO A FUNCTIONAL TESTER
Raoul Velazco, Didier Conard, A. Guyot, and Haissam Ziade (Tripoli Univ., Libya) *In* Institut National Polytechnique, Test and Diagnosis of Programmable Integrated Circuits 1990 p 185-19 Repr. from Microelectronic Engineering 12, 1990 (For primary document see N92-11253 02-33)
Avail: NTIS HC/MF A10

A diagnosis system devoted to precise failure analysis of complex integrated circuits (IC) was built up by coupling an electron beam tester, a functional tester, and a test program generator. The electron beam tester CAMECA ST15 is a microscope specially designed for the integrated circuit test. Its charactertistics are given. The diagnosis strategy is presented. In order to prove the implementation feasibility of the presented top down diagnosis approach, it is applied to a set of faulty 68000 microprocessors, for which functional diagnosis were already stated. ESA

N92-11265# Grenoble-1 Univ. (France).
AUTOMATIC TOOLS FOR MICROPROCESSOR FAILURE ANALYSIS
Didier Conard, J. Laurent, Raoul Velazco, Haissam Ziade, J. Cabestany, and F. Sala (Universidad Politecnica de Barcelona, Spain) *In* Institut National Polytechnique, Test and Diagnosis of Programmable Integrated Circuits 1990 p 195-20 Presented at the International Conference on Microelectronics, Damas, Syria, Oct. 1990 (For primary document see N92-11253 02-33)
Avail: NTIS HC/MF A10

A new approach for fault location when testing microprocessors is presented. The startpoint for the backtracing analysis converging to the failure is constituted by the automatic localization of a reduced area. Automatic image comparison based on pattern recognition is performed by means of an electron beam tester. The developed hardware and software tools allow large circuit areas to be covered offering powerful diagnosis capabilities to the user. The validation of this technique was performed on faulty 68000 microprocessors. It shows the feasibility of the automation of the first and most important step of failure analysis: fault location at the chip surface. ESA

N92-11266# Grenoble-1 Univ. (France). Unite Genie Materiel.
COMPARISON BETWEEN CALIFORNIUM AND CYCLOTRON HEAVY ION TESTS [COMPARAISON ENTRE LES TESTS D'IONS LOURDS SOUS CALIFORNIUM ET AU CYCLOTRON]
Raoul Velazco and Antoine Provost-Grellier *In* Institut National Polytechnique, Test and Diagnosis of Programmable Integrated Circuits 1990 p 209-22 Repr. from Annales de Physique, Colloque No. 2, v. 14, no. 6, Dec. 1989 In FRENCH; ENGLISH summary Prepared in cooperation with Centre National d'Etudes Spatiales, Toulouse, France (For primary document see N92-11253 02-33)
Avail: NTIS HC/MF A10

Experimental equipment which performs heavy ion tests for programmable integrated circuits is presented. This equipment is used along with two different means of heavy ion simulator to perform Single Event Upset (SEU) tests on representative circuits: A dedicated Cf 252 fission decay source and a cyclotron. The validity of using californium source to simulate high LET particles is questioned by the discrepancies observed between Cf 252 and cyclotron results. ESA

N92-11267# Grenoble-1 Univ. (France). Lab. de Genie Informatique.
COMPARISON BETWEEN CALIFORNIUM AND CYCLOTRON SEU TESTS
Raoul Velazco, Antoine Provost-Grellier, T. Chapuis, M. Labrunee, D. Falguere, and R. Koga (Aerospace Corp., Los Angeles, CA.) *In* Institut National Polytechnique, Test and Diagnosis of Programmable Integrated Circuits 1990 p 227-23 Repr. from IEEE Transactions on Nuclear Science, v. 36, no. 6, Dec. 1989 (For primary document see N92-11253 02-33)
Avail: NTIS HC/MF A10

Experimental equipment which performs heavy ion testing for programmable integrated circuits is presented. This equipment is used along with two different means of heavy ion simulator to perform Single Event Upset (SEU) tests on representative circuits: a dedicated Cf 252 fission decay source to simulate high LET particles is questioned by the discrepancies observed between Cf 252 and cyclotron results. ESA

N92-11268# Grenoble-1 Univ. (France). Lab. de Genie Informatique.
AN A PRIORI APPROACH TO THE EVALUATION OF SIGNATURE ANALYSIS EFFICIENCY
Paul Caspi, Jacek Piotrowski (Poznan Technical Univ., Poland), and Raoul Velazco *In* Institut National Polytechnique, Test and Diagnosis of Programmable Integrated Circuits 1990 p 239-25 Submitted for publication (For primary document see N92-11253 02-33)
Avail: NTIS HC/MF A10

The evaluation of signature analysis efficiency presented does

not rely on assumptions on the distribution of the analyzed error sequences. An a priori randomization technique is used, which leads to choosing Linear Feedback Signature Registers (LSFRs) corresponding to randomly chosen prime polynomials of a given degree. The proposed evaluation is more pessimistic than the usual ones as it does not make use of assumptions on the error distribution. The length of the analyzed sequence is taken into account. It is shown to be valuable when the efficiency of signature analysis is to be guaranteed. In this case, LSFRs of length 32 seems to be a practical choice, with respect to both the maximum length of the analyzed sequences and the aliasing error probability. ESA

N92-11269# National Inst. of Standards and Technology, Gaithersburg, MD.
SEMICONDUCTOR MEASUREMENT TECHNOLOGY: NIST LIST OF PUBLICATIONS, 1962-1989 (REVISED MARCH 1990)
1991 130 p
(PB91-193961; NIST/SP-400/72) Avail: NTIS HC/MF A07 CSCL 09C

The list of publications contains reports of work performed at the National Institute of Standards and Technology (NIST) in the field of semiconductor measurement technology. Most of the publications resulted from work carried out as part of the NIST Semiconductor Technology Program (STP). The STP serves to focus NIST research on improved measurement technology for the use of the semiconductor device community in specifying materials, equipment, and devices in national and international commerce, and in monitoring and controlling device fabrication and assembly. The research leads to carefully evaluated, well-documented measurement methods, data, reference artifacts, models and theory, and associated technology which when applied by the industry are expected to contribute to higher yields, lower costs, and higher reliability of semiconductor devices and to provide a basis for controlled environments in fabrication processes and device performance. GRA

N92-11270# Oregon State Univ., Corvallis. Dept. of Electrical and Computer Engineering.
HIGH EFFICIENCY MOTOR REWIND STUDY
A. K. Wallace and R. Spee Feb. 1991 73 p
(Contract DE-BI79-90BP-06048)
(DE91-017162; DOE/BP-06048/1) Avail: NTIS HC/MF A04

The objective of performing this work was to evaluate a new technology used for rewinding electric motors. Motor performance evaluation was conducted at the motor test facility at Oregon State University. The test program consisted of comparing new high efficiency motor technology and standard rewind technology with the Unity-Plus system. The Unity-Plus configuration exhibited reduced efficiency over the complete load range compared to the other motors. Appropriately sized capacitors connected to the terminals of the conventional induction motor produced the same power factor improvement as the Unity-Plus system. Torque production and torque pulsation were very similar for all systems. The Unity-Plus configuration drew lower starting currents but the duration of the starting transient was increased. Motor temperature rise was about the same for all systems. Noise levels were about the same in all systems. Although determination of time to failure was not undertaken, the expected lifetime of the Unit-Plus system is probably less due to higher capacitor stress and higher insulation stress. The investigation concludes that a conventional induction motor with terminal capacitors is the most acceptable way of obtaining good efficiency and power factor and the Unity-Plus system cannot be recommended on the basis of any of the evaluation criteria used in this study. DOE

N92-11271# Superconducting Super Collider Lab., Dallas, TX.
COIL SHAPES TOWARDS PURE MULTIPOLES IN CIRCULAR REGIONS: A NUMERICAL APPROACH
V. Thiagarajan Apr. 1991 40 p
(Contract DE-AC35-89ER-40486)
(DE91-017239; SSCL-399-Rev-1) Avail: NTIS HC/MF A03

Coil shapes to produce pure multipole fields in circular regions have been studied and numerically evaluated. Coil shapes have been assumed as functions of unknown coefficients (and prescribed constraining parameters) and cosine functions. The coefficients have been numerically determined to produce the required multipole, simultaneously reducing the other multipoles to zero, or to negligible values. DOE

N92-11272*# Arizona State Univ., Tempe. Dept. of Electrical Engineering.
DESIGN OF A FAST COMPUTER-BASED PARTIAL DISCHARGE DIAGNOSTIC SYSTEM Final Report
Jose R. Oliva, G. G. Karady, and Stan Domitz Aug. 1991 100 p
(Grant NAG3-1139)
(NASA-CR-189057; NAS 1.26:189057) Avail: NTIS HC/MF A05 CSCL 09A

Partial discharges cause progressive deterioration of insulating materials working in high voltage conditions and may lead ultimately to insulator failure. Experimental findings indicate that deterioration increases with the number of discharges and is consequently proportional to the magnitude and frequency of the applied voltage. In order to obtain a better understanding of the mechanisms of deterioration produced by partial discharges, instrumentation capable of individual pulse resolution is required. A new computer-based partial discharge detection system was designed and constructed to conduct long duration tests on sample capacitors. This system is capable of recording large number of pulses without dead time and producing valuable information related to amplitude, polarity, and charge content of the discharges. The operation of the system is automatic and no human supervision is required during the testing stage. Ceramic capacitors were tested at high voltage in long duration tests. The obtained results indicated that the charge content of partial discharges shift towards high levels of charge as the level of deterioration in the capacitor increases. Author

N92-11273# Materials Research Labs., Melbourne (Australia).
APPROXIMATE EXPRESSIONS FOR THE MAGNETIC FIELD FROM AN ELECTRIC CURRENT SOURCE IN A LAYERED CONDUCTING MEDIUM
A. G. Theobald 1991 22 p
(MRL-TR-91-5; AR-006-351) Copyright Avail: NTIS HC/MF A03

An electric current source comprising point horizontal electric dipoles is proposed. An approximate description of the magnetic field from such a source is given. The environments considered are two-layer (2 semi-infinite media, typically the air and the sea) and three-layer (2 semi-infinite layers separated by a conducting slab, typically the air, sea, and sea bed). Author

N92-11274# University of Southern California, Los Angeles. Electronic Sciences Lab.
JOINT SERVICES ELECTRONICS PROGRAM RESEARCH IN ELECTRONICS Final Report, 1 Apr. 1988 - 31 Mar. 1991
W. H. Steier 31 May 1991 11 p
(Contract F49620-88-C-0067)
(AD-A240155; AFOSR-91-0748TR) Avail: NTIS HC/MF A03 CSCL 20/12

During this period thirteen research projects were supported under this program in the areas of Solid State Electronics, Quantum Electronics, and Information Electronics. This three year period has been a very productive one from the scientific results achieved and the transfer of the results to industry and government laboratories. The results are documented in the scientific publications that have resulted from this research. Perhaps the best mode of technology transfer is through students who graduate and carry the technology with them to other laboratories and industry. Fifteen students received degrees while supported by JSEP during this period. GRA

N92-11275# Yale Univ., New Haven, CT. Dept. of Applied Physics.
PHYSICS OF ULTRASMALL SUPERCONDUCTING CIRCUITS Final Report, 1 Aug. 1988 - 31 Jul. 1990
Daniel E. Prober 30 Jun. 1991 9 p
(Grant AF-AFOSR-0270-88; AF Proj. 2305)
(AD-A240156; AFOSR-91-0746TR) Avail: NTIS HC/MF A02 CSCL 09/1

The collaboration between Yale and the Westinghouse Science and Technology Center produced high quality, sub-micron, superconducting Nb trilayer tunnel junctions. These junctions were made using a fabrication process developed at Westinghouse as a result of this collaboration. The junctions were fabricated on thin (2 mil) quartz substrates using the existing facilities at Westinghouse. The quality of these devices compares favorably with others reported, particularly in the sub-micron size range. These junction were used as receiving elements in a broad-band 80-120 GHz mixer receiver. This receiver had no mechanical tuning elements. The noise of this receiver using these devices is among the lowest reported in the 80-120 GHz frequency band, particularly among those with no mechanical tuning elements. GRA

N92-11276# Department of the Navy, Washington, DC.
MICROCHANNEL ELECTRON SOURCE Patent Application
Kevin Boulais, inventor (to Navy) and John Choe, inventor (to Navy) 8 Feb. 1991 18 p
(AD-D014956; US-Patent-Appl-SN-652821; Navy-Case-73010)
Avail: NTIS HC/MF A03 CSCL 09/1

A microchannel plate device utilizing a semiconducting bulk material is characterized by electron emissions of high output current density and efficiency. The channel passages in the plate device which are square in cross-section accommodates a larger open area ratio at the input and output plate surfaces. An extended range of high electron emission applications for the plate device is provided. Such applications may include a photocathode installation to which a modulation pulse input is applied under low voltages isolated from high post-accelerating voltages. GRA

N92-11277 Department of the Navy, Washington, DC.
CIRCUIT PROBING SYSTEM Patent
Anthony M. Marques, inventor (to Navy) 11 Jun. 1991 7 p
Filed 4 Jun. 1990
(AD-D014966; US-Patent-5,023,545; US-Patent-Appl-SN-532416; US-Patent-Class-324-158P) Avail: US Patent and Trademark Office CSCL 14/2

A probing system for determining a voltage at a node during normal operation of a circuit is discussed. An input driver drives the circuit normally. A normal output on an output line associated with the node, is recorded. A probe is brought in contact with the node. Various node voltages are applied to the probe and thus to the node, until the output on the output line matches the recorded output. The probe voltage that creates the match is the voltage at the node, during normal operation of circuit. Author (GRA)

N92-11278# Naval Postgraduate School, Monterey, CA.
VHDL SIMULATION OF THE IMPLEMENTATION OF A COSTFUNCTION CIRCUIT M.S. Thesis
Imvidhaya Ming Sep. 1990 85 p
(AD-A240430) Avail: NTIS HC/MF A05 CSCL 12/5

Since VHDL is a DoD standard hardware description language, it is widely used in the design of logic circuits at different levels. VHDL can be used to do behavioral modeling which is desirable in top-down system design. A cost function calculation in a graph partition algorithm is used here as an example to test the VHDL design methodology. Subroutines or statements in the software can be implemented into hardware if the subroutines or the statements in that software are suitably grouped. While the design of hardware is considered, high density integration of circuit is also the primary goal. Parts of an old design were condensed using programmable EPLDs which were programmed by commercial software development tools. The methodology of implementation goes from a register transfer language description to data flow design and control flow design. The costfunction calculation was successfully put into 4 EP1800 chips and the design was simulated in VHDL. The primary goal of integration was achieved at the expense of speed. To support the total simulation several behavior models were created. Results of simulation revealed that the adder circuit in the EP1800 can be further improved. Experiences of using VHDL are discussed in this thesis. GRA

N92-11279# Technische Univ., Berlin (Germany, F.R.). Fachbereich Elektrotechnik.
INSULATED GATE BIPOLAR TRANSISTORS (IGBT) MODELIZATION FOR CIRCUIT SIMULATION AND UTILIZATION IN PULSE MODULATED INVERTERS Ph.D. Thesis [INSULATED GATE BIPOLAR TRANSISTOREN: MODELLIERUNG ZUR SCHALTUNGSSIMULATION UND ANWENDUNG IN PULSWECHSELRICHTERN]
Ernst-Karl Behr 1990 194 p In GERMAN
(ETN-91-90149) Avail: NTIS HC/MF A09

A model is developed for the IGBT, which can be used on components for the simulation of power electronics circuits. The use of IGBT in a typical utilization case is examined, e.g., a quick switching pulse inverter for the control of asynchronous machines. The starting point of IGBT model production is an equivalent circuit from a bipolar transistor and from a controlling field effect transistor. The stationary behavior of the bipolar transistor is described by analytically produced nonlinear equations. Available model equations are collected in a dynamic IGBT model. New and modified processes are developed, with which all relevant IGBT parameters can be obtained by electrical measurements in simple test circuits. The validity of the developed IGBT model is demonstrated, using typical load conditions, by comparison with simulation and measurement results. ESA

N92-11280# Max-Planck-Inst. fuer Physik und Astrophysik, Garching (Germany, F.R.). Inst. fuer Extraterrestrische Physik.
LIMITS OF ENERGY DISSIPATION FOR X RAY SENSITIVE pn CHARGE COUPLED DEVICES (CCDs) Thesis - Technische Univ. [GRENZEN DER ENERGIEAUFLOESUNG ROENTGENEMPFINDLICHER PN-CCDS]
Wolfgang Schreiber May 1990 61 p In GERMAN
(MPE-224; ISSN-0178-0719; ETN-91-90200) Copyright Avail: NTIS HC/MF A04

The noise behavior of integrated electronics is examined, with regard to fully depleted pn CCDs in order to determine the limits of energy dissipation ability of the detectors. A review of semiconductor detectors and of the important physical principles of integrated electronics is given. The function principle of fully depletable pn CCDs and of chip electronics is defined. The noise of integrated electronics is determined, using measurements, and the spectral dissociation ability obtainable with the CCD is evaluated. The pn CCDs described are intended as focal detectors for the XMM satellite mission. ESA

N92-11281# Max-Planck-Inst. fuer Physik und Astrophysik, Garching (Germany, F.R.). Inst. fuer Physik und Astrophysik.
DIFFUSION AND DRIFT OF CHARGES IN SEMICONDUCTOR DETECTORS Thesis - Technische Univ. [DIFFUSION UND DRIFT VON LADUNGEN IN HALBLEITER-DETEKTOREN]
Norbert Meidinger Jan. 1991 75 p In GERMAN
(MBE-225; ISSN-0178-0719; ETN-91-90201) Copyright Avail: NTIS HC/MF A04

It is shown that the dissemination of a signal charge bundle produced by a photon in a semiconductor is calculable with numerical methods, and formulable analytically, with regard to diffusion and Coulomb repulsion. For fully depletable pn Charge Coupled Devices (CCDs), calculations were carried out for various temperatures, photon energies and drift times. Results are given. For the CCDs used, low splitting probabilities, between 20 to 30 pct. accrue from a pixel sized 150 by 150 microns. Charge splitting can also occur only at photon incidence immediately at the boundary pixels. It is shown that this new type of X ray photon detector has excellent possibilities with regard to energy disspation,

and that the charge splitting effect can be used for an increase of local dissipation. ESA

N92-11282# Sandia National Labs., Albuquerque, NM.
NONAQUEOUS SECONDARY BATTERIES
Takayuki Yamahira and Masanori Anzai (Sony Corp. Tokyo, Japan) 24 Apr. 1991 16 p Transl. into ENGLISH of Japanese Patent Application No. 294372, (28 Nov. 1989)
(Contract DE-AC04-76DP-00789)
(DE91-017788; ALS/TR-91-007) Avail: NTIS HC/MF A03

The object of the present invention is to make possible the repeated use for a long period of time of nonaqueous secondary battery that contains in the battery case a negative electrode of a carbonized organic substance, a positive electrode with Li(x)MO2 (where M is at least one of Co and Ni; x being 0.05 less than or = x less than or = 1.10) and an electrolytic solution. The method comprises at least one charging operation of the battery before the sealing of their cells to inhibit the gas generation that would occur in the finished battery in its charging and discharging. DOE

N92-11283# Sandia National Labs., Albuquerque, NM.
CASE HISTORY: FAILURE ANALYSIS OF A CMOS SRAM WITH AN INTERMITTENT OPEN CONTACT
A. N. Campbell, E. I. Cole, Jr., C. L. Henderson, and M. R. Taylor 1991 9 p Presented at the 17th International Symposium for Testing and Failure Analysis, Los Angeles, CA, 11-15 Nov. 1991
(Contract DE-AC04-76DP-00789)
(DE91-018811; SAND-91-0741C; CONF-911115-2) Avail: NTIS HC/MF A02

Analysis of an intermittent failure to write the 1 state to a particular memory location at low temperature (-55 C) in a 16K x 1 CMOS SRAM is presented. The failure was found to be due to an open metallization at a metal-to-silicon contact. The root cause of the failure was poor step coverage of the metallization over an oxide step. A variety of failure analysis techniques including dynamic electron beam analysis at low temperature using a Peltier cold stage were employed to study the intermittently failing SRAM. The failure site was located by using capacitive coupling voltage contrast analysis. PSPICE simulation, light emission microscopy, scanning electron microscopy, and focused-ion beam techniques were used to confirm the failure mechanism and location. The write cycle time of the failed IC was abnormally long, but within the allowable tester limit. The vulnerability of other ICs to failure by open metallization in metal-to-silicon contacts is reviewed. DOE

N92-11284*# Michigan Univ., Ann Arbor. Space Physics Research Lab.
ADVANCED LANGMUIR PROBE (LP) Final Report
N. R. Voronka, B. P. Block, and G. R. Carignan 1991 142 p
(Grant NAG5-419)
(NASA-CR-180084; NAS 1.26:180084) Avail: NTIS HC/MF A07 CSCL 09A

The dynamic response of the MK-2 version of the Langmuir probe amplifier was studied. The settling time of the step response is increased by: (1) stray node-to-ground capacitance at series connections between high value feedback resistors; and (2) input capacitance due to the input cable, FET switches, and input source follower. The stray node-to-ground capacitances can be reduced to tolerable levels by elevating the string of feedback resistors above the printing board. A new feedback network was considered, with promising results. The design uses resistances having much lower nominal values, thereby minimizing the effect of stray capacitances. Faster settling times can be achieved by using an operational amplifier having a higher gain-bandwidth product. Author

34 FLUID MECHANICS AND HEAT TRANSFER

Includes boundary layers; hydrodynamics; fluidics; mass transfer; and ablation cooling.

For related information see also *02 Aerodynamics* and *77 Thermodynamics and Statistical Physics.*

N92-11285*# National Aeronautics and Space Administration. Langley Research Center, Hampton, VA.
CALCULATIONS AND CURVE FITS OF THERMODYNAMIC AND TRANSPORT PROPERTIES FOR EQUILIBRIUM AIR TO 30000 K
Roop N. Gupta, Kam-Pui Lee, Richard A. Thompson, and Jerrold M. Yos (Textron Defense Systems, Wilmington, MA.) Washington Oct. 1991 76 p
(NASA-RP-1260; L-16907; NAS 1.61:1260) Avail: NTIS HC/MF A05 CSCL 20D

A self-consistent set of equilibrium air values were computed for enthalpy, total specific heat at constant pressure, compressibility factor, viscosity, total thermal conductivity, and total Prandtl number from 500 to 30,000 K over a range of 10(exp -4) atm to 10(exp 2) atm. The mixture values are calculated from the transport and thermodynamic properties of the individual species provided in a recent study by the authors. The concentrations of the individual species, required in the mixture relations, are obtained from a free energy minimization calculation procedure. Present calculations are based on an 11-species air model. For pressures less than 10(exp -2) atm and temperatures of about 15,000 K and greater, the concentrations of N(++) and O(++) become important, and consequently, they are included in the calculations determining the various properties. The computed properties are curve fitted as a function of temperature at a constant value of pressure. These curve fits reproduce the computed values within 5 percent for the entire temperature range considered here at specific pressures and provide an efficient means for computing the flowfield properties of equilibrium air, provided the elemental composition remains constant at 0.24 for oxygen and 0.76 for nitrogen by mass. Author

N92-11286*# National Aeronautics and Space Administration. Ames Research Center, Moffett Field, CA.
COOLING APPARATUS AND COUPLINGS THEREFOR Patent Application
Curtis Lomax, inventor (to NASA) and Bruce Webbon, inventor (to NASA) 21 May 1989 25 p
(NASA-Case-ARC-11921-1; NAS 1.71:ARC-11921-1; US-Patent-Appl-SN-703649) Avail: NTIS HC/MF A03 CSCL 20D

The present invention relates generally to the field of thermal transfer and, more specifically, to a direct-interface, fusible heat sink for non-venting, regenerable, and self-contained thermal regulation. A quick connect coupling includes a male and a female portion. The female portion is frozen in a container of solid-phase coolant fluid, i.e., water, so that passages in the housing are blocked by ice initially. The ice is melted by direct interface with liquid coolant fluid delivered from the male portion. The present invention has advantages in that the phase change material remains sealed at all times, including during regeneration. Also, it uses quick-disconnect couplings that allow the phase change material to completely fill the container and is easily handled in microgravity without spills, leakage or handling of phase change material. NASA

N92-11287# Institut National des Sciences Appliquees de Rouen, Mont Saint Aignan (France). Lab. d'Energetique des Systemes et de Procedes.
THEORETICAL STUDY (LAGRANGIAN MODELING) OF TURBULENT PARTICULATE DISPERSION [ETUDE THEORIQUE (MODELISATION LAGRANGIENNE) DE LA DISPERSION PARTICULAIRE TURBULENTE]
A. Berlemont, M. S. Grancher, and P. Desjonqueres 1990

48 p In FRENCH
(Contract DRET-88-218)
(ETN-91-99909) Avail: NTIS HC/MF A03

A study aimed at improving the prediction and knowledge of two phase phenomena in a turbomachine is presented. A code to three dimensionally simulate particle dispersion, taking account of turbulent droplet evaporation, and which can be easily integrated into the DIAMANT code, is developed. Lagrangian modeling of particle dispersion is used. The influence of turbulence on evaporation appears to be non-negligible and must therefore be taken into account in droplet turbulent transfer problems. ESA

N92-11288# Association Aeronautique et Astronautique de France, Paris.
PRELIMINARY STUDIES FOR AUTOMIZING THERMAL FLUX MEASUREMENT EXAMINATION BY THERMOSENSITIVE COLORING [ETUDES PRELIMINAIRES POUR L'AUTOMATISATION DU DEPOUILLEMENT DES MESURES DE FLUX THERMIQUES PAR PEINTURE THERMOSENSIBLE]
M. Girard, J. C. Bohl, and P. Baumann (Office National d'Etudes et de Recherches Aerospatiales, Paris, France) 1989 29 p In FRENCH Presented at the 26th Colloque d'Aerodynamique Appliquee, Toulouse, France, 23-25 Oct. 1990 Previously announced in IAA as A90-22439
(AAAF-NT-89-28; ISBN-2-7170-0961-2; ISSN-0243-0177; ETN-91-99969) Avail: NTIS HC/MF A03; CEDOCAR, Section des Diffusions, 26 Blvd Victor, 75996 Paris Armees, France, HC 30 francs

The automatization of thermal wall flow data analysis measurement by thermosensitive coloring in gust wind tunnel is addressed. The study was directed towards more sophisticated imaging techniques based on the use of video cameras. The extraction of shade change lines was examined. Satisfactory results were obtained with an optical filter relating to software including mathematical morphology ideas. The digitization and image processing technologies likely to be applied to Thermocolor test examinations are reviewed. A simple and evolutive solution would be to digitize then process silver films currently in use. ESA

N92-11289# Imperial Coll. of Science and Technology, London (England). Dept. of Aeronautics.
RECIPROCITY THEORY OF GAS SURFACE INTERACTIONS
Adolf A. Agbormbai Nov. 1989 38 p
(IC-Aero-89-04; ISSN-0308-7247; ETN-91-99880) Avail: NTIS HC/MF A03

Since the Direct Simulation Monte Carlo (DSMC) method has established itself as a standard technique for numerically computing rarefied gas flows, it follows that to develop the theory of rarefied gas dynamics a framework for its fundamental microscopic processes needs to be formulated, i.e., intermolecular collisions and gas surface interactions, which lead to rigorous statistical models that can be utilized in the code. In this report attention is focussed on the mechanism of gas surface interactions. A reciprocity theory for it, which leads to models that can be utilized in the DSMC code, is formulated. ESA

N92-11290*# Research Inst. for Advanced Computer Science, Moffett Field, CA.
APPLICATION OF KRYLOV EXPONENTIAL PROPAGATION TO FLUID DYNAMICS EQUATIONS
Youcef Saad and David Semeraro (Illinois Univ., Urbana-Champaign.) 23 Jan. 1991 14 p Previously announced in IAA as A91-40741
(Contract NCC2-387)
(NASA-CR-188887; NAS 1.26:188887; RIACS-TR-91-06) Avail: NTIS HC/MF A03 CSCL 20D

An application of matrix exponentiation via Krylov subspace projection to the solution of fluid dynamics problems is presented. The main idea is to approximate the operation exp(A)v by means of a projection-like process onto a krylov subspace. This results in a computation of an exponential matrix vector product similar to the one above but of a much smaller size. Time integration schemes can then be devised to exploit this basic computational kernel. The motivation of this approach is to provide time-integration schemes that are essentially of an explicit nature but which have good stability properties. Author

N92-11291# Argonne National Lab., IL. Energy Systems Div.
DIRECT-CONTACT HEAT EXCHANGER FOR SWIRLING COUNTERCURRENT FLOW OF HOT GAS AND FINELY DIVIDED SOLIDS: A PARAMETRIC STUDY
K. J. Bell and B. Arman Jun. 1991 36 p
(Contract W-31-109-eng-38)
(DE91-017229; ANL/ESD/TM-16) Avail: NTIS HC/MF A03

A vertically oriented solid-to-gas direct-contact heat exchanger (DCHX) has been proposed for heat recovery in high temperature plants that process finely divided solids. The flows are countercurrent, with the inlet gas flow entering on the centerline and swirling strongly. Swirling enhances heat transfer and centrifuges the solid particles from the center to the wall in order to minimize entrainment and permit gravity separation. A computer program was written to calculate particle trajectories and heat transfer rates (and, therefore, temperature profiles) for gas and solid phases. The flow model considers interactions between the particles and the flow field of the gas. The results of the computer program showed that the introduction of swirl significantly reduced the vertical distance required to achieve a given thermal efficiency. The countercurrent flow arrangement achieves high thermal efficiency in one contacting stage, unlike existing cocurrent suspension preheater systems, which require four or five stages. The practical application of this design to the cement industry appears unlikely, because very low gas velocities and correspondingly large areas of cross-sectional flow are required to prevent elutriation of the 74 micron particles required for the chemical reactions. The computer program can be modified for spray-dryer applications by the addition of mass transfer terms and a spray-formation model. In addition, the concept of a swirling flow heat exchanger may be applicable to other processes in which larger and heavier particles are used. DOE

N92-11292 North Carolina State Univ., Raleigh.
A NEWTON'S METHOD SOLVER FOR THE TWO-DIMENSIONAL AND AXISYMMETRIC NAVIER-STOKES EQUATIONS Ph.D. Thesis
Paul David Orkwis 1990 149 p
Avail: Univ. Microfilms Order No. DA9121973

A method for calculating the 2-D or axisymmetric, laminar or turbulent Navier-Stokes equations are approximated by finite differences using Roe's flux difference splitting (FDS) with Glaister's approach used to extend Roe's scheme to the axisymmetric equations. This method makes use of the exact Jacobian of the full discretized equation set. The freestream reproduction criteria is satisfied for the axisymmetric solver through the addition of a geometric conservation law like term similar to that used by Gielda and McRae. Higher order accuracy is attained through Spekreijse's interpolation approach, with Van Albada's limiter used to reduce spurious oscillations. Expansion shocks are eliminated by use of Harten and Hymans's entropy correction. Turbulent flows are calculated using the Baldwin-Lomax turbulence model. Nonoptimal initial conditions are overcome by the addition of a time like term to the Jacobian matrix diagonal. The symbolic manipulation package MACSYMA is used to determine the Jacobian matrix entries and to write the FORTRAN code. Numerical results are presented and compared with available exact solutions and experimental data for various supersonic laminar flat plate and flat plate/wedge geometries, and turbulent projectile type flows. Dissert. Abstr.

N92-11293 Missouri Univ., Rolla.
MIXED CONVECTION IN TWO-DIMENSIONAL LAMINAR AIR FLOW WITH REVERSE FLOW REGIONS Ph.D. Thesis
Byung Joon Baek 1990 109 p
Avail: Univ. Microfilms Order No. DA9114842

Measurements and predictions of mixed convection heat transfer and flow characteristics for two dimensional laminar flow with flow reversal are reported. Two different geometries with

reverse flow regions were examined. One of these geometries involves a reverse flow that is caused by the buoyancy force effect in a vertical asymmetrically heated parallel-plate duct flow. The reverse flow occurred adjacent to the cooler wall from the top exit section of the duct as the duct flow was starved by restricting the inlet air flow to a level below the natural convection value while increasing the heating rate of the hotter wall. The effects of increasing asymmetric heating, increasing interwall spacing, and inlet air velocity on the flow and heat transfer characteristics were measured and predicted. The other geometry has a reverse flow that is caused by a sudden expansion of the flow cross section. The fluid flow fails to follow the sudden changes in the boundary contour and separates from the surface, forming a recirculation region. In this part, the focus is on a geometry with a backward-facing step. The effects of buoyancy forces on the flow characteristics in the recirculation region, along with the reattachment length and heat transfer were measured and predicted. The experimental measurements for velocities, temperature, and heat fluxes compare well with numerical predictions. Dissert. Abstr.

N92-11294*# Wisconsin Univ., Madison. Nuclear Engineering and Engineering Physics Div.
SUPERFLUID HELIUM DYNAMICS Final Technical Report, 15 Jan. - 31 Dec. 1990
Steven W. VanSciver 31 Dec. 1990 16 p
(Grant NAG5-1031)
(NASA-CR-188814; NAS 1.26:188814) Avail: NTIS HC/MF A03 CSCL 20D

Two papers on cryogenics are presented. The first is entitled, Characterizing He II Flow Through Porous Materials Using Counterflow Data. The second paper is entitled, Thermal Behavior of the SHOOT Gallery Arm. Both papers were presented at the Cryogenic Engineering Conference in Huntsville, AL. For individual titles, see N92-11295 through N92-11296.

N92-11295*# Wisconsin Univ., Madison. Applied Superconductivity Center.
CHARACTERIZING He II FLOW THROUGH POROUS MATERIALS USING COUNTERFLOW DATA
J. R. Maddocks, Jr. and Steven W. VanSciver *In its* Superfluid Helium Dynamics 31 Dec. 1990 8 p Presented at the Cryogenic Engineering Conference, Huntsville, AL, 1991 (For primary document see N92-11294 02-34)
(CD-4) Avail: NTIS HC/MF A03 CSCL 20D

Proposed space applications, such as the cooling of infrared and x ray telescopes, have generated substantial interest in the behavior of He II flowing in porous materials. For design purposes, classical porous media correlations and room temperature data are often used to obtain order of magnitude estimates of expected pressure drops, while the attendant temperature differences are either ignored or estimated using smooth tube correlations. A more accurate alternative to this procedure is suggested by an empirical extension of the two fluid model. It is shown that four empirical parameters are necessary to describe the pressure and temperature differences induced by He II flow through a porous sample. The three parameters required to determine pressure differences are measured in counterflow and found to compare favorably with those for isothermal flow. The fourth parameter, the Gorter-Mellink constant, differs substantially from smooth tube values. It is concluded that parameter values determined from counterflow can be used to predict pressure and temperature differences in a variety of flows to an accuracy of about + or - 20 pct. Author

N92-11296*# Wisconsin Univ., Madison. Applied Superconductivity Center.
THERMAL BEHAVIOR OF THE SHOOT GALLERY ARM
J. A. Nissen and Steven W. VanSciver *In its* Superfluid Helium Dynamics 31 Dec. 1990 7 p Presented at the Cryogenic Engineering Conference, Huntsville, AL, 1991 (For primary document see N92-11294 02-34)
(CD-21) Avail: NTIS HC/MF A03 CSCL 20D

The planned Superfluid Helium On-Orbit Transfer (SHOOT) experiment will show the feasibility of resupplying orbiting facilities with liquid helium. The SHOOT experiment, designed for transfer rates of 300 to 800 liters/hr, will use a thermomechanical pump and four screen covered flow channels for fluid acquisition. Cavitation and thermal behavior was examined in ground based tests of the pump and of a full sized channel. A model for estimating the temperature profile at the pump inlet is presented. Large temperature increases in this region can significantly degrade the performance of the fountain pump. Author

N92-11297*# United Technologies Research Center, East Hartford, CT.
THE EFFECTS OF REYNOLDS NUMBER, ROTOR INCIDENCE ANGLE AND SURFACE ROUGHNESS ON THE HEAT TRANSFER DISTRIBUTION IN A LARGE-SCALE TURBINE ROTOR PASSAGE Final Report
M. F. Blair Nov. 1991 228 p Original contains color illustrations
(Contract NAS8-38870)
(NASA-CR-187693; NAS 1.26:187693; UTRC/R91-970057-3)
Avail: NTIS HC/MF A11; 5 functional color pages CSCL 20D

A combined experimental and computational program was conducted to examine the heat transfer distribution in a turbine rotor passage geometrically similar to the Space Shuttle Main Engine (SSME) High Pressure Fuel Turbopump (HPFTP). Heat transfer was measured and computed for both the full span suction and pressure surfaces of the rotor airfoil as well as for the hub endwall surface. The objective of the program was to provide a benchmark-quality database for the assessment of rotor heat transfer computational techniques. The experimental portion of the study was conducted in a large scale, ambient temperature, rotating turbine model. The computational portion consisted of the application of a well-posed parabolized Navier-Stokes analysis of the calculation of the three-dimensional viscous flow through ducts simulating a gas turbine package. The results of this assessment indicate that the procedure has the potential to predict the aerodynamics and the heat transfer in a gas turbine passage and can be used to develop detailed three dimensional turbulence models for the prediction of skin friction and heat transfer in complex three dimensional flow passages. Author

N92-11298# National Aerospace Lab., Tokyo (Japan).
THEORETICAL ESTIMATION OF THE VISCOUS DAMPING FROM LIQUID TRANSIENT MOTION IN TANKS
Keiji Komatsu and Jyun-ichirou Shimizu (Tsukuba Univ., Japan) Feb. 1991 12 p In JAPANESE; ENGLISH summary
(NAL-TR-1095; ISSN-0389-4010) Avail: NTIS HC/MF A03

The dynamic behavior of liquid propellants in launch vehicles and spacecraft has been of great importance in generating vehicle designs. Presented here is a method to estimate the viscous dissipative force for the transient motion of liquid propellants in tanks. The estimation algorithm is combined into the Large Amplitude Sloshing (LAMPS) algorithm, where the dissipative values have been approximated from test data. Analytical predictions show excellent agreement with existing test results. Author

N92-11299*# National Aeronautics and Space Administration. Lewis Research Center, Cleveland, OH.
MODELING OF THE HEAT TRANSFER IN BYPASS TRANSITIONAL BOUNDARY-LAYER FLOWS
Frederick F. Simon and Craig A. Stephens (PRC Kentron, Inc., Edwards, CA.) Washington Oct. 1991 15 p
(NASA-TP-3170; E-6046; NAS 1.60:3170) Avail: NTIS HC/MF A03 CSCL 20D

A low Reynolds number k-epsilon turbulence model and conditioned momentum, energy and turbulence equations were used to predict bypass transition heat transfer on a flat plate in a high-disturbance environment with zero pressure gradient. The use of conditioned equations was demonstrated to be an improvement over the use of the global-time-averaged equations for the calculation of velocity profiles and turbulence intensity profiles in the transition region of a boundary layer. The approach of

conditioned equations is extended to include heat transfer and a modeling of transition events is used to predict transition onset and the extent of transition on a flat plate. The events, which describe the boundary layer at the leading edge, result in boundary-layer regions consisting of: (1) the laminar, (2) pseudolaminar, (3) transitional, and (4) turbulent boundary layers. The modeled transition events were incorporated into the TEXSTAN 2-D boundary-layer code which is used to numerically predict the heat transfer. The numerical predictions in general compared well with the experimental data and revealed areas where additional experimental information is needed. Author

N92-11300*# National Aeronautics and Space Administration. Langley Research Center, Hampton, VA.
COMPUTER CODES FOR THE EVALUATION OF THERMODYNAMIC AND TRANSPORT PROPERTIES FOR EQUILIBRIUM AIR TO 30000 K
Richard A. Thompson, Kam-Pui Lee (Vigyan Research Associates, Inc., Hampton, VA.), and Roop N. Gupta Sep. 1991 27 p
(NASA-TM-104107; NAS 1.15:104107) Avail: NTIS HC/MF A03 CSCL 20D

The computer codes developed here provide self-consistent thermodynamic and transport properties for equilibrium air for temperatures from 500 to 30000 K over a temperature range of 10 (exp -4) to 10 (exp -2) atm. These properties are computed through the use of temperature dependent curve fits for discrete values of pressure. Interpolation is employed for intermediate values of pressure. The curve fits are based on mixture values calculated from an 11-species air model. Individual species properties used in the mixture relations are obtained from a recent study by the present authors. A review and discussion of the sources and accuracy of the curve fitted data used herein are given in NASA RP 1260. Author

N92-11301*# National Aeronautics and Space Administration. Hugh L. Dryden Flight Research Facility, Edwards, CA.
AEROTHERMAL TEST RESULTS FROM THE FIRST FLIGHT OF THE PEGASUS AIR-LAUNCHED SPACE BOOSTER
Gregory K. Noffz, Robert E. Curry, Edward A. Haering, Jr., and Paul Kolodziej (National Aeronautics and Space Administration. Ames Research Center, Moffett Field, CA.) Oct. 1991 53 p
(NASA-TM-4330; H-1672; NAS 1.15:4330) Avail: NTIS HC/MF A04 CSCL 20D

A survey of temperature measurements at speeds through Mach 8.0 on the first flight of the Pegasus air-launched booster system is discussed. In addition, heating rates were derived from the temperature data obtained on the fuselage in the vicinity of the wing shock interaction. Sensors were distributed on the wing surfaces, leading edge, and on the wing-body fairing or fillet. Side-by-side evaluations were obtained for a variety of sensor installations. Details of the trajectory reconstruction through first-stage separation are provided. Given here are indepth descriptions of the sensor installations, temperature measurements, and derived heating rates along with interpretations of the results. Author

N92-11302*# National Aeronautics and Space Administration. Lewis Research Center, Cleveland, OH.
ON THE BASIC EQUATIONS FOR THE SECOND-ORDER MODELING OF COMPRESSIBLE TURBULENCE
W. W. Liou and T.-H. Shih Oct. 1991 28 p
(NASA Order C-99066-G)
(NASA-TM-105277; ICOMP-91-19; CMOTT-91-08; E-6600; NAS 1.15:105277) Avail: NTIS HC/MF A03 CSCL 20D

Equations for the mean and turbulent quantities for compressible turbulent flows are derived. Both the conventional Reynolds average and the mass-weighted, Favre average were employed to decompose the flow variable into a mean and a turbulent quality. These equations are to be used later in developing second order Reynolds stress models for high speed compressible flows. A few recent advances in modeling some of the terms in the equations due to compressibility effects are also summarized. Author

N92-11303*# National Aeronautics and Space Administration. Ames Research Center, Moffett Field, CA.
THE THREE-DIMENSIONAL EVOLUTION OF A PLANE MIXING LAYER. PART 1: THE KELVIN-HELMHOLTZ ROLL-UP
Michael M. Rogers and Robert D. Moser Sep. 1991 87 p
(NASA-TM-103856; A-91115-Pt-1; NAS 1.15:103856) Avail: NTIS HC/MF A05 CSCL 20D

The Kelvin Helmholtz roll up of three dimensional, temporally evolving, plane mixing layers were simulated numerically. All simulations were begun from a few low wavenumber disturbances, usually derived from linear stability theory, in addition to the mean velocity profile. The spanwise disturbance wavelength was taken to be less than or equal to the streamwise wavelength associated with the Kelvin Helmholtz roll up. A standard set of clean structures develop in most of the simulations. The spanwise vorticity rolls up into a corrugated spanwise roller, with vortex stretching creating strong spanwise vorticity in a cup shaped region at the vends of the roller. Predominantly streamwise rib vortices develop in the braid region between the rollers. For sufficiently strong initial three dimensional disturbances, these ribs collapse into compact axisymmetric vortices. The rib vortex lines connect to neighboring ribs and are kinked in the opposite direction of the roller vortex lines. Because of this, these two sets of vortex lines remain distinct. For certain initial conditions, persistent ribs do not develop. In such cases the development of significant three dimensionality is delayed. When the initial three dimensional disturbance energy is about equal to, or less than, the two dimensional fundamental disturbance energy, the evolution of the three dimensional disturbance is nearly linear (with respect to the mean and the two dimensional disturbances), at least until the first Kelvin Helmholtz roll up is completed. Author

N92-11304# Naval Research Lab., Washington, DC.
NUMERICAL SIMULATIONS OF DETONATION TRANSMISSION Memorandum Report
Elaine S. Oran, David A. Jones, and Martin Sichel 3 Sep. 1991 49 p
(NRL Proj. RR0-1109)
(AD-A240560; NRL-MR-6884) Avail: NTIS HC/MF A03 CSCL 19/9

The complex, dynamic shock-detonation structure formed by the glancing interaction of a primary detonation with a secondary explosive is studied using time-dependent two-dimensional simulations and related experiments. The materials considered in the simulations are stoichiometric and lean mixtures of hydrogen and oxygen diluted with argon. Related experiments have used undiluted hydrogen and oxygen as well as other gases. The conditions simulated are: (1) the primary mixture is stoichiometric and the secondary inert; (2) both the primary and secondary mixtures are the same and stoichiometric; (3) the primary mixture is lean and the secondary is stoichiometric; and (4) the primary mixture is stoichiometric and the secondary is lean. For cases 2 and 4, comparisons are also made between simulations in which the primary mixture is overdriven and when it is a Chapman-Jouguet detonation. For the overdriven stoichiometric primary detonation interacting with the lean mixture, a complex detonation structure forms and quickly asymptotes to the detonation velocity of the primary mixture. For the same case, but when the primary detonation is initially at Chapman-Jouguet velocity, the detonation appears to die but then reignites due to a series of shock reflections and then propagates as a complex structure. The lowest velocity of the complex structure is always greater than the Chapman-Jouguet velocity of the lean mixture and it increases in time, appearing to approach the Chapman-Jouguet velocity of the stoichiometric mixture. The dynamics of the decay of reignition process are described and discussed in detail. GRA

N92-11305# Naval Postgraduate School, Monterey, CA.
HEAT TRANSFER, ADIABATIC EFFECTIVENESS, AND INJECTANT DISTRIBUTIONS DOWNSTREAM OF SINGLE AND DOUBLE ROWS OF FILM-COOLING HOLES WITH SIMPLE AND COMPOUND ANGLES M.S. Thesis

Salvatore Ciriello, Jr. 28 Mar. 1991 287 p
(MIPR-FY1455-89-N0670)
(AD-A240743) Avail: NTIS HC/MF A13 CSCL 20/4

Experimental results are presented which describe the development and structure of flow downstream of single and double rows of film cooling holes with both simple and compound angle orientations. Two configurations are investigated, a simple angle injection system in which the injectant is introduced into the freestream parallel to the main flow (as viewed in streamwise/spanwise planes), and a compound angle injection system in which the injectant is introduced with spanwise velocity components. Results indicate that effectiveness depends mostly on four parameters: simple or compound angle injection, spanwise hole spacing, one or two rows of holes, and blowing ratio. In general, for a given m, for all the configurations tested, effectiveness is greatest at low x/d values, and decreases with increasing x/d. As blowing ratio increases, effectiveness generally decreases, particularly at low x/d values because of lift-off effects. Iso-energetic Stanton number ratios vary between 1.0 and 1.25 for all cases, and generally increase with increasing blowing ratio at any given x/d. Effectiveness values measured downstream of two rows of holes are higher than values measured downstream of one row of holes. Adiabatic film cooling effectiveness data for both the compound angle injection system and the simple angle injection collapse with minimal scatter in n/m vs xl/s coordinates. GRA

N92-11306# Centre d'Etudes et de Recherches, Toulouse (France). Dept. d'Etudes et de Recherches en Aerothermodynamique.
SECONDARY INSTABILITY OF THE THREE DIMENSIONAL LAMINAR BOUNDARY LAYER IN INCOMPRESSIBLE FLOW: DESCRIPTION OF THE CALCULATION CODE [INSTABILITE SECONDAIRE DE LA COUCHE LIMITE LAMINAIRE TRIDIMENSIONNELLE EN ECOULEMENT INCOMPRESSIBLE: DESCRIPTION DU CODE DE CALCUL]
G. Casalis Apr. 1991 73 p In FRENCH
(CERT-RT-63/5618-54; ETN-91-90079) Avail: NTIS HC/MF A04

A calculation code for resolving stability equations of the three dimensional laminar boundary layer in incompressible flow is presented. Secondary instability and the Floquet theorem are addressed. The code is based on a spectal Galerkin type method using Chebyshev polynomials. The theory is explained and as detailed use as possible of the code is shown. ESA

N92-11307# Centre d'Etudes et de Recherches, Toulouse (France). Dept. d'Etudes et de Recherches en Aerodynamique.
RESOLUTION OF THE NAVIER-STOKES EQUATIONS APPLIED TO THE COMPUTATION OF THE LAMINAR FLOW AROUND A TWO DIMENSIONAL WING PROFILE [RESOLUTION DES EQUATIONS DE NAVIER-STOKES APPLIQUEE AU CALCUL DE L'ECOULEMENT LAMINAIRE AUTOUR D'UN PROFIL D'AILE BIDIMENSIONNEL]
X. deSaint-Victor Dec. 1990 48 p In FRENCH
(CERT-RT-65/5604-35; ETN-91-90080) Avail: NTIS HC/MF A03

A two dimensional Navier-Stokes equation computation code of the laminar flow around a wing profile is presented. The equations are discretized by finite volume method. The motion quantity equations are resolved by an alternate direction method and the pressure correction equation by the conjugate gradient method with preconditining. Results of calculations on a NACA0012 and an AS239 profile at different incidences are presented. A comparison with a boundary layer computation code is carried out. ESA

N92-11308# Office National d'Etudes et de Recherches Aerospatiales, Paris (France). Direction de l'Aerodynamique.
HYDRODYNAMIC TUNNEL STUDY OF THE MARGINAL VORTEX BREAKDOWN IN THE PRESSURE FIELD OF A WING PROFILE Final Summary Report [ETUDE AU TUNNEL HYDRODYNAMIQUE DE L'ECLATEMENT D'UN TOURBILLON MARGINAL DANS LE CAMP DE PRESSION D'UN PROFIL D'AILE. RAPPORT DE SYNTHESE FINAL]
J. L. Solignac and M. Gallon Nov. 1990 26 p In FRENCH
(Contract DRET-89-34-001)
(ONERA-RSF-44/1147-AY-144A; ETN-91-90084) Avail: NTIS HC/MF A03

Tests carried out in a hydrodynamic tunnel with a view to revealing the susceptible breakdown at the time of the passage of a marginal vortex of an eliptic wind in proximity to the flight edge of an even profile are reported. Laser velocimetry measurements can precise the qualitative aspect of visualizations and conclude the abscence of breakdown in real conditions of tests carried out at very low Reynolds number. ESA

N92-11309# Centre d'Etudes et de Recherches, Toulouse (France). Dept. d'Etudes et de Recherches en Aerothermodynamique.
TURBULENT FRICTION DRAG REDUCTION: BOUNDARY LAYER MANIPULATORS Final Summary Report [REDUCTION DE TRAINEE DE FROTTEMENT TURBULENT: MANIPULATEURS DE COUCHE LIMITE. RAPPORT DE SYNTHESE FINAL]
E. Coustols Mar. 1990 61 p In FRENCH
(Contract STPA-85-95-009-51)
(CERT-RSF-DERAT-62/5004-31; ETN-91-90085) Avail: NTIS HC/MF A04

Internal manipulation by slant of thin longitudinal riblets is addressed experimentally in three dimensional flow. An ONERA D profile mounted between the lateral walls of a subsonic wind tunnel is maintained at an angle sweep of 22.5 degrees and at incidence 0 degrees. When the profile is recovered by different models of ribleted walls the variations on the drag coefficient are estimated by wake explorations and compared to the drag of the profile encased in a smooth sheet of equivalent thickness. ESA

N92-11310# Office National d'Etudes et de Recherches Aerospatiales, Paris (France). Direction de l'Aerodynamique.
RESOLUTION OF NAVIER-STOKES EQUATIONS AROUND PROFILES: DRAG EVOLUTION [RESOLUTION DES EQUATIONS DE NAVIER-STOKES AUTOUR DE PROFILS: EVALUATION DE LA TRAINEE. RAPPORT TECHNIQUE DE SYNTHESE]
F. Montigny-Rannou and J. P. Veuillot Sep. 1990 51 p In FRENCH
(Contract DRET-89-34-001)
(ONERA-RTS-86/1685-AY-156A; ETN-91-90086) Avail: NTIS HC/MF A04

Modifications on the two dimensional Navier-Stokes equations resolution code are presented. A numerical viscocity model was introduced which allowed more difficult cases than before to be addressed. The drag around supercritical profiles is evaluated transonically and at low speeds. A comparison with experimental results is presented. Difficulties encountered are outlined and paths to explore are described. ESA

N92-11311# Office National d'Etudes et de Recherches Aerospatiales, Paris (France). Direction Scientifique de la Resistance des Structures.
PERFECT COMPRESSIBLE TWO DIMENSIONAL BOUNDARY LAYER STRONG FLUID COUPLING IN THE CASE OF SHARP LEADING EDGE PROFILES. UNSTEADY CASE OF ISOLATED PROFILES AND STEADY CASE OF BLADE GRIDS Final Report [COUPLAGE FORT FLUIDE PARFAIT-COUCHE LIMITE 2D COMPRESSIBLE DANS LE CAS DES PROFILS A BORD D'ATTAQUE AIGU. CAS INSTATIONNAIRE DES PROFILS ISOLES ET CAS STATIONNAIRE DES GRILLES D'AUBES]
C. Soize Jan. 1991 73 p In FRENCH

(Contract DRET-89-34-01)
(ONERA-RT-43/1621-RY-006-R; ETN-91-90094) Avail: NTIS HC/MF A04

In the frame of studies of blade grid aeroelasticity, the perfect boundary layer strong fluid coupling is studied, the outer boundary layer being disengaged in leading edge and reengaged over the profile. The study is the fifth phase of a study to understand the development of the compressible code and its experimental validation, for unsteady isolated profiles and steady blade grids. ESA

N92-11312# Office National d'Etudes et de Recherches Aerospatiales, Paris (France). Direction de l'Aerodynamique.
HYDRODYNAMIC FLOW VISUALIZATION AROUND AN OSCILLATING VANE. EXTENSION OF STUDY TO THE CASE OF HIGHER INCIDENCES AND AMPLITUDES AND THE STARTING OFF PHASE FROM PERMANENT REGIME [VISUALISATION HYDRODYNAMIQUE DE L'ECOULEMENT AUTOUR D'UNE PALE OSCILLANTE. EXTENSION DE L'ETUDE AU CAS DES INCIDENCES ET AMPLITUDE ELEVEES A LA PHASE DE MISE EN MOUVEMENT A PARTIR DU REGIME PERMANENT]
H. Werle Jan. 1976 41 p In FRENCH
(ONERA-RT-56/1369-AN; ETN-91-90095) Avail: NTIS HC/MF A03

Visualizations obtained in a hydrodynamic tunnel contributed to the specification of the running of phenomena characterizing the unsteady breakdown on a profile under large amplitude harmonic oscillations. The starting phase of the oscillations was observed around a minimally zero incidence starting off profile and compared to the well established periodic regime; the visualizations further reveal the evolution of the phenomena as a function of the Reynolds number, the frequency and amplitude of the oscillations as well as the influence of the pitching and mean incidence axis position. ESA

N92-11313# Centre d'Etudes Aerodynamiques et Thermiques, Poitiers (France).
EUROMECH 260: ADVANCED NON-INTRUSIVE EXPERIMENTAL TECHNIQUES IN FLUID AND PLASMA FLOWS
1990 84 p Colloquium held in Poitiers, France, 5-7 Sep. 1990 Sponsored by CNRS; Poitiers Univ.; Dept. de la Vienne; Poitou-Charentes Region; and UFR CEAT
(Contract DRET-90-1430/A000)
(ETN-91-90104) Avail: NTIS HC/MF A05

The following topics are discussed: coherent anti-Stokes and elastic Rayleigh scattering; elastic scattering and non linear dynamics; fluorescence; molecular tracking techniques and particle image velocimetry. ESA

N92-11314# Technische Univ., Eindhoven (Netherlands). Dept. of Physics.
CRITICAL VELOCITIES AND MUTUAL FRICTION IN He-3-He-4 II MIXTURES AT TEMPERATURES BELOW 100 mK Ph.D. Thesis
Josephus Catharina H Zeegers 1991 171 p Sponsored in part by Stichting voor Fundamenteel Onderzoek der Materie and Netherlands Organization for the Advancement of Scientific Research
(ETN-91-90132) Avail: NTIS HC/MF A08

A study of the flow properties of liquid He-3 He-4 II mixtures at temperatures between 10 and 200 mK near the mixing chamber of a dilution refrigerator is presented. The temperature rise if He-3 flows through superfluid He-4 II in capillaries with a diameter between 50 microns and 5 mm under adiabatic conditions is investigated. Measurements of the temperature increase, the concentration decrease and pressure difference are used to calculate the chemical potential of He-4. Results are compared to previous models. Above a critical velocity, dissipation appears because of a mutual friction between the He-3 and He-4 together with the viscous dissipation which is always present. The influence of wall material and the diameter of the capillaries on the critical velocity are studied. Data on the vortex line density for velocities above the critical velocity is obtained. The flow phenomena of He-3 through a background of superfluid He-4 resemble those in He-4 counterflow. A viscosity meter is developed to measure the viscosity of the He-3 He-4 mixture between 7 and 200 mK and a value of viscosity which influences the calculated pressure difference is found. ESA

N92-11315# Technische Univ., Eindhoven (Netherlands).
DEFORMATION AND BREAKUP OF DROPS IN SIMPLE SHEAR FLOWS Ph.D. Thesis
Robert Antonie deBruijn 1991 281 p Sponsored in part by Commission of the European Communities
(ETN-91-90143) Avail: NTIS HC/MF A13

In an investigation aimed at modeling the operation of emulsifying devices in the food industry, some aspects of the viscous breakup of drops in simple shear flows are described: the breakup of nonNewtonian drops, the deformation and breakup of drops in transient shear flows and the origin of the tipstreaming phenomenon observed in simple shear flow. The basic equations and scaling laws for the flow of emulsions are presented for use in experimental and numerical investigations. A Couette device is developed and used to study the breakup of non-Newtonian droplets in quasi-steady simple shear flows. ESA

N92-11316# Heidelberg Univ. (Germany, F.R.). Naturwissenschaftlich-Mathematischen Gesamtfakultaet.
MEASUREMENT OF TURBULENT FLOW BENEATH THE WIND WAVE INDUCED WATER SURFACE, USING PICTURE REPETITION ANALYSIS Ph.D. Thesis [MESSUNG TURBULENTER STROEMUNGEN UNTERHALB DER WIND-WELLENBEWEGTEN WASSEROBERFLAECHE MITTELS BILDFOLGENANALYSE]
Dietmar Wierzimok 1990 146 p In GERMAN
(ETN-91-90203) Avail: NTIS HC/MF A07

A process for two dimensional examination of turbulent flows in laboratory is developed, which allows quantitative area flow measurements beneath the free wind wave induced water surface, using an automatic image analysis process. The process allows a detailed flow analysis of Euler and Lagrange velocity fields, by tracking flow tracer particles in film sequences by means of digital picture repetition analysis. The correspondence between particles in sequential pictures is determined using heuristic criteria. A reliability of correspondence of about 95 pct. is obtained, taking into consideration flowing physical particle properties, velocity and acceleration. The reconstruction of particle velocity ensues by displacing the center of gravity of particle tracers between two successive pictures. ESA

N92-11317*# National Aeronautics and Space Administration. Lewis Research Center, Cleveland, OH.
TURBULENT FLUID MOTION 3: BASIC CONTINUUM EQUATIONS
Robert G. Deissler Oct. 1991 20 p
(NASA-TM-104386; E-6196; NAS 1.15:104386) Avail: NTIS HC/MF A03 CSCL 20D

A derivation of the continuum equations used for the analysis of turbulence is given. These equations include the continuity equation, the Navier-Stokes equations, and the heat transfer or energy equation. An experimental justification for using a continuum approach for the study of turbulence is given. Author

N92-11318*# Colorado State Univ., Fort Collins.
EVALUATION OF HIGH REYNOLDS NUMBER FLOW IN A 180 DEGREE TURN-AROUND-DUCT
V. A. Sandborn and S. J. Marcy 1991 26 p
(Contract NAS8-38186)
(NASA-CR-184243; NAS 1.26:184243) Avail: NTIS HC/MF A03 CSCL 20D

Mean and turbulent velocities were measured for the flow in a 180 degree turn-around-duct over a Reynolds number range from 600,000 to greater than 900,000. The measurements were made in water using a forward scattering laser velocimeter. A duct of

100 x 10 cm constant cross-section, with a mean radius of curvature (centerline) of 10 cm was employed for the study. The measurements are in agreement with previous studies in that the use of local bulk velocity to nondimensionalize the mean and turbulent velocities reduce the Reynolds number variations. The basic phenomenon of relaminarization along the inner surface at the exit of the turn are similar to the flow observed at low Reynolds numbers. The separation bubble region shows a systematic variation with Reynolds number, however the Reynolds number effect may be of second order in the calculation of the overall flow. Large tangential, radial, and lateral turbulent velocities are measured along the outer surface of the turn. Author

N92-11319*# Calspan-Buffalo Univ. Research Center, NY.
STUDIES OF AEROTHERMAL LOADS GENERATED IN REGIONS OF SHOCK/SHOCK INTERACTION IN HYPERSONIC FLOW Final Report
Michael S. Holden, John R. Moselle, and Jinho Lee Oct. 1991 339 p
(Contract NAS1-17721)
(NASA-CR-181893; NAS 1.26:181893) Avail: NTIS HC/MF A15 CSCL 20D

Experimental studies were conducted to examine the aerothermal characteristics of shock/shock/boundary layer interaction regions generated by single and multiple incident shocks. The presented experimental studies were conducted over a Mach number range from 6 to 19 for a range of Reynolds numbers to obtain both laminar and turbulent interaction regions. Detailed heat transfer and pressure measurements were made for a range of interaction types and incident shock strengths over a transverse cylinder, with emphasis on the 3 and 4 type interaction regions. The measurements were compared with the simple Edney, Keyes, and Hains models for a range of interaction configurations and freestream conditions. The complex flowfields and aerothermal loads generated by multiple-shock impingement, while not generating as large peak loads, provide important test cases for code prediction. The detailed heat transfer and pressure measurements proved a good basis for evaluating the accuracy of simple prediction methods and detailed numerical solutions for laminar and transitional regions or shock/shock interactions.
Author

N92-11320*# National Aeronautics and Space Administration. Lewis Research Center, Cleveland, OH.
AN EFFICIENT AND ROBUST ALGORITHM FOR TWO DIMENSIONAL TIME DEPENDENT INCOMPRESSIBLE NAVIER-STOKES EQUATIONS: HIGH REYNOLDS NUMBER FLOWS
John W. Goodrich 1991 17 p Presented at the Seventh International Conference on Numerical Methods in Laminar and Turbulent Flow, Stanford, CA, 15-19 Jul. 1991; sponsored by LMSC, Stanford Univ., International Journal for Numerical Methods in Fluids, and International Journal for Computational Methods in Heat and Fluid Flow
(NASA-TM-104424; E-6257; NAS 1.15:104424) Avail: NTIS HC/MF A03 CSCL 20D

An algorithm is presented for unsteady two-dimensional incompressible Navier-Stokes calculations. This algorithm is based on the fourth order partial differential equation for incompressible fluid flow which uses the streamfunction as the only dependent variable. The algorithm is second order accurate in both time and space. It uses a multigrid solver at each time step. It is extremely efficient with respect to the use of both CPU time and physical memory. It is extremely robust with respect to Reynolds number.
Author

N92-11321# Argonne National Lab., IL. Multiphase Flow Research Inst.
IMPLEMENTATION OF THE FLOW-MODULATED SKEW-UPWARD DIFFERENCE SCHEME IN THE MOMENTUM EQUATION OF THE COMMIX-1C PROGRAM: A FIRST ASSESSMENT
Y. Shen, M. Bottoni, and W. T. Sha Feb. 1991 99 p
(Contract W-31-109-eng-38)
(DE91-018013; ANL/MFRI-8) Avail: NTIS HC/MF A05

Based on the concept of feedback sensitivity in the analysis of stability behavior of discretized partial differential equations, central differences, when applied to even-order derivatives yield stable algorithms, while applied to odd-order derivatives they yield algorithms without inherent stability. In a low-convection, diffusion-dominated flow, in which both convective and diffusive terms are discretized with central differences, the stabilizing effect of the diffusion term is sufficient to allow stability; in a flow dominated by convection, the stabilizing effect of the diffusion term becomes weaker and cannot prevent wiggles that finally lead to instability. In the case of two-dimensional flow, numerical diffusion depends on the skewness of the flow with respect to the grids. The numerical diffusion can be reduced by considering upstream values of the dependent transported variables, taken following the stream lines. Variants of the skew-upwind difference (SUD) scheme have been obtained by taking into account either mass flows or cell surface areas or cell volumes to properly weight the contributions of the cells involved in the discretization process. The mass-flow-weighted SUD scheme has been developed in the three-dimensional case and implemented in the energy equation of the COMMIX-1A code. The volume-weighted SUD scheme was likewise implemented in the three-dimensional energy equation of the variant COMMIX-1B. Problems in the application of the SUD scheme arise when the flow is so skewed that the contributions of upwind cells become much smaller than the contributions of neighboring cells. The problem has been tackled with the development of a new algorithm, the flow-modulated skew-upwind difference (FMSUD) scheme. The report explains test cases in which the implementation of the FMSUD scheme has been applied. DOE

N92-11322# Argonne National Lab., IL.
LOCAL INTERFACIAL AREA CONCENTRATION MEASUREMENT IN BUBBLY FLOW
M. Ishii and S. T. Revankar (Purdue Univ., West Lafayette, IN.) Oct. 1990 71 p
(Contract W-31-109-eng-38)
(DE91-018702; ANL-90/51) Avail: NTIS HC/MF A04

The interfacial area concentration is one of the most important parameters in a thermal-hydraulic analysis of two-phase flow systems based on the two-fluid model. A theoretical foundation of the measurement method for the time averaged local interfacial area using a double sensor probe is presented. Based on this theory, the double sensor resistivity probe was employed for the measurement of local properties of two-phase flow such as the interfacial velocity, local interfacial area concentration and void fraction in vertical air-water bubbly flow. Experimental data are presented on the radial profiles of the void fraction, bubble velocity, bubble chord length and interfacial area concentration at various gas flow rates. In addition to these, some statistical information on turbulent motions of bubbles are presented. Each of the double sensors are checked against the global void measurement using a differential pressure. The result is very satisfactory. Furthermore, the area averaged void fraction, and the interfacial area concentration obtained from the double sensor probe measurement compared very well with the photographic measurements. The results show that the double sensor probe method is accurate and reliable for the local measurements of interfacial area and void fraction in bubbly two-phase flow. Results of the measurement of interfacial area concentration with the double sensor probe in forced flow loop are presented for bubbly flow at different liquid flow rates. The data indicate that the radial profiles of the interfacial area concentration show similar dependence on the liquid and gas flow rate like radial profiles of void fraction in the bubbly flow regime. DOE

N92-11323# Gosudarstvennyi Komitet po Ispolzovaniyu Atomnoi Energii, Obninsk (USSR). Fiziko-Ehnergeticheskij Inst.
TO THE ACCOUNT OF FINITE VELOCITY OF THERMAL DIFFUSION IN TURBULENT FLOWS

V. I. Mikhin 1989 15 p In RUSSIAN
(DE91-635593; FEI-1981) Avail: NTIS HC/MF A03

Derivation of heat transfer equations taking account of effects of finite velocity of heat propagation in processes of turbulent diffusion is given. Quantitative estimations of the effects of finite velocity of heat propagation is presented. DOE

N92-11324# Gosudarstvennyi Komitet po Ispolzovaniyu Atomnoi Energii, Obninsk (USSR). Fiziko-Ehnergeticheskij Inst.
HEAT TRANSFER IN CHANNELS WITH UNIFORMLY SWIRLED FLOW
S. G. Kalyakin and A. N. Yarkin 1989 9 p In RUSSIAN
(DE91-635594; FEI-2017) Avail: NTIS HC/MF A02

Equations for calculation of the heat transfer coefficient in uniformly swirled flows in the range of P(sub r) number change from 1 to 100 and from 0.004 to 0.04 are obtained on the basis of semiempirical models of turbulent flow. The principle possibility for increasing this range is shown. DOE

N92-11325# Gosudarstvennyi Komitet po Ispolzovaniyu Atomnoi Energii, Obninsk (USSR). Fiziko-Ehnergeticheskij Inst.
DETERMINATION OF NONSTATIONARY TEMPERATURES IN HIGH-STRESSED ELEMENTS WITH PULSED HEAT SOURCES
G. A. Zinina, A. A. Sholokhov, V. N. Petrov, and L. D. Eltsova 1989 17 p In RUSSIAN
(DE91-635705; FEI-2047) Avail: NTIS HC/MF A03

Techniques for calculating nonstationary temperature field in an arbitrary cylindrical area with nonuniform by azimuth boundary condition is described. Thermal-physical properties of the area depend on radial coordinate, heat release depends on radial and axial coordinates and changés in time. The solution is performed in two stages. Firstly nonstationary temperature field in the cross section of a cylindrical body is determined with account of azimuthal temperature distribution nonuniformity. Then axial change of nonstationary coolant temperature is determined using the solution of the problem in axially symmetrical form. The complete solution is the sum of two summands first of which is coolant temperature, the second one - temperature gradient in the cross section normalized to local heat release. The method is illustrated by example of calculating temperatures in fuel element with a defect under pulsed test conditions in a special research reactor. DOE

N92-11326# Technical Research Centre of Finland, Espoo.
MAGNETIC FLUIDS AND THEIR APPLICATIONS
M. Saeynaetjoki Feb. 1991 31 p In FINNISH; ENGLISH summary
(DE92-704012; VTT-TIED-1207) Avail: NTIS HC/MF A03

Magnetic fluids consist of carrier fluid, magnetically active particles and surfactant on each particle preventing the agglomeration of the particles. The fluids acting in the presence of the magnetic field like the ferromagnetic materials, but remaining their fluid properties, are prepared in this way. Potential applications of these fluids are magnetic separation, ink jet printing, sealing, damping, lubrication and heat transfer. So far, the industrial applications of the magnetic fluids are in the seals and bearings of the computer hard disk drives, in the heat transfer and damping of loudspeakers and in the damping of step motors. The other applications are in laboratory and research stage. DOE

N92-11327# Tampere Univ. of Technology (Finland). Thermal Engineering.
THE PHENOMENA OF SCALAR MIXING IN TURBULENT GAS-PARTICLE FLOWS, MEASURING EQUIPMENT, AND MEASUREMENTS
H. Karema and R. Laurila 1989 118 p In FINNISH; ENGLISH summary
(DE92-704034; TTKK-LT-69) Avail: NTIS HC/MF A06

The phenomena of scalar mixing in turbulent gas-particle flows up to the loading ratio two is studied in upward flow conditions using spherical equal sized particles as the dispersed phase and air as the conveying phase. The tracer gas is injected isokineticly and isothermally in the parallel gas-particle flow and the time mean profile of the concentration is measured using a suction probe connected to the infrared analyzer. These profiles are fitted to the similarity solution derived assuming the gradient diffusion model for the mixing process leading to the approximate value of the diffusivity. DOE

N92-11328*# National Aeronautics and Space Administration. Lewis Research Center, Cleveland, OH.
EULER SOLUTIONS FOR AN UNBLADED JET ENGINE CONFIGURATION
Mark E. M. Stewart 1991 9 p Proposed for presentation at the 30th Aerospace Sciences Meeting and Exhibit, Reno, NV, 6-9 Jan. 1991; sponsored by AIAA
(NASA Order C-99066-G)
(NASA-TM-105332; ICOMP-91-23; E-6695; NAS 1.15:105332)
Avail: NTIS HC/MF A02 CSCL 20D

A Euler solution for an axisymmetric jet engine configuration without blade effects is presented. The Euler equations are solved on a multiblock grid which covers a domain including the inlet, bypass duct, core passage, nozzle, and the far field surrounding the engine. The simulation is verified by considering five theoretical properties of the solution. The solution demonstrates both multiblock grid generation techniques and a foundation for a full jet engine throughflow calculation. Author

N92-11118*# National Aeronautics and Space Administration. Langley Research Center, Hampton, VA.
A DETAILED INVESTIGATION OF STAGED NORMAL INJECTION INTO A MACH 2 FLOW
Dean R. Eklund, G. Burton Northam, and Roy J. Hartfield, Jr. (Virginia Univ., Charlottesville.) *In* JHU, The 27th JANNAF Combustion Subcommittee Meeting, Volume 3 Nov. 1990 p 115-129 (For primary document see N92-11117 02-20)
Avail: NTIS HC/MF A99 CSCL 20D

35 INSTRUMENTATION AND PHOTOGRAPHY

Includes remote sensors; measuring instruments and gages; detectors; cameras and photographic supplies; and holography.

For aerial photography see *43 Earth Resources and Remote Sensing*. For related information see also *06 Aircraft Instrumentation*, and *19 Spacecraft Instrumentation*.

N92-11329*# Santa Barbara Research Center, Goleta, CA.
MAPPING PHOTOPOLARIMETER SPECTROMETER INSTRUMENT FEASIBILITY STUDY FOR FUTURE PLANETARY FLIGHT MISSIONS Final Report
Oct. 1990 50 p
(Contract NAS5-30531)
(NASA-CR-189242; NAS 1.26:189242; SBRC-90-1045) Avail: NTIS HC/MF A03 CSCL 14B

Evaluations are summarized directed towards defining optimal instrumentation for performing planetary polarization measurements from a spacecraft platform. An overview of the science rationale for polarimetric measurements is given to point out the importance of such measurements for future studies and exploration of the outer planets. The key instrument features required to perform the needed measurements are discussed and applied to the requirements for the Cassini mission to Saturn. The resultant conceptual design of a spectro-polarimeter photometer for Cassini is described in detail. Author

N92-11330# Argonne National Lab., IL.
CALORIMETRY MEASUREMENTS IN LESS THAN 20 MINUTES
R. B. Perry and T. Cremers 1991 5 p Presented at the 32nd Institute of Nuclear Materials Management (INMM) Annual Meeting, New Orleans, LA, 28-31 Jul. 1991 Prepared in cooperation with Los Alamos National Lab., NM
(Contracts W-31-109-eng-38; W-7405-eng-36)
(DE91-017318; ANL/CP-71984; CONF-910774-76) Avail: NTIS HC/MF A01

Argonne National Laboratory has developed a new series of 10 watt Bulk Plutonium Assay Calorimeters (BPAC10). The calorimeter measures bulk samples of plutonium bearing material in containers up to 5 in. in diameter and 7 in. high. The average measurement time is 19.7 minutes compared to 2-9 hours for the same sample measured in a water bath calorimeter. Measurement precision in the range of 1-10 watts is 1 to 0.1 percent and it is 0.010 watt for sample power less than 1 watt. The BPAC10 series calorimeters are in use in two plutonium facilities at the EG&G Rocky Flats Plant and at the Los Alamos National Laboratory TA55 Plutonium Facility. The paper presents a description of the calorimeter, discusses operating experience at Los Alamos, and presents a comparison of data on typical samples measured with both types of calorimeters. DOE

N92-11331*# Radiation Monitoring Devices, Inc., Watertown, MA.
SOLID STATE NEUTRON DOSIMETER FOR SPACE APPLICATIONS Final Report
Gerald Entine, Vivek Nagargar, and Daud Sharif 17 Aug. 1990 23 p
(Contract NAS9-18328)
(NASA-CR-185633; NAS 1.26:185633) Avail: NTIS HC/MF A03 CSCL 14B

Personnel engaged in space flight are exposed to significant flux of high energy neutrons arising from both primary and secondary sources of ionizing radiation. Presently, there exist no compact neutron sensor capable of being integrated in a flight instrument to provide real time measurement of this radiation flux. A proposal was made to construct such an instrument using special PIN silicon diode which has the property of being insensitive to the other forms of ionizing radiation. Studies were performed to determine the design and construction of a better reading system to allow the PIN diode to be read with high precision. The physics of the device was studied, especially with respect to those factors which affect the sensitivity and reproducibility of the neutron response. This information was then used to develop methods to achieve high sensitivity at low neutron doses. The feasibility was shown of enhancing the PIN diode sensitivity to make possible the measurement of the low doses of neutrons encountered in space flights. The new PIN diode will make possible the development of a very compact, accurate, personal neutron dosimeter. Author

N92-11332*# Columbia Univ., New York, NY. Astrophysics Lab.
DEVELOPMENT OF A HIGH RESOLUTION LIQUID XENON IMAGING CHAMBER FOR GAMMA-RAY ASTRONOMY Final Technical Report, 1 May 1988 - 30 Apr. 1990
Elena Aprile Oct. 1991 31 p
(Grant NAGw-1370)
(NASA-CR-188994; NAS 1.26:188994; CAL-1922) Avail: NTIS HC/MF A03 CSCL 14B

The objective was to develop the technology of liquid xenon (LXe) detectors for spectroscopy and imaging of gamma rays from astrophysical sources emitting in the low to medium energy regime. In particular, the technical challenges and the physical processes relevant to the realization of the LXe detector operated as a Time Projection Chamber (TPC) were addressed and studied. Experimental results were obtained on the following topics: (1) long distance drift of free electrons in LXe (purity); (2) scintillation light yield for electrons and alphas in LXe (triggering); and (3) ionization yield for electrons and gamma rays in LXe (energy resolution). The major results from the investigations are summarized. Author

N92-11333# Virginia Univ., Charlottesville. Dept. of Electrical Engineering.
DISTRIBUTED SENSOR SYSTEM DECISION ANALYSIS USING TEAM STRATEGIES Final Report, Feb. 1988 - Jan. 1989
Howard C. Choe and Dimitri Kazakos Jul. 1991 145 p
(Contract F30602-81-C-0169)
(AD-A240250; RL-TR-91-116) Avail: NTIS HC/MF A07 CSCL 17/11

A distributed (or decentralized) multiple sensor system is considered under binary hypothesis environments. The system is deployed with a host sensor and multiple slave sensors. All sensors have their own independent decision makers (DM) which are capable of declaring local decisions based only on their own observation of the environment. The communication between the host sensor (HS) and the slave sensors (SS) is conditional upon the host sensor's command. Each communication that takes place involves a communication cost which plays an important role in approaches taken in this study. The conditional communication with cost initiates the team strategy in making the final decisions at the host sensor. The objectives are not only to apply the team strategy method in the decision making process, but also to minimize the expected system cost (or the probability or error in making decisions) by optimizing thresholds in the host sensor. The analytical expression of the expected system cost is numerically evaluated for Gaussian statistics over threshold locations in the host sensor to find an optimal threshold location for a given communication cost. The computer simulations of various sensor systems for Gaussian observations are also performed to understand the behavior of each system with respect to correct detections, false alarms, and target misses.
Author (GRA)

N92-11334# Naval Research Lab., Washington, DC.
LINEAR THEORY OF A QUASIOPTICAL GYROKLYSTRON WITH NONUNIFORM MAGNETIC FIELD Memorandum Report
R. P. Fischer, W. M. Manheimer, T. A. Hargreaves, and A. W. Fliflet 3 Sep. 1991 26 p
(AD-A240264; NRL-MR-6881) Avail: NTIS HC/MF A03 CSCL 09/1

A linear analysis of a two-resonator quasioptical gyroklystron is presented which examines the effect of the experimental magnetic field profile and velocity spread of the electron beam. The slow time scale equations of motion are used to determine the effect of a magnetic field taper in the prebunching resonator. Velocity spread is considered by calculating the linear efficiency in the presence of gyrophase mixing in the drift region. The linear efficiency can be made independent of velocity spread to first order by detuning the cyclotron frequencies in the two resonators.
GRA

N92-11335# Naval Research Lab., Washington, DC.
TILTED RESONATOR EXPERIMENTS ON A QUASIOPTICAL GYROTRON Memorandum Report
T. A. Hargreaves, A. W. Fliflet, R. P. Fischer, M. L. Barsanti, and W. M. Manheimer 16 Sep. 1991 27 p
(AD-A240680; NRL-MR-6887) Avail: NTIS HC/MF A03 CSCL 09/5

Tilting the resonator axis slightly with respect to the magnetic field axis in the quasioptical gyrotron (QOG) is predicted to greatly enlarge the parameter space available for stable, single-mode operation. Greater interaction efficiency is also predicted for single-mode operation. A resonator with a 2 degree tilt has been tested on the QOG experiment. The operation of this resonator has been compared to an untilted, but otherwise identical resonator. Multimode operation of the two resonators was very similar, in contrast to predictions. However, an output power of 600 kW was produced at an efficiency of 8 percent and a frequency of 120 GHz. At lower power, efficiencies above 12 percent were observed. The efficiency of single-mode operation appears to be raised significantly by tilting the resonator axis. GRA

N92-11336*# National Aeronautics and Space Administration. Langley Research Center, Hampton, VA.
SCHLIEREN SYSTEM FOR VISUALIZING THE FLOW WITHIN A PIPE OF CIRCULAR CROSS-SECTION Patent Application
Robert C. Costen, inventor (to NASA), David B. Rhodes, inventor (to NASA), and Stephen B. Jones, inventor (to NASA) 15 Aug. 1991 14 p

(NASA-Case-LAR-13944-1; NAS 1.71:LAR-13944-1; US-Patent-Appl-SN-747152) Avail: NTIS HC/MF A03 CSCL 14B

An on-axis Schlieren system is provided for visualizing the flow within a straight pipe having a circular cross-section. A point source is directed through a collimator to produce a parallel beam of light. A first convergent cylindrical lens converges this exiting beam to a substantially parallel beam which then passes through a reverse collimator and is focused back to a light point. A knife edge is perpendicularly oriented relative to the axis of symmetry of the pipe to block a portion of the light. The unblocked portion of light is then focused and projected into a viewing sensor or film for visualization. The two convergent cylindrical lenses may be replaced by either a single double strength convergent cylindrical lens located between the collimator and the test cell or a single double strength convergent cylindrical lens located between the test cell and the reverse collimator. NASA

N92-11337# Ecole Nationale Superieure des Telecommunications, Paris (France). Groupe Optique.
CONOSCOPIC HOLOGRAPHY. 1: BASIC PRINCIPLES AND PHYSICAL BASIS. 2: RIGOROUS DERIVATION
Gabriel Y. Sirat 7 Feb. 1991 96 p Submitted for publication
(TELECOM-Paris-91-C-001; ISSN-0751-1337; ETN-91-90115) Copyright Avail: NTIS HC/MF A05

A simplified version of the theory of conoscopic holography is presented. The Point Spread Function (PSF) and the transfer function of the conoscopic system are developed using simple arguments, and the conoscopic hologram is defined. The basic schemes for reconstructing (i.e., retrieving, optically or numerically) this three dimensional information about the object from the recorded hologram is presented. The resolution of the system is quantified. ESA

N92-11338*# Lockheed Engineering and Sciences Co., Hampton, VA.
ATTITUDE IDENTIFICATION FOR SCOLE USING TWO INFRARED CAMERAS Interim Report
Joram Shenhar Washington NASA Oct. 1991 64 p
(Contract NAS1-19000)
(NASA-CR-4397; NAS 1.26:4397) Avail: NTIS HC/MF A04 CSCL 14E

An algorithm is presented that incorporates real time data from two infrared cameras and computes the attitude parameters of the Spacecraft COntrol Lab Experiment (SCOLE), a lab apparatus representing an offset feed antenna attached to the Space Shuttle by a flexible mast. The algorithm uses camera position data of three miniature light emitting diodes (LEDs), mounted on the SCOLE platform, permitting arbitrary camera placement and an on-line attitude extraction. The continuous nature of the algorithm allows identification of the placement of the two cameras with respect to some initial position of the three reference LEDs, followed by on-line six degrees of freedom attitude tracking, regardless of the attitude time history. A description is provided of the algorithm in the camera identification mode as well as the mode of target tracking. Experimental data from a reduced size SCOLE-like lab model, reflecting the performance of the camera identification and the tracking processes, are presented. Computer code for camera placement identification and SCOLE attitude tracking is listed. Author

N92-11339*# Georgia Inst. of Tech., Atlanta.
MEASUREMENT OF FREQUENCY RESPONSE IN SHORT THERMOCOUPLE WIRES Progress Report, May - Oct. 1991
L. J. Forney, E. L. Meeks, and J. Ma Nov. 1991 29 p
(Contract NCC3-135)
(NASA-CR-187821; NAS 1.26:187821) Avail: NTIS HC/MF A03 CSCL 14B

Experimental measurements are made for the steady-state frequency response of a supported thermocouple wire. In particular, the effects of axial heat conduction are demonstrated for both a supported one material wire (type K) and a two material wire (type T) with unequal material properties across the junction. The data for the amplitude ratio and phase angle are correlated to within 10 percent with the theoretical predictions of Fralick and Forney (1991). This is accomplished by choosing a natural frequency omega(sub n) for the wire data to correlate the first order response at large gas temperature frequencies. It is found that a large bead size, however, will increase the amplitude ratio at low frequencies but decreas the natural frequency of the wire. The phase angle data are also distorted for imperfect junctions. Author

N92-11340*# National Aeronautics and Space Administration. Langley Research Center, Hampton, VA.
TECHNIQUE FOR CALIBRATING ANGULAR MEASUREMENT DEVICES WHEN CALIBRATION STANDARDS ARE UNAVAILABLE
Tom D. Finley Aug. 1991 19 p
(NASA-TM-104148; NAS 1.15:104148) Avail: NTIS HC/MF A03 CSCL 14B

A calibration technique is proposed that will allow the calibration of certain angular measurement devices without requiring the use of absolute standard. The technique assumes that the device to be calibrated has deterministic bias errors. A comparison device must be available that meets the same requirements. The two devices are compared; one device is then rotated with respect to the other, and a second comparison is performed. If the data are reduced using the described technique, the individual errors of the two devices can be determined. Author

36 LASERS AND MASERS

Includes parametric amplifiers.
For related information see also *76 Solid-State Physics.*

N92-11341*# Laser Photonics, Inc., Bedford, MA. Analytics Div.
LONG WAVELENGTH SEMICONDUCTOR LASERS DEVELOPMENT FOR INFRARED HETERODYNE APPLICATIONS Final Report
Zeev Feit and Douglas Kostyk 15 Dec. 1989 13 p
(Contract NAS5-30445)
(NASA-CR-189243; NAS 1.26:189243) Avail: NTIS HC/MF A03 CSCL 20E

PbSnTe single crystals were grown in a new 3 zone furnace. Molecular beam epitaxy (MBE) growth parameters have been established, including beam flux vs. temperature, and growth rates and dopant vs. PbTe flux ratios for the various effusion sources involved. Lattice matching studies were conducted and doping studies were completed. Broad area Pb(1-x)Sn(x)Te double heterostructure lasers were fabricated with active layer compositions up to x equals 0.04 at percent Sn in the active layers. Electrical and optical test data are presented. Author

N92-11342 National Physical Lab., Teddington (England). Div. of Quantum Metrology.
FEASIBILITY STUDY ON THE COLD HYDROGEN MASER (CHM)
Ruzbeh Mossavati Apr. 1991 23 p
(NPL-QU-89; ISSN-0309-3050; ETN-91-99865) Copyright Avail: National Physical Lab., Teddington, Middlesex TW11 OLW, England

The feasibility of assembling and operating a Cold Hydrogen Maser (CHM) is discussed. The hydrogen maser is the most stable of all atomic frequency standards for short and intermediate measuring times. A survey of frequency stabilities is given and the principle of the CHM is considered. The advantages of a low temperature operation and the basic elements of the CHM are looked into. Suggestions for research are given. ESA

N92-11343# Department of the Navy, Washington, DC.
ANTIRESONANT NONLINEAR MIRROR FOR PASSIVE LASER MODE LOCKING Patent Application
Irl Duling, inventor (to Navy) and Thomas F. Carruthers, inventor

(to Navy) 28 Dec. 1990 14 p
(AD-D014951; US-Patent-Appl-SN-635016) Avail: NTIS HC/MF A03 CSCL 20/6

The present invention relates in general to nonlinear mirrors, and in particular to antiresonant nonlinear mirrors for passive mode locking of lasers which do not require active length stabilization. GRA

N92-11344# Lawrence Livermore National Lab., CA.
TRENDS IN LASER-PLASMA-INSTABILITY EXPERIMENTS FOR LASER FUSION
R. P. Drake (California Univ., Davis.) Jun. 1991 13 p Presented at the International Conference on Research Trends in Inertial Confinement Fusion, La Jolla, CA, 4-6 Feb. 1991
(Contract W-7405-eng-48)
(DE91-016923; UCRL-JC-105909; CONF-910247-3) Avail: NTIS HC/MF A03

Laser plasma instability experiments for laser fusion have followed three developments. These are advances in the technology and design of experiments, advances in diagnostics, and evolution of the design of high-gain targets. This paper traces the history of these three topics and discusses their present state. Today one is substantially able to produce controlled plasma conditions and to diagnose specific instabilities within such plasmas. Experiments today address issues that will matter for future laser facilities. Such facilities will irradiate targets with approx. 1 MJ of visible or UV light pulses that are tens of nanoseconds in duration, very likely with a high degree of spatial and temporal incoherence. DOE

N92-11345# California Univ., Santa Barbara. Dept. of Electrical and Computer Engineering.
ELECTRON ACCELERATION BY LASER FIELDS IN A GAS
J. R. Fontana 1 Sep. 1991 14 p
(Contract DE-FG03-90ER-40545)
(DE91-018477; DOE/ER-40545/T1) Avail: NTIS HC/MF A03

The strong fields lasers can produce allow high energy acceleration of charged particles. As the phase velocity of the fields cannot be matched in vacuum to the particle velocity, cumulative interaction over arbitrarily long straight trajectories is impossible. However, over limited regions a large energy gain as well as considerable focusing action can be achieved with suitably shaped laser beams. Away from boundaries, all laser fields consist of superpositions of plane wave components. We describe the properties of several practical configurations, beginning with a single plane wave. Only straight particle trajectories are considered in this analysis and it is assumed the energy is large enough so their speed is nearly constant and very close to that of light. The particles considered are electrons. The physical limitation of the interaction region may be obtained by reflecting surfaces which generate no evanescent waves, with the electron beam crossing the boundaries through holes small enough not to disturb the fields. The laser power density over these reflectors could impose a practical limit to field intensity in the interaction region. An alternative way to limit the interaction range is by bending magnets to deflect the electrons; but the energy radiated must then be taken into consideration. In the rest of this paper, no further discussion is given of interaction region boundaries, although they must be present in every case. This paper contains a quantitative analysis of the acceleration and focusing properties of a particular laser configuration, and discusses means of extending the useful interaction range by phase compensation surfaces. DOE

N92-11346# SRI International Corp., Menlo Park, CA.
NOVEL NONLINEAR LASER DIAGNOSTIC TECHNIQUES
Annual Technical Report, 1 Jun. 1990 - 31 May 1991
Gregory W. Faris, Jay B. Jeffries, and D. L. Huestis 26 Jun. 1991 35 p
(Contract F49620-90-C-0044)
(AD-A240193; SRI-MP-91-160; AFOSR-91-0706TR) Avail: NTIS HC/MF A03 CSCL 09/3

This report describes research on novel laser-based diagnostic techniques in two areas: (1) extension of laser-based diagnostics to shorter wavelengths, allowing two-photon detection of atomic ions; and (2) investigation of the feasibility of obtaining quantitative concentration and velocity measurements using amplified spontaneous emission (ASE). For the first task, we have developed a high power VUV source based on two-photon-resonant difference frequency mixing of a ArF excimer laser and a frequency-doubled Nd:YAG-pumped dye laser in krypton gas. Up to 6 micro-J at 147 nm have been generated, and the characteristics of the mixing process have been studied. On the second task, we have performed the first measurement of the ASE bandwidth, indicating that temperature and velocity measurements may be possible. Measurement of ASE in a variety of flames demonstrate that the ASE signal intensity can be influenced by gas collisions. GRA

N92-11347 Department of the Navy, Washington, DC.
LASER DIODE PUMPED, ERBIUM-DOPED, SOLID STATE LASER WITH HIGH SLOPE EFFICIENCY Patent
Leon Esterowitz, inventor (to NAVY), Roger E. Allen, inventor (to NAVY), and Gregory J. Kintz, inventor (to Navy) 7 May 1991 7 p Filed 31 Oct. 1989 Supersedes AD-D014482
(AD-D014968; US-Patent-5,014,279; US-Patent-Appl-SN-429426)
Avail: US Patent and Trademark Office CSCL 09/3

A laser and method for producing a laser emission at a wavelength of substantially 2.8 microns is disclosed. In a preferred embodiment of the invention, the laser comprises laser diode means for emitting a pump beam at a preselected wavelength; a crystal; and a laser cavity defined by first and second reflective elements at opposing ends of the crystal to form a reflective path there between. The crystal has a preselected host material doped with a predetermined percent concentration of erbium activator ions sufficient to produce a laser emission at substantially 2.8 microns when the crystal is pumped by the laser diode means. A portion of the laser emission at substantially 2.8 microns is outputted from one of the first and second reflective elements at a slope efficiency of at least 5 percent, but preferably 10 percent, when the crystal is pumped by the pump beam. GRA

N92-11348# Lawrence Livermore National Lab., CA.
IRRADIANCE COMPENSATION CONTROL FOR HIGH-ENERGY LASER PROPAGATION, PART 2
D. T. Gavel 18 Apr. 1991 17 p
(Contract W-7405-eng-48)
(DE91-018489; UCRL-ID-107112-Pt-2) Avail: NTIS HC/MF A03

The quality of propagated Laser light strongly depends on the degree of phase uniformity across the beam at its source. When propagating through turbulent atmosphere, a Strehl ratio of nearly 0.9 is possible if phase correction is made at all spatial scales greater than approx. r sub o, the Fried atmospheric cell size. Therefore r sub o is a reasonable choice for actuator spacing on the phase compensating adaptive optics. However, analysis of high energy laser propagation has shown that a control law designed to compensate only for atomspheric index fluctuations will drive thermal blooming instabilities. Small initial perturbations in beam irradiance will grow exponentially until the beam breaks up. Therefore it is necessary also to compensate for irradiance perturbations at the same spatial scale as the compensation for phase. Combined phase and irradiance compensation of an HEL has been shown to be stable in theory. Irradiance control can be accomplished with a pair of deformable mirrors spaced apart over a propagation path. Laser light reflected off of the first deformable mirror surface at z = 0 will result in magnitude perturbations some distance away at z = L. The second deformable mirror then recollimates the light. The purpose of simulating the irradiance compensation system is to test the baseline design in such a way that the effect of discrete actuator/sensors and beam edge effects is taken into account in a more realistic manner than can be performed by a 2-D fourier analysis. DOE

N92-11349# Korea Advanced Energy Research Inst., Daeduk (Republic of Korea).
STUDIES ON LASER ATOMIC SPECTROSCOPY
Jong Min Lee, Young Gie Ohr, and Byung Heon Cha (Korea

Advanced Energy Research Inst., Daeduk, Republic of Korea) Jan. 1990 145 p In KOREAN
(DE91-628172; KAERI/RR-830/89) Avail: NTIS HC/MF A07

Laser atomic spectroscopy has been studied both theoretically and experimentally. In the theoretical parts, the energy levels and the transition probabilities of Hg atom were calculated by using MCDF (Multi-Configuration Dirac-Fork) code which considered the relativistic effect of electrons in Hg atom. Also, theoretical studies on the interactions between atom and atom or between atom and photon, and collisional dynamics have been carried out. In the experimental parts, the equipments used in the first year (1988) such as a Q-switched Nd:YAG laser, a high power tunable dye laser, a vacuum system, an ionization cell, and an ion current detection system have been improved in order to execute resonant multiphoton ionization (RMPI) efficiently. The RMPI characteristics in Hg atoms have been measured and analyzed. AC stark shifts, linewidth changes, and nonlinearity for the four photon resonant five photon ionization (4+1) and the two photon resonant three photon ionization (2+1) processes are observed, and autoionization level was detected by the double resonant process which was caused by the AC stark shift in the (4+1) process. Using those results, we have estimated the optimum conditions to ionize atoms efficiently. DOE

N92-11350# Brookhaven National Lab., Upton, NY.
REDUCTION OF FEL GAIN DUE TO WIGGLER ERRORS
L. H. Yu, S. Krinsky, A. Friedman, R. L. Gluckstern, and J. B. J. vanZeijts (Maryland Univ., College Park.) 1991 10 p Presented at the 13th International Free-Electron Laser (FEL) Conference, Santa Fe, NM, 25-30 Aug. 1991
(Contract DE-AC02-76CH-00016)
(DE92-000482; BNL-46582; CONF-9108118-7) Avail: NTIS HC/MF A02

For an FEL operating in the exponential regime before saturation, we consider the effect on the gain of longitudinal velocity variations arising from wiggler field errors. The average gain reduction and the width of the output power distribution are expressed in terms of the mean square average of the ponderomotive phase shift per gain length. A scheme for correcting the electron trajectory using position monitors and dipole correctors is analyzed. Analytic results are compared with numerical simulations. Our work is directly applicable to the design of FEL amplifiers and the results are encouraging for the feasibility of such devices. DOE

N92-11351# Brookhaven National Lab., Upton, NY.
THE EFFECT OF WIGGLER ERRORS ON FEL GAIN
L. H. Yu, S. Krinsky, R. L. Gluckstern, and J. B. J. vanZeijts (Maryland Univ., College Park.) 1991 34 p Presented at the 13th International Free-Electron Laser (FEL) Conference, Santa Fe, NM, 25-30 Aug. 1991
(Contract DE-AC02-76CH-00016)
(DE92-000483; BNL-46608; CONF-9108118-8) Avail: NTIS HC/MF A03

For a free electron laser (FEL) operating in the exponential regime before saturation, we present an analytic description of the effect on the gain of longitudinal velocity variations arising from wiggler field errors. The average gain reduction and the width of the output power distribution are expressed in terms of the mean square average of the ponderomotive phase shift per gain length. A scheme for correcting the electron trajectory using position monitors and dipole correctors is analyzed. Our work is directly applicable to the design of FEL amplifiers and the results are encouraging for their feasibility. DOE

37 MECHANICAL ENGINEERING

Includes auxiliary systems (nonpower); machine elements and processes; and mechanical equipment.

N92-11352# Southwest Research Inst., San Antonio, TX. Dept. of Engine and Vehicle Research.
PISTON TEMPERATURE MEASUREMENT IN A NATURAL GAS ENGINE Topical Report, Jan. - Dec. 1990
R. W. Burrahm and J. K. Davis Apr. 1991 40 p Original contains color illustrations
(Contract GRI-5089-293-1848)
(PB91-194357; SWRI-3178-1.6.1; GETA-91-02; GRI-91/0070)
Avail: NTIS HC/MF A03 CSCL 13I

The objective was to determine piston operating temperatures in a high-output natural gas-fueled 454 Chevrolet engine using a Southwest Research Institute (SwRI) developed telemetry-based system and to perform validation testing to verify the effect of piston cooling on engine durability. The projects was part of a program to develop a cost effective natural gas-fueled prime mover in the 300 hp range. The problem of piston cracking with the development piston in this natural gas engine can be overcome if sufficient data is accumulated to allow a better piston to be designed. Adequate piston temperature data are prerequisite to performing finite element analysis (FEA) modeling during the design of new pistons. The particular project was directed at obtaining this data as well as exploring the effects of piston cooling and operating conditions on piston temperatures. Piston temperature data was obtained at various engine speeds and loads including 300 hp at 3,600 rpm. Crown temperatures were recorded in excess of 500 F while piston pin boss and skirt temperatures remained at or below 300 F. The effects of limited piston cooling were explored at 300 hp. At low piston cooling oil flow rates, no decrease in piston crown temperatures were observed. Author

N92-11353# Argonne National Lab., IL. Energy Systems Div.
COMPONENT COST ANALYSIS FOR COMPRESSED NATURAL GAS VEHICLES
J. B. Rajan and R. R. Sekar Jun. 1991 25 p
(Contract W-31-109-eng-38)
(DE91-017230; ANL/ESD/TM-18) Avail: NTIS HC/MF A03

Use of compressed natural gas (CNG) fuel in engine applications dominated by gasoline and diesel fuels has well known advantages. It is a clean burning, low cost fuel available from domestic sources. In addition, a pipeline distribution infrastructure already exists in the United States. Although the cost of converting a small number of gasoline or diesel powered vehicles for CNG use is generally known, no estimates have been published for the cost of producing a large number of these vehicles. Only the costs of converting or producing gasoline vehicles able to operate on dual fuels (gasoline and CNG) were considered in this study. Cost estimates of the various components needed to convert light duty gasoline vehicles to dual fuel vehicles were obtained and consolidated under the following three categories: CNG cylinders, interface kits, and installation labor. An economies-of-scale model was used to fit the data gathered from the various sources, and total cost premium curves were generated for the production of CNG vehicles. The results indicate that, at production levels of 50000 to 100000 units, a cost premium of $600 to $800 per vehicle would be incurred. DOE

N92-11354*# National Aeronautics and Space Administration. Langley Research Center, Hampton, VA.
BLIND FASTENING APPARATUS Patent Application
Norman F. Willey, inventor (to NASA) and James F. Linker, inventor (to NASA) 8 Aug. 1991 14 p
(NASA-Case-LAR-14542-1; NAS 1.71:LAR-14542-1; US-Patent-Appl-SN-743489) Avail: NTIS HC/MF A03 CSCL 13K

An anchor nut insert is provided having external threads for engaging an internally threaded receptacle of a fixture to be installed. The fixture also has two side wings flanking the receptacle and having fastener holes. An insert driver is provided having a projecting blade which engages a slot in the anchor nut insert for

driving the insert. A guide member, such as a wire, passes through symmetry axes of the anchor nut insert and insert driver such that the anchor nut insert is located between the inser driver and a first terminal end of the guide wire. A swag is provided on this terminal end to prevent the anchor nut insert and insert driver from sliding off the end. The fixture with the installed anchor nut insert is fed through the central hole in a structure wall having a blind side. The fixture is rotated until the wing holes are aligned with side holes in the wall and then the fixture is pulled flush against the blind side via the guide wire. Fasteners are then inserted through the hole and the anchor nut insert removed via the driver, exposing the fixed threaded receptacle for engagement as desired. NASA

N92-11355# Sandia National Labs., Albuquerque, NM.
MELTING EFFICIENCY IN FUSION WELDING
P. W. Fuerschbach 1991 29 p Presented at the Fall Meeting of the Minerals, Metals, and Materials Society of AIME and Materials Week of the American Society of Metals, Cincinnati, OH, 20-24 Oct. 1991
(Contract DE-AC04-76DP-00789)
(DE91-017988; SAND-91-1326C; CONF-911003-9) Avail: NTIS HC/MF A03

Basic to our knowledge of the science of welding is an understanding of the melting efficiency, which indicates how much of the heat deposited by the welding process is used to produce melting. Recent calorimetric studies of GTAW, PAW, and LBW processes have measured the net heat input to the part thereby quantifying the energy transfer efficiency and in turn permitting an accurate determination of the melting efficiency. It is indicated that the weld process variables can dramatically affect the melting efficiency. This limiting value is shown to depend on the weld heat flow geometry as predicted by analytical solutions to the heat flow equation and as demonstrated by the recent empirical data. A new dimensionless parameter is used to predict the melting efficiency and is shown to correlate extremely well with recent empirical data. This simple prediction methodology is notable because it requires only a knowledge of the weld schedule and the material properties in order to estimate melting efficiency. DOE

N92-11356# Department of the Navy, Washington, DC.
IN-LINE HYDRAULIC DASHPOT Patent Application
Paul E. Moody, inventor (to Navy) 25 Mar. 1991 16 p
(AD-D014955; US-Patent-Appl-SN-674638; Navy-Case-72996)
Avail: NTIS HC/MF A03 CSCL 13/7

An in-line hydraulic dashpot is disclosed that effectively decelerates the piston of a power cylinder by controllably choking off the oil which is providing pressure to the piston. The in-line hydraulic dashpot of the invention includes a valve spool member movable between an open and closed position along a fluid flow path that supplies oil to the power cylinder. An actuator rod is cooperative with the valve spool member and the piston shaft of the power cylinder to move the valve spool member between its open and closed positions. The in-line hydraulic dashpot eliminates the clashing of mechanical parts and eliminates the noise that would otherwise be generated. The in-line hydraulic dashpot of the present invention makes possible the adaptation of a fixed stroke power cylinder to applications that call for a variable stroke length. GRA

N92-11357# Coordinating Research Council, Inc., Atlanta, GA.
EFFECT OF GASOLINE OCTANE QUALITY ON VEHICLE ACCELERATION PERFORMANCE
Jul. 1991 70 p
(AD-A240433; CRC-574) Avail: NTIS HC/MF A04 CSCL 21/4

A study was conducted under the auspices of the Coordinating Research Council, Inc. (CRC) to assess the potential effects of gasoline octane quality on vehicle acceleration performance. Twelve participating laboratories, representing both the oil and the automotive industries, tested a total of 182 vehicles as part of the 1989 CRC Octane Number Requirement Survey. The vehicles consisted of 78 with electronic knock control systems and 104 without. All testing was performed using the 1989/1990 CRC Full Boiling Range Unleaded (FBRU) fuel series. The results showed that acceleration performance of vehicles with knock sensors was significantly affected by gasoline octane quality. Octane effects on acceleration performance were most pronounced at maximum-throttle (detent) conditions and at octane levels below the vehicles' octane requirements; however, some knock-sensor vehicles did show improved acceleration performance with fuels at octane levels above the octane number requirement. Acceleration performance in non-knock sensor vehicles was unaffected by octane quality. GRA

N92-11358*# Carnegie-Mellon Univ., Pittsburgh, PA. Robotics Inst.
LEVELING OF THE AMBLER WALKING MACHINE: A COMPARISON OF METHODS
Pablo GonzalezdeSantos, Peter V. Nagy, and William L. Whittaker
Jul. 1991 44 p
(Grant NAGw-1175)
(NASA-CR-189015; NAS 1.26:189015; AD-A240766;
CMU-RI-TR-91-13) Avail: NTIS HC/MF A03 CSCL 13/9

For orthogonally-decoupled machines, such as the AMBLER, power efficiency is contingent upon keeping the body level. There are several ways of accomplishing this, which trade-off approximations of the complete phenomena versus simplicity of the implementation. In this report the effectiveness of four different strategies are evaluated for body attitude control. One of these uses vertical actuations to level the body ignoring the secondary geometric effects. Two alternate methods actuate only the vertical axes, but additionally utilize part of the horizontal kinematic information to calculate the required vertical displacements. Another method actuates both the horizontal and vertical joints in order to obtain ideally correct kinematic motion, but at the cost of higher energy expenditure. In this document the simulation of these methods and their implementation on the AMBLER are reported. This research shows that leveling methods that use only the vertical axes are most appropriate. The Simple Z-axes leveling method works satisfactorily to level using only six concurrent motions, ignoring the complexity of higher order kinematic calculations. The Z-axes method that is derived from the All-axes method has the consequence that the body drops when these equations are used to tilt the body. The Isoaltitude method performs slightly better than the Simple Z-axes method, by maintaining constant body height during both leveling and tilting maneuvers. GRA

N92-11359*# National Aeronautics and Space Administration. Lyndon B. Johnson Space Center, Houston, TX.
QUICK APPLICATION/RELEASE NUT WITH ENGAGEMENT INDICATOR Patent Application
Jay M. Wright, inventor (to NASA) 13 Sep. 1991 18 p
(NASA-Case-MSC-21799-1; NAS 1.71:MSC-21799-1;
US-Patent-Appl-SN-759367) Avail: NTIS HC/MF A03 CSCL 13K

A composite nut is shown which permits a fastener to be inserted or removed from either side with an indicator of fastener engagement. The nut has a plurality of segments, preferably at least three segments, which are internally threaded, spring loaded apart by an internal spring, and has detents on opposite sides which force the nut segments into operative engagements with a threaded member when pushed in and release the segments for quick insertion or removal of the nut when moved out. When the nut is installed, end pressure on one of the detents presses the nut segments into operative engagement with a threaded member where continued rotation locks the structure together with the detents depressed to indicate positive locking engagement of the nut. On removal, counterclockwise rotation of the nut relieves the endwise pressure on the detents permitting internal springs to force the detents outward and allowing the nut segments to move outward and separate to permit quick removal of the fastener. NASA

N92-11360# Technische Univ., Berlin (Germany, F.R.). Inst. fuer Luft- und Raumfahrt.
DEVELOPMENT OF A PERSONAL COMPUTER PROGRAM FOR MILLING THE SHAPES OF WIND TURBINE BLADES. THEORY AND APPLICATION Thesis [ENTWICKLUNG EINES PC-PROGRAMMS ZUM FRAESEN DER FORMEN FUER WINDTURBINENBLAETTER: THEORIE UND ANWENDUNG]
Jens Paape 1990 75 p In GERMAN
(ILR-Mitt-243(1990); ETN-91-90204) Avail: NTIS HC/MF A04

A wind power installation is developed, which is characterized by its low costs, high quality, simple construction, ease of operation, and low maintenance costs. The profile is a special profile developed for low Reynolds number. The mill is a three axle mill. The general task can be divided into three groups: the development of a transition from profile to axle, the production of a personal computer program allowing the three dimensional coordinates of the rotor to be calculated and transformed into data records that can be treated by the mill, and the fabrication of the shapes and the production of the rotor blades. This program is to be modified so that it can be universally used in the fabrication of any rotor.
ESA

N92-11361*# Rockwell International Corp., Canoga Park, CA. Rocketdyne Div.
HYDRODYNAMIC DESIGN OF GENERIC PUMP COMPONENTS Final Technical Report, Jun. 1991
A. H. J. Eastland and H. C. Dodson 28 Jun. 1991 232 p
(Contract NAS8-38863)
(NASA-CR-184252; NAS 1.26:184252; RI-RD-91-193; Rept-91RC11706) Avail: NTIS HC/MF A11 CSCL 13I

Inducer and impellar base geometries were defined for a fuel pump for a generic generator cycle. Blade surface data and inlet flowfield definition are available in sufficient detail to allow computational fluid dynamic analysis of the two components.
Author

N92-11362# Sandia National Labs., Albuquerque, NM.
OVERLOOKED FUNDAMENTALS OF RESISTANCE WELDING
G. A. Knorovsky 1991 20 p Presented at the Fall Meeting of the Minerals, Metals, and Materials Society of AIME and Materials Week of the American Society of Metals, Cincinnati, OH, 20-24 Oct. 1991
(Contract DE-AC04-76DP-00789)
(DE91-018814; SAND-91-1756C; CONF-911003-15) Avail: NTIS HC/MF A03

Resistance Welding (RW) has been known for about a century and in common use for much of that time. Much knowledge has been accumulated concerning many aspects of the process. However, upon examining contemporary RW handbooks, a few subjects that have been overlooked were found. Usually, this oversight will not be important; however, when the RW process is being applied at its limits, these factors may become critical. In this paper we will discuss such overlooked factors as the Peltier and Thomson effects, and the dynamics of welding head motions and how they are affected by the current pulse. Examples taken from sheet metal and microwelding applications will be given as examples.
DOE

38 QUALITY ASSURANCE AND RELIABILITY

Includes product sampling procedures and techniques; and quality control.

N92-11363# Advanced Research and Applications Corp., Sunnyvale, CA.
A NEW RADIOGRAPHIC CORROSION INSPECTION CAPABILITY Final Report, Sep. 1985 - Apr. 1988
Robert N. Yancey and James H. Stanley 3 Feb. 1989 29 p
(Contract F33615-85-C-5151)
(AD-A231476; ARACOR-FR469-88; AFWAL-TR-88-4234) Avail: NTIS HC/MF A03 CSCL 14/4

Corrosion of equipment and material costs the Armed Forces billions of dollars each year. A need currently exists for a cost effective nondestructive inspection tool able to detect corrosion within military equipment. Dual Energy Radiography was proposed as a potential NDE corrosion inspection method. A program was undertaken to construct a preprototype dual energy scan system. An effective dual energy detector system was designed and fabricated, dual energy software was coded, and a complete dual energy system also capable of laminography was constructed. The results of this program are a fully operational preprototype Dual Energy/Laminography system.
Author

N92-11364# Industrial Quality, Inc., Gaithersburg, MD.
DEVELOPMENT OF DATA FILE STANDARDS FOR AUTOMATED ULTRASONIC SCANNING SYSTEMS. EXCHANGE METHODS FOR DIGITAL ULTRASONIC INSPECTION DATA Final Report, Jul. 1989 - Jul. 1991
Harold Berger, T. S. Jones, E. S. Gaynor, and T. M. Hsieh 26 Jul. 1991 55 p
(Contract N00019-89-C-0275)
(AD-A240075; IQI-F-91-0726) Avail: NTIS HC/MF A04 CSCL 12/5

Ultransonic scanning inspection data has been exchanged among an Automated Ultrasonic Scanning System (AUSS-V) unit at McDonnell Aircraft, a DuPont CalData system at the North Island Naval Aviation Depot (NADEP) and a Sigma system at the Cherry Point NADEP. The exchange of ultrasonic data for these three incompatible equipments has been accomplished using a neutral format medium compatible with the Standard for the Exchange of Product Model Data (STEP), the exchange specification now under development as the international specification for the exchange of all manufacturing and life cycle data. A commercial product for the exchange of digital nondestructive test data is planned.
GRA

N92-11365# Advanced Research and Applications Corp., Sunnyvale, CA.
SUPERVOLTAGE NDE TECHNIQUES FOR LARGE AEROSPACE STRUCTURES Final Report, Feb. 1989 - Jan. 1991
Paul D. Tonner and James H. Stanley Jul. 1991 49 p
(Contract F33615-88-C-5511)
(AD-A240625; ARACOR-FR-743-91; WL-TR-91-4036) Avail: NTIS HC/MF A03 CSCL 14/2

Innovative technical approaches for detecting and characterizing defects in aerospace structures like large solid rocket boosters or jet engines are urgently needed. Unfortunately, in fully assembled components, zones which are the most critical to system reliability are often the most inaccessible to standard examination techniques. A computed tomography (CT) system can provide excellent images of otherwise inaccessible areas but the size and opacity of large aerospace components preclude the use of even the most energetic industrial CT systems produced to date with power extended for the largest solid rocket boosters to peak energies in the 40- to 60-MV range. The use of these supervoltage energies for CT completes the logical extension since material attenuations begin to increase for higher energies. A Phase 1 effort verified the feasibility of the concept by resolving key questions relating to operation at supervoltage energies. The key objective of the Phase 2 program was to obtain a supervoltage CT image of an aerospace structure which, because of its size and opacity, could not be imaged with current CT technology. Supervoltage CT images of many configurations of a simulated 3.9-m-diameter, 12-mm steel case solid rocket booster, obtained on a pre-prototype supervoltage CT scanner specially designed for this purpose, conclusively demonstrate that supervoltage CT is feasible and completes the extension of CT to the highest possible X-ray energies. Furthermore, analysis of the supervoltage images provides convincing evidence that CT dynamic range, contrast sensitivity, and defect detectability are not dismissed, and may in some cases be enhanced, at supervoltage energies.
GRA

N92-11366# Army Engineer Waterways Experiment Station, Vicksburg, MS. Geotechnical Lab.
DEVELOPMENT OF A RELIABILITY-BASED METHOD FOR EVALUATING A PAVEMENT FEATURE Final Technical Report
William P. Grogan Jul. 1991 156 p
(AD-A240747; WES/TR/GL-91-14) Avail: NTIS HC/MF A08 CSCL 13/13

Nondestructive testing (NDT) is used to evaluate the structural capacity of in-place pavements. NDT is accomplished with the use of a falling weight deflectometer (FWD). The data obtained with the FWD are used to determine the modulus value of the layers in the pavement system. The modulus values are used to determine the structural capacity of the pavements in terms of allowable load, allowable passes, and overlay thickness requirements. Because NDT provides a means of rapidly testing a pavement, many tests are conducted on a pavement feature. Currently, the method for evaluating a pavement feature uses the mean NDT. This study was conducted to investigate the effect of using the mean NDT. The results of this investigation provide a statistical approach for evaluating a pavement feature using NDT procedures at a user-defined level of reliability. GRA

N92-11367# Netrologic, Inc., San Diego, CA.
ROBOTIC NON-DESTRUCTIVE INSPECTION OF AIRCRAFT, PHASE 1 Final Report
Joel Davis 5 Sep. 1991 39 p
(Contract N00014-91-C-0095)
(AD-A240777) Avail: NTIS HC/MF A03 CSCL 01/3

Non-Destructive Inspection (NDI) of aircraft is known to be a time consuming, boring, and an error prone task for human inspectors. A method is needed for looking (inspecting) at an aircraft without reliability problems due to boredom while minimizing aircraft total inspection time during the life of the aircraft. The application of robotics to the NDI of aircraft was investigated. It was found that it is feasible to transform the Navy's robotic deriveter to a neural network based NDI robot. A feedforward multilayer neural network was found to be very reliable at detecting cracks around rivets. In addition, an efficient new manipulator path planning method using neural networks was found to be useful for the robotic aircraft NDI. GRA

N92-11368# Lawrence Livermore National Lab., CA.
CONTINUUM X RAY GAUGING OF MULTIPLE-ELEMENT MATERIALS
D. L. Lewis, C. M. Logan, and M. R. Gabel (Minnesota Mining and Mfg. Co., Saint Paul.) Feb. 1991 6 p Presented at the American Society for Nondestructive Testing Spring Conference, Oakland, CA, 18-22 Mar. 1991
(Contract W-7405-eng-48)
(DE91-017429; UCRL-JC-104111-Rev-1; CONF-910399-3-Rev-1)
Avail: NTIS HC/MF A02

We have developed a system for elemental quantification of materials with known constituents. It utilizes an x ray tube to generate a photon spectrum and an energy dispersive detector to measure the photon transmission of a material at selected energies. The abundance of each element is then iteratively extracted using characteristic attenuation coefficients and the material bulk density and thickness. DOE

39 STRUCTURAL MECHANICS

Includes structural element design and weight analysis; fatigue; and thermal stress.

For applications see *05 Aircraft Design, Testing and Performance* and *18 Spacecraft Design, Testing and Performance.*

N92-11369# Sydney Univ. (Australia). Dept. of Aeronautical Engineering.
STUDIES IN THE FORM OF FINITE ELEMENT MASS MATRICES FOR BEAMS, PLATES AND SHELLS
J. R. Ghidella and G. P. Steven Jun. 1991 46 p
(Aero-TN-9101) Avail: NTIS HC/MF A03

A variety of different mass matrices are presented for beam and plate elements, and the resulting eigenvalues are compared which were obtained from each of the different mass matrices. From the results, it is clear that no one mass matrix formulation gives the correct results for natural frequencies. For beam elements, it was found that the consistent mass matrices give more accurate results, for the examples tested, than did the diagonal mass matrices. Noting that for the axial and torsional modes, the modified consistent mass matrix, whose axial and torsional terms are the average of the consistent and HRZ diagonal terms, gave the most accurate results. Whereas with the bending modes, the consistent and modified consistent mass matrices both give the most accurate results, remembering that the modified consistent has the same bending term as the consistent mass matrix. With the plate elements, the diagonal mass matrices seemed to produce the better values, even the lumped diagonal mass matrix, which has no rotational terms gave results that are as good as and sometimes better than the consistent mass matrices. Yet all plate element mass matrices needed high numbers of elements to produce accurate results. Author

N92-11370 National Physical Lab., Teddington (England). Div. of Materials Metrology.
APPROXIMATE LARGE DEFLECTION ANALYSIS OF CIRCULAR PLATES LOADED SYMMETRICALLY
D. H. Ferriss Apr. 1991 13 p
(NPL-DMM(A)-25; ISSN-0959-2423; ETN-91-99878) Copyright Avail: National Physical Lab., Teddington, Middlesex TW11 OLW, England

Equations describing the large deflection of circular plates subjected to transverse uniform and center point loading are oriented. Two types of edge boundary conditions are considered, one in which the disc edge is simply supported with zero in plain restraint and the other in which the edge is clamped with full in plane constraint. An approximate solution is determined using a Galerkin technique involving simple polynomial and logarithmic functions. Results are presented in terms of simple cubic design equations. ESA

N92-11371 Colorado Univ., Boulder.
A COMPUTATIONAL PROCEDURE FOR THE DYNAMICS OF FLEXIBLE BEAMS WITHIN MULTIBODY SYSTEMS Ph.D. Thesis
Janice Diane Downer 1990 217 p
Avail: Univ. Microfilms Order No. DA9123442

The dynamic analysis of 3-D elastic beams which experience large rotational and deformational motions are examined. The beam motion is modeled using an inertial reference for the translational displacements and a body fixed reference for the rotational quantities. Finite strain rod theories are then defined in conjunction with the beam kinematic description which accounts for the effects of stretching, bending, torsion, and transverse shear deformations. A convected coordinate representation of the Cauchy stress tensor and a conjugate strain definition is introduced to model the beam deformation. To treat the beam dynamics, a two stage change of the central difference algorithm is presented to integrate the translational coordinates and the application of an implicit integration algorithm to the Euler parameter/angular velocity kinematical relation. The combined developments of the objective internal force computation with the dynamic solution procedures result in the computational preservation of total energy for undamped systems. The present method is also intended to model the dynamics of deployment or retrieval of the flexible members. Dissert. Abstr.

N92-11372# Sandia National Labs., Albuquerque, NM.
MICROSTRUCTURAL EVOLUTION DURING THE THERMOMECHANICAL FATIGUE OF SOLDER JOINTS
D. R. Frear 1991 10 p Presented at the Fall Meeting of the Minerals, Metals, and Materials Society of AIME and Materials Week of the American Society of Metals, Cincinnati, OH, 20-24

Oct. 1991
(Contract DE-AC04-76DP-00789)
(DE91-017309; SAND-91-1461C; CONF-911003-8) Avail: NTIS HC/MF A02

Solder joints in electronic packages are electrical interconnections that also function as mechanical bonds. The solder often constrains materials of different coefficients of thermal expansion that, when thermal fluctuations are encountered, causes the solder joint to experience cyclical deformation. Due to the catastrophic consequences of electrical or mechanical failure of solder joints, a great deal of work has been performed to develop a better understanding of the metallurgical response of solder joints subjected to thermomechanical fatigue. This work reviews the microstructural and mechanical evolution that occurs in solder joints during thermomechanical fatigue. The eutectic Sn-Pb solder alloy is highlighted. Unlike most materials that experience thermomechanical fatigue, solder is commonly used at temperatures of up to nine-tenths of its melting point. Therefore extensive creep, solid state diffusion, recrystallization and grain growth occur in this alloy resulting in the evolution of a heterogeneous coarsened band through which failure eventually takes place. Two other solder alloys are compared with the Sn-Pb eutectic, a Pb-rich Sn-Pb alloy and a ternary near eutectic (40In-40Sn-20Pb, all alloys are given in wt. percent). The Pb-rich alloy is a precipitated single phase matrix that does not evolve during thermomechanical fatigue and subsequently has a shorter lifetime. Conversely, the 40In-40Sn-20Pb solder is a two phase eutectic in which the microstructures refines during thermomechanical fatigue giving it a longer lifetime than the eutectic Sn-Pb solder. The microstructural processes that occur during thermomechanical fatigue and final fracture behavior are discussed for the three solder alloys. DOE

N92-11373*# National Aeronautics and Space Administration. Lewis Research Center, Cleveland, OH.
FIRST-PASSAGE PROBLEMS: A PROBABILISTIC DYNAMIC ANALYSIS FOR DEGRADED STRUCTURES
Michael C. Shiao (Sverdrup Technology, Inc., Brook Park, OH.) and Christos C. Chamis 1990 17 p Presented at the 2nd International Conference on Stochastic Structural Dynamics, Boca Raton, FL, 9-11 May 1990
(NASA-TM-103755; E-6011; NAS 1.15:103755) Avail: NTIS HC/MF A03 CSCL 20K

Structures subjected to random excitations with uncertain system parameters degraded by surrounding environments (a random time history) are studied. Methods are developed to determine the statistics of dynamic responses, such as the time-varying mean, the standard deviation, the autocorrelation functions, and the joint probability density function of any response and its derivative. Moreover, the first-passage problems with deterministic and stationary/evolutionary random barriers are evaluated. The time-varying (joint) mean crossing rate and the probability density function of the first-passage time for various random barriers are derived. Author

N92-11374*# National Aeronautics and Space Administration. Langley Research Center, Hampton, VA.
CONDUCTIVE GAGE FOR CRACK LENGTH MEASUREMENT Patent Application
Ramamurthy Prabhakaran, inventor (to NASA) (Old Dominion Univ., Norfolk, VA.) and Osveldo F. Lopez, inventor (to NASA) 24 May 1991 22 p
(NASA-Case-LAR-14480-1-CU; NAS 1.71:LAR-14480-1-CU; US-Patent-Appl-SN-705474) Avail: NTIS HC/MF A03 CSCL 20K

The determination of crack lengths in an accurate and straight forward manner is very useful in studying and preventing load created flaws and cracks. A crack length sensor according to the present invention is fabricated in a rectangular or other geometrical form from a conductive powder impregnated polymer material. The long edges of the sensor are silver painted on both sides and the sensor is then bonded to a test specimen via an adhesive having sufficient thickness to also serve as an insulator. A lead wire is connected to each of the two outwardly facing silver painted edges. The resistance across the sensor changes as a function of the crack length in the specimen and sensor. The novel aspect of the present invention include the use of relatively uncomplicated sensors and instrumentation to effectively measure the length of generated cracks. NASA

N92-11375*# Akron Univ., OH. Dept. of Civil Engineering.
ON THE SYMBOLIC MANIPULATION AND CODE GENERATION FOR ELASTO-PLASTIC MATERIAL MATRICES Final Report
T. Y. Chang, A. F. Saleeb, P. S. Wang, and H. Q. Tan (Kent State Univ., OH.) Oct. 1991 29 p
(Grants NAG3-307; NAG3-298)
(NASA-CR-187223; NAS 1.26:187223) Avail: NTIS HC/MF A03 CSCL 20K

A computerized procedure for symbolic manipulations and FORTRAN code generation of an elasto-plastic material matrix for finite element applications is presented. Special emphasis is placed on expression simplifications during intermediate derivations, optimal code generation, and interface with the main program. A systematic procedure is outlined to avoid redundant algebraic manipulations. Symbolic expressions of the derived material stiffness matrix are automatically converted to RATFOR code which is then translated into FORTRAN statements through a preprocessor. To minimize the interface problem with the main program, a template file is prepared so that the translated FORTRAN statements can be merged into the file to form a subroutine (or a submodule). Three constitutive models; namely, von Mises plasticity, Drucker-Prager model, and a concrete plasticity model, are used as illustrative examples. Author

N92-11376# Aeronautical Research Labs., Melbourne (Australia).
CRITICAL APPRAISAL OF THE MCDONNELL DOUGLAS CLOSURE MODEL FOR PREDICTING FATIGUE CRACK GROWTH
M. J. Bos Sep. 1991 93 p
(ARL-STRUC-R-444; AR-006-626) Copyright Avail: NTIS HC/MF A05

The McDonnell-Douglas fatigue crack growth model CNTKM8 has been used to predict crack growth in Carbon-Carbon Technology (CCT) specimens with through cracks under four different load sequences, including a flight-by-flight sequence and two stress levels. The predictions were compared against experimental data. The results ranged from fairly good for the more structured sequences to rather poor for the more random sequences. The experimental trend of the structured sequences was not predicted correctly. An enhanced model was proposed and tested. The predictions of this model were more consistent with the experimental data, and the above mentioned experimental trend was also predicted correctly. Author

N92-11377*# Technion Research and Development Foundation Ltd., Haifa (Israel). Faculty of Aerospace Engineering.
MULTI-DISCIPLINARY OPTIMIZATION OF AEROSERVOELASTIC SYSTEMS Annual Report, 1 Oct. 1990 - 30 Sep. 1991
Mordechay Karpel 21 Oct. 1991 18 p
(Grant NAGw-1708)
(NASA-CR-188983; NAS 1.26:188983; Rept-160-573) Avail: NTIS HC/MF A03 CSCL 20K

New methods were developed for efficient aeroservoelastic analysis and optimization. The main target was to develop a method for investigating large structural variations using a single set of modal coordinates. This task was accomplished by basing the structural modal coordinates on normal modes calculated with a set of fictitious masses loading the locations of anticipated structural changes. The following subject areas are covered: (1) modal coordinates for aeroelastic analysis with large local structural variations; and (2) time simulation of flutter with large stiffness changes. Author

N92-11378*# Massachusetts Inst. of Tech., Cambridge. Dept. of Aeronautics and Astronautics.
ADVANCED STRESS ANALYSIS METHODS APPLICABLE TO TURBINE ENGINE STRUCTURES Final Report
Theodore H. H. Pian Oct. 1991 43 p
(Grant NAG3-33)
(NASA-CR-187235; NAS 1.26:187235) Avail: NTIS HC/MF A03 CSCL 20K

The following tasks on the study of advanced stress analysis methods applicable to turbine engine structures are described: (1) constructions of special elements which contain traction-free circular boundaries; (2) formulation of new version of mixed variational principles and new version of hybrid stress elements; (3) establishment of methods for suppression of kinematic deformation modes; (4) construction of semiLoof plate and shell elements by assumed stress hybrid method; and (5) elastic-plastic analysis by viscoplasticity theory using the mechanical subelement model. Author

N92-11379*# Akron Univ., OH. Dept. of Mechanical and Civil Engineering.
ENGINE DYNAMIC ANALYSIS WITH GENERAL NONLINEAR FINITE ELEMENT CODES Final Report
M. L. Adams, J. Padovan, and D. G. Fertis Oct. 1991 93 p
(Grant NsG-3283)
(NASA-CR-187222; NAS 1.26:187222) Avail: NTIS HC/MF A05 CSCL 20K

A general engine dynamic analysis as a standard design study computational tool is described for the prediction and understanding of complex engine dynamic behavior. Improved definition of engine dynamic response provides valuable information and insights leading to reduced maintenance and overhaul costs on existing engine configurations. Application of advanced engine dynamic simulation methods provides a considerable cost reduction in the development of new engine designs by eliminating some of the trial and error process done with engine hardware development. Author

N92-11380# California Univ., Los Angeles. Dept. of Civil Engineering.
FATIGUE CRACK INITIATION Final Technical Report
T. H. Lin 1991 25 p
(Contract N00014-86-K-0153)
(AD-A240196) Avail: NTIS HC/MF A03 CSCL 20/11

Partial contents include dependency of slip on resolved shear stress and previous theories; present micromechanic theory - - analog of inelastic strain and applied forces, initial stress field, gating mechanism provided by stress field, and supporting experimental observations; and research summaries on fatigue crack initiation under cyclic torsion, fatigue crack initiation under combined cyclic axial loading and torsion, interaction of two slip planes in fatigue crack initiation, interaction of fatigue and creep in high-cycle fatigue crack initiation, overload effect on the retardation of fatigue crack initiation, and fatigue crack initiation in ordered alloys. GRA

N92-11381# David Taylor Research Center, Bethesda, MD. Ship Materials Engineering Dept.
ANALYSIS OF STRAIN DEPENDENT DAMPING IN MATERIALS VIA MODELING OF MATERIAL POINT HYSTERESIS
E. J. Graesser and C. R. Wong Jul. 1991 72 p
(AD-A240298; DTRC/SME-91/34) Avail: NTIS HC/MF A04 CSCL 20/4

A constitutive relationship was used to model the cyclic material response of damping test samples in separate bending and torsion configurations. This was done in order to better understand variations in reported values of damping for materials possessing strain dependent characteristics. The constitutive equations are based on a model of shape memory alloy stress strain behavior and have been adapted especially for the study of nonlinear hysteresis and the problem of strain dependent damping. Experimental measurements and analytical material response analyses of separate bending and torsion test samples indicated that when the damping of a single nonlinear material is plotted against the one-dimensional local strain of the sample, results are produced which are difficult to compare. However, when the same results are plotted against an invariant measure of three dimensional distortion the means by which one may compare the data is more straightforward. Also, the approach allows for a quantitative comparison of the damping at a material point to the overall damping. The method can be applied to any homogeneous isotropic nonlinear damping material. GRA

N92-11382# Virginia Univ., Charlottesville.
LARGE DEFORMATION INDUCED FAILURES IN NONLINEAR SOLIDS Final Report, 1 Sep. 1989 - 31 Jul. 1991
Cornelius O. Horgan 31 Jul. 1991 10 p
(Grant AF-AFOSR-0470-89)
(AD-A240369; AFOSR-91-0751TR) Avail: NTIS HC/MF A02 CSCL 20/11

This work is concerned with the fundamental mechanics and mathematics of large deformation induced failures in nonlinear solids. The specific area investigated was that of void nucleation and growth due to large deformation in nonlinear solids. Research on cavitation phenomena, which serve as a precursor to fracture, is crucial to understanding failure mechanisms in rubber-like solids. (e.g., polymers, solid rocket propellants) and of ductile fracture processes in metals. Mathematically, the work involved investigation of singular solutions of the second-order quasilinear system of partial differential equations describing equilibrium states of nonlinearly elastic bodies. For radially symmetric deformations, the basic problem reduces to a bifurcation problem for a single second-order nonlinear ordinary differential equation. Particular emphasis was placed on the effect of material inhomogeneity, compressibility, and anisotropy on void nucleation and growth. Studies on the micromechanics of particles, in particular the correlation of inclusions to void formation, are receiving much attention from the solid mechanics, applied mathematics, and materials science communities. The work has impact on failure mechanisms due to large deformations in anisotropic and composite materials. Compared to the vast amount of information available on small deformations of such materials, results on large deformations remain virtually unexplored. Considerations of large deformations in anisotropic or composite materials often lead to striking differences from predictions of corresponding linearized theories. In view of the rapid utilization of advanced composite materials in present day Air Force technology, studies on the fundamental mechanics and mathematics of large deformations of such materials promise to have widespread impact on the AFOSR mission. GRA

N92-11383# Wright Lab., Wright-Patterson AFB, OH.
NONLINEAR ASPECTS OF AEROSPACE STRUCTURES AT HIGH EXCITATION LEVELS FLAT ALUMINUM BEAMS AND PLATES STUDIED Progress Report, Oct. 1989 - Sep. 1990
Howard F. Wolfe May 1991 61 p
(AD-A240600; WL-TM-91-311-FIBG) Avail: NTIS HC/MF A04 CSCL 13/13

Nonlinear multimodal response of flat aluminum clamped beams and plates was studied theoretically and experimentally together with associated signal processing effects. Theoretical models were evaluated to determine the various methods investigated and which methods might yield new information if further development with specific applications were pursued. The test methods and transducer suitability were carefully scrutinized. Beam tests were performed with sinusoidal and random excitation using a coil-magnet exciter. Clamped flat plate tests were performed using high intensity acoustic excitation from low levels to high levels. Data processing and analysis were investigated to determine their suitability. The hard spring nonlinearity or jump phenomena was apparent from the beam test results. The beam and plate were instrumented to separate the bending and axial components from the total strain. Displacement shapes of the beam were completed. The beam tests and the acoustic tests with the plate have been completed. GRA

N92-11384*# National Aeronautics and Space Administration. Langley Research Center, Hampton, VA.
METHOD OF RECERTIFYING A LOADED BEARING MEMBER USING A PHASE POINT Patent Application
Joseph S. Heyman, inventor (to NASA) 19 Jun. 1991 25 p
(NASA-CASE-LAR-14741-1; NAS 1.71:LAR-14741-1; US-Patent-Appl-SN-720153) Avail: NTIS HC/MF A03 CSCL 20K

A method of recertifying a load on a bearing member using a pulsed phase locked loop (P2L2) system is disclosed. A first tone burst signal with a corresponding first phase signal is generated in the bearing member in a first load condition. The sample/hold of the P2L2 is adjusted to a determined phase point on the first phase signal and then the P2L2 is locked at this phase period to determine a first load measurement. Next, the phase sample point is correlated with a corresponding position, w, on the first tone burst signal. A second tone burst with a corresponding second phase signal is then generated at some later time in the bearing member in a second load condition. The sample/hold is adjusted to the sample/hold phase point as before and then the output frequency of the P2L2 is adjusted until the sample/hold is positioned at the previously determined phase point corresponding to position w on th second tone burst signal. The P2L2 is then locked at this phase point to determine a frequency indicative of the load of the second loading condition. NASA

N92-11385# Technische Univ., Berlin (Germany, F.R.). Inst. fuer Luft- und Raumfahrt.
EXPERIMENTAL DETERMINATION OF THE MATERIAL PARAMETER OF TWO VISCOELASTIC SYNTHETIC MATERIALS, USING CREEP TESTS Thesis [EXPERIMENTELLE BESTMMUNG DER MATERIALPARAMETER ZWEIER VISKOELASTISCHER KUNSTSTOFFE MIT HILFE VON KRIECHVERSUCHEN]
Heike Jansen Jun. 1990 74 p In GERMAN
(ILR-Mitt-244(1990); ETN-91-90205) Avail: NTIS HC/MF A04

In the framework of a calculation in the field of rolling contact, requisite material parameters for two different viscoelastic materials, e.g., polyamide and thermoplastic polyurethane are to be determined. On account of the great number of influence factors on the material behavior of viscoelastic synthetic materials, many tests and experimental methods are required, in order to obtain a complete knowledge of material behavior. These tests allow only a statistical statement on material behavior. This complexity does not allow all influence factors to be taken into account. Essential influences are examined in order to obtain a fundamental insight into material behavior. In a quasistatic test, material parameters are obtained for different loads, and in a cyclical test the influence of initial loads is examined. ESA

N92-11386# Technische Univ., Berlin (Germany, F.R.). Isnt. fuer Luft- und Raumfahrt.
CALCULATION OF GENERAL SHELLS OF REVOLUTION, USING A SEMI ANALYTICAL PROCESS Thesis [ZUR BERECHNUNG ALLGEMEINER ROTATIONSSCHALEN MIT EINEM HALBANALYTISCHEN VERFAHREN]
Kim Kose 1991 33 p In GERMAN
(ILR-Mitt-262(1991); ETN-91-90208) Avail: NTIS HC/MF A03

A process is presented, which allows the static deformations and strains of shells of revolution to be calculated at relatively low cost. Contrary to ring elements from multipurpose finite element method programs, exact matrices are constructed for the static case, up to numerical inaccuracies. Using the procedure recommended it is possible to determine the homogeneous and particular cutting forces even inside the elements. Comparisons with results obtained analytically show excellent agreement. ESA

N92-11387*# Akron Univ., OH. Dept. of Civil Engineering.
LIMIT PRESSURE OF A CIRCUMFERENTIALLY REINFORCED SiC/Ti RING Final Report
D. N. Robinson and M. S. Pastor Oct. 1991 27 p
(Grant NAG3-379)
(NASA-CR-187211; NAS 1.26:187211) Avail: NTIS HC/MF A03 CSCL 20K

Limit loads under plane stress and plane strain are found for a circumferentially reinforced elastoplastic ring subjected to interior pressure. These are used as bounds on an estimate of the failure pressure of a SiC/Ti test rig that is being fabricated and tested. The ring is to serve as a benchmark against which deformation and failure analysis methods can be assessed. An anisotropic perfect plasticity idealization of the SiC/Ti ring material is made and used in the limit load calculations. An estimate of the failure pressure of the NASA/PW benchmark test ring is given. Author

N92-11388*# Textron Bell Aerospace Co., Buffalo, NY.
SLAVE FINITE ELEMENT FOR NON-LINEAR ANALYSIS OF ENGINE STRUCTURES. VOLUME 2: PROGRAMMER'S MANUAL AND USER'S MANUAL
D. L. Witkop, B. J. Dale, and S. Gellin Oct. 1991 124 p
(Contract NAS3-23279)
(NASA-CR-187225; NAS 1.26:187225) Avail: NTIS HC/MF A06 CSCL 20K

The programming aspects of SFENES are described in the User's Manual. The information presented is provided for the installation programmer. It is sufficient to fully describe the general program logic and required peripheral storage. All element generated data is stored externally to reduce required memory allocation. A separate section is devoted to the description of these files thereby permitting the optimization of Input/Output (I/O) time through efficient buffer descriptions. Individual subroutine descriptions are presented along with the complete Fortran source listings. A short description of the major control, computation, and I/O phases is included to aid in obtaining an overall familiarity with the program's components. Finally, a discussion of the suggested overlay structure which allows the program to execute with a reasonable amount of memory allocation is presented. Author

N92-11389# Oak Ridge National Lab., TN.
PROPAGATION BEHAVIOR OF SMALL CRACKS IN 304 STAINLESS STEEL UNDER BIAXIAL LOW-CYCLE FATIGUE AT ELEVATED TEMPERATURE
Takashi Ogata, Akito Nitta (Central Research Inst. of Electric Power Industry, Tokyo, Japan), and J. J. Blass 1991 26 p Presented at the American Society for Testing and Materials (ASTM) Symposium on Thermo-Mechanical Fatigue: Behavior of Materials, San Diego, CA, 14-17 Oct. 1991
(Contract DE-AC05-84OR-21400)
(DE91-018863; CONF-911048-1) Avail: NTIS HC/MF A03

To investigate the propagation behavior of small cracks and the relationship between crack propagation and fatigue life, strain-controlled in-phase and 90 degrees out-of-phase axial-torsional fatigue tests were conducted at 550 C using tubular specimens of 304 stainless steel with and without surface notches. During the tests, observations of crack initiation and propagation were frequently made using replica films and an optical microscope. Most of the fatigue life was spent in the propagation of small cracks less than 2 mm long. Regardless of loading conditions, the crack propagation rate correlated well with the equivalent shear strain range defined as a function of maximum shear strain range and normal strain range on the plane of the maximum shear strain range. The biaxial low-cycle fatigue life could be estimated from the relationship between the crack propagation rate and the equivalent shear strain range. DOE

N92-11390# Lawrence Livermore National Lab., CA.
GEOMETRICALLY EXACT SHELLS MODELS: FOUNDATION AND COMPUTATIONAL ASPECTS WITH SPECIAL REFERENCE TO IMPLICIT LARGE-SCALE CALCULATIONS
J. C. Simo, F. Armero, C. Miehe, T. Laursen, and R. L. Taylor (California Univ., Berkeley.) Feb. 1991 23 p
(Contract W-7405-eng-48)
(DE91-019014; UCRL-CR-107856) Avail: NTIS HC/MF A03

A rigorous nonlinear stability analysis for a class of return

mapping algorithms in elastoviscoplasticity based on the generalized mid-point rule is presented. In contrast with previous developments, the analysis is performed directly on the system of variational inequalities governing the problem and shown to hold for non-smooth convex elastic domains. To motivate the approach, a similar analysis is performed on the nonlinear heat-conduction equation. DOE

N92-11391*# Washington Univ., Seattle.
THERMOVISCOPLASTIC RESPONSE OF Ti-15-3 UNDER VARIOUS LOADING CONDITIONS
M. E. Tuttle and J. Rogacki Oct. 1991 151 p
(Grant NAG1-974)
(NASA-CR-187621; NAS 1.26:187621) Avail: NTIS HC/MF A08 CSCL 20K

Metal matrix composites (MMC's) are candidate materials for use in high temperature, high loading applications. In particular, an MMC consisting of a titanium alloy reinforced with silicon-carbide fibers is being considered for use on the National Aerospace Plane (NASP). Compared to other metals and metallic alloys, titanium alloys retain relatively high stiffness, strength, and corrosion resistance at elevated temperatures. However, above roughly 316 C titanium exhibits a significant thermoviscoplastic (creep) response. Since the temperatures encountered in many regions of the NASP are expected to exceed 316 C, the potential thermoviscoplastic behavior of titanium-based MMC's at elevated temperatures must be thoroughly investigated. Author

N92-11392*# National Aeronautics and Space Administration. Langley Research Center, Hampton, VA.
SENSITIVITY OF SPACE STATION ALPHA JOINT ROBUST CONTROLLER TO STRUCTURAL MODAL PARAMETER VARIATIONS
Renjith R. Kumar, Paul A. Cooper, and Tae W. Lim (Lockheed Engineering and Sciences Co., Hampton, VA.) Aug. 1991 12 p Presented at the AIAA Guidance, Navigation and Control Conference, 12-14 Aug. 1991 Previously announced in IAA as A91-49636
(NASA-TM-104153; NAS 1.15:104153) Avail: NTIS HC/MF A03 CSCL 20K

The photovoltaic array sun tracking control system of Space Station Freedom is described. A synthesis procedure for determining optimized values of the design variables of the control system is developed using a constrained optimization technique. The synthesis is performed to provide a given level of stability margin, to achieve the most responsive tracking performance, and to meet other design requirements. Performance of the baseline design, which is synthesized using predicted structural characteristics, is discussed and the sensitivity of the stability margin is examined for variations of the frequencies, mode shapes and damping ratios of dominant structural modes. The design provides enough robustness to tolerate a sizeable error in the predicted modal parameters. A study was made of the sensitivity of performance indicators as the modal parameters of the dominant modes vary. The design variables are resynthesized for varying modal parameters in order to achieve the most responsive tracking performance while satisfying the design requirements. This procedure of reoptimization design parameters would be useful in improving the control system performance if accurate model data are provided. Author

42 GEOSCIENCES (GENERAL)

No abstracts in this category.

43 EARTH RESOURCES AND REMOTE SENSING

Includes remote sensing of earth resources by aircraft and spacecraft; photogrammetry; and aerial photography.

For instrumentation see *35 Instrumentation and Photography.*

N92-11393*# International Space Univ., Inc., Cambridge, MA.
INTERNATIONAL PROGRAM FOR EARTH OBSERVATIONS Final Report
1990 380 p Presented at the Summer Session of the Inst. for Space and Terrestrial Science, Toronto, Ontario, 1990
(Grant NAG5-1469)
(NASA-CR-188799; NAS 1.26:188799) Copyright Avail: NTIS HC/MF A17; 2 functional color pages CSCL 08B

During the 1990 summer session of the International Space University, graduate students of many different countries and with various academic backgrounds carried out a design project that focused on how to meet the most pressing environmental information requirements of the 1990's. The International Program for Earth Observations (IPEO) is the result of the students labor. The IPEO report examines the legal and institutional, scientific, engineering and systems, financial and economic, and market development approaches needed to improve international earth observations and information systems to deal with environmental issues of global importance. The IPEO scenario is based on the production of a group of lightweight satellites to be used in global remote sensing programs. The design and function of the satellite is described in detail. M.G.

N92-11394# European Space Agency, Paris (France).
PHYSICAL MEASUREMENTS AND SIGNATURES IN REMOTE SENSING, VOLUME 1
James J. Hunt, ed. May 1991 452 p In ENGLISH and FRENCH The 5th International Colloquium was held in Courchevel, France, 14-18 Jan. 1991; sponsored by CNES, CNRS, Inst. National de la Recherche Agronomique, and Inst. Francais de la Recherche pour l'Exploitation de la Mer
(ESA-SP-319-Vol-1; ISBN-92-9092-118-8; ISSN-0379-6566; ETN-91-90063) Copyright Avail: NTIS HC/MF A20; ESA, EPD, ESTEC, Noordwijk, Netherlands, HC 150 Dutch guilders (2 vols)

The analysis of the relationships between the specific properties of a target (vegetative canopy, soil, rock, water surface, snow, ice etc.) and its spectral characteristics in different wavelength ranges (from ultraviolet to microwaves), the determination of factors affecting the spectral response of an object (atmospheric effects, measuring techniques etc.) and the development of intepretation models were addressed. A good survey of research in progress in the domain of the application of remote sensing to the study of Earth resources, with in depth investigations into atmospheric corrections, high spectral resolution, active microwaves, passive microwaves and thermal infrared, and directional and polarimetric effects in the optical domain, is offered. For individual titles, see N92-11395 through N92-11487.

N92-11395# Water Conservation Lab., Phoenix, AZ.
COMPARISON OF ATMOSPHERIC CORRECTION PROCEDURES FOR VISIBLE AND NEAR-IR SATELLITE SENSOR OUTPUT
M. Susan Moran, R. D. Jackson, P. N. Slater, and Philippe M. Teillet (Canada Centre for Remote Sensing, Ottawa, Ontario) *In* ESA, Physical Measurements and Signatures in Remote Sensing, Volume 1 May 1991 p 7-12 Sponsored in part by Maricopa Agricultural Center (For primary document see N92-11394 02-43)
Copyright Avail: NTIS HC/MF A20; ESA, EPD, ESTEC, Noordwijk, Netherlands, HC 150 Dutch guilders (2 vols)

An experiment to assess the accuracy of several atmospheric correction procedures, including four Radiative Transfer Codes (RTCs) and Dark Object Subtraction (DOS), for retrieval of surface reflectance factors from LANDSAT Thematic Mapper data in the

visible and near IR spectrum is reported. The most accurate results (approx. + or - 0.01 reflectance) were obtained using RTCs with on site measurements of Mie, Rayleigh and ozone optical depths. Acceptable results (+ or - 0.02 reflectance) were achieved with less complex techniques, based on RTCs using reasonable estimates of atmospheric conditions. The DOS technique was the least accurate method, producing greater error in the near IR spectrum than no correction at all. ESA

N92-11396# Akademiya Nauk BSSR, Minsk. Inst. of Physics.
MODELING OF VISIBLE AND UV RADIATIVE TRANSFER IN THE OCEAN-ATMOSPHERE SYSTEM CONCEPTS, MODELS, AND PROGRAMS
E. P. Zege, A. S. Prikhach, and L. I. Chaikovskaya *In* ESA, Physical Measurements and Signatures in Remote Sensing, Volume 1 May 1991 p 13-18 (For primary document see N92-11394 02-43)
Copyright Avail: NTIS HC/MF A20; ESA, EPD, ESTEC, Noordwijk, Netherlands, HC 150 Dutch guilders (2 vols)

A simple and convenient tool to investigate radiative characteristics of the atmosphere-ocean system, including spectral polarization ones, called the ATMOTOOLS package and implemented for an IBM personal computer and synthesizing up to date optical ocean and atmosphere models, new procedures of refining these models by different experimental data and special radiation calculation procedures, is described. Special attention is paid to aerosol models and organization of data banks on optical aerosol properties. The calculation procedures for radiative transfer are developed with regard to atmosphere stratification, light polarization, multiple scattering and so on. Examples of investigating different problems connected with remote sensing of ocean bioproductivity using ATMOTOOLS are given. ESA

N92-11397*# Jet Propulsion Lab., California Inst. of Tech., Pasadena.
DETERMINATION OF THE IN-FLIGHT SPECTRAL AND RADIOMETRIC CHARACTERISTICS OF THE AIRBORNE VISIBLE/INFRARED IMAGING SPECTROMETER (AVIRIS)
Robert O. Green, James E. Conel, Veronique Carrere, Carol J. Bruegge, Jack S. Margolis, Michael Rast, and Gordon Hoover *In* ESA, Physical Measurements and Signatures in Remote Sensing, Volume 1 May 1991 p 19-28 (For primary document see N92-11394 02-43)
Copyright Avail: NTIS HC/MF A20; ESA, EPD, ESTEC, Noordwijk, Netherlands, HC 150 Dutch guilders (2 vols) CSCL 08B

AVIRIS is a science research imaging spectrometer that measures radiance in 224 channels between 400 to 2450 nm in the electromagnetic spectrum. To determine the inflight spectral and radiometric characteristics of AVIRIS a validation and calibration experiment was performed. Five data sets were acquired over a calibration site on the homogeneous playa of Rogers Dry Lake, California, U.S. Surface reflectance, atmospheric optical depths, and atmospheric water vapor measurements were acquired concurrently with the overflights. These in situ measurements were used to constrain the LOWTRAN 7 radiative transfer code to predict the total spectral radiance incident at the AVIRIS aperture. These predicted radiances and the AVIRIS measured radiances were analyzed to validate the inflight characteristics. Inflight spectral channel positions and response functions over the AVIRIS spectral range were derived. Radiometric calibration coefficients were calculated for each channel as well as radiometric accuracy, intraflight stability, and noise equivalent delta radiance. ESA

N92-11398# Office National d'Etudes et de Recherches Aerospatiales, Toulouse (France). Lab. d'Etudes et de Recherches en Teledetection Spatiale.
ATMOSPHERIC CORRECTION IN THE THERMAL INFRARED: AVHRR CASE [CORRECTIONS ATMOSPHERIQUES DANS L'INFRA-ROUGE THERMIQUE: CAS DE L'AVHRR]
Yann H. Kerr *In* ESA, Physical Measurements and Signatures in Remote Sensing, Volume 1 May 1991 p 29-34 In FRENCH (For primary document see N92-11394 02-43)
Copyright Avail: NTIS HC/MF A20; ESA, EPD, ESTEC, Noordwijk, Netherlands, HC 150 Dutch guilders (2 vols)

The two thermal infrared channels of AVHRR (Advanced Very High Resolution Radiometer) can measure surface temperature with atmospheric correction of data. Reliable surface temperatures can be obtained using the split window method for atmospheric correction on ocean surfaces. However, for emerged terrain, temperature estimations can be erroneous. Different atmospheric correction methods are investigated for analyzing the causes of errors on terrestrial surfaces. The split window method is analyzed in detail and several causes of errors related to surface type are studied to get a reliable atmospheric correction methodology. The associated errors are presented and the results obtained by the different methods are compared to ground measurements. ESA

N92-11399# Institut National de la Recherche Agronomique, Avignon (France). Station de Bioclimatologie.
ESTIMATION OF THE AEROSOL OPTICAL THICKNESS FROM BROADBAND TURBIDITY MEASUREMENTS: APPLICATION TO THE ATMOSPHERIC CORRECTION OF SPOT IMAGES
Clement Atzberger (Trier Univ., Trier-Tarforst, Germany, F.R.), Martine Guerif, and Xing-Fa Gu *In* ESA, Physical Measurements and Signatures in Remote Sensing, Volume 1 May 1991 p 37-40 (For primary document see N92-11394 02-43)
Copyright Avail: NTIS HC/MF A20; ESA, EPD, ESTEC, Noordwijk, Netherlands, HC 150 Dutch guilders (2 vols)

The development of a method to determine the Spectral Aerosol Optical Thickness (SAOT) from broadband turbidity measurements of the World Turbidity Network is reported. The determination of the aerosol size distribution was determined without referring to spectral irradiance measurements. The methods included a correction for errors in the determined SAOT due to forward scattered light measured with the direct beam. The interest of this method was tested through the use of an atmospheric corrections model to estimate ground reflectances from SPOT data. Data analysis indicated that: the errors in the determined SAOT could be reduced by this method by the factor of two or more as compared with the usual estimation from the visibility; using this estimation of SAOT, the ground reflectance of agricultural fields was estimated from multitemporal SPOT images with a precision of 0.0089 (XS2) to 0.0198 (XS3); compared to the reflectance estimations using the visibility method, an error reduction of 8 pct. (XS2) to 24 pct. (XS3) was found. ESA

N92-11400# Vrije Univ., Amsterdam (Netherlands). Dept. of Physics and Astronomy.
ATMOSPHERIC CORRECTION OF SATELLITE BORNE IMAGERY INVESTIGATED BY MEANS OF A SENSITIVITY ANALYSIS OF THE ENTIRE REMOTE SENSING PROCESS
Johan F. deHaan, V. L. Dolman, and J. W. Hovenier *In* ESA, Physical Measurements and Signatures in Remote Sensing, Volume 1 May 1991 p 41-44 (For primary document see N92-11394 02-43)
Copyright Avail: NTIS HC/MF A20; ESA, EPD, ESTEC, Noordwijk, Netherlands, HC 150 Dutch guilders (2 vols)

The problem of atmospheric correction is reduced to a form that can be handled by computer simulations, employing radiative transfer calculations. A remote sensing image is created, assuming actual surface reflection properties and actual optical properties of atmospheric constituents. Atmospheric correction is performed repeatedly, each time using different aerosol properties. This yields the error in the derived target reflectance due to innaccurate knowledge of aerosol properties. The merits of additional measurements during satellite passage are investigated. Surface irradiance measurements strongly reduce the error for bright surfaces and low solar elevations. Atmospheric path radiance measurements (i.e., simplified version of Gordon's correction method) give small errors for dark surfaces only. ESA

N92-11401# Institut National de la Recherche Agronomique, Montfavet (France). Station de Bioclimatologie.
INTER-CALIBRATING OF SPOT1-HRV, LANDSAT5-TM, AND NOA11-AVHRR IN THE VISIBLE AND NEAR INFRARED FIELD S [INTER-ETALONNAGE DE SPOT1-HRV, LANDSAT5-TM ET NOAA11-AVHRR DANS LES DOMAINES DU VISIBLE ET DU PROCHE INFRAROUGE]
Xing-Fa Gu, Michel Verbrugghe, and Gerard Guyot *In* ESA, Physical Measurements and Signatures in Remote Sensing, Volume 1 May 1991 p 45-48 In FRENCH (For primary document see N92-11394 02-43)
(Contract PNTS-AI/0693/1769)
Copyright Avail: NTIS HC/MF A20; ESA, EPD, ESTEC, Noordwijk, Netherlands, HC 150 Dutch guilders (2 vols)

The intercalibrating of the SPOT 1 HRV, LANDSAT 5 Thematic Mapper (TM) and NOAA AVHRR satellite sensors over the stony La Crau plain in south east France is reported. The method involved choosing clear days during which La Crau was covered by the satellites and determining the ground reflectance and the optical thicknesses of the atmospheric parameters at the time of each image acquisition. From these data the calibrating and intercalibrating coefficients of the satellite instruments were determined. Results show that the methods led to stable results and can be considered operational. ESA

N92-11402# Centre d'Etudes et de Recherches, Toulouse (France).
CHARACTERIZATION OF AFRICAN DESERT SITES FOR THE RELATIVE CALIBRATING OF WIDE FIELD SATELLITE OPTICAL SENSORS [CARACTERISATION DES SITES DESERTIQUES AFRICAINS POUR L'ETALONNAGE RELATIF DES CAPTEURS OPTIQUES SPATIAUX A GRAND CHAMP]
L. Delphin, Xavier Briottet, Eric Vermote, and Marc Leroy (Centre National d'Etudes Spatiales, Toulouse, France) *In* ESA, Physical Measurements and Signatures in Remote Sensing, Volume 1 May 1991 p 49-52 In FRENCH (For primary document see N92-11394 02-43)
Copyright Avail: NTIS HC/MF A20; ESA, EPD, ESTEC, Noordwijk, Netherlands, HC 150 Dutch guilders (2 vols)

Alternatives to onboard calibrating methods for sufficiently accurate intercalibrating of different wide field (1000 to 2000 km sweep) satellite sensor detectors, equipped with connecting strips or charged coupled devices, such as VEGETATION, MODIS, POLDER, MERIS, were investigated. Aiming at particular terrestrial targets as such an alternative method was addressed. The principle is to intercalibrate the detector responses over calibrate terrestrial sites presenting the following qualities: temporal stability, interesting surface, spatial homogeneity, low directional effects, low spectral effects, few atmospheric perturbations (clouds and aerosols). The suitability of certain African desert sites is studied. ESA

N92-11403# Institut National de la Recherche Agronomique, Montfavet (France). Station de Bioclimatologie.
USE OF OPERATION ART-SPOT TO TEST THE 5S MODEL AND THE MTF OF THE SPOT [UTILISATION DE L'OPERATION ART-SPOT POUR TESTER LE MODELE 5S ET LA FTM DU SATELLITE SPOT]
Xing-Fa Gu, Gerard Guyot, and Michel Verbrugghe *In* ESA, Physical Measurements and Signatures in Remote Sensing, Volume 1 May 1991 p 53-56 In FRENCH (For primary document see N92-11394 02-43)
(Contract CNES-833/87/4891/02)
Copyright Avail: NTIS HC/MF A20; ESA, EPD, ESTEC, Noordwijk, Netherlands, HC 150 Dutch guilders (2 vols)

For operation ARTSPOT 16 by 60 m black squares were installed over a 1.5 by 1.0 km surface in La Crau (south east France). These small sized surfaces presented a strong contrast with their environment and showed the effects of the SPOT HRV MTF (Modulation Transfer Function) on the acquired image, experimentally validating its value to the Nyquist frequency provided by SPOT IMAGE. The experiment also validated the atmospheric correction estimation function and the 5S model atmospheric transfer environment. ESA

N92-11404# Rijkswaterstaat, Delft (Netherlands). Survey Dept.
COMPARISON OF IN SITU, AIRCRAFT- AND SATELLITE-DERIVED SURFACE REFLECTANCES IN FLEVOLAND (NETHERLANDS)
J. M. M. Kokke *In* ESA, Physical Measurements and Signatures in Remote Sensing, Volume 1 May 1991 p 57-60 Sponsored in part by Begleidingscommisse Remote Sensing (For primary document see N92-11394 02-43)
Copyright Avail: NTIS HC/MF A20; ESA, EPD, ESTEC, Noordwijk, Netherlands, HC 150 Dutch guilders (2 vols)

A validation campaign set up in one of the Dutch polders to evaluate a complete atmospheric correction method for multispectral satellite borne imagery is reported. A ground based radiometer measured total and diffuse spectral irradiance simultaneous with Thematic Mapper data acquisition for purposes of atmospheric correction of observed satellite radiances. The experiment included the use of data of the Dutch airborne scanner CAESAR to compare measured reflectances from several altitude levels. To assess the surface reflectance factors in the test area, a hand held field radiometer was used. Reference panels with known reflectances served for calibration of in situ and airborne data. Differences between satellite derived reflectances and ground based reflectances were quite small. Somewhat larger deviations occurred in airborne derived reflectances, which could not accurately be explained because of insufficient knowledge of some instrumental factors, e.g., field radiometer spectral response. ESA

N92-11405# Centre d'Etudes de Meteorologie Spatiale, Lannion (France).
ROUTINE MAPPING OF VEGETATION INDEX WITH THE AVHRR OF NOAA11
P. Brunel, M. Derrien, H. Legleau, and A. Marsouin *In* ESA, Physical Measurements and Signatures in Remote Sensing, Volume 1 May 1991 p 61-64 (For primary document see N92-11394 02-43)
Copyright Avail: NTIS HC/MF A20; ESA, EPD, ESTEC, Noordwijk, Netherlands, HC 150 Dutch guilders (2 vols)

Daytime and nightime AVHRR (Advanced Very High Resolution Radiometer) data from NOAA 11 are routinely processed for different meteorological purposes, such as the cloud cover description. The use of this automatic scheme to achieve vegetation index mapping is described. The first step is a fully automated cloud detection applied to all the AVHRR pixels of the orbit. The AVHRR channels and the cloud mask are then located by automatic landmarks recognition (one pixel accuracy is achieved) and then remapped on stereographic projection at 4 km resolution over an area covering France and Spain. The visible and near infrared channels are then corrected from atmospheric effects (except from aerosol) with the water vapor content derived from the radiosonde measurements and the vegetation index is computed. ESA

N92-11406# Lille Univ. (France). Lab. d'Optique Atmospherique.
INFLIGHT CALIBRATION OF CHANNELS 1 AND 2 OF AVHRR USING DESERTIC SITES AND CLOUDS
Richard Santer, M. Asmami, Eric Vermote, and Martin Sharman (Joint Research Centre of the European Communities, Ispra, Italy) *In* ESA, Physical Measurements and Signatures in Remote Sensing, Volume 1 May 1991 p 65-68 (For primary document se N92-11394 02-43)
Copyright Avail: NTIS HC/MF A20; ESA, EPD, ESTEC, Noordwijk, Netherlands, HC 150 Dutch guilders (2 vols)

The measurement of the loss of sensitivity of the odd numbered AVHRRs is based on the stability of desert sites. For the interband calibration, high reflective clouds are used. For channel 1 of NOAA 7 and NOAA 9 resuits are in agreement with the published results. For channel 2 of NOAA 7 the observed degradation seems higher by 2 pct. per year than the result reported by Holben et al (1989). For NOAA 11, rapid degradation of the signal over the first six months was followed by relative stability of the response. ESA

N92-11407# Deutsche Forschungsanstalt fuer Luft- und Raumfahrt, Wessling (Germany, F.R.). Inst. for Optoelectronics.
CORRECTION OF ATMOSPHERIC AND TOPOGRAPHIC EFFECTS IN LANDSAT TM IMAGES
R. Richter, Frank Lehmann, and Sabine Tischler *In* ESA, Physical Measurements and Signatures in Remote Sensing, Volume 1 May 1991 p 69-71 (For primary document see N92-11394 02-43)
Copyright Avail: NTIS HC/MF A20; ESA, EPD, ESTEC, Noordwijk, Netherlands, HC 150 Dutch guilders (2 vols)

In the solar reflective region (0.4 to 3 microns) the signal of satellite sensors viewing mountainous terrain strongly depends on topographics effects, solar illumination, and atmospheric parameters. An algorithm which calculates the surface reflectance for each pixel of an image employing a digital terrain model and the altitude profile of atmospheric data (standard atmosphere or measured data, e.g., radiosonde) is proposed. As a final step the adjacency effect can be accounted for in approximate manner. Results for a LANDSAT Thematic Mapper (TM) scene of the Black Forest (Fed. Republic of Germany) are given. ESA

N92-11408# Sherbrooke Univ. (Quebec). Centre d'Applications et de Recherches en Teledetection.
EVALUATION OF ATMOSPHERIC EFFECTS IN HIGH SPECTRAL RESOLUTION AIRBORNE IMAGES [EVALUATION DES EFFETS ATMOSPHERIQUES DANS LES IMAGES AEROPORTEES A HAUTE RESOLUTION SPECTRALE]
Alain Royer, Norman T. ONeill, Daniel Williams, John R. Miller, and Jim Freemantle (York Univ., Downsview, Ontario) *In* ESA, Physical Measurements and Signatures in Remote Sensing, Volume 1 May 1991 p 73-76 In FRENCH; ENGLISH summary Sponsored by CRSNG, and Ministere de l'Enseignement Superieur et de la Science (For primary document see N92-11394 02-43)
Copyright Avail: NTIS HC/MF A20; ESA, EPD, ESTEC, Noordwijk, Netherlands, HC 150 Dutch guilders (2 vols)

An analysis of the 5S and LOWTRAN 7 simulation models modified for the two Canadian FLI (Fluorescence Line Imager) spectrometers for spectral reflectance correction or to study atmospheric optical properties is presented. The results show that the mode of smoothing of raw spectra affects the simulations (position of absorption peaks). The simulated spectra for several atmospheric visibilities are compared to FLI and CASI measurements. The differences observed (problem of calibrating and absorption peak correspondence) are shown. ESA

N92-11409# Lille Univ. (France). Lab. d'Optique Atmospherique.
SPOT CALIBRATION ON THE TEST SITE LA CRAU (FRANCE)
Richard Santer, J.-L. Deuze, C. Devaux, Eric Vermote, Gerard Guyot, Xing-Fa Gu, Michel Verbrugghe, and Marc Leroy (Centre National d'Etudes Spatiales, Toulouse, France) *In* ESA, Physical Measurements and Signatures in Remote Sensing, Volume 1 May 1991 p 77-80 (For primary document see N92-11394 02-43)
(Contract CNES-833/89/5935/00)
Copyright Avail: NTIS HC/MF A20; ESA, EPD, ESTEC, Noordwijk, Netherlands, HC 150 Dutch guilders (2 vols)

Inflight calibration of SPOT 1 performed using a French site located in La Crau is reported. A full description of the procedure which includes both the characterization of the ground and of the atmosphere is presented. To predict the radiance at the satellite level, the non Lambertian properties of the test site and the surround contribution were taken into account. The three calibrations performed are self consistent and are in close agreement with calibration data obtained for B2 and B3. A discrepancy of 8 pct. is observed for B1 and its origin is under study. ESA

N92-11410# Valencia Univ. (Spain). Dept. of Thermodynamics.
A SPLIT-WINDOW METHOD FOR OBTAINING CROP TEMPERATURES
Cesar Coll, Jose A. Sobrino, and Vicente Caselles *In* ESA, Physical Measurements and Signatures in Remote Sensing, Volume 1 May 1991 p 81-84 (For primary document see N92-11394 02-43)
(Contract CICYT-ESP-89-0436)
Copyright Avail: NTIS HC/MF A20; ESA, EPD, ESTEC, Noordwijk, Netherlands, HC 150 Dutch guilders (2 vols)

A model that relates the land surface temperature with the temperatures measured by thermal infrared channels was derived by linearization of Planck's function and atmospheric transmittance. In this way a split window equation was obtained in which the angular dependence can be avoided while the total water vapor dependence must be retained. The emissivity dependence was analyzed for several atmospheric models and it was linearized in terms of the channel emissivity and the channel emissivity differences. An application of the split window method for vegetated areas is given. ESA

N92-11411# Musee Royal de l'Afrique Centrale, Tervuren (Belgium). Lab. de Teledetection Aerospatiale.
SUPPRESSION OF AEROSOLS ON LANDSAT THEMATIC MAPPER IMAGERY [SUPPRESSION DES AEROSOLS SUR L'IMAGERIE LANDSAT THEMATIC MAPPER]
Johan Lavreau *In* ESA, Physical Measurements and Signatures in Remote Sensing, Volume 1 May 1991 p 85-88 In FRENCH (For primary document see N92-11394 02-43)
Copyright Avail: NTIS HC/MF A20; ESA, EPD, ESTEC, Noordwijk, Netherlands, HC 150 Dutch guilders (2 vols)

A numerical count (DN) correction was carried out in each spectral band of LANDSAT Thematic Mapper after estimating the abundance of aerosols covering each pixel by the 4th parameter of the tasseled cap transformations. The corrected DN is calculated using equations established over test zones considered as homogenous at ground, but affected by a variable density aerosol cover. ESA

N92-11412# Centre National de Recherches Meteorologiques, Toulouse (France).
TIMS CALIBRATION CORRECTION BY COMPARISON WITH PRT5
Magali Stoll, Thierry Phulpin, and Thomas Schmugge (Agricultural Research Service, Beltsville, MD.) *In* ESA, Physical Measurements and Signatures in Remote Sensing, Volume 1 May 1991 p 89-93 (For primary document see N92-11394 02-43)
Copyright Avail: NTIS HC/MF A20; ESA, EPD, ESTEC, Noordwijk, Netherlands, HC 150 Dutch guilders (2 vols)

An analysis of the data acquired by TIMS (Thermal Infrared Multispectral Scanner) operating from the NASA C-130 during HAPEX (Hydrologic Atmospheric Experiment) showed systematic errors in brightness temperatures for all 6 channels with a magnitude depending on the aircraft altitude. The TIMS correction depends on estimating the actual temperatures of the cold (Tc) and hot (Th) blackbody references. The TIMS data is compared with those obtained by the broadband nonscanning PRT5 by using a method of maximum correlation between corresponding radiances. The correlations were always greater than 0.92. To correct the TIMS calibration, a relation between TIMS surface brightness temperatures, Ti, and PRT5 surface brightness temperature, T, taking into account emissivities variations was used. Tc and Th are deduced from the slope and origin of the regression between corresponding surface brightness temperatures. The final accuracy on brightness temperatures varies from 0.3 to 1.3 degrees. ESA

N92-11413# Canada Centre for Remote Sensing, Ottawa (Ontario).
ALTITUDE DEPENDENCE IN A SEMI-ANALYTICAL ATMOSPHERIC CODE
Philippe M. Teillet and Richard P. Santer (Lille Univ., France) *In* ESA, Physical Measurements and Signatures in Remote Sensing, Volume 1 May 1991 p 95-100 (For primary document see N92-11394 02-43)
Copyright Avail: NTIS HC/MF A20; ESA, EPD, ESTEC, Noordwijk, Netherlands, HC 150 Dutch guilders (2 vols)

Variable terrain elevation and sensor altitude capabilities were incorporated into the 5S atmospheric code. The approach and the equations used to refine the code in order to provide this

new capability are described. Several examples illustrate the effect of varying the terrain elevation and the dependence of results from the code on sensor altitude. ESA

N92-11414# Canada Centre for Remote Sensing, Ottawa (Ontario).
RADIOMETRIC AND ATMOSPHERIC CORRECTION PROCEDURES FOR AVHRR PREPROCESSING IN THE SOLAR REFLECTIVE CHANNELS
Philippe M. Teillet *In* ESA, Physical Measurements and Signatures in Remote Sensing, Volume 1 May 1991 p 101-104 (For primary document see N92-11394 02-43)
Copyright Avail: NTIS HC/MF A20; ESA, EPD, ESTEC, Noordwijk, Netherlands, HC 150 Dutch guilders (2 vols)

Radiometric and atmospheric corrections are formulated with a view to computing vegetation indices such as the Normalized Difference Vegetation Index (NDVI) from surface reflectances rather than the digital signal levels recorded at the sensor. In particular, Look Up Table (LUT) results from an atmospheric radiative transfer code are used to save time and avoid the complexities of running and maintaining such a code in a production environment. The data flow for radiometric image correction is very similar to commonly used geometric correction data flows. The role of terrain elevation in the atmospheric correction process is discussed. ESA

N92-11415*# Jet Propulsion Lab., California Inst. of Tech., Pasadena.
COMPARISON OF TWO ATMOSPHERIC CORRECTION MODELS FOR A VEGETATED AIRBORNE VISIBLE/INFRARED IMAGING SPECTROMETER (AVIRIS) SCENE
Jeannette Marie vandenBosch (California Univ., Santa Barbara.) and R. E. Alley *In* ESA, Physical Measurements and Signatures in Remote Sensing, Volume 1 May 1991 p 105-107 (For primary document see N92-11394 02-43)
Copyright Avail: NTIS HC/MF A20; ESA, EPD, ESTEC, Noordwijk, Netherlands, HC 150 Dutch guilders (2 vols)

Current atmospheric correction models applied to imaging spectroscopy data include such methods as residual (scene average) and flat field correction, regression method, and the LOWTRAN 7 method. Due to the limitations of using residual and flat field corrections on vegetated scenes, regression and LOWTRAN 7 are compared. Field measured targets taken at the time of the 13 April, 1989 AVIRIS overflight of Jasper Ridge, California (U.S.) were used to formulate the regression atmospheric correction. Assuming the regressed image represents ground truth, results show that the LOWTRAN 7 method with radiosonde data does not compensate as well for atmospheric water vapor as the regression method, but it may be easier to obtain a posteriori information to perform the LOWTRAN 7 atmospheric correction. ESA

N92-11416# Lille Univ. (France). Lab. d'Optique Atmospherique.
IN FLIGHT CALIBRATION OF LARGE FIELD OF VIEW SENSORS AT SHORT WAVELENGTH USING THE RAYLEIGH SCATTERING
Eric Vermote, Richard Santer, Pierre-Yves Deschamps, and M. Herman *In* ESA, Physical Measurements and Signatures in Remote Sensing, Volume 1 May 1991 p 109-113 Sponsored by CNES (For primary document see N92-11394 02-43)
Copyright Avail: NTIS HC/MF A20; ESA, EPD, ESTEC, Noordwijk, Netherlands, HC 150 Dutch guilders (2 vols)

In case of sea observations at short wavelengths, the well known Rayleigh scattering dominates the signal received by a satellite sensor. This predictable signature is used to calibrate the visible channels of satellite sensor while in flight. A first method is examined which consists in directly relating the measured numerical signal to the predicted reflectance. This direct method is improved by using a second channel at a larger wavelength in order to take into account the aerosol contribution. These two methods are applied to SPOT, both for the channel B0 of VEGETATION, planned to be set up on SPOT and for the present channel B1 of HRV. The error analysis shows that accuracies of 3 and 6 pct. respectively can be achieved for B0 and B1. A validation of the error analysis using HRV SPOT data is given. ESA

N92-11417# Akademiya Nauk BSSR, Minsk. Inst. of Physics.
ITERATIVE PROCEDURES FOR ATMOSPHERIC CORRECTION
E. P. Zege and A. S. Prikhach *In* ESA, Physical Measurements and Signatures in Remote Sensing, Volume 1 May 1991 p 115-118 (For primary document see N92-11394 02-43)
Copyright Avail: NTIS HC/MF A20; ESA, EPD, ESTEC, Noordwijk, Netherlands, HC 150 Dutch guilders (2 vols)

The methods of reconstructing an optical aerosol local model of atmosphere above ocean are presented. They resulted from refinement of regional models and use of different meteorological and spectral data. Some iterative methods of atmospheric correction including multiple scattering are proposed. The investigation proves to be successful on account of the ATMOTOOLS package which was developed and includes specially arranged aerosol data banks and procedures of radiative transfer computation. ESA

N92-11418# Institut National de la Recherche Agronomique, Montfavet (France). Station de Bioclimatolgie.
ON THE NATURE OF SPECTRAL SHIFTS: MODELING AND COMPARISON TO INFORMATION CONTAINED IN WIDE BANDS [DE LA NATURE DES GLISSEMENTS SPECTRAUX: MODELISATION ET COMPARAISON A L'INFORMATION CONTENUE DANS LES BANDES LARGES]
Frederic Baret, Stephane Jacquemoud, Gerard Guyot, and Catherine E. Leprieur (Office National d'Etudes et de Recherches Aerospatiales, Toulouse, France) *In* ESA, Physical Measurements and Signatures in Remote Sensing, Volume 1 May 1991 p 121-129 In FRENCH Sponsored in part by CNES; CNRS; and Institut Francais de la Recherche pour l'Exploitation de la Mer (For primary document see N92-11394 02-43)
Copyright Avail: NTIS HC/MF A20; ESA, EPD, ESTEC, Noordwijk, Netherlands, HC 150 Dutch guilders (2 vols)

The leaf optical properties model PROSPECT, the vegetation cover reflectance model SAIL, and the atmospheric effects simulation model 5S were coupled in order to analyze the spectral shift characterized by the inflection point lambda sub i of the red edge (670 to 780 nm). If this spectral index is equivalent to the knowledge of wideband red and near infrared reflectance at the level of the leaf, there will not be any at the level of the cover. It appears that lambda sub i is very sensitive to the foliar index and to the cholorophyll concentration, and relatively little dependent on the ground optical properties and atmospheric effects. This would therefore be a good indicator of the photosynthetic capacity of the vegetation. On the other hand, its dynamic weakness necessitates complementary studies in relation to sensor noise and computation methods. ESA

N92-11419# Agricultural Research Service, Beltsville, MD.
ON THE VALUE OF HIGH SPECTRAL RESOLUTION MEASUREMENTS IN THE VISIBLE AND NEAR-INFRARED
John C. Price *In* ESA, Physical Measurements and Signatures in Remote Sensing, Volume 1 May 1991 p 131-136 (For primary document see N92-11394 02-43)
Copyright Avail: NTIS HC/MF A20; ESA, EPD, ESTEC, Noordwijk, Netherlands, HC 150 Dutch guilders (2 vols)

Due to spectral correlations, the number of independent variables in high resolution reflectance spectra is much smaller than the number of data points describing the spectra. Examination of data sets shows that the number of independent variables describing data sets comprised of 160 to 300,000 spectra, is generally in the range of 5 to 10. When data sets are combined this number is increased to 10 to 20, with the signal to noise ratio of the data acquisition system being the limiting factor. It appears that the principal value of high resolution spectra is for establishing energy levels and absorption characteristics of natural substances, e.g., plants, soils, rocks, etc., i.e., for determining the solutions of the Schroedinger equation. Remote sensing objectives

are better achieved by instrumentation with relatively low spectral resolution (15 to 20 bands at 0.04 to 0.10 micrometer bandwith) and high signal to noise. ESA

N92-11420*# Jet Propulsion Lab., California Inst. of Tech., Pasadena.

USE OF HIGH SPECTRAL RESOLUTION AIRBORNE VISIBLE/INFRARED IMAGING SPECTROMETER DATA FOR GEOLOGIC MAPPING: AN OVERVIEW

Veronique Carrere *In* ESA, Physical Measurements and Signatures in Remote Sensing, Volume 1 May 1991 p 137-143 (For primary document see N92-11394 02-43)

Copyright Avail: NTIS HC/MF A20; ESA, EPD, ESTEC, Noordwijk, Netherlands, HC 150 Dutch guilders (2 vols) CSCL 08B

Specific examples of the use of AVIRIS (Airborne Visible/Infrared Imaging Spectrometer) high spectral resolution data for mapping, alteration related to ore deposition and to hydrocarbon seepage, and alluvial fans are presented. Correction for atmospheric effects was performed using flat field correction, log residuals, and radiative transfer modeling. Minerals of interest (alunite, kaolinite, gypsum, carbonate iron oxides, etc.) were mapped based upon the wavelength position, depth and width of characteristic absorption features. Results were checked by comparing to existing maps, results from other sensors (Thematic Mapper (TM) and TIMS (Thermal Infrared Multispectral Scanner)), and laboratory spectra of samples collected in the field. Alteration minerals were identified and mapped. The signal to noise ratio of acquired AVIRIS data, long to 2.0 microns, was insufficient to map minerals of interest. ESA

N92-11421# Laboratoire de Meteorologie Dynamique, Paris (France).

SPACE OBSERVATION OF THE LAND-OCEAN-ATMOSPHERE SYSTEM AT HIGH SPECTRAL RESOLUTION IN THE INFRARED: PERSPECTIVES AND PROBLEMS Abstract Only [OBSERVATION SPATIALE DU SYSTEME TERRE-OCEAN-ATMOSPHERE A HAUTE RESOLUTION SPECTRALE DANS L'INFRAROUGE: PERSPECTIVES ET PROBLEMES]

A. Chedin and N. A. Scott *In* ESA, Physical Measurements and Signatures in Remote Sensing, Volume 1 May 1991 p 145 In FRENCH (For primary document see N92-11394 02-43)

Copyright Avail: NTIS HC/MF A20; ESA, EPD, ESTEC, Noordwijk, Netherlands, HC 150 Dutch guilders (2 vols)

A summary of space observation with high infrared spectral resolution instruments is presented. Perspectives offered by projects such as AIRS (Advanced Infrared Sounder on EOS/NASA/JPL polar platforms) and SAAS (French acronym for atmospheric sounding by spectral analysis) and problems to be resolved to gain greater advantage were addressed. Future numerical prediction models of weather and climate are cited. ESA

N92-11422# European Space Agency. European Space Research and Technology Center, ESTEC, Noordwijk (Netherlands).

THE PERFORMANCE OF THE ESA MEDIUM RESOLUTION IMAGING SPECTROMETER (MERIS)

Michael Rast, Jean-Loup Bezy, M. Morel, and O. FantondAndon (ACRI S.A., Sophia Antipolis, France) *In its* Physical Measurements and Signatures in Remote Sensing, Volume 1 May 1991 p 147-152 (For primary document see N92-11394 02-43)

Copyright Avail: NTIS HC/MF A20; ESA, EPD, ESTEC, Noordwijk, Netherlands, HC 150 Dutch guilders (2 vols)

An overview of the MERIS system, its mission plan and requirements and the sun illumination conditions affecting the utlization of MERIS, is given. Radiometric signal simulations are being performed which consider the observation geometry and time, as well as the instrument characteristics. Results of these analyses and the related performance to be expected from MERIS are presented. The mission goals of MERIS include: biophysical oceanography; phytoplankton biomass and productivity by measuring chlorophyll and yellow substance concentrations; atmospheric investigations on cloud and aerosol parameters; and land surface processes- global scale vegetation monitoring, distribution, extent and condition. ESA

N92-11423# Joanneum Research Centre, Graz (Austria). Inst. for Image Processing and Computer Graphics.

PHENOLOGICAL CHANGES IN THE RED EDGE SHIFT OF NORWAY SPRUCE NEEDLES AND THEIR RELATIONSHIP TO NEEDLE CHLOROPHYLL CONTENT

Cliff Banninger *In* ESA, Physical Measurements and Signatures in Remote Sensing, Volume 1 May 1991 p 155-158 (For primary document see N92-11394 02-43)

Copyright Avail: NTIS HC/MF A20; ESA, EPD, ESTEC, Noordwijk, Netherlands, HC 150 Dutch guilders (2 vols)

Laboratory reflectance and chlorophyll measurements of first and second year metal stressed and nonstressed Norway spruce needles showed little change in the position of the red edge between first year stressed and nonstressed needles and between second year stressed and nonstressed needles over the growing season from May to November. Total chlorophyll content (chlorophyll a + b) of the needles displayed little variation over the growing period between their respective growth years and stress categories, indicating an adaptation of the spruce trees to the prevailing metal stress conditions with respect to their foliar chlorophyll production. ESA

N92-11424# Hebrew Univ. of Jerusalem, Rehovot (Israel). Dept. of Soil and Water Sciences.

SIMULTANEOUS DETERMINATION OF SIX SOIL PROPERTIES FROM THE SOIL DIFFUSE REFLECTANCE SPECTRUM IN THE NEAR INFRARED REGION (1-2.5 MICRONS)

Eyal Ben-Dor, A. Banin, and A. Singer *In* ESA, Physical Measurements and Signatures in Remote Sensing, Volume 1 May 1991 p 159-164 (For primary document see N92-11394 02-43)

Copyright Avail: NTIS HC/MF A20; ESA, EPD, ESTEC, Noordwijk, Netherlands, HC 150 Dutch guilders (2 vols)

High resolution diffuse reflectance spectra (3113 spectral points) in the near infrared region were recorded for 91 soil samples. Six soil properties (clay content, specific surface area, cation exchange capacity, hygroscopic moisture content, organic matter content, and carbonate content) were measured by routine methods employed in soil laboratories. An empirical model to predict each property from its spectral signature was developed by adapting a Near Infrared Analysis (NIRA) technique. Several data manipulations were used in order to obtained optimum performance. The optimum performance of all properties was found to be at 25 to 63 spectral points. Strong support for the NIRA capability was provided by the ability to explain most of the spectral assignments. NIRA is shown to be a very good tool for rapid and nondestructive analysis of soil materials as well as for better utilization of high resolution remote sensing data. ESA

N92-11425# Wageningen Agricultural Univ. (Netherlands). Dept. of Land Surveying and Remote Sensing.

FEASIBILITY OF THE RED EDGE INDEX FOR THE DETECTION OF NITROGEN DEFICIENCY

J. G. P. W. Clevers and Cordt Bueker (Bonn Univ., Germany, F.R.) *In* ESA, Physical Measurements and Signatures in Remote Sensing, Volume 1 May 1991 p 165-168 (For primary document see N92-11394 02-43)

Copyright Avail: NTIS HC/MF A20; ESA, EPD, ESTEC, Noordwijk, Netherlands, HC 150 Dutch guilders (2 vols)

The SAIL canopy reflectance model is used for evaluating the influence of varying crop parameters, such as LAI (Leaf Area Index) and leaf angle distribution, and external parameters, such as soil reflectance and irradiation conditions on the theoretical position of the red edge. Results show that the position of the red edge is independent of soil background, but is largely influenced by LAI. Field spectroradiometer data of field trials are analyzed to study the effects of nitrogen deficiency in a barley crop. Results show a shift of the red edge for two distinct barley crops at the same LAI

due to nitrogen stress. During the EISAC'89 campaign, data of a nitrogen experiment at the Somerset test site (United Kingdom), recorded with the Programmable Multispectral Imager (PLI), were analyzed. Again, a clear spectral shift of the red edge occurred as a result of nitrogen deficiency. ESA

N92-11426# Salford Univ. (England). Dept. of Geography.
MULTI-TEMPORAL MONITORING OF LAKE WATER QUALITY
F. Mark Danson, A. L. Heathwaite, and S. T. Trudgill (Sheffield Univ., England) *In* ESA, Physical Measurements and Signatures in Remote Sensing, Volume 1 May 1991 p 169-172 (For primary document see N92-11394 02-43)
Copyright Avail: NTIS HC/MF A20; ESA, EPD, ESTEC, Noordwijk, Netherlands, HC 150 Dutch guilders (2 vols)

Airborne Thematic Mapper data were collected on three dates over a eutrophic lake in south west England. Simultaneous surveys of lake water quality were undertaken and point estimates of chlorophyll-a concentration were obtained. It was not possible to relate the remotely sensed radiance directly to the estimates of chlorophyll-a concentration but the image data exhibited spatial structures related to water quality. ESA

N92-11427# Colorado Univ., Boulder. Center for the Study of Earth from Space.
RETRIEVALS OF COLUMN ATMOSPHERIC WATER VAPOR, VEGETATION LIQUID WATER, AND CLOUD COVER FRACTION FROM AVIRIS DATA
Bo-Cai Gao and Alexander F. H. Goetz *In* ESA, Physical Measurements and Signatures in Remote Sensing, Volume 1 May 1991 p 173-176 (For primary document see N92-11394 02-43)
Copyright Avail: NTIS HC/MF A20; ESA, EPD, ESTEC, Noordwijk, Netherlands, HC 150 Dutch guilders (2 vols)

The Airbone Visible/Infrared Imaging Spectrometer (AVIRIS) collects spectral imaging data in the 0.4 to 2.5 micron region in 10 nm bands and has a ground instantaneous field of view of 20 by 20 from an altitude of 20 km. Column atmospheric water vapor amounts were derived from AVIRIS data by curve fitting observed spectra with calculated spectra in the 0.94 and 1.14 micron water vapor band absorption regions using an atmospheric model, a narrow band spectral model, and a nonlinear least squares fitting technique. Curve fitting of spectra near 1 micron from areas covered with vegetation indicates that both the amount of atmospheric water vapor and the moisture content of vegetation can be retrieved simultaneously. The fractional cloud area is derived by ratioing radiances near the 0.94 and the 1.14 micron water vapor band centers against those in the intermediate atmospheric window regions. The band ratioing technique effectively discriminates among clouds and surface areas having similar reflectance values. ESA

N92-11428# Vrije Univ., Amsterdam (Netherlands). Section Hydrology.
A MULTI-SENSOR APPROACH TO SPECTRAL SIGNATURE ANALYSIS OF INLAND WATERS
A. G. Dekker, T. J. Malthus (Nottingham Univ., England), M. M. Wijnen, and E. Seyhan *In* ESA, Physical Measurements and Signatures in Remote Sensing, Volume 1 May 1991 p 177-180 (For primary document see N92-11394 02-43)
Copyright Avail: NTIS HC/MF A20; ESA, EPD, ESTEC, Noordwijk, Netherlands, HC 150 Dutch guilders (2 vols)

Several remote sensing systems (PMI/FLI, CAESAR, CASI, the Thematic Mapper, and SPOT) were used to assess their potential for inland water quality detection and monitoring. Airborne imaging spectrometry was acquired. Simultaneous (sub)surface spectroradiometric and laboratory based spectrophotometric measurements allowed an accurate description of the underwater lightfield through determination of the inherent and apparent optical properties. Spectral signature simulation of various systems increased understanding of the performances and led to the development of an inland water quality spectral band set for the CAESAR system. These results are relevant for operationalization of high resolution airborne systems and for future satellite systems such as MERIS, MODIS, and HIRIS, especially in the area of data reduction and the development of algorithms. ESA

N92-11429# Colorado Univ., Boulder. Center for the Study of Earth from Space.
SPECTRAL IDENTIFICATION (1.2-2.5 MICRONS) AND CHARACTERIZATION OF PARIS (FRANCE) BASIN KAOLINITE/SMECTITE CLAYS USING A FIELD SPECTROMETER
Fred A. Kruse, Medard Thiry (Ecole Nationale Superieure des Mines, Fontainebleau, France), and Phoebe L. Hauff *In* ESA, Physical Measurements and Signatures in Remote Sensing, Volume 1 May 1991 p 181-184 (For primary document see N92-11394 02-43)
Copyright Avail: NTIS HC/MF A20; ESA, EPD, ESTEC, Noordwijk, Netherlands, HC 150 Dutch guilders (2 vols)

Kaolinite/smectite interstratified clays are globally distributed and provide a means of determining conditions of deposition, local and regional weathering environments, and paleoclimate in stratigraphic sequences. A methodology is under development that integrates the classical techniques of X-Ray Diffraction (XRD) with laboratory, field, and airborne infrared (1.2 to 2.5 micron) reflectance spectroscopy. Field and laboratory spectra from Paris basin (France) samples are used to demonstrate the method's potential as an analytical tool for rapidly mapping mineral distribution and paragenic sequences in the field. Reflectance spectra were collected in situ during Jul. 1990 and compared against laboratory spectra. Preliminary results are presented. ESA

N92-11430# Joint Research Centre of the European Communities, Ispra (Italy). Land Use Planning and Environmental Protection Program.
THE USE OF IMAGING SPECTROMETRY IN MEDITERRANEAN LAND DEGRADATION AND SOIL EROSION HAZARD ASSESSMENTS
Joachim Hill and Jacques Megier *In* ESA, Physical Measurements and Signatures in Remote Sensing, Volume 1 May 1991 p 185-188 (For primary document see N92-11394 02-43)
Copyright Avail: NTIS HC/MF A20; ESA, EPD, ESTEC, Noordwijk, Netherlands, HC 150 Dutch guilders (2 vols)

Mediterranean lands are characterized by a high diversity of topography, lithology, soils, and microclimate, resulting in a range of various ecosystems. It is a highly sensitive natural environment with vegetation types that are almost entirely anthropogenically degraded forms, and the remaining areas of this quasinatural vegetation are highly vulnerable to further destruction. An interdisciplinary cooperation of research institutes was formed to integrate their specific expertise in remote sensing, geology, soil science, and geobotany. Their development of a specific interest in remotely sensed data from high spectral resolution imagers for the observation of Mediteranean land degradation and soil erosion is reported. ESA

N92-11431# Deutsche Forschungsanstalt fuer Luft- und Raumfahrt, Oberpfaffenhofen (Germany, F.R.). Inst. for Optoelectronics.
THE COMPARISON OF AIRBORNE IMAGING SPECTROMETRY AND GEOCHEMICAL GROUND SURVEY FOR THE ANALYSIS OF VEGETATION ANOMALIES OVER WASTE DEPOSITS
Harald Rothfuss, Frank Lehmann, and R. Richter *In* ESA, Physical Measurements and Signatures in Remote Sensing, Volume 1 May 1991 p 189-191 (For primary document see N92-11394 02-43)
Copyright Avail: NTIS HC/MF A20; ESA, EPD, ESTEC, Noordwijk, Netherlands, HC 150 Dutch guilders (2 vols)

Atmospherically corrected GER 2 imaging spectrometry data acquired during the European Airborne Imaging Spectrometry Campaign (EISAC) in May 1989 are employed for the spectral analysis of vegetation growing over a former waste deposit southern Bavaria (Fed. Republic of Germany). Spectral anomalies were observed in the vegetation cover which are likely to be attributed to the buried material. The result of a scene classification based

on the spectral signatures shows a correlation with infill structures on the formally open site. Geochemical sampling over the site revealed high heavy metal concentrations as a probable source for the spectral differences. This environmental application of imaging spectrometry data with new quantitative evaluation methods could reduce extensive ground surveys and be of economical interest if developed to an operational state. ESA

N92-11432# Deutsche Forschungsanstalt fuer Luft- und Raumfahrt, Oberpfaffenhofen (Germany, F.R.). Inst. for Optoelectronics.

THE SPECTRAL REFLECTION BEHAVIOUR OF BRANCHES AND BRANCH COMPONENTS OF HEALTHY AND DAMAGED BEECH TREES

Harald Hoffmann and W. Kirchhof *In* ESA, Physical Measurements and Signatures in Remote Sensing, Volume 1 May 1991 p 193-196 (For primary document see N92-11394 02-43)

Copyright Avail: NTIS HC/MF A20; ESA, EPD, ESTEC, Noordwijk, Netherlands, HC 150 Dutch guilders (2 vols)

Spectral measurements of beech branches and branch components were performed in the laboratory from 0.5 to 2.5 microns. The measurements focused on primary effects influencing the spectral signature of healthy and damaged beech trees. Saturation of the reflected radiance is reached with a stack of 5 to 7 layers for branches and leaves. Differences between branch and leaf spectra can be attributed to the amount of bark, nuts, etc. Their contribution to the spectral reflectance is also responsible for the possibility to discriminate between healthy and damaged beech branches in the NIR and SWIR. Leaves of different degree of damage can be distinguished in the VIS. The spectral veriations observed in the region are similar to those observed for healthy and damaged branches. ESA

N92-11433# Deutsche Forschungsanstalt fuer Luft- und Raumfahrt, Oberpfaffenhofen (Germany, F.R.). Inst. for Optoelectronics.

EVALUATION OF HIGH SPECTRAL RESOLUTION LABORATORY REFLECTANCE DATA OF HEALTHY AND DAMAGED BEECH AND SPRUCE BRANCHES FOR THE IMPROVEMENT OF FOREST DAMAGE CLASSIFICATION

W. Kirchhof and Harald Hoffmann *In* ESA, Physical Measurements and Signatures in Remote Sensing, Volume 1 May 1991 p 197-200 (For primary document see N92-11394 02-43)

Copyright Avail: NTIS HC/MF A20; ESA, EPD, ESTEC, Noordwijk, Netherlands, HC 150 Dutch guilders (2 vols)

In the past decade forest damage became a serious environmental problem in Germany. In support of a research project for the development of multispectral forest damage monitoring, high spectral monitoring, high spectral resolution measurements on 1 to 7 stacked beech and spruce branches of different degrees of damage were performed in the laboratory. The influence of primary effects of damage on spectral reflectance was measured in the 0.49 to 2.50 microns region. In the visible, the reflectance peak raises with increasing damage. Red shift of the reflectance peak and a variation of the shape at the beginning to the NIR slope was observed. In the IR, reflectance decreases with the increase of damage. These results provide valuable information for spectral band selection and optimization of forest damage classification with multispectral scanner data. ESA

N92-11434# Office National d'Etudes et de Recherches Aerospatiales, Toulouse (France). Lab. d'Etudes et de Recherches en Teledetection Spatiale.

MODELING THE BEHAVIOR OF A VEGETATION COVER IN THE MIR, CONTRIBUTION OF HIGH SPECTRAL RESOLUTION [MODELISATION DU COMPORTEMENT D'UN COUVERT VEGETAL DANS LE MIR, APPORT DE LA HAUTE RESOLUTION SPECTRALE]

Catherine E. Leprieur and Frederic Baret (Institut National de la Recherche Agronomique, Montfavet, France) *In* ESA, Physical Measurements and Signatures in Remote Sensing, Volume 1 May 1991 p 201-204 In FRENCH (For primary document see N92-11394 02-43)

Copyright Avail: NTIS HC/MF A20; ESA, EPD, ESTEC, Noordwijk, Netherlands, HC 150 Dutch guilders (2 vols)

Factors affecting the behavior of vegetation cover in the medium infrared (MIR) are analyzed by means of spectra generated between 500 to 2500 nm when combining the TUCKER optical leaf model with the SAIL cover reflectance model. The relation between the spectral convexity and the mean reflectance is shown not to be univocal and expresses a different sensitivity to the studied variables (leaf water retention, cover architecture, and ground optical response). The use of this convexity coupled with mean reflectance values in the near and medium infrared can improve the evaluation of cover water content and give a relation dependent on the leaf water retention. ESA

N92-11435# Nottingham Univ. (England). Dept. of Physiology and Environmental Science.

CANDIDATE HIGH SPECTRAL RESOLUTION DERIVATIVE INDICES FOR THE PREDICTION OF CROP COVER

T. J. Malthus, Bruno Andrieu, Frederic Baret, J. A. Clark, F. Mark Danson, K. W. Jaggard, A. C. Madeira (Lisbon Univ., Portugal), and M. D. Steven *In* ESA, Physical Measurements and Signatures in Remote Sensing, Volume 1 May 1991 p 205-208 Sponsored in cooperation with the British Council and Natural Environmental Research Council (For primary document see N92-11394 02-43)

(Grants AFRC-PG42/328; NERC-GR3/6373)

Copyright Avail: NTIS HC/MF A20; ESA, EPD, ESTEC, Noordwijk, Netherlands, HC 150 Dutch guilders (2 vols)

Part of the results of collaborative experiment to measure high resolution reflectance spectra of crop canopies are presented. One aim of the experiment was to test candidate high spectral resolution indices for vegetation cover for sensitivity to variations in both canopy and soil background color. Measurements of first and second derivative candidate indices, which are compared to the conventional NIR/R ratio for their ability to estimate canopy cover, are presented. Derivative indices related to the red edge were significantly influenced by both canopy color and soil background, as well as the NIR/IR ratio. Several derivative indices in the infrared showed good correlations with canopy color effects. Several derivatives warrant further study, although those indices showing the highest correlations with canopy cover were also significantly affected by soil background color. ESA

N92-11436# Paris VI Univ. (France). Lab. Mineralogie-Cristallographie.

MOISTURE EFFECTS ON SPECTRAL SIGNATURES AND CIE-COLOR OF LATERITIC SOILS

Ali Bedidi, B. Cervelle, and J. Madeira (Office de la Recherche Scientifique et Technique, Bondy, France) *In* ESA, Physical Measurements and Signatures in Remote Sensing, Volume 1 May 1991 p 209-212 (For primary document see N92-11394 02-43)

Copyright Avail: NTIS HC/MF A20; ESA, EPD, ESTEC, Noordwijk, Netherlands, HC 150 Dutch guilders (2 vols)

Soil samples from a lateritic cover were placed in a pressure chamber and subjected to soil suction pressures pF: 2.0, 2.5, 2.8, 3.0, and 4.2. The CIE color values, intensity, hue saturation, were calculated from the diffuse reflectance spectra. The dominant wavelength (hue) increases with moisture content; as the lateritic soil becomes more colored by iron oxihydroxides, this increase becomes more pronouced. The purity Pe (saturation) decreases systemically with increasing moisture content. When the moisture content increases, air in the sample is progressively replaced by water. Therefore, the refractive index of the immersion medium changes from N = 1 (air) to N = 1.33 (water). This change in the refractive index causes an increase in the volumetric diffuse reflectance, especially in the weak absorption regions, and a decrease in the specular reflectance. Contrary to the generally accepted assumption, diffuse reflectance spectra of soils at different moisture rates undergo nonhomothetic changes, leading to a wavelength dependency of the intensity and displacement in the spectral extremas of the bands. ESA

N92-11437# Ludwig-Maximilians-Univ., Munich (Germany, F.R.). Inst. of Landscape Techniques.

HIGH RESOLUTION SPECTRAL MEASUREMENTS OF VEGETATION AND SOIL IN FIELD AND LABORATORY

U. Ammer, B. Koch, T. Schneider, and Helge Wittmeier *In* ESA, Physical Measurements and Signatures in Remote Sensing, Volume 1 May 1991 p 213-217 (For primary document see N92-11394 02-43)

Copyright Avail: NTIS HC/MF A20; ESA, EPD, ESTEC, Noordwijk, Netherlands, HC 150 Dutch guilders (2 vols)

A project to analyze the variations of spectral reflection characteristics on laboratory and field conditions is reported. The future objective is to combine spectrometry with laser fluorescence methods. Signatures of crops measured in their natural environment during the vegetation period with a field spectroradiometer measuring from 400 to 2200 microns in 58 channels are shown. Method and results of spectral measurements of a laboratory experiment are described. The objective of the experiment was the early reconnaissance of stress (water deficiency) of wheat and maize plants. The soil of the plants was measured. The spectroradiometer used has 864 channels in the wavelength region 400 to 2500 microns. ESA

N92-11438# Observatoire de Midi-Pyresnees, Toulouse (France). Groupe de Recherche de Geodesie Spatiale.

NEAR-INFRARED IMAGING SPECTROSCOPY: LEARNING FROM PLANETARY GEOLOGY

Patrick Pinet and Serge Chevrel *In* ESA, Physical Measurements and Signatures in Remote Sensing, Volume 1 May 1991 p 219-222 (For primary document see N92-11394 02-43)

Copyright Avail: NTIS HC/MF A20; ESA, EPD, ESTEC, Noordwijk, Netherlands, HC 150 Dutch guilders (2 vols)

More advanced techniques in the field of planetary geology, orbital and telescopic imaging spectroscopy have already been used for geological applications in the case of Moon and Mars exploration. Examples which illustrate how such techniques are powerful investigation tools to study planetary volcanism, surface alteration processes, and to characterize the composition, vertical stratification, and lateral heterogeneities of planetary crusts, are described. For terrestrial applications, given the high complexity of the natural surfaces and variability of environmental factors, it is necessary to develop new strategies and methods (spectromixing models and image endmember techniques) for the processing, analysis, and interpretation of the next coming spectral data, either airborne or spaceborne. ESA

N92-11439# Canada Centre for Remote Sensing, Ottawa (Ontario).

SPECTROSCOPIC ANALYSIS OF IMAGING SPECTROMETER DATA FOR CLASSIFICATION PURPOSES

Karl Staenz and D. G. Goodenough *In* ESA, Physical Measurements and Signatures in Remote Sensing, Volume 1 May 1991 p 223-227 (For primary document see N92-11394 02-43)

Copyright Avail: NTIS HC/MF A20; ESA, EPD, ESTEC, Noordwijk, Netherlands, HC 150 Dutch guilders (2 vols)

Results for a spectroscopic analysis with an agricultural data set acquired with the Programmable Multispectral Imager (PMI) near Zurich (Switzerland) are presented. In order to reduce the spectral dimensionality of the 288 band data for classification purposes, an eight band data set was derived using an automated data reduction procedure, the band moment analysis concept. Classification accuracies of approximately 80 percent would be achieved with this method. The preprocessing steps which address problems due to the sensor, the calibration, and the transcription of the data, and the flat field normalization method of the MI data, are described. ESA

N92-11440# Centre National de la Recherche Scientifique, Meudon-Bellevue (France). Lab. de Geographie Physique.

PRELIMINARY RESULTS OF A SPECTRO-IMAGERY EXPERIMENT (GER) OVER THE ADRIATIC COASTLINE OF THE VENICE LAGOON [RESULTATS PRELIMINAIRES D'UNE EXPERIENCE DE SPECTRO-IMAGERIE (GER) SUR LE LITTORAL ADRIATIQUE DE LA LAGUNE DE VENISE]

Regina Zbinden and L. Alberotanza (Venice Univ., Italy) *In* ESA, Physical Measurements and Signatures in Remote Sensing, Volume 1 May 1991 p 229-232 In FRENCH Sponsored by ATP Teledetection Spatiale (For primary document see N92-11394 02-43)

Copyright Avail: NTIS HC/MF A20; ESA, EPD, ESTEC, Noordwijk, Netherlands, HC 150 Dutch guilders (2 vols)

A study to characterize the spectral signatures of different water masses and to analyze their distribution and difficulties related to pollution, is reported. A ground validation, using amongst others, radiometric and atmospheric optical thickness measurements, was carried out at the same time. Results show the need for radiometric correction before all other processing. The data currently available to validate the GER instrument results shows that, once this is carried out, classifications based on the spectral signatures of observed targets can be developed. ESA

N92-11441*# Jet Propulsion Lab., California Inst. of Tech., Pasadena.

CURRENT STATUS AND FUTURE DEVELOPMENTS IN RADAR REMOTE SENSING

Diane L. Evans *In* ESA, Physical Measurements and Signatures in Remote Sensing, Volume 1 May 1991 p 235-240 (For primary document see N92-11394 02-43)

Copyright Avail: NTIS HC/MF A20; ESA, EPD, ESTEC, Noordwijk, Netherlands, HC 150 Dutch guilders (2 vols)

Some of the major initiatives and directions of remote sensing using SAR (Synthetic Aperture Radar) data alone and in conjunction with other sensors for Earth science investigations are outlined. Specific emphasis is on areas key to global monitoring using SAR data from spaceborne platforms: calibration, geophysical processing, and generation of digital elevation models. Calibration as used here encompasses end to end system characterization over the life of a sensor and characterization of data products relative to past and future sensors. Geophysical processing is defined here to include any processing which results in derived geophysical units. An additional data type, topography, which is required to complete the three dimensional view of surface properties and correct for distortions inherent in SAR is discussed. Future challenges in radar remote sensing include development of strategies to extrapolate from regional to global scale models and development of new sensor technology. ESA

N92-11442# Marconi Co. Ltd., Great Baddow (England).

MODELING OF RADAR BACKSCATTERING FROM THE SEA SURFACE USING POLARIMETRIC-SAR OBSERVATIONS

J. A. Conway, R. A. Cordey, and J. T. Macklin *In* ESA, Physical Measurements and Signatures in Remote Sensing, Volume 1 May 1991 p 241-246 Sponsored in part by RAE (For primary document see N92-11394 02-43)

Copyright Avail: NTIS HC/MF A20; ESA, EPD, ESTEC, Noordwijk, Netherlands, HC 150 Dutch guilders (2 vols)

Three images obtained from airborne polarimetric SAR (Synthetic Aperture Radar) systems are analyzed to test the composite surface model of radar backscattering from the sea surface. Theoretical predictions are compared with observational data in three tests, involving the dependence of relative radar cross section on incidence angle, polarization signatures, and the distribution of the relative phase difference between HH and VV channels. Calibration errors are taken into account, and it is found that cross talk can dominate over the very weak backscatter expected from the sea surface in HV polarization. All the data sets are consistent with the composite surface model, assuming low to moderate wind speeds, consistent with the environmental conditions at the times of imaging. One of the scenes shows a

well developed swell system propagating in the azimuth direction, together with harmonics of this system a predicted by the nonlinear velocity bunching mechanism. ESA

N92-11443# Physics and Electronics Lab. TNO, The Hague (Netherlands).
DUAL-POLARIZED SCATTEROMETER MEASUREMENTS OF WIND AND MECHANICALLY GENERATED WAVES IN A VERY LARGE WIND/WAVE FLUME, THE VIERS-1 PROJECT
D. vanHalsema, C. Calkoen, W. A. Oost, P. Snoeij, J. Vogelzang, and B. Jaehne (Scripps Institution of Oceanography, La Jolla, CA.) *In* ESA, Physical Measurements and Signatures in Remote Sensing, Volume 1 May 1991 p 247-252 (For primary document see N92-11394 02-43)
Copyright Avail: NTIS HC/MF A20; ESA, EPD, ESTEC, Noordwijk, Netherlands, HC 150 Dutch guilders (2 vols)

In preparation for the launch of the ERS-1 satellite, a study to improve the wind extraction algorithms for the scatterometer was started. The creation of a model for wind retrieval based on physics was addressed. The study consists of a theoretical effort together with two experiments in large wind/wave flume as well as a verification experiment from an ocean based platform. Results of the comparison of the first test model and the flume measurements of the first experiment are given. Results of second flume experiment, dealing especially with the modulation of the backscatter by the long waves, are presented. ESA

N92-11444# Centre for Agrobiological Research, Wageningen (Netherlands).
MULTIFREQUENCY RADAR MEASUREMENTS OF POTATO, BEET, AND WHEAT DURING THE AGRISCATT-88 CAMPAIGN IN THE NETHERLANDS
B. A. M. Bouman, M. A. M. Vissers, and D. Uenk *In* ESA, Physical Measurements and Signatures in Remote Sensing, Volume 1 May 1991 p 255-258 Sponsored in part by Begeleidingscommisse Remote Sensing (For primary document see N92-11394 02-43)
Copyright Avail: NTIS HC/MF A20; ESA, EPD, ESTEC, Noordwijk, Netherlands, HC 150 Dutch guilders (2 vols)

Multitemporal, multifrequency DUTSCAT (1.2 to 17.3 GHz) data collected over the Flevoland test site during Agriscatt 1988, were analyzed in relation to crop type and crop growth of potato, sugar beet and winter wheat. Bare soil types of potato (ridges), beet (flat) and wheat (approximately 0.55 cover, 30 cm height) were well discriminated in the L and S band, and closed crop covers in the high frequencies X, Ku 1 or Ku 2 band. For potato and beet, the wavelength increased 10 to 12 dB in all frequencies (40 degrees incidence angle, VV polarization) from bare soil to the closing of the canopy. For wheat, no radar growth curves were recognized at any frequency. There was no single frequency band most suitable for growth monitoring. For overall application in agriculture, radar observations in one low frequency and in one high frequency seem to suffice (for potato, beet and wheat). ESA

N92-11445# Institut National de la Recherche Agronomique, Montfavet (France). Station de Science du Sol.
ESTIMATION OF THE GROUND HUMIDITY UNDER VEGETATION: APPLICATIONS OF SEMI-EMPIRICAL MODELS [ESTIMATION DE L'HUMIDITE DU SOL SOUS VEGETATION: APPLICATIONS DE MODELES SEMI-EMPIRIQUES]
Patrick Bertuzzi and Laurent Bruckler *In* ESA, Physical Measurements and Signatures in Remote Sensing, Volume 1 May 1991 p 259-264 In FRENCH; ENGLISH summary (For primary document see N92-11394 02-43)
Copyright Avail: NTIS HC/MF A20; ESA, EPD, ESTEC, Noordwijk, Netherlands, HC 150 Dutch guilders (2 vols)

C Band scatterometer measurements (15 degrees HH, 23 degrees HH, 23 degrees VV) were made from Jul. to Oct. 1989 during the growing season of a soybean, concurrently with measurements of soil moisture and growth canopy descriptors. Seven formulations of semi empirical cloud models were fitted to experimental data. Results showed that all models were similar. The nonlinear estimation procedure gave satisfactory but slightly biased results. The inversion procedure of such models did not give accurate estimates of surface soil moisture for the 23 degrees VV configuration of the ERS1 satellite. ESA

N92-11446# Paris VI Univ. (France). Lab. de Geologie Structurale et Teledetection.
RADAR IMAGE SIMULATION TO STUDY THE VISUAL APTITUDE OF OBSERVING SLOPE AND ROUGHNESS EFFECTS [SIMULATION D'IMAGES RADAR POUR ETUDIER L'APTITUDE VISUELLE A OBSERVER LES EFFETS DE PENTE ET DE RUGOSITE]
H. Chakroun, E. Monjoux, and Jean-Paul Rudant *In* ESA, Physical Measurements and Signatures in Remote Sensing, Volume 1 May 1991 p 265-267 In FRENCH (For primary document see N92-11394 02-43)
Copyright Avail: NTIS HC/MF A20; ESA, EPD, ESTEC, Noordwijk, Netherlands, HC 150 Dutch guilders (2 vols)

The study of visually differentiating morpholithological faces by radar image simulation was addressed. Theoretical and experimental microwave backscatter coefficients are used as problem parameters. ESA

N92-11447# Joint Research Centre of the European Communities, Ispra (Italy).
GENERALIZED FORMULATION FOR SEMI-EMPIRICAL RADAR MODELS REPRESENTING CROP BACKSCATTERING
Isabelle Champion and Gerard Guyot (Institut National de la Recherche Agronomique, Montfavet, France) *In* ESA, Physical Measurements and Signatures in Remote Sensing, Volume 1 May 1991 p 269-272 (For primary document see N92-11394 02-43)
Copyright Avail: NTIS HC/MF A20; ESA, EPD, ESTEC, Noordwijk, Netherlands, HC 150 Dutch guilders (2 vols)

Two one layer cloud droplet models, working with the leaf area index as a vegetation biomass variable are used in a generalized formulation, initially adapted to different crop geometries for one frequency range to fit correctly at all frequencies/polarization configurations through a varying scattering term. A difference of crop geometry or a variation of frequency is concluded to play a similar role in regard to the analytical form of the cloud model. The important factor, which determines the form of radar signal evolution versus the biomass variable, is the ratio between the wavelength of the radar signal and the characteristic crop scattering length. The significance of the adjusted parameters of the model are discussed in terms of scattering and attenuation and of their relative weight in the radar signal as a function of the varying combinations of crop/measurement geometries. ESA

N92-11448# Paris VI Univ. (France). Lab. de Geologie Structurale et Teledetection.
CONTRIBUTION OF ACTIVE MICROWAVES TO THE STRUCTURAL ANALYSIS OF EPICONTINENTAL SHELF-FORMS: EXAMPLE OF THE ENGLISH CHANNEL [APPORT DES HYPERFREQUENCES ACTIVES A L'ANALYSE STRUCTURALE DES PLATES-FORMES EPICONTINENTALES: EXEMPLE DE LA MANCHE]
Jean-Paul Rudant, Jean-Paul Deroin, and Alain Wadsworth (Institut Francais du Petrole, Rueil-Malmaison.) *In* ESA, Physical Measurements and Signatures in Remote Sensing, Volume 1 May 1991 p 273-276 In FRENCH (For primary document see N92-11394 02-43)
Copyright Avail: NTIS HC/MF A20; ESA, EPD, ESTEC, Noordwijk, Netherlands, HC 150 Dutch guilders (2 vols)

The interpretation of a Seasat image taken over the Isle of Wight (English Channel) and its neighboring environment shows the continuity of geological structures on land and at sea. Such submarine structures cause perturbations in the velocity field of marine currents which, by their interaction with moderate winds, modulate ultragravitational wave fields at the surface; this induces backscatter variations as a function of water depth. ESA

N92-11449# Groupement Scientifique de Teledetection Spatiale de Toulouse (France).

ANALYSIS OF RADAR POLARIMETRIC DATA FOR THE DISCRIMINATION AND MONITORING OF FOREST COVERS

Stephane Goze, T. LeToan, E. Mougin, A. Lopes, and R. Touzi *In* ESA, Physical Measurements and Signatures in Remote Sensing, Volume 1 May 1991 p 277-281 Sponsored by Alcatel Espace; Joint Research Centre of the European Communities; and PNTS (For primary document see N92-11394 02-43)

Copyright Avail: NTIS HC/MF A20; ESA, EPD, ESTEC, Noordwijk, Netherlands, HC 150 Dutch guilders (2 vols)

In order to assess the use of polarimetric SAR (Synthetic Aperture Radar) images for forest monitoring and for retrieval of forest biophysical parameters, a study conducted with the polarimetric L band NASA/JPL SAR image acquired during the 1988 Alaskan campaign was undertaken. Radar measurements retrieved from the image include polarimetric signatures and new polarimetric indices, in addition to the radar backscattering coefficients. The analysis of the polarimetric signatures gives more insight into the scattering mechanisms. The different radar measurements are studied as a function of vegetation parameters. The preliminary results seem to be promising for identification and monitoring of forest covers. ESA

N92-11450*# Jet Propulsion Lab., California Inst. of Tech., Pasadena.

AIRBORNE PRECURSOR MISSIONS IN SUPPORT OF SIR-C/X-SAR

D. Evans, H. Oettl, and P. Pampaloni (Consiglio Nazionale delle Ricerche, Florence, Italy) *In* ESA, Physical Measurements and Signatures in Remote Sensing, Volume 1 May 1991 p 283-284 (For primary document see N92-11394 02-43)

Copyright Avail: NTIS HC/MF A20; ESA, EPD, ESTEC, Noordwijk, Netherlands, HC 150 Dutch guilders (2 vols) CSCL 08B

The NASA DC-8 and DLR E-SAR airborne imaging radars have been deployed over several sites in Europe and the U.S. in support of SIR-C/X-SAR (Shuttle Imaging Radar-C/X-Synthetic Aperture Radar) science team investigations. To date, data have been acquired in support of studies of alpine glaciers, forests, geology, oceanography, and calibration. An experimental campaign with airborne sensors will take place in Europe in June to July 1991 which will allow multitemporal surveys of several Europeans sites. Current plans are for calibration and ecology experiments to be undertaken in Germany, the Netherlands, Italy, France, and the United Kingdom. Coordinated multitemporal aircraft and ground campaigns are planned in support of hydrology experiments in Italy, the United Kingdom, and Austria. Data will also be acquired in support of oceanogrqhy in the Gulf of Genova, North Atlantic, Straits of Messina and the North Sea. Geology sites will include Campi Flegrei and Vesuvio, Italy. ESA

N92-11451# Academy of Sciences (USSR), Gorky. Inst. of Applied Physics.

NONLINEAR THEORY OF SYNTHETIC APERTURE RADAR SEA WAVE IMAGING

M. B. Kanevsky *In* ESA, Physical Measurements and Signatures in Remote Sensing, Volume 1 May 1991 p 285-287 (For primary document see N92-11394 02-43)

Copyright Avail: NTIS HC/MF A20; ESA, EPD, ESTEC, Noordwijk, Netherlands, HC 150 Dutch guilders (2 vols)

The Synthetic Aperture Radar (SAR) sea wave imaging mechanism is shown to be nonlinear for any sea wave directions except for the nearly radial one. The SAR image spectrum for azimuthally traveling waves is found with the speckle noise taken into account. ESA

N92-11452# Joint Research Centre of the European Communities, Ispra (Italy). Inst. for Remote Sensing Applications.

DUAL POLARIZATION MICROWAVE BACKSCATTER SIGNATURES OF BARE AND VEGETATED SOILS

G. G. Lemoine *In* ESA, Physical Measurements and Signatures in Remote Sensing, Volume 1 May 1991 p 289-292 Sponsored in part by Beleidscommissie Remote Sensing (For primary document see N92-11394 02-43)

Copyright Avail: NTIS HC/MF A20; ESA, EPD, ESTEC, Noordwijk, Netherlands, HC 150 Dutch guilders (2 vols)

The ratio between the VV and HH polarized radar cross sections of bare and vegetated soils is discussed. Trends predicted by microwave backscatter models for slightly rough surfaces show an increase in the ratio towards the higher incidence angles. This is due to the Brewster angle effect. The magnitude and position of the maximum ratio depends on the dielectric permittivity of soil material. Since the dielectric permittivity of soil material largely depends on the moisture content, the ratio can serve as an indicator for soil moisture content close to the surface. The theoretical predictions are supported by high incidence angle scatterometer data. An interesting observation is that the ratio at high incidence angles decreases when crops emerge, and remains rather constant until the crop dries out or is harvested at the end of the season, when it increases again. Hence, the ratio can be used as qualitative classifier to separate bare and vegetated areas in SAR (Synthetic Aperture Radar) data. As an example, a composite image taken over the Dutch Flevoland site on September 8th 1987, is shown. ESA

N92-11453# Institut National de la Recherche Agronomique, Rennes (France). Dept. de Science du Sol.

HUMIDITY MEASUREMENT OF NAKED GROUND BY RADAR IN CONDITIONS OF EXCESSIVE WATER [MESURE DE L'HUMIDITE D'UN SOL NU PAR RADAR DANS DES CONDITIONS D'EXCES D'EAU]

P. Merot and Andre Chanzy (Institut National de la Recherche Agronomique, Avignon, France) *In* ESA, Physical Measurements and Signatures in Remote Sensing, Volume 1 May 1991 p 293-296 In FRENCH (For primary document see N92-11394 02-43)

Copyright Avail: NTIS HC/MF A20; ESA, EPD, ESTEC, Noordwijk, Netherlands, HC 150 Dutch guilders (2 vols)

Radar response to the prescence of an excess of water was addressed. The surface saturation was measured over two parcels, one smooth, one rugged; it changed from 50 to 0 percent. Characterization of the surface saturation was done simultaneously by radar and by photographs. The following are shown: relevance of a variable such as the percentage of saturated surface to explain the backscatter signal decrease; the identical character of the decrease for the two types of surface; the strong amplitude of signal amplitude in excess water conditions (several dB); the necessity of removing the ambiguity between measurements in excess water and in dry or dried conditions. ESA

N92-11454# Centre Machinisme Agricole Genie Rural Eaux Forets, Antony (France). Div. Hydrologie.

ACTIVE MICROWAVE REMOTE SENSING AND GROUND HYDRIC STATE. AGRISCATT '88 AIRBORNE CAMPAIGN OVER THE ORGEVAL BASIN (FRANCE) [TELEDETECTION EN HYPERFREQUENCES ACTIVES ET ETAT HYDRIQUE SUPERFICIEL DU SOL. A LA CAMPAGNE AEROPORTEE AGRISCATT'88 SUR LE BASSIN DE L'ORGEVAL]

M. Normand, Sylvie Galle, M. Benallegue, M. Dechambre, O. Taconet, Daniel Vidal-Madjar, and Laurent Prevot (Institut National de la Recherche Agronomique, Montfavet, France) *In* ESA, Physical Measurements and Signatures in Remote Sensing, Volume 1 May 1991 p 297-300 In FRENCH Sponsored by ESA (For primary document see N92-11394 02-43)

Copyright Avail: NTIS HC/MF A20; ESA, EPD, ESTEC, Noordwijk, Netherlands, HC 150 Dutch guilders (2 vols)

The objectives of the campaign are presented and experiments over the Orgeval basin are described. Ground truth operations were carried out on the superficial humidity of ground and vegetation over 17 land parcels. The correlation coefficient between the backscattered radar signal and the ground humidity volume is optimal for the configuration band C, HH, 20 degrees, and is little influenced by incidence angle. It can be improved however by combining bands C and X (multiple correlations) data. Analysis of band C, 20 degree results shows temporal and spatial variability

of the signal along the flight axis, where the parcels appear as entities with regard to the surface humidity, and validates this remote sensing method for the hydric state of sloping basins.
ESA

N92-11455# Office de la Recherche Scientifique et Technique Outre-Mer, Montpellier (France).
AIRBORNE SAR HAREM CAMPAIGN: RESULTS, TARGETS FEATURES, ERS1 SIMULATIONS, AND OPERATIONAL SATELLITE EXPLOITATION
Michel Petit, Jean-Michel Stretta, Henri Farrugio, and Alain Wadsworth (Institut Francais du Petrole, Rueil-Malmaison.) *In* ESA, Physical Measurements and Signatures in Remote Sensing, Volume 1 May 1991 p 301-304 (For primary document see N92-11394 02-43)
Copyright Avail: NTIS HC/MF A20; ESA, EPD, ESTEC, Noordwijk, Netherlands, HC 150 Dutch guilders (2 vols)

During the Halieutics Radar Experimentation Mediterranean sea (HAREM) campaign, Synthetic Aperture Radar (SAR) images of the sea and lagoon surface and concurrent ground truth observations and measurements were collected in order to test the potential of some applications of SAR imaging theories to halieutics. These theories were developed to explain the SAR signal modulation in relationship with small variations of water roughness induced by internal wave or current or wind field variations. Analysis of the HAREM data indicates that the marine surface life (tuna schools and marine mammals) and fishing activities (nets and fish traps) can generate a SAR signal modulation of the comparable order of magnitude for the C band (5.3 GHz). This confirmed the expectation of SAR, after the preliminary experiment made in X band (9.6 GHz). From the HAREM data, the results of satellite simulations, considering ERS1 characteristics, are presented and show good promises for fishing activity surveys. This high detection power of SAR provides unique opportunities to obtain direct information on fishing and surface marine life activities in large survey areas. From that, the aerial SAR data and, under certain conditions, satellite SAR data is assumed to perhaps dramatically enhance and complement classical methods (statistics) used in fishery management, the essential goal in halieutics. ESA

N92-11456# Institut National de la Recherche Agronomique, Thiverval-Grignon (France). Station de Bioclimatologie.
EVALUATION OF VEGETATION COVER CHARACTERISTICS USING AN AIRBORNE MICROWAVE SCATTEROMETER [ESTIMATION DE CARACTERISTIQUES DE COUVERTS VEGETAUX A L'AIDE D'UN DIFFUSIOMETRE HYPERFREQUENCE AEROPORTE]
Laurent Prevot, M. Dechambre, O. Taconet, Daniel Vidal-Madjar, M. Normand, and Sylvie Galle (Office de la Recherche Scientifique et Technique Outre-Mer, Montpellier, France) *In* ESA, Physical Measurements and Signatures in Remote Sensing, Volume 1 May 1991 p 305-308 In FRENCH; ENGLISH summary Sponsored by Programme National de Teledetection Spatiale and CNES (For primary document see N92-11394 02-43)
Copyright Avail: NTIS HC/MF A20; ESA, EPD, ESTEC, Noordwijk, Netherlands, HC 150 Dutch guilders (2 vols)

Possible use of SAR (Synthetic Aperture Radar) for monitoring agricultural canopies is investigated. Data were acquired on the Orgeval watershed (France) during the Agriscatt'88 campaign. Simultaneous ground truth measurements (soil moisture, leaf area index, water content of the canopy) were conducted on 11 wheat fields. Backscattering coefficients of the canopy are interpretated in the framework of semi empirical watercloud models. A simple parametrization of the angular effect of soil roughness is introduced, allowing the use of simultaneous multi-incidence angle radar data. It is shown that in this case attenuation is the dominant effect of the vegetation and an inversion algorithm is proposed for estimating the water content of vegetation. Different combinations of radar configurations are tested. ESA

N92-11457# Aerospatiale, Cannes (France).
LAND COVER CLASSIFICATION BY MULTIPOLARIZED SAR IMAGERY [CLASSIFICATION DE COUVERTS DE TERRAINS PAR IMAGERIE SAR MULTIPOLARISEE]
Sabine Caillault-Voyer *In* ESA, Physical Measurements and Signatures in Remote Sensing, Volume 1 May 1991 p 309-312 In FRENCH (For primary document see N92-11394 02-43)
Copyright Avail: NTIS HC/MF A20; ESA, EPD, ESTEC, Noordwijk, Netherlands, HC 150 Dutch guilders (2 vols)

Data which can be extracted from SAR (Synthetic Aperture Radar) is statistically analyzed for classification of different types of land cover. Important steps are to define an optimal classification vector and define adapted classification methods. Principles of each classification technique are described. Applications on multipolarized SAR images are presented. ESA

N92-11458*# National Aeronautics and Space Administration. Goddard Space Flight Center, Greenbelt, MD.
PASSIVE MICROWAVE REMOTE SENSING OF SOIL MOISTURE: RESULTS FROM HAPEX, FIFE, AND MONSOON 90
Thomas Schmugge, T. J. Jackson, and J. R. Wang (Department of Agriculture, Beltsville, MD.) *In* ESA, Physical Measurements and Signatures in Remote Sensing, Volume 1 May 1991 p 315-319 (For primary document see N92-11394 02-43)
Copyright Avail: NTIS HC/MF A20; ESA, EPD, ESTEC, Noordwijk, Netherlands, HC 150 Dutch guilders (2 vols) CSCL 08B

HAPEX (Hydrologic Atmospheric Pilot Experiment), FIFE (First ISLSCP Field Experiment) and MONSOON 90 which used an imaging microwave radiometer operating at a frequency of 1.42 GHz are reported. For FIFE and MONSOON 90, a wide range of moisture conditions were present and it was possible to observe the drydown of the soil following heavy rain and to map its spatial variation. The quantitive agreement of microwave observations and ground measurements was very good. In HAPEX there were no significant rains and conditions were generally rather dry, however, moisture variations due to irrigation were observed. ESA

N92-11459# Princeton Univ., NJ. Water Resources Program.
COMPARISON OF PASSIVE MICROWAVE AND MODEL DERIVED ESTIMATES FOR SOIL MOISTURE FIELDS
J. S. Famiglietti and Eric F. Wood *In* ESA, Physical Measurements and Signatures in Remote Sensing, Volume 1 May 1991 p 321-326 (For primary document see N92-11394 02-43)
Copyright Avail: NTIS HC/MF A20; ESA, EPD, ESTEC, Noordwijk, Netherlands, HC 150 Dutch guilders (2 vols)

Techniques to incorporate remotely sensed soil moisture data in a distributed hydrologic model are investigated. Specifically, the use of remotely sensed surface soil moisture maps for calibration and validation of the model is explored. The distributed water balance model used in the study is reviewed. Remotely sensed soil moisture maps from FIFE (First ISLSCP Field Experiment) are used to calibrate and validate the model on a small catchment at the experiment site. Results indicate that maps or remotely sensed soil moisture are useful tools for the calibration and verification of hydrological models. Problems due to the resolution of the remotely sensed, modeled, and observed data are discussed. ESA

N92-11460# Consiglio Nazionale delle Ricerche, Florence (Italy). Ist. di Ricerca sulle Onde Elettromagnetiche.
PASSIVE MICROWAVE REMOTE SENSING OF VEGETATION CANOPIES: EXPERIMENTAL AND MODELING RESULTS
Simonetta Paloscia and P. Pampaloni *In* ESA, Physical Measurements and Signatures in Remote Sensing, Volume 1 May 1991 p 327-332 (For primary document see N92-11394 02-43)
Copyright Avail: NTIS HC/MF A20; ESA, EPD, ESTEC, Noordwijk, Netherlands, HC 150 Dutch guilders (2 vols)

The potentials of some microwave vegetation parameters in describing vegetation characteristics are discussed. Thermal infrared and microwave brightness temperatures (at 10 GHz, 36 GHz) of agricultural surfaces are combined to compute some

microwave parameters. These parameters are correlated to vegeta-leaf area index and plant water content of corn and alfalfa. The experimental relationships are explained, at least partially, by means of a model which treats vegetation as a slab of uniform material upon the soil surface. ESA

N92-11461*# Jet Propulsion Lab., California Inst. of Tech., Pasadena.

ON THE USE OF PASSIVE MICROWAVES AT 37 GHz

Yann H. Kerr (Office National d'Etudes et de Recherches Aerospatiales, Toulouse, France) and Eni G. Njoku *In* ESA, Physical Measurements and Signatures in Remote Sensing, Volume 1 May 1991 p 333-337 (For primary document see N92-11394 02-43)

Copyright Avail: NTIS HC/MF A20; ESA, EPD, ESTEC, Noordwijk, Netherlands, HC 150 Dutch guilders (2 vols)

Recently a number of studies have been presented on the use of the 37 GHz channels of the Scanning Multichannel Microwave Radiometer (SMMR) on board the Nimbus 7 satellite, and on the synergisms between the SNMMR and the AVHRR (Advanced Very High Resolution Radiometer). The approaches are interesting but raise a number of questions on the validity of the interpretation of the results. A study to analyze the Microwave Polarization Difference Temperature (MPDT) in terms of sensitivity to surface and atmospheric parameters is presented. For this a radiative transfer model is used so as to depict the shortcomings of this index. Another approach, using lower frequencies is described and compared to the 37 GHz MPDT. ESA

N92-11462# Groupement Scientifique de Teledetection de Strasbourg (France).

EXPERIMENTAL APPROACH TO EMISSIVITY PROBLEMS AND SURFACE TEMPERATURE IN THERMAL INFRARED REMOTE SENSING [APPROCHE EXPERIMENTALE DES PROBLEMES D'EMISSIVITE ET TEMPERATURE DE SURFACE EN TELEDETECTION INFRAROUGE THERMIQUE]

M. P. Stoll, Francoise Nerry, Jelila Labed, and N. Kologo *In* ESA, Physical Measurements and Signatures in Remote Sensing, Volume 1 May 1991 p 339-344 In FRENCH (For primary document see N92-11394 02-43)

Copyright Avail: NTIS HC/MF A20; ESA, EPD, ESTEC, Noordwijk, Netherlands, HC 150 Dutch guilders (2 vols)

Emission and reflection approaches are used in an experimental study of surface properties in the thermal IR. Techniques and results obtained concerning absolute emissivity signatures, angular variation of ground emissivity in the thermal IR, and ground diffuse reflection at 10.6 microns are described. In situ spectroradiometric measurements are examined and an operational procedure to pass from local scale to pixel scale and obtain spectral signature and surface temperature is proposed. Accuracy is discussed and the total error on the effective temperature is shown to be perhaps less than 0.8 K. ESA

N92-11463# Centre National de la Recherche Scientifique, Grenoble (France). Lab. de Glaciologie et de Geophysique de l'Environnement.

LARGE SCALE STUDY OF THE MICROWAVE SIGNATURE OF THE ANTARCTIC ICE SHEET

Michel Fily and J. P. Benoist *In* ESA, Physical Measurements and Signatures in Remote Sensing, Volume 1 May 1991 p 347-350 (For primary document see N92-11394 02-43)
(Contract ATP-87/CNES/1254)

Copyright Avail: NTIS HC/MF A20; ESA, EPD, ESTEC, Noordwijk, Netherlands, HC 150 Dutch guilders (2 vols)

Data from the Scanning Multichannel Microwave Radiometer are analyzed over the Antarctic ice sheet. A principal component analysis reveals the importance of the polarization difference at 6.6 GHz and of the gradient between 6.6 and 18 GHz brightness temperatures. Distinct areas appear from the spatial distribution of these parameters. Differences are related to surface snow characteristics as stratification, due to a distinct temperature-snow accumulation ratio. Temporal variations throughout one year are used to derive a map related to the topography. The analysis of data over seven years indicates a remarkable stability without any particular long term trend. ESA

N92-11464# Centre National de la Recherche Scientifique, Grenoble (France). Lab. de Glaciologie et de Geophysique de l'Environnement.

COMPARISON BETWEEN THE OBSERVED MICROWAVE SPECTRAL SIGNATURES OVER THE ANTARCTIC ICE SHEET AND A SNOW EMISSIVITY MODEL

Sylviane Surdyk and Michel Fily *In* ESA, Physical Measurements and Signatures in Remote Sensing, Volume 1 May 1991 p 351-354 (For primary document see N92-11394 02-43)
(Contract ATP-87/CNES/1254)

Copyright Avail: NTIS HC/MF A20; ESA, EPD, ESTEC, Noordwijk, Netherlands, HC 150 Dutch guilders (2 vols)

The Scanning Multichannel Microwave Radiometer data are compared with the snow characteristics measured during a Japanese traverse made in 1968-1969 from Syowa (69 degrees south, 39 degrees 35 minutes east) to the South Pole on the Antarctic ice sheet. The results from a snow emissivity model based on the strong fluctuation theory are used to help with the interpretation of data. The polarization difference is mainly affected by the stratification of snow where its density is low. The brightness temperature versus frequency gradient is linked to the distributions of grain sizes as determined from detailed stratigraphies. ESA

N92-11465# Academy of Sciences of the Estonian SSR, Tartu. Inst. of Astrophysics and Atmospheric Physics.

INFLUENCE OF THE CROP ARCHITECTURE PARAMETERS ON CROP BRDF: A MONTE CARLO SIMULATION

Juhan Ross and Alexander L. Marshak (Goettingen Univ., Germany, F.R.) *In* ESA, Physical Measurements and Signatures in Remote Sensing, Volume 1 May 1991 p 357-360 (For primary document see N92-11394 02-43)

Copyright Avail: NTIS HC/MF A20; ESA, EPD, ESTEC, Noordwijk, Netherlands, HC 150 Dutch guilders (2 vols)

To calculate the plant canopy Bidirectional Reflectance Distribution Function (BRDF), a powerful Monte Carlo algorithm, was developed. The plant canopy is presented by a rather universal opticogeometrical model, which allows illumination conditions, plant architecture parameters, plant and soil optical properties and their influence on the shape of the canopy BRDF as a function of solar and view directions to be considered. A series of numerical experiments was carried out to analyze the influence of input parameters on the canopy BRDF. ESA

N92-11466*# National Aeronautics and Space Administration, Washington, DC.

A THREE DIMENSIONAL RADIATIVE TRANSFER METHOD FOR OPTICAL REMOTE SENSING OF VEGETATED LAND SURFACES

Ghassem Asrar, Ranga B. Myneni, and Bhaskar J. Choudhury (National Aeronautics and Space Administration. Goddard Space Flight Center, Greenbelt, MD.) *In* ESA, Physical Measurements and Signatures in Remote Sensing, Volume 1 May 1991 p 361-367 (For primary document see N92-11394 02-43)

Copyright Avail: NTIS HC/MF A20; ESA, EPD, ESTEC, Noordwijk, Netherlands, HC 150 Dutch guilders (2 vols)

In the application of remote sensing at optical wavelengths to vegetated surfaces from satellite borne high resolution instruments, an understanding of the various physical mechanisms that contribute to the measured signal is important. A numerical method of solving the radiative transfer equation in three dimensions is reported. The reliability of coding and accuracy of the algorithm are evaluated by benchmarching. Parametrization of the methods and results of a simulation are presented. The method is tested with experimental data of canopy bidirectional reflectance factors. The effect of spatial heterogeneity on the relationship between the simple ratio and normalized vrs absorbed Photosynthetically Active Radiation (PAR) is discussed. ESA

N92-11467*# California Univ., Davis. Dept. of Land, Air and Water Resources.

ANISOTROPY OF THERMAL INFRARED EXITANCE ABOVE AND WITHIN PLANT CANOPIES

Kyaw Tha PawU (Institut National de la Recherche Agronomique, Thiverval-Grignon, France) *In* ESA, Physical Measurements and Signatures in Remote Sensing, Volume 1 May 1991 p 369-374 Sponsored by NASA, Washington and Institut National de la Recherche Agronomique (For primary document see N92-11394 02-43)

Copyright Avail: NTIS HC/MF A20; ESA, EPD, ESTEC, Noordwijk, Netherlands, HC 150 Dutch guilders (2 vols)

Any significant angular dependence of the emitted long wave radiation could result in errors in remotely estimated energy budgets or evapotranspiration. Empirical data and thermal infrared radiation models are reviewed in reference to anisotropic emissions from the plant canopy. The biometeorological aspects of linking longwave models with plant canopy energy budgets and micrometeorology are discussed. A new soil plant atmosphere model applied to anisotropic longwave emissions from a canopy is presented. Time variation of thermal infrared emission measurements is discussed. ESA

N92-11468# University Coll., London (England). Dept. of Geography.

MEASUREMENT, SIMULATION, AND ANALYSIS OF THE DIRECTIONAL REFLECTANCE PROPERTIES OF EARTH SURFACE MATERIALS

Mike J. Barnsley and Jan-Peter Muller *In* ESA, Physical Measurements and Signatures in Remote Sensing, Volume 1 May 1991 p 375-382 (For primary document see N92-11394 02-43)

(Grants NERC-GR3/7020; NERC-GR3/7901)

Copyright Avail: NTIS HC/MF A20; ESA, EPD, ESTEC, Noordwijk, Netherlands, HC 150 Dutch guilders (2 vols)

The directional reflectance properties of Earth surface materials are believed to contain unique information relating to their biophysical characteristics and three dimensional geometric structure that cannot be inferred from multispectral analyses alone. Various aspects of the measurement and analysis of directional reflectance data using ground based, airborne and satellite sensors are examined. The numerical simulation of directional reflectance data at a variety of spatial scales is explored using ray racing techniques applied to Digital Elevation Models (DEMs) of surface microtopography and three dimensional models of vegetation canopies, both derived from close range stereo photogrammetry. The potential application of directional reflectance data to infer a number of biophysical and climatological parameters is discussed. ESA

N92-11469# Office National d'Etudes et de Recherches Aerospatiales, Toulouse (France). Lab. d'Etudes et de Recherches en Teledetection Spatiale.

BIDIRECTIONAL REFLECTANCE AND SURFACE ALBEDO: PHYSICAL MODELING AND INVERSION

Bernard Pinty and Michel M. Verstraete (Joint Research Centre of the European Communities, Ispra, Italy) *In* ESA, Physical Measurements and Signatures in Remote Sensing, Volume 1 May 1991 p 383-386 (For primary document see N92-11394 02-43)

Copyright Avail: NTIS HC/MF A20; ESA, EPD, ESTEC, Noordwijk, Netherlands, HC 150 Dutch guilders (2 vols)

The need to obtain surface albedo measurements for climate models, and the desire to use remote sensing tools to describe the nature and evolution of terrestrial ecosystems both hinge on the capability to describe the bidirectional reflectance of natural surfaces, as it is observed on board satellites. The various radiation models applied to these problems, either in direct mode to generate the reflectance and the albedo of known porous media, or in inverse mode to retrieve the characteristics of the surface from remote sensing measurements are reviewed. Issues related to the validation and to the inversion of these models are discussed, and outstanding challenges are outlined. ESA

N92-11470*# Scripps Institution of Oceanography, La Jolla, CA. Space Inst.

BI-DIRECTIONAL REFLECTANCE OF FINITE AND INFINITE CLOUDS

Francois-Marie Breon and Catherine Gautier (California Univ., Santa Barbara.) *In* ESA, Physical Measurements and Signatures in Remote Sensing, Volume 1 May 1991 p 389-392 (For primary document see N92-11394 02-43)

(Grant NAG1-889)

Copyright Avail: NTIS HC/MF A20; ESA, EPD, ESTEC, Noordwijk, Netherlands, HC 150 Dutch guilders (2 vols)

The transfer of solar irradiance in plane parallel and broken cloud fields is modeled using a Monte Carlo method. The angular distribution pattern of radiances exiting the cloud layer is studied with varying cloud geometries, optical thicknesses, cloudiness and solar zenith angles. A rather large anisotropy of the reflected flux is found, usually increasing with solar zenith angle and with patterns that strongly depend on cloud geometry. The main features are: a local maximum of reflected intensity in the forward direction for all cases; a limb darkening for the plane parallel case; and a limb brightening and a local maximum of reflected intensity in the backward direction for broken clouds. The method is used to study the cloud reflectance sensitivity to various parameters. A more precise description of cloud field internal and external structure is needed in order to obtain accurate bi directional reflectance diagrams. ESA

N92-11471# Lille-1 Univ., Villeneuve-d'Asoq (France). Lab. d'Optique Atmospherique.

AIRCRAFT SIMULATIONS OF THE POLDER EXPERIMENT: FIRST RESULTS

J.-L. Deuze, Jean-Yves Balois, C. Devaux, L. Gonzalez, M. Herman, P. Lecomte, and Christian Verwarde *In* ESA, Physical Measurements and Signatures in Remote Sensing, Volume 1 May 1991 p 393-396 (For primary document see N92-11394 02-43)

Copyright Avail: NTIS HC/MF A20; ESA, EPD, ESTEC, Noordwijk, Netherlands, HC 150 Dutch guilders (2 vols)

The POLDER (Polarization and Directionality of the Earth's Reflectances) instrument is a new device designed to measure from space, with different viewing angles, the reflectance and polarization of the solar radiation, reflected by the Earth atmosphere system, at visible and near infrared wavelengths. Measurements performed in June 1990 during the first aircraft experimentation of the POLDER simulator, over the region of La Crau (south east of France) are presented. ESA

N92-11472# Nottingham Univ. (England). Dept. of Geography.

THE EFFECT OF THE DISTRIBUTION OF CHLOROTIC MATERIAL ON THE REFLECTANCE OF MIXED CANOPIES

J. A. Eastwood and M. D. Steven *In* ESA, Physical Measurements and Signatures in Remote Sensing, Volume 1 May 1991 p 397-400 Sponsored by Natural Environmental Research Council and Remote Sensing Society (For primary document see N92-11394 02-43)

Copyright Avail: NTIS HC/MF A20; ESA, EPD, ESTEC, Noordwijk, Netherlands, HC 150 Dutch guilders (2 vols)

The effect on canopy reflectance of the spatial distribution of chlorotic material within plant stands was simulated using the SAIL model. Three idealized distributions of chlorotic and green leaves were investigated: a completely random mixture, a green layer below a chlorotic layer, and a chlorotic layer below a green layer. The model predicted differences in red canopy reflectance and NDVI (Normalized Difference Vegetation Index) between the three distributions which diverged with increasing leaf area index or solar zenith angle. Reflectance and NDVI were shown to depend upon soil reflectance, canopy geometry and the percentage of chlorotic material present, with maximum separation of the three cases occurring when the amounts of green and yellow material were equal. Field data from semichlorotic canopies were obtained from stands of stressed sugar beet. The fit of modeled NDVI to the measured data was improved when the chlorotic material was assumed to be at the top of the canopy. ESA

N92-11473# Office de la Recherche Scientifique et Technique Outre-Mer, Paris (France).

INFLUENCE OF THE VIEWING GEOMETRY ON THE SPECTRAL PROPERTIES (HIGH RESOLUTION VISIBLE AND NIR) OF SELECTED SOILS FROM ARIZONA

Richard Escadafal and Alfredo R. Huete (Arizona Univ., Tucson.) *In* ESA, Physical Measurements and Signatures in Remote Sensing, Volume 1 May 1991 p 401-404 (For primary document see N92-11394 02-43)

Copyright Avail: NTIS HC/MF A20; ESA, EPD, ESTEC, Noordwijk, Netherlands, HC 150 Dutch guilders (2 vols)

The influence of view angle on the spectral signature of bare soils was investigated during a field campaign over five sites. Bidirectional Reflectance Factors (BRF) in the 400 to 900 nm wavelength range and color coefficients were computed from measurements made along the principal plane of the Sun with a portable spectrocardiometer. A strong backscatter effect was observed in the antisolar direction. This nonlambertian behavior is related to the surface roughness and can be interpreted with existing models. Viewing geometry also influenced the shape of the soil spectral reflectance curves and resulted in an increase in color hue in the antisolar direction and maximum color saturation at nadir. This was attributed to multiple reflections of direct light and diffuse illumination of the shadowed parts of rough surfaces. These viewing effects on soil surface spectral signatures are relatively small when compared to spectral variances normally encountered among soils. ESA

N92-11474*# National Aeronautics and Space Administration, Washington, DC.

OPTIMUM COMBINATIONS OF VISIBLE AND NEAR-INFRARED REFLECTANCES FOR ESTIMATING THE FRACTION OF PHOTOSYNTHETICALLY AVAILABLE RADIATION ABSORBED BY PLANTS

Alain Podaire, Pierre-Yves Deschamps, R. Frouin (Scripps Institution of Oceanography, La Jolla, CA.), and Ghassem Asrar *In* ESA, Physical Measurements and Signatures in Remote Sensing, Volume 1 May 1991 p 405-408 (For primary document see N92-11394 02-43)

(Grants NAG5-900; NAGw-1968; CS-76-90)

Copyright Avail: NTIS HC/MF A20; ESA, EPD, ESTEC, Noordwijk, Netherlands, HC 150 Dutch guilders (2 vols) CSCL 08B

A useful parameter to estimate terrestrial primary productivity, that can be sensed from space, is the daily averaged fraction of Photosynthetically Available Radiation (PAR) absorbed by plants. To evaluate this parameter, investigators have relied on the fact that the relative amount of radiation reflected by a vegetated surface in the visible and near infrared depends on the fraction of the surface covered by the vegetation and therefore, correlates with absorbed PAR. They have used vegetation indices, namely normalized difference and simple ratio, to derive absorbed PAR. The problem with normalized difference and simple ratio is first, they are non linear functions of radiance or reflectance and therefore, cannot be readily applied to heterogeneous targets, second, they are used in generally nonlinear relationships, which make time integrals of the indices not proportional to primary productivity, and third, the relationships depend strongly on the type of canopy and background. To remove these limitations, linear combinations of visible and near infrared reflectances at optimum (one or two) viewing zenith angles are proposed. ESA

N92-11475*# State Univ. of New York, Binghamton.

VEGETATION CANOPIES AND OBJECTS OF ARBITRARY SHAPES: COMPUTER GENERATION AND BIDIRECTIONAL REFLECTANCE CALCULATIONS

Narenda S. Goel, I. Rozehnal, and R. L. Thompson *In* ESA, Physical Measurements and Signatures in Remote Sensing, Volume 1 May 1991 p 409-413 Sponsored in part by NASA, Washington (For primary document see N92-11394 02-43)

Copyright Avail: NTIS HC/MF A20; ESA, EPD, ESTEC, Noordwijk, Netherlands, HC 150 Dutch guilders (2 vols) CSCL 08B

A general computer graphics based model is presented for computer generation of objects of arbitrary shape and for calculating Bidirectional Reflectance Factor (BRF) and scattering from them, in the optical region. The computer generation uses a modified Lindemayer system (L system) approach. For rendering on a computer screen, the object is divided into polygons, and innovative computer graphics techniques are used to display the object and to calculate the scattering and reflectance from the object. The use of the technique is illustrated with scattering from canopies of simulated corn plants and from a snow covered mountain. The scattering is quantified using measures like BRF and albedo and by rendering the objects with brightness of each of the two facets of a polygon proportional to the amount of light scattered from the object in the viewer's direction. ESA

N92-11476# Groupement d'Etudes et de Recherches pour le Developpement de l'Agronomie Tropicale, Paris (France). Lab. de Modelisation.

RADIATIVE TRANSFER SIMULATION ON COMPUTER MODELS OF VEGETATION COVER [SIMULATION DES TRANFERTS RADIATIFS SUR MAQUETTES INFORMATIQUES DE COUVERTS VEGETAUX]

Jean Dauzat and O. Hautecoeur *In* ESA, Physical Measurements and Signatures in Remote Sensing, Volume 1 May 1991 p 415-418 In FRENCH (For primary document see N92-11394 02-43)

Copyright Avail: NTIS HC/MF A20; ESA, EPD, ESTEC, Noordwijk, Netherlands, HC 150 Dutch guilders (2 vols)

The AMAP plant growth simulation software allows construction of realistic computer models of vegetation formation. Radiative transfers are simulated by a beam thrower integrating spectral reflectance at the level of leaves and ground. This approach reproduces as faithfully as possible radiative phenomena at the plant-atmosphere interface. The model is used to analyze the radiometric response of a millet culture. The reflectance appears very anisotropic in some conditions. Ground specular reflection pre dominates for weak foliar indexes and backscattering for higher foliar indexes. ESA

N92-11477# Arizona Univ., Tucson. Dept. of Soil and Water Science.

NORMALIZATION OF MULTIDIRECTIONAL RED AND NIR REFLECTANCES WITH THE SAVI

Alfredo R. Huete, J. Qi, A. Chehbouni (Office National d'Etudes et de Recherches Aerospatiales, Toulouse, France), W. Leeuwen, and G. Hua *In* ESA, Physical Measurements and Signatures in Remote Sensing, Volume 1 May 1991 p 419-422 (For primary document see N92-11394 02-43)

Copyright Avail: NTIS HC/MF A20; ESA, EPD, ESTEC, Noordwijk, Netherlands, HC 150 Dutch guilders (2 vols)

Directional reflectance measurements were made over a semi-desert gramma grassland at various times of the growing season. View angle measurements from +40 to -40 degrees were made at various solar zenith angles and soil moisture conditions. The sensitivity of the Normalized Difference Vegetation Index (NDVI) and the Soil Adjusted Vegetation Index (SAVI) to bidirectional measurements was assessed for purposes of improving remote temporal monitoring of vegetation dynamics. The SAVI view angle response was found to be symmetric about nadir while the NDVI response was strongly anisotropic. This enabled the view angle behavior of the SAVI to be normalized with a cosine function. In constrast to the NDVI, the SAVI was able to minimize soil moisture and shadow influences for all measurement conditions. ESA

N92-11478# Academy of Sciences (USSR), Moscow. Inst. of Applied Mathematics.

MULTIANGULAR APPROACH TO SOLUTION OF ATMOSPHERE OPTICS REVERSE PROBLEMS

A. A. Ioltukhovski *In* ESA, Physical Measurements and Signatures in Remote Sensing, Volume 1 May 1991 p 423-425 (For primary document see N92-11394 02-43)

Copyright Avail: NTIS HC/MF A20; ESA, EPD, ESTEC, Noordwijk, Netherlands, HC 150 Dutch guilders (2 vols)

An approach to identifying the atmosphere and surface optical characteristics based upon accurate formalism of the transport theory is addressed. Measurement of radiation intensity in different directions enables to solve the following problems: identification of full optical thickness using measurement of intensity abrupt changes (instrumentation resolution impact upon identification error is discussed); identification of the mean characteristics of atmosphere and mean albedo on the basis of a priori information concerning relationship between these characteristics and optical parameters of atmosphere, as well as using parametrization of transmission function; identification of inhomogeneous albedo for optical thin atmosphere. This method enables to obtain a spectrum of optical characteristics of the atmosphere and albedo. ESA

N92-11479# Institut National de la Recherche Agronomique, Montfavet (France). Station de Bioclimatologie.

VALIDATION OF A GROUND SPECTRAL AND DIRECTIONAL REFLECTANCE MODEL [VALIDATION D'UN MODELE DE REFLECTANCE SPECTRALE ET DIRECTIONNELLE DE SOL]

Stephane Jacquemoud, Frederic Baret, and J. F. Hanocq *In* ESA, Physical Measurements and Signatures in Remote Sensing, Volume 1 May 1991 p 427-430 In FRENCH Sponsored in part by CNES; CNRS; Institut National de la Recherche Agronomique; and Institut Francais de la Recherche pour l'Exploitation de la Mer (For primary document see N92-11394 02-43)

Copyright Avail: NTIS HC/MF A20; ESA, EPD, ESTEC, Noordwijk, Netherlands, HC 150 Dutch guilders (2 vols)

The spectral and directional reflectance of 26 ground surfaces were measured in laboratory using a spectrometer, (100 spectral bands between 450 to 2450 nm) and a radiometer (5 wideband Thematic Mapper). A radiative transfer model, whose input parameters are a simple scattering albedo, a particle phase function and a characteristic variable of the surface, was tested. The Hapke model was used to adjust the parameters by inversion. Results show that only the simple scattering albedo depends on the wavelength, the other parameters possibly being considered as constants for a given ground surface. ESA

N92-11480# Office National d'Etudes et de Recherches Aerospatiales, Toulouse (France). Lab. d'Etudes et de Recherches en Teledetection Spatiale.

NORMALIZATION OF BIDIRECTIONAL EFFECTS OF SURFACE REFLECTANCE ON A SERIES OF MULTITEMPORAL NOAA/AVHRRR DATA [NORMALISATION DES EFFETS BIDIRECTIONNELS DE LA REFLECTANCE DE SURFACE SUR UNE SERIE DE DONNEES MULTITEMPORELLES NOAA/AVHRR]

Jean-Louis Roujean and Marc Leroy (Centre National d'Etudes Spatiales, Toulouse, France) *In* ESA, Physical Measurements and Signatures in Remote Sensing, Volume 1 May 1991 p 431-434 In FRENCH (For primary document see N92-11394 02-43)

Copyright Avail: NTIS HC/MF A20; ESA, EPD, ESTEC, Noordwijk, Netherlands, HC 150 Dutch guilders (2 vols)

Bidirectional effects of surface on a satellite data set acquired over three sites in France were addressed. A data normalization method is proposed using a semi empirical correction model for bidirectional effects. The results are preliminary in that the residual dispersion of the normalized data is not completely included and it appears difficult to accurately predict the results. ESA

N92-11481# Goettingen Univ. (Germany, F.R.). Inst. fuer Bioklimatologie.

MONTE CARLO MODEL FOR TRANSPORT EQUATION IN A PLANT CANOPY AND ITS INVERSION

Alexander L. Marshak and Victor S. Antyufeev (Academy of Sciences, USSR, Novosibirsk) *In* ESA, Physical Measurements and Signatures in Remote Sensing, Volume 1 May 1991 p 435-438 (For primary document see N92-11394 02-43)

Copyright Avail: NTIS HC/MF A20; ESA, EPD, ESTEC, Noordwijk, Netherlands, HC 150 Dutch guilders (2 vols)

Plant canopy reflectance is calculated using the governing equation for photon transport. The integral equation of transfer is solved by the Monte Carlo method. The main emphasis is on statistical estimation and simulation of the Markov chain. The leaf dimensions are taken into account in obtaining the hot spot effect of the canopy. New coefficients of extinction and scattering are obtained to consider the transport theory for a leaf canopy with finite dimensional scattering centers. Numerical results for the transport equation obtained by the Monte Carlo method are compared with those obtained by using other methods. A general inversion technique for estimating model parameters is presented. The method of calculating derivatives of the bidirectional reflectance factor with respect to unknown parameters using the same photon trajectories as in the solution of the direct problem is developed. ESA

N92-11482*# Jet Propulsion Lab., California Inst. of Tech., Pasadena.

SPECTRAL REFLECTANCE OF THIN SNOW

Anne W. Nolin and Jeff Dozier (National Aeronautics and Space Administration. Goddard Space Flight Center, Greenbelt, MD.) *In* ESA, Physical Measurements and Signatures in Remote Sensing, Volume 1 May 1991 p 439-442 (For primary document see N92-11394 02-43)

Copyright Avail: NTIS HC/MF A20; ESA, EPD, ESTEC, Noordwijk, Netherlands, HC 150 Dutch guilders (2 vols)

A radiative transfer model was used to calculate the spectral reflectance of thin snow overlying dark soil. Model results show that directional hemispherical reflectance depends on density, grain size, and solar and viewing geometries. Measurements of thin snow spectral Bidirectional Reflectance Distribution Function (BRDF) show that the reflectance in the visible wavelengths is reduced when the sensor is near nadir yet, at a viewing zenith of 75 degrees the same snowpack will appear to be optically thick. If the snow is sufficiently thin and snow grains are large, the spectral signature of the substrate may influence snow reflectance. This phenomenon was also detected in reflectance data collected using the ground based PIDAS (Portable Instantaneous Display and Analysis Spectrometer). Concurrent airborne data from the AVIRIS instrument (Advanced Visible/Infrared Imaging Spectrometer) show effects of thin snow and mixed pixels for areas of thin and patchy spring snow. ESA

N92-11483# British National Space Centre, Huntingdon (England). Remote Sensing Applications Development Unit.

ASSESSMENT OF THE EFFECT OF SPECULAR REFLECTANCE ON THE RELATIONSHIPS BETWEEN VEGETATION INDICES AND BIOMASS

S. E. Plummer *In* ESA, Physical Measurements and Signatures in Remote Sensing, Volume 1 May 1991 p 443-446 (For primary document see N92-11394 02-43)

Copyright Avail: NTIS HC/MF A20; ESA, EPD, ESTEC, Noordwijk, Netherlands, HC 150 Dutch guilders (2 vols)

Vegetation indices like the near Infrared/Red Ratio (VDI) or the Normalized Difference Vegetation Index (NDVI) are commonly used to estimate vegetation parameters like fresh biomass or leaf area index. Since vegetation canopies are nonlambertian reflectors, these indices are calculated using radiation from the cuticle (specular reflection) and from the internal leaf structure (bulk reflection). Specular reflection, however, is primarily a function of canopy roughness and has no relationship with the determinants of photosynthetic capacity that these indices attempt to measure. The reduction of the amount of specular reflection is hypothesized to result in increased correlation between vegetation indices and fresh biomass. The results indicate that for perennial ryegrass, over the variation in canopy geometry considered, reduction of the specular reflection does lead to increases in the correlation between fresh biomass and both RVI and NDVI. ESA

N92-11484# Universite des Sciences et Techniques de Lille (France). Lab. d'Optique Atmospherique.

SPECULAR AND DIFFUSE COMPONENTS OF PLANT CANOPY REFLECTANCE AT THE WAVELENGTHS OF 550 AND 630 NM

Genevieve Rondeaux and M. Herman *In* ESA, Physical

Measurements and Signatures in Remote Sensing, Volume 1 May 1991 p 447-452 (For primary document see N92-11394 02-43)
Copyright Avail: NTIS HC/MF A20; ESA, EPD, ESTEC, Noordwijk, Netherlands, HC 150 Dutch guilders (2 vols)

Polarization data allow quantification of that portion of the canopy reflectance which represents light specularly reflected by the leaf surfaces. Polarization is particularly sensitive to the variations of the architectural characteristics of the canopy during its development. The polarization decreased 10 to 20 when the corn canopy tasseled and the soybean canopy was water stressed. These results show that remotely sensed polarization data provide information, complementary to the reflectance data, for following the plant canopy phenological development. The radiation transport process in the plant canopy is modeled by adapting the successive orders method used in atmospheric radiation transport. The first results of this model give a good estimate of the diffuse component of the bidirectional reflectance factor of plant canopy. Estimates of these two components are interesting to both plant scientists who study the photosynthetic capacity of a canopy and to remote sensing scientists who use the knowledge of the directional effects to improve the quality of multitemporal observations of vegetation. ESA

N92-11485*# National Aeronautics and Space Administration. Lyndon B. Johnson Space Center, Houston, TX.
OBSERVATIONS OF THE EARTH IN POLARIZED LIGHT FROM THE US SPACE SHUTTLE
Jean-Claude Roger, Richard Santer, M. Herman, J.-L. Deuze (Universite des Sciences et Techniques de Lille, France), and V. C. Whitehead *In* ESA, Physical Measurements and Signatures in Remote Sensing, Volume 1 May 1991 p 453-457 (For primary document see N92-11394 02-43)
(Contract CNES-833/CNES/885527)
Copyright Avail: NTIS HC/MF A20; ESA, EPD, ESTEC, Noordwijk, Netherlands, HC 150 Dutch guilders (2 vols) CSCL 08B

During the four American Space Shuttle missions of year 1985, the crewmembers took pictures of the Earth in polarized light. Different problems were encountered in the quantitative use of the data: induced polarization by the shuttle window, lack of calibration correction of the window polarization and enveloped in flight calibration methods. The analysis of the selected data first confirmed the previous observation over snow and sand. A low polarization on these surfaces was observed. On the other hand, the measurements show the potentiability of the polarization for agricultural inventory. Contamination of the atmosphere is well characterized. ESA

N92-11486*# Boston Univ., MA. Center for Remote Sensing.
CALCULATING THE BIDIRECTIONAL REFLECTANCE OF NATURAL VEGETATION COVERS USING BOOLEAN MODELS AND GEOMETRIC OPTICS
Alan H. Strahler, Xiao-Wen Li, and David L. B. Jupp (Commonwealth Scientific and Industrial Research Organization, Linfield, Australia) *In* ESA, Physical Measurements and Signatures in Remote Sensing, Volume 1 May 1991 p 459-462 (For primary document see N92-11394 02-43)
(Grant NAGw-1474)
Copyright Avail: NTIS HC/MF A20; ESA, EPD, ESTEC, Noordwijk, Netherlands, HC 150 Dutch guilders (2 vols)

The bidirectional radiance or reflectance of a forest or woodland can be modeled using principles of geometric optics and Boolean models for random sets in a three dimensional space. This model may be defined at two levels, the scene includes four components; sunlight and shadowed canopy, and sunlit and shadowed background. The reflectance of the scene is modeled as the sum of the reflectances of the individual components as weighted by their areal proportions in the field of view. At the leaf level, the canopy envelope is an assemblage of leaves, and thus the reflectance is a function of the areal proportions of sunlit and shadowed leaf, and sunlit and shadowed background. Because the proportions of scene components are dependent upon the directions of irradiance and exitance, the model accounts for the hotspot that is well known in leaf and tree canopies. ESA

N92-11487# British National Space Centre, Huntingdon (England). Remote Sensing Applications Development Unit.
ATLAS: AN AUTO-TRACKING LAND AND ATMOSPHERE SENSOR FOR RETRIEVAL OF ATMOSPHERIC OPTICAL PARAMETERS AND ACQUISITION OF BIDIRECTIONAL SURFACE REFLECTANCE
A. K. Wilson *In* ESA, Physical Measurements and Signatures in Remote Sensing, Volume 1 May 1991 p 463-466 (For primary document see N92-11394 02-43)
Copyright Avail: NTIS HC/MF A20; ESA, EPD, ESTEC, Noordwijk, Netherlands, HC 150 Dutch guilders (2 vols)

ATLAS is being developed to provide the necessary measurements of atmospheric optical parameters and surface bidirectional reflectance, required in the retrieval of quantitative information from remotely sensed data. Its main task, in support of airborne remote sensing campaigns, is to retrieve atmospheric optical parameters for input to atmospheric correction algorithms. It will be used to develop a database of multispectral directional reflectances from a variety of nonlambertian surfaces such as vegetation canopies. The design characteristics of this instrument are reviewed and its measurement capabilities discussed. ESA

N92-11488# European Space Agency, Paris (France).
PHYSICAL MEASUREMENTS AND SIGNATURES IN REMOTE SENSING, VOLUME 2
James J. Hunt, ed. May 1991 367 p In ENGLISH and FRENCH The 5th International Colloquium was held in Courchevel, France, 14-18 Jan. 1991; sponsored by CNES, CNRS, Inst. National de la Recherche Agronomique, and Inst. Francais de la Recherche pour l'Exploitation de la Mer
(ESA-SP-319-Vol-2; ISBN-92-9092-118-8; ISSN-0379-6566; ETN-91-90064) Copyright Avail: NTIS HC/MF A16; ESA, EPD, ESTEC, Noordwijk, Netherlands, HC 150 Dutch guilders (2 vols)

The analysis of the relationships between the specific properties of a target (vegetative canopy, soil, rock, water surface, snow, ice etc.) and its spectral characteristics in different wavelength ranges (from ultraviolet to microwaves) the determination of factors affecting the spectral response of an object (atmospheric effects, measuring techniques etc.) and the development of interpretation models were addressed. A good survey is offered of research in progress in the domain of the application of remote sensing to the study of Earth resources, with in-depth investigation into synergy between observations in different wavelength domains and active laser remote sensing. For individual titles, see N92-11489 through N92-11558.

N92-11489*# National Aeronautics and Space Administration. Goddard Space Flight Center, Greenbelt, MD.
SYNERGISTIC USE OF MULTISPECTRAL SATELLITE DATA FOR MONITORING LAND SURFACE CHANGE
Bhaskar J. Choudhury *In* ESA, Physical Measurements and Signatures in Remote Sensing, Volume 2 May 1991 p 469-473 (For primary document see N92-11488 02-43)
Copyright Avail: NTIS HC/MF A16; ESA, EPD, ESTEC, Noordwijk, Netherlands, HC 150 Dutch guilders (2 vols) CSCL 08B

Observations by the Advanced Very High Resolution Radiometer (AVHRR) onboard the NOAA satellites were used to compute visible and near infrared reflectances and surface temperature, while passive microwave observations at 37 GHz frequency by the Scanning Multichannel Microwave Radiometer (SMMR) and Special Sensor Microwave Imager (SSM/I) on board, respectively, the Nimbus-7 and DMSP-F8 satellites were used to compute polarization difference. These observations were analyzed along transects from rainforest to desert over northern Africa for the period 1979-1987, which included an unprecedented drought during 1984 over the Sahel zone. Model simulations were made to understand the interrelationship among multispectral data. ESA

N92-11490# Groupement Scientifique de Teledetection de Strasbourg (France).
COMPLEMENTARITY OF TEMPERATURE INDEPENDENT THERMAL INFRARED SPECTRAL INDICES (TISI) AND NDVI: COMPARED PROPERTIES AND COMBINED USE FOR SOIL AND VEGETATION DISCRIMINATION
Francois Becker and Zhao-Liang Li *In* ESA, Physical Measurements and Signatures in Remote Sensing, Volume 2 May 1991 p 475-480 (For primary document see N92-11488 02-43)
Copyright Avail: NTIS HC/MF A16; ESA, EPD, ESTEC, Noordwijk, Netherlands, HC 150 Dutch guilders (2 vols)

The definition of temperature independent Thermal Infrared Spectral Indices (TISI) is recalled and examples of such indices based upon channels 3, 4, 5 of TIMS (Thermal Infrared Multispectral Scanner) are given. Several properties of these indices are discussed. The correlations between TISI derived from the TIMS data and respectively NDVI (Normalized Difference Vegetation Index) derived from the data of NS001 and surface temperature (Ts) show very interesting features. In the example discussed, the results showed that TISI and NDVI have more sensitivity to surface characteristics. TISI is more sensitive to bare soil characteristics than NDVI which is, in turn, more sensitive to vegetation and vegetation cover. Therefore the combined use of TISI, NDVI, and Ts should increase the accuracy of soils and vegetation discrimination as well as the understanding of their energetic behavior effects. A method to retrieve surface temperature and surface emissivities from AVHRR data is proposed. The preliminary results derived from AVHRR over La Crau (France) are in good agreement with in situ measurements. ESA

N92-11491*# Colorado Univ., Boulder. Center for the Study of Earth from Space.
INTEGRATION OF VISIBLE-THROUGH MICROWAVE-RANGE MULTISPECTRAL IMAGE DATA SETS FOR GEOLOGIC MAPPING
Fred A. Kruse and John B. Dietz *In* ESA, Physical Measurements and Signatures in Remote Sensing, Volume 2 May 1991 p 481-486 (For primary document see N92-11488 02-43)
(Contract JPL-958456; NAGw-1143; NAGw-1601)
Copyright Avail: NTIS HC/MF A16; ESA, EPD, ESTEC, Noordwijk, Netherlands, HC 150 Dutch guilders (2 vols) CSCL 08B

Multispectral remote sensing data sets collected during the Geologic Remote Sensing Field Experiment (GRSFE) conducted during 1989 in the southwestern U.S. were used to produce thematic image maps showing details of the surface geology. LANDSAT TM (Thematic Mapper) images were used to map the distribution of clays, carbonates, and iron oxides. AVIRIS (Airborne Visible/Infrared Imaging Spectrometer) data were used to identify and map calcite, dolomite, sericite, hematite, and geothite, including mixtures. TIMS (Thermal Infrared Multispectral Scanner) data were used to map the distribution of igneous rock phases and carbonates based on their silica contents. AIRSAR (Airborne Synthetic Aperture Radar) data were used to map surface textures related to the scale of surface roughness. The AIRSAR also allowed identification of previously unmapped fault segments and structural control of lithology and minerology. Because all of the above data sets were geographically referenced, combination of different data types and direct comparison of the results with conventional field and laboratory data sets allowed improved geologic mapping of the test site. ESA

N92-11492# Academy of Sciences (USSR), Moscow. Inst. of Radioengineering and Electronics.
AIRBORNE PASSIVE MICROWAVE REMOTE SENSING OF LAND AND WATER SURFACE
Anatoli M. Shutko, E. A. Reutov, B. M. Liberman, A. G. Grankov, A. A. Milshin, G. G. Yazerian, A. A. Haldin, and S. P. Golovachev *In* ESA, Physical Measurements and Signatures in Remote Sensing, Volume 2 May 1991 p 487-489 (For primary document see N92-11488 02-43)
Copyright Avail: NTIS HC/MF A16; ESA, EPD, ESTEC, Noordwijk, Netherlands, HC 150 Dutch guilders (2 vols)

The scientific activity of the research team working on passive microwaves is presented. The characteristics of the instruments used are given as well as some examples of the obtained results concerning estimations of soil moistures content, depth of shallow water table, salt and pollutant concentration in water, vegetation biomass. ESA

N92-11493# Sherbrooke Univ. (Quebec). Centre d'Applications et de Recherches en Teledetection.
EVALUATION OF THE QUALITY OF URBAN BIOTYPES BY REMOTE SENSING [EVALUATION DE LA QUALITE DES BIOTOPES URBAINS PAR TELEDETECTION]
L. Charbonneau, Alain Royer, Mario Hinse, A. Coulombe, and E. Lambert *In* ESA, Physical Measurements and Signatures in Remote Sensing, Volume 2 May 1991 p 493-496 In FRENCH Sponsored in part by the Communaute Urbaine de Montreal (For primary document see N92-11488 02-43)
(Contract CRSNG-GP-8643)
Copyright Avail: NTIS HC/MF A16; ESA, EPD, ESTEC, Noordwijk, Netherlands, HC 150 Dutch guilders (2 vols)

A study to characterize the environmental quality of urban Montreal (Canada) using integration vegetation and thermal index data from LANDSAT 5 Thematic Mapper imagery is presented. The analysis gives discrimation of different vegetal (woods, lawns, cemeteries, golf courses) and mineralized (small and large built up residential zones) regions. The decrease in temperature from high vegetation index parks can reach 6 to 8 C in relation to strongly mineralized neighboring zones (town center). Emphasis is placed on two studies specifically concerning land use inventory and the quality of natural spaces on one hand and mapping of urban heat islands on the other. Distinct geographic areas could be distinguished by interrelating the two studies. ESA

N92-11494# Office National d'Etudes et de Recherches Aerospatiales, Toulouse (France). Lab. d'Etudes et de Recherches en Teledetection Spatiale.
COMBINED USE OF EARTH OBSERVATION SATELLITE AND METEOROLOGICAL SATELLITE FOR CROP ASSESSMENT IN SEMIARID ENVIRONMENTS
Sabine deBrisis, Martine Guerif, Alain Podaire, and Bernard Seguin (Institut National de la Recherche Agronomique, Montfavet, France) *In* ESA, Physical Measurements and Signatures in Remote Sensing, Volume 2 May 1991 p 497-500 (For primary document see N92-11488 02-43)
Copyright Avail: NTIS HC/MF A16; ESA, EPD, ESTEC, Noordwijk, Netherlands, HC 150 Dutch guilders (2 vols)

Satellite thermal visible and near infrared information is used to drive crop assessment in semiarid environment considering crop dependency to environmental conditions. The soil temperature, which leads to the 'water use balance' by means of the expression Ts-Ta (Ts: soil temperature, Ta: air temperature), and the NDVI index which leads to actual photosynthesis because of its correlation with the Active Photosynthetically Absorbed Radiation (APAR), are two important variables that can provide crop growth assessment. Their cumulation over the crop cycle, taking into account NDVI's and (Ts - Ta)'s temporal evolution, is used to explain biomass production and yield of cereals in Sidi-Bel-Abbes (Algeria). ESA

N92-11495# Valencia Univ. (Spain). Dept. de Geografia.
NOAA-AVHRR CONTRIBUTION TO THE ANALYSIS OR URBAN HEAT ISLANDS
M. J. LopezGarcia, Vicente Caselles, J. Melia (Valencia Univ., Burjassot, Spain), and A. J. PerezCueva *In* ESA, Physical Measurements and Signatures in Remote Sensing, Volume 2 May 1991 p 501-504 Sponsored by DGICyT (For primary document see N92-11488 02-43)
Copyright Avail: NTIS HC/MF A16; ESA, EPD, ESTEC, Noordwijk, Netherlands, HC 150 Dutch guilders (2 vols)

The heat island effect of the city of Valencia (Spain) is analyzed by means of traditional techniques and NOAA AVHRR data.

Satellite images were corrected for atmospheric and emissivity effects by using a split window method for rough and heterogeneous media. An effective emissivity is obtained for every pixel from the emissivity values of its constituent surfaces. The intensity of the effect detected from satellite data is about 60 pct. higher than those obtained from air temperature. The difference is due to the distinct nature of the measurements. ESA

N92-11496# Paris VI Univ. (France). Lab. de Geologie-Geomorphologie Structurale et Teledetection.
SYNERGY OF HIGH RESOLUTION SPATIAL MICROWAVE IMAGERY AND GEOMORPHOLOGICAL OPTICS [SYNERGIE DES IMAGERIES A HAUTE RESOLUTION SPATIALE HYPERFREQUENCES ET OPTIQUES EN GEOMORPHOLOGIE]
Ali Mekarnia, Jean-Paul Rudant, Jean Chorowicz, and Christophe Charron *In* ESA, Physical Measurements and Signatures in Remote Sensing, Volume 2 May 1991 p 505-508 In FRENCH (For primary document see N92-11488 02-43)
Copyright Avail: NTIS HC/MF A16; ESA, EPD, ESTEC, Noordwijk, Netherlands, HC 150 Dutch guilders (2 vols)

SPOT satellite and VARAN airborne radar over the Sainte-Victoire mountain (Provence, France) is addressed. The radar information shows the slope effect at the instance that the morphology is confirmed and the nature of land use. The examples show the perfect synergy of two types of very different radiometric data. Their local growth in particular give a better characterization of the landsliding forms. ESA

N92-11497# Kagoshima Univ. (Japan). Faculty of Agriculture.
A STUDY ON THE EFFECTS OF MT. SAKURAJIMA'S FALLING ASH OVER CROP AND FOREST AREAS USING IMAGE PROCESSING FOR LANDSAT-5, MOS-1, AND JAFSA DIGITAL DATA
E. Ishiguro, Krishna Kumar Mishra, Y. Hidaka, and M. Miyazato *In* ESA, Physical Measurements and Signatures in Remote Sensing, Volume 2 May 1991 p 509-512 (For primary document see N92-11488 02-43)
Copyright Avail: NTIS HC/MF A16; ESA, EPD, ESTEC, Noordwijk, Netherlands, HC 150 Dutch guilders (2 vols)

Mount Sakurajima is one of the most active volcanic mountains in Japan. It causes severe damage to the surrounding living environment by erupting huge amounts of volcanic ash. The importance of this was realized and the effects were evaluated of falling ash over agricultural fields, forests and cities using this remote sensing techniques. The changes in the spectral characteristics of vegetables covered with and without ash were measured by a spectroradiometer. The information was utilized for identifying the volcanic smoke and the areas affected by falling ash using a personal computer, an image processor for the LANDSAT 5, MOS-1, and Jafsa digital data. The results indicate the probability in evaluating the amount of falling ash. ESA

N92-11498# Open Univ., Milton (England). Dept. of Earth Sciences.
MONITORING VOLCANOES USING SHORT WAVELENGTH INFRARED IMAGES
David A. Rothery and Clive Oppenheimer *In* ESA, Physical Measurements and Signatures in Remote Sensing, Volume 2 May 1991 p 513-516 (For primary document see N92-11488 02-43)
(Grants NERC-GR9/14; NERC-GT4/88/GS/87)
Copyright Avail: NTIS HC/MF A16; ESA, EPD, ESTEC, Noordwijk, Netherlands, HC 150 Dutch guilders (2 vols)

By measuring radiance in LANDSAT TM (Thematic Mapper) bands 7 (2.08 to 2.35 microns) and band 5 (1.55 to 1.75 microns) the subpixel temperature distribution of a hot volcanic surface can be calculated. LANDAT TM data acquired by day and by night was used to measure the radiated energy flux of volcanoes, in particular of the hot dome in the summit crater of volcan Lascar in Chile. This is believed to be the first ever use of the Short Wavelength Infrared (SWIR) bands of this instrument by night. The considerable potential value of SWIR instruments in forthcoming remote sensing programs (notably JERS-1 and the Earth Observing System) to monitor volcanic activity in a quantitive fashion is demonstrated. ESA

N92-11499# Groupement Scientifique de Teledetection de Strasbourg (France). Inst. de Geologie.
INTEGRATION OF SEASAT AND SPOT DATA, CONTRIBUTION TO STRUCTURAL GEOLOGY MAPPING IN TEMPERATURE ENVIRONMENT [INTEGRATION DES DONNEES SATELLITAIRES SEASAT ET SPOT, CONTRIBUTION A LA CARTOGRAPHIE GEOLOGIQUE STRUCTURALE EN MILIEU TEMPERE]
Herve Yesou, Y. Besnus, J. Rolet (Brest Univ., France), and J. C. Pion *In* ESA, Physical Measurements and Signatures in Remote Sensing, Volume 2 May 1991 p 517-520 In FRENCH (For primary document see N92-11488 02-43)
Copyright Avail: NTIS HC/MF A16; ESA, EPD, ESTEC, Noordwijk, Netherlands, HC 150 Dutch guilders (2 vols)

After speckle reduction and geometric correction, Seasat data was combined with a SPOT image and with tests of the photographic and numeric integration processes. The best results are obtained when combining RVB, respectively XS3, Seasat and XS1, or Seasat, XS3, XS2. The numerical methods comprise linear combinations, IHS transformations and ACP analyses. ACP gives very good results working on the SPOT XS channels and Seasat data, centered and reduced. The numerical method offers the advantage of mastering the relative weight accorded to radar data in relation to the multispectral SPOT data. ESA

N92-11500*# National Aeronautics and Space Administration. Goddard Space Flight Center, Greenbelt, MD.
URBAN HEAT ISLAND
Hongsuk H. Kim *In* ESA, Physical Measurements and Signatures in Remote Sensing, Volume 2 May 1991 p 521-525 (For primary document see N92-11488 02-43)
Copyright Avail: NTIS HC/MF A16; ESA, EPD, ESTEC, Noordwijk, Netherlands, HC 150 Dutch guilders (2 vols) CSCL 08B

The phenomenon of urban heat island was investigated by the use of LANDSAT Thematic Mapper data sets collected over the metropolitan area of Washington DC (U.S.). By combining the retrieved spectral albedos and temperatures, urban modification on radiation budgets of five surface categories were analyzed. The surface radiation budget imagery of the area show that urban heating is attributable to a large heat flux from the rapidly heating surfaces of asphalt, bare soil and short grass. In summer, symptoms of diurnal heating begin to appear by mid morning and can be about 10 degrees warmer than nearby woodlands in summer. ESA

N92-11501# Institut National de la Recherche Agronomique, Montfavet (France). Station de Bioclimatologie.
JOINT USE OF REMOTE SENSING AND AGRICULTURAL PRODUCTION ESTIMATION MODELS: CURRENT TRENDS [L'UTILISATION CONJOINTE DE LA TELEDETECTION ET DES MODELES D'ESTIMATION DES PRODUCTIONS AGRICOLES: TENDANCES ACTUELLES]
Richard Delecolle, Frederic Baret, Martine Guerif, and S. J. Maas (Department of Agriculture, Weslaco, TX.) *In* ESA, Physical Measurements and Signatures in Remote Sensing, Volume 2 May 1991 p 529-534 In FRENCH (For primary document see N92-11488 02-43)
Copyright Avail: NTIS HC/MF A16; ESA, EPD, ESTEC, Noordwijk, Netherlands, HC 150 Dutch guilders (2 vols)

Empirical and dynamic models and corresponding time and space scales are presented. Principal methods for using satellite information to estimate the same predictions are described and the joint use of satellite data and dynamic models is shown as preferable. The simultaneous use of these models and remote sensing data is examined while attempting to determine the optimum spatial scale for each method. Constraints induced (not of time, necessitating and independent phenological scale) are discussed. ESA

N92-11502# Office National d'Etudes et de Recherches Aerospatiales, Toulouse (France). Lab. d'Etudes et de Recherches en Teledetection Spatiale.

INTEGRATION OF QUALITATIVE KNOWLEDGE ON OPERATIONAL MODELS FOR FOLLOWING VEGETATION USING TEMPORAL SERIES OF REMOTE SENSING IMAGES [INTEGRATION DE CONNAISSANCES QUALITATIVES SUR LES MODELES DE FONCTIONNEMENT POUR LE SUIVI DE LA VEGETATION A PARTIR DE SERIES TEMPORELLES D'IMAGES DE TELEDETECTION]

Nicolas Viovy and G. Saint *In* ESA, Physical Measurements and Signatures in Remote Sensing, Volume 2 May 1991 p 535-540 In FRENCH (For primary document see N92-11488 02-43)

Copyright Avail: NTIS HC/MF A16; ESA, EPD, ESTEC, Noordwijk, Netherlands, HC 150 Dutch guilders (2 vols)

Vegetation cover evolutions submit to environmental conditions: remote sensing measurements depending on the state of the cover can thus characterize at least partly the way in which the cover responds to external forcing. A method for vegetation discrimination characterized by a model which describes the cover responses to rain gaging in sahelian environment is presented. ESA

N92-11503# Centre National de Recherches Meteorologiques, Toulouse (France).

SOME EXAMPLES OF SATELLITE DATA UTILIZATION FOR ATMOSPHERIC MODELING AT MEDIUM SCALE [QUELQUES EXEMPLES D'UTILISATION DES DONNEES SATELLITAIRES POUR LA MODELISATION ATMOSPHERIQUE A MOYENNE ECHELLE]

Joel Noilhan, J. P. Jullien, P. Lacarrere, Thierry Phulpin (Centre National d'Etudes Spatiales, Toulouse, France), and Magali Stoll *In* ESA, Physical Measurements and Signatures in Remote Sensing, Volume 2 May 1991 p 541-546 In FRENCH; ENGLISH summary (For primary document see N92-11488 02-43)

Copyright Avail: NTIS HC/MF A16; ESA, EPD, ESTEC, Noordwijk, Netherlands, HC 150 Dutch guilders (2 vols)

Examples of the use of satellite data in atmospheric modeling are presented. The mesoscale model of the French Weather Service is used to simulate clear days of the Hapex-Mobilhy (85-86) experiment which took place in South Western France. In addition to the classical physical package of parameterizations, a simple land surface scheme was implemented in the model in order to handle the regional effects related to land surface processes. Images of NDVI (Normalized Difference Vegetation Index) from AVHRR/NOAA9 are used to classify the vegetation within the simulation domain and to derive maps of two surface parameters: the fraction of vegetation (veg) and the minimum surface resistance (R smin). An analysis of the time variation of NDVI during three months of the experiment allows veg to be prescribed from the relation veg = 1.1 (NDVI)(exp 0.65) in the case of short vegetation during the growing season. On the other hand, the time decrease of vegetation indices for mature crops or semi desertic area is used to prescribe a high value of R smin. Maps of veg and (R smin) are used as input to the mesoscale model. Examples of validation of three dimensional integrations are given from the comparison between remotely sensed and predicted surface temperature and cloudiness. ESA

N92-11504# Institut de Recherche en Agronomie Tropicale, Montpellier (France).

ESTIMATION OF THE PRIMARY PRODUCTION IN SAHELIAN REGION FROM RADIOMETRIC DATA [ESTIMATION DE LA PRODUCTION PRIMAIRE EN ZONE SAHELIENNE A PARTIR DE DONNEES RADIOMETRIQUES]

Agnes Begue, J. Imbernon, and J. F. Desprat *In* ESA, Physical Measurements and Signatures in Remote Sensing, Volume 2 May 1991 p 549-552 In FRENCH (For primary document see N92-11488 02-43)

Copyright Avail: NTIS HC/MF A16; ESA, EPD, ESTEC, Noordwijk, Netherlands, HC 150 Dutch guilders (2 vols)

A radiative transfer model to study the relation of Photosynthetic Active Radiation (PAR) absorption efficiency and vegetation cover reflectance over sahelian region discontinuous cover is studied. The model is validated using experimental data acquired over millet. The relation is shown to have a strong variability linked to the source-sensor configuration. Absorption efficiency is introduced into the production model based on Monteith determinism. Biological data and data acquired over millet at the Niger (Nigeria) allowed model parameters to be calculated and showed the sensitivity of efficiency of conversion to frequent hydric stress in sahelian zone. ESA

N92-11505# Institut National de la Recherche Agronomique, Thiverval-Grignon (France). Station de Bioclimatologie.

CONSTRUCTION OF GROUND COVER CHARTS OF A WHEAT CANOPY FROM REFLECTANCE MEASUREMENTS

Paul Boissard, J. G. Pointel, and J. Tranchefort (Institut Technique des Cereales et Fourrages, Boigneville, France) *In* ESA, Physical Measurements and Signatures in Remote Sensing, Volume 2 May 1991 p 553-556 (For primary document see N92-11488 02-43)

(Contract ATP-88/50/N/5111)

Copyright Avail: NTIS HC/MF A16; ESA, EPD, ESTEC, Noordwijk, Netherlands, HC 150 Dutch guilders (2 vols)

The ground cover ratio of a partial covering early winter wheat crop at the 1 cm stem + spike stage was evaluated using a three channel CIMEL radiometer which simulated the SPOT satellite observation bands. During short periods guaranteeing constant illumination, the reflectance of experimental plots was linearly correlated to the plants ground cover ratio within a range from 0 to 57 pct. This result was used to construct charts to allow the estimation of the ground cover ratio of a given area from reflectance measurements in the red and infrared bands. ESA

N92-11506# Institut National de la Recherche Agronomique, Thiverval-Grignon (France). Station de Bioclimatologie.

USING THE RADIATIVE SURFACE TEMPERATURE IN ENERGY BUDGET STUDIES OVER PLANT CANOPIES

Yves Brunet, Kyaw Tha PawU (California Univ., Davis.), and Laurent Prevot *In* ESA, Physical Measurements and Signatures in Remote Sensing, Volume 2 May 1991 p 557-560 (For primary document see N92-11488 02-43)

Copyright Avail: NTIS HC/MF A16; ESA, EPD, ESTEC, Noordwijk, Netherlands, HC 150 Dutch guilders (2 vols)

The infrared surface temperature has been extensively used over the past few years in the determination of the energy balance of plant canopies. However, the surface temperature required by turbulent transfer equations is a priori defined from purely aerodynamic considerations. It is therefore of importance to investigate the differences between these two surface temperatures, in order to use correctly the radiative temperature in flux calculations. For this purpose, simulations were performed with a multilayer higher order closure model describing the radiative and turbulent processes within and above a plant canopy, for given climatic conditions and various canopy structures. The radiative temperature values calculated for all azimuth and zenith angles of the sensor are presented. The differences obtained between radiative and aerodynamic temperatures are interpreted in terms of an excess resistance. The consequences on the possible heat flux calculation are discussed. ESA

N92-11507# Valencia Univ., Burjassot (Spain). Dept. of Thermodynamics.

MAXIMUM EVAPOTRANSPIRATION MONITORING OVER LA MANCHA, SPAIN, USING NOAA-AVHRR DATA

Vicente Caselles, Jesus Delegido, E. Hurtado (Polytechnical Coll. of Albacete, Spain), and Jose A. Sobrino *In* ESA, Physical Measurements and Signatures in Remote Sensing, Volume 2 May 1991 p 561-564 Sponsored by Comission Interministerial de Ciencia y Tecnologia (For primary document see N92-11488 02-43)

Copyright Avail: NTIS HC/MF A16; ESA, EPD, ESTEC, Noordwijk, Netherlands, HC 150 Dutch guilders (2 vols)

Evaporation (ET) monitoring is of great interest in agricultural areas, like La Mancha, where irrigation is practiced. Accurate

information in crop water use is essential for improving the efficiency of watering systems. NOAA satellites with a spatial resolution of 1 sq km are suitable to estimate ET at regional scale (1 to 10,000 sq km). A model using remote sensing, meteorological and agronomical data, such as near midday NOAA albedo and temperature, maximum air temperature, and crop coefficients, is proposed. The maximum ET is determined with an acceptable precision (approx. 1.2 mm/day). ESA

N92-11508# Katholieke Univ. te Leuven (Belgium). Lab. for Land Management, Remote Sensing and Land Information.
AN INTEGRATED MODELLING APPROACH FOR THE SPECTRAL IDENTIFICATION OF CROPS
Herman Eerens, Tine Hemelings, and Roland Gombeer *In* ESA, Physical Measurements and Signatures in Remote Sensing, Volume 2 May 1991 p 565-568 (For primary document see N92-11488 02-43)
Copyright Avail: NTIS HC/MF A16; ESA, EPD, ESTEC, Noordwijk, Netherlands, HC 150 Dutch guilders (2 vols)

The phenological evolution of the spectral reflectance of agricultural crops is simulated by the association of a canopy reflectance and a crop growth model. Potential applications regarding image classification and the optimization of scene purchase strategies are discussed. ESA

N92-11509# Institut National de la Recherche Agronomique, Villenave d'Ornon (France). Station de Bioclimatologie.
ACTUAL DAILY EVAPOTRANSPIRATION MONITORING USING NOAA-AVHRR DATA FROM THE HAPEX-MOBILHY CAMPAIGNS [SUIVI DE L'EVAPOTRANSPIRATION REELLE JOURNALIERE A PARTIR DES DONNEES NOAA-AVHRR LORS DE LA CAMPAGNE HAPEX-MOBILHY]
Jean-Pierre Lagouarde and Yves Brunet (Institut National de la Recherche Agronomique, Thiverval-Grignon, France) *In* ESA, Physical Measurements and Signatures in Remote Sensing, Volume 2 May 1991 p 569-572 In FRENCH; ENGLISH summary (For primary document see N92-11488 02-43)
Copyright Avail: NTIS HC/MF A16; ESA, EPD, ESTEC, Noordwijk, Netherlands, HC 150 Dutch guilders (2 vols)

Two methods for estimating and mapping the actual evapotranspiration are described. The first is based on a linear statistical relationship between the daily evaporation and the surface temperature acquired in the beginning of the afternoon at the NOAA satellite overpass time. The coefficients of the relationship depend on the roughness length of the surface and on mean wind speed. The second method is based on a simple modeling of the planetary boundary coupled with Penman-Monteith type surface equations. Examples of mapping of daily evaporation obtained with both methods on the southwest of France are given for two dates. ESA

N92-11510# Institut National de la Recherche Agronomique, Montfavet (France). Station de Bioclimatologie.
SPECTRAL ESTIMATES OF PAR INTERCEPTION AND BIOMASS PRODUCTION OF IRRIGATED RICE CROPS. 2: MODEL VALIDATION WITH SPOT DATA
Brigitte Leblon and Martine Guerif *In* ESA, Physical Measurements and Signatures in Remote Sensing, Volume 2 May 1991 p 573-576 (For primary document see N92-11488 02-43)
Copyright Avail: NTIS HC/MF A16; ESA, EPD, ESTEC, Noordwijk, Netherlands, HC 150 Dutch guilders (2 vols)

A model of biomass and yield estimation, based on an energetic yield approach for biomass production in which light interception profile is estimated from the spectral profile in the visible and near infrared spectrum, was proposed for rice crops. A validation of the model, in the same region, but a different year, on different fields and using SPOT data to generate the spectral profiles is presented. Although the variability of cultural conditions was greater, the model gave biomass estimates at different phenological stages which were in good agreement with the measured ones. ESA

N92-11511# Centre National d'Etudes des Telecommunications, Issy-les-Moulineaux (France).
CALIBRATION AND VALIDATION OF A SURFACE FLUX MODEL IN THE FRAMEWORK OF THE HAPEX-MOBILHY EXPERIMENT. APPLICATION TO ESTIMATING THE COVER RESISTANCE [ETALONNAGE ET VALIDATION D'UN MODELE DE FLUX DE SURFACE DANS LE CAS DE L'EXPERIENCE HAPEX-MOBILHY. APPLICATION A L'ESTIMATION DE LA RESISTANCE D'UN COUVERT]
Meryem Ben-Mehrez, O. Taconet, and Daniel Vidal-Madjar *In* ESA, Physical Measurements and Signatures in Remote Sensing, Volume 2 May 1991 p 577-580 In FRENCH (For primary document see N92-11488 02-43)
Copyright Avail: NTIS HC/MF A16; ESA, EPD, ESTEC, Noordwijk, Netherlands, HC 150 Dutch guilders (2 vols)

A surface flux model that describes mass and energy transfers between the ground, vegetation, and atmosphere which is capable of assimilating the remotely sensed data to estimate the fluxes and the surface characteristics is presented. The model is validated locally over different surfaces. Using the model, ground evaporation can be separated from cover transpiration and the cover resistance can be calculated for all phenological stages. ESA

N92-11512# Centre for Agrobiological Research, Wageningen (Netherlands).
THE LINKING OF CROP GROWTH MODELS AND MULTI-SENSOR REMOTE SENSING DATA
B. A. M. Bouman *In* ESA, Physical Measurements and Signatures in Remote Sensing, Volume 2 May 1991 p 583-588 (For primary document see N92-11488 02-43)
Copyright Avail: NTIS HC/MF A16; ESA, EPD, ESTEC, Noordwijk, Netherlands, HC 150 Dutch guilders (2 vols)

The crop growth simulation model, SUCROS, was extended with the cloud equations for radar backscattering, and with the EXTRAD model for canopy reflectance. A numerical optimization procedure was used to re-parameterize SUCROS-Cloud-EXTRAD to fit simulated X band radar backscattering and optical reflectance to measured values. The simulated canopy biomass with the parameterized model, was compared to simulations with standard SUCROS, and with field measurements for 11 fields of sugar beet. The seasonal average error in simulated canopy biomass was smaller with the parameterized model (225 to 475 kg/ha), than with standard SUCROS (390 to 700 kg/ha). ESA

N92-11513# Institut National de la Recherche Agronomique, Montfavet (France). Station de Bioclimatologie.
TEMPORAL SIGNATURES USING NOAA-AVHRR AND LAND USE MAPPING [SIGNATURES TEMPORELLES A PARTIR DE NOAA-AVHRR ET CARTOGRAPHIE DE L'OCCUPATION DU SOL]
Bernard Seguin, Alberte Fischer, Sami Louahala, Alain Podaire (Office National d'Etudes et de Recherches Aerospatiales, Toulouse, France), and Y. Wang *In* ESA, Physical Measurements and Signatures in Remote Sensing, Volume 2 May 1991 p 589-594 In FRENCH (For primary document see N92-11488 02-43)
(Contract EEC-3444-88-08)
Copyright Avail: NTIS HC/MF A16; ESA, EPD, ESTEC, Noordwijk, Netherlands, HC 150 Dutch guilders (2 vols)

The mapping of temporal series of vegetative indices from NOAA-AVHRR data is addressed. The reflectances are modeled at the NOAA level allowing scale transfer using SPOT land parcel information. The infrared thermal imagery is also analyzed. ESA

N92-11514# Institut National de la Recherche Agronomique, Thiverval-Grignon (France).
SIMULATION STUDY OF VEGETATION INDICES SENSITIVITY USING THE MIDDLE INFRARED [ETUDE PAR SIMULATION DE LA SENSIBILITE D'INDICES DE VEGETATION UTILISANT LE MOYEN INFRAROUGE]
Bruno Andrieu and Frederic Baret *In* ESA, Physical Measurements and Signatures in Remote Sensing, Volume 2 May 1991 p 597-600 In FRENCH; ENGLISH summary Sponsored by

Programme National de Teledetection Spatiale (For primary document see N92-11488 02-43)
Copyright Avail: NTIS HC/MF A16; ESA, EPD, ESTEC, Noordwijk, Netherlands, HC 150 Dutch guilders (2 vols)

Reflectance models are used to compare vegetation indices (VI) using middle infrared (MIR) and near infrared (NIR) reflectance, to usual VI based on visible (VIS) and NIR reflectance. Sensitivity of VI to LAI (leaf area index) leaf water and pigment content, soil reflectance, and atmospheric diffusion, is studied. The MIR and NIR indices appear to predict LAI as well as, or better than (VISNIR) indices, when soil and leaf optical properties are variable. The use of MIR instead of VIS decreases strongly the effect of the atmosphere on remote sensing measurements. ESA

N92-11515# Institut National de la Recherche Agronomique, Montfavet (France). Station de Bioclimatologie.
STUDY OF THE SPATIAL VARIABILITY OF THE HYDRODYNAMIC BEHAVIOR OF GROUNDS AT THE NIGER (AFRICA) USING SATELLITE IMAGES [ETUDE DE LA VARIABILITE SPATIALE DU COMPORTEMENT HYDRODYNAMIQUE DES SOLS AU NIGER A PARTIR D'IMAGES SATELLITAIRES]
Dominique Courault, J.-M. DHerbes, C. Valentin, and D. Remy (Office de la Recherche Scientifique et Technique, Bondy, France) *In* ESA, Physical Measurements and Signatures in Remote Sensing, Volume 2 May 1991 p 601-604 In FRENCH; ENGLISH summary (For primary document see N92-11488 02-43)
Copyright Avail: NTIS HC/MF A16; ESA, EPD, ESTEC, Noordwijk, Netherlands, HC 150 Dutch guilders (2 vols)

A study to analyze the exchanges of water and energy on an area of 100/100 km in the Niger area is presented. Before measuring different flux between soil and atmosphere, spatial variability of landscapes must be studied. Different documents were used: topographic and pedologic maps, NOAA, MSS, and SPOT images. Their combination was made by a GIS (Geographic Information System). The methodology is to stratify space in three levels. Field observations and radiometric measurements were made, using a special topology to characterize surface states in relation with infiltration and runoff coefficients. Three classifications levels are proposed: five large physiographic domains resulting from NOAA and pedologic map analyses; geomorphologic features and the watershed delimitation from topographic maps and MSS images studies; and surface states obtained from SPOT classifications. This methodology allows spatial variability of surface organizations at each perception level to be integrated. ESA

N92-11516# Salford Univ. (England). Dept. of Geography.
STRUCTURAL CONTROLS ON THE REMOTELY SENSED RESPONSE OF A CONIFEROUS FOREST PLANTATION
F. Mark Danson and P. J. Curran (University Coll. of Swansea, Wales) *In* ESA, Physical Measurements and Signatures in Remote Sensing, Volume 2 May 1991 p 605-609 Sponsored in part by Sheffield Univ. (For primary document see N92-11488 02-43)
Copyright Avail: NTIS HC/MF A16; ESA, EPD, ESTEC, Noordwijk, Netherlands, HC 150 Dutch guilders (2 vols)

Airborne Thematic Mapper (ATM) and SPOT-1 HRV data were used to determine the effects of structural variation on the remotely sensed response of a coniferous forest plantation in the United Kingdom. Red and near infrared radiance were strongly and negatively correlated with a range of structural properties. A composite variable, related to the volume of the canopy, accounted for over 75 percent of the variation in near infrared radiance. A model that relates forest structural parameters to the remotely sensed response was offered as a means of understanding this response from a coniferous forest plantation. ESA

N92-11517# Centre d'Etudes et de Recherches, Toulouse (France).
DATABASE OF SPOT HISTROGRAMS [BASE DE DONNEES DE HISTOGRAMMES SPOT]
Magdeleine Dinguirard and Patrice Henry (Centre National d'Etudes Spatiales, Toulouse, France) *In* ESA, Physical Measurements and Signatures in Remote Sensing, Volume 2 May 1991 p 611-614 In FRENCH (For primary document see N92-11488 02-43)
Copyright Avail: NTIS HC/MF A16; ESA, EPD, ESTEC, Noordwijk, Netherlands, HC 150 Dutch guilders (2 vols)

The functional scheme of the SPOT histogram database and its processing possibilities are described. Results after three years of storage are presented. They give a good estimation of luminances over Europe (station visibilities) and with SPOT 4 a world coverage can be foreseen. ESA

N92-11518# Office National d'Etudes et de Recherches Aerospatiales, Toulouse (France). Lab. d'Etudes et de Recherches en Teledetection Spatiale.
MODELING TEMPORAL EVOLUTION OF THE RADIOMETRIC RESPONSE MEASURED BY WIDEBAND SENSORS OVER TEMPERATE AGRICULTURAL REGIONS [MODELISATION DE L'EVOLUTION TEMPORELLE DE LA REPONSE RADIOMETRIQUE MESUREE PAR LES CAPTEURS A LARGE CHAMP SUR LES REGIONS AGRICOLES TEMPEREES]
Alberte Fischer, Alain Podaire, Frederic Baret, and Richard Delecolle (Institut National de la Recherche Agronomique, Montfavet, France) *In* ESA, Physical Measurements and Signatures in Remote Sensing, Volume 2 May 1991 p 615-618 In FRENCH (For primary document see N92-11488 02-43)
(Contract EEC-3447-88-08-ES-ISPF)
Copyright Avail: NTIS HC/MF A16; ESA, EPD, ESTEC, Noordwijk, Netherlands, HC 150 Dutch guilders (2 vols)

Temporal evolution modeling of visible and near infrared AVHRR data helps understand the significance of the NDVI (Normalized Difference Vegetative Index) over agricultural regions. The composition of two different cycles of cultures over the region of Beauce (France) was processed to discover the real NDVI cycle of each of these two cycles. ESA

N92-11519# Ecole Polytechnique Federale de Lausanne (Switzerland). Inst. d'Amenagement des Terres et des Eaux.
TEXTURE INDICES SENSITIVITY TO SPATIAL AND SPECTRAL RESOLUTIONS IN SEMI-URBAN ENVIRONMENTS [SENSIBILITE D'INDICES DE TEXTURE AUX RESOLUTIONS SPATIALE ET SPECTRALE EN MILIEUX SEMI-URBAINS]
Thomas J. Blaser, Regis Caloz, Guillemette Willemin, Claude Collet, Ronald J. P. Lyon, Frank R. Honey, and Christopher D. Elvidge (Desert Research Inst., Reno, NV.) *In* ESA, Physical Measurements and Signatures in Remote Sensing, Volume 2 May 1991 p 619-623 In FRENCH (For primary document see N92-11488 02-43)
Copyright Avail: NTIS HC/MF A16; ESA, EPD, ESTEC, Noordwijk, Netherlands, HC 150 Dutch guilders (2 vols)

An analysis of semi urban environments by a texture indices approach is presented. The sensitivity of four indices to different spatial and spectral resolutions was examined. The initial image is produced by the Geascan radiometer and presents a resolution of about 5 by 5 m with 30 nm width bands on average. ESA

N92-11520# Bureau de Recherches Geologiques et Minieres, Orleans (France).
CONTRIBUTION OF NOAA-AVHRR SATELLITE DATA IN FOREST VEGETATION MONITORING [APPORT DES DONNEES SATELLITAIRES NOAA-AVHRR DANS LE SUIVI DE LA VEGETATION FORESTIERE]
J. F. Gouyet, C. King, H. LeGleau, J. F. Malon, Thierry Phulpin, and J. C. Valette (Institut National de la Recherche Agronomique, Avignon, France) *In* ESA, Physical Measurements and Signatures in Remote Sensing, Volume 2 May 1991 p 625-629 In FRENCH (For primary document see N92-11488 02-43)
Copyright Avail: NTIS HC/MF A16; ESA, EPD, ESTEC, Noordwijk, Netherlands, HC 150 Dutch guilders (2 vols)

A temporal series of NOAA-AVHRR data was processed over south east France during the 1989 drought. The vegetative index and surface temperature were calculated over five forest masses and several agricultural sites. Significant modifications are seen to

appear in the cover response. Combination of this data with climatic and biological data results collected in situ confirm coherence in detectable alarm thresholds and suggests that it may be possible to identify a critical period for forest vegetation. ESA

N92-11521# Centre Machinisme Agricole Genie Rural Eaux Forets, Montpellier (France).
MULTIDATE ANALYSIS OF NOAA-AVHRR DATA OVER FRANCE: RELATIONSHIP WITH AGROCLIMATIC CHARACTERISTICS [ANALYSE MULTIDATE DE SCENES NOAA-AVHRR SUR LA FRANCE: RELATION AVEC LES CARACTERISTIQUES AGROCLIMATIQUES]
Herve Kerdiles, Sami Louahala, A. Vidal, and Bernard Seguin (Institut National de la Recherche Agronomique, Montfavet, France) *In* ESA, Physical Measurements and Signatures in Remote Sensing, Volume 2 May 1991 p 631-634 (For primary document see N92-11488 02-43)
Copyright Avail: NTIS HC/MF A16; ESA, EPD, ESTEC, Noordwijk, Netherlands, HC 150 Dutch guilders (2 vols)

Results from a statistical analysis of multidate data aimed at establishing the effects of climatic accidents (essential drought) are presented. A preliminary study showed different responses in vegetative index and surface temperature of the predominantly winter culture zones to summer culture zones, and for the latter, of the irrigated zones to the dry cultures. A later analysis on data converted by slope synthesis was carried out in relationship with the availability of land use data and precisely spaced yield scales. ESA

N92-11522# Institut National de la Recherche Agronomique, Montfavet (France). Station de Bioclimatologie.
SPECTRAL ESTIMATES OF PAR INTERCEPTION AND BIOMASS PRODUCTION OF IRRIGATED RICE CROPS. 1: MODEL ELABORATION WITH GROUND DATA
Brigitte Leblon, Martine Guerif, and Frederic Baret *In* ESA, Physical Measurements and Signatures in Remote Sensing, Volume 2 May 1991 p 635-638 (For primary document see N92-11488 02-43)
Copyright Avail: NTIS HC/MF A16; ESA, EPD, ESTEC, Noordwijk, Netherlands, HC 150 Dutch guilders (2 vols)

A model of biomass production for irrigated rice crops, based on an energetic yield approach (Monteith's model), in which light interception efficiency (LIE) is estimated from the normalized difference (ND) vegetation index calculated from canopy reflectances in the visible and near infrared wavelengths, is proposed. The relationship between LIE (measured from hemispherical photographs) and ND results from coupling reflectance and PAR interception models based on Lambert-Beer's extinction law is examined. The background reflectance is determined through the temporal evolution of the water state and height, and takes into account the senescent vegetation after anthesis. Given the spectral profile of the crop, its PAR absorption profile can be estimated. The light use efficiency (LUE) is then calculated as the ratio of total absorbed PAR to total synthesized biomass during every homogeneous phenological period. In the case of irrigated rice, the root extraction and biomass evaluation are rather easy and a more realistic value can be estimated for LUE. Some obtained LUE values agree well with those of the literature. Varietal observed differences agree with experimental evaluation of cultivar photosynthetic capabilties. ESA

N92-11523# Grenoble-1 Univ. (France). Lab. de Geologie-Geomorphologie Structurale et Teledetection.
ANALYSIS OF THE SURFACE STATE OF TWO SUB-POLAR GLACIERS USING SPOT DATA AND A NUMERICAL TERRAIN MODEL [ANALYSE DE L'ETAT DE SURFACE DE DEUX GLACIERS SUB-POLAIRES A L'AIDE DES DONNEES SPOT ET D'UN MODELE NUMERIQUE DE TERRAIN]
Bernard Lefauconnier, N. Lyberis, and J. F. Parrot (Office de la Recherche Scientifique et Technique, Bondy, France) *In* ESA, Physical Measurements and Signatures in Remote Sensing, Volume 2 May 1991 p 639-642 In FRENCH (For primary document see N92-11488 02-43)
Copyright Avail: NTIS HC/MF A16; ESA, EPD, ESTEC, Noordwijk, Netherlands, HC 150 Dutch guilders (2 vols)

Radiometric XS1 and XS2 values of a SPOT image of two Spitsberg subpolar glaciers were combined with a numerical terrain model. Using the two dimensional histogram, radiometric correction values of the topographic effect were obtained: a neochannel no longer presented discontinuities between the shade and light zones. On this neochannel, the pixel values were validated by terrain measurements. From the summit at the front of the glaciers studied, the values of the neochannel decrease lightly, the limits between two surfaces states being little marked. ESA

N92-11524# Institut Francais de Recherche Scientifique pour le Developpement en Cooperation, Paris (France).
MULTITEMPORAL STUDY OF THE GUYANA COASTLINE AND ESTUARIES USING SPOT AND LANDSAT IMAGERY [ETUDE MULTITEMPORELLE DU LITTORAL ET DES ESTUAIRES GUYANAIS UTILISANT L'IMAGERIE SPOT ET LANDSAT]
C. Charron, Marc Lointier, M. T. Prost, and Jean-Paul Rudant (Paris VI Univ., France) *In* ESA, Physical Measurements and Signatures in Remote Sensing, Volume 2 May 1991 p 643-646 In FRENCH (For primary document see N92-11488 02-43)
Copyright Avail: NTIS HC/MF A16; ESA, EPD, ESTEC, Noordwijk, Netherlands, HC 150 Dutch guilders (2 vols)

The dynamically changing coasts of Guyana were studied with different data using different techniques (historical and topographic map comparisons and photointerpretation). The accuracy of these measurements is variable: in many cases it is a question of estimations given the quality of the documents and the difficulty of defining a shoreline on a constantly changing coastal feature. Remote sensing and ground truth data were used to calculate the actual accretion and retreat of the shoreline. ESA

N92-11525# Office National d'Etudes et de Recherches Aerospatiales, Toulouse (France). Lab. d'Etudes et de Recherches en Teledetection Spatiale.
NOAA-AVHRR NDVI TEMPORAL PROFILE CLASSIFICATION AND SENSITIVITY TO LAND USE AND CLIMATIC CONDITIONS IN TEMPERATE REGION [CLASSIFICATION DE PROFILS TEMPORELS DE NDVI AVHRR/NOAA ET SENSIBILITE A L'OCCUPATION DU SOL ET AUX CONDITIONS CLIMATIQUES EN REGION TEMPEREE]
Sami Louahala, Alberte Fisher, Alain Podaire, and Nicolas Viovy *In* ESA, Physical Measurements and Signatures in Remote Sensing, Volume 2 May 1991 p 647-650 In FRENCH (For primary document see N92-11488 02-43)
(Contract EEC-3444-88-08-ES-IPF)
Copyright Avail: NTIS HC/MF A16; ESA, EPD, ESTEC, Noordwijk, Netherlands, HC 150 Dutch guilders (2 vols)

Three years of NOAA AVHRR data were processed to map land use in south west France. The corrected NDVI (Normalized Difference Vegetative Index) of atmospheric effects was filtered by a simple algorithm, then smoothed by fast Fourier Transform, to obtain temporal profiles. Land use differences and climatic events are clearly perceived. The profiles are classified automatically by a dynamic cloud type algorithm. Combining the results allows the sensitivity of the AVHRR profiles to be evaluated with the land use. ESA

N92-11526# Stockholm Univ. (Sweden). Dept. of Physical Geography.
NIGHT-TIME LANDSAT THERMAL INFRARED IMAGERY AS A TOOL FOR CLIMATOLOGICAL STUDIES
Bengt Lunden and Maj-Liz Nordberg *In* ESA, Physical Measurements and Signatures in Remote Sensing, Volume 2 May 1991 p 651-654 Sponsored by Swedish Board for Space Activities and Swedish Natural Science Research Council (For primary document see N92-11488 02-43)
Copyright Avail: NTIS HC/MF A16; ESA, EPD, ESTEC, Noordwijk, Netherlands, HC 150 Dutch guilders (2 vols)

An analysis of a LANDSAT 5 TM (Thematic Mapper) band 6

image from an Oct. night, 1988, is reported. With radiosonde data and an atmospheric propagation model, definite temperatures are determined. Examples of how the imagery can be used for analyses of some hydrological phenomena, like fast radiative cooling of lake water surfaces, and coastal upwelling, are given. The satellite derived temperature patterns on clear cuts are examined, especially with the relation to elevation, aspect and slope. ESA

N92-11527# Institut Francais de Recherche Scientifique pour le Developpement en Cooperation, Paris (France).
SPATIAL AND SPECTRAL ANALYSIS OF A DEGRADED MANGROVE IN SOUTH SENEGAL [ANALYSE SPATIALE ET SPECTRALE D'UNE MANGROVE DEGRADEE AU SUD DU SENEGAL]
Bernard Mougenot *In* ESA, Physical Measurements and Signatures in Remote Sensing, Volume 2 May 1991 p 655-657 In FRENCH; ENGLISH summary (For primary document see N92-11488 02-43)
Copyright Avail: NTIS HC/MF A16; ESA, EPD, ESTEC, Noordwijk, Netherlands, HC 150 Dutch guilders (2 vols)

Radiometric ground data were acquired on a degraded mangrove parcel in south Senegal and processed with geostatistical methods. A weak spatial structure is observed with important nugget and drift effects. Kriging maps were edited after variogram modelization. The analysis of pedological and SPOT satellite data produced similar results: increasing of drift effect and random tendancy whatever the distance. Spatial variability of various data can be compared. ESA

N92-11528# Sherbrooke Univ. (Quebec). Centre d'Applications et de Recherches en Teledetection.
EVALUATION OF GROUND COVER IN AGRICULTURAL ENVIRONMENT BY IN SITU MEASUREMENTS AND MULTITEMPORAL IMAGES FOR MODELING HYDRIC EROSION [EVALUATION DE LA COUVERTURE DU SOL EN MILIEU AGRICOLE PAR MESURES IN-SITU ET IMAGES MULTITEMPORELLES POUR LA MODELISATION DE L'EROSION HYDRIQUE]
Linda Cyr, Sylvain Perras, Ferdinand Bonn, Alain Pesant, and Thierry Willm (Groupement Scientifique de Teledetection de Strasbourg, France) *In* ESA, Physical Measurements and Signatures in Remote Sensing, Volume 2 May 1991 p 659-662 In FRENCH; ENGLISH summary Sponsored by Ministere de l'Agriculture, des Pecheries et de l'Alimentation and CRSNG (For primary document see N92-11488 02-43)
Copyright Avail: NTIS HC/MF A16; ESA, EPD, ESTEC, Noordwijk, Netherlands, HC 150 Dutch guilders (2 vols)

In erosion models such as the Universal Soil Loss Equation, soil protective cover and its variations throughout the phenological cycle plays a major role. A supervised classification based on 2 SPOT images (Spring, Summer, Fall) allowed the establishment of a fine classification of crops. A normalized difference vegetation index was calculated on the training sites for each of the crop classes. Soil cover values and vegetation indexes were obtained at 10 day intervals during the growing season by radiometric field measurements and digitization of low altitude photographs. The relationship between soil cover and vegetation index as well as between ground and satellite data is examined. Evaluation of soil protective cover with vegetation indexes gives a good correlation as long as the vegetation is green, but gives less satisfactory results for vegetation in the senescence stage. Soil cover data was integrated in a soil loss model within a geographic information system. ESA

N92-11529# Toulouse Univ. (France). Lab. d'Aerologie.
DETECTION AND CHARACTERIZATION OF ACTIVE FIRES IN WEST AFRICA WITH LANDSAT THEMATIC MAPPER AND NOAA
J. M. Brustet, J. B. Vickos, J. Fontan, Alain Podaire, and Francois Lavenu (Office National d'Etudes et de Recherches Aerospatiales, Toulouse, France) *In* ESA, Physical Measurements and Signatures in Remote Sensing, Volume 2 May 1991 p 663-670 (For primary document see N92-11488 02-43)
Copyright Avail: NTIS HC/MF A16; ESA, EPD, ESTEC, Noordwijk, Netherlands, HC 150 Dutch guilders (2 vols)

Data from LANDSAT Thematic Mapper was used to study some characteristics of fires: temperature, surface, shape. The radiance of fire can be separated from that of the environment on channels TM5 and TM7. The smoke present over the fires has to be taken into account. A first estimation of the emission of some constituents of a mean fire is given. NOAA AVHRR can give the number of fires at a larger scale. The radiances of fires are analyzed using channels 3 and 4. Generally, the separation of radiance of fires and of the environment is easy with the channel 3. In some cases, when the reflectance and emission of the environment are too large, the radiance given by the two can be imbricated, but, nevertheless, it is possible to have most of fires. ESA

N92-11530# Montreal Univ. (Quebec). Dept. de Geographie.
STUDY OF THE SPATIAL SIGNATURE OF FOREST COVERS BY GEOMETRIC-OPTIC MODELING [ETUDE DE LA SIGNATURE SPATIALE DES COUVERTS FORESTIERS PAR MODELISATION GEOMETRIQUE-OPTIQUE]
Benoit St.Onge, F. Cavayas, and Philippe M. Teillet (Canada Centre for Remote Sensing, Ottawa, Ontario) *In* ESA, Physical Measurements and Signatures in Remote Sensing, Volume 2 May 1991 p 671-674 In FRENCH (For primary document see N92-11488 02-43)
Copyright Avail: NTIS HC/MF A16; ESA, EPD, ESTEC, Noordwijk, Netherlands, HC 150 Dutch guilders (2 vols)

The potential of a texture based approach to study spatial resolution of digital night images of complex surfaces such as forests was addressed. A semivariogram was used for measuring on computer simulated images using a geometric optics process and mathematical models of trees. Results show that the texture reveals a lot of information on the height and density of the trees, especially when the spatial resolution and solar elevation are taken. ESA

N92-11531# Polish Academy of Sciences, Warsaw.
FROM EVAPOTRANSPIRATION TO SOIL MOISTURE INVESTIGATION BASED ON NOAA THERMAL INFRARED DATA, CASE STUDY: POLAND
K. Dabrowska-Zielinska, M. Gruszczynska, and Stanislaw Lewinski *In* ESA, Physical Measurements and Signatures in Remote Sensing, Volume 2 May 1991 p 675-678 Sponsored by United Nations Development Program/FAO (For primary document see N92-11488 02-43)
Copyright Avail: NTIS HC/MF A16; ESA, EPD, ESTEC, Noordwijk, Netherlands, HC 150 Dutch guilders (2 vols)

Grassland evapotranspiration was assessed as a residual from the energy budget equation, from which the surface temperature was extracted from NOAA AVHRR channel 4 and 5 and corrected for atmospheric absorption. The ratio of sensible to latent heat was used as an index for soil moisture, wet biomass and leaf area index assessment. The ratio of calculated evapotranspiration to net radiation was applied for predicting biomass dry. The normalized difference vegetative index calculated from NOAA data can be used as an indicator of the height of grass, one of the factors influencing the value of evapotranspiration. ESA

N92-11532# Paris XI Univ., Orsay (France). Lab. pour l'Utilisation du Rayonnement Electromagnetique.
CONTROL OF THE PHYSIOLOGICAL STATE OF VEGETATION COVER BY REMOTE SENSING OF FLUORESCENT EMISSION IN THE BLUE AND RED VISIBLE SPECTRUM REGIONS [CONTROLE DE L'ETAT PHYSIOLOGIQUE DES COUVERTS VEGETAUX PAR TELEDETECTION DES EMISSIONS DE FLUORESCENCE DANS LES REGIONS BLEUE ET ROUGE DU SPECTRE VISIBLE]
Ismael Moya, Yves Goulas, Gerard Guyot, Bruno Bertolini, and Guido Schmuck (Joint Research Centre of the European Communities, Ispra, Italy) *In* ESA, Physical Measurements and Signatures in Remote Sensing, Volume 2 May 1991 p 681-685 In FRENCH (For primary document see N92-11488

02-43)
Copyright Avail: NTIS HC/MF A16; ESA, EPD, ESTEC, Noordwijk, Netherlands, HC 150 Dutch guilders (2 vols)

Techniques currently envisaged for fluorescence remote sensing are addressed. Active and passive laser induced fluorescence for detecting vegetation cover fluorescence are reviewed. Possibilities for satellite detection are also considered. ESA

N92-11533# Consiglio Nazionale delle Ricerche, Florence (Italy). Ist. di Ricerca sulle Onde Elettromagnetiche.
VEGETATION MONITORING BY MEANS OF SPECTRAL RESOLVED FLUORESCENCE LIDAR
Giovanna Cecchi and Luca Pantani *In* ESA, Physical Measurements and Signatures in Remote Sensing, Volume 2 May 1991 p 687-689 (For primary document see N92-11488 02-43)
Copyright Avail: NTIS HC/MF A16; ESA, EPD, ESTEC, Noordwijk, Netherlands, HC 150 Dutch guilders (2 vols)

Fluorescence lidar is introduced with its principles and the type of spectroscopy which is carried out with lidar systems is described. Vegetation monitoring is presented and discussed in relation with chlorophyll fluorescence. ESA

N92-11534# Academy of Sciences (USSR), Leningrad. Inst. for Lake Research.
LASER ACTIVE REMOTE SENSING OF PHYTOPLANKTON IN INLAND WATERS
K. Y. Kondratyev and D. V. Pozdnyakov *In* ESA, Physical Measurements and Signatures in Remote Sensing, Volume 2 May 1991 p 691-696 (For primary document see N92-11488 02-43)
Copyright Avail: NTIS HC/MF A16; ESA, EPD, ESTEC, Noordwijk, Netherlands, HC 150 Dutch guilders (2 vols)

Large scale limnological applications of active optical remote sensing techniques are described. An airborne Nd:YAG laser with frequency doubling and tripling facilities is used. Information on spatial distribution of both phytoplankton chlorophyll and dissolved organic matter concentrations is retrieved together with the data on macrophytes littoral invasions. The analysis of specific features of two dimensional fields of chlorophyll concentrations is liable to give an insight into some thermohydrodynamic processes in the waterbody. ESA

N92-11535# Deutsche Forschungsanstalt fuer Luft- und Raumfahrt, Oberpfaffenhofen (Germany, F.R.). Inst. for Optoelectronics.
CO2 LASER ACTIVE REMOTE SENSING FROM 9 TO 11 MICRONS: AIRBORNE AND LABORATORY APPLICATION
P. Hausknecht and L. B. Whitbourn (Commonwealth Scientific and Industrial Research Organization, Linfield, Australia) *In* ESA, Physical Measurements and Signatures in Remote Sensing, Volume 2 May 1991 p 697-701 (For primary document see N92-11488 02-43)
Copyright Avail: NTIS HC/MF A16; ESA, EPD, ESTEC, Noordwijk, Netherlands, HC 150 Dutch guilders (2 vols)

An active airborne remote sensing system using a rapidly tuned CO2 laser, which covers the region between 9.2 and 11.1 microns with up to 90 lines of different wavelengths is reported. The system was designed to produce a contiguous line profile with 2 m diameter footprints at a range of 500 m and an aircraft speed of 80 m/s. Results of airborne tests are presented. The first series was performed in October 1989 in south east New South Wales (Australia). These data sets show recognizable spectral reflectance signatures over a number of sites. The second series was carried out in Oct. 1990 in Western Australia and the data show an improved signal to noise ratio and data quality. The acquired profiles of ground spectra are very promising, and good results are expected after a more detailed analysis. ESA

N92-11536*# National Aeronautics and Space Administration. Goddard Space Flight Center, Greenbelt, MD.
WAVELENGTH SHIFTS IN FLUORESCENCE MAXIMA OF STRESSED AND NON-STRESSED NORWAY SPRUCE NEEDLES OVER THE GROWING SEASON
Cliff Banninger (Joanneum Research Centre, Graz, Austria) and E. Chappelle *In* ESA, Physical Measurements and Signatures in Remote Sensing, Volume 2 May 1991 p 705-710 (For primary document see N92-11488 02-43)
Copyright Avail: NTIS HC/MF A16; ESA, EPD, ESTEC, Noordwijk, Netherlands, HC 150 Dutch guilders (2 vols)

Laboratory fluorescence measurements of first and third year metal stressed and non stressed Norway spruce needles collected in May, Jul. Sep. and Nov. display significant wavelength shifts in the intensity maxima in the blue, green, red, and near infrared spectral regions, with the largest shifts occurring in the blue spectral region for both first and third year needles from Nov. Smaller, but the otherwise significant shifts also take place in the blue spectral region for first year needles from Sep. in the red spectral region for third year neddles from May, Jul. and Sep. and in the near infrared spectral region for first and third year needles from Jul. and Sep. Wavelength shifts in needle fluorescence maxima over the growing season are greatest in the blue and to a lesser extent, greenspectral regions from Sep. to Nov. but are also significant in the red and near infrared spectral regions from Jul. to Sep. and Sep. to Nov., and in the near infrared spectral region also from May to Jul. ESA

N92-11537# MPB Technologies, Inc., Dorval (Quebec).
LASER-INDUCED SPECTRAL SIGNATURES IN INVESTIGATIONS OF SEA UPPER LAYER
Alexander Dudelzak, S. M. Babichenko, L. V. Poryvkina, and J. Lapimaa (Academy of Sciences of the Estonian SSR, Tallinn.) *In* ESA, Physical Measurements and Signatures in Remote Sensing, Volume 2 May 1991 p 711-714 (For primary document see N92-11488 02-43)
Copyright Avail: NTIS HC/MF A16; ESA, EPD, ESTEC, Noordwijk, Netherlands, HC 150 Dutch guilders (2 vols)

The results of applying the Total Luminescent Spectroscopy (TLS) to the diagnostics of natural water conditions and a study of spatial variability of sea phytoplankton and dissolved organic water using a laser technique are presented. Two dimensional TLS signatures can serve as representative indicators of both statistically normal state of water and of departures from it. With the aid of laboratory catalogs of laser induced signatures, it is possible to detect oils in water at levels substantially below those of spoils and to determine different water types according to specific spectral signatures of dissolved organic matter. Regularities in sea surface phytoplankton spatial distribution were found. The block diagram of a tunable laser remote spectrometer developed by the authors is presented. ESA

N92-11538# Institut National de la Recherche Agronomique, Montfavet (France).
TIME-RESOLVED SPECTROSCOPY OF THE BLUE FLUORESCENCE OF SPINACH LEAVES
Yves Goulas, Ismael Moya, and Guido Schmuck (Joint Research Centre of the European Communities, Ispra, Italy) *In* ESA, Physical Measurements and Signatures in Remote Sensing, Volume 2 May 1991 p 715-718 Sponsored by Applications de la Recherche en Photonique Society (For primary document see N92-11488 02-43)
Copyright Avail: NTIS HC/MF A16; ESA, EPD, ESTEC, Noordwijk, Netherlands, HC 150 Dutch guilders (2 vols)

Upon excitation by ultraviolet radiation, leaves of a great number of species of higher plants exhibit emission of blue fluorescence, comparable in intensity to the well known red emission of cholorophyll. The fluorescence decay of the blue emission of spinach leaves recorded by single photon counting techniques is decomposed into exponential components and it is shown that at least three different components are present. The lifetime of the three components does not show significant variations with the excitation or emission wavelengths. The excitation and emission

spectra of each component were determined. The nature of the chemical compounds which cause this emission is discussed in relation to these spectra. ESA

N92-11539# Consiglio Nazionale delle Richerche Olivicoltura, Perugia (Italy).
SIMULTANEOUS DETECTION IN BLUE AND RED BANDS OF LASER INDUCED VEGETATION FLUORESCENCE [DETECTION SIMULTANEE DANS LES BANDES BLEUE ET ROUGE DE LA FLUORESCENCE INDUITE PAR LASER DES VEGETAUX]
Guido Bongi, Yves Goulas, Ismael Moya, and Guido Schmuck (Joint Research Centre of the European Communities, Ispra, Italy) *In* ESA, Physical Measurements and Signatures in Remote Sensing, Volume 2 May 1991 p 719-722 In FRENCH (For primary document see N92-11488 02-43)
Copyright Avail: NTIS HC/MF A16; ESA, EPD, ESTEC, Noordwijk, Netherlands, HC 150 Dutch guilders (2 vols)

The development of an impulse fluorimeter, measuring in four channels, 440, 515, 690 and 730 nm, and insensitive to continuous light, is reported. Emissions at 440 and 515 nm are shown for the first time to be unchanged, at the time of variations in the photosynthetic activity produced by the light of by photosynthesis inhibitors, in the accessible time field (100 ms to a few mn). The measurements showed a very sensitive signal dependence at 440 and 515 nm with the foliar temperature between 0 and 40 C, leading to up to 60 of fall of these transmissions, when the temperature increased. ESA

N92-11540# Deutsche Forschungsanstalt fuer Luft- und Raumfahrt, Oberpfaffenhofen (Germany, F.R.). Inst. for Optoelectronics.
DESIGN AND TESTING OF A SPECTRAL-RESOLVING FLUORESCENCE LIDAR SYSTEM FOR REMOTE SENSING OF VEGETATION
Kurt P. Guenther, Wilhelm Luedeker, and H.-G. Dahn *In* ESA, Physical Measurements and Signatures in Remote Sensing, Volume 2 May 1991 p 723-726 (For primary document see N92-11488 02-43)
(Contract BMFT-0339290A)
Copyright Avail: NTIS HC/MF A16; ESA, EPD, ESTEC, Noordwijk, Netherlands, HC 150 Dutch guilders (2 vols)

In the frame of the EUREKA project LASFLEUR (EU 380), an experimental high resolution laser remote sensing system for the detection of chlorophyll fluorescence of vegetation is reported. The main aim of the LASFLEUR project is to correlate laser excited fluorescence data of different vegetation with simultaneous measured elementary physiological parameters as e.g., pigment concentration, gas exchange and fluorescence induction kinetics. The future target will be to find a new approach for remote sensing the state of vegetation. The compact lidar system can be used in the laboratory and in the field. For far distance measurements in the field the system may be operated ground based or mounted on towers. The performance of the new lidar is demonstrated and data sets of stressed and non stressed leaves and canopies are discussed. ESA

N92-11541# Karlsruhe Univ. (Germany, F.R.). Plant Physiology and Plant Biochemistry.
LASER-INDUCED BLUE FLUORESCENCE AND RED CHLOROPHYLL FLUORESCENCE SIGNATURES OF DIFFERENTLY PIGMENTED LEAVES
Hartmut K. Lichtenthaler, Michael Lang, and Fred Stober *In* ESA, Physical Measurements and Signatures in Remote Sensing, Volume 2 May 1991 p 727-730 Sponsored in part by BMFT and PEF (For primary document see N92-11488 02-43)
Copyright Avail: NTIS HC/MF A16; ESA, EPD, ESTEC, Noordwijk, Netherlands, HC 150 Dutch guilders (2 vols)

The laser induced red chlorophyll fluorescence spectra of green leaves were determined using a dye laser/OMA III system. The ratio of the two chlorophyll fluorescence maxima F690/F735 exhibits a curvilinear correlation to the chlorophyll content, as was shown here during the autumnal chlorophyll breakdown. When UV light is applied for excitatioin, in addition to Red chlorophyll Fluorescence (RF), a Blue Fluorescence (BF) is obtained with a maximum near 450 nm and a shoulder/maximum near 520 nm. Upper and lower leaf sides differ in their fluorescence intensity and in the ratio F450/F690 (BF/RF). The BF of plants appears to be a mixed signal composed of the fluorescence of various phenolic substances from the epidermal layers such as chlorogenic acid, caffeic acid, berberine and possibly also NADPH. Whether the intensity of the blue fluorescence and the ratio F450/F690 can be used as a stress indicator has yet to be determined. ESA

N92-11542# Karlsruhe Univ. (Germany, F.R.). Plant Physiology and Plant Chemistry.
THE LASER-INDUCED CHLOROPHYLL FLUORESCENCE RATIO F690/F735 OF SPRUCE NEEDLES AND BEECH LEAVES DURING THE COURSE OF A YEAR
U. Rinderle, C. Schindler, and Hartmut K. Lichtenthaler *In* ESA, Physical Measurements and Signatures in Remote Sensing, Volume 2 May 1991 p 731-734 Sponsored in part by PEF (For primary document see N92-11488 02-43)
Copyright Avail: NTIS HC/MF A16; ESA, EPD, ESTEC, Noordwijk, Netherlands, HC 150 Dutch guilders (2 vols)

The shapes of the in vivo chlorophyll fluorescence emission spectra of spruce needles and beech leaves with different chlorophyll content were determined under steady state conditions of chlorophyll fluorescence and photosynthesis. The chlorophyll fluorescence emission of green plant tissue is characterized by two maxima in the 690 and 735 nm region. The ratio of the intensity of the two fluorescence maxima F690/F735 varies depending on the chlorophyll content of leaves. Yellowish green needles of damaged spruces, which are affected by the first decline, show higher values for F690/F735 and lower chlorophyll content than green needles of healthy trees. The differences in F690/F735 during the course of a year are mainly due to changes in the chlorophyll content of needles. The possible application of this ratio in remote sensing of vegetation is discussed. ESA

N92-11543# Centre Machinisme Agricole Genie Rural Eaux Forets, Montpellier (France). Lab. Commun de Teledetection.
A SIMPLE MODEL OF CANOPY FLUORESCENCE
Albert Olioso, Maurice Methy, and Bernard Lacaze (Centre National de la Recherche Scientifique, Montpellier, France) *In* ESA, Physical Measurements and Signatures in Remote Sensing, Volume 2 May 1991 p 735-738 (For primary document see N92-11488 02-43)
Copyright Avail: NTIS HC/MF A16; ESA, EPD, ESTEC, Noordwijk, Netherlands, HC 150 Dutch guilders (2 vols)

Canopy chlorophyll fluorescence depends on the variation of individual leaf response inside the canopy, the attenuation of incident exciting radiation and the scattering of emitted radiation toward the sensor. A simple model, which takes into account the leaf fluorescence profile inside the canopy and structural variations of the canopy and background reflection is presented. Analysis shows that canopy fluorescence is strongly affected by these parameters. However, the ratio of both maximum chlorophyll fluorescence at 690 and 730 nm limits these effects. ESA

N92-11544# Consiglio Nazionale delle Ricerche, Florence (Italy). Ist. di Ricerca sulle Onde Elettromagnetiche.
TARGET SIGNATURE BY DIFFERENTIAL REFLECTANCE LIDAR, A FEASIBILITY STUDY
Luca Pantani, I. Pippi, B. Radicati, and P. VujkovicCvijin (Institute of Physics, Zemun, Yugoslavia) *In* ESA, Physical Measurements and Signatures in Remote Sensing, Volume 2 May 1991 p 739-742 (For primary document see N92-11488 02-43)
Copyright Avail: NTIS HC/MF A16; ESA, EPD, ESTEC, Noordwijk, Netherlands, HC 150 Dutch guilders (2 vols)

A feasibility study to determine the usefulness of differential reflectance lidars in the remote sensing of the Earth surface is reported. The study is based on a spectral library built by laboratory measurements in the visible and infrared performed by a lidar simulator and commercial interferometer and spectrometer. ESA

N92-11545# Environmental Analysis and Remote Sensing, Delft (Netherlands).
MODELING OF FLUORESCENCE LIGHT-CANOPY INTERACTION
Andries Rosema and W. Verhoef (National Aerospace Lab., Emmeloord, Netherlands) *In* ESA, Physical Measurements and Signatures in Remote Sensing, Volume 2 May 1991 p 743-748 Sponsored by Begeleidingscommissee Remote Sensing (For primary document see N92-11488 02-43)
Copyright Avail: NTIS HC/MF A16; ESA, EPD, ESTEC, Noordwijk, Netherlands, HC 150 Dutch guilders (2 vols)

The development of an operational field instrument for the measurement of laser induced fluorescence of vegetation (LEAF) is reported. Plant physiological and remote sensing research carried out to support this new remote sensing instrument is reported. An introduction to the subject of laser induced fluorescence is presented. The development of a leaf and a canopy fluorescence model are reported. With these models a sensitivity study was carried out. A 690 nm fluorescence appears to be most suitable to obtain information on photosynthesis and stress. ESA

N92-11546# Wageningen Agricultural Univ. (Netherlands). Dept. of Plant Physiological Research.
(L)EAF: A REMOTE SENSING FLUORESENSOR
J. Schroote and J. F. H. Snel *In* ESA, Physical Measurements and Signatures in Remote Sensing, Volume 2 May 1991 p 749-752 Sponsored by Begeleidingscommisse Remote Sensing (For primary document see N92-11488 02-43)
Copyright Avail: NTIS HC/MF A16; ESA, EPD, ESTEC, Noordwijk, Netherlands, HC 150 Dutch guilders (2 vols)

The development of an operational field instrument for the measurement of laser induced fluorescence of plants (LEAF) is reported. Plant physiological and remote sensing research is carried out to support this new remote sensing instrument. A simulator of the LEAF instrument (EAF) is built for the plant physiological research under laboratory conditions. A description of the EAF instrument, an introduction of the interpretation of chlorophyll fluorescence in plant physiological terms and some preliminary measurements showing that stress induced changes in chlorophyll fluorescence can be detected with this new instrument, are given. ESA

N92-11547# Kisarazu National Coll. of Technology (Japan).
LASER INDUCED FLUORESCENCE OF GROWING CAMPHOR TREE LEAVES: INFLUENCE OF CHLOROPHYLL CONTENT ON LIF SPECTRAL SIGNATURE
Kunio Takahashi, T. Nakamura, M. Koizumi (National Inst. of Agrobiological Resources, Ibaraki, Japan), H. Kano, and S. Suzuki *In* ESA, Physical Measurements and Signatures in Remote Sensing, Volume 2 May 1991 p 753-756 (For primary document see N92-11488 02-43)
Copyright Avail: NTIS HC/MF A16; ESA, EPD, ESTEC, Noordwijk, Netherlands, HC 150 Dutch guilders (2 vols)

Fluorescence spectra induced by a laser light (Ar-laser, 477 nm and 488 nm, 3.5 mW) in intact camphor tree leaves were measured at room temperature by an Optical Multichannel Spectrometer (OMS) equipped with an image intensifier. Two peaks were observed in the fluorescence spectra. Resolution of peaks to emitter components with Gaussian shapes suggested that the peak near 685 nm were the bands related to photosystem 2 and that those near 740 nm were related to photosystem 1. The ratio increased along with progession of growth stages of the leaf associated with the increase of chlorophyll content. It was considered that fluorescence from photosystem 2 was reabsorbed by photosystem 1. Self absorption of fluorescence raises the conversion efficiency of solar energy to photochemical reactions in the leaves with dense chlorophyll. ESA

N92-11548# Joint Research Centre of the European Communities, Ispra (Italy). Inst. for Remote Sensing Applications.
THE USE OF A TIME-RESOLVED LIDAR TO STUDY THE WATER COLUMN
Bruno Bertolini, C. Koechler, and Jean Verdebout *In* ESA, Physical Measurements and Signatures in Remote Sensing, Volume 2 May 1991 p 757-761 (For primary document see N92-11488 02-43)
Copyright Avail: NTIS HC/MF A16; ESA, EPD, ESTEC, Noordwijk, Netherlands, HC 150 Dutch guilders (2 vols)

Remote measurements performed on an artificial water column with a fully time resolved lidar technique are presented. The results are discussed in view of the possibility of evaluating the attenuation coefficient from the temporal dependence of the various signals (backscattering, water Raman diffusion and dissolved organic matter fluorescence). The results are analyzed on the basis of the most simple model which completely neglects multiple scattering and the experimental values are found to be 10 to 30 lower then the beam attenuation coefficient measured with a spectrophotometer. Considering the characteristics of the experimental system and the type of water measured, this is in accordance with published Monte Carlo simulations. ESA

N92-11549# Joint Research Centre of the European Communities, Ispra (Italy).
OBSERVATION OF DOM COMPOSITION BY SYNCHRONOUS FLUORESCENCE SPECTROSCOPY
A. Vodacek *In* ESA, Physical Measurements and Signatures in Remote Sensing, Volume 2 May 1991 p 763-766 (For primary document see N92-11488 02-43)
Copyright Avail: NTIS HC/MF A16; ESA, EPD, ESTEC, Noordwijk, Netherlands, HC 150 Dutch guilders (2 vols)

Dilute solutions of model compounds of lignin degradation products and a freshwater pond sample were studied using synchronous fluorescence spectroscopy. Synchronous fluorescence spectra of the model compounds and of a caffeic acid and pond water during titration are analyzed with respect to the relation between molecular electronic structure and fluorescence. An empirical model of the composition dependent fluorecence characteristics of lignin derived Dissolved Organic Matter (DOM) is described. These results link several previous DOM fluorescence studies in a consistent manner. ESA

N92-11550# State Univ. of New York, Binghamton.
BIOSPHERIC MODELS, MEASUREMENTS, AND REMOTE SENSING OF VEGETATION
Narenda S. Goel and J. M. Norman (Wisconsin Univ., Madison.) *In* ESA, Physical Measurements and Signatures in Remote Sensing, Volume 2 May 1991 p 769-775 (For primary document see N92-11488 02-43)
Copyright Avail: NTIS HC/MF A16; ESA, EPD, ESTEC, Noordwijk, Netherlands, HC 150 Dutch guilders (2 vols)

The roles of biospheric models and measurements in developing a practical technique for remote sensing of vegetation are discussed. An approach to develop models for biospheric processes is presented. Such biopheric models require component models for radiation interception in optical and thermal infrared regions, for soil plant atmosphere interaction, and for plant growth. These models and the techniques to measure relevant soil, vegetation, and atmospheric parameters occurring in these models are reviewed. Some directions for future research for modeling and measurements in connection with successful remote sensing of vegetation are suggested. ESA

N92-11551# Colorado Univ., Boulder. Center for the Study of Earth from Space.
A CONCEPTUAL FRAMEWORK FOR ECOSYSTEM MODELING USING REMOTELY SENSED INPUTS
Carol A. Wessman, Brian Curtiss, Bo-Cai Gao, and Susan L. Ustin (California Univ., Davis.) *In* ESA, Physical Measurements and Signatures in Remote Sensing, Volume 2 May 1991 p 777-782 (For primary document see N92-11488 02-43)
Copyright Avail: NTIS HC/MF A16; ESA, EPD, ESTEC, Noordwijk, Netherlands, HC 150 Dutch guilders (2 vols)

Ecosystem models utilizing input parameters obtained from remote sensing measurements will improve the simulation of ecosystem dynamics in ths spatial domain and provide the means to describe and monitor the state of the biosphere at regional to

global scales. Landscape processes affecting remote sensing data occur at a range of spatial and temporal scales. Thus, ecosystem models utilizing remote sensing inputs must be parameterized not only on leaf scale properties, but also on canopy properties that are modulated at much larger scales. It is only through the modeling of both large and small scale canopy properties that ecosystem parameters can be accurately inferred. A conceptual framework that allows the analysis of ecosystem processes using models that rely on new physical parameters to be derived from the suite of instruments available on the Earth Observing System and other proposed remote sensing platforms is presented. ESA

N92-11552# Arizona Univ., Tucson. Dept. of Soil and Water Science.

VIEW-ATMOSPHERE-SOIL EFFECTS ON VEGETATION INDICES DERIVED FROM SPOT IMAGES

J. Qi, M. Susan Moran, Alfredo R. Huete, R. D. Jackson, and A. Chehbouni (Office National d'Etudes et de Recherches Aerospatiales, Toulouse, France) *In* ESA, Physical Measurements and Signatures in Remote Sensing, Volume 2 May 1991 p 785-790 (For primary document see N92-11488 02-43)

Copyright Avail: NTIS HC/MF A16; ESA, EPD, ESTEC, Noordwijk, Netherlands, HC 150 Dutch guilders (2 vols)

A temporal sequence of 15 SPOT high resolution visible (HRV) images and aircraft data were obtained over cotton at the Maricopa Agricultural Center, Arizona (U.S.) from April to October 1989. The SPOT data included different view angles (-28 to +24 degrees) and the aircraft data were obtained with a nadir viewing radiometer equipped with SPOT filters. View angle/direction, atmosphere, and soil influences were observed in the SPOT data. The relative magnitude among the 3 influences was dependent on surface conditions varied with canopy growth, and was different for reflectances versus Vegetation Indices (VI). View effects were most pronounced with the red and NIR bands but became secondary with the use of VI's. Soil and view variations on VI's were most important in partial canopies while atmospheric influences became dominant with increase in vegetation. ESA

N92-11553*# Jet Propulsion Lab., California Inst. of Tech., Pasadena.

NEOTECTONIC STUDIES OF NORTHERN BAJA CALIFORNIA, MEXICO, WITH LANDSAT THEMATIC MAPPER AND SPOT PANCHROMATIC IMAGERY: PARTITIONING OF DEXTRAL AND EXTENSIONAL STRAIN AT THE PACIFIC-NORTH AMERICA PLATE BOUNDARY

M. Meghan Miller, Robert E. Crippen, and Timothy H. Dixon *In* ESA, Physical Measurements and Signatures in Remote Sensing, Volume 2 May 1991 p 791-796 (For primary document see N92-11488 02-43)

Copyright Avail: NTIS HC/MF A16; ESA, EPD, ESTEC, Noordwijk, Netherlands, HC 150 Dutch guilders (2 vols) CSCL 08B

Numerous studies of active faulting in southern California indicate that the San Jacinto, Elsinore, and adjacent faults west of the San Andreas fault accommodate a significant proportion of Pacific-North America relative plate motion. Because of the complex distribution of slip, little is known about the activities of these and similar structures in northern Baja California and the southward transition to the oceanic ridge transform-fault system in the Gulf of California. SPOT and LANDSAT Thematic Mapper imagery for northern Baja California was processed to optimize discrimination of lithologic and structural features. This data was used to suggest a preliminary kinematic framework for distribution of relative plate motion between 31 and 33 degrees north, in which continental borderland tectonics play an important role in partitioning of plate motion. ESA

N92-11554*# National Aeronautics and Space Administration, Washington, DC.

USE OF MULTITEMPORAL SPOT DATA IN FIRST ISLSCP FIELD EXPERIMENT

Ghassem Asrar, R. E. Murphy, F. G. Hall, and P. J. Sellers (National Aeronautics and Space Administration. Goddard Space Flight Center, Greenbelt, MD.) *In* ESA, Physical Measurements and Signatures in Remote Sensing, Volume 2 May 1991 p 797-801 (For primary document see N92-11488 02-43)

Copyright Avail: NTIS HC/MF A16; ESA, EPD, ESTEC, Noordwijk, Netherlands, HC 150 Dutch guilders (2 vols) CSCL 08B

The use of multitemporal SPOT data in a coordinated field experiment is described with objectives to understand the processes that control the biosphere-atmosphere exchanges of heat, mass, momentum and radiation at a range of spatial and temporal scales; and quantify processes associated with these biosphere-atmosphere exchanges with the aid of multispectral and multitemporal remotely sensed data. The study was conducted in a 15 sq km area located in the tall grass prairie region of midwestern U.S. over a period of three years from 1987 through 1989. A combination of ground based, airborne and space based remotely sensed data were used in a variety of interdisciplinary investigations. An overview of the results from studies that used SPOT multispectral and multitemporal data is presented. ESA

N92-11555*# National Aeronautics and Space Administration, Washington, DC.

SPACE OBSERVATIONS FOR GLOBAL CHANGE Abstract Only

S. I. Rasool *In* ESA, Physical Measurements and Signatures in Remote Sensing, Volume 2 May 1991 p 805 (For primary document see N92-11488 02-43)

Copyright Avail: NTIS HC/MF A16; ESA, EPD, ESTEC, Noordwijk, Netherlands, HC 150 Dutch guilders (2 vols)

There is now compelling evidence that man's activities are changing both the composition of the atmospheric and the global landscape quite drastically. The consequences of these changes on the global climate of the 21st century is currently a hotly debated subject. Global models of a coupled Earth-ocean-atmosphere system are still very primitive and progress in this area appears largely data limited, specially over the global biosphere. A concerted effort on monitoring biospheric functions on scales from pixels to global and days to decades needs to be coordinated on an international scale in order to address the questions related to global change. An international program of space observations and ground research was described. ESA

N92-11556# California Univ., Santa Barbara. Center for Remote Sensing and Environmental Optics.

LOOKING AHEAD TO EOS: UPDATE ON NASA'S EARTH OBSERVING PROGRAM Abstract Only

Jeff Dozier *In* ESA, Physical Measurements and Signatures in Remote Sensing, Volume 2 May 1991 p 807 (For primary document see N92-11488 02-43)

Copyright Avail: NTIS HC/MF A16; ESA, EPD, ESTEC, Noordwijk, Netherlands, HC 150 Dutch guilders (2 vols)

NASA's Earth Observing System (EOS) is a pivotal part of the U.S. Global Change Research Program, and hence of the international effort to understand global change and the increasing demands of human activity. EOS consists of a space based observing system, a Data and Information System (EOSDIS), and a scientific research program. The space component will consist of two series of polar orbiting platforms, the first scheduled for launch in late 1997 and followed by launches every 2 1/2 years, that will collect data for 15 years. EOS will be supplemented by European and Japanese platforms and continuing operational and commercial satellites. ESA

N92-11557# Centre National de Recherches Meteorologiques, Toulouse (France).

REMOTE SENSING CONTRIBUTION TO THE APEX MOBILHY PROGRAM [APPORT DE LA TELEDETECTION AU PROGRAMME HAPEX-MOBILHY]

J. P. Goutorbe, J. C. Andre, and Thierry Phulpin (Centre National d'Etudes Spatiales, Toulouse, France) *In* ESA, Physical Measurements and Signatures in Remote Sensing, Volume 2 May 1991 p 809-813 In FRENCH (For primary document see N92-11488 02-43)

Copyright Avail: NTIS HC/MF A16; ESA, EPD, ESTEC, Noordwijk, Netherlands, HC 150 Dutch guilders (2 vols)

The program is a regional scale study of evaporation and hydric effect on an averagely heterogeneous continental surface. The aim is to improve the ground link of the water cycle in climate models. A variety of evaporation measurements techniques are used. The contribution of airborne and satellite remote sensing to the interpretation of in situ measurements and to modeling is examined. ESA

N92-11558# Southampton Univ. (England). Dept. of Geography.

THE UK NATURAL ENVIRONMENT RESEARCH COUNCIL EQUIPMENT POOL FOR FIELD SPECTROSCOPY (NERC-EPFS)

E. M. Rollin and E. J. Milton *In* ESA, Physical Measurements and Signatures in Remote Sensing, Volume 2 May 1991 p 837-839 (For primary document see N92-11488 02-43)

Copyright Avail: NTIS HC/MF A16; ESA, EPD, ESTEC, Noordwijk, Netherlands, HC 150 Dutch guilders (2 vols)

Access to high performance spectroradiometers for research and training in remote sensing is described. Five intercalibrated field portable spectroradiometers are available for loan for supported research, or hire for commissioned research projects. Equipment loan supports a wide range of projects covering applications in terrestrial and freshwater, Earth, marine, atmospheric and life sciences. Several international research programs and special airborne remote sensing campaigns benefit from use of the pool spectroradiometers. ESA

N92-11559*# Virginia Polytechnic Inst. and State Univ., Blacksburg. Dept. of Electrical Engineering.

THE SCIENCE BENEFITS OF AND THE ANTENNA REQUIREMENTS FOR MICROWAVE REMOTE SENSING FROM GEOSTATIONARY ORBIT Final Report

Warren L. Stutzman, ed. and Gary S. Brown, ed. Washington NASA Oct. 1991 62 p

(Contract NAS1-18471)

(NASA-CR-4408; NAS 1.26:4408; EE-SATCOM-91-1) Avail: NTIS HC/MF A04 CSCL 20N

The primary objective of the Large Space Antenna (LSA) Science Panel was to evaluate the science benefits that can be realized with a 25-meter class antenna in a microwave/millimeter wave remote sensing system in geostationary orbit. The panel concluded that a 25-meter or larger antenna in geostationary orbit can serve significant passive remote sensing needs in the 10 to 60 GHz frequency range, including measurements of precipitation, water vapor, atmospheric temperature profile, ocean surface wind speed, oceanic cloud liquid water content, and snow cover. In addition, cloud base height, atmospheric wind profile, and ocean currents can potentially be measured using active sensors with the 25-meter antenna. Other environmental parameters, particularly those that do not require high temporal resolution, are better served by low Earth orbit based sensors. Author

N92-11560*# Ohio State Univ., Columbus. Dept. of Geodetic Science and Surveying.

ESTIMATION OF GEOPOTENTIAL DIFFERENCES OVER INTERCONTINENTAL LOCATIONS USING SATELLITE AND TERRESTRIAL MEASUREMENTS Ph.D. Thesis

Nikolaos K. Pavlis Aug. 1991 166 p Sponsored in cooperation with the Ohio Supercomputer Center

(Grant NAG5-1329; Proj. 723194)

(NASA-CR-188992; NAS 1.26:188992; OSU-409) Avail: NTIS HC/MF A08 CSCL 08B

An error analysis study was conducted in order to assess the current accuracies and the future anticipated improvements in the estimation of geopotential differences over intercontinental locations. An observation/estimation scheme was proposed and studied, whereby gravity disturbance measurements on the Earth's surface, in caps surrounding the estimation points, are combined with corresponding data in caps directly over these points at the altitude of a low orbiting satellite, for the estimation of the geopotential difference between the terrestrial stations. The mathematical modeling required to relate the primary observables to the parameters to be estimated, was studied for the terrestrial data and the data at altitude. Emphasis was placed on the examination of systematic effects and on the corresponding reductions that need to be applied to the measurements to avoid systematic errors. The error estimation for the geopotential differences was performed using both truncation theory and least squares collocation with ring averages, in case observations on the Earth's surface only are used. The error analysis indicated that with the currently available global geopotential model OSU89B and with gravity disturbance data in 2 deg caps surrounding the estimation points, the error of the geopotential difference arising from errors in the reference model and the cap data is about 23 kgal cm, for 30 deg station separation. Author

N92-11561*# Lockheed Engineering and Sciences Co., Houston, TX. Engineering and Science Program.

CATALOG OF SPACE SHUTTLE EARTH OBSERVATIONS HANDHELD PHOTOGRAPHY. SPACE TRANSPORTATION SYSTEM 37 (STS-37) MISSION DATES: APRIL 5-11, 1991

Raymond M. Nelson, Kimberly J. Willis, William J. Daley, and Fred R. Brumbaugh Aug. 1991 250 p

(Contract NAS9-17900)

(NASA-CR-189014; NAS 1.26:189014; AD-A240314; LESC-29483) Avail: NTIS HC/MF A11 CSCL 14/4

This document catalogs Space Shuttle handheld Earth observations photographs which were collected during the Space Transportation System 37 (STS-37) Mission of April 5 through 11, 1991. The catalog includes the following data for each of 4486 frames, 4283 of which are Earth looking: identification number, geographical name, feature description, latitude and longitude, percentage of cloud cover, tilt, lens focal length, exposure evaluation, stereopair availability, and orbit number. GRA

N92-11562# Army Engineer Topographic Labs., Fort Belvoir, VA.

MULTISPECTRAL IMAGE MAPS FROM LANDSAT THEMATIC MAPPER DATA Technical Report, Oct. 1988 - Jun. 1989

Robert S. Rand, John E. Anderson, and Donald A. Davis Sep. 1991 23 p

(AD-A240453; ETL-0590) Avail: NTIS HC/MF A03 CSCL 08/2

This report describes a capability to produce prototype 1:50,000 scale multispectral image maps using LANDSAT Thematic Mapper (TM) data. These image maps are in the standard Universal Transverse Mercator (UTM) projection, contain imbedded 1,000 meter grid lines with labeled UTM coordinates, and can easily be used in conjunction with conventional military maps of the same scale. Annotation that gives the title of the standard DMA map of the area, the LANDSAT TM band combinations, as well as a bar scale and compass were also imbedded into the product. Author (GRA)

N92-11563# Army Engineer Topographic Labs., Fort Belvoir, VA.

A HYBRID METHODOLOGY FOR DETECTING CARTOGRAPHICALLY SIGNIFICANT FEATURES USING LANDSAT TM IMAGERY Technical Report, May - Aug. 1989

Robert S. Rand Sep. 1991 66 p

(AD-A240454; ETL-0589) Avail: NTIS HC/MF A04 CSCL 17/11

A general Change Detection (CD) methodology is investigated that involves a hybrid mix of image processing, spectral transformation, and statistical pattern recognition techniques. The Hybrid Methodology attempts to combine various forms of supporting and conflicting evidence for change into a resulting change map. The approach involves differencing registered multiband scene pairs that have undergone a spectral transformation, generating threshold masks, and applying a classifier to the masked multiband scene pairs. GRA

N92-11564# Army Engineer Topographic Labs., Fort Belvoir, VA.
THERMAL INFRARED SPECTRA OF NATURAL AND MANMADE MATERIALS: IMPLICATIONS FOR REMOTE SENSING Technical Report, Jan. 1985 - Mar. 1989
John W. Eastes Aug. 1991 256 p
(DA Proj. 4A1-61102-B-52-C)
(AD-A240455; ETL-0587) Avail: NTIS HC/MF A12 CSCL 20/5

This report is a compilation of laboratory thermal infrared reflectance spectra recorded over various spectral ranges between 4000 and 400 cm (-1) (2.5-25.0 micrometers) for natural and manmade materials of potential interest to both military and civilian sectors. Knowledge of the position and shape of significant spectral features as detected by remote spectrometers or spectral radiometers is necessary to discriminate between targets on the basis of either spectral emittance or reflectance. Many of the samples in this study display spectral features in either, or both of the 3- to 5- micrometer or the 8- to 14- micrometer regions of the spectrum in which terrestrial remote sensing is possible. Such information can be used to devise image enhancement strategies for data in hand or to design new instruments or experiments utilizing thermal multispectral data. GRA

N92-11565# Sparta, Inc., Lexington, MA.
DEVELOPMENT OF A 3-D TREE THERMAL RESPONSE MODEL FOR ENERGY BUDGET AND SCENE SIMULATION STUDIES
John R. Hummel, James R. Jones, David R. Longtin, and Nanette L. Paul 15 Mar. 1991 48 p
(Contract F19628-88-C-0038)
(AD-A240693; PL-TR-91-2108; SR-8) Avail: NTIS HC/MF A03 CSCL 20/13

Energy budget modeling of vegetated surfaces is complicated by the extreme variability that can be encountered in the species that are present. A three dimensional thermal model of trees is being developed to understand the thermal properties of trees. The model is being developed for leafed (deciduous) and leafless conditions. Primitive solid distribution within each element is then established and material properties assigned. A finite difference calculation of the energy budget is performed in which tree elements are allowed to interact with one another as well as the outside environment. This report describes the development of a three dimensional thermal response model for individual trees. The model can be used for leafed and leafless trees. The thermal balance for woody materials is determined using a 3-heat conduction model for the tree components. The thermal balance of deciduous levels is calculated using an energy balance formulation that takes into account solar and infrared radiative interactions, free or forced convection, and evapotranspiration. Results of sensitivity calculations outlining the importance of various physical processes are given as well as comparisons against field test data. GRA

N92-11566# Surface Optics Corp., San Diego, CA.
SURFACE OPTICAL PROPERTY MEASUREMENTS ON BARK AND LEAF SAMPLES
J. T. Neu, R. S. Dummer, M. Beecroft, P. McKenna, and D. C. Robertson 31 Dec. 1990 392 p
(Contract F19628-89-C-0128)
(AD-A240714; PL-TR-91-2009; SR-2) Avail: NTIS HC/MF A17 CSCL 20/6

This paper presents reflectance data for leaf and bark samples taken from a big leaf aspen tree located near Orono, Maine. Total hemispherical directional reflectance measurements were made for several angles of incidence between 20 and 80 deg. and over the 0.3 to 25.0 microns spectral region. Since the leaves are translucent, transmittance measurements were also made. Bidirectional reflectances were measured for incident angles of 20, 40, and 60 deg. at wavelengths of 1.3, 4.6, and 10.0 microns. In addition, some reflectance data from a concrete runway and adjacent grasses are presented. GRA

44 ENERGY PRODUCTION AND CONVERSION

Includes specific energy conversion systems, e.g., fuel cells; global sources of energy; geophysical conversion; and windpower.

For related information see also *07 Aircraft Propulsion and Power, 20 Spacecraft Propulsion and Power,* and *28 Propellants and Fuels.*

N92-11567# Alaska Univ., Fairbanks. Inst. of Northern Engineering.
PHOTOVOLTAIC ENERGY SYSTEM AT AN ALASKAN SITE
D. K. Das and R. W. Briggs 1991 56 p Sponsored by Alaska Dept. of Transportation and Public Facilities, Fairbanks
(PB91-201350; Rept-86.59; AK-RD-91-05) Avail: NTIS HC/MF A04 CSCL 10A

Information gathered over several years on the availability of solar energy and its utilization by a photovoltaic (PV) system that was installed near Fairbanks, Alaska (65 N latitude) to demonstrate its feasibility is provided. Both theoretical and experimental investigations on the potential of solar energy for interior Alaska are addressed. Three theoretical approaches are described for calculating solar radiation using the American Society of Heating, Refrigerating, and Air Conditioning Engineers, Liu Jordan, and Collares-Pereira and Rabl models. Computer programs for these theories are included in the appendix. The actual test setup of a PV system with all its auxiliary components installed in Haystack (near Fairbanks) and the electrical loads run by it are described in detail. Four and one-half years of solar radiation measurements and operations comparisons are made between the measured solar radiation of previous measurements done at the Geophysical Institute of the University of Alaska Fairbanks, and the calculated values from the three models cited earlier. GRA

N92-11568# Sandia National Labs., Albuquerque, NM.
TODAY'S CENTRAL RECEIVER POWER PLANT
D. J. Alpert, G. J. Kolb, and J. M. Chavez 1991 10 p Presented at the World Congress of the International Solar Energy Society, Denver, CO, 19-23 Aug. 1991
(Contract DE-AC04-76DP-00789)
(DE91-017998; SAND-91-1890C; CONF-910802-2) Avail: NTIS HC/MF A02

For 15 years, the United States Department of Energy has worked with industry, both utilities and manufacturers, to develop the technology of solar central receiver power plants. In this type of plant, sunlight is concentrated by a field of sun-tracking mirrors, called heliostats, onto a centrally located receiver. The solar energy is collected in the form of a heated fluid, which is used to generate steam to power a conventional turbine generator. For a number of reasons, molten nitrate salt is now the preferred heat transfer fluid. Commercial plants will be sized between 100 and 200 MW. The impetus for developing central receivers comes from their unique advantages: (1) they produce clean, reliable, low-cost electricity; (2) they have practical energy storage that provides a high degree of dispatchability (annually up to 60 percent) - without fossil fuels; and (3) they are environmentally benign. Development efforts around the world have brought the technology to the brink of commercialization: The technical feasibility has been proven, and cost, performance, and reliability can be confidently predicted. Plans are currently being developed for the final steps toward commercial central receiver power plants. DOE

N92-11569 Department of the Navy, Washington, DC.
GEOTHERMAL ENERGY CONVERSION SYSTEM Patent
David Goldstein, inventor (to Navy) 2 Apr. 1991 7 p Filed 18 Jun. 1990
(AD-D014979; US-Patent-5,003,779; US-Patent-Appl-SN-539942; US-Patent-Class-GU-527) Avail: US Patent and Trademark Office CSCL 10/1

A generator having a tubular gear made of shape memory alloy in sheet-form floatingly supported for rotation about an axis fixedly spaced from the rotational axis of a roller gear presented.

The tubular gear is sequentially deformed by exposure to a geothermal heat source and meshing engagement with the roller gear. Such sequential deformation of the tubular gear is controlled by a temperature differential to induce and sustain rotation of the gears in response to which the heat energy is converted into electrical energy. GRA

N92-11570# Department of Energy, Washington, DC. Office of Basic Energy Sciences.
OFFICE OF BASIC ENERGY SCIENCES Summary Report, 1991
Sep. 1991 64 p
(DE91-019006; DOE/ER-0507P) Avail: NTIS HC/MF A04

Basic research is an important investment in the future and will help the U.S. maintain and enhance its economic strength. The U.S. Department of Energy Office of Basic Energy Sciences (BES) basic research activities, carried out mainly in universities and Department of Energy (DOE) laboratories, are critical to the Nation's leadership in science, for training future scientists, and to fortify the Nation's foundations for social and economic well-being. Attainment of the national goals (energy self-sufficiency, improved health and quality of life for all, economic growth, national security) depends on both technological research achievements and the ability to exploit them rapidly. Basic research is a necessary element for technology development and economic growth. This report presents the Department of Energy's Office of Basic Energy Sciences program. The BES mission is to develop understanding and to stimulate innovative thinking needed to fortify the Department's missions. The program has two distinct interrelated parts: research and facilities operations and development. In the pursuit of forefront research results, BES designs, builds and operates certain large, complex advanced scientific facilities such as neutron sources and synchrotron radiation sources. These facilities not only provide BES with unique instruments, but these instruments are also made available to all qualified users, even those not supported by BES. Thus, the facilities actually leverage a great deal more research from the national effort. The BES program conducts basic research that will most likely help the Nation's long-term energy goals. BES implements a broad strategy for conducting basic research and contributes strongly towards national energy goals and to national goals of maintaining and enhancing scientific leadership, technological innovation, and economic strength. DOE

N92-11571# Centro Tecnico Aerospacial, San Jose dos Campos (Brazil). Inst. de Estudos Avancados.
TEGEN: A ONE DIMENSIONAL PROGRAM TO CALCULATE A THERMOELECTRIC GENERATOR
M. A. P. Rosa, P. A. Ferreira, and P. DaviddeCastroLobo 19 Jun. 1990 41 p In PORTUGUESE; ENGLISH summary
(DE91-634444; CTA-IEAv-NT-006/90) Avail: NTIS HC/MF A03

A computer program for the solution of the one-dimensional, steady-state temperature equation in the arms of a thermoelectric generator is discussed. The discretized equations obtained through a finite difference scheme are solved by Gaussian Elimination. Due to nonlinearities caused by the temperature dependence of the coefficients of such equations, an iterative procedure is used to obtain the temperature distribution in the arms. Such distributions are used in the calculation of the efficiency, electric power, load voltage and other relevant parameters for the design of a thermoelectric generator. DOE

45 ENVIRONMENT POLLUTION

Includes atmospheric, noise, thermal, and water pollution.

N92-11572*# National Aeronautics and Space Administration. Lyndon B. Johnson Space Center, Houston, TX.
FIELD TRIP GUIDEBOOK ON ENVIRONMENTAL IMPACT OF CLAYS ALONG THE UPPER TEXAS COAST
Theron D. Garcia, Douglas W. Ming, and Lisa Kay Tuck (Sterling Chemicals, Inc., Texas City, TX.) 1991 59 p Presented at the Clay Minerals Society 28th Annual Meeting, Houston, TX, 5-10 Oct. 1991 Original contains color illustrations
(NASA-TM-105097; NAS 1.15:105097) Avail: NTIS HC/MF A04; 2 functional color pages CSCL 13B

The field trip was prepared to provide an opportunity to see first hand some the environmental hazards associated with clays in the Houston, Texas area. Because of the very high clay content in area soils and underlying Beaumont Formation clay, Houston is a fitting location to host the Clay Mineral Society. Examinations were made of (1) expansive soils, (2) subsidence and surface faulting, and (3) a landfill located southeast of Houston at the Gulf Coast Waste Disposal Authority where clay is part of the liner material. Author

N92-11573# Agency for International Development, Washington, DC.
GREENHOUSE GAS EMISSIONS AND THE DEVELOPING COUNTRIES: STRATEGIC OPTIONS AND THE USAID RESPONSE
D. Jhirad and S. Padmanabhan Jul. 1990 162 p
(PB91-209882; AID-PN-ABG-833) Avail: NTIS HC/MF A08 CSCL 13B

This report responds to the Fiscal Year 1990 Foreign Assistance Appropriations Act, which requested the Agency of International Development (AID) to prepare a report that: (1) examines the potential contributions of developing countries to future global emissions of greenhouse gases under different economic growth scenarios; (2) estimates the relative contributions of those countries to global greenhouse gas emissions; and (3) identifies specific key countries that stand to contribute significantly to global greenhouse gas emissions, and in which actions to promote energy efficiency, reliance on renewable resources, and conservation of forest resources could significantly reduce emissions of greenhouse gases. Ongoing programs and new initiatives being considered by AID to promote sustained economic growth in developing countries while minimizing green house gas emissions are presented. Estimates of present and projected emissions, including emission from AID-designated key countries, are based on the work of the Intergovernmental Panel on Climate Change (IPCC). Despite the uncertainties regarding the timing, magnitude, and impacts of global climate change, the issue has dramatized the daunting problems faced by developing countries in achieving sustained economic and social development. Responding to the policy imperative of managing the global commons while accelerating development in individual countries is one of the significant challenges of our time. Author

N92-11574# Yellowstone National Park, WY.
WINTER USE PLAN: ENVIRONMENTAL ASSESSMENT
1991 127 p
(PB91-194027) Avail: NTIS HC/MF A07 CSCL 13B

A winter use plan is described and analyzed along with three alternatives for managing winter use. These four possible plans were developed from a list of alternatives that was reviewed by the public and other agencies operating in the greater Yellowstone area in the fall of 1989. Because of the general nature of the plan, some of the proposed actions will require additional site planning and environmental compliance before they are implemented. The plan is consistent with the master plans for Yellowstone and Grand Teton, the general management plan for Rockefeller Parkway, and the current management plans for the adjacent national forests. Implementation of the Winter Use Plan will occur through more detailed resource management, development, and park operations plans, which will also be coordinated with the U.S. Forest Service and other agencies in the Yellowstone area. Author

N92-11575# Colorado State Univ., Fort Collins.
GRASSLAND/ATMOSPHERE RESPONSE TO CHANGING CLIMATE: COUPLING REGIONAL AND LOCAL SCALES
M. B. Coughenour, T. Kittel, R. A. Pielkel, W. Parton, J. Eastman,

and J. Cram 30 Jul. 1991 46 p
(Contract DE-FG02-90ER-60932)
(DE91-016906; DOE/ER-60932/T1) Avail: NTIS HC/MF A03

This study is an interdisciplinary research designed to increase our understanding of the ecological impacts of changes in climate and atmospheric chemistry projected to occur over the next 50 to 100 years due to globally increasing levels of CO2 and other greenhouse gases. The project study area is the North American Central Grasslands. The objectives are (1) to develop multiscaled modeling systems linking extant state-of-the-art models from the ecological and atmospheric sciences with different spatial and temporal resolutions, and (2) to evaluate the response of grassland ecosystems to atmospheric change at regional and site scales. Responses are to be evaluated in terms of ecosystem function and potential biospheric impacts to climate. We report progress since the last progress report (July 1990), covering the last half of Year 1 and the first 7 months of Year 2. We have (1) refined the high resolution GRASS model, (2) completed parameterization of the GRASS model for three sites, (3) constructed a multi-scaled modeling user interface, (4) conducted preliminary modeling experiments to filter from fine to coarse scale models, (5) implemented a computer-based synoptic classification scheme (synoptic classification processor), a key step in the scale transition of GCM climate change scenarios, and (6) evaluated scale issues associated with linking models. We also used coarse and fine resolution ecosystem models, in a manually linked mode, to simulate ecosystem response to climate and CO2 change. DOE

N92-11576*# National Aeronautics and Space Administration, Washington, DC.
SCIENTIFIC ASSESSMENT OF STRATOSPHERIC OZONE: 1989, VOLUME 1
1989 532 p Prepared in cooperation with Department of the Environment, London (England); NOAA, Washington, DC; United Nations Environment Program, Nairobi, Kenya; and World Meteorological Organization, Geneva, Switzerland Original contains color illustrations
(NASA-TM-105116; NAS 1.15:105116; GORMP-20;
ISBN-92-807-1255-1) Avail: NTIS HC/MF A23; 5 functional color pages CSCL 13B

A review is presented of the current understanding of stratospheric ozone (SO). The focus is on four major current aspects of SO: (1) polar ozone; (2) global trends; (3) theoretical predictions; and (4) halocarbon ozone depleting materials and global warming potentials. Other ozone related topics are also discussed: (1) the trends of stratospheric temperature, stratospheric aerosols, source gases, and surface ultraviolet radiation; and (2) the oxidizing capacity of the troposphere as it pertains to the lifetimes of ozone related chemicals. There have been highly significant advances in the understanding of the impact of human activities on the Earth's protective ozone layer. There are four major findings that each heighten the concern that chlorine and bromine containing chemicals can lead to a significant depletion of SO: (1) Antarctic Ozone Hole; (2) Perturbed Arctic Chemistry; (3) Long-term Ozone Decreases; and (4) Model Limitations.
Author

N92-11577*# National Aeronautics and Space Administration, Washington, DC.
SCIENTIFIC ASSESSMENT OF STRATOSPHERIC OZONE: 1989. VOLUME 2: APPENDIX: AFEAS REPORT
1989 478 p Prepared in cooperation with Department of the Environment, London (England); NOAA, Washington, DC; United Nations Environment Program; and World Meteorological Organization, Geneva, Switzerland
(NASA-TM-105117; NAS 1.15:105117; GORMP-20) Avail: NTIS HC/MF A21 CSCL 13B

The outcome is presented of the Alternative Fluorocarbon Environmental Acceptability Study (AFEAS). AFEAS evaluated the potential effects on the environment of alternative compounds targeted to replace fully halogenated chlorofluorocarbons (CFCs). Emphasis was placed on the following topics: (1) the potential of the compounds to affect stratospheric ozone; (2) their potential to affect tropospheric ozone; (3) their potential to contribute to model calculated global warming; (4) the atmospheric degradation mechanisms of the compounds, in order to identify their products and hence; (5) the potential environmental effects of the decomposition products. The alternative compounds were hydrofluorocarbons (HFCs) with one or two carbon atoms and one or more each of fluorine and hydrogen and hydrochlorofluoro carbons (HCFCs).
Author

N92-11578# Federal Aviation Administration, Washington, DC. Office of Environment and Energy.
EDMS: MICROCOMPUTER POLLUTION MODEL FOR CIVILIAN AIRPORTS AND AIR FORCE BASES, (USER'S GUIDE)
H. M. Segal Jun. 1991 53 p Supersedes DOT/FAA/EE-88-6 Sponsored by AFESC
(AD-A240528; DOT/FAA/EE-91-3; ESL-TR-91-31;
DOT/FAA/EE-88-6) Avail: NTIS HC/MF A04 CSCL 24/1

Before starting an airfield improvement project or changing the numbers, types, or activity of aircraft at an airfield, an air quality assessment is usually required. This assessment is usually made with an emissions/dispersion model. Two emissions/dispersion models were developed in the early 1970s for use at airports and airbases. The United States Air Force (USAF) developed the Air Quality Assessment Model (AQAM) (Rote, et al., 1975), and the Federal Aviation Administration (FAA) developed the Airport Vicinity Air Pollution model (AVAP) (Wang, et al., 1973). However, these models are obsolete (they are expensive to operate, tedious to enter data into), and since they were not approved by the Environmental Protection Agency, had to be sold for each application. Both the FAA and the USAF noticed that microcomputer advances of the 1980s' could significantly improve airfield modeling. They also noticed that the FAA's and the USAF's modeling requirements were quite similar. It was therefore concluded that the FAA and the USAF should join forces to develop a single modeling system that both agencies could use. This single modeling system is called the Emissions and Dispersion Modeling System (EDMS). EDMS is a refined model designed for use on a microcomputer. It employs special table lookup and numerical integration procedures to permit a microcomputer to perform the tasks that had previously been done on a mainframe computer.
GRA

N92-11579# Resources for the Future, Inc., Washington, DC.
PROCESSES FOR IDENTIFYING REGIONAL INFLUENCES OF AND RESPONSES TO INCREASING ATMOSPHERIC CO2 AND CLIMATE CHANGE: THE MINK PROJECT
Aug. 1991 113 p
(Contract DE-AC06-76RL-01830)
(DE91-018601; DOE/RL-01830T-H6) Avail: NTIS HC/MF A06

This is the first of a series of reports of research contributing to the study Processes for Identifying Regional Influences of and Responses to Increasing Atmospheric CO2 and Climate Change, MINK (Missouri-Iowa-Nebraska-Kansas) Project. This Report is intended to provide background information on project organization and methodology. In Sections 2 and 3 the region chosen for study and the scenario of climate change applied to it are described. The remainder of the paper provides information on the current functioning of the region, its demography and macroeconomic characteristics, its major natural resource sectors, and way these sectors interlink among themselves and with other industries and the region's economic base. In the final section projections are made of the demographics and macroeconomic characteristics of the region 20 and 40 years into the future.
DOE

N92-11580# Resources for the Future, Inc., Baltimore, MD.
PROCESSES FOR IDENTIFYING REGIONAL INFLUENCES OF AND RESPONSES TO INCREASING ATMOSPHERIC CO2 AND CLIMATE CHANGE: THE MINK PROJECT
M. D. Bowes and R. A. Sedjo Aug. 1991 123 p
(Contract DE-AC06-76RL-01830)
(DE91-018604; DOE/RL-01830T-H9) Avail: NTIS HC/MF A06

This is the third of a series of reports of research contributing to the study Processes for Identifying Regional Influences of an

Responses to Increasing Atmospheric CO2 and Climate Change, The MINK Project. This report is an analysis of the possible impacts of climatic change on forest resources in the Missouri-Iowa-Nebraska-Kansas (MINK) region. It follows a uniform methodological strategy that is applied to the four resource sectors most likely to be impacted by climate change, i.e., agriculture, forestry, water resources and energy. What makes the forests of this region interesting is their great vulnerability to climate warming. With their position on the fringe of the eastern hardwood forest, bordering the grasslands of the midwest, it might be expected that these forests would be among the first to be affected by a changing climate. The state of the current forest resource are examined as well as, using simulation models, the likely sensitivity of the Missouri forests to a climate warming. The future development of forestry and forest technology in the region is considered. It is concluded that the low productivity of these forests rules out active adaptation to climate change, such as might expected in the region's agricultural sector or in the more productive forest regions of the U.S. southeast or northwest. The forest sector is most likely to begin gradual and passive decline under a climate warming. DOE

46 GEOPHYSICS

Includes aeronomy; upper and lower atmosphere studies; ionospheric and magnetospheric physics; and geomagnetism.

For space radiation see *93 Space Radiation.*

N92-11581*# ECK Research Co., Columbia, MO.
ENERGETICS DIAGNOSIS OF NUMERICAL SIMULATION OF ATMOSPHERIC BLOCKING Final Report, 2 Sep. 1987 - 1 Dec. 1990
Ernest C. Kung 1 Dec. 1990 75 p
(Contract NAS5-30128)
(NASA-CR-183503; NAS 1.26:183503) Avail: NTIS HC/MF A04 CSCL 04A

A series of systematic comprehensive diagnoses of Goddard Laboratory for Atmospheres (GLA) General Circulation Model (GCM) simulation experiments was performed in reference to predictability and energetics of the Northern Hemisphere blocking circulation. The simulation experiments were performed. The following subject areas are also covered: an analysis of simulated summer blocking episodes; energetics examination of winter blocking simulations in the Northern Hemisphere; normal mode energetic and error analysis of GLA GCM simulations with the different horizontal resolutions during a winter month; and simulations of winter blocking episodes using observed sea surface temperatures. Author

N92-11582*# National Academy of Sciences - National Research Council, Washington, DC.
REAL-TIME EARTHQUAKE MONITORING: EARLY WARNING AND RAPID RESPONSE
1991 63 p Sponsored by NASA, Washington; NSF; DOE; Geological Survey; Nuclear Regulatory Commission; Federal Emergency Management Agency; and DARPA
(NASA-CR-186701; NAS 1.26:186701) Avail: NTIS HC/MF A04 CSCL 08K

A panel was established to investigate the subject of real-time earthquake monitoring (RTEM) and suggest recommendations on the feasibility of using a real-time earthquake warning system to mitigate earthquake damage in regions of the United States. The findings of the investigation and the related recommendations are described in this report. A brief review of existing real-time seismic systems is presented with particular emphasis given to the current California seismic networks. Specific applications of a real-time monitoring system are discussed along with issues related to system deployment and technical feasibility. In addition, several non-technical considerations are addressed including cost-benefit analysis, public perceptions, safety, and liability. M.G.

N92-11583*# National Aeronautics and Space Administration. Goddard Space Flight Center, Greenbelt, MD.
ANALYSIS OF ALTIMETRY OVER THE ARAL SEA
Andrew Y. Au, Richard D. Brown (ST Systems Corp., Lanham, MD.), and Jean E. Welker Apr. 1991 32 p
(NASA-TM-100759; Rept-89B00108; NAS 1.15:100759) Avail: NTIS HC/MF A03 CSCL 08C

Satellite based altimetric data taken by GEOS-3, SEASAT, and GEOSAT over the Aral Sea are analyzed and a least squares collocation technique is used to predict the geoid undulations on a 0.25 by 0.25 degree grid and to transform these geoid undulations to free air gravity anomalies. Rapp's 180 by 180 geopotential model is taken as the empirical model. The collocation procedure is performed with a set of local residual empirical covariance functions. For comparison, Rapp's global covariance functions and Jordan's self-consistent theoretical covariance functions based on Jordan's formulation and on locally derived parameters are also used to grid geoid undulations and to predict gravity anomalies. The sensitivity of the collocation results to the choice of covariance functions is discussed. Author

N92-11584*# National Aeronautics and Space Administration. Goddard Space Flight Center, Greenbelt, MD.
LAGEOS GEODETIC ANALYSIS-SL7.1
D. E. Smith, R. Kolenkiewicz, P. J. Dunn, S. M. Klosko, J. W. Robbins, M. H. Torrence, R. G. Williamson, E. C. Pavlis, N. B. Douglas, and S. K. Fricke (RMS Technologies, Inc., Landover, MD.) Sep. 1991 248 p
(NASA-TM-104549; Rept-91B00153; NAS 1.15:104549) Avail: NTIS HC/MF A11 CSCL 08E

Laser ranging measurements to the LAGEOS satellite from 1976 through 1989 are related via geodetic and orbital theories to a variety of geodetic and geodynamic parameters. The SL7.1 analyses are explained of this data set including the estimation process for geodetic parameters such as Earth's gravitational constant (GM), those describing the Earth's elasticity properties (Love numbers), and the temporally varying geodetic parameters such as Earth's orientation (polar motion and Delta UT1) and tracking site horizontal tectonic motions. Descriptions of the reference systems, tectonic models, and adopted geodetic constants are provided; these are the framework within which the SL7.1 solution takes place. Estimates of temporal variations in non-conservative force parameters are included in these SL7.1 analyses as well as parameters describing the orbital states at monthly epochs. This information is useful in further refining models used to describe close-Earth satellite behavior. Estimates of intersite motions and individual tracking site motions computed through the network adjustment scheme are given. Tabulations of tracking site eccentricities, data summaries, estimated monthly orbital and force model parameters, polar motion, Earth rotation, and tracking station coordinate results are also provided. Author

N92-11585# Lockheed Missiles and Space Co., Palo Alto, CA.
RADIATION BELT DYNAMIC AND QUASI-STATIC MODELING BASED ON CRRES DATA
Y. T. Chiu, M. A. Rinaldi, W. E. Francis, R. M. Robinson, and R. W. Nightingale 17 Jun. 1991 57 p
(Contract DAMD17-90-Z-0054; AF Proj. 7601)
(AD-A240392; PL-TR-91-2159; SR-1) Avail: NTIS HC/MF A04 CSCL 03/2

This report summarizes achievements made in the first year of the subject contract. New results on modeling the outer magnetosphere have been derived in order to provide an interpretation of the Combined Release and Radiation Effects Satellite (CRRES) radiation belt data. New features of the outer radiation belt dynamic response to geomagnetic storms are characterized using CRRES data. Detailed analysis of a benchmark event is presented. Author (GRA)

N92-11586# Air Force Environmental Technical Applications Center, Scott AFB, IL.
GROVES MODEL ACCURACY STUDY

Matthew C. Peterson Aug. 1991 70 p
(AD-A240456; USAFETAC/PR-91/012) Avail: NTIS HC/MF A04 CSCL 04/1

The United States Air Force Environmental Technical Applications Center (USAFETAC) was tasked to review the scientific literature for studies of the Groves Neutral Density Climatology Model and compare the Groves Model with others in the 30-60 km range. The tasking included a request to investigate the merits of comparing accuracy of the Groves Model to rocketsonde data. USAFETAC analysts found the Groves Model to be state of the art for middle-atmospheric climatological models. In reviewing previous comparisons with other models and with space shuttle-derived atmospheric densities, good density vs altitude agreement was found in almost all cases. A simple technique involving comparison of the model with range reference atmospheres was found to be the most economical way to compare the Groves Model with rocketsonde data; an example of this type is provided. The Groves 85 Model is used routinely in USAFETAC's Improved Point Analysis Model (IPAM). To create this model, Dr. Gerald Vann Groves produced tabulations of atmospheric density based on data derived from satellite observations and modified by rocketsonde observations. Neutral Density as presented here refers to the monthly mean density in 10-degree latitude bands as a function of altitude. The Groves 85 Model zonal mean density tabulations are given in their entirety. GRA

N92-11587# Naval Postgraduate School, Monterey, CA.
A CALIBRATION OF THE NAVAL POSTGRADUATE SCHOOL MIDDLE ULTRAVIOLET SPECTROGRAPH AND AN ANALYSIS OF THE OII 2470 A AND OI 2972 A EMISSIONS OBTAINED FROM MID-LATITUDE ROCKET OBSERVATIONS M.S. Thesis
Carl K. Andersen Sep. 1990 118 p
(AD-A240686) Avail: NTIS HC/MF A06 CSCL 20/5

The MUSTANG instrument was calibrated using standard techniques to determine the sensitivity and wavelength calibrations and field of view. The instrument was launched aboard a NASA sounding rocket on March 30, 1990. Post-flight tests indicated that the calibration did not change as a result of the rocket experiment. Ultraviolet dayglow spectra of the Earth's ionosphere were obtained from approximately 100 km to 320 km in altitude over a wavelength range of 1800 A to 3400 A. The spectra were divided into 512 pixels of approximately 3.134 A per pixel. Analyses of the data from 2420 A to 2490 A and from 2920 A to 2972 A were conducted to obtain the intensity profiles of the OII 2470.4 A multiplet and the OI 2972.3 A line emission, respectively. The intensity profile of the OII 2470.4 A multiplet was found to have a broad peak of 1.6 kR centered at approximately 250 km. The intensity profile of the OI 2972.3 A line emission shows a general trend of decreasing intensity with altitude. The maximum intensity of 3.6 kR was found at 105 km and the minimum of 137 R at 315 km. A partial layer, with an intensity of 4.1 kR, was evident near 150 km. GRA

N92-11588# Office National d'Etudes et de Recherches Aerospatiales, Paris (France). Direction de la Physique Generale.
ACOUSTIC PROPAGATION AT LOW ALTITUDE: EFFECTS OF ATMOSPHERIC TURBULENCE (VILLEAU (FRANCE) TEST) [PROPAGATION ACOUSTIQUE A BASSE ALTITUDE: EFFETS DE LA TURBULENCE ATMOSPHERIQUE (ESSAI DE VILLEAU)]
S. Canard-Caruana Jul. 1990 57 p In FRENCH
(Contract DRET-89-001-118)
(ONERA-RT-15/3641-PY; ETN-91-90091) Avail: NTIS HC/MF A04

The refraction by wind velocity and temperature profiles and turbulent diffusion, characterized by acoustic level fluctuations, are considered. Interpretation of the results shows the importance of the emitted frequency on one hand in the meteorological gradients effect and on the other in the evaluation of divergent type fluctuations of resonant levels. ESA

47 METEOROLOGY AND CLIMATOLOGY

Includes weather forecasting and modification.

N92-11589*# Space Industries, Inc., Webster, TX.
NONSCANNING CLIMATE SENSOR STUDY Final Report, May 1987 - May 1989
James W. Hoffman and Ronald C. Grush Jul. 1989 66 p
(Contract NAS5-30090)
(NASA-CR-183506; NAS 1.26:183506; SI89-R07JWH001) Avail: NTIS HC/MF A04 CSCL 04B

The Nonscanning Climate Sensor represents a new instrument for climate research and global monitoring of the earth radiation budget. It contains a mosaic of array of detectors which measures the outgoing radiation of the earth in all directions without the need for mechanical scanning. The goal is to eliminate all moving parts and obtain highly calibrated measurements for up to one solar cycle (11 years) without being susceptible to mechanical failure. Over set intervals of time, the angular measurements are integrated up to produce total reflected and emitted flux values from each target area on the Earth. To achieve the require sensitivity while maintaining a flat spectral response, an improved dual cavity detector with digital control loop was developed. The detector is self calibrating to maintain high precision over the life of the instrument. Prototype detectors and a complete set of electronics with a microprocessor controller were fabricated and tested. Measurements show that the new detectors are more than an order of magnitude more sensitive than previous versions. Author

N92-11590*# Research Inst. for Advanced Computer Science, Moffett Field, CA.
WEATHER PREDICTION USING A GENETIC MEMORY
David Rogers Feb. 1990 18 p
(Contracts NCC2-408; NCC2-387)
(NASA-CR-185448; NAS 1.26:185448; RIACS-TR-90-6) Avail: NTIS HC/MF A03 CSCL 04B

Kanaerva's sparse distributed memory (SDM) is an associative memory model based on the mathematical properties of high dimensional binary address spaces. Holland's genetic algorithms are a search technique for high dimensional spaces inspired by evolutional processes of DNA. Genetic Memory is a hybrid of the above two systems, in which the memory uses a genetic algorithm to dynamically reconfigure its physical storage locations to reflect correlations between the stored addresses and data. This architecture is designed to maximize the ability of the system to scale-up to handle real world problems. Author

N92-11591# National Oceanographic Data Center, Washington, DC.
MARINERS WEATHER LOG, VOLUME 35, NUMBER 1, WINTER 1991 Quarterly Report
R. M. DeAngelis 1991 87 p
(PB91-201129) Avail: NTIS HC/MF A05 CSCL 04B

The following features are presented: (1) we fought Cape Horn ... and the Horn Won-- a first hand account of a dramatic attempt to break the 136-year old record set by the Northern Light from San Francisco to Boston via Cape Horn; (2) the second part of the Admiral Beaufort story that involves the evolution of the original scale through the ages; and (3) view from another bridge-- a frightening account of sailing the lower Mississippi River and the Gulf of Mexico, while battling the weather and commercial vessels. GRA

N92-11592# National Oceanographic Data Center, Washington, DC.
MARINERS WEATHER LOG, VOLUME 35, NUMBER 2, SPRING 1991 Quarterly Report
R. M. DeAngelis 1991 104 p
(PB91-202572) Avail: NTIS HC/MF A06 CSCL 04B

The following topics are covered: (1) the Bonner Bridge storm-- the story of the Oct. 1990 storm that caused the problems for residents and visitors on North Carolina's Outer Banks; (2) Soviet-American Sail, 1990-- an historic joint training cruise aboard

a Soviet Tall ship; (3) North Atlantic Hurricanes, 1990-- a year that was active but spared the U.S.; and (4) Eastern North Pacific Hurricanes, 1990-- a year that featured two of the strongest hurricanes ever in this basin. GRA

N92-11593*# Federal Aviation Administration, Washington, DC.
PILOT'S AUTOMATED WEATHER SUPPORT SYSTEM (PAWSS) CONCEPTS DEMONSTRATION PROJECT. PHASE 1: PILOT'S WEATHER INFORMATION REQUIREMENTS AND IMPLICATIONS FOR WEATHER DATA SYSTEMS DESIGN Interim Report, Dec. 1990 - Apr. 1991
Norman L. Crabill and Ernie R. Dash Apr. 1991 19 p Sponsored in part by Diversified International Sciences Corp., Lanham, MD, and by Vigyan Research Associates, Inc., Hampton, VA
(Contracts NAS1-18585; DTFA01-90-4-01019)
(NASA-CR-188228; NAS 1.26:188228; DOT/FAA/RD-91/9)
Avail: NTIS HC/MF A03 CSCL 04B

The weather information requirements for pilots and the deficiencies of the current aviation weather support system in meeting these requirements are defined. As the amount of data available to pilots increases significantly in the near future, expert system technology will be needed to assist pilots in assimilating that information. Some other desirable characteristics of an automation-assisted system for weather data acquisition, dissemination, and assimilation are also described. Author

N92-11594# Air Force Environmental Technical Applications Center, Scott AFB, IL.
A METHOD FOR ESTIMATING MISSING HOURLY TEMPERATURES USING DAILY MAXIMUM AND MINIMUM TEMPERATURES
William R. Schaub, Jr. Aug. 1991 21 p
(AD-A240394; USAFETAC/PR-91/017) Avail: NTIS HC/MF A03 CSCL 04/2

USAFETAC's Engineering Meteorology Section (USAFETAC/ECE) asked USAFETAC/DNO to develop a method for estimating missing hourly temperatures for locations that report only maximum and minimum temperatures, such as those in the NOAA Climatological Data (CD). USAFETAC/ECE required such a temperature estimation technique before they could calculate cooling degree hours (CDH) for stations at which only maximum and minimum temperatures were reported. This study is an extension of work documented by USAFETAC/PR-90/006, Short-Term Hourly Temperature Interpolation, by Maj. Walter F. Miller, December 1990. In his study, Miller described a method for interpolating hourly temperatures when less than 6 consecutive hours of data were missing. Input temperature data, the same for both studies, was taken from stations in different climates to test the temperature filling methods adequately. GRA

N92-11595# Air Force Environmental Technical Applications Center, Scott AFB, IL.
MARCH AFB FORECASTING RULES OF THUMB EVALUATION
Brian M. Bjornson Jul. 1991 20 p
(AD-A240458; USAFETAC/PR-91/013) Avail: NTIS HC/MF A03 CSCL 04/2

This report documents an evaluation of 23 different rules of thumb used in weather forecasting at March AFB, CA. Surface and upper-air data were collected for selected cities in Southern California and Nevada. Pressure differences, dew-point temperature, and 850-mb and 500-mb heights were calculated for the selected locations and used to predict ceiling and/or visibility, wind direction, or rain/drizzle events at March AFB. Predictor and predictand variables were identified. The procedure for determining the probability of the predictand, given the predictor, is described, and the accuracy and statistical significance of the results are tested statistically. Frequency distribution tables for each of the 23 rules-of-thumb are given in an appendix. GRA

N92-11596# Air Force Environmental Technical Applications Center, Scott AFB, IL.
SHORT-TERM HOURLY TEMPERATURE INTERPOLATION
Walter F. Miller Dec. 1990 17 p
(AD-A240489; USAFETAC/PR-90/006) Avail: NTIS HC/MF A03 CSCL 04/2

This report describes the development of a computer method for interpolating missing hourly temperatures in weather observing records. Although a long term interpolation method is under consideration, this report deals with replacing missing temperatures over periods of less than 6 consecutive hours. GRA

N92-11597# Atmospheric and Environmental Research, Inc., Cambridge, MA.
MESOSCALE PREDICTION AND SATELLITE CLOUD ANALYSIS FOR ADVANCED METEOROLOGICAL PROCESSING SYSTEMS Final Report, Apr. 1988 - Dec. 1990
Gary B. Gustafson, Jean-Luc Moncet, Charles F. Ivaldi, Ho-Chun Huang, and Jeanne M. Sparrow 8 Jan. 1991 143 p
(Contract F19628-88-C-0086)
(AD-A240510; PL-TR-91-2008) Avail: NTIS HC/MF A07 CSCL 04/2

Three topics are addressed: mesoscale prediction modeling, improvements and modifications to the Air Force real time nephanalysis program, and on-site support for maintenance and enhancements to the Air Force Interactive Meteorological Processing System (AIMS). Mesoscale model work centered on the GL/LYP prediction model. An investigation of the model revealed several problems and inconsistencies when attempting to reproduce the Aster results. Numerous procedural changes were made to the model program to facilitate operation and interpretation of model results. Nephanalysis work was in a number of areas including: satellite data ingest and data base management, remapping of satellite data, and development of an atmospheric transmission band model to characterize infrared water vapor attenuation. Band model results were inconclusive due to model sensitivity to input data field quality, particularly surface temperature and vertical moisture profiles. AIMS support consisted of system management, technical support, and software development over a time of explosive system growth. During the period of the contract, 11 processing nodes were added to the cluster in addition to numerous peripheral devices and software upgrades. GRA

N92-11598# Air Force Environmental Technical Applications Center, Scott AFB, IL.
PERSIAN GULF CONTRAIL ALTITUDE LIMITS
Gregory J. Reding Jun. 1991 51 p
(AD-A240702; USAFETAC/PR-91/009) Avail: NTIS HC/MF A04 CSCL 04/2

The development of a computer program (DNCONTRL) that determines the mean and extreme upper and lower limits for conditions that favor condensation trail formation over a given upper-air reporting station is described. Output of the DNCONTRL program is provided in tabular form for 19 stations in the Persian Gulf region, not only as upper and lower altitudes for the formation of contrails, but as monthly percent occurrence frequency (POF) for favorable contrail formation at specified altitudes. These results were compared with an earlier, similar, study for the entire northern hemisphere and found to be consistent. GRA

N92-11599# Army Engineer Topographic Labs., Fort Belvoir, VA.
HOURLY AND DAILY PRECIPITATION FREQUENCIES FOR THE UNITED STATES Technical Report, Nov. 1986 - Nov. 1987
Ruth L. Wexler Aug. 1991 60 p
(AD-A240746; ETL-0498) Avail: NTIS HC/MF A04 CSCL 04/2

This report presents daily and hourly precipitation frequencies for an extensive network of stations throughout the United States, from special summaries of observations obtained over the decade 1951-1960. When data are in format of cumulative percent frequency per precipitation rate, the daily and hourly distributions each form a fairly regular progression, per P/D or P/H, respectively (P equals total precipitation, D equals days, H equals hours). The resultant models, in the form of succinct tables, graphs, or computer

programs, provide a ready means for recovering the original observations, or estimating any selected precipitation rate for a wide spectrum of precipitation regimes in the United States, or elsewhere. The models, which serve as a check on data errors, or weather modification, also indicate to the engineer preferred areas testing particular equipment. The methodology for the comparison among stations (or countries) of the actual short-term precipitation distributions, given only routine climatic data, should be highly useful for assessing more accurately a host of factors, as: soil moisture, trafficability, water supply, crop yields, or possible malfunction of electronic equipment. The greatest advantage of the result is that they may be utilized for estimating short-term precipitation in data sparse localities. GRA

N92-11600*# National Aeronautics and Space Administration. Goddard Space Flight Center, Greenbelt, MD.
OPTICALLY THIN CIRRUS CLOUDS OVER OCEANS AND POSSIBLE IMPACT ON SEA SURFACE TEMPERATURE OF WARM POOL IN WESTERN PACIFIC
C. Prabhakara, J.-M. Yoo, G. Dalu, and P. Kratz (Universities Space Research Association, Columbia, MD.) Washington Nov. 1991 40 p
(NASA-TM-104550; NAS 1.15:104550; Rept-92B00006) Avail: NTIS HC/MF A03 CSCL 04B

Over the convectively active tropical ocean regions, the measurement made from space in the IR and visible spectrum have revealed the presence of optically thin cirrus clouds, which are quite transparent in the visible and nearly opaque in the IR. The Nimbus-4 IR Interferometer Spectrometer (IRIS), which has a field of view (FOV) of approximately 100 km, was utilized to examine the IR optical characteristics of these cirrus clouds. From the IRIS data, it was observed that these optically thin cirrus clouds prevail extensively over the warm pool region of the equatorial western Pacific, surrounding Indonesia. It is found that the seasonal cloud cover caused by these thin cirrus clouds exceeds 50 percent near the central regions of the warm pool. For most of these clouds, the optical thickness in the IR is less than or = 2. It is deduced that the dense cold anvil clouds associated with deep convection spread extensively and are responsible for the formation of the thin cirrus clouds. This is supported by the observation that the coverage of the dense anvil clouds is an order of magnitude less than that of the thin cirrus clouds. From these observations, together with a simple radiative-convective model, it is inferred that the optically thin cirrus can provide a greenhouse effect, which can be a significant factor in maintaining the warm pool. In the absence of fluid transports, it is found that these cirrus clouds could lead to a runaway greenhouse effect. The presence of fluid transport processes, however, act to moderate this effect. Thus, if a modest 20 W/sq m energy input is considered to be available to warm the ocean, then it is found that the ocean mixed-layer of a 50-m depth will be heated by approximately 1 C in 100 days. Author

N92-11601# Pacific Northwest Lab., Richland, WA.
AN ASSESSMENT OF THE AVAILABLE WINDY LAND AREA AND WIND ENERGY POTENTIAL IN THE CONTIGUOUS UNITED STATES
D. L. Elliott, L. L. Wendell, and G. L. Gower Aug. 1991 92 p
(Contract DE-AC06-76RL-01830)
(DE91-018887; PNL-7789) Avail: NTIS HC/MF A05

Estimates of land areas with various levels of wind energy resource and resultant wind energy potential have been developed for each state in the contiguous United States. The estimates are based on published wind resource data and account for the exclusion of some windy lands as a result of environmental and land-use considerations. Despite these exclusions, the amount of wind resource estimated over the contiguous United States is surprisingly large and has the potential to supply a substantial fraction of the nation's energy needs, even with the use of today's wind turbine technology. Although this study shows that, after exclusions, only about 0.6 percent of the land area in the contiguous United States is characterized by high wind resource (comparable to that found in windy areas of California where wind energy is being cost-effectively developed), the wind electric potential that could be extracted with today's technology from these areas across the United States is equivalent to about 20 percent of the current U.S. electric consumption. Future advances in wind turbine technology will further enhance the potential of wind energy. As advances in turbine technology allow areas of moderate wind resource to be developed, more than a tenfold increase in the wind energy potential is possible. These areas, which cover large sections of the Great Plains and are widely distributed throughout many other sections of the country, have the potential of producing more than three times the nation's current electric consumption. DOE

48 OCEANOGRAPHY

Includes biological, dynamic, and physical oceanography; and marine resources.

For related information see also *43 Earth Resources and Remote Sensing.*

N92-11602# Joint Oceanographic Inst., Inc., Washington, DC.
THEORY AND MODELING IN GLOBEC: A FIRST STEP
E. Hofmann, T. Osborn, T. Powell, J. Price, B. Rothschild, and J. Roughgarden Feb. 1991 14 p
Avail: NTIS HC/MF A03

Evidence continues to accumulate that the environment of Earth is changing. The changes involve physical, geological, chemical, and biological processes. A great challenge is to assess the direction and magnitude of the response of the planet's environment to these changes. GLOBEC (GLOBal ocean ECosystems dynamics) is an initiative proposed by the oceanographic and fisheries communities to determine the impact of the changes in our global environment on the populations and communities of marine animals. The GLOBEC approach is to develop fundamental information about the basic mechanisms that determine the abundance and distribution of marine animal populations and, most importantly, the variability of these populations about their average values. Through understanding of these fundamental mechanisms reliable predictions of population changes in the face of a shifting global environment can be obtained. The GLOBEC program is detailed. Author

N92-11603*# National Aeronautics and Space Administration, Washington, DC.
GLOBEC: GLOBAL OCEAN ECOSYSTEMS DYNAMICS: A COMPONENT OF THE US GLOBAL CHANGE RESEARCH PROGRAM Initial Science Plan Report No. 1
Feb. 1991 91 p Prepared in cooperation with Joint Oceanographic Inst., Inc., Washington, DC
(NASA-TM-105121; NAS 1.15:105121) Avail: NTIS HC/MF A05 CSCL 08C

GLOBEC (GLOBal ocean ECosystems dynamics) is a research initiative proposed by the oceanographic and fisheries communities to address the question of how changes in global environment are expected to affect the abundance and production of animals in the sea. The approach to this problem is to develop a fundamental understanding of the mechanisms that determine both the abundance of key marine animal populations and their variances in space and time. The assumption is that the physical environment is a major contributor to patterns of abundance and production of marine animals, in large part because the planktonic life stages typical of most marine animals are intrinsically at the mercy of the fluid motions of the medium in which they live. Consequently, the authors reason that a logical approach to predicting the potential impact of a globally changing environment is to understand how the physical environment, both directly and indirectly, contributes to animal abundance and its variability in marine ecosystems. The plans for this coordinated study of of the potential impact of global change on ocean ecosystems dynamics are discussed. Author

N92-11604# Scripps Institution of Oceanography, La Jolla, CA. Marine Research Div.
STUDIES OF THE PHYSICAL AND CHEMICAL STABILITY OF NATURAL SEA-SURFACE FILMS
Peter M. Williams 30 Nov. 1990 3 p
(Contract N00014-87-K-0144)
(AD-A239818) Avail: NTIS HC/MF A01 CSCL 08/3

The major effort was to measure the total dissolved organic content of surface films and the corresponding subsurface waters by high temperature combustion; the ancillary efforts were: to measure the size, diffusive properties and density of colloids and small particulates in seawater; and secondly, to measure the carbon 14 and carbon 13 signatures of marine surface films. Measurements of the dissolved organic carbon (DOC) and nitrogen (DON) have been made on approx. 100 samples of sea surface films and their corresponding 5 to 15 cm subsurface waters. Carbon isotope (C-14, C-13) measurements of DOC were made on surface films and 5 to 15 cm subsurface waters collected off Southern California and southeast of Bermuda, while C-13 and delta N-15 measurements of suspended organic matter were made for samples collected on shore-to-open-ocean transects off the coast of Maine. Using photon correlation spectroscopy (changes in the Doppler shift in frequency of scattered laser light), rapid aggregation of colloidal particles into larger particulates, especially in un-preserved sample has been observed. GRA

N92-11605# Skidaway Inst. of Oceanography, Savannah, GA.
ORGANIC GEOCHEMISTRY OF SEAWATER PARTICULATE MATTER: FINAL DATA ANALYSIS INTERPRETATION Report, 15 Feb. 1990 - 14 Aug. 1991
Stuart G. Wakeham 14 Aug. 1991 7 p
(Contract N00014-90-J-1785)
(AD-A240199) Avail: NTIS HC/MF A02 CSCL 08/3

The purpose of this brief grant was to complete the data analysis and preparation of manuscripts resulting from prior ONR-supported research on the organic geochemistry of particulate matter and surface sediments in the Black Sea. That cruise resulted in a unique set of particle and sediment samples, especially in the region of the oxic-anoxic interface. Analysis of lipid biomarkers in these samples has proven invaluable in interpreting the sources and alteration processes which determine the composition of particulate organic matter in the Black Sea. Of particular interest is the in-growth of bacterial biomarkers at the top of the anoxic zone as particles transit the chemocline. GRA

N92-11606# Naval Research Lab., Washington, DC.
A SURVEY OF SCATTERING, ATTENUATION, AND SIZE SPECTRA STUDIES OF BUBBLE LAYERS AND PLUMES BENEATH THE AIR-SEA INTERFACE Memorandum Report
Edward Powell 30 Aug. 1991 68 p
(AD-A240262; NRL-MR-6823) Avail: NTIS HC/MF A04 CSCL 20/1

Previous and ongoing research relating to acoustic scattering and attenuation by sub-surface oceanic bubble layers and clouds is surveyed within the context of sea surface scattering and the parameters relevant to numerical modeling. Bubble concentration and size spectra measurements are addressed, as are theoretical and numerical studies of bubble cloud (plume) generation processes and scattering mechanisms. Related studies of oceanic processes such as Langmuir circulation, wavebreak plume injection, and the biological bubble component are discussed. Conclusions are drawn regarding the current understanding of phenomena and the availability of sufficient data. GRA

N92-11607# Coastal Engineering Research Center, Vicksburg, MS.
INDEX AND BULK PARAMETERS FOR FREQUENCY-DIRECTION SPECTRA MEASURED AT CERC FIELD RESEARCH FACILITY Final Report, Sep. 1987 - Aug. 1988
Charles E. Long Aug. 1991 70 p
(AD-A240320; CERC-MP-91-7) Avail: NTIS HC/MF A04 CSCL 13/2

The directional distribution of wind-wave energy is an intuitively and demonstrably important aspect of sea state definition in coastal engineering design. A multiyear series of measurements has been undertaken. Cross spectra of surface corrected signals from a linear array of nine bottom mounted pressure sensors have been used in conjunction with an iterative maximum likelihood algorithm to estimate frequency direction spectra. The array was located in about 8 m of water, approximately 900 m offshore. This report provides an index of and describes a means of access to 636 frequency direction spectral observations obtained nominally from September 1987 to August 1988. This period represents the second year of data collection. Actual data are reported only until early January 1988. Damage to the array by fishing trawlers precluded successfully data collection for the remainder of this collection year. In addition to a list of data collection start times are a set of bulk parameters that can be used to characterize the observations. These parameters include characteristic wave height, spectral peak frequency and corresponding peak period, peak wave direction, and directional spread. Time series graphs of these parameters as well as local winds and currents illustrate some of the salient climatology. Observed spectra have been archived on magnetic tape and can be provided to a user on request. This report describes the structure, format, and naming scheme of the data files and lists a FORTRAN program that can be used to read them. GRA

N92-11608# Coastal Engineering Research Center, Vicksburg, MS.
USE OF THEORETICAL WAVE HEIGHT DISTRIBUTIONS IN DIRECTIONAL SEAS Final Report
Charles E. Long Aug. 1991 107 p
(AD-A240411; CERC-TR-91-6) Avail: NTIS HC/MF A06 CSCL 08/3

Knowledge of total water levels, of which the heights of wind waves are an important part, is critical to the successful design of coastal shore protection projects. This report makes a preliminary examination of the behavior of two wave height distribution models using a small but diverse set of test data. Data are derived from a Waverider buoy deployed near the 8-m-depth contour about 1 km offshore of the Coastal Energy Resource Center's (CERC) Field Research Facility near Duck, NC. Data are classified by directional characteristics derived from a high-resolution, linear array, directional wave gage also located near the 8-m contour and just north of the Waverider buoy. The two models are the Rayleigh probability function and the Beta-Rayleigh probability function, introduced to address the problem of wave heights in shallow water. The Beta-Rayleigh model was used in three forms: a deepwater asymptotic form, the formally derived form, and a finite-depth form in which the governing parameters are estimated from the spectrally based characteristic wave height and peak period. Models were tested under the constraints that they be computed exactly as published and with no allowance to adjust parameters to reduce differences with observations. In spite of the stringent requirements of the tests, all models performed remarkably well. GRA

N92-11609# Naval Postgraduate School, Monterey, CA.
A DIAGNOSTIC STUDY OF THE VELOCITY STRUCTURE OF A MEANDERING JET USING A PRIMITIVE EQUATION MODEL WITH DYNAMIC MODE INITIALIZATION M.S. Thesis
Roland E. DeJesus Sep. 1990 77 p
(AD-A240687) Avail: NTIS HC/MF A05 CSCL 08/3

A high resolution, 20-level, primitive equation (PE) model of the California coastal region is initialized using temperature data acquired during the first California Transition Zone (CTZ) cruise from 6 to 12 July 1988 for the purpose of diagnosing the three-dimensional dynamically balanced flow field for the region. The major feature in the region during the cruise period was a strong meandering jet which flowed equatorward and offshore, oriented in a northeast to southwest direction. The quality of data acquired during cruise CTZR1 is sufficiently high to enable diagnosis of the horizontal (baroclinic) and vertical velocity field using the numerical model. The measured (ADCP) currents showed more

details of the flow at deeper depths than the model, which showed a broader baroclinic flow at depth and a level of no motion near 300 m. The maximum surface velocities from model and ADCP cross-sections agreed to within 10 cm/sec except for leg G, in which ADCP velocity was greater than the model velocity by about 30 cm/sec. The sign of vertical velocity agrees very well with independent estimates made from bio-optical data; however, the magnitude calculated by the model is 30 to 60 times larger than that estimated from the bio-optical observations. GRA

51 LIFE SCIENCES (GENERAL)

N92-11610# Joint Publications Research Service, Arlington, VA.
JPRS REPORT: SCIENCE AND TECHNOLOGY. USSR: LIFE SCIENCES
28 Jun. 1991 29 p
(JPRS-ULS-91-015) Avail: NTIS HC/MF A03

Translations are presented of articles from various Russian periodicals. The presentation is divided into the following general categories: agricultural science; biotechnology; epidemiology; genetics; medicine; microbiology; physiology; public health; radiation biology; and virology. Some representative titles might be: Plasticity and Resistance of Barley to Root Rot; Biosynthetic Activity of Wood Destroying Basidiomycetes in Submerged Culture; Drug Resistance and Plasmid Profiles of DNA of Shigella dysenteriae 1 in the USSR and Abroad; Creation of an Integrative Expression Vector and its Use for Introduction of the Recombinant Human Alpha Interferon Gene into Plants; Current Burns Management in Disaster Medicine; Mechanism of Resistance of Methicillin Resistant Staphylococcus aureus to Phages of the International Collection; Visual Perception Training and Changes in Autonomic and Psychophysiological Indicators; Epidemiology of Cerebrovascular Disease in USSR; and Pharmacokinetics of Inhaled Pu-238 Tributyl Phosphate Complex. E.R.

N92-11611# Joint Publications Research Service, Arlington, VA.
JPRS REPORT: SCIENCE AND TECHNOLOGY. USSR: LIFE SCIENCES
3 Jun. 1991 48 p
(JPRS-ULS-91-012) Avail: NTIS HC/MF A03

Translations of articles from various Russian publications are presented in the Life Sciences category. The presentation is divided into the following general topic areas: microbiology; military medicine; molecular biology; pharmacology, toxicology; physiology; and public health. Some representative titles might be: Study of Induction of Tumor Necrosis Factor and Inteleukin-1 with use of Glycopolymers Isolated from Pseudomonas solanacearum and Clavibacter michiganense; Lab Assessment of Quality and Standardization of New Plasma Replacing Protein Saline Solution 'Protesalin' for Shock Therapy; Directed Reconstruction of Influenza Virus Hemagglutinin Gene; Effect of Delta-9 Tetrahydro cannabinol on Receptor and Physicochemical Properties of Rat Cerebral Membranes; Effect of Enkephalins on Associative Processes in Parietal Cortex Neurons; and Work of Belorussian Radiation Medicine Institute Described. E.R.

N92-11612# Illinois Univ., Urbana. Dept. of Chemistry.
BIOCHEMICAL AND BIOPHYSICAL STUDIES OF THE E. COLI RESPIRATORY CHAIN
R. B. Gennis 1991 20 p
(Contract DE-FG02-87ER-13716)
(DE91-016966; DOE/ER-13716/2) Avail: NTIS HC/MF A03

Escherichia coli contains two distinct ubiquinol oxidases but no cytochrome c-dependent branch of its aerobic respiratory chain. The cytochrome d complex has a very high affinity for molecular oxygen and is the predominant oxidase when the cells are grown with limited oxygen. The cytochrome o complex is the predominant oxidase present when E. coli is grown at high aeration. This grant is directed towards characterizing the cytochrome o complex. Substantial progress has been made during the past five years. The single most important results of our work is the demonstration that the E. coli cytochrome o complex is closely related structurally to the family of mitochondrial and bacterial aa(sub 3)-type cytochrome c oxidases. This has revealed the existence of a superfamily of proton-pumping respiratory oxidases that share common structural and mechanistic features, but vary with respect to substrate (cytochrome c vs quinol) and/or heme components (a-type vs protoheme). DOE

N92-11613# Yale Univ., New Haven, CT. Dept. of Psychology.
LONG TERM SYNAPTIC PLASTICITY AND LEARNING IN NEURONAL NETWORKS Final Annual Report, 1 Oct. 1988 - 30 Sep. 1991
Thomas H. Brown 5 Aug. 1991 12 p
(Grant AF-AFOSR-0047-89; AF Proj. 2312)
(AD-A240366; AFOSR-91-0727TR) Avail: NTIS HC/MF A03
CSCL 05/2

The purpose of this project was to understand a form of synaptic plasticity, called long-term potentiation (LTP), that appears to be a good candidate mechanism for rapid learning in mammals. LTP is a persistent form of synaptic enhancement that can be rapidly induced by brief periods of stimulation. As this project evolved, I focused on four aims: (1) methods for studying mechanisms underlying LTP expression in the hippocampus; (2) using these methods to elucidate the mechanisms; (3) developing a suitable system for evaluating the role of LTP in learning; (4) developing and applying methods of computational neuroscience to create a learning theory that is grounded in principles of cellular neurophysiology. GRA

N92-11614# Murcia Univ. (Spain).
THE 4TH INTERNATIONAL WORKSHOP ON MEMBRANE BIOTECHNOLOGY AND MEMBRANE DIOMATERIALS
2 Jun. 1991 79 p Workshop held in LaManga, Murcia, Spain, 29 May - 2 Jun. 1991
(Contract DAJA45-90-M-0034)
(AD-A240481; R/D-6606-BC-02) Avail: NTIS HC/MF A05
CSCL 06/5

This talk describes recent basic studies of polypeptides and proteins using Fourier Transfer Infrared (FTIR) spectroscopic techniques. Signal polypeptides, water soluble and membrane proteins were studied. The qualitative and quantitative information which can be deduced concerning secondary structure will be shown. The possibility of distinguishing a normal alpha-helical structure from a helical structure by this technique will be indicated. Recent technological studies of blood coagulation behaviour in the presence of various lipid polar surfaces, including negative charges, positive charges and Zwitter-ion charges will be described. GRA

N92-11615# Los Alamos National Lab., NM.
BIOLOGICAL EFFECTS OF MINERALS
G. D. Guthrie, Jr. Sep. 1991 46 p
(Contract W-7405-eng-36)
(DE91-018183; LA-12184-MS) Avail: NTIS HC/MF A03

In general, clay materials exhibit a range of biological activities, from apparently inactive or slightly active, such as hematite, to highly fibrogenic and carcinogenic, such as fibrous brucite (nemalite). The zeolites also exhibit such as range, with some mordenite being slightly active and erionite being highly active; however, erionite is the only zeolite that has been studied extensively. The diversity of mineral species holds great potential for probing these mechanisms, especially when mineralogical data are integrated with biological data. Unfortunately, many of the studies reporting data on the biological effects of clays and zeolites fail to report detailed mineralogical information; hence, it is difficult at present to interpret the biological activities of minerals in terms of their physical and chemical properties. Important mineralogical data that are only rarely considered in biological research include exact mineralogy of the specimen (i.e., identification and abundance of contaminants), physical and chemical properties of minerals, and surface properties of minerals. DOE

52 AEROSPACE MEDICINE

Includes physiological factors; biological effects of radiation; and effects of weightlessness on man and animals.

N92-11616# Joint Publications Research Service, Arlington, VA.
JPRS REPORT: SCIENCE AND TECHNOLOGY. USSR: LIFE SCIENCES Abstracts Only
7 Oct. 1991 65 p Transl. into ENGLISH from various Russian articles
(JPRS-ULS-91-017) Avail: NTIS HC/MF A04

Translations from various Russian publications are presented. The areas of general interest are as follows: aerospace medicine; biophysics; biotechnology; epidemiology; immunology; microbiology; physiology; public health; radiation biology; and virology. Some titles of interest are listed as follows: Effects of Prolonged Space Flight on Erythrocyte Metabolism and Membrane Functional Condition; Efficacy of Hyperbaric Oxygenation in Enhancing Flight Tolerance; Toxicity Assessment of Combustion Products in Simulated Space Cabins; and Technical Requirements of Sick Bays Aboard Space Ships. For individual titles, see N92-11617 through N92-11620.

N92-11617# Joint Publications Research Service, Arlington, VA.
EFFECT OF PROLONGED SPACE FLIGHT ON ERYTHROCYTE METABOLISM AND MEMBRANE FUNCTIONAL CONDITION Abstract Only
S. M. Ivanova, S. S. Brantova, O. I. Labetskaya, G. S. Arzamazov, N. V. Delenyan, and T. I. Turkina *In its* JPRS Report: Science and Technology. USSR: Life Sciences 7 Oct. 1991 p 1 Transl. into ENGLISH from Kosmicheskaya Biologiya i Aviakosmicheskaya Meditsina (Moscow, USSR), v. 24, no. 6, Nov. - Dec. 1990 p 18-23 (For primary document see N92-11616 02-52)
Avail: NTIS HC/MF A04

Erythrocyte metabolism was assessed in two cosmonauts following 326 day (cosmo 1) and 160 day (cosmo 2) space flights. Studies on day 1 after landing revealed marked depression of erythrocyte glycolysis and reduced ATP levels in both cosmonauts. On day 9, glycolysis and ATP had returned to baseline levels in cosmo 2, but continued to decline in cosmo 1. Changes in erythrocyte membranes included a significant increase in free cholesterol and cholesterol esters on day 9, while phospholipids were reduced. Furthermore, phosphatidyl ethanolamine showed a significant reduction and an increase in lysophosphatydyl choline in cosmo 1, while cardiolipin was elevated in both cosmos. Further metabolism alterations included a reduction of membrane Na(+), K(+) -ATPase and an increase in Ca(2+), Mg(2+)-ATPase activities. In addition, in the immediate post-flight period the erythrocytes displayed enhanced resistance to acid hemolysis. These observations showed that space flight conditions have a profound effect on the metabolic and physiological status of erythrocytes, resulting in reduced deformability. Accordingly, appropriate measures should be used in-flight and post-flight to insure normal erythrocyte function. Author

N92-11618# Joint Publications Research Service, Arlington, VA.
EFFICACY OF HYPERBARIC OXYGENATION IN ENHANCING FLIGHT TOLERANCE Abstract Only
I. N. Chernyakov, A. A. Shishov, O. A. Vorobyev, V. I. Nekrasov, N. F. Popov, S. M. Razinkin, and A. V. Semenov *In its* JPRS Report: Science and Technology. USSR: Life Sciences 7 Oct. 1991 p 1 Transl. into ENGLISH from Kosmicheskaya Biologiya i Aviakosmicheskaya Meditsina (Moscow, USSR), v. 24, no. 6, Nov. - Dec. 1990 p 21-23 (For primary document see N92-11616 02-52)
Avail: NTIS HC/MF A04

Thirty men, 19 to 48 years old, were used in an assessment of the efficacy of hyperbaric oxygenation (HO; 1 to 10 1 hr sessions at $pO2 = 2$ atm over 10 to 12 days) in enhancing flight tolerance. Assessment of mental and physical performance demonstrated that poor altitude tolerance was improved to the extent that the maximum altitude could be increased by 1 km and reserve time at 5 to 7 km by 3 to 4 min. These improvements persisted for 2 to 3 months. In addition, subjects with average performance on statokinetic tests showed a 2 to 2.5 fold improvement following a course of HO. Finally, fatigue due to repetitive work under adverse conditions (22 to 49 C, 92 to 95 dB noise) was alleviated by HO, in comparison with conventional 2 hr rest periods, to the degree that 15 to 20 pct. more work could be accomplished prior to the onset of intolerable fatigue. On balance, the data demonstrated that HO promotes more efficient recovery from flight related fatigue than seen with simple periods of rest and enhances high altitude tolerance. Author

N92-11619# Joint Publications Research Service, Arlington, VA.
TOXICITY ASSESSMENT OF COMBUSTION PRODUCTS IN SIMULATED SPACE CABINS Abstract Only
V. F. Ushakov, G. I. Solomin, V. P. Savina, S. S. Pashin, L. V. Marchenko, A. I. Gorshunova, E. I. Chukhno, V. M. Zinovyev, N. Ye. Ostasheva, and Ye. A. Demchenko et al *In its* JPRS Report: Science and Technology. USSR: Life Sciences 7 Oct. 1991 p 4 Transl. into ENGLISH from Kosmicheskaya Biologiya i Aviakosmicheskaya Meditsina (Moscow, USSR), v. 24, no. 6, Nov. - Dec. 1990 p 58-60 (For primary document see N92-11616 02-52)
Avail: NTIS HC/MF A04

The toxicity of the combustion products of polymers used in transformers was assessed on outbred albino rats and mice in simulated space cabins. Polyamide-6 and getinaks represented 81.4 pct. of the polymers in the transformer by weight. The resultant data indicated that within the testing parameters, unambiguous toxicity was lacking. It also became apparent that tests reflecting function of the nervous system are the most sensitive indicators of toxicity. Furthermore, tolerance of combustion products may be best assessed by determining the level of hepatic detoxication. The experiments also showed that within a cabin volume of 80 cu m, the concentrations of the most toxic products (hydrocyanic acid, carbon monoxide, ammonia, hydrogen fluoride, and formaldehyde) produced by a transformer fire remained below threshold limit values. Smaller cabins, accordingly, would present greater toxicity risks even on short term exposure. Author

N92-11620# Joint Publications Research Service, Arlington, VA.
TECHNICAL REQUIREMENTS OF SICK BAYS ABOARD SPACE SHIPS Abstract Only **c18**
A. V. Perkovskiy *In its* JPRS Report: Science and Technology. USSR: Life Sciences 7 Oct. 1991 p 5 Transl. into ENGLISH from Kosmicheskaya Biologiya i Aviakosmicheskaya Meditsina (Moscow, USSR), v. 24, no. 6, Nov. - Dec. 1990 p 62-64 (For primary document see N92-11616 02-52)
Avail: NTIS HC/MF A04

The technical components of sick bays aboard space ships must be designed to create an optimal medical environment. Within the close confines of a space ship, air contamination by bacteria is a high priority concern, and systems must be designed to minimize this hygienic factor. Accordingly, cursory description is provided of individual subcomponents of such a system that regulates air temperature, gas composition, relative humidity, air currents, and bacterial counts. In addition, a table is provided of a permissible range of values for every parameter of interest in the different compartments of the space ship. Author

N92-11621* National Aeronautics and Space Administration. Langley Research Center, Hampton, VA.
RAPIDLY QUANTIFYING THE RELATIVE DISTENTION OF A HUMAN BLADDER Patent
John A. Companion, inventor (to NASA), Joseph S. Heyman, inventor (to NASA), Beth A. Mineo, inventor (to NASA), Albert R. Cavalier, inventor (to NASA), and Travis N. Blalock, inventor (to NASA) 22 Oct. 1991 14 p Filed 26 May 1989 Continuation of US-Patent-Appl-SN-118993, filed 10 Nov. 1987 which is a continuation-in-part of abandoned US-Patent-Appl-SN-929869, filed 13 Nov. 1986
(NASA-Case-LAR-13901-2; US-Patent-5,058,591; US-Patent-Appl-SN-358213; US-Patent-Appl-SN-118993; US-Patent-Appl-SN-929869; US-Patent-Class-128-661.03;

Int-Patent-Class-A61B-8/00) Avail: US Patent and Trademark Office CSCL 06B

A device and method was developed to rapidly quantify the relative distention of the bladder of a human subject. An ultrasonic transducer is positioned on the human subject near the bladder. A microprocessor controlled pulser excites the transducer by sending an acoustic wave into the human subject. This wave interacts with the bladder walls and is reflected back to the ultrasonic transducer where it is received, amplified, and processed by the receiver. The resulting signal is digitized by an analog to digital converter, controlled by the microprocessor again, and is stored in data memory. The software in the microprocessor determines the relative distention of the bladder as a function of the propagated ultrasonic energy. Based on programmed scientific measurements and the human subject's past history as contained in program memory, the microprocessor sends out a signal to turn on any or all of the available alarms. The alarm system includes and audible alarm, the visible alarm, the tactile alarm, and the remote wireless alarm.

Official Gazette of the U.S. Patent and Trademark Office

N92-11622# Michigan Univ., Ann Arbor. Div. of Nuclear Medicine.

NON-INVASIVE EVALUATION OF THE CARDIAC AUTONOMIC NERVOUS SYSTEM BY PET

1991 3 p

(Contract DE-FG02-90ER-61091)

(DE91-018476; DOE/ER-61091/1) Avail: NTIS HC/MF A01

Our research efforts in the first funding year concentrated on animal and clinical studies validating C-11 hydroxyephedrine as a marker for norepinephrine uptake and storage in presynaptic sympathetic nerve terminals. In addition to kinetic studies in animals, the first clinical studies have been performed. C-11 hydroxyephedrine provides excellent image quality in the human heart with high myocardium to blood ratios. A canine model with transient intracoronary occlusion of the left anterior descending aorta was used to show decreased retention of tracer with ischemia. Clinical studies of patients with acute myocardial infarction showed an area of decreased retention of tracer exceeding the infarct territory as defined by Rb-82 blood flow imaging. We are also developing tracers for the parasympathetic nervous system. It appears that methyl-TRB is a specific tracer for this system. Studies of C-11 or F-18 benzovesamicol as a potential tracer for parasympathetic presynaptic nerve terminals are under way.

DOE

N92-11623# National Council on Radiation Protection and Measurements, Bethesda, MD.

DEVELOPMENT OF RECOMMENDATIONS IN THE AREA OF IONIZING RADIATIONS

1991 9 p

(Contract DE-FG05-90ER-60951)

(DE91-018527; DOE/ER-60951/2) Avail: NTIS HC/MF A02

This semiannual progress report is for the period 10/30/90 through 8/31/91. It describes the reports, proceedings, commentary, and lectures published by the National Council on Radiation Protection (NCRP) during this period. The reports published were: influence of radiation quality (LET) on relative biological effectiveness; implementation of the principle of as low as reasonably achievable (ALARA) for medical and dental personnel; and conceptual basis for calculations of absorbed dose distributions. The NCRP Proceedings 12, health and ecological implications of radioactively contaminated environments, was published, as was NCRP Commentary 6, radon exposure of the U.S. population -- status of the problem. Taylor Lecture 14, radiation protection and the internal emitter problem, was presented at the 1990 Annual Meeting. Currently there are three reports, one Commentary and one Taylor Lecture in press. DOE

N92-11624# Harvard Univ., Cambridge, MA. Dept. of Psychology.

PET STUDIES OF COMPONENTS OF HIGH-LEVEL VISION Quarterly Report

Stephen M. Kosslyn Aug. 1991 4 p

(Contract N00014-91-J-1243)

(AD-A240202) Avail: NTIS HC/MF A01 CSCL 06/4

We have finished analyzing the data from our first PET experiments and written a report of the results. As noted earlier, we have strong evidence ($p = .0001$) that primary visual cortex is activated selectively during visual mental imagery. In our next PET experiment we will study how objects are identified when seen from unusual points of view. Warrington and Taylor (1973) found that patients with right-parietal lesions have a very difficult time recognizing objects seen from unusual points of view. Kosslyn, Flynn, Amsterdam and Wang (1990) explain this result by positing a top-down, hypothesis testing mechanism that is called into play when a stimulus does not immediately match a stored memory very well. This mechanism not only relies on processes in the parietal lobe to shift attention, but also on processes in the frontal lobe formulate hypotheses. To test these ideas, subjects will see a series of pictures, either of objects seen from a canonical point of view or of objects seen from an unusual point of view. One sec after seeing a picture, a word will be presented, and the subject will decide whether the word names the pictured object. Counterbalancing will ensure that the same objects and words appear equally often in the two conditions. GRA

N92-11625# Naval Submarine Medical Research Lab., Groton, CT.

THE EFFECT OF BLINKING ON SUBSEQUENT DARK ADAPTATION Interim Report

S. M. Luria 14 May 1991 10 p

(AD-A240281; NSMRL-1170) Avail: NTIS HC/MF A02 CSCL 06/1

Night vision is extremely important for all operational forces, no less so for the submarine force. Periscope operators must be able to see at night, and great care is taken to ensure that they will be dark adapted when necessary. The crew in the control center routinely begins to dark adapt well in advance of nightfall. It is, thus, impossible to imagine that a submariner will not be dark adaptated when necessary. Nevertheless, if the dark adaptation process could be speeded up, it would add to the efficiency of submarine operations. For this reason, a claim by Stryker (1990) that an individual will achieve dark adaptation very quickly if he blinks his eyes rapidly and forcefully for 15 to 30 seconds has aroused some interest. The claim was that this technique works for adults half of those individuals who have tried it. GRA

N92-11626# State Univ. of New York, Stony Brook.

TRAINING, MUSCLE FATIGUE AND STRESS FRACTURES Midterm Report, 28 Sep. 1990 - 15 May 1991

Clinton T. Rubin 15 Jun. 1991 30 p

(Contract DAMD17-90-Z-0054; DA Proj. 3M1-61102-BS-15)

(AD-A240386) Avail: NTIS HC/MF A03 CSCL 06/5

The objective of this three year program is to expand and intensify our research efforts on the pathogenesis of the stress fracture lesion, using an animal model to further identify those aspects of the physical regimen which exacerbate this debilitating condition. Thus far, the studies we have undertaken demonstrate that the origins of the lesion stem from tissue remodeling, not material microdamage. As importantly, the site of the lesion, when correlated to the mechanical environment to which the bone is subjected, emphasizes that the pathology predominates in areas of least strain, not those areas subject to greatest deformation. Finally, the pathology observed in the two animal models pursued in the first period of this contract is histologically identical to that which occurs in the human condition, demonstrating the applicability of these studies to the etiology of the human condition. GRA

N92-11627*# National Aeronautics and Space Administration. Lyndon B. Johnson Space Center, Houston, TX.

EXTRA-CORPOREAL BLOOD ACCESS, SENSING, AND RADIATION METHODS AND APPARATUSES Patent Application

Kent D. Castle, inventor (to NASA) 16 Sep. 1991 24 p

(NASA-Case-MSC-21775-1; NAS 1.71:MSC-21775-1; US-Patent-Appl-SN-760633) Avail: NTIS HC/MF A03 CSCL 06B

The described invention is related to extra-corporeal blood access and radiation methods and apparatuses and, in particular, to subjecting flowing blood to energy in variety of forms, including radiation, electromagnetic force fields or atomic particles. It is directed to methods and apparatuses for accessing flowing blood and for subjecting the blood to electrical conductive, electrostatic or electromagnetic fields or for radiating the blood with some type of radiation, e.g., radio waves, ultrasonic or audio waves, microwaves, IR rays, visible light, UV radiation, x-rays, alpha, beta or gamma rays. An apparatus is employed which includes one or more access ports or windows for radiating blood and/or for sensing/analyzing blood. This invention is useful for killing viruses and bacteria in blood, monitoring blood for medical purposes, genetic modification of blood, and analyzing and/or treating blood components. NASA

N92-11628*# National Aeronautics and Space Administration. Lyndon B. Johnson Space Center, Houston, TX.
INTRANASAL SCOPOLAMINE PREPARATION AND METHOD Patent Application
Lakshmi Putcha, inventor (to NASA) and Nitza M. Cintron, inventor (to NASA0 25 Sep. 1991 11 p
(NASA-Case-MSC-21858-1; NAS 1.71:MSC-21858-1; US-Patent-Appl-SN-765615) Avail: NTIS HC/MF A03 CSCL 06E

A new method and preparation for intranasal delivery of scopolamine provides a safe and effective treatment for motion sickness and other conditions requiring anticholinergic therapy. The preparation can be in the form of aqueous nasal drops, mist spray, gel or oinment. Intranasal delivery of scopolamine has similar bioavailability and effect of intravenous delivery and is far superior to oral dosage. Scopolamine is prepared in a buffered saline solution at the desired dosage rate for effective anticholinergic response. NASA

53 BEHAVIORAL SCIENCES

Includes psychological factors; individual and group behavior; crew training and evaluation; and psychiatric research.

N92-11629*# National Aeronautics and Space Administration. Ames Research Center, Moffett Field, CA.
PERCEPTUAL STYLE AND AIR-TO-AIR TRACKING PERFORMANCE
Paul Atchley Jul. 1991 8 p
(NASA-TM-102868; A-91032; NAS 1.15:102868; USAAVSCOM-TR-90-A-004) Avail: NTIS HC/MF A02 CSCL 05I

The relationship between perceptual style and tracking of a target was examined. Four pilots were given the Embedded Figures Test to assess their degree of field dependence or independence. They then flew a helicopter simulator and attempted to track an airborne target. A significant correlation was found between perceptual style and tracking performance. Field independent subjects were able to track the target for longer periods than field dependent subjects. Author

N92-11630# Air Force Human Resources Lab., Brooks AFB, TX. Manpower and Personnel Research Div.
THE DEVELOPMENT OF BEHAVIORALLY ANCHORED RATING SCALES (BARS) FOR EVALUATING USAF PILOT TRAINING PERFORMANCE Interim Technical Paper, Oct. 1989 - Mar. 1991
Thomas R. Carretta and Laurie C. Walters Jul. 1991 32 p
(AD-A239969; AL-TP-1991-0022) Avail: NTIS HC/MF A03 CSCL 05/6

The purpose of this study was to develop Behaviorally Anchored Rating Scales (BARS) which could be used by instructor pilots (IP's) to evaluate their students on eight personality characteristics considered important to flying fighter-type aircraft. IP's generated behavioral examples which reflected good, average, and poor job behaviors for each personality dimension. These job behaviors were randomized and presented to another group of IP's who tried to match each behavior with the personality characteristic it best represented. The IP's demonstrated sufficient agreement to develop BARS for four of the eight personality characteristics (achievement motivation, assertiveness, cooperativeness, and stress tolerance). The behavioral examples generated for the retained personality characteristics were evaluated for their use as scale anchor points. Several uses of BARS in the flying training environment were discussed. GRA

N92-11631# Wisconsin Univ., Madison.
PICTURES AND ANAPHORA Annual Technical Report, 1 Jul. 1990 - 30 Jun. 1991
Arthur M. Glenberg and Peter Kruley 29 Jul. 1991 26 p
(Grant AF-AFOSR-0367-89; AF Proj. 2313)
(AD-A240153; AFOSR-91-0707TR) Avail: NTIS HC/MF A03 CSCL 05/8

Pictures help people to comprehend and remember texts. The goal of this project is to begin to understand how this occurs. Section 1 of this report contains a summary of work on several subgoals. Section 2 contains the report of two experiments testing the assumption that pictures provide an external memory which can assist working memory and thereby facilitate comprehension. We predicted that the availability of a diagram would interact with the difficulty of resolving anaphor references in texts. Resolution of an anaphor distance from its antecedent (which should stress working memory) should benefit greatly from a picture, whereas resolution of an anaphor near to its antecedent should benefit less from a picture. In experiments involving both cumulative and moving window presentations of texts, picture availability and distance separating antecedent from anaphor were manipulated. Although both picture presence and ease of anaphor resolution significantly improved subjects comprehension of the material, no evidence was found for an interaction of these factors. The results are interpreted as consistent with either dual code theory or aspects of working memory management that do not involve anaphor resolution. GRA

N92-11632# Pennsylvania State Univ., Hershey. Dept. of Behavioral Science.
SERIAL AVERAGING IN THE CONSTRUCTION AND VALIDATION OF PERFORMANCE TESTS Final Report, 1 Jun. 1990 - 31 May 1991
Marshall B. Jones 9 Jul. 1991 70 p
(Contract N00014-90-J-1994)
(AD-A240313; TR-90-01) Avail: NTIS HC/MF A04 CSCL 05/8

The advent of the microcomputer has led to a renaissance in performance testing, that is, tests which sample what a person can do (remember, track, aim, detect, recognize, etc.) rather than what he or she knows. Psychometric theory, however, is based on knowledge tests. The unit of analysis is an item and the order of administering the items is arbitrary. In performance testing the unit of analysis is a trial and order of administration is not only nonarbitrary but often the only thing that distinguishes one trial from another. In a knowledge test it is not unreasonable to suppose that mean performance and interitem correlations are independent of order of administration. In a performance test it is. Typically, performance improves with practice and intertrial correlations tend toward a definite pattern as a function of order. The consequences of these differences for theory are drastic. In performance testing, both reliability and temporal stability frequently encounter optima as a test is lengthened. Hence, low reliability or stability may not be corrigible by increasing test length. Further, scoring all trials administered (the usual practice) may not yield the best obtainable predictive validity. Scoring only a subset of consecutive trials (early, middle, or late) frequently yields appreciably higher predictive validities than the conventional practice. GRA

N92-11633# New York Univ., New York. Dept. of Psychology.
PERCEPTION AND MEMORY OF PICTURES Annual Report, 1 Jul. 1989 - 30 Jun. 1990
Joan G. Snodgrass 13 Aug. 1991 15 p
(Grant AF-AFOSR-0442-89; AF Proj. 2313)
(AD-A240364; AFOSR-91-0739TR) Avail: NTIS HC/MF A03 CSCL 12/9

This research is concerned with perception and memory of pictures. The theoretical motivation behind the experiments vary from area to area: in some cases, we want to test predictions of a connectionist model for picture recognition; in others we want to compare pictures with words to determine whether the two surface forms are understood at the same rate; in still others, the pictures are used as a vehicle to study questions about implicit memory. Although there are five areas of research, here I will mention highlights from only two. In the area of perception, interference in identification of a degraded image occurs when even more degraded images of the same object precede it. We tested and rejected an erroneous hypotheses about the object's identity interfering with subsequent recognition in favor of the explanation generated by our connectionist model. This explanation holds that transient activation of perceptual features common to the target and its distractors reduces the signal-to-noise ratio and causes interference. We were able to eliminate interference by having subjects solve math problems between presentations of the more degraded images. In the area of implicit memory, we found that the best priming stimulus for subsequent identification was a moderately fragmented one, as compared to a very fragmented or almost complete stimulus. We developed the perceptual closure hypothesis to account for this effect -- it says that the more difficult perceptual closure or completion of the fragmented figure is to be achieve, the more priming occurs, as long as closure is finally achieved. GRA

N92-11634# Illinois Univ., Urbana. Dept. of Psychology.
REMINDING-BASED LEARNING Annual Report, 21 Jun. 1990 - 20 Jun. 1991
Brian H. Ross 21 Aug. 1991 16 p
(Grant AF-AFOSR-0447-89; AF Proj. 2313)
(AD-A240370; AFOSR-91-0758TR) Avail: NTIS HC/MF A03 CSCL 05/8

When learning new cognitive skills involving problem solving, novices are often reminded of earlier problems. The use of earlier problems is a common means of problem solving and affects the learning of the skill. This project has three aims in understanding this learning. First, the representation of the resulting generalizations is being examined. Generalizations formed from remindings are likely to be conservative, in that they may be more tied to the examples than many current theories allow. A main aim of the project is to distinguish and test different forms of this conservatism. Second, the development of problem solving expertise is examined by focusing on differences in how typical and atypical problems are solved. Third, the effects of such reminding-based learning in everyday problem solving is examined to extend the findings and test some theoretical ideas that are difficult to investigate in more formal domains. GRA

N92-11635# Dayton Univ., OH.
LESSONS LEARNED IN THE DEVELOPMENT OF THE C-130 AIRCREW TRAINING SYSTEM: A SUMMARY OF AIR FORCE ON-SITE EXPERIENCE Final Report, Jan. 1990 - Mar. 1991
Ron Dukes, Marty R. Rockway, and Robert T. Nullmeyer Aug. 1991 47 p
(Contract F33615-90-C-0005)
(AD-A240554; AL-TP-1991-0032) Avail: NTIS HC/MF A03 CSCL 05/9

The current trend within the Air Force is to design aircrew training programs as total integrated systems. This trend has been coupled with a concurrent shift to contracting out the design, delivery and support of aircrew training. These changes have introduced a new set of technical and management issues which impact the design, acquisition, and operation of aircrew training programs. The Aircrew Training Research Division of the Armstrong Laboratory is conducting research and development (R and D) to address several of these issues in order to provide principles, procedures, and user-oriented guidelines to support Air Force acquisition and operational training agencies. This paper is one of a series concerned with the identification of lessons learned by contractor and government personnel directly involved in the acquisition and utilization of contracted aircrew training systems (ATSs). It documents some of the major experiences and lessons learned by Lt Col Ron Dukes of the Military Airlift Command during his long involvement with the C-130 ATS program. The report provides a general description of the C-130 ATS program and summaries Lt Col Dukes' experiences and lessons learned in the areas of courseware, training management, test and evaluation, quality assurance, and configuration management. GRA

N92-11636# Air Force Human Resources Lab., Brooks AFB, TX.
COGNITIVE FACTORS INVOLVED IN THE FIRST STAGE OF PROGRAMMING SKILL ACQUISITION Interim Technical Paper, Mar. 1989 - Mar. 1991
Carmen M. Pena and William C. Tirre Jul. 1991 27 p
(AD-A240566; AL-TP-1991-0018) Avail: NTIS HC/MF A03 CSCL 05/8

This study examined the role of cognitive abilities in the first stage of programming skill acquisition. Three hundred and five Air Force recruits were given 1.5 hours of computer based instruction on PASCAL. They were also administered computer-based tests assessing working memory, general reasoning, programming related knowledge, and component skills underlying algebra word problem solving. Additional test scores reflecting verbal knowledge were available from personnel records. Structural equation modeling was used to test alternative models of PASCAL learning, general cognitive abilities, and algebra word problem solving. The factors resulting from these analyses were then interrelated using structural models. The results showed that a model of PASCAL learning reflecting declarative and procedural factors was not superior in fit to a single factor model. In the general cognitive abilities domain, a three-factor model positing separate working memory, reasoning, and verbal knowledge abilities provided a better fit to the data than a single factor (g) model. Three factors were found to underlie algebra word problem solution. In interrelating the three sets of factors, we found that word problem translation added to significant contributions from more general abilities such as general reasoning, working memory, and verbal knowledge in predicting success in programming skill acquisition. GRA

54 MAN/SYSTEM TECHNOLOGY AND LIFE SUPPORT

Includes human engineering; biotechnology; and space suits and protective clothing.

For related information see also *16 Space Transportation.*

N92-11637*# Vanderbilt Univ., Nashville, TN. Dept. of Electrical Engineering.
ROBOT GRAPHIC SIMULATION TESTBED Final Report
George E. Cook, Janos Sztipanovits, Csaba Biegl, Gabor Karsai, and James F. Springfield Aug. 1991 119 p Original contains color illustrations
(Grant NAG8-690)
(NASA-CR-188998; NAS 1.26:188998) Avail: NTIS HC/MF A06; 12 functional color pages CSCL 06K

The objective of this research was twofold. First, the basic capabilities of ROBOSIM (graphical simulation system) were improved and extended by taking advantage of advanced graphic workstation technology and artificial intelligence programming techniques. Second, the scope of the graphic simulation testbed was extended to include general problems of Space Station automation. Hardware support for 3-D graphics and high processing performance make high resolution solid modeling, collision detection, and simulation of structural dynamics computationally

feasible. The Space Station is a complex system with many interacting subsystems. Design and testing of automation concepts demand modeling of the affected processes, their interactions, and that of the proposed control systems. The automation testbed was designed to facilitate studies in Space Station automation concepts. Author

N92-11638*# National Aeronautics and Space Administration. Ames Research Center, Moffett Field, CA.
HUMAN MACHINE INTERFACES FOR TELEOPERATORS AND VIRTUAL ENVIRONMENTS CONFERENCE
Mar. 1990 175 p Conference held in Santa Barbara, CA, 4-9 Mar. 1990
(NASA-CP-10071; NAS 1.55:10071; AD-A240716) Avail: NTIS HC/MF A08 CSCL 05/8

In a teleoperator system the human operator senses, moves within, and operates upon a remote or hazardous environment by means of a slave mechanism (a mechanism often referred to as a teleoperator). In a virtual environment system the interactive human machine interface is retained but the slave mechanism and its environment are replaced by a computer simulation. Video is replaced by computer graphics. The auditory and force sensations imparted to the human operator are similarly computer generated. In contrast to a teleoperator system, where the purpose is to extend the operator's sensorimotor system in a manner that facilitates exploration and manipulation of the physical environment, in a virtual environment system, the purpose is to train, inform, alter, or study the human operator to modify the state of the computer and the information environment. A major application in which the human operator is the target is that of flight simulation. Although flight simulators have been around for more than a decade, they had little impact outside aviation presumably because the application was so specialized and so expensive. GRA

N92-11639*# National Aeronautics and Space Administration. Lyndon B. Johnson Space Center, Houston, TX.
LUNAR RADIATOR SHADE Patent Application
Michael K. Ewert, inventor (to NASA) 25 Sep. 1991 13 p
(NASA-Case-MSC-21868-1; NAS 1.71:MSC-21868-1; US-Patent-Appl-SN-765273) Avail: NTIS HC/MF A03 CSCL 06K

An apparatus for rejecting waste heat from a system located on or near the lunar equator which utilizes a reflective catenary shaped trough deployed about a vertical radiator to shade the radiator from heat (i.e., infrared radiation) emitted by the hot lunar surface. The catenary shaped trough is constructed from a film material and is aligned relative to the sun so that incoming solar energy is focused to a line just above the vertical radiator and thereby isolate the radiator from the effects of direct sunlight. The film is in a collapsed position between side by side support rods, all of which are in a transport case. To deploy the film and support rods, a set of parallel tracks running perpendicular to length of the support rods are extended out from the transport case. After the support tracks are deployed, the support rods are positioned equidistant from each other along the length of the support tracks so that the flexible film shade between adjacent support rods is unfolded and hangs in a catenary shaped trough. A heat radiator is supported between each pair of support rods above each hanging reflective trough. NASA

N92-11049*# Computer Technology Associates, Inc., Rockville, MD.
HUMAN FACTORS ISSUES IN THE DESIGN OF USER INTERFACES FOR PLANNING AND SCHEDULING
Elizabeth D. Murphy *In* NASA. Goddard Space Flight Center, Space Network Control Conference on Resource Allocation Concepts and Approaches Sep. 1991 p 135-144 (For primary document see N92-11039 02-17)
Avail: NTIS HC/MF A13 CSCL 05H

N92-11051*# Computer Technology Associates, Inc., Rockville, MD.
CHIMES-2: A TOOL FOR AUTOMATED HCI ANALYSIS
William J. Weiland *In* NASA. Goddard Space Flight Center, Space Network Control Conference on Resource Allocation Concepts and Approaches Sep. 1991 p 159-166 (For primary document see N92-11039 02-17)
Avail: NTIS HC/MF A13 CSCL 05H

55 SPACE BIOLOGY

Includes exobiology; planetary biology; and extraterrestrial life.

No abstracts in this category.

59 MATHEMATICAL AND COMPUTER SCIENCES (GENERAL)

N92-11640*# Institute for Computer Applications in Science and Engineering, Hampton, VA.
RESONANT FREQUENCY CALCULATIONS USING A HYBRID PERTURBATION-GALERKIN TECHNIQUE Final Report
James F. Geer and Carl M. Andersen (College of William and Mary, Williamsburg, VA.) Sep. 1991 32 p Submitted for publication
(Contract NAS1-18605)
(NASA-CR-187632; NAS 1.26:187632; ICASE-91-68) Avail: NTIS HC/MF A03 CSCL 12A

A two-step hybrid perturbation Galerkin technique is applied to the problem of determining the resonant frequencies of one or several degree of freedom nonlinear systems involving a parameter. In one step, the Lindstedt-Poincare method is used to determine perturbation solutions which are formally valid about one or more special values of the parameter (e.g., for large or small values of the parameter). In step two, a subset of the perturbation coordinate functions determined in step one is used in Galerkin type approximation. The technique is illustrated for several one degree of freedom systems, including the Duffing and van der Pol oscillators, as well as for the compound pendulum. For all of the examples considered, it is shown that the frequencies obtained by the hybrid technique using only a few terms from the perturbation solutions are significantly more accurate than the perturbation results on which they are based, and they compare very well with frequencies obtained by purely numerical methods. Author

N92-11641*# National Aeronautics and Space Administration. Lyndon B. Johnson Space Center, Houston, TX.
MAKING INTELLIGENT SYSTEMS TEAM PLAYERS: CASE STUDIES AND DESIGN ISSUES. VOLUME 2: FAULT MANAGEMENT SYSTEM CASES
Jane T. Malin, Debra L. Schreckenghost, David D. Woods, Scott S. Potter, Leila Johannesen, and Matthew Holloway (Ohio State Univ., Columbus.) Oct. 1991 230 p Original contains color illustrations
(NASA-TM-104738; S-652; NAS 1.15:104738) Avail: NTIS HC/MF A11; 6 functional color pages CSCL 12A

Observations from a case study of intelligent systems are reported as part of a multi-year, interdisciplinary effort to provide guidance and assistance for designers of intelligent systems and their user interfaces. The objective of this case study was to identify preliminary guidance for the design of effective human-computer interaction (HCI) with intelligent fault management systems in aerospace applications. Fifteen intelligent fault management systems within NASA were studied. Author

60 COMPUTER OPERATIONS AND HARDWARE

Includes hardware for computer graphics, firmware, and data processing.

For components see *33 Electronics and Electrical Engineering.*

N92-11642*# National Aeronautics and Space Administration. Lewis Research Center, Cleveland, OH.
COMPUTERS IN AERONAUTICS AND SPACE RESEARCH AT THE LEWIS RESEARCH CENTER
1991 12 p Prepared in cooperation with Sverdrup Technology, Inc., Cleveland, OH
(NASA-TM-105096; NAS 1.15:105096) Avail: NTIS HC/MF A03; 3 functional color pages CSCL 09B

This brochure presents a general discussion of the role of computers in aerospace research at NASA's Lewis Research Center (LeRC). Four particular areas of computer applications are addressed: computer modeling and simulation, computer assisted engineering, data acquisition and analysis, and computer controlled testing. M.G.

N92-11643*# Research Inst. for Advanced Computer Science, Moffett Field, CA.
SPARSE DISTRIBUTED MEMORY
Peter J. Denning 20 May 1989 14 p Submitted for publication
(Contract NCC2-387)
(NASA-CR-188841; NAS 1.26:188841; RIACS-TR-89-22) Avail: NTIS HC/MF A03 CSCL 09B

Sparse distributed memory was proposed be Pentti Kanerva as a realizable architecture that could store large patterns and retrieve them based on partial matches with patterns representing current sensory inputs. This memory exhibits behaviors, both in theory and in experiment, that resemble those previously unapproached by machines - e.g., rapid recognition of faces or odors, discovery of new connections between seemingly unrelated ideas, continuation of a sequence of events when given a cue from the middle, knowing that one doesn't know, or getting stuck with an answer on the tip of one's tongue. These behaviors are now within reach of machines that can be incorporated into the computing systems of robots capable of seeing, talking, and manipulating. Kanerva's theory is a break with the Western rationalistic tradition, allowing a new interpretation of learning and cognition that respects biology and the mysteries of individual human beings. Author

N92-11644*# Research Inst. for Advanced Computer Science, Moffett Field, CA.
A CLASS OF DESIGNS FOR A SPARSE DISTRIBUTED MEMORY
Louis A. Jaeckel Jul. 1989 42 p
(Contracts NCC2-387; NCC2-408)
(NASA-CR-188849; NAS 1.26:188849; RIACS-TR-89-30) Avail: NTIS HC/MF A03 CSCL 09B

A general class of designs for a space distributed memory (SDM) is described. The author shows that Kanerva's original design and the selected-coordinate design are related, and that there is a series of possible intermediate designs between those two designs. In each such design, the set of addresses that activate a memory location is a sphere in the address space. We can also have hybrid designs, in which the memory locations may be a mixture of those found in the other designs. In some applications, the bits of the read and write addresses that will actually be used might be mostly zeros; that is, the addresses might lie on or near z hyperplane in the address space. The author describes a hyperplane design which is adapted to this situation and compares it to an adaptation of Kanerva's design. To study the performance of these designs, he computes the expected number of memory locations activated by both of two addresses. Author

N92-11645*# Research Inst. for Advanced Computer Science, Moffett Field, CA.
THREATS AND COUNTERMEASURES FOR NETWORK SECURITY
Peter J. Denning 8 Jan. 1991 28 p Presented at the 4th Annual Computer Virus and Security Conference, New York, NY, 14-15 Mar. 1991
(Contract NCC2-387)
(NASA-CR-188883; NAS 1.26:188883; RIACS-TR-91-2) Avail: NTIS HC/MF A03 CSCL 09B

In the late 1980's, the traditional threat of anonymous break-ins to networked computers was joined by viruses and worms, multiplicative surrogates that carry out the bidding of their authors. Technologies for authentication and secrecy, supplemented by good management practices, are the principal countermeasures. Four articles on these subjects are presented. Author

N92-11646 Department of the Navy, Washington, DC.
THIN FILM MAGNETIC MEMORY ELEMENTS Patent
Gary A. Prinz, inventor (to Navy) 18 Jun. 1991 8 p Filed 1 Jun. 1989 Supersedes AD-D014178
(AD-D014971; US-Patent-5,025,416; US-Patent-Appl-SN-360173; US-Patent-Class-365-170) Avail: US Patent and Trademark Office CSCL 12/6

A magnetic memory element is fabricated from a thin magnetic film wherein the magnetic films is grown on a lattice-matched substrate and subsequently patterned to form a closure domain. The closer domain is comprised of a plurality of legs which are joined at the domain walls. The individual legs are patterned in the thin magnetic film to lie parallel to an easy axis of the thin film crystal structure being used. Thus, each closure domain represents a magnetic memory element. Fringing fields about the memory elements are eliminated due to the closure domain design. An array of such closure domains can be grown on a substrate and can be packed to high densities up to the limits of current lithographic technology. Such thin film magnetic memory arrays are non-volatile and are compatible with existing Random Access Memories. GRA

N92-11647# Technische Univ., Berlin (Germany, F.R.). Forschungszentrum fuer Onnovative Rechnersysteme und -Strukturen.
THE ULM: A RISC FOR LISP. SYSTEM ARCHITECTURE Ph.D. Thesis
Reinhard Rasche Mar. 1990 238 p
(ETN-91-90162) Avail: NTIS HC/MF A11

An architecture to execute LISP which combines the benefits of traditional LISP machine designs and Reduced Instruction Set Computer (RISC) processors is presented. The architecture is scalable because some of the special units can be omitted emulating their functionality by software. The processor features hardware support for a rich set of different data types and a set of highly generic instructions suitable to meet LISP requirements. The proposed processor can be either operated as a LISP coprocessor in a host system or as the CPU of a stand alone computer system. Simulation results show that in combination with a highly optimizing complier the dedicated LISP RISC processor allows an architecture superior to those existing LISP machines and LISP supporting RISC based computers. ESA

61 COMPUTER PROGRAMMING AND SOFTWARE

Includes computer programs, routines, alogorithms, and specific applications, e.g., CAD/CAM.

N92-11648*# Simpson Weather Associates, Inc., Charlottesville, VA.
STUDY AND PROTOTYPE OF DATA SYSTEM INTERACTIONS FOR THE EARTH OBSERVING SYSTEM DATA AND INFORMATION SYSTEM Final Report

G. D. Emmitt, S. A. Wood, and M. Morris Dec. 1990 10 p
(Contract NAS5-31180)
(NASA-CR-183505; NAS 1.26:183505) Avail: NTIS HC/MF A02 CSCL 09B

A crucial part of the Earth Observing System (EOS) is its Data and Information System (EOSDIS). The success of EOS depends not only on its instruments and science studies, but also on its ability to help scientists integrate data sets of geophysical and biological measurements taken by various instruments and investigators. NASA contractors have completed Phase B studies of EOSDIS, in particular its architecture, functionality, and user interfacing. At this point in time, it may seem impossible to exercise the EOSDIS or any of its components since they do not exist; i.e., if the EOSDIS is accepted as a totally new system, distinct from any existing DIS. However, if EOSDIS is seen as evolving from existing data systems, then some limited prototyping studies can be conducted by using currently functioning systems. In support of both the EOSDIS Science Advisory Panel and the EOSDIS Project, a prototyping activity was carried out by a cross section of interdisciplinary scientists. That prototyping activity is summarized and some conclusions are drawn that can be used by NASA-Goddard to evaluate and modify the specifications soon to be released in an RFP to build EOSDIS. Author

N92-11649# Massachusetts Inst. of Tech., Cambridge. Artificial Intelligence Lab.
EXPERIENCE WITH ACORE: IMPLEMENTING GHC WITH ACTORS Memorandum Report
Jeff Paumucci, Carl A. Waldspurger, David Duis, and Paul Krause Oct. 1990 42 p
(Contracts N00014-88-K-0460; N00014-85-K-0124)
(AD-A231409; AI-M-1106) Avail: NTIS HC/MF A03 CSCL 12/5

This paper presents a concurrent interpreter for the programming language Guarded Horn Clauses, abbreviated GHC. GHC is a general purpose concurrent logic programming language. It has a clean, simple semantics based upon unification and choice nondeterminism. Unlike typical implementations of GHC in logic programming languages, the interpreter is implemented in the Actor language Acore. The primary motivation for this work was to probe the strengths and weaknesses of Acore as a platform for developing sophisticated programs. We chose to implement a concurrent interpreter for GHC because this large, complex application provided a rich testbed for exploring Actor programming methodology. The interpreter is a pedagogical investigation of the mapping of GHC constructs onto the Actor model. Because we opted for simplicity over efficiency, the interpreter is inefficient in both time and space. GRA

N92-11650# Massachusetts Inst. of Tech., Cambridge. Artificial Intelligence Lab.
THE ITERATE MANUAL Memorandum Report
Jonathan Amsterdam Oct. 1990 32 p
(Contract N00014-85-K-0124)
(AD-A231410; AI-M-1236) Avail: NTIS HC/MF A03 CSCL 12/5

This manual describes iterate, a powerful iteration macro for Common Lisp. Iterate provides abstractions for many common iteration patterns and allows for the definitions of additional patterns. Iterate is a macro that expands into ordinary Lisp at compile-time, so it is more efficient than higher-order functions like map and reduce. While its similar to loop, iterate offers a more Lisp like syntax and enhanced extensibility. GRA

N92-11651# Army Electronic Proving Ground, Fort Huachuca, AZ.
METHODOLOGY INVESTIGATION. PHASE 2: SOFTWARE MATURITY MODEL VALIDATION Final Report
Curtis Massie 4 Sep. 1990 103 p
(AD-A231439) Avail: NTIS HC/MF A06 CSCL 12/5

This report covers phase 2 of an investigation to identify methods of quantitatively assessing software reliability. A set of software reliability models were used in estimating reliability parameters in a developmental testing environment. These methods demonstrated that software reliability models are one tool available to the tester for providing quantitative assessments of software reliability. GRA

N92-11652*# Southwest Research Inst., San Antonio, TX.
CONTINUATION OF RESEARCH INTO LANGUAGE CONCEPTS FOR THE MISSION SUPPORT ENVIRONMENT Final Report
5 Sep. 1991 306 p
(Grant NAG9-435; SwRI Proj. 05-3531)
(NASA-CR-187818; NAS 1.26:187818) Avail: NTIS HC/MF A14 CSCL 09B

A concept for a more intuitive and graphically based Computation (Comp) Builder was developed. The Graphical Comp Builder Prototype was developed, which is an X Window based graphical tool that allows the user to build Comps using graphical symbols. Investigation was conducted to determine the availability and suitability of the Ada programming language for the development of future control center type software. The Space Station Freedom Project identified Ada as the desirable programming language for the development of Space Station Control Center software systems. Author

N92-11653*# Research Inst. for Advanced Computer Science, Moffett Field, CA.
A PARALLEL ALGORITHM FOR THE EIGENVALUES AND EIGENVECTORS FOR A GENERAL COMPLEX MATRIX
Gautam Shroff (Rensselaer Polytechnic Inst., Troy, NY.) Jun. 1989 35 p
(Contracts NCC2-387; N00014-86-K-0610)
(NASA-CR-188854; NAS 1.26:188854; RIACS-TR-89-35) Avail: NTIS HC/MF A03 CSCL 09B

A new parallel Jacobi-like algorithm is developed for computing the eigenvalues of a general complex matrix. Most parallel methods for this parallel typically display only linear convergence. Sequential norm-reducing algorithms also exit and they display quadratic convergence in most cases. The new algorithm is a parallel form of the norm-reducing algorithm due to Eberlein. It is proven that the asymptotic convergence rate of this algorithm is quadratic. Numerical experiments are presented which demonstrate the quadratic convergence of the algorithm and certain situations where the convergence is slow are also identified. The algorithm promises to be very competitive on a variety of parallel architectures. Author

N92-11654*# Research Inst. for Advanced Computer Science, Moffett Field, CA.
MODULA-2*: AN EXTENSION OF MODULA-2 FOR HIGHLY PARALLEL PROGRAMS
Walter F. Tichy and Christian G. Herter (Karlsruhe Univ., Germany, F.R.) Sep. 1989 22 p
(Contract NCC2-387)
(NASA-CR-188855; NAS 1.26:188855; RIACS-TR-89-34) Avail: NTIS HC/MF A03 CSCL 09B

Parallel programs should be machine-independent, i.e., independent of properties that are likely to differ from one parallel computer to the next. Extensions are described of Modula-2 for writing highly parallel, portable programs meeting these requirements. The extensions are: synchronous and asynchronous forms of forall statement; and control of the allocation of data to processors. Sample programs written with the extensions demonstrate the clarity of parallel programs when machine-dependent details are omitted. The principles of efficiently implementing the extensions on SIMD, MIMD, and MSIMD machines are discussed. The extensions are small enough to be integrated easily into other imperative languages. Author

N92-11655*# Research Inst. for Advanced Computer Science, Moffett Field, CA.
FAST SECANT METHODS FOR THE ITERATIVE SOLUTION OF LARGE NONSYMMETRIC LINEAR SYSTEMS
Peter Deuflhard, Roland Freund, and Artur Walter Jul. 1990 41 p

(Contract NCC2-387)
(NASA-CR-188867; NAS 1.26:188867; RIACS-TR-90-31) Avail: NTIS HC/MF A03 CSCL 09B

A family of secant methods based on general rank-1 updates was revisited in view of the construction of iterative solvers for large non-Hermitian linear systems. As it turns out, both Broyden's good and bad update techniques play a special role, but should be associated with two different line search principles. For Broyden's bad update technique, a minimum residual principle is natural, thus making it theoretically comparable with a series of well known algorithms like GMRES. Broyden's good update technique, however, is shown to be naturally linked with a minimum next correction principle, which asymptotically mimics a minimum error principle. The two minimization principles differ significantly for sufficiently large system dimension. Numerical experiments on discretized partial differential equations of convection diffusion type in 2-D with integral layers give a first impression of the possible power of the derived good Broyden variant. Author

N92-11656*# Research Inst. for Advanced Computer Science, Moffett Field, CA.
OPTIMAL PARALLEL SOLUTION OF SPARSE TRIANGULAR SYSTEMS
Fernando L. Alvarado and Robert Schreiber Sep. 1990 34 p Submitted for publication
(Contract NCC2-387; NSF ECS-88-22654; NSF ECS-89-07391)
(NASA-CR-188872; NAS 1.26:188872; RIACS-TR-90-36) Avail: NTIS HC/MF A03 CSCL 09B

A method for the parallel solution of triangular sets of equations is described that is appropriate when there are many right-handed sides. By preprocessing, the method can reduce the number of parallel steps required to solve $Lx = b$ compared to parallel forward or backsolve. Applications are to iterative solvers with triangular preconditioners, to structural analysis, or to power systems applications, where there may be many right-handed sides (not all available a priori). The inverse of L is represented as a product of sparse triangular factors. The problem is to find a factored representation of this inverse of L with the smallest number of factors (or partitions), subject to the requirement that no new nonzero elements be created in the formation of these inverse factors. A method from an earlier reference is shown to solve this problem. This method is improved upon by constructing a permutation of the rows and columns of L that preserves triangularity and allow for the best possible such partition. A number of practical examples and algorithmic details are presented. The parallelism attainable is illustrated by means of elimination trees and clique trees. Author

N92-11657*# Research Inst. for Advanced Computer Science, Moffett Field, CA.
STOPPING COMPUTER CRIMES
Peter J. Denning 28 Nov. 1989 13 p Submitted for publication
(Contract NCC2-387)
(NASA-CR-188896; NAS 1.26:188896; RIACS-TR-89-47) Avail: NTIS HC/MF A03 CSCL 09B

Two new books about intrusions and computer viruses remind us that attacks against our computers on networks are the actions of human beings. Cliff Stoll's book about the hacker who spent a year, beginning in Aug. 1986, attempting to use the Lawrence Berkeley Computer as a stepping-stone for access to military secrets is a spy thriller that illustrates the weaknesses of our password systems and the difficulties in compiling evidence against a hacker engaged in espionage. Pamela Kane's book about viruses that attack IBM PC's shows that viruses are the modern version of the old problem of a Trojan horse attack. It discusses the most famous viruses and their countermeasures, and it comes with a floppy disk of utility programs that will disinfect your PC and thwart future attack. Author

N92-11658*# Research Inst. for Advanced Computer Science, Moffett Field, CA.
SOLVING THE SHALLOW WATER EQUATIONS ON THE CRAY X-MP/48 AND THE CONNECTION MACHINE 2
Paul N. Swarztrauber and Richard K. Sato (National Center for Atmospheric Research, Boulder, CO.) Dec. 1989 19 p
(Contract NCC2-387)
(NASA-CR-188897; NAS 1.26:188897; RIACS-TR-89-48) Avail: NTIS HC/MF A03 CSCL 09B

The shallow water equations in Cartesian coordinates and 2-D are solved on the Connection Machine 2 (CM-2) using both the spectral and finite difference methods. A description of these implementations is presented together with a brief discussion of the CM-2 as it relates to these specific computations. The finite difference code was written both in C* and *LISP and the spectral code was written in *LISP. The performance of the codes is compared with a FORTRAN version that was optimized for the Cray X-MP/48. Author

N92-11659*# Research Inst. for Advanced Computer Science, Moffett Field, CA.
AN O(LOG SUP 2 N) PARALLEL ALGORITHM FOR COMPUTING THE EIGENVALUES OF A SYMMETRIC TRIDIAGONAL MATRIX
Paul N. Swarztrauber (National Center for Atmospheric Research, Boulder, CO.) Dec. 1989 27 p
(Contract NCC2-387)
(NASA-CR-188898; NAS 1.26:188898; RIACS-TR-89-49) Avail: NTIS HC/MF A03 CSCL 09B

An O(log sup 2 N) parallel algorithm is presented for computing the eigenvalues of a symmetric tridiagonal matrix using a parallel algorithm for computing the zeros of the characteristic polynomial. The method is based on a quadratic recurrence in which the characteristic polynomial is constructed on a binary tree from polynomials whose degree doubles at each level. Intervals that contain exactly one zero are determined by the zeros of polynomials at the previous level which ensures that different processors compute different zeros. The exact behavior of the polynomials at the interval endpoints is used to eliminate the usual problems induced by finite precision arithmetic. Author

N92-11660# Argonne National Lab., IL.
LAPACK: LINEAR ALGEBRA SOFTWARE FOR SUPERCOMPUTERS
Christian H. Bischof 1991 17 p Presented at the Optimale Datenstructuren In Ngenieurwissenschaften (ODIN) Symposium, Karlsruhe (Germany), 11-12 Apr. 1991
(Contract W-31-109-eng-38)
(DE91-017316; ANL/CP-73796; CONF-9104290-1) Avail: NTIS HC/MF A03

This paper presents an overview of the LAPACK library, a portable, public-domain library to solve the most common linear algebra problems. This library provides a uniformly designed set of subroutines for solving systems of simultaneous linear equations, least-squares problems, and eigenvalue problems for dense and banded matrices. We elaborate on the design methodologies incorporated to make the LAPACK codes efficient on today's high-performance architectures. In particular, we discuss the use of block algorithms and the reliance on the Basic Linear Algebra Subprograms. We present performance results that show the suitability of the LAPACK approach for vector uniprocessors and shared-memory multiprocessors. We also address some issues that have to be dealt with in tuning LAPACK for specific architectures. Lastly, we present results that show that the LAPACK software can be adapted with little effort to distributed-memory environments, and we discuss future efforts resulting from this project. DOE

N92-11661*# Research Inst. for Advanced Computer Science, Moffett Field, CA.
MODELLING DEFAULT AND LIKELIHOOD REASONING AS PROBABILISTIC REASONING
Wray Buntine Sep. 1990 38 p Prepared in cooperation with

Universities Space Research Association, Columbia, MD
(Contract NCC2-387)
(NASA-CR-188936; NAS 1.26:188936; RIACS-TR-90-50) Avail: NTIS HC/MF A03 CSCL 09B

A probabilistic analysis of plausible reasoning about defaults and about likelihood is presented. Likely and by default are in fact treated as duals in the same sense as possibility and necessity. To model these four forms probabilistically, a qualitative default probabilistic (QDP) logic and its quantitative counterpart DP are derived that allow qualitative and corresponding quantitative reasoning. Consistency and consequent results for subsets of the logics are given that require at most a quadratic number of satisfiability tests in the underlying propositional logic. The quantitative logic shows how to track the propagation error inherent in these reasoning forms. The methodology and sound framework of the system highlights their approximate nature, the dualities, and the need for complementary reasoning about relevance.
Author

N92-11662*# Research Inst. for Advanced Computer Science, Moffett Field, CA.
CLASSIFICATION OF POSTURE MAINTENANCE DATA WITH FUZZY CLUSTERING ALGORITHMS Interim Progress Report
James C. Bezdek (University of West Florida, Pensacola.) 15 Aug. 1991 15 p
(Contract NCC9-16; RICIS Proj. AI-19)
(NASA-CR-188949; NAS 1.26:188949) Avail: NTIS HC/MF A03 CSCL 09B

Sensory inputs from the visual, vestibular, and proprioreceptive systems are integrated by the central nervous system to maintain postural equilibrium. Sustained exposure to microgravity causes neurosensory adaptation during spaceflight, which results in decreased postural stability until readaptation occurs upon return to the terrestrial environment. Data which simulate sensory inputs under various conditions were collected in conjunction with JSC postural control studies using a Tilt-Translation Device (TTD). The University of West Florida proposed applying the Fuzzy C-Means Clustering (FCM) Algorithms to this data with a view towards identifying various states and stages. Data supplied by NASA/JSC were submitted to the FCM algorithms in an attempt to identify and characterize cluster substructure in a mixed ensemble of pre- and post-adaptational TTD data. Following several unsuccessful trials with FCM using a full 11 dimensional data set, a set of two channels (features) were found to enable FCM to separate pre- from post-adaptational TTD data. The main conclusions are that: (1) FCM seems able to separate pre- from post-TTD subject no. 2 on the one trial that was used, but only in certain subintervals of time; and (2) Channels 2 (right rear transducer force) and 8 (hip sway bar) contain better discrimination information than other supersets and combinations of the data that were tried so far.
Author

N92-11663*# Research Inst. for Advanced Computer Science, Moffett Field, CA.
ART/Ada DESIGN PROJECT, PHASE 1: PROJECT PLAN Status Report, Mar. - Oct. 1988
Bradley P. Allen (Inference Corp., Los Angeles, CA.) 24 Oct. 1988 10 p
(Contract NCC9-16; RICIS Proj. SE-19)
(NASA-CR-187313; NAS 1.26:187313) Avail: NTIS HC/MF A02 CSCL 09B

The plan and schedule for Phase 1 of the Ada based ESBT Design Research Project is described. The main platform for the project is a DEC Ada compiler on VAX mini-computers and VAXstations running the Virtual Memory System (VMS) operating system. The Ada effort and lines of code are given in tabular form. A chart is given of the entire project life cycle. Author

N92-11664*# Research Inst. for Advanced Computer Science, Moffett Field, CA.
DEPLOYING EXPERT SYSTEMS IN Ada
S. Daniel Lee and Bradley P. Allen (Inference Corp., Los Angeles, CA.) Oct. 1989 14 p Presented at the TRI-Ada '89 Conference, Pittsburgh, PA, 22-26 Oct. 1989 Submitted for publication
(Contract NCC9-16; RICIS Proj. SE-19)
(NASA-CR-188938; NAS 1.26:188938) Avail: NTIS HC/MF A03 CSCL 09B

As the Department of Defense Ada mandate begins to be enforced actively, interest in deploying expert systems in Ada has increased. A prototype Ada based expert system tool is introduced called ART/Ada. This prototype was built to support research into the language and operational issues of expert systems in Ada. ART/Ada allows applications of a conventional expert system tool called ART-IM (Automated Reasoning Tool for Information Management) to be deployed in various Ada environments with efficient use of time and space. ART-IM, a C-based expert system tool, is used to generate Ada source code which is compiled and linked with an Ada base inference engine to produce an Ada executable image. ART/Ada will be used to implement several prototype expert systems for the Space Station Freedom Program testbeds.
Author

N92-11665*# Research Inst. for Advanced Computer Science, Moffett Field, CA.
ART/Ada DESIGN PROJECT, PHASE 1. TASK 1 REPORT: OVERALL DESIGN Status Report, Mar. - Oct. 1988
Bradley P. Allen (Inference Corp., Los Angeles, CA.) 24 Oct. 1988 18 p
(Contract NCC9-16; RICIS Proj. SE-19)
(NASA-CR-188943; NAS 1.26:188943) Avail: NTIS HC/MF A03 CSCL 09B

The design methodology for the ART/Ada project is introduced, and the selected design for ART/Ada is described in detail. The following topics are included: object-oriented design, reusable software, documentation techniques, impact of Ada, design approach, and differences between ART-IM 1.5 and ART/Ada 1.0 prototype. Also, Ada generator and ART/Ada runtime systems are discussed.
Author

N92-11666*# Research Inst. for Advanced Computer Science, Moffett Field, CA.
ART/Ada DESIGN PROJECT, PHASE 1. TASK 2 REPORT: DETAILED DESIGN Status Report, Mar. - Oct. 1988
Bradley P. Allen (Inference Corp., Los Angeles, CA.) 24 Oct. 1988 106 p
(Contract NCC9-16; RICIS Proj. SE-19)
(NASA-CR-188944; NAS 1.26:188944) Avail: NTIS HC/MF A06 CSCL 09B

Various issues are studied in the context of the design of an Ada based expert system building tool. Using an existing successful design as a starting point, the impact is analyzed of the Ada language and Ada development methodologies on that design, the Ada system is redesigned, and its performance is analyzed using both complexity-theoretic and empirical techniques. The algorithms specified in the overall design are refined, resolving and documenting any open design issues, identifying each system module, documenting the internal architecture and control logic, and describing the primary data structures involved in the module.
Author

N92-11667*# Research Inst. for Advanced Computer Science, Moffett Field, CA.
ART-Ada DESIGN PROJECT, PHASE 2 Final Report
S. Daniel Lee and Bradley P. Allen (Inference Corp., Los Angeles, CA.) Feb. 1990 44 p
(Contract NCC9-16; RICIS Proj. SE-19)
(NASA-CR-188940; NAS 1.26:188940) Copyright Avail: NTIS HC/MF A03 CSCL 09B

Interest in deploying expert systems in Ada has increased. An Ada based expert system tool is described called ART-Ada, which was built to support research into the language and methodological issues of expert systems in Ada. ART-Ada allows applications of an existing expert system tool called ART-IM (Automated Reasoning Tool for Information Management) to be deployed in various Ada environments. ART-IM, a C-based expert system tool, is used to generate Ada source code which is compiled and linked

with an Ada based inference engine to produce an Ada executable image. ART-Ada is being used to implement several expert systems for NASA's Space Station Freedom Program and the U.S. Air Force. Author

N92-11668*# National Aeronautics and Space Administration. Langley Research Center, Hampton, VA.
USER'S MANUAL FOR THE MACINTOSH VERSION OF PASCO
S. H. Lucas and Randall C. Davis Sep. 1991 10 p
(NASA-TM-104115; NAS 1.15:104115) Avail: NTIS HC/MF A02 CSCL 09B

A user's manual for Macintosh PASCO is presented. Macintosh PASCO is an Apple Macintosh version of PASCO, an existing computer code for structural analysis and optimization of longitudinally stiffened composite panels. PASCO combines a rigorous buckling analysis program with a nonlinear mathematical optimization routine to minimize panel mass. Macintosh PASCO accepts the same input as mainframe versions of PASCO. As output, Macintosh PASCO produces a text file and mode shape plots in the form of Apple Macintosh PICT files. Only the user interface for Macintosh is discussed here. Author

N92-11669*# Institute for Computer Applications in Science and Engineering, Hampton, VA.
DISTRIBUTED MEMORY COMPILER METHODS FOR IRREGULAR PROBLEMS: DATA COPY REUSE AND RUNTIME PARTITIONING Final Report
Raja Das, Ravi Ponnusamy (Syracuse Univ., NY.), Joel Saltz, and Dimitri Mavriplis Sep. 1991 36 p Submitted for publication
(Contract NAS1-18605; NSF ASC-88-19374)
(NASA-CR-187635; NAS 1.26:187635; ICASE-91-73) Avail: NTIS HC/MF A03 CSCL 09B

Outlined here are two methods which we believe will play an important role in any distributed memory compiler able to handle sparse and unstructured problems. We describe how to link runtime partitioners to distributed memory compilers. In our scheme, programmers can implicitly specify how data and loop iterations are to be distributed between processors. This insulates users from having to deal explicitly with potentially complex algorithms that carry out work and data partitioning. We also describe a viable mechanism for tracking and reusing copies of off-processor data. In many programs, several loops access the same off-processor memory locations. As long as it can be verified that the values assigned to off-processor memory locations remain unmodified, we show that we can effectively reuse stored off-processor data. We present experimental data from a 3-D unstructured Euler solver run on iPSC/860 to demonstrate the usefulness of our methods. Author

N92-11670*# Institute for Computer Applications in Science and Engineering, Hampton, VA.
VIENNA FORTRAN: A FORTRAN LANGUAGE EXTENSION FOR DISTRIBUTED MEMORY MULTIPROCESSORS Final Report
Barbara Chapman, Piyush Mehrotra, and Hans Zima (Wien Univ., Austria) Sep. 1991 29 p Submitted for publication Sponsored in part by Austrian Research Foundation and Austrian Ministry for Science and Research
(Contract NAS1-18605)
(NASA-CR-187634; NAS 1.26:187634; ICASE-91-72) Avail: NTIS HC/MF A03 CSCL 09B

Exploiting the performance potential of distributed memory machines requires a careful distribution of data across the processors. Vienna FORTRAN is a language extension of FORTRAN which provides the user with a wide range of facilities for such mapping of data structures. However, programs in Vienna FORTRAN are written using global data references. Thus, the user has the advantage of a shared memory programming paradigm while explicitly controlling the placement of data. The basic features of Vienna FORTRAN are presented along with a set of examples illustrating the use of these features. Author

N92-11671*# Pittsburgh Univ., PA.
TRANSIENT FINITE ELEMENT COMPUTATIONS ON A VARIABLE TRANSPUTER SYSTEM
Patrick J. Smolinski and Ireneusz Lapczyk Oct. 1991 90 p
(Grant NAG3-1152)
(NASA-CR-189060; NAS 1.26:189060) Avail: NTIS HC/MF A05 CSCL 09B

A parallel program to analyze transient finite element problems was written and implemented on a system of transputer processors. The program uses the explicit time integration algorithm which eliminates the need for equation solving, making it more suitable for parallel computations. An interprocessor communication scheme was developed for arbitrary two dimensional grid processor configurations. Several 3-D problems were analyzed on a system with a small number of processors. Author

N92-11672*# Institute for Computer Applications in Science and Engineering, Hampton, VA.
OPTIMAL PROCESSOR ASSIGNMENT FOR PIPELINE COMPUTATIONS Final Report
David M. Nicol, Rahul Simha, Alok N. Choudhury, and Bhagirath Narahari (George Washington Univ., Washington, DC.) Oct. 1991 37 p Submitted for publication
(Contract NAS1-18605)
(NASA-CR-189047; NAS 1.26:189047; ICASE-91-79) Avail: NTIS HC/MF A03 CSCL 09B

The availability of large scale multitasked parallel architectures introduces the following processor assignment problem for pipelined computations. Given a set of tasks and their precedence constraints, along with their experimentally determined individual responses times for different processor sizes, find an assignment of processor to tasks. Two objectives are of interest: minimal response given a throughput requirement, and maximal throughput given a response time requirement. These assignment problems differ considerably from the classical mapping problem in which several tasks share a processor; instead, it is assumed that a large number of processors are to be assigned to a relatively small number of tasks. Efficient assignment algorithms were developed for different classes of task structures. For a p processor system and a series parallel precedence graph with n constituent tasks, an O(np2) algorithm is provided that finds the optimal assignment for the response time optimization problem; it was found that the assignment optimizing the constrained throughput in O(np2log p) time. Special cases of linear, independent, and tree graphs are also considered. Author

N92-11673*# National Aeronautics and Space Administration. Ames Research Center, Moffett Field, CA.
COMPUTER INTEGRATED DOCUMENTATION
Guy Boy Sep. 1991 129 p
(Contract NAS2-13210)
(NASA-TM-103870; A-91167; NAS 1.15:103870) Avail: NTIS HC/MF A07 CSCL 09B

The main technical issues of the Computer Integrated Documentation (CID) project are presented. The problem of automation of documents management and maintenance is analyzed both from an artificial intelligence viewpoint and from a human factors viewpoint. Possible technologies for CID are reviewed: conventional approaches to indexing and information retrieval; hypertext; and knowledge based systems. A particular effort was made to provide an appropriate representation for contextual knowledge. This representation is used to generate context on hypertext links. Thus, indexing in CID is context sensitive. The implementation of the current version of CID is described. It includes a hypertext data base, a knowledge based management and maintenance system, and a user interface. A series is also presented of theoretical considerations as navigation in hyperspace, acquisition of indexing knowledge, generation and maintenance of a large documentation, and relation to other work. Author

N92-11674# Brunel Univ., Uxbridge (England). Inst. of Computational Mathematics.
WORKSHOPS ON EFFICIENT USE OF SCIENTIFIC COMPUTING
Ben Noble and J. R. Whiteman 2 Aug. 1991 5 p Workshops held in Watervliet, NY, 15-16 Nov. 1990; and in Natick, MA, 22-23 May 1991
(Contract DAJA45-90-M-0298)
(AD-A240175; R/D-6490-MA-93) Avail: NTIS HC/MF A01
CSCL 12/5

Two 2-day workshops were held. These concentrated on MATLAB, which is a high-level computer language for scientific and engineering calculations. It is extremely useful for many exploratory investigations, and for problems that need efficient use of matrices. Some of the advantages of MATLAB over lower-level languages like FORTRAN are: (1) the essentials can be learned very easily - one day; (2) programs tend to be short, easy to write and read; (3) MATLAB is interactive, which makes it easy to debug and make changes in programs; (4) excellent, easy-to-use graphics; and (5) tedious aspects of lower-level languages are eliminated. GRA

N92-11675# Michigan Univ., Ann Arbor. Dept. of Electrical Engineering and Computer Science.
FAST ALGORITHMS FOR LINEAR LEAST-SQUARES ESTIMATION OF MULTI-DIMENSIONAL RANDOM FIELDS Final Report, 1 Nov. 1988 - 31 May 1991
Andrew E. Yagle 31 Jul. 1991 149 p
(Grant AF-AFOSR-0017-89; AF Proj. 2304)
(AD-A240249; AFOSR-91-0741) Avail: NTIS HC/MF A07
CSCL 12/1

This report develops fast algorithms for computing filters for linear least squares estimation of one, two, and three dimensional random fields. The algorithms generalize the split Levinson and Schur algorithms to two and three dimensions; however, they are applicable to a more general Toeplitz plus Hankel structure in the covariance function. A discrete version of the Bellman Siegert Krein resolvent identity is developed for smoothing problems in one and two dimensions. Applications to linear predictive coding, and restoration and smoothing, of isotropic random fields on a polar raster are demonstrated. In addition, two new algorithms are developed for spectral estimation on a two-dimensional polar raster. Both use the Radon transform to map the two dimensional problem into one dimensional problems. Interpolating functions for computing the Radon transform, positive definite covariance extensions, and correlation matching are all considered. GRA

N92-11676# Defense Systems Management School, Fort Belvoir, VA.
PROCEEDINGS OF THE ACQUISITION RESEARCH SYMPOSIUM: IMAGNINATION, INNOVATION, AND IMPLEMENTATION, 1991, VOLUME 1
1991 390 p Symposium held in Washington, DC, 1991
(AD-A240260) Avail: NTIS HC/MF A17 CSCL 15/5

The proceedings of the symposium are presented. Some areas of discussion are as follows: Acquisition Keyed to a Specific Program; ADP Hardware and Software; Automated Procurement; Industrial Preparedness; International Aspects of Acquisition; Manpower, Personnel, and Training Acquisition Work Force; Program Management from A to Z; Research, Reforms, and Trends in Acquisition; Total Quality Management (TQM) and Total Quality Control (TQC). GRA

N92-11677# Defense Systems Management School, Fort Belvoir, VA.
PROCEEDINGS OF THE ACQUISITION RESEARCH SYMPOSIUM: ACQUISITION FOR THE FUTURE, IMAGINATION, INNOVATION, AND IMPLEMENTATION, 1991, VOLUME 2
1991 602 p Symposium held in Washington, DC, 1991
(AD-A240261) Avail: NTIS HC/MF A99 CSCL 15/5

The proceedings of the symposium are presented. Some areas of discussions are as follows: Acquisition Keyed to a Specific Program; ADP Hardware and Software; Automated Procurement; Budget and Costs; Industrial Preparedness; International Aspects of Acquisition; Manpower, Personnel, and Training Acquisition Workforce; Program Management from A to Z; Research, Reforms, and Trends in Acquisition; Total Quality Management (TQM) and Total Quality Control (TQC); Miscellaneous. GRA

N92-11678# Illinois Univ., Urbana. Coordinated Science Lab.
PERCEPTUAL GROUPING AND SHAPE FROM TEXTURE Final Report, 1 Dec. 1989 - 30 Nov. 1990
Narendra Ahuja 30 Nov. 1990 3 p
(Grant AF-AFOSR-0061-90; AF Proj. 2304)
(AD-A240358; AFOSR-91-0721TR) Avail: NTIS HC/MF A01
CSCL 12/3

This report summarizes the progress made during the year 1990 under grant AFOSR-90-0061. During the grant period of December 1989 to November 1990, we have concentrated on the projects on motion through textured environment and perceptual structure and reliable computing. In the first project, we have made process on the estimation of three-dimensional structure from (1) two perspective, monocular views of a dynamic scene, and (2) a sequence of perspective, monocular views of a dynamic scene. Towards (1), we have developed an algorithm that estimates the three-dimensional motion and structure of a moving piecewise textured surface from two perspective views. The algorithm has two major steps. Here, the local planar nature of the surface is used to obtain polynomial expressions for image plane displacements of features. Using regions as moving features, the image is segmented using Hough transform such that the regions in each segment have the same polynomial coefficients. The values of these coefficients and region properties (e.g., area) are then used to identify region correspondences. In the second step, for each planar surface, the region correspondences are used to compute the corresponding motion parameters and surface orientation in closed form. GRA

N92-11679# Carnegie-Mellon Univ., Pittsburgh, PA. Robotics Inst.
APPEARANCE SIMULATOR FOR COMPUTER VISION RESEARCH
Yoshimasa Fujiwara, Shree Nayer, and Katsushi Ikeuchi Aug. 1991 35 p
(Contract F33615-87-C-1499; DARPA Order 4976)
(AD-A240506; CMU-RI-TR-91-16) Avail: NTIS HC/MF A03
CSCL 12/5

Computer vision research needs a flexible and robust method to obtain accurate appearance of a scene. Such needs include generating test data, using a simulator as a part of an algorithm, and generating model data for object recognition and inspection. A sophisticated and reasonable mechanism for generating scene appearance is a technique known as ray tracing. However, current ray tracers are mainly developed for computer graphic research. They are based on ad hoc reflectance mechanisms; their algorithms emphasize computational costs by choosing computational expediency at the expense of an appearance grounded in physics. We are developing an appearance simulator to be able to produce a scene according to the laws of physics. By combining the reflectance theory based on physics and the technique of ray tracing, we are able to produce scene appearances that are adequate and realistic enough for computer vision. First, we will briefly describe our reflectance model to be used in our simulator. Then, we will discuss several implementation issues how to embody the model into real algorithms. Finally, we will generate several scene appearances to verify the performance of our system and illustrate applications of this system. GRA

N92-11680# Netrologic, Inc., San Diego, CA.
FRACTAL IMAGE COMPRESSION Quarterly Progress Report
Yuval Fisher, Ben Bielefeld, Albert Lawrence, and Dan Greenwood 12 Aug. 1991 6 p
(Contract N00014-91-C-0117)
(AD-A240636) Avail: NTIS HC/MF A02 CSCL 12/9

Efforts were concentrated in three areas, a survey of

applications, algorithm development and theory. Specific applications have been selected for the compression algorithms. The selection process is based on information gained through technical discussions with commercial groups selling image compression hardware and software, literature reviews and performance figures on commercially available software. The industry standard (JPEG) for image compression is based on the discrete cosine transform. One evaluates the suitability of the fractal method in comparison with this transform. Several key differences are apparent. GRA

N92-11681# Harris Corp., Melbourne, FL.
TESTER INDEPENDENT SUPPORT SOFTWARE SYSTEM (TISSS) Final Report, Sep. 1985 - Jun. 1989
Robert Rolfe, Amy Pierce, and David Lehtonen Aug. 1991 135 p
(Contract F30602-84-C-0168)
(AD-A240668; RL-TR-91-163) Avail: NTIS HC/MF A07 CSCL 12/5

This report defines the objectives and technical accomplishments of the Tester Independent Support Software System (TISSS) software development effort. The objectives of this software development effort were to define, develop, and implement a software system for the automated generation and maintenance of electrical test specifications and test programs for complex Very High Speed Integrated Circuits (VHSIC) and other Very Large Scale Integrated Circuits (VLSI) devices. This was accomplished through the development of the TISSS Software system and necessary information representation languages. The TISSS provides a capability for the Government to capture design data in a standardized electronic form and use this information in a standard, transportable, and computer-accessible format and to automatically generate Automatic Microcircuit Test Equipment (AMTE) test programs for lifecycle support of VHSIC and VLSI devices. GRA

N92-11682# Mitre Corp., Bedford, MA.
TECHNOLOGY ASSESSMENT OF THE SOFTWARE LIFE CYCLE SUPPORT ENVIRONMENT (SLCSE) Final Report, Sep. 1989 - Sep. 1990
R. W. Baldwin and D. E. Emery Aug. 1991 75 p
(Contract F19628-89-C-0001)
(AD-A240673; RL-TR-91-166) Avail: NTIS HC/MF A04 CSCL 12/5

This report summarizes the technology assessment of the Rome Laboratory Software Life Cycle Support Environment (SLCSE) performed by the MITRE Corporation. MITRE assesses the SLCSE for applicability to Electronic Systems Division (ESD) System Program Offices (SPOs) and their contractors, and identifies changes required to tailor the SLCSE to ESD requirements. The report also includes a plan for transfer of the SLCSE from the Command Center Evaluation System (CCES) to various SPOs and changes that may be necessary to productize SLCSE, in particular, for use on large scale C3I software development efforts. GRA

N92-11683# Massachusetts Inst. of Tech., Lexington. Lincoln Lab.
AN EFFICIENT A* STACK DECODER ALGORITHM FOR CONTINUOUS SPEECH RECOGNITION WITH A STOCHASTIC LANGUAGE MODEL
D. B. Paul 18 Jul. 1991 21 p
(Contract F19628-90-C-0002)
(AD-A240745; TR-930; ESD-TR-91-111) Avail: NTIS HC/MF A03 CSCL 05/7

The stack decoder is an attractive algorithm for controlling the acoustic and language model matching in a continuous speech recognizer. It implements a best-first tree search to find the best match to both the language model and the observed speech. A previous paper described a near-optimal admissible Viterbi A asterisk search algorithms for use with non-cross-word acoustic models and no-grammar language models. This report extends this algorithm to include unigram language models and describes a modified version of the algorithm which includes the full (forward) decoder, cross-word acoustic models and longer-span language models. The resultant algorithm is not admissible, but has been demonstrated to be very efficient. GRA

N92-11684# Technische Univ., Eindhoven (Netherlands).
ON THE CAPACITY REGION FOR DETERMINISTIC TWO-WAY CHANNELS AND WRITE-UNIDIRECTIONAL MEMORIES Ph.D. Thesis
Wilhelmina Maria Cor vanOverveld 25 Jan. 1991 220 p
(ETN-91-90147) Copyright Avail: NTIS HC/MF A10

Two Way Channels (TWCs) and Write Unidirectional Memories (WUMs) of information theory are addressed. Old results are collected into one theory called the graphical representation, which relates communication over the channel to the partitioning of the unit square. This method can be used for a large class of channels and good lower bounds for the capacity region can be derived. Connections between TWCs and WUMs are studied. Since the capacity region for the binary WUM in two cases is equal to a fundamental outer bound for the capacity of the binary multiplying channel, a generalization of this phenomenon over arbitrary alphabets is sought. This gives rise to a generalization of TWCs with q users, for which some properties are derived. ESA

N92-11685*# National Aeronautics and Space Administration. Langley Research Center, Hampton, VA.
CELLULAR REPAIR/MISREPAIR TRACK MODEL
John W. Wilson and Francis A. Cucinotta Washington Nov. 1991 11 p
(NASA-TP-3124; L-16949; NAS 1.60:3124) Avail: NTIS HC/MF A03 CSCL 09B

A repair/misrepair cell kinetics model is superimposed onto the track structure model of Katz to provide for a repair mechanism. The model is tested on the repair-dependent data of Yang et al. and provides an adequate description of that data. The misrepair rate determines the maximum relative biological effectiveness (RBE), but similar results could arise from indirect X-ray lethality not include in the present model. Author

N92-11686# State Univ. of New York, Albany.
THE MODELING OF COMPLEX CONTINUA: FUNDAMENTAL OBSTACLES AND GRAND CHALLENGES
Sep. 1991 10 p
(Contract DE-FG02-90ER-25084)
(DE91-018806; DOE/ER-25084/2) Avail: NTIS HC/MF A02

The focus of this research program is to achieve quantitatively correct computations in the modeling of complex continua. The central theme of the effort is to continue the development of a coherent approach that is independent of any one particular application. This is done by abstracting important mathematical concepts and computational methods from individual applications which generalize to all applications involving complex continua. The generic difficulties in the modeling of continua that guide this abstraction are associated with (1) multiple length and time scales, often involving sharply defined internal layers of boundaries, (2) high dimensional descriptions of the solution variables, (3) microstructures such as droplets, vortices and crystal defects, and (4) chaotic or random phenomena described by a statistical formulation. The scientific goal is achieved by identifying critical research areas and, within them, focusing the development of the theory necessary to support computation. The mathematical concepts and computational methods thus developed are generalized where possible and added to an integrated framework for general use in complex continua problems. DOE

N92-11687# Pacific Northwest Lab., Richland, WA.
EDUCATION IN COMPUTATIONAL SCIENCE: ROLE OF THE NATIONAL LABORATORIES
T. H. Dunning, Jr. Apr. 1991 9 p Presented at the Workshop on Undergraduate and Graduate Education in Computational Science, Baton Rouge, LA, 29-30 Apr. 1991
(Contract DE-AC06-76RL-01830)
(DE91-018823; PNL-SA-19923; CONF-9104258-2) Avail: NTIS HC/MF A02

The National Laboratories operated by the U.S. Department of Energy have, since their very beginning, been at the forefront of research in computational science. Computational physics is at the core of the Department's programs to design nuclear weapons and to tame the fusion process. And, and the focal points of this research and development effort, the Los Alamos and Lawrence Livermore National Laboratories, support two of the largest computer centers in the world. More recently, the Office of Energy Research established the National Energy Research Supercomputer Center at Lawrence National Laboratory and cosponsored the Supercomputer Research Institute at Florida State University. These Centers provide supercomputer access to DOE's basic research programs, including chemistry, materials science, solid state physics nuclear physics, high energy physics, biology and environmental science. The availability of these resources has had a profound impact on these activities, permitting the solution of problems which have heretofore intractable. There is now underway at DOE's Pacific Northwest Laboratory a new research initiative which will have a profound impact on computational molecular science. The computing demands of new research programs are expected to grow dramatically over the next few years as new projects involving such as the molecular systems of increasing size and complexity are undertaken, new staff are added to the program, and extensive collabortive projects are initiated. To provide for the computing needs of these efforts, the computer hardware and software will need to provide state-of-the-art high performance computational and visualization capabilities for simulations while enabling the evaluation and exploitation of promising new computer technologies. DOE

N92-11688# Arizona State Univ., Tempe. Dept. of Chemical Engineering.
COMPUTER AIDED SURFACE REPRESENTATION
R. E. Barnhill 2 Apr. 1991 20 p
(Contract DE-FG02-87ER-25041)
(DE91-018872; DOE/ER-25041/4) Avail: NTIS HC/MF A03

Modern computing resources permit the generation of large amounts of numerical data. These large data sets, if left in numerical form, can be overwhelming. Such large data sets are usually discrete points from some underlying physical phenomenon. Because we need to evaluate the phenomenon at places where we don't have data, a continuous representation (a surface) is required. A simple example is a weather map obtained from a discrete set of weather stations. (For more examples including multi-dimensional ones, see the article by Dr. Rosemary Chang in the enclosed IRIS Universe.) In order to create a scientific structure encompassing the data, we construct an interpolating mathematical surface which can evaluate at arbitrary locations. We can also display and analyze the results via interactive computer graphics. In our research we construct a very wide variety of surfaces for applied geometry problems that have sound theoretical foundations. However, our surfaces have the distinguishing feature that they are constructed to solve short or long term practical problems. This DOE-funded project has developed the premiere research team in the subject of constructing surfaces (3D and higher dimensional) that provide smooth representations of real scientific and engineering information, including state of the art computer graphics visualizations. However, our main contribution is in the development of fundamental constructive mathematical methods and visualization techniques which can be incorporated into a wide variety of applications. This project combines constructive mathematics, algorithms, and computer graphics, all applied to real problems. The project is a unique resource, considered by our peers to be a de facto national center for this type of research. DOE

N92-11689# Illinois Univ., Urbana. Center for Supercomputing Research and Development.
CEDAR PROJECT: ORIGINAL GOALS AND PROGRESS TO DATE
G. Cybenko, D. Kuck, D. Padua, and E. Gallopoulos Sep. 1991 64 p
(Contract DE-FG02-85ER-25001)
(DE92-000032; DOE/ER-25001/T6) Avail: NTIS HC/MF A04

The following subject areas are covered: Cedar system hardware; compiler and software issues on memory management; operating systems; compilers; and multiprocessor performance on algorithms and applications. DOE

N92-11690# Lawrence Livermore National Lab., CA.
A DOMAIN DECOMPOSITION ALGORITHM FOR SOLVING LARGE ELLIPTIC PROBLEMS Ph.D. Thesis
M. P. Nolan Jan. 1991 114 p
(Contract W-7405-eng-48)
(DE92-000096; UCRL-LR-108186) Avail: NTIS HC/MF A06

An algorithm which efficiently solves large systems of equations arising from the discretization of a single second-order elliptic partial differential equation is discussed. The global domain is partitioned into not necessarily disjoint subdomains which are traversed using the Schwarz Alternating Procedure. On each subdomain the multigrid method is used to advance the solution. The algorithm has the potential to decrease solution time when data is stored across multiple levels of a memory hierarchy. Results are presented for a virtual memory, vector multiprocessor architecture. A study of choice of inner iteration procedure and subdomain overlap is presented for a model problem, solved with two and four subdomains, sequentially and in parallel. Microtasking multiprocessing results are reported for multigrid on the Alliant FX-8 vector-multiprocessor. A convergence proof for a class of matrix splittings for the two-dimensional Helmholtz equation is given. DOE

N92-11691*# National Aeronautics and Space Administration. Lewis Research Center, Cleveland, OH.
COMPUTER PROGRAM FOR BESSEL AND HANKEL FUNCTIONS
Kevin L. Kreider (Akron Univ., OH.), Arthur V. Saule, Edward J. Rice, and Bruce J. Clark Oct. 1991 66 p
(NASA-TM-105154; E-6439; NAS 1.15:105154) Avail: NTIS HC/MF A04 CSCL 09B

A set of FORTRAN subroutines for calculating Bessel and Hankel functions is presented. The routines calculate Bessel and Hankel functions of the first and second kinds, as well as their derivatives, for wide ranges of integer order and real or complex argument in single or double precision. Depending on the order and argument, one of three evaluation methods is used: the power series definition, an Airy function expansion, or an asymptotic expansion. Routines to calculate Airy functions and their derivatives are also included. Author

N92-11056*# Computer Sciences Corp., Greenbelt, MD.
POLYNOMIAL OPTIMIZATION TECHNIQUES FOR ACTIVITY SCHEDULING. OPTIMIZATION BASED PROTOTYPE SCHEDULER
Surender Reddy *In* NASA. Goddard Space Flight Center, Space Network Control Conference on Resource Allocation Concepts and Approaches Sep. 1991 p 207-215 (For primary document see N92-11039 02-17)
Avail: NTIS HC/MF A13 CSCL 09B

N92-11060*# McDonnell-Douglas Space Systems Co., Houston, TX.
RESOURCE REPRESENTATION IN COMPASS
Barry R. Fox *In* NASA. Goddard Space Flight Center, Space Network Control Conference on Resource Allocation Concepts and Approaches Sep. 1991 p 241-256 (For primary document see N92-11039 02-17)
Avail: NTIS HC/MF A13 CSCL 09B

N92-11063*# National Aeronautics and Space Administration. Goddard Space Flight Center, Greenbelt, MD.
A PLANNING LANGUAGE FOR ACTIVITY SCHEDULING
David R. Zoch, David LaVallee, Stuart Weinstein (Ford Aerospace and Communications Corp., Seabrook, MD.), and G. Michael Tong *In its* Space Network Control Conference on Resource

Allocation Concepts and Approaches Sep. 1991 p 285-294
(For primary document see N92-11039 02-17)
Avail: NTIS HC/MF A13 CSCL 09B

N92-11735*# Massachusetts Inst. of Tech., Cambridge.
NESTED OCEAN MODELS: WORK IN PROGRESS
A. Louise Perkins *In* ICASE, Proceedings for the ICASE Workshop on Heterogeneous Boundary Conditions Aug. 1991 p 60-69
(For primary document see N92-11728 02-64)
Avail: NTIS HC/MF A05 CSCL 09B

62 COMPUTER SYSTEMS

Includes computer networks and special application computer systems.

N92-11692*# Research Inst. for Advanced Computer Science, Moffett Field, CA.
SOME FAST ELLIPTIC SOLVERS ON PARALLEL ARCHITECTURES AND THEIR COMPLEXITIES
E. Gallopoulos (Illinois Univ. at Urbana-Champaign, Savoy.) and Youcef Saad Apr. 1989 32 p Previously announced in IAA as A90-18679 Sponsored in cooperation with AT&T
(Contract NCC2-387; NSF MIP-84-10110; NSF DCR-85-09970; NSF CCR-87-17942)
(NASA-CR-188840; NAS 1.26:188840; RIACS-TR-89-16) Avail: NTIS HC/MF A03 CSCL 09B

The discretization of separable elliptic partial differential equations leads to linear systems with special block triangular matrices. Several methods are known to solve these systems, the most general of which is the Block Cyclic Reduction (BCR) algorithm which handles equations with nonconsistant coefficients. A method was recently proposed to parallelize and vectorize BCR. Here, the mapping of BCR on distributed memory architectures is discussed, and its complexity is compared with that of other approaches, including the Alternating-Direction method. A fast parallel solver is also described, based on an explicit formula for the solution, which has parallel computational complexity lower than that of parallel BCR. Author

N92-11693*# Research Inst. for Advanced Computer Science, Moffett Field, CA.
EFFICIENT ICCG ON A SHARED MEMORY MULTIPROCESSOR
Steven W. Hammond (Rensselaer Polytechnic Inst., Troy, NY.) and Robert Schreiber May 1989 33 p Submitted for publication
(Contract NCC2-387)
(NASA-CR-188843; NAS 1.26:188843; RIACS-TR-89-24) Avail: NTIS HC/MF A03 CSCL 09B

Different approaches are discussed for exploiting parallelism in the ICCG (Incomplete Cholesky Conjugate Gradient) method for solving large sparse symmetric positive definite systems of equations on a shared memory parallel computer. Techniques for efficiently solving triangular systems and computing sparse matrix-vector products are explored. Three methods for scheduling the tasks in solving triangular systems are implemented on the Sequent Balance 21000. Sample problems that are representative of a large class of problems solved using iterative methods are used. We show that a static analysis to determine data dependences in the triangular solve can greatly improve its parallel efficiency. We also show that ignoring symmetry and storing the whole matrix can reduce solution time substantially. Author

N92-11694*# Research Inst. for Advanced Computer Science, Moffett Field, CA.
POLICY ISSUES IN INTERCONNECTING NETWORKS
Barry M. Leiner Jun. 1989 49 p
(Contract NCC2-387)
(NASA-CR-188844; NAS 1.26:188844; RIACS-TR-89-25) Avail: NTIS HC/MF A03 CSCL 09B

To support the activities of the Federal Research Coordinating Committee (FRICC) in creating an interconnected set of networks to serve the research community, two workshops were held to address the technical support of policy issues that arise when interconnecting such networks. The workshops addressed the required and feasible technologies and architectures that could be used to satisfy the desired policies for interconnection. The results of the workshop are documented. Author

N92-11695*# Research Inst. for Advanced Computer Science, Moffett Field, CA.
THE ARPANET AFTER TWENTY YEARS
Peter J. Denning 20 Sep. 1989 15 p Submitted for publication
(Contract NCC2-387)
(NASA-CR-188853; NAS 1.26:188853; RIACS-TR-89-38) Avail: NTIS HC/MF A03 CSCL 09B

The ARPANET began operations in 1969 with four nodes as an experiment in resource sharing among computers. It has evolved into a worldwide research network of over 60,000 nodes, influencing the design of other networks in business, education, and government. It demonstrated the speed and reliability of packet-switching networks. Its protocols have served as the models for international standards. And yet the significance of the ARPANET lies not in its technology, but in the profound alterations networking has produced in human practices. Network designers must now turn their attention to the discourses of scientific technology, business, education, and government that are being mixed together in the milieux of networking, and in particular the conflicts and misunderstandings that arise from the different world views of these discourses. Author

N92-11696*# Research Inst. for Advanced Computer Science, Moffett Field, CA.
OPTIMAL EXPRESSION EVALUATION FOR DATA PARALLEL ARCHITECTURES
John R. Gilbert (Xerox Palo Alto Research Center, CA.) and Robert Schreiber 24 Apr. 1990 19 p Sponsored in part by USRA
(Contract NCC2-387)
(NASA-CR-187773; NAS 1.26:187773; RIACS-TR-90-15) Avail: NTIS HC/MF A03 CSCL 09B

A data parallel machine represents an array or other composite data structure by allocating one processor (at least conceptually) per data item. A pointwise operation can be performed between two such arrays in unit time, provided their corresponding elements are allocated in the same processors. If the arrays are not aligned in this fashion, the cost of moving one or both of them is part of the cost of the operation. The choice of where to perform the operation then affects this cost. If an expression with several operands is to be evaluated, there may be many choices of where to perform the intermediate operations. An efficient algorithm is given to find the minimum-cost way to evaluate an expression, for several different data parallel architectures. This algorithm applies to any architecture in which the metric describing the cost of moving an array is robust. This encompasses most of the common data parallel communication architectures, including meshes of arbitrary dimension and hypercubes. Remarks are made on several variations of the problem, some of which are solved and some of which remain open. Author

N92-11697*# Research Inst. for Advanced Computer Science, Moffett Field, CA.
NEURAL NETWORKS AND MIMD-MULTIPROCESSORS
Jukka Vanhala and Kimmo Kaski Feb. 1990 17 p Sponsored in part by the Center for Technological Development in Finland (TEKES)
(Contract NCC2-387)
(NASA-CR-188481; NAS 1.26:188481; RIACS-TR-90-9) Avail: NTIS HC/MF A03 CSCL 09B

Two artificial neural network models are compared. They are the Hopfield Neural Network Model and the Sparse Distributed Memory model. Distributed algorithms for both of them are designed and implemented. The run time characteristics of the algorithms are analyzed theoretically and tested in practice. The storage

capacities of the networks are compared. Implementations are done using a distributed multiprocessor system. Author

N92-11698*# Research Inst. for Advanced Computer Science, Moffett Field, CA.
HIGHLY PARALLEL COMPUTATION
Peter J. Denning and Walter F. Tichy (Karlsruhe Univ., Germany, F.R.) 19 Aug. 1990 34 p Submitted for publication
(Contract NCC2-387)
(NASA-CR-188871; NAS 1.26:188871; RIACS-TR-90-35) Avail: NTIS HC/MF A03 CSCL 09B

Highly parallel computing architectures are the only means to achieve the computation rates demanded by advanced scientific problems. A decade of research has demonstrated the feasibility of such machines and current research focuses on which architectures designated as multiple instruction multiple datastream (MIMD) and single instruction multiple datastream (SIMD) have produced the best results to date; neither shows a decisive advantage for most near-homogeneous scientific problems. For scientific problems with many dissimilar parts, more speculative architectures such as neural networks or data flow may be needed. Author

N92-11699*# Research Inst. for Advanced Computer Science, Moffett Field, CA.
TOTAL RECALL IN DISTRIBUTIVE ASSOCIATIVE MEMORIES
Douglas G. Danforth 23 Jan. 1991 52 p
(Contracts NCC2-408; NCC2-387)
(NASA-CR-188884; NAS 1.26:188884; RIACS-TR-91-03) Avail: NTIS HC/MF A04 CSCL 09B

Iterative error correction of asymptotically large associative memories is equivalent to a one-step learning rule. This rule is the inverse of the activation function of the memory. Spectral representations of nonlinear activation functions are used to obtain the inverse in closed form for Sparse Distributed Memory, Selected-Coordinate Design, and Radial Basis Functions. Author

N92-11700*# Research Inst. for Advanced Computer Science, Moffett Field, CA.
ORDERED FAST FOURIER TRANSFORMS ON A MASSIVELY PARALLEL HYPERCUBE MULTIPROCESSOR
Charles Tong and Paul N. Swarztrauber (National Center for Atmospheric Research, Boulder, CO.) Dec. 1989 30 p
(Contract NCC2-387)
(NASA-CR-188899; NAS 1.26:188899; RIACS-TR-89-50) Avail: NTIS HC/MF A03 CSCL 09B

Design alternatives for ordered Fast Fourier Transformation (FFT) algorithms were examined on massively parallel hypercube multiprocessors such as the Connection Machine. Particular emphasis is placed on reducing communication which is known to dominate the overall computing time. To this end, the order and computational phases of the FFT were combined, and the sequence to processor maps that reduce communication were used. The class of ordered transforms is expanded to include any FFT in which the order of the transform is the same as that of the input sequence. Two such orderings are examined, namely, standard-order and A-order which can be implemented with equal ease on the Connection Machine where orderings are determined by geometries and priorities. If the sequence has $N = 2 \exp r$ elements and the hypercube has $P = 2 \exp d$ processors, then a standard-order FFT can be implemented with $d + r/2 + 1$ parallel transmissions. An A-order sequence can be transformed with $2d - r/2$ parallel transmissions which is $r - d + 1$ fewer than the standard order. A parallel method for computing the trigonometric coefficients is presented that does not use trigonometric functions or interprocessor communication. A performance of 0.9 GFLOPS was obtained for an A-order transform on the Connection Machine. Author

N92-11701*# Research Inst. for Advanced Computer Science, Moffett Field, CA.
ANALYSIS OF A PARALLEL MULTIGRID ALGORITHM
Tony F. Chan and Ray S. Tuminaro (Stanford Univ., CA.) Oct. 1989 24 p Previously announced in IAA as A90-29130
(Contracts NCC2-387; NCA2-233; DE-FG03-87ER-25037; DAAL03-88-K-0085; NSF DMS-87-14612)
(NASA-CR-188906; NAS 1.26:188906; RIACS-TR-89-41) Avail: NTIS HC/MF A03 CSCL 09B

The parallel multigrid algorithm of Frederickson and McBryan (1987) is considered. This algorithm uses multiple coarse-grid problems (instead of one problem) in the hope of accelerating convergence and is found to have a close relationship to traditional multigrid methods. Specifically, the parallel coarse-grid correction operator is identical to a traditional multigrid coarse-grid correction operator, except that the mixing of high and low frequencies caused by aliasing error is removed. Appropriate relaxation operators can be chosen to take advantage of this property. Comparisons between the standard multigrid and the new method are made. Author

N92-11702*# Research Inst. for Advanced Computer Science, Moffett Field, CA.
GROUND SYSTEMS DEVELOPMENT ENVIRONMENT (GSDE) INTERFACE REQUIREMENTS ANALYSIS Final Report
Victor E. Church, John Philips, Ray Hartenstein, Mitchell Bassman, Leslie Ruskin, and Alfredo Perez-Davila Jun. 1991 106 p Prepared in cooperation with Computer Sciences Corp., Beltsville, MD and Computer Sciences Corp., and Computer Sciences Corp., Falls Church, VA
(Contract NCC9-16; RICIS Proj. SE-34)
(NASA-CR-188822; NAS 1.26:188822; CSC/TM-91/6102) Avail: NTIS HC/MF A06 CSCL 09B

A set of procedural and functional requirements are presented for the interface between software development environments and software integration and test systems used for space station ground systems software. The requirements focus on the need for centralized configuration management of software as it is transitioned from development to formal, target based testing. This concludes the GSDE Interface Requirements study. A summary is presented of findings concerning the interface itself, possible interface and prototyping directions for further study, and results of the investigation of the Cronus distributed applications environment. Author

N92-11703# Superconducting Super Collider Lab., Dallas, TX.
BCD/CPS: AN EVENT-LEVEL GEANT3 PARALLELIZATION VIA CPS
L. A. Roberts Apr. 1991 47 p
(Contract DE-AC35-89ER-40486)
(DE91-017238; SSCL-413) Avail: NTIS HC/MF A03

BCD/CPS is an implementation of the Bottom Collider Detector GEANT3 simulation for CPS processor ranches. BCD/CPS demonstrates some of the capabilities of event-parallel applications applicable to current SSC detector simulations using the CPS and CZ/CPS communications protocols. Design, implementation and usage of the BCD/CPS simulation are presented along with extensive source listings for novice GEANT3/CPS programmers. DOE

N92-11704*# Draper (Charles Stark) Lab., Inc., Cambridge, MA.
ADVANCED INFORMATION PROCESSING SYSTEM FOR ADVANCED LAUNCH SYSTEM: AVIONICS ARCHITECTURE SYNTHESIS
Jaynarayan H. Lala, Richard E. Harper, Kenneth R. Jaskowiak, Gene Rosch, Linda S. Alger, and Andrei L. Schor Sep. 1991 155 p Original contains color illustrations
(Contract NAS1-18565)
(NASA-CR-187554; NAS 1.26:187554) Avail: NTIS HC/MF A08; 1 functional color page CSCL 09B

The Advanced Information Processing System (AIPS) is a fault-tolerant distributed computer system architecture that was developed to meet the real time computational needs of advanced aerospace vehicles. One such vehicle is the Advanced Launch System (ALS) being developed jointly by NASA and the Department of Defense to launch heavy payloads into low earth orbit at one tenth the cost (per pound of payload) of the current launch vehicles.

An avionics architecture that utilizes the AIPS hardware and software building blocks was synthesized for ALS. The AIPS for ALS architecture synthesis process starting with the ALS mission requirements and ending with an analysis of the candidate ALS avionics architecture is described. Author

N92-11705*# Draper (Charles Stark) Lab., Inc., Cambridge, MA.
ADVANCED INFORMATION PROCESSING SYSTEM FOR ADVANCED LAUNCH SYSTEM: HARDWARE TECHNOLOGY SURVEY AND PROJECTIONS
Richard Cole Sep. 1991 76 p
(Contract NAS1-18565)
(NASA-CR-187555; NAS 1.26:187555) Avail: NTIS HC/MF A05 CSCL 09B

The major goals of this effort are as follows: (1) to examine technology insertion options to optimize Advanced Information Processing System (AIPS) performance in the Advanced Launch System (ALS) environment; (2) to examine the AIPS concepts to ensure that valuable new technologies are not excluded from the AIPS/ALS implementations; (3) to examine advanced microprocessors applicable to AIPS/ALS, (4) to examine radiation hardening technologies applicable to AIPS/ALS; (5) to reach conclusions on AIPS hardware building blocks implementation technologies; and (6) reach conclusions on appropriate architectural improvements. The hardware building blocks are the Fault-Tolerant Processor, the Input/Output Sequencers (IOS), and the Intercomputer Interface Sequencers (ICIS). Author

N92-11706*# Draper (Charles Stark) Lab., Inc., Cambridge, MA.
ADVANCED INFORMATION PROCESSING SYSTEM: INTER-COMPUTER COMMUNICATION SERVICES
Laura Burkhardt, Tom Masotto, J. Terry Sims, Roy Whittredge, and Linda S. Alger Sep. 1991 340 p Original contains color illustrations
(Contract NAS1-18565)
(NASA-CR-187556; NAS 1.26:187556) Avail: NTIS HC/MF A15; 1 functional color page CSCL 09B

The purpose is to document the functional requirements and detailed specifications for the Inter-Computer Communications Services (ICCS) of the Advanced Information Processing System (AIPS). An introductory section is provided to outline the overall architecture and functional requirements of the AIPS and to present an overview of the ICCS. An overview of the AIPS architecture as well as a brief description of the AIPS software is given. The guarantees of the ICCS are provided, and the ICCS is described as a seven-layered International Standards Organization (ISO) Model. The ICCS functional requirements, functional design, and detailed specifications as well as each layer of the ICCS are also described. A summary of results and suggestions for future work are presented. Author

N92-11707# Connecticut Univ., Storrs. Dept. of Mathematics.
CONVERGENCE AND PERFORMANCE OF SYNCHRONOUS AND ASYNCHRONOUS PARALLEL AND CONVENTIONAL ITERATIVE METHODS Final Report, 1 Nov. 1987 - 30 Jun. 1991
Michael Neumann Aug. 1991 29 p
(Grant AF-AFOSR-0047-88)
(AD-A240286; AFOSR-91-0750TR) Avail: NTIS HC/MF A03 CSCL 12/1

Parallel and sequential iterative methods for linear and nonlinear systems are investigated. Much of the work on this topic concentrated on the convergence and rate of convergence of parallel asynchronized methods for solving linear systems arising, on the one hand, from the numerical solution to partial differential equations and, on the other hand, from least squares solution to rectangular systems which arise in application such as image reconstruction from incomplete tomographical data. The mathematics behind the analysis of these two applications of the asynchronized parallel methods is quite different. Recently they have been able to extend their convergence results to asynchronized methods for solving nonlinear systems. One application now consists of tomographic reconstruction from incomplete data where the image is constrained to lie in a bounded convex set such as an n dimensional box. GRA

N92-11708# Technische Univ., Berlin (Germany, F.R.). Fachbereich Informatik.
A SYNCHRONIZATION AND CHARGE DISTRIBUTION PROCESS FOR THE PARALLEL MULTILEVEL LOGIC SIMULATION Ph.D. Thesis [EIN VERFAHREN ZUR SYNCHRONISATION UND LASTVERTEILUNG FUER DIE PARALLELE MEHREBENENLOGIKSIMULATION]
Fiedrich Hoppe 1991 165 p In GERMAN
(ETN-91-90152) Avail: NTIS HC/MF A08

A parallel multilevel simulator kernel is designed for digital circuits, which allows the combination of simulation models on the levels of register transfer, block function, gate, and switch. A variant of a so called time warp method is realized. Charge distribution is determined by the communication structure of the partial system, and the activity of the elements. The actual charge distribution in the system is determined during the simulation. An adaptive and semi-adaptive process is developed for the rearrangement of elements. It is shown that, by using the charge distribution process, the simulation velocity can be increased from 2 to 38. ESA

N92-11709# Lawrence Livermore National Lab., CA.
HARNESSING THE KILLER MICROS: APPLICATIONS FROM LLNL'S MASSIVELY PARALLEL COMPUTING INITIATIVE
J. F. Belak Jul. 1991 13 p Presented at the Workshop on Parallel Computation in Chemistry, Willowbrook, IL, 17-19 Jul. 1991
(Contract W-7405-eng-48)
(DE91-018721; UCRL-JC-108197; CONF-910799-1) Avail: NTIS HC/MF A03

Recent developments in microprocessor technology have led to performance on scalar applications exceeding traditional supercomputers. This suggests that coupling hundreds or even thousands of these killer-micros (all working on a single physical problem) may lead to performance on vector applications in excess of vector supercomputers. Also, future generation killer-micros are expected to have vector floating point units as well. The purpose of this paper is to present an overview of the parallel computing environment at Lawrence Livermore National Laboratory. However, the perspective is necessarily quite narrow and most of the examples are taken from the author's implementation of a large scale molecular dynamics code on the BBN-TC2000 at LLNL. Parallelism is achieved through a geometric domain decomposition -- each processor is assigned a distinct region of space and all atoms contained therein. As the atomic positions evolve, the processors must exchange ownership of specific atoms. This geometric domain decomposition proves to be quite general and we highlight its application to image processing and hydrodynamics simulations as well. DOE

N92-11710# Argonne National Lab., IL.
STUDYING PARALLEL PROGRAM BEHAVIOR WITH UPSHOT
V. Herrarte and E. Lusk Aug. 1991 11 p
(Contract W-31-109-eng-38)
(DE91-019072; ANL-91/15) Avail: NTIS HC/MF A03

This is a description of and a user's manual for upshot, an X-based graphics tool for viewing log files produced by parallel programs. DOE

63 CYBERNETICS

Includes feedback and control theory, artificial intelligence, robotics and expert systems.

For related information see also *54 Man/System Technology and Life Support.*

N92-11711*# Research Inst. for Advanced Computer Science, Moffett Field, CA.

LEARNING TO READ ALOUD: A NEURAL NETWORK APPROACH USING SPARSE DISTRIBUTED MEMORY

Umesh Dwarkanath Joglekar Jul. 1989 99 p

(Contracts NCC2-387; NCC2-408)

(NASA-CR-188846; NAS 1.26:188846; RIACS-TR-89-27) Avail: NTIS HC/MF A05 CSCL 09B

An attempt to solve a problem of text-to-phoneme mapping is described which does not appear amenable to solution by use of standard algorithmic procedures. Experiments based on a model of distributed processing are also described. This model (sparse distributed memory (SDM)) can be used in an iterative supervised learning mode to solve the problem. Additional improvements aimed at obtaining better performance are suggested. Author

N92-11712*# National Inst. of Standards and Technology, Gaithersburg, MD. Intelligent Controls Group.

GENERATION OF SMOOTH TRAJECTORIES WITHOUT PLANNING

John C. Fiala Nov. 1988 19 p

(NASA Order S-28187-D)

(NASA-CR-189013; NAS 1.26:189013; PB91-217414; NISTIR-4622) Avail: NTIS HC/MF A03 CSCL 09B

A technique for generating smooth trajectories of a system is presented. The approach is to find a dynamical equation with the desired transient behavior and use it as the basis of the control algorithm. It is shown that an appropriate dynamical equation can be obtained by varying the position and velocity gains of a proportional derivative control loop over the duration of the movement. The dynamical equation can be used to generate trajectories online with minimal planning. The resulting manipulator control system responds to path errors in a more reasonable fashion than traditional approaches to trajectory control since explicit planning is not required. Author

N92-11713# Office National d'Etudes et de Recherches Aerospatiales, Paris (France). Direction Scientifique de la Resistance des Structures.

OPTIMAL CONTROL BY WIDEBAND FREQUENCY. APPLICATION TO ACOUSTIC CONTROL BY PIEZOELECTRIC TECHNIQUE Final Report [CONTROLE OPTIMAL PAR LARGE BANDE DE FREQUENCE. APPLICATION AU CONTROLE ACOUSTIQUE PAR TECHNIQUE PIEZOELECTRIQUE. RAPPORT FINAL]

N. Meidinger Nov. 1990 78 p In FRENCH

(Contract DRET-89-34-001)

(ONERA-RT-6/3654-RY-006-R; ETN-91-90089) Avail: NTIS HC/MF A05

The definition of the problem of wideband frequency optimal control for a large class of variably complex dynamical systems is addressed. Existence and uniqueness of the solutions are examined. The problem is discretized by finite elements. The numerical resolution is optimized, proceeded by narrowband frequency. Relationships between optimal and physically realizable control are focussed. A closed loop numerical simulation method calling up causative stable control filters is detailed. The wideband optimal control is applied to acoustic control via a piezoelectric technique operating on a plate noise source. ESA

64 NUMERICAL ANALYSIS

Includes iteration, difference equations, and numerical approximation.

N92-11714# Grenoble-1 Univ. (France). Lab. de Modelisation et Calcul.

ON THE THEORY AND NUMERICAL APPROXIMATION OF NONLINEAR HYPERBOLIC PROBLEMS Ph.D. Thesis - Constantine Univ. [SUR LA THEORIE ET L'APPROXIMATION NUMERIQUE DE PROBLEMES HYPERBOLIQUES NON LINEAIRES]

Abdallah Chalabi 1990 208 p In ENGLISH and FRENCH

(ETN-91-99898) Avail: NTIS HC/MF A10

Scalar conservation laws are addressed. The stability and convergence of quasi order two schemes of Van Leer type for homogeneous and inhomogeneous laws are studied. The theoretical and numerical study of Saint Vernant system is carried out. The existence and the uniqueness of the solution of the viscous problem are established by a compacity method and Gronwall inequality. The numerical approximation is carried out by the finite element method. A monotone method proves the existence and the uniqueness of the solution in the case of a perfect fluid. The Riemann problem is resolved in a monodimensional case. The method of fractional steps and its consistency with entropic condition is presented, as well as the convergence of associated schemes. For individual titles, see N92-11715 through N92-11721.

N92-11715# Grenoble-1 Univ. (France). Tech. de l'Informatique, des Math., de la Microelectronique et de la Microscopie Quantitative.

ON A CLASS OF IMPLICIT AND EXPLICIT SCHEMES OF VAN-LEER TYPE FOR SCALAR CONSERVATION LAWS

Abdallah Chalabi and J. P. Vila (Centre Machinisme Agricole Genie Rural Eaux Forets, Saint-Martin d'Heres, France) *In its* On the Theory and Numerical Approximation of Nonlinear Hyperbolic Problems 1990 26 p Repr. from M2AN, v. 23, 1989 pp 261-282 (For primary document see N92-11714 02-64)

Avail: NTIS HC/MF A10

Physical problems where flux is the physical variable are addressed. The convergence of second order accurate schemes towards the entropy solution of scalar conservation law is studied. The Van Leer method is used to obtain an affine approximation of the flux. The construction procedure leads to Total Variation Diminishing (TVD) schemes in the implicit and in the explicit cases. The proposed schemes can be presented as corrected upwind schemes. ESA

N92-11716# Grenoble-1 Univ. (France). Tech. de l'Informatique, des Math., de la Microelectronique et de la Microscopie Quantitative.

STABLE UPWIND SCHEMES FOR HYPERBOLIC CONSERVATION LAWS FOR WITH SOURCE TERMS

Abdallah Chalabi *In its* On the Theory and Numerical Approximation of Nonlinear Hyperbolic Problems 1990 41 p Submitted for publication (For primary document see N92-11714 02-64)

Avail: NTIS HC/MF A10

A class of stable upwind schemes for the numerical solution of nonhomogeneous hyperbolic conservation laws is given. Explicit and implicit explicit schemes of first and second order accuracy are studied. Stationary solutions are used as data in the first order case. The constructed schemes are not Total Variation Diminishing (TVD) schemes, on account of the source term effect. They are locally Total Variation Bounded (TVB) schemes. The convergence of the numerical solution towards the entropy solution is proved. ESA

N92-11717# Grenoble-1 Univ. (France). Tech. de l'Informatique, des Math., de la Microelectronique et de la Microscopie Quantitative.

AN ANALYSIS OF UPWIND SCHEMES FOR INHOMOGENEOUS TWO DIMENSIONAL CONSERVATION LAWS

Abdallah Chalabi *In its* On the Theory and Numerical Approximation of Nonlinear Hyperbolic Problems 1990 17 p In FRENCH; ENGLISH summary Submitted for publication (For primary document see N92-11714 02-64)
Avail: NTIS HC/MF A10

The proposed schemes are first and second order accurate. The stability and the convergence of upwind schemes for two dimensional conservation laws with source term are reported. Preliminaries concerning the entropy solution are recalled. The convergence of first order implicit and explicit schemes is studied. The quasi order two scheme stability in space is examined. Numerical results are given. ESA

N92-11718# Grenoble-1 Univ. (France). Tech. de l'Informatique, des Math., de la Microelectronique et de la Microscopie Quantitative.
AN ANALYSIS OF SOME HYPERBOLIC PROBLEMS RELATED TO THE SHALLOW WATER MODEL (CHAPTER 6)
Abdallah Chalabi *In its* On the Theory and Numerical Approximation of Nonlinear Hyperbolic Problems 1990 19 p (For primary document see N92-11714 02-64)
(IMAG-RR-579) Avail: NTIS HC/MF A10

The system of the shallow water model is strictly hyperbolic and admits a strict convex entropy function. An analysis of the three possible formulations of the model is given together with the study of the Riemann problem. The uniqueness of the regular solution for the two dimensional case is stated. Problems of long waves in shallow water are examined. Various cases are studied in Eulerian and Lagrange coordinates. A nonreflecting boundary condition is given for the one dimensional problem. ESA

N92-11719# Grenoble-1 Univ. (France). Tech. de l'Informatique, des Math., de la Microelectronique et de la Microscopie Quantitative.
OPERATOR SPLITTING, FRACTIONAL STEPS, METHOD AND ENTROPY CONDITION FOR NONLINEAR HYPERBOLIC SYSTEMS [ECLATEMENT D'OPERATEUR, METHODE A PAS FRACTIONNAIRES ET CONDITION D'ENTROPIE POUR LES SYSTEMES HYPERBOLIQUES NON LINEAIRES (CHAPITRE 7)]
J. P. Vila *In its* On the Theory and Numerical Approximation of Nonlinear Hyperbolic Problems 1990 12 p In FRENCH Presented at the Colloque International sur les Problemes Hyperboliques, Uppsala, Sweden, Jun. 1990 (For primary document see N92-11714 02-64)
Avail: NTIS HC/MF A10

A characterization of proper splitting is given, in order to obtain hyperbolic subsystems which have the same entropy as initial systems. It is shown that, in the conservative case, if the solution obtained by the fractional steps converges, it converges towards an entropy solution of the initial problem. Splitting is considered for a nonlinear hyperbolic problem. Conservative splitting is studied. Two types of scheme are proposed, for which the convergence towards an entropy solution is studied. A procedure for the construction of allowable splitting leading to conservative subsystems is given. ESA

N92-11720# Grenoble-1 Univ. (France). Lab. de Mathematiques Appliquees.
NUMERICAL ANALYSIS OF THE PROBLEM OF LONG WAVES IN SHALLOW WATER [ANALYSE NUMERIQUE DU PROBLEME DES ONDES LONGUES EN EAU PEU PROFONDE (CHAPITRE 8)]
Abdallah Chalabi (Constantine Univ., Algeria) *In its* On the Theory and Numerical Approximation of Nonlinear Hyperbolic Problems 1990 21 p Repr. from Calcolo, v. 19, fasc. 3, Jul. - Sep. 1982 p 269-288 In FRENCH; ENGLISH summary (For primary document see N92-11714 02-64)
Avail: NTIS HC/MF A10

The problem of long waves in viscous shallow water is considered. A result of existence and uniqueness is given for this problem, thus extending a one dimensional result to a bidimensional case. A compacity method is used. The stability of the implicit scheme proposed, and the convergence towards the continuous problem solution are shown. The boundary conditions are homogeneous for the two components of velocity, on account of the boundary layer neighboring the border. It is shown that the boundary condition on liquid total deepness can be inhomogeneous. ESA

N92-11721# Grenoble-1 Univ. (France).
ON THE SOLUTION FOR THE PROBLEM OF LONG WAVES IN A PERFECT FLUID [SUR LA RESOLUTION DU PROBLEME DES ONDES LONGUES DANS UN FLUIDE PARFAIT]
Abdallah Chalabi (Constantine Univ., Algeria) *In its* On the Theory and Numerical Approximation of Nonlinear Hyperbolic Problems 1990 20 p Repr. from Afrika Matematika, v. 6, 1984 pp 31-48 In FRENCH; ENGLISH summary (For primary document see N92-11714 02-64)
Avail: NTIS HC/MF A10

The existence and the uniqueness of the solution for the problem of long waves in a perfect fluid are established. A theoretical study is presented for damped long waves in a perfect fluid. An example of positive maximal boundary condition is given. Monotone method is used for the treatment of the nonlinear part of the equations. Friction force is taken into account. ESA

N92-11722*# Research Inst. for Advanced Computer Science, Moffett Field, CA.
OPTIMAL CHEBYSHEV POLYNOMIALS ON ELLIPSES IN THE COMPLEX PLANE
Bernd Fischer and Roland Freund (Wuerzburg Univ., Germany, F.R.) Feb. 1989 8 p
(Contract NCC2-387)
(NASA-CR-188836; NAS 1.26:188836; RIACS-TR-89-5) Avail: NTIS HC/MF A02 CSCL 12A

The design of iterative schemes for sparse matrix computations often leads to constrained polynomial approximation problems on sets in the complex plane. For the case of ellipses, we introduce a new class of complex polynomials which are in general very good approximations to the best polynomials and even optimal in most cases. Author

N92-11723*# Research Inst. for Advanced Computer Science, Moffett Field, CA.
AN IMPROVED NEWTON ITERATION FOR THE GENERALIZED INVERSE OF A MATRIX, WITH APPLICATIONS
Victor Pan (State Univ. of New York, Albany.) and Robert Schreiber Mar. 1990 40 p Prepared in cooperation with Lehman (Herbert H.) Coll., Bronx, NY, and Rensselaer Polytechnic Inst.,Troy, NY Submitted for publication
(Contracts NCC2-387; N00014-86-K-0610; NSF CCR-88-05782; DAAL03-86-K-0112)
(NASA-CR-186983; NAS 1.26:186983; RIACS-TR-90-16) Avail: NTIS HC/MF A03 CSCL 12A

The purpose here is to clarify and illustrate the potential for the use of variants of Newton's method of solving problems of practical interest on highly personal computers. The authors show how to accelerate the method substantially and how to modify it successfully to cope with ill-conditioned matrices. The authors conclude that Newton's method can be of value for some interesting computations, especially in parallel and other computing environments in which matrix products are especially easy to work with. Author

N92-11724*# Research Inst. for Advanced Computer Science, Moffett Field, CA.
NEW BERNSTEIN TYPE INEQUALITIES FOR POLYNOMIALS ON ELLIPSES
Roland Freund and Bernd Fischer (Hamburg Univ., Germany, F.R.) Mar. 1990 23 p Sponsored in part by the German Research Association
(Contract NCC2-387)
(NASA-CR-186626; NAS 1.26:186626; RIACS-TR-90-12) Avail: NTIS HC/MF A03 CSCL 12A

New and sharp estimates are derived for the growth in the complex plane of polynomials known to have a curved majorant

on a given ellipse. These so-called Bernstein type inequalities are closely connected with certain constrained Chebyshev approximation problems on ellipses. Also presented are some new results for approximation problems of this type. Author

N92-11725# Oak Ridge National Lab., TN.
GORTER-MELLINK PULSED-SOURCE PROBLEM IN CYLINDRICAL AND SPHERICAL GEOMETRY
L. Dresner 1991 15 p Presented at the 2nd US-Japan Joint Seminar on Basic Mechanisms of Helium Heat Transfer and Related Influence on Stability, Los Angeles, CA, 26-30 Aug. 1991
(Contract DE-AC05-84OR-21400)
(DE91-017249; CONF-9108132-1) Avail: NTIS HC/MF A03

An exact solution to the Gorter-Mellink pulsed source problem is known in plane geometry. According to this solution, the central temperature falls as t(exp -3/2), where t is the elapsed time after an instantaneous, plane pulse. No such exact solutions are known to the pulsed source problem in cylindrical and spherical geometry. But in cylindrical geometry, it can be shown that if the initial condition is an instantaneous temperature rise (Delta)T inside a cylinder of radius R, the central temperature is bounded from above by a decreasing exponential function of time. The relaxation time of this exponential is related to (Delta)T and R. In spherical geometry, it can be shown that if the initial condition is an instantaneous temperature rise (Delta)T inside a sphere of radius R, the central temperature is bounded from above by a function proportional to (t sub 0 -t)(exp 9/2). The extinction time t sub 0 is related to (Delta)T and R. These predictions have not been tested by experiment, and the author recommends such experiments. DOE

N92-11726# Argonne National Lab., IL.
ISSUES IN PARALLEL AUTOMATIC DIFFERENTIATION
Christian H. Bischof 1991 14 p Presented at the Society for Industrial and Applied Mathematics (SIAM) Workshop on Automatic Differentiation of Algorithms: Theory, Implementation, and Application, Breckenridge, CO, 6-8 Jan. 1991
(Contract W-31-109-eng-38)
(DE91-017311; ANL/CP-73798; CONF-910189-2) Avail: NTIS HC/MF A03

In this paper we show how first-order derivatives can be computed in parallel by considering the computational graph that underlies the evaluation of the target function. We show how this graph can be generated efficiently from the ADOL-C computational trace, and how is can be used to automatically deduce the structure of the Jacobian matrix, and compute the Jacobian using the reverse mode of automatic differentiation. By employing well-known graph coloring techniques, we drastically decrease the number of reverse passes required, and the resulting implementation performs well on the Sequent Symmetry and BBN Butterfly TC2000 shared-memory multiprocessors. Lastly, we give an outlook on the problems that have to be tackled to make automatic differentiation the commonplace computing tool it deserves to be, and to allow for efficient implementations on high-performance computers. In our view, the key lies in finding better ways to incorporate user and/or compile-time information about the behavior of the program into the automatic differentiation approach. DOE

N92-11727# National Inst. of Standards and Technology, Gaithersburg, MD. Computing and Applied Mathematics Lab.
PORTABLE VECTORIZED SOFTWARE FOR BESSEL FUNCTION EVALUATION
Ronald F. Boisvert and Bonita V. Saunders 19 Jun. 1991 18 p
(PB91-216598; NISTIR-4615) Avail: NTIS HC/MF A03 CSCL 12A

A suite of computer programs for the evaluation of Bessel functions and modified Bessel functions of orders zero and one for a vector of real arguments is described. Distinguishing characteristics of these programs are that they are portable across a wide range of machines, and they are vectorized in the case where multiple function evaluations are to be performed. The performance of the new programs are compared with software from the FNLIB collection of Fullerton on which the new software is based. Author

N92-11728*# Institute for Computer Applications in Science and Engineering, Hampton, VA.
PROCEEDINGS FOR THE ICASE WORKSHOP ON HETEROGENEOUS BOUNDARY CONDITIONS Final Report
A. Louise Perkins and Jeffrey S. Scroggs (North Carolina State Univ., Raleigh.) Aug. 1991 79 p Workshop held in Hampton, VA, Aug. 1991
(Contract NAS1-18605)
(NASA-CR-187630; NAS 1.26:187630; ICASE-IR-19) Avail: NTIS HC/MF A05 CSCL 12A

Domain Decomposition is a complex problem with many interesting aspects. The choice of decomposition can be made based on many different criteria, and the choice of interface of internal boundary conditions are numerous. The various regions under study may have different dynamical balances, indicating that different physical processes are dominating the flow in these regions. This conference was called in recognition of the need to more clearly define the nature of these complex problems. This proceedings is a collection of the presentations and the discussion groups. For individual titles, see N92-11729 through N92-11735.

N92-11729*# Massachusetts Inst. of Tech., Cambridge.
MODEL PROBLEM **c74**
A. Louise Perkins *In* ICASE, Proceedings for the ICASE Workshop on Heterogeneous Boundary Conditions Aug. 1991 p 1-6 (For primary document see N92-11728 02-64)
Avail: NTIS HC/MF A05 CSCL 20F

Our purpose in examining this test problem is to measure directly the effect of mesh refinement and the resulting mesh interfaces on a known wave that is sensitive to phase errors, while concurrently being able to visually display a meaningful picture of the effects of the refinement induced error on the solution. The refined mesh must be able to adequately capture the diffraction behavior, so that the plane wave front bends as it passes through the slit. Given that the coarse and refined meshes are sufficiently accurate, the phase errors introduced during the problem solution will be a function of th sound speed on the two grids plus the coarse/refined grid interaction errors. Author

N92-11730*# Texas Univ., Houston.
DISCUSSION SUMMARY: FICTITIOUS DOMAIN METHODS
Rowland Glowinski and Garry Rodrigue (California Univ., Davis.) *In* ICASE, Proceedings for the ICASE Workshop on Heterogeneous Boundary Conditions Aug. 1991 p 7-8 (For primary document see N92-11728 02-64)
Avail: NTIS HC/MF A05 CSCL 12A

Fictitious Domain methods are constructed in the following manner: Suppose a partial differential equation is to be solved on an open bounded set, Omega, in 2-D or 3-D. Let R be a rectangle domain containing the closure of Omega. The partial differential equation is first solved on R. Using the solution on R, the solution of the equation on Omega is then recovered by some procedure. The advantage of the fictitious domain method is that in many cases the solution of a partial differential equation on a rectangular region is easier to compute than on a nonrectangular region. Fictitious domain methods for solving elliptic PDEs on general regions are also very efficient when used on a parallel computer. The reason is that one can use the many domain decomposition methods that are available for solving the PDE on the fictitious rectangular region. The discussion on fictitious domain methods began with a talk by R. Glowinski in which he gave some examples of a variational approach to ficititious domain methods for solving the Helmholtz and Navier-Stokes equations. Author

N92-11731*# California Univ., Los Angeles. Dept. of Mathematics.
DOMAIN-DECOMPOSED PRECONDITIONINGS FOR TRANSPORT OPERATORS
Tony F. Chan, William D. Gropp, and David E. Keyes (Yale Univ.,

New Haven, CT.) *In* ICASE, Proceedings for the ICASE Workshop on Heterogeneous Boundary Conditions Aug. 1991 p 9-27 Presented at the Third International Symposium on Domain Decomposition Methods, Siam, 1990 p 245-262 (For primary document see N92-11728 02-64)
(Contracts NAS1-18605; DE-FG03-87ER-25037; DAAL03-88-K-0085; W-31-109-eng-38; NSF ASC-90-03002; NSF ECS-89-57475)
Avail: NTIS HC/MF A05 CSCL 12A

The performance was tested of five different interface preconditionings for domain decomposed convection diffusion problems, including a novel one known as the spectral probe, while varying mesh parameters, Reynolds number, ratio of subdomain diffusion coefficients, and domain aspect ratio. The preconditioners are representative of the range of practically computable possibilities that have appeared in the domain decomposition literature for the treatment of nonoverlapping subdomains. It is shown that through a large number of numerical examples that no single preconditioner can be considered uniformly superior or uniformly inferior to the rest, but that knowledge of particulars, including the shape and strength of the convection, is important in selecting among them in a given problem. Author

N92-11732*# Los Alamos National Lab., NM. Computing and Communications Div.
LAYER TRACKING, ASYMPTOTICS, AND DOMAIN DECOMPOSITION
D. L. Brown, R. C. Y. Chin, G. W. Hedstrom, and T. A. Manteuffel (Colorado Univ., Denver.) *In* ICASE, Proceedings for the ICASE Workshop on Heterogeneous Boundary Conditions Aug. 1991 p 28-43 Previously announced as N91-21462 (For primary document see N92-11728 02-64)
Avail: NTIS HC/MF A05 CSCL 12A

A preliminary report is presented on the work on the tracking of internal layers in a singularly-perturbed convection-diffusion equation. It is shown why such tracking may be desirable, and it is also shown how to do it using domain decomposition based on asymptotic analysis. Author

N92-11733*# North Carolina State Univ., Raleigh. Dept. of Mathematics.
INTERFACE CONDITIONS FOR DOMAIN DECOMPOSITION WITH RADICAL GRID REFINEMENT
Jeffrey S. Scroggs *In* ICASE, Proceedings for the ICASE Workshop on Heterogeneous Boundary Conditions Aug. 1991 p 44-54 (For primary document see N92-11728 02-64)
(Contract NAS1-18605)
Avail: NTIS HC/MF A05 CSCL 12A

Interface conditions for coupling the domains in a physically motivated domain decomposition method are discussed. The domain decomposition is based on an asymptotic-induced method for the numerical solution of hyperbolic conservation laws with small viscosity. The method consists of multiple stages. The first stage is to obtain a first approximation using a first-order method, such as the Godunov scheme. Subsequent stages of the method involve solving internal-layer problem via a domain decomposition. The method is derived and justified via singular perturbation techniques. Author

N92-11734*# Naval Oceanographic and Atmospheric Research Lab., Bay Saint Louis, MS.
ONE-WAY NESTING FOR A PRIMITIVE EQUATION OCEAN MODEL
D. W. Blake *In* ICASE, Proceedings for the ICASE Workshop on Heterogeneous Boundary Conditions Aug. 1991 p 55-59 (For primary document see N92-11728 02-64)
Avail: NTIS HC/MF A05 CSCL 12A

Prognostic numerical models for atmospheric and oceanic circulations require initial fields, boundary conditions, and forcing functions in addition to a consistent set of partial differential equations, including a state relation and equations expressing conservation of mass, momentum, and energy. Depending on the horizontal domain to be modeled, the horizontal boundary conditions are either physically obvious or extremely difficult to specify consistently. If the entire atmosphere is modeled, periodic horizontal boundary conditions are appropriate. On the other hand, the physical horizontal boundaries on the entire ocean are solid walls. Obviously, the normal velocity at a solid wall is zero while the specification of the tangential velocity depends on the mathematical treatment of the horizontal viscous terms. Limitations imposed by computer capacity and cost, as well as research interests, have led to the use of limited area models to study flows in the atmosphere and ocean. The limited area models do not have physical horizontal boundaries, merely numerical ones. Correctly determining these open boundary conditions for limited-area numerical models has both intrigued and frustrated numerical modelers for decades. One common approach is to use the closed or solid wall boundary conditions for a limited-area model. The argument given for this approach is that the boundary conditions affect flow near the walls but that none of these effects are propagated into the interior. Therefore, one chooses a big enough domain that the central region of interest is not corrupted by the boundary flow. Research in progress to model the North Atlantic circulation vividly illustrates the pitfalls of this approach. Two model runs are compared: (1) the southern boundary at 20S between latitudes 0 and 40W is artificially closed; and (2) the same boundary is specified as open with an inward transport of 15 Sv (determined from a global model with the same physics) uniformly spread across the boundary. A comparison of both runs is presented. Author

N92-11735*# Massachusetts Inst. of Tech., Cambridge.
NESTED OCEAN MODELS: WORK IN PROGRESS **c61**
A. Louise Perkins *In* ICASE, Proceedings for the ICASE Workshop on Heterogeneous Boundary Conditions Aug. 1991 p 60-69 (For primary document see N92-11728 02-64)
Avail: NTIS HC/MF A05 CSCL 09B

The ongoing work of combining three existing software programs into a nested grid oceanography model is detailed. The HYPER domain decomposition program, the SPEM ocean modeling program, and a quasi-geostrophic model written in England are being combined into a general ocean modeling facility. This facility will be used to test the viability and the capability of two-way nested grids in the North Atlantic. Author

N92-11736*# Institute for Computer Applications in Science and Engineering, Hampton, VA.
MULTI-RESOLUTION ANALYSIS FOR ENO SCHEMES Final Report
Ami Harten (Tel-Aviv Univ., Israel) Sep. 1991 17 p Submitted for publication Sponsored in part by DARPA
(Contracts NAS1-18605; N00014-86-K-0691; NSF DMS-88-11863) (NASA-CR-189043; NAS 1.26:189043; ICASE-91-77) Avail: NTIS HC/MF A03 CSCL 12A

Given an function, u(x), which is represented by its cell-averages in cells which are formed by some unstructured grid, we show how to decompose the function into various scales of variation. This is done by considering a set of nested grids in which the given grid is the finest, and identifying in each locality the coarsest grid in the set from which u(x) can be recovered to a prescribed accuracy. This multi-resolution analysis was applied to essentially non-oscillatory (ENO) schemes in order to advance the solution by one time-step. This is accomplished by decomposing the numerical solution at the beginning of each time-step into levels of resolution, and performing the computation in each locality at the appropriate coarser grid. An efficient algorithm for implementing this program in the 1-D case is presented; this algorithm can be extended to the multi-dimensional case with Cartesian grids.
Author

N92-11737# Strathclyde Univ., Glasgow (Scotland).
INVERSE PROBLEMS AND IMAGING (PITMAN RESEARCH NOTES IN MATHEMATICS SERIES NUMBER 245)
G. F. Roach 1991 279 p
(Contract DAJA45-89-M-0086)

(AD-A240333; R/D-6105-MA-02) Avail: NTIS HC/MF A13 CSCL 12/1

Some topics of research are as follows: Partial Measurement and reconstruction in electrical impedance tomography; Polarization in electromagnetic inverse problems; Inverse thermoelastic Rayleight scattering by a rigid ellipsoid; An inverse moving boundary problem for Laplace's equation; The scattering of velocity fields by an airfoil in compressible flow; and Boundary problems in electrical impedance tomography. GRA

N92-11738# Naval Ocean Systems Center, San Diego, CA.
CONDITIONAL EVENT ALGEBRAS: TWO NEW CHARACTERIZATIONS AND THEIR RELATIONS TO BAYESIAN ANALYSIS
I. R. Goodman Aug. 1991 2 p
(AD-A240378) Avail: NTIS HC/MF A01 CSCL 12/1

The standard approach in developing conditional probability is a numerically oriented one, although one notable exception has been efforts in the area of qualitative (comparative-preference ordering) probability theory, as developed by Suppes, Domotor, Fishburn, and others. However, the latter aspect of probability requires, in general, the preference ordering to be equivalent to the probability ordering. But, this is obviously too restrictive to be compatible with the basic monotonicity property of probability, relative to the usual partial subclass order for events. On the other hand, Koopman's approach to qualitative probability is not as restrictive and does yield a preference relation, which if suitably modified, is compatible with the natural subclass partial order. In the work here, it is shown that a qualitative concept of conditional probability can be established on a thoroughly rigorous algebraic basis which can be directly related to Koopman qualitative conditional probability. In addition, it is shown that conditional events which must be certain principal ideal cosets of events from the initial boolean algebra of events: they can be compared, contrasted, and combined by any boolean operations, even if the events have distinctly different antecedents. In addition, conditional events form a conditional event algebra which in structure is midway between a pseudocomplemented distributive lattice and a full boolean algebra. This richness of structure allows for: the development of an associated sound and complete conditional probability logic of propositions; deep structural relations with three-valued logic and Definett's previous concept of partial indicator functions; and an interpretation of Bayesian analysis from a qualitative/syntactic viewpoint. GRA

N92-11739# Technische Univ., Berlin (Germany, F.R.). Fachbereich Informatik.
EXTENDED ALGEBRAIC GRAPH TRANSFORMATION Ph.D. Thesis
Michael Loewe 11 Feb. 1991 184 p
(ETN-91-90151) Avail: NTIS HC/MF A09

Further developments and adjustments of algebraic graph transformation methods are suggested in order to increase their applicability in the everyday practice of software engineers. The aim is to bring theoretical and practical aspects closer together. The starting point for the investigation is the algebraic approach to graph transformation. The following are considered: partial morphisms and graph structures, pushout based transformations, pullback based transformations, and computing by graph transformation. ESA

N92-11740# Technische Hochschule, Darmstadt (Germany, F.R.). Fachbereich Mathematik.
ORIENTED MATROIDS AND PROJECTIVE INVARIANT THEORY Ph.D. Thesis
Antonio GuedesdeOliveira 1990 117 p
(ETN-91-90181) Avail: NTIS HC/MF A06

The Graussmann manifold of k dimensional linear space over a field K is isomorphic. A similar statement is proved for matroids and oriented matroids. Matroids and oriented matroids are proven to be definable as varieties, over the Galois fields in order 2 and 3, by a set of polynomials in a one to one canonical correspondence with the Grassmann-Pluecker polynomials. Hence a new light is cast over the (close) connection between the Grassmann variety, matroids and oriented matroids. As a result of this, certain theorems of invariant theory can be carried out to one or both of these structures, and between them as well. ESA

N92-11741# Technische Univ., Berlin (Germany, F.R.). Fachbereich Mathematik.
REPRESENTATION OF PHI MEROMORPHIC FUNCTIONS, WHEN PHI AND A LINEAR DIFFERENTIAL POLYNOMIAL IN PHI HAVE MAXIMUM FINITE ZEROS Ph.D. Thesis [DARSTELLUNGSSAETZE MEROMORPHER FUNKTIONEN PHI, WENN PHI EIN LINEARES DIFFERENTIUALPOLYNOM IN PHI HOECHSTENS ENDLICH VIELE NULLSTELLEN HABEN]
Michael Heckner 1991 74 p In GERMAN
(ETN-91-90202) Avail: NTIS HC/MF A04

Differential polynomials with rational coefficients are considered. The fundamental principles of truth distribution science and the theory of conventional differential equations are presented. Linear differential equations and Wronski determinants are examined. Results are demonstrated and discussed. ESA

N92-11742*# National Aeronautics and Space Administration. Langley Research Center, Hampton, VA.
A FOURIER COLLOCATION TIME DOMAIN METHOD FOR NUMERICALLY SOLVING MAXWELL'S EQUATIONS
John V. Shebalin Oct. 1991 19 p
(NASA-TM-104162; NAS 1.15:104162) Avail: NTIS HC/MF A03 CSCL 12A

A new method for solving Maxwell's equations in the time domain for arbitrary values of permittivity, conductivity, and permeability is presented. Spatial derivatives are found by a Fourier transform method and time integration is performed using a second order, semi-implicit procedure. Electric and magnetic fields are collocated on the same grid points, rather than on interleaved points, as in the Finite Difference Time Domain (FDTD) method. Numerical results are presented for the propagation of a 2-D Transverse Electromagnetic (TEM) mode out of a parallel plate waveguide and into a dielectric and conducting medium. Author

65 STATISTICS AND PROBABILITY

Includes data sampling and smoothing; Monte Carlo method; and stochastic processes.

N92-11743*# Research Inst. for Advanced Computer Science, Moffett Field, CA.
STATISTICAL PREDICTION WITH KANERVA'S SPARSE DISTRIBUTED MEMORY
David Rogers Jan. 1989 10 p
(Contracts NCC2-378; NCC2-408)
(NASA-CR-187314; NAS 1.26:187314; RIACS-TR-89-02) Avail: NTIS HC/MF A02 CSCL 12A

A new viewpoint of the processing performed by Kanerva's sparse distributed memory (SDM) is presented. In conditions of near- or over-capacity, where the associative-memory behavior of the model breaks down, the processing performed by the model can be interpreted as that of a statistical predictor. Mathematical results are presented which serve as the framework for a new statistical viewpoint of sparse distributed memory and for which the standard formulation of SDM is a special case. This viewpoint suggests possible enhancements to the SDM model, including a procedure for improving the predictiveness of the system based on Holland's work with genetic algorithms, and a method for improving the capacity of SDM even when used as an associative memory. Author

N92-11744*# Research Inst. for Advanced Computer Science, Moffett Field, CA.
NUMERICAL METHODS IN MARKOV CHAIN MODELING
Bernard Philippe, Youcef Saad, and William J. Stewart (North Carolina State Univ., Raleigh.) Oct. 1989 42 p Sponsored by CNRS

(Contract NCC2-387; NSF INT-86-13332)
(NASA-CR-188908; NAS 1.26:188908; RIACS-TR-89-39) Avail: NTIS HC/MF A03 CSCL 12A

Several methods for computing stationary probability distributions of Markov chains are described and compared. The main linear algebra problem consists of computing an eigenvector of a sparse, usually nonsymmetric, matrix associated with a known eigenvalue. It can also be cast as a problem of solving a homogeneous singular linear system. Several methods based on combinations of Krylov subspace techniques are presented. The performance of these methods on some realistic problems are compared. Author

N92-11745*# National Aeronautics and Space Administration. Ames Research Center, Moffett Field, CA.
TABLES OF SQUARE-LAW SIGNAL DETECTION STATISTICS FOR HANN SPECTRA WITH 50 PERCENT OVERLAP
Stanley R. Deans (University of South Florida, Tampa.) and D. Kent Cullers Sep. 1991 20 p
(NASA-TM-103830; A-91037; NAS 1.15:103830) Avail: NTIS HC/MF A03 CSCL 12A

The Search for Extraterrestrial Intelligence, currently being planned by NASA, will require that an enormous amount of data be analyzed in real time by special purpose hardware. It is expected that overlapped Hann data windows will play an important role in this analysis. In order to understand the statistical implication of this approach, it has been necessary to compute detection statistics for overlapped Hann spectra. Tables of signal detection statistics are given for false alarm rates from 10(exp -14) to 10(exp -1) and signal detection probabilities from 0.50 to 0.99; the number of computed spectra ranges from 4 to 2000. Author

N92-11746# Naval Ocean Systems Center, San Diego, CA.
A RE-EXAMINATION OF THE RELATIONSHIP BETWEEN FUZZY SET THEORY AND PROBABILITY THEORY
I. R. Goodman and V. M. Bier Aug. 1991 3 p
(AD-A240243) Avail: NTIS HC/MF A01 CSCL 12/2

Recently, a number of articles have appeared in newspapers and popular magazines and journals emphasizing a dichotomy in regard to fuzzy sets: the great potential benefit of using an intuitively appealing and simple approach to modeling uncertainties and its almost universal rejection or avoidance by orthodox scientists in the United States trained in probability theory. Thus, once more, it is of some interest to attempt to determine dispassionately what relations, if any, exist between fuzzy sets and probabilities. Previously, Goodman et al. were the first to point out that rather basic connections do indeed exist between fuzzy set theory and probability theory via random sets and their one point coverage functions. But relatively few individuals have utilized these connections (Dubois and Prade on occasion and Oblow emphasizing full random set representations through his hybrid O-Theory), mainly due to the foreboding complex structure of random sets as compared to the relatively simple form of random variables or random vectors. Even the relatively recent contributions of Lindley, Klir, and others in comparing the roles and game theoretic admissibility properties of fuzzy sets and probabilities do not address the deeper relations between the two areas. GRA

N92-11747# Naval Ocean Systems Center, San Diego, CA.
ASSIGNMENT OF SINGLE VALUES TO PROBABILITY INTERVALS, EVALUATION OF CONDITIONAL EVENTS, AND APPLICATIONS TO COMBINATION OF EVIDENCE Professional Paper
I. R. Goodman Aug. 1991 4 p
(AD-A240258) Avail: NTIS HC/MF A01 CSCL 12/3

A long unrecognized problem in probability and statistics has been the inability to treat inference statements (such as if b then a or a given b) so that logical combinations of them can be evaluated, compatible with conditional probability. Thus, in the situation where no conditioning occurs, or everything is conditioned on a common antecedent, statements such as if b then a or if b then c can be readily addressed with the typical evaluation: p(a v c / b) = p sub b (a v c) = p sub b (a) + p sub b (c) - p sub b (a.c), etc., for any probability measure p over the space of events. GRA

N92-11748# College of William and Mary, Williamsburg, VA. Dept. of Mathematics and Computer Science.
ALGEBRAIC ASPECTS OF NETWORK RELIABILITY PROBLEMS Final Report, 1 Dec. 1988 - 31 May 1991
Douglas R. Shier 31 May 1991 10 p
(Grant AF-AFOSR-0071-89; AF Proj. 2304)
(AD-A240365; AFOSR-91-0717TR) Avail: NTIS HC/MF A02 CSCL 13/8

This research addresses both theoretical and computational aspects of evaluating the reliability of a complex system in terms of its structure and the reliability of its individual components. This type of problem frequently arises in the design and evaluation of telecommunication, logistics, and distribution systems, which are commonly modelled using networks. The present research employs an algebraic approach for studying the reliability of such network systems. This approach has not only unified a variety of theoretical results but has also produced a number of new algorithms for calculating various measures of system reliability. Based on this approach, both exact and approximate computational schemes have been developed, together with supporting data structures for implementing the necessary computations in an efficient manner. Approximation schemes, also based on an underlying algebraic structure, have also been developed for evaluating more general measures of system performance, such as average delay or throughput in stochastic systems. In addition this research has recently led to the study of efficient methods for generating cutsets in networks and has produced substantial improvements relative to existing methods for this fundamental task. Author (GRA)

N92-11749# Georgia Univ., Athens. Dept. of Psychology.
CIRCULAR STATISTICAL METHODS: APPLICATIONS IN SPATIAL AND TEMPORAL PERFORMANCE ANALYSIS Final Report, Jun. - Oct. 1990
Robert P. Mahan Apr. 1991 53 p
(Contract DAAL03-86-D-0001)
(AD-A240751; ARI-SR-16) Avail: NTIS HC/MF A04 CSCL 12/3

This report surveys methods used for analyzing data generated from circular scales. The focus is on dimensions of simulation network training and development data that may be inaccessible to linear-based analyses. Several problem areas are identified that may lead to erroneous conclusions and/or loss of information when applying traditional analytic procedures to spatial and temporal performance measures. For example, the arithmetic mean and standard deviation are shown to be inappropriate descriptive measures for circular data. In addition, the use of average absolute deviations to measure directional errors of judgment can lead to loss of directional information. Finally, the usual methods of statistical inference are shown to fail in accounting for circularity when it exists. Therefore, these methods are subject to serious, often unknown and unrecognized errors in stated probabilities associated with Type 1 error rates, loss of statistical power, or both. Statistical methods are presented that help circumvent these problems. GRA

N92-11750# Technische Univ., Berlin (Germany, F.R.). Fachbereich Mathematik.
ON THE MAXIMUM ENTROPY PRINCIPLE FOR MARKOV CHAINS AND PROCESSES Ph.D. Thesis
Uwe Schmock 1990 114 p
(ETN-91-90150) Avail: NTIS HC/MF A06

The determination of the distribution of those paths which provide the main contribution to an expression of the form E(exp(TH(L sub T))) as T tends to infinity is addressed. Here, H denotes a measurable, extended real valued function; (L sub T) denotes an empirical process; and E denotes expectation with respect to a Markovian path measure. Considerations motivated by the asymptotics of the Froelich polaron functional integral, which

has its origin in the quantum mechanics of an electron coupled to a polar crystal, are addressed. The problem of the one dimensional Wiener sausage is addressed, and results are generalized to more complicated empirical processes by putting more restrictive assumptions on the functional H of the empirical process. ESA

N92-11751# Mohammed V Univ., Rabat (Morocco). Faculte des Sciences.
THE CONSIDERING OF THE SLOWING DOWN EFFECT IN THE FORMALISM OF PROBABILITY TABLES. APPLICATION TO THE EFFECTIVE CROSS SECTION CALCULATION Ph.D. Thesis
O. K. A. Bouhelal 2 Nov. 1990 199 p
(DE91-626722; INIS-MF-12808) Avail: NTIS HC/MF A09

The exact determination of the effective multigroup cross sections imposes the numerical solution of the slowing down equation on a very fine energy mesh. Given the complexity of these calculations, different approximation methods have been developed but without a satisfactory treatment of the slowing-down effect. The usual methods are essentially based on interpolations using precalculated tables. The models that use the probability tables allow one to reduce the amount of data and the computational effort. A variety of methods proposed by Soviets, then by Americans, and finally by the French, based on the moments of a probability distribution, are incontestably valid within the framework of the statistical hypothesis. This stipulates that the collision densities do not depend on cross section and there is no ambiguity in the effective cross section calculation. The objective of our work is to show that the non-statistical phenomena, such as the slowing-down effect which is taken into account, can be described by probability tables which are able to represent the neutronic values and collision densities. The formalism involved in the statistical hypothesis, is based on the Gauss quadrature of the cross sections moments. In the non-statistical hypothesis we introduce the crossed probability tables using the quadratures of double integrals of cross sections. Moreover, a mathematical formalism allowing one to establish a relationship between the crossed probability tables and the collision densities was developed. This method was applied on uranium-238 in the range of resolved resonances where the slowing down effect is significant. Validity of the method and the analysis of the obtained results are studied through a reference calculation based on a solution of a discretized slowing down equation using a very fine mesh in which each microgroup can be correctly defined via the statistical probability tables. DOE

66 SYSTEMS ANALYSIS

Includes mathematical modeling; network analysis; and operations research.

N92-11752# Naval War Coll., Newport, RI. Dept. of Operations.
INSURANCE AGAINST CATASTROPHE: SDI AND THE 3RD WORLD NUCLEAR PROLIFERATION PROBLEM Final Report
David W. Swindle 21 Jun. 1991 39 p
(AD-A240429) Avail: NTIS HC/MF A03 CSCL 15/3

The Strategic Defense Initiative (SDI) employing a space-based ballistic missile defense (BMD) system of approximately 30 percent effectiveness will offer protection from emerging third world nuclear powers. A 30 percent effective BMD system will eliminate the possibility of attack by a third world nuclear power or state that sponsors terrorism and reduce the potential for being held hostage by a politically fragmented nation. While this paper does examine a number of controversial issues surrounding the SDI, it focuses primarily on the political impact of a BMD system on the third world vice the traditional possibility of conflict with the Soviet Union. A 30 percent effective BMD system would protect the United States and our allies from sustaining damage from a third world nuclear power for the next 15 to 20 years. The United States should build such a system before third world countries amass a large enough arsenal to make the transitioning process an unstable activity. GRA

67 THEORETICAL MATHEMATICS

Includes topology and number theory.

No abstracts in this category.

70 PHYSICS (GENERAL)

For precision time and time interval (PTTI) see *35 Instrumentation and Photography;* for geophysics, astrophysics or solar physics see *46 Geophysics, 90 Astrophysics,* or *92 Solar Physics.*

N92-11753*# Research Inst. for Advanced Computer Science, Moffett Field, CA.
ABOUT TIME
Peter J. Denning 14 May 1990 17 p
(Contract NCC2-387)
(NASA-CR-188870; NAS 1.26:188870; RIACS-TR-90-34) Avail: NTIS HC/MF A03 CSCL 20C

Time has historically been a measure of progress of recurrent physical processes. Coordination of future actions, prediction of future events, and assigning order to events are three practical reasons for implementing clocks and signalling mechanisms. In large networks of computers, these needs lead to the problem of synchronizing the clocks throughout the network. Recent methods allow this to be done in large networks with precision around 1 millisecond despite mean message exchange times near 5 milliseconds. These methods are discussed. Author

N92-11754# California Univ., Berkeley. Lawrence Berkeley Lab.
CHARACTERIZATION OF RARE EARTH PERMANENT MAGNETS
A. Huetten and G. Thomas Jun. 1991 20 p Presented at the 11th International Workshop on Rare Earth Magnets and Their Applications and 6th International Symposium on Magnetic Anisotropy and Coercivity in Rare Earth-Transition Metal Alloys, Pittsburgh, PA, 21-24 Oct. 1990
(Contract DE-AC03-76SF-00098)
(DE91-017010; LBL-29553; CONF-901059-1) Avail: NTIS HC/MF A03

Recently developed alloys based either on ternary phases such as Nd2Fe14B(2-14) or on iron-rich pseudobinaries with the ThMn12-structure combine excellent intrinsic magnetic properties with the appropriate microstructure for applications as hard magnetic materials. In order to understand the magnetic behavior of these materials, systematic microstructural characterization has been performed using microdiffraction, x-ray microanalyses, and high resolution electron microscopy. The magnetic behavior of three types of NdFeB specimens, namely sintered, mechanically alloyed, and melt-spun, is correlated to their microstructure. The effect of minority phases on the magnetization and the coercivity in these materials is investigated. The ease with which the nonmagnetic Nd-rich grain boundary phase decouples hard magnetic 2-14 matrix grains depends on their average grain size which is related to the different preparation processes. DOE

N92-11755# Office National d'Etudes et de Recherches Aerospatiales, Paris (France). Direction Scientifique de la Resistance des Structures.
SIMULATION OF A NONLINEAR TWO DEGREES OF FREEDOM SYSTEM. STUDY OF THE TEMPORAL RESPONSE TO A HARMONIC ATTRACTION [SIMULATION D'UN SYSTEME A DEUX DEGRES DE LIBERTE NON LINEAIRE. ETUDE DE LA REPONSE TEMPORELLE A UNE SOLLICITATION HARMONIQUE]
B. Guillermin Oct. 1990 43 p In FRENCH
(Contract STPA-BT-85-95-004)
(ONERA-RT-17/1677-RY-091-R; ETN-91-90092) Avail: NTIS HC/MF A03

Following previous studies on the nonlinear behavior of structures, the temporal response of a nonlinear two degrees of freedom system is modeled. The model is shown to translate the response for different types of nonlinearity (stiffness and damping). The Angelini method is used to determine the linear model characteristics. The robustness of this method is tested by function of nonlinear factor importance in the case of a stiff cubic law. The temporal signal study leads to the consideration of a criteria of detection called harmonic distortion representing the part of the response outside excitation frequency in the system behavior. ESA

N92-11756# Technische Univ., Eindhoven (Netherlands).
LIGHT SCATTERING EXPERIMENTS ON BROWNIAN MOTION IN SHEAR FLOW AND IN COLLOIDAL CRYSTALS Ph.D. Thesis
Jacobus Johannes Derksen 1991 112 p
(ETN-91-90134) Avail: NTIS HC/MF A06

The interaction between fluid flow and Brownian motion and the dynamics of so called colloidal crystals are investigated. The technique of dynamic light scattering is reviewed and results of tests with an optical set up for heterodyne experiments are presented. Results of cross correlation experiments are given. Colloidal crystal theory is reviewed and light scattering experiments and results are presented. Experiments focused on long wavelength transverse modes showed that the walls of the sample cell have a strong impact on the dynamics of the crystal in regions of reciprocal space characterized by weak damping. This leads to a better understanding of discrepancies between theory and experiments observed earlier. Measurements of the damping of long wavelength transverse modes directly (without interference of the elastic properties of the crystal) showed significant wall effects. ESA

N92-11757# Technische Univ., Berlin (Germany, F.R.). Fachbereich Mathematik.
THE STRONG COUPLING LIMIT FOR POLARON MODELS Ph.D. Thesis
Ulrich Mansmann 1991 124 p
(ETN-91-90163) Avail: NTIS HC/MF A06

A polaron like asymptote is shown to be given for a class of functions called of decreasing interaction and nicely approximable with respect to the Wiener process. Using large deviation techniques, the asymptotics for the strong coupling limit are shown to be given by a meanfield model and can be described by a variational problem. A one dimensional analogon to the Froelich polaron is considered. This is called a Dirac polaron because Dirac's delta function is used to model the interaction. Brownian local time is used to give a rigorous definition of the Dirac polaron. Using large deviation techniques, the asymptotics for the strong coupling limit for the Dirac polaron is shown to be given by a meanfield model and can be described by a variational problem. ESA

71 ACOUSTICS

Includes sound generation, transmission and attenuation. For noise pollution see *45 Environmental Pollution.*

N92-11758*# National Aeronautics and Space Administration. Langley Research Center, Hampton, VA.
ANNOYANCE CAUSED BY ADVANCED TURBOPROP AIRCRAFT FLYOVER NOISE: COMPARISON OF DIFFERENT PROPELLER CONFIGURATIONS
David A. McCurdy Washington Oct. 1991 69 p
(NASA-TP-3104; L-16850; NAS 1.60:3104) Avail: NTIS HC/MF A04 CSCL 20A

A laboratory experiment was conducted to compare the annoyance of flyover noise from advanced turboprop aircraft having different propeller configurations with the annoyance of conventional turboprop and turbofan aircraft flyover noise. A computer synthesis system was used to generate 40 realistic, time varying simulations of advanced turboprop takeoff noise. Of the 40 noises, single-rotating propeller configurations (8) and counter-rotating propeller configurations with an equal (12) and unequal (20) number of blades on each rotor were represented. Analyses found that advanced turboprops with single-rotating propellers were, on average, slightly less annoying than the other aircraft. Fundamental frequency and tone-to-broadband noise ratio affected annoyance response to advanced turboprops, but the effects varied with propeller configuration and noise metric. The addition of duration corrections and corrections for tones above 500 Hz to the noise measurement procedures improved annoyance prediction ability. Author

N92-11759*# National Aeronautics and Space Administration. Langley Research Center, Hampton, VA.
A NEW SIMULATOR FOR ASSESSING SUBJECTIVE EFFECTS OF SONIC BOOMS
Jack D. Leatherwood, Kevin P. Shepherd, and Brenda M. Sullivan (Lockheed Engineering and Sciences Co., Hampton, VA.) Sep. 1991 34 p
(NASA-TM-104150; NAS 1.15:104150) Avail: NTIS HC/MF A03 CSCL 20A

A man rated and computer driven sonic boom simulator which has been constructed and placed in operational use at NASA-Langley is described. The simulator is used to study human subjective reactions to sonic booms and has the capability of producing a wide range of signatures under controlled conditions. Results are presented to illustrate the capability of the simulator to generate user specified N-wave and shaped booms having rise times as low as 0.5 milliseconds and peak overpressures up to 191 Pa (4 psf). The validity of the simulator as a lab research tool for studying human subjective response to sonic booms was demonstrated by successful completion of a preliminary test designed to compare loudness of N-wave sonic booms with results obtained by other investigators. Excellent agreement of the preliminary test data with existing data was observed. This provided confidence in the experimental methodology and established the simulator as a viable tool for performing detailed evaluations of sonic boom loudness and acceptability within the lab. environment. Author

N92-11760# Department of the Navy, Washington, DC.
ACOUSTIC TRANSPONDER RECEIVER CIRCUIT Patent
Reginald Cyr, inventor (to Navy) 16 Apr. 1991 8 p Filed 7 Dec. 1988
(AD-D014965; US-Patent-5,008,859; US-Patent-Appl-SN-281139; US-Patent-Class-367-2) Avail: US Patent and Trademark Office CSCL 20/1

A transponder that responds differently to two different input signals is discussed. The first input signal is at a first frequency. The first input signal is detected by a first powered detector that operates at the first frequency. The transponder responses in a first mode to the first input signal. The second input signal consists of short pulses at the first frequency and at a second frequency. The transponder responds to short pulses at the first frequency

by powering a second detector. The first and second detector then detect the second input signal. The transponder responds in a second mode to the second input signal. Author (GRA)

N92-11761# Washington State Univ., Pullman. Dept. of Physics.
QUANTITATIVE RAY METHODS FOR SCATTERING OF SOUND BY SPHERICAL SHELLS Technical Report, 16 May 1987 - 31 Jul. 1990
S. G. Kargl 1 Aug. 1991 189 p
(Contract N00014-85-C-0141)
(AD-A240255) Avail: NTIS HC/MF A09 CSCL 20/1

The application of ray methods to the scattering of high-frequency plane waves from evacuated elastic spherical shells is investigated. The investigation of ray methods for spherical shells is a precursor to the application of such methods to shells having more complicated shapes. Ray models are developed to synthesize the form function f(Theta, ka) where k is the wavenumber of the incident wave and Theta is the scattering angle. The forward scattering amplitude, f(Theta equals 0), is related to the extinction cross section, sigma sub e by the optical theorem. If the absorption by the scatterer is negligible, the sigma sub e is equal to the total scattering cross section sigma sub t. A ray synthesis partition f(Theta equals 0) into a component for ordinary forward diffraction about the shell, f sub FD, and contributions from surface guided elastic waves. For high-frequency scattering, the relevant surface guided elastic waves are leaky Lamb waves. A similar ray synthesis of the backscattering amplitude f(Theta equals pi) contains a specular reflection component, f sub sp(Theta equals pi), and leaky Lamb wave contributions. A generalization of the geometrical theory of diffraction is employed to synthesize f sub l(Theta equals 0, ka) and f sub l (Theta equals pi, ka) for the lth leaky Lamb wave contribution. The syntheses for forward and backwards scattering correctly describe the leaky Lamb wave contributions and are expressible in a Fabry-Perot resonator form. While the ray description of backscattering GRA

N92-11762# Army Aeromedical Research Lab., Fort Rucker, AL.
THE HAZARD OF EXPOSURE TO IMPULSE NOISE AS A FUNCTION OF FREQUENCY, VOLUME 2 Final Report
James H. Patterson, Jr., Melvin Carrier, Jr., Kevin Bordwell, Ilia M. Lomba, and Roger P. Gautier Jun. 1991 365 p
(DA Proj. 3E1-62777-A-878; DA Proj. 3M1-61102-BS-15)
(AD-A240530; USAARL-91-18-Vol-2) Avail: NTIS HC/MF A16 CSCL 06/10

The energy spectrum of a noise is known to be an important variable in determining the effects of a traumatic exposure. However, existing criteria for exposure to impulse noise do not consider the frequency spectrum of an impulse as a variable in the evaluation of the hazards to the auditory system. This report presents the results of a study that was designed to determine the relative potential that impulsive energy concentrated at different frequencies has in causing auditory systems trauma. One hundred and eighteen (118) chinchilla, divided into 20 groups with 5 to 7 animals per group, were used in these experiments. Pre- and post-exposure hearing thresholds were measured at 10 test frequencies between 0.125 and 8 kHz on each animal using avoidance conditioning procedures. Quantitative histology (cochleograms) was used to determine the extent and pattern of the sensory cell damage. The noise exposure stimuli consisted of six different computer-generated narrow band tone bursts having center frequencies located at 0.260, 0.775, 1.025, 1.350, 2.450, and 3.550 kHz. Each narrow band exposure stimulus was presented at two to four different intensities. An analysis of the audiometric and histological data allowed a frequency weighting function to be derived. The weighting function clearly demonstrates that equivalent amounts of impulsive energy concentrated at different frequencies is not equally hazardous to auditory function. GRA

N92-11763# Washington State Univ., Pullman. Dept. of Physics.
WAVEFIELDS NEAR TRANSVERSE CUSP CAUSTICS PRODUCED BY REFLECTING ULTRASONIC TRANSIENTS AND TONE BURSTS FROM CURVED SURFACES Ph.D. Thesis
Carl K. Frederickson 16 Aug. 1991 248 p
(Contract N00014-85-C-0141)
(AD-A240641; TR-11) Avail: NTIS HC/MF A11 CSCL 20/1

Ultrasonic wavefields reflected from curved surfaces were studied in the vicinity of caustics. Acoustical and optical transverse cusp diffraction catastrophes produced by reflections from a curved metal surface in water were imaged by displaying the amplitude or intensity in an observation plane transverse to the general direction of propagation. The optical image was used to locate the cusp point in the observation plane. Acoustical diffraction patterns for sine waves, described by the Pearcey function, were calculated with the parameters determined by the experimental setup leaving no adjustable scaling parameters. The calculated and experimental acoustical diffraction patterns showed good agreement near the cusp point. The acoustical diffraction pattern showed the expected mirror symmetry about an axis. The pattern was shown to scale properly with frequency. The transverse cusp caustic separates space into a region with three rays and a region with one ray. Inside the caustic there are three rays on the curve; two of the rays merge and disappear leaving one ray outside. Transient signals reflected from curved surfaces exhibited the merging and disappearance of rays on the caustic. Relative arrival times for signals in calculated and recorded time traces agree well. The relation to the wavefront parameters of the temporal orientation of the travel time surface is discussed. The general shape of the travel time surface is that of the swallow tail caustic surface. GRA

N92-11764# Washington State Univ., Pullman. Dept. of Physics.
SCATTERING OF TONE BURSTS FROM SPHERICAL SHELLS: COMPUTATIONS BASED ON FOURIER TRANSFORM METHOD M.S. Thesis
Ligang G. Zhang 30 Aug. 1991 156 p
(Contract N00014-89-J-3088)
(AD-A240642; TR-1) Avail: NTIS HC/MF A08 CSCL 20/1

An algorithm to compute the transient scattering of sound by elastic spheres and shells has been developed and tested. Short tone bursts incident on elastic spherical shells under various conditions have been investigated. Previous experiment results for elastic spheres and shells have been confirmed. Some interesting physical aspects concerning the basics of the scattering mechanism have been detected. A mid-frequency enhancement has been examined for thin shells and compared with the ray model results. The ray model is found to closely approximate the enhanced backscattering for tone bursts associated with a subsonic wave on thin shells. A related filter-like effect of thin shells for the selected frequencies of the enhancement has been detected and quantitatively described, and the impulse response has been computed. The subsonic wave associated with the mid-frequency enhancement is referred to as the Scholte Stoneley wave by some authors. The present computations can be of practical use and can be compared with observations or ray models of the scattering from shells under the same conditions if such observations or models become available later on. The scattering of tome bursts from shells was calculated when the carrier frequency is at or close to the frequency of resonance associated with a reverberation of longitudinal waves across the thickness of the shell. When the shell is a fluid, the results are easily interpreted in terms of an existing ray model. When the shell is elastic, they suggest the presence of a mechanism for prompt radiation noninvolving complete circumnavigation of the sphere by guided elastic waves. GRA

N92-11765*# National Aeronautics and Space Administration. Langley Research Center, Hampton, VA.
A LOUDNESS CALCULATION PROCEDURE APPLIED TO SHAPED SONIC BOOMS

Kevin P. Shepherd and Brenda M. Sullivan (Lockheed Engineering and Sciences Co., Hampton, VA.) Washington Nov. 1991 13 p
(NASA-TP-3134; L-16913; NAS 1.60:3134) Avail: NTIS HC/MF A03 CSCL 20A

Described here is a procedure that can be used to calculate the loudness of sonic booms. The procedure is applied to a wide range of sonic booms, both classical N-waves and a variety of other shapes of booms. The loudness of N-waves is controlled by overpressure and the associated rise time. The loudness of shaped booms is highly dependent on the characteristics of the initial shock. A comparison of the calculated loudness values indicates that shaped booms may have significantly reduced loudness relative to N-waves having the same peak overpressure. This result implies that a supersonic transport designed to yield minimized sonic booms may be substantially more acceptable than an unconstrained design. Author

72 ATOMIC AND MOLECULAR PHYSICS

Includes atomic structure, electron properties, and molecular spectra.

N92-11766 National Physical Lab., Teddington (England). Div. of Radiation Science and Acoustics.
INTERCOMPARISON OF THE MEDIUM ENERGY PRIMARY STANDARDS FOR X RAY EXPOSURE OF NPL AND ENEA, ITALY
C. J. Moretti, Julie A. Heaton, R. F. Laitano, and Maria Pia Toni (Ente Nazionale per l'Energia Elettrica, Rome, Italy) Apr. 1991 20 p
(NPL-RSA(EXT)-18; ISSN-0955-9655; ETN-91-99871) Copyright Avail: National Physical Lab., Teddington, Middlesex TW11 OLW, England

An intercomparison between the primary standards of exposure for medium energy X rays held by the National Physics Laboratory (NPL) (United Kingdom) and ENEA is described. The intercomparison used four different transfer chambers. Measurements were made at four therapy level qualities, with Half Value Layers (HDL) of 0.15, 0.5, 1.0 and 2.5 mm Cu (nominal generating voltages of 100, 135, 180 and 250 kV respectively. At the 2.5 mm Cu HVL quality the primary standards were found to agree to within about 0.8 percent, for the other three qualities the chambers differed by no more than 0.3percent. ESA

N92-11767 National Physical Lab., Teddington (England). Div. of Radiation Science and Acoustics.
INTERCOMPARISON OF THE LOW ENERGY PRIMARY STANDARDS FOR X RAY EXPOSURE OF NPL AND ENEA, ITALY
C. J. Moretti, Julie A. Heaton, R. F. Laitano, and Maria Pia Toni (Ente Nazionale per l'Energia Elettrica, Rome, Italy) 15 May 1991 15 p
(NPL-RSA(EXT)-19; ISSN-0955-9655; ETN-91-99872) Copyright Avail: National Physical Lab., Teddington, Middlesex TW11 OLW, England

An intercomparison between the primary standards of X rays exposure for low energy X rays held by National Physics Laboratory (NPL) (United Kingdom) and ENEA is described. The intercomparison directly between the two standard chambers took place at NPL during December 1989. Measurements were made at three therapy level qualities with half value layers of 0.036, 0.25 and 1.00 mm Al (nominal generating voltages of 10, 24 and 50 kV respectively). The two primary standards agreed to within + or - 0.3 percent. ESA

N92-11768# Rutherford Appleton Lab., Chilton (England). Theory Div.
ON THE POLARISATION OF TENSOR MESONS IN PSI RADIATIVE DECAYS AND POSSIBLE IMPLICATIONS FOR THE GLUONIC CONTENT OF THE THETA(1720)
F. E. Close and Z. P. Li (Tennessee Univ., Knoxville.) Dec. 1990 13 p Sponsored in part by State of Tennessee Science Alliance Center
(Contract DE-AS05-76ER-04936)
(RAL-90-091; UTK-90-14; ETN-91-99882) Avail: NTIS HC/MF A03

It is shown how perturbative Quantum Chromodynamics (QCD) can successfully describe the data on the helicity structure of tensor mesons produced in psi to gamma T decay. The new feature is that the diagrams are separated according to their different topologies, the corresponding helicity structures being analyzed for each diagram in the quark model via a correspondence principle. Different topologies appear to dominate the f sub 2 (1270, 1525) quark-antiquark production and the theta/f sub 2 (1720) production. ESA

N92-11769*# BSA Services, Houston, TX.
[SPECTRAL FITTING, SHOCK LAYER MODELING, AND PRODUCTION OF NITROGEN OXIDES AND EXCITED NITROGEN] Final Report, 24 Oct. 1990 - 31 Jun. 1991
H. E. Blackwell 30 Jun. 1991 41 p
(Contract NAS9-18493)
(NASA-CR-185664; NAS 1.26:185664) Avail: NTIS HC/MF A03 CSCL 20H

An analysis was made of N2 emission from 8.72 MJ/kg shock layer at 2.54, 1.91, and 1.27 cm positions and vibrational state distributions, temperatures, and relative electronic state populations was obtained from data sets. Other recorded arc jet N2 and air spectral data were reviewed and NO emission characteristics were studied. A review of operational procedures of the DSMC code was made. Information on other appropriate codes and modifications, including ionization, were made as well as a determination of the applicability of codes reviewed to task requirement. A review was also made of computational procedures used in CFD codes of Li and other codes on JSC computers. An analysis was made of problems associated with integration of specific chemical kinetics applicable to task into CFD codes. Author

N92-11770*# Research Inst. for Advanced Computer Science, Moffett Field, CA.
COLLISION INTEGRALS AND HIGH TEMPERATURE TRANSPORT PROPERTIES FOR N-N, O-O, AND N-O
E. Levin, Harry Partridge, and J. R. Stallcop (National Aeronautics and Space Administration. Ames Research Center, Moffett Field, CA.) Nov. 1989 31 p
(Contract NCC2-387)
(NASA-CR-188907; NAS 1.26:188907; RIACS-TR-89-43) Avail: NTIS HC/MF A03 CSCL 20H

Accurate collision integrals are reported for the interactions of N(4 S 0) + N(4 S 0), O(3 P), and N(4 S 0) + O(3 P). These are computed from a semiclassical formulation of the scattering using the best available representations of all of the potential energy curves needed to describe the collisions. Experimental RKR curves and other accurate measured data are used where available; the results of accurate ab initio electronic structure calculations are used to determine the remaining potential curves. The high-lying states are found to give the largest contributions to the collision cross sections. The nine collision integrals, needed to determine transport properties to second order, are tabulated for translational temperatures in the range 250 K to 100,000 K. These results are intended to reduce the uncertainty in future predictions of the transport properties of nonequilibrium air, particularly at high temperatures. The viscosity, thermal conductivity, diffusion coefficient, and thermal diffusion factor for a gas composed of nitrogen and oxygen atoms in thermal equilibrium are calculated. It was found that the second order contribution to the transport properties is small. Graphs of these transport properties for various mixture ratios are presented for temperatures in the range 5000 to 15000 K. Author

N92-11771# Lawrence Livermore National Lab., CA.
CRITICAL PROPERTIES OF STRONGLY INTERACTING BOSONS ON A LATTICE

G. G. Batrouni Feb. 1991 22 p Presented at the 4th Annual Workshop on the Recent Development of Computer Simulation Studies in Condensed Matter Physics, Athens, GA, 18-22 Feb. 1991
(Contract W-7405-eng-48)
(DE91-016926; UCRL-JC-106331; CONF-910298-2) Avail: NTIS HC/MF A03

We use quantum Monte Carlo techniques to study the critical properties of an interacting boson model in one dimension with and without disorder in the absences of disorder, the phase diagram consists of a Mott insulating phase at commensurate fillings and a superfluid phase. The effect of disorder is to shrink the Mott insulator phase and to cause the emergence of two new insulating regions. Our simulations are the first to demonstrate the existence and study the properties of the predicted Bose glass phase as well as an unanticipated Anderson-like insulating regime. For the uniform system, we study the critical behavior of the superfluid density and the compressibility, and measure the exponents v and z, which agree with predictions based on a scaling analysis. DOE

N92-11772# California Univ., Berkeley. Lawrence Berkeley Lab.
COLLISIONAL ENERGY TRANSFER FROM EXCITED NITROGEN DIOXIDE Ph.D. Thesis
K. O. Patten May 1991 244 p
(Contract DE-AC03-76SF-00098)
(DE91-016989; LBL-30599) Avail: NTIS HC/MF A11

The radiative lifetimes of gaseous nitrogen dioxide excited by pulsed, tunable dye laser radiation are determined for excitation wavelengths ranging from 400 to 750 nm. When the data are expressed in the form of zero-pressure radiative rate constants (k(sub 0)/s exp -1), they fit a linear equation with respect to excitation energy. This fit predicts a radiative lifetime of 64 microseconds for 400 nm excitation and 102 microseconds at 750 nm. The effects of pressure, observation delay time, and wavelength range of the fluorescence detection apparatus are determined for both radiative lifetime and quenching constant. Dispersed fluorescence spectra from excited nitrogen dioxide are analyzed into three-parameter functions that approximate the corresponding excited state population distributions. Energy transfer from nitrogen dioxide excited at 532 nm and colliding with thirteen buffer gases is studied by this population deconvolution method. The energy removal rate constants increase in the order Ne, Ar, Kr, Xe, He, CO, N2, O2, NO, NO2, CO2, SF6, SO2. The energy transfer rate constant is strongly correlated with the number of degrees of freedom of the buffer molecule and with low vibrational frequencies of the buffer molecule. Population deconvolution from excited nitrogen dioxide fluorescence spectra is again employed to find energy removal rate constants for the NO2*-NO2 collisions, excited by dye laser at 475.34, 435.04, and 400.00 nm. The energy transfer rate constant increases with decreasing excitation wavelength. The energy removal rate constant between 400 and 532 nm excitation increases as the (3.6 +/- 0.4) power of the excitation photon energy. DOE

N92-11773# Ceskoslovenska Akademie Ved, Prague. Inst. of Plasma Physics.
RADIATION FORCES TO ELECTRONS IN LASER FIELDS EXPLAINED AS SCATTERING FOR PONDEROMOTIVE MOMENTUM TRANSFERS
V. Petrzilka and H. Hora (New South Wales Univ., Kensington, Australia) Feb. 1991 10 p
(IPPCZ-308) Avail: NTIS HC/MF A02

The forces acting on electrons and/or plasmas in strong electromagnetic fields are very important phenomena in laser produced plasmas and in similar interactions with intense microwaves. These forces are known as ponderomotive forces. We present here a derivation of these forces as a scattering process. While Thomson scattering or that of Bremsstrahlung is weak and mostly neglected for the balance of the strong nonlinear forces acting on the electrons, it turns out that the compensation of momentum can be explained as a momentum exchange with the field - a kind of scattering process. This gives fundamental insights into the radiation pressure. Author

N92-11774*# Fermi National Accelerator Lab., Batavia, IL.
GLOBAL ANALYSIS OF FERMION MIXING WITH EXOTICS
Enrico Nardi, Esteban Roulet, and Daniele Tommasini (International School for Advanced Studies, Trieste, Italy) Aug. 1991 34 p Sponsored in part by DOE
(Grant NAGw-1340)
(NASA-CR-189006; NAS 1.26:189006; FERMILAB-Pub-91/207-A; SISSA-104/91/EP) Avail: NTIS HC/MF A03 CSCL 20H

The limits are analyzed on deviation of the lepton and quark weak-couplings from their standard model values in a general class of models where the known fermions are allowed to mix with new heavy particles with exotic SU(2) x U(1) quantum number assignments (left-handed singlets or right-handed doublets). These mixings appear in many extensions of the electroweak theory such as models with mirror fermions, E(sub 6) models, etc. The results update previous analyses and improve considerably the existing bounds. Author

N92-11775# Science Applications International Corp., McLean, VA.
PARTICLE ACCELERATION IN SPACE AND RADIATION BELT DEPLETION Final Technical Report, 1 Mar. 1987 - 28 Feb. 1991
C. R. Menyuk and D. Papadopoulos 30 Apr. 1991 134 p
(Contract F19628-87-C-0085)
(AD-A240311; PL-TR-91-2104) Avail: NTIS HC/MF A07 CSCL 09/3

Particle acceleration and the accompanying radiation belt depletion are studied theoretically. The effect of stochastic particle acceleration on a distribution of electrons is studied using a finite element method, combined with resonance overlap techniques. In particular cases, these are also studied using particle simulations and good agreement is found. We next focus on particle acceleration in the Alfven wave maser. It is shown that the maser is naturally well-confined but will not lead to significant acceleration. It is shown, however, that the kinetic Alfven wave will lead to significant acceleration, although it has to be ducted to remain confined. An experimental approach to stimulate these waves artificially by heating electrons is then proposed. GRA

N92-11776# Oregon State Univ., Corvallis.
MATTER-WAVE INTERFEROMETRY WITH LASER COOLED ATOMS Progress Report
David McIntyre Jul. 1991 6 p
(Contract N00014-91-J-1198)
(AD-A240531) Avail: NTIS HC/MF A02 CSCL 20/5

This program is investigating matter wave interferometry with laser cooled atoms. A slow beam of laser cooled rubidium atoms will be used as the matter wave source. The atom optical elements will be microfabricated amplitude transmission gratings which will be used in a three-grating interferometer to split and recombine the rubidium beam. The interferometer will be a useful new tool for precision atomic physics and a sensitive inertial sensor. GRA

N92-11777# Argonne National Lab., IL.
CONTROL OF ELECTRON TRANSFER RATES BY MOTIONS OF ATOMS AND MOLECULES
J. R. Miller 1990 21 p Presented at the Conference on Photochemical Processes in Organized Molecular Systems, Yokohama (Japan), 22-24 Sep. 1990
(Contract W-31-109-eng-38)
(DE91-018575; ANL/CP-73037; CONF-9009427-1) Avail: NTIS HC/MF A03

Recently measurements have been made of the temperature dependence of long distance intramolecular electron transfer reactions in molecules in which donor and acceptor groups are held at a fixed distance apart. For very highly exoergic electron transfer reactions, the rates show a remarkable independence of temperature. This temperature independence can be predicted

quite precisely from the results of previous experiments which measured only the dependence of rates on free energy change. The temperature dependence can be ascribed to nuclear tunneling in high frequency vibrational modes which are coupled to the electron transfer reaction. While this is not surprising, the dominance of even a small coupling to high frequency modes in determining the temperature dependence is surprising. The importance of the high frequency modes is likely to be apparent in other contexts, particularly cases in which dynamic solvent effects occur for electron transfer reactions in highly viscous media. DOE

N92-11778# Argonne National Lab., IL.
VARIATIONAL MONTE CARLO CALCULATIONS OF FINITE NUCLEI
R. B. Wiringa 1991 10 p Presented at the Recent Progress in Many-Body Theories, Minneapolis, MN, 26-31 Aug. 1991
(Contract W-31-109-eng-38)
(DE91-018895; ANL/CP-74237; CONF-9108142-2) Avail: NTIS HC/MF A02

A major goal in nuclear physics is to understand how nuclear structure comes about from the underlying interactions between nucleons. This requires modelling nuclei as collections of strongly interacting particles. Using realistic nucleon-nucleon potentials, supplemented with consistent three-nucleon potentials and two-body electroweak current operators, we calculate nuclear ground-state properties, such as the binding energy, electromagnetic form factors, and momentum distributions. Other properties such as excited states and low-energy reactions are also calculable in this framework. DOE

N92-11779# Oak Ridge National Lab., TN.
NEW DIMENSIONS IN ATOM PROBE ANALYSIS
A. Cerezo, J. M. Hyde, G. Beverini, R. P. Setna, P. J. Warren, G. D. W. Smith (Oxford Univ., England), and M. K. Miller 1991 27 p Presented at the 38th International Field Emission Symposium, Vienna (Austria), 5-9 Aug. 1991
(Contract DE-AC05-84OR-21400)
(DE91-018926; CONF-9108160-1) Avail: NTIS HC/MF A03

A new class of atom probe instruments has recently been developed which combine single atom sensitivity mass spectrometry with position sensing, and have the potential of reconstructing nanometer-scale composition variations in 3-D. These techniques will be very powerful in the study of the early stages of phase transformations, and surface and interface segregation. Some recent results obtained with the first of the instruments, the position-sensitive atom probe, are described. Difficulties arise in this instrument when more than one ion is evaporated from the analysis area on a single field evaporation pulse, which can limit the accuracy of analysis performed on the resultant data. Other 3-D atom probe instruments currently under development are described, and their expected performance in this respect is discussed. The significance of defining composition on the sub-nanometer scale is addressed, and the importance of atomic-scale modelling of the phenomena under investigation is indicated. DOE

N92-11780# Flinders Univ., Bedford Park (Australia). Electronic Structure of Materials Centre.
COUPLED-CHANNEL OPTICAL CALCULATION OF ELECTRON-HYDROGEN SCATTERING: ELASTIC SCATTERING FROM 0.5 TO 30 eV
I. Bray, D. A. Konovalov, and I. E. McCarthy Jan. 1991 22 p
(DE91-634157; ESM-28) Avail: NTIS HC/MF A03

A coupled-channel optical method for electron-atomic hydrogen scattering is presented in a form that treats both the projectile and the target electrons symmetrically. Elastic differential cross sections are calculated at a range of energies from 0.5 to 30 eV and are found to be in complete agreement with the absolute measurements that were previously reported. Total and total ionization cross sections are also presented. DOE

N92-11781# Lawrence Livermore National Lab., CA.
POSITRON LIFETIMES IN SOLIDS FROM FIRST PRINCIPLES CALCULATIONS
P. A. Sterne, J. C. OBrien, R. H. Howell, and J. H. Kaiser (Texas Univ., Arlington.) Aug. 1991 10 p Presented at the 9th International Conference on Positron Annihilation, Szombathely (Hungary), 26-31 Aug. 1991
(Contract W-7405-eng-48)
(DE92-000088; UCRL-JC-106988; CONF-9108150-2) Avail: NTIS HC/MF A02

We present a first principles method for calculating positron lifetimes in solids, based on self-consistent calculations using the Linear Muffin-Tin Orbital method. Local density approximations are used for both electron-electron and electron-positron interactions. Results are presented for a variety of elemental metals and vacancies to demonstrate the reliability of this approach. Theoretical calculations of positron lifetimes can be used to interpret experimental data. As an examples of this, we interpret our experimental lifetime data for the oxide superconductor Ba(1-x)K(x)BiO(3) using calculations based on this method. DOE

73 NUCLEAR AND HIGH-ENERGY PHYSICS

Includes elementary and nuclear particles; and reactor theory.

For space radiation see *93 Space Radiation.*

N92-11782# Kent State Univ., OH.
THEORETICAL INTERPRETATION OF HIGH-ENERGY NUCLEAR COLLISIONS
G. Fai Jul. 1991 11 p
(Contract DE-FG02-86ER-40251)
(DE91-016965; DOE/ER-40251/6) Avail: NTIS HC/MF A03

Nuclear collision data are interpreted theoretically. The nuclear equation of state is investigated with particular emphasis on momentum dependent mean field effects. Subnucleonic degrees of freedom are invoked at high energies and densities, and a short length-scales. A nontopological soliton model for baryons is studied in which effective meson fields are generated from extended quark-antiquark pairs. The major objective of this nuclear theory project is a better understanding of the properties of strongly interacting matter on the nuclear energy scale, as manifested in high energy heavy ion collisions. DOE

N92-11783*# National Aeronautics and Space Administration, Washington, DC.
FUSION ENERGY FOR SPACE MISSIONS IN THE 21ST CENTURY
Norman R. Schulze Aug. 1991 477 p
(NASA-TM-4298; NAS 1.15:4298) Avail: NTIS HC/MF A21 CSCL 18K

Future space missions were hypothesized and analyzed and the energy source for their accomplishment investigated. The mission included manned Mars, scientific outposts to and robotic sample return missions from the outer planets and asteroids, as well as fly-by and rendezvous mission with the Oort Cloud and the nearest star, Alpha Centauri. Space system parametric requirements and operational features were established. The energy means for accomplishing the High Energy Space Mission were investigated. Potential energy options which could provide the propulsion and electric power system and operational requirements were reviewed and evaluated. Fusion energy was considered to be the preferred option and was analyzed in depth. Candidate fusion fuels were evaluated based upon the energy output and neutron flux. Reactors exhibiting a highly efficient use of magnetic fields for space use while at the same time offering efficient coupling to an exhaust propellant or to a direct energy convertor for efficient electrical production were examined. Near term approaches were identified. Author

N92-11784# Brookhaven National Lab., Upton, NY.
PHOTON STIMULATED DESORPTION OF NEUTRAL SPECIES FROM ALUMINUM
T. S. Chou 1991 4 p Presented at the 1991 Institute of Electrical and Electronics Engineers (IEEE) Particle Accelerator Conference (PAC), San Francisco, CA, 6-9 May 1991
(Contract DE-AC02-76CH-00016)
(DE91-017004; BNL-46474; CONF-910505-396) Avail: NTIS HC/MF A01

Photon Simulated Desorption of neutral species (PSD) is the major dynamic gas load in electron synchrotron light source. In the National Synchrotron Light Source, PSD presented initial machine commissioning difficulty. Sensitivity to surface contamination on PSD had been experienced during an incident of Fomblin Oil contamination. The U10B-Photon Stimulated Desorption Experimental Station is constructed to investigate: (1) the degree of the contribution to the photon stimulated desorption (PSD) from primary photon flux and scattered secondary photon flux, (2) the underlying mechanism for photon stimulated desorption, and (3) criteria to chose the proper beam tube material for a future accelerator such as the Superconducting X-Ray Lithography Source (SXLS), Free Electron Laser (FEL), Superconducting Super Collider (SSC), Advanced Light Source (ALS), etc. In this report, only photon stimulated desorption of neutral species (PSD) from aluminum with different surface treatments is reported to show the great potential for this station to investigate beam tube material selection. DOE

N92-11785# Argonne National Lab., IL.
MESON-EXCHANGE CALCULATION OF THE d(GAMMA,p)n IN THE GeV ENERGY REGION
T. S. H. Lee 1991 14 p
(Contract W-31-109-eng-38)
(DE91-017994; ANL/PP-64910) Avail: NTIS HC/MF A03

We show that a meson-exchange model of the d(gamma,p) reaction can be constructed to reproduce the energy-dependence of the existing data for the differential cross section at 90 deg. The prediction of the model in the GeV energy region is found to be radically different from the QCD prediction by Brodsky and Hiller. The results will be compared with the new data presented in a companion paper. DOE

N92-11786# Lawrence Livermore National Lab., CA.
A REALISTIC, GRADUAL AND ECONOMICAL APPROACH TO FUSION POWER
A. Szoeke and R. W. Moir 15 Jun. 1991 12 p Presented at the 6th International Conference on Emerging Nuclear Energy Systems, Monterey, CA, 16-21 Jun. 1991
(Contract W-7405-eng-48)
(DE91-018464; UCRL-JC-106443; CONF-910626-12) Avail: NTIS HC/MF A03

This article describes, in broad outline, a nuclear power plant that generates power by means of repetitive, low-yield explosions in an underground chamber. Such a plant can be built in the near future by using modest extensions of existing technology, and it could be economically competitive if certain parts of the cost are controlled. This is in contrast to magnetic and inertial confinement fusion, of which the technical and economic feasibility will remain highly uncertain for the foreseeable future. Technical improvements of the envisioned plant can be introduced gradually with corresponding reductions in cost of power production. With advancing technology, an increasingly larger fraction of the power can be extracted from fusion reactions, thus providing a smooth transition to a fusion-based economy. Eventually, pure (inertial) fusion schemes could be incorporated into the power plant in a natural way, thereby shortening the time required to achieve large-scale use of fusion power, possibly by decades. This article considers both the technical aspects of this route to fusion power and the relevant issues of public policy. DOE

N92-11787# Phillips Lab., Edwards AFB, CA.
SHIELDING REQUIREMENTS FOR PARTICLE BED PROPULSION SYSTEMS Special Report, May 1990 - Mar. 1991
S. J. Gruneisen Jun. 1991 88 p
(AD-A240780; PL-TR-91-3018) Avail: NTIS HC/MF A05
CSCL 21/6

Nuclear Thermal Propulsion systems present unique challenges in reliability and safety. Due to the radiation incident upon all components of the propulsion system, shielding must be used to keep nuclear heating in the materials within limits; in addition, electronic control systems must be protected. This report analyzes the nuclear heating due to the radiation and the shielding required to meet the established criteria while also minimizing the shield mass. Heating rates were determined in a 2000 MWt Particle Bed Reactor (PBR) system for all materials in the interstage region, between the reactor vessel and the propellant tank, with special emphasis on meeting the silicon dose criteria. Using a Lithium Hydride/Tungsten shield, the optimum shield design was found to be: 50 cm LiH/2 cm W on the axial reflector in the reactor vessel and 50 cm LiH/2 cm W in a collar extension of the inside shield outside of the pressure vessel. Within these parameters, the radiation doses in all of the components in the interstage and lower tank regions would be within acceptable limits for mission requirements. GRA

74 OPTICS

Includes light phenomena; and optical devices.
For lasers see *36 Lasers and Masers.*

N92-11788# Department of the Navy, Washington, DC.
MICRO PHOTOREFLECTANCE SEMICONDUCTOR WAFER ANALYZER Patent Application
Nicholas Bottka, inventor (to Navy) 21 Dec. 1990 22 p
(AD-D014950; US-Patent-Appl-SN-635215) Avail: NTIS HC/MF A03 CSCL 20/12

An apparatus for measuring local carrier concentration in a preselected area of a semiconductor is shown and described. An exciting light (preferably a laser) alters the sample's band-gap by photo injecting electron hole pairs in the area being measured. Because of the Franz-Keldysh effect, the photo injected carriers alter the sample's reflectivity. An optical fiber conducts a broad band source of probing light to the excited area on the sample. The sample reflects some of the broad band light back into a fiber that conducts the reflected light to an optical analyzer. The optical analyzer includes a dispersive element that disperses the reflected light onto a linear array of detectors. The analyzer thus simultaneously samples multiple wavelengths in the reflected spectrum. From the resulting samples, a computer deconvolutes the spectral line shape into a measurement of the local electric field and the local carrier concentration. Author (GRA)

N92-11789# Lawrence Livermore National Lab., CA.
OPTICAL DESIGN OF A HIGH POWER FIBER OPTIC COUPLER
R. E. English, Jr., J. M. Halpin, F. A. House, and R. D. Paris 19 Jun. 1991 8 p Presented at the Society of Photo-Optical Instrumentation Engineers (SPIE) Meeting, San Diego, CA, 21-26 Jul. 1991
(Contract W-7405-eng-48)
(DE91-016924; UCRL-JC-107591; CONF-9107115-26) Avail: NTIS HC/MF A02

Fiber optic beam delivery systems are replacing conventional mirror delivery systems for many reasons (e.g., system flexibility and redundancy, stability, and ease of alignment). Commercial products are available that use fiber optic delivery for laser surgery and materials processing. Also, pump light of dye lasers can be delivered by optical fibers. Many laser wavelengths have been transported via optical fibers; high power delivery has been reported for argon, Nd:YAG, and excimer. We have been developing fiber optic beam delivery systems for copper vapor laser light; many of the fundamental properties of these systems are applicable to other high power delivery applications. A key element of fiber optic beam delivery systems is the coupling of laser light into the optical fiber. For our application, this optical coupler must be robust

to a range of operating parameters and laser characteristics. We have access to a high power copper vapor laser beam that is generated by a master oscillator/power amplifier (MOPA) chain comprised of three amplifiers. The light has a pulse width of 40 to 50 nsec with a repetition rate of about 4 kHz. The average power (nominal) to be injected into a fiber is 200 W. (We will refer to average power in this paper.) In practice, the laser beam's direction and collimation change with time. These characteristics plus other mechanical and operational constraints make it difficult for our coupler to be opto-mechanically referenced to the laser beam. We describe specifications, design, and operation of an optical system that couples a high power copper vapor laser beam into a large core, multimode fiber. The approach used and observations reported are applicable to fiber optic delivery applications. DOE

N92-11790 Georgia Inst. of Tech., Atlanta.
ILLUMINATION, OPTICS, AND RETROREFLECTORS FOR EFFICIENT LANDMARK TRACKING Thesis
Eun Ho Lee 1991 181 p
Avail: Univ. Microfilms Order No. DA9124535

The design methods for a Landmark Tracking System (LTS) is a non-contact position measurement sensor. It is a totally self-contained vision system that does not need an additional image processor or frame grabber. The characteristics of a retroreflector, especially the case of a sheet type retroreflector which utilizes coated glass beads, are investigated. An analysis of the glass bead retroreflector shows that its retroreflective characteristics are closely related to the refractive index of the glass material. The nature of retroreflection requires a special illumination design. Two illumination methods, which are the coaxial illumination and the edge illumination, are compared in terms of their relative light power of the landmark image on the charge-coupled device (CCD) sensor surface. Also, the irradiance pattern of a landmark image on the sensor surface is derived. As the optics for the LTS, a pinhole is selected. The quality of the image from a pinhole optics is related to pinhole size. The optimal size of the pinhole is derived using a numerical method. The method is based on a criterion that minimizes the size of the image from a point target. Various sources may cause errors in the position estimation output of the LTS. Several possible error sources and their effects on the position measurement calculation are analyzed. These include the image's nonuniform irradiance levels, the thickness of the pinhole, and light backscattering. Experiments are performed with a prototype of the LTS. First, the characteristics of the CCD sensor and the electronic components of the system are measured. The CCD sensor's dark current characteristics and the light sensitivities are measured. Secondly, the irradiance pattern on the detector of the LTS of retroreflective materials is measured, and compared with the analytical results. In addition, the light backscattering effect is measured with respect to the light source power and the distance from the light source to the optical axis. Finally, the performance in landmark tracking is determined. The repeatability and accuracy of position measurements are taken as measures of performance. Author

N92-11791*# National Aeronautics and Space Administration. Pasadena Office, CA.
DUAL FREQUENCY OPTICAL CARRIER TECHNIQUE FOR TRANSMISSION OF REFERENCE FREQUENCIES IN DISPERSIVE MEDIA Patent Application
Lutfollah Maleki, inventor (to NASA) (Jet Propulsion Lab., California Inst. of Tech., Pasadena.) 20 May 1991 14 p
(Contract NAS7-918)
(NASA-Case-NPO-18007-1-CU; NAS 1.71:NPO-18007-1-CU; US-Patent-Appl-SN-703238) Avail: NTIS HC/MF A03 CSCL 20F

This invention relates to stabilized frequency distribution links, suitable for guided wave and free space applications, and immune to degradations resulting from the variations of the dispersive properties of the propagation medium. In this system two different carrier frequencies modulated by a reference frequency are transmitted to each receiver in order to be synchronized. Each receiver is constructed to respond to local phase differences between the two received signals and to correct the phase of one them (the signals) so as to maintain the corrected signal as a reliable synchronization reference. NASA

N92-11792 Department of the Navy, Washington, DC.
COMPACT OPTICAL RF SPECTRUM ANALYZER Patent
John N. Lee, inventor (to Navy) and Carl M. Verber, inventor (to Navy) 25 Jun. 1991 11 p Filed 10 Jan. 1990 Supersedes AD-D014481
(AD-D014962; US-Patent-5,027,055; US-Patent-Appl-SN-463063; US-Patent-Class-324-77K) Avail: US Patent and Trademark Office CSCL 20/1

An improved compact optical and rugged laser-driven RF spectrum analyzer being made up of slab-like waveguide means is discussed. The waveguide means has at one end enhanced surface diffraction grating means for intercepting and selectively diffracting a laser source beam so that the diffracted laser beam is deflected, expanded and focussed to converge toward the other end and in relation to both a surface acoustic wave (SAW) and detector array means. The waveguide means includes novel combined signal detection and arcuate-shaped transducer (CSD/AT) means between its ends for forming and directing the SAW in response to a detected RF (microwave) signal to be analyzed such that the SAW optically intercepts, interacts and further diffracts in Bragg-Cell-like fashion that converging beam so as to deflect same relative to detector array means at the other end of the waveguide means. The detector array means normally analyzes a series of differently deflected beams so as to provide frequency distribution and intensity of one or more detected signals. GRA

N92-11793# Sandia National Labs., Albuquerque, NM.
PROCESS FOR CONTROLLING THE THICKNESS OF AN ANTIREFLECTION COATING, AND EMBODYING APPARATUS
J. Landreau and Hisao Nakajima (Centre National d'Etudes des Telecommunications, Issy-les-Moulineaux, France) 30 May 1991 11 p Transl. into ENGLISH of European Patent Application No. 0407298A1 (9 Jan. 1991)
(Contract DE-AC04-76DP-00789)
(DE91-017634; ALS/TR-91-015) Avail: NTIS HC/MF A03

The object of this invention is a process for controlling the thickness of an antireflection coating, and an embodying apparatus. It is applicable in the antireflection processing of facets of semiconductor lasers. It is known that an antireflection coating whose index n satisfies the equation n(exp 2) = n(sub 0), where n(sub 0) is the index of the substrate onto which it is deposited, the thickness of which is equal to lambda/4n, where lambda is the wavelength. For any given material, the thickness can be adjusted to obtain a good antireflection coating. It is considered that a good antireflection coating is a coating whose reflectivity is less than 10(exp -3). This very low value imposes severe constraints on the thickness, which must be adjusted to better than 10(exp -2). It is therefore relatively difficult to produce good antireflection coatings. DOE

N92-11794# Lawrence Livermore National Lab., CA.
STRAY LIGHT REDUCTION IN A WFOV STAR TRACKER LENS
I. T. Lewis, A. G. Ledebuhr, T. S. Axelrod, and S. A. Ruddell 23 Jul. 1991 21 p Presented at the Society of Photo-Optical Instrumentation Engineers (SPIE) Meeting, San Diego, CA, 21-26 Jul. 1991
(Contract W-7405-eng-48)
(DE91-018460; UCRL-JC-106888; CONF-9107115-46) Avail: NTIS HC/MF A03

Lawrence Livermore National Laboratory (LLNL) has recently developed a wide field-of-view 28 x 44 degs. camera for use as a star tracker navigational sensor. As for all seasons, stray light rejection performance is critical. Due to the baffle dimensions dictated by the large field angles, the 2-part sunshade/baffle configuration commonly seen on spaceborn telescopes is impractical. Meeting the required stray light rejection performance

(of 10(exp -7) Point Source Transmittance, (PST)) with a 1-part baffle required iterative APART modeling (APART is an industry standard stray light evaluation program), hardware testing, and mechanical design correction. This paper presents a chronology of lens and baffle improvements that resulted in the meeting of the stray light rejection goal outside the solar exclusion angle of the baffle stage. Comparisons with APART analyses are given, and future improvements in mechanical design are discussed. Stray light testing methods and associated experimental difficulties are presented. DOE

N92-11729*# Massachusetts Inst. of Tech., Cambridge.
MODEL PROBLEM
A. Louise Perkins *In* ICASE, Proceedings for the ICASE Workshop on Heterogeneous Boundary Conditions Aug. 1991 p 1-6 (For primary document see N92-11728 02-64)
Avail: NTIS HC/MF A05 CSCL 20F

75 PLASMA PHYSICS

Includes magnetohydrodynamics and plasma fusion.

For ionospheric plasmas see *46 Geophysics*. For space plasmas see *90 Astrophysics*.

N92-11795*# TRW Space Technology Labs., Redondo Beach, CA. Applied Technology Div.
ISEE/ICE PLASMA WAVE DATA ANALYSIS Final Report, Jan. 1985 - Oct. 1989
E. W. Greenstadt Oct. 1989 89 p
(Contract NAS5-28703)
(NASA-CR-189244; NAS 1.26:189244; TRW-46179-6041-UT-00)
Avail: NTIS HC/MF A05 CSCL 20I

The work performed for the period 1 Jan. 1985 to 30 Oct. 1989 is presented. The objective was to provide reduction and analysis of data from a scientific instrument designed to study solar wind and plasma wave phenomena on the International Sun Earth Explorer 3 (ISEE-3)/International Cometary Explorer (ICE) missions. Author

N92-11796# National Inst. for Fusion Science, Nagoya (Japan).
ON RADIAL ELECTRIC FIELD STRUCTURE IN CHS TORSATRON/HELIOTRON
H. Sanuki, Kimitaka Itoh, Katsumi Ida, and Sanae-I. Itoh Jun. 1991 33 p
(NIFS-94; ISSN-0915-633X) Avail: NTIS HC/MF A03

The radial electric field structure in helical systems is discussed taking into account the effects of the orbit loss and charge exchange loss in addition to the neoclassical fluxes. Analysis is made for the CHS torsatron/heliotron, in which the radial electric field was estimated experimentally. It was found that the fast ion orbit loss and charge exchange loss have strong influence on the profile of the radial electric field, particularly near the plasma periphery. The absolute value of the radial electric field in the experiments is still more negative than the theoretical prediction. Author

N92-11797# National Inst. for Fusion Science, Nagoya (Japan).
INFLUENCE OF FAST ION LOSS ON RADIAL ELECTRIC FIELD IN WENDELSTEIN 7-A STELLARATOR
Kimitaka Itoh, H. Sanuki, and Sanae-I. Itoh Jun. 1991 22 p
(NIFS-95; ISSN-0915-633X) Avail: NTIS HC/MF A03

A theoretical model is developed to determine the radial electric field and the fast ion loss simultaneously in stellarators, and is applied to the Wendelstein 7-A Stellarator. The predicted value of the radial electric field is closer to experiments than the purely neoclassical calculation. The loss rate, which is determined simultaneously, is in the range of experimental observations. Author

N92-11798# National Inst. for Fusion Science, Nagoya (Japan).
SYMPOSIUM ON DEVELOPMENT AND APPLICATIONS OF INTENSE PULSED PARTICLE BEAMS
Kiyoshi Yatsui, ed. Jun. 1991 143 p Symposium held in Nagoya, Japan, 6-7 Dec. 1990
(NIFS-PROC-8; ISSN-0915-6348) Avail: NTIS HC/MF A07

Papers from the symposium are presented. The following topics are covered: (1) light ion beam interaction with target of indirect driven ICF; (2) ion-beam power amplification through x ray conversion; (3) proton beam fusion; (4) developments for high performance light ion beams; (5) generation and focusing of a proton beam by an inverse pinch ion diode; (6) optimization of a self-magnetically insulated plasma focus diode; (7) diagnostics and evaluation of an anode plasma in a point pinch diode; (8) an experimental study on the spectrum of microwave radiation from intense relativistic electron beam (IREB)-plasma interactions; (9) characteristics of plasma injection type pulsed ion diodes; (10) development of intense negative ion sources; (11) production of pulsed beams of negative light-heavy ions; (12) pulsed power generation by an inductive energy storage system; (13) generation of relativistic electron beams by pulsed power generation using an inductive storage system; and (14) intense beams of highly-ionized metallic ions generated in the point pinch diode. Author

N92-11799# National Inst. for Fusion Science, Nagoya (Japan).
PROCEEDINGS OF THE FIRST INTERNATIONAL TOKI CONFERENCE ON PLASMA PHYSICS AND CONTROLLED NUCLEAR FUSION: NEXT GENERATION EXPERIMENTS IN HELICAL SYSTEMS
Mar. 1990 292 p Conference held in Toki, Japan, 4-7 Dec. 1989 Submitted for publication
(NIFS-Proc-3; ISSN-0915-6348) Avail: NTIS HC/MF A13

The First International Conference on Plasma Physics and Controlled Nuclear Fusion was held on 4-7 December 1989, in Tokishi Bunka Plasa. Topics discussed include the status of the Large Helical Device, the design of the Compact Auburn Torsatron, magnetohydrodynamic stability, drift optimization in helical systems, plasma transport in advanced stellarators, tokamak devices, and the Advanced Toroidal Facility. For individual titles, see N92-11800 through N92-11870.

N92-11800# National Inst. for Fusion Science, Nagoya (Japan). LHD Design Group.
PRESENT STATUS OF THE LARGE HELICAL DEVICE PROJECT
Osamu Motojima *In its* Proceedings of the First International Toki Conference on Plasma Physics and Controlled Nuclear Fusion: Next Generation Experiments in Helical Systems Mar. 1990 p 3-6 (For primary document see N92-11799 02-75)
Avail: NTIS HC/MF A13

The National Institute for Fusion Science is a new large fusion research institute in Japan. It is responsible for the joint university researches of plasma physics and fusion technology. The major experimental facility of the institute is the Large Helical Device (LHD), which is now in the phase of practical design. Described here is the design study of the LHD. The goal is the demonstration of high energy and high bar-beta' plasma production in the helical device, which is a necessary step toward the realization of the helical reactor system. Author

N92-11801# Max-Planck-Inst. fuer Plasmaphysik, Garching (Germany, F.R.).
STATUS OF THE WENDELSTEIN VII-X PROJECT
Gunter Grieger *In* National Inst. for Fusion Science, Proceedings of the First International Toki Conference on Plasma Physics and Controlled Nuclear Fusion: Next Generation Experiments in Helical Systems Mar. 1990 p 7-10 (For primary document see N92-11799 02-75)
Avail: NTIS HC/MF A13

The objectives of the Wendelstein VII-X project are to demonstrate the reactor potential of Advanced Stellarators, including the following items: to demonstrate plasma build-up by non-ohmic means; to prove that plasma confinement is adequate; to show that stability can be achieved at high enough beta; to demonstrate stationary operation, controlled by refuelling and

exhaust only; and to prove that magnet technology is feasible and simple. The Wendelstein VII-X promises good confinement, a negligible loss cone, stability at high enough beta, good prospects for stationary operation, low bootstrap current, moderate shear, a feasible magnet technology, and seems to be compatible with present budget constraints. Author

N92-11802# Oak Ridge National Lab., TN.
OVERVIEW OF THE ATF-II STUDIES
James F. Lyon, Brian A. Carreras, L. Dresner, S. P. Hirshman, R. N. Morris, S. L. Painter, and J. A. Rome *In* National Inst. for Fusion Science, Proceedings of the First International Toki Conference on Plasma Physics and Controlled Nuclear Fusion: Next Generation Experiments in Helical Systems Mar. 1990 p 11-15 (For primary document see N92-11799 02-75)
(Contract DE-AC05-84OR-21400)
Avail: NTIS HC/MF A13

Design studies focusing on critical physics and engineering issues for a low aspect ratio, large next generation stellarator, ATF-II, are described. The Compact Torsatron approach is the most developed one, but there are concerns about energetic orbit confinement. An integrated (magnetohydrodynamics plus orbit) optimization may lead to a better magnetic configuration. Author

N92-11803# Centro de Investigaciones Energeticas, Madrid (Spain).
REVIEW OF THE TJ-II FLEXIBLE HELIAC PROJECT Abstract Only
Carlos L. Alejaldre, L. Almoguera, J. Alonso, E. Anabitarte, E. Ascasibar, M. Blaumoser (Max-Planck-Inst. fuer Plasmaphysik, Garching, Germany, F.R.), J. Botija, B. G. Castaner, F. Castejon, and J. R. Cepero et al *In* National Inst. for Fusion Science, Proceedings of the First International Toki Conference on Plasma Physics and Controlled Nuclear Fusion: Next Generation Experiments in Helical Systems Mar. 1990 p 16 (For primary document see N92-11799 02-75)
Avail: NTIS HC/MF A13

The TJ-II is a device oriented to the study of the properties of helical magnetic axis plasmas in a wide range of configurations. The design of the device was tailored to provide as much flexibility as possible in the magnetic structure. Design parameters are R sub 0 equals 1.5 m and B sub 0 equals 1 T in a 4-periods symmetry. A central core composed of two different coils enables the attainment, by adequate setting of the current in each coil, of different magnetic configurations with the following flexibility ranges: 1/M approximately equals 0.24 to 0.62, plasma radius approximately equals 0.2 - 0.1 m, shear approximately equals -1 percent to + 10 percent, and magnetic well approximately equals 0 to 6 percent. Plasma start-up and heating will be based on electron cyclotron heating (ECH) by using 2 gyrotrons of 200 kw each, CW at 53.2 GHz. Here, we review the physics for such configurations in different areas: equilibrium, deducing the operational space for TJ-II; stability, with special emphasis on beta limits and access to the second stability regime; heating, discussing the optimization of absorption and the adopted ECH scheme; and transport, deducing confinement properties for the different heating scenarios. In addition, the experimental program to develop this device and the engineering solutions found for the most critical elements of the TJ-II heliac during its detailed design are discussed. Author

N92-11804# Australian National Univ., Canberra. Dept. of Theoretical Physics.
THE ANU HELIAC PROGRAM
Robert L. Dewar, H. J. Gardner, G. J. Cooper, S. M. Hamberger, L. E. Sharp, B. D. Blackwell, T. Y. Tou, G. D. Conway, X.-H. Shi, and D.-F. Zhou et al *In* National Inst. for Fusion Science, Proceedings of the First International Toki Conference on Plasma Physics and Controlled Nuclear Fusion: Next Generation Experiments in Helical Systems Mar. 1990 p 17-20 Previously announced as N90-20843 (For primary document see N92-11799 02-75)
Avail: NTIS HC/MF A13

The history and current status of theoretical and experimental work on heliacs at the Australian National University are reviewed. A plasma containment device, helical control windings, and reactor design are discussed. Author

N92-11805# Auburn Univ., AL. Dept. of Physics.
DESIGN OF THE COMPACT AUBURN TORSATRON
Rex F. Gandy, M. A. Henderson, J. D. Hanson, T. Schneider, D. G. Swanson, and J. R. Cary (Colorado Univ., Boulder.) *In* National Inst. for Fusion Science, Proceedings of the First International Toki Conference on Plasma Physics and Controlled Nuclear Fusion: Next Generation Experiments in Helical Systems Mar. 1990 p 21-25 Sponsored by Maxwell Labs., Inc.; TRW, Inc.; and Allied-Signal Corp. (For primary document see N92-11799 02-75)
(Contracts DE-FG02-85ER-53207; DE-FG85-85ER-53192; NSF PHY-84-51275)
Avail: NTIS HC/MF A13

The Compact Auburn Torsatron (CAT) is a low aspect ratio, continuous coil, toroidal magnetic fusion device. CAT has two main helical coils: an l equals 2, m equals 5 coil, and an l equals 1, m equals 5 coil. The machine has a major radius of 56 cm, an average plasma radius of 11 cm, and a steady state magnetic field of 1 kG. CAT was designed using an optimization scheme which employs the coil positions and coil winding laws as parameters. Once CAT is operational, the research program will focus on the study of magnetic flux surfaces and ion cyclotron heating. Author

N92-11806# Max-Planck-Inst. fuer Plasmaphysik, Garching (Germany, F.R.).
OPTIMIZATION OF HELIAS CONFIGURATIONS
Jurgen Nuehrenberg *In* National Inst. for Fusion Science, Proceedings of the First International Toki Conference on Plasma Physics and Controlled Nuclear Fusion: Next Generation Experiments in Helical Systems Mar. 1990 p 29-32 (For primary document see N92-11799 02-75)
Avail: NTIS HC/MF A13

The Helias optimization procedure is outlined. Evidence for the convergence behavior in stellarator configurational space is presented. The hierarchy of optimization is described. Details of the optimization of Helias configurations for W VII-X, i.e., the attainability and compatibility of seven stellarator specific goodness criteria, are given in the subsequent workshop. Author

N92-11807# Centro de Investigaciones Energeticas, Madrid (Spain).
SECOND STABILITY STUDIES IN A HELICAL AXIS DEVICE: TJ-II
Carlos L. Alejaldre, A. Varias, A. Lopez-Fraguas, Brian A. Carreras, N. Dominguez, and V. E. Lynch (Oak Ridge National Lab., TN.) *In* National Inst. for Fusion Science, Proceedings of the First International Toki Conference on Plasma Physics and Controlled Nuclear Fusion: Next Generation Experiments in Helical Systems Mar. 1990 p 33-36 (For primary document see N92-11799 02-75)
Avail: NTIS HC/MF A13

The helical hard core in the four period TJ-II heliac permits access to a variety of magnetic configurations with very different magnetohydrodynamic properties. Here, a particular set of shearless configurations is presented with similar rotational transform at the magnetic axis, approximately equals 1.20, and slightly different values of the magnetic well that exhibit self-stabilization behavior to Mercier modes characteristic of a second stability regime. Author

N92-11808# National Inst. for Fusion Science, Nagoya (Japan).
THE 3-D EQUILIBRIA OF HELICAL SYSTEMS: MAGNETIC ISLANDS AND THEIR CONTROL
Takaya Hayashi *In its* Proceedings of the First International Toki Conference on Plasma Physics and Controlled Nuclear Fusion: Next Generation Experiments in Helical Systems Mar. 1990

p 37-40 (For primary document see N92-11799 02-75)
Avail: NTIS HC/MF A13

Three dimensional equilibrium and breaking of magnetic surfaces due to the finite beta effect in a 1 equals 2 heliotron configuration are studied by using a newly developed three-dimensional equilibrium code. Several methods to suppress the breaking are discussed. Author

N92-11809# Oak Ridge National Lab., TN.
RESISTIVE MHD STABILITY STUDIES FOR ATF PLASMAS DURING OPERATION IN THE SECOND STABILITY REGIME
Lowell A. Charlton, J. N. Leboeuf, Brian A. Carreras, N. Dominguez, and V. E. Lynch *In* National Inst. for Fusion Science, Proceedings of the First International Toki Conference on Plasma Physics and Controlled Nuclear Fusion: Next Generation Experiments in Helical Systems Mar. 1990 p 41-44 (For primary document see N92-11799 02-75)
(Contract DE-AC05-84OR-21400)
Avail: NTIS HC/MF A13

In the initial period of operation of the Advanced Toroidal Facility (ATF) stellarator device, the beta self-stabilization effect on fluctuations was observed. The measured magnetic fluctuations increased with beta up to beta sub 0 equals 1.5 percent, and decreased for higher beta values. This indicated that the AFT was operating in a regime where beta self-stabilization effects were dominant. AFT was designed to operate in the second stability regime with respect to ideal magnetohydrodynamics. It was shown that resistive instabilities remain in the second stability regime, but they can be affected by beta self-stabilization effects. Researchers present the results of detailed nonlinear studies of these instabilities for equilibrium parameters corresponding to those of the AFT. The results show a reduction in the magnetic perturbations at high beta, as observed in the experiment. The beta self-stabilization effect is also seen in the simulations from a sharp reduction in the turbulence inside the plasma core at high beta and a decrease in the saturation level of the kinetic energy. Author

N92-11810# Kyoto Univ., Uji (Japan). Plasma Physics Lab.
DRIFT OPTIMIZATION OF HELICAL SYSTEMS
Kiyoshi Hanatani *In* National Inst. for Fusion Science, Proceedings of the First International Toki Conference on Plasma Physics and Controlled Nuclear Fusion: Next Generation Experiments in Helical Systems Mar. 1990 p 45-48 (For primary document see N92-11799 02-75)
Avail: NTIS HC/MF A13

The minimization of the particle loss region of heliotron/torsatron configurations is considered. Both Heliotron E (high aspect ratio) and Large Helical Device (LHD) (low aspect ratio) configurations are examined and compared. In the drift optimization of Heliotron E, the vertical field B sub v is used to minimize the loss region. The ultimate shift of magnetic axis delta sub v (opt) and operation window with respect to B sub v are predicted and compared with Heliotron E experiments. Correlations between the theoretical prediction and experimental observations are discussed. As for the LHD configuration, modulations of the helical field (HF) coil and multipole moments from the poloidal field (PF) coil set are used to minimize the loss region. It is shown that the loss region of a LHD configuration can be reduced as narrowly as that of the standard Heliotron E configuration by simultaneous control of the vertical and quadrupole field. Author

N92-11811# Max-Planck-Inst. fuer Plasmaphysik, Garching (Germany, F.R.).
PLASMA TRANSPORT IN ADVANCED STELLARATORS
Horst Wobig *In* National Inst. for Fusion Science, Proceedings of the First International Toki Conference on Plasma Physics and Controlled Nuclear Fusion: Next Generation Experiments in Helical Systems Mar. 1990 p 49-52 (For primary document see N92-11799 02-75)
Avail: NTIS HC/MF A13

Reformulated here is the neoclassical theory of general toroidal equilibria. The relevant geometrical parameters are identified and it is shown how the reduction of Pfirsch-Schluter currents affects neoclassical transport and bootstrap effects. The influence of turbulent electromagnetic fluctuations is also discussed. Since a toroidal loop voltage is included, the theory is valid for all toroidal systems. Author

N92-11812# Japan Atomic Energy Research Inst., Naka. Fusion Research Establishment.
RECENT EXPERIMENTS IN JT-60
Hiroshi Kishimoto *In* National Inst. for Fusion Science, Proceedings of the First International Toki Conference on Plasma Physics and Controlled Nuclear Fusion: Next Generation Experiments in Helical Systems Mar. 1990 p 53-56 (For primary document see N92-11799 02-75)
Avail: NTIS HC/MF A13

Recent experiments in JT-60 have been conducted mainly on the plasma parameter improvement and the current drive optimization. Energy confinement can be improved by pellet injection. High beta sub p (less than or equal to 3) discharges are obtained with high power neutral beam (NB) heating and then the bootstrap current becomes dominant in the plasma current. Lower hybrid (LH) current drive efficiency is improved up to 3.4 times 10 (exp 19) m (exp -2) MA/MW with a multijunction launcher. Sawtooth activity is suppressed successfully by the LH wave. Author

N92-11813# Hokkaido Univ., Sapporo (Japan). Dept. of Nuclear Engineering.
GRAPHITES AS PLASMA FACING MATERIAL OF A LARGE FUSION DEVICE
Tomoaki Hino and Toshiro Yamashina *In* National Inst. for Fusion Science, Proceedings of the First International Toki Conference on Plasma Physics and Controlled Nuclear Fusion: Next Generation Experiments in Helical Systems Mar. 1990 p 57-60 (For primary document see N92-11799 02-75)
Avail: NTIS HC/MF A13

Several graphites, such as the first wall materials of the Large Helical System, are evaluated in terms of erosion, thermal shock resistance, and recycling. Adequate graphites are suggested, and the required conditions such as baking, cooling, and the discharge cleaning are discussed. Author

N92-11814# Academia Sinica, Hefei (China). Inst. of Plasma Physics.
THE MAIN FUSION ACTIVITIES IN INSTITUTE OF PLASMA PHYSICS, ACADEMIA SINICA
Wang Shao-Hu *In* National Inst. for Fusion Science, Proceedings of the First International Toki Conference on Plasma Physics and Controlled Nuclear Fusion: Next Generation Experiments in Helical Systems Mar. 1990 p 61-64 (For primary document see N92-11799 02-75)
Avail: NTIS HC/MF A13

The Academy Sinica of the Institute of Plasma Physics (ASIPP), established in 1978, is one of the most important research centers in China. Two tokamak devices are in operation. It was found that a resonant helical field can significantly suppress the magnetohydrodynamic modes and improve the confinement of the plasma. A middle sized tokamak device will be put into operation in 1991. Since 1987, ASIPP has been conducting a national high technology program, the Fusion Fission Hybrid Reactor Program. Author

N92-11815# Kyoto Univ., Uji (Japan). Plasma Physics Lab.
ANALYSIS OF SCRAPE-OFF LAYER IN TOROIDAL HELICAL SYSTEMS
Kazunobu Nagasaki, Kimitaka Itoh, Sanae-I. Itoh, and Atsushi Fukuyama (Okayama Univ., Japan) *In* National Inst. for Fusion Science, Proceedings of the First International Toki Conference on Plasma Physics and Controlled Nuclear Fusion: Next Generation Experiments in Helical Systems Mar. 1990 p 65-68 (For primary document see N92-11799 02-75)
Avail: NTIS HC/MF A13

Magnetic field structure of the scrape-off layer region in toroidal helical systems is analyzed by using toroidal harmonic functions.

The connection length of the field line to the wall is calculated for various configurations. It is found that L has a logarythmic dependence on the distance from the outermost magnetic surface or from the residual magnetic islands. The effect of the axisymmetric fields on the stress structure is also discussed.
Author

N92-11816# Princeton Univ., NJ. Plasma Physics Lab.
DETACHED PLASMA AND DENSITY LIMIT OF TOKAMAKS Abstract Only
Shoichi Yoshikawa *In* National Inst. for Fusion Science, Proceedings of the First International Toki Conference on Plasma Physics and Controlled Nuclear Fusion: Next Generation Experiments in Helical Systems Mar. 1990 p 69 (For primary document see N92-11799 02-75)
Avail: NTIS HC/MF A13

An analytical solution of detached plasmas in a tokamak plasma is assumed at the plasma edge. The additional condition that the safety factor of the plasma must be over 2 leads to the density limit. Thus, a tokamak plasma can be classified into (1) limiter or divertor limited, (2) detached plasmas, and (3) disruptive plasmas, as the plasma density increases from 1 to 3. Author

N92-11817# National Inst. for Fusion Science, Nagoya (Japan).
CONFINEMENT IMPROVEMENT BY EDGE CONTROL
Naruyoshi Ohyabu *In its* Proceedings of the First International Toki Conference on Plasma Physics and Controlled Nuclear Fusion: Next Generation Experiments in Helical Systems Mar. 1990 p 70-72 (For primary document see N92-11799 02-75)
Avail: NTIS HC/MF A13

Three types of diverter operation were considered to improve the plasma performance, particularly the energy confinement in the Large Helical Diverter (LHD) device. They are (1) high density, cold diverter plasma operation for reducing the purity sputtering; (2) H-mode type operation for minimizing the deterioration of the energy confinement at high input power; and (3) high temperature divertor plasma operation for further enhancement of the energy confinement. The major goal of the helical diverter system is that a wide range of divertor operation modes or scenarios can be attempted to optimize overall plasma performance. Author

N92-11818# National Inst. for Fusion Science, Nagoya (Japan).
EFFECTS OF PERTURBING HELICAL FIELDS ON CONFINEMENT OF HELIOTRON DR PLASMA
Shigeyuki Morimoto, M. Nakasuga, N. Yanagi, Motoyasu Sato, and Tokuhiro Obiki (Kyoto Univ., Uji, Japan) *In its* Proceedings of the First International Toki Conference on Plasma Physics and Controlled Nuclear Fusion: Next Generation Experiments in Helical Systems Mar. 1990 p 73-76 (For primary document see N92-11799 02-75)
Avail: NTIS HC/MF A13

Two types of perturbing helical fields were applied to Heliotron DR plasma: type A makes a large m=n=1 magnetic island at r/a sub p is similar to 0.5; whereas type B makes a set of many islands with high mode numbers (m=5, 4, 3,; n=5, 6, 7, 8, 9, 10) at 0.5 similar to or less than r/a sub p similar to or less than 1. Deterioration of plasma confinement due to the type A perturbation was observed at B sub 1, sub 1/B sub t similar to 3 x 10(exp -4), where B sub 1, sub 1 and B sub t are the Fourier component of m=n=1 and the confining toroidal field, respectively. The plasma performance is less sensitive to the type B perturbation and the confinement deterioration was not found even at zeta greater than 1, where zeta is the overlapping parameters of the magnetic islands. Author

N92-11819# Oak Ridge National Lab., TN.
OVERVIEW OF RECENT RESULTS FROM THE ADVANCED TOROIDAL FACILITY
Masanori Murakami, E. Anabitarte, F. S. B. Anderson, G. L. Bell, J. D. Bell, T. S. Bigelow, Brian A. Carreras, Lowell A. Charlton, T. L. Clark (Tennessee Univ., Knoxville.), and R. J. Colchin et al *In* National Inst. for Fusion Science, Proceedings of the First International Toki Conference on Plasma Physics and Controlled Nuclear Fusion: Next Generation Experiments in Helical Systems Mar. 1990 p 77-80 Previously announced as N90-19853 (For primary document see N92-11799 02-75)
(Contract DE-AC05-84OR-21400)
Avail: NTIS HC/MF A13

An overview of recent experimental results from the Advanced Toroidal Facility (ATF) is presented. Beam heated plasmas with bar n sub e of 10(exp 20)/cu m and tau sub E* of approx. 20 ms were achieved. Thermal collapse of the plasmas is mitigated by wall conditioning and particle fueling. Confinement time scales positively with density and magnetic field, offsetting deterioration with power. Results fit the LHD scaling and the drift wave turbulence scaling. Bootstrap currents observed during electron cyclotron heating (ECH) agree with neoclassical theory in magnitude and parameter dependences. Fast reciprocating Langmuir probe measurements show that edge fluctuations in ATF have many similarities to those in the TEXT tokamak. The location of magnetic flux instabilities has shifted outward in radius, consistent with the broader pressure profiles. Author

N92-11820# Max-Planck-Inst. fuer Plasmaphysik, Garching (Germany, F.R.).
STATUS OF THE WVII-AS PROGRAM
Heinz Ringler, E. Anabitarte, E. Ascasibar, Sakae Besshou (Kyoto Univ., Japan), R. Brakel, R. Burhenn, G. Cattanei, A. Dodhy, D. Dorst, and A. Elsner et al *In* National Inst. for Fusion Science, Proceedings of the First International Toki Conference on Plasma Physics and Controlled Nuclear Fusion: Next Generation Experiments in Helical Systems Mar. 1990 p 81-84 (For primary document see N92-11799 02-75)
Avail: NTIS HC/MF A13

The first experimental campaign aimed at plasma production and confinement studies was successfully finished on Aug. 2, 1989. All standard diagnostics, the data acquisition and data handling system were available form the start up phase. The development of the 140 GHz system at KfK is on schedule. At the end of the year power supplies and a quasioptical transmission line will be supplied by IPP/IPF. KfK is testing a prototype at 140 GHz (TE sub 03 Mode, 200 kW, less than 100 ms). The complete system was expected to be operational in summer of 1990. Author

N92-11821# Wisconsin Univ., Madison. Torsatron/Stellarator Lab.
STATUS OF THE TORSATRON/STELLARATOR PROGRAM
Juda L. Shohet *In* National Inst. for Fusion Science, Proceedings of the First International Toki Conference on Plasma Physics and Controlled Nuclear Fusion: Next Generation Experiments in Helical Systems Mar. 1990 p 85-88 (For primary document see N92-11799 02-75)
(Contract DE-FG02-86ER-53216; ORNL Order 19X-3591-C)
Avail: NTIS HC/MF A13

Experimental research in the Torsatron/Stellarator Lab. has concentrated on two main areas: transport and divertor operation. Measurements were made in the Interchangeable Module Stellarator (IMS) with Langmuir probes to ascertain the extent to which the plasma pressure and potential varies on a magnetic surface. The degree to which the divertor flow could be altered in IMS was studied by means of electron injection into the divertor region. Also, the flux of particles streaming into the continuous coil Proto-Cleo Stellarator divertor was measured as a function of poloidal angle along the helical divertor path. Author

N92-11822# Kyoto Univ. (Japan). Plasma Physics Lab.
REVIEW OF HELIOTRON E EXPERIMENT
Tokuhiro Obiki, Hideki Zushi, Fumimichi Sano, Shigeru Sudo, Katsumi Kondo, Motoyasu Sato, M. Nakasuga, T. Mizuuchi, Sakae Besshou, and H. Okada et al *In* National Inst. for Fusion Science, Proceedings of the First International Toki Conference on Plasma Physics and Controlled Nuclear Fusion: Next Generation Experiments in Helical Systems Mar. 1990 p 89-92 (For primary document see N92-11799 02-75)
Avail: NTIS HC/MF A13

The effects of the magnetic configuration on edge plasma

parameters, plasma wall interaction, transport improvement, MHD activities, and fast ion confinement are studied by varying the vertical field and the toroidal field. The role of the vertical field is a change in the magnetic well/hill formation and the helical ripple localization by the axis shift vertical Delta. With toroidal field, the shape and size of the plasma cross section, the rotational transform and, as a consequence, shear are changed. The conclusions are summarized as follows: (1) results of edge diagnostics qualitatively agree with the change in the magnetic limiter configuration by the toroidal field; (2) the transport improvement is found in the inward shift case with a small toroidal field; (3) the stabilization effect of the toroidal field on the m=2/n=1 and m=1/n=1 modes is found; and (4) observed inward shifted CX flux distribution agrees well with the trapped particle orbit theory. Author

N92-11823# National Inst. for Fusion Science, Nagoya (Japan).
REVIEW OF CHS EXPERIMENT
Keisuke Matsuoka, Masami Fujiwara, J. H. Harris, Minolu Hosokawa, Katsumi Ida, H. Idei, Harukazu Iguchi, Osamu Kaneko, Shin Kubo, and K. Masai (Nagoya Univ., Japan) et al *In its* Proceedings of the First International Toki Conference on Plasma Physics and Controlled Nuclear Fusion: Next Generation Experiments in Helical Systems Mar. 1990 p 93-96 (For primary document see N92-11799 02-75)
Avail: NTIS HC/MF A13

Heating experiments with 28 GHz/53 GHz Electron Cyclotron Heating (ECH) and Neutral Beam Injection (NBI) were done under the following conditions: the field strength of the toroidal field from 0.46T to 1.5T, heating powers up to 150 kW and 1.1 MW for ECH and NBI respectively. The line averaged electron density bar n sub e is 0.1 similar to 10 x 10(exp 13)/cu cm, electron and ion temperatures are up to about 1.1 keV and 600 eV respectively: the collisionality ranges from the plateau to 1/upsilon regime. Magnetic field configuration study, where the magnetic axis position is scanned from the viewpoint of loss cone, shows that the confinement characteristics improve at an inward shifted axis position. Global energy confinement time is found to follow the Large Helical Device (LHD) scaling and to be improved compared with the scaling in some discharges. Author

N92-11824# Tohoku Univ., Sendai (Japan). Dept. of Nuclear Engineering.
EXPERIMENTAL STUDIES OF A HELICAL AXIS STELLARATOR (TU-HELIAC)
Sumio Kitajima, M. Takayama, T. Zama, M. Takahashi, N. Takeuchi, and Hirosige Watanabe *In* National Inst. for Fusion Science, Proceedings of the First International Toki Conference on Plasma Physics and Controlled Nuclear Fusion: Next Generation Experiments in Helical Systems Mar. 1990 p 97-100 (For primary document see N92-11799 02-75)
Avail: NTIS HC/MF A13

The recent experimental results are presented on TU-Heliac. TU-Heliac is a helical axis stellarator of heliac type and was built at Sendai in July 1988. The device description is given elsewhere. TU-Heliac has 4 periods, 48 cm of major radius, maximum toroidal field of 3.5 kG, and an average plasma radius of 6 to 8 cm. The swing radius of TF coil is 8 cm. The topics presented deal with measurements of the vacuum magnetic surfaces of TU-Heliac by three different kinds of electron beam methods, and measurements of 2-D contour of the plasma pressure to ensure the existence of the plasma equilibrium in a heliac and brief analytical calculation of the toroidal heliac equilibria. Author

N92-11825# Wisconsin Univ., Madison. Torsatron/Stellarator Lab.
DIVERTED PARTICLE-FLUX STUDIES IN THE IMS AND PROTO-CLEO STELLARATORS
Juda L. Shohet, D. T. Anderson, F. S. B. Anderson, P. G. Matthews, and Joseph N. Talmadge *In* National Inst. for Fusion Science, Proceedings of the First International Toki Conference on Plasma Physics and Controlled Nuclear Fusion: Next Generation Experiments in Helical Systems Mar. 1990 p 101-104 (For primary document see N92-11799 02-75)
Avail: NTIS HC/MF A13

Diverted particle fluxes were measured under varying conditions in electron cyclotron resonance produced and heated plasmas in both the Interchangeable Module Stellarator (IMS) and the Proto-Cleo 1=3, seven field period conventional stellarator. Flow patterns are observed to be dependent on magnetic field strength in IMS, with abrupt changes observed as the central field strength passes through resonance with the microwaves. Electron injection into the IMS diverted-flux areas, using a strongly emissive filament, was used to map connections between various diverted flux areas and to the scrape-off layer. Electron injection can also significantly alter observed divertor flows, in a fashion similar to previous results with divertor strike-plate biasing. Scoping studies of the diverted particle flux pattern were made in the Proto-Cleo Stellarator. Asymmetries are observed in the strength of the diverted flux along the path of the helical coil. These asymmetries are not strongly dependent on moderate levels of applied external vertical magnetic fields. Author

N92-11826# Wisconsin Univ., Madison. Torsatron/Stellarator Lab.
PRESSURE AND POTENTIAL MEASUREMENTS IN IMS DURING ELECTRON CYCLOTRON HEATING
Joseph N. Talmadge, D. T. Anderson, F. S. B. Anderson, B. J. Peterson, and Juda L. Shohet *In* National Inst. for Fusion Science, Proceedings of the First International Toki Conference on Plasma Physics and Controlled Nuclear Fusion: Next Generation Experiments in Helical Systems Mar. 1990 p 105-108 (For primary document see N92-11799 02-75)
(Contract DE-FG02-86ER-53216)
Avail: NTIS HC/MF A13

Two dimensional measurements of the plasma pressure were made in the Interchangeable Module Stellarator (IMS) at two separate toroidal locations. The results indicate that the profile is hollow during Electron Cyclotron Heating (ECH) and that there is a significant variation of the plasma pressure on the magnetic surfaces towards the plasma edge. Also, two emissive probes are aligned along a magnetic field line in vacuum by using one probe to detect the emitted electrons from the other. The locus of detected peaks in the current agree well with the numerical calculation of the magnetic surface. Measurements of the space potential on a flux surface indicate a maximum on the outboard side of the torus and a possible m=1 structure. Author

N92-11827# Washington Univ., Seattle.
NUMERICAL AND EXPERIMENTAL STUDIES OF SIMULATED TOROIDICITY EFFECTS IN A LINEAR HIGH-BETA HELIAC
Brian A. Nelson, G. Spanjers, F. L. Ribe, D. C. Barnes, and R. Bishop (Texas Univ., Austin.) *In* National Inst. for Fusion Science, Proceedings of the First International Toki Conference on Plasma Physics and Controlled Nuclear Fusion: Next Generation Experiments in Helical Systems Mar. 1990 p 109-112 (For primary document see N92-11799 02-75)
Avail: NTIS HC/MF A13

Formation and equilibrium studies of a linear high beta were performed, showing an axial current is induced. Vacuum field numerical studies have shown that when the hardcore center conductor is shifted, the magnetic field structure is similar to a large aspect ratio toroidal heliac. An experiment in a hardcore theta pinch has shown that programming of the hardcore current can significantly reduce the induced axial current. Finite beta effects were incorporated into a code to study the evolution of plasma on a shifted hardcore heliac. These results will be used in an experimental study of simulated toroidicity in a shifted hardcore linear heliac. Author

N92-11828# Centro de Investigaciones Energeticas, Madrid (Spain).
THEORY OF ELECTRON CYCLOTRON HEATING IN THE FLEXIBLE HELIAC TJ-II
Carlos L. Alejaldre, F. Castejon, V. Krivenski, and V. Tribaldos *In* National Inst. for Fusion Science, Proceedings of the First

International Toki Conference on Plasma Physics and Controlled Nuclear Fusion: Next Generation Experiments in Helical Systems Mar. 1990 p 113-116 (For primary document see N92-11799 02-75)
Avail: NTIS HC/MF A13

A theoretical model was developed to study microwave absorption in the presence of non-Maxwellian electron distribution functions, that can easily be incorporated in existing ray tracing codes. A TJ-II and a CHS/ATF magnetic configuration are used to illustrate the results obtained with the model. To fully understand ECH in TJ-II, quasilinear effects are taken into account by means of a flux averaged quasilinear Fokker-Planck code. The modification of the electron distribution function is presented for central and off axis heating in the second harmonic. Author

N92-11829# Centro de Investigaciones Energeticas, Madrid (Spain).
STORM: A LOW ASPECT RATIO TORSATRON FOR PLASMA STABILITY Abstract Only
A. P. Navarro, J. Guasp, Carlos L. Alejaldre, J. Alonso, E. Ascasibar, J. Botija, F. Castejon, J. R. Cepero, A. L. Fraguas, and L. Garcia et al *In* National Inst. for Fusion Science, Proceedings of the First International Toki Conference on Plasma Physics and Controlled Nuclear Fusion: Next Generation Experiments in Helical Systems Mar. 1990 p 117 (For primary document see N92-11799 02-75)
Avail: NTIS HC/MF A13

STORM is a low aspect ratio torsatron currently under construction. Main configuration parameters are t(0)=0.3, shearless, magnetic well depth approx. = 7 pct. and helical axis elongation approx. = 0.025 m. Plasma start-up and heating is based on electron cyclotron heating (ECH) using a 2nd harmonic heating squeme, with a 200 kw gyrotron at 28 GHz. This device is described in detail and the configuration studies are discussed which were made for the selection of the configuration. Predictions from stability and transport analysis for the plasma behavior in the device is also presented together with microwave absorption studies, made with ray tracing codes to optimize the heating squeme. Changing currents in the vertical field coils, some flexibility in the configuration parameters is obtained. This device flexibility allows the study of stability properties with and without magnetic well. In the case of the configuration without magnetic well, a high fraction of the energetic particles, generated by injection of ECH, could be trapped in the plasma. So, the effect of these particles on stability could be also experimentally studied in STORM. Theoretical estimations made for all these experiments are presented. Author

N92-11830# Oak Ridge National Lab., TN.
DISSIPATIVE TRAPPED ELECTRON MODES IN L = 2 TORSATRONS
Brian A. Carreras, N. Dominguez, V. E. Lynch, and P. H. Diamond (California Univ., San Diego.) *In* National Inst. for Fusion Science, Proceedings of the First International Toki Conference on Plasma Physics and Controlled Nuclear Fusion: Next Generation Experiments in Helical Systems Mar. 1990 p 118-121 Previously announced as N90-18256 (For primary document see N92-11799 02-75)
(Contract DE-AC05-86OR-21400)
Avail: NTIS HC/MF A13

Trapped electron modes in stellarators can be more unstable than those in tokamaks. They could be easier to detect in a stellarator and may be responsible for anomalous losses in the low collisionality regime. Author

N92-11831# Universidad Complutense, Madrid (Spain).
LOW-n STABILITY CALCULATIONS FOR THREE DIMENSIONAL STELLARATOR CONFIGURATIONS Abstract Only
L. Garcia, Brian A. Carreras, N. Dominguez, J. N. Leboeuf, and V. E. Lynch (Oak Ridge National Lab., TN.) *In* National Inst. for Fusion Science, Proceedings of the First International Toki Conference on Plasma Physics and Controlled Nuclear Fusion: Next Generation Experiments in Helical Systems Mar. 1990 p 122 (For primary document see N92-11799 02-75)
Avail: NTIS HC/MF A13

The MHD equilibrium and stability stellarator calculations are complex because of the intrinsic 3-D character of these configurations. The stellarator expansion can be applied to low n stability for modes which varies along field lines and is slow compared with the variation of the stellarator terms. A reduced set of MHD stellarator equations was derived by Strauss, and was implemented in different stability codes. The accuracy of the method was tested and demonstrated by comparing with 3-D stability results. The averaging method was applied to an equilibrium represented in a straight field line coordinate system. This will allow the extension of the low n stability calculations to helical axis systems and hopefully improve the accuracy of the low n stability for any type of configuration. The exact 3-D equilibrium is taken as the lowest order of the expansion, and it is assumed that this equilibrium is given in Boozer coordinates. Numerical solutions are shown to agree well with marginal stability boundaries given by the classical stellarator expansion in the planar magnetic axis case. Author

N92-11832# National Inst. for Fusion Science, Nagoya (Japan).
DESTRUCTION OF MAGNETIC SURFACES IN HELICAL TORUS
Jiro Todoroki *In its* Proceedings of the First International Toki Conference on Plasma Physics and Controlled Nuclear Fusion: Next Generation Experiments in Helical Systems Mar. 1990 p 123-126 Sponsored by Ministry of Education, Science and Culture (For primary document see N92-11799 02-75)
Avail: NTIS HC/MF A13

The toroidal magnetic field is decomposed into two parts, the field consisting of the magnetic surfaces, and the field part destroying the magnetic surfaces. The structure of the surface destroying part is determined only by the helical coils, and determines the bound of the magnetic surface, as well as the structure of the divertor magnetic field lines. Author

N92-11833# National Inst. for Fusion Science, Nagoya (Japan).
RIPPLE DIFFUSION AND BOOTSTRAP CURRENT IN LHD
Tsuneo Amano, Masao Okamoto, Noriyoshi Nakjima, Yuichi Ogawa, Kozo Yamazaki, S. P. Hirshman, and W. I. vanRij (Oak Ridge National Lab., TN.) *In its* Proceedings of the First International Toki Conference on Plasma Physics and Controlled Nuclear Fusion: Next Generation Experiments in Helical Systems Mar. 1990 p 127-129 (For primary document see N92-11799 02-75)
Avail: NTIS HC/MF A13

Ripple diffusion and bootstrap current are calculated for the plasma of Large Helical Device (LHD) with L = 2, M = 10, R = 4 m, and B = 4T. The ripple diffusion is calculated by using GIOTA and DKES codes. GIOTA code calculates the diffusion coefficient in 1/v regime very quickly and DKES calculates the neoclassical transport coefficients in all collisionality regime by solving drift kinetic equation. Bootstrap current is evaluated by using the formulation given in refs 3 and 4. Author

N92-11834# National Inst. for Fusion Science, Nagoya (Japan).
NUMERICAL ANALYSIS OF TEMPORAL DEVELOPMENT OF RF-HEATED PLASMA
Tsuguhiro Watanabe *In its* Proceedings of the First International Toki Conference on Plasma Physics and Controlled Nuclear Fusion: Next Generation Experiments in Helical Systems Mar. 1990 p 130-133 (For primary document see N92-11799 02-75)
Avail: NTIS HC/MF A13

Numerical calculation of an overall temporal development of an RF heated straight plasma cylinder is tried by a new numerical method HIDM (Higher order Implicit Difference Method). The plasma is described by electron, ion, and neutral atom fluids (3 fluid model), with ionization, recombination, and charge exchange processes being taken into account. Author

N92-11835# Max-Planck-Inst. fuer Plasmaphysik, Garching (Germany, F.R.).
ISLAND STUDIES FOR HELIAS CONFIGURATIONS
Peter Merkel *In* National Inst. for Fusion Science, Proceedings of the First International Toki Conference on Plasma Physics and Controlled Nuclear Fusion: Next Generation Experiments in Helical Systems Mar. 1990 p 134-137 (For primary document see N92-11799 02-75)
Avail: NTIS HC/MF A13

In the framework of the NESCOIL code, a method analogous to the procedure of Cary and Hanson was developed to eliminate islands and more generally to control the size and phase of islands. The method was applied to Helias stellerator vacuum fields in order to determine configurations with a dense set of flux surfaces in the plasma region and an island chain at the boundary which may serve as a basis for a divertor concept. Author

N92-11836# Institut za Nuklearne Nauke Boris Kidric, Belgrade (Yugoslavia).
ON STRONG RF PLASMA TURBULENCE Abstract Only
Milos M. Skoric *In* National Inst. for Fusion Science, Proceedings of the First International Toki Conference on Plasma Physics and Controlled Nuclear Fusion: Next Generation Experiments in Helical Systems Mar. 1990 p 138 (For primary document see N92-11799 02-75)
Avail: NTIS HC/MF A13

There is a sound theoretical and experimental evidence of strong nonlinear effects associated with RF heating of toroidal plasmas. In particular, concerning high power lower hybrid heating schemes, it is expected that nonlinear, strongly turbulent effects can become important. Basic features are discussed of strong RF plasma turbulence of upper hybrid and lower hybrid waves. Model equations are presented, having a Hamiltonian structure, and it is shown that in those nonlinear systems, the nonexistence of 3-D soliton wave solution is superseded by wave collapse phenomena, governed by strong ponderomotive nonlinearity. Collapse of RF waves as a unique self focusing type phenomena plays a role of an effective dissipation, determining basic microfeatures of emerging strong plasma turbulence. Moreover, it is shown that there exists a hierarchy of wave collapse regimes, starting from a weak collapse case which formally preserves zero energy into the final collapse stage and concluding with strong collapse, where the trapped RF energy remains finite. In this way, collapse classification appears significant concerning the plasma heating efficiency. Author

N92-11837# Toshiba Corp., Yokohama (Japan).
STRUCTURAL DESIGN OF LARGE HELICAL DEVICE
K. Kitamura, Masanao Shibui, Keiichi Yamamoto, S. Nakamoto, S. Mizumaki, H. Takano, Y. Wachi, T. Hamajima, T. Sasaki, and Osamu Motojima (National Inst. for Fusion Science, Nagoya, Japan) et al *In* National Inst. for Fusion Science, Proceedings of the First International Toki Conference on Plasma Physics and Controlled Nuclear Fusion: Next Generation Experiments in Helical Systems Mar. 1990 p 139-142 (For primary document see N92-11799 02-75)
Avail: NTIS HC/MF A13

A structural design of the Large Helical Device (LHD) was performed with proposals of: (1) application to forced flow superconductor to helical and poloidal coils; (2) toroidal shell for support structure of the coils; and (3) corrugated vacuum vessel with high temperature difference between inner and outer skins. Structural analyses of these components were also carried out to understand their mechanical behaviors including load transmission and to assess the structural reliabilities of the LHD. Author

N92-11838# Toshiba Corp., Yokohama (Japan).
RESEARCH AND DEVELOPMENT OF FORCED FLOW SUPERCONDUCTING COILS FOR LARGE HELICAL DEVICE
Shigenori Tsuruga, Keiichi Yamamoto, K. Nakamoto, S. Mizumaki, H. Takano, Masanao Shibui, K. Kitamura, T. Uchida, Y. Wachi, and Shigeru Ioka et al *In* National Inst. for Fusion Science, Proceedings of the First International Toki Conference on Plasma Physics and Controlled Nuclear Fusion: Next Generation Experiments in Helical Systems Mar. 1990 p 143-146 (For primary document see N92-11799 02-75)
Avail: NTIS HC/MF A13

A forced flow superconducting coil was proposed for application to coils of the Large Helical Device (LHD). The main objectives of R&D are to study characteristics of a forced flow superconducting coil and to examine fabricability of a large helical coil for the LHD. A R&D facility consists of a cryostat with 30 kA power leads and two types of R&D coils. Cable-in-conduit type superconductors using NbTi/Cu are adopted for the coils. A computer controlled winding machine was developed in order to fabricate the TOKI TF (helical coil). The design features of the R&D facility are presented. Author

N92-11839# Hitachi Ltd. (Japan).
POOL-COOLED SUPERCONDUCTING MAGNET DESIGN OF LARGE HELICAL DEVICE
S. Suzuki, H. Miyazawa, R. Saito, F. Iida, H. Ogata, Y. Yamazaki, Osamu Motojima, Junya Yamamoto, Masami Fujiwara, and M. Takeo (Kyushu Univ., Fukuoka, Japan) *In* National Inst. for Fusion Science, Proceedings of the First International Toki Conference on Plasma Physics and Controlled Nuclear Fusion: Next Generation Experiments in Helical Systems Mar. 1990 p 147-150 (For primary document see N92-11799 02-75)
Avail: NTIS HC/MF A13

The Large Helical Device is the next generation in helical equipment for nuclear fusion. The large scale superconducting magnets are going to be applied to these coils. The major and minor radius of the helical coil system are 4 and 0.96 m respectively and the magnetic field is 4 T at the plasma center and 8 T at the coil surface. The coil system stores about 2 GJ of total energy. The superconductor of the helical coil is pure aluminum stabilized Nb-Ti compacted strand cable with copper housing. The coils have a stainless-steel helium can that is filled with liquid helium. This pool-cooled superconducting helical coil system satisfies the fully stabilized condition. The superconducting poloidal coils are composed of six (three pairs) circular coils and use forced-cooled superconductors to reduce the eddy current losses by the field changing operation. The helical and poloidal coil system are built in the large bell-jar (vacuum vessel for thermal insulation) with outer diameter of 13 m. Conductor design and stability of superconducting magnets for helical and poloidal coil systems are described. Author

N92-11840# Hitachi Ltd. (Japan). Energy Research Lab.
BEHAVIOR OF VACUUM VESSEL EDDY CURRENT IN LARGE HELICAL DEVICE
Hideshi Fukumoto, Shigeyoshi Kinoshita, Michio Otsuka, Nobuyoshi Ohyabu, Nobuaki Noda, Kozo Yamzaki, and Osamu Motojima (National Inst. for Fusion Science, Nagoya, Japan) *In* National Inst. for Fusion Science, Proceedings of the First International Toki Conference on Plasma Physics and Controlled Nuclear Fusion: Next Generation Experiments in Helical Systems Mar. 1990 p 151-154 (For primary document see N92-11799 02-75)
Avail: NTIS HC/MF A13

The eddy current on a Large Helical Device was analyzed to understand its flow pattern on the vacuum vessel with helical structure in the existence of helical field or poloidal field change. The magnetic field in the plasma region and the electromagnetic force induced by the eddy current were also evaluated. Author

N92-11841# Mitsubishi Fusion Center, Tokyo (Japan).
FUNDAMENTAL DESIGN ON LHD WITH BATH COOLING METHOD
Shigeru Tado, Katsuhiro Shimizu, B. Ikeda, A. Kameari, R. Saito, M. Tomita, Tadanori Tsukamoto, K. Kuno, K. Toyota, and T. Satow (Mitsubishi Electric Co., Kobe, Japan) et al *In* National Inst. for Fusion Science, Proceedings of the First International Toki Conference on Plasma Physics and Controlled Nuclear Fusion: Next Generation Experiments in Helical Systems Mar. 1990 p 155-158 (For primary document see N92-11799 02-75)
Avail: NTIS HC/MF A13

The Large Helical Device (LHD) is a fusion experimental device of heliotron type. The results of the structural analyses which were made on the superconducting magnetic coil support structure and the vacuum vessel are described as a preliminary design study of the LHD. Author

N92-11842# Mitsubishi Electric Co., Kobe (Japan).
A COMPACT HELICAL DEVICE FOR A SUPERCONDUCTING LARGE HELICAL COIL
Yoshiyuki Tsuda, K. Toyoda, T. Hirayama, S. Kida, K. Kuno, T. Mito, Junya Yamamoto, K. Takahata, M. Takeo, and I. Ohtake (National Inst. for Fusion Science, Nagoya, Japan) et al *In* National Inst. for Fusion Science, Proceedings of the First International Toki Conference on Plasma Physics and Controlled Nuclear Fusion: Next Generation Experiments in Helical Systems Mar. 1990 p 159-162 (For primary document see N92-11799 02-75)
Avail: NTIS HC/MF A13

A superconducting helical coil was constructed. The fabricated coil has a major radius of 300 mm and a minor radius of 62.7mm. In order to simulate the construction technique of a large helical coil, the small-scale coil was wound with the computer controlled winding machine that was developed for the automatic helical winding. Useful technical data was gained about the fabrication of a superconducting helical coil, and the feasibility of fabricating a large helical coil was confirmed. Author

N92-11843# National Inst. for Fusion Science, Nagoya (Japan).
OPTIMIZATION OF DESIGN PARAMETERS FOR LARGE HELICAL DEVICE
Kozo Yamazaki, Makoto Asao (Kobe Steel Ltd., Japan), and Osamu Motojima *In its* Proceedings of the First International Toki Conference on Plasma Physics and Controlled Nuclear Fusion: Next Generation Experiments in Helical Systems Mar. 1990 p 163-166 (For primary document see N92-11799 02-75)
Avail: NTIS HC/MF A13

The convenient scaling formula for plasma configurations and engineering design parameters of l = 2 helical systems are derived from a wide range of computations. Using these formula, optimized designs of heliotron/torsatron experimental devices with NbTi superconducting coils are surveyed for the next generation of machines. An l = 2/ m = 10/ gamma approximately = 1.2 system with a coil current density of approximately 40 A/sq mm is found as an optimized higher-beta better-confinement configuration with respect to the clean divertor installation, the coil engineering requirements, and the cost optimization. Author

N92-11844# National Inst. for Fusion Science, Nagoya (Japan).
EFFECT OF MULTI-LAYER OPERATION OF HELICAL COIL IN LARGE HELICAL DEVICE
Makoto Asao (Kobe Steel Ltd., Japan), Kozo Yamazaki, and Osamu Motojima *In its* Proceedings of the First International Toki Conference on Plasma Physics and Controlled Nuclear Fusion: Next Generation Experiments in Helical Systems Mar. 1990 p 167-170 (For primary document see N92-11799 02-75)
Avail: NTIS HC/MF A13

One of the main objectives of the Large Helical Device Project is to investigate the fundamental properties of a helical torus system in wide plasma parameter range. Therefore, it is necessary to design the flexible coil system to obtain various magnetic field configurations. For this purpose, a helical coil is divided into multi-layers to change the helical pitch parameter. A variety of configurations with different rotational transform and minor radius are obtained by this multi-layer operation of the helical coil. Author

N92-11845# National Inst. for Fusion Science, Nagoya (Japan).
ECH SYSTEM IN THE LARGE HELICAL DEVICE
Kunizo Ohkubo, Minolu Hosokawa, Shin Kubo, Takashi Mutoh, Motoyasu Sato (Kyoto Univ., Japan), Ryuhei Kumazawa, Tetsuo Watari, and Tsutomu Kuroda *In its* Proceedings of the First International Toki Conference on Plasma Physics and Controlled Nuclear Fusion: Next Generation Experiments in Helical Systems Mar. 1990 p 171-174 (For primary document see N92-11799 02-75)
Avail: NTIS HC/MF A13

The electron cyclotron heating system will provide 10 MW of RF power for the large helical device. The RF power will be generated by ten 1 MW gyrotrons and transmitted via the mirror system and/or the corrugated waveguide. High voltage dc power to the electron cyclotron heating equipment will be supplied from approximately 80 kV power supplies with CW and 10 sec pulsewidth. A control system will interface to the supervisory control system for the large helical device. Author

N92-11846# National Inst. for Fusion Science, Nagoya (Japan).
ICRF HEATING PROGRAM OF THE LARGE HELICAL DEVICE
Takashi Mutoh, Atsushi Fukuyama, Tetsuo Watari, Ryuhei Kumazawa, Hiroyuki Okada, Masashi Ohnishi (Kyoto Univ., Uji, Japan), Masao Okamoto, Kiyohiko Nishimura, and Tsutomu Kuroda *In its* Proceedings of the First International Toki Conference on Plasma Physics and Controlled Nuclear Fusion: Next Generation Experiments in Helical Systems Mar. 1990 p 175-178 (For primary document see N92-11799 02-75)
Avail: NTIS HC/MF A13

Ion Cyclotron Radio Frequency (ICRF) Heating Programs of the Large Helical Device (LHD) are discussed. The ICRF heating is considered as one of the additional heating methods to achieve the objective plasma parameters and as the useful tool to study the various physics subjects. Theoretical analysis methods were developed, and parameter surveys were carried out to determine optimum heating conditions. Wave propagation and Fokker-Planck analyses are used to evaluate the heating deposition profiles and direct orbit loss effect. Monte-Carlo calculation is also used to confirm the above results. An alpha particle simulation program using ICRF is studied, and it can be examined to a certain extent by forming a similar distribution function in ion velocity space. From these analyses, it becomes clear that the ICRF heating has high potentiality as a useful heating tool, even if the loss cone exists at the radial range of r/a sub p greater than or = 0.4. Author

N92-11847# Delhi Univ. (India). Dept. of Physics and Astrophysics.
MOTION OF CHARGED PARTICLE IN HELICAL SYSTEMS
Mahesh P. Srivastava *In* National Inst. for Fusion Science, Proceedings of the First International Toki Conference on Plasma Physics and Controlled Nuclear Fusion: Next Genration Experiments in Helical Systems Mar. 1990 p 179-182 (For primary document see N92-11799 02-75)
Avail: NTIS HC/MF A13

The motion of a charged particle in an axially symmetric magnetic field such as found in straight helical systems is studied. The three dimensional motion of a charged particle is reduced into a two dimensional one by introducing an effective potential. It was possible to classify the motion into an off axis motion and an encircling motion in the r-z plane. Author

N92-11848# Nihon Univ., Tokyo (Japan). Atomic Energy Research Inst.
EQUILIBRIUM, STABILITY, AND TRANSPORT IN L = 1 COMPACT HELICAL AXIS CONFIGURATION
Hitoshi Kikuchi, Hikaru Ueno, Masamitsu Aizawa, Kiyomitsu Suzuki, Hirokazu Gesso, Katsunori Saito, Ichiro Kawakami, and Shoichi Shiina *In* National Inst. for Fusion Science, Proceedings of the First International Toki Conference on Plasma Physics and Controlled Nuclear Fusion: Next Generation Experiments in Helical Systems Mar. 1990 p 183-187 (For primary document see N92-11799 02-75)
Avail: NTIS HC/MF A13

The L = 1 torsatron is modified by two methods to improve the plasma stability. The first one is the negative pitch modulation of coil winding. The second is the superposition of a relatively weak L = -1 torsatron field. These modifications give rise to a local magnetic well keeping a positive magnetic shear. The

equilibrium, stability, and transport of plasma in these modified L = 1 torsatrons are described and discussed. Author

N92-11849# Auburn Univ., AL. Dept. of Physics.
ELECTRON TEMPERATURE MEASUREMENTS ON ATF USING ELECTRON CYCLOTRON EMISSION
Rex F. Gandy, G. L. Bell, J. B. Wilgen, T. S. Bigelow, and D. A. Rasmussen (Oak Ridge National Lab., TN.) *In* National Inst. for Fusion Science, Proceedings of the First International Toki Conference on Plasma Physics and Controlled Nuclear Fusion: Next Generation Experiments in Helical Systems Mar. 1990 p 188-191 (For primary document see N92-11799 02-75)
(Contract DE-AC05-84OR-21400)
Avail: NTIS HC/MF A13

Second and third harmonic electron cyclotron emission measurements were carried out on the Advanced Toroidal Facility (ATF). The ATF is a l = 2, m = 12 torsatron with a major radius of 2.1 m and an average plasma radius of 0.3 m. At the standard magnetic field values of 1 and 2 T, heterodyne receivers were used monitor the electron temperature profile as a function of time. The optically thin third harmonic emission was used to measure the central electron temperature during electron cyclotron heating and neutral beam injection. Results from both harmonics agree well with the Thomson scattering data. Calculations of the width of the resonance zones indicate values from 1 cm at the edge to 5 cm centrally. An in situ absolute calibration of the system using a liquid nitrogen source was performed. The beam pattern of the system was also measured in-situ and agrees well with theoretical calculations. A beam viewing dump was installed to reduce the wall reflection problem for the optically thin emission. Author

N92-11850# Kyoto Univ., Uji (Japan). Plasma Physics Lab.
CONFINEMENT STUDIES OF HELIOTRON E PLASMAS IN MAGNETIC SURFACE VARIATION EXPERIMENTS
Fumimichi Sano *In* National Inst. for Fusion Science, Proceedings of the First International Toki Conference on Plasma Physics and Controlled Nuclear Fusion: Next Generation Experiments in Helical Systems Mar. 1990 p 192-195 (For primary document see N92-11799 02-75)
Avail: NTIS HC/MF A13

Confinement studies of Heliotron-E neutral beam heated plasmas were carried out with reference to magnetic surface variation by using additional toroidal field, B sub t, as well as additional vertical field, B sub v. The variation of alpha* (= B sub t/ B sub h; B sub h helical field on axis) causes mainly a change in mean plasma radius a sub p and in rotational transform t(r), while that of beta* (= B sub v/ B sub h) causes a shift of magnetic axis (delta sub v) and a variation of shear parameter (theta). In the standard configuration (alpha*, beta*) = (0,-0.185), the gross energy confinement time, tau sup G sub E, is given empirically as tau(sup G sub E)(ms) = 13 x n sup -0.53 sub e(10 exp 14/cc) x P(sup -0.71 sub heat)(MW) x B sup 0.35(T) for neutral beam injection (NBI) plasmas and then the anomalous electron thermal diffusivity chi sup an sub e associated with the above power-degradating scaling is now the crucial problem to be settled. Therefore, from the viewpoint of confinement improvement in the helical system, the investigation of confinement properties as functions of magnetic surface quantities such as a sub p, delta sub v, or theta is of special importance in order to find out the physical mechanism of anomalous diffusivity. The experimental studies of the effects of a sub p on transport with special regard to NBI plasma are described. Author

N92-11851# Kyoto Univ., Uji (Japan). Plasma Physics Lab.
PROFILE MEASUREMENTS IN MAGNETIC SURFACE VARIATION EXPERIMENTS/MULTIPLE PELLET INJECTION EXPERIMENTS
Shigeru Sudo, T. Baba, Motoyasu Sato, Katsumi Kondo, Hideki Zushi, T. Mizuuchi, H. Okada, Sakae Besshou, Masahiro Wakatani, and Tokuhiro Obiki *In* National Inst. for Fusion Science, Proceedings of the First International Toki Conference on Plasma Physics and Controlled Nuclear Fusion: Next Generation Experiments in Helical Systems Mar. 1990 p 196-199 (For primary document see N92-11799 02-75)
Avail: NTIS HC/MF A13

Temperature and density profile measurements by the Thomson scattering method in magnetic surface variation experiments are presented. The density profile becomes peaked when alpha* (identical with B sub T0/ B sub H0) decreases, while the central electron temperature changes little. This property is common in neutral beam injection (NBI) plasmas. Apart from the alpha* value, there is optimization when beta* (identical with B sub V0/ B sub H0) = -0.192(delta sub v = -2 cm). When beta* = -0.192, there is optimization when alpha* = 0.05 to approximately 0.10. In this case, the edge plasma is observed to expand when alpha* is increased from 0 to approximately 0.10. Density clamping of electron cyclotron heating (ECH) plasmas (P sub ECH of approximately 450 kW) is stopped under the condition of alpha* greater than 0. The optimum condition is when alpha* is approximately 0.05 with beta* = -0.192. A quasi-steady state plasma with a density of n bar sub e = 4 x 10(exp 19)/cubic meters, which is higher than the cut-off density of n sub e approximately = 3.5 x 10(exp 19) cubic meters, can be produced under the condition of T sub e(0) approximately = 350 eV in the case of alpha* = 0.05 and beta* = -0.192. Multiple pellet injection experiments on Heliotron E are described. By multiple pellet injection, the regime of n - T diagram is expanded in the high density region. As a result of high nT plasma production, magnetohydrodynamic (MHD) instability has appeared first in case of B = 1.9 T under the standard configuration. A peaked density profile with high density is achieved by pellet injection, which cannot be obtained merely by gas puffing. The behavior of pellet-injected plasma is also studied under the magnetic surface variation.
Author

N92-11852# Kyoto Univ., Uji (Japan). Plasma Physics Lab.
IMPURITY BEHAVIOR IN HELIOTRON E
Katsumi Kondo, T. Oda, and K. Miyake (Kyoto Univ., Japan) *In* National Inst. for Fusion Science, Proceedings of the First International Toki Conference on Plasma Physics and Controlled Nuclear Fusion: Next Generation Experiments in Helical Systems Mar. 1990 p 200-203 (For primary document see N92-11799 02-75)
Avail: NTIS HC/MF A13

Impurity behavior in the Heliotron E plasma was studied by a vacuum ultraviolet spectrometer in various magnetic configurations with or without a carbon coating on the vacuum chamber wall.
Author

N92-11853# Kyoto Univ., Uji (Japan). Plasma Physics Lab.
EDGE PLASMA STUDY IN HELIOTRON E
T. Mizuuchi, Hiroto Matsuura, A. Komori, Mitsuru Harada, S. Nagai (Kyushu Univ., Fukuoka, Japan), Hideki Zushi, Fumimichi Sano, Katsumi Kondo, Shigeru Sudo, and Sotoyasu Sato et al *In* National Inst. for Fusion Science, Proceedings of the First International Toki Conference on Plasma Physics and Controlled Nuclear Fusion: Next Generation Experiments in Helical Systems Mar. 1990 p 204-207 (For primary document see N92-11799 02-75)
Avail: NTIS HC/MF A13

The magnetic field configuration of Heliotron E can be controlled by additional toroidal field and/or vertical field. The change of the configuration, especially in the edge region, is experimentally confirmed by measurement of the edge plasma profile and by measurement of the vacuum magnetic surface with the beam impedance method. Author

N92-11854# Kyoto Univ., Uji (Japan). Plasma Physics Lab.
RECENT DIAMAGNETIC MEASUREMENTS OF TOROIDAL COIL EXPERIMENTS ON HELIOTRON E
Sakae Besshou *In* National Inst. for Fusion Science, Proceedings of the First International Toki Conference on Plasma Physics and Controlled Nuclear Fusion: Next Generation Experiments in Helical Systems Mar. 1990 p 208-211 (For primary document see N92-11799 02-75)
Avail: NTIS HC/MF A13

Recent results (Jul.-Nov. 1989) on diamagnetic measurements of Heliotron E toroidal coil experiments are described. The status of the system is described, including calibration and electronic signal compensation. Recent results are presented showing the behavior of the stored plasma energy or average beta with additional toroidal field, vertical field, and heating powers. Author

N92-11855# Kyoto Univ., Uji (Japan). Plasma Physics Lab.
STUDY OF RESISTIVE INTERCHANGE MODE IN HELIOTRON E
Hideki Zushi *In* National Inst. for Fusion Science, Proceedings of the First International Toki Conference on Plasma Physics and Controlled Nuclear Fusion: Next Generation Experiments in Helical Systems Mar. 1990 p 212-215 (For primary document see N92-11799 02-75)
Avail: NTIS HC/MF A13

The effects of magnetic axis shift snd the toroidal field on pressure driven instabilities are studied. It is found that the internal disruption caused by the interchange modes is sensitive to the magnetic well formation near the magnetic axis. It is also observed that the additional toroidal field (B(sub t)/B(sub h) approximately 5 percent) is effective to stabilize it. Dominant instability modes are changed from m=2/n=1 or m=3/n=2 modes (0 less than r/a less than 0.3) to the m=1/n=1 mode (0.6 less than r/a less than 0.7) as beta increases. Author

N92-11856# Kyoto Univ., Uji (Japan). Plasma Physics Lab.
MEASUREMENT OF MAGNETIC FLUCTUATIONS IN HELIOTRON E
Mitsuru Harada, Hideki Zushi, Fumimichi Sano, T. Mizuuchi, M. Nakasuga, Shigeru Sudo, Katsumi Kondo, Sakae Besshou, Motoyasu Sato, and Hiroshi Kaneko (National Inst. for Fusion Science, Nagoya, Japan) et al *In* National Inst. for Fusion Science, Proceedings of the First International Toki Conference on Plasma Physics and Controlled Nuclear Fusion: Next Generation Experiments in Helical Systems Mar. 1990 p 216-219 (For primary document see N92-11799 02-75)
Avail: NTIS HC/MF A13

In Heliotron E, it was found that pressure driven internal disruptions occur in high beta plasmas. Magnetic fluctuations are thought to have relation to pressure driven instabilities. The cross-correlation analysis of magnetic fluctuations in Heliotron E is presented, and the properties of coherent magnetic oscillations related with magnetohydrodynamic activities affected by the magnetic configurations are discussed. Author

N92-11857# National Inst. for Fusion Science, Nagoya (Japan).
TRANSPORT STUDY OF ECH AND NBI PLASMAS IN CHS
Hiroshi Yamada, Harukazu Iguchi, H. C. Howe, Yasuhiko Takeiri, Shin Kubo, Shoichi Okamura, R. N. Morris, and D. K. Lee (Oak Ridge National Lab., TN.) *In its* Proceedings of the First International Toki Conference on Plasma Physics and Controlled Nuclear Fusion: Next Generation Experiments in Helical Systems Mar. 1990 p 220-223 (For primary document see N92-11799 02-75)
(Contract DE-AC05-84OR-21400)
Avail: NTIS HC/MF A13

Power balance of ECR (Electron-Cyclotron Resonance) and NBI (Neutral Beam Injector) heated plasmas in CHS (Compact Helical System) was analyzed using the time-dependent transport code PROCTR-mod. The power losses in the ECH (Electron Cyclotron Heated) plasma are dominated by electron heat conduction which is typically larger than the prediction from the neoclassical theory by a factor of 4, while that for the NBI plasmas is several-tens times larger than the prediction from the neoclassical theory. Author

N92-11858# National Inst. for Fusion Science, Nagoya (Japan).
EFFECT OF MAGNETIC AXIS SHIFT ON CHS PLASMA CHARACTERISTICS
Shoichi Okamura and Harukazu Iguchi *In its* Proceedings of the First International Toki Conference on Plasma Physics and Controlled Nuclear Fusion: Next Generation Experiments in Helical Systems Mar. 1990 p 224-227 (For primary document see N92-11799 02-75)
Avail: NTIS HC/MF A13

For the study of plasma transport in helical systems, the comparison of the confinement for different magnetic configurations can give us a lot of useful information for understanding the transport mechanism as well as scaling studies for various plasma parameters. The poloidal coil system of CHS (Compact Helical Systems) device consists of four pairs of hoop coils. Three of them are energized by independent power supplies which make it possible to realize a wide variation of poloidal field configuration. It is possible to decompose the poloidal field structure into a sum of multipole components. We chose the values of dipole (vertical) and quadrupole components as two free parameters to determine the poloidal coil current settings. To determine the third free parameter, we set the condition of minimizing the stray field around the machine with which we can reduce the perturbing field that is brought by the magnetic material around the machine. Author

N92-11859# National Inst. for Fusion Science, Nagoya (Japan).
A STUDY OF RADIATION COLLAPSE IN CHS PLASMAS
Shigeru Morita *In its* Proceedings of the First International Toki Conference on Plasma Physics and Controlled Nuclear Fusion: Next Generation Experiments in Helical Systems Mar. 1990 p 228-231 (For primary document see N92-11799 02-75)
Avail: NTIS HC/MF A13

It is found that ECH (Electron Cyclotron Heated) plasmas without Ti gettering cause radiation collapse at some magnetic configurations in which plasma-wall distance is extremely decreasing. In NBI plasmas the radiation collapse can be observed even in the Ti-flashed discharges, when strong gas puffing is carried out. Spectroscopic results and analysis indicate that the radiation collapse is caused by the oxygen buildup reaching 10-20 percent and 3-5 percent of electron density in ECH and NBI plasmas, respectively. These critical values decrease because of a flat or hollow electron density profile of the CHS plasmas. In addition, hydrocarbon pellets are injected into the NBI plasmas to make these phenomena clear. The spherical pellet injection of 0.46 mm dia. corresponding to 5 percent carbon fraction of electron density causes the radiation collapse. However, the pellet injection of 0.32 mm dia. corresponding to 2.3 percent of electron density does not cause the collapse. The results show good agreement with the analysis. Author

N92-11860# National Inst. for Fusion Science, Nagoya (Japan).
ION TEMPERATURE AND POLOIDAL ROTATION PROFILES FOR NBI HEATED PLASMA IN CHS
Katsumi Ida and S. Hidekuma *In its* Proceedings of the First International Toki Conference on Plasma Physics and Controlled Nuclear Fusion: Next Generation Experiments in Helical Systems Mar. 1990 p 232-235 (For primary document see N92-11799 02-75)
Avail: NTIS HC/MF A13

Ion temperature and poloidal rotation velocity profiles are measured with 68 channel space resolved spectrometer using beam emission spectroscopy techniques in CHS. The electric field near the plasma edge derived from poloidal rotation velocity is 15 V/cm for low density 28 GHz ECH plasma, and -35 V/cm for high density NBI plasma. The peak of the ion temperature os shifted from the vacuum magnetic axis and becomes larger as the magnetic axis moves toward the tangential major radius of the heating neutral beam. This shift is larger than that estimated from finite beta calculation by a factor of two or less. Presumably, the shift is due to a significant parallel beam pressure as well as thermal component. Author

N92-11861# National Inst. for Fusion Science, Nagoya (Japan).
DRIVEN CURRENTS IN NEUTRAL BEAM HEATED PLASMA
Osamu Kaneko, Yasuhiko Takeiri, Hiroshi Yamada, Harukazu Iguchi, Shoichi Okamura, and Keisuke Matsuoka *In its* Proceedings of the First International Toki Conference on Plasma Physics and Controlled Nuclear Fusion: Next Generation

Experiments in Helical Systems Mar. 1990 p 236-239 (For primary document see N92-11799 02-75)
Avail: NTIS HC/MF A13

Plasma currents, which are observed in the tangential neutral beam heated plasma, are studied under the various plasma conditions in CHS. The plasma current is mainly driven by high energy beam when the plasma density is low, while the bootstrap current seems to be dominant in the dense plasma. Author

N92-11862# National Inst. for Fusion Science, Nagoya (Japan).
POWER DEPOSITION DURING ECH IN CHS
Shin Kubo, Minolu Hosokawa, Y. Takita, and H. Idei *In its* Proceedings of the First International Toki Conference on Plasma Physics and Controlled Nuclear Fusion: Next Generation Experiments in Helical Systems Mar. 1990 p 240-243 (For primary document see N92-11799 02-75)
Avail: NTIS HC/MF A13

Power deposition profile and the total absorbed power during electron cyclotron heating (ECH) in CHS are estimated from the resonance structure at each flux surface. The dependence of the central electron temperature on the magnetic field can be well accounted for by this method. Total deposited power into the plasma is estimated from the measurement of the leaking power around the torus. Using this power deposition profile, preliminary confinement analysis of the electron is done. Author

N92-11863# Associazione EURATOM-CNEN Sulla Fusione, Frascati (Italy).
A POSSIBLE MODIFICATION OF THE FT TOKAMAK INTO A COMPACT HIGH FIELD STELLARATOR WITH SEPARATRICES
F. Alladio, P. Buratti, F. Crisanti, S. Mancuso, and P. Micozzi *In* National Inst. for Fusion Science, Proceedings of the First International Toki Conference on Plasma Physics and Controlled Nuclear Fusion: Next Generation Experiments in Helical Systems Mar. 1990 p 244-247 (For primary document see N92-11799 02-75)
Avail: NTIS HC/MF A13

A possible modification of the FT Tokamak could be to transform it into a compact high field stellarator experiment. The removal of the copper shell and of the secondary liner would leave space (9 cm) between the inside of the toroidal magnet (r=29 cm) and possible vacuum vessel with r=20 cm. This space could be used for helical windings. As the toroidal magnet is built by 12 sectors a rather attractive possibility could be an l=2 m=6 stellarator. Author

N92-11864# National Inst. for Fusion Science, Nagoya (Japan).
ENGINEERING DESIGN OF LARGE HELICAL DEVICE
Junya Yamamoto and Osamu Motojima *In its* Proceedings of the First International Toki Conference on Plasma Physics and Controlled Nuclear Fusion: Next Generation Experiments in Helical Systems Mar. 1990 p 248-251 (For primary document see N92-11799 02-75)
Avail: NTIS HC/MF A13

Engineering design of Large Helical Device and technical subject to realize the device are described. Research and development works of superconducting coils are also introduced. Author

N92-11865# National Inst. for Fusion Science, Nagoya (Japan).
OPERATION SCENARIO AND STRUCTURAL DESIGN ANALYSIS OF LHD (LARGE HELICAL DEVICE) COILS
Kozo Yamazaki and Osamu Motojima *In its* Proceedings of the First International Toki Conference on Plasma Physics and Controlled Nuclear Fusion: Next Generation Experiments in Helical Systems Mar. 1990 p 252-255 (For primary document see N92-11799 02-75)
Avail: NTIS HC/MF A13

Flexible operation modes of coil system are presented for the Large Helical Device (LHD) with m(field period)=10, 4-layer HFC (Helical Field Coil) and 3-pair PFC (Poloidal Field Coil) superconducting systems. For these operation modes, electromagnetic force and stress analyses are carried out, and it is clarified that coil supporting system within the permissible stress level is possible with adequate stiffness to keep clean magnetic surface without large magnetic islands. Author

N92-11866# National Inst. for Fusion Science, Nagoya (Japan).
ENGINEERING DESIGN OF LHD VACUUM VESSEL
Naruyoshi Ohyabu and Nobuaki Noda *In its* Proceedings of the First International Toki Conference on Plasma Physics and Controlled Nuclear Fusion: Next Generation Experiments in Helical Systems Mar. 1990 p 256-259 (For primary document see N92-11799 02-75)
Avail: NTIS HC/MF A13

There are two key issues in designing the LHD vacuum vessel: (1) how to accommodate a closed helical divertor system, and (2) how to assemble the vessel. The assembly procedure is quite different, depending on whether it is done before or after the coil winding. The conceptual design of the LHD vacuum vessel is discussed. Author

N92-11867# National Inst. for Fusion Science, Nagoya (Japan).
DEVELOPMENT OF SUPERCONDUCTOR FOR LARGE HELICAL DEVICE
Toshiyuki Mito, Junya Yamamoto, K. Takahata, Osamu Motojima, and F. Sumiyoshi (Kagoshima Univ., Japan) *In its* Proceedings of the First International Toki Conference on Plasma Physics and Controlled Nuclear Fusion: Next Generation Experiments in Helical Systems Mar. 1990 p 260-263 (For primary document see N92-11799 02-75)
Avail: NTIS HC/MF A13

The present situation of the design and construction of R&D superconducting conductors for Large Helical Device is reported. The required properties for the conductor of LHD and the design criteria of the conductors are mentioned. The designed patterns of the cross sections of R&D conductors are shown. The test and estimation items of conductors are listed. The R&D schedules are shown. Author

N92-11868# Max-Planck-Inst. fuer Plasmaphysik, Garching (Germany, F.R.).
OVERVIEW OF ENGINEERING DESIGN OF WENDELSTEIN VII-X
Jorg Sapper *In* National Inst. for Fusion Science, Proceedings of the First International Toki Conference on Plasma Physics and Controlled Nuclear Fusion: Next Generation Experiments in Helical Systems Mar. 1990 p 264-267 (For primary document see N92-11799 02-75)
Avail: NTIS HC/MF A13

The Experiment Wendelstein VII-X is a large machine in which the plasma to be studied should be representative of the future Stellarator reactors. The main parameters are: major radius R(sub 0) = 5.5 m, magnetic induction B(sub 0) = 3T, stored magnetic energy W approximately 600 MJ. The average plasma radius will be 0.53 m. Following the Garching development line, the confinement field will be generated by one set of nonplanar coils, modularly arranged in toroidal periods. Additional planar coils will allow experimental flexibility which will not be necessary later on in an optimized reactor design with fixed operational conditions. Under the constraint of a required pulse-length of more than 10 sec. for the experiment, superconductivity is the technical solution for the coil design. In the first step the technical features of the machine were studied together with competent industrial companies. Author

N92-11869# Kyoto Univ., Uji (Japan). Plasma Physics Lab.
THE 100 GHz HALF MEGAWATT MICROWAVE TRANSMISSION SYSTEM DEVELOPMENT WITH WHISPERING GALLERY MODE
Motoyasu Sato, M. Iima, S. Kobayashi, Shigeru Sudo, Fumimichi Sano, Hideki Zushi, Tokuhiro Obiki, M. Nakajima, Shin Kubo, and Minolu Hosokawa (National Inst. for Fusion Science, Nagoya, Japan) et al *In* National Inst. for Fusion Science, Proceedings of the First International Toki Conference on Plasma Physics and Controlled Nuclear Fusion: Next Generation Experiments in Helical

Systems Mar. 1990 p 268-271 (For primary document see N92-11799 02-75)
Avail: NTIS HC/MF A13

The 106 GHz half megawatt ECRH (Electron Cyclotron Resonance Heating) is under the final stage of development and will serve for the future one megawatt design. The following subject areas are covered: gyratron tube, quasi-optional mode converter development, and transmission line. Author

N92-11870# National Inst. for Fusion Science, Nagoya (Japan).
NBI SYSTEM WITH NEGATIVE ION SOURCE IN LARGE HELICAL DEVICE
Yasuhiko Takeiri, Osamu Kaneko, Fumimichi Sano, A. Ando, Yoshihide Oka, Tokuhiro Obiki, Tsutomu Kuroda, and Kiyoshi Hanatani (Kyoto Univ., Uji, Japan) *In its* Proceedings of the First International Toki Conference on Plasma Physics and Controlled Nuclear Fusion: Next Generation Experiments in Helical Systems Mar. 1990 p 272-275 (For primary document see N92-11799 02-75)
Avail: NTIS HC/MF A13

Negative-ion-based NBI (Neutral Beam Injector) system is designed for Large Helical Device. Injection energy is 125 keV for hydrogen beam and total injection power is 20 MW which is provided by four tangential injectors with two ion sources. Design concept for the system performance and hardware system design are described. Author

N92-11871# Argonne National Lab., IL.
ITER DIVERTOR SPUTTERING EROSION: RECENT ANALYSIS FOR CARBON, BERYLLIUM, TUNGSTEN, AND NIOBIUM SURFACES
Jeffrey N. Brooks Jul. 1991 11 p
(Contract W-31-109-eng-38)
(DE91-017235; ANL/FPP/TM-255) Avail: NTIS HC/MF A03

ITER divertor plate sputtering erosion has been analyzed using current design information and updated impurity transport models. The REDEP erosion/redeposition code was used to compute erosion for a very low plasma divertor temperature (T sub e sub 0 approx. 12 eV) physics phase reference case, and for other plasma conditions. A high surface temperature case (T sub s sub 0 = 1800 C) is analyzed for a carbon surface. Niobium is analyzed using WBC near-surface transport code results for the redeposited charge state. The REDEP results show high net erosion rates approx. greater than 20 cm/burn(sm bullet)yr for beryllium and carbon, even at low plasma temperatures. Net erosion rates are low to moderate for niobium (approx. 0 to 3 cm/burn(sm bullet)yr), depending on plasma conditions, and low for tungsten (approx. 0 to 0.2 cm/burn(sm bullet)yr). DOE

N92-11872# Texas Univ., Austin. Inst. for Fusion Studies.
POWER-LAW ENERGY SPECTRUM AND ORBITAL STOCHASTICITY
K. Mima, W. Horton, T. Tajima, and A. Hasegawa (Bell Telephone Labs., Inc., Murray Hill, NJ.) Jun. 1991 14 p
(Contract DE-FG05-80ET-53088)
(DE91-017387; DOE/ET-53088/503; IFSR-503) Avail: NTIS HC/MF A03

The power-law energy distributions are observed in space and fusion plasmas. The power law decay of the two-time velocity correlation function and the corresponding frequency spectrum of the correlation function are shown to be related to the power law distribution of the time interval of acceleration, which produces a power-law energy distribution. In particular, the two time correlation function, the distribution of acceleration duration, (namely the distribution of the trapping time of the quasi-trapped orbits in the vicinity of the magnetic null such as the geomagnetic tail configurations) are shown to produce a power law energy distribution function. The statistical property is applicable under conditions given here to the energy spectra of cosmic rays, electrons in laser-plasma interaction, and the radio-frequency heated confined plasmas. DOE

N92-11873# Lawrence Livermore National Lab., CA.
AN IFE DEVELOPMENT STRATEGY
W. J. Hogan, E. Storm, and J. D. Lindl 16 Jul. 1991 11 p Presented at the International Atomic Energy Agency (IAEA) Technical Committee Meeting on Drivers for Inertial Confinement Fusion (ICF), Osaka (Japan), 15-19 Apr. 1991
(Contract W-7405-eng-48)
(DE91-016918; UCRL-JC-105833; CONF-9104210-7) Avail: NTIS HC/MF A03

The development of inertial fusion as a power source will require achieving four principal milestones: ignition and propagating burn; high gain at low drive energy for the reactor driver; pulse repetition rates of a few Hz; and long-term reliability and economics of a reactor. To keep development time and costs to a minimum, these should be accomplished with as few major facilities as possible. A viable scenario for the Inertial Fusion Energy (IFE) Program would include establishing the first milestone in a Nova Upgrade for ignition and gain and the latter three in an upgradable, low-power Engineering Test Facility (ETF)/Demonstration Power Plant (DPP), i.e., two major facilities. To be successful in as short a time as possible operations at the major facilities would have to be supported by off-line reactor driver and other reactor technology development efforts. These efforts would evaluate and prioritize the myriad of options available at present for power plant and subsystem concepts. This paper describes the elements of such a program that could make the first commercial power available in the decade of the 2020's and estimates the resources needed. This program would be carried out in phases with major go/no-go decision points before each large funding change. Cost estimates are presented. DOE

N92-11874# Lawrence Livermore National Lab., CA.
LASER PRODUCED PLASMA SOFT X RAY GENERATION
C. Cerjan and M. D. Rosen 20 May 1991 6 p Presented at the Soft-X Ray Projection Lithography Topical Meeting, Monterey, CA, 10-12 Apr. 1991
(Contract W-7405-eng-48)
(DE91-016925; UCRL-JC-107382; CONF-9104203-5) Avail: NTIS HC/MF A02

The efficiency of soft x-ray production from laser-irradiated plasmas is simulated for two different spectral regions. These two regions, 14 A +/- 15 percent and 130 A +/- 1 percent, were chosen for proximity mask or point-projection technological applications. Relatively large conversion efficiencies were obtained from irradiation of a stainless steel target using the conditions suggested by recent Hampshire Instruments' experiments for proximity masking. Pulse-width and laser frequency parameter studies were performed for point-projection applications which suggest that the conversion efficiency is sensitive to pulse-width but not to laser frequency. One of the critical components of any x-ray lithographic scheme is of course the x-ray laser source. There are two primary contenders for a reliable, efficient source currently: synchrotron radiation and spectral emission from laser produced plasma. The dominant issue for laser-plasma emission is the conversion efficiency -- output in the intended operating spectral region relative the required incident laser energy. Simulations are described in the following for both high and low energy spectral regions which have been suggested by either the proximity masking or point-projection technology. DOE

N92-11875# Washington Univ., Seattle. Aerospace and Energetics Research Program.
COAXIAL SLOW SOURCE
R. D. Brooks and T. R. Jarboe 1990 40 p
(Contract DE-FG06-87ER-53243)
(DE91-016947; DOE/ER-53243/4; UWAERP-33) Avail: NTIS HC/MF A03

Field reversed configurations (FRC's) are a class of compact toroid with no toroidal field. The field reversed theta pinch technique has been successfully used for formation of FRC's since their inception in 1958. In this method an initial bias field is produced. After ionization of the fill gas, the current in the coil is rapidly reversed producing the radial implosion of a current sheath. At

the ends of the coil the reversed field lines rapidly tear and reconnect with the bias field lines until no more bias flux remains. At this point, vacuum reversed field accumulates around the configuration which contracts axially until an equilibrium is reached. When extrapolating the use of such a technique to reactor size plasmas two main shortcomings are found. First, the initial bias field, and hence flux in a given device, which can be reconnected to form the configuration is limited from above by destructive axial dynamics. Second, the voltages required to produce rapid current reversal in the coil are very large. Clearly, a low voltage formation technique without limitations on flux addition is desirable. The Coaxial Slow Source (CSS) device was designed to meet this need. It has two coaxial theta pinch coils. Coaxial coil geometry allows for the addition of as much magnetic flux to the annular plasma between them as can be generated inside the inner coil. Furthermore the device can be operated at charging voltages less than 10 kV and on resistive diffusion, rather than implosive time scales. The inner coil is a novel, concentric, helical design so as to allow it to be cantilevered on one end to permit translation of the plasma. Following translation off the inner coil the Annular Field Reversed Configuration would be re-formed as a true FRC. In this paper, we investigate the formation process in the new parallel configuration, CSSP, in which the inner and outer coils are connected in parallel to the main capacitor bank. DOE

N92-11876# Lawrence Livermore National Lab., CA.
PARTICLE TRAJECTORIES THROUGH MIRRORTRON CONFIGURATIONS
D. J. Larson (California Univ., Davis.) and D. W. Hewett Jun. 1991 3 p Presented at the 1991 Institute of Electrical and Electronics Engineers (IEEE) Particle Accelerator Conference (PAC), San Francisco, CA, 6-9 May 1991
(Contract W-7405-eng-48)
(DE91-017084; UCRL-JC-106273; CONF-910505-399) Avail: NTIS HC/MF A01

Numerical simulation using the r-z code GYMNOS shows the time evolution of the focusing and accelerating potentials found in Post's MIRRORTRON. Formed in a strongly anisotropic loss cone plasma, the transient potential is generated by the application of an additional local mirror field produced by a strap coil. The current rise time in the strap coil must be on the order of tens of nanoseconds in order for the plasma ions to remain inertially confined while the hot electrons respond to the local mirror force. The plasma density is low in order to facilitate the penetration of the magnetic field into the plasma. Typical plasma densities in a Mirrortron are 10(exp 10) - 10(exp 11) cm(exp -3) with electron temperatures in the hundred keV to several MeV range. The magnitude of the potential produced is on the order of the electron temperature. We follow the formation of this potential peak and project test ions through the resulting fields in order to evaluate the feasibility of using a Mirrortron as a heavy ion accelerator. DOE

N92-11877# National Inst. for Fusion Science, Nagoya (Japan).
EXPERIMENTS AND APPLICATIONS OF SOLITON PHYSICS
Yoshi H. Ichikawa Jun. 1990 30 p Presented at the Fourth Tropical Coll. on Applied Physics, Kuala Lumpur, Malaysia, 28 May - 16 Jun. 1990
(NIFS-32; ISSN-0915-633X) Avail: NTIS HC/MF A03

Solitons are everywhere in the nature. Various soliton phenomena are surveyed, after giving the mathematical foundation to define solitons. Laboratory devices for the studies of plasma soliton phenomena are described together with experimental results. The most interesting application of soliton physics is illustrated in the discussion of soliton propagation in optical fibers. Topics on chaotic behavior in nonlinear dynamical systems are also briefly discussed. Author

N92-11878# National Inst. for Fusion Science, Nagoya (Japan).
EFFECTS OF ELECTRIC FIELD ON PARTICLE DRIFT ORBITS IN A l = 2 TORSATRON
H. Sanuki, T. Kamimura, Kiyoshi Hanatani (Kyoto Univ., Uji, Japan), Kimitaka Itoh, and Jiro Todoroki May 1990 39 p
(NIFS-31; ISSN-0915-633X) Avail: NTIS HC/MF A03

Particle orbits and loss regions in both real and velocity spaces are studied on the basis of the guiding center drift equations im magnetic coordinates. The boundary of loss region in pitch angle-radius (chi-rho) plane is determined from the condition whether the drift surfaces for helically trapped and transition particles reach the outermost magnetic surface or not. The loss boundaries for the absolute particle confinement within of which boundary no particles are lost, is evaluated. Effects of the radial electric field, E(sub r) on drift orbits and loss regions are discussed in detail. When ion motion is considered, the poloidal rotation modified by a positive E(sub r) reduces a number of trapped particles and consequently it leads the improvement of particle confinement. For a small negative E(sub r), there is a possible particle loss caused by the helical resonance. The loss rate of ions caused by loss cone in collisionless limit is evaluated in the presence of E(sub r). Effect of ripple modulation on the loss region is also discussed briefly. Author

N92-11879# National Inst. for Fusion Science, Nagoya (Japan).
FOKKER-PLANCK EQUATION IN THE PRESENCE OF ANOMALOUS DIFFUSION
Sanae-I. Itoh, A. Fukuyama (Okayama Univ., Japan), and Kimitaka Itoh May 1990 27 p Sponsored in part by Ministry of Education
(NIFS-29; ISSN-0915-633X) Avail: NTIS HC/MF A03

Spatial and temporal evolution of the distribution function is theoretically discussed in the presence of the RF waves and microscopic fluctuations. Using the quasilinear formulation, Fokker-Planck equation is derived in terms of the parallel and perpendicular energies and the distance across the magnetic surface. The energy dependence of the anomalous spatial diffusion term is studied for the case of the drift wave fluctuations. Cases for the intense ICRF (Ion Cyclotron Range of Frequencies) heating is also discussed. Author

N92-11880# National Inst. for Fusion Science, Nagoya (Japan).
CALCULATION OF MAGNETIC FIELD OF HELICAL COILS
Jiro Todoroki Feb. 1990 11 p Submitted for publication Sponsored by Ministry of Education, Science and Culture
(NIFS-18; ISSN-0915-633X) Avail: NTIS HC/MF A03

Formulae of magnetic field calculations of finite helical coils with rectangular cross sections are extended to the case where the size of the coil, or the relative position to the guiding curve, varies along the arc length of the guiding curve. The error caused by the inappropriate formulae or inappropriate current model is discussed. Author

N92-11881# Ceskoslovenska Akademie Ved, Prague. Inst. of Plasma Physics.
LHCD EXPERIMENTS ON TOKAMAK CASTOR
F. Zacek, J. Badalec, K. Jakubka, L. Kryska, J. Preinhaelter, J. Stoeckel, M. Valovic, S. Nanobashvili, L. Weixelbaum, and U. Wenzel (Academy of Sciences, Berlin, German D.R.) et al Oct. 1990 33 p
(IPPCZ-304) Avail: NTIS HC/MF A03

A short survey of experimental activity on the small Prague tokamak CASTOR is given. This activity concerns the lower hybrid current drive (LHCD) using multijunction waveguide grills as launching antennae. During the last two years, the effort has concentrated on the investigation of the electrostatic and magnetic fluctuations under conditions of combined inductive/LHCD regimes and linking of those fluctuation levels with the anomalous particle transport in the tokamak CASTOR. Author

N92-11882# National Inst. for Fusion Science, Nagoya (Japan).
ELMy-H MODE AS LIMIT CYCLE AND CHAOTIC OSCILLATIONS IN TOKAMAK PLASMAS
Sanae-I. Itoh, Kimitaka Itoh, Atsushi Fukuyama, and Yukitoshi Miura (Japan Atomic Energy Research Inst., Tokai.) May 1991 20 p
(NIFS-87; ISSN-0915-633X) Avail: NTIS HC/MF A03

A model of edge localized modes (ELMs) in tokamak plasmas

is presented. A limit cycle solution is found in the transport equation (time-dependent Ginzburg-Landau type), which has an hysteresis curve between the gradient and flux. Periodic oscillation of the particle outflux and L/H intermediate state are predicted near the L/H transition boundary. A mesophase in spatial structure appears near the edge. Chaotic oscillation is also predicted. Author

N92-11883# National Inst. for Fusion Science, Nagoya (Japan).
NONLINEAR BEHAVIOR OF MULTIPLE-HELICITY RESISTIVE INTERCHANGE MODES NEAR MARGINALLY STABLE STATES
Hideo Sugama, Noriyoshi Nakajima, and Masahiro Wakatani (Kyoto Univ., Uji, Japan) May 1991 35 p
(NIFS-89; ISSN-0915-633X) Avail: NTIS HC/MF A03

Nonlinear behavior of resistive interchange modes near marginally stable states is studied under the multiple-helicity condition. Reduced fluid equations in the sheared slab configuration are used in order to treat a local transport problem. With the use of the invariance property of local reduced fluid model equations under a transformation between the modes with different rational surfaces, weakly nonlinear theories for single-helical modes by Hamaguchi and Nakajima are extended to the multiple-helicity case and applied to the resistive interchange modes. We derive the nonlinear amplitude equations of the multiple-helicity modes, from which the convective transport in the saturated state is obtained. It is shown how the convective transport is enhanced by nonlinear interaction between modes with different rational surfaces compared with the single-helicity case. We confirm that theoretical results are in good agreement with direct numerical simulations. Author

N92-11884# National Inst. for Fusion Science, Nagoya (Japan).
FLUID DESCRIPTION OF PONDEROMOTIVE FORCE COMPATIBLE WITH THE KINETIC ONE IN A WARM PLASMA
Hitoshi Hojo, Tomoko Ogawa, and Mitsuo Kono (Kyushu Univ., Fukuoka, Japan) Jul. 1991 11 p Sponsored in part by Ministry of Education, Science and Culture
(NIFS-100; ISSN-0915-633X) Avail: NTIS HC/MF A03

The ponderomotive effects of electromagnetic wave fields are of great practical importance in such cases as radio frequency (RF) stabilization, RF-induced transport in magnetically confined plasmas, etc. Theoretically, however, there are still discrepancies among expressions derived by a number of authors. Attention is restricted to the discrepancy between fluid and kinetic expressions of the ponderomotive force often found in literature dealing with warm plasma. Where it stems from and how it is resolved are discussed. Author

N92-11885# National Inst. for Fusion Science, Nagoya (Japan).
ROTATIONS OF BULK IONS AND IMPURITIES IN NON-AXISYMMETRIC TOROIDAL SYSTEMS
Noriyoshi Nakajima and Masao Okamoto Jul. 1991 21 p Submitted for publication
(NIFS-102; ISSN-0915-633X) Avail: NTIS HC/MF A03

Neoclassical rotations are studied theoretically for a plasma consisting of electrons, bulk ions, and impurities in nonaxisymmetric toroidal systems. Impurity ions are assumed to lie in the Pfirsch-Schlueter collisionality regime. The results include the case of tokamaks. It is found that the rotations of impurities are generally different from those of bulk ions. The difference comes from mainly the different diamagnetic flows between bulk ion and impurities. In the 1/delta regime or banana regime, the gradient of bulk ion temperature may be another cause for the different rotations between two species. However, in the region where the configuration is far from the axisymmetry, the cause of different rotations is just the different diamagnetic flows. As the poloidal rotations depend on the radial electric field contrary to the axisymmetric system, a relationship, which does not include the radial electric field, can be derived between poloidal and toroidal rotations. By estimating this relationship based on the measured rotations, the present neoclassical theory can be validated without knowledge of radial electric field. Author

N92-11886# Office of Naval Research, Arlington, VA.
A COMPACT LASER PHOTOCATHODE DRIVEN ACCELERATOR FOR THE PLASMA WAKE FIELD ACCELERATOR PROGRAM AT UCLA Annual Progress Report, 1 Jun. 1990 - 31 May 1991
31 May 1991 76 p
(Contract N00014-90-J-1952)
(AD-A240646) Avail: NTIS HC/MF A05 CSCL 20/9

The plasma wake field accelerator requires a plasma density of 5 x 10(exp 13) to 5 x 10(exp 14) cc in order to achieve a significant wake field amplitude (eE greater than 10 Mev/m/nCoul). Our earlier attempts with RF produced plasmas and BaO coated cathodes resulted in plasma densities which approached 9 x 10(exp 12)cc. In this report, we will describe the preliminary measurements of a plasma produced by an indirectly heated lanthanum hexaboride cathode. The main advantages of lanthanum hexaboride (LaB6) are that: (1) LaB6 has a high emission current density (20 A/sq cm at 1700 C); (2) it has a low evaporation rate (almost two order of magnitudes lower than tungsten); and (3) it is immune to accidental exposure to air. GRA

N92-11887# Technische Univ., Berlin (Germany, F.R.). Fachbereich Elektrotechnik.
THE RECOMBINATION BEHAVIOR OF A LASER INDUCED ELECTRON HOLE PLASMA IN PIN DIODES AND SILICON BASE MATERIAL Ph.D. Thesis [DAS REKOMBINATIONSVERAHLTEN EINES LASERINDUZIERTEN ELEKTRON-LOCH-PLASMA IN PIN-DIODEN UND SILIZIUM-AUSGANGSMATERIAL]
Andreas C. Brockelt 1990 180 p In GERMAN
(ETN-91-90153) Avail: NTIS HC/MF A09

The examination took place in a large zone in the excess beam concentration. Particular attention was given to high injection effects. Specially prepared pin diodes and pieces of base material, from which the structural elements were fabricated, were used as test objects. Besides the measurements of the absorption of free charged particles, the recombination radiation test method, photoconductivity measurements, and open circuit voltage measurements were chosen as test methods. The test method of absorption of optically generated free charged paticles prevails over other test methods, as it shows higher sensitivity when examining transient processes, and as the influence of surface recombination on the experimental accessible complete recombination is widely reduced. This can be verified by comparison with corresponding recombination radiation measurements. ESA

N92-11888# Argonne National Lab., IL.
CURRENT PROFILE CONTROL FOR ITER WITH RF CURRENT DRIVE
D. A. Ehst and D. L. Pearlstein (Lawrence Livermore National Lab., CA.) Aug. 1991 5 p Presented at the 9th Topical Conference on Radio Frequency Power in Plasmas, Charleston, SC, 12-14 Aug. 1991
(Contract W-31-109-eng-38)
(DE91-018597; ANL/CP-73548; CONF-910869-5) Avail: NTIS HC/MF A01

Self-consistent MHD equilibria are found with the RIP computer code, which traces lower hybrid and fast wave rays in two dimensions; the tokamak flux surfaces are generated by LHCD, FWCD and the bootstrap effect. The bootstrap current dominates at the mid-minor radius, the FWCD provides the seed current and LHCD is effective only in the surface region of a fusion-grade tokamak. The bootstrap fraction maximizes by operating at high central safety factor, q (0) approx. = 2, that is, with rather minimal FWCD; while the total current is effectively controlled by LHCD. There is potentially considerable flexibility to affect the current profile and MHD stability by appropriate adjustments to the RF power spectra. Current drive on ITER is more attractive at higher aspect ratios, and results are presented for A = 4.0. DOE

N92-11889# Oak Ridge National Lab., TN.
ECH EXPERIMENTS ON ATF
T. S. Bigelow, J. B. Wilgen, L. R. Baylor, Masanori Murakami, C.

R. Schaich, and R. Lindley (Michigan Univ., Ann Arbor.) 1991 6 p Presented at the 9th Topical Conference on Radio Frequency Power in Plasmas, Charleston, SC, 12-14 Aug. 1991
(Contract DE-AC05-84OR-21400)
(DE91-018845; CONF-910869-10) Avail: NTIS HC/MF A02

Several electron cyclotron heating (ECH) experiments have been completed on the Advanced Toroidal Facility (ATF) at Oak Ridge National Laboratory (ORNL) under a variety of operating conditions and launch polarizations. ECH power is launched using a polarization-controlled beam launcher and microwave detectors are used to measure absorption of first-pass and multiply-reflected power. Measurements show that first-pass absorption efficiency at low plasma density is highly dependent on magnetic field, polarization, and plasma conditions. Wave polarization rotation has been detected; it is caused by the large magnetic field shear on ATF. Detector signals indicate that absorption efficiency is relatively high for medium plasma density at either fundamental or second harmonic operation. Plasmas have also been sustained using the third harmonic cyclotron resonance where absorption efficiency is much lower. Gyrotron power modulation and turn-off experiments have been performed to study power deposition and transport using plasma diagnostics. These experiments show that power absorption is fairly efficient. However, the power deposition profile is rather broad despite the relatively narrow launcher beam. This effect can be attributed to several factors including the broad extent of the resonant surface and the approximately 45 percent of power contained in both low-level sidelobes outside the launcher beam and in the wrong plasma mode. DOE

N92-11890# Texas Univ., Austin. Inst. for Fusion Studies.
CONTINUUM DAMPING OF HIGH MODE NUMBER TOROIDAL ALFVEN WAVES
M. N. Rosenbluth (California Univ., San Diego, La Jolla.), H. L. Berk, D. M. Lindberg, and J. W. VanDam Aug. 1991 11 p
(Contracts DE-FG05-80ET-53088; DE-FG03-88ER-53275)
(DE91-018891; DOE/ET-53088/518; IFSR-518) Avail: NTIS HC/MF A03

An asymptotic theory is developed to determine the continuum damping of short-wavelength Toroidal Alfven Eigenmodes, which is essential for ascertaining thresholds for alpha particle driven instability in ignited tokamaks. DOE

N92-11891# New York Univ., New York. Inst. of Mathematical Sciences.
PLASMA PROPERTIES
H. Weitzner Aug. 1991 11 p
(Contract DE-FG02-86ER-53223)
(DE91-018913; DOE/ER-53223/169) Avail: NTIS HC/MF A03

This report discusses the following topics on plasma physics: kinetic modelling; fluid modelling; development of a non-maxwellian plasma transport theory; development of neoclassical theories near a tokamak edge; improvement of the usual neoclassical formula; ballooning modes; and the alfven spectrum. DOE

N92-11892# Tri-Univ. Meson Facility, Vancouver (British Columbia).
COMPARATIVE STUDY OF FINAL STATE INTERACTION CONTRIBUTIONS TO THE DYNAMIC RESPONSE OF QUANTUM FLUIDS
A. S. Rinat (Weizmann Inst. of Science, Rehovoth, Israel) and M. N. Butler Feb. 1989 10 p
(DE91-631020; TRI-PP-89-6) Avail: NTIS HC/MF A02

The expression for the final state interaction part of the dynamic response S(q,omega) as given by Silver is derived from a multiple scattering theory. We first discuss the single scattering term which has the same form in the analyses of Silver and Rinat. Next, we indicate the approximations which permit a summation of the full scattering series in the form given by Silver, but we argue that under currently prevailing conditions the approximated sun for S is dominated by the first two terms. In order to determine the better approach, we suggest as a test a comparison of the part of S odd in the variable y. DOE

N92-11893# Colorado Univ., Boulder.
APPLICATION OF MODERN MATHEMATICAL CONCEPTS TO PLASMA CONFINEMENT
J. R. Cary Aug. 1991 4 p
(Contract DE-FG02-85ER-53207)
(DE92-000053; DOE/ER-53207/6) Avail: NTIS HC/MF A01

Progress in three research areas has been achieved. (1) A new expression for the trapping probability for transitioning particles in asymmetric toroidal plasma confinement devices (e.g., stellarators and rippled tokamaks) has been derived. Comparison with numerical integrations shows that this new expression is more accurate than those of previous workers. (2) Simulations show that the dynamical enhancement of the turbulent diffusion coefficient over quasilinear observed in test particle simulations occurs also in self consistent plasma turbulence. (3) The simple method for calculating magnetic island widths discussed in the previous report has been published. DOE

N92-11894# Oak Ridge National Lab., TN.
FULL-WAVE CALCULATION OF FAST-WAVE CURRENT DRIVE IN TOKAMAKS INCLUDING K(PARALLEL) VARIATIONS
E. F Jaeger and D. B. Batchelor 1991 10 p Presented at the International Workshop on Fast Wave Current Drive in Reactor Scale Tokamaks Synergy and Complementarity With LHCD and ECRH, Cadarache (France), 23-25 Sep. 1991
(Contract DE-AC05-84OR-21400)
(DE92-000076; CONF-9109200-1) Avail: NTIS HC/MF A02

When fast waves propagate inward from the edge of a tokamak toward the plasma center, the k(perpendicular) spectrum produced by the antenna is not maintained but is shifted and deformed due to the presence of the finite poloidal magnetic field. This k(perpendicular) shift causes a variation in the parallel phase speed of the wave and can therefore have a strong effect on electron damping and current drive efficiency. In this paper, we include this effect in a new full-wave calculation (PICES) which represents the wave fields as a superposition of poloidal modes, thereby reducing k(perpendicular) to an algebraic operator. The wave equation is solved in general flux coordinates, including a full (non-perturbative) solution for E(perpendicular) and a reduced-order dielectric formulation to eliminate short-wavelength ion Bernstein modes. A simplified current drive model which includes particle trapping is used to estimate the effect of the k(perpendicular) shift on current drive efficiency in ITER and D3-D. Results suggest that when single-pass absorption is weak, reflected power may drive current nearly as efficiently as that absorbed on the first pass. DOE

N92-11895# California Univ., Los Angeles.
THE TITAN REVERSED-FIELD-PINCH FUSION REACTOR STUDY, VOLUME 4
1990 349 p Prepared in cooperation with General Atomics Technologies Corp., San Diego, CA; Los Alamos National Lab., NM; and Rensselaer Polytechnic Inst., Troy, NY
(Contracts DE-FG03-86ER-52126; DE-AC03-84ER-53158; DE-FG02-85ER-52118; W-7405-eng-36)
(DE92-000138; UCLA/PPG-1200-Vol-4) Avail: NTIS HC/MF A15

The following subject areas are discussed: overview of TITAN-2 design; TITAN-2 fusion-power-core engineering; TITAN-2 divertor engineering; TITAN-2 tritium systems; TITAN-2 safety design and radioactive-waste disposal; and TITAN-2 maintenance procedures. DOE

N92-11896# California Univ., Los Angeles.
THE TITAN REVERSED-FIELD-PINCH FUSION REACTOR STUDY, VOLUME 2
1990 431 p Prepared in cooperation with General Atomics Technologies Corp., San Diego, CA; Los Alamos National Lab., NM; and Rensselaer Polytechnic Inst., Troy, NY
(Contracts DE-FG03-86ER-52126; DE-AC03-84ER-53158; DE-FG02-85ER-52118; W-7405-eng-36)

(DE92-000140; UCLA/PPG-1200-Vol-2) Avail: NTIS HC/MF A19

This paper on TITAN plasma engineering contains papers on the following topics: reversed-field pinch as a fusion reactor; parametric systems studies; magnetics; burning-plasma simulations; plasma transient operations; current drive; and physics issues for compact RFP reactors. DOE

N92-11897# California Univ., Los Angeles.
THE TITAN REVERSED-FIELD-PINCH FUSION REACTOR STUDY, VOLUME 1
1990 202 p Prepared in cooperation with General Atomics Technologies Corp., San Diego, CA; Los Alamos National Lab., NM; and Rensselaer Polytechnic Inst., Troy, NY
(Contracts DE-FG03-86ER-52126; DE-AC03-84ER-53158; DE-FG02-85ER-52118; W-7405-eng-36)
(DE92-000141; UCLA/PPG-1200-Vol-1) Avail: NTIS HC/MF A10

This paper contains the executive summary of the titan revised-field-find fusion reactor study. The general topics covered are: overview of titan plasma engineering; overview of titan-1 fusion power core; and overview of titan-2 fusion power core. DOE

N92-11898*# Southwest Research Inst., San Antonio, TX.
A SIMULATION STUDY OF INTERACTIONS OF SPACE-SHUTTLE GENERATED ELECTRON BEAMS WITH AMBIENT PLASMA AND NEUTRAL GAS Annual Progress Report, Nov. 1990 - Nov. 1991
Nov. 1991 26 p
(Grant NAGw-1936; SwRI Proj. 15-3399)
(NASA-CR-189025; NAS 1.26:189025) Avail: NTIS HC/MF A03 CSCL 20I

The object was to conduct large scale simulations of electron beams injected into space. The study of active injection of electron beams from spacecraft is important since it provides valuable insight into beam-plasma interactions and the development of current systems in the ionosphere. However, the beam injection itself is not simple, being constrained by the ability of the spacecraft to draw return current from the ambient plasma. The generation of these return currents is dependent on several factors, including the density of the ambient plasma relative to the beam density, the presence of neutrals around the spacecraft, the configuration of the spacecraft, and the motion of the spacecraft through the plasma. Two dimensional particle simulations with collisional processes included are used to show how these different and often coupled processes can be utilized to enhance beam propagation from the spacecraft. To understand the radical expansion of mechanism of an electron beam from a highly charged spacecraft, two dimensional particle in cell simulations were conducted for a high density electron beam injected parallel to magnetic fields from an isolated equipotential conductor into a cold background plasma. The simulations indicate that charge buildup at the beam stagnation point causes the beam to expand radially to the beam electron gyroradius. Author

76 SOLID-STATE PHYSICS

Includes superconductivity.

For related information, see also *33 Electronics and Electrical Engineering* and *36 Lasers and Masers.*

N92-11899# Sandia National Labs., Albuquerque, NM.
NEW HIGH-T(SUB c) BENCHMARKS FOR ORGANIC AND FULLERENE SUPERCONDUCTORS
J. M. Williams, H. H. Wang, K. D. Carlson, A. M. Kini, U. Geiser, A. J. Schultz, W. K. Kwok, U. Welp, G. W. Crabtree, and S. Fleshler (Argonne National Lab., IL.) et al 1991 5 p Presented at the International Conference on Materials and Mechanisms of Superconductivity, Kanazawa (Japan), 22-26 Jul. 1991
(Contracts DE-AC04-76DP-00789; W-31-109-eng-38; DE-FG05-86ER-45259)
(DE91-016406; SAND-91-1728C; CONF-910736-7) Avail: NTIS HC/MF A01

Superconductivity in the highest-T(sub c) radical cation kappa-(ET)2Cu(N(CN)2)X, X = Br(T(sub c)=11.6 K), X = Cl(T(sub c) = 12.8 K, 0.3 kbar) and radical anion (kappa(sub x)C60(T(sub c) = 18.0K), Rb(sub x)C60(T(sub c) = 28.6 K)) organic superconductors is discussed. Over 20 ET based superconductors are now known. Two doped fullerene superconductors have been reported. Current status of both ET and fullerene high T(sub c) (greater than 11.5 K) research is reviewed. DOE

N92-11900# Argonne National Lab., IL.
RADIATION INDUCED GROWTH OF MICRO CRYSTALLITES
D. Meisel 1991 6 p Presented at the 9th International Congress of Radiation Research (ICRR) Conference, Toronto (Canada), 7-12 Jul. 1991
(Contract W-31-109-eng-38)
(DE91-016516; ANL/CP-72218; CONF-9107136-6) Avail: NTIS HC/MF A02

Generation of colloidal particles during the radiolysis of aqueous solutions was already observed in the early days of radiation chemistry. Systematic studies using radiation chemistry techniques as synthetic tools in the preparation of colloidal particles, primarily metallic particles, were begun approximately a decade ago in conjunction since they were found to catalyze multi-electron redox processes. A large number of metallic colloidal particles were then synthesized, including silver, gold, platinum, iridium, nickel, cadmium, and others. More recently, attention has turned to semiconductor colloidal particles. The stimulus to these studies is the observation of quantum size effects in small semiconductor particles that exhibit hybrid properties between those of the molecular species and the solid state bulk material. In the following we discuss our own observations on the evolution of semiconductor particles whose growth has been initiated by pulse radiolysis. DOE

N92-11901# Sandia National Labs., Albuquerque, NM.
ELECTROOPTIC EFFECTS AND PHOTOSENSITIVITIES OF PLZT THIN FILMS
D. Dimos, C. E. Land, and R. W. Schwartz 1991 24 p Presented at the 93rd Annual Meeting and Exposition of the American Ceramic Society (ACerS), Cincinnati, OH, 28 Apr. - 2 May 1991
(Contract DE-AC04-76DP-00789)
(DE91-017067; SAND-91-1506C; CONF-910430-19) Avail: NTIS HC/MF A03

Although the feasibility of using PZT and PLZT films for optical data processing applications, such as optical storage disks, image comparators, and spatial light modulators, has clearly been established, most of the critical parameters related to the storage and readout processes still need to be evaluated. Optical readout techniques capable of nondestructively determining the value of polarization are based either on the quadratic electrooptic effect or on a photocurrent response. In reflection, large electrooptic retardations (greater than 60 degrees) have now been achieved with thin PZT films (approximately = 0.5 microns) under conditions that optimize interference effects. These results are quite attractive for device applications. Model calculations, based on the equations of reflection ellipsometry, have been used to develop a framework for understanding those results. The magnitude of the photocurrent response has also been used to determine the polarization state. However, the photocurrent always has the same sign, regardless of the sign of the polarization, which suggests the presence of a strong bias field due to at least one of the interfaces. In addition, the accumulation of space charge after a succession of measurements suppresses the photocurrent transient, which severely limits the utility of a photocurrent based readout. DOE

N92-11902*# Clemson Univ., SC. Dept. of Ceramic Engineering.
DEVELOPMENT OF HIGH Tc (GREATER THAN 110K) Bi, Tl AND Y-BASED MATERIALS AS SUPERCONDUCTING CIRCUIT ELEMENTS Semiannual Report, Feb. - Oct. 1991
Gene Haertling, Gregory Grabert, and Phillip Gilmour 11 Nov.

1991 46 p
(Grant NAG1-1108)
(NASA-CR-188999; NAS 1.26:188999) Avail: NTIS HC/MF A03 CSCL 20L

Experimental work was continued on the development and characterization of bulk and hot pressed powders and tapecast materials in the Bi-Sr-Ca-Cu-O and Tl-Ba-Ca-Cu-O systems. A process for producing warp-free, sintered, superconducting tapes of Bi composition Bi1Sr2Ca2 Cu3O(x) was established. The procedure requires a triple calcination at 830 C for 24 hours and sintering at 845 C from 20 to 200 hours. Hot pressing the triple calcined powder at 845 C for 6 hours at 5000 psi yielded a dense material, which on further heat treatment at 845 C for 24 hours, exhibited a Tc of 108.2K. The Bi compositions were found to be much less oxygen sensitive than the Y compositions. This was especially noted in the case of the hot pressed materials which were superconducting as hot pressed, a condition that could not be achieved in the Y compositions. Safire-type grounding links are in the process of being fabricated from these materials.

Author

N92-11903# Ames Lab., IA.
PHOTOEMISSION STUDY OF Ce/Ta(110) AND Ce/W(110) INTERFACES AND THE CATALYTIC OXIDATION EFFECT
Ph.D. Thesis
Chun Gu Aug. 1991 86 p
(Contract W-7405-eng-82)
(DE91-018167; IS-T-1494) Avail: NTIS HC/MF A05

Photoemission spectroscopy was used to study Ce/Ta(110) and Ce/W(110) interfaces, and the catalytic oxidation effect on both surfaces. A weak Ce/Ta interface reaction is illustrated by the reduced Ta 4f surface core-level shift (SCS) upon Ce adsorption. No Ce/Ta interdiffusion was found. The Ce layer may greatly enhance the oxidation of Ta(110). Oxidation of Ce/Ta(110) at 300 K yields on monolayer (ML) of Ta suboxide (approximately TaO), followed by the rapid formations of Ta2O5. Ce/W(110) adsorption patterns were determined by low-energy electron diffraction. For Theta less than or equal to 0.5 ML, the adsorption structure is characterized by one-dimensional commensuration along the zone axes (1'10) direction. It changes abruptly to a hexagonal pattern after 0.5 ML. The interatomic spacing shrinks continuously from 9 percent larger than that for gamma-Ce to 3 percent smaller than that for alpha-Ce. Correspondingly the Ce 4f photoelectron spectrum evolves to resemble that of alpha-Ce. W 4f core levels are also correlated to the adsorption. A significantly widened W SCS is found at low Ce coverages. After the formation of the hexagonal patterns, the Ce-W registration is lost, and the interaction within the Ce layer increases. The SCS for the top layer of W is partially restored. Electronic charge polarization from Ce toward the W (or Ta) substrate is believed to be the key mechanism for the Ce-induced SCS.

DOE

N92-11904# Oak Ridge National Lab., TN.
HIGH l STATE POPULATION IN O(7+) PRODUCED IN ION-SOLID COLLISIONS
J. Kemmler, J. Bourgdoerfer, and C. O. Reinhold (Tennessee Univ., Knoxville.) 1991 13 p Presented at the 14th International Conference on Atomic Collisions in Solids, Salford, England, 29 Jul. - 2 Aug. 1991
(Contract DE-AC05-84OR-21400)
(DE91-018169; CONF-9107155-2) Avail: NTIS HC/MF A03

The high l-state population of fast ions excited in ion-solid interactions is very different from l-state populations produced under single collision conditions. A study of the population dynamics of electronic excitation and transport within the framework of a classical transport theory for O(2+) (2 MeV/u) ions traversing carbon foils shows good agreement with experimental results from delayed photon emission spectroscopy. We investigate the dependence of the characteristic exponent for the power-law decay of delayed Ly(sub alpha) and Ly(sub beta) radiation on the initial n,l distribution. From our simulations we find evidence that the very high l-state populations produced in ion-solid collision are the consequence of a high l-state diffusion under the influence of multiple inelastic and elastic collisions in the bulk of the solid.

DOE

N92-11905# Oak Ridge National Lab., TN.
PROGRESS IN PHOTON SCANNING-TUNNELING MICROSCOPY (PSTM)
T. L. Ferrell, S. L. Sharp, and R. J. Warmack 1991 18 p Presented at the 1991 Scanning Tunneling Microscopy, Interlaken, Switzerland, 12-16 Aug. 1991
(Contract DE-AC05-84OR-21400)
(DE91-018174; CONF-9108153-1) Avail: NTIS HC/MF A03

Tunneling of either electrons or photons from a sample to a probe tip yields an exponential signal that permits subwavelength tangential resolution and even better resolution of the tip-to-sample distance. Photon Scanning Tunneling Microscopy (PSTM) provides images of both insulators and conductors that are either thin or not too strongly absorbing at the wavelength used. Scanning Tunneling Microscopy (STM) provides better spatial resolution but poorer spectroscopic resolution, so there are complementary aspects for the two instruments. Our recent progress with the PSTM includes adding a zoom capability, detection of surface-enhanced Raman signals, imaging of photolithographically prepared arrays of isolated silver particles, and studies of tunneling effects on films of photoresist.

DOE

N92-11906# Oak Ridge National Lab., TN.
NEUTRON DIFFRACTION FROM THE FLUX LINE LATTICE
E. M. Forgan, S. L. Lee, R. Cubitt, J. S. Abell, F. Gencer, D. M. Paul (Warwick Univ., Coventry, England), and H. A. Mook 1991 6 p Presented at the International Conference on Materials and Mechanisms of Superconductivity, Kanazawa, Japan, 22-26 Jul. 1991
(Contract DE-AC05-84OR-21400)
(DE91-018175; CONF-910736-17) Avail: NTIS HC/MF A02

We review the detection of flux lattice structure by neutron diffraction and describe recent results of this technique in YBa2Cu3O(7-delta). We have observed flux lattice structures in fields up to 4T, which is the highest field at which the mixed state has been imaged in any superconductor. There is strong pinning of flux lattice planes to twin planes and no clear signs of melting of the flux lattice in this material. The distortion of the flux lattice structure by the crystal anisotropy has also been observed.

DOE

N92-11907# Missouri Univ., Saint Louis. Dept. of Physics.
QUANTUM 1/f NOISE IN HIGH TECHNOLOGY APPLICATIONS INCLUDING ULTRASMALL STRUCTURES AND DEVICES
Annual Report No. 2, 15 Jun. 1990 - 14 Jun. 1991
Peter H. Handel 15 Jul. 1991 33 p
(Grant AF-AFOSR-0416-89; AF Proj. 2305)
(AD-A240152; AFOSR-91-0742TR) Avail: NTIS HC/MF A03 CSCL 09/1

This report summarizes progress achieved this year both in the more general formulation of our new criterion for nonlinear systems which allows us to tell right away if a chaotic system will exhibit a l/f spectrum, and in the application and further study of the quantum l/f effect. The general criterion was applied to a one-dimensional crystal with anharmonic interactions, predicting for the first time a l/f phonon number spectrum in the chaotic regime at very low frequencies and always when cubic terms are dominant in the potential energy. The quantum l/f theory was applied to a quartz resonator directly for the first time, providing both an explanation for the observed l/f frequency fluctuations and optimization means. Our new formula for collector l/f noise in ultrasmall BJT's was found to agree reasonably with the experiment.

GRA

N92-11908# Washington State Univ., Pullman. Dept. of Chemistry.
CHEMICAL REACTIVITY AND ELECTRONIC STRUCTURE OF SILICON MICROCLUSTERS
Daniel A. Jelski, Tapio T. Rantala, and Thomas F. George Sep.

1991 22 p
(Contract N00014-90-J-1193)
(AD-A240276; WSU/DC/91/TR-62) Avail: NTIS HC/MF A03 CSCL 07/4

The tight-binding model is used to study the structure and chemical reactivity of medium sized clusters, Si10-Si60. First, the validity of the model is established with a comparison to existing experimental and other calculated data. A new stable structure for the Si10 cluster is found. Second, the strong cluster size dependency in the reactivity with ammonia and methanol for Si30(+)-Si45(+) is modeled in terms of stacked, six-membered ring structures. This accounts for the periodicity of six in the reactivity pattern. Finally the photofragmentation of Si60(+) indicating mainly Si10(+) daughters is considered. It is suggested that Si60 consists of stacked ten-atom naphthalene-like rings.
GRA

N92-11909# Washington State Univ., Pullman. Dept. of Chemistry.
STRUCTURE OF THE Si45 CLUSTER
Daniel A. Jelski, Brian L. Swift, Tapio T. Rantala, Xinfu Xia, and Thomas F. George Sep. 1991 32 p
(Contract N00014-90-J-1193)
(AD-A240278; WSU-DC/91/TR-61) Avail: NTIS HC/MF A03 CSCL 07/4

There has been much interest in the Silicon cluster, both from an experimental and theoretical point of view. The original impetus to this effort was the astounding experimental results compiled by Elkind et al, which reported a reactivity difference between various silicon clusters spanning two orders of magnitude. Silicon ions were found to be unreactive with ammonia and methanol. This implies a periodicity of six atoms in the reactivity pattern for clusters ranging form 30 to 45 atoms. For clusters larger than 45 atoms the reactivity appeared to monotonically increase. J. C. Phillips suggested that silicon forms six-membered rings in a carbon-like fashion and proposed a structure of stacked rings with a three-atom cap. We took this suggestion literally, and in what we believe to be the first calculation which tried to explain this data, proposed a series of stacked benzene rings and attempted to show that this accounted for the experiment.
GRA

N92-11910# California Univ., Irvine.
SUPERIONICS Final Technical Report, 1 May 1988 - 30 Apr. 1991
Richard F. Wallis 30 Apr. 1991 133 p
(Contract N00014-88-K-0392; DARPA Order 9526)
(AD-A240352) Avail: NTIS HC/MF A07 CSCL 10/3

This research concerns the investigation of the physical properties of the components of a new solid state microbattery. This battery consists of a lithium metal anode, a lithium borate glass separator, and a cathode of the layer compound indium selenide which readily intercalates lithium ions and which is also an electronic conductor. The battery operates by the passage of lithium ions between the electrodes through the borate glass separator and the passage of electrons between the electrodes via the external circuit. A single battery of this type produces a voltage of 2.7 V, can be discharged with a current density of 50 microamps/sq cm and can achieve a specific energy of 300 watt hours. It is the ultimate objective of this project to produce systems composed of many microbatteries for applications requiring high voltage, high current density, and/or high energy density. In order to achieve this objective, it is necessary to have a fundamental understanding of fast ion transport in the lithium borate glasses and of both fast ion and electron transport in the layer compound.
GRA

N92-11911# Illinois Univ., Urbana.
PHOTOREFLECTANCE AND H2O ADSORPTION ON GaAs(100) M.S. Thesis
William F. Buechter 1991 131 p
(AD-A240391) Avail: NTIS HC/MF A07 CSCL 09/1

Compound semiconductors possess the essential characteristics for the next technologically advanced generation of the semiconductor industry. Gallium arsenide (GaAs) in particular demonstrates considerable promise in the development of twenty first century ultrahigh speed computers, microwave generation and optical transmission. The unique properties of GaAs in comparison to silicon, the current mainstay of the electronic industry, are its enhanced optical properties and considerably higher electron velocity, which provide intrinsically higher speeds, greater operating frequencies, lower power requirements, higher resistance to high energy radiation and dramatic optoelectronic capabilities. The enhanced performance of GaAs makes it an essential component for certain aspects of future commercial and military electronic systems. However, as with any new material, manufacturing technologies for compound semiconductors are still in their early stages of development.
GRA

N92-11912# Cornell Univ., Ithaca, NY. Dept. of Chemistry.
SYNTHESIS OF NOVEL CONDUCTING SOLIDS Final Report, Nov. 1987 - Nov. 1990
Francis J. DiSalvo 12 Sep. 1991 5 p
(Contracts N00014-88-K-0139; N00014-91-J-1269)
(AD-A240468) Avail: NTIS HC/MF A01 CSCL 07/4

A large family of novel nitride materials has been discovered and examined. Unusual structural, electrical and magnetic properties were found. Work continues in this field to better understand the scope of nitride chemistry in solids and the chemical and physical properties of these unique materials. The synthesis of new oxides, sulfides and nitrides was undertaken with the objective of discovering novel conducting properties. One goal is to discover new classes of compounds that could be high temperature superconductors. Such discovery is hoped to lead to materials with better mechanical and electrical properties than the copper oxides and possible to provide new perspectives on the mechanism of high temperature superconductivity. A second goal is to investigate little studied classes of materials for new chemical or physical behavior. While oxides as a class have been extensively studied, compounds such as ternary nitrides are almost completely unexplored.
GRA

N92-11913# Technische Univ., Eindhoven (Netherlands).
SURFACE ANALYSIS OF CATALYSTS BY LOW-ENERGY ION SCATTERING Ph.D. Thesis
Gerrit Cornelis vanLeerdam 18 Jan. 1991 138 p Sponsored in part by Netherlands Foundation of Chemical Research and Netherlands Organization for the Advancement of Scientific Research
(ETN-91-90133) Avail: NTIS HC/MF A07

The characterization of catalyst surfaces using Low Energy Ion Scattering (LEIS) is described. The structure of a catalyst is generally described in conjunction with the different spectroscopic techniques used to characterize them. LEIS is discussed in detail. The importance of the different mechanisms for a number of elements is discussed and related to the total shape of a LEIS spectrum. The consequences for quantitative surface composition analysis are addressed. The absence of signals for tetragonally coordinated cations in the surface of gamma Al2O3 is argued to be due to the preferential exposure of crystallographic planes which contain exclusively octahedral sites. The insight makes it possible to propose a detailed model for the surface structure of gamma Al2O3 and the position of deposited metaloxides there upon. The location of molybdenum strongly depends on the amount deposited and the calcination temperature. The addition of lanthanum making gamma Al2O3 more thermostable is investigated. A series of silica supported molybdenum oxide catalysts is investigated toexplain the remarkable behavior to the selective oxidation of ammonia.
ESA

N92-11914# Technische Univ., Eindhoven (Netherlands).
SPECTROSCOPIC STUDIES OF LAYERED AND BULK SEMICONDUCTOR MATERIALS Ph.D. Thesis
Edwin Andre Montie 1991 126 p Prepared in cooperation with Philips Gloeilampenfabrieken N.V., Eindhoven, Netherlands
(ETN-91-90145) Avail: NTIS HC/MF A07

Spectroscopic studies of semiconductor materials investigating

both bulk and layered structure properties are described. The spectroscopic techniques used, Raman scattering, photoluminescence and optically detected magnetic resonance, are reviewed. The modeling of lattice matched In(x)Ga(1-x)As(y)P(1-y)/InP quantum wells for application in 1.5 micron telecommunication lasers, and the effects of strain in non lattice matched In(x)Ga(1-x)As/InP quantum wells, are described. Raman spectroscopy of Si/Ge superlattices is described. An optically detected magnetic resonance study of the effective mass donor system in Al(x)Ga(1-x)As is presented. The results of a photoluminescence study of Zn diffused InP are given. ESA

N92-11915# Technische Univ., Berlin (Germany, F.R.). Inst. fuer Festkoerperphysik.
THERMAL ANNEALING STUDIES OF Fe AND Ti IMPLANTED IN GaAs AND InP Ph.D. Thesis
Salah M. D. Darwish 1990 120 p Sponsored by Egypt Studienmission
(ETN-91-90148) Avail: NTIS HC/MF A06

Fe and Ti as a deep transition metal was implanted with energies of 400 keV and 150 keV and with doses of 1 x 10(exp 14)/sq cm and 4 x 10(exp 14)/sq cm respectively. The optical (photoluminescence) and electrical (capacitance voltage) properties were systematically investigated after various annealing conditions. The redistribution of Fe and Ti was investigated by Secondary Ion Mass Spectrometer (SIMS). Results are given. ESA

N92-11916# Argonne National Lab., IL.
VORTEX-LATTICE STATES OF A TWO-DIMENSIONAL ELECTRON SYSTEM AT STRONG MAGNETIC FIELDS
H. Akera, A. H. MacDonald (Indiana Univ., Bloomington.), and M. R. Norman 1991 10 p Presented at the CAP-NSERC Workshop on Theoretical Physics, Ontario (Canada), 28 Jul. - 3 Aug. 1991
(Contracts W-31-109-eng-38; DE-FG02-86ER-45247)
(DE91-018551; ANL/CP-74020; CONF-9107170-1) Avail: NTIS HC/MF A02

To explore a possible superconducting phase, the microscopic mean-field equations are solved for the case of a two-dimensional electron system in the strong magnetic field limit where the Landau level quantization invalidates the semiclassical approximations in the Ginzburg-Landau (GL) theory. For delta function attractive interactions there exist n + 1 pairing channels in the n - th Landau level. For n greater than or = 1 the order parameter differs markedly from expectations based on the GL theory and the excitation spectrum has a zero gap. DOE

N92-11917# Korea Advanced Energy Research Inst., Daeduk (Republic of Korea).
A STUDY ON THE DEVELOPMENT OF HIGH T(SUB c) SUPERCONDUCTING MATERIALS
Dong Yeon Won, Hee Gyoun Lee, and Chan Joong Kim (Korea Advanced Energy Research Inst., Daeduk, Republic of Korea) Jan. 1990 57 p In KOREAN
(DE91-629755; KAERI/RR-837/89) Avail: NTIS HC/MF A04

The microstructure, crystal structure and formation kinetics for the superconducting phases were studied in the lead-doped BiSrCaCuO system. The formation kinetics was also investigated in the samples with different Pb/Bi ratio and it was observed that the 30 percent Pb addition is most preferable for the formation of the high T(sub c) phase. The formation of the high T(sub c) phase was delayed by the excessive addition of Pb. The lattice parameter (c) of the unit cell of both low T(sub c) and high T(sub c) phases increased with increasing Pb content. Superconducting thin film was successfully prepared by chemical vapor deposition (CVD). Film deposited on MgO substrate showed a T(sub c), onset of 85 K and did not reach to zero resistivity down to 77 K. Superconducting 124 phase in Y-system, which is more stable than 123 phase at high temperature showed a T(sub c), onset of 84 K. Additionally, 0.1 mole of Pb, Sn and Ca was substituted for yttrium in 124 phase, respectively. For Pb and Sn-subsituted specimens, 124 phase was formed and for Ca substituted specimen, 124 phase was not formed and revealed no superconductivity down to 77 K. For Sn-substituted specimens, 124 phase was formed but showed no superconductivity down to 77 K. DOE

77 THERMODYNAMICS AND STATISTICAL PHYSICS

Includes quantum mechanics; theoretical physics; and Bose and Fermi statistics.

For related information see also *25 Inorganic and Physical Chemistry* and *34 Fluid Mechanics and Heat Transfer.*

No abstracts in this category.

80 SOCIAL SCIENCES (GENERAL)

Includes educational matters.

No abstracts in this category.

81 ADMINISTRATION AND MANAGEMENT

Includes management planning and research.

N92-11918*# Research Inst. for Advanced Computer Science, Moffett Field, CA.
AN APPLICATION FOR MULTI-PERSON TASK SYNCHRONIZATION
Robert L. Brown and Dee Doyle Jul. 1990 14 p
(Contract NCC2-387)
(NASA-CR-187712; NAS 1.26:187712; RIACS-TR-90-24) Avail: NTIS HC/MF A03 CSCL 05A

Computer applications are studied that will enable a group of people to synchronize their actions when following a predefined task sequence. It is assumed that the people involved only have computer workstations available to them for communication. Hence, the approach is to study how the computer can be used to help a group remain synchronized. A series of applications were designed and developed that can be used as vehicles for experimentation. An example of how this technique can be used for a remote coaching capability is explained in a report describing an experiment that simulated a Life Sciences experiment on-board Space Station Freedom, with a ground based principal investigator providing the expertise by coaching the on-orbit mission specialist. Author

N92-11919# Technische Univ., Eindhoven (Netherlands).
MODELLING PRODUCT STRUCTURES BY GENERIC BILLS-OF-MATERIAL Ph.D. Thesis
Eelco Anthonie vanVeen 11 Jan. 1991 214 p
(ETN-91-90146) Avail: NTIS HC/MF A10

The way in which products and their Bills Of Material (BOM) are represented in typical Material Resource Planning (MRP) based Production Control Information Systems (PICS) is described and the role they play for the major important business functions is characterized. The basics of coordinated goods flow control are described, different production control environments are typified and the requirements they place on product data and BOM are characterized. The problems of representing products and their BOM are characterized. The problems of representing products and their BOM in the case of large product variety are explored. A framework for specifying products and obtaining their BOM, and a number of recently developed concepts and systems which

support parts of this functional architecture are described. The Generic BOM, a new concept in BOM theory, is described. A case in which the new set of concepts and terms is applied to describe a dedicated solution developed by a company with an enormous product variety is described. ESA

N92-11042*# National Aeronautics and Space Administration, Washington, DC.
CONCEPTS, REQUIREMENTS, AND DESIGN APPROACHES FOR BUILDING SUCCESSFUL PLANNING AND SCHEDULING SYSTEMS
Rhoda Shaller Hornstein and John K. Willoughby (Information Sciences, Inc., Englewood, CO.) *In* NASA. Goddard Space Flight Center, Space Network Control Conference on Resource Allocation Concepts and Approaches Sep. 1991 p 69-84 (For primary document see N92-11039 02-17)
Avail: NTIS HC/MF A13 CSCL 05A

N92-11043*# National Aeronautics and Space Administration. Goddard Space Flight Center, Greenbelt, MD.
PROPOSED PLANNING AND SCHEDULING SERVICES FOR THE SNC IN THE CDOS ERA
Todd Welden *In its* Space Network Control Conference on Resource Allocation Concepts and Approaches Sep. 1991 p 85-91 (For primary document see N92-11039 02-17)
Avail: NTIS HC/MF A13 CSCL 05A

N92-11044*# National Aeronautics and Space Administration. Goddard Space Flight Center, Greenbelt, MD.
AN RF INTERFERENCE MITIGATION METHODOLOGY WITH POTENTIAL APPLICATIONS IN SCHEDULING
Yen F. Wong and James L. Rash *In its* Space Network Control Conference on Resource Allocation Concepts and Approaches Sep. 1991 p 93-106 (For primary document see N92-11039 02-17)
Avail: NTIS HC/MF A13 CSCL 05A

N92-11045*# TRW Systems Group, Redondo Beach, CA. Systems Development Div.
AUTOMATED CONFLICT RESOLUTION ISSUES
Jeffrey S. Wike *In* NASA. Goddard Space Flight Center, Space Network Control Conference on Resource Allocation Concepts and Approaches Sep. 1991 p 107-113 (For primary document see N92-11039 02-17)
Avail: NTIS HC/MF A13 CSCL 05A

N92-11055*# Space Industries, Inc., Webster, TX. Intelligent Systems.
INTELLIGENT PERTURBATION ALGORITHMS FOR SPACE SCHEDULING OPTIMIZATION
Clifford R. Kurtzman *In* NASA. Goddard Space Flight Center, Space Network Control Conference on Resource Allocation Concepts and Approaches Sep. 1991 p 193-205 (For primary document see N92-11039 02-17)
Avail: NTIS HC/MF A13 CSCL 05A

N92-11057*# Mitre Corp., McLean, VA.
RANGE SCHEDULING AID (RSA)
J. R. Logan and M. K. Pulvermacher *In* NASA. Goddard Space Flight Center, Space Network Control Conference on Resource Allocation Concepts and Approaches Sep. 1991 p 217-223 (For primary document see N92-11039 02-17)
Avail: NTIS HC/MF A13 CSCL 05A

N92-11058*# Ford Aerospace and Communications Corp., Seabrook, MD. Systems, Engineering, and Analysis Support.
SCHEDULING TECHNIQUES IN THE REQUEST ORIENTED SCHEDULING ENGINE (ROSE)
David R. Zoch *In* NASA. Goddard Space Flight Center, Space Network Control Conference on Resource Allocation Concepts and Approaches Sep. 1991 p 225-232 (For primary document see N92-11039 02-17)
Avail: NTIS HC/MF A13 CSCL 05A

N92-11059*# Martin Marietta Aerospace, Denver, CO. Information Systems Group.
MANAGING TEMPORAL RELATIONS IN THE MAESTRO SCHEDULING SYSTEM
Daniel L. Britt *In* NASA. Goddard Space Flight Center, Space Network Control Conference on Resource Allocation Concepts and Approaches Sep. 1991 p 233-240 Submitted for publication (For primary document see N92-11039 02-17)
Avail: NTIS HC/MF A13 CSCL 05A

N92-11061*# TRW, Inc., Redondo Beach, CA.
AUTOMATING THE CONFLICT RESOLUTION PROCESS
Jeffrey S. Wike *In* NASA. Goddard Space Flight Center, Space Network Control Conference on Resource Allocation Concepts and Approaches Sep. 1991 p 265-269 (For primary document see N92-11039 02-17)
Avail: NTIS HC/MF A13 CSCL 05A

N92-11064*# Space Industries, Inc., Webster, TX. Intelligent Systems.
INTELLIGENT PERTURBATION ALGORITHMS TO SPACE SCHEDULING OPTIMIZATION
Clifford R. Kurtzman *In* NASA. Goddard Space Flight Center, Space Network Control Conference on Resource Allocation Concepts and Approaches Sep. 1991 p 295-298 (For primary document see N92-11039 02-17)
Avail: NTIS HC/MF A13 CSCL 05A

82 DOCUMENTATION AND INFORMATION SCIENCE

Includes information management; information storage and retrieval technology; technical writing; graphic arts; and micrography.

For computer documentation see *61 Computer Programming and Software*.

N92-11920*# Wanderman (Ken) and Associates, Inc., Staten Island, NY.
A GENERALIZED STRATEGY FOR BUILDING RESIDENT DATABASE INTERFACES Final Report
Marsha Moroh and Ken Wanderman 12 May 1990 130 p (Contract NAS5-30304)
(NASA-CR-189246; NAS 1.26:189246) Avail: NTIS HC/MF A07 CSCL 05B

A strategy for building resident interfaces to host heterogeneous distributed data base management systems is developed. The strategy is used to construct several interfaces. A set of guidelines is developed for users to construct their own interfaces. Author

N92-11921*# National Aeronautics and Space Administration. Goddard Space Flight Center, Greenbelt, MD.
NSSDC DATA LISTING
Richard Horowitz Aug. 1991 125 p
(NASA-TM-105010; NAS 1.15:105010; NSSDC/WDC-A-R/S-91-19) Avail: NTIS HC/MF A06 CSCL 05B

The purpose here is to identify, in a highly summarized way, data available from the National Space Science Data Center (NSSDC). Most data are maintained as offline data sets gathered from individual instruments carried on spacecraft; these comprise the Satellite Data Listing. Descriptive names, time spans, data form, and quality of these data sets are identified in the listing, which is sorted alphabetically, first by spacecraft name and then by the principal investigator's or team leader's last name. Several data sets not associated with individual spaceflight instruments are identified in separate listings following the Satellite Data Listing. These include composite spacecraft data sets, ground based data, models, and computer routines. NSSDC also offers data via special services and systems in a number of areas, including the Astronomical Data Center, Coordinated Data Analysis Workshops,

NASA Climate Data System, Pilot Land Data System, and Crustal Dynamics Data Information System. Author

N92-11922 Rutgers - The State Univ., New Brunswick, NJ.
AN INVESTIGATION TO FIND APPROPRIATE MEASURES FOR EVALUATING INTERACTIVE INFORMATION RETRIEVAL Ph.D. Thesis
Louise T. Su 1991 307 p
Avail: Univ. Microfilms Order No. DA9125400

Several criteria and measures are proposed to evaluate interactive information retrieval (IR) performance. This study aims to identify appropriate measures for evaluating interactive IR performance, i.e., evaluative measures that can best reflect system's success in providing help for users' needs or problems. Twenty measures of IR performance were selected for study, representing four major evaluation criteria: relevance, utility, user satisfaction, and efficiency. Four nonperformance characteristics were also selected for subgroup analysis. User's judgment of system success in a realistic IR situation was used as the devised criterion measure with which all other 20 measures were to be correlated. A computer search was conducted by a searcher in the normal manner, for each individual problem, in the user's presence and with his/her participation. The end-users were each responsible for the cost of his/her own search. This study showed that value of search results as a whole is the best single measure of interactive IR performance among the 20 measures selected. It is strongly correlated with other significant correlates of success: user's satisfaction with completeness of search results, and user's satisfaction with precision of the search. Precision, one of the most important traditional measures of effectiveness, was found to be not significantly correlated with success. Users appeared to be more concerned with absolute recall then with precision of the search. Seventeen new success categories are suggested for further investigation. Dissert. Abstr.

N92-11923# Department of Energy, Washington, DC.
FEDIX: THE ON-LINE DATABASE RETRIEVAL SERVICE OF GOVERNMENT INFORMATION FOR COLLEGES, UNIVERSITIES, AND OTHER ORGANIZATIONS
1991 79 p
(DE91-018496; DOE/ER-0500) Avail: NTIS HC/MF A05

The FEDIX is an on-line information service that links the education community and the Federal government to facilitate research, education, and services. The system provides accurate and timely Federal agency information to colleges, universities, and other research organizations. There are no registration fees and no access charges for using FEDIX. The only cost involved is that of a phone call. Agencies participating in the FEDIX system include: Department of Energy (DOE), Federal Aviation Administration (FAA), National Aeronautics and Space Administration (NASA), Office of Naval Research (ONR), National Science Foundation (NSF), National Security Agency (NSA), Department of Commerce (DOC), Department of Education (DOEd), and Department of Housing and Urban Development (HUD). Additional government agencies are expected to join FEDIX in the near future. This guide is intended to help users access and utilize the FEDIX system. Because the system requires frequent updating, some menus and tables used as examples in this publication may not exactly match those displayed on the on-line system. DOE

N92-11924# Department of Energy, Washington, DC. RCRA/CERCLA Div.
INTEGRATED RISK INFORMATION SYSTEM
Jun. 1991 46 p
(DE91-018503; DOE/EH-0194) Avail: NTIS HC/MF A03

The Resource Conservation of Recovery Act of 1976 (RCRA) established a regulatory program for cradle-to-grave management of hazardous wastes; the Comprehensive Environmental Response, Compensation, and Liability Act of 1980 (CERCLA) established a federal program to assess and respond to unpermitted or uncontrolled releases of hazardous substances into the environment. The overall performance measure of these two regulatory programs is protection of human health and the environment. In order to assess the threats to human health posed by RCRA hazardous wastes and CERCLA hazardous substances, a quantitative measure of the adverse impact of hazardous constituents on persons exposed and potentially exposed is required. The quantitative assessment of threats to human health is called 'risk assessment' and this is an integral part of both the RCRA and CERCLA regulatory programs. To facilitate the quantification of risks under the RCRA, CERCLA, and other regulatory programs, the US Environmental Protection Agency (EPA) developed the Integrated Risk Information System (IRIS). Its purpose is to provide an authoritative source of risk information for chemicals of environmental and public health concern. The IRIS is an one-line database of risk summaries for over 370 chemicals. It provides information on the relationship between chemical exposure and estimated human health effects. This information is based on EPA reviews of available studies. The risk values provided in IRIS are reviewed and agreed upon by scientists throughout EPA. As such, these values represent an agency-wide scientific consensus. The IRIS was designed to provide information for performing EPA human health risk assessments. Such risk assessments are divided into four steps: (1) hazard identification, (2) dose-response assessment, (3) exposure assessment, and (4) risk characterization. the IRIS's risk values are used during the hazard identification and dose-response assessment steps. DOE

N92-11925# Naval Ocean Systems Center, San Diego, CA.
DATABASE MANAGEMENT SYSTEM INTERFACE STANDARD FOR NAVY NEXT GENERATION COMPUTING RESOURCES
D. L. Small, M. C. Butterbrodt, and R. M. Bergman Aug. 1991 16 p
(AD-A240432) Avail: NTIS HC/MF A03 CSCL 12/7

This paper is a snapshot of the Navy's use of database management system (DBMS) technology for Command, Control and Combat Systems. Our long-term goal is to contribute to the development of a standard DBMS interface (DBMSIF) to promote interoperability among Navy systems. This paper is an excerpt from the paper that was developed under Naval Ocean Systems Center (NOSC) tasking for the SPAWAR 3243, Next Generation Computer Resources (NGCR) Program. Navy systems have a requirement for managing a massive command, control, communications, and intelligence (C3I) system encompassing land, surface, subsurface, air, and space data elements. These systems ultimately control thousands of complex sensor, combat direction and weapon systems aboard hundreds of tactical units. Driving such systems are significant requirements for management of such objects, discriminating the real threats among them, and tracking them with realtime updates using an intelligent analysis of which objects are benign (friendly, neutral or decoys) and which are threats. The systems are necessarily distributed and require substantial data which must be consistent through time, often requiring the meeting of a hard realtime deadline schedule for data availability and accessibility. GRA

N92-11926# Carnegie-Mellon Univ., Pittsburgh, PA. Software Engineering Inst.
ISSUES IN REAL-TIME DATA MANAGEMENT Final Report
Marc H. Graham Jul. 1991 27 p
(Contract F19628-90-C-0003)
(AD-A240712; CMU/SEI-91-TR-17; ESD-91-TR-17) Avail: NTIS HC/MF A03 CSCL 12/7

This report explores issues related to the use of database management technology in support of real time system programming. It describes the potential benefits of database support for real time systems, and it describes the state of the art in database technologies relevant to real time. The report concludes that more research and development will be needed before the benefits of database management can be applied to real time system development. GRA

N92-11927# Centre d'Etudes et de Recherches, Toulouse (France). Dept. d'Etudes et de Recherches en Automatique.
MODELING OF FLEXIBLE POLYARTICULATE CHAINS: BIBLIOGRAPHIC SYNTHESIS Interim Report [MODELISATION DES CHAINES POLYARTICULEES FLEXIBLES: SYNTHESE BIBLIOGRAPHIQUE. RAPPORT INTERMEDIAIRE]
Jean-Pierre Chretien Oct. 1990 53 p In FRENCH
(CERT-DERA-1/7735; ETN-91-90081) Avail: NTIS HC/MF A04

The problem of dynamic modeling of flexible polyarticulate systems is addressed in an assimilation of related documents. Techniques of modeling reviewed cover the finite element method, modal approach, modeling by imaginery articulations, modeling by bond graph, modal impedance approach and the problem of premature linearization. Relevant conclusions are made. ESA

N92-11928# Technische Univ., Berlin (Germany, F.R.). Fachbereich Informatik.
OPEN DOCUMENT PROCESSING AND THE ISOTEXT SYSTEM Ph.D. Thesis
Carsten Bormann 1991 291 p
(ETN-91-90160) Copyright Avail: NTIS HC/MF A13

A common foundation for Open Document Processing (ODP) systems as well as for future standardization of this area is adressed. An overview of the current technological base for ODP, including the standards ODA (Open Document Architecture) and SGML (Standard Generalized Markup Language) and other related standards is presented. Results of the ISOTEXT project, a major document processing system implementation effort based on ODA and making use of SGML technology, which produced an ODA based interactive what you see is what you get editor/formatter for ODP are reported. The future of ODP, looking at both an important document interchange format controlled by a vendor and the further development of ODA and of the SGML related standards, is discussed. ESA

83 ECONOMICS AND COST ANALYSIS

Includes cost effectiveness studies.

No abstracts in this category.

84 LAW, POLITICAL SCIENCE AND SPACE POLICY

Includes NASA appropriation hearings; aviation law; space law and policy; international law; international cooperation; and patent policy.

No abstracts in this category.

85 URBAN TECHNOLOGY AND TRANSPORTATION

Includes applications of space technology to urban problems; technology transfer; technology assessment; and surface and mass transportation.

For related information see also *03 Air Transportation and Safety, 16 Space Transportation,* and *44 Energy Production and Conversion.*

No abstracts in this category.

88 SPACE SCIENCES (GENERAL)

N92-11929*# National Aeronautics and Space Administration, Washington, DC.
A BIBLIOGRAPHY OF PLANETARY GEOLOGY AND GEOPHYSICS PRINCIPAL INVESTIGATORS AND THEIR ASSOCIATES, 1990-1991
Oct. 1991 49 p
(NASA-TM-4299; NAS 1.15:4299) Avail: NTIS HC/MF A03 CSCL 03A

A compilation of selected bibliographic data specifically relating to recent publications submitted by principal investigators and their associates, supported through the NASA Office of Space Science and Applications, Solar System Exploration Division, Planetary Geology and Geophysics Program is presented. Author

N92-11930*# National Aeronautics and Space Administration. Lyndon B. Johnson Space Center, Houston, TX.
THE MICROGRAVITY ENVIRONMENT OF THE SPACE SHUTTLE COLUMBIA MIDDECK DURING STS-32
Bonnie J. Dunbar, Donald A. Thomas, and Jeff N. Schoess (Honeywell, Inc., Bloomington, MN.) Washington Nov. 1991 59 p
(NASA-TP-3140; S-640; NAS 1.60:3140) Avail: NTIS HC/MF A04 CSCL 22B

Four hours of three-axis microgravity accelerometer data were successfully measured at the MA9F locker location in the Orbiter middeck of Columbia as part of the Microgravity Disturbances Experiment (MDE) on STS-32. These data were measured using the Honeywell In-Space Accelerometer, a small three-axis accelerometer that was hard-mounted onto the Fluid Experiment Apparatus to record the microgravity environment at the exact location of the MDE. Data were recorded during specific mission events such as Orbiter quiescent periods, crew exercise on the treadmill, and numerous Orbiter engine burns. Orbiter background levels were measured to be in the 3 x 10(exp -5) to 2 x 10(exp -4) G range, treadmill operations in the 6 x 10(exp -4) to 5 x 10(exp -3) G range, and Orbiter engine burns from 4 x 10(exp -3) to in excess of 1 x 10(exp -2) G. These data represent some of the first microgravity accelerometer data ever recorded in the middeck area of the Orbiter. Author

N92-11931*# National Aeronautics and Space Administration. Lyndon B. Johnson Space Center, Houston, TX.
THE MICROGRAVITY ENVIRONMENT OF THE SPACE SHUTTLE COLUMBIA PAYLOAD BAY DURING STS-32
Bonnie J. Dunbar, Robert L. Giesecke, and Donald A. Thomas Washington Nov. 1991 51 p
(NASA-TP-3141; S-641; NAS 1.60:3141) Avail: NTIS HC/MF A04 CSCL 22B

Over 11 hours of three-axis microgravity accelerometer data were successfully measured in the payload bay of Space Shuttle Columbia as part of the Microgravity Disturbances Experiment on STS-32. These data were measured using the High Resolution Accelerometer Package and the Aerodynamic Coefficient Identification Package which were mounted on the Orbiter keel in the aft payload bay. Data were recorded during specific mission events such as Orbiter quiescent periods, crew exercise on the treadmill, and numerous Orbiter engine burns. Orbiter background levels were measured in the 10(exp -5) G range, treadmill operations in the 10(exp -3) G range, and the Orbiter engine burns in the 10(exp -2) G range. Induced acceleration levels resulting from the SYNCOM satellite deploy were in the 10 (exp -2) G range, and operations during the pre-entry Flight Control System checkout were in the 10(exp -2) to 10(exp -1) G range. Author

89 ASTRONOMY

Includes radio, gamma-ray, and infrared astronomy, and astrometry.

N92-11932 Council for National Academic Awards (England).
INFRARED TO MILLIMETRE OBSERVATIONS OF ACTIVE GALAXIES Ph.D. Thesis
David Handel Hughes 1990 176 p
Avail: Univ. Microfilms Order No. BRDX92803

Measurements of the continuum emission at infrared (IR) to millimeter wavelengths from the nuclear regions of a number of active galaxies are presented. Many observations have been made for the first time in the submillimeter regime. The observing methods at these wavelengths are described. The central 1.5 kpc of the starburst galaxy M82 was mapped at 800 and 1100 microns. The far infrared (FIR) to millimeter continuum is due to thermal reradiation from dust grains at a temperature of 47 K, and the spatial distribution of the thermal emission shows a halo of grains extending to 500 pc from the plane of the galaxy centered on the 2.2 micron nucleus. The similar morphologies of the millimeter, radio, and X-ray emissions suggests that inverse Compton scattering of FIR photons dominates the observed X-ray luminosity of M82. An improved method of background subtraction from the IRAS database has been developed and applied to a 2 deg square field of the Leo Triplet, an interacting system of galaxies. The success of the technique is demonstrated by the detection of a low surface brightness FIR counterpart to the optical and HI tidal plume associated with NGC3628. The most sensitive submillimeter observations to date of radio quiet quasars are described. Although no detections were obtained, the upper limits were sufficient to show that for one quasar, PG0710 + 457, nonthermal emission is unlikely to be the source of the FIR luminosity. Submillimeter detection of a less luminous active emission line galaxy, Mkn1183, was achieved at a level of 69 mJy at 800 microns. In this instance the FIR luminosity was attributable to thermal emission from dust. Dissert. Abstr.

N92-11933# Naval Observatory, Washington, DC.
PROCEEDINGS OF THE 127TH COLLOQUIUM OF THE INTERNATIONAL ASTRONOMICAL UNION REFERENCE SYSTEMS
James A. Hughes, Clayton A. Smith, and George H. Kaplan 1991 433 p Colloquium held in Virginia Beach, VA, 14-20 Oct. 1990
(AD-A240207) Avail: NTIS HC/MF A19 CSCL 03/1

Both invited oral and poster papers were presented on topics ranging from theoretical relativistic considerations to new observational programs and results. Partial contents include a report of the Subgroup on Time; preliminary report of the work of the Subgroup on Coordinate Frames and Origins; activity report of the IAU Working Group on reference system: subgroup on astronomical constants; relativistic hierarchy of reference systems and time scales; relativistic celestial mechanics and reference frames; current status of the astrometric capabilities of the Hubble Space Telescope fine guidance sensors; necessary procedures to reach an agreeable reference frame: counterproposal to the circular letter no. 4 of Kovalevsky; stability of the extragalactic reference frame realized by VLBI; The ZMOA-1990 nutation series; and long-period perturbations in terrestrial reference frames. GRA

N92-11054*# Space Telescope Science Inst., Baltimore, MD. Advance Planning Systems Branch.
SPIKE: AI SCHEDULING TECHNIQUES FOR HUBBLE SPACE TELESCOPE
Mark D. Johnston *In* NASA. Goddard Space Flight Center, Space Network Control Conference on Resource Allocation Concepts and Approaches Sep. 1991 p 183-192 (For primary document see N92-11039 02-17)
Avail: NTIS HC/MF A13 CSCL 03A

90 ASTROPHYSICS

Includes cosmology; celestial mechanics; space plasmas; and interstellar and interplanetary gases and dust.
For related information see also *75 Plasma Physics*.

N92-11934*# Washington Univ., Seattle.
REPORT ON CARBON AND NITROGEN ABUNDANCE STUDIES Research Report, Oct. 1990 - Sep. 1991
Erika Boehm-Vitense Sep. 1991 70 p
(Grant NAG5-1255)
(NASA-CR-188803; NAS 1.26:188803) Avail: NTIS HC/MF A04 CSCL 03B

The aim of the proposal was to determine the nitrogen to carbon abundance ratios from transition layer lines in stars with different T(sub eff) and luminosities. The equations which give the surface emission line fluxes and the measured ratio of the NV to CIV emission line fluxes are presented and explained. The abundance results are compared with those of photospheric abundance studies for stars in common with the photospheric investigations. The results show that the analyses are at least as accurate as the photospheric determinations. These studies can be extended to F and early G stars for which photospheric abundance determinations for giants are hard to do because molecular bands become too weak. The abundance determination in the context of stellar evolution is addressed. The N/C abundance ratio increases steeply at the point of evolution for which the convection zone reaches deepest. Looking at the evolution of the rotation velocities v sin i, a steep decrease in v sin i is related to the increasing depth of the convection zone. It is concluded that the decrease in v sin i for T(sub eff) less than or approximately = 5800 K is most probably due to the rearrangement of the angular momentum in the stars due to deep convective mixing. It appears that the convection zone is rotating with nearly depth independent angular momentum. Other research results and ongoing projects are discussed. Author

N92-11935# State Univ. of New York, Stony Brook. Dept. of Earth and Space Sciences.
EFFECTS OF THE EQUATION OF STATE IN NEUTRON STARS AND IN STELLAR COLLAPSE
J. M. Lattimer and A. Burrows (Arizona Univ., Tucson.) 1990 13 p Presented at the ESO/EIPC Workshop: SN1987A and Other Supernova, Isola d'Elba, Italy, 17-22 Sep. 1990
(Contract DE-FG02-87ER-40317)
(DE91-014534; DOE/ER-40317/7; CONF-9009320-2) Avail: NTIS HC/MF A03

Some effects of the equation of state of dense matter on the structure of neutron stars and on gravitational collapse supernovae are discussed. We discuss which nuclear parameters are most important for the equation of state, and constraints on them that have been obtained from lab experiments. We then discuss how neutron stars and supernovae depend upon and, therefore, could constrain, these parameters. Some structural constraints on neutron stars are available from observations, but these cannot, at present, set limits on important nuclear parameters such as the bulk incompressibility parameter or the bulk symmetry energy. However, the mechanism of Type 2, or gravitational collapse, supernovae depends crucially on these nuclear parameters and upon other aspects of the equation of the state. We examine the equation of state in the important regime just below nuclear density in which nuclei become deformed and undergo possible phase transitions to other shapes such as an inside-out bubble phase, and a phase transition to uniform nuclear matter. The pressure and adiabatic index in this density regime is sensitive chiefly to the incompressibility parameter of bulk nuclear matter. Author

N92-11936*# Research Inst. for Advanced Computer Science, Moffett Field, CA.
INFORMATION TECHNOLOGIES FOR ASTROPHYSICS CIRCA 2001
Peter J. Denning 23 May 1990 26 p Presented at a NASA Workshop on Astrophysical Information Systems, Moffett Field, CA, 23-25 May 1990

(Contract NCC2-387)
(NASA-CR-188868; NAS 1.26:188868; RIACS-TR-90-33) Avail: NTIS HC/MF A03 CSCL 03B

It is easy to extrapolate current trends to see where technologies relating to information systems in astrophysics and other disciplines will be by the end of the decade. These technologies include mineaturization, multiprocessing, software technology, networking, databases, graphics, pattern computation, and interdisciplinary studies. It is easy to see what limits our current paradigms place on our thinking about technologies that will allow us to understand the laws governing very large systems about which we have large datasets. Three limiting paradigms are saving all the bits collected by instruments or generated by supercomputers; obtaining technology for information compression, storage and retrieval off the shelf; and the linear mode of innovation. We must extend these paradigms to meet our goals for information technology at the end of the decade. Author

N92-11937 Princeton Univ., NJ.
KINEMATICS AND DYNAMICS OF BARRED GALAXIES Ph.D. Thesis
Kevin Long 1991 137 p
Avail: Univ. Microfilms Order No. DA9124901

Methods of interpreting observations of velocity fields are investigated. If streamlines in a bar have the same symmetry as the bar, the velocity field can be recovered. This inversion is singular when the line of nodes of projection corresponds to one of the axes of symmetry of the bar. Near these viewing geometries, the velocity field cannot be inverted; it is important to select target galaxies far from these singular points. Fitting to circular motion alone can lead to large systematic errors (approximately 50 percent or more) in the rotation curve. Formulae for estimating forces from a noncircular velocity field are derived. These methods were tested on synthesized observations of a N-body bar. Williams' Fabry-Perot observations of the projected velocity field for NGC 1832 were analyzed. The bar is near a singular point of projection, yet there are large asymmetries in the projected field. The velocity field can more reasonably be explained by a combination of barlike streaming motion (approximately v(sub c)/2) and a slight (approximately 10-20 deg) warp. A method for computing analytical approximations to the potentials of nearly spherical galaxies is presented. The accuracy and the effect on orbital structure were tested. For the models tested, the approximations were accurate for axis ratios less than approx.= 1.4, and surfaces of section were not significantly altered. A computer program for automatic computation of these approximate formulae is presented. A self consistent field method for the calculation of equilibrium models of rotating bars is presented. The closed orbits in a potential are integrated and each response density is calculated. A new density model is computed. This model is then used to generate a new potential, and the process is iterated until convergence.
Dissert. Abstr.

N92-11938 Florida Univ., Gainesville.
A THEORY OF THE EARTH'S PRECESSION RELATIVE TO THE INVARIABLE PLANE OF THE SOLAR SYSTEM Ph.D. Thesis
William Mann Owen, Jr. 1990 276 p
Avail: Univ. Microfilms Order No. DA9121640

The usual formulas for the application of general precession use three successive small rotations by which the equatorial coordinate system at epoch is aligned with the equatorial system of date. An alternate method is presented in which the rotation angles are intimately tied to the invariable plane of the Solar System. Constructing this theory divides into three parts. First, the newest planetary ephemeris from the JPL allows one to infer the orientation of the invariable plane with a standard error. Second, the coefficients in the approximation polynomials for the new angles are found in terms of their counterparts in the currently accepted IAU theory; this short term theory is valid for a few centuries. Third, the motion of the Earth's north pole is integrated numerically over a million year time span; values for both the standard precession angles and the new ones are inferred at discrete times from the integration, and Chebyshev polynomials are fit to these values (long term theory). Both long and short theories are simpler to use than the current ones. A comparison of both theories reveals two possible improvements to the IAU system of constants. These are detailed. Dissert. Abstr.

N92-11939# Lawrence Livermore National Lab., CA.
OPAL OPACITIES FOR ASTROPHYSICAL APPLICATIONS
C. A. Iglesias and F. J. Rogers May 1991 7 p Presented at the International Workshop on Radiative Properties of Hot Dense Matter, Sarasota, FL, 22-26 Oct. 1990
(Contract W-7405-eng-48)
(DE91-016922; UCRL-JC-107495; CONF-9010298-12) Avail: NTIS HC/MF A02

The OPAL opacity code developed at LLNL has been applied to astrophysical problems. The computed Rosseland mean opacities show significant differences when compared to the Los Alamos results. These differences have been traced to both atomic and equation of state improvements in the OPAL code. Furthermore, preliminary work suggest that the OPAL calculations considerably improve the agreement between observations and stellar models. DOE

N92-11940# Lawrence Livermore National Lab., CA.
MODELING UV AND X RAY OXYGEN EMISSION IN ASTROPHYSICAL PLASMAS
P. Vitello, M. Dunning, C. Cerjan, and J. Nash 2 May 1991 6 p Presented at the 20th International Conference on Phenomena in Ionized Gases, Barga, Italy, 8-12 Jul. 1991
(Contract W-7405-eng-48)
(DE91-016927; UCRL-JC-107117; CONF-910711-7) Avail: NTIS HC/MF A02

The advent of high resolution, high sensitivity X ray spectroscopy from Astro-D and AXAF missions will provide a wealth of highly detailed spectral information. The successful analysis of this data will depend on the use of nonequilibrium ionization descriptions of the radiating plasma, using accurate and complete atomic physics data sets. We present here simulated UV and X ray Oxygen spectra calculated from a time dependent, nonequilibrium hydrodynamic model using extremely detailed atomic physics data bases. Emission from static plasmas and radiative shocks are considered. We discuss the sensitivity of the calculated spectra to modeling assumptions and to approximations made in generating the atomic rates. DOE

N92-11941*# Fermi National Accelerator Lab., Batavia, IL.
PERTURBATIONS FROM STRINGS DON'T LOOK LIKE STRINGS!
Andreas Albrecht and Albert Stebbins Aug. 1991 3 p Sponsored in part by DOE
(Grant NAGw-1340)
(NASA-CR-189012; NAS 1.26:189012; FERMILAB-Conf-91/214-A) Avail: NTIS HC/MF A01 CSCL 03B

A systematic analysis is challenging popular ideas about perturbation from cosmic strings. One way in which the picture has changed is reviewed. It is concluded that, while the scaling properties of cosmic strings figure significantly in the analysis, care must be taken when thinking in terms of single time snapshots. The process of seeding density perturbations is not fundamentally localized in time, and this fact can wash out many of the details which appear in a single snapshot. Author

N92-11942*# Fermi National Accelerator Lab., Batavia, IL.
SUPERFLUID-LIKE TURBULENCE IN COSMOLOGY
Ben-Ami Gradwohl Sep. 1991 7 p Presented at the Sixth Marcel Grossmann Meeting on General Relativity, Kyoto, Japan, 24-29 Jun. 1991 Sponsored in part by DOE
(Grant NAGw-1340)
(NASA-CR-189011; NAS 1.26:189011; FERMILAB-Conf-91/239-A) Avail: NTIS HC/MF A02 CSCL 03B

A network of vortices in a superfluid system exhibits turbulent behavior. It is argued that the universe may have experienced such a phase of superfluid-like turbulence due to the existence of

a coherent state with non-topological charge and a network of global strings. The unique feature of a distribution of turbulent domains is that it can yield non-gravitationally induced large-scale coherent velocities. It may be difficult, however, to relate these velocities to the observed large-scale bulk motion. Author

N92-11943*# Fermi National Accelerator Lab., Batavia, IL.
COSMOLOGICAL CONSTRAINTS ON PSEUDO-NAMBU-GOLDSTONE BOSONS
Joshua A. Frieman and Andrew H. Jaffe (Chicago Univ., IL.) Sep. 1991 27 p Sponsored in part by DOE
(Grant NAGw-1340)
(NASA-CR-189010; NAS 1.26:189010; FERMILAB-Pub-91/240-A)
Avail: NTIS HC/MF A03 CSCL 03B

Particle physics models with pseudo-Nambu-Goldstone bosons (PNGBs) are characterized by two mass scales: a global spontaneous symmetry breaking scale, f, and a soft (explicit) symmetry breaking scale, Lambda. General model insensitive constraints were studied on this 2-D parameter space arising from the cosmological and astrophysical effects of PNGBs. In particular, constraints were studied arising from vacuum misalignment and thermal production of PNGBs, topological defects, and the cosmological effects of PNGB decay products, as well as astrophysical constraints from stellar PNGB emission. Bounds on the Peccei-Quinn axion scale, 10(exp 10) GeV approx. = or less than f sub pq approx. = or less than 10(exp 10) to 10(exp 12) GeV, emerge as a special case, where the soft breaking scale is fixed at Lambda sub QCD approx. = 100 MeV. Author

N92-11944*# Fermi National Accelerator Lab., Batavia, IL.
RE-IONIZATION AND DECAYING DARK MATTER
Scott Dodelson and Jay M. Jubas (Massachusetts Inst. of Tech., Cambridge.) Sep. 1991 37 p Sponsored in part by DOE, NSF and the Sloan Foundation
(Contract NAGw-1340; DE-FG02-84ER-40158)
(NASA-CR-189009; NAS 1.26:189009; FERMILAB-Pub-91/260-A)
Avail: NTIS HC/MF A03 CSCL 03B

Gunn-Peterson tests suggest that the Universe was reionized after the standard recombination epoch. A systematic treatment is presented of the ionization process by deriving the Boltzmann equations appropriate to this regime. A compact solution for the photon spectrum is found in terms of the ionization ratio. These equations are then solved numerically for the Decaying Dark Matter scenario, wherein neutrinos with mass of order 30 eV radiatively decay producing photons which ionize the intergalactic medium. It was found that the neutrino mass and lifetime are severely constrained by Gunn-Peterson tests, observations of the diffuse photon spectrum in the ultraviolet regime, and the Hubble parameter. Author

N92-11945*# Fermi National Accelerator Lab., Batavia, IL.
CONVERTING NEUTRON STARS INTO STRANGE STARS
A. V. Olinto (Chicago Univ., IL.) Jul. 1991 11 p Presented at Strange Quark Matter in Physics and Astrophysics, Aarhus, Denmark, 1991
(Contract NAGw-1340; DE-FG02-90ER-40606; NSF AST-22595)
(NASA-CR-189008; NAS 1.26:189008; FERMILAB-Conf-91/202-A)
Avail: NTIS HC/MF A03 CSCL 03B

If strange matter is formed in the interior of a neutron star, it will convert the entire neutron star into a strange star. The proposed mechanisms are reviewed for strange matter seeding and the possible strange matter contamination of neutron star progenitors. The conversion process that follows seeding and the recent calculations of the conversion timescale are discussed. Author

N92-11946*# Fermi National Accelerator Lab., Batavia, IL.
COSMOLOGICAL STRUCTURE FORMATION
David N. Schramm (Chicago Univ., IL.) Sep. 1991 18 p Presented at the Second International Symposium on Particles, Strings, and Cosmology, Boston, MA, Mar. 1991
(Contract NAGw-1321; NAGw-1340; DE-FG02-91ER-40606; NSF AST-88-22595)
(NASA-CR-189007; NAS 1.26:189007; FERMILAB-Conf-91/266-A)
Avail: NTIS HC/MF A03 CSCL 03B

A summary of the current forefront problem of physical cosmology, the formation of structures (galaxies, clusters, great walls, etc.) in the universe is presented. Solutions require two key ingredients: (1) matter; and (2) seeds. Regarding the matter, it now seems clear that both baryonic and non-baryonic matter are required. Whether the non-baryonic matter is hot or cold depends on the choice of seeds. Regarding the seeds, both density fluctuations and topological defects are discussed. The combination of isotropy of the microwave background and the recent observations indicating more power on large scales have severly constrained, if not eliminated, Gaussian fluctuations with equal power on all scales, regardless of the eventual resolution of both the matter and seed questions. It is important to note that all current structure formation ideas require new physics beyond SU(3) x SU(2) x U(1). Author

N92-11947*# Fermi National Accelerator Lab., Batavia, IL.
NON SCALE-INVARIANT DENSITY PERTURBATIONS FROM CHAOTIC EXTENDED INFLATION
Silvia Mollerach and Sabino Matarrese (Padua Univ., Italy) Aug. 1991 28 p Sponsored in part by DOE
(Grant NAGw-1340)
(NASA-CR-189004; NAS 1.26:189004; FERMILAB-Pub-91/203-A)
Avail: NTIS HC/MF A03 CSCL 03B

Chaotic inflation is analyzed in the frame of scalar-tensor theories of gravity. Fluctuations in the energy density arise from quantum fluctuations of the Brans-Dicke field and of the inflation field. The spectrum of perturbations is studied for a class of models: it is non scale-invarient and, for certain values of the parameters, it has a peak. If the peak appears at astrophysically interesting scales, it may help to reconcile the Cold Dark Matter scenario for structure formation with large scale observations. Author

N92-11948# Tri-Univ. Meson Facility, Vancouver (British Columbia).
ON THE EVOLUTION OF A SUPERCONDUCTING COSMIC STRING NETWORK
M. N. Butler, R. A. Malaney, and M. B. Mijic (British Columbia Univ., Vancouver.) Feb. 1989 20 p
(DE91-630995; TRI-PP-89-7) Avail: NTIS HC/MF A03

Until now, it has been assumed that the evolution of a cosmic string network is independent of whether or not the strings are superconducting. We show here how the evolution of a superconducting cosmic string (SCS) network may in fact be dramatically effected by the electromagnetic interactions of the SCS's. Specifically, we find that a scaling solution may be possible for smaller loop self-intersection probabilities than allowed for normal strings, resulting in a modification of the loop number density. In fact, we find that the number density of loops can be enhanced by an order of magnitude. The consequences of this for primordial nucleosynthesis are discussed. DOE

91 LUNAR AND PLANETARY EXPLORATION

Includes planetology; and manned and unmanned flights.

For spacecraft design or space stations see *18 Spacecraft Design, Testing and Performance.*

N92-11949 Arizona Univ., Tucson.
DIFFUSION IN THE IO PLASMA TORUS AND ITS RELATION TO THE TORUS SPATIAL STRUCTURE Ph.D. Thesis
Eric Wesley Davis 1991 137 p
Avail: Univ. Microfilms Order No. DA9123473

Plasma diffusion processes relevant to the physical nature of the Io plasma torus at Jupiter were studied. Centrifugally driven flux tube interchange instability, the only published theory of Io torus plasma diffusion, was examined and found to be an invalid mechanism in the plasma torus. The collisional nature of the hot torus plasma is observed through its extreme ultraviolet (EUV)

emissions and is characterized in the long mean free path regime where classical transport theory breaks down. Further, the torus plasma parameters fall in the range of values satisfying the criteria for the use of collisional transport theory to derive a collisional diffusion coefficient. The Chapman Enskog method of calculating the plasma diffusion coefficient from a solution of the Boltzmann equation is used. Simplifying approximations of a fully ionized plasma dominated by Coulomb elastic charged particle collisions are made to derive an ad hoc nonclassical diffusion coefficient which results in slow differential diffusion rates for the various sulfur and oxygen ions in the plasma torus. The radial spatial structure and energetics of the plasma torus are modeled by employing the collisional diffusion coefficient in a computer model calculation of collisional ionization diffusive equilibrium and energy branching. The computer model uses the known significant plasma reactions involving the torus sulfur and oxygen species, utilizing the most recently available atomic parameters. Neutral Cloud Theory fails to adequately power the copious amounts of UV radiation emitted by the Io plasma torus. The radial plasma model was used to investigate this 'energy crisis'. The application of the plasma model to a proposed heterogeneous source of energetic electrons and a proposal of inward diffusing energetic outer magnetospheric O2 and S2 ions as ad hoc heat inputs to the plasma torus electrons in order to maintain a steady state energy balance, are investigated. Dissert. Abstr.

N92-11950 Arizona Univ., Tucson.
LABORATORY MEASUREMENTS OF THE SINGLE-SCATTERING PROPERTIES OF AMMONIA ICE CRYSTALS Ph.D. Thesis
Shelly Kay Pope 1991 130 p
Avail: Univ. Microfilms Order No. DA9123146

Scattering measurements and photographs are presented of ammonia ice crystals grown at temperatures from 130 to 180 K. The prime candidate for the material making up the visible clouds of Jupiter and Saturn is ammonia ice. Spacecraft observations of these planets have constrained the single scattering properties of the cloud particles. To further study the nature of these particles, ammonia ice crystals were grown under conditions simulating the atmosphere of Jupiter and Saturn. The experimental apparatus used to make these measurements include a glass walled cylindrical chamber which permits measurement of the scattered light over a wide range of scattering angles and a temperature control system which uses a liquid nitrogen reservoir combined with heaters. A variety of crystal shapes and phase functions were seen. A representative selection of scattering measurements and photographs are presented. The data can be used to rule out some models for Jupiter's and Saturn's atmospheres and to guide future modeling efforts. For Jupiter, models with a cloud of ammonia crystals of size parameter equal to about 5 (in the red) are suggested. Dissert. Abstr.

N92-11951*# Sverdrup Technology, Inc., Brook Park, OH.
LUNAR DUST TRANSPORT AND POTENTIAL INTERACTIONS WITH POWER SYSTEM COMPONENTS Final Report
Cynthia M. Katzan and Jonathan L. Edwards (Marshall Univ., Huntington, WV.) Washington NASA Nov. 1991 42 p Sponsored in part by Case Western Reserve Univ.
(Contract NAS3-25266)
(NASA-CR-4404; E-6145; NAS 1.26:4404) Avail: NTIS HC/MF A03 CSCL 03B

The lunar surface is covered by a thick blanket of fine dust. This dust may be readily suspended from the surface and transported by a variety of mechanisms. As a consequence, lunar dust can accumulate on sensitive power components, such as photovoltaic arrays and radiator surfaces, reducing their performance. In addition to natural mechanisms, human activities on the Moon will disturb significant amounts of lunar dust. Of all the mechanisms identified, the most serious is rocket launch and landing. The return of components from the Surveyor 3 provided a rare opportunity to observe the effects of the nearby landing of the Apollo 12 Lunar Module. The evidence proved that significant dust accumulation occurred on the Surveyor at a distance of 155 m. From available information on particle suspension and transport mechanisms, a series of models was developed to predict dust accumulation as a function of distance from the lunar module. The accumulation distribution was extrapolated to a future Lunar Lander scenario. These models indicate that accumulation is expected to be substantial even as far as 2 km from the landing site. Estimates of the performance penalties associated with lunar dust coverage and photovoltaic arrays are presented. Because of the lunar dust adhesive and cohesive properties, the most practical dust defensive strategy appears to be the protection of sensitive components from the arrival of lunar dust by location, orientation, or barriers. Author

92 SOLAR PHYSICS

Includes solar activity, solar flares, solar radiation and sunspots.

For related information see *93 Space Radiation.*

N92-11952 Michigan Univ., Ann Arbor.
ELECTRON DISTRIBUTIONS AND SOLAR WIND INTERACTION WITH NONMAGNETIC PLANETS Ph.D. Thesis
Lu Gan 1991 255 p
Avail: Univ. Microfilms Order No. DA9124009

A two stream transport model for suprathermal electrons and a time dependent energy equation for themal electrons are used to find the electron distributions at the solar wind planetary atmosphere boundary regions of comet Halley, Venus, and Titan. The model equations of the inner coma of comet Halley have demonstrated the existence of a sharp transition boundary, called the thermal electron collisionopause, near a cometocentric distance of about 1.5 x 10(exp 4) km. Inside this boundary, a cold (T less than 10(exp 4) K) thermal electron component exists along with suprathermal electrons of solar wind and photoelectron origin. Outside, there is no cold thermal electron component, and the electrons are isothermal along magnetic field lines. The model of Venus' dayside upper ionosphere and the mantle region has give suprathermal electron distributions as functions of altitude, solar zenith angle, and the solar wind boundary conditions. The calculated electron temperatures agree very well with Pioneer Venus Orbiter (PVO) measurements in the mantle region, as well as in the magnetized ionosphere, suggesting that horizontal energy transport is an adequate mechanism for the energy deposition in this case. The model of the interaction region between Saturn's magnetosphere and Titan's ionosphere leads to the conclusion that air-glow emission due to photoelectron impact is a much more important process than that produced by magnetospheric electron interactions. The photoelectrons also make a much larger contribution to the ion productions than the magnetospheric electrons. Dissert. Abstr.

N92-11953# Ceskoslovenska Akademie Ved, Prague. Astronomical Inst.
SPECTRAL OBSERVATIONS OF SOLAR RADIO BURSTS IN THE RANGE OF 2.0-4.5 GHz Report, Apr. - Dec. 1989
A. Tlamicha 1990 131 p Original contains color illustrations
(CAS-Publ-76) Avail: NTIS HC/MF A07

Solar radio spectra in the range of 2.0-4.5 GHz observed by using a digital radio spectrometer at the Astronomical Observatory Ondrejov are presented. A brief description of the observational equipment is given. Solar radio spectra observed during the period 10 Apr. to 29 Dec. 1989 are presented, including the first flares 22/MAX 1991 Campaign No. 1. Author

N92-11954# Ceskoslovenska Akademie Ved, Prague. Astonomical Inst.
SPECTRAL OBSERVATIONS OF SOLAR RADIO BURSTS AT 2.0-4.5 GHz Report, Jan. - Dec. 1990
A. Tlamicha, Z. Ambrozova, and T. Sigmund 1991 100 p
(CAS-Publ-77) Avail: NTIS HC/MF A05

Spectral observations of solar radio burst at 2.0-4.5 GHz taken at the Astronomical Observatory Ondrejov between Jan. and Dec.

1990 are presented. Also, tables and computer outputs are given in equidensities and in time intensity profiles of the bursts. Author

N92-11955*# Rochester Univ., NY. Dept. of Mechanical Engineering.
SUNSPOT DYNAMICS Final Technical Report, 1 Oct. 1978 - 30 Sep. 1990
John H. Thomas 30 Sep. 1990 14 p
(Grants NsG-7562; NAGw-2123)
(NASA-CR-188978; NAS 1.26:188978) Avail: NTIS HC/MF A03 CSCL 03B

The goal of this research was the understanding of the various oscillatory, transient, and quasi-steady motions in sunspots and the basic structure of a sunspot. The research involved both theoretical modeling (based on thermohydrodynamic theory) and observations of dynamical phenomena in sunspots. The principal topics of the research were sunspot seismology (the interaction of solar p-modes with a sunspot as a probe of the subsurface structure of a sunspot); three minute umbral oscillations and their relation to the structure of the umbral atmosphere; siphon flows in isolated magnetic flux tubes and their relation to the photospheric Evershed flow and to intense magnetic elements outside of sunspots; and more general theoretical work on magneto-atmospheric waves. Here, a summary of results is given. Author

N92-11956*# Fermi National Accelerator Lab., Batavia, IL.
E SUB 6 LEPTOQUARKS AND THE SOLAR NEUTRINO PROBLEM
Esteban Roulet Aug. 1991 7 p Sponsored in part by DOE (Grant NAGw-1340)
(NASA-CR-189005; NAS 1.26:189005; FERMILAB-Pub-91/206-A) Avail: NTIS HC/MF A02 CSCL 03B

The possibility that non-conventional neutrino oscillations take place in the superstring inspired E sub 6 models is considered. In this context, the influence of leptoquark mediated interactions of the neutrinos with nucleons in the resonant flavor conversion is discussed. It is shown that this effect can be significant for v sub e - v sub tau oscillations if these neutrinos have masses required in the ordinary Mikheyev-Smirnov-Wolfenstein (MSW) effect, and may lead to a solution of the solar neutrino problem even in the absence of vacuum mixings. On the other hand, this model cannot lead to a resonant behavior in the sun if the neutrinos are massless. Author

N92-11957# Yale Univ., New Haven, CT. Center for Solar and Space Research.
DEVELOPMENT OF A SYSTEM FOR ACCURATE FORECASTING OF SOLAR ACTIVITY Final Report, 15 Oct. 1987 - 14 Oct. 1990
Sabatino Sofia 11 Jul. 1991 14 p
(Grant AF-AFOSR-0054-88; AF Proj. 2311)
(AD-A240359; AFOSR-91-0728TR) Avail: NTIS HC/MF A03 CSCL 03/2

This is a continuing effort which has empirical, theoretical and experimental components related to the physics of solar activity. The empirical forecasting scheme, developed under this grant, has been very successful for solar cycle 22. Important elements of a highly sophisticated theoretical scheme to model the solar activity cycle have been produced and tested. The Solar Disk Sextant experiment is progressing well. In addition to the Principal Investigator, this work involves five students and two research associates. GRA

N92-11958# Air Force Environmental Technical Applications Center, Scott AFB, IL.
CONDITIONAL CLIMATOLOGY OF AP: THE RELATIONSHIP BETWEEN VARIOUS SOLAR EVENTS (SURGES, PROMINENCES, FILAMENTS, RADIO BURSTS, X RAY EPISODES) AND GEOMAGNETIC STORMS
Donald L. Wilson Aug. 1991 56 p
(AD-A240457; USAFETAC/TN-91/006) Avail: NTIS HC/MF A04 CSCL 03/2

This report is a continuation of USAFETAC/TN-90/001 (AD-A222574). This report documents the relationship between Goettingen's planetary geomagnetic index (Ap) and various other solar events, such as surges, prominences, filaments, radio bursts and X-ray events. The study is based on solar and Ap data with an 11-year period of record (1975 to 1986--Solar Cycle 21). Solar reports were merged with 3-hour Ap values for 7 days after each event. The resultant datasets were analyzed with respect to type, position on the sun, and size. Contingency tables of means and percent frequency distribution summarize the results. GRA

93 SPACE RADIATION

Includes cosmic radiation; and inner and outer earth's radiation belts.

For biological effects of radiation see *52 Aerospace Medicine.* For theory see *73 Nuclear and High-Energy Physics.*

N92-11959 California Univ., Los Angeles.
UNDERLYING GENERATION MECHANISMS FOR THE EXTRAGALACTIC GAMMA RAY BACKGROUND AND THEIR IMPLICATIONS FOR HIGH-RESOLUTION GAMMA RAY COSMOLOGY Ph.D. Thesis
Yi-Tian Gao 1991 81 p
Avail: Univ. Microfilms Order No. DA9122727

The cosmological effects and observational consequences of various proposed extragalactic gamma ray background (EGB) generation mechanisms are investigated. It is claimed that the fine-scale EGB anisotropies can form a unique test for the active galactic nuclei (AGN) mechanism. Some effects independent of the AGN evolution models are found. It is argued that more than one type of underlying generation mechanism for the EGB appears to be called for. It is shown that cosmological antimatter may contribute large-scale anisotropies to the EGB. Linking the EGB spectrum and large-scale anisotropies, a combined test likely to be very powerful in determining the role of antimatter in the early Universe is proposed. Furthermore, it is found that the radiative decays of 4th-family neutrinos in the early Universe may yield a bump or spike in the EGB spectrum, around 10 to approximately 10(exp 2) MeV. The cosmological annihilation of the lightest supersymmetric particle (LSP) as a major contributor to the observed EGB is eliminated. Author

N92-11960 Louisiana State Univ., Baton Rouge.
NEUTRON STAR MAGNETIC FIELDS AND IMPLICATIONS FOR PULSARS AND GAMMA RAY BURSTS Ph.D. Thesis
Yeming Sang 1990 145 p
Avail: Univ. Microfilms Order No. DA9123236

Calculations of ohmic decay of neutron star dipolar magnetic fields which are confined to the neutron star crust are carried out. Results indicate that the field does not decay exponentially as has been assumed in most analyses of pulsar observations. Additionally, it is shown that the surface magnetic fields of young pulsars may fluctuate and even change polarities on time scales much shorter than their secular decay time scale. Through a detailed statistical analysis, it is shown that nonexponential field decay is consistent with the current understanding of radio pulsars. Since the field decays nonexponentially and may retain a substantial fraction of its initial strength at ages greater than or equal to 10(exp 9) years, it may also provide a natural explanation for the magnetic fields of millisecond pulsars, which are thought to be old objects. Strong magnetic fields may be present on the surface of neutron stars associated with gamma ray bursts. The possibility that the cyclotron emissions from plasmas in neutron star magnetospheres, which are heated through Compton process by high energy gamma rays, may produce observable optical flashes is examined. It is concluded that, under certain magnetospheric conditions, the model is capable of explaining the historical flashes found within modern gamma ray burst error

boxes. The cyclotron radiative transfer calculations in high temperature (k(sub b)T is approximately 100 keV) plasmas require a fast and accurate code to compute the cyclotron opacities. A numerical code based on the steepest descent path method, first devised by Trubnikov, was developed. The results are in general agreement with those obtained using the Chanmugam and Dulk method. Dissert. Abstr.

N92-11961# Los Alamos National Lab., NM.
CYGNUS COLLABORATION CONTRIBUTIONS TO THE TWENTY-SECOND ICRC
D. E. Alexandreas, S. Biller, G. M. Dion, X. Q. Lu, G. B. Yodh (California Univ., Irvine.), D. Berley, C. Y. Chang, B. L. Dingus, C. Dion, and J. A. Goodman et al Aug. 1991 20 p Conference held in Dublin, Ireland, 11-23 Aug. 1991
(Contract W-7405-eng-36)
(DE92-000258; LA-UR-91-2911; CONF-9108141-2-Exc) Avail: NTIS HC/MF A03

This report contains short papers on the cygnus experiments on the detection of cosmic air showers from distant sources such as nebulae, galaxies, x ray sources, etc. DOE

99 GENERAL

N92-11962# Purdue Univ., West Lafayette, IN. School of Electrical Engineering.
ANNUAL RESEARCH SUMMARY, JULY 1, 1990 - JUNE 30, 1991
1991 280 p
(DE91-017408; PUR-91017408) Avail: NTIS HC/MF A13

This document summarizes the research activities within the School of Electrical Engineering of Purdue University for July 1, 1990 to June 30, 1991. It is intended as a reference document for colleagues, prospective graduate students and organizations interested in electrical engineering research. The research activities of Part 1 are organized according to ten areas. The first eight of these are areas in which the Purdue Electrical Engineering graduate program is divided for administrative purposes. The ten areas are: automatic controls; electromagnetic fields; bioengineering; energy source and systems; circuit theory; solid state devices and materials; communications and signal processing; engineering education; and computer engineering. DOE

N92-11963# Office National d'Etudes et de Recherches Aerospatiales, Paris (France).
EIGHTY YEARS OF AEROSPACE TECHNIQUE THROUGH ATMA BULLETINS [80 ANS DE TECHNIQUE AEROSPATIALE A TRAVERS LES BULLETINS DE L'ATMA]
J.-P. Marec 1990 123 p In FRENCH; ENGLISH summary
(ETN-91-90097) Avail: NTIS HC/MF A06

The history of aerospace techniques during the last 80 years is reviewed from the rapid analysis of the memoirs presented at the sessions of ATMA (French acronym for the French association of maritime and aeronautical techniques) during this period. The main headings reviewed are: aerodynamics and hydrodynamics, flight mechanics, structures and materials, equipment, navigation, different types of vehicles, engines, aerospace programs and miscellaneous problems including safety. Some particularly significant passages of the memoirs are quoted and the text is abundantly illustrated by figures taken from the memoirs. A chronological index and an analytical index of the memoirs are given as appendices. ESA

N92-11964# Max-Planck-Inst. fuer Aeronomie, Katlenburg-Lindau (Germany, F.R.).
[ACTIVITIES REPORT OF THE MAX-PLANCK INSTITUTE FOR AERONOMY] Annual Report, 1990 [MAX-PLANCK FUER AERONOMIE, TAETIGKEITSBERICHT FUER DAS JAHR 1990]
H. Schwentek and S. Deutsch Apr. 1991 206 p In GERMAN
(ETN-91-90233) Copyright Avail: NTIS HC/MF A10

The main points in the activity of the Institute during year 1990 were the launching of spatial sonde Ulysses, the launching of the Combined Release and Radiation Effects Satellite (CRRES) in a geostationary transfer orbit and the achievement of the last capacity stage of the largest antenna of the heating project installation. The Ulysses neutral gas experiment was successful in giving information on properties in interstellar neutral gases. The Energetic Particle Composition (EPAC) experiment and the Solar Wind Ion Composition (EPAC) experiment and the Solar Wind Ion Composition Sensor (SWICS) on board the NASA satellite WIND delivered new data on the behavior of particles from solar flares. Success is also to be mentioned for ground projects, such as lidar developments, and polar light radar system. ESA

N92-11965# Rochester Univ., NY. Lab. for Laser Energetics.
LLE REVIEW Quarterly Report, Apr. - Jun. 1991
P. A. Jaanimagi, ed. 1991 72 p
(Contract DE-FC03-85DP-40200)
(DE91-018828; DOE/DP-40200/166) Avail: NTIS HC/MF A04

This volume of the LLE (Laboratory for Laser Energetics) Review, covering the period April to June 1991, contains articles on the production and characterization of hot, long-scale-length laser plasmas, a new x-ray spectroscopic method for diagnosing laser-driven target implosions, and two-dimensional (2-D) simulation results that confirm the dominance of kinetic thermal filamentation over ponderomotive filamentation. The section on advanced technology includes a report on the time-domain characterization of bent coplanar waveguides, and a study of the surface disordering of Pb(100) at temperatures below the bulk-melting temperature. Finally, the activities of the National Laser Users Facility and the Gas Dynamics Laboratory (GDL) and OMEGA laser facilities are summarized. DOE

Typical Subject Index Listing

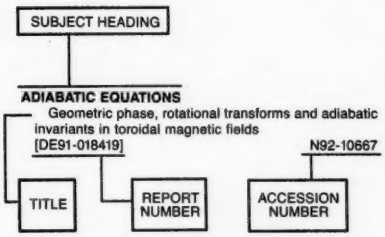

The subject heading is a key to the subject content of the document. Titles, report numbers, and accession numbers of pertinent documents are provided under each subject heading. When the title is insufficiently descriptive of the document content, a title extension has been added, separated from the title by three hyphens. The report number helps to indicate the type of document cited (e.g., NASA report, NASA translation, NASA contractor report). The accession number is the number by which the document abstracts are arranged in this journal and by which the document is sold or requested. The titles, with title extensions if present, are arranged under each subject heading in ascending accession number order. The subject headings have been selected from the latest revision of the *NASA Thesaurus*.

A

ABSORPTION SPECTRA
Photothermal deflection spectroscopy of conjugated polymers
[DE91-018318] N92-11204

ABSORPTION SPECTROSCOPY
Polarized x ray absorption spectroscopy for the study of superconductors and magnetic materials
[DE91-017990] N92-11163

ABUNDANCE
Continuum x ray gauging of multiple-element materials
[DE91-017429] N92-11368
Report on carbon and nitrogen abundance studies
[NASA-CR-188803] N92-11934

ACCELERATION (PHYSICS)
Effect of gasoline octane quality on vehicle acceleration performance
[AD-A240433] N92-11357
The microgravity environment of the Space Shuttle Columbia middeck during STS-32
[NASA-TP-3140] N92-11930
The microgravity environment of the Space Shuttle Columbia payload bay during STS-32
[NASA-TP-3141] N92-11931

ACCELEROMETERS
The microgravity environment of the Space Shuttle Columbia middeck during STS-32
[NASA-TP-3140] N92-11930
The microgravity environment of the Space Shuttle Columbia payload bay during STS-32
[NASA-TP-3141] N92-11931

ACCEPTABILITY
Discharge system tests of Halon 1301 test gas simulants
[AD-A240679] N92-11193

ACCURACY
Groves model accuracy study
[AD-A240456] N92-11586

ACETALS
Synthesis and reactivity of silyl-ketene acetal-modified polysiloxanes preparation of polysiloxanes with high dielectric constraints
[AD-A240754] N92-11196

ACOUSTIC ATTENUATION
A survey of scattering, attenuation, and size spectra studies of bubble layers and plumes beneath the air-sea interface
[AD-A240262] N92-11606

ACOUSTIC EXCITATION
Nonlinear aspects of aerospace structures at high excitation levels flat aluminum beams and plates studied
[AD-A240600] N92-11383

ACOUSTIC PROPAGATION
Acoustic propagation at low altitude: Effects of atmospheric turbulence (Villeau (France) test)
[ONERA-RT-15/3641-PY] N92-11588

ACOUSTIC SCATTERING
Discrete ARMA model for natural resonances in electromagnetic and acoustic scattering
[AD-A240656] N92-11241
A survey of scattering, attenuation, and size spectra studies of bubble layers and plumes beneath the air-sea interface
[AD-A240262] N92-11606
Quantitative ray methods for scattering of sound by spherical shells
[AD-A240255] N92-11761
Scattering of tone bursts from spherical shells: Computations based on Fourier transform method
[AD-A240642] N92-11764

ACOUSTICS
Optimal control by wideband frequency. Application to acoustic control by piezoelectric technique
[ONERA-RT-6/3654-RY-006-R] N92-11713

ACQUISITION
Proceedings of the Acquisition Research Symposium: Imagination, Innovation, and Implementation, 1991, volume 1
[AD-A240260] N92-11676
Proceedings of the Acquisition Research Symposium: Acquisition for the Future, Imagination, Innovation, and Implementation, 1991, volume 2
[AD-A240261] N92-11677

ACTIVE CONTROL
Analysis of open loop higher harmonic control at high airspeeds on a modern four-bladed articulated rotor
[NASA-TM-103876] N92-11000
Active vibration damping of the Space Shuttle remote manipulator system
[NASA-TM-104149] N92-11073
Microgravity vibration isolation: An optimal control law for the one-dimensional case
[NASA-TM-105146] N92-11217

ACTIVE GALACTIC NUCLEI
Underlying generation mechanisms for the extragalactic gamma ray background and their implications for high-resolution gamma ray cosmology N92-11959

ACTIVE GALAXIES
Infrared to millimetre observations of active galaxies N92-11932

ACTIVITY (BIOLOGY)
Theory and modeling in GLOBEC: A first step N92-11602

ACTUATION
Leveling of the AMBLER walking machine: A comparison of methods
[NASA-CR-189015] N92-11358

ADA (PROGRAMMING LANGUAGE)
ART/Ada design project, phase 1: Project plan
[NASA-CR-187313] N92-11663
Deploying expert systems in Ada
[NASA-CR-188938] N92-11664
ART/Ada design project, phase 1. Task 1 report: Overall design
[NASA-CR-188943] N92-11665
ART/Ada design project, phase 1. Task 2 report: Detailed design
[NASA-CR-188944] N92-11666
ART-Ada design project, phase 2
[NASA-CR-188940] N92-11667

ADAPTATION
Classification of posture maintenance data with fuzzy clustering algorithms
[NASA-CR-188949] N92-11662

ADAPTIVE OPTICS
Irradiance compensation control for high-energy laser propagation, part 2
[DE91-018489] N92-11348

ADDITIVES
High-T sub c fluorine-doped YBa2Cu3O(y) films on ceramic substrates by screen printing
[NASA-TM-105296] N92-11188
Properties of aircraft fuels and related materials
[AD-A240650] N92-11213

ADHESION
Contact angle and work of adhesion between Ni-based melts and non-metallic solids
[NPL-DMM(A)-23] N92-11171

ADHESIVE BONDING
Conductive gage for crack length measurement
[NASA-CASE-LAR-14480-1-CU] N92-11374

ADIABATIC CONDITIONS
Heat transfer, adiabatic effectiveness, and injectant distributions downstream of single and double rows of film-cooling holes with simple and compound angles
[AD-A240743] N92-11305

ADRIATIC SEA
Preliminary results of a spectro-imagery experiment (GER) over the Adriatic coastline of the Venice lagoon N92-11440

ADSORPTION
Photoemission study of Ce/Ta(110) and Ce/W(110) interfaces and the catalytic oxidation effect
[DE91-018167] N92-11903
Photoreflectance and H2O adsorption on GaAs(100)
[AD-A240391] N92-11911

ADVANCED LAUNCH SYSTEM (STS)
Advanced information processing system for advanced launch system: Avionics architecture synthesis
[NASA-CR-187554] N92-11704
Advanced information processing system for advanced launch system: Hardware technology survey and projections
[NASA-CR-187555] N92-11705

ADVANCED VERY HIGH RESOLUTION RADIOMETER
Inter-calibrating of SPOT1-HRV, LANDSAT5-TM, and NOA11-AVHRR in the visible and near infrared field s N92-11401
Routine mapping of vegetation index with the AVHRR of NOAA11 N92-11405
On the use of passive microwaves at 37 GHz N92-11461
NOAA-AVHRR contribution to the analysis or urban heat islands N92-11495
Maximum evapotranspiration monitoring over La Mancha, Spain, using NOAA-AVHRR data N92-11507
Contribution of NOAA-AVHRR satellite data in forest vegetation monitoring N92-11520

AEROACOUSTICS
Development of unsteady aerodynamic analyses for turbomachinery aeroelastic and aeroacoustic applications
[NASA-CR-4405] N92-10979

AEROASSIST
Prediction of the pattern performance for the Aeroassist Flight Experiment (AFE) spacecraft
[NASA-CR-4409] N92-11065

AERODYNAMIC CHARACTERISTICS
Subsonic wind tunnel testing handbook
[AD-A240263] N92-10986

AERODYNAMIC COEFFICIENTS
Drag coefficients with applications to satellite orbits N92-11069

AERODYNAMIC CONFIGURATIONS
Unsteady aerodynamic calculations for general configurations by the double-point method
[NAL-TR-1101T] N92-10980
Aerodynamic calculations related to tethered sub-satellite experiments
[NASA-CR-188964] N92-11071

AERODYNAMIC DRAG
Drag coefficients with applications to satellite orbits N92-11069
Resolution of Navier-Stokes equations around profiles: Drag evolution
[ONERA-RTS-86/1685-AY-156A] N92-11310
AERODYNAMIC FORCES
A methodology to assess the Best Estimate Trajectory (BET) results generated for the Kwajalein Missile Range
[AD-A240770] N92-11083
AERODYNAMIC INTERFERENCE
Experimental study of an independently deflected wingtip mounted on a semispan wing
[NASA-TM-102842] N92-10983
Model representation in the PANCOR wall interference assessment code
[NASA-TM-104152] N92-11022
AERODYNAMIC LOADS
Experimental study of an independently deflected wingtip mounted on a semispan wing
[NASA-TM-102842] N92-10983
Studies of aerothermal loads generated in regions of shock/shock interaction in hypersonic flow
[NASA-CR-181893] N92-11319
Multi-disciplinary optimization of aeroservoelastic systems
[NASA-CR-188983] N92-11377
AERODYNAMIC NOISE
Annoyance caused by advanced turboprop aircraft flyover noise: Comparison of different propeller configurations
[NASA-TP-3104] N92-11758
AERODYNAMIC STABILITY
Rotorcraft system identification
[AGARD-AR-280] N92-11001
Aerodynamic calculations related to tethered sub-satellite experiments
[NASA-CR-188964] N92-11071
AERODYNAMICS
Aeronautical engineering: A continuing bibliography with indexes (supplement 270)
[NASA-SP-7037(270)] N92-10973
Aeronautical engineering: A continuing bibliography with indexes (supplement 269)
[NASA-SP-7037(269)] N92-10974
The effects of Reynolds number, rotor incidence angle and surface roughness on the heat transfer distribution in a large-scale turbine rotor passage
[NASA-CR-187693] N92-11297
AEROELASTICITY
Development of unsteady aerodynamic analyses for turbomachinery aeroelastic and aeroacoustic applications
[NASA-CR-4405] N92-10979
Three dimensional numerical method for resolving small transonic perturbations in unstructured mesh
[ONERA-RT-56/3064-RY-006-R] N92-10989
Perfect compressible two dimensional boundary layer strong fluid coupling in the case of sharp leading edge profiles. Unsteady case of isolated profiles and steady case of blade grids
[ONERA-RT-43/1621-RY-006-R] N92-11311
Multi-disciplinary optimization of aeroservoelastic systems
[NASA-CR-188983] N92-11377
AERONAUTICAL ENGINEERING
Study of alternatives: Dayton's Aviation heritage, Ohio
[PB91-202275] N92-10972
Aeronautical engineering: A continuing bibliography with indexes (supplement 270)
[NASA-SP-7037(270)] N92-10973
Aeronautical engineering: A continuing bibliography with indexes (supplement 269)
[NASA-SP-7037(269)] N92-10974
AERONOMY
Activities report of the Max-Planck Institute for Aeronomy
[ETN-91-90233] N92-11964
AEROSOLS
Modeling of visible and UV radiative transfer in the ocean-atmosphere system concepts, models, and programs N92-11396
Estimation of the aerosol optical thickness from broadband turbidity measurements: Application to the atmospheric correction of SPOT images N92-11399
Atmospheric correction of satellite borne imagery investigated by means of a sensitivity analysis of the entire remote sensing process N92-11400
Suppression of aerosols on LANDSAT thematic mapper imagery N92-11411
In flight calibration of large field of view sensors at short wavelength using the Rayleigh scattering N92-11416
Iterative procedures for atmospheric correction N92-11417
ATLAS: An Auto-Tracking Land and Atmosphere Sensor for retrieval of atmospheric optical parameters and acquisition of bidirectional surface reflectance N92-11487
AEROSPACE ENGINEERING
Space engineering
[NASA-CR-187820] N92-11215
Supervoltage NDE techniques for large aerospace structures
[AD-A240625] N92-11365
Robot graphic simulation testbed
[NASA-CR-188998] N92-11637
Computers in aeronautics and space research at the Lewis Research Center
[NASA-TM-105096] N92-11642
Eighty years of aerospace technique through ATMA bulletins
[ETN-91-90097] N92-11963
AEROSPACE MEDICINE
JPRS report: Science and technology. USSR: Life sciences
[JPRS-ULS-91-017] N92-11616
AEROSPACE PLANES
Overview of the Beta II Two-Stage-To-Orbit vehicle design
[NASA-TM-105298] N92-11034
AEROSPACE SAFETY
Safety issues N92-11115
AEROSPACE SCIENCES
Eighty years of aerospace technique through ATMA bulletins
[ETN-91-90097] N92-11963
AEROSPACE SYSTEMS
New insulation constructions for aerospace wiring applications. Volume 1: Testing and evaluation
[AD-A240638] N92-11006
New insulation constructions for aerospace wiring applications. Volume 2: The 270 VDC arc tracking testing with power controllers
[AD-A240639] N92-11007
OPUS: Optimal Projection for Uncertain Systems, volume 2
[AD-A240373] N92-11081
Supervoltage NDE techniques for large aerospace structures
[AD-A240625] N92-11365
Making intelligent systems team players: Case studies and design issues. Volume 2: Fault management system cases
[NASA-TM-104738] N92-11641
AEROSPACE VEHICLES
New methods in robust control
[AD-A240221] N92-11018
AEROTHERMODYNAMICS
Application of infrared thermography to thermal flux measurement in wind tunnels
[AAAF-NT-89-12] N92-11020
Aerodynamic calculations related to tethered sub-satellite experiments
[NASA-CR-188964] N92-11071
Aerothermal test results from the first flight of the Pegasus air-launched space booster
[NASA-TM-4330] N92-11301
Studies of aerothermal loads generated in regions of shock/shock interaction in hypersonic flow
[NASA-CR-181893] N92-11319
AFRICA
Detection and characterization of active fires in west Africa with LANDSAT thematic mapper and NOAA N92-11529
AFTERBODIES
Viscous computations of cold air/air flow around scramjet nozzle afterbody
[NASA-CR-4406] N92-10982
AGING (MATERIALS)
Investigation of the stability of the spectral responsitivity of silicon photodiodes
[NPL-QU-87] N92-11184
Physical ageing and creep in PVC
[NPL-DMM(A)-21] N92-11185
AGRICULTURE
Joint use of remote sensing and agricultural production estimation models: Current trends N92-11501
Modeling temporal evolution of the radiometric response measured by wideband sensors over temperate agricultural regions N92-11518
JPRS report: Science and technology. USSR: Life sciences
[JPRS-ULS-91-015] N92-11610
AIR
Calculations and curve fits of thermodynamic and transport properties for equilibrium air to 30000 K
[NASA-RP-1260] N92-11285
Computer codes for the evaluation of thermodynamic and transport properties for equilibrium air to 30000 K
[NASA-TM-104107] N92-11300
AIR BREATHING BOOSTERS
Mach 6.5 air induction system design for the Beta 2 two-stage-to-orbit booster vehicle
[NASA-CR-187233] N92-11013
AIR BREATHING ENGINES
Overview of the Beta II Two-Stage-To-Orbit vehicle design
[NASA-TM-105298] N92-11034
AIR FLOW
Mixed convection in two-dimensional laminar air flow with reverse flow regions N92-11293
AIR INTAKES
Mach 6.5 air induction system design for the Beta 2 two-stage-to-orbit booster vehicle
[NASA-CR-187233] N92-11013
AIR JETS
Numerical simulation of the reactive flow in advanced (HSR) combustors using KIVA-2
[NASA-CR-188996] N92-11014
A detailed investigation of staged normal injection into a Mach 2 flow N92-11118
AIR LAND INTERACTIONS
Biospheric models, measurements, and remote sensing of vegetation N92-11550
AIR NAVIGATION
The electronic aeronautical chart for general aeronautics: A system specification
[ILR-MITT-263(1991)] N92-10997
AIR POLLUTION
Low volatile organic compound paints
[DE91-017984] N92-11203
EDMS: Microcomputer pollution model for civilian airports and Air Force bases, (user's guide)
[AD-A240528] N92-11578
Technical requirements of sick bays aboard space ships N92-11620
AIR QUALITY
EDMS: Microcomputer pollution model for civilian airports and Air Force bases, (user's guide)
[AD-A240528] N92-11578
AIR TO AIR MISSILES
An examination of the factors affecting the use of infra-red search and track systems in the air-to-air role
[ETN-91-99987] N92-11222
AIR TRAFFIC
A systematic formulation, as an approach to air traffic
[MBB-Z-0371-91-PUB] N92-10996
AIR TRANSPORTATION
Personal air transport: State of the art
[PB91-204768] N92-10991
AIR WATER INTERACTIONS
Local interfacial area concentration measurement in bubbly flow
[DE91-018702] N92-11322
Modeling of visible and UV radiative transfer in the ocean-atmosphere system concepts, models, and programs N92-11396
A survey of scattering, attenuation, and size spectra studies of bubble layers and plumes beneath the air-sea interface
[AD-A240262] N92-11606
AIRBORNE EQUIPMENT
Airborne SAR HAREM campaign: Results, targets features, ERS1 simulations, and operational satellite exploitation N92-11455
Laser active remote sensing of phytoplankton in inland waters N92-11534
AIRBORNE/SPACEBORNE COMPUTERS
Advanced information processing system for advanced launch system: Avionics architecture synthesis
[NASA-CR-187554] N92-11704
Advanced information processing system for advanced launch system: Hardware technology survey and projections
[NASA-CR-187555] N92-11705
Advanced information processing system: Inter-computer communication services
[NASA-CR-187556] N92-11706
AIRCRAFT CONFIGURATIONS
Static internal performance of ventral and rear nozzle concepts for short-takeoff and vertical-landing aircraft
[NASA-TP-3103] N92-10975
Technology needs for high speed rotorcraft (3)
[NASA-CR-186433] N92-10999
AIRCRAFT CONSTRUCTION MATERIALS
Critical appraisal of the McDonnell Douglas closure model for predicting fatigue crack growth
[ARL-STRUC-R-444] N92-11376
AIRCRAFT CONTROL
Maximized gust loads for a nonlinear airplane using matched filter theory and constrained optimization
[NASA-TM-104138] N92-11010

AIRCRAFT DESIGN
Development of unsteady aerodynamic analyses for turbomachinery aeroelastic and aeroacoustic applications
[NASA-CR-4405] N92-10979
AIRCRAFT DETECTION
The role of stealth in naval aviation and joint/combined operations
[AD-A240595] N92-11005
AIRCRAFT ENGINES
Numerical simulation of the reactive flow in advanced (HSR) combustors using KIVA-2
[NASA-CR-188996] N92-11014
Properties of aircraft fuels and related materials
[AD-A240650] N92-11213
AIRCRAFT EQUIPMENT
Concept evaluation of the UH-60 externally mounted rescue hoist
[AD-A240545] N92-11004
AIRCRAFT FUELS
Properties of aircraft fuels and related materials
[AD-A240650] N92-11213
AIRCRAFT LANDING
Evaluation of two high-speed runway exits
[DOT/FAA/CT-TN91/36] N92-11021
Prototype runway hold-short lighting system
[DOT/FAA/CT-TN91/43] N92-11028
AIRCRAFT MAINTENANCE
Program plan: National aging aircraft research program
[DOT/FAA/CT-88/32-1] N92-10992
AIRCRAFT MANEUVERS
Development of a 1/7th scale fighter UAV for flight research
[AD-A240703] N92-11008
AIRCRAFT MODELS
Model representation in the PANCOR wall interference assessment code
[NASA-TM-104152] N92-11022
AIRCRAFT NOISE
Annoyance caused by advanced turboprop aircraft flyover noise: Comparison of different propeller configurations
[NASA-TP-3104] N92-11758
A new simulator for assessing subjective effects of sonic booms
[NASA-TM-104150] N92-11759
AIRCRAFT PERFORMANCE
Technology needs for high speed rotorcraft (3)
[NASA-CR-186433] N92-10999
AIRCRAFT PILOTS
Pilot's Automated Weather Support System (PAWSS) concepts demonstration project. Phase 1: Pilot's weather information requirements and implications for weather data systems design
[NASA-CR-188228] N92-11593
AIRCRAFT RELIABILITY
Program plan: National aging aircraft research program
[DOT/FAA/CT-88/32-1] N92-10992
Robotic non-destructive inspection of aircraft, phase 1
[AD-A240777] N92-11367
AIRCRAFT SAFETY
Program plan: National aging aircraft research program
[DOT/FAA/CT-88/32-1] N92-10992
AIRCRAFT STRUCTURES
Nonlinear aspects of aerospace structures at high excitation levels flat aluminum beams and plates studied
[AD-A240600] N92-11383
AIRFIELD SURFACE MOVEMENTS
Evaluation of two high-speed runway exits
[DOT/FAA/CT-TN91/36] N92-11021
Surface painted taxiway markings at Seattle-Tacoma International Airport
[DOT/FAA/CT-TN91/49] N92-11029
AIRFOIL PROFILES
Resolution of Navier-Stokes equations around profiles: Drag evolution
[ONERA-RTS-86/1685-AY-156A] N92-11310
Hydrodynamic flow visualization around an oscillating vane. Extension of study to the case of higher incidences and amplitudes and the starting off phase from permanent regime
[ONERA-RT-56/1369-AN] N92-11312
AIRFOILS
Perfect compressible two dimensional boundary layer strong fluid coupling in the case of sharp leading edge profiles. Unsteady case of isolated profiles and steady case of blade grids
[ONERA-RT-43/1621-RY-006-R] N92-11311
AIRLINE OPERATIONS
Program plan: National aging aircraft research program
[DOT/FAA/CT-88/32-1] N92-10992
Parameter identification studies on the NASA/Ames Research Center Advanced Concepts Flight Simulator
[NASA-TM-105126] N92-11024
Prototype runway hold-short lighting system
[DOT/FAA/CT-TN91/43] N92-11028
Surface painted taxiway markings at Seattle-Tacoma International Airport
[DOT/FAA/CT-TN91/49] N92-11029
AIRPORT LIGHTS
Prototype runway hold-short lighting system
[DOT/FAA/CT-TN91/43] N92-11028
AIRPORTS
Surface painted taxiway markings at Seattle-Tacoma International Airport
[DOT/FAA/CT-TN91/49] N92-11029
EDMS: Microcomputer pollution model for civilian airports and Air Force bases, (user's guide)
[AD-A240528] N92-11578
AIRY FUNCTION
Computer program for Bessel and Hankel functions
[NASA-TM-105154] N92-11691
ALASKA
Photovoltaic energy system at an Alaskan site
[PB91-201350] N92-11567
ALCOHOLS
Alternative fuels for heavy duty engines: Status of fleet trials
[DE91-018474] N92-11210
ALGEBRA
LAPACK: Linear algebra software for supercomputers
[DE91-017316] N92-11660
Conditional event algebras: Two new characterizations and their relations to Bayesian analysis
[AD-A240378] N92-11738
Extended algebraic graph transformation
[ETN-91-90151] N92-11739
Algebraic aspects of network reliability problems
[AD-A240365] N92-11748
ALGORITHMS
A fast sorting algorithm for a hypersonic rarefied flow particle simulation on the connection machine
[NASA-CR-188903] N92-10977
A comparison of airborne wake vortex detection measurements with values predicted from potential theory
[NASA-TP-3125] N92-10994
Real-time fault diagnosis for propulsion systems
[NASA-TM-105303] N92-11017
Space Network Control Conference on Resource Allocation Concepts and Approaches
[NASA-CP-3124] N92-11039
Space Network Control (SNC) Conference on Resource Allocation Concepts and Approaches. Overview N92-11040
Intelligent perturbation algorithms for space scheduling optimization N92-11055
Intelligent perturbation algorithms to space scheduling optimization N92-11064
Precision pointing control of the spinning Gravity Probe B spacecraft N92-11068
A generalized method for multiple robotic manipulator programming applied to vertical-up welding
[NASA-TP-3163] N92-11218
Dispersion and stability of two electromagnetic solvers for triangular meshes
[DE91-016607] N92-11227
A fast algorithm for plotting antenna and scattering patterns in three dimensions
[AD-A240410] N92-11233
A conjugate gradient based algorithm to minimize the sidelobe level of planar arrays with element failures
[AD-A240667] N92-11242
Enhanced clutter suppression apparatus for use with an infrared search and surveillance system
[AD-D014984] N92-11247
VHDL simulation of the implementation of a costfunction circuit
[AD-A240430] N92-11278
Resolution of the Navier-Stokes equations applied to the computation of the laminar flow around a two dimensional wing profile
[CERT-RT-65/5604-35] N92-11307
An efficient and robust algorithm for two dimensional time dependent incompressible Navier-Stokes equations: High Reynolds number flows
[NASA-TM-104424] N92-11320
Implementation of the flow-modulated skew-upward difference scheme in the momentum equation of the COMMIX-1C program: A first assessment
[DE91-018013] N92-11321
Attitude identification for SCOLE using two infrared cameras
[NASA-CR-4397] N92-11338
Irradiance compensation control for high-energy laser propagation, part 2
[DE91-018489] N92-11348
A computational procedure for the dynamics of flexible beams within multibody systems N92-11371
Slave finite element for non-linear analysis of engine structures. Volume 2: Programmer's manual and user's manual
[NASA-CR-187225] N92-11388
Geometrically exact shells models: Foundation and computational aspects with special reference to implicit large-scale calculations
[DE91-019014] N92-11390
Atmospheric correction in the thermal infrared: AVHRR case N92-11398
Correction of atmospheric and topographic effects in LANDSAT TM images N92-11407
Weather prediction using a genetic memory
[NASA-CR-185448] N92-11590
Index and bulk parameters for frequency-direction spectra measured at CERC field research facility
[AD-A240320] N92-11607
A parallel algorithm for the eigenvalues and eigenvectors for a general complex matrix
[NASA-CR-188854] N92-11653
Modula-2*: An extension of Modula-2 for highly parallel programs
[NASA-CR-188855] N92-11654
Fast secant methods for the iterative solution of large nonsymmetric linear systems
[NASA-CR-188867] N92-11655
Optimal parallel solution of sparse triangular systems
[NASA-CR-188872] N92-11656
An O(log sup 2 N) parallel algorithm for computing the eigenvalues of a symmetric tridiagonal matrix
[NASA-CR-188898] N92-11659
Classification of posture maintenance data with fuzzy clustering algorithms
[NASA-CR-188949] N92-11662
ART/Ada design project, phase 1. Task 2 report: Detailed design
[NASA-CR-188944] N92-11666
Optimal processor assignment for pipeline computations
[NASA-CR-189047] N92-11672
Fast algorithms for linear least-squares estimation of multi-dimensional random fields
[AD-A240249] N92-11675
Perceptual grouping and shape from texture
[AD-A240358] N92-11678
Appearance simulator for computer vision research
[AD-A240506] N92-11679
Fractal image compression
[AD-A240636] N92-11680
An efficient A* stack decoder algorithm for continuous speech recognition with a stochastic language model
[AD-A240745] N92-11683
Cedar Project: Original goals and progress to date
[DE92-000032] N92-11689
A domain decomposition algorithm for solving large elliptic problems
[DE92-000096] N92-11690
Optimal expression evaluation for data parallel architectures
[NASA-CR-187773] N92-11696
Analysis of a parallel multigrid algorithm
[NASA-CR-188906] N92-11701
Learning to read aloud: A neural network approach using sparse distributed memory
[NASA-CR-188846] N92-11711
Discussion summary: Fictitious domain methods N92-11730
Algebraic aspects of network reliability problems
[AD-A240365] N92-11748
Scattering of tone bursts from spherical shells: Computations based on Fourier transform method
[AD-A240642] N92-11764
ALKENES
Conversion of ethane and of propane to higher olefin hydrocarbons
[DE91-016896] N92-11160
Synthesis and reactivity of silyl-ketene acetal-modified polysiloxanes preparation of polysiloxanes with high dielectric constraints
[AD-A240754] N92-11196
ALLOYING
Strengthening of an AISI 1020 steel by aluminum-microalloying during liquid dynamic compaction
[DE91-018745] N92-11182
ALPHA PARTICLES
Continuum damping of high mode number toroidal Alfven waves
[DE91-018891] N92-11890
ALTIMETERS
C-29A aircraft altimeter errors
[AD-A240486] N92-11011

ALTIMETRY
Analysis of altimetry over the Aral Sea
[NASA-TM-100759] N92-11583
ALTITUDE
Altitude dependence in a semi-analytical atmospheric code N92-11413
Persian Gulf contrail altitude limits
[AD-A240702] N92-11598
ALTITUDE TOLERANCE
Efficacy of hyperbaric oxygenation in enhancing flight tolerance N92-11618
ALUMINIDES
Alloy modeling and experimental correlation for ductility enhancement in near stoichiometric single crystal nickel aluminide
[AD-A240151] N92-11175
Oxidation of titanium aluminide and its XD composite
[AD-A240401] N92-11177
ALUMINUM
Centrifugal casting of composites
[AD-D014981] N92-11144
Nonlinear aspects of aerospace structures at high excitation levels flat aluminum beams and plates studied
[AD-A240600] N92-11383
Photon stimulated desorption of neutral species from aluminum
[DE91-017004] N92-11784
ALUMINUM NITRIDES
Strengthening of an AISI 1020 steel by aluminum-microalloying during liquid dynamic compaction
[DE91-018745] N92-11182
ALUMINUM-LITHIUM ALLOYS
A comparison of single cycle overload effect on Al-Li 2091-T81 plate and 2091-T83 sheet
[AD-A240627] N92-11179
AMBIENT TEMPERATURE
Strategic air command contrail formation study
[AD-A240467] N92-11003
Moisture-induced environmental embrittlement of ordered intermetallic alloys at ambient temperatures
[DE91-018852] N92-11183
AMIDES
Diphenylmethane-containing dianhydride and polyimides prepared therefrom
[NASA-CASE-LAR-14487-1] N92-11200
AMINES
Polyimides with imprcved compression moldability
[NASA-CASE-LAR-14457-1-CU] N92-11198
AMMONIA
Laboratory measurements of the single-scattering properties of ammonia ice crystals N92-11950
AMMONIUM CHLORIDES
New polymer electrolyte hosts and their tetrabutylammonium chloride complexes. Relationships among concentration of polar groups, ESR spin probe response, and ionic conductivity
[AD-A240497] N92-11190
AMPLIFICATION
The effect of wiggler errors on FEL gain
[DE92-000483] N92-11351
AMPLITUDES
Hydrodynamic flow visualization around an oscillating vane. Extension of study to the case of higher incidences and amplitudes and the starting off phase from permanent regime
[ONERA-RT-56/1369-AN] N92-11312
ANALYSIS (MATHEMATICS)
Stable upwind schemes for hyperbolic conservation laws for with source terms N92-11716
An analysis of upwind schemes for inhomogeneous two dimensional conservation laws N92-11717
An analysis of some hyperbolic problems related to the shallow water model (chapter 6)
[IMAG-RR-579] N92-11718
ANCHORS (FASTENERS)
Blind fastening apparatus
[NASA-CASE-LAR-14542-1] N92-11354
ANGLES (GEOMETRY)
Technique for calibrating angular measurement devices when calibration standards are unavailable
[NASA-TM-104148] N92-11340
ANGULAR VELOCITY
Ion temperature and poloidal rotation profiles for NBI heated plasma in CHS N92-11860
ANHYDRIDES
Polyimides with improved compression moldability
[NASA-CASE-LAR-14457-1-CU] N92-11198
Diphenylmethane-containing dianhydride and polyimides prepared therefrom
[NASA-CASE-LAR-14487-1] N92-11200
A process for preparing an assembly of an article and a polyimide which resists dimensional change, delamination, and debonding when exposed to changes in temperature
[NASA-CASE-LAR-14538-1] N92-11201
ANIMALS
Television image compression and small animal remote monitoring
[NASA-CR-186614] N92-11223
ANISOTROPIC MEDIA
Effects of anisotropic conduction and heat pipe interaction on minimum mass space radiators
[NASA-TM-105297] N92-11138
ANISOTROPY
The notion of artificial satellites in the anisotropic gravitational field of a uniformly rotating solid Earth model. A second order analytical solution
[SER-C-357] N92-11072
Anisotropy of thermal infrared exitance above and within plant canopies N92-11467
Bidirectional reflectance and surface albedo: Physical modeling and inversion N92-11469
ANNEALING
High-T sub c fluorine-doped YBa2Cu3O(y) films on ceramic substrates by screen printing
[NASA-TM-105296] N92-11188
Thermal annealing studies of Fe and Ti implanted in GaAs and InP
[ETN-91-90148] N92-11915
ANNOTATIONS
Magnetic suspension and balance systems: A comprehensive, annotated bibliography
[NASA-TM-4318] N92-11030
ANTARCTIC REGIONS
Large scale study of the microwave signature of the Antarctic ice sheet N92-11463
Comparison between the observed microwave spectral signatures over the Antarctic ice sheet and a snow emissivity model N92-11464
ANTENNA ARRAYS
Programmable beam transform and beam steering control system for a phased array radar antenna
[AD-D014970] N92-11230
A conjugate gradient based algorithm to minimize the sidelobe level of planar arrays with element failures
[AD-A240667] N92-11242
A thinned high frequency linear antenna array to study ionospheric structure
[AD-A240764] N92-11243
ANTENNA COMPONENTS
Programmable beam transform and beam steering control system for a phased array radar antenna
[AD-D014970] N92-11230
ANTENNA DESIGN
Large deployable antenna program. Phase 1: Technology assessment and mission architecture
[NASA-CR-4410] N92-11036
Shipboard antenna concepts: Structurally independent 2- to 6-MHz transmit antenna design
[AD-A240544] N92-11236
A thinned high frequency linear antenna array to study ionospheric structure
[AD-A240764] N92-11243
Multiple beam antenna/switch system study
[NASA-CR-183496] N92-11251
ANTENNA RADIATION PATTERNS
A fast algorithm for plotting antenna and scattering patterns in three dimensions
[AD-A240410] N92-11233
A thinned high frequency linear antenna array to study ionospheric structure
[AD-A240764] N92-11243
ANTENNAS
A fast algorithm for plotting antenna and scattering patterns in three dimensions
[AD-A240410] N92-11233
Three-dimensional calculations of fields and loading for loop and folded waveguide ICRF antennas
[DE92-000065] N92-11250
ANTICHOLINERGICS
Intranasal scopolamine preparation and method
[NASA-CASE-MSC-21858-1] N92-11628
ANTIMATTER
Underlying generation mechanisms for the extragalactic gamma ray background and their implications for high-resolution gamma ray cosmology N92-11959
ANTIMISSILE DEFENSE
Insurance against catastrophe: SDI and the 3rd World nuclear proliferation problem
[AD-A240429] N92-11752
ANTIRADAR COATINGS
Active radar stealth device
[AD-D014980] N92-11246
ANTIREFLECTION COATINGS
Process for controlling the thickness of an antireflection coating, and embodying apparatus
[DE91-017634] N92-11793
ANTISHIP MISSILES
Specification of difficult to test radar performance
[AD-A240398] N92-11232
APPLICATIONS PROGRAMS (COMPUTERS)
LV software support for supersonic flow analysis
[NASA-CR-188914] N92-10978
Numerical simulation of the reactive flow in advanced (HSR) combustors using KIVA-2
[NASA-CR-188996] N92-11014
On the symbolic manipulation and code generation for elasto-plastic material matrices
[NASA-CR-187223] N92-11375
APPROPRIATIONS
Greenhouse gas emissions and the developing countries: Strategic options and the USAID response
[PB91-209882] N92-11573
APPROXIMATION
On the theory and numerical approximation of nonlinear hyperbolic problems
[ETN-91-99898] N92-11714
On a class of implicit and explicit schemes of Van-Leer type for scalar conservation laws N92-11715
AQUEOUS SOLUTIONS
Mixing effects in aqueous solutions at elevated temperatures
[DE91-017695] N92-11168
ARC DISCHARGES
New insulation constructions for aerospace wiring applications. Volume 2: The 270 VDC arc tracking testing with power controllers
[AD-A240639] N92-11007
ARCHITECTURE (COMPUTERS)
SPIKE: AI scheduling techniques for Hubble Space Telescope N92-11054
Range Scheduling Aid (RSA) N92-11057
The ULM: A RISC for LISP. System architecture
[ETN-91-90162] N92-11647
ART/Ada design project, phase 1. Task 1 report: Overall design
[NASA-CR-188943] N92-11665
Optimal processor assignment for pipeline computations
[NASA-CR-189047] N92-11672
Education in computational science: Role of the National Laboratories
[DE91-018823] N92-11687
A domain decomposition algorithm for solving large elliptic problems
[DE92-000096] N92-11690
Some fast elliptic solvers on parallel architectures and their complexities
[NASA-CR-188840] N92-11692
Policy issues in interconnecting networks
[NASA-CR-188844] N92-11694
Optimal expression evaluation for data parallel architectures
[NASA-CR-187773] N92-11696
Ground Systems Development Environment (GSDE) interface requirements analysis
[NASA-CR-188822] N92-11702
Advanced information processing system for advanced launch system: Avionics architecture synthesis
[NASA-CR-187554] N92-11704
Advanced information processing system for advanced launch system: Hardware technology survey and projections
[NASA-CR-187555] N92-11705
Advanced information processing system: Inter-computer communication services
[NASA-CR-187556] N92-11706
ARID LANDS
Combined use of Earth observation satellite and meteorological satellite for crop assessment in semiarid environments N92-11494
ARITHMETIC
Circular Statistical methods: Applications in spatial and temporal performance analysis
[AD-A240751] N92-11749
ARPA COMPUTER NETWORK
The ARPANET after twenty years
[NASA-CR-188853] N92-11695
ARTIFICIAL INTELLIGENCE
Intelligent perturbation algorithms for space scheduling optimization N92-11055
Integration of qualitative knowledge on operational models for following vegetation using temporal series of remote sensing images N92-11502
Robot graphic simulation testbed
[NASA-CR-188998] N92-11637
Sparse distributed memory
[NASA-CR-188841] N92-11643
Computer integrated documentation
[NASA-TM-103870] N92-11673
ARTIFICIAL SATELLITES
The notion of artificial satellites in the anisotropic gravitational field of a uniformly rotating solid Earth model. A second order analytical solution
[SER-C-357] N92-11072

ASHES
A study on the effects of Mt. Sakurajima's falling ash over crop and forest areas using image processing for LANDSAT-5, MOS-1, and Jafsa digital data N92-11497
ASPECT RATIO
Numerical and experimental studies of simulated toroidicity effects in a linear high-beta heliac N92-11827
ASSAYING
Calorimetry measurements in less than 20 minutes [DE91-017318] N92-11330
ASSEMBLY
Blind fastening apparatus [NASA-CASE-LAR-14542-1] N92-11354
ASTRODYNAMICS
Kinematics and dynamics of barred galaxies N92-11937
ASTRONOMICAL COORDINATES
Proceedings of the 127th Colloquium of the International Astronomical Union Reference Systems [AD-A240207] N92-11933
ASTRONOMICAL SPECTROSCOPY
Development of a high resolution liquid xenon imaging chamber for gamma-ray astronomy [NASA-CR-188994] N92-11332
ASTRONOMY
NSSDC data listing [NASA-TM-105010] N92-11921
Proceedings of the 127th Colloquium of the International Astronomical Union Reference Systems [AD-A240207] N92-11933
ASTROPHYSICS
The great observatories for space astrophysics [NASA-NP-128] N92-11066
Information technologies for astrophysics circa 2001 [NASA-CR-188868] N92-11936
OPAL opacities for astrophysical applications [DE91-016922] N92-11939
Modeling UV and x ray oxygen emission in astrophysical plasmas [DE91-016927] N92-11940
Cosmological structure formation [NASA-CR-189007] N92-11946
Non scale-invariant density perturbations from chaotic extended inflation [NASA-CR-189004] N92-11947
ASYMPTOTES
The strong coupling limit for polaron models [ETN-91-90163] N92-11757
ASYMPTOTIC SERIES
Layer tracking, asymptotics, and domain decomposition N92-11732
Interface conditions for domain decomposition with radical grid refinement N92-11733
Continuum damping of high mode number toroidal Alfven waves [DE91-018891] N92-11890
ATLANTIC OCEAN
Mariners Weather Log, Volume 35, Number 2, Spring 1991 [PB91-202572] N92-11592
ATMOSPHERIC ATTENUATION
Evaluation of atmospheric effects in high spectral resolution airborne images N92-11408
ATMOSPHERIC CHEMISTRY
Upper Atmosphere Research Satellite (UARS): A program to study global ozone change [NASA-TM-105100] N92-11067
Grassland/atmosphere response to changing climate: Coupling regional and local scales [DE91-016906] N92-11575
ATMOSPHERIC CIRCULATION
Energetics diagnosis of numerical simulation of atmospheric blocking [NASA-CR-183503] N92-11581
Optically thin cirrus clouds over oceans and possible impact on sea surface temperature of warm pool in western Pacific [NASA-TM-104550] N92-11600
A diagnostic study of the velocity structure of a meandering jet using a primitive equation model with dynamic mode initialization [AD-A240687] N92-11609
ATMOSPHERIC COMPOSITION
Grassland/atmosphere response to changing climate: Coupling regional and local scales [DE91-016906] N92-11575
Scientific assessment of stratospheric ozone: 1989, volume 1 [NASA-TM-105116] N92-11576
Scientific assessment of stratospheric ozone: 1989. Volume 2: Appendix: AFEAS report [NASA-TM-105117] N92-11577
Processes for identifying regional influences of and responses to increasing atmospheric CO2 and climate change: The MINK Project [DE91-018601] N92-11579
Processes for identifying regional influences of and responses to increasing atmospheric CO2 and climate change: The MINK Project [DE91-018604] N92-11580
ATMOSPHERIC CORRECTION
Comparison of atmospheric correction procedures for visible and near-IR satellite sensor output N92-11395
Atmospheric correction in the thermal infrared: AVHRR case N92-11398
Estimation of the aerosol optical thickness from broadband turbidity measurements: Application to the atmospheric correction of SPOT images N92-11399
Atmospheric correction of satellite borne imagery investigated by means of a sensitivity analysis of the entire remote sensing process N92-11400
Use of operation ART-SPOT to test the 5S model and the MTF of the SPOT N92-11403
Comparison of in situ, aircraft- and satellite-derived surface reflectances in Flevoland (Netherlands) N92-11404
Routine mapping of vegetation index with the AVHRR of NOAA11 N92-11405
Correction of atmospheric and topographic effects in LANDSAT TM images N92-11407
Evaluation of atmospheric effects in high spectral resolution airborne images N92-11408
Suppression of aerosols on LANDSAT thematic mapper imagery N92-11411
TIMS calibration correction by comparison with PRT5 N92-11412
Radiometric and atmospheric correction procedures for AVHRR preprocessing in the solar reflective channels N92-11414
Comparison of two atmospheric correction models for a vegetated Airborne Visible/Infrared Imaging Spectrometer (AVIRIS) scene N92-11415
Iterative procedures for atmospheric correction N92-11417
Use of high spectral resolution airborne visible/infrared imaging spectrometer data for geologic mapping: An overview N92-11420
ATLAS: An Auto-Tracking Land and Atmosphere Sensor for retrieval of atmospheric optical parameters and acquisition of bidirectional surface reflectance N92-11487
Physical Measurements and Signatures in Remote Sensing, volume 2 [ESA-SP-319-VOL-2] N92-11488
NOAA-AVHRR contribution to the analysis or urban heat islands N92-11495
NOAA-AVHRR NDVI temporal profile classification and sensitivity to land use and climatic conditions in temperate region N92-11525
ATMOSPHERIC DENSITY
Groves model accuracy study [AD-A240456] N92-11586
ATMOSPHERIC DIFFUSION
Evaluation of atmospheric effects in high spectral resolution airborne images N92-11408
ATMOSPHERIC EFFECTS
Physical Measurements and Signatures in Remote Sensing, volume 2 [ESA-SP-319-VOL-2] N92-11488
ATMOSPHERIC GENERAL CIRCULATION MODELS
Energetics diagnosis of numerical simulation of atmospheric blocking [NASA-CR-183503] N92-11581
ATMOSPHERIC MODELS
Modeling of visible and UV radiative transfer in the ocean-atmosphere system concepts, models, and programs N92-11396
Estimation of the aerosol optical thickness from broadband turbidity measurements: Application to the atmospheric correction of SPOT images N92-11399
A split-window method for obtaining crop temperatures N92-11410
Altitude dependence in a semi-analytical atmospheric code N92-11413
Comparison of two atmospheric correction models for a vegetated Airborne Visible/Infrared Imaging Spectrometer (AVIRIS) scene N92-11415
On the use of passive microwaves at 37 GHz N92-11461
Some examples of satellite data utilization for atmospheric modeling at medium scale N92-11503
Grassland/atmosphere response to changing climate: Coupling regional and local scales [DE91-016906] N92-11575
Processes for identifying regional influences of and responses to increasing atmospheric CO2 and climate change: The MINK Project [DE91-018601] N92-11579
Processes for identifying regional influences of and responses to increasing atmospheric CO2 and climate change: The MINK Project [DE91-018604] N92-11580
Groves model accuracy study [AD-A240456] N92-11586
ATMOSPHERIC MOISTURE
Determination of the in-flight spectral and radiometric characteristics of the Airborne Visible/Infrared Imaging Spectrometer (AVIRIS) N92-11397
Retrievals of column atmospheric water vapor, vegetation liquid water, and cloud cover fraction from AVIRIS data N92-11427
ATMOSPHERIC OPTICS
Multiangular approach to solution of atmosphere optics reverse problems N92-11478
ATMOSPHERIC PRESSURE
C-29A aircraft altimeter errors [AD-A240486] N92-11011
ATMOSPHERIC REFRACTION
Acoustic propagation at low altitude: Effects of atmospheric turbulence (Villeau (France) test) [ONERA-RT-15/3641-PY] N92-11588
ATMOSPHERIC SCATTERING
Design and operation of the GL/OPA mobile Doppler lidar [AD-A240257] N92-11231
ATMOSPHERIC SOUNDING
Space observation of the land-ocean-atmosphere system at high spectral resolution in the infrared: Perspectives and problems N92-11421
ATMOSPHERIC TEMPERATURE
Combined use of Earth observation satellite and meteorological satellite for crop assessment in semiarid environments N92-11494
A method for estimating missing hourly temperatures using daily maximum and minimum temperatures [AD-A240394] N92-11594
March AFB forecasting rules of thumb evaluation [AD-A240458] N92-11595
Short-term hourly temperature interpolation [AD-A240489] N92-11596
ATMOSPHERIC TURBULENCE
Acoustic propagation at low altitude: Effects of atmospheric turbulence (Villeau (France) test) [ONERA-RT-15/3641-PY] N92-11588
ATOMIC CLOCKS
Feasibility study on the Cold Hydrogen Maser (CHM) [NPL-QU-89] N92-11342
ATOMIC COLLISIONS
Collision integrals and high temperature transport properties for N-N, O-O, and N-O [NASA-CR-188907] N92-11770
ATOMIC EXCITATIONS
High I state population in O(7+) produced in ion-solid collisions [DE91-018169] N92-11904
ATOMIC SPECTRA
Studies on laser atomic spectroscopy [DE91-628172] N92-11349
ATOMIC STRUCTURE
OPAL opacities for astrophysical applications [DE91-016922] N92-11939
ATOMIZING
LOX/hydrogen coaxial injector atomization test program N92-11121
ATOMS
Novel nonlinear laser diagnostic techniques [AD-A240193] N92-11346
Matter-wave interferometry with laser cooled atoms [AD-A240531] N92-11776
Control of electron transfer rates by motions of atoms and molecules [DE91-018575] N92-11777
ATTENUATION
The use of a time-resolved lidar to study the water column N92-11548
ATTITUDE (INCLINATION)
Tilted resonator experiments on a quasioptical gyrotron [AD-A240680] N92-11335
Attitude identification for SCOLE using two infrared cameras [NASA-CR-4397] N92-11338
ATTITUDE CONTROL
Precision pointing control of the spinning Gravity Probe B spacecraft N92-11068
Attitude control of flexible structures [AD-A240520] N92-11082
Leveling of the AMBLER walking machine: A comparison of methods [NASA-CR-189015] N92-11358
ATTITUDE INDICATORS
Pinhole cameras as sensors for atomic oxygen in orbit; application to attitude determination of the LDEF N92-11078

AUDIO EQUIPMENT
An efficient A* stack decoder algorithm for continuous speech recognition with a stochastic language model
[AD-A240745] N92-11683
AUDITORY PERCEPTION
The hazard of exposure to impulse noise as a function of frequency, volume 2
[AD-A240530] N92-11762
AUGMENTATION
Erosive augmentation of solid propellant burning rate: Motor size scaling effect N92-11125
AUTOCORRELATION
First-passage problems: A probabilistic dynamic analysis for degraded structures
[NASA-TM-103755] N92-11373
AUTOMATIC CONTROL
Automatic tools for microprocessor failure analysis N92-11265
Pilot's Automated Weather Support System (PAWSS) concepts demonstration project. Phase 1: Pilot's weather information requirements and implications for weather data systems design
[NASA-CR-188228] N92-11593
Issues in parallel automatic differentiation
[DE91-017311] N92-11726
AUTOMATIC TEST EQUIPMENT
Automatic generation of microprocessor test programs N92-11256
Hardware and software tools for microprocessor functional test N92-11257
Taking into account asynchronous signals in functional test of complex circuits N92-11259
A microprocessor test approach allowing fault localisation N92-11261
Towards an automated system for the verification and diagnosis of intelligent VLSI circuits N92-11262
A method and tools for microprocessor validation: High safety function applications N92-11263
AUTOMOBILE FUELS
Alternative fuels for heavy duty engines: Status of fleet trials
[DE91-018474] N92-11210
AUTOMOBILES
Component cost analysis for compressed natural gas vehicles
[DE91-017230] N92-11353
Effect of gasoline octane quality on vehicle acceleration performance
[AD-A240433] N92-11357
AUTONOMIC NERVOUS SYSTEM
Non-invasive evaluation of the cardiac autonomic nervous system by PET
[DE91-018476] N92-11622
AVIATION METEOROLOGY
Pilot's Automated Weather Support System (PAWSS) concepts demonstration project. Phase 1: Pilot's weather information requirements and implications for weather data systems design
[NASA-CR-188228] N92-11593
AVIONICS
Advanced information processing system for advanced launch system: Avionics architecture synthesis
[NASA-CR-187554] N92-11704
Advanced information processing system for advanced launch system: Hardware technology survey and projections
[NASA-CR-187555] N92-11705
AXISYMMETRIC FLOW
A Newton's method solver for the two-dimensional and axisymmetric Navier-Stokes equations N92-11292
Motion of charged particle in helical systems N92-11847
AZIMUTH
A thinned high frequency linear antenna array to study ionospheric structure
[AD-A240764] N92-11243

B

BACILLUS
Time-resolved analytical pyrolysis mass spectrometry of biomaterials
[AD-A240624] N92-11167
BACKGROUND RADIATION
Underlying generation mechanisms for the extragalactic gamma ray background and their implications for high-resolution gamma ray cosmology N92-11959
BACKSCATTERING
Modeling of radar backscattering from the sea surface using polarimetric-SAR observations N92-11442
Dual-polarized scatterometer measurements of wind and mechanically generated waves in a very large wind/wave flume, the VIERS-1 project N92-11443
Multifrequency radar measurements of potato, beet, and wheat during the AGRISCATT-88 campaign in the Netherlands N92-11444
Radar image simulation to study the visual aptitude of observing slope and roughness effects N92-11446
Generalized formulation for semi-empirical radar models representing crop backscattering N92-11447
Contribution of active microwaves to the structural analysis of epicontinental shelf-forms: Example of the English Channel N92-11448
Dual polarization microwave backscatter signatures of bare and vegetated soils N92-11452
Humidity measurement of naked ground by radar in conditions of excessive water N92-11453
Evaluation of vegetation cover characteristics using an airborne microwave scatterometer N92-11456
Quantitative ray methods for scattering of sound by spherical shells
[AD-A240255] N92-11761
BACKWARD FACING STEPS
A detailed investigation of staged normal injection into a Mach 2 flow N92-11118
BACTERIA
Biochemical and biophysical studies of the E. coli respiratory chain
[DE91-016966] N92-11612
BACTERIOLOGY
Biochemical and biophysical studies of the E. coli respiratory chain
[DE91-016966] N92-11612
BAFFLES
Stray light reduction in a WFOV star tracker lens
[DE91-018460] N92-11794
BALANCE
Further developments relating to the NASA Langley Research Center 13-inch magnetic suspension and balance system
[NASA-CR-188995] N92-11023
BALLOON FLIGHT
Engineering and instrumentation support of GL Research Balloon Program
[AD-A240616] N92-10987
BALLOON-BORNE INSTRUMENTS
Engineering and instrumentation support of GL Research Balloon Program
[AD-A240616] N92-10987
BALLOONING MODES
Plasma properties
[DE91-018913] N92-11891
BAND STRUCTURE OF SOLIDS
Alloy modeling and experimental correlation for ductility enhancement in near stoichiometric single crystal nickel aluminide
[AD-A240151] N92-11175
Positron lifetimes in solids from first principles calculations
[DE92-000088] N92-11781
BARIUM
High-T sub c fluorine-doped YBa2Cu3O(y) films on ceramic substrates by screen printing
[NASA-TM-105296] N92-11188
BARIUM OXIDES
Neutron diffraction from the flux line lattice
[DE91-018175] N92-11906
BARLEY
Feasibility of the red edge index for the detection of nitrogen deficiency N92-11425
BARRED GALAXIES
Kinematics and dynamics of barred galaxies N92-11937
BARYONS
Theoretical interpretation of high-energy nuclear collisions
[DE91-016965] N92-11782
Superfluid-like turbulence in cosmology
[NASA-CR-189011] N92-11942
Cosmological structure formation
[NASA-CR-189007] N92-11946
BAYES THEOREM
Conditional event algebras: Two new characterizations and their relations to Bayesian analysis
[AD-A240378] N92-11738
BAYS (STRUCTURAL UNITS)
The microgravity environment of the Space Shuttle Columbia payload bay during STS-32
[NASA-TP-3141] N92-11931
BEAM INJECTION
Review of CHS experiment N92-11823
Diverted particle-flux studies in the IMS and Proto-Cleo stellarators N92-11825
Electron temperature measurements on ATF using electron cyclotron emission N92-11849
Confinement studies of Heliotron E plasmas in magnetic surface variation experiments N92-11850
Transport study of ECH and NBI plasmas in CHS N92-11857
A study of radiation collapse in CHS plasmas N92-11859
Driven currents in neutral beam heated plasma N92-11861
NBI system with negative ion source in large helical device N92-11870
A simulation study of interactions of Space-Shuttle generated electron beams with ambient plasma and neutral gas
[NASA-CR-189025] N92-11898
BEAMS (RADIATION)
Schlieren system for visualizing the flow within a pipe of circular cross-section
[NASA-CASE-LAR-13944-1] N92-11336
BEAMS (SUPPORTS)
Studies in the form of finite element mass matrices for beams, plates and shells
[AERO-TN-9101] N92-11369
Nonlinear aspects of aerospace structures at high excitation levels flat aluminum beams and plates studied
[AD-A240600] N92-11383
BERYLLIUM ISOTOPES
The interactions of atmospheric cosmogenic radionuclides with spacecraft surfaces N92-11075
BERYLLIUM OXIDES
Physicochemical properties and dissolution in simulated biological fluids of particles of beryllium-powered rocket motor exhaust and pure beryllium oxides calcined at low and high temperature
[AD-A240288] N92-11134
BESSEL FUNCTIONS
Computer program for Bessel and Hankel functions
[NASA-TM-105154] N92-11691
Portable vectorized software for Bessel function evaluation
[PB91-216598] N92-11727
BIAS
Technique for calibrating angular measurement devices when calibration standards are unavailable
[NASA-TM-104148] N92-11340
BIBLIOGRAPHIES
Aeronautical engineering: A continuing bibliography with indexes (supplement 270)
[NASA-SP-7037(270)] N92-10973
Aeronautical engineering: A continuing bibliography with indexes (supplement 269)
[NASA-SP-7037(269)] N92-10974
Magnetic suspension and balance systems: A comprehensive, annotated bibliography
[NASA-TM-4318] N92-11030
A bibliography of planetary geology and geophysics principal investigators and their associates, 1990-1991
[NASA-TM-4299] N92-11929
BIG BANG COSMOLOGY
On the evolution of a superconducting cosmic string network
[DE91-630995] N92-11948
BINARY ALLOYS
Characterization of rare earth permanent magnets
[DE91-017010] N92-11754
BINARY DATA
On the capacity region for deterministic two-way channels and write-unidirectional memories
[ETN-91-90147] N92-11684
BINARY FLUIDS
Heat exchanger thermal performance for two nonazeotropic refrigerant mixtures
[DE91-017250] N92-11216
BIOCHEMISTRY
Time-resolved analytical pyrolysis mass spectrometry of biomaterials
[AD-A240624] N92-11167
Biochemical and biophysical studies of the E. coli respiratory chain
[DE91-016966] N92-11612
BIODYNAMICS
Theory and modeling in GLOBEC: A first step N92-11602
BIOLOGICAL EFFECTS
Biological effects of minerals
[DE91-018183] N92-11615
Extra-corporeal blood access, sensing, and radiation methods and apparatuses
[NASA-CASE-MSC-21775-1] N92-11627
Cellular repair/misrepair track model
[NASA-TP-3124] N92-11685
BIOLOGICAL MODELS (MATHEMATICS)
Spectral estimates of PAR interception and biomass production of irrigated rice crops. 1: Model elaboration with ground data N92-11522
BIOMASS
Assessment of the effect of specular reflectance on the relationships between vegetation indices and biomass N92-11483
Airborne passive microwave remote sensing of land and water surface N92-11492

Combined use of Earth observation satellite and meteorological satellite for crop assessment in semiarid environments N92-11494
Spectral estimates of PAR interception and biomass production of irrigated rice crops. 2: Model validation with SPOT data N92-11510
Spectral estimates of PAR interception and biomass production of irrigated rice crops. 1: Model elaboration with ground data N92-11522
From evapotranspiration to soil moisture investigation based on NOAA thermal infrared data, case study: Poland N92-11531

BIOPHYSICS
Biochemical and biophysical studies of the E. coli respiratory chain
[DE91-016966] N92-11612
JPRS report: Science and technology. USSR: Life sciences
[JPRS-ULS-91-017] N92-11616

BIOSPHERE
Biospheric models, measurements, and remote sensing of vegetation N92-11550
Use of multitemporal SPOT data in first ISLSCP field experiment N92-11554

BIOTECHNOLOGY
JPRS report: Science and technology. USSR: Life sciences
[JPRS-ULS-91-015] N92-11610
The 4th International Workshop on Membrane Biotechnology and Membrane Diomaterials
[AD-A240481] N92-11614
JPRS report: Science and technology. USSR: Life sciences
[JPRS-ULS-91-017] N92-11616
Rapidly quantifying the relative distention of a human bladder
[NASA-CASE-LAR-13901-2] N92-11621

BIPOLAR TRANSISTORS
Insulated Gate Bipolar Transistors (IGBT) modelization for circuit simulation and utilization in pulse modulated inverters
[ETN-91-90149] N92-11279

BLADDER
Rapidly quantifying the relative distention of a human bladder
[NASA-CASE-LAR-13901-2] N92-11621

BLADE TIPS
Experimental study of an independently deflected wingtip mounted on a semispan wing
[NASA-TM-102842] N92-10983
High pressure turbine blade life extension
[AD-A240654] N92-11180

BLOCKING
Energetics diagnosis of numerical simulation of atmospheric blocking
[NASA-CR-183503] N92-11581

BLOOD
Extra-corporeal blood access, sensing, and radiation methods and apparatuses
[NASA-CASE-MSC-21775-1] N92-11627

BLOOD COAGULATION
The 4th International Workshop on Membrane Biotechnology and Membrane Diomaterials
[AD-A240481] N92-11614

BLOWING
Experimental investigation of the effects of blowing on bursting of strake vortices
[AD-A240256] N92-10985

BODIES OF REVOLUTION
Calculation of general shells of revolution, using a semi analytical process
[ILR-MITT-262(1991)] N92-11386

BODY CENTERED CUBIC LATTICES
Moisture-induced environmental embrittlement of ordered intermetallic alloys at ambient temperatures
[DE91-018852] N92-11183

BODY FLUIDS
Physicochemical properties and dissolution in simulated biological fluids of particles of beryllium-powered rocket motor exhaust and pure beryllium oxides calcined at low and high temperature
[AD-A240288] N92-11134

BODY-WING CONFIGURATIONS
Aerothermal test results from the first flight of the Pegasus air-launched space booster
[NASA-TM-4330] N92-11301

BOEING 757 AIRCRAFT
Parameter identification studies on the NASA/Ames Research Center Advanced Concepts Flight Simulator
[NASA-TM-105126] N92-11024

BOEING 767 AIRCRAFT
Parameter identification studies on the NASA/Ames Research Center Advanced Concepts Flight Simulator
[NASA-TM-105126] N92-11024

BOLTZMANN TRANSPORT EQUATION
Diffusion in the Io plasma torus and its relation to the torus spatial structure N92-11949

BOND GRAPHS
Modeling of flexible polyarticulate chains: Bibliographic synthesis
[CERT-DERA-1/7735] N92-11927

BONES
Training, muscle fatigue and stress fractures
[AD-A240386] N92-11626

BOOLEAN ALGEBRA
Calculating the bidirectional reflectance of natural vegetation covers using Boolean models and geometric optics N92-11486
Conditional event algebras: Two new characterizations and their relations to Bayesian analysis
[AD-A240378] N92-11738

BOSONS
Critical properties of strongly interacting bosons on a lattice
[DE91-016926] N92-11771
Cosmological constraints on pseudo-Nambu-Goldstone bosons
[NASA-CR-189010] N92-11943

BOUNDARY CONDITIONS
Determination of nonstationary temperatures in high-stressed elements with pulsed heat sources
[DE91-635705] N92-11325
Proceedings for the ICASE Workshop on Heterogeneous Boundary Conditions
[NASA-CR-187630] N92-11728
One-way nesting for a primitive equation ocean model N92-11734

BOUNDARY INTEGRAL METHOD
A new technique for simulating composite material
[NASA-CR-188792] N92-11140

BOUNDARY LAYER CONTROL
Results from computational analysis of a mixed compression supersonic inlet
[NASA-TM-104475] N92-10976

BOUNDARY LAYER FLOW
Modeling of the heat transfer in bypass transitional boundary-layer flows
[NASA-TP-3170] N92-11299
Studies of aerothermal loads generated in regions of shock/shock interaction in hypersonic flow
[NASA-CR-181893] N92-11319

BOUNDARY LAYER STABILITY
Secondary instability of the three dimensional laminar boundary layer in incompressible flow: Description of the calculation code
[CERT-RT-63/5618-54] N92-11306

BOUNDARY LAYER TRANSITION
Modeling of the heat transfer in bypass transitional boundary-layer flows
[NASA-TP-3170] N92-11299
Secondary instability of the three dimensional laminar boundary layer in incompressible flow: Description of the calculation code
[CERT-RT-63/5618-54] N92-11306
Perfect compressible two dimensional boundary layer strong fluid coupling in the case of sharp leading edge profiles. Unsteady case of isolated profiles and steady case of blade grids
[ONERA-RT-43/1621-RY-006-R] N92-11311

BOUNDARY LAYERS
A grid-free method for high Reynolds number flow around an immersed elastic structure
[AD-A240048] N92-10984
Layer tracking, asymptotics, and domain decomposition N92-11732

BOUNDARY VALUE PROBLEMS
Multi-resolution analysis for ENO schemes
[NASA-CR-189043] N92-11736

BRAIN
PET studies of components of high-level vision
[AD-A240202] N92-11624

BREADBOARD MODELS
Development of a ninety string solar array simulator
[NASA-TM-105278] N92-11086

BRIGHTNESS TEMPERATURE
TIMS calibration correction by comparison with PRT5 N92-11412

BROADBAND
The design of broadband radar absorbing surfaces
[AD-A240521] N92-11235

BROKEN SYMMETRY
Cosmological constraints on pseudo-Nambu-Goldstone bosons
[NASA-CR-189010] N92-11943

BROWNIAN MOVEMENTS
Light scattering experiments on Brownian motion in shear flow and in colloidal crystals
[ETN-91-90134] N92-11756

BUBBLES
Local interfacial area concentration measurement in bubbly flow
[DE91-018702] N92-11322
A survey of scattering, attenuation, and size spectra studies of bubble layers and plumes beneath the air-sea interface
[AD-A240262] N92-11606

BUCKLING
Delamination propagation in a composite panel under compressive stress
[ONERA-RT-23/3542-RY-093-R] N92-11146
Buckling values and optimization of carbon fiber reinforced compression chord plates with rectangular stringers
[ILR-MITT-259(1991)] N92-11148

BUDGETING
The Space Shuttle: An attempt at low-cost, routine access to space
[AD-A240589] N92-11037

BURNING RATE
Erosive augmentation of solid propellant burning rate: Motor size scaling effect N92-11125

BURSTS
Scattering of tone bursts from spherical shells: Computations based on Fourier transform method
[AD-A240642] N92-11764

BYPASSES
Modeling of the heat transfer in bypass transitional boundary-layer flows
[NASA-TP-3170] N92-11299

C

C BAND
Estimation of the ground humidity under vegetation: Applications of semi-empirical models N92-11445
Active microwave remote sensing and ground hydric state. Agriscatt '88 airborne campaign over the Orgeval basin (France) N92-11454

CADMIUM COMPOUNDS
Solid lubricants on pretreated surfaces
[NASA-CASE-LEW-14474-2] N92-11186

CALIBRATING
Calibration of turbine flowmeters for storable bipropellant engines
[NAL-TR-1091] N92-11127
Technique for calibrating angular measurement devices when calibration standards are unavailable
[NASA-TM-104148] N92-11340
Inter-calibrating of SPOT1-HRV, LANDSAT5-TM, and NOA11-AVHRR in the visible and near infrared field s N92-11401
Characterization of African desert sites for the relative calibrating of wide field satellite optical sensors N92-11402
Inflight calibration of channels 1 and 2 of AVHRR using desertic sites and clouds N92-11406
SPOT calibration on the test site La Crau (France) N92-11409
TIMS calibration correction by comparison with PRT5 N92-11412
In flight calibration of large field of view sensors at short wavelength using the Rayleigh scattering N92-11416
Spectroscopic analysis of imaging spectrometer data for classification purposes N92-11439
Observations of the Earth in polarized light from the US Space Shuttle N92-11485
A calibration of the Naval Postgraduate School middle ultraviolet spectrograph and an analysis of the OII 2470 A and OI 2972 A emissions obtained from mid-latitude rocket observations
[AD-A240686] N92-11587
Recent diamagnetic measurements of toroidal coil experiments on Heliotron E N92-11854

CALIFORNIA
Neotectonic studies of northern Baja California, Mexico, with LANDSAT thematic mapper and SPOT panchromatic imagery: Partitioning of dextral and extensional strain at the Pacific-North America plate boundary N92-11553
March AFB forecasting rules of thumb evaluation
[AD-A240458] N92-11595

CALIFORNIUM
Comparison between californium and cyclotron heavy ion tests N92-11266
Comparison between californium and cyclotron SEU tests N92-11267

CALORIMETERS
Calorimetry measurements in less than 20 minutes
[DE91-017318] N92-11330

CAMERAS
Attitude identification for SCOLE using two infrared cameras
[NASA-CR-4397] N92-11338

Stray light reduction in a WFOV star tracker lens
[DE91-018460] N92-11794

CANCELLATION
Pulse compression degradation due to open loop adaptive cancellation, part 1
[AD-A240552] N92-11238
Pulse compression degradation due to open loop adaptive cancellation, part 3
[AD-A240553] N92-11239

CANOPIES (VEGETATION)
Feasibility of the red edge index for the detection of nitrogen deficiency N92-11425
Modeling the behavior of a vegetation cover in the MIR, contribution of high spectral resolution N92-11434
Candidate high spectral resolution derivative indices for the prediction of crop cover N92-11435
Estimation of the ground humidity under vegetation: Applications of semi-empirical models N92-11445
Evaluation of vegetation cover characteristics using an airborne microwave scatterometer N92-11456
Passive microwave remote sensing of vegetation canopies: Experimental and modeling results N92-11460
Influence of the crop architecture parameters on crop BRDF: A Monte Carlo simulation N92-11465
A three dimensional radiative transfer method for optical remote sensing of vegetated land surfaces N92-11466
Anisotropy of thermal infrared exitance above and within plant canopies N92-11467
Measurement, simulation, and analysis of the directional reflectance properties of Earth surface materials N92-11468
The effect of the distribution of chlorotic material on the reflectance of mixed canopies N92-11472
Vegetation canopies and objects of arbitrary shapes: Computer generation and bidirectional reflectance calculations N92-11475
Monte Carlo model for transport equation in a plant canopy and its inversion N92-11481
Specular and diffuse components of plant canopy reflectance at the wavelengths of 550 and 630 nm N92-11484
Calculating the bidirectional reflectance of natural vegetation covers using Boolean models and geometric optics N92-11486
Integration of qualitative knowledge on operational models for following vegetation using temporal series of remote sensing images N92-11502
Construction of ground cover charts of a wheat canopy from reflectance measurements N92-11505
Using the radiative surface temperature in energy budget studies over plant canopies N92-11506
An integrated modelling approach for the spectral identification of crops N92-11508
Calibration and validation of a surface flux model in the framework of the HAPEX-MOBILHY experiment. Application to estimating the cover resistance N92-11511
A simple model of canopy fluorescence N92-11543
Modeling of fluorescence light-canopy interaction N92-11545
View-atmosphere-soil effects on vegetation indices derived from SPOT images N92-11552

CAPACITANCE
On the nature of bulk electrical relaxation in silicate glasses
[DE92-000077] N92-11206
Advanced Langmuir Probe (LP)
[NASA-CR-180084] N92-11284

CAPACITORS
Design of a fast computer-based partial discharge diagnostic system
[NASA-CR-189057] N92-11272

CARBIDES
Contact angle and work of adhesion between Ni-based melts and non-metallic solids
[NPL-DMM(A)-23] N92-11171

CARBON
Effects of hydrogen and carbon on thermally activated deformation in nickel
[AD-A240496] N92-11178
Report on carbon and nitrogen abundance studies
[NASA-CR-188803] N92-11934

CARBON DIOXIDE
Nuclear rocket using indigenous Martian fuel NIMF N92-11098

CARBON DIOXIDE CONCENTRATION
Grassland/atmosphere response to changing climate: Coupling regional and local scales
[DE91-016906] N92-11575
Processes for identifying regional influences of and responses to increasing atmospheric CO2 and climate change: The MINK Project
[DE91-018601] N92-11579
Processes for identifying regional influences of and responses to increasing atmospheric CO2 and climate change: The MINK Project
[DE91-018604] N92-11580

CARBON DIOXIDE LASERS
CO2 laser active remote sensing from 9 to 11 microns: Airborne and laboratory application N92-11535

CARBON FIBERS
Buckling values and optimization of carbon fiber reinforced compression chord plates with rectangular stringers
[ILR-MITT-259(1991)] N92-11148

CARBON ISOTOPES
Studies of the physical and chemical stability of natural sea-surface films
[AD-A239818] N92-11604

CARBON-CARBON COMPOSITES
Fracture toughness of carbon/carbon composites
[AD-A240200] N92-11143
Critical appraisal of the McDonnell Douglas closure model for predicting fatigue crack growth
[ARL-STRUC-R-444] N92-11376

CARDIOLOGY
Non-invasive evaluation of the cardiac autonomic nervous system by PET
[DE91-018476] N92-11622

CARRIER DENSITY (SOLID STATE)
Micro photoreflectance semiconductor wafer analyzer
[AD-D014950] N92-11788

CARRIER FREQUENCIES
Dual frequency optical carrier technique for transmission of reference frequencies in dispersive media
[NASA-CASE-NPO-18007-1-CU] N92-11791

CARTESIAN COORDINATES
Solving the shallow water equations on the Cray X-MP/48 and the connection machine 2
[NASA-CR-188897] N92-11658

CASSINI MISSION
Mapping photopolarimeter spectrometer instrument feasibility study for future planetary flight missions
[NASA-CR-189242] N92-11329

CATALOGS (PUBLICATIONS)
Catalog of space shuttle earth observations handheld photography. Space transportation system 37 (STS-37) mission dates: April 5-11, 1991
[NASA-CR-189014] N92-11561

CATALYSTS
Conversion of ethane and of propane to higher olefin hydrocarbons
[DE91-016896] N92-11160
Surface analysis of catalysts by low-energy ion scattering
[ETN-91-90133] N92-11913

CATALYTIC ACTIVITY
Photoemission study of Ce/Ta(110) and Ce/W(110) interfaces and the catalytic oxidation effect
[DE91-018167] N92-11903

CATIONS
High-T sub c fluorine-doped YBa2Cu3O(y) films on ceramic substrates by screen printing
[NASA-TM-105296] N92-11188

CAVITATION FLOW
Thermal behavior of the SHOOT gallery arm
[CD-21] N92-11296

CEILINGS (METEOROLOGY)
March AFB forecasting rules of thumb evaluation
[AD-A240458] N92-11595

CELESTIAL MECHANICS
The notion of artificial satellites in the anisotropic gravitational field of a uniformly rotating solid Earth model. A second order analytical solution
[SER-C-357] N92-11072
Proceedings of the 127th Colloquium of the International Astronomical Union Reference Systems
[AD-A240207] N92-11933

CELL MEMBRANES (BIOLOGY)
Effect of prolonged space flight on erythrocyte metabolism and membrane functional condition N92-11617

CELLS (BIOLOGY)
Cellular repair/misrepair track model
[NASA-TP-3124] N92-11685

CENTRIFUGAL CASTING
Centrifugal casting of composites
[AD-D014981] N92-11144

CERAMIC NUCLEAR FUELS
A cermet fuel reactor for nuclear thermal propulsion N92-11096
Dumbo: A pachydermal rocket motor N92-11100

CERAMICS
High-T sub c fluorine-doped YBa2Cu3O(y) films on ceramic substrates by screen printing
[NASA-TM-105296] N92-11188

CEREBRAL CORTEX
PET studies of components of high-level vision
[AD-A240202] N92-11624

CERIUM
Photoemission study of Ce/Ta(110) and Ce/W(110) interfaces and the catalytic oxidation effect
[DE91-018167] N92-11903

CERMETS
A cermet fuel reactor for nuclear thermal propulsion N92-11096
Dumbo: A pachydermal rocket motor N92-11100

CHANGE DETECTION
A hybrid methodology for detecting cartographically significant features using LANDSAT TM imagery
[AD-A240454] N92-11563

CHANNEL FLOW
Heat transfer in channels with uniformly swirled flow
[DE91-635594] N92-11324

CHAPMAN-ENSKOG THEORY
Diffusion in the Io plasma torus and its relation to the torus spatial structure N92-11949

CHARGE COUPLED DEVICES
Limits of energy dissipation for x ray sensitive pn Charge Coupled Devices (CCDs)
[MPE-224] N92-11280
Diffusion and drift of charges in semiconductor detectors
[MBE-225] N92-11281
Illumination, optics, and retroreflectors for efficient landmark tracking N92-11790

CHARGE DISTRIBUTION
Diffusion and drift of charges in semiconductor detectors
[MBE-225] N92-11281
A synchronization and charge distribution process for the parallel multilevel logic simulation
[ETN-91-90152] N92-11708

CHARGE EXCHANGE
Numerical analysis of temporal development of RF-heated plasma N92-11834

CHARGED PARTICLES
Motion of charged particle in helical systems N92-11847

CHARGING
Nonaqueous secondary batteries
[DE91-017788] N92-11282

CHARRING
Evaluation of Kapton pyrolysis, arc tracking, and arc propagation on the Space Station Freedom (SSF) solar array Flexible Current Carrier (FCC)
[NASA-CR-189056] N92-11139

CHARTS
The electronic aeronautical chart for general aeronautics: A system specification
[ILR-MITT-263(1991)] N92-10997

CHEBYSHEV APPROXIMATION
Optimal Chebyshev polynomials on ellipses in the complex plane
[NASA-CR-188836] N92-11722
New Bernstein type inequalities for polynomials on ellipses
[NASA-CR-186626] N92-11724
A theory of the earth's precession relative to the invariable plane of the solar system N92-11938

CHECKOUT
Technology readiness assessment of advanced space engine integrated controls and health monitoring
[NASA-TM-105255] N92-11130

CHEMICAL ANALYSIS
New dimensions in atom probe analysis
[DE91-018926] N92-11779

CHEMICAL COMPOSITION
Laser Raman diagnostics in subsonic and supersonic turbulent jet diffusion flames N92-11159
Glass formation, properties, and structure of soda-yttria-silicate glasses
[NASA-TM-104488] N92-11202
Continuum x ray gauging of multiple-element materials
[DE91-017429] N92-11368
Observation of DOM composition by synchronous fluorescence spectroscopy N92-11549
Surface analysis of catalysts by low-energy ion scattering
[ETN-91-90133] N92-11913

CHEMICAL PROPERTIES
Physicochemical properties and dissolution in simulated biological fluids of particles of beryllium-powered rocket motor exhaust and pure beryllium oxides calcined at low and high temperature
[AD-A240288] N92-11134
Magnetic fluids and their applications
[DE92-704012] N92-11326
Synthesis of novel conducting solids
[AD-A240468] N92-11912

CHEMICAL PROPULSION
Nuclear thermal propulsion program overview N92-11089
Hybrid propulsion systems for space exploration missions N92-11097

CHEMICAL REACTIONS
Conversion of ethane and of propane to higher olefin hydrocarbons
[DE91-016896] N92-11160
Study of silanization of silica and fiberglass using ESR spectroscopy and spin labelling
[AD-A240767] N92-11197
Diphenylmethane-containing dianhydride and polyimides prepared therefrom
[NASA-CASE-LAR-14487-1] N92-11200
Chemical reactivity and electronic structure of silicon microclusters
[AD-A240276] N92-11908
Structure of the Si45 cluster
[AD-A240278] N92-11909
CHLORINE COMPOUNDS
High density energetic materials
[AD-D014959] N92-11212
CHLOROCARBONS
Scientific assessment of stratospheric ozone: 1989. Volume 2: Appendix: AFEAS report
[NASA-TM-105117] N92-11577
CHLOROFORMATE
High density energetic materials
[AD-D014959] N92-11212
CHLOROPHYLLS
Phenological changes in the red edge shift of Norway spruce needles and their relationship to needle chlorophyll content N92-11423
Design and testing of a spectral-resolving fluorescence lidar system for remote sensing of vegetation N92-11540
Laser-induced blue fluorescence and red chlorophyll fluorescence signatures of differently pigmented leaves N92-11541
The laser-induced chlorophyll fluorescence ratio F690/F735 of spruce needles and beech leaves during the course of a year N92-11542
(L)EAF: A remote sensing fluoresensor N92-11546
Laser induced fluorescence of growing camphor tree leaves: Influence of chlorophyll content on LIF spectral signature N92-11547
CHOLESKY FACTORIZATION
Efficient ICCG on a shared memory multiprocessor
[NASA-CR-188843] N92-11693
CHROMIUM STEELS
Creep response of a 9Cr-1Mo-V-Nb steel to varying stresses and temperatures
[DE91-017871] N92-11181
CIRCLES (GEOMETRY)
Circular Statistical methods: Applications in spatial and temporal performance analysis
[AD-A240751] N92-11749
CIRCUIT PROTECTION
New insulation constructions for aerospace wiring applications. Volume 2: The 270 VDC arc tracking testing with power controllers
[AD-A240639] N92-11007
CIRCUITS
Communications interface and system for radiation recovery of a microprocessor portion thereof
[AD-D014977] N92-11245
Taking into account asynchronous signals in functional test of complex circuits N92-11259
Automatic tools for microprocessor failure analysis N92-11265
Circuit probing system
[AD-D014966] N92-11277
Insulated Gate Bipolar Transistors (IGBT) modelization for circuit simulation and utilization in pulse modulated inverters
[ETN-91-90149] N92-11279
Acoustic transponder receiver circuit
[AD-D014965] N92-11760
Development of high Tc (greater than 110K) Bi, Tl and Y-based materials as superconducting circuit elements
[NASA-CR-188999] N92-11902
CIRCULAR PLATES
Approximate large deflection analysis of circular plates loaded symmetrically
[NPL-DMM(A)-25] N92-11370
CIRCULAR POLARIZATION
Polarized x ray absorption spectroscopy for the study of superconductors and magnetic materials
[DE91-017990] N92-11163
CIRRUS CLOUDS
Optically thin cirrus clouds over oceans and possible impact on sea surface temperature of warm pool in western Pacific
[NASA-TM-104550] N92-11600
CITIES
Evaluation of the quality of urban biotypes by remote sensing N92-11493
NOAA-AVHRR contribution to the analysis or urban heat islands N92-11495
Urban heat island N92-11500
Texture indices sensitivity to spatial and spectral resolutions in semi-urban environments N92-11519
CIVIL AVIATION
Personal air transport: State of the art
[PB91-204768] N92-10991
A systematic formulation, as an approach to air traffic
[MBB-Z-0371-91-PUB] N92-10996
CLASSIFICATIONS
Spectroscopic analysis of imaging spectrometer data for classification purposes N92-11439
Study of the spatial variability of the hydrodynamic behavior of grounds at the Niger (Africa) using satellite images N92-11515
CLAYS
Spectral identification (1.2-2.5 microns) and characterization of Paris (France) Basin kaolinite/smectite clays using a field spectrometer N92-11429
Field trip guidebook on environmental impact of clays along the upper Texas coast
[NASA-TM-105097] N92-11572
Biological effects of minerals
[DE91-018183] N92-11615
CLIMATE
NOAA-AVHRR NDVI temporal profile classification and sensitivity to land use and climatic conditions in temperate region N92-11525
Nonscanning climate sensor study
[NASA-CR-183506] N92-11589
Hourly and daily precipitation frequencies for the United States
[AD-A240746] N92-11599
NSSDC data listing
[NASA-TM-105010] N92-11921
CLIMATE CHANGE
Space observations for global change N92-11555
Greenhouse gas emissions and the developing countries: Strategic options and the USAID response
[PB91-209882] N92-11573
Grassland/atmosphere response to changing climate: Coupling regional and local scales
[DE91-016906] N92-11575
Processes for identifying regional influences of and responses to increasing atmospheric CO2 and climate change: The MINK Project
[DE91-018601] N92-11579
Processes for identifying regional influences of and responses to increasing atmospheric CO2 and climate change: The MINK Project
[DE91-018604] N92-11580
CLIMATOLOGY
Multidate analysis of NOAA-AVHRR data over France: Relationship with agroclimatic characteristics N92-11521
Night-time LANDSAT thermal infrared imagery as a tool for climatological studies N92-11526
Groves model accuracy study
[AD-A240456] N92-11586
Index and bulk parameters for frequency-direction spectra measured at CERC field research facility
[AD-A240320] N92-11607
Conditional climatology of Ap: The relationship between various solar events (surges, prominences, filaments, radio bursts, x ray episodes) and geomagnetic storms
[AD-A240457] N92-11958
CLOCKS
About time
[NASA-CR-188870] N92-11753
CLOSED CYCLES
Nuclear light bulb N92-11110
CLOUD COVER
Retrievals of column atmospheric water vapor, vegetation liquid water, and cloud cover fraction from AVIRIS data N92-11427
Catalog of space shuttle earth observations handheld photography. Space transportation system 37 (STS-37) mission dates: April 5-11, 1991
[NASA-CR-189014] N92-11561
Optically thin cirrus clouds over oceans and possible impact on sea surface temperature of warm pool in western Pacific
[NASA-TM-104550] N92-11600
CLOUD PHYSICS
Mesoscale prediction and satellite cloud analysis for advanced meteorological processing systems
[AD-A240510] N92-11597
CLOUDS
Inflight calibration of channels 1 and 2 of AVHRR using desertic sites and clouds N92-11406
Bi-directional reflectance of finite and infinite clouds N92-11470
CLOUDS (METEOROLOGY)
Estimation of the ground humidity under vegetation: Applications of semi-empirical models N92-11445
Generalized formulation for semi-empirical radar models representing crop backscattering N92-11447
CLUMPS
Chemical reactivity and electronic structure of silicon microclusters
[AD-A240276] N92-11908
Structure of the Si45 cluster
[AD-A240278] N92-11909
CLUSTER ANALYSIS
Classification of posture maintenance data with fuzzy clustering algorithms
[NASA-CR-188949] N92-11662
CLUTTER
Enhanced clutter suppression apparatus for use with an infrared search and surveillance system
[AD-D014984] N92-11247
CMOS
Case history: Failure analysis of a CMOS SRAM with an intermittent open contact
[DE91-018811] N92-11283
COASTAL WATER
Use of theoretical wave height distributions in directional seas
[AD-A240411] N92-11608
COATINGS
Nuclear fuels status N92-11113
Evaluation of Kapton pyrolysis, arc tracking, and arc propagation on the Space Station Freedom (SSF) solar array Flexible Current Carrier (FCC)
[NASA-CR-189056] N92-11139
The design of broadband radar absorbing surfaces
[AD-A240521] N92-11235
COBALT
The 23 to 300 C demagnetization resistance of samarium-cobalt permanent magnets
[NASA-TP-3119] N92-11252
CODING
The probability of multiple correct packet receptions in a multireceiver frequency-hopped spread-spectrum system
[AD-A240655] N92-11240
Fast algorithms for linear least-squares estimation of multi-dimensional random fields
[AD-A240249] N92-11675
COGNITION
Pictures and anaphora
[AD-A240153] N92-11631
Cognitive factors involved in the first stage of programming skill acquisition
[AD-A240566] N92-11636
COGNITIVE PSYCHOLOGY
Pictures and anaphora
[AD-A240153] N92-11631
Perception and memory of pictures
[AD-A240364] N92-11633
COLD FLOW TESTS
Viscous computations of cold air/air flow around scramjet nozzle afterbody
[NASA-CR-4406] N92-10982
COLD GAS
Feasibility study on the Cold Hydrogen Maser (CHM)
[NPL-QU-89] N92-11342
COLD PLASMAS
Confinement improvement by edge control N92-11817
A simulation study of interactions of Space-Shuttle generated electron beams with ambient plasma and neutral gas
[NASA-CR-189025] N92-11898
COLLAPSE
A study of radiation collapse in CHS plasmas N92-11859
COLLIMATION
Programmable beam transform and beam steering control system for a phased array radar antenna
[AD-D014970] N92-11230
COLLIMATORS
Schlieren system for visualizing the flow within a pipe of circular cross-section
[NASA-CASE-LAR-13944-1] N92-11336
COLLISION PARAMETERS
Collision integrals and high temperature transport properties for N-N, O-O, and N-O
[NASA-CR-188907] N92-11770
Meson-exchange calculation of the d(gamma,p)n in the GeV energy region
[DE91-017994] N92-11785
High I state population in O(7+) produced in ion-solid collisions
[DE91-018169] N92-11904
COLLISIONAL PLASMAS
Diffusion in the Io plasma torus and its relation to the torus spatial structure N92-11949
COLLOCATION
A Fourier collocation time domain method for numerically solving Maxwell's equations
[NASA-TM-104162] N92-11742

COLLOIDS
Studies of the physical and chemical stability of natural sea-surface films
[AD-A239818] N92-11604
Light scattering experiments on Brownian motion in shear flow and in colloidal crystals
[ETN-91-90134] N92-11756
Radiation induced growth of micro crystallites
[DE91-016516] N92-11900

COLOR
Effects on LDEF exposed copper film and bulk N92-11076
Moisture effects on spectral signatures and CIE-color of lateritic soils N92-11436
The effect of the distribution of chlorotic material on the reflectance of mixed canopies N92-11472
Influence of the viewing geometry on the spectral properties (high resolution visible and NIR) of selected soils from Arizona N92-11473

COLORIMETRY
Preliminary studies for automizing thermal flux measurement examination by thermosensitive coloring
[AAAF-NT-89-28] N92-11288

COLUMBIA (ORBITER)
The microgravity environment of the Space Shuttle Columbia middeck during STS-32
[NASA-TP-3140] N92-11930
The microgravity environment of the Space Shuttle Columbia payload bay during STS-32
[NASA-TP-3141] N92-11931

COMBUSTIBLE FLOW
Numerical simulation of the reactive flow in advanced (HSR) combustors using KIVA-2
[NASA-CR-188996] N92-11014
Navier-Stokes entropy controlled combustion instability analysis for liquid propellants N92-11122

COMBUSTION CHAMBERS
Numerical simulation of the reactive flow in advanced (HSR) combustors using KIVA-2
[NASA-CR-188996] N92-11014

COMBUSTION PHYSICS
JANNAF Combustion Instability Panel Workshop report: Numerical methods in combustion instability N92-11123
A systematic approach to combustion model reduction and lumping
[AD-A240195] N92-11164

COMBUSTION PRODUCTS
Toxicity assessment of combustion products in simulated space cabins N92-11619

COMBUSTION STABILITY
Navier-Stokes entropy controlled combustion instability analysis for liquid propellants N92-11122
JANNAF Combustion Instability Panel Workshop report: Numerical methods in combustion instability N92-11123
JANNAF Liquid Rocket Combustion Instability Panel research recommendations N92-11124
Numerical prediction of turbulent flame stability in premixed/prevaporized (HSCT) combustors
[NASA-CR-188991] N92-11161

COMMERCIAL AIRCRAFT
Program plan: National aging aircraft research program
[DOT/FAA/CT-88/32-1] N92-10992
Technology needs for high speed rotorcraft (3)
[NASA-CR-186433] N92-10999
Parameter identification studies on the NASA/Ames Research Center Advanced Concepts Flight Simulator
[NASA-TM-105126] N92-11024

COMMUNICATION NETWORKS
Telescience workstation
[NASA-CR-188878] N92-11033
Space Network Control (SNC) Conference on Resource Allocation Concepts and Approaches. Overview N92-11040
What we were asked to do N92-11041
Proposed planning and scheduling services for the SNC in the CDOS era N92-11043
An RF interference mitigation methodology with potential applications in scheduling N92-11044
Automated conflict resolution issues N92-11045
Effect of locus of resource control on operational efficiency in distributed operations N92-11046
The probability of multiple correct packet receptions in a multireceiver frequency-hopped spread-spectrum system
[AD-A240655] N92-11240
Communications interface and system for radiation recovery of a microprocessor portion thereof
[AD-D014977] N92-11245
Algebraic aspects of network reliability problems
[AD-A240365] N92-11748

COMMUNICATION SATELLITES
Basic concepts of low Earth orbit satellite systems for communications
[TELECOM-PARIS-91-D-001] N92-11248

COMPACTING
Strengthening of an AISI 1020 steel by aluminum-microalloying during liquid dynamic compaction
[DE91-018745] N92-11182

COMPARISON
Comparison of a new refiner with a conventional refiner N92-11156
Failure coverage of functional test methods: A comparative experimental evaluation N92-11255
Comparison between californium and cyclotron heavy ion tests N92-11266
Groves model accuracy study
[AD-A240456] N92-11586

COMPENSATORS
Linear quadratic servo control of a reusable rocket engine
[NASA-TM-105291] N92-11128

COMPILERS
ART/Ada design project, phase 1: Project plan
[NASA-CR-187313] N92-11663
ART/Ada design project, phase 1. Task 1 report: Overall design
[NASA-CR-188943] N92-11665
Distributed memory compiler methods for irregular problems: Data copy reuse and runtime partitioning
[NASA-CR-187635] N92-11669
Cedar Project: Original goals and progress to date
[DE92-000032] N92-11689
Optimal expression evaluation for data parallel architectures
[NASA-CR-187773] N92-11696

COMPLEX SYSTEMS
Analysis of experimental results on functional testing and diagnosis of complex circuits N92-11254
Taking into account asynchronous signals in functional test of complex circuits N92-11259
Fault localization when testing complex circuits N92-11260
A method and tools for microprocessor validation: High safety function applications N92-11263
Algebraic aspects of network reliability problems
[AD-A240365] N92-11748

COMPLEX VARIABLES
Optimal Chebyshev polynomials on ellipses in the complex plane
[NASA-CR-188836] N92-11722

COMPOSITE MATERIALS
A new technique for simulating composite material
[NASA-CR-188792] N92-11140
Numerical simulation of the degradation of the folds of a laminated composite structure. Study of the importance of residual firing constraints
[ONERA-RT-8/7256-RY-094-R] N92-11145
Damage evolution in filled elastomers
[AD-A240532] N92-11191

COMPOSITE STRUCTURES
New insulation constructions for aerospace wiring applications. Volume 1: Testing and evaluation
[AD-A240638] N92-11006
A new technique for simulating composite material
[NASA-CR-188792] N92-11140
Numerical simulation of the degradation of the folds of a laminated composite structure. Study of the importance of residual firing constraints
[ONERA-RT-8/7256-RY-094-R] N92-11145
Delamination propagation in a composite panel under compressive stress
[ONERA-RT-23/3542-RY-093-R] N92-11146
The behaviour of fire-exposed composite steel/concrete slabs
[ISBN-90-386-0031-3] N92-11147
User's manual for the Macintosh version of PASCO
[NASA-TM-104115] N92-11668

COMPRESSED GAS
Component cost analysis for compressed natural gas vehicles
[DE91-017230] N92-11353

COMPRESSIBILITY EFFECTS
On the basic equations for the second-order modeling of compressible turbulence
[NASA-TM-105277] N92-11302

COMPRESSIBLE FLOW
Perfect compressible two dimensional boundary layer strong fluid coupling in the case of sharp leading edge profiles. Unsteady case of isolated profiles and steady case of blade grids
[ONERA-RT-43/1621-RY-006-R] N92-11311
Layer tracking, asymptotics, and domain decomposition N92-11732

COMPRESSING
Polyimides with improved compression moldability
[NASA-CASE-LAR-14457-1-CU] N92-11198
Improved compression molding technology for continuous fiber reinforced composite laminates. Part 2: AS-4/Polyimidesulfone prepreg system
[NASA-TM-104133] N92-11207

COMPRESSION LOADS
Effects of elevated temperature on the viscoplastic modeling of graphite/polymeric composites
[NASA-TM-104160] N92-11149

COMPUTATION
Continuation of research into language concepts for the mission support environment
[NASA-CR-187818] N92-11652
The considering of the slowing down effect in the formalism of probability tables. Application to the effective cross section calculation
[DE91-626722] N92-11751
Calculation of magnetic field of helical coils
[NIFS-18] N92-11880
Information technologies for astrophysics circa 2001
[NASA-CR-188868] N92-11936

COMPUTATIONAL ASTROPHYSICS
Kinematics and dynamics of barred galaxies N92-11937
Neutron star magnetic fields and implications for pulsars and gamma ray bursts N92-11960

COMPUTATIONAL FLUID DYNAMICS
Viscous computations of cold air/air flow around scramjet nozzle afterbody
[NASA-CR-4406] N92-10982
Numerical simulation of the reactive flow in advanced (HSR) combustors using KIVA-2
[NASA-CR-188996] N92-11014
CFD code survey for thrust chamber application N92-11119
Numerical prediction of turbulent flame stability in premixed/prevaporized (HSCT) combustors
[NASA-CR-188991] N92-11161
The three-dimensional evolution of a plane mixing layer. Part 1: The Kelvin-Helmholtz roll-up
[NASA-TM-103856] N92-11303
Hydrodynamic design of generic pump components
[NASA-CR-184252] N92-11361
Proceedings for the ICASE Workshop on Heterogeneous Boundary Conditions
[NASA-CR-187630] N92-11728

COMPUTATIONAL GRIDS
A grid-free method for high Reynolds number flow around an immersed elastic structure
[AD-A240048] N92-10984
Three dimensional numerical method for resolving small transonic perturbations in unstructured mesh
[ONERA-RT-56/3064-RY-006-R] N92-10989
A new technique for simulating composite material
[NASA-CR-188792] N92-11140
Dispersion and stability of two electromagnetic solvers for triangular meshes
[DE91-016607] N92-11227
Domain-decomposed preconditionings for transport operators N92-11731
Interface conditions for domain decomposition with radical grid refinement N92-11733
Nested ocean models: Work in progress N92-11735
Multi-resolution analysis for ENO schemes
[NASA-CR-189043] N92-11736

COMPUTER AIDED DESIGN
Developments in REDES: The Rocket Engine Design Expert System N92-11120
VHDL simulation of the implementation of a costfunction circuit
[AD-A240430] N92-11278
Computers in aeronautics and space research at the Lewis Research Center
[NASA-TM-105096] N92-11642

COMPUTER AIDED MAPPING
Ground penetrating radar data acquisition system
[AD-A240765] N92-11244

COMPUTER AIDED TOMOGRAPHY
Supervoltage NDE techniques for large aerospace structures
[AD-A240625] N92-11365

COMPUTER ASSISTED INSTRUCTION
Cognitive factors involved in the first stage of programming skill acquisition
[AD-A240566] N92-11636

COMPUTER GRAPHICS
CHIMES-2: A tool for automated HCI analysis N92-11051
Network Control Center User Planning System (NCC UPS) N92-11053
SPIKE: AI scheduling techniques for Hubble Space Telescope N92-11054
Scheduling techniques in the Request Oriented Scheduling Engine (ROSE) N92-11058

Vegetation canopies and objects of arbitrary shapes: Computer generation and bidirectional reflectance calculations N92-11475
Robot graphic simulation testbed [NASA-CR-188998] N92-11637
Continuation of research into language concepts for the mission support environment [NASA-CR-187818] N92-11652
Workshops on Efficient Use of Scientific Computing [AD-A240175] N92-11674
Appearance simulator for computer vision research [AD-A240506] N92-11679
Education in computational science: Role of the National Laboratories [DE91-018823] N92-11687
Computer aided surface representation [DE91-018872] N92-11688
Studying parallel program behavior with upshot [DE91-019072] N92-11710
Extended algebraic graph transformation [ETN-91-90151] N92-11739

COMPUTER INFORMATION SECURITY
Threats and countermeasures for network security [NASA-CR-188883] N92-11645
Stopping computer crimes [NASA-CR-188896] N92-11657

COMPUTER NETWORKS
Telescience workstation [NASA-CR-188878] N92-11033
Threats and countermeasures for network security [NASA-CR-188883] N92-11645
ART-Ada design project, phase 2 [NASA-CR-188940] N92-11667
Education in computational science: Role of the National Laboratories [DE91-018823] N92-11687
Policy issues in interconnecting networks [NASA-CR-188844] N92-11694
Neural networks and MIMD-multiprocessors [NASA-CR-188481] N92-11697
Highly parallel computation [NASA-CR-188871] N92-11698
Total recall in distributive associative memories [NASA-CR-188884] N92-11699
Advanced information processing system for advanced launch system: Hardware technology survey and projections [NASA-CR-187555] N92-11705
Advanced information processing system: Inter-computer communication services [NASA-CR-187556] N92-11706
Learning to read aloud: A neural network approach using sparse distributed memory [NASA-CR-188846] N92-11711
Algebraic aspects of network reliability problems [AD-A240365] N92-11748
About time [NASA-CR-188870] N92-11753
An application for multi-person task synchronization [NASA-CR-187712] N92-11918

COMPUTER PROGRAM INTEGRITY
Methodology investigation. Phase 2: Software maturity model validation [AD-A231439] N92-11651

COMPUTER PROGRAMMING
LV software support for supersonic flow analysis [NASA-CR-188914] N92-10978
Experience with Acore: Implementing GHC with actors [AD-A231409] N92-11649
Modula-2*: An extension of Modula-2 for highly parallel programs [NASA-CR-188855] N92-11654
Computer integrated documentation [NASA-TM-103870] N92-11673
Workshops on Efficient Use of Scientific Computing [AD-A240175] N92-11674
Technology assessment of the Software Life Cycle Support Environment (SLCSE) [AD-A240673] N92-11682
Education in computational science: Role of the National Laboratories [DE91-018823] N92-11687
Ground Systems Development Environment (GSDE) interface requirements analysis [NASA-CR-188822] N92-11702
Extended algebraic graph transformation [ETN-91-90151] N92-11739
Issues in real-time data management [AD-A240712] N92-11926

COMPUTER PROGRAMS
Development of unsteady aerodynamic analyses for turbomachinery aeroelastic and aeroacoustic applications [NASA-CR-4405] N92-10979
Model representation in the PANCOR wall interference assessment code [NASA-TM-104152] N92-11022
Parameter identification studies on the NASA/Ames Research Center Advanced Concepts Flight Simulator [NASA-TM-105126] N92-11024
Calibration of the Naval Postgraduate School 3.5' x 5.0' academic wind tunnel [AD-A240614] N92-11025
Managing temporal relations in the MAESTRO scheduling system N92-11059
Resource representation in COMPASS N92-11060
Automating the conflict resolution process N92-11061
MLITemp: A computer program to predict the thermal effects associated with hypervelocity impact damage to space station MLI [NASA-CR-184245] N92-11079
CFD code survey for thrust chamber application N92-11119
Developments in REDES: The Rocket Engine Design Expert System N92-11120
Compression response of laminated composite panels containing multiple delaminations N92-11141
A thinned high frequency linear antenna array to study ionospheric structure [AD-A240764] N92-11243
Three-dimensional calculations of fields and loading for loop and folded waveguide ICRF antennas [DE92-000065] N92-11250
Test and diagnosis of programmable integrated circuits [ETN-91-99483] N92-11253
Automatic generation of microprocessor test programs N92-11256
Hardware and software tools for microprocessor functional test N92-11257
The GAPT system: A chain of test for microprocessors N92-11258
A microprocessor test approach allowing fault localisation N92-11261
Coil shapes towards pure multipoles in circular regions: A numerical approach [DE91-017239] N92-11271
Theoretical study (Lagrangian modeling) of turbulent particulate dispersion [ETN-91-99909] N92-11287
Computer codes for the evaluation of thermodynamic and transport properties for equilibrium air to 30000 K [NASA-TM-104107] N92-11300
Secondary instability of the three dimensional laminar boundary layer in incompressible flow: Description of the calculation code [CERT-RT-63/5618-54] N92-11306
Resolution of the Navier-Stokes equations applied to the computation of the laminar flow around a two dimensional wing profile [CERT-RT-65/5604-35] N92-11307
Implementation of the flow-modulated skew-upward difference scheme in the momentum equation of the COMMIX-1C program: A first assessment [DE91-018013] N92-11321
Attitude identification for SCOLE using two infrared cameras [NASA-CR-4397] N92-11338
Development of a personal computer program for milling the shapes of wind turbine blades. Theory and application [ILR-MITT-243(1990)] N92-11360
Slave finite element for non-linear analysis of engine structures. Volume 2: Programmer's manual and user's manual [NASA-CR-187225] N92-11388
Altitude dependence in a semi-analytical atmospheric code N92-11413
Radiometric and atmospheric correction procedures for AVHRR preprocessing in the solar reflective channels N92-11414
ATLAS: An Auto-Tracking Land and Atmosphere Sensor for retrieval of atmospheric optical parameters and acquisition of bidirectional surface reflectance N92-11487
Photovoltaic energy system at an Alaskan site [PB91-201350] N92-11567
TEGEN: A one dimensional program to calculate a thermoelectric generator [DE91-634444] N92-11571
Mesoscale prediction and satellite cloud analysis for advanced meteorological processing systems [AD-A240510] N92-11597
Persian Gulf contrail altitude limits [AD-A240702] N92-11598
Hourly and daily precipitation frequencies for the United States [AD-A240746] N92-11599
Methodology investigation. Phase 2: Software maturity model validation [AD-A231439] N92-11651
Deploying expert systems in Ada [NASA-CR-188938] N92-11664
ART/Ada design project, phase 1. Task 1 report: Overall design [NASA-CR-188943] N92-11665
ART-Ada design project, phase 2 [NASA-CR-188940] N92-11667
User's manual for the Macintosh version of PASCO [NASA-TM-104115] N92-11668
Workshops on Efficient Use of Scientific Computing [AD-A240175] N92-11674
Proceedings of the Acquisition Research Symposium: Imagnination, Innovation, and Implementation, 1991, volume 1 [AD-A240260] N92-11676
Proceedings of the Acquisition Research Symposium: Acquisition for the Future, Imagination, Innovation, and Implementation, 1991, volume 2 [AD-A240261] N92-11677
Fractal image compression [AD-A240636] N92-11680
Tester Independent Support Software System (TISSS) [AD-A240668] N92-11681
Cedar Project: Original goals and progress to date [DE92-000032] N92-11689
Computer program for Bessel and Hankel functions [NASA-TM-105154] N92-11691
BCD/CPS: An event-level GEANT3 parallelization via CPS [DE91-017238] N92-11703
Portable vectorized software for Bessel function evaluation [PB91-216598] N92-11727
Nested ocean models: Work in progress N92-11735
Extended algebraic graph transformation [ETN-91-90151] N92-11739
The considering of the slowing down effect in the formalism of probability tables. Application to the effective cross section calculation [DE91-626722] N92-11751
Transport study of ECH and NBI plasmas in CHS N92-11857
A generalized strategy for building resident database interfaces [NASA-CR-189246] N92-11920
NSSDC data listing [NASA-TM-105010] N92-11921
Kinematics and dynamics of barred galaxies N92-11937
OPAL opacities for astrophysical applications [DE91-016922] N92-11939

COMPUTER STORAGE DEVICES
Communications interface and system for radiation recovery of a microprocessor portion thereof [AD-D014977] N92-11245
Case history: Failure analysis of a CMOS SRAM with an intermittent open contact [DE91-018811] N92-11283
PET studies of components of high-level vision [AD-A240202] N92-11624
Thin film magnetic memory elements [AD-D014971] N92-11646

COMPUTER SYSTEMS DESIGN
The electronic aeronautical chart for general aeronautics: A system specification [ILR-MITT-263(1991)] N92-10997
Intelligent perturbation algorithms to space scheduling optimization N92-11064
Sparse distributed memory [NASA-CR-188841] N92-11643
ART/Ada design project, phase 1. Task 1 report: Overall design [NASA-CR-188943] N92-11665
Ground Systems Development Environment (GSDE) interface requirements analysis [NASA-CR-188822] N92-11702

COMPUTER SYSTEMS PERFORMANCE
Parallel processing applications for gas turbine engine control N92-11012
Hardware and software tools for microprocessor functional test N92-11257
The GAPT system: A chain of test for microprocessors N92-11258
Taking into account asynchronous signals in functional test of complex circuits N92-11259
Fault localization when testing complex circuits N92-11260
A microprocessor test approach allowing fault localisation N92-11261
Towards an automated system for the verification and diagnosis of intelligent VLSI circuits N92-11262
A method and tools for microprocessor validation: High safety function applications N92-11263

Short-term hourly temperature interpolation
[AD-A240489] N92-11596
Study and prototype of data system interactions for the Earth Observing System Data and Information System
[NASA-CR-183505] N92-11648
Experience with Acore: Implementing GHC with actors
[AD-A231409] N92-11649
Optimal processor assignment for pipeline computations
[NASA-CR-189047] N92-11672
Efficient ICCG on a shared memory multiprocessor
[NASA-CR-188843] N92-11693
Ground Systems Development Environment (GSDE) interface requirements analysis
[NASA-CR-188822] N92-11702
Discussion summary: Fictitious domain methods N92-11730

COMPUTER SYSTEMS PROGRAMS
Modula-2*: An extension of Modula-2 for highly parallel programs
[NASA-CR-188855] N92-11654
Ground Systems Development Environment (GSDE) interface requirements analysis
[NASA-CR-188822] N92-11702

COMPUTER TECHNIQUES
Calibration of the Naval Postgraduate School 3.5' x 5.0' academic wind tunnel
[AD-A240614] N92-11025
Space station tracking requirements feasibility study, volume 2
[NASA-CR-185641-VOL-2] N92-11084
Design of a fast computer-based partial discharge diagnostic system
[NASA-CR-189057] N92-11272
Analysis of strain dependent damping in materials via modeling of material point hysteresis
[AD-A240298] N92-11381
Computers in aeronautics and space research at the Lewis Research Center
[NASA-TM-105096] N92-11642
Computer aided surface representation
[DE91-018872] N92-11688
The ARPANET after twenty years
[NASA-CR-188853] N92-11695
An application for multi-person task synchronization
[NASA-CR-187712] N92-11918

COMPUTER VIRUSES
Threats and countermeasures for network security
[NASA-CR-188883] N92-11645
Stopping computer crimes
[NASA-CR-188896] N92-11657

COMPUTER VISION
Appearance simulator for computer vision research
[AD-A240506] N92-11679

COMPUTERIZED SIMULATION
Results from computational analysis of a mixed compression supersonic inlet
[NASA-TM-104475] N92-10976
A fast sorting algorithm for a hypersonic rarefied flow particle simulation on the connection machine
[NASA-CR-188903] N92-10977
Numerical simulation of the reactive flow in advanced (HSR) combustors using KIVA-2
[NASA-CR-188996] N92-11014
User modeling techniques for enhanced usability of OPSMODEL operations simulation software
[NASA-TM-4306] N92-11035
JANNAF Combustion Instability Panel Workshop report: Numerical methods in combustion instability N92-11123
A new technique for simulating composite material
[NASA-CR-188792] N92-11140
Compression response of laminated composite panels containing multiple delaminations N92-11141
Numerical simulation of the degradation of the folds of a laminated composite structure. Study of the importance of residual firing constraints
[ONERA-RT-8/7256-RY-094-R] N92-11145
Specification of difficult to test radar performance
[AD-A240398] N92-11232
A thinned high frequency linear antenna array to study ionospheric structure
[AD-A240764] N92-11243
VHDL simulation of the implementation of a costfunction circuit
[AD-A240430] N92-11278
Modeling of the heat transfer in bypass transitional boundary-layer flows
[NASA-TP-3170] N92-11299
Numerical simulations of detonation transmission
[AD-A240560] N92-11304
To the account of finite velocity of thermal diffusion in turbulent flows
[DE91-635593] N92-11323
Distributed sensor system decision analysis using team strategies
[AD-A240250] N92-11333
Multi-disciplinary optimization of aeroservoelastic systems
[NASA-CR-188983] N92-11377
Advanced stress analysis methods applicable to turbine engine structures
[NASA-CR-187235] N92-11378
Atmospheric correction of satellite borne imagery investigated by means of a sensitivity analysis of the entire remote sensing process N92-11400
Study of the spatial signature of forest covers by geometric-optic modeling N92-11530
Processes for identifying regional influences of and responses to increasing atmospheric CO2 and climate change: The MINK Project
[DE91-018604] N92-11580
Energetics diagnosis of numerical simulation of atmospheric blocking
[NASA-CR-183503] N92-11581
Robot graphic simulation testbed
[NASA-CR-188998] N92-11637
Human Machine Interfaces for Teleoperators and Virtual Environments Conference
[NASA-CP-10071] N92-11638
Computers in aeronautics and space research at the Lewis Research Center
[NASA-TM-105096] N92-11642
Computer aided surface representation
[DE91-018872] N92-11688
BCD/CPS: An event-level GEANT3 parallelization via CPS
[DE91-017238] N92-11703
Harnessing the killer micros: Applications from LLNL's massively parallel computing initiative
[DE91-018721] N92-11709
A new simulator for assessing subjective effects of sonic booms
[NASA-TM-104150] N92-11759
Critical properties of strongly interacting bosons on a lattice
[DE91-016926] N92-11771
Effects of electric field on particle drift orbits in a l = 2 torsatron
[NIFS-31] N92-11878

COMPUTERS
Education in computational science: Role of the National Laboratories
[DE91-018823] N92-11687
Database management system interface standard for Navy next generation computing resources
[AD-A240432] N92-11925

CONCRETE STRUCTURES
The behaviour of fire-exposed composite steel/concrete slabs
[ISBN-90-386-0031-3] N92-11147

CONDENSATES
Bose-condensation in liquid helium under pressure
[DE91-634504] N92-11170

CONDUCTING POLYMERS
New polymer electrolyte hosts and their tetrabutylammonium chloride complexes. Relationships among concentration of polar groups, ESR spin probe response, and ionic conductivity
[AD-A240497] N92-11190

CONDUCTIVE HEAT TRANSFER
Effects of anisotropic conduction and heat pipe interaction on minimum mass space radiators
[NASA-TM-105297] N92-11138
Measurement of frequency response in short thermocouple wires
[NASA-CR-187821] N92-11339

CONDUCTIVITY
Conductive gage for crack length measurement
[NASA-CASE-LAR-14480-1-CU] N92-11374

CONDUCTORS
Approximate expressions for the magnetic field from an electric current source in a layered conducting medium
[MRL-TR-91-5] N92-11273

CONFERENCES
The 4th International Workshop on Membrane Biotechnology and Membrane Diomaterials
[AD-A240481] N92-11614
Policy issues in interconnecting networks
[NASA-CR-188844] N92-11694
Proceedings for the ICASE Workshop on Heterogeneous Boundary Conditions
[NASA-CR-187630] N92-11728
Symposium on Development and Applications of Intense Pulsed Particle Beams
[NIFS-PROC-8] N92-11798
Proceedings of the First International Toki Conference on Plasma Physics and Controlled Nuclear Fusion: Next Generation Experiments in Helical Systems
[NIFS-PROC-3] N92-11799
Proceedings of the 127th Colloquium of the International Astronomical Union Reference Systems
[AD-A240207] N92-11933

CONFIGURATION INTERACTION
Attitude control of flexible structures
[AD-A240520] N92-11082
Decomposition pathways of tetrahydrogen
[AD-A240623] N92-11166

CONIFERS
Phenological changes in the red edge shift of Norway spruce needles and their relationship to needle chlorophyll content N92-11423
Structural controls on the remotely sensed response of a coniferous forest plantation N92-11516
Wavelength shifts in fluorescence maxima of stressed and non-stressed Norway spruce needles over the growing season N92-11536

CONJUGATE GRADIENT METHOD
A conjugate gradient based algorithm to minimize the sidelobe level of planar arrays with element failures
[AD-A240667] N92-11242
Efficient ICCG on a shared memory multiprocessor
[NASA-CR-188843] N92-11693

CONJUGATION
Photothermal deflection spectroscopy of conjugated polymers
[DE91-018318] N92-11204

CONSERVATION LAWS
On the theory and numerical approximation of nonlinear hyperbolic problems
[ETN-91-99898] N92-11714
On a class of implicit and explicit schemes of Van-Leer type for scalar conservation laws N92-11715
Stable upwind schemes for hyperbolic conservation laws for with source terms N92-11716
An analysis of upwind schemes for inhomogeneous two dimensional conservation laws N92-11717
Interface conditions for domain decomposition with radical grid refinement N92-11733
Multi-resolution analysis for ENO schemes
[NASA-CR-189043] N92-11736

CONTAINMENT
Nuclear light bulb N92-11110

CONTAMINANTS
Ground penetrating radar data acquisition system
[AD-A240765] N92-11244

CONTEXT
Computer integrated documentation
[NASA-TM-103870] N92-11673

CONTINENTAL SHELVES
Contribution of active microwaves to the structural analysis of epicontinental shelf-forms: Example of the English Channel N92-11448

CONTINUITY EQUATION
Turbulent fluid motion 3: Basic continuum equations
[NASA-TM-104386] N92-11317

CONTINUOUS RADIATION
Efficient detection of a CW signal with a linear frequency drift
[NASA-CR-188900] N92-11224
Review of the TJ-II Flexible Heliac Project N92-11803

CONTINUOUS SPECTRA
Infrared to millimetre observations of active galaxies N92-11932

CONTINUUMS
Continuum x ray gauging of multiple-element materials
[DE91-017429] N92-11368
Continuum damping of high mode number toroidal Alfven waves
[DE91-018891] N92-11890

CONTRAILS
Strategic air command contrail formation study
[AD-A240467] N92-11003
Persian Gulf contrail altitude limits
[AD-A240702] N92-11598

CONTROL EQUIPMENT
In-line hydraulic dashpot
[AD-D014955] N92-11356

CONTROL STABILITY
OPUS: Optimal Projection for Uncertain Systems. Volume 1
[AD-A240372] N92-11080
OPUS: Optimal Projection for Uncertain Systems, volume 2
[AD-A240373] N92-11081

CONTROL SURFACES
Prediction of forces and moments for hypersonic flight vehicle control effectors
[NASA-CR-188954] N92-11070

CONTROL SYSTEMS DESIGN
Engineering and instrumentation support of GL Research Balloon Program
[AD-A240616] N92-10987

Initial design study of existing flight control system of RPH and feasibility study of implementing HHC on the SH-60B
[AD-A240522] N92-11019
Precision pointing control of the spinning Gravity Probe B spacecraft N92-11068
OPUS: Optimal Projection for Uncertain Systems. Volume 1
[AD-A240372] N92-11080
OPUS: Optimal Projection for Uncertain Systems, volume 2
[AD-A240373] N92-11081
Multidisciplinary optimization of controlled space structures with global sensitivity equations
[NASA-TP-3130] N92-11087
Linear quadratic servo control of a reusable rocket engine
[NASA-TM-105291] N92-11128
Effect of control variables and length of refining zone on the refining result with a new pilot refiner N92-11155
Programmable beam transform and beam steering control system for a phased array radar antenna
[AD-D014970] N92-11230
Automatic tools for microprocessor failure analysis N92-11265
Robot graphic simulation testbed
[NASA-CR-188998] N92-11637
ECH system in the large helical device N92-11845

CONTROL THEORY
Microgravity vibration isolation: An optimal control law for the one-dimensional case
[NASA-TM-105146] N92-11217

CONTROLLED FUSION
On radial electric field structure in CHS torsatron/heliotron
[NIFS-94] N92-11796
Influence of fast ion loss on radial electric field in Wendelstein 7-A stellarator
[NIFS-95] N92-11797
Symposium on Development and Applications of Intense Pulsed Particle Beams
[NIFS-PROC-8] N92-11798
Proceedings of the First International Toki Conference on Plasma Physics and Controlled Nuclear Fusion: Next Generation Experiments in Helical Systems
[NIFS-PROC-3] N92-11799
Present status of the Large Helical Device Project N92-11800
Drift optimization of helical systems N92-11810
Structural design of large helical device N92-11837
Research and development of forced flow superconducting coils for large helical device N92-11838
Pool-cooled superconducting magnet design of large helical device N92-11839
ICRF heating program of the large helical device N92-11846
Particle trajectories through MIRRORTRON configurations
[DE91-017084] N92-11876
Fluid description of ponderomotive force compatible with the kinetic one in a warm plasma
[NIFS-100] N92-11884

CONTROLLERS
New insulation constructions for aerospace wiring applications. Volume 2: The 270 VDC arc tracking testing with power controllers
[AD-A240639] N92-11007
Parallel processing applications for gas turbine engine control N92-11012
OPUS: Optimal Projection for Uncertain Systems. Volume 1
[AD-A240372] N92-11080
OPUS: Optimal Projection for Uncertain Systems, volume 2
[AD-A240373] N92-11081

CONVECTION-DIFFUSION EQUATION
Layer tracking, asymptotics, and domain decomposition N92-11732

CONVECTIVE FLOW
Mixed convection in two-dimensional laminar air flow with reverse flow regions N92-11293
Domain-decomposed preconditionings for transport operators N92-11731

CONVECTIVE HEAT TRANSFER
Mixed convection in two-dimensional laminar air flow with reverse flow regions N92-11293

CONVERGENCE
A parallel algorithm for the eigenvalues and eigenvectors for a general complex matrix
[NASA-CR-188854] N92-11653
Analysis of a parallel multigrid algorithm
[NASA-CR-188906] N92-11701
Convergence and performance of synchronous and asynchronous parallel and conventional iterative methods
[AD-A240286] N92-11707

CONVERGENT-DIVERGENT NOZZLES
Analytical study of nozzle performance for nuclear thermal rockets
[NASA-TM-105251] N92-11126

COOLANTS
Cooling apparatus and couplings therefor
[NASA-CASE-ARC-11921-1] N92-11286

COOLING
Characterizing He II flow through porous materials using counterflow data
[CD-4] N92-11295
A method for estimating missing hourly temperatures using daily maximum and minimum temperatures
[AD-A240394] N92-11594
Matter-wave interferometry with laser cooled atoms
[AD-A240531] N92-11776

COOLING FINS
Effects of anisotropic conduction and heat pipe interaction on minimum mass space radiators
[NASA-TM-105297] N92-11138

COOLING SYSTEMS
Cooling apparatus and couplings therefor
[NASA-CASE-ARC-11921-1] N92-11286
Pool-cooled superconducting magnet design of large helical device N92-11839
Fundamental design on LHD with bath cooling method N92-11841
Engineering design of large helical device N92-11864

COORDINATES
Multi-disciplinary optimization of aeroservoelastic systems
[NASA-CR-188983] N92-11377

COPPER
Effects on LDEF exposed copper film and bulk N92-11076
High-T sub c fluorine-doped YBa2Cu3O(y) films on ceramic substrates by screen printing
[NASA-TM-105296] N92-11188
Synthesis of novel conducting solids
[AD-A240468] N92-11912

COPPER OXIDES
Neutron diffraction from the flux line lattice
[DE91-018175] N92-11906

CORN
High resolution spectral measurements of vegetation and soil in field and laboratory N92-11437

CORRECTION
Normalization of bidirectional effects of surface reflectance on a series of multitemporal NOAA/AVHRRR data N92-11480

CORROSION
A new radiographic corrosion inspection capability
[AD-A231476] N92-11363

CORROSION TESTS
Analysis of surfaces from the LDEF A0114, phase 4
[NASA-CR-188990] N92-11074

COSMIC RAY SHOWERS
CYGNUS collaboration contributions to the twenty-second ICRC
[DE92-000258] N92-11961

COSMIC X RAYS
CYGNUS collaboration contributions to the twenty-second ICRC
[DE92-000258] N92-11961

COSMOLOGY
Perturbations from strings don't look like strings!
[NASA-CR-189012] N92-11941
Superfluid-like turbulence in cosmology
[NASA-CR-189011] N92-11942
Cosmological constraints on pseudo-Nambu-Goldstone bosons
[NASA-CR-189010] N92-11943
Cosmological structure formation
[NASA-CR-189007] N92-11946
Non scale-invariant density perturbations from chaotic extended inflation
[NASA-CR-189004] N92-11947
Underlying generation mechanisms for the extragalactic gamma ray background and their implications for high-resolution gamma ray cosmology N92-11959

COST ANALYSIS
Component cost analysis for compressed natural gas vehicles
[DE91-017230] N92-11353
A realistic, gradual and economical approach to fusion power
[DE91-018464] N92-11786

COST EFFECTIVENESS
The Space Shuttle: An attempt at low-cost, routine access to space
[AD-A240589] N92-11037

COST ESTIMATES
Definition, technology readiness, and development cost of the orbit transfer vehicle engine integrated control and health monitoring system elements
[NASA-CR-187123] N92-11132
Component cost analysis for compressed natural gas vehicles
[DE91-017230] N92-11353
An IFE development strategy
[DE91-016918] N92-11873

COSTS
VHDL simulation of the implementation of a costfunction circuit
[AD-A240430] N92-11278

COUETTE FLOW
Deformation and breakup of drops in simple shear flows
[ETN-91-90143] N92-11315

COUNTER ROTATION
Calibration of the Naval Postgraduate School 3.5' x 5.0' academic wind tunnel
[AD-A240614] N92-11025

COUPLING
Top down IC failure analysis using an E-beam system coupled to a functional tester N92-11264
Coupled-channel optical calculation of electron-hydrogen scattering: Elastic scattering from 0.5 to 30 eV
[DE91-634157] N92-11780

COUPLINGS
Cooling apparatus and couplings therefor
[NASA-CASE-ARC-11921-1] N92-11286

COVARIANCE
Analysis of altimetry over the Aral Sea
[NASA-TM-100759] N92-11583
Fast algorithms for linear least-squares estimation of multi-dimensional random fields
[AD-A240249] N92-11675

CRACK GEOMETRY
Fracture toughness of carbon/carbon composites
[AD-A240200] N92-11143

CRACK INITIATION
Fracture toughness of carbon/carbon composites
[AD-A240200] N92-11143
Fatigue crack initiation
[AD-A240196] N92-11380

CRACK PROPAGATION
Numerical simulation of the degradation of the folds of a laminated composite structure. Study of the importance of residual firing constraints
[ONERA-RT-8/7256-RY-094-R] N92-11145
A probabilistic model of intergranular stress corrosion cracking
[DE91-017986] N92-11173
A comparison of single cycle overload effect on Al-Li 2091-T81 plate and 2091-T83 sheet
[AD-A240627] N92-11179
Conductive gage for crack length measurement
[NASA-CASE-LAR-14480-1-CU] N92-11374
Critical appraisal of the McDonnell Douglas closure model for predicting fatigue crack growth
[ARL-STRUC-R-444] N92-11376
Propagation behavior of small cracks in 304 stainless steel under biaxial low-cycle fatigue at elevated temperature
[DE91-018863] N92-11389

CRACKING (FRACTURING)
Fatigue crack initiation
[AD-A240196] N92-11380

CRACKS
Conductive gage for crack length measurement
[NASA-CASE-LAR-14480-1-CU] N92-11374
Critical appraisal of the McDonnell Douglas closure model for predicting fatigue crack growth
[ARL-STRUC-R-444] N92-11376
Propagation behavior of small cracks in 304 stainless steel under biaxial low-cycle fatigue at elevated temperature
[DE91-018863] N92-11389

CRAY COMPUTERS
Solving the shallow water equations on the Cray X-MP/48 and the connection machine 2
[NASA-CR-188897] N92-11658

CREEP PROPERTIES
Effects of elevated temperature on the viscoplastic modeling of graphite/polymeric composites
[NASA-TM-104160] N92-11149
Creep response of a 9Cr-1Mo-V-Nb steel to varying stresses and temperatures
[DE91-017871] N92-11181
Microstructural evolution during the thermomechanical fatigue of solder joints
[DE91-017309] N92-11372
Thermoviscoplastic response of Ti-15-3 under various loading conditions
[NASA-CR-187621] N92-11391

CREEP TESTS
Creep response of a 9Cr-1Mo-V-Nb steel to varying stresses and temperatures
[DE91-017871] N92-11181
Experimental determination of the material parameter of two viscoelastic synthetic materials, using creep tests
[ILR-MITT-244(1990)] N92-11385
CRIME
Stopping computer crimes
[NASA-CR-188896] N92-11657
CRITICAL FLOW
Results from computational analysis of a mixed compression supersonic inlet
[NASA-TM-104475] N92-10976
CRITICAL TEMPERATURE
Development of an experimental database and theories for prediction of thermodynamic properties of aqueous electrolytes and nonelectrolytes of geochemical significance at supercritical temperatures and pressures
[DE91-018493] N92-11169
A study on the development of high T(sub c) superconducting materials
[DE91-629755] N92-11917
CRITICAL VELOCITY
Critical velocities and mutual friction in He-3-He-4 II mixtures at temperatures below 100 mK
[ETN-91-90132] N92-11314
CROP GROWTH
A split-window method for obtaining crop temperatures N92-11410
Combined use of Earth observation satellite and meteorological satellite for crop assessment in semiarid environments N92-11494
Joint use of remote sensing and agricultural production estimation models: Current trends N92-11501
Estimation of the primary production in Sahelian region from radiometric data N92-11504
Maximum evapotranspiration monitoring over La Mancha, Spain, using NOAA-AVHRR data N92-11507
The linking of crop growth models and multi-sensor remote sensing data N92-11512
CROSS CORRELATION
Measurement of magnetic fluctuations in Heliotron E N92-11856
CROSS FLOW
Model representation in the PANCOR wall interference assessment code
[NASA-TM-104152] N92-11022
CRYOGENIC EQUIPMENT
Description of Liquid Nitrogen Experimental Test Facility
[NASA-TM-105215] N92-11208
CRYOGENIC FLUID STORAGE
Improved thermodynamic modeling of the no-vent fill process and correlation with experimental data
[NASA-TM-104492] N92-11129
CRYOGENICS
Benefits of slush hydrogen for space missions
[NASA-TM-104503] N92-11214
Superfluid helium dynamics
[NASA-CR-188814] N92-11294
Characterizing He II flow through porous materials using counterflow data
[CD-4] N92-11295
CRYOPUMPING
Thermal behavior of the SHOOT gallery arm
[CD-21] N92-11296
CRYSTAL DISLOCATIONS
Direct imaging of deformation and disorder in extended-chain polymer fibers
[AD-A240651] N92-11192
CRYSTAL GROWTH
Non-equilibrium microstructures produced during electron-beam and laser-beam surface modification of metallic alloys
[DE91-018466] N92-11174
Radiation induced growth of micro crystallites
[DE91-016516] N92-11900
Laboratory measurements of the single-scattering properties of ammonia ice crystals N92-11950
CRYSTAL LATTICES
Neutron diffraction from the flux line lattice
[DE91-018175] N92-11906
CRYSTAL STRUCTURE
Direct imaging of deformation and disorder in extended-chain polymer fibers
[AD-A240651] N92-11192
Biological effects of minerals
[DE91-018183] N92-11615
Neutron diffraction from the flux line lattice
[DE91-018175] N92-11906
Surface analysis of catalysts by low-energy ion scattering
[ETN-91-90133] N92-11913
A study on the development of high T(sub c) superconducting materials
[DE91-629755] N92-11917
CRYSTAL SURFACES
Surface analysis of catalysts by low-energy ion scattering
[ETN-91-90133] N92-11913
CRYSTALLITES
Direct imaging of deformation and disorder in extended-chain polymer fibers
[AD-A240651] N92-11192
Radiation induced growth of micro crystallites
[DE91-016516] N92-11900
CRYSTALS
Light scattering experiments on Brownian motion in shear flow and in colloidal crystals
[ETN-91-90134] N92-11756
Quantum 1/f noise in high technology applications including ultrasmall structures and devices
[AD-A240152] N92-11907
CURRENT DENSITY
Coil shapes towards pure multipoles in circular regions: A numerical approach
[DE91-017239] N92-11271
Microchannel electron source
[AD-D014956] N92-11276
Full-wave calculation of fast-wave current drive in tokamaks including k(parallel) variations
[DE92-000076] N92-11894
CURRENT DISTRIBUTION
Current profile control for ITER with RF current drive
[DE91-018597] N92-11888
CURVE FITTING
Calculations and curve fits of thermodynamic and transport properties for equilibrium air to 30000 K
[NASA-RP-1260] N92-11285
CYCLIC LOADS
Thermoviscoplastic response of Ti-15-3 under various loading conditions
[NASA-CR-187621] N92-11391
CYCLOTRON FREQUENCY
ICRF heating program of the large helical device N92-11846
Fokker-Planck equation in the presence of anomalous diffusion
[NIFS-29] N92-11879
CYCLOTRON RADIATION
Transport study of ECH and NBI plasmas in CHS N92-11857
Neutron star magnetic fields and implications for pulsars and gamma ray bursts N92-11960
CYCLOTRON RESONANCE
Diverted particle-flux studies in the IMS and Proto-Cleo stellarators N92-11825
Transport study of ECH and NBI plasmas in CHS N92-11857
The 100 GHz half megawatt microwave transmission system development with whispering gallery mode N92-11869
CYCLOTRON RESONANCE DEVICES
Tilted resonator experiments on a quasioptical gyrotron
[AD-A240680] N92-11335
Review of the TJ-II Flexible Heliac Project N92-11803
ECH system in the large helical device N92-11845
CYCLOTRONS
Comparison between californium and cyclotron heavy ion tests N92-11266
Comparison between californium and cyclotron SEU tests N92-11267
CYLINDRICAL BODIES
Determination of nonstationary temperatures in high-stressed elements with pulsed heat sources
[DE91-635705] N92-11325
In-line hydraulic dashpot
[AD-D014955] N92-11356
Gorter-Mellink pulsed-source problem in cylindrical and spherical geometry
[DE91-017249] N92-11725
CYLINDRICAL TANKS
Description of Liquid Nitrogen Experimental Test Facility
[NASA-TM-105215] N92-11208
CYTOCHROMES
Biochemical and biophysical studies of the E. coli respiratory chain
[DE91-016966] N92-11612
CZECHOSLOVAKIA
Spectral observations of solar radio bursts at 2.0-4.5 GHz
[CAS-PUBL-77] N92-11954

D

DAMAGE
Debris/ice/TPS assessment and photographic analysis for Shuttle Mission STS-43
[NASA-TM-103823] N92-11038
An examination of the damage tolerance enhancement of carbon/epoxy using an outer lamina of spectra (R)
[NASA-TP-3160] N92-11142
Delamination propagation in a composite panel under compressive stress
[ONERA-RT-23/3542-RY-093-R] N92-11146
Damage evolution in filled elastomers
[AD-A240532] N92-11191
DAMAGE ASSESSMENT
The spectral reflection behaviour of branches and branch components of healthy and damaged beech trees N92-11432
Evaluation of high spectral resolution laboratory reflectance data of healthy and damaged beech and spruce branches for the improvement of forest damage classification N92-11433
DAMPING
Magnetic fluids and their applications
[DE92-704012] N92-11326
Analysis of strain dependent damping in materials via modeling of material point hysteresis
[AD-A240298] N92-11381
Continuum damping of high mode number toroidal Alfven waves
[DE91-018891] N92-11890
DARK ADAPTATION
The effect of blinking on subsequent dark adaptation
[AD-A240281] N92-11625
DARK MATTER
Perturbations from strings don't look like strings!
[NASA-CR-189012] N92-11941
Superfluid-like turbulence in cosmology
[NASA-CR-189011] N92-11942
Re-ionization and decaying dark matter
[NASA-CR-189009] N92-11944
Converting neutron stars into strange stars
[NASA-CR-189008] N92-11945
Non scale-invariant density perturbations from chaotic extended inflation
[NASA-CR-189004] N92-11947
DATA ACQUISITION
Engineering and instrumentation support of GL Research Balloon Program
[AD-A240616] N92-10987
Ground penetrating radar data acquisition system
[AD-A240765] N92-11244
International program for Earth observations
[NASA-CR-188799] N92-11393
Comparison of in situ, aircraft- and satellite-derived surface reflectances in Flevoland (Netherlands) N92-11404
SPOT calibration on the test site La Crau (France) N92-11409
Spectroscopic analysis of imaging spectrometer data for classification purposes N92-11439
DATA BASE MANAGEMENT SYSTEMS
Proposed planning and scheduling services for the SNC in the CDOS era N92-11043
A generalized strategy for building resident database interfaces
[NASA-CR-189246] N92-11920
FEDIX: The on-line database retrieval service of Government information for colleges, universities, and other organizations
[DE91-018496] N92-11923
Integrated Risk Information System
[DE91-018503] N92-11924
Database management system interface standard for Navy next generation computing resources
[AD-A240432] N92-11925
Issues in real-time data management
[AD-A240712] N92-11926
DATA BASES
World Geodetic System 1984 (WGS-84) consolidated database for test ranges
[AD-A240621] N92-11026
Network Control Center User Planning System (NCC UPS) N92-11053
Development of an experimental database and theories for prediction of thermodynamic properties of aqueous electrolytes and nonelectrolytes of geochemical significance at supercritical temperatures and pressures
[DE91-018493] N92-11169
Development of data file standards for automated ultrasonic scanning systems. Exchange methods for digital ultrasonic inspection data
[AD-A240075] N92-11364
Database of SPOT histrograms N92-11517

A generalized strategy for building resident database interfaces
[NASA-CR-189246] N92-11920
FEDIX: The on-line database retrieval service of Government information for colleges, universities, and other organizations
[DE91-018496] N92-11923
DATA FLOW ANALYSIS
Pulse compression degradation due to open loop adaptive cancellation, part 1
[AD-A240552] N92-11238
Pulse compression degradation due to open loop adaptive cancellation, part 3
[AD-A240553] N92-11239
DATA INTEGRATION
VHDL simulation of the implementation of a costfunction circuit
[AD-A240430] N92-11278
DATA LINKS
Space Network Control Conference on Resource Allocation Concepts and Approaches
[NASA-CP-3124] N92-11039
TRUST: TDRSS Resource User Support Tool N92-11052
A method for interference mitigation in space communications scheduling N92-11062
Prediction of the pattern performance for the Aeroassist Flight Experiment (AFE) spacecraft
[NASA-CR-4409] N92-11065
Communications interface and system for radiation recovery of a microprocessor portion thereof
[AD-D014977] N92-11245
Basic concepts of low Earth orbit satellite systems for communications
[TELECOM-PARIS-91-D-001] N92-11248
Policy issues in interconnecting networks
[NASA-CR-188844] N92-11694
Advanced information processing system: Inter-computer communication services
[NASA-CR-187556] N92-11706
DATA PROCESSING
Spectroscopic analysis of imaging spectrometer data for classification purposes N92-11439
ISEE/ICE plasma wave data analysis
[NASA-CR-189244] N92-11795
Open document processing and the ISOTEXT system
[ETN-91-90160] N92-11928
DATA PROCESSING EQUIPMENT
Modula-2*: An extension of Modula-2 for highly parallel programs
[NASA-CR-188855] N92-11654
DATA REDUCTION
ISEE/ICE plasma wave data analysis
[NASA-CR-189244] N92-11795
DATA RETRIEVAL
A class of designs for a sparse distributed memory
[NASA-CR-188849] N92-11644
DATA SAMPLING
Pulse compression degradation due to open loop adaptive cancellation, part 3
[AD-A240553] N92-11239
DATA STORAGE
A class of designs for a sparse distributed memory
[NASA-CR-188849] N92-11644
A domain decomposition algorithm for solving large elliptic problems
[DE92-000096] N92-11690
Information technologies for astrophysics circa 2001
[NASA-CR-188868] N92-11936
DATA STRUCTURES
Vienna FORTRAN: A FORTRAN language extension for distributed memory multiprocessors
[NASA-CR-187634] N92-11670
Optimal expression evaluation for data parallel architectures
[NASA-CR-187773] N92-11696
DATA SYSTEMS
Development of data file standards for automated ultrasonic scanning systems. Exchange methods for digital ultrasonic inspection data
[AD-A240075] N92-11364
Study and prototype of data system interactions for the Earth Observing System Data and Information System
[NASA-CR-183505] N92-11648
NSSDC data listing
[NASA-TM-105010] N92-11921
DATA TRANSMISSION
A brief introduction to the universal documentation system. Universal documentation system handbook
[AD-A240622] N92-11027
Multiple beam antenna/switch system study
[NASA-CR-183496] N92-11251
The ARPANET after twenty years
[NASA-CR-188853] N92-11695
Optimal expression evaluation for data parallel architectures
[NASA-CR-187773] N92-11696
Dual frequency optical carrier technique for transmission of reference frequencies in dispersive media
[NASA-CASE-NPO-18007-1-CU] N92-11791
DAYGLOW
A calibration of the Naval Postgraduate School middle ultraviolet spectrograph and an analysis of the OII 2470 A and OI 2972 A emissions obtained from mid-latitude rocket observations
[AD-A240686] N92-11587
DEBRIS
Debris/ice/TPS assessment and photographic analysis for Shuttle Mission STS-43
[NASA-TM-103823] N92-11038
DECAY RATES
Neutron star magnetic fields and implications for pulsars and gamma ray bursts N92-11960
DECIDUOUS TREES
The spectral reflection behaviour of branches and branch components of healthy and damaged beech trees N92-11432
Evaluation of high spectral resolution laboratory reflectance data of healthy and damaged beech and spruce branches for the improvement of forest damage classification N92-11433
DECISION MAKING
Distributed sensor system decision analysis using team strategies
[AD-A240250] N92-11333
DECISION THEORY
Distributed sensor system decision analysis using team strategies
[AD-A240250] N92-11333
DECODERS
An efficient A* stack decoder algorithm for continuous speech recognition with a stochastic language model
[AD-A240745] N92-11683
DECOMPOSITION
Decomposition pathways of tetrahydrogen
[AD-A240623] N92-11166
A domain decomposition algorithm for solving large elliptic problems
[DE92-000096] N92-11690
Proceedings for the ICASE Workshop on Heterogeneous Boundary Conditions
[NASA-CR-187630] N92-11728
DEEP SPACE NETWORK
Resource allocation planning helper (RALPH) N92-11047
DEEP WATER
Use of theoretical wave height distributions in directional seas
[AD-A240411] N92-11608
DEFECTS
Failure coverage of functional test methods: A comparative experimental evaluation N92-11255
DEFLAGRATION
KA-111, Phase C, M-1 propellant tests: Deflagration in partial confinement
[AD-A240185] N92-11211
DEFLECTION
Experimental study of an independently deflected wingtip mounted on a semispan wing
[NASA-TM-102842] N92-10983
Photothermal deflection spectroscopy of conjugated polymers
[DE91-018318] N92-11204
Approximate large deflection analysis of circular plates loaded symmetrically
[NPL-DMM(A)-25] N92-11370
DEFORMATION
Compression response of laminated composite panels containing multiple delaminations N92-11141
Effects of hydrogen and carbon on thermally activated deformation in nickel
[AD-A240496] N92-11178
Deformation of isodamp (A polyvinyl chloride-based elastomer) at various loading rates
[AD-A240393] N92-11189
Direct imaging of deformation and disorder in extended-chain polymer fibers
[AD-A240651] N92-11192
A computational procedure for the dynamics of flexible beams within multibody systems N92-11371
Large deformation induced failures in nonlinear solids
[AD-A240369] N92-11382
DEGRADATION
Effect of particle size of Martian dust on the degradation of photovoltaic cell performance
[NASA-TM-105232] N92-11133
Pulse compression degradation due to open loop adaptive cancellation, part 3
[AD-A240553] N92-11239
DELAMINATING
Compression response of laminated composite panels containing multiple delaminations N92-11141
Numerical simulation of the degradation of the folds of a laminated composite structure. Study of the importance of residual firing constraints
[ONERA-RT-8/7256-RY-094-R] N92-11145
Delamination propagation in a composite panel under compressive stress
[ONERA-RT-23/3542-RY-093-R] N92-11146
DELTA WINGS
Computational study of the aerodynamics and control by blowing of asymmetric vortical flows over delta wings
[NASA-CR-187979] N92-10990
DEMAGNETIZATION
The 23 to 300 C demagnetization resistance of samarium-cobalt permanent magnets
[NASA-TP-3119] N92-11252
DENDRITIC CRYSTALS
Non-equilibrium microstructures produced during electron-beam and laser-beam surface modification of metallic alloys
[DE91-018466] N92-11174
DENSE PLASMAS
Driven currents in neutral beam heated plasma N92-11861
DENSITY MEASUREMENT
Micro photoreflectance semiconductor wafer analyzer
[AD-D014950] N92-11788
Profile measurements in magnetic surface variation experiments/multiple pellet injection experiments N92-11851
DEPLETION
Particle acceleration in space and radiation belt depletion
[AD-A240311] N92-11775
DEPLOYMENT
Aerodynamic calculations related to tethered sub-satellite experiments
[NASA-CR-188964] N92-11071
DEPOSITION
Strengthening of an AISI 1020 steel by aluminum-microalloying during liquid dynamic compaction
[DE91-018745] N92-11182
DESERTS
Characterization of African desert sites for the relative calibrating of wide field satellite optical sensors N92-11402
DESIGN ANALYSIS
Development of unsteady aerodynamic analyses for turbomachinery aeroelastic and aeroacoustic applications
[NASA-CR-4405] N92-10979
JANNAF Combustion Instability Panel Workshop report: Numerical methods in combustion instability N92-11123
Definition, technology readiness, and development cost of the orbit transfer vehicle engine integrated control and health monitoring system elements
[NASA-CR-187123] N92-11132
Hydrodynamic design of generic pump components
[NASA-CR-184252] N92-11361
ART/Ada design project, phase 1. Task 1 report: Overall design
[NASA-CR-188943] N92-11665
Optimization of Helias configurations N92-11806
Fundamental design on LHD with bath cooling method N92-11841
Optimization of design parameters for large helical device N92-11843
DESORPTION
Photon stimulated desorption of neutral species from aluminum
[DE91-017004] N92-11784
DETECTION
Specification of difficult to test radar performance
[AD-A240398] N92-11232
A hybrid methodology for detecting cartographically significant features using LANDSAT TM imagery
[AD-A240454] N92-11563
DETECTORS
ISEE/ICE plasma wave data analysis
[NASA-CR-189244] N92-11795
DETERIORATION
Design of a fast computer-based partial discharge diagnostic system
[NASA-CR-189057] N92-11272
DETONATION
KA-111, Phase C, M-1 propellant tests: Deflagration in partial confinement
[AD-A240185] N92-11211
Numerical simulations of detonation transmission
[AD-A240560] N92-11304

DETONATION WAVES
Numerical simulations of detonation transmission
[AD-A240560] N92-11304
DEVELOPING NATIONS
Greenhouse gas emissions and the developing countries: Strategic options and the USAID response
[PB91-209882] N92-11573
Insurance against catastrophe: SDI and the 3rd World nuclear proliferation problem
[AD-A240429] N92-11752
DEVIATION
The strong coupling limit for polaron models
[ETN-91-90163] N92-11757
DEW POINT
March AFB forecasting rules of thumb evaluation
[AD-A240458] N92-11595
DIAMAGNETISM
Recent diamagnetic measurements of toroidal coil experiments on Heliotron E N92-11854
Rotations of bulk ions and impurities in non-axisymmetric toroidal systems
[NIFS-102] N92-11885
DIAMINES
Diphenylmethane-containing dianhydride and polyimides prepared therefrom
[NASA-CASE-LAR-14487-1] N92-11200
A process for preparing an assembly of an article and a polyimide which resists dimensional change, delamination, and debonding when exposed to changes in temperature
[NASA-CASE-LAR-14538-1] N92-11201
DIFFERENTIAL CALCULUS
Issues in parallel automatic differentiation
[DE91-017311] N92-11726
DIFFERENTIAL EQUATIONS
Issues in parallel automatic differentiation
[DE91-017311] N92-11726
Representation of phi meromorphic functions, when phi and a linear differential polynomial in phi have maximum finite zeros
[ETN-91-90202] N92-11741
DIFFERENTIATION
Issues in parallel automatic differentiation
[DE91-017311] N92-11726
DIFFRACTION
Model problem N92-11729
DIFFRACTION PATTERNS
Wavefields near transverse cusp caustics produced by reflecting ultrasonic transients and tone bursts from curved surfaces
[AD-A240641] N92-11763
DIFFUSE RADIATION
Specular and diffuse components of plant canopy reflectance at the wavelengths of 550 and 630 nm N92-11484
DIFFUSION
Diffusion and drift of charges in semiconductor detectors
[MBE-225] N92-11281
Domain-decomposed preconditionings for transport operators N92-11731
Fokker-Planck equation in the presence of anomalous diffusion
[NIFS-29] N92-11879
DIFFUSION COEFFICIENT
Domain-decomposed preconditionings for transport operators N92-11731
Ripple diffusion and bootstrap current in LHD N92-11833
Diffusion in the Io plasma torus and its relation to the torus spatial structure N92-11949
DIFFUSION FLAMES
Laser Raman diagnostics in subsonic and supersonic turbulent jet diffusion flames N92-11159
Ignition and structure of a laminar diffusion flame in the field of a vortex
[NASA-CR-189042] N92-11162
DIGITAL COMPUTERS
Advanced information processing system for advanced launch system: Avionics architecture synthesis
[NASA-CR-187554] N92-11704
DIGITAL DATA
Development of data file standards for automated ultrasonic scanning systems. Exchange methods for digital ultrasonic inspection data
[AD-A240075] N92-11364
DIGITAL ELECTRONICS
A synchronization and charge distribution process for the parallel multilevel logic simulation
[ETN-91-90152] N92-11708
DIGITAL SIMULATION
Evaluation of atmospheric effects in high spectral resolution airborne images N92-11408
Comparison of two atmospheric correction models for a vegetated Airborne Visible/Infrared Imaging Spectrometer (AVIRIS) scene N92-11415
On the nature of spectral shifts: Modeling and comparison to information contained in wide bands N92-11418
Measurement, simulation, and analysis of the directional reflectance properties of Earth surface materials N92-11468
Vegetation canopies and objects of arbitrary shapes: Computer generation and bidirectional reflectance calculations N92-11475
Radiative transfer simulation on computer models of vegetation cover N92-11476
An integrated modelling approach for the spectral identification of crops N92-11508
A simple model of canopy fluorescence N92-11543
Modeling of fluorescence light-canopy interaction N92-11545
DIGITAL SYSTEMS
Development of data file standards for automated ultrasonic scanning systems. Exchange methods for digital ultrasonic inspection data
[AD-A240075] N92-11364
DIMENSIONAL MEASUREMENT
Conductive gage for crack length measurement
[NASA-CASE-LAR-14480-1-CU] N92-11374
DIODES
Solid state neutron dosimeter for space applications
[NASA-CR-185633] N92-11331
The recombination behavior of a laser induced electron hole plasma in pin diodes and silicon base material
[ETN-91-90153] N92-11887
DIRAC EQUATION
The strong coupling limit for polaron models
[ETN-91-90163] N92-11757
DIRECTION FINDING
Using a discrete Fourier transform to estimate phase in interferometric direction finding
[AD-A231414] N92-10995
DIRECTIONAL SOLIDIFICATION (CRYSTALS)
High pressure turbine blade life extension
[AD-A240654] N92-11180
DIRECTIVITY
Aircraft simulations of the POLDER experiment: First results N92-11471
Normalization of multidirectional red and NIR reflectances with the SAVI N92-11477
Validation of a ground spectral and directional reflectance model N92-11479
Normalization of bidirectional effects of surface reflectance on a series of multitemporal NOAA/AVHRRR data N92-11480
Calculating the bidirectional reflectance of natural vegetation covers using Boolean models and geometric optics N92-11486
DISASTERS
Guidelines for integrating helicopter assets into emergency planning
[SCT-91RR-18] N92-10993
DISCRETE FUNCTIONS
Using a discrete Fourier transform to estimate phase in interferometric direction finding
[AD-A231414] N92-10995
DISCRIMINATION
Television image compression and small animal remote monitoring
[NASA-CR-186614] N92-11223
DISPERSING
Development of a fundamentally new refining method. Part 1: Basic design considerations N92-11153
EDMS: Microcomputer pollution model for civilian airports and Air Force bases, (user's guide)
[AD-A240528] N92-11578
DISPERSION
Dispersion and stability of two electromagnetic solvers for triangular meshes
[DE91-016607] N92-11227
DISPLACEMENT
A computational procedure for the dynamics of flexible beams within multibody systems N92-11371
DISPLAY DEVICES
Human factors issues in the design of user interfaces for planning and scheduling N92-11049
High definition systems in Japan
[NASA-TM-105108] N92-11225
DISPOSAL
Discharge system tests of Halon 1301 test gas simulants
[AD-A240679] N92-11193
DISSOLVING
Physicochemical properties and dissolution in simulated biological fluids of particles of beryllium-powered rocket motor exhaust and pure beryllium oxides calcined at low and high temperature
[AD-A240288] N92-11134
Observation of DOM composition by synchronous fluorescence spectroscopy N92-11549
Studies of the physical and chemical stability of natural sea-surface films
[AD-A239818] N92-11604
DISTORTION
Ignition and structure of a laminar diffusion flame in the field of a vortex
[NASA-CR-189042] N92-11162
Simulation of a nonlinear two degrees of freedom system. Study of the temporal response to a harmonic attraction
[ONERA-RT-17/1677-RY-091-R] N92-11755
DISTRIBUTED PROCESSING
Sparse distributed memory
[NASA-CR-188841] N92-11643
Vienna FORTRAN: A FORTRAN language extension for distributed memory multiprocessors
[NASA-CR-187634] N92-11670
Total recall in distributive associative memories
[NASA-CR-188884] N92-11699
Advanced information processing system for advanced launch system: Avionics architecture synthesis
[NASA-CR-187554] N92-11704
Advanced information processing system for advanced launch system: Hardware technology survey and projections
[NASA-CR-187555] N92-11705
Advanced information processing system: Inter-computer communication services
[NASA-CR-187556] N92-11706
Learning to read aloud: A neural network approach using sparse distributed memory
[NASA-CR-188846] N92-11711
Statistical prediction with Kanerva's sparse distributed memory
[NASA-CR-187314] N92-11743
DISTRIBUTION FUNCTIONS
Spectral reflectance of thin snow N92-11482
March AFB forecasting rules of thumb evaluation
[AD-A240458] N92-11595
On the maximum entropy principle for Markov chains and processes
[ETN-91-90150] N92-11750
The strong coupling limit for polaron models
[ETN-91-90163] N92-11757
Fokker-Planck equation in the presence of anomalous diffusion
[NIFS-29] N92-11879
Conditional climatology of Ap: The relationship between various solar events (surges, prominences, filaments, radio bursts, x ray episodes) and geomagnetic storms
[AD-A240457] N92-11958
DIVERTERS
Confinement improvement by edge control N92-11817
Status of the Torsatron/Stellarator Program N92-11821
Destruction of magnetic surfaces in helical torus N92-11832
Island studies for Helias Configurations N92-11835
Engineering design of LHD vacuum vessel N92-11866
ITER divertor sputtering erosion: Recent analysis for carbon, beryllium, tungsten, and niobium surfaces
[DE91-017235] N92-11871
The TITAN reversed-field-pinch fusion reactor study, volume 4
[DE92-000138] N92-11895
DOCUMENT STORAGE
Development of data file standards for automated ultrasonic scanning systems. Exchange methods for digital ultrasonic inspection data
[AD-A240075] N92-11364
DOCUMENTATION
Computer integrated documentation
[NASA-TM-103870] N92-11673
DOCUMENTS
A brief introduction to the universal documentation system. Universal documentation system handbook
[AD-A240622] N92-11027
Open document processing and the ISOTEXT system
[ETN-91-90160] N92-11928
DOMAINS
Interface conditions for domain decomposition with radical grid refinement N92-11733
DOPED CRYSTALS
Laser diode pumped, erbium-doped, solid state laser with high slope efficiency
[AD-D014968] N92-11347
A study on the development of high T(sub c) superconducting materials
[DE91-629755] N92-11917
DOPPLER RADAR
Design and operation of the GL/OPA mobile Doppler lidar
[AD-A240257] N92-11231

DOSIMETERS
Solid state neutron dosimeter for space applications
[NASA-CR-185633] N92-11331
DOWNLINKING
Multiple beam antenna/switch system study
[NASA-CR-183496] N92-11251
DRAG REDUCTION
Experimental study of an independently deflected wingtip mounted on a semispan wing
[NASA-TM-102842] N92-10983
Turbulent friction drag reduction: Boundary layer manipulators
[CERT-RSF-DERAT-62/5004-31] N92-11309
DRIFT (INSTRUMENTATION)
Diffusion and drift of charges in semiconductor detectors
[MBE-225] N92-11281
DRONE AIRCRAFT
Development of a 1/7th scale fighter UAV for flight research
[AD-A240703] N92-11008
DROP SIZE
LOX/hydrogen coaxial injector atomization test program N92-11121
Deformation and breakup of drops in simple shear flows
[ETN-91-90143] N92-11315
DROPS (LIQUIDS)
Droplet Core Nuclear Rocket (DLNR) N92-11105
Generalized formulation for semi-empirical radar models representing crop backscattering N92-11447
DROUGHT
Contribution of NOAA-AVHRR satellite data in forest vegetation monitoring N92-11520
Multidate analysis of NOAA-AVHRR data over France: Relationship with agroclimatic characteristics N92-11521
DRY CELLS
Nonaqueous secondary batteries
[DE91-017788] N92-11282
DUCTED FLOW
Mixed convection in two-dimensional laminar air flow with reverse flow regions N92-11293
Evaluation of high Reynolds number flow in a 180 degree turn-around-duct
[NASA-CR-184243] N92-11318
DUCTILITY
Alloy modeling and experimental correlation for ductility enhancement in near stoichiometric single crystal nickel aluminide
[AD-A240151] N92-11175
Moisture-induced environmental embrittlement of ordered intermetallic alloys at ambient temperatures
[DE91-018852] N92-11183
DUMP COMBUSTORS
Numerical prediction of turbulent flame stability in premixed/prevaporized (HSCT) combustors
[NASA-CR-188991] N92-11161
DURABILITY
Properties of aircraft fuels and related materials
[AD-A240650] N92-11213
Piston temperature measurement in a natural gas engine
[PB91-194357] N92-11352
DUST STORMS
Effect of particle size of Martian dust on the degradation of photovoltaic cell performance
[NASA-TM-105232] N92-11133
DYE LASERS
Novel nonlinear laser diagnostic techniques
[AD-A240193] N92-11346
DYNAMIC CHARACTERISTICS
Perceptual grouping and shape from texture
[AD-A240358] N92-11678
DYNAMIC CONTROL
New methods in robust control
[AD-A240221] N92-11018
OPUS: Optimal Projection for Uncertain Systems. Volume 1
[AD-A240372] N92-11080
DYNAMIC LOADS
Deformation of isodamp (A polyvinyl chloride-based elastomer) at various loading rates
[AD-A240393] N92-11189
Photon stimulated desorption of neutral species from aluminum
[DE91-017004] N92-11784
DYNAMIC MODELS
Modeling of flexible polyarticulate chains: Bibliographic synthesis
[CERT-DERA-1/7735] N92-11927
DYNAMIC RESPONSE
Advanced Langmuir Probe (LP)
[NASA-CR-180084] N92-11284
A computational procedure for the dynamics of flexible beams within multibody systems N92-11371
First-passage problems: A probabilistic dynamic analysis for degraded structures
[NASA-TM-103755] N92-11373
Engine dynamic analysis with general nonlinear finite element codes
[NASA-CR-187222] N92-11379
A diagnostic study of the velocity structure of a meandering jet using a primitive equation model with dynamic mode initialization
[AD-A240687] N92-11609
Simulation of a nonlinear two degrees of freedom system. Study of the temporal response to a harmonic attraction
[ONERA-RT-17/1677-RY-091-R] N92-11755
Comparative study of final state interaction contributions to the dynamic response of quantum fluids
[DE91-631020] N92-11892
DYNAMIC STABILITY
New methods in robust control
[AD-A240221] N92-11018
DYNAMIC STRUCTURAL ANALYSIS
A computational procedure for the dynamics of flexible beams within multibody systems N92-11371
First-passage problems: A probabilistic dynamic analysis for degraded structures
[NASA-TM-103755] N92-11373

E

EARLY WARNING SYSTEMS
Real-time earthquake monitoring: Early warning and rapid response
[NASA-CR-186701] N92-11582
EARTH (PLANET)
The notion of artificial satellites in the anisotropic gravitational field of a uniformly rotating solid Earth model. A second order analytical solution
[SER-C-357] N92-11072
Theory and modeling in GLOBEC: A first step N92-11602
EARTH ALBEDO
Bidirectional reflectance and surface albedo: Physical modeling and inversion N92-11469
Aircraft simulations of the POLDER experiment: First results N92-11471
Multiangular approach to solution of atmosphere optics reverse problems N92-11478
Validation of a ground spectral and directional reflectance model N92-11479
EARTH ATMOSPHERE
Use of multitemporal SPOT data in first ISLSCP field experiment N92-11554
Space observations for global change N92-11555
EARTH IONOSPHERE
A calibration of the Naval Postgraduate School middle ultraviolet spectrograph and an analysis of the OII 2470 A and OI 2972 A emissions obtained from mid-latitude rocket observations
[AD-A240686] N92-11587
EARTH MOVEMENTS
Neotectonic studies of northern Baja California, Mexico, with LANDSAT thematic mapper and SPOT panchromatic imagery: Partitioning of dextral and extensional strain at the Pacific-North America plate boundary N92-11553
LAGEOS geodetic analysis-SL7.1
[NASA-TM-104549] N92-11584
EARTH OBSERVATIONS (FROM SPACE)
Observations of the Earth in polarized light from the US Space Shuttle N92-11485
Combined use of Earth observation satellite and meteorological satellite for crop assessment in semiarid environments N92-11494
Catalog of space shuttle earth observations handheld photography. Space transportation system 37 (STS-37) mission dates: April 5-11, 1991
[NASA-CR-189014] N92-11561
EARTH OBSERVING SYSTEM (EOS)
Space observation of the land-ocean-atmosphere system at high spectral resolution in the infrared: Perspectives and problems N92-11421
Looking ahead to EOS: Update on NASA's Earth Observing Program N92-11556
Study and prototype of data system interactions for the Earth Observing System Data and Information System
[NASA-CR-183505] N92-11648
EARTH ORBITAL ENVIRONMENTS
Analysis of surfaces from the LDEF A0114, phase 4
[NASA-CR-188990] N92-11074
The interactions of atmospheric cosmogenic radionuclides with spacecraft surfaces N92-11075
EARTH ORBITS
Measurements of erosion characteristics for metal and polymer surfaces using profilometry N92-11077
EARTH RADIATION BUDGET
Nonscanning climate sensor study
[NASA-CR-183506] N92-11589
EARTH SURFACE
A split-window method for obtaining crop temperatures N92-11410
Influence of the viewing geometry on the spectral properties (high resolution visible and NIR) of selected soils from Arizona N92-11473
Validation of a ground spectral and directional reflectance model N92-11479
Target signature by differential reflectance lidar, a feasibility study N92-11544
EARTHQUAKES
Real-time earthquake monitoring: Early warning and rapid response
[NASA-CR-186701] N92-11582
ECOLOGY
Grassland/atmosphere response to changing climate: Coupling regional and local scales
[DE91-016906] N92-11575
Processes for identifying regional influences of and responses to increasing atmospheric CO2 and climate change: The MINK Project
[DE91-018601] N92-11579
ECONOMIC ANALYSIS
High definition systems in Japan
[NASA-TM-105108] N92-11225
A realistic, gradual and economical approach to fusion power
[DE91-018464] N92-11786
ECONOMIC DEVELOPMENT
Greenhouse gas emissions and the developing countries: Strategic options and the USAID response
[PB91-209882] N92-11573
ECONOMICS
Processes for identifying regional influences of and responses to increasing atmospheric CO2 and climate change: The MINK Project
[DE91-018601] N92-11579
ECOSYSTEMS
A conceptual framework for ecosystem modeling using remotely sensed inputs N92-11551
Grassland/atmosphere response to changing climate: Coupling regional and local scales
[DE91-016906] N92-11575
Theory and modeling in GLOBEC: A first step N92-11602
GLOBEC: Global Ocean Ecosystems Dynamics: A component of the US Global Change Research Program
[NASA-TM-105121] N92-11603
Development of recommendations in the area of ionizing radiations
[DE91-018527] N92-11623
EDDY CURRENTS
Behavior of vacuum vessel eddy current in large helical device N92-11840
EDGE DISLOCATIONS
Effects of hydrogen and carbon on thermally activated deformation in nickel
[AD-A240496] N92-11178
EDGE LOADING
Approximate large deflection analysis of circular plates loaded symmetrically
[NPL-DMM(A)-25] N92-11370
EDUCATION
Lessons learned in the development of the C-130 aircrew training system: A summary of Air Force on-site experience
[AD-A240554] N92-11635
Annual research summary, July 1, 1990 - June 30, 1991
[DE91-017408] N92-11962
EIGENVALUES
Studies in the form of finite element mass matrices for beams, plates and shells
[AERO-TN-9101] N92-11369
A parallel algorithm for the eigenvalues and eigenvectors for a general complex matrix
[NASA-CR-188854] N92-11653
An O(log sup 2 N) parallel algorithm for computing the eigenvalues of a symmetric tridiagonal matrix
[NASA-CR-188898] N92-11659
LAPACK: Linear algebra software for supercomputers
[DE91-017316] N92-11660
Numerical methods in Markov chain modeling
[NASA-CR-188908] N92-11744
EIGENVECTORS
A parallel algorithm for the eigenvalues and eigenvectors for a general complex matrix
[NASA-CR-188854] N92-11653
Numerical methods in Markov chain modeling
[NASA-CR-188908] N92-11744

ELASTIC PLATES
A grid-free method for high Reynolds number flow around an immersed elastic structure
[AD-A240048] N92-10984
ELASTIC SCATTERING
Euromech 260: Advanced non-intrusive experimental techniques in fluid and plasma flows
[ETN-91-90104] N92-11313
The considering of the slowing down effect in the formalism of probability tables. Application to the effective cross section calculation
[DE91-626722] N92-11751
Coupled-channel optical calculation of electron-hydrogen scattering: Elastic scattering from 0.5 to 30 eV
[DE91-634157] N92-11780
ELASTIC SHELLS
Quantitative ray methods for scattering of sound by spherical shells
[AD-A240255] N92-11761
Scattering of tone bursts from spherical shells: Computations based on Fourier transform method
[AD-A240642] N92-11764
ELASTIC WAVES
Deformation of isodamp (A polyvinyl chloride-based elastomer) at various loading rates
[AD-A240393] N92-11189
Quantitative ray methods for scattering of sound by spherical shells
[AD-A240255] N92-11761
ELASTOMERS
Deformation of isodamp (A polyvinyl chloride-based elastomer) at various loading rates
[AD-A240393] N92-11189
Damage evolution in filled elastomers
[AD-A240532] N92-11191
ELASTOPLASTICITY
On the symbolic manipulation and code generation for elasto-plastic material matrices
[NASA-CR-187223] N92-11375
Limit pressure of a circumferentially reinforced SiC/Ti ring
[NASA-CR-187211] N92-11387
ELECTRIC ARCS
New insulation constructions for aerospace wiring applications. Volume 2: The 270 VDC arc tracking testing with power controllers
[AD-A240639] N92-11007
Evaluation of Kapton pyrolysis, arc tracking, and arc propagation on the Space Station Freedom (SSF) solar array Flexible Current Carrier (FCC)
[NASA-CR-189056] N92-11139
ELECTRIC BATTERIES
Superionics
[AD-A240352] N92-11910
ELECTRIC CHARGE
Nonaqueous secondary batteries
[DE91-017788] N92-11282
ELECTRIC CONDUCTORS
Progress in Photon Scanning-Tunneling Microscopy (PSTM)
[DE91-018174] N92-11905
ELECTRIC CURRENT
Approximate expressions for the magnetic field from an electric current source in a layered conducting medium
[MRL-TR-91-5] N92-11273
ELECTRIC DISCHARGES
Design of a fast computer-based partial discharge diagnostic system
[NASA-CR-189057] N92-11272
ELECTRIC FIELDS
On radial electric field structure in CHS torsatron/heliotron
[NIFS-94] N92-11796
Influence of fast ion loss on radial electric field in Wendelstein 7-A stellarator
[NIFS-95] N92-11797
Ion temperature and poloidal rotation profiles for NBI heated plasma in CHS N92-11860
Effects of electric field on particle drift orbits in a l = 2 torsatron
[NIFS-31] N92-11878
ELMy-H mode as limit cycle and chaotic oscillations in tokamak plasmas
[NIFS-87] N92-11882
Rotations of bulk ions and impurities in non-axisymmetric toroidal systems
[NIFS-102] N92-11885
ELECTRIC GENERATORS
Geothermal energy conversion system
[AD-D014979] N92-11569
ELECTRIC MOTORS
High efficiency motor rewind study
[DE91-017162] N92-11270
ELECTRIC POWER
Geothermal energy conversion system
[AD-D014979] N92-11569
ELECTRIC POWER PLANTS
Today's central receiver power plant
[DE91-017998] N92-11568
ELECTRIC PROPULSION
Test facilities for high power electric propulsion
[NASA-TM-105247] N92-11136
ELECTRIC WELDING
Overlooked fundamentals of resistance welding
[DE91-018814] N92-11362
ELECTRIC WIRE
New insulation constructions for aerospace wiring applications. Volume 1: Testing and evaluation
[AD-A240638] N92-11006
New insulation constructions for aerospace wiring applications. Volume 2: The 270 VDC arc tracking testing with power controllers
[AD-A240639] N92-11007
Measurement of frequency response in short thermocouple wires
[NASA-CR-187821] N92-11339
ELECTRICAL ENGINEERING
Annual research summary, July 1, 1990 - June 30, 1991
[DE91-017408] N92-11962
ELECTRICAL FAULTS
Design of a fast computer-based partial discharge diagnostic system
[NASA-CR-189057] N92-11272
ELECTRICAL IMPEDANCE
Inverse problems and imaging (Pitman research notes in mathematics series Number 245)
[AD-A240333] N92-11737
ELECTRICAL INSULATION
New insulation constructions for aerospace wiring applications. Volume 1: Testing and evaluation
[AD-A240638] N92-11006
New insulation constructions for aerospace wiring applications. Volume 2: The 270 VDC arc tracking testing with power controllers
[AD-A240639] N92-11007
Progress in Photon Scanning-Tunneling Microscopy (PSTM)
[DE91-018174] N92-11905
ELECTRICAL PROPERTIES
Tester Independent Support Software System (TISSS)
[AD-A240668] N92-11681
Synthesis of novel conducting solids
[AD-A240468] N92-11912
Thermal annealing studies of Fe and Ti implanted in GaAs and InP
[ETN-91-90148] N92-11915
ELECTRICAL RESISTIVITY
On the nature of bulk electrical relaxation in silicate glasses
[DE92-000077] N92-11206
ELECTRO-OPTICAL EFFECT
Electrooptic effects and photosensitivities of PLZT thin films
[DE91-017067] N92-11901
ELECTRODES
Overlooked fundamentals of resistance welding
[DE91-018814] N92-11362
ELECTROLYTES
Mixing effects in aqueous solutions at elevated temperatures
[DE91-017695] N92-11168
Development of an experimental database and theories for prediction of thermodynamic properties of aqueous electrolytes and nonelectrolytes of geochemical significance at supercritical temperatures and pressures
[DE91-018493] N92-11169
New polymer electrolyte hosts and their tetrabutylammonium chloride complexes. Relationships among concentration of polar groups, ESR spin probe response, and ionic conductivity
[AD-A240497] N92-11190
Nonaqueous secondary batteries
[DE91-017788] N92-11282
ELECTROMAGNETIC ABSORPTION
Active radar stealth device
[AD-D014980] N92-11246
ELECTROMAGNETIC COMPATIBILITY
Conformity Assessment Workshop on Electromagnetic Compatibility
[PB91-192989] N92-11226
ELECTROMAGNETIC FIELDS
Behavior of vacuum vessel eddy current in large helical device N92-11840
A compact laser photocathode driven accelerator for the Plasma Wake Field Accelerator Program at UCLA
[AD-A240646] N92-11886
ELECTROMAGNETIC INTERACTIONS
On the evolution of a superconducting cosmic string network
[DE91-630995] N92-11948
ELECTROMAGNETIC MEASUREMENT
Inverse problems and imaging (Pitman research notes in mathematics series Number 245)
[AD-A240333] N92-11737
ELECTROMAGNETIC SCATTERING
Dispersion and stability of two electromagnetic solvers for triangular meshes
[DE91-016607] N92-11227
Discrete ARMA model for natural resonances in electromagnetic and acoustic scattering
[AD-A240656] N92-11241
Nonlinear theory of synthetic aperture radar sea wave imaging N92-11451
ELECTROMAGNETIC SPECTRA
The great observatories for space astrophysics
[NASA-NP-128] N92-11066
ELECTROMAGNETISM
A Fourier collocation time domain method for numerically solving Maxwell's equations
[NASA-TM-104162] N92-11742
ELECTRON ACCELERATION
Electron acceleration by laser fields in a gas
[DE91-018477] N92-11345
ELECTRON BEAMS
Non-equilibrium microstructures produced during electron-beam and laser-beam surface modification of metallic alloys
[DE91-018466] N92-11174
Top down IC failure analysis using an E-beam system coupled to a functional tester N92-11264
Electron acceleration by laser fields in a gas
[DE91-018477] N92-11345
Reduction of FEL gain due to wiggler errors
[DE92-000482] N92-11350
The effect of wiggler errors on FEL gain
[DE92-000483] N92-11351
Experimental studies of a helical axis stellarator (TU-Heliac) N92-11824
A simulation study of interactions of Space-Shuttle generated electron beams with ambient plasma and neutral gas
[NASA-CR-189025] N92-11898
ELECTRON CYCLOTRON HEATING
Review of the TJ-II Flexible Heliac Project N92-11803
Review of CHS experiment N92-11823
Pressure and potential measurements in IMS during electron cyclotron heating N92-11826
Theory of electron cyclotron heating in the flexible heliac TJ-II N92-11828
STORM: A low aspect ratio torsatron for plasma stability N92-11829
ECH system in the large helical device N92-11845
Electron temperature measurements on ATF using electron cyclotron emission N92-11849
Profile measurements in magnetic surface variation experiments/multiple pellet injection experiments N92-11851
Transport study of ECH and NBI plasmas in CHS N92-11857
A study of radiation collapse in CHS plasmas N92-11859
Ion temperature and poloidal rotation profiles for NBI heated plasma in CHS N92-11860
Power deposition during ECH in CHS N92-11862
The 100 GHz half megawatt microwave transmission system development with whispering gallery mode N92-11869
ECH experiments on ATF
[DE91-018845] N92-11889
ELECTRON DIFFRACTION
Photoemission study of Ce/Ta(110) and Ce/W(110) interfaces and the catalytic oxidation effect
[DE91-018167] N92-11903
ELECTRON DISTRIBUTION
Particle acceleration in space and radiation belt depletion
[AD-A240311] N92-11775
Electron distributions and solar wind interaction with nonmagnetic planets N92-11952
ELECTRON EMISSION
Microchannel electron source
[AD-D014956] N92-11276
ELECTRON ENERGY
Electron temperature measurements on ATF using electron cyclotron emission N92-11849
Profile measurements in magnetic surface variation experiments/multiple pellet injection experiments N92-11851
A study of radiation collapse in CHS plasmas N92-11859
Power deposition during ECH in CHS N92-11862

ITER divertor sputtering erosion: Recent analysis for carbon, beryllium, tungsten, and niobium surfaces
[DE91-017235] N92-11871

ELECTRON IMPACT
Electron distributions and solar wind interaction with nonmagnetic planets N92-11952

ELECTRON ORBITALS
Positron lifetimes in solids from first principles calculations
[DE92-000088] N92-11781

ELECTRON PARAMAGNETIC RESONANCE
New polymer electrolyte hosts and their tetrabutylammonium chloride complexes. Relationships among concentration of polar groups, ESR spin probe response, and ionic conductivity
[AD-A240497] N92-11190
Study of silanization of silica and fiberglass using ESR spectroscopy and spin labelling
[AD-A240767] N92-11197

ELECTRON SCATTERING
Coupled-channel optical calculation of electron-hydrogen scattering: Elastic scattering from 0.5 to 30 eV
[DE91-634157] N92-11780

ELECTRON SOURCES
Microchannel electron source
[AD-D014956] N92-11276
Photon stimulated desorption of neutral species from aluminum
[DE91-017004] N92-11784

ELECTRON STATES
Spectral fitting, shock layer modeling, and production of nitrogen oxides and excited nitrogen
[NASA-CR-185664] N92-11769
High I state population in O(7+) produced in ion-solid collisions
[DE91-018169] N92-11904

ELECTRON TRANSFER
Control of electron transfer rates by motions of atoms and molecules
[DE91-018575] N92-11777

ELECTRON TRANSITIONS
Studies on laser atomic spectroscopy
[DE91-628172] N92-11349
High I state population in O(7+) produced in ion-solid collisions
[DE91-018169] N92-11904

ELECTRON TUNNELING
Physics of ultrasmall superconducting circuits
[AD-A240156] N92-11275
Progress in Photon Scanning-Tunneling Microscopy (PSTM)
[DE91-018174] N92-11905

ELECTRONIC EQUIPMENT
The electronic aeronautical chart for general aeronautics: A system specification
[ILR-MITT-263(1991)] N92-10997

ELECTRONICS
Joint services electronics program research in electronics
[AD-A240155] N92-11274

ELECTRONS
Radiation forces to electrons in laser fields explained as scattering for ponderomotive momentum transfers
[IPPCZ-308] N92-11773
Rotations of bulk ions and impurities in non-axisymmetric toroidal systems
[NIFS-102] N92-11885
Vortex-lattice states of a two-dimensional electron system at strong magnetic fields
[DE91-018551] N92-11916

ELECTROSTATIC PROBES
Advanced Langmuir Probe (LP)
[NASA-CR-180084] N92-11284
Status of the Torsatron/Stellarator Program N92-11821
LHCD experiments on tokamak CASTOR
[IPPCZ-304] N92-11881

ELEMENTARY PARTICLES
Theoretical interpretation of high-energy nuclear collisions
[DE91-016965] N92-11782

ELEVATION
Altitude dependence in a semi-analytical atmospheric code N92-11413

ELLIPSES
Optimal Chebyshev polynomials on ellipses in the complex plane
[NASA-CR-188836] N92-11722
New Bernstein type inequalities for polynomials on ellipses
[NASA-CR-186626] N92-11724

ELLIPTIC DIFFERENTIAL EQUATIONS
Some fast elliptic solvers on parallel architectures and their complexities
[NASA-CR-188840] N92-11692

EMBRITTLEMENT
Moisture-induced environmental embrittlement of ordered intermetallic alloys at ambient temperatures
[DE91-018852] N92-11183

EMERGENCIES
Guidelines for integrating helicopter assets into emergency planning
[SCT-91RR-18] N92-10993

EMISSION
EDMS: Microcomputer pollution model for civilian airports and Air Force bases, (user's guide)
[AD-A240528] N92-11578

EMISSION SPECTRA
Continuum x ray gauging of multiple-element materials
[DE91-017429] N92-11368
Time-resolved spectroscopy of the blue fluorescence of spinach leaves N92-11538
Simultaneous detection in blue and red bands of laser induced vegetation fluorescence N92-11539
Laser-induced blue fluorescence and red chlorophyll fluorescence signatures of differently pigmented leaves N92-11541
The laser-induced chlorophyll fluorescence ratio F690/F735 of spruce needles and beech leaves during the course of a year N92-11542
A simple model of canopy fluorescence N92-11543
Laser induced fluorescence of growing camphor tree leaves: Influence of chlorophyll content on LIF spectral signature N92-11547
Spectral fitting, shock layer modeling, and production of nitrogen oxides and excited nitrogen
[NASA-CR-185664] N92-11769

EMISSIVITY
Experimental approach to emissivity problems and surface temperature in thermal infrared remote sensing N92-11462
Complementarity of temperature independent Thermal Infrared Spectral Indices (TISI) and NDVI: Compared properties and combined use for soil and vegetation discrimination N92-11490
NOAA-AVHRR contribution to the analysis or urban heat islands N92-11495

EMULSIONS
Deformation and breakup of drops in simple shear flows
[ETN-91-90143] N92-11315

ENERGY BUDGETS
Development of a 3-D tree thermal response model for energy budget and scene simulation studies
[AD-A240693] N92-11565

ENERGY CONSERVATION
Office of Basic Energy Sciences
[DE91-019006] N92-11570

ENERGY CONSUMPTION
Effect of control variables and length of refining zone on the refining result with a new pilot refiner N92-11155
An assessment of the available windy land area and wind energy potential in the contiguous United States
[DE91-018887] N92-11601

ENERGY CONVERSION
Enabling the space exploration initiative: NASA's exploration technology program in space power
[NASA-TM-4325] N92-11131

ENERGY CONVERSION EFFICIENCY
High efficiency motor rewind study
[DE91-017162] N92-11270
Office of Basic Energy Sciences
[DE91-019006] N92-11570
Laser produced plasma soft x ray generation
[DE91-016925] N92-11874

ENERGY DISSIPATION
Limits of energy dissipation for x ray sensitive pn Charge Coupled Devices (CCDs)
[MPE-224] N92-11280

ENERGY DISTRIBUTION
Index and bulk parameters for frequency-direction spectra measured at CERC field research facility
[AD-A240320] N92-11607
Power-law energy spectrum and orbital stochasticity
[DE91-017387] N92-11872

ENERGY LEVELS
Studies on laser atomic spectroscopy
[DE91-628172] N92-11349

ENERGY POLICY
Greenhouse gas emissions and the developing countries: Strategic options and the USAID response
[PB91-209882] N92-11573
A realistic, gradual and economical approach to fusion power
[DE91-018464] N92-11786

ENERGY SPECTRA
Index and bulk parameters for frequency-direction spectra measured at CERC field research facility
[AD-A240320] N92-11607
The hazard of exposure to impulse noise as a function of frequency, volume 2
[AD-A240530] N92-11762
Power-law energy spectrum and orbital stochasticity
[DE91-017387] N92-11872

ENERGY TRANSFER
Melting efficiency in fusion welding
[DE91-017988] N92-11355
Calibration and validation of a surface flux model in the framework of the HAPEX-MOBILHY experiment. Application to estimating the cover resistance N92-11511
Collisional energy transfer from excited nitrogen dioxide
[DE91-016989] N92-11772
Effects of perturbing helical fields on confinement of Heliotron DR plasma N92-11818

ENGINE CONTROL
Parallel processing applications for gas turbine engine control N92-11012
Technology readiness assessment of advanced space engine integrated controls and health monitoring
[NASA-TM-105255] N92-11130
Definition, technology readiness, and development cost of the orbit transfer vehicle engine integrated control and health monitoring system elements
[NASA-CR-187123] N92-11132

ENGINE DESIGN
Mach 6.5 air induction system design for the Beta 2 two-stage-to-orbit booster vehicle
[NASA-CR-187233] N92-11013
Structural tailoring of advanced turboprops (STAT): User's manual
[NASA-CR-187101] N92-11016
Wire core reactor for NTP N92-11099
Fission fragment assisted reactor concept for space propulsion: Foil reactor N92-11103
JANNAF Combustion Instability Panel Workshop report: Numerical methods in combustion instability N92-11123
JANNAF Liquid Rocket Combustion Instability Panel research recommendations N92-11124
An overview of tested and analyzed NTP concepts
[NASA-TM-105252] N92-11137
Piston temperature measurement in a natural gas engine
[PB91-194357] N92-11352
Engine dynamic analysis with general nonlinear finite element codes
[NASA-CR-187222] N92-11379

ENGINE MONITORING INSTRUMENTS
Technology readiness assessment of advanced space engine integrated controls and health monitoring
[NASA-TM-105255] N92-11130
Definition, technology readiness, and development cost of the orbit transfer vehicle engine integrated control and health monitoring system elements
[NASA-CR-187123] N92-11132

ENGINE TESTS
Upgraded NERVA systems: Enabler nuclear system N92-11093
Nuclear light bulb N92-11110

ENTHALPY
Effects of hydrogen and carbon on thermally activated deformation in nickel
[AD-A240496] N92-11178
Calculations and curve fits of thermodynamic and transport properties for equilibrium air to 30000 K
[NASA-RP-1260] N92-11285

ENTROPY
Navier-Stokes entropy controlled combustion instability analysis for liquid propellants N92-11122
On a class of implicit and explicit schemes of Van-Leer type for scalar conservation laws N92-11715
Stable upwind schemes for hyperbolic conservation laws for with source terms N92-11716
An analysis of some hyperbolic problems related to the shallow water model (chapter 6)
[IMAG-RR-579] N92-11718
Operator splitting, fractional steps, method and entropy condition for nonlinear hyperbolic systems N92-11719

ENVIRONMENT EFFECTS
The comparison of airborne imaging spectrometry and geochemical ground survey for the analysis of vegetation anomalies over waste deposits N92-11431
Field trip guidebook on environmental impact of clays along the upper Texas coast
[NASA-TM-105097] N92-11572
Winter use plan: Environmental assessment
[PB91-194027] N92-11574
Scientific assessment of stratospheric ozone: 1989. Volume 2: Appendix: AFEAS report
[NASA-TM-105117] N92-11577

Processes for identifying regional influences of and responses to increasing atmospheric CO2 and climate change: The MINK Project
[DE91-018601] N92-11579
Processes for identifying regional influences of and responses to increasing atmospheric CO2 and climate change: The MINK Project
[DE91-018604] N92-11580
Optically thin cirrus clouds over oceans and possible impact on sea surface temperature of warm pool in western Pacific
[NASA-TM-104550] N92-11600

ENVIRONMENT MANAGEMENT
Winter use plan: Environmental assessment
[PB91-194027] N92-11574

ENVIRONMENT MODELS
Actual daily evapotranspiration monitoring using NOAA-AVHRR data from the HAPEX-MOBILHY campaigns N92-11509
Spectral estimates of PAR interception and biomass production of irrigated rice crops. 2: Model validation with SPOT data N92-11510
Calibration and validation of a surface flux model in the framework of the HAPEX-MOBILHY experiment. Application to estimating the cover resistance N92-11511
The linking of crop growth models and multi-sensor remote sensing data N92-11512
Development of a 3-D tree thermal response model for energy budget and scene simulation studies
[AD-A240693] N92-11565

ENVIRONMENT PROTECTION
Integrated Risk Information System
[DE91-018503] N92-11924

ENVIRONMENTAL MONITORING
International program for Earth observations
[NASA-CR-188799] N92-11393
Current status and future developments in radar remote sensing N92-11441
Vegetation monitoring by means of spectral resolved fluorescence lidar N92-11533
The UK Natural Environment Research Council Equipment Pool for Field Spectroscopy (NERC-EPFS) N92-11558

ENVIRONMENTAL SURVEYS
The comparison of airborne imaging spectrometry and geochemical ground survey for the analysis of vegetation anomalies over waste deposits N92-11431
Field trip guidebook on environmental impact of clays along the upper Texas coast
[NASA-TM-105097] N92-11572

ENVIRONMENTAL TESTS
Analysis of surfaces from the LDEF A0114, phase 4
[NASA-CR-188990] N92-11074
The interactions of atmospheric cosmogenic radionuclides with spacecraft surfaces N92-11075

EPHEMERIDES
A theory of the earth's precession relative to the invariable plane of the solar system N92-11938

EPIDEMIOLOGY
JPRS report: Science and technology. USSR: Life sciences
[JPRS-ULS-91-015] N92-11610
JPRS report: Science and technology. USSR: Life sciences
[JPRS-ULS-91-017] N92-11616

EPITAXY
Ultra high vacuum sputtering system
[AD-A240157] N92-11176

EPOXY MATRIX COMPOSITES
An examination of the damage tolerance enhancement of carbon/epoxy using an outer lamina of spectra (R)
[NASA-TP-3160] N92-11142

EQUATIONS OF MOTION
Effects of electric field on particle drift orbits in a l = 2 torsatron
[NIFS-31] N92-11878

EQUATIONS OF STATE
Theoretical interpretation of high-energy nuclear collisions
[DE91-016965] N92-11782
Effects of the equation of state in neutron stars and in stellar collapse
[DE91-014534] N92-11935
OPAL opacities for astrophysical applications
[DE91-016922] N92-11939

EQUATORS
A theory of the earth's precession relative to the invariable plane of the solar system N92-11938

EQUILIBRIUM FLOW
Computational study of the aerodynamics and control by blowing of asymmetric vortical flows over delta wings
[NASA-CR-187979] N92-10990
Computer codes for the evaluation of thermodynamic and transport properties for equilibrium air to 30000 K
[NASA-TM-104107] N92-11300

EQUIVALENT CIRCUITS
Insulated Gate Bipolar Transistors (IGBT) modelization for circuit simulation and utilization in pulse modulated inverters
[ETN-91-90149] N92-11279

ERBIUM
Laser diode pumped, erbium-doped, solid state laser with high slope efficiency
[AD-D014968] N92-11347

EROSION
Measurements of erosion characteristics for metal and polymer surfaces using profilometry N92-11077
Erosive augmentation of solid propellant burning rate: Motor size scaling effect N92-11125
Graphites as plasma facing material of a large fusion device N92-11813
ITER divertor sputtering erosion: Recent analysis for carbon, beryllium, tungsten, and niobium surfaces
[DE91-017235] N92-11871

EROSIVE BURNING
Erosive augmentation of solid propellant burning rate: Motor size scaling effect N92-11125

ERROR ANALYSIS
Error control techniques for satellite and space communications
[NASA-CR-188997] N92-11228
An a priori approach to the evaluation of signature analysis efficiency N92-11268
In flight calibration of large field of view sensors at short wavelength using the Rayleigh scattering N92-11416
Estimation of geopotential differences over intercontinental locations using satellite and terrestrial measurements
[NASA-CR-188992] N92-11560

ERROR CORRECTING CODES
Total recall in distributive associative memories
[NASA-CR-188884] N92-11699

ERRORS
Test and diagnosis of programmable integrated circuits
[ETN-91-99483] N92-11253
Analysis of experimental results on functional testing and diagnosis of complex circuits N92-11254
The effect of wiggler errors on FEL gain
[DE92-000483] N92-11351

ERS-1 (ESA SATELLITE)
Dual-polarized scatterometer measurements of wind and mechanically generated waves in a very large wind/wave flume, the VIERS-1 project N92-11443

ERYTHROCYTES
Effect of prolonged space flight on erythrocyte metabolism and membrane functional condition N92-11617

ESCHERICHIA
Time-resolved analytical pyrolysis mass spectrometry of biomaterials
[AD-A240624] N92-11167
Biochemical and biophysical studies of the E. coli respiratory chain
[DE91-016966] N92-11612

ESSENTIALLY NON-OSCILLATORY SCHEMES
Multi-resolution analysis for ENO schemes
[NASA-CR-189043] N92-11736

ESTIMATES
Theoretical estimation of the viscous damping from liquid transient motion in tanks
[NAL-TR-1095] N92-11298
A method for estimating missing hourly temperatures using daily maximum and minimum temperatures
[AD-A240394] N92-11594

ESTIMATING
A method for estimating missing hourly temperatures using daily maximum and minimum temperatures
[AD-A240394] N92-11594

ETCHING
Solid lubricants on pretreated surfaces
[NASA-CASE-LEW-14474-2] N92-11186

ETHANE
Conversion of ethane and of propane to higher olefin hydrocarbons
[DE91-016896] N92-11160

ETHYL COMPOUNDS
High density energetic materials
[AD-D014959] N92-11212

EULER EQUATIONS OF MOTION
Numerical resolution of three dimensional Euler equations in totally unstructured mesh
[CERT-RF-1/3369-00/DERI-GAN] N92-10988
Euler solutions for an unbladed jet engine configuration
[NASA-TM-105332] N92-11328

EUROPE
Conformity Assessment Workshop on Electromagnetic Compatibility
[PB91-192989] N92-11226

EUTECTIC ALLOYS
Microstructural evolution during the thermomechanical fatigue of solder joints
[DE91-017309] N92-11372

EVALUATION
Test and diagnosis of programmable integrated circuits
[ETN-91-99483] N92-11253
Failure coverage of functional test methods: A comparative experimental evaluation N92-11255
Portable vectorized software for Bessel function evaluation
[PB91-216598] N92-11727
An investigation to find appropriate measures for evaluating interactive information retrieval N92-11922

EVAPORATION
Remote sensing contribution to the APEX MOBILHY program N92-11557

EVAPOTRANSPIRATION
Maximum evapotranspiration monitoring over La Mancha, Spain, using NOAA-AVHRR data N92-11507
Actual daily evapotranspiration monitoring using NOAA-AVHRR data from the HAPEX-MOBILHY campaigns N92-11509
Calibration and validation of a surface flux model in the framework of the HAPEX-MOBILHY experiment. Application to estimating the cover resistance N92-11511
From evapotranspiration to soil moisture investigation based on NOAA thermal infrared data, case study: Poland N92-11531

EXCIMER LASERS
Novel nonlinear laser diagnostic techniques
[AD-A240193] N92-11346

EXHAUST NOZZLES
Static internal performance of ventral and rear nozzle concepts for short-takeoff and vertical-landing aircraft
[NASA-TP-3103] N92-10975

EXHAUST SYSTEMS
Static internal performance of ventral and rear nozzle concepts for short-takeoff and vertical-landing aircraft
[NASA-TP-3103] N92-10975

EXISTENCE THEOREMS
On the solution for the problem of long waves in a perfect fluid N92-11721

EXOTHERMIC REACTIONS
Oxidation of titanium aluminide and its XD composite
[AD-A240401] N92-11177

EXPERT SYSTEMS
TRUST: TDRSS Resource User Support Tool N92-11052
Developments in REDES: The Rocket Engine Design Expert System N92-11120
Making intelligent systems team players: Case studies and design issues. Volume 2: Fault management system cases
[NASA-TM-104738] N92-11641
Deploying expert systems in Ada
[NASA-CR-188938] N92-11664
ART/Ada design project, phase 1. Task 1 report: Overall design
[NASA-CR-188943] N92-11665
ART/Ada design project, phase 1. Task 2 report: Detailed design
[NASA-CR-188944] N92-11666
ART-Ada design project, phase 2
[NASA-CR-188940] N92-11667

EXPLOSIVES
An investigation of the material hazard of some insensitive high explosives
[MRL-TR-91-22] N92-11209
KA-111, Phase C, M-1 propellant tests: Deflagration in partial confinement
[AD-A240185] N92-11211
High density energetic materials
[AD-D014959] N92-11212
Numerical simulations of detonation transmission
[AD-A240560] N92-11304

EXPONENTIAL FUNCTIONS
Application of Krylov exponential propagation to fluid dynamics equations
[NASA-CR-188887] N92-11290
Neutron star magnetic fields and implications for pulsars and gamma ray bursts N92-11960

EXTRATERRESTRIAL MATTER
Non scale-invariant density perturbations from chaotic extended inflation
[NASA-CR-189004] N92-11947

EXTRATERRESTRIAL RADIATION
Underlying generation mechanisms for the extragalactic gamma ray background and their implications for high-resolution gamma ray cosmology N92-11959

EYE MOVEMENTS
The effect of blinking on subsequent dark adaptation
[AD-A240281] N92-11625

F

FABRICATION
Long wavelength semiconductor lasers development for infrared heterodyne applications
[NASA-CR-189243] N92-11341
A compact helical device for a superconducting large helical coil N92-11842
Development of high Tc (greater than 110K) Bi, Tl and Y-based materials as superconducting circuit elements
[NASA-CR-188999] N92-11902

FABRICS
Woven angle ply fabric and apparatus and method for producing such fabrics
[NASA-CASE-LAR-14048-1] N92-11220

FAILURE ANALYSIS
A probabilistic model of intergranular stress corrosion cracking
[DE91-017986] N92-11173
Thermal verification testing of commercial printed-circuit boards for spaceflight
[NASA-TM-105261] N92-11221
Test and diagnosis of programmable integrated circuits
[ETN-91-99483] N92-11253
Analysis of experimental results on functional testing and diagnosis of complex circuits N92-11254
Failure coverage of functional test methods: A comparative experimental evaluation N92-11255
Fault localization when testing complex circuits N92-11260
A microprocessor test approach allowing fault localisation N92-11261
Towards an automated system for the verification and diagnosis of intelligent VLSI circuits N92-11262
Top down IC failure analysis using an E-beam system coupled to a functional tester N92-11264
Automatic tools for microprocessor failure analysis N92-11265
Design of a fast computer-based partial discharge diagnostic system
[NASA-CR-189057] N92-11272
Case history: Failure analysis of a CMOS SRAM with an intermittent open contact
[DE91-018811] N92-11283
Large deformation induced failures in nonlinear solids
[AD-A240369] N92-11382
Making intelligent systems team players: Case studies and design issues. Volume 2: Fault management system cases
[NASA-TM-104738] N92-11641

FAILURE MODES
Case history: Failure analysis of a CMOS SRAM with an intermittent open contact
[DE91-018811] N92-11283

FAR INFRARED RADIATION
Infrared to millimetre observations of active galaxies N92-11932

FARM CROPS
Multifrequency radar measurements of potato, beet, and wheat during the AGRISCATT-88 campaign in the Netherlands N92-11444
Specular and diffuse components of plant canopy reflectance at the wavelengths of 550 and 630 nm N92-11484
Estimation of the primary production in Sahelian region from radiometric data N92-11504

FAST FOURIER TRANSFORMATIONS
Efficient detection of a CW signal with a linear frequency drift
[NASA-CR-188900] N92-11224
Ordered fast fourier transforms on a massively parallel hypercube multiprocessor
[NASA-CR-188899] N92-11700

FASTENERS
Blind fastening apparatus
[NASA-CASE-LAR-14542-1] N92-11354

FATIGUE (MATERIALS)
Critical appraisal of the McDonnell Douglas closure model for predicting fatigue crack growth
[ARL-STRUC-R-444] N92-11376
Fatigue crack initiation
[AD-A240196] N92-11380

FATIGUE LIFE
Propagation behavior of small cracks in 304 stainless steel under biaxial low-cycle fatigue at elevated temperature
[DE91-018863] N92-11389

FATIGUE TESTS
A comparison of single cycle overload effect on Al-Li 2091-T81 plate and 2091-T83 sheet
[AD-A240627] N92-11179

FAULT TOLERANCE
Parallel processing applications for gas turbine engine control N92-11012
Real-time fault diagnosis for propulsion systems
[NASA-TM-105303] N92-11017
Thermal verification testing of commercial printed-circuit boards for spaceflight
[NASA-TM-105261] N92-11221
Communications interface and system for radiation recovery of a microprocessor portion thereof
[AD-D014977] N92-11245
The GAPT system: A chain of test for microprocessors N92-11258
Fault localization when testing complex circuits N92-11260
Making intelligent systems team players: Case studies and design issues. Volume 2: Fault management system cases
[NASA-TM-104738] N92-11641
Advanced information processing system for advanced launch system: Avionics architecture synthesis
[NASA-CR-187554] N92-11704
Advanced information processing system for advanced launch system: Hardware technology survey and projections
[NASA-CR-187555] N92-11705
Advanced information processing system: Inter-computer communication services
[NASA-CR-187556] N92-11706

FEASIBILITY ANALYSIS
Space station tracking requirements feasibility study, volume 2
[NASA-CR-185641-VOL-2] N92-11084
Space station tracking requirements feasibility study, volume 1
[NASA-CR-185641-VOL-1] N92-11085
Automatic tools for microprocessor failure analysis N92-11265
Photovoltaic energy system at an Alaskan site
[PB91-201350] N92-11567

FEED SYSTEMS
Propulsion system needs N92-11112

FEEDBACK CONTROL
Active vibration damping of the Space Shuttle remote manipulator system
[NASA-TM-104149] N92-11073
Linear quadratic servo control of a reusable rocket engine
[NASA-TM-105291] N92-11128

FERMIONS
Global analysis of fermion mixing with exotics
[NASA-CR-189006] N92-11774

FERROFLUIDS
Magnetic fluids and their applications
[DE92-704012] N92-11326

FIBER COMPOSITES
Improved compression molding technology for continuous fiber reinforced composite laminates. Part 2: AS-4/Polyimidesulfone prepreg system
[NASA-TM-104133] N92-11207

FIBER OPTICS
Optical design of a high power fiber optic coupler
[DE91-016924] N92-11789

FIBERS
The role of fiber flocculation in chemical pulp refining
[ETN-91-90025] N92-11150
Fundamental aspects of the refining process N92-11151
A new hypothesis for the mechanics of refining N92-11152
Development of a fundamentally new refining method. Part 1: Basic design considerations N92-11153
Development of a fundamentally new refining method. Part 2: Operating conditions of the new refiner N92-11154
Homogeneity of refining action; effects on fiber and paper structure N92-11157

FIELD COILS
STORM: A low aspect ratio torsatron for plasma stability N92-11829
Structural design of large helical device N92-11837
Pool-cooled superconducting magnet design of large helical device N92-11839
Recent diamagnetic measurements of toroidal coil experiments on Heliotron E N92-11854

FIELD EFFECT TRANSISTORS
Insulated Gate Bipolar Transistors (IGBT) modelization for circuit simulation and utilization in pulse modulated inverters
[ETN-91-90149] N92-11279
Advanced Langmuir Probe (LP)
[NASA-CR-180084] N92-11284

FIELD STRENGTH
Review of CHS experiment N92-11823
Diverted particle-flux studies in the IMS and Proto-Cleo stellarators N92-11825

FIGHTER AIRCRAFT
Static internal performance of ventral and rear nozzle concepts for short-takeoff and vertical-landing aircraft
[NASA-TP-3103] N92-10975
Development of a 1/7th scale fighter UAV for flight research
[AD-A240703] N92-11008

FILM COOLING
Heat transfer, adiabatic effectiveness, and injectant distributions downstream of single and double rows of film-cooling holes with simple and compound angles
[AD-A240743] N92-11305

FILM THICKNESS
Effects on LDEF exposed copper film and bulk N92-11076

FINISHES
Low volatile organic compound paints
[DE91-017984] N92-11203

FINITE DIFFERENCE THEORY
Three-dimensional calculations of fields and loading for loop and folded waveguide ICRF antennas
[DE92-000065] N92-11250
A Newton's method solver for the two-dimensional and axisymmetric Navier-Stokes equations N92-11292
Development of a 3-D tree thermal response model for energy budget and scene simulation studies
[AD-A240693] N92-11565
TEGEN: A one dimensional program to calculate a thermoelectric generator
[DE91-634444] N92-11571

FINITE ELEMENT METHOD
Numerical resolution of three dimensional Euler equations in totally unstructured mesh
[CERT-RF-1/3369-00/DERI-GAN] N92-10988
Structural tailoring of advanced turboprops (STAT): User's manual
[NASA-CR-187101] N92-11016
A new technique for simulating composite material
[NASA-CR-188792] N92-11140
Delamination propagation in a composite panel under compressive stress
[ONERA-RT-23/3542-RY-093-R] N92-11146
Studies in the form of finite element mass matrices for beams, plates and shells
[AERO-TN-9101] N92-11369
On the symbolic manipulation and code generation for elasto-plastic material matrices
[NASA-CR-187223] N92-11375
Engine dynamic analysis with general nonlinear finite element codes
[NASA-CR-187222] N92-11379
Slave finite element for non-linear analysis of engine structures. Volume 2: Programmer's manual and user's manual
[NASA-CR-187225] N92-11388
Transient finite element computations on a variable transputer system
[NASA-CR-189060] N92-11671
Optimal control by wideband frequency. Application to acoustic control by piezoelectric technique
[ONERA-RT-6/3654-RY-006-R] N92-11713
Particle acceleration in space and radiation belt depletion
[AD-A240311] N92-11775

FINITE VOLUME METHOD
Viscous computations of cold air/air flow around scramjet nozzle afterbody
[NASA-CR-4406] N92-10982
Numerical prediction of turbulent flame stability in premixed/prevaporized (HSCT) combustors
[NASA-CR-188991] N92-11161
Modeling of flexible polyarticulate chains: Bibliographic synthesis
[CERT-DERA-1/7735] N92-11927

FIREPROOFING
The behaviour of fire-exposed composite steel/concrete slabs
[ISBN-90-386-0031-3] N92-11147

FIRES
Detection and characterization of active fires in west Africa with LANDSAT thematic mapper and NOAA N92-11529

FISSION
Fission fragment assisted reactor concept for space propulsion: Foil reactor N92-11103
Open cycle gas core nuclear rockets N92-11108

FISSION PRODUCTS
Liquid annulus N92-11104

FIXTURES
Blind fastening apparatus
[NASA-CASE-LAR-14542-1] N92-11354

FLAME STABILITY
Numerical prediction of turbulent flame stability in premixed/prevaporized (HSCT) combustors
[NASA-CR-188991] N92-11161

FLAMES
Ignition and structure of a laminar diffusion flame in the field of a vortex
[NASA-CR-189042] N92-11162
FLASH
Explicit determination of the vapor fraction in flash calculations
[AD-A240376] N92-11165
FLASHBACK
Numerical prediction of turbulent flame stability in premixed/prevaporized (HSCT) combustors
[NASA-CR-188991] N92-11161
FLASHING (VAPORIZING)
Explicit determination of the vapor fraction in flash calculations
[AD-A240376] N92-11165
FLAT PLATES
Nonlinear aspects of aerospace structures at high excitation levels flat aluminum beams and plates studied
[AD-A240600] N92-11383
FLAVOR (PARTICLE PHYSICS)
E sub 6 leptoquarks and the solar neutrino problem
[NASA-CR-189005] N92-11956
FLEXIBLE BODIES
OPUS: Optimal Projection for Uncertain Systems. Volume 1
[AD-A240372] N92-11080
OPUS: Optimal Projection for Uncertain Systems, volume 2
[AD-A240373] N92-11081
Attitude control of flexible structures
[AD-A240520] N92-11082
A computational procedure for the dynamics of flexible beams within multibody systems N92-11371
Modeling of flexible polyarticulate chains: Bibliographic synthesis
[CERT-DERA-1/7735] N92-11927
FLIGHT CONTROL
Development of a 1/7th scale fighter UAV for flight research
[AD-A240703] N92-11008
New methods in robust control
[AD-A240221] N92-11018
Initial design study of existing flight control system of RPH and feasibility study of implementing HHC on the SH-60B
[AD-A240522] N92-11019
Prediction of forces and moments for hypersonic flight vehicle control effectors
[NASA-CR-188954] N92-11070
FLIGHT CREWS
Lessons learned in the development of the C-130 aircrew training system: A summary of Air Force on-site experience
[AD-A240554] N92-11635
FLIGHT SAFETY
A comparison of airborne wake vortex detection measurements with values predicted from potential theory
[NASA-TP-3125] N92-10994
FLIGHT SIMULATION
Human Machine Interfaces for Teleoperators and Virtual Environments Conference
[NASA-CP-10071] N92-11638
FLIGHT SIMULATORS
Parameter identification studies on the NASA/Ames Research Center Advanced Concepts Flight Simulator
[NASA-TM-105126] N92-11024
Perceptual style and air-to-air tracking performance
[NASA-TM-102868] N92-11629
FLIGHT TESTS
Rotorcraft system identification
[AGARD-AR-280] N92-11001
Developmental flight testing of a half scale unmanned air vehicle
[AD-A240347] N92-11002
Development of a 1/7th scale fighter UAV for flight research
[AD-A240703] N92-11008
FLIGHT TRAINING
The development of Behaviorally Anchored Rating Scales (BARS) for evaluating USAF pilot training performance
[AD-A239969] N92-11630
Lessons learned in the development of the C-130 aircrew training system: A summary of Air Force on-site experience
[AD-A240554] N92-11635
FLOCCULATING
The role of fiber flocculation in chemical pulp refining
[ETN-91-90025] N92-11150
FLOW DISTRIBUTION
Results from computational analysis of a mixed compression supersonic inlet
[NASA-TM-104475] N92-10976
Viscous computations of cold air/air flow around scramjet nozzle afterbody
[NASA-CR-4406] N92-10982
A grid-free method for high Reynolds number flow around an immersed elastic structure
[AD-A240048] N92-10984
Computational study of the aerodynamics and control by blowing of asymmetric vortical flows over delta wings
[NASA-CR-187979] N92-10990
A comparison of airborne wake vortex detection measurements with values predicted from potential theory
[NASA-TP-3125] N92-10994
Numerical simulation of the reactive flow in advanced (HSR) combustors using KIVA-2
[NASA-CR-188996] N92-11014
Prediction of forces and moments for hypersonic flight vehicle control effectors
[NASA-CR-188954] N92-11070
Aerodynamic calculations related to tethered sub-satellite experiments
[NASA-CR-188964] N92-11071
CFD code survey for thrust chamber application N92-11119
Navier-Stokes entropy controlled combustion instability analysis for liquid propellants N92-11122
Numerical prediction of turbulent flame stability in premixed/prevaporized (HSCT) combustors
[NASA-CR-188991] N92-11161
Calculations and curve fits of thermodynamic and transport properties for equilibrium air to 30000 K
[NASA-RP-1260] N92-11285
Direct-contact heat exchanger for swirling countercurrent flow of hot gas and finely divided solids: A parametric study
[DE91-017229] N92-11291
Heat transfer, adiabatic effectiveness, and injectant distributions downstream of single and double rows of film-cooling holes with simple and compound angles
[AD-A240743] N92-11305
Diverted particle-flux studies in the IMS and Proto-Cleo stellarators N92-11825
FLOW EQUATIONS
Application of Krylov exponential propagation to fluid dynamics equations
[NASA-CR-188887] N92-11290
Solving the shallow water equations on the Cray X-MP/48 and the connection machine 2
[NASA-CR-188897] N92-11658
FLOW MEASUREMENT
LV software support for supersonic flow analysis
[NASA-CR-188914] N92-10978
Preliminary studies for automizing thermal flux measurement examination by thermosensitive coloring
[AAAF-NT-89-28] N92-11288
Measurement of turbulent flow beneath the wind wave induced water surface, using picture repetition analysis
[ETN-91-90203] N92-11316
Evaluation of high Reynolds number flow in a 180 degree turn-around-duct
[NASA-CR-184243] N92-11318
The phenomena of scalar mixing in turbulent gas-particle flows, measuring equipment, and measurements
[DE92-704034] N92-11327
FLOW STABILITY
Application of Krylov exponential propagation to fluid dynamics equations
[NASA-CR-188887] N92-11290
The three-dimensional evolution of a plane mixing layer. Part 1: The Kelvin-Helmholtz roll-up
[NASA-TM-103856] N92-11303
FLOW VELOCITY
Calibration of turbine flowmeters for storable bipropellant engines
[NAL-TR-1091] N92-11127
Numerical prediction of turbulent flame stability in premixed/prevaporized (HSCT) combustors
[NASA-CR-188991] N92-11161
Evaluation of high Reynolds number flow in a 180 degree turn-around-duct
[NASA-CR-184243] N92-11318
A diagnostic study of the velocity structure of a meandering jet using a primitive equation model with dynamic mode initialization
[AD-A240687] N92-11609
FLOW VISUALIZATION
Experimental investigation of the effects of blowing on bursting of strake vortices
[AD-A240256] N92-10985
Theoretical study (Lagrangian modeling) of turbulent particulate dispersion
[ETN-91-99909] N92-11287
Hydrodynamic tunnel study of the marginal vortex breakdown in the pressure field of a wing profile
[ONERA-RSF-44/1147-AY-144A] N92-11308
Hydrodynamic flow visualization around an oscillating vane. Extension of study to the case of higher incidences and amplitudes and the starting off phase from permanent regime
[ONERA-RT-56/1369-AN] N92-11312
Schlieren system for visualizing the flow within a pipe of circular cross-section
[NASA-CASE-LAR-13944-1] N92-11336
FLOWMETERS
Calibration of turbine flowmeters for storable bipropellant engines
[NAL-TR-1091] N92-11127
FLUID DYNAMICS
Application of Krylov exponential propagation to fluid dynamics equations
[NASA-CR-188887] N92-11290
Superfluid helium dynamics
[NASA-CR-188814] N92-11294
Turbulent fluid motion 3: Basic continuum equations
[NASA-TM-104386] N92-11317
An efficient and robust algorithm for two dimensional time dependent incompressible Navier-Stokes equations: High Reynolds number flows
[NASA-TM-104424] N92-11320
FLUID FLOW
Thermal behavior of the SHOOT gallery arm
[CD-21] N92-11296
Euromech 260: Advanced non-intrusive experimental techniques in fluid and plasma flows
[ETN-91-90104] N92-11313
An efficient and robust algorithm for two dimensional time dependent incompressible Navier-Stokes equations: High Reynolds number flows
[NASA-TM-104424] N92-11320
In-line hydraulic dashpot
[AD-D014955] N92-11356
The modeling of complex continua: Fundamental obstacles and grand challenges
[DE91-018806] N92-11686
FLUID MANAGEMENT
Improved thermodynamic modeling of the no-vent fill process and correlation with experimental data
[NASA-TM-104492] N92-11129
FLUID MECHANICS
Critical velocities and mutual friction in He-3-He-4 II mixtures at temperatures below 100 mK
[ETN-91-90132] N92-11314
FLUORESCENCE
Euromech 260: Advanced non-intrusive experimental techniques in fluid and plasma flows
[ETN-91-90104] N92-11313
Control of the physiological state of vegetation cover by remote sensing of fluorescent emission in the blue and red visible spectrum regions N92-11532
Wavelength shifts in fluorescence maxima of stressed and non-stressed Norway spruce needles over the growing season N92-11536
Time-resolved spectroscopy of the blue fluorescence of spinach leaves N92-11538
A simple model of canopy fluorescence N92-11543
Observation of DOM composition by synchronous fluorescence spectroscopy N92-11549
FLUORIDES
Vapor core propulsion reactors N92-11109
FLUORINE
High-T sub c fluorine-doped YBa2Cu3O(y) films on ceramic substrates by screen printing
[NASA-TM-105296] N92-11188
FLUOROCARBONS
Scientific assessment of stratospheric ozone: 1989. Volume 2: Appendix: AFEAS report
[NASA-TM-105117] N92-11577
FLUX (RATE)
On a class of implicit and explicit schemes of Van-Leer type for scalar conservation laws N92-11715
FLUX QUANTIZATION
Nonscanning climate sensor study
[NASA-CR-183506] N92-11589
FOKKER-PLANCK EQUATION
Fokker-Planck equation in the presence of anomalous diffusion
[NIFS-29] N92-11879
FORECASTING
Strategic air command contrail formation study
[AD-A240467] N92-11003
Development of a system for accurate forecasting of solar activity
[AD-A240359] N92-11957
FORESTS
The spectral reflection behaviour of branches and branch components of healthy and damaged beech trees N92-11432
Evaluation of high spectral resolution laboratory reflectance data of healthy and damaged beech and spruce branches for the improvement of forest damage classification N92-11433

Analysis of radar polarimetric data for the discrimination and monitoring of forest covers N92-11449
Structural controls on the remotely sensed response of a coniferous forest plantation N92-11516
Contribution of NOAA-AVHRR satellite data in forest vegetation monitoring N92-11520
Study of the spatial signature of forest covers by geometric-optic modeling N92-11530
Processes for identifying regional influences of and responses to increasing atmospheric CO2 and climate change: The MINK Project
[DE91-018604] N92-11580

FORMAT
Development of data file standards for automated ultrasonic scanning systems. Exchange methods for digital ultrasonic inspection data
[AD-A240075] N92-11364

FORTRAN
Vienna FORTRAN: A FORTRAN language extension for distributed memory multiprocessors
[NASA-CR-187634] N92-11670
Computer program for Bessel and Hankel functions
[NASA-TM-105154] N92-11691

FORWARD SCATTERING
Quantitative ray methods for scattering of sound by spherical shells
[AD-A240255] N92-11761

FOURIER ANALYSIS
Three-dimensional calculations of fields and loading for loop and folded waveguide ICRF antennas
[DE92-000065] N92-11250

FOURIER TRANSFORMATION
Using a discrete Fourier transform to estimate phase in interferometric direction finding
[AD-A231414] N92-10995
A Fourier collocation time domain method for numerically solving Maxwell's equations
[NASA-TM-104162] N92-11742
Scattering of tone bursts from spherical shells: Computations based on Fourier transform method
[AD-A240642] N92-11764

FRACTALS
Fractal image compression
[AD-A240636] N92-11680

FRACTURE MECHANICS
Critical appraisal of the McDonnell Douglas closure model for predicting fatigue crack growth
[ARL-STRUC-R-444] N92-11376
Fatigue crack initiation
[AD-A240196] N92-11380
Large deformation induced failures in nonlinear solids
[AD-A240369] N92-11382
Propagation behavior of small cracks in 304 stainless steel under biaxial low-cycle fatigue at elevated temperature
[DE91-018863] N92-11389
Training, muscle fatigue and stress fractures
[AD-A240386] N92-11626

FRACTURE STRENGTH
Fracture toughness of carbon/carbon composites
[AD-A240200] N92-11143
Strengthening of an AISI 1020 steel by aluminum-microalloying during liquid dynamic compaction
[DE91-018745] N92-11182
The effects of specimen geometry and size on the fracture toughness of nuclear graphites
[DE92-000056] N92-11205

FRACTURES (MATERIALS)
Training, muscle fatigue and stress fractures
[AD-A240386] N92-11626

FRAUNHOFER LINE DISCRIMINATORS
Control of the physiological state of vegetation cover by remote sensing of fluorescent emission in the blue and red visible spectrum regions N92-11532

FREE ELECTRON LASERS
Reduction of FEL gain due to wiggler errors
[DE92-000482] N92-11350
The effect of wiggler errors on FEL gain
[DE92-000483] N92-11351

FREE MOLECULAR FLOW
Drag coefficients with applications to satellite orbits N92-11069

FREQUENCIES
The hazard of exposure to impulse noise as a function of frequency, volume 2
[AD-A240530] N92-11762

FREQUENCY CONTROL
Dual frequency optical carrier technique for transmission of reference frequencies in dispersive media
[NASA-CASE-NPO-18007-1-CU] N92-11791

FREQUENCY DISTRIBUTION
Hourly and daily precipitation frequencies for the United States
[AD-A240746] N92-11599

FREQUENCY HOPPING
The probability of multiple correct packet receptions in a multireceiver frequency-hopped spread-spectrum system
[AD-A240655] N92-11240

FREQUENCY MEASUREMENT
Measurement of frequency response in short thermocouple wires
[NASA-CR-187821] N92-11339

FREQUENCY RESPONSE
Measurement of frequency response in short thermocouple wires
[NASA-CR-187821] N92-11339

FREQUENCY SHIFT
Wavelength shifts in fluorescence maxima of stressed and non-stressed Norway spruce needles over the growing season N92-11536

FREQUENCY STABILITY
Dual frequency optical carrier technique for transmission of reference frequencies in dispersive media
[NASA-CASE-NPO-18007-1-CU] N92-11791

FREQUENCY STANDARDS
Feasibility study on the Cold Hydrogen Maser (CHM)
[NPL-QU-89] N92-11342
Dual frequency optical carrier technique for transmission of reference frequencies in dispersive media
[NASA-CASE-NPO-18007-1-CU] N92-11791

FRESH WATER
Observation of DOM composition by synchronous fluorescence spectroscopy N92-11549

FRICTION
Critical velocities and mutual friction in He-3-He-4 II mixtures at temperatures below 100 mK
[ETN-91-90132] N92-11314

FRICTION DRAG
Turbulent friction drag reduction: Boundary layer manipulators
[CERT-RSF-DERAT-62/5004-31] N92-11309

FUEL FLOW
Dumbo: A pachydermal rocket motor N92-11100
Calibration of turbine flowmeters for storable bipropellant engines
[NAL-TR-1091] N92-11127

FUEL PUMPS
Hydrodynamic design of generic pump components
[NASA-CR-184252] N92-11361

FUEL SPRAYS
LOX/hydrogen coaxial injector atomization test program N92-11121

FUEL SYSTEMS
Properties of aircraft fuels and related materials
[AD-A240650] N92-11213

FULLERENES
New high-T(sub c) benchmarks for organic and fullerene superconductors
[DE91-016406] N92-11899

FUNCTIONAL ANALYSIS
Test and diagnosis of programmable integrated circuits
[ETN-91-99483] N92-11253
Failure coverage of functional test methods: A comparative experimental evaluation N92-11255
Hardware and software tools for microprocessor functional test N92-11257
The GAPT system: A chain of test for microprocessors N92-11258
Taking into account asynchronous signals in functional test of complex circuits N92-11259
Top down IC failure analysis using an E-beam system coupled to a functional tester N92-11264

FUNCTIONAL DESIGN SPECIFICATIONS
Network Control Center User Planning System (NCC UPS) N92-11053
Advanced information processing system: Inter-computer communication services
[NASA-CR-187556] N92-11706

FUSION
Power-law energy spectrum and orbital stochasticity
[DE91-017387] N92-11872

FUSION REACTORS
Graphites as plasma facing material of a large fusion device N92-11813
The main fusion activities in Institute of Plasma Physics, Academia Sinica N92-11814
The TITAN reversed-field-pinch fusion reactor study, volume 4
[DE92-000138] N92-11895
The TITAN reversed-field-pinch fusion reactor study, volume 2
[DE92-000140] N92-11896
The TITAN reversed-field-pinch fusion reactor study, volume 1
[DE92-000141] N92-11897
LLE review
[DE91-018828] N92-11965

FUSION WELDING
Melting efficiency in fusion welding
[DE91-017988] N92-11355

FUZZY SETS
A re-examination of the relationship between fuzzy set theory and probability theory
[AD-A240243] N92-11746

FUZZY SYSTEMS
Classification of posture maintenance data with fuzzy clustering algorithms
[NASA-CR-188949] N92-11662

G

GALACTIC CLUSTERS
Cosmological structure formation
[NASA-CR-189007] N92-11946

GALACTIC EVOLUTION
Perturbations from strings don't look like strings!
[NASA-CR-189012] N92-11941
Cosmological structure formation
[NASA-CR-189007] N92-11946

GALACTIC STRUCTURE
Cosmological structure formation
[NASA-CR-189007] N92-11946

GALERKIN METHOD
Resonant frequency calculations using a hybrid perturbation-Galerkin technique
[NASA-CR-187632] N92-11640

GALLIUM ARSENIDES
Photoreflectance and H2O adsorption on GaAs(100)
[AD-A240391] N92-11911
Spectroscopic studies of layered and bulk semiconductor materials
[ETN-91-90145] N92-11914
Thermal annealing studies of Fe and Ti implanted in GaAs and InP
[ETN-91-90148] N92-11915

GAMMA RAY ASTRONOMY
Development of a high resolution liquid xenon imaging chamber for gamma-ray astronomy
[NASA-CR-188994] N92-11332

GAMMA RAY BURSTS
Neutron star magnetic fields and implications for pulsars and gamma ray bursts N92-11960

GAMMA RAY OBSERVATORY
The great observatories for space astrophysics
[NASA-NP-128] N92-11066

GAMMA RAY SPECTRA
Underlying generation mechanisms for the extragalactic gamma ray background and their implications for high-resolution gamma ray cosmology N92-11959

GAMMA RAYS
Communications interface and system for radiation recovery of a microprocessor portion thereof
[AD-D014977] N92-11245
Development of a high resolution liquid xenon imaging chamber for gamma-ray astronomy
[NASA-CR-188994] N92-11332
Underlying generation mechanisms for the extragalactic gamma ray background and their implications for high-resolution gamma ray cosmology N92-11959

GAS FLOW
Reciprocity theory of gas surface interactions
[IC-AERO-89-04] N92-11289
Direct-contact heat exchanger for swirling countercurrent flow of hot gas and finely divided solids: A parametric study
[DE91-017229] N92-11291
Local interfacial area concentration measurement in bubbly flow
[DE91-018702] N92-11322
The phenomena of scalar mixing in turbulent gas-particle flows, measuring equipment, and measurements
[DE92-704034] N92-11327

GAS INJECTION
Numerical simulation of the reactive flow in advanced (HSR) combustors using KIVA-2
[NASA-CR-188996] N92-11014

GAS MIXTURES
Numerical resolution of three dimensional Euler equations in totally unstructured mesh
[CERT-RF-1/3369-00/DERI-GAN] N92-10988
Explicit determination of the vapor fraction in flash calculations
[AD-A240376] N92-11165
Collision integrals and high temperature transport properties for N-N, O-O, and N-O
[NASA-CR-188907] N92-11770

GAS PRESSURE
Droplet Core Nuclear Rocket (DLNR) N92-11105
Bose-condensation in liquid helium under pressure
[DE91-634504] N92-11170

KA-111, Phase C, M-1 propellant tests: Deflagration in partial confinement
[AD-A240185] N92-11211
GAS TUNGSTEN ARC WELDING
Melting efficiency in fusion welding
[DE91-017988] N92-11355
GAS TURBINE ENGINES
Parallel processing applications for gas turbine engine control N92-11012
Engine dynamic analysis with general nonlinear finite element codes
[NASA-CR-187222] N92-11379
GAS TURBINES
Radial inflow turbine study
[AD-A240169] N92-11015
The effects of Reynolds number, rotor incidence angle and surface roughness on the heat transfer distribution in a large-scale turbine rotor passage
[NASA-CR-187693] N92-11297
GAS-METAL INTERACTIONS
Effects of hydrogen and carbon on thermally activated deformation in nickel
[AD-A240496] N92-11178
GAS-SOLID INTERACTIONS
Drag coefficients with applications to satellite orbits N92-11069
GASEOUS FISSION REACTORS
Nuclear light bulb N92-11110
GASOLINE
Effect of gasoline octane quality on vehicle acceleration performance
[AD-A240433] N92-11357
GATES (CIRCUITS)
Insulated Gate Bipolar Transistors (IGBT) modelization for circuit simulation and utilization in pulse modulated inverters
[ETN-91-90149] N92-11279
GAUSSIAN ELIMINATION
TEGEN: A one dimensional program to calculate a thermoelectric generator
[DE91-634444] N92-11571
GENERAL AVIATION AIRCRAFT
Personal air transport: State of the art
[PB91-204768] N92-10991
GENETICS
Weather prediction using a genetic memory
[NASA-CR-185448] N92-11590
JPRS report: Science and technology. USSR: Life sciences
[JPRS-ULS-91-015] N92-11610
GEOBOTANY
The use of imaging spectrometry in Mediterranean land degradation and soil erosion hazard assessments N92-11430
GEOCENTRIC COORDINATES
A theory of the earth's precession relative to the invariable plane of the solar system N92-11938
GEOCHEMISTRY
Development of an experimental database and theories for prediction of thermodynamic properties of aqueous electrolytes and nonelectrolytes of geochemical significance at supercritical temperatures and pressures
[DE91-018493] N92-11169
The comparison of airborne imaging spectrometry and geochemical ground survey for the analysis of vegetation anomalies over waste deposits N92-11431
Organic geochemistry of seawater particulate matter: Final data analysis interpretation
[AD-A240199] N92-11605
GEODESY
World Geodetic System 1984 (WGS-84) consolidated database for test ranges
[AD-A240621] N92-11026
GEODETIC ACCURACY
Estimation of geopotential differences over intercontinental locations using satellite and terrestrial measurements
[NASA-CR-188992] N92-11560
GEODETIC SURVEYS
LAGEOS geodetic analysis-SL7.1
[NASA-TM-104549] N92-11584
GEODYNAMICS
LAGEOS geodetic analysis-SL7.1
[NASA-TM-104549] N92-11584
GEOLOGY
The use of imaging spectrometry in Mediterranean land degradation and soil erosion hazard assessments N92-11430
Target signature by differential reflectance lidar, a feasibility study N92-11544
Field trip guidebook on environmental impact of clays along the upper Texas coast
[NASA-TM-105097] N92-11572
Theory and modeling in GLOBEC: A first step N92-11602
GEOMETRIC RECTIFICATION (IMAGERY)
Integration of Seasat and SPOT data, contribution to structural geology mapping in temperature environment N92-11499
GEOMETRICAL OPTICS
Measurement, simulation, and analysis of the directional reflectance properties of Earth surface materials N92-11468
Calculating the bidirectional reflectance of natural vegetation covers using Boolean models and geometric optics N92-11486
Synergy of high resolution spatial microwave imagery and geomorphological optics N92-11496
Study of the spatial signature of forest covers by geometric-optic modeling N92-11530
GEOMETRICAL THEORY OF DIFFRACTION
Quantitative ray methods for scattering of sound by spherical shells
[AD-A240255] N92-11761
GEOMETRY
Computer aided surface representation
[DE91-018872] N92-11688
GEOMORPHOLOGY
Contribution of active microwaves to the structural analysis of epicontinental shelf-forms: Example of the English Channel N92-11448
Synergy of high resolution spatial microwave imagery and geomorphological optics N92-11496
GEOPHYSICS
Current status and future developments in radar remote sensing N92-11441
A bibliography of planetary geology and geophysics principal investigators and their associates, 1990-1991
[NASA-TM-4299] N92-11929
GEOPOTENTIAL
Estimation of geopotential differences over intercontinental locations using satellite and terrestrial measurements
[NASA-CR-188992] N92-11560
Analysis of altimetry over the Aral Sea
[NASA-TM-100759] N92-11583
GEOS 3 SATELLITE
Analysis of altimetry over the Aral Sea
[NASA-TM-100759] N92-11583
GEOSYNCHRONOUS ORBITS
Large deployable antenna program. Phase 1: Technology assessment and mission architecture
[NASA-CR-4410] N92-11036
GEOTHERMAL ENERGY CONVERSION
Geothermal energy conversion system
[AD-D014979] N92-11569
GETTERS
A study of radiation collapse in CHS plasmas N92-11859
GLACIERS
Analysis of the surface state of two sub-polar glaciers using SPOT data and a numerical terrain model N92-11523
GLASS
Glass formation, properties, and structure of soda-yttria-silicate glasses
[NASA-TM-104488] N92-11202
On the nature of bulk electrical relaxation in silicate glasses
[DE92-000077] N92-11206
GLASS COATINGS
Effect of particle size of Martian dust on the degradation of photovoltaic cell performance
[NASA-TM-105232] N92-11133
GLASS FIBERS
Study of silanization of silica and fiberglass using ESR spectroscopy and spin labelling
[AD-A240767] N92-11197
GLOBAL AIR POLLUTION
Greenhouse gas emissions and the developing countries: Strategic options and the USAID response
[PB91-209882] N92-11573
GLOBAL POSITIONING SYSTEM
Space station tracking requirements feasibility study, volume 2
[NASA-CR-185641-VOL-2] N92-11084
Space station tracking requirements feasibility study, volume 1
[NASA-CR-185641-VOL-1] N92-11085
GLOBAL WARMING
Space observations for global change N92-11555
GLUONS
On the polarisation of tensor mesons in psi radiative decays and possible implications for the gluonic content of the theta(1720)
[RAL-90-091] N92-11768
GRAIN BOUNDARIES
A probabilistic model of intergranular stress corrosion cracking
[DE91-017986] N92-11173
New dimensions in atom probe analysis
[DE91-018926] N92-11779
GRAMMARS
Extended algebraic graph transformation
[ETN-91-90151] N92-11739
GRAPH THEORY
Extended algebraic graph transformation
[ETN-91-90151] N92-11739
GRAPHITE
The effects of specimen geometry and size on the fracture toughness of nuclear graphites
[DE92-000056] N92-11205
Graphites as plasma facing material of a large fusion device N92-11813
GRAPHITE-EPOXY COMPOSITES
Compression response of laminated composite panels containing multiple delaminations N92-11141
GRAPHS (CHARTS)
Extended algebraic graph transformation
[ETN-91-90151] N92-11739
Spectral observations of solar radio bursts in the range of 2.0-4.5 GHz
[CAS-PUBL-76] N92-11953
Spectral observations of solar radio bursts at 2.0-4.5 GHz
[CAS-PUBL-77] N92-11954
GRASSLANDS
Use of multitemporal SPOT data in first ISLSCP field experiment N92-11554
GRATINGS (SPECTRA)
Compact optical RF spectrum analyzer
[AD-D014962] N92-11792
GRAVITATION
Non scale-invariant density perturbations from chaotic extended inflation
[NASA-CR-189004] N92-11947
GRAVITATIONAL COLLAPSE
Effects of the equation of state in neutron stars and in stellar collapse
[DE91-014534] N92-11935
GRAVITATIONAL EFFECTS
The microgravity environment of the Space Shuttle Columbia payload bay during STS-32
[NASA-TP-3141] N92-11931
GRAVITATIONAL FIELDS
The notion of artificial satellites in the anisotropic gravitational field of a uniformly rotating solid Earth model. A second order analytical solution
[SER-C-357] N92-11072
Estimation of geopotential differences over intercontinental locations using satellite and terrestrial measurements
[NASA-CR-188992] N92-11560
GRAVITATIONAL PHYSIOLOGY
Classification of posture maintenance data with fuzzy clustering algorithms
[NASA-CR-188949] N92-11662
GRAVITY ANOMALIES
Analysis of altimetry over the Aral Sea
[NASA-TM-100759] N92-11583
GRAVITY PROBE B
Precision pointing control of the spinning Gravity Probe B spacecraft N92-11068
GREENHOUSE EFFECT
Greenhouse gas emissions and the developing countries: Strategic options and the USAID response
[PB91-209882] N92-11573
Processes for identifying regional influences of and responses to increasing atmospheric CO2 and climate change: The MINK Project
[DE91-018601] N92-11579
Optically thin cirrus clouds over oceans and possible impact on sea surface temperature of warm pool in western Pacific
[NASA-TM-104550] N92-11600
GRID GENERATION (MATHEMATICS)
Numerical resolution of three dimensional Euler equations in totally unstructured mesh
[CERT-RF-1/3369-00/DERI-GAN] N92-10988
Computational study of the aerodynamics and control by blowing of asymmetric vortical flows over delta wings
[NASA-CR-187979] N92-10990
A new technique for simulating composite material
[NASA-CR-188792] N92-11140
Dispersion and stability of two electromagnetic solvers for triangular meshes
[DE91-016607] N92-11227
Euler solutions for an unbladed jet engine configuration
[NASA-TM-105332] N92-11328
Model problem N92-11729
GROUND BASED CONTROL
Engineering and instrumentation support of GL Research Balloon Program
[AD-A240616] N92-10987

GROUND TESTS
Ground penetrating radar data acquisition system [AD-A240765] N92-11244
GROUND TRUTH
Active microwave remote sensing and ground hydric state. Agriscatt '88 airborne campaign over the Orgeval basin (France) N92-11454
Airborne SAR HAREM campaign: Results, targets features, ERS1 simulations, and operational satellite exploitation N92-11455
Multitemporal study of the Guyana coastline and estuaries using SPOT and LANDSAT imagery N92-11524
GUIDANCE (MOTION)
Quantitative ray methods for scattering of sound by spherical shells [AD-A240255] N92-11761
GUST LOADS
Maximized gust loads for a nonlinear airplane using matched filter theory and constrained optimization [NASA-TM-104138] N92-11010
GUYANA
Multitemporal study of the Guyana coastline and estuaries using SPOT and LANDSAT imagery N92-11524
GYRATORS
Linear theory of a quasioptical gyroklystron with nonuniform magnetic field [AD-A240264] N92-11334
GYROSCOPES
Navigation and positioning of mobile robots [DE92-704014] N92-10998

H

HALLEY'S COMET
Electron distributions and solar wind interaction with nonmagnetic planets N92-11952
HALOCARBONS
Scientific assessment of stratospheric ozone: 1989, volume 1 [NASA-TM-105116] N92-11576
HANDBOOKS
A brief introduction to the universal documentation system. Universal documentation system handbook [AD-A240622] N92-11027
A generalized strategy for building resident database interfaces [NASA-CR-189246] N92-11920
HANKEL FUNCTIONS
Computer program for Bessel and Hankel functions [NASA-TM-105154] N92-11691
HARMONIC CONTROL
Analysis of open loop higher harmonic control at high airspeeds on a modern four-bladed articulated rotor [NASA-TM-103876] N92-11000
Initial design study of existing flight control system of RPH and feasibility study of implementing HHC on the SH-60B [AD-A240522] N92-11019
HARMONIC FUNCTIONS
Analysis of scrape-off layer in toroidal helical systems N92-11815
HARMONIC RADIATION
Electron temperature measurements on ATF using electron cyclotron emission N92-11849
HARMONICS
Simulation of a nonlinear two degrees of freedom system. Study of the temporal response to a harmonic attraction [ONERA-RT-17/1677-RY-091-R] N92-11755
HAZARDOUS MATERIAL DISPOSAL (IN SPACE)
Disposal methods N92-11116
HAZARDS
Safety issues N92-11115
An investigation of the material hazard of some insensitive high explosives [MRL-TR-91-22] N92-11209
HEART
Non-invasive evaluation of the cardiac autonomic nervous system by PET [DE91-018476] N92-11622
HEAT EXCHANGERS
Heat exchanger thermal performance for two nonazeotropic refrigerant mixtures [DE91-017250] N92-11216
Direct-contact heat exchanger for swirling countercurrent flow of hot gas and finely divided solids: A parametric study [DE91-017229] N92-11291
HEAT FLUX
To the account of finite velocity of thermal diffusion in turbulent flows [DE91-635593] N92-11323
HEAT ISLANDS
NOAA-AVHRR contribution to the analysis or urban heat islands N92-11495
Urban heat island N92-11500
HEAT MEASUREMENT
Calorimetry measurements in less than 20 minutes [DE91-017318] N92-11330
HEAT PIPES
Effects of anisotropic conduction and heat pipe interaction on minimum mass space radiators [NASA-TM-105297] N92-11138
HEAT RADIATORS
Lunar radiator shade [NASA-CASE-MSC-21868-1] N92-11639
HEAT RESISTANT ALLOYS
High pressure turbine blade life extension [AD-A240654] N92-11180
Thermoviscoplastic response of Ti-15-3 under various loading conditions [NASA-CR-187621] N92-11391
HEAT SHIELDING
Shielding requirements for particle bed propulsion systems [AD-A240780] N92-11787
HEAT SINKS
Cooling apparatus and couplings therefor [NASA-CASE-ARC-11921-1] N92-11286
HEAT SOURCES
Determination of nonstationary temperatures in high-stressed elements with pulsed heat sources [DE91-635705] N92-11325
HEAT TRANSFER
Direct-contact heat exchanger for swirling countercurrent flow of hot gas and finely divided solids: A parametric study [DE91-017229] N92-11291
Thermal behavior of the SHOOT gallery arm [CD-21] N92-11296
The effects of Reynolds number, rotor incidence angle and surface roughness on the heat transfer distribution in a large-scale turbine rotor passage [NASA-CR-187693] N92-11297
Modeling of the heat transfer in bypass transitional boundary-layer flows [NASA-TP-3170] N92-11299
Heat transfer, adiabatic effectiveness, and injectant distributions downstream of single and double rows of film-cooling holes with simple and compound angles [AD-A240743] N92-11305
Turbulent fluid motion 3: Basic continuum equations [NASA-TM-104386] N92-11317
To the account of finite velocity of thermal diffusion in turbulent flows [DE91-635593] N92-11323
Heat transfer in channels with uniformly swirled flow [DE91-635594] N92-11324
Geometrically exact shells models: Foundation and computational aspects with special reference to implicit large-scale calculations [DE91-019014] N92-11390
Using the radiative surface temperature in energy budget studies over plant canopies N92-11506
Gorter-Mellink pulsed-source problem in cylindrical and spherical geometry [DE91-017249] N92-11725
HEAT TRANSMISSION
Melting efficiency in fusion welding [DE91-017988] N92-11355
HEAT TREATMENT
Low toxicity high temperature PMR polyimides [NASA-CASE-LAR-14639-1] N92-11199
Development of high Tc (greater than 110K) Bi, Tl and Y-based materials as superconducting circuit elements [NASA-CR-188999] N92-11902
HEATING
Aerothermal test results from the first flight of the Pegasus air-launched space booster [NASA-TM-4330] N92-11301
HEATING EQUIPMENT
ECH system in the large helical device N92-11845
HEAVY IONS
Comparison between californium and cyclotron heavy ion tests N92-11266
Comparison between californium and cyclotron SEU tests N92-11267
HELICAL WINDINGS
On radial electric field structure in CHS torsatron/heliotron [NIFS-94] N92-11796
The ANU Heliac Program N92-11804
Experimental studies of a helical axis stellarator (TU-Heliac) N92-11824
Numerical and experimental studies of simulated toroidicity effects in a linear high-beta heliac N92-11827
Destruction of magnetic surfaces in helical torus N92-11832
Ripple diffusion and bootstrap current in LHD N92-11833
Island studies for Helias Configurations N92-11835
Structural design of large helical device N92-11837
Research and development of forced flow superconducting coils for large helical device N92-11838
Pool-cooled superconducting magnet design of large helical device N92-11839
A compact helical device for a superconducting large helical coil N92-11842
Optimization of design parameters for large helical device N92-11843
Effect of multi-layer operation of helical coil in large helical device N92-11844
Motion of charged particle in helical systems N92-11847
Equilibrium, stability, and transport in L = 1 compact helical axis configuration N92-11848
A possible modification of the FT Tokamak into a compact high field stellarator with separatrices N92-11863
Engineering design of LHD vacuum vessel N92-11866
Calculation of magnetic field of helical coils [NIFS-18] N92-11880
HELICOPTER CONTROL
Analysis of open loop higher harmonic control at high airspeeds on a modern four-bladed articulated rotor [NASA-TM-103876] N92-11000
Rotorcraft system identification [AGARD-AR-280] N92-11001
Initial design study of existing flight control system of RPH and feasibility study of implementing HHC on the SH-60B [AD-A240522] N92-11019
HELICOPTER PERFORMANCE
Concept evaluation of the UH-60 externally mounted rescue hoist [AD-A240545] N92-11004
HELICOPTERS
Guidelines for integrating helicopter assets into emergency planning [SCT-91RR-18] N92-10993
Perceptual style and air-to-air tracking performance [NASA-TM-102868] N92-11629
HELIOSTATS
Today's central receiver power plant [DE91-017998] N92-11568
HELIOTRONS
On radial electric field structure in CHS torsatron/heliotron [NIFS-94] N92-11796
Present status of the Large Helical Device Project N92-11800
Review of the TJ-II Flexible Heliac Project N92-11803
The 3-D equilibria of helical systems: Magnetic islands and their control N92-11808
Drift optimization of helical systems N92-11810
Graphites as plasma facing material of a large fusion device N92-11813
Analysis of scrape-off layer in toroidal helical systems N92-11815
Effects of perturbing helical fields on confinement of Heliotron DR plasma N92-11818
Review of Heliotron E experiment N92-11822
Structural design of large helical device N92-11837
Research and development of forced flow superconducting coils for large helical device N92-11838
Pool-cooled superconducting magnet design of large helical device N92-11839
Behavior of vacuum vessel eddy current in large helical device N92-11840
Fundamental design on LHD with bath cooling method N92-11841
A compact helical device for a superconducting large helical coil N92-11842
Optimization of design parameters for large helical device N92-11843
Effect of multi-layer operation of helical coil in large helical device N92-11844
ECH system in the large helical device N92-11845
ICRF heating program of the large helical device N92-11846
Confinement studies of Heliotron E plasmas in magnetic surface variation experiments N92-11850
Profile measurements in magnetic surface variation experiments/multiple pellet injection experiments N92-11851
Impurity behavior in Heliotron E N92-11852
Edge plasma study in Heliotron E N92-11853

Recent diamagnetic measurements of toroidal coil experiments on Heliotron E N92-11854
Study of resistive interchange mode in Heliotron E N92-11855
Measurement of magnetic fluctuations in Heliotron E N92-11856
Transport study of ECH and NBI plasmas in CHS N92-11857
Effect of magnetic axis shift on CHS plasma characteristics N92-11858
Ion temperature and poloidal rotation profiles for NBI heated plasma in CHS N92-11860
Engineering design of large helical device N92-11864
Operation scenario and structural design analysis of LHD (Large Helical Device) coils N92-11865
Engineering design of LHD vacuum vessel N92-11866
Development of superconductor for large helical device N92-11867
NBI system with negative ion source in large helical device N92-11870

HELIUM ISOTOPES
Bose-condensation in liquid helium under pressure [DE91-634504] N92-11170
Critical velocities and mutual friction in He-3-He-4 II mixtures at temperatures below 100 mK [ETN-91-90132] N92-11314
Gorter-Mellink pulsed-source problem in cylindrical and spherical geometry [DE91-017249] N92-11725

HELMHOLTZ EQUATIONS
A domain decomposition algorithm for solving large elliptic problems [DE92-000096] N92-11690

HEMOLYSIS
Effect of prolonged space flight on erythrocyte metabolism and membrane functional condition N92-11617

HERMITIAN POLYNOMIAL
Fast secant methods for the iterative solution of large nonsymmetric linear systems [NASA-CR-188867] N92-11655

HETERODYNING
Design and operation of the GL/OPA mobile Doppler lidar [AD-A240257] N92-11231
Long wavelength semiconductor lasers development for infrared heterodyne applications [NASA-CR-189243] N92-11341

HETEROGENEITY
Control of the heterogeneity of the refining action N92-11158
Proceedings for the ICASE Workshop on Heterogeneous Boundary Conditions [NASA-CR-187630] N92-11728
A generalized strategy for building resident database interfaces [NASA-CR-189246] N92-11920

HEURISTIC METHODS
Intelligent perturbation algorithms for space scheduling optimization N92-11055

HIERARCHIES
CHIMES-2: A tool for automated HCI analysis N92-11051

HIGH CURRENT
Microchannel electron source [AD-D014956] N92-11276

HIGH DEFINITION TELEVISION
High definition systems in Japan [NASA-TM-105108] N92-11225

HIGH ENERGY ELECTRONS
Photoreflectance and H2O adsorption on GaAs(100) [AD-A240391] N92-11911

HIGH FREQUENCIES
A thinned high frequency linear antenna array to study ionospheric structure [AD-A240764] N92-11243

HIGH LEVEL LANGUAGES
Workshops on Efficient Use of Scientific Computing [AD-A240175] N92-11674

HIGH POWER LASERS
Novel nonlinear laser diagnostic techniques [AD-A240193] N92-11346

HIGH PRESSURE
High pressure turbine blade life extension [AD-A240654] N92-11180

HIGH RESOLUTION
A multi-sensor approach to spectral signature analysis of inland waters N92-11428
Evaluation of high spectral resolution laboratory reflectance data of healthy and damaged beech and spruce branches for the improvement of forest damage classification N92-11433
Candidate high spectral resolution derivative indices for the prediction of crop cover N92-11435
High resolution spectral measurements of vegetation and soil in field and laboratory N92-11437

HIGH REYNOLDS NUMBER
A grid-free method for high Reynolds number flow around an immersed elastic structure [AD-A240048] N92-10984
Evaluation of high Reynolds number flow in a 180 degree turn-around-duct [NASA-CR-184243] N92-11318

HIGH SPEED
Technology needs for high speed rotorcraft (3) [NASA-CR-186433] N92-10999
Evaluation of two high-speed runway exits [DOT/FAA/CT-TN91/36] N92-11021

HIGH SPEED PHOTOGRAPHY
Debris/ice/TPS assessment and photographic analysis for Shuttle Mission STS-43 [NASA-TM-103823] N92-11038

HIGH TEMPERATURE
Mixing effects in aqueous solutions at elevated temperatures [DE91-017695] N92-11168
Low toxicity high temperature PMR polyimides [NASA-CASE-LAR-14639-1] N92-11199

HIGH TEMPERATURE AIR
Collision integrals and high temperature transport properties for N-N, O-O, and N-O [NASA-CR-188907] N92-11770

HIGH TEMPERATURE GAS COOLED REACTORS
Nuclear fuels status N92-11113

HIGH TEMPERATURE PLASMAS
Confinement improvement by edge control N92-11817
Diffusion in the Io plasma torus and its relation to the torus spatial structure N92-11949

HIGH TEMPERATURE SUPERCONDUCTORS
Critical properties of strongly interacting bosons on a lattice [DE91-016926] N92-11771
Positron lifetimes in solids from first principles calculations [DE92-000088] N92-11781
New high-T(sub c) benchmarks for organic and fullerene superconductors [DE91-016406] N92-11899
Synthesis of novel conducting solids [AD-A240468] N92-11912
A study on the development of high T(sub c) superconducting materials [DE91-629755] N92-11917

HIGH VOLTAGES
Supervoltage NDE techniques for large aerospace structures [AD-A240625] N92-11365

HIPPOCAMPUS
Long term synaptic plasticity and learning in neuronal networks [AD-A240366] N92-11613

HISTOGRAMS
Database of SPOT histograms N92-11517

HISTORIES
Study of alternatives: Dayton's Aviation heritage, Ohio [PB91-202275] N92-10972
Dumbo: A pachydermal rocket motor N92-11100
Mariners Weather Log, Volume 35, Number 1, Winter 1991 [PB91-201129] N92-11591
Eighty years of aerospace technique through ATMA bulletins [ETN-91-90097] N92-11963

HOLE DISTRIBUTION (ELECTRONICS)
The recombination behavior of a laser induced electron hole plasma in pin diodes and silicon base material [ETN-91-90153] N92-11887

HOLES (ELECTRON DEFICIENCIES)
The recombination behavior of a laser induced electron hole plasma in pin diodes and silicon base material [ETN-91-90153] N92-11887

HOLES (MECHANICS)
Heat transfer, adiabatic effectiveness, and injectant distributions downstream of single and double rows of film-cooling holes with simple and compound angles [AD-A240743] N92-11305

HOLOGRAPHY
Conoscopic holography. 1: Basic principles and physical basis. 2: Rigorous derivation [TELECOM-PARIS-91-C-001] N92-11337

HOSPITALS
Technical requirements of sick bays aboard space ships N92-11620

HOT PRESSING
Development of high Tc (greater than 110K) Bi, Tl and Y-based materials as superconducting circuit elements [NASA-CR-188999] N92-11902

HOUSINGS
Cooling apparatus and couplings therefor [NASA-CASE-ARC-11921-1] N92-11286

HUBBLE SPACE TELESCOPE
SPIKE: AI scheduling techniques for Hubble Space Telescope N92-11054
The great observatories for space astrophysics [NASA-NP-128] N92-11066

HUMAN BEINGS
Rapidly quantifying the relative distention of a human bladder [NASA-CASE-LAR-13901-2] N92-11621

HUMAN FACTORS ENGINEERING
Parameter identification studies on the NASA/Ames Research Center Advanced Concepts Flight Simulator [NASA-TM-105126] N92-11024
Telescience workstation [NASA-CR-188878] N92-11033
User interface issues in supporting human-computer integrated scheduling N92-11048
Human factors issues in the design of user interfaces for planning and scheduling N92-11049
CHIMES-2: A tool for automated HCI analysis N92-11051
Safety issues N92-11115
Space engineering [NASA-CR-187820] N92-11215
Cognitive factors involved in the first stage of programming skill acquisition [AD-A240566] N92-11636

HUMAN PERFORMANCE
Space engineering [NASA-CR-187820] N92-11215
Efficacy of hyperbaric oxygenation in enhancing flight tolerance N92-11618
The effect of blinking on subsequent dark adaptation [AD-A240281] N92-11625
Serial averaging in the construction and validation of performance tests [AD-A240313] N92-11632

HUMAN REACTIONS
A new simulator for assessing subjective effects of sonic booms [NASA-TM-104150] N92-11759

HURRICANES
Mariners Weather Log, Volume 35, Number 2, Spring 1991 [PB91-202572] N92-11592

HYBRID PROPULSION
Hybrid propulsion systems for space exploration missions N92-11097

HYDRAULIC CONTROL
In-line hydraulic dashpot [AD-D014955] N92-11356

HYDRAULIC EQUIPMENT
In-line hydraulic dashpot [AD-D014955] N92-11356

HYDROCARBONS
Conversion of ethane and of propane to higher olefin hydrocarbons [DE91-016896] N92-11160
Explicit determination of the vapor fraction in flash calculations [AD-A240376] N92-11165
Scientific assessment of stratospheric ozone: 1989. Volume 2: Appendix: AFEAS report [NASA-TM-105117] N92-11577

HYDRODYNAMICS
Hydrodynamic design of generic pump components [NASA-CR-184252] N92-11361
Study of the spatial variability of the hydrodynamic behavior of grounds at the Niger (Africa) using satellite images N92-11515
Harnessing the killer micros: Applications from LLNL's massively parallel computing initiative [DE91-018721] N92-11709

HYDROGEN
Open cycle gas core nuclear rockets N92-11108
Decomposition pathways of tetrahydrogen [AD-A240623] N92-11166
Effects of hydrogen and carbon on thermally activated deformation in nickel [AD-A240496] N92-11178
Coupled-channel optical calculation of electron-hydrogen scattering: Elastic scattering from 0.5 to 30 eV [DE91-634157] N92-11780

HYDROGEN ATOMS
Feasibility study on the Cold Hydrogen Maser (CHM) [NPL-QU-89] N92-11342

HYDROGEN ENGINES
Nuclear rocket using indigenous Martian fuel NIMF N92-11098

HYDROGEN FUELS
Benefits of slush hydrogen for space missions [NASA-TM-104503] N92-11214

HYDROGEN MASERS
Feasibility study on the Cold Hydrogen Maser (CHM)
[NPL-QU-89] N92-11342
HYDROGEN OXYGEN ENGINES
Technology readiness assessment of advanced space engine integrated controls and health monitoring
[NASA-TM-105255] N92-11130
HYDROLOGICAL CYCLE
Remote sensing contribution to the APEX MOBILHY program N92-11557
HYDROLOGY
Humidity measurement of naked ground by radar in conditions of excessive water N92-11453
Passive microwave remote sensing of soil moisture: Results from HAPEX, FIFE, and MONSOON 90 N92-11458
HYDROLOGY MODELS
Comparison of passive microwave and model derived estimates for soil moisture fields N92-11459
HYOSCINE
Intranasal scopolamine preparation and method
[NASA-CASE-MSC-21858-1] N92-11628
HYPERBOLIC FUNCTIONS
On the theory and numerical approximation of nonlinear hyperbolic problems
[ETN-91-99898] N92-11714
Stable upwind schemes for hyperbolic conservation laws for with source terms N92-11716
An analysis of some hyperbolic problems related to the shallow water model (chapter 6)
[IMAG-RR-579] N92-11718
Operator splitting, fractional steps, method and entropy condition for nonlinear hyperbolic systems N92-11719
HYPERCUBE MULTIPROCESSORS
Some fast elliptic solvers on parallel architectures and their complexities
[NASA-CR-188840] N92-11692
Ordered fast fourier transforms on a massively parallel hypercube multiprocessor
[NASA-CR-188899] N92-11700
HYPERPLANES
A class of designs for a sparse distributed memory
[NASA-CR-188849] N92-11644
HYPERSONIC FLOW
A fast sorting algorithm for a hypersonic rarefied flow particle simulation on the connection machine
[NASA-CR-188903] N92-10977
Numerical resolution of three dimensional Euler equations in totally unstructured mesh
[CERT-RF-1/3369-00/DERI-GAN] N92-10988
Prediction of forces and moments for hypersonic flight vehicle control effectors
[NASA-CR-188954] N92-11070
Studies of aerothermal loads generated in regions of shock/shock interaction in hypersonic flow
[NASA-CR-181893] N92-11319
HYPERSONIC VEHICLES
Viscous computations of cold air/air flow around scramjet nozzle afterbody
[NASA-CR-4406] N92-10982
Mach 6.5 air induction system design for the Beta 2 two-stage-to-orbit booster vehicle
[NASA-CR-187233] N92-11013
Prediction of forces and moments for hypersonic flight vehicle control effectors
[NASA-CR-188954] N92-11070
HYPERVELOCITY IMPACT
MLITemp: A computer program to predict the thermal effects associated with hypervelocity impact damage to space station MLI
[NASA-CR-184245] N92-11079
HYSTERESIS
Analysis of strain dependent damping in materials via modeling of material point hysteresis
[AD-A240298] N92-11381

I

ICE
Laboratory measurements of the single-scattering properties of ammonia ice crystals N92-11950
ICE ENVIRONMENTS
Large scale study of the microwave signature of the Antarctic ice sheet N92-11463
Comparison between the observed microwave spectral signatures over the Antarctic ice sheet and a snow emissivity model N92-11464
IDEAL FLUIDS
On the solution for the problem of long waves in a perfect fluid N92-11721
IGNITION
Ignition and structure of a laminar diffusion flame in the field of a vortex
[NASA-CR-189042] N92-11162
An investigation of the material hazard of some insensitive high explosives
[MRL-TR-91-22] N92-11209
ILLUMINATION
Illumination, optics, and retroreflectors for efficient landmark tracking N92-11790
IMAGE ANALYSIS
Measurement of turbulent flow beneath the wind wave induced water surface, using picture repetition analysis
[ETN-91-90203] N92-11316
Multifrequency radar measurements of potato, beet, and wheat during the AGRISCATT-88 campaign in the Netherlands N92-11444
Contribution of active microwaves to the structural analysis of epicontinental shelf-forms: Example of the English Channel N92-11448
Analysis of radar polarimetric data for the discrimination and monitoring of forest covers N92-11449
Nonlinear theory of synthetic aperture radar sea wave imaging N92-11451
Humidity measurement of naked ground by radar in conditions of excessive water N92-11453
Land cover classification by multipolarized SAR imagery N92-11457
Synergistic use of multispectral satellite data for monitoring land surface change N92-11489
Integration of visible-through microwave-range multispectral image data sets for geologic mapping N92-11491
Evaluation of the quality of urban biotypes by remote sensing N92-11493
Urban heat island N92-11500
Temporal signatures using NOAA-AVHRR and land use mapping N92-11513
Perceptual grouping and shape from texture
[AD-A240358] N92-11678
IMAGE PROCESSING
Ground penetrating radar data acquisition system
[AD-A240765] N92-11244
Preliminary studies for automizing thermal flux measurement examination by thermosensitive coloring
[AAAF-NT-89-28] N92-11288
Characterization of African desert sites for the relative calibrating of wide field satellite optical sensors N92-11402
Use of operation ART-SPOT to test the 5S model and the MTF of the SPOT N92-11403
Routine mapping of vegetation index with the AVHRR of NOAA11 N92-11405
Near-infrared imaging spectroscopy: Learning from planetary geology N92-11438
Preliminary results of a spectro-imagery experiment (GER) over the Adriatic coastline of the Venice lagoon N92-11440
A study on the effects of Mt. Sakurajima's falling ash over crop and forest areas using image processing for LANDSAT-5, MOS-1, and Jafsa digital data N92-11497
Integration of Seasat and SPOT data, contribution to structural geology mapping in temperature environment N92-11499
Spectral estimates of PAR interception and biomass production of irrigated rice crops. 2: Model validation with SPOT data N92-11510
Study of the spatial variability of the hydrodynamic behavior of grounds at the Niger (Africa) using satellite images N92-11515
Structural controls on the remotely sensed response of a coniferous forest plantation N92-11516
Database of SPOT histrograms N92-11517
Texture indices sensitivity to spatial and spectral resolutions in semi-urban environments N92-11519
Multitemporal study of the Guyana coastline and estuaries using SPOT and LANDSAT imagery N92-11524
NOAA-AVHRR NDVI temporal profile classification and sensitivity to land use and climatic conditions in temperate region N92-11525
A hybrid methodology for detecting cartographically significant features using LANDSAT TM imagery
[AD-A240454] N92-11563
Thermal infrared spectra of natural and manmade materials: Implications for remote sensing
[AD-A240455] N92-11564
Perceptual grouping and shape from texture
[AD-A240358] N92-11678
Fractal image compression
[AD-A240636] N92-11680
Harnessing the killer micros: Applications from LLNL's massively parallel computing initiative
[DE91-018721] N92-11709
Progress in Photon Scanning-Tunneling Microscopy (PSTM)
[DE91-018174] N92-11905
IMAGE RECONSTRUCTION
Iterative procedures for atmospheric correction N92-11417
Appearance simulator for computer vision research
[AD-A240506] N92-11679
Inverse problems and imaging (Pitman research notes in mathematics series Number 245)
[AD-A240333] N92-11737
IMAGE RESOLUTION
Television image compression and small animal remote monitoring
[NASA-CR-186614] N92-11223
IMAGES
Multispectral image maps from LANDSAT thematic mapper data
[AD-A240453] N92-11562
Pictures and anaphora
[AD-A240153] N92-11631
Perceptual grouping and shape from texture
[AD-A240358] N92-11678
Wavefields near transverse cusp caustics produced by reflecting ultrasonic transients and tone bursts from curved surfaces
[AD-A240641] N92-11763
IMAGING SPECTROMETERS
Determination of the in-flight spectral and radiometric characteristics of the Airborne Visible/Infrared Imaging Spectrometer (AVIRIS) N92-11397
Evaluation of atmospheric effects in high spectral resolution airborne images N92-11408
Comparison of two atmospheric correction models for a vegetated Airborne Visible/Infrared Imaging Spectrometer (AVIRIS) scene N92-11415
Use of high spectral resolution airborne visible/infrared imaging spectrometer data for geologic mapping: An overview N92-11420
The performance of the ESA Medium Resolution Imaging Spectrometer (MERIS) N92-11422
The use of imaging spectrometry in Mediterranean land degradation and soil erosion hazard assessments N92-11430
The comparison of airborne imaging spectrometry and geochemical ground survey for the analysis of vegetation anomalies over waste deposits N92-11431
Near-infrared imaging spectroscopy: Learning from planetary geology N92-11438
Spectroscopic analysis of imaging spectrometer data for classification purposes N92-11439
Preliminary results of a spectro-imagery experiment (GER) over the Adriatic coastline of the Venice lagoon N92-11440
IMAGING TECHNIQUES
Direct imaging of deformation and disorder in extended-chain polymer fibers
[AD-A240651] N92-11192
Development of a high resolution liquid xenon imaging chamber for gamma-ray astronomy
[NASA-CR-188994] N92-11332
Near-infrared imaging spectroscopy: Learning from planetary geology N92-11438
Dual polarization microwave backscatter signatures of bare and vegetated soils N92-11452
Integration of Seasat and SPOT data, contribution to structural geology mapping in temperature environment N92-11499
Non-invasive evaluation of the cardiac autonomic nervous system by PET
[DE91-018476] N92-11622
Inverse problems and imaging (Pitman research notes in mathematics series Number 245)
[AD-A240333] N92-11737
Illumination, optics, and retroreflectors for efficient landmark tracking N92-11790
IMMUNOLOGY
JPRS report: Science and technology. USSR: Life sciences
[JPRS-ULS-91-017] N92-11616
IMPACT DAMAGE
MLITemp: A computer program to predict the thermal effects associated with hypervelocity impact damage to space station MLI
[NASA-CR-184245] N92-11079
IMPACT TESTS
An examination of the damage tolerance enhancement of carbon/epoxy using an outer lamina of spectra (R)
[NASA-TP-3160] N92-11142
An investigation of the material hazard of some insensitive high explosives
[MRL-TR-91-22] N92-11209
IMPEDANCE
Modeling of flexible polyarticulate chains: Bibliographic synthesis
[CERT-DERA-1/7735] N92-11927
IMPREGNATING
Conductive gage for crack length measurement
[NASA-CASE-LAR-14480-1-CU] N92-11374
IMPURITIES
Impurity behavior in Heliotron E N92-11852

Rotations of bulk ions and impurities in non-axisymmetric toroidal systems
[NIFS-102] N92-11885
IN-FLIGHT MONITORING
A comparison of airborne wake vortex detection measurements with values predicted from potential theory
[NASA-TP-3125] N92-10994
INCIDENCE
Hydrodynamic flow visualization around an oscillating vane. Extension of study to the case of higher incidences and amplitudes and the starting off phase from permanent regime
[ONERA-RT-56/1369-AN] N92-11312
INCOMPRESSIBLE FLOW
An efficient and robust algorithm for two dimensional time dependent incompressible Navier-Stokes equations: High Reynolds number flows
[NASA-TM-104424] N92-11320
INCOMPRESSIBLE FLUIDS
An efficient and robust algorithm for two dimensional time dependent incompressible Navier-Stokes equations: High Reynolds number flows
[NASA-TM-104424] N92-11320
INDEPENDENT VARIABLES
On the value of high spectral resolution measurements in the visible and near-infrared N92-11419
INDEXES (DOCUMENTATION)
Aeronautical engineering: A continuing bibliography with indexes (supplement 270)
[NASA-SP-7037(270)] N92-10973
Aeronautical engineering: A continuing bibliography with indexes (supplement 269)
[NASA-SP-7037(269)] N92-10974
Magnetic suspension and balance systems: A comprehensive, annotated bibliography
[NASA-TM-4318] N92-11030
INDIUM PHOSPHIDES
Spectroscopic studies of layered and bulk semiconductor materials
[ETN-91-90145] N92-11914
Thermal annealing studies of Fe and Ti implanted in GaAs and InP
[ETN-91-90148] N92-11915
INDUSTRIAL WASTES
Integrated Risk Information System
[DE91-018503] N92-11924
INELASTIC SCATTERING
Global analysis of fermion mixing with exotics
[NASA-CR-189006] N92-11774
INEQUALITIES
New Bernstein type inequalities for polynomials on ellipses
[NASA-CR-186626] N92-11724
INERTIAL CONFINEMENT FUSION
An IFE development strategy
[DE91-016918] N92-11873
INERTIAL FUSION (REACTOR)
An IFE development strategy
[DE91-016918] N92-11873
INFERENCE
Assignment of single values to probability intervals, evaluation of conditional events, and applications to combination of evidence
[AD-A240258] N92-11747
Circular Statistical methods: Applications in spatial and temporal performance analysis
[AD-A240751] N92-11749
INFORMATION DISSEMINATION
A brief introduction to the universal documentation system. Universal documentation system handbook
[AD-A240622] N92-11027
Alternative fuels for heavy duty engines: Status of fleet trials
[DE91-018474] N92-11210
Real-time earthquake monitoring: Early warning and rapid response
[NASA-CR-186701] N92-11582
Education in computational science: Role of the National Laboratories
[DE91-018823] N92-11687
INFORMATION FLOW
Highly parallel computation
[NASA-CR-188871] N92-11698
INFORMATION MANAGEMENT
A brief introduction to the universal documentation system. Universal documentation system handbook
[AD-A240622] N92-11027
Deploying expert systems in Ada
[NASA-CR-188938] N92-11664
ART-Ada design project, phase 2
[NASA-CR-188940] N92-11667
INFORMATION RETRIEVAL
Conoscopic holography. 1: Basic principles and physical basis. 2: Rigorous derivation
[TELECOM-PARIS-91-C-001] N92-11337
Computer integrated documentation
[NASA-TM-103870] N92-11673
An investigation to find appropriate measures for evaluating interactive information retrieval N92-11922
FEDIX: The on-line database retrieval service of Government information for colleges, universities, and other organizations
[DE91-018496] N92-11923
Integrated Risk Information System
[DE91-018503] N92-11924
INFORMATION SYSTEMS
A systematic formulation, as an approach to air traffic
[MBB-Z-0371-91-PUB] N92-10996
Joint services electronics program research in electronics
[AD-A240155] N92-11274
Study and prototype of data system interactions for the Earth Observing System Data and Information System
[NASA-CR-183505] N92-11648
Advanced information processing system for advanced launch system: Avionics architecture synthesis
[NASA-CR-187554] N92-11704
Advanced information processing system for advanced launch system: Hardware technology survey and projections
[NASA-CR-187555] N92-11705
Advanced information processing system: Inter-computer communication services
[NASA-CR-187556] N92-11706
Modelling product structures by generic bills-of-material
[ETN-91-90146] N92-11919
NSSDC data listing
[NASA-TM-105010] N92-11921
FEDIX: The on-line database retrieval service of Government information for colleges, universities, and other organizations
[DE91-018496] N92-11923
Integrated Risk Information System
[DE91-018503] N92-11924
Database management system interface standard for Navy next generation computing resources
[AD-A240432] N92-11925
Information technologies for astrophysics circa 2001
[NASA-CR-188868] N92-11936
INFORMATION THEORY
On the capacity region for deterministic two-way channels and write-unidirectional memories
[ETN-91-90147] N92-11684
INFRARED ASTRONOMY
Infrared to millimetre observations of active galaxies N92-11932
INFRARED DETECTORS
An examination of the factors affecting the use of infra-red search and track systems in the air-to-air role
[ETN-91-99987] N92-11222
INFRARED IMAGERY
Application of infrared thermography to thermal flux measurement in wind tunnels
[AAAF-NT-89-12] N92-11020
Use of high spectral resolution airborne visible/infrared imaging spectrometer data for geologic mapping: An overview N92-11420
Monitoring volcanoes using short wavelength infrared images N92-11498
Temporal signatures using NOAA-AVHRR and land use mapping N92-11513
Night-time LANDSAT thermal infrared imagery as a tool for climatological studies N92-11526
INFRARED RADIATION
Enhanced clutter suppression apparatus for use with an infrared search and surveillance system
[AD-D014984] N92-11247
Long wavelength semiconductor lasers development for infrared heterodyne applications
[NASA-CR-189243] N92-11341
Determination of the in-flight spectral and radiometric characteristics of the Airborne Visible/Infrared Imaging Spectrometer (AVIRIS) N92-11397
Atmospheric correction in the thermal infrared: AVHRR case N92-11398
TIMS calibration correction by comparison with PRT5 N92-11412
Experimental approach to emissivity problems and surface temperature in thermal infrared remote sensing N92-11462
Anisotropy of thermal infrared exitance above and within plant canopies N92-11467
Complementarity of temperature independent Thermal Infrared Spectral Indices (TISI) and NDVI: Compared properties and combined use for soil and vegetation discrimination N92-11490
Using the radiative surface temperature in energy budget studies over plant canopies N92-11506
Simulation study of vegetation indices sensitivity using the middle infrared N92-11514
Lunar radiator shade
[NASA-CASE-MSC-21868-1] N92-11639
INFRARED REFLECTION
Simulation study of vegetation indices sensitivity using the middle infrared N92-11514
INFRARED SCANNERS
Thermal verification testing of commercial printed-circuit boards for spaceflight
[NASA-TM-105261] N92-11221
INFRARED SIGNATURES
Simultaneous determination of six soil properties from the soil diffuse reflectance spectrum in the near infrared region (1-2.5 microns) N92-11424
INFRARED SPECTRA
On the value of high spectral resolution measurements in the visible and near-infrared N92-11419
Space observation of the land-ocean-atmosphere system at high spectral resolution in the infrared: Perspectives and problems N92-11421
Modeling the behavior of a vegetation cover in the MIR, contribution of high spectral resolution N92-11434
Thermal infrared spectra of natural and manmade materials: Implications for remote sensing
[AD-A240455] N92-11564
INFRARED SPECTROSCOPY
Feasibility of the red edge index for the detection of nitrogen deficiency N92-11425
Spectral identification (1.2-2.5 microns) and characterization of Paris (France) Basin kaolinite/smectite clays using a field spectrometer N92-11429
The 4th International Workshop on Membrane Biotechnology and Membrane Biomaterials
[AD-A240481] N92-11614
INFRARED TELESCOPES
The great observatories for space astrophysics
[NASA-NP-128] N92-11066
INFRARED TRACKING
An examination of the factors affecting the use of infra-red search and track systems in the air-to-air role
[ETN-91-99987] N92-11222
Attitude identification for SCOLE using two infrared cameras
[NASA-CR-4397] N92-11338
INHOMOGENEITY
Stable upwind schemes for hyperbolic conservation laws for with source terms N92-11716
An analysis of upwind schemes for inhomogeneous two dimensional conservation laws N92-11717
INJECTION
A detailed investigation of staged normal injection into a Mach 2 flow N92-11118
Profile measurements in magnetic surface variation experiments/multiple pellet injection experiments N92-11851
INJECTORS
LOX/hydrogen coaxial injector atomization test program N92-11121
Driven currents in neutral beam heated plasma N92-11861
INLAND WATERS
A multi-sensor approach to spectral signature analysis of inland waters N92-11428
Laser active remote sensing of phytoplankton in inland waters N92-11534
INLET FLOW
Radial inflow turbine study
[AD-A240169] N92-11015
INSERTS
Blind fastening apparatus
[NASA-CASE-LAR-14542-1] N92-11354
INSPECTION
Debris/ice/TPS assessment and photographic analysis for Shuttle Mission STS-43
[NASA-TM-103823] N92-11038
INSTRUCTION SETS (COMPUTERS)
The ULM: A RISC for LISP. System architecture
[ETN-91-90162] N92-11647
INSTRUCTORS
The development of Behaviorally Anchored Rating Scales (BARS) for evaluating USAF pilot training performance
[AD-A239969] N92-11630
INSTRUMENT ERRORS
C-29A aircraft altimeter errors
[AD-A240486] N92-11011
Reduction of FEL gain due to wiggler errors
[DE92-000482] N92-11350
INSULATION
Design of a fast computer-based partial discharge diagnostic system
[NASA-CR-189057] N92-11272
INSULATORS
Design of a fast computer-based partial discharge diagnostic system
[NASA-CR-189057] N92-11272

INTEGRAL EQUATIONS
Collision integrals and high temperature transport properties for N-N, O-O, and N-O
[NASA-CR-188907] N92-11770
INTEGRATED CIRCUITS
Test and diagnosis of programmable integrated circuits
[ETN-91-99483] N92-11253
Fault localization when testing complex circuits N92-11260
A microprocessor test approach allowing fault localisation N92-11261
A method and tools for microprocessor validation: High safety function applications N92-11263
Top down IC failure analysis using an E-beam system coupled to a functional tester N92-11264
Comparison between californium and cyclotron SEU tests N92-11267
Limits of energy dissipation for x ray sensitive pn Charge Coupled Devices (CCDs)
[MPE-224] N92-11280
INTEGRATED MISSION CONTROL CENTER
Engineering and instrumentation support of GL Research Balloon Program
[AD-A240616] N92-10987
INTERACTIONAL AERODYNAMICS
Experimental investigation of the effects of blowing on bursting of strake vortices
[AD-A240256] N92-10985
Studies of aerothermal loads generated in regions of shock/shock interaction in hypersonic flow
[NASA-CR-181893] N92-11319
Robot graphic simulation testbed
[NASA-CR-188998] N92-11637
INTERACTIONS
Use of multitemporal SPOT data in first ISLSCP field experiment N92-11554
INTERFACES
Local interfacial area concentration measurement in bubbly flow
[DE91-018702] N92-11322
INTERFEROMETRY
Using a discrete Fourier transform to estimate phase in interferometric direction finding
[AD-A231414] N92-10995
INTERGALACTIC MEDIA
Re-ionization and decaying dark matter
[NASA-CR-189009] N92-11944
INTERGRANULAR CORROSION
A probabilistic model of intergranular stress corrosion cracking
[DE91-017986] N92-11173
INTERMETALLICS
Oxidation of titanium aluminide and its XD composite
[AD-A240401] N92-11177
Moisture-induced environmental embrittlement of ordered intermetallic alloys at ambient temperatures
[DE91-018852] N92-11183
INTERNAL COMBUSTION ENGINES
Alternative fuels for heavy duty engines: Status of fleet trials
[DE91-018474] N92-11210
Piston temperature measurement in a natural gas engine
[PB91-194357] N92-11352
INTERNATIONAL COOPERATION
International program for Earth observations
[NASA-CR-188799] N92-11393
INTERNATIONAL SUN EARTH EXPLORER 3
ISEE/ICE plasma wave data analysis
[NASA-CR-189244] N92-11795
INTERPLANETARY SPACECRAFT
Quick trips to Mars N92-11111
INTERPOLATION
A method for estimating missing hourly temperatures using daily maximum and minimum temperatures
[AD-A240394] N92-11594
Short-term hourly temperature interpolation
[AD-A240489] N92-11596
INTERPROCESSOR COMMUNICATION
Transient finite element computations on a variable transputer system
[NASA-CR-189060] N92-11671
Ordered fast fourier transforms on a massively parallel hypercube multiprocessor
[NASA-CR-188899] N92-11700
An application for multi-person task synchronization
[NASA-CR-187712] N92-11918
INTRAVENOUS PROCEDURES
Intranasal scopolamine preparation and method
[NASA-CASE-MSC-21858-1] N92-11628
INVERSE SCATTERING
Evaluation of vegetation cover characteristics using an airborne microwave scatterometer N92-11456
INVERSIONS
Inverse problems and imaging (Pitman research notes in mathematics series Number 245)
[AD-A240333] N92-11737
INVERTERS
Insulated Gate Bipolar Transistors (IGBT) modelization for circuit simulation and utilization in pulse modulated inverters
[ETN-91-90149] N92-11279
IO
Diffusion in the Io plasma torus and its relation to the torus spatial structure N92-11949
ION ACCELERATORS
Particle trajectories through MIRRORTRON configurations
[DE91-017084] N92-11876
ION BEAMS
Ultra high vacuum sputtering system
[AD-A240157] N92-11176
ION CURRENTS
New polymer electrolyte hosts and their tetrabutylammonium chloride complexes. Relationships among concentration of polar groups, ESR spin probe response, and ionic conductivity
[AD-A240497] N92-11190
ION CYCLOTRON RADIATION
Comparison between californium and cyclotron heavy ion tests N92-11266
Comparison between californium and cyclotron SEU tests N92-11267
Design of the compact Auburn torsatron N92-11805
ICRF heating program of the large helical device N92-11846
Fokker-Planck equation in the presence of anomalous diffusion
[NIFS-29] N92-11879
ION EXCHANGING
Superionics
[AD-A240352] N92-11910
ION PROBES
New dimensions in atom probe analysis
[DE91-018926] N92-11779
ION SCATTERING
Surface analysis of catalysts by low-energy ion scattering
[ETN-91-90133] N92-11913
ION SOURCES
NBI system with negative ion source in large helical device N92-11870
ION TEMPERATURE
Ion temperature and poloidal rotation profiles for NBI heated plasma in CHS N92-11860
IONIC COLLISIONS
High l state population in O(7+) produced in ion-solid collisions
[DE91-018169] N92-11904
IONIZATION
Studies on laser atomic spectroscopy
[DE91-628172] N92-11349
Spectral fitting, shock layer modeling, and production of nitrogen oxides and excited nitrogen
[NASA-CR-185664] N92-11769
Numerical analysis of temporal development of RF-heated plasma N92-11834
Re-ionization and decaying dark matter
[NASA-CR-189009] N92-11944
Electron distributions and solar wind interaction with nonmagnetic planets N92-11952
IONIZATION CROSS SECTIONS
Coupled-channel optical calculation of electron-hydrogen scattering: Elastic scattering from 0.5 to 30 eV
[DE91-634157] N92-11780
IONIZING RADIATION
Solid state neutron dosimeter for space applications
[NASA-CR-185633] N92-11331
Development of recommendations in the area of ionizing radiations
[DE91-018527] N92-11623
IONOSPHERIC ELECTRON DENSITY
Electron distributions and solar wind interaction with nonmagnetic planets N92-11952
IONS
Mixing effects in aqueous solutions at elevated temperatures
[DE91-017695] N92-11168
Novel nonlinear laser diagnostic techniques
[AD-A240193] N92-11346
Influence of fast ion loss on radial electric field in Wendelstein 7-A stellarator
[NIFS-95] N92-11797
Rotations of bulk ions and impurities in non-axisymmetric toroidal systems
[NIFS-102] N92-11885
IRRADIANCE
Irradiance compensation control for high-energy laser propagation, part 2
[DE91-018489] N92-11348
Comparison of in situ, aircraft- and satellite-derived surface reflectances in Flevoland (Netherlands) N92-11404
IRRADIATION
Extra-corporeal blood access, sensing, and radiation methods and apparatuses
[NASA-CASE-MSC-21775-1] N92-11627
IRRIGATION
Maximum evapotranspiration monitoring over La Mancha, Spain, using NOAA-AVHRR data N92-11507
Spectral estimates of PAR interception and biomass production of irrigated rice crops. 1: Model elaboration with ground data N92-11522
ISOTOPIC LABELING
Non-invasive evaluation of the cardiac autonomic nervous system by PET
[DE91-018476] N92-11622
ITERATION
Iterative procedures for atmospheric correction N92-11417
The iterate manual
[AD-A231410] N92-11650
An improved Newton iteration for the generalized inverse of a matrix, with applications
[NASA-CR-186983] N92-11723
Discussion summary: Fictitious domain methods N92-11730
ITERATIVE SOLUTION
Fast secant methods for the iterative solution of large nonsymmetric linear systems
[NASA-CR-188867] N92-11655
Optimal parallel solution of sparse triangular systems
[NASA-CR-188872] N92-11656
A domain decomposition algorithm for solving large elliptic problems
[DE92-000096] N92-11690
Convergence and performance of synchronous and asynchronous parallel and conventional iterative methods
[AD-A240286] N92-11707
Harnessing the killer micros: Applications from LLNL's massively parallel computing initiative
[DE91-018721] N92-11709
Optimal Chebyshev polynomials on ellipses in the complex plane
[NASA-CR-188836] N92-11722

J

JACOBI MATRIX METHOD
A Newton's method solver for the two-dimensional and axisymmetric Navier-Stokes equations N92-11292
Issues in parallel automatic differentiation
[DE91-017311] N92-11726
JAPAN
High definition systems in Japan
[NASA-TM-105108] N92-11225
JET ENGINES
Euler solutions for an unbladed jet engine configuration
[NASA-TM-105332] N92-11328
Supervoltage NDE techniques for large aerospace structures
[AD-A240625] N92-11365
JET FLOW
Experimental investigation of the effects of blowing on bursting of strake vortices
[AD-A240256] N92-10985
Laser Raman diagnostics in subsonic and supersonic turbulent jet diffusion flames N92-11159
JET MIXING FLOW
Viscous computations of cold air/air flow around scramjet nozzle afterbody
[NASA-CR-4406] N92-10982
Numerical simulation of the reactive flow in advanced (HSR) combustors using KIVA-2
[NASA-CR-188996] N92-11014
JET STREAMS (METEOROLOGY)
A diagnostic study of the velocity structure of a meandering jet using a primitive equation model with dynamic mode initialization
[AD-A240687] N92-11609
JOSEPHSON JUNCTIONS
Physics of ultrasmall superconducting circuits
[AD-A240156] N92-11275
JUDGMENTS
Television image compression and small animal remote monitoring
[NASA-CR-186614] N92-11223

JUPITER ATMOSPHERE
Laboratory measurements of the single-scattering properties of ammonia ice crystals N92-11950

K

K-EPSILON TURBULENCE MODEL
Numerical prediction of turbulent flame stability in premixed/prevaporized (HSCT) combustors [NASA-CR-188991] N92-11161
Modeling of the heat transfer in bypass transitional boundary-layer flows [NASA-TP-3170] N92-11299
KAPTON (TRADEMARK)
Evaluation of Kapton pyrolysis, arc tracking, and arc propagation on the Space Station Freedom (SSF) solar array Flexible Current Carrier (FCC) [NASA-CR-189056] N92-11139
KELVIN-HELMHOLTZ INSTABILITY
The three-dimensional evolution of a plane mixing layer. Part 1: The Kelvin-Helmholtz roll-up [NASA-TM-103856] N92-11303
KETENES
Synthesis and reactivity of silyl-ketene acetal-modified polysiloxanes preparation of polysiloxanes with high dielectric constraints [AD-A240754] N92-11196
KINEMATICS
A computational procedure for the dynamics of flexible beams within multibody systems N92-11371
Advanced stress analysis methods applicable to turbine engine structures [NASA-CR-187235] N92-11378
Kinematics and dynamics of barred galaxies N92-11937
KINETIC EQUATIONS
Ripple diffusion and bootstrap current in LHD N92-11833
KINETICS
Cellular repair/misrepair track model [NASA-TP-3124] N92-11685
Fluid description of ponderomotive force compatible with the kinetic one in a warm plasma [NIFS-100] N92-11884
KLYSTRONS
Linear theory of a quasioptical gyroklystron with nonuniform magnetic field [AD-A240264] N92-11334
KNOWLEDGE BASES (ARTIFICIAL INTELLIGENCE)
Range Scheduling Aid (RSA) N92-11057
KRAFT PROCESS (WOODPULP)
Control of the heterogeneity of the refining action N92-11158

L

LABORATORIES
Education in computational science: Role of the National Laboratories [DE91-018823] N92-11687
Activities report of the Max-Planck Institute for Aeronomy [ETN-91-90233] N92-11964
LAGEOS (SATELLITE)
LAGEOS geodetic analysis-SL7.1 [NASA-TM-104549] N92-11584
LAKES
Multi-temporal monitoring of lake water quality N92-11426
Retrievals of column atmospheric water vapor, vegetation liquid water, and cloud cover fraction from AVIRIS data N92-11427
LAMBERT SURFACE
SPOT calibration on the test site La Crau (France) N92-11409
LAMINAR BOUNDARY LAYER
Secondary instability of the three dimensional laminar boundary layer in incompressible flow: Description of the calculation code [CERT-RT-63/5618-54] N92-11306
LAMINAR FLOW
Ignition and structure of a laminar diffusion flame in the field of a vortex [NASA-CR-189042] N92-11162
A Newton's method solver for the two-dimensional and axisymmetric Navier-Stokes equations N92-11292
Mixed convection in two-dimensional laminar air flow with reverse flow regions N92-11293
Resolution of the Navier-Stokes equations applied to the computation of the laminar flow around a two dimensional wing profile [CERT-RT-65/5604-35] N92-11307
Evaluation of high Reynolds number flow in a 180 degree turn-around-duct [NASA-CR-184243] N92-11318
LAMINATES
Compression response of laminated composite panels containing multiple delaminations N92-11141
Numerical simulation of the degradation of the folds of a laminated composite structure. Study of the importance of residual firing constraints [ONERA-RT-8/7256-RY-094-R] N92-11145
Improved compression molding technology for continuous fiber reinforced composite laminates. Part 2: AS-4/Polyimidesulfone prepreg system [NASA-TM-104133] N92-11207
LAND MANAGEMENT
Winter use plan: Environmental assessment [PB91-194027] N92-11574
LAND USE
A split-window method for obtaining crop temperatures N92-11410
The use of imaging spectrometry in Mediterranean land degradation and soil erosion hazard assessments N92-11430
Evaluation of the quality of urban biotypes by remote sensing N92-11493
Combined use of Earth observation satellite and meteorological satellite for crop assessment in semiarid environments N92-11494
Synergy of high resolution spatial microwave imagery and geomorphological optics N92-11496
NOAA-AVHRR NDVI temporal profile classification and sensitivity to land use and climatic conditions in temperate region N92-11525
LANDAU-GINZBURG EQUATIONS
Vortex-lattice states of a two-dimensional electron system at strong magnetic fields [DE91-018551] N92-11916
LANDMARKS
Study of alternatives: Dayton's Aviation heritage, Ohio [PB91-202275] N92-10972
Illumination, optics, and retroreflectors for efficient landmark tracking N92-11790
LANDSAT SATELLITES
A hybrid methodology for detecting cartographically significant features using LANDSAT TM imagery [AD-A240454] N92-11563
LANDSAT 5
Inter-calibrating of SPOT1-HRV, LANDSAT5-TM, and NOA11-AVHRR in the visible and near infrared field s N92-11401
LARGE SCALE INTEGRATION
Tester Independent Support Software System (TISSS) [AD-A240668] N92-11681
LARGE SPACE STRUCTURES
Large deployable antenna program. Phase 1: Technology assessment and mission architecture [NASA-CR-4410] N92-11036
OPUS: Optimal Projection for Uncertain Systems. Volume 1 [AD-A240372] N92-11080
OPUS: Optimal Projection for Uncertain Systems, volume 2 [AD-A240373] N92-11081
Multidisciplinary optimization of controlled space structures with global sensitivity equations [NASA-TP-3130] N92-11087
Supervoltage NDE techniques for large aerospace structures [AD-A240625] N92-11365
LASER APPLICATIONS
Antiresonant nonlinear mirror for passive laser mode locking [AD-D014951] N92-11343
Electron acceleration by laser fields in a gas [DE91-018477] N92-11345
Laser produced plasma soft x ray generation [DE91-016925] N92-11874
A compact laser photocathode driven accelerator for the Plasma Wake Field Accelerator Program at UCLA [AD-A240646] N92-11886
LASER BEAMS
Non-equilibrium microstructures produced during electron-beam and laser-beam surface modification of metallic alloys [DE91-018466] N92-11174
Electron acceleration by laser fields in a gas [DE91-018477] N92-11345
Irradiance compensation control for high-energy laser propagation, part 2 [DE91-018489] N92-11348
Collisional energy transfer from excited nitrogen dioxide [DE91-016989] N92-11772
Matter-wave interferometry with laser cooled atoms [AD-A240531] N92-11776
Optical design of a high power fiber optic coupler [DE91-016924] N92-11789
Compact optical RF spectrum analyzer [AD-D014962] N92-11792
LASER CAVITIES
Laser diode pumped, erbium-doped, solid state laser with high slope efficiency [AD-D014968] N92-11347
LASER DOPPLER VELOCIMETERS
LV software support for supersonic flow analysis [NASA-CR-188914] N92-10978
Experimental investigation of the effects of blowing on bursting of strake vortices [AD-A240256] N92-10985
LASER FUSION
LLE review [DE91-018828] N92-11965
LASER INDUCED FLUORESCENCE
Laser Raman diagnostics in subsonic and supersonic turbulent jet diffusion flames N92-11159
Vegetation monitoring by means of spectral resolved fluorescence lidar N92-11533
Laser-induced spectral signatures in investigations of sea upper layer N92-11537
Simultaneous detection in blue and red bands of laser induced vegetation fluorescence N92-11539
Laser-induced blue fluorescence and red chlorophyll fluorescence signatures of differently pigmented leaves N92-11541
The laser-induced chlorophyll fluorescence ratio F690/F735 of spruce needles and beech leaves during the course of a year N92-11542
Modeling of fluorescence light-canopy interaction N92-11545
(L)EAF: A remote sensing fluoresensor N92-11546
Laser induced fluorescence of growing camphor tree leaves: Influence of chlorophyll content on LIF spectral signature N92-11547
Collisional energy transfer from excited nitrogen dioxide [DE91-016989] N92-11772
LASER INTERFEROMETRY
Matter-wave interferometry with laser cooled atoms [AD-A240531] N92-11776
LASER MODE LOCKING
Antiresonant nonlinear mirror for passive laser mode locking [AD-D014951] N92-11343
LASER OUTPUTS
Laser diode pumped, erbium-doped, solid state laser with high slope efficiency [AD-D014968] N92-11347
Radiation forces to electrons in laser fields explained as scattering for ponderomotive momentum transfers [IPPCZ-308] N92-11773
LASER PLASMAS
Trends in laser-plasma-instability experiments for laser fusion [DE91-016923] N92-11344
Laser produced plasma soft x ray generation [DE91-016925] N92-11874
The recombination behavior of a laser induced electron hole plasma in pin diodes and silicon base material [ETN-91-90153] N92-11887
LLE review [DE91-018828] N92-11965
LASER POWER BEAMING
Enabling the space exploration initiative: NASA's exploration technology program in space power [NASA-TM-4325] N92-11131
LASER PUMPING
Laser diode pumped, erbium-doped, solid state laser with high slope efficiency [AD-D014968] N92-11347
LASER RANGE FINDERS
LAGEOS geodetic analysis-SL7.1 [NASA-TM-104549] N92-11584
LASER SPECTROSCOPY
Studies on laser atomic spectroscopy [DE91-628172] N92-11349
LASER TARGETS
Trends in laser-plasma-instability experiments for laser fusion [DE91-016923] N92-11344
LASERS
Navigation and positioning of mobile robots [DE92-704014] N92-10998
A fast algorithm for plotting antenna and scattering patterns in three dimensions [AD-A240410] N92-11233
Radiation forces to electrons in laser fields explained as scattering for ponderomotive momentum transfers [IPPCZ-308] N92-11773
A compact laser photocathode driven accelerator for the Plasma Wake Field Accelerator Program at UCLA [AD-A240646] N92-11886

LATERITES
Moisture effects on spectral signatures and CIE-color of lateritic soils N92-11436
LATTICE PARAMETERS
A study on the development of high T(sub c) superconducting materials
[DE91-629755] N92-11917
LAUNCH VEHICLE CONFIGURATIONS
Overview of the Beta II Two-Stage-To-Orbit vehicle design
[NASA-TM-105298] N92-11034
LEAD (METAL)
A study on the development of high T(sub c) superconducting materials
[DE91-629755] N92-11917
LEAD ZIRCONATE TITANATES
Electrooptic effects and photosensitivities of PLZT thin films
[DE91-017067] N92-11901
LEADING EDGES
Modeling of the heat transfer in bypass transitional boundary-layer flows
[NASA-TP-3170] N92-11299
LEAF AREA INDEX
On the nature of spectral shifts: Modeling and comparison to information contained in wide bands N92-11418
Feasibility of the red edge index for the detection of nitrogen deficiency N92-11425
Passive microwave remote sensing of vegetation canopies: Experimental and modeling results N92-11460
Monte Carlo model for transport equation in a plant canopy and its inversion N92-11481
Specular and diffuse components of plant canopy reflectance at the wavelengths of 550 and 630 nm N92-11484
An integrated modelling approach for the spectral identification of crops N92-11508
Simulation study of vegetation indices sensitivity using the middle infrared N92-11514
From evapotranspiration to soil moisture investigation based on NOAA thermal infrared data, case study: Poland N92-11531
LEARNING THEORY
Long term synaptic plasticity and learning in neuronal networks
[AD-A240366] N92-11613
Reminding-based learning
[AD-A240370] N92-11634
LEAST SQUARES METHOD
LAPACK: Linear algebra software for supercomputers
[DE91-017316] N92-11660
Fast algorithms for linear least-squares estimation of multi-dimensional random fields
[AD-A240249] N92-11675
LEAVES
Time-resolved spectroscopy of the blue fluorescence of spinach leaves N92-11538
The laser-induced chlorophyll fluorescence ratio F690/F735 of spruce needles and beech leaves during the course of a year N92-11542
Laser induced fluorescence of growing camphor tree leaves: Influence of chlorophyll content on LIF spectral signature N92-11547
Surface optical property measurements on bark and leaf samples
[AD-A240714] N92-11566
LENGTH
Conductive gage for crack length measurement
[NASA-CASE-LAR-14480-1-CU] N92-11374
LENSES
Stray light reduction in a WFOV star tracker lens
[DE91-018460] N92-11794
LEPTONS
Global analysis of fermion mixing with exotics
[NASA-CR-189006] N92-11774
E sub 6 leptoquarks and the solar neutrino problem
[NASA-CR-189005] N92-11956
LESIONS
Training, muscle fatigue and stress fractures
[AD-A240386] N92-11626
LETHALITY
Cellular repair/misrepair track model
[NASA-TP-3124] N92-11685
LEVELING
Leveling of the AMBLER walking machine: A comparison of methods
[NASA-CR-189015] N92-11358
LIE GROUPS
A systematic approach to combustion model reduction and lumping
[AD-A240195] N92-11164
LIFE SCIENCES
JPRS report: Science and technology. USSR: Life sciences
[JPRS-ULS-91-015] N92-11610
JPRS report: Science and technology. USSR: Life sciences
[JPRS-ULS-91-012] N92-11611
JPRS report: Science and technology. USSR: Life sciences
[JPRS-ULS-91-017] N92-11616
LIFE SUPPORT SYSTEMS
Technical requirements of sick bays aboard space ships N92-11620
LIFT
Model representation in the PANCOR wall interference assessment code
[NASA-TM-104152] N92-11022
LIGHT (VISIBLE RADIATION)
Schlieren system for visualizing the flow within a pipe of circular cross-section
[NASA-CASE-LAR-13944-1] N92-11336
Comparison of atmospheric correction procedures for visible and near-IR satellite sensor output N92-11395
Inter-calibrating of SPOT1-HRV, LANDSAT5-TM, and NOA11-AVHRR in the visible and near infrared field s N92-11401
Optimum combinations of visible and near-infrared reflectances for estimating the fraction of photosynthetically available radiation absorbed by plants N92-11474
Modeling of fluorescence light-canopy interaction N92-11545
Compact optical RF spectrum analyzer
[AD-D014962] N92-11792
Stray light reduction in a WFOV star tracker lens
[DE91-018460] N92-11794
LIGHT BEAMS
The effect of wiggler errors on FEL gain
[DE92-000483] N92-11351
LIGHT SCATTERING
Estimation of the aerosol optical thickness from broadband turbidity measurements: Application to the atmospheric correction of SPOT images N92-11399
Vegetation canopies and objects of arbitrary shapes: Computer generation and bidirectional reflectance calculations N92-11475
Light scattering experiments on Brownian motion in shear flow and in colloidal crystals
[ETN-91-90134] N92-11756
Stray light reduction in a WFOV star tracker lens
[DE91-018460] N92-11794
Laboratory measurements of the single-scattering properties of ammonia ice crystals N92-11950
LIGHT SOURCES
Photon stimulated desorption of neutral species from aluminum
[DE91-017004] N92-11784
LINE SPECTRA
Report on carbon and nitrogen abundance studies
[NASA-CR-188803] N92-11934
LINEAR ARRAYS
A thinned high frequency linear antenna array to study ionospheric structure
[AD-A240764] N92-11243
LINEAR ENERGY TRANSFER (LET)
Comparison between californium and cyclotron SEU tests N92-11267
LINEAR EQUATIONS
Fast secant methods for the iterative solution of large nonsymmetric linear systems
[NASA-CR-188867] N92-11655
LAPACK: Linear algebra software for supercomputers
[DE91-017316] N92-11660
Fast algorithms for linear least-squares estimation of multi-dimensional random fields
[AD-A240249] N92-11675
Representation of phi meromorphic functions, when phi and a linear differential polynomial in phi have maximum finite zeros
[ETN-91-90202] N92-11741
LINEAR PREDICTION
Fast algorithms for linear least-squares estimation of multi-dimensional random fields
[AD-A240249] N92-11675
LINEAR QUADRATIC REGULATOR
Linear quadratic servo control of a reusable rocket engine
[NASA-TM-105291] N92-11128
Microgravity vibration isolation: An optimal control law for the one-dimensional case
[NASA-TM-105146] N92-11217
LINEAR SYSTEMS
Linear theory of a quasioptical gyroklystron with nonuniform magnetic field
[AD-A240264] N92-11334
Convergence and performance of synchronous and asynchronous parallel and conventional iterative methods
[AD-A240286] N92-11707
LIPIDS
The 4th International Workshop on Membrane Biotechnology and Membrane Biomaterials
[AD-A240481] N92-11614
LIQUEFIED GASES
Development of a high resolution liquid xenon imaging chamber for gamma-ray astronomy
[NASA-CR-188994] N92-11332
LIQUID FUELS
Droplet Core Nuclear Rocket (DLNR) N92-11105
LIQUID HELIUM
Bose-condensation in liquid helium under pressure
[DE91-634504] N92-11170
Characterizing He II flow through porous materials using counterflow data
[CD-4] N92-11295
Critical velocities and mutual friction in He-3-He-4 II mixtures at temperatures below 100 mK
[ETN-91-90132] N92-11314
LIQUID HELIUM 2
Superfluid helium dynamics
[NASA-CR-188814] N92-11294
Thermal behavior of the SHOOT gallery arm
[CD-21] N92-11296
LIQUID HYDROGEN
Improved thermodynamic modeling of the no-vent fill process and correlation with experimental data
[NASA-TM-104492] N92-11129
LIQUID NITROGEN
Description of Liquid Nitrogen Experimental Test Facility
[NASA-TM-105215] N92-11208
LIQUID OXYGEN
Improved thermodynamic modeling of the no-vent fill process and correlation with experimental data
[NASA-TM-104492] N92-11129
LIQUID PROPELLANT ROCKET ENGINES
The 27th JANNAF Combustion Subcommittee Meeting, Volume 3
[CPIA-PUBL-557-VOL-3] N92-11117
Developments in REDES: The Rocket Engine Design Expert System N92-11120
LOX/hydrogen coaxial injector atomization test program N92-11121
JANNAF Combustion Instability Panel Workshop report: Numerical methods in combustion instability N92-11123
JANNAF Liquid Rocket Combustion Instability Panel research recommendations N92-11124
Calibration of turbine flowmeters for storable bipropellant engines
[NAL-TR-1091] N92-11127
LIQUID ROCKET PROPELLANTS
The 27th JANNAF Combustion Subcommittee Meeting, Volume 3
[CPIA-PUBL-557-VOL-3] N92-11117
Navier-Stokes entropy controlled combustion instability analysis for liquid propellants N92-11122
Calibration of turbine flowmeters for storable bipropellant engines
[NAL-TR-1091] N92-11127
Improved thermodynamic modeling of the no-vent fill process and correlation with experimental data
[NASA-TM-104492] N92-11129
LIQUID SLOSHING
Theoretical estimation of the viscous damping from liquid transient motion in tanks
[NAL-TR-1095] N92-11298
LISP (PROGRAMMING LANGUAGE)
The ULM: A RISC for LISP. System architecture
[ETN-91-90162] N92-11647
The iterate manual
[AD-A231410] N92-11650
LITHIUM HYDRIDES
Shielding requirements for particle bed propulsion systems
[AD-A240780] N92-11787
LITHOLOGY
Radar image simulation to study the visual aptitude of observing slope and roughness effects N92-11446
LOAD DISTRIBUTION (FORCES)
Experimental study of an independently deflected wingtip mounted on a semispan wing
[NASA-TM-102842] N92-10983
Buckling values and optimization of carbon fiber reinforced compression chord plates with rectangular stringers
[ILR-MITT-259(1991)] N92-11148
Approximate large deflection analysis of circular plates loaded symmetrically
[NPL-DMM(A)-25] N92-11370

Method of recertifying a loaded bearing member using a phase point
[NASA-CASE-LAR-14741-1] N92-11384
Limit pressure of a circumferentially reinforced SiC/Ti ring
[NASA-CR-187211] N92-11387

LOAD TESTS
Creep response of a 9Cr-1Mo-V-Nb steel to varying stresses and temperatures
[DE91-017871] N92-11181

LOADING RATE
Deformation of isodamp (A polyvinyl chloride-based elastomer) at various loading rates
[AD-A240393] N92-11189

LOADS (FORCES)
Critical appraisal of the McDonnell Douglas closure model for predicting fatigue crack growth
[ARL-STRUC-R-444] N92-11376
Method of recertifying a loaded bearing member using a phase point
[NASA-CASE-LAR-14741-1] N92-11384

LOCKING
Quick application/release nut with engagement indicator
[NASA-CASE-MSC-21799-1] N92-11359

LOGIC CIRCUITS
VHDL simulation of the implementation of a costfunction circuit
[AD-A240430] N92-11278
Experience with Acore: Implementing GHC with actors
[AD-A231409] N92-11649
A synchronization and charge distribution process for the parallel multilevel logic simulation
[ETN-91-90152] N92-11708

LOGIC PROGRAMMING
Parameter identification studies on the NASA/Ames Research Center Advanced Concepts Flight Simulator
[NASA-TM-105126] N92-11024

LONG DURATION EXPOSURE FACILITY
Analysis of surfaces from the LDEF A0114, phase 4
[NASA-CR-188990] N92-11074
The interactions of atmospheric cosmogenic radionuclides with spacecraft surfaces N92-11075
Effects on LDEF exposed copper film and bulk N92-11076
Pinhole cameras as sensors for atomic oxygen in orbit; application to attitude determination of the LDEF N92-11078

LONG DURATION SPACE FLIGHT
Effect of prolonged space flight on erythrocyte metabolism and membrane functional condition N92-11617

LONG WAVE RADIATION
Anisotropy of thermal infrared exitance above and within plant canopies N92-11467

LOOP ANTENNAS
Three-dimensional calculations of fields and loading for loop and folded waveguide ICRF antennas
[DE92-000065] N92-11250

LOUDNESS
A loudness calculation procedure applied to shaped sonic booms
[NASA-TP-3134] N92-11765

LOW ALTITUDE
Acoustic propagation at low altitude: Effects of atmospheric turbulence (Villeau (France) test)
[ONERA-RT-15/3641-PY] N92-11588

LOW ASPECT RATIO
Overview of the ATF-II studies N92-11802
Design of the compact Auburn torsatron N92-11805
STORM: A low aspect ratio torsatron for plasma stability N92-11829

LOW COST
The Space Shuttle: An attempt at low-cost, routine access to space
[AD-A240589] N92-11037

LOW PRESSURE
Low Pressure Nuclear Thermal Rocket (LPNTR) concept N92-11094

LOW SPEED
NACA 0015 wing pressure and trailing vortex measurements
[NASA-TP-3151] N92-10981

LOW THRUST
Liquid annulus N92-11104

LOW VISIBILITY
Surface painted taxiway markings at Seattle-Tacoma International Airport
[DOT/FAA/CT-TN91/49] N92-11029

LUBRICATION
Magnetic fluids and their applications
[DE92-704012] N92-11326

LUMINESCENCE
Laser-induced spectral signatures in investigations of sea upper layer N92-11537

LUMINOUS INTENSITY
Infrared to millimetre observations of active galaxies N92-11932

LUNAR BASED EQUIPMENT
Lunar dust transport and potential interactions with power system components
[NASA-CR-4404] N92-11951

LUNAR DUST
Lunar dust transport and potential interactions with power system components
[NASA-CR-4404] N92-11951

LUNAR SURFACE
Lunar radiator shade
[NASA-CASE-MSC-21868-1] N92-11639

M

MACH NUMBER
Mach 6.5 air induction system design for the Beta 2 two-stage-to-orbit booster vehicle
[NASA-CR-187233] N92-11013

MAGNETIC COILS
Coil shapes towards pure multipoles in circular regions: A numerical approach
[DE91-017239] N92-11271
Status of the WVII-AS Program N92-11820
Destruction of magnetic surfaces in helical torus N92-11832
Island studies for Helias Configurations N92-11835
Research and development of forced flow superconducting coils for large helical device N92-11838
Fundamental design on LHD with bath cooling method N92-11841
A compact helical device for a superconducting large helical coil N92-11842
Optimization of design parameters for large helical device N92-11843
Effect of multi-layer operation of helical coil in large helical device N92-11844
Motion of charged particle in helical systems N92-11847
Equilibrium, stability, and transport in L = 1 compact helical axis configuration N92-11848
A possible modification of the FT Tokamak into a compact high field stellarator with separatrices N92-11863
Engineering design of large helical device N92-11864
Operation scenario and structural design analysis of LHD (Large Helical Device) coils N92-11865
Engineering design of LHD vacuum vessel N92-11866
Development of superconductor for large helical device N92-11867
Overview of engineering design of Wendelstein VII-X N92-11868
Coaxial slow source
[DE91-016947] N92-11875

MAGNETIC DIPOLES
Neutron star magnetic fields and implications for pulsars and gamma ray bursts N92-11960

MAGNETIC EFFECTS
Linear theory of a quasioptical gyroklystron with nonuniform magnetic field
[AD-A240264] N92-11334

MAGNETIC FIELD CONFIGURATIONS
Review of the TJ-II Flexible Heliac Project N92-11803
Analysis of scrape-off layer in toroidal helical systems N92-11815
Review of CHS experiment N92-11823
Pressure and potential measurements in IMS during electron cyclotron heating N92-11826
Numerical and experimental studies of simulated toroidicity effects in a linear high-beta heliac N92-11827
Island studies for Helias Configurations N92-11835
Behavior of vacuum vessel eddy current in large helical device N92-11840
Equilibrium, stability, and transport in L = 1 compact helical axis configuration N92-11848
Edge plasma study in Heliotron E N92-11853
Study of resistive interchange mode in Heliotron E N92-11855
Measurement of magnetic fluctuations in Heliotron E N92-11856
Effect of magnetic axis shift on CHS plasma characteristics N92-11858
Effects of electric field on particle drift orbits in a l = 2 torsatron
[NIFS-31] N92-11878
Application of modern mathematical concepts to plasma confinement
[DE92-000053] N92-11893

MAGNETIC FIELDS
Nuclear transparency and double beta decay of molybdenum 100
[DE91-016963] N92-11172
Three-dimensional calculations of fields and loading for loop and folded waveguide ICRF antennas
[DE92-000065] N92-11250
Coil shapes towards pure multipoles in circular regions: A numerical approach
[DE91-017239] N92-11271
Approximate expressions for the magnetic field from an electric current source in a layered conducting medium
[MRL-TR-91-5] N92-11273
The 3-D equilibria of helical systems: Magnetic islands and their control N92-11808
Overview of recent results from the Advanced Toroidal Facility N92-11819
Status of the WVII-AS Program N92-11820
Destruction of magnetic surfaces in helical torus N92-11832
Behavior of vacuum vessel eddy current in large helical device N92-11840
Motion of charged particle in helical systems N92-11847
Edge plasma study in Heliotron E N92-11853
Operation scenario and structural design analysis of LHD (Large Helical Device) coils N92-11865
Calculation of magnetic field of helical coils
[NIFS-18] N92-11880
ECH experiments on ATF
[DE91-018845] N92-11889
Application of modern mathematical concepts to plasma confinement
[DE92-000053] N92-11893
Full-wave calculation of fast-wave current drive in tokamaks including k(parallel) variations
[DE92-000076] N92-11894
Vortex-lattice states of a two-dimensional electron system at strong magnetic fields
[DE91-018551] N92-11916

MAGNETIC FILMS
Ultra high vacuum sputtering system
[AD-A240157] N92-11176
Thin film magnetic memory elements
[AD-D014971] N92-11646

MAGNETIC FLUX
Design of the compact Auburn torsatron N92-11805
Overview of recent results from the Advanced Toroidal Facility N92-11819
Diverted particle-flux studies in the IMS and Proto-Cleo stellarators N92-11825
Neutron diffraction from the flux line lattice
[DE91-018175] N92-11906
Sunspot dynamics
[NASA-CR-188978] N92-11955

MAGNETIC INDUCTION
Overview of engineering design of Wendelstein VII-X N92-11868

MAGNETIC MATERIALS
Polarized x ray absorption spectroscopy for the study of superconductors and magnetic materials
[DE91-017990] N92-11163
Characterization of rare earth permanent magnets
[DE91-017010] N92-11754
The TITAN reversed-field-pinch fusion reactor study, volume 2
[DE92-000140] N92-11896

MAGNETIC MEASUREMENT
Recent diamagnetic measurements of toroidal coil experiments on Heliotron E N92-11854
Measurement of magnetic fluctuations in Heliotron E N92-11856

MAGNETIC MIRRORS
Particle trajectories through MIRRORTRON configurations
[DE91-017084] N92-11876

MAGNETIC PROPERTIES
Ultra high vacuum sputtering system
[AD-A240157] N92-11176
Magnetic fluids and their applications
[DE92-704012] N92-11326
Characterization of rare earth permanent magnets
[DE91-017010] N92-11754
Confinement studies of Heliotron E plasmas in magnetic surface variation experiments N92-11850
Synthesis of novel conducting solids
[AD-A240468] N92-11912

MAGNETIC STORAGE
Thin film magnetic memory elements
[AD-D014971] N92-11646

MAGNETIC STORMS
Conditional climatology of Ap: The relationship between various solar events (surges, prominences, filaments, radio bursts, x ray episodes) and geomagnetic storms
[AD-A240457] N92-11958

MAGNETIC SUSPENSION
Further developments relating to the NASA Langley Research Center 13-inch magnetic suspension and balance system
[NASA-CR-188995] N92-11023
Magnetic suspension and balance systems: A comprehensive, annotated bibliography
[NASA-TM-4318] N92-11030
MAGNETIC VARIATIONS
Measurement of magnetic fluctuations in Heliotron E N92-11856
MAGNETOHYDRODYNAMIC FLOW
Euromech 260: Advanced non-intrusive experimental techniques in fluid and plasma flows
[ETN-91-90104] N92-11313
Equilibrium, stability, and transport in L = 1 compact helical axis configuration N92-11848
MAGNETOHYDRODYNAMIC STABILITY
Trends in laser-plasma-instability experiments for laser fusion
[DE91-016923] N92-11344
Proceedings of the First International Toki Conference on Plasma Physics and Controlled Nuclear Fusion: Next Generation Experiments in Helical Systems
[NIFS-PROC-3] N92-11799
Status of the Wendelstein VII-X Project N92-11801
Overview of the ATF-II studies N92-11802
Second stability studies in a helical axis device: TJ-II N92-11807
The 3-D equilibria of helical systems: Magnetic islands and their control N92-11808
Resistive MHD stability studies for ATF plasmas during operation in the second stability regime N92-11809
Overview of recent results from the Advanced Toroidal Facility N92-11819
Review of Heliotron E experiment N92-11822
STORM: A low aspect ratio torsatron for plasma stability N92-11829
Dissipative trapped electron modes in l = 2 torsatrons N92-11830
Low-n stability calculations for three dimensional stellarator configurations N92-11831
Equilibrium, stability, and transport in L = 1 compact helical axis configuration N92-11848
Profile measurements in magnetic surface variation experiments/multiple pellet injection experiments N92-11851
Study of resistive interchange mode in Heliotron E N92-11855
Measurement of magnetic fluctuations in Heliotron E N92-11856
Effects of electric field on particle drift orbits in a l = 2 torsatron
[NIFS-31] N92-11878
ELMy-H mode as limit cycle and chaotic oscillations in tokamak plasmas
[NIFS-87] N92-11882
Nonlinear behavior of multiple-helicity resistive interchange modes near marginally stable states
[NIFS-89] N92-11883
Current profile control for ITER with RF current drive
[DE91-018597] N92-11888
Plasma properties
[DE91-018913] N92-11891
MAGNETOHYDRODYNAMIC WAVES
Continuum damping of high mode number toroidal Alfven waves
[DE91-018891] N92-11890
Plasma properties
[DE91-018913] N92-11891
MAGNETOHYDRODYNAMICS
Second stability studies in a helical axis device: TJ-II N92-11807
Resistive MHD stability studies for ATF plasmas during operation in the second stability regime N92-11809
The main fusion activities in Institute of Plasma Physics, Academia Sinica N92-11814
LHCD experiments on tokamak CASTOR
[IPPCZ-304] N92-11881
MAGNETOSPHERIC ELECTRON DENSITY
Electron distributions and solar wind interaction with nonmagnetic planets N92-11952
MAGNETRONS
Ultra high vacuum sputtering system
[AD-A240157] N92-11176
MAINTENANCE
Classification of posture maintenance data with fuzzy clustering algorithms
[NASA-CR-188949] N92-11662
MAMMALS
Long term synaptic plasticity and learning in neuronal networks
[AD-A240366] N92-11613
MAN MACHINE SYSTEMS
Telescience workstation
[NASA-CR-188878] N92-11033
CHIMES-2: A tool for automated HCI analysis N92-11051
MAN-COMPUTER INTERFACE
Telescience workstation
[NASA-CR-188878] N92-11033
Space Network Control (SNC) Conference on Resource Allocation Concepts and Approaches. Overview N92-11040
Concepts, requirements, and design approaches for building successful planning and scheduling systems N92-11042
User interface issues in supporting human-computer integrated scheduling N92-11048
Human factors issues in the design of user interfaces for planning and scheduling N92-11049
CHIMES-2: A tool for automated HCI analysis N92-11051
SPIKE: AI scheduling techniques for Hubble Space Telescope N92-11054
Range Scheduling Aid (RSA) N92-11057
Scheduling techniques in the Request Oriented Scheduling Engine (ROSE) N92-11058
Human Machine Interfaces for Teleoperators and Virtual Environments Conference
[NASA-CP-10071] N92-11638
Making intelligent systems team players: Case studies and design issues. Volume 2: Fault management system cases
[NASA-TM-104738] N92-11641
Computer integrated documentation
[NASA-TM-103870] N92-11673
MANAGEMENT ANALYSIS
High definition systems in Japan
[NASA-TM-105108] N92-11225
MANAGEMENT METHODS
Lessons learned in the development of the C-130 aircrew training system: A summary of Air Force on-site experience
[AD-A240554] N92-11635
MANAGEMENT SYSTEMS
Making intelligent systems team players: Case studies and design issues. Volume 2: Fault management system cases
[NASA-TM-104738] N92-11641
MANEUVERABILITY
Developmental flight testing of a half scale unmanned air vehicle
[AD-A240347] N92-11002
Development of a 1/7th scale fighter UAV for flight research
[AD-A240703] N92-11008
MANIFOLDS (MATHEMATICS)
Oriented matroids and projective invariant theory
[ETN-91-90181] N92-11740
MANIPULATORS
A generalized method for multiple robotic manipulator programming applied to vertical-up welding
[NASA-TP-3163] N92-11218
Generation of smooth trajectories without planning
[NASA-CR-189013] N92-11712
MANNED MARS MISSIONS
NERVA upgrade: Non-nuclear components N92-11092
Nuclear rocket using indigenous Martian fuel NIMF N92-11098
MANNED SPACE FLIGHT
Safety issues N92-11115
MANUALS
FEDIX: The on-line database retrieval service of Government information for colleges, universities, and other organizations
[DE91-018496] N92-11923
MAPPING
Three dimensional migration and forward modelling of ground penetrating radar data
[AD-A240505] N92-11234
Routine mapping of vegetation index with the AVHRR of NOAA11 N92-11405
Spectral identification (1.2-2.5 microns) and characterization of Paris (France) Basin kaolinite/smectite clays using a field spectrometer N92-11429
Comparison of passive microwave and model derived estimates for soil moisture fields N92-11459
Actual daily evapotranspiration monitoring using NOAA-AVHRR data from the HAPEX-MOBILHY campaigns N92-11509
Multispectral image maps from LANDSAT thematic mapper data
[AD-A240453] N92-11562
MAPS
Multispectral image maps from LANDSAT thematic mapper data
[AD-A240453] N92-11562
MARINE BIOLOGY
Airborne SAR HAREM campaign: Results, targets features, ERS1 simulations, and operational satellite exploitation N92-11455
Theory and modeling in GLOBEC: A first step N92-11602
GLOBEC: Global Ocean Ecosystems Dynamics: A component of the US Global Change Research Program
[NASA-TM-105121] N92-11603
MARINE METEOROLOGY
Mariners Weather Log, Volume 35, Number 1, Winter 1991
[PB91-201129] N92-11591
Mariners Weather Log, Volume 35, Number 2, Spring 1991
[PB91-202572] N92-11592
MARINE RESOURCES
Airborne SAR HAREM campaign: Results, targets features, ERS1 simulations, and operational satellite exploitation N92-11455
MARKERS
Surface painted taxiway markings at Seattle-Tacoma International Airport
[DOT/FAA/CT-TN91/49] N92-11029
MARKET RESEARCH
Conformity Assessment Workshop on Electromagnetic Compatibility
[PB91-192989] N92-11226
MARKOV CHAINS
Integration of qualitative knowledge on operational models for following vegetation using temporal series of remote sensing images N92-11502
Numerical methods in Markov chain modeling
[NASA-CR-188908] N92-11744
On the maximum entropy principle for Markov chains and processes
[ETN-91-90150] N92-11750
MARS (PLANET)
Nuclear rocket using indigenous Martian fuel NIMF N92-11098
Quick trips to Mars N92-11111
MARS ATMOSPHERE
Nuclear rocket using indigenous Martian fuel NIMF N92-11098
MARS ENVIRONMENT
Effect of particle size of Martian dust on the degradation of photovoltaic cell performance
[NASA-TM-105232] N92-11133
MARS EXCURSION MODULE
Quick trips to Mars N92-11111
MARS SURFACE
Effect of particle size of Martian dust on the degradation of photovoltaic cell performance
[NASA-TM-105232] N92-11133
MARTENSITIC TRANSFORMATION
Alloy modeling and experimental correlation for ductility enhancement in near stoichiometric single crystal nickel aluminide
[AD-A240151] N92-11175
MASERS
Particle acceleration in space and radiation belt depletion
[AD-A240311] N92-11775
MASKING
Laser produced plasma soft x ray generation
[DE91-016925] N92-11874
MASS SPECTROSCOPY
Time-resolved analytical pyrolysis mass spectrometry of biomaterials
[AD-A240624] N92-11167
New dimensions in atom probe analysis
[DE91-018926] N92-11779
MASS TRANSFER
Calibration and validation of a surface flux model in the framework of the HAPEX-MOBILHY experiment. Application to estimating the cover resistance N92-11511
MASSIVELY PARALLEL PROCESSORS
Solving the shallow water equations on the Cray X-MP/48 and the connection machine 2
[NASA-CR-188897] N92-11658
Ordered fast fourier transforms on a massively parallel hypercube multiprocessor
[NASA-CR-188899] N92-11700
Analysis of a parallel multigrid algorithm
[NASA-CR-188906] N92-11701
MATCHED FILTERS
Maximized gust loads for a nonlinear airplane using matched filter theory and constrained optimization
[NASA-TM-104138] N92-11010
MATERIALS TESTS
New insulation constructions for aerospace wiring applications. Volume 1: Testing and evaluation
[AD-A240638] N92-11006

MATHEMATICAL LOGIC
Modeling default and likelihood reasoning as probabilistic reasoning
[NASA-CR-188936] N92-11661
MATHEMATICAL MODELS
Rotorcraft system identification
[AGARD-AR-280] N92-11001
Numerical simulation of the reactive flow in advanced (HSR) combustors using KIVA-2
[NASA-CR-188996] N92-11014
LOX/hydrogen coaxial injector atomization test program N92-11121
JANNAF Combustion Instability Panel Workshop report: Numerical methods in combustion instability N92-11123
Improved thermodynamic modeling of the no-vent fill process and correlation with experimental data
[NASA-TM-104492] N92-11129
Compression response of laminated composite panels containing multiple delaminations N92-11141
The behaviour of fire-exposed composite steel/concrete slabs
[ISBN-90-386-0031-3] N92-11147
Effects of elevated temperature on the viscoplastic modeling of graphite/polymeric composites
[NASA-TM-104160] N92-11149
Ignition and structure of a laminar diffusion flame in the field of a vortex
[NASA-CR-189042] N92-11162
A systematic approach to combustion model reduction and lumping
[AD-A240195] N92-11164
A probabilistic model of intergranular stress corrosion cracking
[DE91-017986] N92-11173
Damage evolution in filled elastomers
[AD-A240532] N92-11191
Discrete ARMA model for natural resonances in electromagnetic and acoustic scattering
[AD-A240656] N92-11241
High efficiency motor rewind study
[DE91-017162] N92-11270
Approximate expressions for the magnetic field from an electric current source in a layered conducting medium
[MRL-TR-91-5] N92-11273
Insulated Gate Bipolar Transistors (IGBT) modelization for circuit simulation and utilization in pulse modulated inverters
[ETN-91-90149] N92-11279
Theoretical study (Lagrangian modeling) of turbulent particulate dispersion
[ETN-91-99909] N92-11287
Reciprocity theory of gas surface interactions
[IC-AERO-89-04] N92-11289
Deformation and breakup of drops in simple shear flows
[ETN-91-90143] N92-11315
Implementation of the flow-modulated skew-upward difference scheme in the momentum equation of the COMMIX-1C program: A first assessment
[DE91-018013] N92-11321
To the account of finite velocity of thermal diffusion in turbulent flows
[DE91-635593] N92-11323
Heat transfer in channels with uniformly swirled flow
[DE91-635594] N92-11324
On the symbolic manipulation and code generation for elasto-plastic material matrices
[NASA-CR-187223] N92-11375
Critical appraisal of the McDonnell Douglas closure model for predicting fatigue crack growth
[ARL-STRUC-R-444] N92-11376
Advanced stress analysis methods applicable to turbine engine structures
[NASA-CR-187235] N92-11378
Analysis of strain dependent damping in materials via modeling of material point hysteresis
[AD-A240298] N92-11381
Nonlinear aspects of aerospace structures at high excitation levels flat aluminum beams and plates studied
[AD-A240600] N92-11383
Calculation of general shells of revolution, using a semi analytical process
[ILR-MITT-262(1991)] N92-11386
Modeling the behavior of a vegetation cover in the MIR, contribution of high spectral resolution N92-11434
Modeling of radar backscattering from the sea surface using polarimetric-SAR observations N92-11442
Dual-polarized scatterometer measurements of wind and mechanically generated waves in a very large wind/wave flume, the VIERS-1 project N92-11443
Generalized formulation for semi-empirical radar models representing crop backscattering N92-11447
Nonlinear theory of synthetic aperture radar sea wave imaging N92-11451
Influence of the crop architecture parameters on crop BRDF: A Monte Carlo simulation N92-11465
A three dimensional radiative transfer method for optical remote sensing of vegetated land surfaces N92-11466
Bidirectional reflectance and surface albedo: Physical modeling and inversion N92-11469
Joint use of remote sensing and agricultural production estimation models: Current trends N92-11501
Integration of qualitative knowledge on operational models for following vegetation using temporal series of remote sensing images N92-11502
Estimation of the primary production in Sahelian region from radiometric data N92-11504
Maximum evapotranspiration monitoring over La Mancha, Spain, using NOAA-AVHRR data N92-11507
Actual daily evapotranspiration monitoring using NOAA-AVHRR data from the HAPEX-MOBILHY campaigns N92-11509
The linking of crop growth models and multi-sensor remote sensing data N92-11512
Analysis of the surface state of two sub-polar glaciers using SPOT data and a numerical terrain model N92-11523
Study of the spatial signature of forest covers by geometric-optic modeling N92-11530
Estimation of geopotential differences over intercontinental locations using satellite and terrestrial measurements
[NASA-CR-188992] N92-11560
Development of a 3-D tree thermal response model for energy budget and scene simulation studies
[AD-A240693] N92-11565
Photovoltaic energy system at an Alaskan site
[PB91-201350] N92-11567
LAGEOS geodetic analysis-SL7.1
[NASA-TM-104549] N92-11584
Radiation belt dynamic and quasi-static modeling based on CRRES data
[AD-A240392] N92-11585
Mesoscale prediction and satellite cloud analysis for advanced meteorological processing systems
[AD-A240510] N92-11597
A survey of scattering, attenuation, and size spectra studies of bubble layers and plumes beneath the air-sea interface
[AD-A240262] N92-11606
Use of theoretical wave height distributions in directional seas
[AD-A240411] N92-11608
A diagnostic study of the velocity structure of a meandering jet using a primitive equation model with dynamic mode initialization
[AD-A240687] N92-11609
Cognitive factors involved in the first stage of programming skill acquisition
[AD-A240566] N92-11636
Modelling default and likelihood reasoning as probabilistic reasoning
[NASA-CR-188936] N92-11661
The modeling of complex continua: Fundamental obstacles and grand challenges
[DE91-018806] N92-11686
An analysis of some hyperbolic problems related to the shallow water model (chapter 6)
[IMAG-RR-579] N92-11718
One-way nesting for a primitive equation ocean model N92-11734
Nested ocean models: Work in progress N92-11735
Numerical methods in Markov chain modeling
[NASA-CR-188908] N92-11744
Variational Monte Carlo calculations of finite nuclei
[DE91-018895] N92-11778
Meson-exchange calculation of the d(gamma,p)n in the GeV energy region
[DE91-017994] N92-11785
Influence of fast ion loss on radial electric field in Wendelstein 7-A stellarator
[NIFS-95] N92-11797
Theory of electron cyclotron heating in the flexible heliac TJ-II N92-11828
Experiments and applications of soliton physics
[NIFS-32] N92-11877
Comparative study of final state interaction contributions to the dynamic response of quantum fluids
[DE91-631020] N92-11892
Chemical reactivity and electronic structure of silicon microclusters
[AD-A240276] N92-11908
Spectroscopic studies of layered and bulk semiconductor materials
[ETN-91-90145] N92-11914
Modelling product structures by generic bills-of-material
[ETN-91-90146] N92-11919
Cosmological constraints on pseudo-Nambu-Goldstone bosons
[NASA-CR-189010] N92-11943
MATRICES (MATHEMATICS)
Studies in the form of finite element mass matrices for beams, plates and shells
[AERO-TN-9101] N92-11369
Optimal parallel solution of sparse triangular systems
[NASA-CR-188872] N92-11656
An O(log sup 2 N) parallel algorithm for computing the eigenvalues of a symmetric tridiagonal matrix
[NASA-CR-188898] N92-11659
LAPACK: Linear algebra software for supercomputers
[DE91-017316] N92-11660
Optimal Chebyshev polynomials on ellipses in the complex plane
[NASA-CR-188836] N92-11722
An improved Newton iteration for the generalized inverse of a matrix, with applications
[NASA-CR-186983] N92-11723
Oriented matroids and projective invariant theory
[ETN-91-90181] N92-11740
Numerical methods in Markov chain modeling
[NASA-CR-188908] N92-11744
MATRIX MATERIALS
Oxidation of titanium aluminide and its XD composite
[AD-A240401] N92-11177
Low toxicity high temperature PMR polyimides
[NASA-CASE-LAR-14639-1] N92-11199
Improved compression molding technology for continuous fiber reinforced composite laminates. Part 2: AS-4/Polyimidesulfone prepreg system
[NASA-TM-104133] N92-11207
MATRIX METHODS
Application of Krylov exponential propagation to fluid dynamics equations
[NASA-CR-188887] N92-11290
MAXIMUM ENTROPY METHOD
On the maximum entropy principle for Markov chains and processes
[ETN-91-90150] N92-11750
MAXIMUM LIKELIHOOD ESTIMATES
Modelling default and likelihood reasoning as probabilistic reasoning
[NASA-CR-188936] N92-11661
MAXWELL EQUATION
A Fourier collocation time domain method for numerically solving Maxwell's equations
[NASA-TM-104162] N92-11742
MEASURE AND INTEGRATION
Transient finite element computations on a variable transputer system
[NASA-CR-189060] N92-11671
MEASURING INSTRUMENTS
Description of Liquid Nitrogen Experimental Test Facility
[NASA-TM-105215] N92-11208
Semiconductor measurement technology: NIST list of publications, 1962-1989 (revised March 1990)
[PB91-193961] N92-11269
The phenomena of scalar mixing in turbulent gas-particle flows, measuring equipment, and measurements
[DE92-704034] N92-11327
Technique for calibrating angular measurement devices when calibration standards are unavailable
[NASA-TM-104148] N92-11340
Conductive gage for crack length measurement
[NASA-CASE-LAR-14480-1-CU] N92-11374
Simultaneous detection in blue and red bands of laser induced vegetation fluorescence N92-11539
Micro photoreflectance semiconductor wafer analyzer
[AD-D014950] N92-11788
Process for controlling the thickness of an antireflection coating, and embodying apparatus
[DE91-017634] N92-11793
MECHANICAL DEVICES
Integral fill yarn insertion and beatup method
[NASA-CASE-LAR-14046-1] N92-11219
Woven angle ply fabric and apparatus and method for producing such fabrics
[NASA-CASE-LAR-14048-1] N92-11220
In-line hydraulic dashpot
[AD-D014955] N92-11356
MECHANICAL PROPERTIES
Mechanical properties of a porous mullite material
[NASA-TM-104547] N92-11187
Development of a reliability-based method for evaluating a pavement feature
[AD-A240747] N92-11366
MEDICAL EQUIPMENT
Rapidly quantifying the relative distention of a human bladder
[NASA-CASE-LAR-13901-2] N92-11621
MELTING
Melting efficiency in fusion welding
[DE91-017988] N92-11355

MEMBRANES
The 4th International Workshop on Membrane Biotechnology and Membrane Diomaterials
[AD-A240481] N92-11614
MEMORY
Pictures and anaphora
[AD-A240153] N92-11631
Perception and memory of pictures
[AD-A240364] N92-11633
Cognitive factors involved in the first stage of programming skill acquisition
[AD-A240566] N92-11636
MEMORY (COMPUTERS)
Weather prediction using a genetic memory
[NASA-CR-185448] N92-11590
Sparse distributed memory
[NASA-CR-188841] N92-11643
A class of designs for a sparse distributed memory
[NASA-CR-188849] N92-11644
Thin film magnetic memory elements
[AD-D014971] N92-11646
Distributed memory compiler methods for irregular problems: Data copy reuse and runtime partitioning
[NASA-CR-187635] N92-11669
Vienna FORTRAN: A FORTRAN language extension for distributed memory multiprocessors
[NASA-CR-187634] N92-11670
On the capacity region for deterministic two-way channels and write-unidirectional memories
[ETN-91-90147] N92-11684
Cedar Project: Original goals and progress to date
[DE92-000032] N92-11689
Some fast elliptic solvers on parallel architectures and their complexities
[NASA-CR-188840] N92-11692
Efficient ICCG on a shared memory multiprocessor
[NASA-CR-188843] N92-11693
Neural networks and MIMD-multiprocessors
[NASA-CR-188481] N92-11697
Total recall in distributive associative memories
[NASA-CR-188884] N92-11699
Learning to read aloud: A neural network approach using sparse distributed memory
[NASA-CR-188846] N92-11711
Statistical prediction with Kanerva's sparse distributed memory
[NASA-CR-187314] N92-11743
MENTAL PERFORMANCE
Efficacy of hyperbaric oxygenation in enhancing flight tolerance N92-11618
PET studies of components of high-level vision
[AD-A240202] N92-11624
Cognitive factors involved in the first stage of programming skill acquisition
[AD-A240566] N92-11636
MERCURY (METAL)
Studies on laser atomic spectroscopy
[DE91-628172] N92-11349
MEROMORPHIC FUNCTIONS
Representation of phi meromorphic functions, when phi and a linear differential polynomial in phi have maximum finite zeros
[ETN-91-90202] N92-11741
MESOMETEOROLOGY
Mesoscale prediction and satellite cloud analysis for advanced meteorological processing systems
[AD-A240510] N92-11597
MESONS
On the polarisation of tensor mesons in psi radiative decays and possible implications for the gluonic content of the theta(1720)
[RAL-90-091] N92-11768
Meson-exchange calculation of the d(gamma,p)n in the GeV energy region
[DE91-017994] N92-11785
MESOSCALE PHENOMENA
Some examples of satellite data utilization for atmospheric modeling at medium scale N92-11503
METABOLISM
Effect of prolonged space flight on erythrocyte metabolism and membrane functional condition N92-11617
METAL FATIGUE
Microstructural evolution during the thermomechanical fatigue of solder joints
[DE91-017309] N92-11372
Propagation behavior of small cracks in 304 stainless steel under biaxial low-cycle fatigue at elevated temperature
[DE91-018863] N92-11389
METAL FILMS
Effects on LDEF exposed copper film and bulk N92-11076
METAL IONS
Superionics
[AD-A240352] N92-11910
METAL MATRIX COMPOSITES
Effects of anisotropic conduction and heat pipe interaction on minimum mass space radiators
[NASA-TM-105297] N92-11138
Centrifugal casting of composites
[AD-D014981] N92-11144
Oxidation of titanium aluminide and its XD composite
[AD-A240401] N92-11177
Limit pressure of a circumferentially reinforced SiC/Ti ring
[NASA-CR-187211] N92-11387
Thermoviscoplastic response of Ti-15-3 under various loading conditions
[NASA-CR-187621] N92-11391
METAL OXIDES
Oxidation of titanium aluminide and its XD composite
[AD-A240401] N92-11177
METAL PLATES
A comparison of single cycle overload effect on Al-Li 2091-T81 plate and 2091-T83 sheet
[AD-A240627] N92-11179
Nonlinear aspects of aerospace structures at high excitation levels flat aluminum beams and plates studied
[AD-A240600] N92-11383
METAL SHEETS
A comparison of single cycle overload effect on Al-Li 2091-T81 plate and 2091-T83 sheet
[AD-A240627] N92-11179
METAL SURFACES
Measurements of erosion characteristics for metal and polymer surfaces using profilometry N92-11077
Non-equilibrium microstructures produced during electron-beam and laser-beam surface modification of metallic alloys
[DE91-018466] N92-11174
A comparison of single cycle overload effect on Al-Li 2091-T81 plate and 2091-T83 sheet
[AD-A240627] N92-11179
METAL VAPOR LASERS
Optical design of a high power fiber optic coupler
[DE91-016924] N92-11789
METALS
Positron lifetimes in solids from first principles calculations
[DE92-000088] N92-11781
METEOROLOGICAL PARAMETERS
The science benefits of and the antenna requirements for microwave remote sensing from geostationary orbit
[NASA-CR-4408] N92-11559
METEOROLOGICAL SERVICES
Pilot's Automated Weather Support System (PAWSS) concepts demonstration project. Phase 1: Pilot's weather information requirements and implications for weather data systems design
[NASA-CR-188228] N92-11593
METEOROLOGY
A method for estimating missing hourly temperatures using daily maximum and minimum temperatures
[AD-A240394] N92-11594
MICROBIOLOGY
JPRS report: Science and technology. USSR: Life sciences
[JPRS-ULS-91-015] N92-11610
JPRS report: Science and technology. USSR: Life sciences
[JPRS-ULS-91-012] N92-11611
JPRS report: Science and technology. USSR: Life sciences
[JPRS-ULS-91-017] N92-11616
MICROCHANNEL PLATES
Microchannel electron source
[AD-D014956] N92-11276
MICROCOMPUTERS
EDMS: Microcomputer pollution model for civilian airports and Air Force bases, (user's guide)
[AD-A240528] N92-11578
MICROCRACKS
Damage evolution in filled elastomers
[AD-A240532] N92-11191
MICROELECTRONICS
Physics of ultrasmall superconducting circuits
[AD-A240156] N92-11275
Tester Independent Support Software System (TISSS)
[AD-A240668] N92-11681
Superionics
[AD-A240352] N92-11910
MICROGRAVITY APPLICATIONS
Microgravity vibration isolation: An optimal control law for the one-dimensional case
[NASA-TM-105146] N92-11217
Cooling apparatus and couplings therefor
[NASA-CASE-ARC-11921-1] N92-11286
MICROORGANISMS
Time-resolved analytical pyrolysis mass spectrometry of biomaterials
[AD-A240624] N92-11167
MICROPROCESSORS
Communications interface and system for radiation recovery of a microprocessor portion thereof
[AD-D014977] N92-11245
Analysis of experimental results on functional testing and diagnosis of complex circuits N92-11254
Failure coverage of functional test methods: A comparative experimental evaluation N92-11255
Automatic generation of microprocessor test programs N92-11256
Hardware and software tools for microprocessor functional test N92-11257
The GAPT system: A chain of test for microprocessors N92-11258
A microprocessor test approach allowing fault localisation N92-11261
Towards an automated system for the verification and diagnosis of intelligent VLSI circuits N92-11262
A method and tools for microprocessor validation: High safety function applications N92-11263
Automatic tools for microprocessor failure analysis N92-11265
Rapidly quantifying the relative distention of a human bladder
[NASA-CASE-LAR-13901-2] N92-11621
MICROSTRUCTURE
Non-equilibrium microstructures produced during electron-beam and laser-beam surface modification of metallic alloys
[DE91-018466] N92-11174
Moisture-induced environmental embrittlement of ordered intermetallic alloys at ambient temperatures
[DE91-018852] N92-11183
Microstructural evolution during the thermomechanical fatigue of solder joints
[DE91-017309] N92-11372
Characterization of rare earth permanent magnets
[DE91-017010] N92-11754
New dimensions in atom probe analysis
[DE91-018926] N92-11779
Chemical reactivity and electronic structure of silicon microclusters
[AD-A240276] N92-11908
A study on the development of high T(sub c) superconducting materials
[DE91-629755] N92-11917
MICROWAVE ABSORPTION
Theory of electron cyclotron heating in the flexible heliac TJ-II N92-11828
STORM: A low aspect ratio torsatron for plasma stability N92-11829
MICROWAVE AMPLIFIERS
ECH experiments on ATF
[DE91-018845] N92-11889
MICROWAVE ANTENNAS
Large deployable antenna program. Phase 1: Technology assessment and mission architecture
[NASA-CR-4410] N92-11036
The science benefits of and the antenna requirements for microwave remote sensing from geostationary orbit
[NASA-CR-4408] N92-11559
MICROWAVE IMAGERY
The science benefits of and the antenna requirements for microwave remote sensing from geostationary orbit
[NASA-CR-4408] N92-11559
MICROWAVE RADIOMETERS
Passive microwave remote sensing of soil moisture: Results from HAPEX, FIFE, and MONSOON 90 N92-11458
Large scale study of the microwave signature of the Antarctic ice sheet N92-11463
Comparison between the observed microwave spectral signatures over the Antarctic ice sheet and a snow emissivity model N92-11464
Synergistic use of multispectral satellite data for monitoring land surface change N92-11489
Airborne passive microwave remote sensing of land and water surface N92-11492
MICROWAVE SCATTERING
Evaluation of vegetation cover characteristics using an airborne microwave scatterometer N92-11456
MICROWAVE SIGNATURES
Dual polarization microwave backscatter signatures of bare and vegetated soils N92-11452
Large scale study of the microwave signature of the Antarctic ice sheet N92-11463
Comparison between the observed microwave spectral signatures over the Antarctic ice sheet and a snow emissivity model N92-11464
MICROWAVE TRANSMISSION
The 100 GHz half megawatt microwave transmission system development with whispering gallery mode N92-11869
MICROWAVES
Navigation and positioning of mobile robots
[DE92-704014] N92-10998

The design of broadband radar absorbing surfaces [AD-A240521] N92-11235
Active radar stealth device [AD-D014980] N92-11246
Generalized formulation for semi-empirical radar models representing crop backscattering N92-11447
Active microwave remote sensing and ground hydric state. Agriscatt '88 airborne campaign over the Orgeval basin (France) N92-11454
Passive microwave remote sensing of vegetation canopies: Experimental and modeling results N92-11460
On the use of passive microwaves at 37 GHz N92-11461
Synergy of high resolution spatial microwave imagery and geomorphological optics N92-11496
Radiation forces to electrons in laser fields explained as scattering for ponderomotive momentum transfers [IPPCZ-308] N92-11773

MIGRATION
Three dimensional migration and forward modelling of ground penetrating radar data [AD-A240505] N92-11234

MILITARY AIR FACILITIES
EDMS: Microcomputer pollution model for civilian airports and Air Force bases, (user's guide) [AD-A240528] N92-11578

MILITARY AIRCRAFT
The role of stealth in naval aviation and joint/combined operations [AD-A240595] N92-11005

MILITARY OPERATIONS
The role of stealth in naval aviation and joint/combined operations [AD-A240595] N92-11005

MILITARY TECHNOLOGY
The role of stealth in naval aviation and joint/combined operations [AD-A240595] N92-11005

MILLIMETER WAVES
The science benefits of and the antenna requirements for microwave remote sensing from geostationary orbit [NASA-CR-4408] N92-11559
Infrared to millimetre observations of active galaxies N92-11932

MILLING (MACHINING)
Development of a personal computer program for milling the shapes of wind turbine blades. Theory and application [ILR-MITT-243(1990)] N92-11360

MIMD (COMPUTERS)
Neural networks and MIMD-multiprocessors [NASA-CR-188481] N92-11697
Highly parallel computation [NASA-CR-188871] N92-11698

MINERAL EXPLORATION
Use of high spectral resolution airborne visible/infrared imaging spectrometer data for geologic mapping: An overview N92-11420
Spectral identification (1.2-2.5 microns) and characterization of Paris (France) Basin kaolinite/smectite clays using a field spectrometer N92-11429

MINERALOGY
Evaluation of the quality of urban biotypes by remote sensing N92-11493

MINERALS
Field trip guidebook on environmental impact of clays along the upper Texas coast [NASA-TM-105097] N92-11572
Biological effects of minerals [DE91-018183] N92-11615

MIRROR FUSION
Particle trajectories through MIRRORTRON configurations [DE91-017084] N92-11876

MIRRORS
Antiresonant nonlinear mirror for passive laser mode locking [AD-D014951] N92-11343

MISSILE TRACKING
A methodology to assess the Best Estimate Trajectory (BET) results generated for the Kwajalein Missile Range [AD-A240770] N92-11083

MISSILE TRAJECTORIES
A methodology to assess the Best Estimate Trajectory (BET) results generated for the Kwajalein Missile Range [AD-A240770] N92-11083

MISSION PLANNING
What we were asked to do N92-11041
Concepts, requirements, and design approaches for building successful planning and scheduling systems N92-11042
Proposed planning and scheduling services for the SNC in the CDOS era N92-11043
An RF interference mitigation methodology with potential applications in scheduling N92-11044
Automated conflict resolution issues N92-11045
User interface issues in supporting human-computer integrated scheduling N92-11048
SPIKE: AI scheduling techniques for Hubble Space Telescope N92-11054
A planning language for activity scheduling N92-11063
Nuclear thermal propulsion program overview N92-11089
Nuclear thermal propulsion workshop overview N92-11090
Nuclear thermal rocket workshop reference system Rover/NERVA N92-11091
Airborne precursor missions in support of SIR-C/X-SAR N92-11450
Looking ahead to EOS: Update on NASA's Earth Observing Program N92-11556
Fusion energy for space missions in the 21st Century [NASA-TM-4298] N92-11783

MIXED OXIDES
A study on the development of high T(sub c) superconducting materials [DE91-629755] N92-11917

MIXING
Mixing effects in aqueous solutions at elevated temperatures [DE91-017695] N92-11168

MIXING CIRCUITS
Physics of ultrasmall superconducting circuits [AD-A240156] N92-11275

MIXING LAYERS (FLUIDS)
The three-dimensional evolution of a plane mixing layer. Part 1: The Kelvin-Helmholtz roll-up [NASA-TM-103856] N92-11303

MIXING LENGTH FLOW THEORY
A detailed investigation of staged normal injection into a Mach 2 flow N92-11118

MOBILITY
Navigation and positioning of mobile robots [DE92-704014] N92-10998

MODAL RESPONSE
Multi-disciplinary optimization of aeroservoelastic systems [NASA-CR-188983] N92-11377
Sensitivity of Space Station alpha joint robust controller to structural modal parameter variations [NASA-TM-104153] N92-11392
A diagnostic study of the velocity structure of a meandering jet using a primitive equation model with dynamic mode initialization [AD-A240687] N92-11609

MODELS
A conceptual framework for ecosystem modeling using remotely sensed inputs N92-11551

MODULATION TRANSFER FUNCTION
Use of operation ART-SPOT to test the 5S model and the MTF of the SPOT N92-11403

MOISTURE
Strategic air command contrail formation study [AD-A240467] N92-11003
Moisture-induced environmental embrittlement of ordered intermetallic alloys at ambient temperatures [DE91-018852] N92-11183

MOISTURE CONTENT
Retrievals of column atmospheric water vapor, vegetation liquid water, and cloud cover fraction from AVIRIS data N92-11427
Modeling the behavior of a vegetation cover in the MIR, contribution of high spectral resolution N92-11434
Moisture effects on spectral signatures and CIE-color of lateritic soils N92-11436
Humidity measurement of naked ground by radar in conditions of excessive water N92-11453
Active microwave remote sensing and ground hydric state. Agriscatt '88 airborne campaign over the Orgeval basin (France) N92-11454
Passive microwave remote sensing of soil moisture: Results from HAPEX, FIFE, and MONSOON 90 N92-11458
Comparison of passive microwave and model derived estimates for soil moisture fields N92-11459
Passive microwave remote sensing of vegetation canopies: Experimental and modeling results N92-11460
From evapotranspiration to soil moisture investigation based on NOAA thermal infrared data, case study: Poland N92-11531

MOLDING MATERIALS
Improved compression molding technology for continuous fiber reinforced composite laminates. Part 2: AS-4/Polyimidesulfone prepreg system [NASA-TM-104133] N92-11207

MOLDS
Improved compression molding technology for continuous fiber reinforced composite laminates. Part 2: AS-4/Polyimidesulfone prepreg system [NASA-TM-104133] N92-11207

MOLECULAR BEAM EPITAXY
Long wavelength semiconductor lasers development for infrared heterodyne applications [NASA-CR-189243] N92-11341

MOLECULAR BIOLOGY
JPRS report: Science and technology. USSR: Life sciences [JPRS-ULS-91-012] N92-11611

MOLECULAR CHAINS
Direct imaging of deformation and disorder in extended-chain polymer fibers [AD-A240651] N92-11192

MOLECULAR EXCITATION
Decomposition pathways of tetrahydrogen [AD-A240623] N92-11166
Collisional energy transfer from excited nitrogen dioxide [DE91-016989] N92-11772

MOLECULAR GASES
Collisional energy transfer from excited nitrogen dioxide [DE91-016989] N92-11772

MOLECULAR INTERACTIONS
Decomposition pathways of tetrahydrogen [AD-A240623] N92-11166

MOLECULAR STRUCTURE
Decomposition pathways of tetrahydrogen [AD-A240623] N92-11166
Structure of the Si45 cluster [AD-A240278] N92-11909

MOLECULAR WEIGHT
Liquid annulus N92-11104

MOLECULES
Control of electron transfer rates by motions of atoms and molecules [DE91-018575] N92-11777

MOLYBDENUM ISOTOPES
Nuclear transparency and double beta decay of molybdenum 100 [DE91-016963] N92-11172

MOMENTS
Prediction of forces and moments for hypersonic flight vehicle control effectors [NASA-CR-188954] N92-11070

MOMENTUM
Implementation of the flow-modulated skew-upward difference scheme in the momentum equation of the COMMIX-1C program: A first assessment [DE91-018013] N92-11321
Radiation forces to electrons in laser fields explained as scattering for ponderomotive momentum transfers [IPPCZ-308] N92-11773

MONITORS
Television image compression and small animal remote monitoring [NASA-CR-186614] N92-11223

MONOMERS
Polyimides with improved compression moldability [NASA-CASE-LAR-14457-1-CU] N92-11198

MONOTONE FUNCTIONS
On the solution for the problem of long waves in a perfect fluid N92-11721

MONTE CARLO METHOD
Influence of the crop architecture parameters on crop BRDF: A Monte Carlo simulation N92-11465
Bi-directional reflectance of finite and infinite clouds N92-11470
Monte Carlo model for transport equation in a plant canopy and its inversion N92-11481
Variational Monte Carlo calculations of finite nuclei [DE91-018895] N92-11778

MOTION PERCEPTION
Perceptual grouping and shape from texture [AD-A240358] N92-11678

MOTION SICKNESS
Intranasal scopolamine preparation and method [NASA-CASE-MSC-21858-1] N92-11628

MOVING TARGET INDICATORS
Impulse transmitter and quantum detection radar system [AD-D014958] N92-11229

MULLITES
Mechanical properties of a porous mullite material [NASA-TM-104547] N92-11187

MULTIENGINE VEHICLES
Overview of the Beta II Two-Stage-To-Orbit vehicle design [NASA-TM-105298] N92-11034

MULTIGRID METHODS
Euler solutions for an unbladed jet engine configuration
[NASA-TM-105332] N92-11328
Analysis of a parallel multigrid algorithm
[NASA-CR-188906] N92-11701
MULTILAYER INSULATION
MLITemp: A computer program to predict the thermal effects associated with hypervelocity impact damage to space station MLI
[NASA-CR-184245] N92-11079
MULTIMODE RESONATORS
Tilted resonator experiments on a quasioptical gyrotron
[AD-A240680] N92-11335
MULTIPOLES
Coil shapes towards pure multipoles in circular regions: A numerical approach
[DE91-017239] N92-11271
MULTIPROCESSING (COMPUTERS)
Parallel processing applications for gas turbine engine control N92-11012
Distributed memory compiler methods for irregular problems: Data copy reuse and runtime partitioning
[NASA-CR-187635] N92-11669
Vienna FORTRAN: A FORTRAN language extension for distributed memory multiprocessors
[NASA-CR-187634] N92-11670
Cedar Project: Original goals and progress to date
[DE92-000032] N92-11689
A domain decomposition algorithm for solving large elliptic problems
[DE92-000096] N92-11690
Efficient ICCG on a shared memory multiprocessor
[NASA-CR-188843] N92-11693
Neural networks and MIMD-multiprocessors
[NASA-CR-188481] N92-11697
Harnessing the killer micros: Applications from LLNL's massively parallel computing initiative
[DE91-018721] N92-11709
Issues in parallel automatic differentiation
[DE91-017311] N92-11726
MULTISENSOR APPLICATIONS
A multi-sensor approach to spectral signature analysis of inland waters N92-11428
The linking of crop growth models and multi-sensor remote sensing data N92-11512
MULTISPECTRAL BAND SCANNERS
TIMS calibration correction by comparison with PRT5 N92-11412
On the use of passive microwaves at 37 GHz N92-11461
ATLAS: An Auto-Tracking Land and Atmosphere Sensor for retrieval of atmospheric optical parameters and acquisition of bidirectional surface reflectance N92-11487
Integration of visible-through microwave-range multispectral image data sets for geologic mapping N92-11491
MULTISPECTRAL RADAR
Multifrequency radar measurements of potato, beet, and wheat during the AGRISCATT-88 campaign in the Netherlands N92-11444
Land cover classification by multipolarized SAR imagery N92-11457
MULTISTAGE ROCKET VEHICLES
Overview of the Beta II Two-Stage-To-Orbit vehicle design
[NASA-TM-105298] N92-11034
MUSCULAR FATIGUE
Training, muscle fatigue and stress fractures
[AD-A240386] N92-11626

N

N-TYPE SEMICONDUCTORS
Limits of energy dissipation for x ray sensitive pn Charge Coupled Devices (CCDs)
[MPE-224] N92-11280
Diffusion and drift of charges in semiconductor detectors
[MBE-225] N92-11281
NASA PROGRAMS
Safety issues N92-11115
NATIONAL PARKS
Study of alternatives: Dayton's Aviation heritage, Ohio
[PB91-202275] N92-10972
NATURAL GAS
Alternative fuels for heavy duty engines: Status of fleet trials
[DE91-018474] N92-11210
Piston temperature measurement in a natural gas engine
[PB91-194357] N92-11352
Component cost analysis for compressed natural gas vehicles
[DE91-017230] N92-11353
NAVIER-STOKES EQUATION
Viscous computations of cold air/air flow around scramjet nozzle afterbody
[NASA-CR-4406] N92-10982
A detailed investigation of staged normal injection into a Mach 2 flow N92-11118
Navier-Stokes entropy controlled combustion instability analysis for liquid propellants N92-11122
Application of Krylov exponential propagation to fluid dynamics equations
[NASA-CR-188887] N92-11290
A Newton's method solver for the two-dimensional and axisymmetric Navier-Stokes equations N92-11292
Resolution of the Navier-Stokes equations applied to the computation of the laminar flow around a two dimensional wing profile
[CERT-RT-65/5604-35] N92-11307
Resolution of Navier-Stokes equations around profiles: Drag evolution
[ONERA-RTS-86/1685-AY-156A] N92-11310
An efficient and robust algorithm for two dimensional time dependent incompressible Navier-Stokes equations: High Reynolds number flows
[NASA-TM-104424] N92-11320
NAVIGATION
Engineering and instrumentation support of GL Research Balloon Program
[AD-A240616] N92-10987
Navigation and positioning of mobile robots
[DE92-704014] N92-10998
NEAR INFRARED RADIATION
Comparison of atmospheric correction procedures for visible and near-IR satellite sensor output N92-11395
On the value of high spectral resolution measurements in the visible and near-infrared N92-11419
Simultaneous determination of six soil properties from the soil diffuse reflectance spectrum in the near infrared region (1-2.5 microns) N92-11424
Near-infrared imaging spectroscopy: Learning from planetary geology N92-11438
Optimum combinations of visible and near-infrared reflectances for estimating the fraction of photosynthetically available radiation absorbed by plants N92-11474
Normalization of multidirectional red and NIR reflectances with the SAVI N92-11477
Structural controls on the remotely sensed response of a coniferous forest plantation N92-11516
Wavelength shifts in fluorescence maxima of stressed and non-stressed Norway spruce needles over the growing season N92-11536
NEAR WAKES
A comparison of airborne wake vortex detection measurements with values predicted from potential theory
[NASA-TP-3125] N92-10994
NEEDLES
Phenological changes in the red edge shift of Norway spruce needles and their relationship to needle chlorophyll content N92-11423
NEGATIVE IONS
NBI system with negative ion source in large helical device N92-11870
NEODYMIUM LASERS
Novel nonlinear laser diagnostic techniques
[AD-A240193] N92-11346
NEPHANALYSIS
Mesoscale prediction and satellite cloud analysis for advanced meteorological processing systems
[AD-A240510] N92-11597
NETWORK ANALYSIS
Automated conflict resolution issues N92-11045
Algebraic aspects of network reliability problems
[AD-A240365] N92-11748
NETWORK CONTROL
Space Network Control Conference on Resource Allocation Concepts and Approaches
[NASA-CP-3124] N92-11039
Space Network Control (SNC) Conference on Resource Allocation Concepts and Approaches. Overview N92-11040
Effect of locus of resource control on operational efficiency in distributed operations N92-11046
Flexible Envelope Request Notation (FERN) N92-11050
Network Control Center User Planning System (NCC UPS) N92-11053
Polynomial optimization techniques for activity scheduling. Optimization based prototype scheduler N92-11056
Range Scheduling Aid (RSA) N92-11057
Scheduling techniques in the Request Oriented Scheduling Engine (ROSE) N92-11058
A method for interference mitigation in space communications scheduling N92-11062
Real-time earthquake monitoring: Early warning and rapid response
[NASA-CR-186701] N92-11582
NEURAL NETS
SPIKE: AI scheduling techniques for Hubble Space Telescope N92-11054
Robotic non-destructive inspection of aircraft, phase 1
[AD-A240777] N92-11367
Weather prediction using a genetic memory
[NASA-CR-185448] N92-11590
Long term synaptic plasticity and learning in neuronal networks
[AD-A240366] N92-11613
Neural networks and MIMD-multiprocessors
[NASA-CR-188481] N92-11697
Highly parallel computation
[NASA-CR-188871] N92-11698
Total recall in distributive associative memories
[NASA-CR-188884] N92-11699
Learning to read aloud: A neural network approach using sparse distributed memory
[NASA-CR-188846] N92-11711
NEUROLOGY
Long term synaptic plasticity and learning in neuronal networks
[AD-A240366] N92-11613
NEUROPHYSIOLOGY
Long term synaptic plasticity and learning in neuronal networks
[AD-A240366] N92-11613
NEUTRAL ATOMS
Numerical analysis of temporal development of RF-heated plasma N92-11834
NEUTRAL BEAMS
Recent experiments in JT-60 N92-11812
Confinement studies of Heliotron E plasmas in magnetic surface variation experiments N92-11850
Transport study of ECH and NBI plasmas in CHS N92-11857
Ion temperature and poloidal rotation profiles for NBI heated plasma in CHS N92-11860
Driven currents in neutral beam heated plasma N92-11861
NBI system with negative ion source in large helical device N92-11870
NEUTRAL BUOYANCY SIMULATION
Space engineering
[NASA-CR-187820] N92-11215
NEUTRON BEAMS
A study of radiation collapse in CHS plasmas N92-11859
NEUTRON COUNTERS
Solid state neutron dosimeter for space applications
[NASA-CR-185633] N92-11331
NEUTRON DIFFRACTION
Neutron diffraction from the flux line lattice
[DE91-018175] N92-11906
NEUTRON DISTRIBUTION
The considering of the slowing down effect in the formalism of probability tables. Application to the effective cross section calculation
[DE91-626722] N92-11751
NEUTRON EMISSION
Solid state neutron dosimeter for space applications
[NASA-CR-185633] N92-11331
NEUTRON STARS
Effects of the equation of state in neutron stars and in stellar collapse
[DE91-014534] N92-11935
Converting neutron stars into strange stars
[NASA-CR-189008] N92-11945
NEUTRONS
Bose-condensation in liquid helium under pressure
[DE91-634504] N92-11170
The considering of the slowing down effect in the formalism of probability tables. Application to the effective cross section calculation
[DE91-626722] N92-11751
NEVADA
March AFB forecasting rules of thumb evaluation
[AD-A240458] N92-11595
NEWTON METHODS
A Newton's method solver for the two-dimensional and axisymmetric Navier-Stokes equations N92-11292
NICKEL
Effects of hydrogen and carbon on thermally activated deformation in nickel
[AD-A240496] N92-11178
NICKEL ALLOYS
Contact angle and work of adhesion between Ni-based melts and non-metallic solids
[NPL-DMM(A)-23] N92-11171

Alloy modeling and experimental correlation for ductility enhancement in near stoichiometric single crystal nickel aluminide
[AD-A240151] N92-11175

NIGHT VISION
The effect of blinking on subsequent dark adaptation
[AD-A240281] N92-11625

NITROFORMATES
High density energetic materials
[AD-D014959] N92-11212

NITROGEN
Calculations and curve fits of thermodynamic and transport properties for equilibrium air to 30000 K
[NASA-RP-1260] N92-11285
Feasibility of the red edge index for the detection of nitrogen deficiency N92-11425
Report on carbon and nitrogen abundance studies
[NASA-CR-188803] N92-11934

NITROGEN ATOMS
Collision integrals and high temperature transport properties for N-N, O-O, and N-O
[NASA-CR-188907] N92-11770

NITROGEN DIOXIDE
Collisional energy transfer from excited nitrogen dioxide
[DE91-016989] N92-11772

NITROGEN OXIDES
Spectral fitting, shock layer modeling, and production of nitrogen oxides and excited nitrogen
[NASA-CR-185664] N92-11769

NOAA SATELLITES
Modeling temporal evolution of the radiometric response measured by wideband sensors over temperate agricultural regions N92-11518
Contribution of NOAA-AVHRR satellite data in forest vegetation monitoring N92-11520
Detection and characterization of active fires in west Africa with LANDSAT thematic mapper and NOAA N92-11529
From evapotranspiration to soil moisture investigation based on NOAA thermal infrared data, case study: Poland N92-11531

NOISE INJURIES
The hazard of exposure to impulse noise as a function of frequency, volume 2
[AD-A240530] N92-11762

NOISE SPECTRA
The hazard of exposure to impulse noise as a function of frequency, volume 2
[AD-A240530] N92-11762

NONDESTRUCTIVE TESTS
A new radiographic corrosion inspection capability
[AD-A231476] N92-11363
Supervoltage NDE techniques for large aerospace structures
[AD-A240625] N92-11365
Development of a reliability-based method for evaluating a pavement feature
[AD-A240747] N92-11366
Robotic non-destructive inspection of aircraft, phase 1
[AD-A240777] N92-11367

NONELECTROLYTES
Development of an experimental database and theories for prediction of thermodynamic properties of aqueous electrolytes and nonelectrolytes of geochemical significance at supercritical temperatures and pressures
[DE91-018493] N92-11169

NONEQUILIBRIUM PLASMAS
Modeling UV and x ray oxygen emission in astrophysical plasmas
[DE91-016927] N92-11940

NONLINEAR SYSTEMS
Nonlinear optical properties of semiconducting polymers
[AD-A240753] N92-11195
Antiresonant nonlinear mirror for passive laser mode locking
[AD-D014951] N92-11343
Novel nonlinear laser diagnostic techniques
[AD-A240193] N92-11346
Analysis of strain dependent damping in materials via modeling of material point hysteresis
[AD-A240298] N92-11381
Geometrically exact shells models: Foundation and computational aspects with special reference to implicit large-scale calculations
[DE91-019014] N92-11390
Resonant frequency calculations using a hybrid perturbation-Galerkin technique
[NASA-CR-187632] N92-11640
Convergence and performance of synchronous and asynchronous parallel and conventional iterative methods
[AD-A240286] N92-11707
On the theory and numerical approximation of nonlinear hyperbolic problems
[ETN-91-99898] N92-11714
Operator splitting, fractional steps, method and entropy condition for nonlinear hyperbolic systems N92-11719
Nonlinear behavior of multiple-helicity resistive interchange modes near marginally stable states
[NIFS-89] N92-11883
Quantum 1/f noise in high technology applications including ultrasmall structures and devices
[AD-A240152] N92-11907

NONLINEARITY
Nonlinear optical properties of semiconducting polymers
[AD-A240753] N92-11195
Engine dynamic analysis with general nonlinear finite element codes
[NASA-CR-187222] N92-11379
Large deformation induced failures in nonlinear solids
[AD-A240369] N92-11382
Nonlinear aspects of aerospace structures at high excitation levels flat aluminum beams and plates studied
[AD-A240600] N92-11383
Nonlinear theory of synthetic aperture radar sea wave imaging N92-11451
Operator splitting, fractional steps, method and entropy condition for nonlinear hyperbolic systems N92-11719
Simulation of a nonlinear two degrees of freedom system. Study of the temporal response to a harmonic attraction
[ONERA-RT-17/1677-RY-091-R] N92-11755
Nonlinear behavior of multiple-helicity resistive interchange modes near marginally stable states
[NIFS-89] N92-11883

NONNEWTONIAN FLUIDS
Deformation and breakup of drops in simple shear flows
[ETN-91-90143] N92-11315

NONUNIFORM MAGNETIC FIELDS
Linear theory of a quasioptical gyroklystron with nonuniform magnetic field
[AD-A240264] N92-11334

NOREPINEPHRINE
Non-invasive evaluation of the cardiac autonomic nervous system by PET
[DE91-018476] N92-11622

NORMALIZING (STATISTICS)
Normalization of multidirectional red and NIR reflectances with the SAVI N92-11477
Normalization of bidirectional effects of surface reflectance on a series of multitemporal NOAA/AVHRRR data N92-11480

NOZZLE DESIGN
Viscous computations of cold air/air flow around scramjet nozzle afterbody
[NASA-CR-4406] N92-10982
Analytical study of nozzle performance for nuclear thermal rockets
[NASA-TM-105251] N92-11126

NOZZLE FLOW
Viscous computations of cold air/air flow around scramjet nozzle afterbody
[NASA-CR-4406] N92-10982

NUCLEAR ELECTRIC PROPULSION
Hybrid propulsion systems for space exploration missions N92-11097
Enabling the space exploration initiative: NASA's exploration technology program in space power
[NASA-TM-4325] N92-11131

NUCLEAR ENERGY
An IFE development strategy
[DE91-016918] N92-11873

NUCLEAR ENGINE FOR ROCKET VEHICLES
Nuclear Thermal Propulsion: A Joint NASA/DOE/DOD Workshop
[NASA-CP-10079] N92-11088
Nuclear thermal rocket workshop reference system Rover/NERVA N92-11091
NERVA upgrade: Non-nuclear components N92-11092
Upgraded NERVA systems: Enabler nuclear system N92-11093
Low Pressure Nuclear Thermal Rocket (LPNTR) concept N92-11094
Particle bed reactor nuclear rocket concept N92-11095
Nuclear thermal/nuclear electric hybrids N92-11107
Quick trips to Mars N92-11111
Nuclear safety N92-11114
An overview of tested and analyzed NTP concepts
[NASA-TM-105252] N92-11137

NUCLEAR EXPLOSIONS
A realistic, gradual and economical approach to fusion power
[DE91-018464] N92-11786

NUCLEAR FISSION
Vapor core propulsion reactors N92-11109

NUCLEAR FUEL REPROCESSING
The TITAN reversed-field-pinch fusion reactor study, volume 1
[DE92-000141] N92-11897

NUCLEAR FUELS
Pellet bed reactor for nuclear propelled vehicles: Part 1: Reactor technology N92-11101
Liquid annulus N92-11104
Open cycle gas core nuclear rockets N92-11108
Nuclear light bulb N92-11110
Nuclear fuels status N92-11113
The TITAN reversed-field-pinch fusion reactor study, volume 1
[DE92-000141] N92-11897

NUCLEAR FUSION
Fusion energy for space missions in the 21st Century
[NASA-TM-4298] N92-11783
A realistic, gradual and economical approach to fusion power
[DE91-018464] N92-11786
Design of the compact Auburn torsatron N92-11805
On the evolution of a superconducting cosmic string network
[DE91-630995] N92-11948

NUCLEAR HEAT
Shielding requirements for particle bed propulsion systems
[AD-A240780] N92-11787

NUCLEAR MEDICINE
JPRS report: Science and technology. USSR: Life sciences
[JPRS-ULS-91-012] N92-11611

NUCLEAR MODELS
Global analysis of fermion mixing with exotics
[NASA-CR-189006] N92-11774
Variational Monte Carlo calculations of finite nuclei
[DE91-018895] N92-11778

NUCLEAR PHYSICS
Variational Monte Carlo calculations of finite nuclei
[DE91-018895] N92-11778
Theoretical interpretation of high-energy nuclear collisions
[DE91-016965] N92-11782
Converting neutron stars into strange stars
[NASA-CR-189008] N92-11945

NUCLEAR POWER PLANTS
A realistic, gradual and economical approach to fusion power
[DE91-018464] N92-11786

NUCLEAR POWER REACTORS
Nuclear thermal/nuclear electric hybrids N92-11107

NUCLEAR PROPULSION
Nuclear Thermal Propulsion: A Joint NASA/DOE/DOD Workshop
[NASA-CP-10079] N92-11088
Nuclear thermal propulsion program overview N92-11089
Nuclear thermal propulsion workshop overview N92-11090
Nuclear thermal rocket workshop reference system Rover/NERVA N92-11091
NERVA upgrade: Non-nuclear components N92-11092
Upgraded NERVA systems: Enabler nuclear system N92-11093
Low Pressure Nuclear Thermal Rocket (LPNTR) concept N92-11094
Particle bed reactor nuclear rocket concept N92-11095
A cermet fuel reactor for nuclear thermal propulsion N92-11096
Wire core reactor for NTP N92-11099
Pellet bed reactor for nuclear propelled vehicles: Part 1: Reactor technology N92-11101
Pellet bed reactor for nuclear propelled vehicles: Part 2: Missions and vehicle integration trades N92-11102
Fission fragment assisted reactor concept for space propulsion: Foil reactor N92-11103
Liquid annulus N92-11104
Droplet Core Nuclear Rocket (DLNR) N92-11105
Comments on dual-mode nuclear space power and propulsion system concepts N92-11106
Nuclear thermal/nuclear electric hybrids N92-11107
Open cycle gas core nuclear rockets N92-11108
Vapor core propulsion reactors N92-11109
Quick trips to Mars N92-11111
Propulsion system needs N92-11112
Nuclear safety N92-11114
Disposal methods N92-11116
Analytical study of nozzle performance for nuclear thermal rockets
[NASA-TM-105251] N92-11126
An overview of tested and analyzed NTP concepts
[NASA-TM-105252] N92-11137

Fusion energy for space missions in the 21st Century [NASA-TM-4298] N92-11783
NUCLEAR PUMPED LASERS
Fission fragment assisted reactor concept for space propulsion: Foil reactor N92-11103
NUCLEAR REACTORS
Dumbo: A pachydermal rocket motor N92-11100
Droplet Core Nuclear Rocket (DLNR) N92-11105
Vapor core propulsion reactors N92-11109
ITER divertor sputtering erosion: Recent analysis for carbon, beryllium, tungsten, and niobium surfaces [DE91-017235] N92-11871
NUCLEAR ROCKET ENGINES
Nuclear rocket using indigenous Martian fuel NIMF N92-11098
Nuclear light bulb N92-11110
Quick trips to Mars N92-11111
Propulsion system needs N92-11112
Disposal methods N92-11116
Analytical study of nozzle performance for nuclear thermal rockets [NASA-TM-105251] N92-11126
NUCLEAR STRUCTURE
Variational Monte Carlo calculations of finite nuclei [DE91-018895] N92-11778
NUCLEAR WEAPONS
Insurance against catastrophe: SDI and the 3rd World nuclear proliferation problem [AD-A240429] N92-11752
NUCLEATION
Large deformation induced failures in nonlinear solids [AD-A240369] N92-11382
NUCLEON-NUCLEON INTERACTIONS
Variational Monte Carlo calculations of finite nuclei [DE91-018895] N92-11778
NUCLEONS
Meson-exchange calculation of the d(gamma,p)n in the GeV energy region [DE91-017994] N92-11785
NUMERICAL ANALYSIS
JANNAF Combustion Instability Panel Workshop report: Numerical methods in combustion instability N92-11123
TEGEN: A one dimensional program to calculate a thermoelectric generator [DE91-634444] N92-11571
Convergence and performance of synchronous and asynchronous parallel and conventional iterative methods [AD-A240286] N92-11707
On the theory and numerical approximation of nonlinear hyperbolic problems [ETN-91-99898] N92-11714
Numerical analysis of the problem of long waves in shallow water N92-11720
Interface conditions for domain decomposition with radical grid refinement N92-11733
On the evolution of a superconducting cosmic string network [DE91-630995] N92-11948
NUMERICAL CONTROL
A generalized method for multiple robotic manipulator programming applied to vertical-up welding [NASA-TP-3163] N92-11218
NUMERICAL STABILITY
Implementation of the flow-modulated skew-upward difference scheme in the momentum equation of the COMMIX-1C program: A first assessment [DE91-018013] N92-11321
NUMERICAL WEATHER FORECASTING
Energetics diagnosis of numerical simulation of atmospheric blocking [NASA-CR-183503] N92-11581
NUTS (FASTENERS)
Quick application/release nut with engagement indicator [NASA-CASE-MSC-21799-1] N92-11359

O

OBSTACLE AVOIDANCE
Navigation and positioning of mobile robots [DE92-704014] N92-10998
OCEAN CURRENTS
One-way nesting for a primitive equation ocean model N92-11734
OCEAN DYNAMICS
Theory and modeling in GLOBEC: A first step N92-11602
GLOBEC: Global Ocean Ecosystems Dynamics: A component of the US Global Change Research Program [NASA-TM-105121] N92-11603
One-way nesting for a primitive equation ocean model N92-11734
OCEAN MODELS
Modeling of visible and UV radiative transfer in the ocean-atmosphere system concepts, models, and programs N92-11396
One-way nesting for a primitive equation ocean model N92-11734
Nested ocean models: Work in progress N92-11735
OCEAN SURFACE
Modeling of radar backscattering from the sea surface using polarimetric-SAR observations N92-11442
Nonlinear theory of synthetic aperture radar sea wave imaging N92-11451
Studies of the physical and chemical stability of natural sea-surface films [AD-A239818] N92-11604
A survey of scattering, attenuation, and size spectra studies of bubble layers and plumes beneath the air-sea interface [AD-A240262] N92-11606
OCEANOGRAPHY
In flight calibration of large field of view sensors at short wavelength using the Rayleigh scattering N92-11416
Space observation of the land-ocean-atmosphere system at high spectral resolution in the infrared: Perspectives and problems N92-11421
GLOBEC: Global Ocean Ecosystems Dynamics: A component of the US Global Change Research Program [NASA-TM-105121] N92-11603
OCEANS
Use of theoretical wave height distributions in directional seas [AD-A240411] N92-11608
OCTANE
Effect of gasoline octane quality on vehicle acceleration performance [AD-A240433] N92-11357
OHIO
Study of alternatives: Dayton's Aviation heritage, Ohio [PB91-202275] N92-10972
OILS
In-line hydraulic dashpot [AD-D014955] N92-11356
ON-LINE SYSTEMS
Study and prototype of data system interactions for the Earth Observing System Data and Information System [NASA-CR-183505] N92-11648
An investigation to find appropriate measures for evaluating interactive information retrieval N92-11922
FEDIX: The on-line database retrieval service of Government information for colleges, universities, and other organizations [DE91-018496] N92-11923
OPACITY
OPAL opacities for astrophysical applications [DE91-016922] N92-11939
OPERATING SYSTEMS (COMPUTERS)
Cedar Project: Original goals and progress to date [DE92-000032] N92-11689
OPERATING TEMPERATURE
Piston temperature measurement in a natural gas engine [PB91-194357] N92-11352
OPERATIONAL AMPLIFIERS
Advanced Langmuir Probe (LP) [NASA-CR-180084] N92-11284
OPERATIONS RESEARCH
Development of a fundamentally new refining method. Part 2: Operating conditions of the new refiner N92-11154
OPERATORS (MATHEMATICS)
Operator splitting, fractional steps, method and entropy condition for nonlinear hyperbolic systems N92-11719
Domain-decomposed preconditionings for transport operators N92-11731
OPERATORS (PERSONNEL)
Human Machine Interfaces for Teleoperators and Virtual Environments Conference [NASA-CP-10071] N92-11638
OPTICAL COMMUNICATION
Dual frequency optical carrier technique for transmission of reference frequencies in dispersive media [NASA-CASE-NPO-18007-1-CU] N92-11791
OPTICAL DENSITY
Effects on LDEF exposed copper film and bulk N92-11076
OPTICAL EQUIPMENT
Micro photoreflectance semiconductor wafer analyzer [AD-D014950] N92-11788
Process for controlling the thickness of an antireflection coating, and embodying apparatus [DE91-017634] N92-11793
OPTICAL FIBERS
Optical design of a high power fiber optic coupler [DE91-016924] N92-11789
Experiments and applications of soliton physics [NIFS-32] N92-11877
OPTICAL MEASUREMENT
Aircraft lidar sensitivity study for measuring water vapor [AD-A240549] N92-11237
Euromech 260: Advanced non-intrusive experimental techniques in fluid and plasma flows [ETN-91-90104] N92-11313
OPTICAL PATHS
Aircraft lidar sensitivity study for measuring water vapor [AD-A240549] N92-11237
OPTICAL PROPERTIES
Strategic air command contrail formation study [AD-A240467] N92-11003
Nonlinear optical properties of semiconducting polymers [AD-A240753] N92-11195
Multiangular approach to solution of atmosphere optics reverse problems N92-11478
Optically thin cirrus clouds over oceans and possible impact on sea surface temperature of warm pool in western Pacific [NASA-TM-104550] N92-11600
Thermal annealing studies of Fe and Ti implanted in GaAs and InP [ETN-91-90148] N92-11915
OPTICAL RADAR
Design and operation of the GL/OPA mobile Doppler lidar [AD-A240257] N92-11231
Aircraft lidar sensitivity study for measuring water vapor [AD-A240549] N92-11237
Vegetation monitoring by means of spectral resolved fluorescence lidar N92-11533
Laser active remote sensing of phytoplankton in inland waters N92-11534
Laser-induced spectral signatures in investigations of sea upper layer N92-11537
Design and testing of a spectral-resolving fluorescence lidar system for remote sensing of vegetation N92-11540
Target signature by differential reflectance lidar, a feasibility study N92-11544
The use of a time-resolved lidar to study the water column N92-11548
OPTICAL REFLECTION
Micro photoreflectance semiconductor wafer analyzer [AD-D014950] N92-11788
OPTICAL RESONANCE
Antiresonant nonlinear mirror for passive laser mode locking [AD-D014951] N92-11343
OPTICAL THICKNESS
ATLAS: An Auto-Tracking Land and Atmosphere Sensor for retrieval of atmospheric optical parameters and acquisition of bidirectional surface reflectance N92-11487
Optically thin cirrus clouds over oceans and possible impact on sea surface temperature of warm pool in western Pacific [NASA-TM-104550] N92-11600
OPTICAL TRACKING
A methodology to assess the Best Estimate Trajectory (BET) results generated for the Kwajalein Missile Range [AD-A240770] N92-11083
Illumination, optics, and retroreflectors for efficient landmark tracking N92-11790
OPTIMAL CONTROL
Microgravity vibration isolation: An optimal control law for the one-dimensional case [NASA-TM-105146] N92-11217
Optimal control by wideband frequency. Application to acoustic control by piezoelectric technique [ONERA-RT-6/3654-RY-006-R] N92-11713
OPTIMIZATION
Maximized gust loads for a nonlinear airplane using matched filter theory and constrained optimization [NASA-TM-104138] N92-11010
Structural tailoring of advanced turboprops (STAT): User's manual [NASA-CR-187101] N92-11016
Intelligent perturbation algorithms for space scheduling optimization N92-11055
Polynomial optimization techniques for activity scheduling. Optimization based prototype scheduler N92-11056
Intelligent perturbation algorithms to space scheduling optimization N92-11064
Multidisciplinary optimization of controlled space structures with global sensitivity equations [NASA-TP-3130] N92-11087
A systematic approach to combustion model reduction and lumping [AD-A240195] N92-11164

Multi-disciplinary optimization of aeroservoelastic systems
[NASA-CR-188983] N92-11377
User's manual for the Macintosh version of PASCO
[NASA-TM-104115] N92-11668
Review of the TJ-II Flexible Heliac Project N92-11803
Optimization of Helias configurations N92-11806
Drift optimization of helical systems N92-11810
Quantum 1/f noise in high technology applications including ultrasmall structures and devices
[AD-A240152] N92-11907

ORBIT TRANSFER VEHICLES
Mach 6.5 air induction system design for the Beta 2 two-stage-to-orbit booster vehicle
[NASA-CR-187233] N92-11013
Prediction of the pattern performance for the Aeroassist Flight Experiment (AFE) spacecraft
[NASA-CR-4409] N92-11065
Pellet bed reactor for nuclear propelled vehicles: Part 2: Missions and vehicle integration trades N92-11102
Definition, technology readiness, and development cost of the orbit transfer vehicle engine integrated control and health monitoring system elements
[NASA-CR-187123] N92-11132

ORBITAL ASSEMBLY
Space engineering
[NASA-CR-187820] N92-11215
Quick application/release nut with engagement indicator
[NASA-CASE-MSC-21799-1] N92-11359

ORBITS
Power-law energy spectrum and orbital stochasticity
[DE91-017387] N92-11872

ORGANIC CHARGE TRANSFER SALTS
New high-T(sub c) benchmarks for organic and fullerene superconductors
[DE91-016406] N92-11899

ORGANIC CHEMISTRY
Organic geochemistry of seawater particulate matter: Final data analysis interpretation
[AD-A240199] N92-11605

ORGANIC COMPOUNDS
Study of silanization of silica and fiberglass using ESR spectroscopy and spin labelling
[AD-A240767] N92-11197
Low volatile organic compound paints
[DE91-017984] N92-11203

ORGANIC MATERIALS
Observation of DOM composition by synchronous fluorescence spectroscopy N92-11549

ORGANIC SUPERCONDUCTORS
New high-T(sub c) benchmarks for organic and fullerene superconductors
[DE91-016406] N92-11899

OSCILLATIONS
Navier-Stokes entropy controlled combustion instability analysis for liquid propellants N92-11122
E sub 6 leptoquarks and the solar neutrino problem
[NASA-CR-189005] N92-11956

OUTER RADIATION BELT
Radiation belt dynamic and quasi-static modeling based on CRRES data
[AD-A240392] N92-11585

OXIDASE
Biochemical and biophysical studies of the E. coli respiratory chain
[DE91-016966] N92-11612

OXIDATION
Oxidation of titanium aluminide and its XD composite
[AD-A240401] N92-11177
Scientific assessment of stratospheric ozone: 1989, volume 1
[NASA-TM-105116] N92-11576
Photoemission study of Ce/Ta(110) and Ce/W(110) interfaces and the catalytic oxidation effect
[DE91-018167] N92-11903

OXIDES
Contact angle and work of adhesion between Ni-based melts and non-metallic solids
[NPL-DMM(A)-23] N92-11171
Solid lubricants on pretreated surfaces
[NASA-CASE-LEW-14474-2] N92-11186

OXYGEN
Calculations and curve fits of thermodynamic and transport properties for equilibrium air to 30000 K
[NASA-RP-1260] N92-11285
Development of high Tc (greater than 110K) Bi, Tl and Y-based materials as superconducting circuit elements
[NASA-CR-188999] N92-11902

OXYGEN ATOMS
Measurements of erosion characteristics for metal and polymer surfaces using profilometry N92-11077
Pinhole cameras as sensors for atomic oxygen in orbit; application to attitude determination of the LDEF N92-11078
Collision integrals and high temperature transport properties for N-N, O-O, and N-O
[NASA-CR-188907] N92-11770

OXYGEN IONS
High I state population in O(7+) produced in ion-solid collisions
[DE91-018169] N92-11904

OXYGEN PLASMA
Modeling UV and x ray oxygen emission in astrophysical plasmas
[DE91-016927] N92-11940

OXYGEN PRODUCTION
Spectral fitting, shock layer modeling, and production of nitrogen oxides and excited nitrogen
[NASA-CR-185664] N92-11769

OXYGENATION
Efficacy of hyperbaric oxygenation in enhancing flight tolerance N92-11618

OZONE
Scientific assessment of stratospheric ozone: 1989, volume 1
[NASA-TM-105116] N92-11576

OZONE DEPLETION
Upper Atmosphere Research Satellite (UARS): A program to study global ozone change
[NASA-TM-105100] N92-11067
Scientific assessment of stratospheric ozone: 1989, volume 1
[NASA-TM-105116] N92-11576

P

P-I-N JUNCTIONS
Solid state neutron dosimeter for space applications
[NASA-CR-185633] N92-11331

P-TYPE SEMICONDUCTORS
Limits of energy dissipation for x ray sensitive pn Charge Coupled Devices (CCDs)
[MPE-224] N92-11280
Diffusion and drift of charges in semiconductor detectors
[MBE-225] N92-11281

PACIFIC OCEAN
Mariners Weather Log, Volume 35, Number 2, Spring 1991
[PB91-202572] N92-11592

PACKET SWITCHING
The ARPANET after twenty years
[NASA-CR-188853] N92-11695

PACKET TRANSMISSION
The probability of multiple correct packet receptions in a multireceiver frequency-hopped spread-spectrum system
[AD-A240655] N92-11240

PACKETS (COMMUNICATION)
The probability of multiple correct packet receptions in a multireceiver frequency-hopped spread-spectrum system
[AD-A240655] N92-11240

PAINTS
Low volatile organic compound paints
[DE91-017984] N92-11203
Conductive gage for crack length measurement
[NASA-CASE-LAR-14480-1-CU] N92-11374

PANEL METHOD (FLUID DYNAMICS)
Prediction of forces and moments for hypersonic flight vehicle control effectors
[NASA-CR-188954] N92-11070

PANELS
Compression response of laminated composite panels containing multiple delaminations N92-11141
Delamination propagation in a composite panel under compressive stress
[ONERA-RT-23/3542-RY-093-R] N92-11146
User's manual for the Macintosh version of PASCO
[NASA-TM-104115] N92-11668

PAPER (MATERIAL)
The role of fiber flocculation in chemical pulp refining
[ETN-91-90025] N92-11150
Fundamental aspects of the refining process N92-11151
A new hypothesis for the mechanics of refining N92-11152
Development of a fundamentally new refining method. Part 1: Basic design considerations N92-11153
Development of a fundamentally new refining method. Part 2: Operating conditions of the new refiner N92-11154
Effect of control variables and length of refining zone on the refining result with a new pilot refiner N92-11155
Comparison of a new refiner with a conventional refiner N92-11156
Homogeneity of refining action; effects on fiber and paper structure N92-11157
Control of the heterogeneity of the refining action N92-11158

PARALLEL COMPUTERS
Modula-2*: An extension of Modula-2 for highly parallel programs
[NASA-CR-188855] N92-11654
Efficient ICCG on a shared memory multiprocessor
[NASA-CR-188843] N92-11693

PARALLEL PROCESSING (COMPUTERS)
Parallel processing applications for gas turbine engine control N92-11012
A parallel algorithm for the eigenvalues and eigenvectors for a general complex matrix
[NASA-CR-188854] N92-11653
Modula-2*: An extension of Modula-2 for highly parallel programs
[NASA-CR-188855] N92-11654
An O(log sup 2 N) parallel algorithm for computing the eigenvalues of a symmetric tridiagonal matrix
[NASA-CR-188898] N92-11659
Transient finite element computations on a variable transputer system
[NASA-CR-189060] N92-11671
Optimal processor assignment for pipeline computations
[NASA-CR-189047] N92-11672
Some fast elliptic solvers on parallel architectures and their complexities
[NASA-CR-188840] N92-11692
Optimal expression evaluation for data parallel architectures
[NASA-CR-187773] N92-11696
Highly parallel computation
[NASA-CR-188871] N92-11698
Ordered fast fourier transforms on a massively parallel hypercube multiprocessor
[NASA-CR-188899] N92-11700
BCD/CPS: An event-level GEANT3 parallelization via CPS
[DE91-017238] N92-11703
A synchronization and charge distribution process for the parallel multilevel logic simulation
[ETN-91-90152] N92-11708
Harnessing the killer micros: Applications from LLNL's massively parallel computing initiative
[DE91-018721] N92-11709
Studying parallel program behavior with upshot
[DE91-019072] N92-11710
Learning to read aloud: A neural network approach using sparse distributed memory
[NASA-CR-188846] N92-11711
Issues in parallel automatic differentiation
[DE91-017311] N92-11726
Discussion summary: Fictitious domain methods N92-11730

PARALLEL PROGRAMMING
Optimal parallel solution of sparse triangular systems
[NASA-CR-188872] N92-11656
An O(log sup 2 N) parallel algorithm for computing the eigenvalues of a symmetric tridiagonal matrix
[NASA-CR-188898] N92-11659
Analysis of a parallel multigrid algorithm
[NASA-CR-188906] N92-11701

PARAMETER IDENTIFICATION
Parameter identification studies on the NASA/Ames Research Center Advanced Concepts Flight Simulator
[NASA-TM-105126] N92-11024
Simulation of a nonlinear two degrees of freedom system. Study of the temporal response to a harmonic attraction
[ONERA-RT-17/1677-RY-091-R] N92-11755

PARAMETERIZATION
Experimental determination of the material parameter of two viscoelastic synthetic materials, using creep tests
[ILR-MITT-244(1990)] N92-11385

PARTIAL DIFFERENTIAL EQUATIONS
An efficient and robust algorithm for two dimensional time dependent incompressible Navier-Stokes equations: High Reynolds number flows
[NASA-TM-104424] N92-11320
Implementation of the flow-modulated skew-upward difference scheme in the momentum equation of the COMMIX-1C program: A first assessment
[DE91-018013] N92-11321
Fast secant methods for the iterative solution of large nonsymmetric linear systems
[NASA-CR-188867] N92-11655
Convergence and performance of synchronous and asynchronous parallel and conventional iterative methods
[AD-A240286] N92-11707
Discussion summary: Fictitious domain methods N92-11730

PARTICLE ACCELERATION
Particle acceleration in space and radiation belt depletion
[AD-A240311] N92-11775
Power-law energy spectrum and orbital stochasticity
[DE91-017387] N92-11872
PARTICLE ACCELERATORS
Particle acceleration in space and radiation belt depletion
[AD-A240311] N92-11775
PARTICLE BEAMS
Symposium on Development and Applications of Intense Pulsed Particle Beams
[NIFS-PROC-8] N92-11798
PARTICLE COLLISIONS
Theoretical interpretation of high-energy nuclear collisions
[DE91-016965] N92-11782
Meson-exchange calculation of the d(gamma,p)n in the GeV energy region
[DE91-017994] N92-11785
PARTICLE DENSITY (CONCENTRATION)
Studies of the physical and chemical stability of natural sea-surface films
[AD-A239818] N92-11604
PARTICLE ENERGY
The considering of the slowing down effect in the formalism of probability tables. Application to the effective cross section calculation
[DE91-626722] N92-11751
PARTICLE INTERACTIONS
Electron acceleration by laser fields in a gas
[DE91-018477] N92-11345
Studies on laser atomic spectroscopy
[DE91-628172] N92-11349
Positron lifetimes in solids from first principles calculations
[DE92-000088] N92-11781
Comparative study of final state interaction contributions to the dynamic response of quantum fluids
[DE91-631020] N92-11892
PARTICLE MOTION
Theoretical study (Lagrangian modeling) of turbulent particulate dispersion
[ETN-91-99909] N92-11287
The phenomena of scalar mixing in turbulent gas-particle flows, measuring equipment, and measurements
[DE92-704034] N92-11327
Control of electron transfer rates by motions of atoms and molecules
[DE91-018575] N92-11777
Motion of charged particle in helical systems N92-11847
Effects of electric field on particle drift orbits in a l = 2 torsatron
[NIFS-31] N92-11878
Superfluid-like turbulence in cosmology
[NASA-CR-189011] N92-11942
PARTICLE THEORY
Review of Heliotron E experiment N92-11822
Cosmological constraints on pseudo-Nambu-Goldstone bosons
[NASA-CR-189010] N92-11943
PARTICLE TRAJECTORIES
Electron acceleration by laser fields in a gas
[DE91-018477] N92-11345
Particle trajectories through MIRRORTRON configurations
[DE91-017084] N92-11876
PARTICULATE SAMPLING
Studies of the physical and chemical stability of natural sea-surface films
[AD-A239818] N92-11604
Organic geochemistry of seawater particulate matter: Final data analysis interpretation
[AD-A240199] N92-11605
PASCAL (PROGRAMMING LANGUAGE)
Cognitive factors involved in the first stage of programming skill acquisition
[AD-A240566] N92-11636
PATHOGENESIS
Training, muscle fatigue and stress fractures
[AD-A240386] N92-11626
PATTERN RECOGNITION
A hybrid methodology for detecting cartographically significant features using LANDSAT TM imagery
[AD-A240454] N92-11563
Perception and memory of pictures
[AD-A240364] N92-11633
Sparse distributed memory
[NASA-CR-188841] N92-11643
Appearance simulator for computer vision research
[AD-A240506] N92-11679
PAVEMENTS
Development of a reliability-based method for evaluating a pavement feature
[AD-A240747] N92-11366
PAYLOADS
Safety issues N92-11115
PEBBLE BED REACTORS
Particle bed reactor nuclear rocket concept N92-11095
Shielding requirements for particle bed propulsion systems
[AD-A240780] N92-11787
PEGASUS AIR-LAUNCHED BOOSTER
Aerothermal test results from the first flight of the Pegasus air-launched space booster
[NASA-TM-4330] N92-11301
PELLETS
Pellet bed reactor for nuclear propelled vehicles: Part 1: Reactor technology N92-11101
Pellet bed reactor for nuclear propelled vehicles: Part 2: Missions and vehicle integration trades N92-11102
Recent experiments in JT-60 N92-11812
Profile measurements in magnetic surface variation experiments/multiple pellet injection experiments N92-11851
PENDULUMS
Resonant frequency calculations using a hybrid perturbation-Galerkin technique
[NASA-CR-187632] N92-11640
PERFORMANCE PREDICTION
Prediction of the pattern performance for the Aeroassist Flight Experiment (AFE) spacecraft
[NASA-CR-4409] N92-11065
CFD code survey for thrust chamber application N92-11119
Analytical study of nozzle performance for nuclear thermal rockets
[NASA-TM-105251] N92-11126
Effect of particle size of Martian dust on the degradation of photovoltaic cell performance
[NASA-TM-105232] N92-11133
PERFORMANCE TESTS
New insulation constructions for aerospace wiring applications. Volume 1: Testing and evaluation
[AD-A240638] N92-11006
Test facilities for high power electric propulsion
[NASA-TM-105247] N92-11136
Effect of control variables and length of refining zone on the refining result with a new pilot refiner N92-11155
Discharge system tests of Halon 1301 test gas simulants
[AD-A240679] N92-11193
A microprocessor test approach allowing fault localisation N92-11261
Towards an automated system for the verification and diagnosis of intelligent VLSI circuits N92-11262
A method and tools for microprocessor validation: High safety function applications N92-11263
Comparison between californium and cyclotron heavy ion tests N92-11266
PERIODIC VARIATIONS
Anisotropy of thermal infrared exitance above and within plant canopies N92-11467
Normalization of bidirectional effects of surface reflectance on a series of multitemporal NOAA/AVHRRR data N92-11480
PERMANENT MAGNETS
The 23 to 300 C demagnetization resistance of samarium-cobalt permanent magnets
[NASA-TP-3119] N92-11252
Characterization of rare earth permanent magnets
[DE91-017010] N92-11754
PERMEABILITY
A Fourier collocation time domain method for numerically solving Maxwell's equations
[NASA-TM-104162] N92-11742
PERMITTIVITY
The design of broadband radar absorbing surfaces
[AD-A240521] N92-11235
A Fourier collocation time domain method for numerically solving Maxwell's equations
[NASA-TM-104162] N92-11742
PERMUTATIONS
Optimal parallel solution of sparse triangular systems
[NASA-CR-188872] N92-11656
PERSIAN GULF
Persian Gulf contrail altitude limits
[AD-A240702] N92-11598
PERSONAL COMPUTERS
An improved Newton iteration for the generalized inverse of a matrix, with applications
[NASA-CR-186983] N92-11723
PERTURBATION
Intelligent perturbation algorithms for space scheduling optimization N92-11055
Intelligent perturbation algorithms for space scheduling optimization N92-11064
Resistive MHD stability studies for ATF plasmas during operation in the second stability regime N92-11809
Non scale-invariant density perturbations from chaotic extended inflation
[NASA-CR-189004] N92-11947
PERTURBATION THEORY
Resonant frequency calculations using a hybrid perturbation-Galerkin technique
[NASA-CR-187632] N92-11640
Interface conditions for domain decomposition with radical grid refinement N92-11733
Perturbations from strings don't look like strings!
[NASA-CR-189012] N92-11941
PHARMACOLOGY
JPRS report: Science and technology. USSR: Life sciences
[JPRS-ULS-91-012] N92-11611
PHASE CHANGE MATERIALS
Heat exchanger thermal performance for two nonazeotropic refrigerant mixtures
[DE91-017250] N92-11216
PHASE DIAGRAMS
Critical properties of strongly interacting bosons on a lattice
[DE91-016926] N92-11771
PHASE ERROR
Model problem N92-11729
PHASE LOCKED SYSTEMS
Method of recertifying a loaded bearing member using a phase point
[NASA-CASE-LAR-14741-1] N92-11384
PHASE SHIFT
The effect of wiggler errors on FEL gain
[DE92-000483] N92-11351
PHASE SHIFT KEYING
Error control techniques for satellite and space communications
[NASA-CR-188997] N92-11228
PHASE TRANSFORMATIONS
Effects of the equation of state in neutron stars and in stellar collapse
[DE91-014534] N92-11935
PHASED ARRAYS
Programmable beam transform and beam steering control system for a phased array radar antenna
[AD-D014970] N92-11230
PHENOLOGY
Phenological changes in the red edge shift of Norway spruce needles and their relationship to needle chlorophyll content N92-11423
PHOTOCATHODES
A compact laser photocathode driven accelerator for the Plasma Wake Field Accelerator Program at UCLA
[AD-A240646] N92-11886
PHOTOCHEMICAL REACTIONS
Solid lubricants on pretreated surfaces
[NASA-CASE-LEW-14474-2] N92-11186
Photothermal deflection spectroscopy of conjugated polymers
[DE91-018318] N92-11204
PHOTODIODES
Investigation of the stability of the spectral responsitivity of silicon photodiodes
[NPL-QU-87] N92-11184
PHOTODISSOCIATION
Chemical reactivity and electronic structure of silicon microclusters
[AD-A240276] N92-11908
PHOTOELECTRIC EMISSION
Photoemission study of Ce/Ta(110) and Ce/W(110) interfaces and the catalytic oxidation effect
[DE91-018167] N92-11903
PHOTOGRAMMETRY
Measurement, simulation, and analysis of the directional reflectance properties of Earth surface materials N92-11468
PHOTOGRAPHS
Debris/ice/TPS assessment and photographic analysis for Shuttle Mission STS-43
[NASA-TM-103823] N92-11038
Observations of the Earth in polarized light from the US Space Shuttle N92-11485
PHOTOINTERPRETATION
Enhanced clutter suppression apparatus for use with an infrared search and surveillance system
[AD-D014984] N92-11247
Synergistic use of multispectral satellite data for monitoring land surface change N92-11489
PHOTOLUMINESCENCE
Spectroscopic studies of layered and bulk semiconductor materials
[ETN-91-90145] N92-11914

PHOTOMETERS
Mapping photopolarimeter spectrometer instrument feasibility study for future planetary flight missions
[NASA-CR-189242] N92-11329
PHOTONS
Studies on laser atomic spectroscopy
[DE91-628172] N92-11349
Continuum x ray gauging of multiple-element materials
[DE91-017429] N92-11368
Photon stimulated desorption of neutral species from aluminum
[DE91-017004] N92-11784
Progress in Photon Scanning-Tunneling Microscopy (PSTM)
[DE91-018174] N92-11905
PHOTOSENSITIVITY
Electrooptic effects and photosensitivities of PLZT thin films
[DE91-017067] N92-11901
PHOTOSYNTHESIS
Optimum combinations of visible and near-infrared reflectances for estimating the fraction of photosynthetically available radiation absorbed by plants N92-11474
Simultaneous detection in blue and red bands of laser induced vegetation fluorescence N92-11539
Modeling of fluorescence light-canopy interaction N92-11545
(L)EAF: A remote sensing fluoresensor N92-11546
PHOTOVOLTAIC CELLS
Enabling the space exploration initiative: NASA's exploration technology program in space power
[NASA-TM-4325] N92-11131
Effect of particle size of Martian dust on the degradation of photovoltaic cell performance
[NASA-TM-105232] N92-11133
Sensitivity of Space Station alpha joint robust controller to structural modal parameter variations
[NASA-TM-104153] N92-11392
Lunar dust transport and potential interactions with power system components
[NASA-CR-4404] N92-11951
PHOTOVOLTAIC CONVERSION
Photovoltaic energy system at an Alaskan site
[PB91-201350] N92-11567
PHYSICAL CHEMISTRY
Physicochemical properties and dissolution in simulated biological fluids of particles of beryllium-powered rocket motor exhaust and pure beryllium oxides calcined at low and high temperature
[AD-A240288] N92-11134
PHYSICAL OPTICS
The effect of wiggler errors on FEL gain
[DE92-000483] N92-11351
PHYSICAL PROPERTIES
Physicochemical properties and dissolution in simulated biological fluids of particles of beryllium-powered rocket motor exhaust and pure beryllium oxides calcined at low and high temperature
[AD-A240288] N92-11134
PHYSIOLOGICAL EFFECTS
Effect of prolonged space flight on erythrocyte metabolism and membrane functional condition N92-11617
Efficacy of hyperbaric oxygenation in enhancing flight tolerance N92-11618
Toxicity assessment of combustion products in simulated space cabins N92-11619
Extra-corporeal blood access, sensing, and radiation methods and apparatuses
[NASA-CASE-MSC-21775-1] N92-11627
Classification of posture maintenance data with fuzzy clustering algorithms
[NASA-CR-188949] N92-11662
The hazard of exposure to impulse noise as a function of frequency, volume 2
[AD-A240530] N92-11762
PHYTOPLANKTON
Multi-temporal monitoring of lake water quality N92-11426
Laser active remote sensing of phytoplankton in inland waters N92-11534
Laser-induced spectral signatures in investigations of sea upper layer N92-11537
PIEZOELECTRICITY
Optimal control by wideband frequency. Application to acoustic control by piezoelectric technique
[ONERA-RT-6/3654-RY-006-R] N92-11713
PIGMENTS
Laser-induced blue fluorescence and red chlorophyll fluorescence signatures of differently pigmented leaves N92-11541
PILOT PERFORMANCE
Perceptual style and air-to-air tracking performance
[NASA-TM-102868] N92-11629
The development of Behaviorally Anchored Rating Scales (BARS) for evaluating USAF pilot training performance
[AD-A239969] N92-11630
PILOT TRAINING
The development of Behaviorally Anchored Rating Scales (BARS) for evaluating USAF pilot training performance
[AD-A239969] N92-11630
Lessons learned in the development of the C-130 aircrew training system: A summary of Air Force on-site experience
[AD-A240554] N92-11635
PINHOLE CAMERAS
Pinhole cameras as sensors for atomic oxygen in orbit; application to attitude determination of the LDEF N92-11078
PINHOLES
Illumination, optics, and retroreflectors for efficient landmark tracking N92-11790
PIONEER SPACE PROBES
Developmental flight testing of a half scale unmanned air vehicle
[AD-A240347] N92-11002
PIPE FLOW
Schlieren system for visualizing the flow within a pipe of circular cross-section
[NASA-CASE-LAR-13944-1] N92-11336
PIPELINING (COMPUTERS)
Optimal processor assignment for pipeline computations
[NASA-CR-189047] N92-11672
PIPES (TUBES)
A probabilistic model of intergranular stress corrosion cracking
[DE91-017986] N92-11173
PISTON ENGINES
Piston temperature measurement in a natural gas engine
[PB91-194357] N92-11352
PISTONS
Piston temperature measurement in a natural gas engine
[PB91-194357] N92-11352
In-line hydraulic dashpot
[AD-D014955] N92-11356
PITCH
Scattering of tone bursts from spherical shells: Computations based on Fourier transform method
[AD-A240642] N92-11764
PITCHING MOMENTS
Experimental study of an independently deflected wingtip mounted on a semispan wing
[NASA-TM-102842] N92-10983
PLANAR STRUCTURES
Perceptual grouping and shape from texture
[AD-A240358] N92-11678
PLANE STRAIN
Limit pressure of a circumferentially reinforced SiC/Ti ring
[NASA-CR-187211] N92-11387
PLANE STRESS
Limit pressure of a circumferentially reinforced SiC/Ti ring
[NASA-CR-187211] N92-11387
PLANE WAVES
Electron acceleration by laser fields in a gas
[DE91-018477] N92-11345
Model problem N92-11729
Quantitative ray methods for scattering of sound by spherical shells
[AD-A240255] N92-11761
PLANETARY GEOLOGY
Near-infrared imaging spectroscopy: Learning from planetary geology N92-11438
A bibliography of planetary geology and geophysics principal investigators and their associates, 1990-1991
[NASA-TM-4299] N92-11929
PLANNING
Human factors issues in the design of user interfaces for planning and scheduling N92-11049
Flexible Envelope Request Notation (FERN) N92-11050
Resource representation in COMPASS N92-11060
PLANT DISEASES
The effect of the distribution of chlorotic material on the reflectance of mixed canopies N92-11472
PLANT STRESS
(L)EAF: A remote sensing fluoresensor N92-11546
PLANTS (BOTANY)
Optimum combinations of visible and near-infrared reflectances for estimating the fraction of photosynthetically available radiation absorbed by plants N92-11474
Radiative transfer simulation on computer models of vegetation cover N92-11476
Monte Carlo model for transport equation in a plant canopy and its inversion N92-11481
Assessment of the effect of specular reflectance on the relationships between vegetation indices and biomass N92-11483
PLASMA ACCELERATORS
A compact laser photocathode driven accelerator for the Plasma Wake Field Accelerator Program at UCLA
[AD-A240646] N92-11886
PLASMA ARC WELDING
A generalized method for multiple robotic manipulator programming applied to vertical-up welding
[NASA-TP-3163] N92-11218
Melting efficiency in fusion welding
[DE91-017988] N92-11355
PLASMA COMPOSITION
ITER divertor sputtering erosion: Recent analysis for carbon, beryllium, tungsten, and niobium surfaces
[DE91-017235] N92-11871
The TITAN reversed-field-pinch fusion reactor study, volume 2
[DE92-000140] N92-11896
The TITAN reversed-field-pinch fusion reactor study, volume 1
[DE92-000141] N92-11897
PLASMA CONTROL
Trends in laser-plasma-instability experiments for laser fusion
[DE91-016923] N92-11344
On radial electric field structure in CHS torsatron/heliotron
[NIFS-94] N92-11796
Influence of fast ion loss on radial electric field in Wendelstein 7-A stellarator
[NIFS-95] N92-11797
Proceedings of the First International Toki Conference on Plasma Physics and Controlled Nuclear Fusion: Next Generation Experiments in Helical Systems
[NIFS-PROC-3] N92-11799
Present status of the Large Helical Device Project N92-11800
Status of the Wendelstein VII-X Project N92-11801
Overview of the ATF-II studies N92-11802
Review of the TJ-II Flexible Heliac Project N92-11803
The ANU Heliac Program N92-11804
The 3-D equilibria of helical systems: Magnetic islands and their control N92-11808
Recent experiments in JT-60 N92-11812
Confinement improvement by edge control N92-11817
Effects of perturbing helical fields on confinement of Heliotron DR plasma N92-11818
Overview of recent results from the Advanced Toroidal Facility N92-11819
Status of the WVII-AS Program N92-11820
Status of the Torsatron/Stellarator Program N92-11821
Review of Heliotron E experiment N92-11822
Review of CHS experiment N92-11823
Experimental studies of a helical axis stellarator (TU-Heliac) N92-11824
Pressure and potential measurements in IMS during electron cyclotron heating N92-11826
Numerical and experimental studies of simulated toroidicity effects in a linear high-beta heliac N92-11827
Theory of electron cyclotron heating in the flexible heliac TJ-II N92-11828
Dissipative trapped electron modes in l = 2 torsatrons N92-11830
Low-n stability calculations for three dimensional stellarator configurations N92-11831
Destruction of magnetic surfaces in helical torus N92-11832
Ripple diffusion and bootstrap current in LHD N92-11833
Numerical analysis of temporal development of RF-heated plasma N92-11834
Island studies for Helias Configurations N92-11835
On strong RF plasma turbulence N92-11836
Structural design of large helical device N92-11837
Research and development of forced flow superconducting coils for large helical device N92-11838
Behavior of vacuum vessel eddy current in large helical device N92-11840
Optimization of design parameters for large helical device N92-11843
Equilibrium, stability, and transport in L = 1 compact helical axis configuration N92-11848
Electron temperature measurements on ATF using electron cyclotron emission N92-11849
Confinement studies of Heliotron E plasmas in magnetic surface variation experiments N92-11850
Impurity behavior in Heliotron E N92-11852

Edge plasma study in Heliotron E N92-11853
Study of resistive interchange mode in Heliotron E N92-11855
Effect of magnetic axis shift on CHS plasma characteristics N92-11858
Power deposition during ECH in CHS N92-11862
A possible modification of the FT Tokamak into a compact high field stellarator with separatrices N92-11863
Overview of engineering design of Wendelstein VII-X N92-11868
Power-law energy spectrum and orbital stochasticity [DE91-017387] N92-11872
Coaxial slow source [DE91-016947] N92-11875
Particle trajectories through MIRRORTRON configurations [DE91-017084] N92-11876
Effects of electric field on particle drift orbits in a l = 2 torsatron [NIFS-31] N92-11878
Nonlinear behavior of multiple-helicity resistive interchange modes near marginally stable states [NIFS-89] N92-11883
Fluid description of ponderomotive force compatible with the kinetic one in a warm plasma [NIFS-100] N92-11884
Current profile control for ITER with RF current drive [DE91-018597] N92-11888
Application of modern mathematical concepts to plasma confinement [DE92-000053] N92-11893

PLASMA CURRENTS
Driven currents in neutral beam heated plasma N92-11861
Current profile control for ITER with RF current drive [DE91-018597] N92-11888

PLASMA CYLINDERS
Numerical analysis of temporal development of RF-heated plasma N92-11834

PLASMA DENSITY
Detached plasma and density limit of Tokamaks N92-11816
Particle trajectories through MIRRORTRON configurations [DE91-017084] N92-11876
ELMy-H mode as limit cycle and chaotic oscillations in tokamak plasmas [NIFS-87] N92-11882
A compact laser photocathode driven accelerator for the Plasma Wake Field Accelerator Program at UCLA [AD-A240646] N92-11886

PLASMA DIAGNOSTICS
Trends in laser-plasma-instability experiments for laser fusion [DE91-016923] N92-11344
Status of the WVII-AS Program N92-11820
Review of Heliotron E experiment N92-11822
LHCD experiments on tokamak CASTOR [IPPCZ-304] N92-11881
ECH experiments on ATF [DE91-018845] N92-11889

PLASMA DIFFUSION
Diffusion in the Io plasma torus and its relation to the torus spatial structure N92-11949

PLASMA DIODES
Symposium on Development and Applications of Intense Pulsed Particle Beams [NIFS-PROC-8] N92-11798

PLASMA EQUILIBRIUM
Experimental studies of a helical axis stellarator (TU-Heliac) N92-11824
Low-n stability calculations for three dimensional stellarator configurations N92-11831
Equilibrium, stability, and transport in L = 1 compact helical axis configuration N92-11848
Current profile control for ITER with RF current drive [DE91-018597] N92-11888

PLASMA HEATING
Results of folded waveguide tests on RFTF [DE91-018930] N92-11249
Confinement improvement by edge control N92-11817
Status of the WVII-AS Program N92-11820
Review of CHS experiment N92-11823
Theory of electron cyclotron heating in the flexible heliac TJ-II N92-11828
STORM: A low aspect ratio torsatron for plasma stability N92-11829
On strong RF plasma turbulence N92-11836
ICRF heating program of the large helical device N92-11846
Electron temperature measurements on ATF using electron cyclotron emission N92-11849
Profile measurements in magnetic surface variation experiments/multiple pellet injection experiments N92-11851
Recent diamagnetic measurements of toroidal coil experiments on Heliotron E N92-11854
Transport study of ECH and NBI plasmas in CHS N92-11857
A study of radiation collapse in CHS plasmas N92-11859
Ion temperature and poloidal rotation profiles for NBI heated plasma in CHS N92-11860
Driven currents in neutral beam heated plasma N92-11861
Power deposition during ECH in CHS N92-11862
The 100 GHz half megawatt microwave transmission system development with whispering gallery mode N92-11869
NBI system with negative ion source in large helical device N92-11870

PLASMA JET WIND TUNNELS
Hydrodynamic flow visualization around an oscillating vane. Extension of study to the case of higher incidences and amplitudes and the starting off phase from permanent regime [ONERA-RT-56/1369-AN] N92-11312

PLASMA OSCILLATIONS
ELMy-H mode as limit cycle and chaotic oscillations in tokamak plasmas [NIFS-87] N92-11882

PLASMA PHYSICS
Dispersion and stability of two electromagnetic solvers for triangular meshes [DE91-016607] N92-11227
Proceedings of the First International Toki Conference on Plasma Physics and Controlled Nuclear Fusion: Next Generation Experiments in Helical Systems [NIFS-PROC-3] N92-11799
Present status of the Large Helical Device Project N92-11800
The main fusion activities in Institute of Plasma Physics, Academia Sinica N92-11814
A study of radiation collapse in CHS plasmas N92-11859
Operation scenario and structural design analysis of LHD (Large Helical Device) coils N92-11865
Nonlinear behavior of multiple-helicity resistive interchange modes near marginally stable states [NIFS-89] N92-11883
Fluid description of ponderomotive force compatible with the kinetic one in a warm plasma [NIFS-100] N92-11884
Plasma properties [DE91-018913] N92-11891
The TITAN reversed-field-pinch fusion reactor study, volume 2 [DE92-000140] N92-11896

PLASMA PINCH
Symposium on Development and Applications of Intense Pulsed Particle Beams [NIFS-PROC-8] N92-11798
Ripple diffusion and bootstrap current in LHD N92-11833

PLASMA POTENTIALS
Particle trajectories through MIRRORTRON configurations [DE91-017084] N92-11876

PLASMA PRESSURE
Status of the Torsatron/Stellarator Program N92-11821
Pressure and potential measurements in IMS during electron cyclotron heating N92-11826

PLASMA RADIATION
Laser produced plasma soft x ray generation [DE91-016925] N92-11874

PLASMA SPECTRA
Plasma properties [DE91-018913] N92-11891

PLASMA TURBULENCE
On strong RF plasma turbulence N92-11836

PLASMA WAVES
ISEE/ICE plasma wave data analysis [NASA-CR-189244] N92-11795

PLASMAS (PHYSICS)
Prediction of the pattern performance for the Aeroassist Flight Experiment (AFE) spacecraft [NASA-CR-4409] N92-11065
Radiation forces to electrons in laser fields explained as scattering for ponderomotive momentum transfers [IPPCZ-308] N92-11773
Proceedings of the First International Toki Conference on Plasma Physics and Controlled Nuclear Fusion: Next Generation Experiments in Helical Systems [NIFS-PROC-3] N92-11799
Present status of the Large Helical Device Project N92-11800
Status of the Wendelstein VII-X Project N92-11801
Review of the TJ-II Flexible Heliac Project N92-11803
Design of the compact Auburn torsatron N92-11805
Recent experiments in JT-60 N92-11812
Graphites as plasma facing material of a large fusion device N92-11813
The main fusion activities in Institute of Plasma Physics, Academia Sinica N92-11814
Detached plasma and density limit of Tokamaks N92-11816
Overview of engineering design of Wendelstein VII-X N92-11868
Experiments and applications of soliton physics [NIFS-32] N92-11877
LHCD experiments on tokamak CASTOR [IPPCZ-304] N92-11881
ELMy-H mode as limit cycle and chaotic oscillations in tokamak plasmas [NIFS-87] N92-11882
Nonlinear behavior of multiple-helicity resistive interchange modes near marginally stable states [NIFS-89] N92-11883
Application of modern mathematical concepts to plasma confinement [DE92-000053] N92-11893
LLE review [DE91-018828] N92-11965

PLASTIC PROPERTIES
Polyimides with improved compression moldability [NASA-CASE-LAR-14457-1-CU] N92-11198
Long term synaptic plasticity and learning in neuronal networks [AD-A240366] N92-11613

PLATES (STRUCTURAL MEMBERS)
An examination of the damage tolerance enhancement of carbon/epoxy using an outer lamina of spectra (R) [NASA-TP-3160] N92-11142
Buckling values and optimization of carbon fiber reinforced compression chord plates with rectangular stringers [ILR-MITT-259(1991)] N92-11148
Studies in the form of finite element mass matrices for beams, plates and shells [AERO-TN-9101] N92-11369

PLOTTING
A fast algorithm for plotting antenna and scattering patterns in three dimensions [AD-A240410] N92-11233

PLUTONIUM
Calorimetry measurements in less than 20 minutes [DE91-017318] N92-11330

PNEUMATIC EQUIPMENT
Woven angle ply fabric and apparatus and method for producing such fabrics [NASA-CASE-LAR-14048-1] N92-11220

POINT SPREAD FUNCTIONS
Conoscopic holography. 1: Basic principles and physical basis. 2: Rigorous derivation [TELECOM-PARIS-91-C-001] N92-11337

POINTING CONTROL SYSTEMS
Precision pointing control of the spinning Gravity Probe B spacecraft N92-11068
Sensitivity of Space Station alpha joint robust controller to structural modal parameter variations [NASA-TM-104153] N92-11392

POLAR ORBITS
Overview of the Beta II Two-Stage-To-Orbit vehicle design [NASA-TM-105298] N92-11034

POLARIMETERS
Mapping photopolarimeter spectrometer instrument feasibility study for future planetary flight missions [NASA-CR-189242] N92-11329

POLARIMETRY
Mapping photopolarimeter spectrometer instrument feasibility study for future planetary flight missions [NASA-CR-189242] N92-11329
Modeling of radar backscattering from the sea surface using polarimetric-SAR observations N92-11442
Analysis of radar polarimetric data for the discrimination and monitoring of forest covers N92-11449

POLARIZATION (SPIN ALIGNMENT)
Coupled-channel optical calculation of electron-hydrogen scattering: Elastic scattering from 0.5 to 30 eV [DE91-634157] N92-11780

POLARIZATION (WAVES)
Dual-polarized scatterometer measurements of wind and mechanically generated waves in a very large wind/wave flume, the VIERS-1 project N92-11443

POLARIZATION CHARACTERISTICS
Dual polarization microwave backscatter signatures of bare and vegetated soils N92-11452
Aircraft simulations of the POLDER experiment: First results N92-11471

POLARIZED LIGHT
Observations of the Earth in polarized light from the US Space Shuttle N92-11485
POLARIZED RADIATION
Polarized x ray absorption spectroscopy for the study of superconductors and magnetic materials [DE91-017990] N92-11163
POLARONS
On the maximum entropy principle for Markov chains and processes [ETN-91-90150] N92-11750
The strong coupling limit for polaron models [ETN-91-90163] N92-11757
POLLUTION CONTROL
Low volatile organic compound paints [DE91-017984] N92-11203
Greenhouse gas emissions and the developing countries: Strategic options and the USAID response [PB91-209882] N92-11573
POLLUTION MONITORING
The comparison of airborne imaging spectrometry and geochemical ground survey for the analysis of vegetation anomalies over waste deposits N92-11431
POLOIDAL FLUX
Ion temperature and poloidal rotation profiles for NBI heated plasma in CHS N92-11860
POLYAMIDE RESINS
Polyimides with improved compression moldability [NASA-CASE-LAR-14457-1-CU] N92-11198
Experimental determination of the material parameter of two viscoelastic synthetic materials, using creep tests [ILR-MITT-244(1990)] N92-11385
POLYETHYLENES
An examination of the damage tolerance enhancement of carbon/epoxy using an outer lamina of spectra (R) [NASA-TP-3160] N92-11142
POLYIMIDES
Evaluation of Kapton pyrolysis, arc tracking, and arc propagation on the Space Station Freedom (SSF) solar array Flexible Current Carrier (FCC) [NASA-CR-189056] N92-11139
Polyimides with improved compression moldability [NASA-CASE-LAR-14457-1-CU] N92-11198
Low toxicity high temperature PMR polyimides [NASA-CASE-LAR-14639-1] N92-11199
Diphenylmethane-containing dianhydride and polyimides prepared therefrom [NASA-CASE-LAR-14487-1] N92-11200
A process for preparing an assembly of an article and a polyimide which resists dimensional change, delamination, and debonding when exposed to changes in temperature [NASA-CASE-LAR-14538-1] N92-11201
Improved compression molding technology for continuous fiber reinforced composite laminates. Part 2: AS-4/Polyimidesulfone prepreg system [NASA-TM-104133] N92-11207
POLYMER CHEMISTRY
Polyimides with improved compression moldability [NASA-CASE-LAR-14457-1-CU] N92-11198
Diphenylmethane-containing dianhydride and polyimides prepared therefrom [NASA-CASE-LAR-14487-1] N92-11200
POLYMER MATRIX COMPOSITES
Effects of elevated temperature on the viscoplastic modeling of graphite/polymeric composites [NASA-TM-104160] N92-11149
POLYMERIZATION
New polymer electrolyte hosts and their tetrabutylammonium chloride complexes. Relationships among concentration of polar groups, ESR spin probe response, and ionic conductivity [AD-A240497] N92-11190
Synthesis of novel polysiloxanes bearing polar groups [AD-A240722] N92-11194
Low toxicity high temperature PMR polyimides [NASA-CASE-LAR-14639-1] N92-11199
A process for preparing an assembly of an article and a polyimide which resists dimensional change, delamination, and debonding when exposed to changes in temperature [NASA-CASE-LAR-14538-1] N92-11201
POLYMERS
Measurements of erosion characteristics for metal and polymer surfaces using profilometry N92-11077
Direct imaging of deformation and disorder in extended-chain polymer fibers [AD-A240651] N92-11192
Nonlinear optical properties of semiconducting polymers [AD-A240753] N92-11195
Conductive gage for crack length measurement [NASA-CASE-LAR-14480-1-CU] N92-11374
POLYNOMIALS
Polynomial optimization techniques for activity scheduling. Optimization based prototype scheduler N92-11056
An O(log sup 2 N) parallel algorithm for computing the eigenvalues of a symmetric tridiagonal matrix [NASA-CR-188898] N92-11659
Optimal Chebyshev polynomials on ellipses in the complex plane [NASA-CR-188836] N92-11722
New Bernstein type inequalities for polynomials on ellipses [NASA-CR-186626] N92-11724
Representation of phi meromorphic functions, when phi and a linear differential polynomial in phi have maximum finite zeros [ETN-91-90202] N92-11741
POLYPEPTIDES
The 4th International Workshop on Membrane Biotechnology and Membrane Biomaterials [AD-A240481] N92-11614
POLYPHENYLS
Photothermal deflection spectroscopy of conjugated polymers [DE91-018318] N92-11204
POLYSILOXANES
New polymer electrolyte hosts and their tetrabutylammonium chloride complexes. Relationships among concentration of polar groups, ESR spin probe response, and ionic conductivity [AD-A240497] N92-11190
Synthesis of novel polysiloxanes bearing polar groups [AD-A240722] N92-11194
Synthesis and reactivity of silyl-ketene acetal-modified polysiloxanes preparation of polysiloxanes with high dielectric constraints [AD-A240754] N92-11196
POLYURETHANE RESINS
Experimental determination of the material parameter of two viscoelastic synthetic materials, using creep tests [ILR-MITT-244(1990)] N92-11385
POLYVINYL CHLORIDE
Physical ageing and creep in PVC [NPL-DMM(A)-21] N92-11185
PONDEROMOTIVE FORCES
Radiation forces to electrons in laser fields explained as scattering for ponderomotive momentum transfers [IPPCZ-308] N92-11773
Fluid description of ponderomotive force compatible with the kinetic one in a warm plasma [NIFS-100] N92-11884
PONDS
Observation of DOM composition by synchronous fluorescence spectroscopy N92-11549
POPULATIONS
GLOBEC: Global Ocean Ecosystems Dynamics: A component of the US Global Change Research Program [NASA-TM-105121] N92-11603
POROUS MATERIALS
Mechanical properties of a porous mullite material [NASA-TM-104547] N92-11187
Characterizing He II flow through porous materials using counterflow data [CD-4] N92-11295
POSITION (LOCATION)
Fault localization when testing complex circuits N92-11260
Distributed sensor system decision analysis using team strategies [AD-A240250] N92-11333
Estimation of geopotential differences over intercontinental locations using satellite and terrestrial measurements [NASA-CR-188992] N92-11560
POSITION SENSING
Further developments relating to the NASA Langley Research Center 13-inch magnetic suspension and balance system [NASA-CR-188995] N92-11023
New dimensions in atom probe analysis [DE91-018926] N92-11779
POSITIONING
Navigation and positioning of mobile robots [DE92-704014] N92-10998
POSITIVE IONS
High l state population in O(7+) produced in ion-solid collisions [DE91-018169] N92-11904
Chemical reactivity and electronic structure of silicon microclusters [AD-A240276] N92-11908
POSITRONS
Non-invasive evaluation of the cardiac autonomic nervous system by PET [DE91-018476] N92-11622
Positron lifetimes in solids from first principles calculations [DE92-000088] N92-11781
POSTURE
Classification of posture maintenance data with fuzzy clustering algorithms [NASA-CR-188949] N92-11662
POTENTIAL ENERGY
Quantum 1/f noise in high technology applications including ultrasmall structures and devices [AD-A240152] N92-11907
POWDER (PARTICLES)
Development of high Tc (greater than 110K) Bi, Tl and Y-based materials as superconducting circuit elements [NASA-CR-188999] N92-11902
POWER EFFICIENCY
Leveling of the AMBLER walking machine: A comparison of methods [NASA-CR-189015] N92-11358
POWER FACTOR CONTROLLERS
High efficiency motor rewind study [DE91-017162] N92-11270
PRECESSION
A theory of the earth's precession relative to the invariable plane of the solar system N92-11938
PRECIPITATION (METEOROLOGY)
Hourly and daily precipitation frequencies for the United States [AD-A240746] N92-11599
PRECISION
An investigation to find appropriate measures for evaluating interactive information retrieval N92-11922
PRECONDITIONING
Domain-decomposed preconditionings for transport operators N92-11731
PREDICTION ANALYSIS TECHNIQUES
Development of unsteady aerodynamic analyses for turbomachinery aeroelastic and aeroacoustic applications [NASA-CR-4405] N92-10979
Analysis of open loop higher harmonic control at high airspeeds on a modern four-bladed articulated rotor [NASA-TM-103876] N92-11000
MLITemp: A computer program to predict the thermal effects associated with hypervelocity impact damage to space station MLI [NASA-CR-184245] N92-11079
Mixing effects in aqueous solutions at elevated temperatures [DE91-017695] N92-11168
Mixed convection in two-dimensional laminar air flow with reverse flow regions N92-11293
Theoretical estimation of the viscous damping from liquid transient motion in tanks [NAL-TR-1095] N92-11298
Modeling of the heat transfer in bypass transitional boundary-layer flows [NASA-TP-3170] N92-11299
Studies of aerothermal loads generated in regions of shock/shock interaction in hypersonic flow [NASA-CR-181893] N92-11319
Candidate high spectral resolution derivative indices for the prediction of crop cover N92-11435
Mesoscale prediction and satellite cloud analysis for advanced meteorological processing systems [AD-A240510] N92-11597
Statistical prediction with Kanerva's sparse distributed memory [NASA-CR-187314] N92-11743
PREDICTIONS
Critical appraisal of the McDonnell Douglas closure model for predicting fatigue crack growth [ARL-STRUC-R-444] N92-11376
GLOBEC: Global Ocean Ecosystems Dynamics: A component of the US Global Change Research Program [NASA-TM-105121] N92-11603
PREFORMS
Woven angle ply fabric and apparatus and method for producing such fabrics [NASA-CASE-LAR-14048-1] N92-11220
PREMIXING
Numerical prediction of turbulent flame stability in premixed/prevaporized (HSCT) combustors [NASA-CR-188991] N92-11161
PREPROCESSING
Pulse compression degradation due to open loop adaptive cancellation, part 1 [AD-A240552] N92-11238
On the symbolic manipulation and code generation for elasto-plastic material matrices [NASA-CR-187223] N92-11375
Optimal parallel solution of sparse triangular systems [NASA-CR-188872] N92-11656
PRESSURE EFFECTS
Efficacy of hyperbaric oxygenation in enhancing flight tolerance N92-11618

PRESSURE GRADIENTS
Characterizing He II flow through porous materials using counterflow data
[CD-4] N92-11295
PRESSURE MEASUREMENT
NACA 0015 wing pressure and trailing vortex measurements
[NASA-TP-3151] N92-10981
PRIMITIVE EQUATIONS
A diagnostic study of the velocity structure of a meandering jet using a primitive equation model with dynamic mode initialization
[AD-A240687] N92-11609
One-way nesting for a primitive equation ocean model N92-11734
PRINTED CIRCUITS
Thermal verification testing of commercial printed-circuit boards for spaceflight
[NASA-TM-105261] N92-11221
Advanced Langmuir Probe (LP)
[NASA-CR-180084] N92-11284
PRINTING
High-T sub c fluorine-doped YBa2Cu3O(y) films on ceramic substrates by screen printing
[NASA-TM-105296] N92-11188
PRIORITIES
User modeling techniques for enhanced usability of OPSMODEL operations simulation software
[NASA-TM-4306] N92-11035
PROBABILITY THEORY
A probabilistic model of intergranular stress corrosion cracking
[DE91-017986] N92-11173
The probability of multiple correct packet receptions in a multireceiver frequency-hopped spread-spectrum system
[AD-A240655] N92-11240
Use of theoretical wave height distributions in directional seas
[AD-A240411] N92-11608
Modelling default and likelihood reasoning as probabilistic reasoning
[NASA-CR-188936] N92-11661
Conditional event algebras: Two new characterizations and their relations to Bayesian analysis
[AD-A240378] N92-11738
Numerical methods in Markov chain modeling
[NASA-CR-188908] N92-11744
Tables of square-law signal detection statistics for Hann spectra with 50 percent overlap
[NASA-TM-103830] N92-11745
A re-examination of the relationship between fuzzy set theory and probability theory
[AD-A240243] N92-11746
Assignment of single values to probability intervals, evaluation of conditional events, and applications to combination of evidence
[AD-A240258] N92-11747
The considering of the slowing down effect in the formalism of probability tables. Application to the effective cross section calculation
[DE91-626722] N92-11751
On the evolution of a superconducting cosmic string network
[DE91-630995] N92-11948
PROBES
Circuit probing system
[AD-D014966] N92-11277
PROBLEM SOLVING
Automating the conflict resolution process N92-11061
Reminding-based learning
[AD-A240370] N92-11634
Stable upwind schemes for hyperbolic conservation laws for with source terms N92-11716
Discussion summary: Fictitious domain methods N92-11730
PROCESS CONTROL (INDUSTRY)
Polyimides with improved compression moldability
[NASA-CASE-LAR-14457-1-CU] N92-11198
Diphenylmethane-containing dianhydride and polyimides prepared therefrom
[NASA-CASE-LAR-14487-1] N92-11200
Process for controlling the thickness of an antireflection coating, and embodying apparatus
[DE91-017634] N92-11793
PROCUREMENT MANAGEMENT
Proceedings of the Acquisition Research Symposium: Imagnination, Innovation, and Implementation, 1991, volume 1
[AD-A240260] N92-11676
Proceedings of the Acquisition Research Symposium: Acquisition for the Future, Imagination, Innovation, and Implementation, 1991, volume 2
[AD-A240261] N92-11677
PRODUCT DEVELOPMENT
Fundamental aspects of the refining process N92-11151
A new hypothesis for the mechanics of refining N92-11152
Development of a fundamentally new refining method. Part 1: Basic design considerations N92-11153
PRODUCTION ENGINEERING
Proceedings of the Acquisition Research Symposium: Imagnination, Innovation, and Implementation, 1991, volume 1
[AD-A240260] N92-11676
Modelling product structures by generic bills-of-material
[ETN-91-90146] N92-11919
PRODUCTION MANAGEMENT
Modelling product structures by generic bills-of-material
[ETN-91-90146] N92-11919
PRODUCTIVITY
Space engineering
[NASA-CR-187820] N92-11215
PROGRAM VERIFICATION (COMPUTERS)
Methodology investigation. Phase 2: Software maturity model validation
[AD-A231439] N92-11651
Workshops on Efficient Use of Scientific Computing
[AD-A240175] N92-11674
PROGRAMMING LANGUAGES
Flexible Envelope Request Notation (FERN) N92-11050
A planning language for activity scheduling N92-11063
Test and diagnosis of programmable integrated circuits
[ETN-91-99483] N92-11253
VHDL simulation of the implementation of a costfunction circuit
[AD-A240430] N92-11278
Experience with Acore: Implementing GHC with actors
[AD-A231409] N92-11649
Continuation of research into language concepts for the mission support environment
[NASA-CR-187818] N92-11652
Tester Independent Support Software System (TISSS)
[AD-A240668] N92-11681
PROJECT MANAGEMENT
Nuclear Thermal Propulsion: A Joint NASA/DOE/DOD Workshop
[NASA-CP-10079] N92-11088
Upgraded NERVA systems: Enabler nuclear system N92-11093
Low Pressure Nuclear Thermal Rocket (LPNTR) concept N92-11094
PROJECT PLANNING
Study of alternatives: Dayton's Aviation heritage, Ohio
[PB91-202275] N92-10972
Program plan: National aging aircraft research program
[DOT/FAA/CT-88/32-1] N92-10992
Resource allocation planning helper (RALPH) N92-11047
Nuclear Thermal Propulsion: A Joint NASA/DOE/DOD Workshop
[NASA-CP-10079] N92-11088
Nuclear thermal propulsion workshop overview N92-11090
Nuclear thermal rocket workshop reference system Rover/NERVA N92-11091
Upgraded NERVA systems: Enabler nuclear system N92-11093
JANNAF Liquid Rocket Combustion Instability Panel research recommendations N92-11124
ART/Ada design project, phase 1: Project plan
[NASA-CR-187313] N92-11663
An IFE development strategy
[DE91-016918] N92-11873
PROJECT SETI
Tables of square-law signal detection statistics for Hann spectra with 50 percent overlap
[NASA-TM-103830] N92-11745
PROPAGATION VELOCITY
Numerical simulations of detonation transmission
[AD-A240560] N92-11304
PROPANE
Conversion of ethane and of propane to higher olefin hydrocarbons
[DE91-016896] N92-11160
PROPELLANT COMBUSTION
The 27th JANNAF Combustion Subcommittee Meeting, Volume 3
[CPIA-PUBL-557-VOL-3] N92-11117
Erosive augmentation of solid propellant burning rate: Motor size scaling effect N92-11125
KA-111, Phase C, M-1 propellant tests: Deflagration in partial confinement
[AD-A240185] N92-11211
PROPELLANT PROPERTIES
Properties of aircraft fuels and related materials
[AD-A240650] N92-11213
PROPELLANT STORAGE
KA-111, Phase C, M-1 propellant tests: Deflagration in partial confinement
[AD-A240185] N92-11211
PROPELLANT TANKS
Theoretical estimation of the viscous damping from liquid transient motion in tanks
[NAL-TR-1095] N92-11298
PROPELLANT TESTS
KA-111, Phase C, M-1 propellant tests: Deflagration in partial confinement
[AD-A240185] N92-11211
PROPELLANT TRANSFER
Improved thermodynamic modeling of the no-vent fill process and correlation with experimental data
[NASA-TM-104492] N92-11129
PROPELLANTS
Nuclear rocket using indigenous Martian fuel NIMF N92-11098
Theoretical estimation of the viscous damping from liquid transient motion in tanks
[NAL-TR-1095] N92-11298
PROPELLER NOISE
Annoyance caused by advanced turboprop aircraft flyover noise: Comparison of different propeller configurations
[NASA-TP-3104] N92-11758
PROPELLERS
Annoyance caused by advanced turboprop aircraft flyover noise: Comparison of different propeller configurations
[NASA-TP-3104] N92-11758
PROPORTIONAL CONTROL
Generation of smooth trajectories without planning
[NASA-CR-189013] N92-11712
PROPULSION
Dumbo: A pachydermal rocket motor N92-11100
PROPULSION SYSTEM CONFIGURATIONS
Static internal performance of ventral and rear nozzle concepts for short-takeoff and vertical-landing aircraft
[NASA-TP-3103] N92-10975
Nuclear Thermal Propulsion: A Joint NASA/DOE/DOD Workshop
[NASA-CP-10079] N92-11088
Nuclear thermal propulsion program overview N92-11089
Nuclear thermal rocket workshop reference system Rover/NERVA N92-11091
NERVA upgrade: Non-nuclear components N92-11092
Low Pressure Nuclear Thermal Rocket (LPNTR) concept N92-11094
Particle bed reactor nuclear rocket concept N92-11095
A cermet fuel reactor for nuclear thermal propulsion N92-11096
Hybrid propulsion systems for space exploration missions N92-11097
Plans for the development of cryogenic engines for space exploration
[NASA-TM-105250] N92-11135
An overview of tested and analyzed NTP concepts
[NASA-TM-105252] N92-11137
Fusion energy for space missions in the 21st Century
[NASA-TM-4298] N92-11783
PROPULSION SYSTEM PERFORMANCE
Real-time fault diagnosis for propulsion systems
[NASA-TM-105303] N92-11017
Nuclear Thermal Propulsion: A Joint NASA/DOE/DOD Workshop
[NASA-CP-10079] N92-11088
Nuclear thermal propulsion program overview N92-11089
Nuclear thermal rocket workshop reference system Rover/NERVA N92-11091
NERVA upgrade: Non-nuclear components N92-11092
Low Pressure Nuclear Thermal Rocket (LPNTR) concept N92-11094
Particle bed reactor nuclear rocket concept N92-11095
A cermet fuel reactor for nuclear thermal propulsion N92-11096
CFD code survey for thrust chamber application N92-11119
Plans for the development of cryogenic engines for space exploration
[NASA-TM-105250] N92-11135
An overview of tested and analyzed NTP concepts
[NASA-TM-105252] N92-11137

Properties of aircraft fuels and related materials
[AD-A240650] N92-11213
Engine dynamic analysis with general nonlinear finite element codes
[NASA-CR-187222] N92-11379
Fusion energy for space missions in the 21st Century
[NASA-TM-4298] N92-11783

PROTEINS
The 4th International Workshop on Membrane Biotechnology and Membrane Biomaterials
[AD-A240481] N92-11614

PROTOCOL (COMPUTERS)
The ARPANET after twenty years
[NASA-CR-188853] N92-11695
BCD/CPS: An event-level GEANT3 parallelization via CPS
[DE91-017238] N92-11703

PROTOTYPES
Polynomial optimization techniques for activity scheduling. Optimization based prototype scheduler N92-11056
Development of a ninety string solar array simulator
[NASA-TM-105278] N92-11086
Continuation of research into language concepts for the mission support environment
[NASA-CR-187818] N92-11652

PROVING
A method and tools for microprocessor validation: High safety function applications N92-11263

PSYCHOACOUSTICS
Annoyance caused by advanced turboprop aircraft flyover noise: Comparison of different propeller configurations
[NASA-TP-3104] N92-11758

PSYCHOLOGICAL TESTS
Serial averaging in the construction and validation of performance tests
[AD-A240313] N92-11632

PSYCHOMETRICS
Serial averaging in the construction and validation of performance tests
[AD-A240313] N92-11632

PSYCHOPHYSIOLOGY
JPRS report: Science and technology. USSR: Life sciences
[JPRS-ULS-91-015] N92-11610

PUBLIC HEALTH
JPRS report: Science and technology. USSR: Life sciences
[JPRS-ULS-91-015] N92-11610
JPRS report: Science and technology. USSR: Life sciences
[JPRS-ULS-91-012] N92-11611
JPRS report: Science and technology. USSR: Life sciences
[JPRS-ULS-91-017] N92-11616
Integrated Risk Information System
[DE91-018503] N92-11924

PULSARS
Neutron star magnetic fields and implications for pulsars and gamma ray bursts N92-11960

PULSE COMPRESSION
Pulse compression degradation due to open loop adaptive cancellation, part 1
[AD-A240552] N92-11238
Pulse compression degradation due to open loop adaptive cancellation, part 3
[AD-A240553] N92-11239

PULSE DURATION
Acoustic transponder receiver circuit
[AD-D014965] N92-11760

PULSE RADAR
Impulse transmitter and quantum detection radar system
[AD-D014958] N92-11229

PULSED RADIATION
Symposium on Development and Applications of Intense Pulsed Particle Beams
[NIFS-PROC-8] N92-11798

PUMP IMPELLERS
Hydrodynamic design of generic pump components
[NASA-CR-184252] N92-11361

PYROLYSIS
Evaluation of Kapton pyrolysis, arc tracking, and arc propagation on the Space Station Freedom (SSF) solar array Flexible Current Carrier (FCC)
[NASA-CR-189056] N92-11139
Time-resolved analytical pyrolysis mass spectrometry of biomaterials
[AD-A240624] N92-11167

Q

QUALITY CONTROL
Proceedings of the Acquisition Research Symposium: Imagination, Innovation, and Implementation, 1991, volume 1
[AD-A240260] N92-11676
Proceedings of the Acquisition Research Symposium: Acquisition for the Future, Imagination, Innovation, and Implementation, 1991, volume 2
[AD-A240261] N92-11677

QUANTUM CHROMODYNAMICS
Nuclear transparency and double beta decay of molybdenum 100
[DE91-016963] N92-11172
On the polarisation of tensor mesons in psi radiative decays and possible implications for the gluonic content of the theta(1720)
[RAL-90-091] N92-11768
Meson-exchange calculation of the d(gamma,p)n in the GeV energy region
[DE91-017994] N92-11785
Cosmological constraints on pseudo-Nambu-Goldstone bosons
[NASA-CR-189010] N92-11943

QUANTUM COUNTERS
Impulse transmitter and quantum detection radar system
[AD-D014958] N92-11229

QUANTUM ELECTRONICS
Joint services electronics program research in electronics
[AD-A240155] N92-11274

QUANTUM THEORY
Global analysis of fermion mixing with exotics
[NASA-CR-189006] N92-11774
Comparative study of final state interaction contributions to the dynamic response of quantum fluids
[DE91-631020] N92-11892
Quantum 1/f noise in high technology applications including ultrasmall structures and devices
[AD-A240152] N92-11907

QUARKS
Global analysis of fermion mixing with exotics
[NASA-CR-189006] N92-11774
E sub 6 leptoquarks and the solar neutrino problem
[NASA-CR-189005] N92-11956

QUASARS
Infrared to millimetre observations of active galaxies N92-11932

R

RADAR
Specification of difficult to test radar performance
[AD-A240398] N92-11232

RADAR ABSORBERS
The design of broadband radar absorbing surfaces
[AD-A240521] N92-11235

RADAR ANTENNAS
Programmable beam transform and beam steering control system for a phased array radar antenna
[AD-D014970] N92-11230

RADAR BEAMS
Active radar stealth device
[AD-D014980] N92-11246

RADAR CROSS SECTIONS
Active radar stealth device
[AD-D014980] N92-11246
Modeling of radar backscattering from the sea surface using polarimetric-SAR observations N92-11442
Dual polarization microwave backscatter signatures of bare and vegetated soils N92-11452

RADAR DATA
Three dimensional migration and forward modelling of ground penetrating radar data
[AD-A240505] N92-11234
Ground penetrating radar data acquisition system
[AD-A240765] N92-11244
Modeling of radar backscattering from the sea surface using polarimetric-SAR observations N92-11442
Multifrequency radar measurements of potato, beet, and wheat during the AGRISCATT-88 campaign in the Netherlands N92-11444
Analysis of radar polarimetric data for the discrimination and monitoring of forest covers N92-11449
Airborne precursor missions in support of SIR-C/X-SAR N92-11450
Land cover classification by multipolarized SAR imagery N92-11457

RADAR DETECTION
Impulse transmitter and quantum detection radar system
[AD-D014958] N92-11229
Three dimensional migration and forward modelling of ground penetrating radar data
[AD-A240505] N92-11234

RADAR ECHOES
Impulse transmitter and quantum detection radar system
[AD-D014958] N92-11229
The linking of crop growth models and multi-sensor remote sensing data N92-11512

RADAR GEOLOGY
Integration of visible-through microwave-range multispectral image data sets for geologic mapping N92-11491

RADAR IMAGERY
Multifrequency radar measurements of potato, beet, and wheat during the AGRISCATT-88 campaign in the Netherlands N92-11444
Radar image simulation to study the visual aptitude of observing slope and roughness effects N92-11446
Analysis of radar polarimetric data for the discrimination and monitoring of forest covers N92-11449
Airborne precursor missions in support of SIR-C/X-SAR N92-11450
Nonlinear theory of synthetic aperture radar sea wave imaging N92-11451
Dual polarization microwave backscatter signatures of bare and vegetated soils N92-11452
Humidity measurement of naked ground by radar in conditions of excessive water N92-11453
Airborne SAR HAREM campaign: Results, targets features, ERS1 simulations, and operational satellite exploitation N92-11455
Evaluation of vegetation cover characteristics using an airborne microwave scatterometer N92-11456
Passive microwave remote sensing of soil moisture: Results from HAPEX, FIFE, and MONSOON 90 N92-11458
Synergy of high resolution spatial microwave imagery and geomorphological optics N92-11496
The linking of crop growth models and multi-sensor remote sensing data N92-11512

RADAR MEASUREMENT
Aircraft lidar sensitivity study for measuring water vapor
[AD-A240549] N92-11237

RADAR SCATTERING
Discrete ARMA model for natural resonances in electromagnetic and acoustic scattering
[AD-A240656] N92-11241

RADAR SIGNATURES
Discrete ARMA model for natural resonances in electromagnetic and acoustic scattering
[AD-A240656] N92-11241
Analysis of radar polarimetric data for the discrimination and monitoring of forest covers N92-11449

RADAR TARGETS
Discrete ARMA model for natural resonances in electromagnetic and acoustic scattering
[AD-A240656] N92-11241
Active radar stealth device
[AD-D014980] N92-11246

RADAR TRACKING
Space station tracking requirements feasibility study, volume 2
[NASA-CR-185641-VOL-2] N92-11084
Space station tracking requirements feasibility study, volume 1
[NASA-CR-185641-VOL-1] N92-11085
An examination of the factors affecting the use of infra-red search and track systems in the air-to-air role
[ETN-91-99987] N92-11222
Impulse transmitter and quantum detection radar system
[AD-D014958] N92-11229

RADAR TRANSMISSION
Dual-polarized scatterometer measurements of wind and mechanically generated waves in a very large wind/wave flume, the VIERS-1 project N92-11443
Generalized formulation for semi-empirical radar models representing crop backscattering N92-11447

RADAR TRANSMITTERS
Impulse transmitter and quantum detection radar system
[AD-D014958] N92-11229

RADIAL DISTRIBUTION
On radial electric field structure in CHS torsatron/heliotron
[NIFS-94] N92-11796
Influence of fast ion loss on radial electric field in Wendelstein 7-A stellarator
[NIFS-95] N92-11797

RADIAL FLOW
Radial inflow turbine study
[AD-A240169] N92-11015

RADIAL VELOCITY
Evaluation of high Reynolds number flow in a 180 degree turn-around-duct
[NASA-CR-184243] N92-11318
RADIANCE
Determination of the in-flight spectral and radiometric characteristics of the Airborne Visible/Infrared Imaging Spectrometer (AVIRIS) N92-11397
SPOT calibration on the test site La Crau (France) N92-11409
Monitoring volcanoes using short wavelength infrared images N92-11498
RADIANT FLUX DENSITY
Multiangular approach to solution of atmosphere optics reverse problems N92-11478
RADIATION ABSORPTION
Optimum combinations of visible and near-infrared reflectances for estimating the fraction of photosynthetically available radiation absorbed by plants N92-11474
Extra-corporeal blood access, sensing, and radiation methods and apparatuses
[NASA-CASE-MSC-21775-1] N92-11627
RADIATION BELTS
Particle acceleration in space and radiation belt depletion
[AD-A240311] N92-11775
RADIATION CHEMISTRY
Radiation induced growth of micro crystallites
[DE91-016516] N92-11900
RADIATION COUNTERS
CYGNUS collaboration contributions to the twenty-second ICRC
[DE92-000258] N92-11961
RADIATION DETECTORS
Nonscanning climate sensor study
[NASA-CR-183506] N92-11589
RADIATION DISTRIBUTION
Extra-corporeal blood access, sensing, and radiation methods and apparatuses
[NASA-CASE-MSC-21775-1] N92-11627
Wavefields near transverse cusp caustics produced by reflecting ultrasonic transients and tone bursts from curved surfaces
[AD-A240641] N92-11763
RADIATION DOSAGE
Pellet bed reactor for nuclear propelled vehicles: Part 2: Missions and vehicle integration trades N92-11102
Development of recommendations in the area of ionizing radiations
[DE91-018527] N92-11623
Extra-corporeal blood access, sensing, and radiation methods and apparatuses
[NASA-CASE-MSC-21775-1] N92-11627
Intercomparison of the medium energy primary standards for x ray exposure of NPL and ENEA, Italy
[NPL-RSA(EXT)-18] N92-11766
Intercomparison of the low energy primary standards for x ray exposure of NPL and ENEA, Italy
[NPL-RSA(EXT)-19] N92-11767
RADIATION EFFECTS
The interactions of atmospheric cosmogenic radionuclides with spacecraft surfaces N92-11075
Effects on LDEF exposed copper film and bulk N92-11076
Radiation belt dynamic and quasi-static modeling based on CRRES data
[AD-A240392] N92-11585
Development of recommendations in the area of ionizing radiations
[DE91-018527] N92-11623
Extra-corporeal blood access, sensing, and radiation methods and apparatuses
[NASA-CASE-MSC-21775-1] N92-11627
Cellular repair/misrepair track model
[NASA-TP-3124] N92-11685
Collisional energy transfer from excited nitrogen dioxide
[DE91-016989] N92-11772
Radiation induced growth of micro crystallites
[DE91-016516] N92-11900
RADIATION MEASUREMENT
Physical Measurements and Signatures in Remote Sensing, volume 1
[ESA-SP-319-VOL-1] N92-11394
Comparison of in situ, aircraft- and satellite-derived surface reflectances in Flevoland (Netherlands) N92-11404
SPOT calibration on the test site La Crau (France) N92-11409
Aircraft simulations of the POLDER experiment: First results N92-11471
Physical Measurements and Signatures in Remote Sensing, volume 2
[ESA-SP-319-VOL-2] N92-11488
RADIATION PROTECTION
Nuclear safety N92-11114
Communications interface and system for radiation recovery of a microprocessor portion thereof
[AD-D014977] N92-11245
Development of recommendations in the area of ionizing radiations
[DE91-018527] N92-11623
RADIATION SHIELDING
Shielding requirements for particle bed propulsion systems
[AD-A240780] N92-11787
RADIATION SOURCES
CYGNUS collaboration contributions to the twenty-second ICRC
[DE92-000258] N92-11961
RADIATIVE LIFETIME
On the polarisation of tensor mesons in psi radiative decays and possible implications for the gluonic content of the theta(1720)
[RAL-90-091] N92-11768
Collisional energy transfer from excited nitrogen dioxide
[DE91-016989] N92-11772
RADIATIVE TRANSFER
Comparison of atmospheric correction procedures for visible and near-IR satellite sensor output N92-11395
Modeling of visible and UV radiative transfer in the ocean-atmosphere system concepts, models, and programs N92-11396
Determination of the in-flight spectral and radiometric characteristics of the Airborne Visible/Infrared Imaging Spectrometer (AVIRIS) N92-11397
Atmospheric correction of satellite borne imagery investigated by means of a sensitivity analysis of the entire remote sensing process N92-11400
On the use of passive microwaves at 37 GHz N92-11461
A three dimensional radiative transfer method for optical remote sensing of vegetated land surfaces N92-11466
Bi-directional reflectance of finite and infinite clouds N92-11470
Radiative transfer simulation on computer models of vegetation cover N92-11476
Validation of a ground spectral and directional reflectance model N92-11479
Spectral reflectance of thin snow N92-11482
Specular and diffuse components of plant canopy reflectance at the wavelengths of 550 and 630 nm N92-11484
Estimation of the primary production in Sahelian region from radiometric data N92-11504
Using the radiative surface temperature in energy budget studies over plant canopies N92-11506
RADIATORS
Lunar dust transport and potential interactions with power system components
[NASA-CR-4404] N92-11951
RADICALS
A simulation study of interactions of Space-Shuttle generated electron beams with ambient plasma and neutral gas
[NASA-CR-189025] N92-11898
RADII
Detached plasma and density limit of Tokamaks N92-11816
RADIO ASTRONOMY
Infrared to millimetre observations of active galaxies N92-11932
RADIO BURSTS
Conditional climatology of Ap: The relationship between various solar events (surges, prominences, filaments, radio bursts, x ray episodes) and geomagnetic storms
[AD-A240457] N92-11958
RADIO FREQUENCIES
An RF interference mitigation methodology with potential applications in scheduling N92-11044
Results of folded waveguide tests on RFTF
[DE91-018930] N92-11249
Compact optical RF spectrum analyzer
[AD-D014962] N92-11792
Numerical analysis of temporal development of RF-heated plasma N92-11834
On strong RF plasma turbulence N92-11836
Fokker-Planck equation in the presence of anomalous diffusion
[NIFS-29] N92-11879
Current profile control for ITER with RF current drive
[DE91-018597] N92-11888
RADIO FREQUENCY HEATING
ECH system in the large helical device N92-11845
ICRF heating program of the large helical device N92-11846
RADIO FREQUENCY INTERFERENCE
An RF interference mitigation methodology with potential applications in scheduling N92-11044
RADIO RECEIVERS
Physics of ultrasmall superconducting circuits
[AD-A240156] N92-11275
RADIO SPECTRA
Spectral observations of solar radio bursts in the range of 2.0-4.5 GHz
[CAS-PUBL-76] N92-11953
Spectral observations of solar radio bursts at 2.0-4.5 GHz
[CAS-PUBL-77] N92-11954
RADIOACTIVE DECAY
Nuclear transparency and double beta decay of molybdenum 100
[DE91-016963] N92-11172
On the polarisation of tensor mesons in psi radiative decays and possible implications for the gluonic content of the theta(1720)
[RAL-90-091] N92-11768
Re-ionization and decaying dark matter
[NASA-CR-189009] N92-11944
RADIOACTIVE ISOTOPES
The interactions of atmospheric cosmogenic radionuclides with spacecraft surfaces N92-11075
RADIOACTIVE WASTES
Disposal methods N92-11116
RADIOBIOLOGY
Development of recommendations in the area of ionizing radiations
[DE91-018527] N92-11623
Extra-corporeal blood access, sensing, and radiation methods and apparatuses
[NASA-CASE-MSC-21775-1] N92-11627
RADIOGRAPHY
A new radiographic corrosion inspection capability
[AD-A231476] N92-11363
RADIOLYSIS
Radiation induced growth of micro crystallites
[DE91-016516] N92-11900
RADIOMETERS
Validation of a ground spectral and directional reflectance model N92-11479
RADIOMETRIC CORRECTION
Radiometric and atmospheric correction procedures for AVHRR preprocessing in the solar reflective channels N92-11414
Preliminary results of a spectro-imagery experiment (GER) over the Adriatic coastline of the Venice lagoon N92-11440
Analysis of the surface state of two sub-polar glaciers using SPOT data and a numerical terrain model N92-11523
Evaluation of ground cover in agricultural environment by in situ measurements and multitemporal images for modeling hydric erosion N92-11528
RADIOMETRIC RESOLUTION
Synergy of high resolution spatial microwave imagery and geomorphological optics N92-11496
Modeling temporal evolution of the radiometric response measured by wideband sensors over temperate agricultural regions N92-11518
Evaluation of ground cover in agricultural environment by in situ measurements and multitemporal images for modeling hydric erosion N92-11528
RADON
Development of recommendations in the area of ionizing radiations
[DE91-018527] N92-11623
RAIN
March AFB forecasting rules of thumb evaluation
[AD-A240458] N92-11595
RAMAN SPECTRA
Laser Raman diagnostics in subsonic and supersonic turbulent jet diffusion flames N92-11159
Progress in Photon Scanning-Tunneling Microscopy (PSTM)
[DE91-018174] N92-11905
Spectroscopic studies of layered and bulk semiconductor materials
[ETN-91-90145] N92-11914
RAMAN SPECTROSCOPY
Spectroscopic studies of layered and bulk semiconductor materials
[ETN-91-90145] N92-11914
RANDOM ACCESS
An a priori approach to the evaluation of signature analysis efficiency N92-11268
RANDOM PROCESSES
First-passage problems: A probabilistic dynamic analysis for degraded structures
[NASA-TM-103755] N92-11373
The modeling of complex continua: Fundamental obstacles and grand challenges
[DE91-018806] N92-11686

RAPID QUENCHING (METALLURGY)
Non-equilibrium microstructures produced during electron-beam and laser-beam surface modification of metallic alloys
[DE91-018466] N92-11174
RARE EARTH ALLOYS
Characterization of rare earth permanent magnets
[DE91-017010] N92-11754
RAREFIED GAS DYNAMICS
A fast sorting algorithm for a hypersonic rarefied flow particle simulation on the connection machine
[NASA-CR-188903] N92-10977
Drag coefficients with applications to satellite orbits N92-11069
Reciprocity theory of gas surface interactions
[IC-AERO-89-04] N92-11289
RATINGS
The development of Behaviorally Anchored Rating Scales (BARS) for evaluating USAF pilot training performance
[AD-A239969] N92-11630
RAY TRACING
Appearance simulator for computer vision research
[AD-A240506] N92-11679
RAYLEIGH SCATTERING
Euromech 260: Advanced non-intrusive experimental techniques in fluid and plasma flows
[ETN-91-90104] N92-11313
In flight calibration of large field of view sensors at short wavelength using the Rayleigh scattering N92-11416
REACTING FLOW
Navier-Stokes entropy controlled combustion instability analysis for liquid propellants N92-11122
REACTION KINETICS
Conversion of ethane and of propane to higher olefin hydrocarbons
[DE91-016896] N92-11160
Study of silanization of silica and fiberglass using ESR spectroscopy and spin labelling
[AD-A240767] N92-11197
Spectral fitting, shock layer modeling, and production of nitrogen oxides and excited nitrogen
[NASA-CR-185664] N92-11769
A study on the development of high T(sub c) superconducting materials
[DE91-629755] N92-11917
REACTIVITY
Synthesis and reactivity of silyl-ketene acetal-modified polysiloxanes preparation of polysiloxanes with high dielectric constraints
[AD-A240754] N92-11196
Chemical reactivity and electronic structure of silicon microclusters
[AD-A240276] N92-11908
Structure of the Si45 cluster
[AD-A240278] N92-11909
REACTOR CORES
The TITAN reversed-field-pinch fusion reactor study, volume 4
[DE92-000138] N92-11895
The TITAN reversed-field-pinch fusion reactor study, volume 1
[DE92-000141] N92-11897
REACTOR DESIGN
Nuclear Thermal Propulsion: A Joint NASA/DOE/DOD Workshop
[NASA-CP-10079] N92-11088
NERVA upgrade: Non-nuclear components N92-11092
Particle bed reactor nuclear rocket concept N92-11095
The ANU Heliac Program N92-11804
Structural design of large helical device N92-11837
Pool-cooled superconducting magnet design of large helical device N92-11839
Fundamental design on LHD with bath cooling method N92-11841
Optimization of design parameters for large helical device N92-11843
Effect of multi-layer operation of helical coil in large helical device N92-11844
ECH system in the large helical device N92-11845
ICRF heating program of the large helical device N92-11846
Overview of engineering design of Wendelstein VII-X N92-11868
The TITAN reversed-field-pinch fusion reactor study, volume 4
[DE92-000138] N92-11895
REACTOR MATERIALS
Shielding requirements for particle bed propulsion systems
[AD-A240780] N92-11787
REACTOR SAFETY
Nuclear safety N92-11114
REACTOR TECHNOLOGY
Nuclear Thermal Propulsion: A Joint NASA/DOE/DOD Workshop
[NASA-CP-10079] N92-11088
Pellet bed reactor for nuclear propelled vehicles: Part 1: Reactor technology N92-11101
Nuclear fuels status N92-11113
An IFE development strategy
[DE91-016918] N92-11873
READERS
Learning to read aloud: A neural network approach using sparse distributed memory
[NASA-CR-188846] N92-11711
READING
Pictures and anaphora
[AD-A240153] N92-11631
REAL TIME OPERATION
Real-time fault diagnosis for propulsion systems
[NASA-TM-105303] N92-11017
Attitude identification for SCOLE using two infrared cameras
[NASA-CR-4397] N92-11338
Real-time earthquake monitoring: Early warning and rapid response
[NASA-CR-186701] N92-11582
Database management system interface standard for Navy next generation computing resources
[AD-A240432] N92-11925
Issues in real-time data management
[AD-A240712] N92-11926
RECEIVERS
The probability of multiple correct packet receptions in a multireceiver frequency-hopped spread-spectrum system
[AD-A240655] N92-11240
Acoustic transponder receiver circuit
[AD-D014965] N92-11760
RECIPROCITY THEOREM
Reciprocity theory of gas surface interactions
[IC-AERO-89-04] N92-11289
RECOMBINATION REACTIONS
The recombination behavior of a laser induced electron hole plasma in pin diodes and silicon base material
[ETN-91-90153] N92-11887
Re-ionization and decaying dark matter
[NASA-CR-189009] N92-11944
RECTANGULAR WINGS
Unsteady aerodynamic calculations for general configurations by the double-point method
[NAL-TR-1101T] N92-10980
RED SHIFT
On the nature of spectral shifts: Modeling and comparison to information contained in wide bands N92-11418
Phenological changes in the red edge shift of Norway spruce needles and their relationship to needle chlorophyll content N92-11423
Feasibility of the red edge index for the detection of nitrogen deficiency N92-11425
Normalization of multidirectional red and NIR reflectances with the SAVI N92-11477
REDUCED GRAVITY
The microgravity environment of the Space Shuttle Columbia middeck during STS-32
[NASA-TP-3140] N92-11930
The microgravity environment of the Space Shuttle Columbia payload bay during STS-32
[NASA-TP-3141] N92-11931
REDUNDANCY
Real-time fault diagnosis for propulsion systems
[NASA-TM-105303] N92-11017
REENTRY
Disposal methods N92-11116
REENTRY VEHICLES
A methodology to assess the Best Estimate Trajectory (BET) results generated for the Kwajalein Missile Range
[AD-A240770] N92-11083
REFINING
The role of fiber flocculation in chemical pulp refining
[ETN-91-90025] N92-11150
Fundamental aspects of the refining process N92-11151
A new hypothesis for the mechanics of refining N92-11152
Development of a fundamentally new refining method. Part 1: Basic design considerations N92-11153
Development of a fundamentally new refining method. Part 2: Operating conditions of the new refiner N92-11154
Effect of control variables and length of refining zone on the refining result with a new pilot refiner N92-11155
Comparison of a new refiner with a conventional refiner N92-11156
Homogeneity of refining action; effects on fiber and paper structure N92-11157
Control of the heterogeneity of the refining action N92-11158
REFLECTANCE
The design of broadband radar absorbing surfaces
[AD-A240521] N92-11235
Measurement, simulation, and analysis of the directional reflectance properties of Earth surface materials N92-11468
Bidirectional reflectance and surface albedo: Physical modeling and inversion N92-11469
Bi-directional reflectance of finite and infinite clouds N92-11470
Aircraft simulations of the POLDER experiment: First results N92-11471
Micro photoreflectance semiconductor wafer analyzer
[AD-D014950] N92-11788
Photoreflectance and H2O adsorption on GaAs(100)
[AD-A240391] N92-11911
REFLECTOR ANTENNAS
Large deployable antenna program. Phase 1: Technology assessment and mission architecture
[NASA-CR-4410] N92-11036
REFRACTORY MATERIALS
Synthesis of novel conducting solids
[AD-A240468] N92-11912
REFRIGERANTS
Heat exchanger thermal performance for two nonazeotropic refrigerant mixtures
[DE91-017250] N92-11216
REGIONS
Supervoltage NDE techniques for large aerospace structures
[AD-A240625] N92-11365
REINFORCING FIBERS
Buckling values and optimization of carbon fiber reinforced compression chord plates with rectangular stringers
[ILR-MITT-259(1991)] N92-11148
Improved compression molding technology for continuous fiber reinforced composite laminates. Part 2: AS-4/Polyimidesulfone prepreg system
[NASA-TM-104133] N92-11207
REINFORCING MATERIALS
Centrifugal casting of composites
[AD-D014981] N92-11144
RELATIVE BIOLOGICAL EFFECTIVENESS (RBE)
Development of recommendations in the area of ionizing radiations
[DE91-018527] N92-11623
Cellular repair/misrepair track model
[NASA-TP-3124] N92-11685
RELAXATION (MECHANICS)
Physical ageing and creep in PVC
[NPL-DMM(A)-21] N92-11185
On the nature of bulk electrical relaxation in silicate glasses
[DE92-000077] N92-11206
RELAXATION METHOD (MATHEMATICS)
Analysis of a parallel multigrid algorithm
[NASA-CR-188906] N92-11701
Numerical methods in Markov chain modeling
[NASA-CR-188908] N92-11744
RELIABILITY ANALYSIS
Supervoltage NDE techniques for large aerospace structures
[AD-A240625] N92-11365
Algebraic aspects of network reliability problems
[AD-A240365] N92-11748
REMOTE MANIPULATOR SYSTEM
Active vibration damping of the Space Shuttle remote manipulator system
[NASA-TM-104149] N92-11073
REMOTE SENSING
Large deployable antenna program. Phase 1: Technology assessment and mission architecture
[NASA-CR-4410] N92-11036
International program for Earth observations
[NASA-CR-188799] N92-11393
Physical Measurements and Signatures in Remote Sensing, volume 1
[ESA-SP-319-VOL-1] N92-11394
Comparison of in situ, aircraft- and satellite-derived surface reflectances in Flevoland (Netherlands) N92-11404
Altitude dependence in a semi-analytical atmospheric code N92-11413
On the value of high spectral resolution measurements in the visible and near-infrared N92-11419
Use of high spectral resolution airborne visible/infrared imaging spectrometer data for geologic mapping: An overview N92-11420
Space observation of the land-ocean-atmosphere system at high spectral resolution in the infrared: Perspectives and problems N92-11421
The performance of the ESA Medium Resolution Imaging Spectrometer (MERIS) N92-11422

Simultaneous determination of six soil properties from the soil diffuse reflectance spectrum in the near infrared region (1-2.5 microns) N92-11424
Feasibility of the red edge index for the detection of nitrogen deficiency N92-11425
Multi-temporal monitoring of lake water quality N92-11426
Retrievals of column atmospheric water vapor, vegetation liquid water, and cloud cover fraction from AVIRIS data N92-11427
A multi-sensor approach to spectral signature analysis of inland waters N92-11428
Spectral identification (1.2-2.5 microns) and characterization of Paris (France) Basin kaolinite/smectite clays using a field spectrometer N92-11429
The use of imaging spectrometry in Mediterranean land degradation and soil erosion hazard assessments N92-11430
The comparison of airborne imaging spectrometry and geochemical ground survey for the analysis of vegetation anomalies over waste deposits N92-11431
Near-infrared imaging spectroscopy: Learning from planetary geology N92-11438
Spectroscopic analysis of imaging spectrometer data for classification purposes N92-11439
Preliminary results of a spectro-imagery experiment (GER) over the Adriatic coastline of the Venice lagoon N92-11440
Current status and future developments in radar remote sensing N92-11441
Airborne precursor missions in support of SIR-C/X-SAR N92-11450
Active microwave remote sensing and ground hydric state. Agriscatt '88 airborne campaign over the Orgeval basin (France) N92-11454
Airborne SAR HAREM campaign: Results, targets features, ERS1 simulations, and operational satellite exploitation N92-11455
Evaluation of vegetation cover characteristics using an airborne microwave scatterometer N92-11456
Passive microwave remote sensing of soil moisture: Results from HAPEX, FIFE, and MONSOON 90 N92-11458
Comparison of passive microwave and model derived estimates for soil moisture fields N92-11459
On the use of passive microwaves at 37 GHz N92-11461
Experimental approach to emissivity problems and surface temperature in thermal infrared remote sensing N92-11462
Comparison between the observed microwave spectral signatures over the Antarctic ice sheet and a snow emissivity model N92-11464
A three dimensional radiative transfer method for optical remote sensing of vegetated land surfaces N92-11466
Measurement, simulation, and analysis of the directional reflectance properties of Earth surface materials N92-11468
Bidirectional reflectance and surface albedo: Physical modeling and inversion N92-11469
Aircraft simulations of the POLDER experiment: First results N92-11471
The effect of the distribution of chlorotic material on the reflectance of mixed canopies N92-11472
Optimum combinations of visible and near-infrared reflectances for estimating the fraction of photosynthetically available radiation absorbed by plants N92-11474
Radiative transfer simulation on computer models of vegetation cover N92-11476
Normalization of multidirectional red and NIR reflectances with the SAVI N92-11477
Spectral reflectance of thin snow N92-11482
ATLAS: An Auto-Tracking Land and Atmosphere Sensor for retrieval of atmospheric optical parameters and acquisition of bidirectional surface reflectance N92-11487
Physical Measurements and Signatures in Remote Sensing, volume 2
[ESA-SP-319-VOL-2] N92-11488
Integration of visible-through microwave-range multispectral image data sets for geologic mapping N92-11491
Airborne passive microwave remote sensing of land and water surface N92-11492
Construction of ground cover charts of a wheat canopy from reflectance measurements N92-11505
Maximum evapotranspiration monitoring over La Mancha, Spain, using NOAA-AVHRR data N92-11507
Actual daily evapotranspiration monitoring using NOAA-AVHRR data from the HAPEX-MOBILHY campaigns N92-11509
The linking of crop growth models and multi-sensor remote sensing data N92-11512
Simulation study of vegetation indices sensitivity using the middle infrared N92-11514
Study of the spatial variability of the hydrodynamic behavior of grounds at the Niger (Africa) using satellite images N92-11515
Structural controls on the remotely sensed response of a coniferous forest plantation N92-11516
Database of SPOT histrograms N92-11517
Modeling temporal evolution of the radiometric response measured by wideband sensors over temperate agricultural regions N92-11518
Texture indices sensitivity to spatial and spectral resolutions in semi-urban environments N92-11519
Contribution of NOAA-AVHRR satellite data in forest vegetation monitoring N92-11520
Multidate analysis of NOAA-AVHRR data over France: Relationship with agroclimatic characteristics N92-11521
Spectral estimates of PAR interception and biomass production of irrigated rice crops. 1: Model elaboration with ground data N92-11522
Analysis of the surface state of two sub-polar glaciers using SPOT data and a numerical terrain model N92-11523
Multitemporal study of the Guyana coastline and estuaries using SPOT and LANDSAT imagery N92-11524
NOAA-AVHRR NDVI temporal profile classification and sensitivity to land use and climatic conditions in temperate region N92-11525
Spatial and spectral analysis of a degraded mangrove in south Senegal N92-11527
Control of the physiological state of vegetation cover by remote sensing of fluorescent emission in the blue and red visible spectrum regions N92-11532
Laser active remote sensing of phytoplankton in inland waters N92-11534
CO2 laser active remote sensing from 9 to 11 microns: Airborne and laboratory application N92-11535
Laser-induced spectral signatures in investigations of sea upper layer N92-11537
Simultaneous detection in blue and red bands of laser induced vegetation fluorescence N92-11539
Design and testing of a spectral-resolving fluorescence lidar system for remote sensing of vegetation N92-11540
A simple model of canopy fluorescence N92-11543
Target signature by differential reflectance lidar, a feasibility study N92-11544
(L)EAF: A remote sensing fluoresensor N92-11546
The use of a time-resolved lidar to study the water column N92-11548
Observation of DOM composition by synchronous fluorescence spectroscopy N92-11549
Biospheric models, measurements, and remote sensing of vegetation N92-11550
A conceptual framework for ecosystem modeling using remotely sensed inputs N92-11551
View-atmosphere-soil effects on vegetation indices derived from SPOT images N92-11552
Use of multitemporal SPOT data in first ISLSCP field experiment N92-11554
Space observations for global change N92-11555
Looking ahead to EOS: Update on NASA's Earth Observing Program N92-11556
Remote sensing contribution to the APEX MOBILHY program N92-11557
The UK Natural Environment Research Council Equipment Pool for Field Spectroscopy (NERC-EPFS) N92-11558
The science benefits of and the antenna requirements for microwave remote sensing from geostationary orbit
[NASA-CR-4408] N92-11559
Thermal infrared spectra of natural and manmade materials: Implications for remote sensing
[AD-A240455] N92-11564

REMOTE SENSORS
Space station tracking requirements feasibility study, volume 1
[NASA-CR-185641-VOL-1] N92-11085
Airborne precursor missions in support of SIR-C/X-SAR N92-11450
Thermal infrared spectra of natural and manmade materials: Implications for remote sensing
[AD-A240455] N92-11564

REMOTELY PILOTED VEHICLES
Development of a 1/7th scale fighter UAV for flight research
[AD-A240703] N92-11008
Initial design study of existing flight control system of RPH and feasibility study of implementing HHC on the SH-60B
[AD-A240522] N92-11019

REPORTS
Activities report of the Max-Planck Institute for Aeronomy
[ETN-91-90233] N92-11964

REQUIREMENTS
Guidelines for integrating helicopter assets into emergency planning
[SCT-91RR-18] N92-10993
Test facilities for high power electric propulsion
[NASA-TM-105247] N92-11136

RESCUE OPERATIONS
Guidelines for integrating helicopter assets into emergency planning
[SCT-91RR-18] N92-10993
Concept evaluation of the UH-60 externally mounted rescue hoist
[AD-A240545] N92-11004

RESEARCH AIRCRAFT
Development of a 1/7th scale fighter UAV for flight research
[AD-A240703] N92-11008

RESEARCH AND DEVELOPMENT
Nuclear thermal rocket workshop reference system Rover/NERVA N92-11091
JANNAF Liquid Rocket Combustion Instability Panel research recommendations N92-11124
Plans for the development of cryogenic engines for space exploration
[NASA-TM-105250] N92-11135
Engineering design of large helical device N92-11864
Development of superconductor for large helical device N92-11867
Eighty years of aerospace technique through ATMA bulletins
[ETN-91-90097] N92-11963

RESEARCH FACILITIES
Plans for the development of cryogenic engines for space exploration
[NASA-TM-105250] N92-11135
Research and development of forced flow superconducting coils for large helical device N92-11838

RESEARCH MANAGEMENT
Nuclear thermal propulsion program overview N92-11089
Nuclear thermal propulsion workshop overview N92-11090
Office of Basic Energy Sciences
[DE91-019006] N92-11570
Education in computational science: Role of the National Laboratories
[DE91-018823] N92-11687
Annual research summary, July 1, 1990 - June 30, 1991
[DE91-017408] N92-11962
LLE review
[DE91-018828] N92-11965

RESEARCH PROJECTS
Engineering and instrumentation support of GL Research Balloon Program
[AD-A240616] N92-10987
Nuclear Thermal Propulsion: A Joint NASA/DOE/DOD Workshop
[NASA-CP-10079] N92-11088
Nuclear thermal propulsion program overview N92-11089
Nuclear thermal propulsion workshop overview N92-11090
Nuclear thermal rocket workshop reference system Rover/NERVA N92-11091
Upgraded NERVA systems: Enabler nuclear system N92-11093
JANNAF Liquid Rocket Combustion Instability Panel research recommendations N92-11124

RESIDUAL STRENGTH
An examination of the damage tolerance enhancement of carbon/epoxy using an outer lamina of spectra (R)
[NASA-TP-3160] N92-11142

RESIN MATRIX COMPOSITES
Low toxicity high temperature PMR polyimides
[NASA-CASE-LAR-14639-1] N92-11199
Improved compression molding technology for continuous fiber reinforced composite laminates. Part 2: AS-4/Polyimidesulfone prepreg system
[NASA-TM-104133] N92-11207

RESISTORS
Advanced Langmuir Probe (LP)
[NASA-CR-180084] N92-11284

RESONANT FREQUENCIES
Attitude control of flexible structures
[AD-A240520] N92-11082
Discrete ARMA model for natural resonances in electromagnetic and acoustic scattering
[AD-A240656] N92-11241
Measurement of frequency response in short thermocouple wires
[NASA-CR-187821] N92-11339

Studies in the form of finite element mass matrices for beams, plates and shells
[AERO-TN-9101] N92-11369
Resonant frequency calculations using a hybrid perturbation-Galerkin technique
[NASA-CR-187632] N92-11640

RESONATORS
Linear theory of a quasioptical gyroklystron with nonuniform magnetic field
[AD-A240264] N92-11334
Quantitative ray methods for scattering of sound by spherical shells
[AD-A240255] N92-11761
Quantum 1/f noise in high technology applications including ultrasmall structures and devices
[AD-A240152] N92-11907

RESOURCE ALLOCATION
Space Network Control Conference on Resource Allocation Concepts and Approaches
[NASA-CP-3124] N92-11039
Space Network Control (SNC) Conference on Resource Allocation Concepts and Approaches. Overview N92-11040
Resource allocation planning helper (RALPH) N92-11047
Flexible Envelope Request Notation (FERN) N92-11050
Managing temporal relations in the MAESTRO scheduling system N92-11059
Resource representation in COMPASS N92-11060
Automating the conflict resolution process N92-11061

RESOURCES MANAGEMENT
Flexible Envelope Request Notation (FERN) N92-11050
Winter use plan: Environmental assessment
[PB91-194027] N92-11574
Processes for identifying regional influences of and responses to increasing atmospheric CO2 and climate change: The MINK Project
[DE91-018604] N92-11580
Modelling product structures by generic bills-of-material
[ETN-91-90146] N92-11919

RESPIRATORY PHYSIOLOGY
Biochemical and biophysical studies of the E. coli respiratory chain
[DE91-016966] N92-11612

RESPONSE TIME (COMPUTERS)
Optimal processor assignment for pipeline computations
[NASA-CR-189047] N92-11672

RETENTION (PSYCHOLOGY)
Pictures and anaphora
[AD-A240153] N92-11631

RETROFITTING
Discharge system tests of Halon 1301 test gas simulants
[AD-A240679] N92-11193

RETROREFLECTION
Illumination, optics, and retroreflectors for efficient landmark tracking N92-11790

RETROREFLECTORS
Illumination, optics, and retroreflectors for efficient landmark tracking N92-11790

REUSABLE ROCKET ENGINES
Linear quadratic servo control of a reusable rocket engine
[NASA-TM-105291] N92-11128

REVERSE FIELD PINCH
Coaxial slow source
[DE91-016947] N92-11875
The TITAN reversed-field-pinch fusion reactor study, volume 4
[DE92-000138] N92-11895
The TITAN reversed-field-pinch fusion reactor study, volume 2
[DE92-000140] N92-11896
The TITAN reversed-field-pinch fusion reactor study, volume 1
[DE92-000141] N92-11897

REVERSED FLOW
Mixed convection in two-dimensional laminar air flow with reverse flow regions N92-11293

REYNOLDS STRESS
On the basic equations for the second-order modeling of compressible turbulence
[NASA-TM-105277] N92-11302

RICE
Spectral estimates of PAR interception and biomass production of irrigated rice crops. 2: Model validation with SPOT data N92-11510
Spectral estimates of PAR interception and biomass production of irrigated rice crops. 1: Model elaboration with ground data N92-11522

RISK
An investigation of the material hazard of some insensitive high explosives
[MRL-TR-91-22] N92-11209
Integrated Risk Information System
[DE91-018503] N92-11924

ROBOT ARMS
A generalized method for multiple robotic manipulator programming applied to vertical-up welding
[NASA-TP-3163] N92-11218

ROBOT CONTROL
A generalized method for multiple robotic manipulator programming applied to vertical-up welding
[NASA-TP-3163] N92-11218

ROBOT DYNAMICS
A generalized method for multiple robotic manipulator programming applied to vertical-up welding
[NASA-TP-3163] N92-11218

ROBOT SENSORS
Sparse distributed memory
[NASA-CR-188841] N92-11643

ROBOTICS
Ground penetrating radar data acquisition system
[AD-A240765] N92-11244
Robotic non-destructive inspection of aircraft, phase 1
[AD-A240777] N92-11367
Robot graphic simulation testbed
[NASA-CR-188998] N92-11637

ROBOTS
Navigation and positioning of mobile robots
[DE92-704014] N92-10998
Robot graphic simulation testbed
[NASA-CR-188998] N92-11637

ROBUSTNESS (MATHEMATICS)
OPUS: Optimal Projection for Uncertain Systems. Volume 1
[AD-A240372] N92-11080
Optimal expression evaluation for data parallel architectures
[NASA-CR-187773] N92-11696

ROCKET ENGINE CONTROL
Real-time fault diagnosis for propulsion systems
[NASA-TM-105303] N92-11017
Linear quadratic servo control of a reusable rocket engine
[NASA-TM-105291] N92-11128

ROCKET ENGINE DESIGN
Nuclear Thermal Propulsion: A Joint NASA/DOE/DOD Workshop
[NASA-CP-10079] N92-11088
Nuclear thermal rocket workshop reference system Rover/NERVA N92-11091
NERVA upgrade: Non-nuclear components N92-11092
Upgraded NERVA systems: Enabler nuclear system N92-11093
Low Pressure Nuclear Thermal Rocket (LPNTR) concept N92-11094
Nuclear light bulb N92-11110
Propulsion system needs N92-11112
Developments in REDES: The Rocket Engine Design Expert System N92-11120
Analytical study of nozzle performance for nuclear thermal rockets
[NASA-TM-105251] N92-11126
Calibration of turbine flowmeters for storable bipropellant engines
[NAL-TR-1091] N92-11127

ROCKET ENGINES
Dumbo: A pachydermal rocket motor N92-11100

ROCKET EXHAUST
Physicochemical properties and dissolution in simulated biological fluids of particles of beryllium-powered rocket motor exhaust and pure beryllium oxides calcined at low and high temperature
[AD-A240288] N92-11134

ROCKET NOZZLES
Propulsion system needs N92-11112
Analytical study of nozzle performance for nuclear thermal rockets
[NASA-TM-105251] N92-11126

ROCKET THRUST
CFD code survey for thrust chamber application N92-11119

ROTARY WING AIRCRAFT
Rotorcraft system identification
[AGARD-AR-280] N92-11001

ROTARY WINGS
Experimental study of an independently deflected wingtip mounted on a semispan wing
[NASA-TM-102842] N92-10983
Analysis of open loop higher harmonic control at high airspeeds on a modern four-bladed articulated rotor
[NASA-TM-103876] N92-11000

ROTATION
Rotations of bulk ions and impurities in non-axisymmetric toroidal systems
[NIFS-102] N92-11885

ROTOR AERODYNAMICS
Radial inflow turbine study
[AD-A240169] N92-11015

ROTOR BLADES (TURBOMACHINERY)
Hydrodynamic design of generic pump components
[NASA-CR-184252] N92-11361

ROTOR LIFT
Experimental study of an independently deflected wingtip mounted on a semispan wing
[NASA-TM-102842] N92-10983

ROTORCRAFT AIRCRAFT
Technology needs for high speed rotorcraft (3)
[NASA-CR-186433] N92-10999

ROTORS
The effects of Reynolds number, rotor incidence angle and surface roughness on the heat transfer distribution in a large-scale turbine rotor passage
[NASA-CR-187693] N92-11297

RUBIDIUM
Matter-wave interferometry with laser cooled atoms
[AD-A240531] N92-11776

RUN TIME (COMPUTERS)
Distributed memory compiler methods for irregular problems: Data copy reuse and runtime partitioning
[NASA-CR-187635] N92-11669

RUNWAY LIGHTS
Evaluation of two high-speed runway exits
[DOT/FAA/CT-TN91/36] N92-11021

RUNWAYS
Evaluation of two high-speed runway exits
[DOT/FAA/CT-TN91/36] N92-11021
Prototype runway hold-short lighting system
[DOT/FAA/CT-TN91/43] N92-11028
Surface painted taxiway markings at Seattle-Tacoma International Airport
[DOT/FAA/CT-TN91/49] N92-11029

S

SAFETY
KA-111, Phase C, M-1 propellant tests: Deflagration in partial confinement
[AD-A240185] N92-11211

SAFETY FACTORS
Nuclear safety N92-11114
Safety issues N92-11115

SAFETY MANAGEMENT
Program plan: National aging aircraft research program
[DOT/FAA/CT-88/32-1] N92-10992
Nuclear safety N92-11114
Safety issues N92-11115

SAHARA DESERT (AFRICA)
Inflight calibration of channels 1 and 2 of AVHRR using desertic sites and clouds N92-11406

SALINITY
Airborne passive microwave remote sensing of land and water surface N92-11492

SAMARIUM
The 23 to 300 C demagnetization resistance of samarium-cobalt permanent magnets
[NASA-TP-3119] N92-11252

SATELLITE ATTITUDE CONTROL
Pinhole cameras as sensors for atomic oxygen in orbit; application to attitude determination of the LDEF N92-11078

SATELLITE COMMUNICATION
Basic concepts of low Earth orbit satellite systems for communications
[TELECOM-PARIS-91-D-001] N92-11248

SATELLITE CONTROL
Precision pointing control of the spinning Gravity Probe B spacecraft N92-11068

SATELLITE DESIGN
International program for Earth observations
[NASA-CR-188799] N92-11393

SATELLITE IMAGERY
Physical Measurements and Signatures in Remote Sensing, volume 1
[ESA-SP-319-VOL-1] N92-11394
Estimation of the aerosol optical thickness from broadband turbidity measurements: Application to the atmospheric correction of SPOT images N92-11399
Atmospheric correction of satellite borne imagery investigated by means of a sensitivity analysis of the entire remote sensing process N92-11400
Inter-calibrating of SPOT1-HRV, LANDSAT5-TM, and NOA11-AVHRR in the visible and near infrared field s N92-11401

Characterization of African desert sites for the relative calibrating of wide field satellite optical sensors N92-11402
Use of operation ART-SPOT to test the 5S model and the MTF of the SPOT N92-11403
SPOT calibration on the test site La Crau (France) N92-11409
Suppression of aerosols on LANDSAT thematic mapper imagery N92-11411
Radiometric and atmospheric correction procedures for AVHRR preprocessing in the solar reflective channels N92-11414
In flight calibration of large field of view sensors at short wavelength using the Rayleigh scattering N92-11416
Contribution of active microwaves to the structural analysis of epicontinental shelf-forms: Example of the English Channel N92-11448
Normalization of bidirectional effects of surface reflectance on a series of multitemporal NOAA/AVHRRR data N92-11480
Physical Measurements and Signatures in Remote Sensing, volume 2 [ESA-SP-319-VOL-2] N92-11488
Synergistic use of multispectral satellite data for monitoring land surface change N92-11489
Synergy of high resolution spatial microwave imagery and geomorphological optics N92-11496
Joint use of remote sensing and agricultural production estimation models: Current trends N92-11501
Some examples of satellite data utilization for atmospheric modeling at medium scale N92-11503
Actual daily evapotranspiration monitoring using NOAA-AVHRR data from the HAPEX-MOBILHY campaigns N92-11509
Spectral estimates of PAR interception and biomass production of irrigated rice crops. 2: Model validation with SPOT data N92-11510
Temporal signatures using NOAA-AVHRR and land use mapping N92-11513
Simulation study of vegetation indices sensitivity using the middle infrared N92-11514
Study of the spatial variability of the hydrodynamic behavior of grounds at the Niger (Africa) using satellite images N92-11515
Database of SPOT histrograms N92-11517
Contribution of NOAA-AVHRR satellite data in forest vegetation monitoring N92-11520
Analysis of the surface state of two sub-polar glaciers using SPOT data and a numerical terrain model N92-11523
Multitemporal study of the Guyana coastline and estuaries using SPOT and LANDSAT imagery N92-11524
NOAA-AVHRR NDVI temporal profile classification and sensitivity to land use and climatic conditions in temperate region N92-11525
Night-time LANDSAT thermal infrared imagery as a tool for climatological studies N92-11526
Spatial and spectral analysis of a degraded mangrove in south Senegal N92-11527
Detection and characterization of active fires in west Africa with LANDSAT thematic mapper and NOAA N92-11529
View-atmosphere-soil effects on vegetation indices derived from SPOT images N92-11552
Space observations for global change N92-11555
The science benefits of and the antenna requirements for microwave remote sensing from geostationary orbit [NASA-CR-4408] N92-11559
Multispectral image maps from LANDSAT thematic mapper data [AD-A240453] N92-11562
A hybrid methodology for detecting cartographically significant features using LANDSAT TM imagery [AD-A240454] N92-11563

SATELLITE NETWORKS
Effect of locus of resource control on operational efficiency in distributed operations N92-11046
TRUST: TDRSS Resource User Support Tool N92-11052
Network Control Center User Planning System (NCC UPS) N92-11053
Polynomial optimization techniques for activity scheduling. Optimization based prototype scheduler N92-11056
Range Scheduling Aid (RSA) N92-11057
Scheduling techniques in the Request Oriented Scheduling Engine (ROSE) N92-11058
Basic concepts of low Earth orbit satellite systems for communications [TELECOM-PARIS-91-D-001] N92-11248

SATELLITE OBSERVATION
International program for Earth observations [NASA-CR-188799] N92-11393
On the use of passive microwaves at 37 GHz N92-11461
LAGEOS geodetic analysis-SL7.1 [NASA-TM-104549] N92-11584

SATELLITE ORBITS
Drag coefficients with applications to satellite orbits N92-11069

SATELLITE ORIENTATION
Pinhole cameras as sensors for atomic oxygen in orbit; application to attitude determination of the LDEF N92-11078

SATELLITE TRACKING
Estimation of geopotential differences over intercontinental locations using satellite and terrestrial measurements [NASA-CR-188992] N92-11560
LAGEOS geodetic analysis-SL7.1 [NASA-TM-104549] N92-11584

SATELLITE-BORNE RADAR
Space station tracking requirements feasibility study, volume 2 [NASA-CR-185641-VOL-2] N92-11084

SATURN ATMOSPHERE
Electron distributions and solar wind interaction with nonmagnetic planets N92-11952

SCALARS
The phenomena of scalar mixing in turbulent gas-particle flows, measuring equipment, and measurements [DE92-704034] N92-11327

SCALE MODELS
Developmental flight testing of a half scale unmanned air vehicle [AD-A240347] N92-11002

SCALING LAWS
On the theory and numerical approximation of nonlinear hyperbolic problems [ETN-91-99898] N92-11714
On a class of implicit and explicit schemes of Van-Leer type for scalar conservation laws N92-11715
On the evolution of a superconducting cosmic string network [DE91-630995] N92-11948

SCANNERS
A new radiographic corrosion inspection capability [AD-A231476] N92-11363
Development of data file standards for automated ultrasonic scanning systems. Exchange methods for digital ultrasonic inspection data [AD-A240075] N92-11364

SCANNING
Development of data file standards for automated ultrasonic scanning systems. Exchange methods for digital ultrasonic inspection data [AD-A240075] N92-11364

SCANNING TUNNELING MICROSCOPY
Progress in Photon Scanning-Tunneling Microscopy (PSTM) [DE91-018174] N92-11905

SCATTERING
A fast algorithm for plotting antenna and scattering patterns in three dimensions [AD-A240410] N92-11233
Collision integrals and high temperature transport properties for N-N, O-O, and N-O [NASA-CR-188907] N92-11770
Comparative study of final state interaction contributions to the dynamic response of quantum fluids [DE91-631020] N92-11892

SCATTERING AMPLITUDE
Quantitative ray methods for scattering of sound by spherical shells [AD-A240255] N92-11761

SCATTERING CROSS SECTIONS
Quantitative ray methods for scattering of sound by spherical shells [AD-A240255] N92-11761
Coupled-channel optical calculation of electron-hydrogen scattering: Elastic scattering from 0.5 to 30 eV [DE91-634157] N92-11780
Meson-exchange calculation of the d(gamma,p)n in the GeV energy region [DE91-017994] N92-11785

SCATTEROMETERS
Dual-polarized scatterometer measurements of wind and mechanically generated waves in a very large wind/wave flume, the VIERS-1 project N92-11443
Estimation of the ground humidity under vegetation: Applications of semi-empirical models N92-11445

SCENE ANALYSIS
Enhanced clutter suppression apparatus for use with an infrared search and surveillance system [AD-D014984] N92-11247
Comparison of two atmospheric correction models for a vegetated Airborne Visible/Infrared Imaging Spectrometer (AVIRIS) scene N92-11415
Appearance simulator for computer vision research [AD-A240506] N92-11679

SCHEDULES
The Space Shuttle: An attempt at low-cost, routine access to space [AD-A240589] N92-11037
User interface issues in supporting human-computer integrated scheduling N92-11048
Human factors issues in the design of user interfaces for planning and scheduling N92-11049
Flexible Envelope Request Notation (FERN) N92-11050
Intelligent perturbation algorithms for space scheduling optimization N92-11055
Resource representation in COMPASS N92-11060
Automating the conflict resolution process N92-11061
A method for interference mitigation in space communications scheduling N92-11062
A planning language for activity scheduling N92-11063
ART/Ada design project, phase 1: Project plan [NASA-CR-187313] N92-11663

SCHEDULING
What we were asked to do N92-11041
Concepts, requirements, and design approaches for building successful planning and scheduling systems N92-11042
Proposed planning and scheduling services for the SNC in the CDOS era N92-11043
An RF interference mitigation methodology with potential applications in scheduling N92-11044
Automated conflict resolution issues N92-11045
Resource allocation planning helper (RALPH) N92-11047
User interface issues in supporting human-computer integrated scheduling N92-11048
Human factors issues in the design of user interfaces for planning and scheduling N92-11049
Flexible Envelope Request Notation (FERN) N92-11050
TRUST: TDRSS Resource User Support Tool N92-11052
Network Control Center User Planning System (NCC UPS) N92-11053
SPIKE: AI scheduling techniques for Hubble Space Telescope N92-11054
Intelligent perturbation algorithms for space scheduling optimization N92-11055
Polynomial optimization techniques for activity scheduling. Optimization based prototype scheduler N92-11056
Range Scheduling Aid (RSA) N92-11057
Scheduling techniques in the Request Oriented Scheduling Engine (ROSE) N92-11058
Managing temporal relations in the MAESTRO scheduling system N92-11059
Resource representation in COMPASS N92-11060
Automating the conflict resolution process N92-11061
A method for interference mitigation in space communications scheduling N92-11062
A planning language for activity scheduling N92-11063
Intelligent perturbation algorithms to space scheduling optimization N92-11064

SCHLIEREN PHOTOGRAPHY
Schlieren system for visualizing the flow within a pipe of circular cross-section [NASA-CASE-LAR-13944-1] N92-11336

SCIENTIFIC SATELLITES
Radiation belt dynamic and quasi-static modeling based on CRRES data [AD-A240392] N92-11585

SCINTILLATION COUNTERS
Nuclear transparency and double beta decay of molybdenum 100 [DE91-016963] N92-11172
Development of a high resolution liquid xenon imaging chamber for gamma-ray astronomy [NASA-CR-188994] N92-11332

SEA SURFACE TEMPERATURE
Energetics diagnosis of numerical simulation of atmospheric blocking [NASA-CR-183503] N92-11581
Optically thin cirrus clouds over oceans and possible impact on sea surface temperature of warm pool in western Pacific [NASA-TM-104550] N92-11600

SEA WATER
Organic geochemistry of seawater particulate matter: Final data analysis interpretation [AD-A240199] N92-11605

SEARCH PROFILES
Intelligent perturbation algorithms to space scheduling optimization N92-11064
An investigation to find appropriate measures for evaluating interactive information retrieval N92-11922

SEARCH RADAR
An examination of the factors affecting the use of infra-red search and track systems in the air-to-air role
[ETN-91-99987] N92-11222
SEAS
Analysis of altimetry over the Aral Sea
[NASA-TM-100759] N92-11583
Use of theoretical wave height distributions in directional seas
[AD-A240411] N92-11608
SEASAT SATELLITES
Contribution of active microwaves to the structural analysis of epicontinental shelf-forms: Example of the English Channel N92-11448
Analysis of altimetry over the Aral Sea
[NASA-TM-100759] N92-11583
SECONDARY FLOW
Secondary instability of the three dimensional laminar boundary layer in incompressible flow: Description of the calculation code
[CERT-RT-63/5618-54] N92-11306
SEISMIC WAVES
Contribution of active microwaves to the structural analysis of epicontinental shelf-forms: Example of the English Channel N92-11448
SEISMOGRAPHS
Real-time earthquake monitoring: Early warning and rapid response
[NASA-CR-186701] N92-11582
SEISMOLOGY
Sunspot dynamics
[NASA-CR-188978] N92-11955
SELF ABSORPTION
Laser induced fluorescence of growing camphor tree leaves: Influence of chlorophyll content on LIF spectral signature N92-11547
SELF CONSISTENT FIELDS
Kinematics and dynamics of barred galaxies N92-11937
SELF ORGANIZING SYSTEMS
Classification of posture maintenance data with fuzzy clustering algorithms
[NASA-CR-188949] N92-11662
SEMICONDUCTOR DEVICES
Semiconductor measurement technology: NIST list of publications, 1962-1989 (revised March 1990)
[PB91-193961] N92-11269
SEMICONDUCTOR LASERS
Long wavelength semiconductor lasers development for infrared heterodyne applications
[NASA-CR-189243] N92-11341
Laser diode pumped, erbium-doped, solid state laser with high slope efficiency
[AD-D014968] N92-11347
Process for controlling the thickness of an antireflection coating, and embodying apparatus
[DE91-017634] N92-11793
SEMICONDUCTORS (MATERIALS)
Nonlinear optical properties of semiconducting polymers
[AD-A240753] N92-11195
Microchannel electron source
[AD-D014956] N92-11276
Micro photoreflectance semiconductor wafer analyzer
[AD-D014950] N92-11788
Radiation induced growth of micro crystallites
[DE91-016516] N92-11900
Photoreflectance and H2O adsorption on GaAs(100)
[AD-A240391] N92-11911
Spectroscopic studies of layered and bulk semiconductor materials
[ETN-91-90145] N92-11914
SEMISPAN MODELS
NACA 0015 wing pressure and trailing vortex measurements
[NASA-TP-3151] N92-10981
Experimental study of an independently deflected wingtip mounted on a semispan wing
[NASA-TM-102842] N92-10983
SENEGAL
Spatial and spectral analysis of a degraded mangrove in south Senegal N92-11527
SENSORY PERCEPTION
Human Machine Interfaces for Teleoperators and Virtual Environments Conference
[NASA-CP-10071] N92-11638
SEPARATED FLOW
Evaluation of high Reynolds number flow in a 180 degree turn-around-duct
[NASA-CR-184243] N92-11318
SERVICE LIFE
Program plan: National aging aircraft research program
[DOT/FAA/CT-88/32-1] N92-10992
Definition, technology readiness, and development cost of the orbit transfer vehicle engine integrated control and health monitoring system elements
[NASA-CR-187123] N92-11132
High pressure turbine blade life extension
[AD-A240654] N92-11180
High efficiency motor rewind study
[DE91-017162] N92-11270
SERVOCONTROL
Linear quadratic servo control of a reusable rocket engine
[NASA-TM-105291] N92-11128
SERVOMECHANISMS
Linear quadratic servo control of a reusable rocket engine
[NASA-TM-105291] N92-11128
SET THEORY
A re-examination of the relationship between fuzzy set theory and probability theory
[AD-A240243] N92-11746
SHALLOW WATER
Use of theoretical wave height distributions in directional seas
[AD-A240411] N92-11608
Solving the shallow water equations on the Cray X-MP/48 and the connection machine 2
[NASA-CR-188897] N92-11658
An analysis of some hyperbolic problems related to the shallow water model (chapter 6)
[IMAG-RR-579] N92-11718
Numerical analysis of the problem of long waves in shallow water N92-11720
SHAPE MEMORY ALLOYS
Analysis of strain dependent damping in materials via modeling of material point hysteresis
[AD-A240298] N92-11381
SHAPES
Perceptual grouping and shape from texture
[AD-A240358] N92-11678
SHARP LEADING EDGES
Perfect compressible two dimensional boundary layer strong fluid coupling in the case of sharp leading edge profiles. Unsteady case of isolated profiles and steady case of blade grids
[ONERA-RT-43/1621-RY-006-R] N92-11311
SHEAR FLOW
Deformation and breakup of drops in simple shear flows
[ETN-91-90143] N92-11315
Light scattering experiments on Brownian motion in shear flow and in colloidal crystals
[ETN-91-90134] N92-11756
SHELL THEORY
Quantitative ray methods for scattering of sound by spherical shells
[AD-A240255] N92-11761
SHELLS (STRUCTURAL FORMS)
Studies in the form of finite element mass matrices for beams, plates and shells
[AERO-TN-9101] N92-11369
Calculation of general shells of revolution, using a semi analytical process
[ILR-MITT-262(1991)] N92-11386
SHIPS
Discharge system tests of Halon 1301 test gas simulants
[AD-A240679] N92-11193
Shipboard antenna concepts: Structurally independent 2- to 6-MHz transmit antenna design
[AD-A240544] N92-11236
SHOCK ABSORBERS
Deformation of isodamp (A polyvinyl chloride-based elastomer) at various loading rates
[AD-A240393] N92-11189
SHOCK LAYERS
Spectral fitting, shock layer modeling, and production of nitrogen oxides and excited nitrogen
[NASA-CR-185664] N92-11769
SHOCK RESISTANCE
Graphites as plasma facing material of a large fusion device N92-11813
SHOCK WAVE INTERACTION
Numerical simulations of detonation transmission
[AD-A240560] N92-11304
Studies of aerothermal loads generated in regions of shock/shock interaction in hypersonic flow
[NASA-CR-181893] N92-11319
SHOCK WAVE PROPAGATION
Numerical simulations of detonation transmission
[AD-A240560] N92-11304
SHOCK WAVES
Layer tracking, asymptotics, and domain decomposition N92-11732
SHORELINES
Preliminary results of a spectro-imagery experiment (GER) over the Adriatic coastline of the Venice lagoon N92-11440
Multitemporal study of the Guyana coastline and estuaries using SPOT and LANDSAT imagery N92-11524
Use of theoretical wave height distributions in directional seas
[AD-A240411] N92-11608
SHORT CIRCUITS
New insulation constructions for aerospace wiring applications. Volume 2: The 270 VDC arc tracking testing with power controllers
[AD-A240639] N92-11007
Evaluation of Kapton pyrolysis, arc tracking, and arc propagation on the Space Station Freedom (SSF) solar array Flexible Current Carrier (FCC)
[NASA-CR-189056] N92-11139
SHORT TAKEOFF AIRCRAFT
Static internal performance of ventral and rear nozzle concepts for short-takeoff and vertical-landing aircraft
[NASA-TP-3103] N92-10975
SHORT WAVE RADIATION
Monitoring volcanoes using short wavelength infrared images N92-11498
SHUTTLE IMAGING RADAR
Airborne precursor missions in support of SIR-C/X-SAR N92-11450
SIDELOBE REDUCTION
A conjugate gradient based algorithm to minimize the sidelobe level of planar arrays with element failures
[AD-A240667] N92-11242
SIDELOBES
Pulse compression degradation due to open loop adaptive cancellation, part 1
[AD-A240552] N92-11238
Pulse compression degradation due to open loop adaptive cancellation, part 3
[AD-A240553] N92-11239
A conjugate gradient based algorithm to minimize the sidelobe level of planar arrays with element failures
[AD-A240667] N92-11242
SIGNAL ANALYSIS
The performance of the ESA Medium Resolution Imaging Spectrometer (MERIS) N92-11422
SIGNAL DETECTION
Efficient detection of a CW signal with a linear frequency drift
[NASA-CR-188900] N92-11224
Novel nonlinear laser diagnostic techniques
[AD-A240193] N92-11346
Tables of square-law signal detection statistics for Hann spectra with 50 percent overlap
[NASA-TM-103830] N92-11745
Compact optical RF spectrum analyzer
[AD-D014962] N92-11792
SIGNAL DETECTORS
Acoustic transponder receiver circuit
[AD-D014965] N92-11760
Compact optical RF spectrum analyzer
[AD-D014962] N92-11792
SIGNAL PROCESSING
Using a discrete Fourier transform to estimate phase in interferometric direction finding
[AD-A231414] N92-10995
Nonlinear aspects of aerospace structures at high excitation levels flat aluminum beams and plates studied
[AD-A240600] N92-11383
SIGNAL RECEPTION
Multiple beam antenna/switch system study
[NASA-CR-183496] N92-11251
SIGNAL TO NOISE RATIOS
Efficient detection of a CW signal with a linear frequency drift
[NASA-CR-188900] N92-11224
Error control techniques for satellite and space communications
[NASA-CR-188997] N92-11228
On the value of high spectral resolution measurements in the visible and near-infrared N92-11419
SIGNAL TRANSMISSION
Taking into account asynchronous signals in functional test of complex circuits N92-11259
SIGNATURE ANALYSIS
An a priori approach to the evaluation of signature analysis efficiency N92-11268
Simultaneous determination of six soil properties from the soil diffuse reflectance spectrum in the near infrared region (1-2.5 microns) N92-11424
A multi-sensor approach to spectral signature analysis of inland waters N92-11428
The spectral reflection behaviour of branches and branch components of healthy and damaged beech trees N92-11432

Large scale study of the microwave signature of the Antarctic ice sheet N92-11463
Comparison between the observed microwave spectral signatures over the Antarctic ice sheet and a snow emissivity model N92-11464

SIGNATURES
Target signature by differential reflectance lidar, a feasibility study N92-11544

SIKORSKY AIRCRAFT
Analysis of open loop higher harmonic control at high airspeeds on a modern four-bladed articulated rotor [NASA-TM-103876] N92-11000

SILANES
Study of silanization of silica and fiberglass using ESR spectroscopy and spin labelling [AD-A240767] N92-11197

SILICA GLASS
Study of silanization of silica and fiberglass using ESR spectroscopy and spin labelling [AD-A240767] N92-11197

SILICATES
Glass formation, properties, and structure of soda-yttria-silicate glasses [NASA-TM-104488] N92-11202
On the nature of bulk electrical relaxation in silicate glasses [DE92-000077] N92-11206

SILICON
Investigation of the stability of the spectral responsivity of silicon photodiodes [NPL-QU-87] N92-11184
The recombination behavior of a laser induced electron hole plasma in pin diodes and silicon base material [ETN-91-90153] N92-11887
Chemical reactivity and electronic structure of silicon microclusters [AD-A240276] N92-11908
Structure of the Si45 cluster [AD-A240278] N92-11909

SILICON CARBIDES
Centrifugal casting of composites [AD-D014981] N92-11144

SILICON DIOXIDE
Effect of particle size of Martian dust on the degradation of photovoltaic cell performance [NASA-TM-105232] N92-11133
Study of silanization of silica and fiberglass using ESR spectroscopy and spin labelling [AD-A240767] N92-11197

SILICONE RESINS
Synthesis of novel polysiloxanes bearing polar groups [AD-A240722] N92-11194

SILICONES
Synthesis and reactivity of silyl-ketene acetal-modified polysiloxanes preparation of polysiloxanes with high dielectric constraints [AD-A240754] N92-11196

SIMD (COMPUTERS)
Highly parallel computation [NASA-CR-188871] N92-11698

SIMULATION
Aircraft simulations of the POLDER experiment: First results N92-11471
A synchronization and charge distribution process for the parallel multilevel logic simulation [ETN-91-90152] N92-11708
Simulation of a nonlinear two degrees of freedom system. Study of the temporal response to a harmonic attraction [ONERA-RT-17/1677-RY-091-R] N92-11755
A simulation study of interactions of Space-Shuttle generated electron beams with ambient plasma and neutral gas [NASA-CR-189025] N92-11898

SIMULATORS
Development of a ninety string solar array simulator [NASA-TM-105278] N92-11086
Appearance simulator for computer vision research [AD-A240506] N92-11679
A new simulator for assessing subjective effects of sonic booms [NASA-TM-104150] N92-11759

SINGLE CRYSTALS
Long wavelength semiconductor lasers development for infrared heterodyne applications [NASA-CR-189243] N92-11341

SINGLE EVENT UPSETS
Comparison between californium and cyclotron heavy ion tests N92-11266
Comparison between californium and cyclotron SEU tests N92-11267

SINGULARITY (MATHEMATICS)
Interface conditions for domain decomposition with radical grid refinement N92-11733

SINTERING
Development of high Tc (greater than 110K) Bi, Tl and Y-based materials as superconducting circuit elements [NASA-CR-188999] N92-11902

SIZE (DIMENSIONS)
The effects of specimen geometry and size on the fracture toughness of nuclear graphites [DE92-000056] N92-11205

SLOPES
Radar image simulation to study the visual aptitude of observing slope and roughness effects N92-11446

SLOTTED WIND TUNNELS
Model representation in the PANCOR wall interference assessment code [NASA-TM-104152] N92-11022

SLUSH HYDROGEN
Benefits of slush hydrogen for space missions [NASA-TM-104503] N92-11214

SMALL PERTURBATION FLOW
Three dimensional numerical method for resolving small transonic perturbations in unstructured mesh [ONERA-RT-56/3064-RY-006-R] N92-10989
Irradiance compensation control for high-energy laser propagation, part 2 [DE91-018489] N92-11348

SMOKE
A study on the effects of Mt. Sakurajima's falling ash over crop and forest areas using image processing for LANDSAT-5, MOS-1, and Jafsa digital data N92-11497

SNOW
Comparison between the observed microwave spectral signatures over the Antarctic ice sheet and a snow emissivity model N92-11464
Spectral reflectance of thin snow N92-11482

SODIUM PEROXIDES
Glass formation, properties, and structure of soda-yttria-silicate glasses [NASA-TM-104488] N92-11202

SOFTWARE ENGINEERING
Continuation of research into language concepts for the mission support environment [NASA-CR-187818] N92-11652
ART/Ada design project, phase 1. Task 1 report: Overall design [NASA-CR-188943] N92-11665
Fractal image compression [AD-A240636] N92-11680
Technology assessment of the Software Life Cycle Support Environment (SLCSE) [AD-A240673] N92-11682
Ground Systems Development Environment (GSDE) interface requirements analysis [NASA-CR-188822] N92-11702
Information technologies for astrophysics circa 2001 [NASA-CR-188868] N92-11936

SOFTWARE TOOLS
User modeling techniques for enhanced usability of OPSMODEL operations simulation software [NASA-TM-4306] N92-11035
An RF interference mitigation methodology with potential applications in scheduling N92-11044
Range Scheduling Aid (RSA) N92-11057
Scheduling techniques in the Request Oriented Scheduling Engine (ROSE) N92-11058
Hardware and software tools for microprocessor functional test N92-11257
A microprocessor test approach allowing fault localisation N92-11261
Towards an automated system for the verification and diagnosis of intelligent VLSI circuits N92-11262
A method and tools for microprocessor validation: High safety function applications N92-11263
Modeling of visible and UV radiative transfer in the ocean-atmosphere system concepts, models, and programs N92-11396
A split-window method for obtaining crop temperatures N92-11410
Iterative procedures for atmospheric correction N92-11417
Continuation of research into language concepts for the mission support environment [NASA-CR-187818] N92-11652
Deploying expert systems in Ada [NASA-CR-188938] N92-11664
ART-Ada design project, phase 2 [NASA-CR-188940] N92-11667

SOIL EROSION
The use of imaging spectrometry in Mediterranean land degradation and soil erosion hazard assessments N92-11430

SOIL MOISTURE
Estimation of the ground humidity under vegetation: Applications of semi-empirical models N92-11445
Dual polarization microwave backscatter signatures of bare and vegetated soils N92-11452
Active microwave remote sensing and ground hydric state. Agriscatt '88 airborne campaign over the Orgeval basin (France) N92-11454
Evaluation of vegetation cover characteristics using an airborne microwave scatterometer N92-11456
Passive microwave remote sensing of soil moisture: Results from HAPEX, FIFE, and MONSOON 90 N92-11458
Comparison of passive microwave and model derived estimates for soil moisture fields N92-11459
Passive microwave remote sensing of vegetation canopies: Experimental and modeling results N92-11460
Airborne passive microwave remote sensing of land and water surface N92-11492
From evapotranspiration to soil moisture investigation based on NOAA thermal infrared data, case study: Poland N92-11531
Hourly and daily precipitation frequencies for the United States [AD-A240746] N92-11599

SOIL SCIENCE
The use of imaging spectrometry in Mediterranean land degradation and soil erosion hazard assessments N92-11430
Candidate high spectral resolution derivative indices for the prediction of crop cover N92-11435
Moisture effects on spectral signatures and CIE-color of lateritic soils N92-11436

SOILS
Simultaneous determination of six soil properties from the soil diffuse reflectance spectrum in the near infrared region (1-2.5 microns) N92-11424
High resolution spectral measurements of vegetation and soil in field and laboratory N92-11437
Influence of the viewing geometry on the spectral properties (high resolution visible and NIR) of selected soils from Arizona N92-11473
Normalization of multidirectional red and NIR reflectances with the SAVI N92-11477
Spectral reflectance of thin snow N92-11482
Evaluation of ground cover in agricultural environment by in situ measurements and multitemporal images for modeling hydric erosion N92-11528
View-atmosphere-soil effects on vegetation indices derived from SPOT images N92-11552
Field trip guidebook on environmental impact of clays along the upper Texas coast [NASA-TM-105097] N92-11572

SOLAR ACTIVITY
Development of a system for accurate forecasting of solar activity [AD-A240359] N92-11957

SOLAR ARRAYS
Development of a ninety string solar array simulator [NASA-TM-105278] N92-11086
Sensitivity of Space Station alpha joint robust controller to structural modal parameter variations [NASA-TM-104153] N92-11392
Lunar dust transport and potential interactions with power system components [NASA-CR-4404] N92-11951

SOLAR CELLS
Comments on dual-mode nuclear space power and propulsion system concepts N92-11106
Effect of particle size of Martian dust on the degradation of photovoltaic cell performance [NASA-TM-105232] N92-11133

SOLAR COLLECTORS
Today's central receiver power plant [DE91-017998] N92-11568

SOLAR CYCLES
Development of a system for accurate forecasting of solar activity [AD-A240359] N92-11957

SOLAR ENERGY
Photovoltaic energy system at an Alaskan site [PB91-201350] N92-11567
Lunar radiator shade [NASA-CASE-MSC-21868-1] N92-11639

SOLAR ENERGY CONVERSION
Today's central receiver power plant [DE91-017998] N92-11568

SOLAR GENERATORS
Comments on dual-mode nuclear space power and propulsion system concepts N92-11106
Today's central receiver power plant [DE91-017998] N92-11568

SOLAR MAGNETIC FIELD
Sunspot dynamics [NASA-CR-188978] N92-11955

SOLAR NEUTRINOS
OPAL opacities for astrophysical applications [DE91-016922] N92-11939
E sub 6 leptoquarks and the solar neutrino problem [NASA-CR-189005] N92-11956

SOLAR OBSERVATORIES
Spectral observations of solar radio bursts in the range of 2.0-4.5 GHz
[CAS-PUBL-76] N92-11953
Spectral observations of solar radio bursts at 2.0-4.5 GHz
[CAS-PUBL-77] N92-11954
SOLAR PHYSICS
Sunspot dynamics
[NASA-CR-188978] N92-11955
SOLAR PLANETARY INTERACTIONS
Electron distributions and solar wind interaction with nonmagnetic planets N92-11952
SOLAR PROMINENCES
Conditional climatology of Ap: The relationship between various solar events (surges, prominences, filaments, radio bursts, x ray episodes) and geomagnetic storms
[AD-A240457] N92-11958
SOLAR RADIO BURSTS
Spectral observations of solar radio bursts in the range of 2.0-4.5 GHz
[CAS-PUBL-76] N92-11953
Spectral observations of solar radio bursts at 2.0-4.5 GHz
[CAS-PUBL-77] N92-11954
SOLAR SPECTRA
Spectral observations of solar radio bursts in the range of 2.0-4.5 GHz
[CAS-PUBL-76] N92-11953
SOLAR WIND
ISEE/ICE plasma wave data analysis
[NASA-CR-189244] N92-11795
Electron distributions and solar wind interaction with nonmagnetic planets N92-11952
Activities report of the Max-Planck Institute for Aeronomy
[ETN-91-90233] N92-11964
SOLDERED JOINTS
Microstructural evolution during the thermomechanical fatigue of solder joints
[DE91-017309] N92-11372
SOLDERS
Microstructural evolution during the thermomechanical fatigue of solder joints
[DE91-017309] N92-11372
SOLID LUBRICANTS
Solid lubricants on pretreated surfaces
[NASA-CASE-LEW-14474-2] N92-11186
SOLID MECHANICS
Large deformation induced failures in nonlinear solids
[AD-A240369] N92-11382
SOLID PHASES
Cooling apparatus and couplings therefor
[NASA-CASE-ARC-11921-1] N92-11286
SOLID PROPELLANT ROCKET ENGINES
The 27th JANNAF Combustion Subcommittee Meeting, Volume 3
[CPIA-PUBL-557-VOL-3] N92-11117
Erosive augmentation of solid propellant burning rate: Motor size scaling effect N92-11125
SOLID PROPELLANTS
Erosive augmentation of solid propellant burning rate: Motor size scaling effect N92-11125
SOLID ROCKET PROPELLANTS
The 27th JANNAF Combustion Subcommittee Meeting, Volume 3
[CPIA-PUBL-557-VOL-3] N92-11117
SOLID STATE
Superionics
[AD-A240352] N92-11910
SOLID STATE DEVICES
Joint services electronics program research in electronics
[AD-A240155] N92-11274
SOLID-SOLID INTERFACES
Photoemission study of Ce/Ta(110) and Ce/W(110) interfaces and the catalytic oxidation effect
[DE91-018167] N92-11903
SOLIDIFICATION
Strengthening of an AISI 1020 steel by aluminum-microalloying during liquid dynamic compaction
[DE91-018745] N92-11182
SOLIDS
Large deformation induced failures in nonlinear solids
[AD-A240369] N92-11382
Synthesis of novel conducting solids
[AD-A240468] N92-11912
SOLITARY WAVES
On strong RF plasma turbulence N92-11836
Experiments and applications of soliton physics
[NIFS-32] N92-11877
SONIC BOOMS
A new simulator for assessing subjective effects of sonic booms
[NASA-TM-104150] N92-11759
A loudness calculation procedure applied to shaped sonic booms
[NASA-TP-3134] N92-11765
SOUND WAVES
Acoustic transponder receiver circuit
[AD-D014965] N92-11760
Wavefields near transverse cusp caustics produced by reflecting ultrasonic transients and tone bursts from curved surfaces
[AD-A240641] N92-11763
Compact optical RF spectrum analyzer
[AD-D014962] N92-11792
SOUNDING
Wing tip turbine: Analysis of the results of S2MA sounding of marginal vortex of the A320, technical summary
[ONERA-RTS-21/4365-AY-056A] N92-11009
SPACE COMMUNICATION
Space Network Control Conference on Resource Allocation Concepts and Approaches
[NASA-CP-3124] N92-11039
Effect of locus of resource control on operational efficiency in distributed operations N92-11046
A method for interference mitigation in space communications scheduling N92-11062
Error control techniques for satellite and space communications
[NASA-CR-188997] N92-11228
SPACE DEBRIS
MLITemp: A computer program to predict the thermal effects associated with hypervelocity impact damage to space station MLI
[NASA-CR-184245] N92-11079
SPACE EXPLORATION
Space year 1991: The complete record of the year's space events
[ISBN-0-87938-482-4] N92-11031
JPRS report: Science and technology. USSR: Space. Feoktistov's Views on Future Directions for Space Program
[JPRS-USP-91-005] N92-11032
Nuclear thermal propulsion workshop overview N92-11090
Enabling the space exploration initiative: NASA's exploration technology program in space power
[NASA-TM-4325] N92-11131
An overview of tested and analyzed NTP concepts
[NASA-TM-105252] N92-11137
Fusion energy for space missions in the 21st Century
[NASA-TM-4298] N92-11783
A bibliography of planetary geology and geophysics principal investigators and their associates, 1990-1991
[NASA-TM-4299] N92-11929
SPACE FLIGHT
Thermal verification testing of commercial printed-circuit boards for spaceflight
[NASA-TM-105261] N92-11221
SPACE INFRARED TELESCOPE FACILITY
The great observatories for space astrophysics
[NASA-NP-128] N92-11066
SPACE MISSIONS
Space year 1991: The complete record of the year's space events
[ISBN-0-87938-482-4] N92-11031
JPRS report: Science and technology. USSR: Space. Feoktistov's Views on Future Directions for Space Program
[JPRS-USP-91-005] N92-11032
Debris/ice/TPS assessment and photographic analysis for Shuttle Mission STS-43
[NASA-TM-103823] N92-11038
Space Network Control (SNC) Conference on Resource Allocation Concepts and Approaches. Overview N92-11040
What we were asked to do N92-11041
Concepts, requirements, and design approaches for building successful planning and scheduling systems N92-11042
Proposed planning and scheduling services for the SNC in the CDOS era N92-11043
Benefits of slush hydrogen for space missions
[NASA-TM-104503] N92-11214
SPACE PLASMAS
Power-law energy spectrum and orbital stochasticity
[DE91-017387] N92-11872
A simulation study of interactions of Space-Shuttle generated electron beams with ambient plasma and neutral gas
[NASA-CR-189025] N92-11898
SPACE PLATFORMS
Microgravity vibration isolation: An optimal control law for the one-dimensional case
[NASA-TM-105146] N92-11217
Mapping photopolarimeter spectrometer instrument feasibility study for future planetary flight missions
[NASA-CR-189242] N92-11329
Looking ahead to EOS: Update on NASA's Earth Observing Program N92-11556
SPACE POWER REACTORS
Nuclear safety N92-11114
Disposal methods N92-11116
Analytical study of nozzle performance for nuclear thermal rockets
[NASA-TM-105251] N92-11126
Enabling the space exploration initiative: NASA's exploration technology program in space power
[NASA-TM-4325] N92-11131
Fusion energy for space missions in the 21st Century
[NASA-TM-4298] N92-11783
SPACE PROGRAMS
JPRS report: Science and technology. USSR: Space. Feoktistov's Views on Future Directions for Space Program
[JPRS-USP-91-005] N92-11032
Enabling the space exploration initiative: NASA's exploration technology program in space power
[NASA-TM-4325] N92-11131
SPACE SHUTTLE MAIN ENGINE
Overview of the Beta II Two-Stage-To-Orbit vehicle design
[NASA-TM-105298] N92-11034
SPACE SHUTTLE MISSION 61-C
The microgravity environment of the Space Shuttle Columbia payload bay during STS-32
[NASA-TP-3141] N92-11931
SPACE SHUTTLE MISSIONS
Observations of the Earth in polarized light from the US Space Shuttle N92-11485
SPACE SHUTTLE PAYLOADS
A planning language for activity scheduling N92-11063
The microgravity environment of the Space Shuttle Columbia middeck during STS-32
[NASA-TP-3140] N92-11930
The microgravity environment of the Space Shuttle Columbia payload bay during STS-32
[NASA-TP-3141] N92-11931
SPACE SHUTTLES
Space year 1991: The complete record of the year's space events
[ISBN-0-87938-482-4] N92-11031
The Space Shuttle: An attempt at low-cost, routine access to space
[AD-A240589] N92-11037
Prediction of the pattern performance for the Aeroassist Flight Experiment (AFE) spacecraft
[NASA-CR-4409] N92-11065
Active vibration damping of the Space Shuttle remote manipulator system
[NASA-TM-104149] N92-11073
Catalog of space shuttle earth observations handheld photography. Space transportation system 37 (STS-37) mission dates: April 5-11, 1991
[NASA-CR-189014] N92-11561
A simulation study of interactions of Space-Shuttle generated electron beams with ambient plasma and neutral gas
[NASA-CR-189025] N92-11898
SPACE STATION FREEDOM
MLITemp: A computer program to predict the thermal effects associated with hypervelocity impact damage to space station MLI
[NASA-CR-184245] N92-11079
Development of a ninety string solar array simulator
[NASA-TM-105278] N92-11086
Evaluation of Kapton pyrolysis, arc tracking, and arc propagation on the Space Station Freedom (SSF) solar array Flexible Current Carrier (FCC)
[NASA-CR-189056] N92-11139
Television image compression and small animal remote monitoring
[NASA-CR-186614] N92-11223
Sensitivity of Space Station alpha joint robust controller to structural modal parameter variations
[NASA-TM-104153] N92-11392
SPACE STATION POLAR PLATFORMS
The performance of the ESA Medium Resolution Imaging Spectrometer (MERIS) N92-11422
SPACE STATIONS
User modeling techniques for enhanced usability of OPSMODEL operations simulation software
[NASA-TM-4306] N92-11035
Space station tracking requirements feasibility study, volume 2
[NASA-CR-185641-VOL-2] N92-11084
Space station tracking requirements feasibility study, volume 1
[NASA-CR-185641-VOL-1] N92-11085
SPACE TOOLS
Quick application/release nut with engagement indicator
[NASA-CASE-MSC-21799-1] N92-11359

SPACE TRANSPORTATION SYSTEM FLIGHTS
Debris/ice/TPS assessment and photographic analysis for Shuttle Mission STS-43
[NASA-TM-103823] N92-11038
SPACEBORNE EXPERIMENTS
Analysis of surfaces from the LDEF A0114, phase 4
[NASA-CR-188990] N92-11074
The interactions of atmospheric cosmogenic radionuclides with spacecraft surfaces N92-11075
The microgravity environment of the Space Shuttle Columbia middeck during STS-32
[NASA-TP-3140] N92-11930
The microgravity environment of the Space Shuttle Columbia payload bay during STS-32
[NASA-TP-3141] N92-11931
SPACEBORNE PHOTOGRAPHY
Catalog of space shuttle earth observations handheld photography. Space transportation system 37 (STS-37) mission dates: April 5-11, 1991
[NASA-CR-189014] N92-11561
SPACECRAFT ANTENNAS
Prediction of the pattern performance for the Aeroassist Flight Experiment (AFE) spacecraft
[NASA-CR-4409] N92-11065
SPACECRAFT CABIN ATMOSPHERES
Technical requirements of sick bays aboard space ships N92-11620
SPACECRAFT CABINS
Technical requirements of sick bays aboard space ships N92-11620
SPACECRAFT COMPONENTS
Quick trips to Mars N92-11111
SPACECRAFT CONSTRUCTION MATERIALS
Thermoviscoplastic response of Ti-15-3 under various loading conditions
[NASA-CR-187621] N92-11391
SPACECRAFT CONTROL
Attitude control of flexible structures
[AD-A240520] N92-11082
Multidisciplinary optimization of controlled space structures with global sensitivity equations
[NASA-TP-3130] N92-11087
Technology readiness assessment of advanced space engine integrated controls and health monitoring
[NASA-TM-105255] N92-11130
Sensitivity of Space Station alpha joint robust controller to structural modal parameter variations
[NASA-TM-104153] N92-11392
SPACECRAFT DESIGN
Prediction of forces and moments for hypersonic flight vehicle control effectors
[NASA-CR-188954] N92-11070
Multidisciplinary optimization of controlled space structures with global sensitivity equations
[NASA-TP-3130] N92-11087
Technical requirements of sick bays aboard space ships N92-11620
SPACECRAFT ENVIRONMENTS
Toxicity assessment of combustion products in simulated space cabins N92-11619
SPACECRAFT INSTRUMENTS
ISEE/ICE plasma wave data analysis
[NASA-CR-189244] N92-11795
SPACECRAFT LAUNCHING
The Space Shuttle: An attempt at low-cost, routine access to space
[AD-A240589] N92-11037
SPACECRAFT MAINTENANCE
Technology readiness assessment of advanced space engine integrated controls and health monitoring
[NASA-TM-105255] N92-11130
SPACECRAFT MOTION
Aerodynamic calculations related to tethered sub-satellite experiments
[NASA-CR-188964] N92-11071
The notion of artificial satellites in the anisotropic gravitational field of a uniformly rotating solid Earth model. A second order analytical solution
[SER-C-357] N92-11072
SPACECRAFT POWER SUPPLIES
Comments on dual-mode nuclear space power and propulsion system concepts N92-11106
Enabling the space exploration initiative: NASA's exploration technology program in space power
[NASA-TM-4325] N92-11131
Fusion energy for space missions in the 21st Century
[NASA-TM-4298] N92-11783
SPACECRAFT PROPULSION
Nuclear thermal propulsion program overview N92-11089
Quick trips to Mars N92-11111
Propulsion system needs N92-11112
Nuclear safety N92-11114
Disposal methods N92-11116
Plans for the development of cryogenic engines for space exploration
[NASA-TM-105250] N92-11135
Test facilities for high power electric propulsion
[NASA-TM-105247] N92-11136
Fusion energy for space missions in the 21st Century
[NASA-TM-4298] N92-11783
SPACECRAFT RADIATORS
Effects of anisotropic conduction and heat pipe interaction on minimum mass space radiators
[NASA-TM-105297] N92-11138
SPACECRAFT RELIABILITY
Technology readiness assessment of advanced space engine integrated controls and health monitoring
[NASA-TM-105255] N92-11130
SPACECRAFT STABILITY
Developmental flight testing of a half scale unmanned air vehicle
[AD-A240347] N92-11002
SPACECRAFT STRUCTURES
Analysis of surfaces from the LDEF A0114, phase 4
[NASA-CR-188990] N92-11074
The interactions of atmospheric cosmogenic radionuclides with spacecraft surfaces N92-11075
Multidisciplinary optimization of controlled space structures with global sensitivity equations
[NASA-TP-3130] N92-11087
SPACECRAFT TRACKING
Resource allocation planning helper (RALPH) N92-11047
Space station tracking requirements feasibility study, volume 2
[NASA-CR-185641-VOL-2] N92-11084
Space station tracking requirements feasibility study, volume 1
[NASA-CR-185641-VOL-1] N92-11085
SPACECREWS
User modeling techniques for enhanced usability of OPSMODEL operations simulation software
[NASA-TM-4306] N92-11035
SPATIAL DEPENDENCIES
Joint use of remote sensing and agricultural production estimation models: Current trends N92-11501
Study of the spatial variability of the hydrodynamic behavior of grounds at the Niger (Africa) using satellite images N92-11515
SPATIAL DISTRIBUTION
The effect of the distribution of chlorotic material on the reflectance of mixed canopies N92-11472
Spatial and spectral analysis of a degraded mangrove in south Senegal N92-11527
SPATIAL RESOLUTION
Texture indices sensitivity to spatial and spectral resolutions in semi-urban environments N92-11519
SPECIFIC HEAT
Heat exchanger thermal performance for two nonazeotropic refrigerant mixtures
[DE91-017250] N92-11216
SPECIFIC IMPULSE
Particle bed reactor nuclear rocket concept N92-11095
Liquid annulus N92-11104
Open cycle gas core nuclear rockets N92-11108
SPECIFICATIONS
Specification of difficult to test radar performance
[AD-A240398] N92-11232
SPECIMEN GEOMETRY
The effects of specimen geometry and size on the fracture toughness of nuclear graphites
[DE92-000056] N92-11205
SPECTRA
Total recall in distributive associative memories
[NASA-CR-188884] N92-11699
SPECTRAL EMISSION
Thermal infrared spectra of natural and manmade materials: Implications for remote sensing
[AD-A240455] N92-11564
Laser produced plasma soft x ray generation
[DE91-016925] N92-11874
SPECTRAL REFLECTANCE
Physical Measurements and Signatures in Remote Sensing, volume 1
[ESA-SP-319-VOL-1] N92-11394
Comparison of atmospheric correction procedures for visible and near-IR satellite sensor output N92-11395
Determination of the in-flight spectral and radiometric characteristics of the Airborne Visible/Infrared Imaging Spectrometer (AVIRIS) N92-11397
Use of operation ART-SPOT to test the 5S model and the MTF of the SPOT N92-11403
Comparison of in situ, aircraft- and satellite-derived surface reflectances in Flevoland (Netherlands) N92-11404
Inflight calibration of channels 1 and 2 of AVHRR using desertic sites and clouds N92-11406
Correction of atmospheric and topographic effects in LANDSAT TM images N92-11407
Suppression of aerosols on LANDSAT thematic mapper imagery N92-11411
Radiometric and atmospheric correction procedures for AVHRR preprocessing in the solar reflective channels N92-11414
On the nature of spectral shifts: Modeling and comparison to information contained in wide bands N92-11418
On the value of high spectral resolution measurements in the visible and near-infrared N92-11419
Use of high spectral resolution airborne visible/infrared imaging spectrometer data for geologic mapping: An overview N92-11420
Phenological changes in the red edge shift of Norway spruce needles and their relationship to needle chlorophyll content N92-11423
Simultaneous determination of six soil properties from the soil diffuse reflectance spectrum in the near infrared region (1-2.5 microns) N92-11424
Feasibility of the red edge index for the detection of nitrogen deficiency N92-11425
Multi-temporal monitoring of lake water quality N92-11426
Retrievals of column atmospheric water vapor, vegetation liquid water, and cloud cover fraction from AVIRIS data N92-11427
Spectral identification (1.2-2.5 microns) and characterization of Paris (France) Basin kaolinite/smectite clays using a field spectrometer N92-11429
The use of imaging spectrometry in Mediterranean land degradation and soil erosion hazard assessments N92-11430
The comparison of airborne imaging spectrometry and geochemical ground survey for the analysis of vegetation anomalies over waste deposits N92-11431
The spectral reflection behaviour of branches and branch components of healthy and damaged beech trees N92-11432
Evaluation of high spectral resolution laboratory reflectance data of healthy and damaged beech and spruce branches for the improvement of forest damage classification N92-11433
Modeling the behavior of a vegetation cover in the MIR, contribution of high spectral resolution N92-11434
Candidate high spectral resolution derivative indices for the prediction of crop cover N92-11435
Moisture effects on spectral signatures and CIE-color of lateritic soils N92-11436
High resolution spectral measurements of vegetation and soil in field and laboratory N92-11437
Influence of the crop architecture parameters on crop BRDF: A Monte Carlo simulation N92-11465
A three dimensional radiative transfer method for optical remote sensing of vegetated land surfaces N92-11466
The effect of the distribution of chlorotic material on the reflectance of mixed canopies N92-11472
Influence of the viewing geometry on the spectral properties (high resolution visible and NIR) of selected soils from Arizona N92-11473
Optimum combinations of visible and near-infrared reflectances for estimating the fraction of photosynthetically available radiation absorbed by plants N92-11474
Vegetation canopies and objects of arbitrary shapes: Computer generation and bidirectional reflectance calculations N92-11475
Normalization of multidirectional red and NIR reflectances with the SAVI N92-11477
Validation of a ground spectral and directional reflectance model N92-11479
Normalization of bidirectional effects of surface reflectance on a series of multitemporal NOAA/AVHRRR data N92-11480
Monte Carlo model for transport equation in a plant canopy and its inversion N92-11481
Spectral reflectance of thin snow N92-11482
Assessment of the effect of specular reflectance on the relationships between vegetation indices and biomass N92-11483
Specular and diffuse components of plant canopy reflectance at the wavelengths of 550 and 630 nm N92-11484
Calculating the bidirectional reflectance of natural vegetation covers using Boolean models and geometric optics N92-11486
ATLAS: An Auto-Tracking Land and Atmosphere Sensor for retrieval of atmospheric optical parameters and acquisition of bidirectional surface reflectance N92-11487
Physical Measurements and Signatures in Remote Sensing, volume 2
[ESA-SP-319-VOL-2] N92-11488
Synergistic use of multispectral satellite data for monitoring land surface change N92-11489

Joint use of remote sensing and agricultural production estimation models: Current trends N92-11501
Estimation of the primary production in Sahelian region from radiometric data N92-11504
Construction of ground cover charts of a wheat canopy from reflectance measurements N92-11505
An integrated modelling approach for the spectral identification of crops N92-11508
Spectral estimates of PAR interception and biomass production of irrigated rice crops. 2: Model validation with SPOT data N92-11510
Calibration and validation of a surface flux model in the framework of the HAPEX-MOBILHY experiment. Application to estimating the cover resistance N92-11511
The linking of crop growth models and multi-sensor remote sensing data N92-11512
Temporal signatures using NOAA-AVHRR and land use mapping N92-11513
Simulation study of vegetation indices sensitivity using the middle infrared N92-11514
Study of the spatial variability of the hydrodynamic behavior of grounds at the Niger (Africa) using satellite images N92-11515
Structural controls on the remotely sensed response of a coniferous forest plantation N92-11516
Database of SPOT histrograms N92-11517
Spectral estimates of PAR interception and biomass production of irrigated rice crops. 1: Model elaboration with ground data N92-11522
Analysis of the surface state of two sub-polar glaciers using SPOT data and a numerical terrain model N92-11523
Spatial and spectral analysis of a degraded mangrove in south Senegal N92-11527
CO2 laser active remote sensing from 9 to 11 microns: Airborne and laboratory application N92-11535
Thermal infrared spectra of natural and manmade materials: Implications for remote sensing [AD-A240455] N92-11564
Surface optical property measurements on bark and leaf samples [AD-A240714] N92-11566

SPECTRAL RESOLUTION

On the nature of spectral shifts: Modeling and comparison to information contained in wide bands N92-11418
On the value of high spectral resolution measurements in the visible and near-infrared N92-11419
Use of high spectral resolution airborne visible/infrared imaging spectrometer data for geologic mapping: An overview N92-11420
Space observation of the land-ocean-atmosphere system at high spectral resolution in the infrared: Perspectives and problems N92-11421
The performance of the ESA Medium Resolution Imaging Spectrometer (MERIS) N92-11422
Evaluation of high spectral resolution laboratory reflectance data of healthy and damaged beech and spruce branches for the improvement of forest damage classification N92-11433
Modeling the behavior of a vegetation cover in the MIR, contribution of high spectral resolution N92-11434
Candidate high spectral resolution derivative indices for the prediction of crop cover N92-11435
Preliminary results of a spectro-imagery experiment (GER) over the Adriatic coastline of the Venice lagoon N92-11440
Texture indices sensitivity to spatial and spectral resolutions in semi-urban environments N92-11519
Design and testing of a spectral-resolving fluorescence lidar system for remote sensing of vegetation N92-11540

SPECTRAL SENSITIVITY

Investigation of the stability of the spectral responsitivity of silicon photodiodes [NPL-QU-87] N92-11184
On the nature of spectral shifts: Modeling and comparison to information contained in wide bands N92-11418

SPECTRAL SIGNATURES

Physical Measurements and Signatures in Remote Sensing, volume 1 [ESA-SP-319-VOL-1] N92-11394
A multi-sensor approach to spectral signature analysis of inland waters N92-11426
The comparison of airborne imaging spectrometry and geochemical ground survey for the analysis of vegetation anomalies over waste deposits N92-11431
The spectral reflection behaviour of branches and branch components of healthy and damaged beech trees N92-11432
Evaluation of high spectral resolution laboratory reflectance data of healthy and damaged beech and spruce branches for the improvement of forest damage classification N92-11433
Moisture effects on spectral signatures and CIE-color of lateritic soils N92-11436
High resolution spectral measurements of vegetation and soil in field and laboratory N92-11437
Preliminary results of a spectro-imagery experiment (GER) over the Adriatic coastline of the Venice lagoon N92-11440
Experimental approach to emissivity problems and surface temperature in thermal infrared remote sensing N92-11462
The effect of the distribution of chlorotic material on the reflectance of mixed canopies N92-11472
Influence of the viewing geometry on the spectral properties (high resolution visible and NIR) of selected soils from Arizona N92-11473
Physical Measurements and Signatures in Remote Sensing, volume 2 [ESA-SP-319-VOL-2] N92-11488
Spectral estimates of PAR interception and biomass production of irrigated rice crops. 2: Model validation with SPOT data N92-11510
Temporal signatures using NOAA-AVHRR and land use mapping N92-11513
Multidate analysis of NOAA-AVHRR data over France: Relationship with agroclimatic characteristics N92-11521
Study of the spatial signature of forest covers by geometric-optic modeling N92-11530
CO2 laser active remote sensing from 9 to 11 microns: Airborne and laboratory application N92-11535

SPECTROGRAPHS

A calibration of the Naval Postgraduate School middle ultraviolet spectrograph and an analysis of the OII 2470 A and OI 2972 A emissions obtained from mid-latitude rocket observations [AD-A240686] N92-11587

SPECTROMETERS

Mapping photopolarimeter spectrometer instrument feasibility study for future planetary flight missions [NASA-CR-189242] N92-11329
Influence of the viewing geometry on the spectral properties (high resolution visible and NIR) of selected soils from Arizona N92-11473

SPECTRORADIOMETERS

ATLAS: An Auto-Tracking Land and Atmosphere Sensor for retrieval of atmospheric optical parameters and acquisition of bidirectional surface reflectance N92-11487
The UK Natural Environment Research Council Equipment Pool for Field Spectroscopy (NERC-EPFS) N92-11558
Thermal infrared spectra of natural and manmade materials: Implications for remote sensing [AD-A240455] N92-11564

SPECTROSCOPIC ANALYSIS

Spectroscopic analysis of imaging spectrometer data for classification purposes N92-11439

SPECTROSCOPY

High resolution spectral measurements of vegetation and soil in field and laboratory N92-11437
Near-infrared imaging spectroscopy: Learning from planetary geology N92-11438
Laser-induced spectral signatures in investigations of sea upper layer N92-11537
Time-resolved spectroscopy of the blue fluorescence of spinach leaves N92-11538
Observation of DOM composition by synchronous fluorescence spectroscopy N92-11549
The UK Natural Environment Research Council Equipment Pool for Field Spectroscopy (NERC-EPFS) N92-11558

SPECTRUM ANALYSIS

Physical Measurements and Signatures in Remote Sensing, volume 1 [ESA-SP-319-VOL-1] N92-11394
Comparison of atmospheric correction procedures for visible and near-IR satellite sensor output N92-11395
Atmospheric correction of satellite borne imagery investigated by means of a sensitivity analysis of the entire remote sensing process N92-11400
Characterization of African desert sites for the relative calibrating of wide field satellite optical sensors N92-11402
Inflight calibration of channels 1 and 2 of AVHRR using desertic sites and clouds N92-11406
Correction of atmospheric and topographic effects in LANDSAT TM images N92-11407
Evaluation of atmospheric effects in high spectral resolution airborne images N92-11408
SPOT calibration on the test site La Crau (France) N92-11409
Space observation of the land-ocean-atmosphere system at high spectral resolution in the infrared: Perspectives and problems N92-11421
Complementarity of temperature independent Thermal Infrared Spectral Indices (TISI) and NDVI: Compared properties and combined use for soil and vegetation discrimination N92-11490
NOAA-AVHRR contribution to the analysis or urban heat islands N92-11495
Spectral estimates of PAR interception and biomass production of irrigated rice crops. 2: Model validation with SPOT data N92-11510
Spatial and spectral analysis of a degraded mangrove in south Senegal N92-11527
Wavelength shifts in fluorescence maxima of stressed and non-stressed Norway spruce needles over the growing season N92-11536
Time-resolved spectroscopy of the blue fluorescence of spinach leaves N92-11538
The laser-induced chlorophyll fluorescence ratio F690/F735 of spruce needles and beech leaves during the course of a year N92-11542
A calibration of the Naval Postgraduate School middle ultraviolet spectrograph and an analysis of the OII 2470 A and OI 2972 A emissions obtained from mid-latitude rocket observations [AD-A240686] N92-11587
Compact optical RF spectrum analyzer [AD-D014962] N92-11792
Report on carbon and nitrogen abundance studies [NASA-CR-188803] N92-11934

SPECULAR REFLECTION

Assessment of the effect of specular reflectance on the relationships between vegetation indices and biomass N92-11483
Specular and diffuse components of plant canopy reflectance at the wavelengths of 550 and 630 nm N92-11484
Quantitative ray methods for scattering of sound by spherical shells [AD-A240255] N92-11761

SPEECH

Learning to read aloud: A neural network approach using sparse distributed memory [NASA-CR-188846] N92-11711

SPEECH RECOGNITION

An efficient A* stack decoder algorithm for continuous speech recognition with a stochastic language model [AD-A240745] N92-11683

SPHERICAL SHELLS

Quantitative ray methods for scattering of sound by spherical shells [AD-A240255] N92-11761
Scattering of tone bursts from spherical shells: Computations based on Fourier transform method [AD-A240642] N92-11764

SPIN REDUCTION

Precision pointing control of the spinning Gravity Probe B spacecraft N92-11068

SPINACH

Time-resolved spectroscopy of the blue fluorescence of spinach leaves N92-11538

SPLITTING

Operator splitting, fractional steps, method and entropy condition for nonlinear hyperbolic systems N92-11719

SPOT (FRENCH SATELLITE)

Inter-calibrating of SPOT1-HRV, LANDSAT5-TM, and NOA11-AVHRR in the visible and near infrared field s N92-11401
Database of SPOT histrograms N92-11517
Modeling temporal evolution of the radiometric response measured by wideband sensors over temperate agricultural regions N92-11518
View-atmosphere-soil effects on vegetation indices derived from SPOT images N92-11552
Neotectonic studies of northern Baja California, Mexico, with LANDSAT thematic mapper and SPOT panchromatic imagery: Partitioning of dextral and extensional strain at the Pacific-North America plate boundary N92-11553
Use of multitemporal SPOT data in first ISLSCP field experiment N92-11554

SPRAYED COATINGS

Strengthening of an AISI 1020 steel by aluminum-microalloying during liquid dynamic compaction [DE91-018745] N92-11182

SPREAD SPECTRUM TRANSMISSION

The probability of multiple correct packet receptions in a multireceiver frequency-hopped spread-spectrum system [AD-A240655] N92-11240

SPUTTERING

Ultra high vacuum sputtering system [AD-A240157] N92-11176
ITER divertor sputtering erosion: Recent analysis for carbon, beryllium, tungsten, and niobium surfaces [DE91-017235] N92-11871

STABILITY
Dispersion and stability of two electromagnetic solvers for triangular meshes
[DE91-016607] N92-11227
Geometrically exact shells models: Foundation and computational aspects with special reference to implicit large-scale calculations
[DE91-019014] N92-11390
Second stability studies in a helical axis device: TJ-II N92-11807

STABILITY DERIVATIVES
Experimental study of an independently deflected wingtip mounted on a semispan wing
[NASA-TM-102842] N92-10983

STAINLESS STEELS
Propagation behavior of small cracks in 304 stainless steel under biaxial low-cycle fatigue at elevated temperature
[DE91-018863] N92-11389

STANDARD DEVIATION
First-passage problems: A probabilistic dynamic analysis for degraded structures
[NASA-TM-103755] N92-11373
Circular Statistical methods: Applications in spatial and temporal performance analysis
[AD-A240751] N92-11749

STANDARDIZATION
Open document processing and the ISOTEXT system
[ETN-91-90160] N92-11928

STANDARDS
Technique for calibrating angular measurement devices when calibration standards are unavailable
[NASA-TM-104148] N92-11340
Development of data file standards for automated ultrasonic scanning systems. Exchange methods for digital ultrasonic inspection data
[AD-A240075] N92-11364
Intercomparison of the medium energy primary standards for x ray exposure of NPL and ENEA, Italy
[NPL-RSA(EXT)-18] N92-11766
Intercomparison of the low energy primary standards for x ray exposure of NPL and ENEA, Italy
[NPL-RSA(EXT)-19] N92-11767

STAR TRACKERS
Stray light reduction in a WFOV star tracker lens
[DE91-018460] N92-11794

STATIC DEFORMATION
Calculation of general shells of revolution, using a semi analytical process
[ILR-MITT-262(1991)] N92-11386

STATISTICAL ANALYSIS
Land cover classification by multipolarized SAR imagery N92-11457
Large scale study of the microwave signature of the Antarctic ice sheet N92-11463
A study on the effects of Mt. Sakurajima's falling ash over crop and forest areas using image processing for LANDSAT-5, MOS-1, and Jafsa digital data N92-11497
Actual daily evapotranspiration monitoring using NOAA-AVHRR data from the HAPEX-MOBILHY campaigns N92-11509
Multidate analysis of NOAA-AVHRR data over France: Relationship with agroclimatic characteristics N92-11521
Spectral estimates of PAR interception and biomass production of irrigated rice crops. 1: Model elaboration with ground data N92-11522
Spatial and spectral analysis of a degraded mangrove in south Senegal N92-11527
Detection and characterization of active fires in west Africa with LANDSAT thematic mapper and NOAA N92-11529
Statistical prediction with Kanerva's sparse distributed memory
[NASA-CR-187314] N92-11743
Tables of square-law signal detection statistics for Hann spectra with 50 percent overlap
[NASA-TM-103830] N92-11745
Assignment of single values to probability intervals, evaluation of conditional events, and applications to combination of evidence
[AD-A240258] N92-11747

STATISTICAL CORRELATION
Power-law energy spectrum and orbital stochasticity
[DE91-017387] N92-11872

STEADY STATE
Measurement of frequency response in short thermocouple wires
[NASA-CR-187821] N92-11339
TEGEN: A one dimensional program to calculate a thermoelectric generator
[DE91-634444] N92-11571

STEAM
Today's central receiver power plant
[DE91-017998] N92-11568

STEEL STRUCTURES
The behaviour of fire-exposed composite steel/concrete slabs
[ISBN-90-386-0031-3] N92-11147

STEELS
Strengthening of an AISI 1020 steel by aluminum-microalloying during liquid dynamic compaction
[DE91-018745] N92-11182

STEERABLE ANTENNAS
Programmable beam transform and beam steering control system for a phased array radar antenna
[AD-D014970] N92-11230

STELLAR EVOLUTION
Report on carbon and nitrogen abundance studies
[NASA-CR-188803] N92-11934
Converting neutron stars into strange stars
[NASA-CR-189008] N92-11945
Neutron star magnetic fields and implications for pulsars and gamma ray bursts N92-11960

STELLAR LUMINOSITY
Report on carbon and nitrogen abundance studies
[NASA-CR-188803] N92-11934

STELLAR MAGNETIC FIELDS
Neutron star magnetic fields and implications for pulsars and gamma ray bursts N92-11960

STELLAR MAGNETOSPHERES
Neutron star magnetic fields and implications for pulsars and gamma ray bursts N92-11960

STELLAR SPECTRA
Report on carbon and nitrogen abundance studies
[NASA-CR-188803] N92-11934

STELLAR STRUCTURE
Converting neutron stars into strange stars
[NASA-CR-189008] N92-11945

STELLARATORS
On radial electric field structure in CHS torsatron/heliotron
[NIFS-94] N92-11796
Influence of fast ion loss on radial electric field in Wendelstein 7-A stellarator
[NIFS-95] N92-11797
Proceedings of the First International Toki Conference on Plasma Physics and Controlled Nuclear Fusion: Next Generation Experiments in Helical Systems
[NIFS-PROC-3] N92-11799
Status of the Wendelstein VII-X Project N92-11801
Overview of the ATF-II studies N92-11802
The ANU Heliac Program N92-11804
Design of the compact Auburn torsatron N92-11805
Optimization of Helias configurations N92-11806
Second stability studies in a helical axis device: TJ-II N92-11807
Resistive MHD stability studies for ATF plasmas during operation in the second stability regime N92-11809
Plasma transport in advanced stellarators N92-11811
Effects of perturbing helical fields on confinement of Heliotron DR plasma N92-11818
Status of the Torsatron/Stellarator Program N92-11821
Experimental studies of a helical axis stellarator (TU-Heliac) N92-11824
Diverted particle-flux studies in the IMS and Proto-Cleo stellarators N92-11825
Pressure and potential measurements in IMS during electron cyclotron heating N92-11826
Dissipative trapped electron modes in l = 2 torsatrons N92-11830
Low-n stability calculations for three dimensional stellarator configurations N92-11831
Island studies for Helias Configurations N92-11835
Structural design of large helical device N92-11837
Research and development of forced flow superconducting coils for large helical device N92-11838
Pool-cooled superconducting magnet design of large helical device N92-11839
Behavior of vacuum vessel eddy current in large helical device N92-11840
Fundamental design on LHD with bath cooling method N92-11841
A compact helical device for a superconducting large helical coil N92-11842
Optimization of design parameters for large helical device N92-11843
Effect of multi-layer operation of helical coil in large helical device N92-11844
ECH system in the large helical device N92-11845
ICRF heating program of the large helical device N92-11846
Equilibrium, stability, and transport in L = 1 compact helical axis configuration N92-11848
Electron temperature measurements on ATF using electron cyclotron emission N92-11849
A possible modification of the FT Tokamak into a compact high field stellarator with separatrices N92-11863
Overview of engineering design of Wendelstein VII-X N92-11868

STEP FUNCTIONS
Operator splitting, fractional steps, method and entropy condition for nonlinear hyperbolic systems N92-11719

STIFFNESS MATRIX
On the symbolic manipulation and code generation for elasto-plastic material matrices
[NASA-CR-187223] N92-11375

STOCHASTIC PROCESSES
An efficient A* stack decoder algorithm for continuous speech recognition with a stochastic language model
[AD-A240745] N92-11683
Power-law energy spectrum and orbital stochasticity
[DE91-017387] N92-11872

STOICHIOMETRY
Alloy modeling and experimental correlation for ductility enhancement in near stoichiometric single crystal nickel aluminide
[AD-A240151] N92-11175
Polyimides with improved compression moldability
[NASA-CASE-LAR-14457-1-CU] N92-11198
Numerical simulations of detonation transmission
[AD-A240560] N92-11304

STORAGE BATTERIES
Nonaqueous secondary batteries
[DE91-017788] N92-11282

STORAGE STABILITY
Investigation of the stability of the spectral responsitivity of silicon photodiodes
[NPL-QU-87] N92-11184

STORMS (METEOROLOGY)
Mariners Weather Log, Volume 35, Number 2, Spring 1991
[PB91-202572] N92-11592

STRAIN HARDENING
Creep response of a 9Cr-1Mo-V-Nb steel to varying stresses and temperatures
[DE91-017871] N92-11181

STRAIN RATE
Deformation of isodamp (A polyvinyl chloride-based elastomer) at various loading rates
[AD-A240393] N92-11189

STRAKES
Experimental investigation of the effects of blowing on bursting of strake vortices
[AD-A240256] N92-10985

STRANGENESS
Converting neutron stars into strange stars
[NASA-CR-189008] N92-11945

STRATIGRAPHY
Spectral identification (1.2-2.5 microns) and characterization of Paris (France) Basin kaolinite/smectite clays using a field spectrometer N92-11429

STRATOSPHERE
Scientific assessment of stratospheric ozone: 1989, volume 1
[NASA-TM-105116] N92-11576
Scientific assessment of stratospheric ozone: 1989. Volume 2: Appendix: AFEAS report
[NASA-TM-105117] N92-11577

STRESS ANALYSIS
Alloy modeling and experimental correlation for ductility enhancement in near stoichiometric single crystal nickel aluminide
[AD-A240151] N92-11175
High pressure turbine blade life extension
[AD-A240654] N92-11180
Creep response of a 9Cr-1Mo-V-Nb steel to varying stresses and temperatures
[DE91-017871] N92-11181
On the basic equations for the second-order modeling of compressible turbulence
[NASA-TM-105277] N92-11302
Advanced stress analysis methods applicable to turbine engine structures
[NASA-CR-187235] N92-11378

STRESS CORROSION CRACKING
A probabilistic model of intergranular stress corrosion cracking
[DE91-017986] N92-11173

STRESS DISTRIBUTION
Determination of nonstationary temperatures in high-stressed elements with pulsed heat sources
[DE91-635705] N92-11325

STRESS RELAXATION
Effects of elevated temperature on the viscoplastic modeling of graphite/polymeric composites
[NASA-TM-104160] N92-11149
Effects of hydrogen and carbon on thermally activated deformation in nickel
[AD-A240496] N92-11178

STRESS-STRAIN RELATIONSHIPS
Effects of elevated temperature on the viscoplastic modeling of graphite/polymeric composites
[NASA-TM-104160] N92-11149
High pressure turbine blade life extension
[AD-A240654] N92-11180
Analysis of strain dependent damping in materials via modeling of material point hysteresis
[AD-A240298] N92-11381
Limit pressure of a circumferentially reinforced SiC/Ti ring
[NASA-CR-187211] N92-11387
STRESSES
Fracture toughness of carbon/carbon composites
[AD-A240200] N92-11143
Deformation of isodamp (A polyvinyl chloride-based elastomer) at various loading rates
[AD-A240393] N92-11189
STRING THEORY
Perturbations from strings don't look like strings!
[NASA-CR-189012] N92-11941
Superfluid-like turbulence in cosmology
[NASA-CR-189011] N92-11942
On the evolution of a superconducting cosmic string network
[DE91-630995] N92-11948
STRINGERS
Buckling values and optimization of carbon fiber reinforced compression chord plates with rectangular stringers
[ILR-MITT-259(1991)] N92-11148
STRONG INTERACTIONS (FIELD THEORY)
Theoretical interpretation of high-energy nuclear collisions
[DE91-016965] N92-11782
STRUCTURAL ANALYSIS
Development of a reliability-based method for evaluating a pavement feature
[AD-A240747] N92-11366
Slave finite element for non-linear analysis of engine structures. Volume 2: Programmer's manual and user's manual
[NASA-CR-187225] N92-11388
User's manual for the Macintosh version of PASCO
[NASA-TM-104115] N92-11668
STRUCTURAL BASINS
Active microwave remote sensing and ground hydric state. Agriscatt '88 airborne campaign over the Orgeval basin (France) N92-11454
STRUCTURAL DESIGN
Comparison of a new refiner with a conventional refiner N92-11156
Engineering design of large helical device N92-11864
Operation scenario and structural design analysis of LHD (Large Helical Device) coils N92-11865
Engineering design of LHD vacuum vessel N92-11866
Development of superconductor for large helical device N92-11867
STRUCTURAL ENGINEERING
Index and bulk parameters for frequency-direction spectra measured at CERC field research facility
[AD-A240320] N92-11607
STRUCTURAL FAILURE
Developmental flight testing of a half scale unmanned air vehicle
[AD-A240347] N92-11002
STRUCTURAL MEMBERS
Method of recertifying a loaded bearing member using a phase point
[NASA-CASE-LAR-14741-1] N92-11384
STRUCTURAL PROPERTIES (GEOLOGY)
Integration of Seasat and SPOT data, contribution to structural geology mapping in temperature environment N92-11499
STRUCTURAL RELIABILITY
First-passage problems: A probabilistic dynamic analysis for degraded structures
[NASA-TM-103755] N92-11373
STUDENTS
The development of Behaviorally Anchored Rating Scales (BARS) for evaluating USAF pilot training performance
[AD-A239969] N92-11630
SUBJECTS
Magnetic suspension and balance systems: A comprehensive, annotated bibliography
[NASA-TM-4318] N92-11030
SUBMILLIMETER WAVES
Infrared to millimetre observations of active galaxies N92-11932
SUBROUTINE LIBRARIES (COMPUTERS)
LAPACK: Linear algebra software for supercomputers
[DE91-017316] N92-11660
SUBROUTINES
Computer program for Bessel and Hankel functions
[NASA-TM-105154] N92-11691
SUBSONIC WIND TUNNELS
Subsonic wind tunnel testing handbook
[AD-A240263] N92-10986
SUBSTRATES
High-T sub c fluorine-doped YBa2Cu3O(y) films on ceramic substrates by screen printing
[NASA-TM-105296] N92-11188
SULFONES
Improved compression molding technology for continuous fiber reinforced composite laminates. Part 2: AS-4/Polyimidesulfone prepreg system
[NASA-TM-104133] N92-11207
SULFUR FLUORIDES
Discharge system tests of Halon 1301 test gas simulants
[AD-A240679] N92-11193
SUN
Sunspot dynamics
[NASA-CR-188978] N92-11955
E sub 6 leptoquarks and the solar neutrino problem
[NASA-CR-189005] N92-11956
Conditional climatology of Ap: The relationship between various solar events (surges, prominences, filaments, radio bursts, x ray episodes) and geomagnetic storms
[AD-A240457] N92-11958
SUNLIGHT
Lunar radiator shade
[NASA-CASE-MSC-21868-1] N92-11639
SUNSPOTS
Sunspot dynamics
[NASA-CR-188978] N92-11955
SUPERCOMPUTERS
LAPACK: Linear algebra software for supercomputers
[DE91-017316] N92-11660
Highly parallel computation
[NASA-CR-188871] N92-11698
SUPERCONDUCTING MAGNETS
Structural design of large helical device N92-11837
Research and development of forced flow superconducting coils for large helical device N92-11838
Pool-cooled superconducting magnet design of large helical device N92-11839
Fundamental design on LHD with bath cooling method N92-11841
A compact helical device for a superconducting large helical coil N92-11842
Optimization of design parameters for large helical device N92-11843
Effect of multi-layer operation of helical coil in large helical device N92-11844
Engineering design of large helical device N92-11864
Operation scenario and structural design analysis of LHD (Large Helical Device) coils N92-11865
Development of superconductor for large helical device N92-11867
Overview of engineering design of Wendelstein VII-X N92-11868
SUPERCONDUCTING SUPER COLLIDER
BCD/CPS: An event-level GEANT3 parallelization via CPS
[DE91-017238] N92-11703
SUPERCONDUCTIVITY
Physics of ultrasmall superconducting circuits
[AD-A240156] N92-11275
Control of electron transfer rates by motions of atoms and molecules
[DE91-018575] N92-11777
Development of high Tc (greater than 110K) Bi, Tl and Y-based materials as superconducting circuit elements
[NASA-CR-188999] N92-11902
Synthesis of novel conducting solids
[AD-A240468] N92-11912
Vortex-lattice states of a two-dimensional electron system at strong magnetic fields
[DE91-018551] N92-11916
On the evolution of a superconducting cosmic string network
[DE91-630995] N92-11948
SUPERCONDUCTORS
Polarized x ray absorption spectroscopy for the study of superconductors and magnetic materials
[DE91-017990] N92-11163
Physics of ultrasmall superconducting circuits
[AD-A240156] N92-11275
Development of superconductor for large helical device N92-11867
Development of high Tc (greater than 110K) Bi, Tl and Y-based materials as superconducting circuit elements
[NASA-CR-188999] N92-11902
SUPERCRITICAL PRESSURES
Development of an experimental database and theories for prediction of thermodynamic properties of aqueous electrolytes and nonelectrolytes of geochemical significance at supercritical temperatures and pressures
[DE91-018493] N92-11169
SUPERFLUIDITY
Bose-condensation in liquid helium under pressure
[DE91-634504] N92-11170
Superfluid helium dynamics
[NASA-CR-188814] N92-11294
Critical velocities and mutual friction in He-3-He-4 II mixtures at temperatures below 100 mK
[ETN-91-90132] N92-11314
Gorter-Mellink pulsed-source problem in cylindrical and spherical geometry
[DE91-017249] N92-11725
Critical properties of strongly interacting bosons on a lattice
[DE91-016926] N92-11771
Comparative study of final state interaction contributions to the dynamic response of quantum fluids
[DE91-631020] N92-11892
Superfluid-like turbulence in cosmology
[NASA-CR-189011] N92-11942
SUPERNOVAE
Effects of the equation of state in neutron stars and in stellar collapse
[DE91-014534] N92-11935
SUPERSONIC COMBUSTION RAMJET ENGINES
Viscous computations of cold air/air flow around scramjet nozzle afterbody
[NASA-CR-4406] N92-10982
SUPERSONIC FLOW
LV software support for supersonic flow analysis
[NASA-CR-188914] N92-10978
Unsteady aerodynamic calculations for general configurations by the double-point method
[NAL-TR-1101T] N92-10980
Numerical resolution of three dimensional Euler equations in totally unstructured mesh
[CERT-RF-1/3369-00/DERI-GAN] N92-10988
A detailed investigation of staged normal injection into a Mach 2 flow N92-11118
SUPERSONIC INLETS
Results from computational analysis of a mixed compression supersonic inlet
[NASA-TM-104475] N92-10976
SUPERSONIC TRANSPORTS
A loudness calculation procedure applied to shaped sonic booms
[NASA-TP-3134] N92-11765
SUPPORT SYSTEMS
Pilot's Automated Weather Support System (PAWSS) concepts demonstration project. Phase 1: Pilot's weather information requirements and implications for weather data systems design
[NASA-CR-188228] N92-11593
Continuation of research into language concepts for the mission support environment
[NASA-CR-187818] N92-11652
SURFACE FINISHING
The design of broadband radar absorbing surfaces
[AD-A240521] N92-11235
SURFACE LAYERS
Oxidation of titanium aluminide and its XD composite
[AD-A240401] N92-11177
SURFACE PROPERTIES
Analysis of surfaces from the LDEF A0114, phase 4
[NASA-CR-188990] N92-11074
Solid lubricants on pretreated surfaces
[NASA-CASE-LEW-14474-2] N92-11186
Bidirectional reflectance and surface albedo: Physical modeling and inversion N92-11469
Study of the spatial variability of the hydrodynamic behavior of grounds at the Niger (Africa) using satellite images N92-11515
Analysis of the surface state of two sub-polar glaciers using SPOT data and a numerical terrain model N92-11523
Surface optical property measurements on bark and leaf samples
[AD-A240714] N92-11566
Computer aided surface representation
[DE91-018872] N92-11688
Confinement studies of Heliotron E plasmas in magnetic surface variation experiments N92-11850
SURFACE REACTIONS
Drag coefficients with applications to satellite orbits N92-11069
The interactions of atmospheric cosmogenic radionuclides with spacecraft surfaces N92-11075
Reciprocity theory of gas surface interactions
[IC-AERO-89-04] N92-11289

Photon stimulated desorption of neutral species from aluminum
[DE91-017004] N92-11784

SURFACE ROUGHNESS
Measurements of erosion characteristics for metal and polymer surfaces using profilometry N92-11077
Radar image simulation to study the visual aptitude of observing slope and roughness effects N92-11446
Influence of the viewing geometry on the spectral properties (high resolution visible and NIR) of selected soils from Arizona N92-11473

SURFACE TEMPERATURE
Atmospheric correction in the thermal infrared: AVHRR case N92-11398
A split-window method for obtaining crop temperatures N92-11410
TIMS calibration correction by comparison with PRT5 N92-11412
Experimental approach to emissivity problems and surface temperature in thermal infrared remote sensing N92-11462
Synergistic use of multispectral satellite data for monitoring land surface change N92-11489
Complementarity of temperature independent Thermal Infrared Spectral Indices (TISI) and NDVI: Compared properties and combined use for soil and vegetation discrimination N92-11490
Combined use of Earth observation satellite and meteorological satellite for crop assessment in semiarid environments N92-11494
Using the radiative surface temperature in energy budget studies over plant canopies N92-11506
Contribution of NOAA-AVHRR satellite data in forest vegetation monitoring N92-11520
Multidate analysis of NOAA-AVHRR data over France: Relationship with agroclimatic characteristics N92-11521

SURFACE TREATMENT
Non-equilibrium microstructures produced during electron-beam and laser-beam surface modification of metallic alloys
[DE91-018466] N92-11174
Photon stimulated desorption of neutral species from aluminum
[DE91-017004] N92-11784

SURFACE WAVES
Measurement of turbulent flow beneath the wind wave induced water surface, using picture repetition analysis
[ETN-91-90203] N92-11316
Quantitative ray methods for scattering of sound by spherical shells
[AD-A240255] N92-11761
Compact optical RF spectrum analyzer
[AD-D014962] N92-11792

SURGES
Conditional climatology of Ap: The relationship between various solar events (surges, prominences, filaments, radio bursts, x ray episodes) and geomagnetic storms
[AD-A240457] N92-11958

SURVEYOR 3 LUNAR PROBE
Lunar dust transport and potential interactions with power system components
[NASA-CR-4404] N92-11951

SURVEYS
CFD code survey for thrust chamber application N92-11119
Aerothermal test results from the first flight of the Pegasus air-launched space booster
[NASA-TM-4330] N92-11301
Circular Statistical methods: Applications in spatial and temporal performance analysis
[AD-A240751] N92-11749

SWIRLING
Direct-contact heat exchanger for swirling countercurrent flow of hot gas and finely divided solids: A parametric study
[DE91-017229] N92-11291
Heat transfer in channels with uniformly swirled flow
[DE91-635594] N92-11324

SWITCHES
Multiple beam antenna/switch system study
[NASA-CR-183496] N92-11251

SYMBOLIC PROGRAMMING
On the symbolic manipulation and code generation for elasto-plastic material matrices
[NASA-CR-187223] N92-11375

SYMMETRY
Optimization of Helias configurations N92-11806

SYNAPSES
Long term synaptic plasticity and learning in neuronal networks
[AD-A240366] N92-11613

SYNCHRONISM
Convergence and performance of synchronous and asynchronous parallel and conventional iterative methods
[AD-A240286] N92-11707
A synchronization and charge distribution process for the parallel multilevel logic simulation
[ETN-91-90152] N92-11708
About time
[NASA-CR-188870] N92-11753
An application for multi-person task synchronization
[NASA-CR-187712] N92-11918

SYNCHRONOUS SATELLITES
The science benefits of and the antenna requirements for microwave remote sensing from geostationary orbit
[NASA-CR-4408] N92-11559

SYNCHROTRON RADIATION
Polarized x ray absorption spectroscopy for the study of superconductors and magnetic materials
[DE91-017990] N92-11163
Laser produced plasma soft x ray generation
[DE91-016925] N92-11874

SYNCHROTRONS
Photon stimulated desorption of neutral species from aluminum
[DE91-017004] N92-11784

SYNTHESIS (CHEMISTRY)
Synthesis and reactivity of silyl-ketene acetal-modified polysiloxanes preparation of polysiloxanes with high dielectric constraints
[AD-A240754] N92-11196

SYNTHETIC APERTURE RADAR
Current status and future developments in radar remote sensing N92-11441
Modeling of radar backscattering from the sea surface using polarimetric-SAR observations N92-11442
Analysis of radar polarimetric data for the discrimination and monitoring of forest covers N92-11449
Airborne precursor missions in support of SIR-C/X-SAR N92-11450
Nonlinear theory of synthetic aperture radar sea wave imaging N92-11451
Dual polarization microwave backscatter signatures of bare and vegetated soils N92-11452
Airborne SAR HAREM campaign: Results, targets features, ERS1 simulations, and operational satellite exploitation N92-11455
Land cover classification by multipolarized SAR imagery N92-11457

SYNTHETIC FIBERS
Direct imaging of deformation and disorder in extended-chain polymer fibers
[AD-A240651] N92-11192

SYSTEM EFFECTIVENESS
Heat exchanger thermal performance for two nonazeotropic refrigerant mixtures
[DE91-017250] N92-11216

SYSTEM FAILURES
Thermal verification testing of commercial printed-circuit boards for spaceflight
[NASA-TM-105261] N92-11221
A conjugate gradient based algorithm to minimize the sidelobe level of planar arrays with element failures
[AD-A240667] N92-11242
Lunar dust transport and potential interactions with power system components
[NASA-CR-4404] N92-11951

SYSTEM IDENTIFICATION
Rotorcraft system identification
[AGARD-AR-280] N92-11001

SYSTEMS ANALYSIS
Distributed sensor system decision analysis using team strategies
[AD-A240250] N92-11333

SYSTEMS ENGINEERING
A systematic formulation, as an approach to air traffic
[MBB-Z-0371-91-PUB] N92-10996
Calibration of the Naval Postgraduate School 3.5' x 5.0' academic wind tunnel
[AD-A240614] N92-11025
What we were asked to do N92-11041
Concepts, requirements, and design approaches for building successful planning and scheduling systems N92-11042
Network Control Center User Planning System (NCC UPS) N92-11053
The 100 GHz half megawatt microwave transmission system development with whispering gallery mode N92-11869

SYSTEMS INTEGRATION
Pellet bed reactor for nuclear propelled vehicles: Part 2: Missions and vehicle integration trades N92-11102
Technology readiness assessment of advanced space engine integrated controls and health monitoring
[NASA-TM-105255] N92-11130
Definition, technology readiness, and development cost of the orbit transfer vehicle engine integrated control and health monitoring system elements
[NASA-CR-187123] N92-11132
Integration of visible-through microwave-range multispectral image data sets for geologic mapping N92-11491
Lessons learned in the development of the C-130 aircrew training system: A summary of Air Force on-site experience
[AD-A240554] N92-11635
Database management system interface standard for Navy next generation computing resources
[AD-A240432] N92-11925

SYSTEMS MANAGEMENT
Making intelligent systems team players: Case studies and design issues. Volume 2: Fault management system cases
[NASA-TM-104738] N92-11641

T

TABLES (DATA)
The considering of the slowing down effect in the formalism of probability tables. Application to the effective cross section calculation
[DE91-626722] N92-11751

TANTALUM
Photoemission study of Ce/Ta(110) and Ce/W(110) interfaces and the catalytic oxidation effect
[DE91-018167] N92-11903

TARGET RECOGNITION
Discrete ARMA model for natural resonances in electromagnetic and acoustic scattering
[AD-A240656] N92-11241
Enhanced clutter suppression apparatus for use with an infrared search and surveillance system
[AD-D014984] N92-11247

TARGETS
Perceptual style and air-to-air tracking performance
[NASA-TM-102868] N92-11629

TAXIING
Evaluation of two high-speed runway exits
[DOT/FAA/CT-TN91/36] N92-11021
Surface painted taxiway markings at Seattle-Tacoma International Airport
[DOT/FAA/CT-TN91/49] N92-11029

TDR SATELLITES
TRUST: TDRSS Resource User Support Tool N92-11052
Network Control Center User Planning System (NCC UPS) N92-11053
A method for interference mitigation in space communications scheduling N92-11062

TECHNOLOGY ASSESSMENT
Technology needs for high speed rotorcraft (3)
[NASA-CR-186433] N92-10999
The role of stealth in naval aviation and joint/combined operations
[AD-A240595] N92-11005
Large deployable antenna program. Phase 1: Technology assessment and mission architecture
[NASA-CR-4410] N92-11036
Nuclear thermal propulsion workshop overview N92-11090
Upgraded NERVA systems: Enabler nuclear system N92-11093
Low Pressure Nuclear Thermal Rocket (LPNTR) concept N92-11094
Technology readiness assessment of advanced space engine integrated controls and health monitoring
[NASA-TM-105255] N92-11130
Definition, technology readiness, and development cost of the orbit transfer vehicle engine integrated control and health monitoring system elements
[NASA-CR-187123] N92-11132
Plans for the development of cryogenic engines for space exploration
[NASA-TM-105250] N92-11135
High definition systems in Japan
[NASA-TM-105108] N92-11225
Semiconductor measurement technology: NIST list of publications, 1962-1989 (revised March 1990)
[PB91-193961] N92-11269
Current status and future developments in radar remote sensing N92-11441
Today's central receiver power plant
[DE91-017998] N92-11568
Technology assessment of the Software Life Cycle Support Environment (SLCSE)
[AD-A240673] N92-11682
Policy issues in interconnecting networks
[NASA-CR-188844] N92-11694

Eighty years of aerospace technique through ATMA bulletins
[ETN-91-90097] N92-11963

TECHNOLOGY UTILIZATION
Nuclear thermal propulsion workshop overview N92-11090

TECTONICS
Neotectonic studies of northern Baja California, Mexico, with LANDSAT thematic mapper and SPOT panchromatic imagery: Partitioning of dextral and extensional strain at the Pacific-North America plate boundary N92-11553
LAGEOS geodetic analysis-SL7.1
[NASA-TM-104549] N92-11584

TELECOMMUNICATION
Distributed sensor system decision analysis using team strategies
[AD-A240250] N92-11333

TELEMETRY
Further developments relating to the NASA Langley Research Center 13-inch magnetic suspension and balance system
[NASA-CR-188995] N92-11023

TELEOPERATORS
Telescience workstation
[NASA-CR-188878] N92-11033
Space engineering
[NASA-CR-187820] N92-11215
Human Machine Interfaces for Teleoperators and Virtual Environments Conference
[NASA-CP-10071] N92-11638

TELEVISION CAMERAS
Television image compression and small animal remote monitoring
[NASA-CR-186614] N92-11223

TELEVISION SYSTEMS
Television image compression and small animal remote monitoring
[NASA-CR-186614] N92-11223

TEMPERATE REGIONS
Integration of Seasat and SPOT data, contribution to structural geology mapping in temperature environment N92-11499

TEMPERATURE DEPENDENCE
Control of electron transfer rates by motions of atoms and molecules
[DE91-018575] N92-11777

TEMPERATURE DISTRIBUTION
Application of infrared thermography to thermal flux measurement in wind tunnels
[AAAF-NT-89-12] N92-11020
Preliminary studies for automizing thermal flux measurement examination by thermosensitive coloring
[AAAF-NT-89-28] N92-11288
Direct-contact heat exchanger for swirling countercurrent flow of hot gas and finely divided solids: A parametric study
[DE91-017229] N92-11291
Determination of nonstationary temperatures in high-stressed elements with pulsed heat sources
[DE91-635705] N92-11325
Monitoring volcanoes using short wavelength infrared images N92-11498
Energetics diagnosis of numerical simulation of atmospheric blocking
[NASA-CR-183503] N92-11581
Gorter-Mellink pulsed-source problem in cylindrical and spherical geometry
[DE91-017249] N92-11725

TEMPERATURE EFFECTS
MLITemp: A computer program to predict the thermal effects associated with hypervelocity impact damage to space station MLI
[NASA-CR-184245] N92-11079
Conversion of ethane and of propane to higher olefin hydrocarbons
[DE91-016896] N92-11160
Mixing effects in aqueous solutions at elevated temperatures
[DE91-017695] N92-11168
Creep response of a 9Cr-1Mo-V-Nb steel to varying stresses and temperatures
[DE91-017871] N92-11181
The 23 to 300 C demagnetization resistance of samarium-cobalt permanent magnets
[NASA-TP-3119] N92-11252
Measurement of frequency response in short thermocouple wires
[NASA-CR-187821] N92-11339
Piston temperature measurement in a natural gas engine
[PB91-194357] N92-11352
Development of a 3-D tree thermal response model for energy budget and scene simulation studies
[AD-A240693] N92-11565

TEMPERATURE GRADIENTS
Characterizing He II flow through porous materials using counterflow data
[CD-4] N92-11295
Thermal behavior of the SHOOT gallery arm
[CD-21] N92-11296
Gorter-Mellink pulsed-source problem in cylindrical and spherical geometry
[DE91-017249] N92-11725

TEMPERATURE MEASUREMENT
Application of infrared thermography to thermal flux measurement in wind tunnels
[AAAF-NT-89-12] N92-11020
Laser Raman diagnostics in subsonic and supersonic turbulent jet diffusion flames N92-11159
Aerothermal test results from the first flight of the Pegasus air-launched space booster
[NASA-TM-4330] N92-11301
Piston temperature measurement in a natural gas engine
[PB91-194357] N92-11352
NOAA-AVHRR contribution to the analysis or urban heat islands N92-11495
Urban heat island N92-11500
Electron temperature measurements on ATF using electron cyclotron emission N92-11849

TEMPERATURE PROFILES
Thermal behavior of the SHOOT gallery arm
[CD-21] N92-11296
Acoustic propagation at low altitude: Effects of atmospheric turbulence (Villeau (France) test)
[ONERA-RT-15/3641-PY] N92-11588

TEMPERATURE SENSORS
Preliminary studies for automizing thermal flux measurement examination by thermosensitive coloring
[AAAF-NT-89-28] N92-11288

TEMPORAL DISTRIBUTION
Temporal signatures using NOAA-AVHRR and land use mapping N92-11513
Multidate analysis of NOAA-AVHRR data over France: Relationship with agroclimatic characteristics N92-11521
NOAA-AVHRR NDVI temporal profile classification and sensitivity to land use and climatic conditions in temperate region N92-11525

TENSILE CREEP
Physical ageing and creep in PVC
[NPL-DMM(A)-21] N92-11185

TENSORS
On the polarisation of tensor mesons in psi radiative decays and possible implications for the gluonic content of the theta(1720)
[RAL-90-091] N92-11768

TERNARY ALLOYS
Characterization of rare earth permanent magnets
[DE91-017010] N92-11754

TERRAIN
Altitude dependence in a semi-analytical atmospheric code N92-11413
Humidity measurement of naked ground by radar in conditions of excessive water N92-11453

TERRAIN ANALYSIS
Analysis of the surface state of two sub-polar glaciers using SPOT data and a numerical terrain model N92-11523

TERRESTRIAL RADIATION
Nonscanning climate sensor study
[NASA-CR-183506] N92-11589

TEST CHAMBERS
Calibration of the Naval Postgraduate School 3.5' x 5.0' academic wind tunnel
[AD-A240614] N92-11025
Description of Liquid Nitrogen Experimental Test Facility
[NASA-TM-105215] N92-11208

TEST FACILITIES
Test facilities for high power electric propulsion
[NASA-TM-105247] N92-11136
Description of Liquid Nitrogen Experimental Test Facility
[NASA-TM-105215] N92-11208

TEST RANGES
World Geodetic System 1984 (WGS-84) consolidated database for test ranges
[AD-A240621] N92-11026

TETHERED SATELLITES
Aerodynamic calculations related to tethered sub-satellite experiments
[NASA-CR-188964] N92-11071

TEXTS
Pictures and anaphora
[AD-A240153] N92-11631

TEXTURES
Texture indices sensitivity to spatial and spectral resolutions in semi-urban environments N92-11519
Perceptual grouping and shape from texture
[AD-A240358] N92-11678

THEMATIC MAPPERS (LANDSAT)
Inter-calibrating of SPOT1-HRV, LANDSAT5-TM, and NOA11-AVHRR in the visible and near infrared field s N92-11401
Suppression of aerosols on LANDSAT thematic mapper imagery N92-11411
Urban heat island N92-11500
Night-time LANDSAT thermal infrared imagery as a tool for climatological studies N92-11526
Detection and characterization of active fires in west Africa with LANDSAT thematic mapper and NOAA N92-11529
Neotectonic studies of northern Baja California, Mexico, with LANDSAT thematic mapper and SPOT panchromatic imagery: Partitioning of dextral and extensional strain at the Pacific-North America plate boundary N92-11553
Multispectral image maps from LANDSAT thematic mapper data
[AD-A240453] N92-11562
A hybrid methodology for detecting cartographically significant features using LANDSAT TM imagery
[AD-A240454] N92-11563

THEMATIC MAPPING
Correction of atmospheric and topographic effects in LANDSAT TM images N92-11407
Use of high spectral resolution airborne visible/infrared imaging spectrometer data for geologic mapping: An overview N92-11420
Multi-temporal monitoring of lake water quality N92-11426
Integration of visible-through microwave-range multispectral image data sets for geologic mapping N92-11491
Evaluation of the quality of urban biotypes by remote sensing N92-11493
Monitoring volcanoes using short wavelength infrared images N92-11498
Integration of Seasat and SPOT data, contribution to structural geology mapping in temperature environment N92-11499
Structural controls on the remotely sensed response of a coniferous forest plantation N92-11516
A hybrid methodology for detecting cartographically significant features using LANDSAT TM imagery
[AD-A240454] N92-11563

THEOREMS
Oriented matroids and projective invariant theory
[ETN-91-90181] N92-11740

THERMAL CONDUCTIVITY
Calculations and curve fits of thermodynamic and transport properties for equilibrium air to 30000 K
[NASA-RP-1260] N92-11285

THERMAL CYCLING TESTS
Thermal verification testing of commercial printed-circuit boards for spaceflight
[NASA-TM-105261] N92-11221
Microstructural evolution during the thermomechanical fatigue of solder joints
[DE91-017309] N92-11372

THERMAL DIFFUSION
To the account of finite velocity of thermal diffusion in turbulent flows
[DE91-635593] N92-11323

THERMAL EXPANSION
A process for preparing an assembly of an article and a polyimide which resists dimensional change, delamination, and debonding when exposed to changes in temperature
[NASA-CASE-LAR-14538-1] N92-11201

THERMAL FATIGUE
Microstructural evolution during the thermomechanical fatigue of solder joints
[DE91-017309] N92-11372

THERMAL MAPPING
Use of high spectral resolution airborne visible/infrared imaging spectrometer data for geologic mapping: An overview N92-11420

THERMAL PROTECTION
Debris/ice/TPS assessment and photographic analysis for Shuttle Mission STS-43
[NASA-TM-103823] N92-11038

THERMAL RADIATION
An examination of the factors affecting the use of infra-red search and track systems in the air-to-air role
[ETN-91-99987] N92-11222
Atmospheric correction in the thermal infrared: AVHRR case N92-11398
TIMS calibration correction by comparison with PRT5 N92-11412
Experimental approach to emissivity problems and surface temperature in thermal infrared remote sensing N92-11462
Anisotropy of thermal infrared exitance above and within plant canopies N92-11467

Complementarity of temperature independent Thermal Infrared Spectral Indices (TISI) and NDVI: Compared properties and combined use for soil and vegetation discrimination N92-11490
Using the radiative surface temperature in energy budget studies over plant canopies N92-11506
Night-time LANDSAT thermal infrared imagery as a tool for climatological studies N92-11526
Nonscanning climate sensor study [NASA-CR-183506] N92-11589

THERMAL REACTORS
Pellet bed reactor for nuclear propelled vehicles: Part 1: Reactor technology N92-11101
Nuclear thermal/nuclear electric hybrids N92-11107
Open cycle gas core nuclear rockets N92-11108
Shielding requirements for particle bed propulsion systems [AD-A240780] N92-11787

THERMAL STRESSES
Studies of aerothermal loads generated in regions of shock/shock interaction in hypersonic flow [NASA-CR-181893] N92-11319

THERMAL VACUUM TESTS
Thermal verification testing of commercial printed-circuit boards for spaceflight [NASA-TM-105261] N92-11221

THERMOCOUPLES
Measurement of frequency response in short thermocouple wires [NASA-CR-187821] N92-11339

THERMODYNAMIC EFFICIENCY
Heat exchanger thermal performance for two nonazeotropic refrigerant mixtures [DE91-017250] N92-11216

THERMODYNAMIC EQUILIBRIUM
Calculations and curve fits of thermodynamic and transport properties for equilibrium air to 30000 K [NASA-RP-1260] N92-11285

THERMODYNAMIC PROPERTIES
Improved thermodynamic modeling of the no-vent fill process and correlation with experimental data [NASA-TM-104492] N92-11129
Mixing effects in aqueous solutions at elevated temperatures [DE91-017695] N92-11168
Computer codes for the evaluation of thermodynamic and transport properties for equilibrium air to 30000 K [NASA-TM-104107] N92-11300

THERMODYNAMICS
The behaviour of fire-exposed composite steel/concrete slabs [ISBN-90-386-0031-3] N92-11147
Overlooked fundamentals of resistance welding [DE91-018814] N92-11362

THERMOELECTRIC GENERATORS
TEGEN: A one dimensional program to calculate a thermoelectric generator [DE91-634444] N92-11571

THERMOGRAPHY
Application of infrared thermography to thermal flux measurement in wind tunnels [AAAF-NT-89-12] N92-11020

THERMOPLASTICITY
Thermoviscoplastic response of Ti-15-3 under various loading conditions [NASA-CR-187621] N92-11391

THETA PINCH
Numerical and experimental studies of simulated toroidicity effects in a linear high-beta heliac N92-11827
Coaxial slow source [DE91-016947] N92-11875

THICK FILMS
High-T sub c fluorine-doped YBa2Cu3O(y) films on ceramic substrates by screen printing [NASA-TM-105296] N92-11188

THICKNESS
Effects on LDEF exposed copper film and bulk N92-11076
Process for controlling the thickness of an antireflection coating, and embodying apparatus [DE91-017634] N92-11793

THIN FILMS
Effects on LDEF exposed copper film and bulk N92-11076
Ultra high vacuum sputtering system [AD-A240157] N92-11176
Solid lubricants on pretreated surfaces [NASA-CASE-LEW-14474-2] N92-11186
Thin film magnetic memory elements [AD-D014971] N92-11646
Electrooptic effects and photosensitivities of PLZT thin films [DE91-017067] N92-11901

THOMSON SCATTERING
Radiation forces to electrons in laser fields explained as scattering for ponderomotive momentum transfers [IPPCZ-308] N92-11773

THREADS
Blind fastening apparatus [NASA-CASE-LAR-14542-1] N92-11354
Quick application/release nut with engagement indicator [NASA-CASE-MSC-21799-1] N92-11359

THREE DIMENSIONAL BODIES
Advanced stress analysis methods applicable to turbine engine structures [NASA-CR-187235] N92-11378

THREE DIMENSIONAL FLOW
The effects of Reynolds number, rotor incidence angle and surface roughness on the heat transfer distribution in a large-scale turbine rotor passage [NASA-CR-187693] N92-11297
The three-dimensional evolution of a plane mixing layer. Part 1: The Kelvin-Helmholtz roll-up [NASA-TM-103856] N92-11303
Secondary instability of the three dimensional laminar boundary layer in incompressible flow: Description of the calculation code [CERT-RT-63/5618-54] N92-11306
Turbulent friction drag reduction: Boundary layer manipulators [CERT-RSF-DERAT-62/5004-31] N92-11309

THREE DIMENSIONAL MODELS
Determination of nonstationary temperatures in high-stressed elements with pulsed heat sources [DE91-635705] N92-11325
A three dimensional radiative transfer method for optical remote sensing of vegetated land surfaces N92-11466
Development of a 3-D tree thermal response model for energy budget and scene simulation studies [AD-A240693] N92-11565

THREE DIMENSIONAL MOTION
Three-dimensional calculations of fields and loading for loop and folded waveguide ICRF antennas [DE92-000065] N92-11250
Motion of charged particle in helical systems N92-11847

THRUST CHAMBERS
CFD code survey for thrust chamber application N92-11119

THRUST-WEIGHT RATIO
Particle bed reactor nuclear rocket concept N92-11095
Droplet Core Nuclear Rocket (DLNR) N92-11105

TILT ROTOR AIRCRAFT
Technology needs for high speed rotorcraft (3) [NASA-CR-186433] N92-10999

TIME
A Fourier collocation time domain method for numerically solving Maxwell's equations [NASA-TM-104162] N92-11742
About time [NASA-CR-188870] N92-11753

TIME CONSTANT
Simulation of a nonlinear two degrees of freedom system. Study of the temporal response to a harmonic attraction [ONERA-RT-17/1677-RY-091-R] N92-11755

TIME DEPENDENCE
First-passage problems: A probabilistic dynamic analysis for degraded structures [NASA-TM-103755] N92-11373
Joint use of remote sensing and agricultural production estimation models: Current trends N92-11501
Multitemporal study of the Guyana coastline and estuaries using SPOT and LANDSAT imagery N92-11524
The use of a time-resolved lidar to study the water column N92-11548

TIME MEASUREMENT
About time [NASA-CR-188870] N92-11753

TIME SERIES ANALYSIS
Efficient detection of a CW signal with a linear frequency drift [NASA-CR-188900] N92-11224

TISSUES (BIOLOGY)
Training, muscle fatigue and stress fractures [AD-A240386] N92-11626

TITAN
Electron distributions and solar wind interaction with nonmagnetic planets N92-11952

TITANIUM ALLOYS
Oxidation of titanium aluminide and its XD composite [AD-A240401] N92-11177
Thermoviscoplastic response of Ti-15-3 under various loading conditions [NASA-CR-187621] N92-11391

TITANIUM BORIDES
Oxidation of titanium aluminide and its XD composite [AD-A240401] N92-11177

TOKAMAK DEVICES
Results of folded waveguide tests on RFTF [DE91-018930] N92-11249
Proceedings of the First International Toki Conference on Plasma Physics and Controlled Nuclear Fusion: Next Generation Experiments in Helical Systems [NIFS-PROC-3] N92-11799
Recent experiments in JT-60 N92-11812
The main fusion activities in Institute of Plasma Physics, Academia Sinica N92-11814
Detached plasma and density limit of Tokamaks N92-11816
Overview of recent results from the Advanced Toroidal Facility N92-11819
Dissipative trapped electron modes in l = 2 torsatrons N92-11830
A possible modification of the FT Tokamak into a compact high field stellarator with separatrices N92-11863
LHCD experiments on tokamak CASTOR [IPPCZ-304] N92-11861
ELMy-H mode as limit cycle and chaotic oscillations in tokamak plasmas [NIFS-87] N92-11882
Rotations of bulk ions and impurities in non-axisymmetric toroidal systems [NIFS-102] N92-11885
Current profile control for ITER with RF current drive [DE91-018597] N92-11888
Plasma properties [DE91-018913] N92-11891
Application of modern mathematical concepts to plasma confinement [DE92-000053] N92-11893
Full-wave calculation of fast-wave current drive in tokamaks including k(parallel) variations [DE92-000076] N92-11894

TOLERANCES (MECHANICS)
An examination of the damage tolerance enhancement of carbon/epoxy using an outer lamina of spectra (R) [NASA-TP-3160] N92-11142

TOLERANCES (PHYSIOLOGY)
Toxicity assessment of combustion products in simulated space cabins N92-11619

TOMOGRAPHY
Non-invasive evaluation of the cardiac autonomic nervous system by PET [DE91-018476] N92-11622
Inverse problems and imaging (Pitman research notes in mathematics series Number 245) [AD-A240333] N92-11737

TOPOGRAPHY
Correction of atmospheric and topographic effects in LANDSAT TM images N92-11407
Current status and future developments in radar remote sensing N92-11441
Integration of visible-through microwave-range multispectral image data sets for geologic mapping N92-11491

TOROIDAL PLASMAS
Second stability studies in a helical axis device: TJ-II N92-11807
The 3-D equilibria of helical systems: Magnetic islands and their control N92-11808
Resistive MHD stability studies for ATF plasmas during operation in the second stability regime N92-11809
Plasma transport in advanced stellarators N92-11811
Analysis of scrape-off layer in toroidal helical systems N92-11815
Effects of perturbing helical fields on confinement of Heliotron DR plasma N92-11818
Overview of recent results from the Advanced Toroidal Facility N92-11819
Review of Heliotron E experiment N92-11822
Review of CHS experiment N92-11823
Experimental studies of a helical axis stellarator (TU-Heliac) N92-11824
Numerical and experimental studies of simulated toroidicity effects in a linear high-beta heliac N92-11827
Dissipative trapped electron modes in l = 2 torsatrons N92-11830
Destruction of magnetic surfaces in helical torus N92-11832
On strong RF plasma turbulence N92-11836
Confinement studies of Heliotron E plasmas in magnetic surface variation experiments N92-11850
Impurity behavior in Heliotron E N92-11852
Edge plasma study in Heliotron E N92-11853
Recent diamagnetic measurements of toroidal coil experiments on Heliotron E N92-11854

Study of resistive interchange mode in Heliotron E N92-11855
Measurement of magnetic fluctuations in Heliotron E N92-11856
Effect of magnetic axis shift on CHS plasma characteristics N92-11858
Power deposition during ECH in CHS N92-11862
A possible modification of the FT Tokamak into a compact high field stellarator with separatrices N92-11863
Coaxial slow source
[DE91-016947] N92-11875
Continuum damping of high mode number toroidal Alfven waves
[DE91-018891] N92-11890
Plasma properties
[DE91-018913] N92-11891
Diffusion in the Io plasma torus and its relation to the torus spatial structure N92-11949

TOROIDS
Coaxial slow source
[DE91-016947] N92-11875
Application of modern mathematical concepts to plasma confinement
[DE92-000053] N92-11893

TORSION
Analysis of strain dependent damping in materials via modeling of material point hysteresis
[AD-A240298] N92-11381

TOXIC HAZARDS
Ground penetrating radar data acquisition system
[AD-A240765] N92-11244
Integrated Risk Information System
[DE91-018503] N92-11924

TOXICITY
Physicochemical properties and dissolution in simulated biological fluids of particles of beryllium-powered rocket motor exhaust and pure beryllium oxides calcined at low and high temperature
[AD-A240288] N92-11134
Low toxicity high temperature PMR polyimides
[NASA-CASE-LAR-14639-1] N92-11199
Toxicity assessment of combustion products in simulated space cabins N92-11619

TOXICITY AND SAFETY HAZARD
Disposal methods N92-11116
Integrated Risk Information System
[DE91-018503] N92-11924

TOXICOLOGY
JPRS report: Science and technology. USSR: Life sciences
[JPRS-ULS-91-012] N92-11611

TRACKING (POSITION)
Perceptual style and air-to-air tracking performance
[NASA-TM-102868] N92-11629

TRAILING EDGES
NACA 0015 wing pressure and trailing vortex measurements
[NASA-TP-3151] N92-10981

TRAINING DEVICES
Lessons learned in the development of the C-130 aircrew training system: A summary of Air Force on-site experience
[AD-A240554] N92-11635

TRAINING EVALUATION
The development of Behaviorally Anchored Rating Scales (BARS) for evaluating USAF pilot training performance
[AD-A239969] N92-11630

TRAJECTORIES
Generation of smooth trajectories without planning
[NASA-CR-189013] N92-11712

TRAJECTORY CONTROL
Generation of smooth trajectories without planning
[NASA-CR-189013] N92-11712

TRAJECTORY OPTIMIZATION
A methodology to assess the Best Estimate Trajectory (BET) results generated for the Kwajalein Missile Range
[AD-A240770] N92-11083

TRANSFER FUNCTIONS
Conoscopic holography. 1: Basic principles and physical basis. 2: Rigorous derivation
[TELECOM-PARIS-91-C-001] N92-11337

TRANSFORMATIONS (MATHEMATICS)
Extended algebraic graph transformation
[ETN-91-90151] N92-11739

TRANSITION FLOW
Modeling of the heat transfer in bypass transitional boundary-layer flows
[NASA-TP-3170] N92-11299

TRANSITION METALS
Thermal annealing studies of Fe and Ti implanted in GaAs and InP
[ETN-91-90148] N92-11915

TRANSITION PROBABILITIES
Studies on laser atomic spectroscopy
[DE91-628172] N92-11349

TRANSMISSION EFFICIENCY
Dual frequency optical carrier technique for transmission of reference frequencies in dispersive media
[NASA-CASE-NPO-18007-1-CU] N92-11791

TRANSMISSION LOSS
Dual frequency optical carrier technique for transmission of reference frequencies in dispersive media
[NASA-CASE-NPO-18007-1-CU] N92-11791

TRANSMITTERS
Shipboard antenna concepts: Structurally independent 2- to 6-MHz transmit antenna design
[AD-A240544] N92-11236

TRANSONIC FLOW
Three dimensional numerical method for resolving small transonic perturbations in unstructured mesh
[ONERA-RT-56/3064-RY-006-R] N92-10989

TRANSONIC WIND TUNNELS
Model representation in the PANCOR wall interference assessment code
[NASA-TM-104152] N92-11022

TRANSPARENCE
Nuclear transparency and double beta decay of molybdenum 100
[DE91-016963] N92-11172

TRANSPONDERS
Acoustic transponder receiver circuit
[AD-D014965] N92-11760

TRANSPORT AIRCRAFT
Wing tip turbine: Analysis of the results of S2MA sounding of marginal vortex of the A320, technical summary
[ONERA-RTS-21/4365-AY-056A] N92-11009

TRANSPORT PROPERTIES
Calculations and curve fits of thermodynamic and transport properties for equilibrium air to 30000 K
[NASA-RP-1260] N92-11285
Computer codes for the evaluation of thermodynamic and transport properties for equilibrium air to 30000 K
[NASA-TM-104107] N92-11300
Collision integrals and high temperature transport properties for N-N, O-O, and N-O
[NASA-CR-188907] N92-11770
Review of the TJ-II Flexible Heliac Project N92-11803
Ripple diffusion and bootstrap current in LHD N92-11833
Effect of magnetic axis shift on CHS plasma characteristics N92-11858
Power deposition during ECH in CHS N92-11862
Fokker-Planck equation in the presence of anomalous diffusion
[NIFS-29] N92-11879
Nonlinear behavior of multiple-helicity resistive interchange modes near marginally stable states
[NIFS-89] N92-11883
High l state population in O(7+) produced in ion-solid collisions
[DE91-018169] N92-11904
Superionics
[AD-A240352] N92-11910
Lunar dust transport and potential interactions with power system components
[NASA-CR-4404] N92-11951

TRANSPORT THEORY
Multiangular approach to solution of atmosphere optics reverse problems N92-11478
Monte Carlo model for transport equation in a plant canopy and its inversion N92-11481
The considering of the slowing down effect in the formalism of probability tables. Application to the effective cross section calculation
[DE91-626722] N92-11751
Plasma transport in advanced stellarators N92-11811
Plasma properties
[DE91-018913] N92-11891

TRANSPUTERS
Parallel processing applications for gas turbine engine control N92-11012
Transient finite element computations on a variable transputer system
[NASA-CR-189060] N92-11671

TRAPPED PARTICLES
Dissipative trapped electron modes in l = 2 torsatrons N92-11830
Effects of electric field on particle drift orbits in a l = 2 torsatron
[NIFS-31] N92-11878

TREES (PLANTS)
Study of the spatial signature of forest covers by geometric-optic modeling N92-11530
The laser-induced chlorophyll fluorescence ratio F690/F735 of spruce needles and beech leaves during the course of a year N92-11542
Development of a 3-D tree thermal response model for energy budget and scene simulation studies
[AD-A240693] N92-11565
Surface optical property measurements on bark and leaf samples
[AD-A240714] N92-11566

TRELLIS CODING
Error control techniques for satellite and space communications
[NASA-CR-188997] N92-11228

TRENDS
Information technologies for astrophysics circa 2001
[NASA-CR-188868] N92-11936

TRIANGLES
Dispersion and stability of two electromagnetic solvers for triangular meshes
[DE91-016607] N92-11227
Optimal parallel solution of sparse triangular systems
[NASA-CR-188872] N92-11656

TROPICAL REGIONS
Optically thin cirrus clouds over oceans and possible impact on sea surface temperature of warm pool in western Pacific
[NASA-TM-104550] N92-11600

TROPOSPHERE
Scientific assessment of stratospheric ozone: 1989. Volume 2: Appendix: AFEAS report
[NASA-TM-105117] N92-11577

TRUCKS
Component cost analysis for compressed natural gas vehicles
[DE91-017230] N92-11353

TUBES
Centrifugal casting of composites
[AD-D014981] N92-11144

TUNABLE LASERS
CO2 laser active remote sensing from 9 to 11 microns: Airborne and laboratory application N92-11535

TUNGSTEN
Photoemission study of Ce/Ta(110) and Ce/W(110) interfaces and the catalytic oxidation effect
[DE91-018167] N92-11903

TUNGSTEN COMPOUNDS
Shielding requirements for particle bed propulsion systems
[AD-A240780] N92-11787

TURBIDITY
Estimation of the aerosol optical thickness from broadband turbidity measurements: Application to the atmospheric correction of SPOT images N92-11399

TURBINE BLADES
Structural tailoring of advanced turboprops (STAT): User's manual
[NASA-CR-187101] N92-11016
High pressure turbine blade life extension
[AD-A240654] N92-11180
Development of a personal computer program for milling the shapes of wind turbine blades. Theory and application
[ILR-MITT-243(1990)] N92-11360

TURBINE ENGINES
Wing tip turbine: Analysis of the results of S2MA sounding of marginal vortex of the A320, technical summary
[ONERA-RTS-21/4365-AY-056A] N92-11009
Advanced stress analysis methods applicable to turbine engine structures
[NASA-CR-187235] N92-11378

TURBINE INSTRUMENTS
Calibration of turbine flowmeters for storable bipropellant engines
[NAL-TR-1091] N92-11127

TURBINE PUMPS
Propulsion system needs N92-11112
The effects of Reynolds number, rotor incidence angle and surface roughness on the heat transfer distribution in a large-scale turbine rotor passage
[NASA-CR-187693] N92-11297

TURBINES
Today's central receiver power plant
[DE91-017998] N92-11568

TURBOCOMPRESSORS
Radial inflow turbine study
[AD-A240169] N92-11015

TURBOFAN AIRCRAFT
Annoyance caused by advanced turboprop aircraft flyover noise: Comparison of different propeller configurations
[NASA-TP-3104] N92-11758

TURBOMACHINERY
LV software support for supersonic flow analysis
[NASA-CR-188914] N92-10978

Development of unsteady aerodynamic analyses for turbomachinery aeroelastic and aeroacoustic applications
[NASA-CR-4405] N92-10979

TURBOPROP AIRCRAFT
Annoyance caused by advanced turboprop aircraft flyover noise: Comparison of different propeller configurations
[NASA-TP-3104] N92-11758

TURBOPROP ENGINES
Structural tailoring of advanced turboprops (STAT): User's manual
[NASA-CR-187101] N92-11016

TURBULENCE
Overview of recent results from the Advanced Toroidal Facility N92-11819
Application of modern mathematical concepts to plasma confinement
[DE92-000053] N92-11893
Superfluid-like turbulence in cosmology
[NASA-CR-189011] N92-11942

TURBULENCE MODELS
Computational study of the aerodynamics and control by blowing of asymmetric vortical flows over delta wings
[NASA-CR-187979] N92-10990
A detailed investigation of staged normal injection into a Mach 2 flow N92-11118
The effects of Reynolds number, rotor incidence angle and surface roughness on the heat transfer distribution in a large-scale turbine rotor passage
[NASA-CR-187693] N92-11297

TURBULENT BOUNDARY LAYER
Results from computational analysis of a mixed compression supersonic inlet
[NASA-TM-104475] N92-10976
Numerical prediction of turbulent flame stability in premixed/prevaporized (HSCT) combustors
[NASA-CR-188991] N92-11161
Turbulent friction drag reduction: Boundary layer manipulators
[CERT-RSF-DERAT-62/5004-31] N92-11309

TURBULENT DIFFUSION
To the account of finite velocity of thermal diffusion in turbulent flows
[DE91-635593] N92-11323
Application of modern mathematical concepts to plasma confinement
[DE92-000053] N92-11893

TURBULENT FLOW
Theoretical study (Lagrangian modeling) of turbulent particulate dispersion
[ETN-91-99909] N92-11287
A Newton's method solver for the two-dimensional and axisymmetric Navier-Stokes equations N92-11292
On the basic equations for the second-order modeling of compressible turbulence
[NASA-TM-105277] N92-11302
Measurement of turbulent flow beneath the wind wave induced water surface, using picture repetition analysis
[ETN-91-90203] N92-11316
Turbulent fluid motion 3: Basic continuum equations
[NASA-TM-104386] N92-11317
Evaluation of high Reynolds number flow in a 180 degree turn-around-duct
[NASA-CR-184243] N92-11318
To the account of finite velocity of thermal diffusion in turbulent flows
[DE91-635593] N92-11323
Heat transfer in channels with uniformly swirled flow
[DE91-635594] N92-11324
The phenomena of scalar mixing in turbulent gas-particle flows, measuring equipment, and measurements
[DE92-704034] N92-11327
Plasma transport in advanced stellarators N92-11811

TURBULENT MIXING
A detailed investigation of staged normal injection into a Mach 2 flow N92-11118
The phenomena of scalar mixing in turbulent gas-particle flows, measuring equipment, and measurements
[DE92-704034] N92-11327

TURBULENT WAKES
Turbulent friction drag reduction: Boundary layer manipulators
[CERT-RSF-DERAT-62/5004-31] N92-11309

TVD SCHEMES
On a class of implicit and explicit schemes of Van-Leer type for scalar conservation laws N92-11715

TWO DIMENSIONAL BOUNDARY LAYER
Perfect compressible two dimensional boundary layer strong fluid coupling in the case of sharp leading edge profiles. Unsteady case of isolated profiles and steady case of blade grids
[ONERA-RT-43/1621-RY-006-R] N92-11311

TWO DIMENSIONAL FLOW
A Newton's method solver for the two-dimensional and axisymmetric Navier-Stokes equations N92-11292
Mixed convection in two-dimensional laminar air flow with reverse flow regions N92-11293
Resolution of the Navier-Stokes equations applied to the computation of the laminar flow around a two dimensional wing profile
[CERT-RT-65/5604-35] N92-11307
Resolution of Navier-Stokes equations around profiles: Drag evolution
[ONERA-RTS-86/1685-AY-156A] N92-11310

TWO DIMENSIONAL MODELS
An analysis of upwind schemes for inhomogeneous two dimensional conservation laws N92-11717

TWO PHASE FLOW
Theoretical study (Lagrangian modeling) of turbulent particulate dispersion
[ETN-91-99909] N92-11287
Local interfacial area concentration measurement in bubbly flow
[DE91-018702] N92-11322
The phenomena of scalar mixing in turbulent gas-particle flows, measuring equipment, and measurements
[DE92-704034] N92-11327

U

U.S.S.R.
JPRS report: Science and technology. USSR: Space. Feoktistov's Views on Future Directions for Space Program
[JPRS-USP-91-005] N92-11032

UH-60A HELICOPTER
Concept evaluation of the UH-60 externally mounted rescue hoist
[AD-A240545] N92-11004

ULTRAHIGH VACUUM
Ultra high vacuum sputtering system
[AD-A240157] N92-11176

ULTRASONIC FLAW DETECTION
Development of data file standards for automated ultrasonic scanning systems. Exchange methods for digital ultrasonic inspection data
[AD-A240075] N92-11364

ULTRASONIC RADIATION
Wavefields near transverse cusp caustics produced by reflecting ultrasonic transients and tone bursts from curved surfaces
[AD-A240641] N92-11763

ULTRASONIC TESTS
Deformation of isodamp (A polyvinyl chloride-based elastomer) at various loading rates
[AD-A240393] N92-11189
Development of data file standards for automated ultrasonic scanning systems. Exchange methods for digital ultrasonic inspection data
[AD-A240075] N92-11364
Method of recertifying a loaded bearing member using a phase point
[NASA-CASE-LAR-14741-1] N92-11384

ULTRASONIC WAVE TRANSDUCERS
Rapidly quantifying the relative distention of a human bladder
[NASA-CASE-LAR-13901-2] N92-11621

ULTRASONICS
Navigation and positioning of mobile robots
[DE92-704014] N92-10998

ULTRAVIOLET EMISSION
Diffusion in the Io plasma torus and its relation to the torus spatial structure N92-11949

ULTRAVIOLET RADIATION
Modeling UV and x ray oxygen emission in astrophysical plasmas
[DE91-016927] N92-11940

ULTRAVIOLET SPECTRA
A calibration of the Naval Postgraduate School middle ultraviolet spectrograph and an analysis of the OII 2470 A and OI 2972 A emissions obtained from mid-latitude rocket observations
[AD-A240686] N92-11587
Modeling UV and x ray oxygen emission in astrophysical plasmas
[DE91-016927] N92-11940

ULTRAVIOLET SPECTROMETERS
A calibration of the Naval Postgraduate School middle ultraviolet spectrograph and an analysis of the OII 2470 A and OI 2972 A emissions obtained from mid-latitude rocket observations
[AD-A240686] N92-11587
Impurity behavior in Heliotron E N92-11852

ULTRAVIOLET SPECTROSCOPY
A calibration of the Naval Postgraduate School middle ultraviolet spectrograph and an analysis of the OII 2470 A and OI 2972 A emissions obtained from mid-latitude rocket observations
[AD-A240686] N92-11587

ULYSSES MISSION
Activities report of the Max-Planck Institute for Aeronomy
[ETN-91-90233] N92-11964

UNDERWATER PROPULSION
The 27th JANNAF Combustion Subcommittee Meeting, Volume 3
[CPIA-PUBL-557-VOL-3] N92-11117

UNIQUENESS
On the solution for the problem of long waves in a perfect fluid N92-11721

UNIVERSE
Re-ionization and decaying dark matter
[NASA-CR-189009] N92-11944
Cosmological structure formation
[NASA-CR-189007] N92-11946
Non scale-invariant density perturbations from chaotic extended inflation
[NASA-CR-189004] N92-11947
Underlying generation mechanisms for the extragalactic gamma ray background and their implications for high-resolution gamma ray cosmology N92-11959

UNIVERSITY PROGRAM
International program for Earth observations
[NASA-CR-188799] N92-11393

UNSTEADY AERODYNAMICS
Development of unsteady aerodynamic analyses for turbomachinery aeroelastic and aeroacoustic applications
[NASA-CR-4405] N92-10979
Unsteady aerodynamic calculations for general configurations by the double-point method
[NAL-TR-1101T] N92-10980
Three dimensional numerical method for resolving small transonic perturbations in unstructured mesh
[ONERA-RT-56/3064-RY-006-R] N92-10989

UPLINKING
Multiple beam antenna/switch system study
[NASA-CR-183496] N92-11251

UPPER ATMOSPHERE
March AFB forecasting rules of thumb evaluation
[AD-A240458] N92-11595

UPPER ATMOSPHERE RESEARCH SATELLITE (UARS)
Upper Atmosphere Research Satellite (UARS): A program to study global ozone change
[NASA-TM-105100] N92-11067

UPPER SURFACE BLOWING
Computational study of the aerodynamics and control by blowing of asymmetric vortical flows over delta wings
[NASA-CR-187979] N92-10990

URANIUM
Droplet Core Nuclear Rocket (DLNR) N92-11105
Vapor core propulsion reactors N92-11109

URANIUM OXIDES
Fission fragment assisted reactor concept for space propulsion: Foil reactor N92-11103

URANIUM PLASMAS
Open cycle gas core nuclear rockets N92-11108

URINATION
Rapidly quantifying the relative distention of a human bladder
[NASA-CASE-LAR-13901-2] N92-11621

USER MANUALS (COMPUTER PROGRAMS)
Structural tailoring of advanced turboprops (STAT): User's manual
[NASA-CR-187101] N92-11016
Slave finite element for non-linear analysis of engine structures. Volume 2: Programmer's manual and user's manual
[NASA-CR-187225] N92-11388
User's manual for the Macintosh version of PASCO
[NASA-TM-104115] N92-11668
Studying parallel program behavior with upshot
[DE91-019072] N92-11710

USER REQUIREMENTS
User modeling techniques for enhanced usability of OPSMODEL operations simulation software
[NASA-TM-4306] N92-11035
Continuation of research into language concepts for the mission support environment
[NASA-CR-187818] N92-11652
An investigation to find appropriate measures for evaluating interactive information retrieval N92-11922

V

VACANCIES (CRYSTAL DEFECTS)
Positron lifetimes in solids from first principles calculations
[DE92-000088] N92-11781
VACUUM
Edge plasma study in Heliotron E N92-11853
VACUUM CHAMBERS
Test facilities for high power electric propulsion
[NASA-TM-105247] N92-11136
Behavior of vacuum vessel eddy current in large helical device N92-11840
Fundamental design on LHD with bath cooling method N92-11841
Impurity behavior in Heliotron E N92-11852
Engineering design of LHD vacuum vessel N92-11866
VACUUM EFFECTS
Electron acceleration by laser fields in a gas
[DE91-018477] N92-11345
VACUUM SPECTROSCOPY
Impurity behavior in Heliotron E N92-11852
VACUUM SYSTEMS
Ultra high vacuum sputtering system
[AD-A240157] N92-11176
VALUE
An investigation to find appropriate measures for evaluating interactive information retrieval N92-11922
VANES
Hydrodynamic flow visualization around an oscillating vane. Extension of study to the case of higher incidences and amplitudes and the starting off phase from permanent regime
[ONERA-RT-56/1369-AN] N92-11312
VAPORS
Vapor core propulsion reactors N92-11109
Explicit determination of the vapor fraction in flash calculations
[AD-A240376] N92-11165
VARIATIONAL PRINCIPLES
Advanced stress analysis methods applicable to turbine engine structures
[NASA-CR-187235] N92-11378
VECTOR SPACES
Oriented matroids and projective invariant theory
[ETN-91-90181] N92-11740
VECTORS (MATHEMATICS)
Application of Krylov exponential propagation to fluid dynamics equations
[NASA-CR-188887] N92-11290
VEGETATION
Retrievals of column atmospheric water vapor, vegetation liquid water, and cloud cover fraction from AVIRIS data N92-11427
The comparison of airborne imaging spectrometry and geochemical ground survey for the analysis of vegetation anomalies over waste deposits N92-11431
Modeling the behavior of a vegetation cover in the MIR, contribution of high spectral resolution N92-11434
Candidate high spectral resolution derivative indices for the prediction of crop cover N92-11435
High resolution spectral measurements of vegetation and soil in field and laboratory N92-11437
Generalized formulation for semi-empirical radar models representing crop backscattering N92-11447
Land cover classification by multipolarized SAR imagery N92-11457
Construction of ground cover charts of a wheat canopy from reflectance measurements N92-11505
Evaluation of ground cover in agricultural environment by in situ measurements and multitemporal images for modeling hydric erosion N92-11528
Control of the physiological state of vegetation cover by remote sensing of fluorescent emission in the blue and red visible spectrum regions N92-11532
Vegetation monitoring by means of spectral resolved fluorescence lidar N92-11533
Simultaneous detection in blue and red bands of laser induced vegetation fluorescence N92-11539
Design and testing of a spectral-resolving fluorescence lidar system for remote sensing of vegetation N92-11540
Target signature by differential reflectance lidar, a feasibility study N92-11544
Biospheric models, measurements, and remote sensing of vegetation N92-11550
A conceptual framework for ecosystem modeling using remotely sensed inputs N92-11551
VEGETATION GROWTH
On the nature of spectral shifts: Modeling and comparison to information contained in wide bands N92-11418
Estimation of the ground humidity under vegetation: Applications of semi-empirical models N92-11445
Radiative transfer simulation on computer models of vegetation cover N92-11476
Some examples of satellite data utilization for atmospheric modeling at medium scale N92-11503
Wavelength shifts in fluorescence maxima of stressed and non-stressed Norway spruce needles over the growing season N92-11536
VEGETATIVE INDEX
Routine mapping of vegetation index with the AVHRR of NOAA11 N92-11405
Radiometric and atmospheric correction procedures for AVHRR preprocessing in the solar reflective channels N92-11414
Candidate high spectral resolution derivative indices for the prediction of crop cover N92-11435
Passive microwave remote sensing of vegetation canopies: Experimental and modeling results N92-11460
Optimum combinations of visible and near-infrared reflectances for estimating the fraction of photosynthetically available radiation absorbed by plants N92-11474
Normalization of multidirectional red and NIR reflectances with the SAVI N92-11477
Assessment of the effect of specular reflectance on the relationships between vegetation indices and biomass N92-11483
Complementarity of temperature independent Thermal Infrared Spectral Indices (TISI) and NDVI: Compared properties and combined use for soil and vegetation discrimination N92-11490
Airborne passive microwave remote sensing of land and water surface N92-11492
Evaluation of the quality of urban biotypes by remote sensing N92-11493
Integration of qualitative knowledge on operational models for following vegetation using temporal series of remote sensing images N92-11502
Some examples of satellite data utilization for atmospheric modeling at medium scale N92-11503
Estimation of the primary production in Sahelian region from radiometric data N92-11504
An integrated modelling approach for the spectral identification of crops N92-11508
Temporal signatures using NOAA-AVHRR and land use mapping N92-11513
Simulation study of vegetation indices sensitivity using the middle infrared N92-11514
Modeling temporal evolution of the radiometric response measured by wideband sensors over temperate agricultural regions N92-11518
Contribution of NOAA-AVHRR satellite data in forest vegetation monitoring N92-11520
Multidate analysis of NOAA-AVHRR data over France: Relationship with agroclimatic characteristics N92-11521
Spectral estimates of PAR interception and biomass production of irrigated rice crops. 1: Model elaboration with ground data N92-11522
NOAA-AVHRR NDVI temporal profile classification and sensitivity to land use and climatic conditions in temperate region N92-11525
Evaluation of ground cover in agricultural environment by in situ measurements and multitemporal images for modeling hydric erosion N92-11528
View-atmosphere-soil effects on vegetation indices derived from SPOT images N92-11552
VELOCITY COUPLING
Experimental investigation of the effects of blowing on bursting of strake vortices
[AD-A240256] N92-10985
VELOCITY DISTRIBUTION
LOX/hydrogen coaxial injector atomization test program N92-11121
A diagnostic study of the velocity structure of a meandering jet using a primitive equation model with dynamic mode initialization
[AD-A240687] N92-11609
Kinematics and dynamics of barred galaxies N92-11937
VELOCITY MEASUREMENT
NACA 0015 wing pressure and trailing vortex measurements
[NASA-TP-3151] N92-10981
Hydrodynamic tunnel study of the marginal vortex breakdown in the pressure field of a wing profile
[ONERA-RSF-44/1147-AY-144A] N92-11308
VENUS ATMOSPHERE
Electron distributions and solar wind interaction with nonmagnetic planets N92-11952
VERBAL COMMUNICATION
Cognitive factors involved in the first stage of programming skill acquisition
[AD-A240566] N92-11636
VERTICAL LANDING
Static internal performance of ventral and rear nozzle concepts for short-takeoff and vertical-landing aircraft
[NASA-TP-3103] N92-10975
VERY LARGE SCALE INTEGRATION
Test and diagnosis of programmable integrated circuits
[ETN-91-99483] N92-11253
Analysis of experimental results on functional testing and diagnosis of complex circuits N92-11254
Towards an automated system for the verification and diagnosis of intelligent VLSI circuits N92-11262
VHSIC (CIRCUITS)
Tester Independent Support Software System (TISSS)
[AD-A240668] N92-11681
VIBRATION DAMPING
Active vibration damping of the Space Shuttle remote manipulator system
[NASA-TM-104149] N92-11073
Microgravity vibration isolation: An optimal control law for the one-dimensional case
[NASA-TM-105146] N92-11217
Modeling of flexible polyarticulate chains: Bibliographic synthesis
[CERT-DERA-1/7735] N92-11927
VIBRATION ISOLATORS
Microgravity vibration isolation: An optimal control law for the one-dimensional case
[NASA-TM-105146] N92-11217
VIEW EFFECTS
Influence of the viewing geometry on the spectral properties (high resolution visible and NIR) of selected soils from Arizona N92-11473
Normalization of multidirectional red and NIR reflectances with the SAVI N92-11477
View-atmosphere-soil effects on vegetation indices derived from SPOT images N92-11552
VIEWING
View-atmosphere-soil effects on vegetation indices derived from SPOT images N92-11552
VINYL POLYMERS
Deformation of isodamp (A polyvinyl chloride-based elastomer) at various loading rates
[AD-A240393] N92-11189
Photothermal deflection spectroscopy of conjugated polymers
[DE91-018318] N92-11204
VIRTUAL MEMORY SYSTEMS
ART/Ada design project, phase 1: Project plan
[NASA-CR-187313] N92-11663
VISCOELASTICITY
Damage evolution in filled elastomers
[AD-A240532] N92-11191
Experimental determination of the material parameter of two viscoelastic synthetic materials, using creep tests
[ILR-MITT-244(1990)] N92-11385
VISCOPLASTICITY
Effects of elevated temperature on the viscoplastic modeling of graphite/polymeric composites
[NASA-TM-104160] N92-11149
Advanced stress analysis methods applicable to turbine engine structures
[NASA-CR-187235] N92-11378
Geometrically exact shells models: Foundation and computational aspects with special reference to implicit large-scale calculations
[DE91-019014] N92-11390
Thermoviscoplastic response of Ti-15-3 under various loading conditions
[NASA-CR-187621] N92-11391
VISCOSITY
Critical velocities and mutual friction in He-3-He-4 II mixtures at temperatures below 100 mK
[ETN-91-90132] N92-11314
VISCOUS DAMPING
Theoretical estimation of the viscous damping from liquid transient motion in tanks
[NAL-TR-1095] N92-11298
VISCOUS FLOW
Viscous computations of cold air/air flow around scramjet nozzle afterbody
[NASA-CR-4406] N92-10982
The effects of Reynolds number, rotor incidence angle and surface roughness on the heat transfer distribution in a large-scale turbine rotor passage
[NASA-CR-187693] N92-11297
VISCOUS FLUIDS
Numerical analysis of the problem of long waves in shallow water N92-11720
VISIBLE SPECTRUM
On the value of high spectral resolution measurements in the visible and near-infrared N92-11419
Structural controls on the remotely sensed response of a coniferous forest plantation N92-11516

VISION
PET studies of components of high-level vision
[AD-A240202] N92-11624
VISUAL PERCEPTION
PET studies of components of high-level vision
[AD-A240202] N92-11624
The effect of blinking on subsequent dark adaptation
[AD-A240281] N92-11625
Perceptual style and air-to-air tracking performance
[NASA-TM-102868] N92-11629
Perception and memory of pictures
[AD-A240364] N92-11633
VITERBI DECODERS
Error control techniques for satellite and space communications
[NASA-CR-188997] N92-11228
VOIDS
Large deformation induced failures in nonlinear solids
[AD-A240369] N92-11382
VOLATILITY
Low volatile organic compound paints
[DE91-017984] N92-11203
VOLCANOES
A study on the effects of Mt. Sakurajima's falling ash over crop and forest areas using image processing for LANDSAT-5, MOS-1, and Jafsa digital data N92-11497
Monitoring volcanoes using short wavelength infrared images N92-11498
VORTEX BREAKDOWN
Experimental investigation of the effects of blowing on bursting of strake vortices
[AD-A240256] N92-10985
Hydrodynamic tunnel study of the marginal vortex breakdown in the pressure field of a wing profile
[ONERA-RSF-44/1147-AY-144A] N92-11308
VORTICES
NACA 0015 wing pressure and trailing vortex measurements
[NASA-TP-3151] N92-10981
A comparison of airborne wake vortex detection measurements with values predicted from potential theory
[NASA-TP-3125] N92-10994
Wing tip turbine: Analysis of the results of S2MA sounding of marginal vortex of the A320, technical summary
[ONERA-RTS-21/4365-AY-056A] N92-11009
Ignition and structure of a laminar diffusion flame in the field of a vortex
[NASA-CR-189042] N92-11162
The three-dimensional evolution of a plane mixing layer. Part 1: The Kelvin-Helmholtz roll-up
[NASA-TM-103856] N92-11303
Hydrodynamic tunnel study of the marginal vortex breakdown in the pressure field of a wing profile
[ONERA-RSF-44/1147-AY-144A] N92-11308
Vortex-lattice states of a two-dimensional electron system at strong magnetic fields
[DE91-018551] N92-11916
Superfluid-like turbulence in cosmology
[NASA-CR-189011] N92-11942

W

WAFERS
Micro photoreflectance semiconductor wafer analyzer
[AD-D014950] N92-11788
WAKES
A comparison of airborne wake vortex detection measurements with values predicted from potential theory
[NASA-TP-3125] N92-10994
A compact laser photocathode driven accelerator for the Plasma Wake Field Accelerator Program at UCLA
[AD-A240646] N92-11886
WALKING MACHINES
Leveling of the AMBLER walking machine: A comparison of methods
[NASA-CR-189015] N92-11358
WALL FLOW
Model representation in the PANCOR wall interference assessment code
[NASA-TM-104152] N92-11022
WALLS
Graphites as plasma facing material of a large fusion device N92-11813
Analysis of scrape-off layer in toroidal helical systems N92-11815
WARFARE
The role of stealth in naval aviation and joint/combined operations
[AD-A240595] N92-11005
WARNING SYSTEMS
Rapidly quantifying the relative distention of a human bladder
[NASA-CASE-LAR-13901-2] N92-11621
WASTE HEAT
Lunar radiator shade
[NASA-CASE-MSC-21868-1] N92-11639
WASTE TREATMENT
Ground penetrating radar data acquisition system
[AD-A240765] N92-11244
WASTES
Three dimensional migration and forward modelling of ground penetrating radar data
[AD-A240505] N92-11234
WATER
Aircraft lidar sensitivity study for measuring water vapor
[AD-A240549] N92-11237
The use of a time-resolved lidar to study the water column N92-11548
Photoreflectance and H2O adsorption on GaAs(100)
[AD-A240391] N92-11911
WATER EROSION
Evaluation of ground cover in agricultural environment by in situ measurements and multitemporal images for modeling hydric erosion N92-11528
WATER FLOW
Measurement of turbulent flow beneath the wind wave induced water surface, using picture repetition analysis
[ETN-91-90203] N92-11316
WATER POLLUTION
Multi-temporal monitoring of lake water quality N92-11426
WATER QUALITY
Multi-temporal monitoring of lake water quality N92-11426
A multi-sensor approach to spectral signature analysis of inland waters N92-11428
WATER RESOURCES
Combined use of Earth observation satellite and meteorological satellite for crop assessment in semiarid environments N92-11494
Hourly and daily precipitation frequencies for the United States
[AD-A240746] N92-11599
WATER TABLES
Airborne passive microwave remote sensing of land and water surface N92-11492
WATER VAPOR
Aircraft lidar sensitivity study for measuring water vapor
[AD-A240549] N92-11237
Retrievals of column atmospheric water vapor, vegetation liquid water, and cloud cover fraction from AVIRIS data N92-11427
WATER WAVES
Measurement of turbulent flow beneath the wind wave induced water surface, using picture repetition analysis
[ETN-91-90203] N92-11316
Use of theoretical wave height distributions in directional seas
[AD-A240411] N92-11608
Numerical analysis of the problem of long waves in shallow water N92-11720
WATERWAVE ENERGY CONVERSION
Index and bulk parameters for frequency-direction spectra measured at CERC field research facility
[AD-A240320] N92-11607
WAVE INTERACTION
Energetics diagnosis of numerical simulation of atmospheric blocking
[NASA-CR-183503] N92-11581
WAVE PROPAGATION
Irradiance compensation control for high-energy laser propagation, part 2
[DE91-018489] N92-11348
On the solution for the problem of long waves in a perfect fluid N92-11721
Wavefields near transverse cusp caustics produced by reflecting ultrasonic transients and tone bursts from curved surfaces
[AD-A240641] N92-11763
Full-wave calculation of fast-wave current drive in tokamaks including k(parallel) variations
[DE92-000076] N92-11894
WAVE REFLECTION
Active radar stealth device
[AD-D014980] N92-11246
Wavefields near transverse cusp caustics produced by reflecting ultrasonic transients and tone bursts from curved surfaces
[AD-A240641] N92-11763
WAVE SCATTERING
Dual-polarized scatterometer measurements of wind and mechanically generated waves in a very large wind/wave flume, the VIERS-1 project N92-11443
WAVEGUIDE ANTENNAS
Three-dimensional calculations of fields and loading for loop and folded waveguide ICRF antennas
[DE92-000065] N92-11250
WAVEGUIDES
Results of folded waveguide tests on RFTF
[DE91-018930] N92-11249
Three-dimensional calculations of fields and loading for loop and folded waveguide ICRF antennas
[DE92-000065] N92-11250
WEAK INTERACTIONS (FIELD THEORY)
Global analysis of fermion mixing with exotics
[NASA-CR-189006] N92-11774
WEATHER
Mariners Weather Log, Volume 35, Number 1, Winter 1991
[PB91-201129] N92-11591
Mariners Weather Log, Volume 35, Number 2, Spring 1991
[PB91-202572] N92-11592
WEATHER FORECASTING
Space observation of the land-ocean-atmosphere system at high spectral resolution in the infrared: Perspectives and problems N92-11421
Weather prediction using a genetic memory
[NASA-CR-185448] N92-11590
Pilot's Automated Weather Support System (PAWSS) concepts demonstration project. Phase 1: Pilot's weather information requirements and implications for weather data systems design
[NASA-CR-188228] N92-11593
A method for estimating missing hourly temperatures using daily maximum and minimum temperatures
[AD-A240394] N92-11594
March AFB forecasting rules of thumb evaluation
[AD-A240458] N92-11595
Mesoscale prediction and satellite cloud analysis for advanced meteorological processing systems
[AD-A240510] N92-11597
WEATHER MODIFICATION
Hourly and daily precipitation frequencies for the United States
[AD-A240746] N92-11599
WEAVING
Integral fill yarn insertion and beatup method
[NASA-CASE-LAR-14046-1] N92-11219
Woven angle ply fabric and apparatus and method for producing such fabrics
[NASA-CASE-LAR-14048-1] N92-11220
WEIGHT REDUCTION
Multidisciplinary optimization of controlled space structures with global sensitivity equations
[NASA-TP-3130] N92-11087
Effects of anisotropic conduction and heat pipe interaction on minimum mass space radiators
[NASA-TM-105297] N92-11138
WETTING
Contact angle and work of adhesion between Ni-based melts and non-metallic solids
[NPL-DMM(A)-23] N92-11171
WHEAT
High resolution spectral measurements of vegetation and soil in field and laboratory N92-11437
Construction of ground cover charts of a wheat canopy from reflectance measurements N92-11505
WHISPERING GALLERY MODES
The 100 GHz half megawatt microwave transmission system development with whispering gallery mode N92-11869
WIGGLER MAGNETS
Reduction of FEL gain due to wiggler errors
[DE92-000482] N92-11350
The effect of wiggler errors on FEL gain
[DE92-000483] N92-11351
WIND EFFECTS
Contribution of active microwaves to the structural analysis of epicontinental shelf-forms: Example of the English Channel N92-11448
Index and bulk parameters for frequency-direction spectra measured at CERC field research facility
[AD-A240320] N92-11607
WIND MEASUREMENT
An assessment of the available windy land area and wind energy potential in the contiguous United States
[DE91-018887] N92-11601
WIND TUNNEL CALIBRATION
Calibration of the Naval Postgraduate School 3.5' x 5.0' academic wind tunnel
[AD-A240614] N92-11025
WIND TUNNEL MODELS
Model representation in the PANCOR wall interference assessment code
[NASA-TM-104152] N92-11022

WIND TUNNEL TESTS
Experimental study of an independently deflected wingtip mounted on a semispan wing
[NASA-TM-102842] N92-10983
Subsonic wind tunnel testing handbook
[AD-A240263] N92-10986
Application of infrared thermography to thermal flux measurement in wind tunnels
[AAAF-NT-89-12] N92-11020
Further developments relating to the NASA Langley Research Center 13-inch magnetic suspension and balance system
[NASA-CR-188995] N92-11023
Effect of particle size of Martian dust on the degradation of photovoltaic cell performance
[NASA-TM-105232] N92-11133
WIND TUNNELS
Calibration of the Naval Postgraduate School 3.5' x 5.0' academic wind tunnel
[AD-A240614] N92-11025
WIND TURBINES
Development of a personal computer program for milling the shapes of wind turbine blades. Theory and application
[ILR-MITT-243(1990)] N92-11360
An assessment of the available windy land area and wind energy potential in the contiguous United States
[DE91-018887] N92-11601
WIND VELOCITY
Design and operation of the GL/OPA mobile Doppler lidar
[AD-A240257] N92-11231
Acoustic propagation at low altitude: Effects of atmospheric turbulence (Villeau (France) test)
[ONERA-RT-15/3641-PY] N92-11588
WINDPOWER UTILIZATION
Development of a personal computer program for milling the shapes of wind turbine blades. Theory and application
[ILR-MITT-243(1990)] N92-11360
An assessment of the available windy land area and wind energy potential in the contiguous United States
[DE91-018887] N92-11601
WING PROFILES
Computational study of the aerodynamics and control by blowing of asymmetric vortical flows over delta wings
[NASA-CR-187979] N92-10990
Resolution of the Navier-Stokes equations applied to the computation of the laminar flow around a two dimensional wing profile
[CERT-RT-65/5604-35] N92-11307
WING TIPS
NACA 0015 wing pressure and trailing vortex measurements
[NASA-TP-3151] N92-10981
Experimental study of an independently deflected wingtip mounted on a semispan wing
[NASA-TM-102842] N92-10983
Wing tip turbine: Analysis of the results of S2MA sounding of marginal vortex of the A320, technical summary
[ONERA-RTS-21/4365-AY-056A] N92-11009
WINGS
NACA 0015 wing pressure and trailing vortex measurements
[NASA-TP-3151] N92-10981
WINTER
Winter use plan: Environmental assessment
[PB91-194027] N92-11574
WIRE
Wire core reactor for NTP N92-11099
WIRING
New insulation constructions for aerospace wiring applications. Volume 1: Testing and evaluation
[AD-A240638] N92-11006
WORKSTATIONS
Telescience workstation
[NASA-CR-188878] N92-11033
An application for multi-person task synchronization
[NASA-CR-187712] N92-11918

X

X RAY ABSORPTION
Polarized x ray absorption spectroscopy for the study of superconductors and magnetic materials
[DE91-017990] N92-11163
X RAY ASTROPHYSICS FACILITY
The great observatories for space astrophysics
[NASA-NP-128] N92-11066
X RAY DIFFRACTION
Spectral identification (1.2-2.5 microns) and characterization of Paris (France) Basin kaolinite/smectite clays using a field spectrometer N92-11429
X RAY SPECTRA
Modeling UV and x ray oxygen emission in astrophysical plasmas
[DE91-016927] N92-11940
X RAY TUBES
Continuum x ray gauging of multiple-element materials
[DE91-017429] N92-11368
X RAYS
Limits of energy dissipation for x ray sensitive pn Charge Coupled Devices (CCDs)
[MPE-224] N92-11280
Intercomparison of the medium energy primary standards for x ray exposure of NPL and ENEA, Italy
[NPL-RSA(EXT)-18] N92-11766
Intercomparison of the low energy primary standards for x ray exposure of NPL and ENEA, Italy
[NPL-RSA(EXT)-19] N92-11767
Laser produced plasma soft x ray generation
[DE91-016925] N92-11874
Conditional climatology of Ap: The relationship between various solar events (surges, prominences, filaments, radio bursts, x ray episodes) and geomagnetic storms
[AD-A240457] N92-11958
XENON
Development of a high resolution liquid xenon imaging chamber for gamma-ray astronomy
[NASA-CR-188994] N92-11332

Y

YAG LASERS
Novel nonlinear laser diagnostic techniques
[AD-A240193] N92-11346
YARNS
Integral fill yarn insertion and beatup method
[NASA-CASE-LAR-14046-1] N92-11219
Woven angle ply fabric and apparatus and method for producing such fabrics
[NASA-CASE-LAR-14048-1] N92-11220
YTTRIUM
High-T sub c fluorine-doped YBa2Cu3O(y) films on ceramic substrates by screen printing
[NASA-TM-105296] N92-11188
YTTRIUM OXIDES
Glass formation, properties, and structure of soda-yttria-silicate glasses
[NASA-TM-104488] N92-11202
Neutron diffraction from the flux line lattice
[DE91-018175] N92-11906

Z

ZEOLITES
Biological effects of minerals
[DE91-018183] N92-11615

Typical Personal Author Index Listing

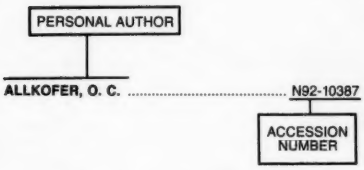

Listings in this index are arranged alphabetically by personal author. The accession number denotes the number by which the citation is identified.

A

ABELL, J. S. N92-11906
ABRAMO, R. S. N92-11236
ADAMS, CATHERINE N92-10993
ADAMS, M. L. N92-11379
AGBORMBAI, ADOLF A. N92-11289
AHUJA, NARENDRA N92-11678
AIZAWA, MASAMITSU N92-11848
AKERA, H. N92-11916
AL-SAADI, JASSIM A. N92-11022
ALBEROTANZA, L. N92-11440
ALBRECHT, ANDREAS N92-11941
ALEJALDRE, CARLOS L. N92-11803
N92-11807
N92-11828
N92-11829
ALEXANDER, HAROLD L. N92-11215
ALEXANDER, MICHAEL G. N92-10986
ALEXANDREAS, D. E. N92-11961
ALGER, LINDA S. N92-11704
N92-11706
ALLADIO, F. N92-11863
ALLAIRE, P. E. N92-11217
ALLEN, BRADLEY P. N92-11663
N92-11664
N92-11665
N92-11666
N92-11667
ALLEN, ROGER E. N92-11347
ALLEY, R. E. N92-11415
ALMOGUERA, L. N92-11803
ALONSO, J. N92-11803
N92-11829
ALP, E. E. N92-11163
ALPERT, D. J. N92-11568
ALTER, JAMES J. N92-11230
ALVARADO, FERNANDO L. N92-11656
AMANO, TSUNEO N92-11833
AMBROZOVA, Z. N92-11954
AMMER, U. N92-11437
AMSTERDAM, JONATHAN N92-11650
ANABITARTE, E. N92-11803
N92-11819
N92-11820
ANDERSEN, CARL K. N92-11587
ANDERSEN, CARL M. N92-11640
ANDERSEN, KRISTINN N92-11218
ANDERSON, D. T. N92-11825
N92-11826
ANDERSON, F. S. B. N92-11819
N92-11825
N92-11826
ANDERSON, JOHN E. N92-11562
ANDO, A. N92-11870
ANDO, T. N92-11182
ANDRE, J. C. N92-11557
ANDRIEU, BRUNO N92-11435
N92-11514
ANGEL, PAUL W. N92-11202
ANGHAIE, SAMIM N92-11105
ANNANPALO, J. N92-10998
ANTYUFEEV, VICTOR S. N92-11481
ANZAI, MASANORI N92-11282
APRILE, ELENA N92-11332
ARMAN, B. N92-11291
ARMERO, F. N92-11390
ARONSON-UNGER, S. N92-11206
ARZAMAZOV, G. S. N92-11617
ASAO, MAKOTO N92-11843
N92-11844
ASCASIBAR, E. N92-11803
N92-11820
N92-11829
ASMAMI, M. N92-11406
ASRAR, GHASSEM N92-11466
N92-11474
N92-11554
ATCHLEY, PAUL N92-11629
ATZBERGER, CLEMENT N92-11399
AU, ANDREW Y. N92-11583
AUKERMAN, CARL A. N92-11135
AXELROD, T. S. N92-11794
AYER, TIMOTHY C. N92-10979

B

BABA, T. N92-11851
BABICHENKO, S. M. N92-11537
BADALEC, J. N92-11881
BAEK, BYUNG JOON N92-11293
BAGOT, KEITH W. N92-11029
BAILEY, DAVID H. N92-11224
BAITY, F. W. N92-11249
N92-11250
BAKER, G. L. N92-11204
BAKER, KARL W. N92-11138
BALAGEAS, D. N92-11020
BALCER, S. N92-11132
BALDWIN, R. W. N92-11682
BALOIS, JEAN-YVES N92-11471
BANGUI, F. N92-10989
BANIN, A. N92-11424
BANNINGER, CLIFF N92-11423
N92-11536
BANSAL, NAROTTAM P. N92-11188
BARET, FREDERIC N92-11418
N92-11434
N92-11435
N92-11479
N92-11501
N92-11514
N92-11518
N92-11522
BARNES, D. C. N92-11827
BARNETT, MARK N92-10979
BARNETT, ROBERT JOEL N92-11218
BARNHILL, R. E. N92-11688
BARNSLEY, MIKE J. N92-11468
BARSANTI, M. L. N92-11335
BASSMAN, MITCHELL N92-11702
BASTIE, J. N92-11184
BATCHELOR, D. B. N92-11250
N92-11894
BATROUNI, G. G. N92-11771
BAUCOM, ROBERT M. N92-11207
BAUMANN, P. N92-11288
BAYLOR, L. R. N92-11889
BAYSAL, OKTAY N92-10982
BECK, ROBERT N92-11234
N92-11244
BECKER, FRANCOIS N92-11490
BEDIDI, ALI N92-11436
BEECROFT, M. N92-11566
BEGUE, AGNES N92-11504
BEHR, ERNST-KARL N92-11279
BELAK, J. F. N92-11709
BELL, G. L. N92-11819
N92-11849
BELL, J. D. N92-11819
BELL, K. J. N92-11291
BELL, WILLIAM A. N92-10978
BELLON, CATHERINE N92-11254
N92-11255
N92-11256
N92-11257
N92-11258
N92-11259
BELTZ, MARK W. N92-11198
BEN-DOR, EYAL N92-11424
BEN-MEHREZ, MERYEM N92-11511
BENALLEGUE, M. N92-11454
BENNETT, GARY L. N92-11089
N92-11131
BENOIST, J. P. N92-11463
BERGER, HAROLD N92-11364
BERGMAN, R. M. N92-11925
BERK, H. L. N92-11890
BERLEMONT, A. N92-11287
BERLEY, D. N92-11961
BERNSTEIN, DENNIS S. N92-11080
N92-11081
BERTHOUMIEUX, P. N92-11020
BERTOLINI, BRUNO N92-11532
N92-11548
BERTUZZI, PATRICK N92-11445
BESNUS, Y. N92-11499
BESSHOU, SAKAE N92-11820
N92-11822
N92-11851
N92-11854
N92-11856
BEVERINI, G. N92-11779
BEZDEK, JAMES C. N92-11662
BEZY, JEAN-LOUP N92-11422
BIDDLE, TEDD B. N92-11213
BIEFELD, ERIC W. N92-11048
BIEGL, CSABA N92-11637
BIELEFELD, BEN N92-11680
BIER, V. M. N92-11746
BIGELOW, T. S. N92-11249
N92-11819
N92-11849
N92-11889
BILLER, S. N92-11961
BIRCHENOUGH, ARTHUR G. N92-11086
BIRNHAM, H. K. N92-11178
BISCHOF, CHRISTIAN H. N92-11660
N92-11726
BISHOP, R. N92-11827
BJORNSON, BRIAN M. N92-11595
BLACKWELL, B. D. N92-11804
BLACKWELL, H. E. N92-11769
BLAIR, M. F. N92-11297
BLAKE, D. W. N92-11734
BLALOCK, TRAVIS N. N92-11621
BLASER, THOMAS J. N92-11519
BLASS, J. J. N92-11389
BLAUMOSER, M. N92-11803
BLOCK, B. P. N92-11284
BOEHM-VITENSE, ERIKA N92-11934
BOHL, J. C. N92-11288
BOISSARD, PAUL N92-11505
BOISVERT, RONALD F. N92-11727
BOMMANNAVAR, A. S. N92-11163
BONGI, GUIDO N92-11539
BONN, FERDINAND N92-11528
BORDWELL, KEVIN N92-11762
BORMANN, CARSTEN N92-11928
BOROWSKI, STANLEY K. N92-11091
BOS, M. J. N92-11376
BOSCHER, D. N92-11020
BOSTON, HAROLD G. N92-11200
BOTIJA, J. N92-11803
N92-11829
BOTTKA, NICHOLAS N92-11788
BOTTONI, M. N92-11321
BOUHELAL, O. K. A. N92-11751
BOULAIS, KEVIN N92-11276
BOUMAN, B. A. M. N92-11444
N92-11512
BOURCIER, R. J. N92-11173
BOURGDOERFER, J. N92-11904
BOWES, M. D. N92-11580
BOY, GUY N92-11673
BRAKEL, R. N92-11820
BRANTOVA, S. S. N92-11617
BRASHEAR, W. T. N92-11134

BRAY, I. N92-11780
BREON, FRANCOIS-MARIE N92-11470
BRIGGS, R. W. N92-11567
BRIOTTET, XAVIER N92-11402
BRITCHER, COLIN P. N92-11023
BRITT, DANIEL L. N92-11059
BROCKELT, ANDREAS C. N92-11887
BROOKS, JEFFREY N. N92-11871
BROOKS, R. D. N92-11875
BROWN, D. L. N92-11732
BROWN, GARY S. N92-11559
BROWN, K. W. N92-11016
BROWN, RICHARD D. N92-11583
BROWN, ROBERT L. N92-11033
N92-11918
BROWN, THOMAS H. N92-11613
BRUCKLER, LAURENT N92-11445
BRUEGGE, CAROL J. N92-11397
BRUMBAUGH, FRED R. N92-11561
BRUNEL, P. N92-11405
BRUNET, YVES N92-11506
N92-11509
BRUSTET, J. M. N92-11529
BUDEN, D. N92-11114
BUECHTER, WILLIAM F. N92-11911
BUEKER, CORDT N92-11425
BUNTINE, WRAY N92-11661
BURATTI, P. N92-11863
BURCHELL, T. D. N92-11205
BURHENN, R. N92-11820
BURKHARDT, LAURA N92-11706
BURRAHM, R. W. N92-11352
BURROWS, A. N92-11935
BUTLER, M. N. N92-11892
N92-11948
BUTTERBRODT, M. C. N92-11925

C

CABESTANY, J. N92-11265
CAILLAULT-VOYER, SABINE N92-11457
CAIN, R. N. N92-11246
CALKOEN, C. N92-11443
CALOZ, REGIS N92-11519
CAMPBELL, A. N. N92-11283
CANARD-CARUANA, S. N92-11588
CANNON, I. N92-11132
CARHART, H. W. N92-11193
CARIGNAN, G. R. N92-11284
CARLSON, K. D. N92-11899
CARRERAS, BRIAN A. N92-11802
N92-11807
N92-11809
N92-11819
N92-11830
N92-11831
CARRERE, VERONIQUE N92-11397
N92-11420
CARRETTA, THOMAS R. N92-11630
CARRIER, MELVIN, JR. N92-11762
CARRUTHERS, THOMAS F. N92-11343
CARSON, GEORGE T., JR. N92-10975
CARTER, M. D. N92-11249
N92-11250
CARY, J. R. N92-11805
N92-11893
CASALIS, G. N92-11306
CASELLES, VICENTE N92-11410
N92-11495
N92-11507
CASPI, PAUL N92-11268
CASTANER, B. G. N92-11803
CASTEJON, F. N92-11803
N92-11828
N92-11829
CASTLE, KENT D. N92-11627
CATTANEI, G. N92-11820
CAVALIER, ALBERT R. N92-11621
CAVAYAS, F. N92-11530
CECCHI, GIOVANNA N92-11533
CEPERO, J. R. N92-11803
N92-11829
CEREZO, A. N92-11779
CERJAN, C. N92-11874
N92-11940
CERVAY, RUSSELL R. N92-11179
CERVELLE, B. N92-11436
CHA, BYUNG HEON N92-11349
CHAIKOVSKAYA, L. I. N92-11396
CHAKROUN, H. N92-11446
CHALABI, ABDALLAH N92-11714
N92-11715
N92-11716
N92-11717
N92-11718
N92-11720
N92-11721
CHAMIS, CHRISTOS C. N92-11373
CHAMPION, ISABELLE N92-11447
CHAN, TONY F. N92-11701
N92-11731
CHANG, C. Y. N92-11961
CHANG, T. Y. N92-11375
CHANZY, ANDRE N92-11453
CHAPMAN, BARBARA N92-11670
CHAPPELLE, E. N92-11536
CHAPUIS, T. N92-11267
CHARBONNEAU, L. N92-11493
CHARLTON, LOWELL A. N92-11809
N92-11819
CHARRON, C. N92-11524
CHARRON, CHRISTOPHE N92-11496
CHATO, DAVID J. N92-11129
CHAVEZ, J. M. N92-11568
CHEDIN, A. N92-11421
CHEHBOUNI, A. N92-11477
N92-11552
CHENG, TSARNG-SHENG N92-11159
CHERNYAKOV, I. N. N92-11618
CHEVREL, SERGE N92-11438
CHIN, R. C. Y. N92-11732
CHIU, Y. T. N92-11585
CHOE, HOWARD C. N92-11333
CHOE, JOHN N92-11276
CHOROWICZ, JEAN N92-11496
CHOU, T. S. N92-11784
CHOUDHURY, ALOK N. N92-11672
CHOUDHURY, BHASKAR J. N92-11466
N92-11489
CHRETIEN, JEAN-PIERRE N92-11927
CHRISTL, LIGIA C. N92-11076
N92-11077
CHUKHNO, E. I. N92-11619
CHUNG, T. J. N92-11122
CHURCH, VICTOR E. N92-11702
CINTRON, NITZA M. N92-11628
CIRIELLO, SALVATORE, JR. N92-11305
CLARK, BRUCE J. N92-11691
CLARK, J. A. N92-11435
CLARK, JOHN S. N92-11088
N92-11090
CLARK, T. L. N92-11819
CLEVERS, J. G. P. W. N92-11425
CLOSE, F. E. N92-11768
COCHRAN, M. N92-11132
COHEN, NORMAN S. N92-11125
COHEN, ROBERT B. N92-11225
COHEN, YUVAL N92-11241
COLCHIN, R. J. N92-11819
COLE, E. I., JR. N92-11283
COLE, RICHARD N92-11705
COLL, CESAR N92-11410
COLLET, CLAUDE N92-11519
COLLIER, DAVID W. N92-11244
COMPANION, JOHN A. N92-11621
CONARD, DIDIER N92-11264
N92-11265
CONEL, JAMES E. N92-11397
CONKLIN, J. C. N92-11216
CONWAY, G. D. N92-11804
CONWAY, J. A. N92-11442
CONWAY, SCOTT N92-10999
COOK, GEORGE E. N92-11218
N92-11637
COOPER, G. J. N92-11804
COOPER, LYNNE P. N92-11048
COOPER, PAUL A. N92-11392
CORDA, ALBERT J. N92-11246
CORDEY, R. A. N92-11442
COSENTINO, JAY N92-11244
COSTELLO, DANIEL J., JR. N92-11228
COSTEN, ROBERT C. N92-11336
COUGHENOUR, M. B. N92-11575
COULOMBE, A. N92-11493
COURAULT, DOMINIQUE N92-11515
COUSTOLS, E. N92-11309
COX, GEORGE B., JR. N92-11123
CRABILL, NORMAN L. N92-11593
CRABTREE, G. W. N92-11899
CRAIG, KEN N92-10990
CRAM, J. N92-11575
CREMERS, T. N92-11330
CRIPPEN, ROBERT E. N92-11553
CRISANTI, F. N92-11863
CUBITT, R. N92-11906
CUCINOTTA, FRANCIS A. N92-11685
CUI, CHUN-FANG N92-11072
CULL, RONALD C. N92-11131
CULLERS, D. KENT N92-11745
CURRAN, P. J. N92-11516
CURRY, ROBERT E. N92-11301
CURTISS, BRIAN N92-11551
CYBENKO, G. N92-11689
CYR, LINDA N92-11528
CYR, REGINALD N92-11760

D

DABROWSKA-ZIELINSKA, K. N92-11531
DAGUM, LEONARDO N92-10977
DAHLBERG, E. D. N92-11176
DAHN, H.-G. N92-11540
DALE, B. J. N92-11388
DALEY, WILLIAM J. N92-11561
DALU, G. N92-11600
DANDEKAR, D. P. N92-11189
DANFORTH, DOUGLAS G. N92-11699
DANSON, F. MARK N92-11426
N92-11435
N92-11516
DAROLIA, R. N92-11175
DAROOKA, D. K. N92-11097
DARWISH, SALAH M. D. N92-11915
DAS, D. K. N92-11567
DAS, RAJA N92-11669
DASH, ERNIE R. N92-11593
DAUZAT, JEAN N92-11476
DAVIDDECASTROLOBO, P. N92-11571
DAVIDIAN, KENNETH O. N92-11120
N92-11126
DAVIS, DONALD A. N92-11562
DAVIS, ERIC WESLEY N92-11949
DAVIS, J. K. N92-11352
DAVIS, JAMES BRADLEY N92-11038
DAVIS, JOEL N92-11367
DAVIS, RANDALL C. N92-11668
DAVIS, WILLIAM T. N92-11035
DAYHOFF, EDWARD S. N92-11247
DAYTON, BIRNEY D. N92-11225
DEALY, BRIAN N92-11053
DEAN, G. D. N92-11185
DEANGELIS, R. M. N92-11591
N92-11592
DEANS, STANLEY R. N92-11745
DEBRISIS, SABINE N92-11494
DEBRUIJN, ROBERT ANTONIE N92-11315
DECHAMBRE, M. N92-11454
N92-11456
DEHAAN, JOHAN F. N92-11400
DEISSLER, ROBERT G. N92-11317
DEJESUS, ROLAND E. N92-11609
DEKKER, A. G. N92-11428
DELAAT, JOHN C. N92-11017
DELECOLLE, RICHARD N92-11501
N92-11518
DELEGIDO, JESUS N92-11507
DELENYAN, N. V. N92-11617
DELORME, PHILIPPE N92-10988
DELPECH, P. N92-11020
DELPHIN, L. N92-11402
DEMCHENKO, YE. A. N92-11619
DEMEO, MARTHA E. N92-11073
DENNING, PETER J. N92-11643
N92-11645
N92-11657
N92-11695
N92-11698
N92-11753
N92-11936
DEOM, A. N92-11020
DERIDDER, JEAN-JACQUES N92-11248
DERKSEN, JACOBUS JOHANNES N92-11756
DEROIN, JEAN-PAUL N92-11448
DERRIEN, M. N92-11405
DESAINT-VICTOR, X. N92-11307
DESCHAMPS, PIERRE-YVES N92-11416
N92-11474
DESJONQUERES, P. N92-11287
DESPRAT, J. F. N92-11504
DETORE, JACK N92-10999
DEUFLHARD, PETER N92-11655
DEUTSCH, S. N92-11964
DEUZE, J.-L. N92-11409
N92-11471
N92-11485
DEVAUX, C. N92-11409
N92-11471
DEWAR, ROBERT L. N92-11804
DHERBES, J.-M. N92-11515
DIAMOND, P. H. N92-11830
DIAZ, NILS J. N92-11109
DIETZ, JOHN B. N92-11491
DIMOS, D. N92-11901
DINENNO, P. J. N92-11193
DINGUIRARD, MAGDELEINE N92-11517
DINGUS, B. L. N92-11961
DION, C. N92-11961

DION, G. M. N92-11961
DISALVO, FRANCIS J. N92-11912
DIVECHA, AMARNATH P. N92-11144
DIXON, TIMOTHY H. N92-11553
DODDS, JAMES N92-11084
N92-11085
DODELSON, SCOTT N92-11944
DODHY, A. N92-11820
DODSON, H. C. N92-11361
DOERFLER, THOMAS N92-11148
DOLMAN, V. L. N92-11400
DOMALEWSKI, STEVE N92-11006
N92-11007
DOMINGUEZ, N. N92-11807
N92-11809
N92-11830
N92-11831
DOMITZ, STAN N92-11272
DORST, D. N92-11820
DOUGLAS, N. B. N92-11584
DOWNER, JANICE DIANE N92-11371
DOYLE, DEE N92-11033
N92-11918
DOYLE, JOHN N92-11018
DOZIER, JEFF N92-11482
N92-11556
DRAKE, R. P. N92-11344
DRESNER, L. N92-11725
N92-11802
DRYER, FREDRICK N92-11164
DUDELZAK, ALEXANDER N92-11537
DUIS, DAVID N92-11649
DUKES, RON N92-11635
DULING, IRL N92-11343
DUMMER, R. S. N92-11566
DUNBAR, BONNIE J. N92-11930
N92-11931
DUNN, P. J. N92-11584
DUNNING, M. N92-11940
DUNNING, T. H., JR. N92-11687
DUYAR, AHMET N92-11017

E

EASTES, JOHN W. N92-11564
EASTLAND, A. H. J. N92-11361
EASTMAN, J. N92-11575
EASTWOOD, J. A. N92-11472
EBELING, KARI N92-11151
N92-11152
N92-11157
N92-11158
EDWARDS, JONATHAN L. N92-11951
EERENS, HERMAN N92-11508
EHST, D. A. N92-11888
EKLUND, DEAN R. N92-11118
EL-GENK, MOHAMED S. N92-11101
ELDER, R. L. N92-11015
ELGERSMA, MIKE N92-11018
ELKUS, RICHARD J., JR. N92-11225
ELLIOTT, D. L. N92-11601
ELMER, J. W. N92-11174
ELSNER, A. N92-11820
ELTSOVA, L. D. N92-11325
ELVIDGE, CHRISTOPHER D. N92-11519
EMERY, D. E. N92-11682
EMMITT, G. D. N92-11648
ENGELUND, WALTER C. N92-10982
ENGLISH, R. E., JR. N92-11789
ENTINE, GERALD N92-11331
ESCADAFAL, RICHARD N92-11473
ESTEROWITZ, LEON N92-11347
EVANS, D. N92-11450
EVANS, DIANE L. N92-11441
EWERT, MICHAEL K. N92-11639

F

FAI, G. N92-11782
FALGUERE, D. N92-11267
FAMIGLIETTI, J. S. N92-11459
FANTONDANDON, O. N92-11422
FARBMAN, GERRY N92-11093
FARIS, GREGORY W. N92-11346
FARLEY, GARY L. N92-11219
N92-11220
FARRUGIO, HENRI N92-11455
FAUCI, LISA J. N92-10984
FEIT, ZEEV N92-11341
FEOKTISTOV, K. P. N92-11032
FERNANDEZ, KENNETH R. N92-11218
FERREIRA, P. A. N92-11571
FERRELL, T. L. N92-11905
FERRISS, D. H. N92-11370
FERTIS, D. G. N92-11379
FIALA, JOHN C. N92-11712
FIELD, R. D. N92-11175
FILY, MICHEL N92-11463
N92-11464
FINDLAY, JOHN T. N92-11083
FINLEY, TOM D. N92-11340
FISCHER, ALBERTE N92-11513
N92-11518
FISCHER, BERND N92-11722
N92-11724
FISCHER, R. P. N92-11334
N92-11335
FISHER, ALBERTE N92-11525
FISHER, YUVAL N92-11680
FISHMAN, G. J. N92-11075
FLECKENSTEIN, H. N92-10996
FLESHLER, S. N92-11899
FLIFLET, A. W. N92-11334
N92-11335
FONTAN, J. N92-11529
FONTANA, J. R. N92-11345
FORGAN, E. M. N92-11906
FORNEY, L. J. N92-11339
FORSSELL, E. W. N92-11193
FOSTER, WILLIAM M., II N92-11221
FOURNIER, J. N92-11020
FOX, BARRY R. N92-11060
FOX, N. P. N92-11184
FRAGUAS, A. L. N92-11829
FRANCIS, W. E. N92-11585
FREAR, D. R. N92-11372
FREDERICKSON, CARL K. N92-11763
FREEMANTLE, JIM N92-11408
FREEMEN, A. J. N92-11175
FREUND, ROLAND N92-11655
N92-11722
N92-11724
FRICKE, S. K. N92-11584
FRIEDLANDER, ALAN N92-11116
N92-11214
FRIEDMAN, A. N92-11350
FRIEMAN, JOSHUA A. N92-11943
FROUIN, R. N92-11474
FUERSCHBACH, P. W. N92-11355
FUJIWARA, MASAMI N92-11823
N92-11839
FUJIWARA, YOSHIMASA N92-11679
FUKUMOTO, HIDESHI N92-11840
FUKUYAMA, A. N92-11879
FUKUYAMA, ATSUSHI N92-11815
N92-11846
N92-11882
FUSARO, ROBERT L. N92-11186

G

GABEL, M. R. N92-11368
GABLEHOUSE, R. DANIEL N92-11052
GAIER, JAMES R. N92-11133
GALLE, SYLVIE N92-11454
N92-11456
GALLON, M. N92-11308
GALLOPOULOS, E. N92-11689
N92-11692
GAN, LU N92-11952
GANDY, REX F. N92-11805
N92-11849
GANNAWAY, MARY T. N92-11117
GAO, BO-CAI N92-11427
N92-11551
GAO, YI-TIAN N92-11959
GARCIA, L. N92-11829
N92-11831
GARCIA, THERON D. N92-11572
GARDETTE, G. N92-11020
GARDNER, H. J. N92-11804
GARDNER, W. L. N92-11249
GATES, THOMAS S. N92-11149
GAUTIER, CATHERINE N92-11470
GAUTIER, ROGER P. N92-11762
GAVEL, D. T. N92-11348
GAYNOR, E. S. N92-11364
GEER, JAMES F. N92-11640
GEISER, U. N92-11899
GELLIN, S. N92-11388
GENCER, F. N92-11906
GENNIS, R. B. N92-11612
GEOFFROY, A. L. N92-11046
GEORGE, THOMAS F. N92-11908
N92-11909
GERANIOTIS, EVAGGELOS N92-11240
GERLACH, KARL N92-11238
N92-11239
GESSO, HIROKAZU N92-11848
GHIDELLA, J. R. N92-11369
GIESECKE, ROBERT L. N92-11931
GILBERT, JOHN R. N92-11696
GILBERT, MICHAEL G. N92-11073
GILMOUR, PHILLIP N92-11902
GIRARD, M. N92-11288
GIRARD, R. N92-11146
GIRIDHARAN, V. N92-11079
GLENBERG, ARTHUR M. N92-11631
GLOWINSKI, ROWLAND N92-11730
GLUCKSTERN, R. L. N92-11350
N92-11351
GOEL, NARENDA S. N92-11475
N92-11550
GOETZ, ALEXANDER F. H. N92-11427
GOLDSTEIN, DAVID N92-11569
GOLOVACHEV, S. P. N92-11492
GOMBEER, ROLAND N92-11508
GONZALEZ, L. N92-11471
GONZALEZDESANTOS, PABLO N92-11358
GOODENOUGH, D. G. N92-11439
GOODMAN, I. R. N92-11738
N92-11746
N92-11747
GOODMAN, J. A. N92-11961
GOODRICH, JOHN W. N92-11320
GORSHUNOVA, A. I. N92-11619
GOULAS, YVES N92-11532
N92-11538
N92-11539
GOULD, ANTHONY J. N92-11243
GOULDING, R. H. N92-11249
GOUTORBE, J. P. N92-11557
GOUYET, J. F. N92-11520
GOWER, G. L. N92-11601
GOZE, STEPHANE N92-11449
GRABERT, GREGORY N92-11902
GRADWOHL, BEN-AMI N92-11942
GRAESSER, E. J. N92-11381
GRAHAM, MARC H. N92-11926
GRANCHER, M. S. N92-11287
GRANKOV, A. G. N92-11492
GRANT, N. J. N92-11182
GRAVES, PHILIP C. N92-11087
GREEN, J. L. N92-11189
GREEN, ROBERT O. N92-11397
GREENSTADT, E. W. N92-11795
GREENWOOD, DAN N92-11680
GREGORY, JOHN C. N92-11074
N92-11075
N92-11076
N92-11077
N92-11078
GREY, JERRY N92-11106
GRIEGER, GUNTER N92-11801
GRILLOT, FRANCOIS N92-11256
GRISNIK, STANLEY P. N92-11136
GRISSOM, MARK P. N92-11005
GRODSINSKY, C. M. N92-11217
GROGAN, WILLIAM P. N92-11366
GROPP, WILLIAM D. N92-11731
GROSS, KLAUS W. N92-11119
GRUNEISEN, S. J. N92-11787
GRUSH, RONALD C. N92-11589
GRUSZCZYNSKA, M. N92-11531
GU, CHUN N92-11903
GU, XING-FA N92-11399
N92-11401
N92-11403
N92-11409
GUASP, J. N92-11829
GUEDESDEOLIVEIRA, ANTONIO N92-11740
GUENTHER, KURT P. N92-11540
GUERIF, MARTINE N92-11399
N92-11494
N92-11501
N92-11510
N92-11522
GUILLERMIN, B. N92-11755
GUNN, STANLEY N92-11092
N92-11112
GUO, TEN-HUEI N92-11017
GUPTA, ROOP N. N92-11285
N92-11300
GUSTAFSON, GARY B. N92-11597
GUTHRIE, G. D., JR. N92-11615
GUYOT, A. N92-11264
GUYOT, GERARD N92-11401
N92-11403
N92-11409
N92-11418
N92-11447
N92-11532

H

HADDAD, WASSIM M. N92-11080
N92-11081
HAERING, EDWARD A., JR. N92-11301
HAERTLING, GENE N92-11902
HAINES, RICHARD F. N92-11033
N92-11223
HALDIN, A. A. N92-11492
HALL, F. G. N92-11554
HALL, KENNETH C. N92-10979
HALOULAKOS, V. E. N92-11102
HALPIN, J. M. N92-11789
HAMAJIMA, T. N92-11837
HAMBERGER, S. M. N92-11804
HAMERLINCK, ALPHONSE FLORENTINUS N92-11147
HAMID, S. N92-11015
HAMMOND, STEVEN W. N92-11693
HAMPTON, R. D. N92-11217
HANATANI, KIYOSHI N92-11810
N92-11870
N92-11878
HANDEL, PETER H. N92-11907
HANKIN, M. N92-11189
HANN, RAIFORD E. N92-11202
HANOCQ, J. F. N92-11479
HANSON, J. D. N92-11805
HARADA, MITSURU N92-11853
N92-11856
HARDY, TERRY L. N92-11214
HARGREAVES, T. A. N92-11334
N92-11335
HARMON, B. A. N92-11075
HARPER, RICHARD E. N92-11704
HARRIS, J. H. N92-11823
HARTEN, AMI N92-11736
HARTENSTEIN, RAY N92-11702
HARTFIELD, ROY J., JR. N92-11118
HARTY, R. B. N92-11099
HASEGAWA, A. N92-11872
HASTE, G. R. N92-11249
N92-11250
HAUFF, PHOEBE L. N92-11429
HAUSKNECHT, P. N92-11535
HAUTECOEUR, O. N92-11476
HAVENS, STEPHEN J. N92-11198
HAYASHI, TAKAYA N92-11808
HEATHWAITE, A. L. N92-11426
HEATON, JULIE A. N92-11766
N92-11767
HECKNER, MICHAEL N92-11741
HEDSTROM, G. W. N92-11732
HEEGER, ALAN J. N92-11195
N92-11204
HEINEMANN, H. N92-11160
HEMELINGS, TINE N92-11508
HENDERSON, C. L. N92-11283
HENDERSON, M. A. N92-11805
HENNINGER, SANDRA N92-10993
HENRY, PATRICE N92-11517
HERGENROTHER, PAUL M. N92-11198
HERMAN, M. N92-11416
N92-11471
N92-11484
N92-11485
HERRARTE, V. N92-11710
HERTER, CHRISTIAN G. N92-11654
HEWETT, D. W. N92-11876
HEYMAN, JOSEPH S. N92-11384
N92-11621
HIDAKA, Y. N92-11497
HIDEKUMA, S. N92-11860
HIETANEN, SOILI N92-11150
N92-11151
N92-11152
N92-11153
N92-11154
N92-11155
N92-11156
N92-11157
N92-11158
HIGGINBOTHAM, SCOTT A. N92-11038
HILL, JOACHIM N92-11430
HINO, TOMOAKI N92-11813
HINSE, MARIO N92-11493
HIRAYAMA, T. N92-11842
HIRSHMAN, S. P. N92-11802
N92-11833
HOFFMAN, D. J. N92-11249
N92-11250
HOFFMAN, JAMES W. N92-11589
HOFFMANN, HARALD N92-11432
N92-11433
HOFMANN, E. N92-11602
HOGAN, W. J. N92-11873
HOJO, HITOSHI N92-11884
HOLDEN, MICHAEL S. N92-11319
HOLLOWAY, MATTHEW N92-11641
HOLMES, H. F. N92-11168
HONEY, FRANK R. N92-11519
HOOVER, GORDON N92-11397
HOPPE, FIEDRICH N92-11708
HORA, H. N92-11773
HORGAN, CORNELIUS O. N92-11382
HORNSTEIN, RHODA SHALLER N92-11042
HORNUNG, R. N92-11111
HOROWITZ, RICHARD N92-11921
HORTON, W. N92-11872
HOSOKAWA, MINOLU N92-11823
N92-11845
N92-11862
N92-11869
HOU, TAN-HUNG N92-11207
HOUSE, F. A. N92-11789
HOVENIER, J. W. N92-11400
HOWE, H. C. N92-11857
HOWE, S. A. N92-11134
HOWELL, R. H. N92-11781
HSIEH, T. M. N92-11364
HUA, G. N92-11477
HUANG, HO-CHUN N92-11597
HUDSON, DAVID F. N92-11229
HUESTIS, D. L. N92-11346
HUETE, ALFREDO R. N92-11473
N92-11477
N92-11552
HUETTEN, A. N92-11754
HUGHES, DAVID HANDEL N92-11932
HUGHES, JAMES A. N92-11933
HUMMEL, JOHN R. N92-11565
HUNT, JAMES J. N92-11394
N92-11488
HURTADO, E. N92-11507
HUSSAINI, M. Y. N92-11162
HYDE, J. M. N92-11779

I

ICHIKAWA, YOSHI H. N92-11877
IDA, KATSUMI N92-11796
N92-11823
N92-11860
IDEI, H. N92-11823
N92-11862
IGLESIAS, C. A. N92-11939
IGUCHI, HARUKAZU N92-11823
N92-11857
N92-11858
N92-11861
IIDA, F. N92-11839
IIMA, M. N92-11869
IKEDA, B. N92-11841
IKEUCHI, KATSUSHI N92-11679
IMBERNON, J. N92-11504
IOKA, SHIGERU N92-11838
IOLTUKHOVSKI, A. A. N92-11478
ISHIGURO, E. N92-11497
ISHII, M. N92-11322
ISSENMAN, M. N92-11256
ITOH, KIMITAKA N92-11796
N92-11797
N92-11815
N92-11878
N92-11879
N92-11882
ITOH, SANAE-I. N92-11796
N92-11797
N92-11815
N92-11879
N92-11882
IVALDI, CHARLES F. N92-11597
IVANOVA, S. M. N92-11617

J

JAANIMAGI, P. A. N92-11965
JACKSON, R. D. N92-11395
N92-11552
JACKSON, ROBERT W. N92-11223
JACKSON, T. J. N92-11458
JACKSON, T. L. N92-11162
JACOBS, RICHARD E. N92-11208
JACQUEMOUD, STEPHANE N92-11418
N92-11479
JAECKEL, LOUIS A. N92-11644
JAEGER, E. F N92-11894
JAEGER, E. F. N92-11250
JAEHNE, B. N92-11443
JAFFE, ANDREW H. N92-11943
JAGGARD, K. W. N92-11435
JAIN, H. N92-11206
JAKUBKA, K. N92-11881
JAMES, BENJAMIN B. N92-11087
JANSEN, HEIKE N92-11385
JARBOE, T. R. N92-11875
JASKOWIAK, KENNETH R. N92-11704
JATA, KUMAR V. N92-11179
JEFFRIES, JAY B. N92-11346
JEGGY, T. N92-11145
JEHLE, ROBERT E. N92-11229
JELSKI, DANIEL A. N92-11908
N92-11909
JHIRAD, D. N92-11573
JOACHIM, CHARLES E. N92-11211
JOGLEKAR, UMESH DWARKANATH N92-11711
JOHANNESEN, LEILA N92-11641
JOHNSTON, MARK D. N92-11054
JONES, DAVID A. N92-11304
JONES, JAMES R. N92-11565
JONES, MARSHALL B. N92-11632
JONES, STEPHEN B. N92-11336
JONES, T. C. E. N92-11184
JONES, T. S. N92-11364
JONES, W. B. N92-11173
JUBAS, JAY M. N92-11944
JULLIEN, J. P. N92-11503
JUPP, DAVID L. B. N92-11486
JURNS, JOHN M. N92-11208

K

KACYNSKI, KENNETH J. N92-11126
KAISER, J. H. N92-11781
KALYAKIN, S. G. N92-11324
KAMEARI, A. N92-11841
KAMIMURA, T. N92-11878
KANEKO, HIROSHI N92-11856
KANEKO, OSAMU N92-11823
N92-11861
N92-11870
KANEVSKY, M. B. N92-11451
KANIA, MICHAEL N92-11113
KANO, H. N92-11547
KAPLAN, GEORGE H. N92-11933
KARADY, G. G. N92-11272
KAREMA, H. N92-11327
KARGL, S. G. N92-11761
KARMARKAR, SUBHASH D. N92-11144
KARPEL, MORDECHAY N92-11377
KARSAI, GABOR N92-11637
KASAKA, KAZUO N92-11127
KASDIN, N. JEREMY N92-11068
KASKI, KIMMO N92-11697
KATNIK, GREGORY N. N92-11038
KATZ, ERIC S. N92-11028
KATZAN, CYNTHIA M. N92-11951
KAWAKAMI, ICHIRO N92-11848
KAZAKOS, DIMITRI N92-11333
KEENE, B. J. N92-11171
KEITH, T. G. N92-10976
KEMMLER, J. N92-11904
KERDILES, HERVE N92-11521
KERR, YANN H. N92-11398
N92-11461
KEYES, DAVID E. N92-11731
KIDA, S. N92-11842
KIDDER, PAUL W. N92-11207
KIKUCHI, HITOSHI N92-11848
KILGORE, ROBERT A. N92-11030
KIM, CHAN JOONG N92-11917
KIM, HONGSUK H. N92-11500
KIMMEL, E. C. N92-11134
KING, C. N92-11520
KINI, A. M. N92-11899
KINOSHITA, SHIGEYOSHI N92-11840
KINTZ, GREGORY J. N92-11347
KIRCHER, THOMAS N92-11177
KIRCHHOF, W. N92-11432
N92-11433
KIRK, BILL N92-11100
KISHIMOTO, HIROSHI N92-11812
KITAJIMA, SUMIO N92-11824
KITAMURA, K. N92-11837
N92-11838
KITTEL, T. N92-11575
KLEM, MARK D. N92-11124
KLOP, J. N92-11132
KLOSKO, S. M. N92-11584
KNOROVSKY, G. A. N92-11362
KNOSPE, C. R. N92-11217
KOBAYASHI, S. N92-11869
KOCH, B. N92-11437
KOECHLER, C. N92-11548
KOGA, R. N92-11267

KOIZUMI, M. N92-11547
KOKKE, J. M. M. N92-11404
KOLB, G. J. N92-11568
KOLENKIEWICZ, R. N92-11584
KOLODZIEJ, PAUL N92-11301
KOLOGO, N. N92-11462
KOLOKITHAS, ERASMIA N92-11258
N92-11261
KOMATSU, KEIJI N92-11298
KOMORI, A. N92-11853
KONDO, KATSUMI N92-11822
N92-11851
N92-11852
N92-11853
N92-11856
KONDRATYEV, K. Y. N92-11534
KONO, MITSUO N92-11884
KONOVALOV, D. A. N92-11780
KOSE, KIM N92-11386
KOSKINEN, K. N92-10998
KOSSLYN, STEPHEN M. N92-11624
KOSTYK, DOUGLAS N92-11341
KOTTAPALLI, SESI N92-11000
KRATZ, P. N92-11600
KRAUSE, PAUL N92-11649
KREIDER, KEVIN L. N92-11691
KRINSKY, S. N92-11350
N92-11351
KRIVENSKI, V. N92-11828
KRUGER, GORDON N92-11096
KRULEY, PETER N92-11631
KRUSE, FRED A. N92-11429
N92-11491
KRYSKA, L. N92-11881
KUBO, SHIN N92-11823
N92-11845
N92-11857
N92-11862
N92-11869
KUCK, D. N92-11689
KULHMAN, JOHN M. N92-10985
KUMAR, RENJITH R. N92-11392
KUMAZAWA, RYUHEI N92-11845
N92-11846
KUNG, ERNEST C. N92-11581
KUNO, K. N92-11841
N92-11842
KURODA, TSUTOMU N92-11845
N92-11846
N92-11870
KURODA, YUKIO N92-11127
KURTZMAN, CLIFFORD R. N92-11055
N92-11064
KUTLU, ZAFER SUKRU N92-11141
KWOK, W. K. N92-11899

L

LABED, JELILA N92-11462
LABETSKAYA, O. I. N92-11617
LABRUNEE, M. N92-11267
LACARRERE, P. N92-11503
LACAZE, BERNARD N92-11543
LAGOUARDE, JEAN-PIERRE N92-11509
LAHRMAN, D. F. N92-11175
LAITANO, R. F. N92-11766
N92-11767
LALA, JAYNARAYAN H. N92-11704
LAMBERT, E. N92-11493
LANCE, D. G. N92-11142
LAND, C. E. N92-11901
LANDREAU, J. N92-11793
LANG, MICHAEL N92-11541
LAPCZYK, IRENEUSZ N92-11671
LAPIMAA, J. N92-11537
LARSON, D. J. N92-11876
LATHAM, TOM N92-11110
LATTIMER, J. M. N92-11935
LAURENT, J. N92-11265
LAURILA, R. N92-11327
LAURSEN, T. N92-11390
LAVALLEE, DAVID N92-11050
N92-11063
LAVENU, FRANCOIS N92-11529
LAVREAU, JOHAN N92-11411
LAWRENCE, ALBERT N92-11680
LAYTON, J. PRESTON N92-11106
LEATHERWOOD, JACK D. N92-11759
LEBLON, BRIGITTE N92-11510
N92-11522
LEBOEUF, J. N. N92-11809
N92-11831
LECOMTE, P. N92-11471
LEDEBUHR, A. G. N92-11794
LEE, D. K. N92-11857
LEE, DANIEL M. N92-11008
LEE, EUN HO N92-11790
LEE, EUN U. N92-11177
LEE, HEE GYOUN N92-11917
LEE, JINHO N92-11319
LEE, JOHN N. N92-11792
LEE, JONG MIN N92-11349
LEE, KAM-PUI N92-11285
N92-11300
LEE, S. DANIEL N92-11664
N92-11667
LEE, S. L. N92-11906
LEE, T. S. H. N92-11785
LEE, W. K. N92-11206
LEEUWEN, W. N92-11477
LEFAUCONNIER, BERNARD N92-11523
LEGLEAU, H. N92-11405
N92-11520
LEHMANN, FRANK N92-11407
N92-11431
LEHTONEN, DAVID N92-11681
LEINER, BARRY M. N92-11694
LEMOINE, G. G. N92-11452
LEMPEREUR, C. N92-11020
LEONARD, J. T. N92-11193
LEPRIEUR, CATHERINE E. N92-11418
N92-11434
LEROY, MARC N92-11402
N92-11409
N92-11480
LESNIAREK-HAMID, J. L. N92-11185
LESTER, WILLIAM A., JR. N92-11166
LETELLIER, JULES P. N92-11230
LETOAN, T. N92-11449
LEVIN, E. N92-11770
LEWINSKI, STANISLAW N92-11531
LEWIS, D. L. N92-11368
LEWIS, D. W. N92-11217
LEWIS, I. T. N92-11794
LEYLAND, JANE N92-11000
LI, XIAO-WEN N92-11486
LI, Z. P. N92-11768
LI, ZHAO-LIANG N92-11490
LIBERMAN, B. M. N92-11492
LICHTENTHALER, HARTMUT K. N92-11541
N92-11542
LICINA, JOSEPH R. N92-11004
LIEBMAN, SHIRLEY A. N92-11167
LIM, TAE W. N92-11392
LIN, T. H. N92-11380
LINDBERG, D. M. N92-11890
LINDL, J. D. N92-11873
LINDLEY, R. N92-11889
LINKER, JAMES F. N92-11354
LIOTHIN, A. N92-11256
LIOU, W. W. N92-11302
LITTLE, DAVID D. N92-10991
LIU, C. T. N92-11183
LIU, J. F. N92-11206
LOEWE, MICHAEL N92-11739
LOGAN, C. M. N92-11368
LOGAN, J. R. N92-11057
LOINTIER, MARC N92-11524
LOMAX, CURTIS N92-11286
LOMBA, ILIA M. N92-11762
LONG, CHARLES E. N92-11607
N92-11608
LONG, KEVIN N92-11937
LONG, LYLE N. N92-11070
LONGTIN, DAVID R. N92-11565
LOPES, A. N92-11449
LOPEZ-FRAGUAS, A. N92-11807
LOPEZ, OSVELDO F. N92-11374
LOPEZGARCIA, M. J. N92-11495
LOUAHALA, SAMI N92-11513
N92-11521
N92-11525
LOUIS, D. N92-11146
LU, X. Q. N92-11961
LUCAS, S. H. N92-11668
LUDEWIG, HANS N92-11095
N92-11104
LUEDEKER, WILHELM N92-11540
LUND, KURT O. N92-11138
LUNDEN, BENGT N92-11526
LURIA, S. M. N92-11625
LUSK, E. N92-11710
LYBERIS, N. N92-11523
LYNCH, V. E. N92-11807
N92-11809
N92-11830
N92-11831
LYON, JAMES F. N92-11802
LYON, RONALD J. P. N92-11519

M

MA, J. N92-11339
MAAS, S. J. N92-11501
MACARAEG, MICHELE G. N92-11162
MACDONALD, A. H. N92-11916
MACKLIN, J. T. N92-11442
MACKNIGHT, NIGEL N92-11031
MADDOCKS, J. R., JR. N92-11295
MADEIRA, A. C. N92-11435
MADEIRA, J. N92-11436
MAEKELAE, H. N92-10998
MAHAN, ROBERT P. N92-11749
MALANEY, R. A. N92-11948
MALEKI, LUTFOLLAH N92-11791
MALIK, R. N92-11197
MALIN, JANE T. N92-11641
MALON, J. F. N92-11520
MALTHUS, T. J. N92-11428
N92-11435
MANCUSO, S. N92-11863
MANHEIMER, W. M. N92-11334
N92-11335
MANIE, F. N92-11009
MANSMANN, ULRICH N92-11757
MANTEUFFEL, T. A. N92-11732
MARAL, GERARD N92-11248
MARCHENKO, L. V. N92-11619
MARCY, S. J. N92-11318
MAREC, J.-P. N92-11963
MARGOLIS, JACK S. N92-11397
MARINELLI, RICK N92-11021
MARQUES, ANTHONY M. N92-11277
MARSHAK, ALEXANDER L. N92-11465
N92-11481
MARSOUIN, A. N92-11405
MARTIN, A. G. N92-11189
MARTIN, D. M. N92-10983
MARTIN, DAVID C. N92-11192
MARTINET, BERNARD N92-11255
MARTINEZ, F. E. N92-11203
MASAI, K. N92-11823
MASOTTO, TOM N92-11706
MASSIE, CURTIS N92-11651
MATARRESE, SABINO N92-11947
MATHE, J. M. N92-11020
MATSUO, S. N92-11182
MATSUOKA, KEISUKE N92-11823
N92-11861
MATSUURA, HIROTO N92-11853
MATTHEWS, P. G. N92-11825
MAUGHMER, MARK D. N92-11070
MAVRIPLIS, DIMITRI N92-11669
MCALISTER, K. W. N92-10981
MCBRANCH, D. N92-11204
MCCARTHY, I. E. N92-11780
MCCURDY, DAVID A. N92-11758
MCINTYRE, DAVID N92-11776
MCKAVITT, THOMAS P., JR. N92-11024
MCKENNA, P. N92-11566
MCNICHOLL, PATRICK J. N92-11231
MEEKS, E. L. N92-11339
MEGIER, JACQUES N92-11430
MEHROTRA, PIYUSH N92-11670
MEIDINGER, N. N92-11713
MEIDINGER, NORBERT N92-11281
MEISEL, D. N92-11900
MEKARNIA, ALI N92-11496
MELIA, J. N92-11495
MENYUK, C. R. N92-11775
MERKEL, PETER N92-11835
MEROT, P. N92-11453
MERRILL, WALTER C. N92-11017
MESMER, R. E. N92-11168
MESSERSCHMITT, DAVID G. N92-11225
METHY, MAURICE N92-11543
MICHEL, D. J. N92-11180
MICOZZI, P. N92-11863
MIDEA, ANTHONY C. N92-11013
MIEHE, C. N92-11390
MIJIC, M. B. N92-11948
MIKHIN, V. I. N92-11323
MILLER, J. R. N92-11777
MILLER, JOHN R. N92-11408
MILLER, M. K. N92-11779
MILLER, M. MEGHAN N92-11553
MILLER, WALTER F. N92-11596
MILLIS, MARC G. N92-11130
MILSHIN, A. A. N92-11492
MILTON, E. J. N92-11558
MIMA, K. N92-11872
MINEO, BETH A. N92-11621
MING, DOUGLAS W. N92-11572
MING, IMVIDHAYA N92-11278
MINI, S. M. N92-11163

MINICK, J. N92-11143
MISHRA, KRISHNA KUMAR N92-11497
MITO, T. N92-11842
MITO, TOSHIYUKI N92-11867
MIURA, YUKITOSHI N92-11882
MIYAJIMA, HIROSHI N92-11127
MIYAKE, K. N92-11852
MIYAZATO, M. N92-11497
MIYAZAWA, H. N92-11839
MIZUMAKI, S. N92-11837
N92-11638
MIZUUCHI, T. N92-11822
N92-11851
N92-11853
N92-11856
MOE, KAREN L. N92-11039
MOESTL, K. N92-11184
MOET, A. N92-11143
MOIR, R. W. N92-11786
MOLLERACH, SILVIA N92-11947
MONCET, JEAN-LUC N92-11597
MONJOUX, E. N92-11446
MONTELLI, LUCIANA N92-11209
MONTIE, EDWIN ANDRE N92-11914
MONTIGNY-RANNOU, F. N92-11310
MOODY, PAUL E. N92-11356
MOOK, H. A. N92-11906
MOORE, DEBORAH L. N92-11030
MORAN, M. SUSAN N92-11395
N92-11552
MOREL, M. N92-11422
MORETTI, C. J. N92-11766
N92-11767
MORIMOTO, SHIGEYUKI N92-11818
MORITA, SHIGERU N92-11859
MOROH, MARSHA N92-11920
MORRIS, M. N92-11648
MORRIS, R. N. N92-11802
N92-11857
MORTON, BLAISE N92-11018
MOSELLE, JOHN R. N92-11319
MOSER, ROBERT D. N92-11303
MOSSAVATI, RUZBEH N92-11342
MOTOJIMA, OSAMU N92-11800
N92-11837
N92-11839
N92-11840
N92-11843
N92-11844
N92-11864
N92-11865
N92-11867
MOUGENOT, BERNARD N92-11527
MOUGIN, E. N92-11449
MOYA, ISMAEL N92-11532
N92-11538
N92-11539
MULLER, JAN-PETER N92-11468
MURAKAMI, MASANORI N92-11819
N92-11889
MURPHY, ELIZABETH D. N92-11049
MURPHY, R. E. N92-11554
MUSGRAVE, JEFFREY L. N92-11128
MUTOH, TAKASHI N92-11845
N92-11846
MYERS, ROGER M. N92-11136
MYNENI, RANGA B. N92-11466

N

NAGAI, S. N92-11853
NAGARGAR, VIVEK N92-11331
NAGASAKI, KAZUNOBU N92-11815
NAGASHIMA, RYUICHI N92-11127
NAGY, PETER V. N92-11358
NAKAJIMA, HISAO N92-11793
NAKAJIMA, M. N92-11869
NAKAJIMA, NORIYOSHI N92-11883
N92-11885
NAKAMOTO, K. N92-11838
NAKAMOTO, S. N92-11837
NAKAMURA, T. N92-11547
NAKASUGA, M. N92-11818
N92-11822
N92-11856
NAKJIMA, NORIYOSHI N92-11833
NANOBASHVILI, S. N92-11881
NARAHARI, BHAGIRATH N92-11672
NARDI, ENRICO N92-11774
NASH, J. N92-11940
NAVARRO, A. P. N92-11829
NAYER, SHREE N92-11679
NEKRASOV, V. I. N92-11618
NELSON, BRIAN A. N92-11827
NELSON, RAYMOND M. N92-11561
NERRY, FRANCOISE N92-11462
NESTOR, DUANE E. N92-11025
NETTLES, A. T. N92-11142
NETTLETON, D. H. N92-11184
NEU, J. T. N92-11566
NEUMANN, MICHAEL N92-11707
NICHOLSON, H. W. N92-11172
NICOL, DAVID M. N92-11672
NIEDRA, JANIS M. N92-11252
NIGHTINGALE, R. W. N92-11585
NISHIMURA, KIYOHIKO N92-11846
NISSEN, J. A. N92-11296
NITTA, AKITO N92-11389
NJOKU, ENI G. N92-11461
NOBLE, BEN N92-11674
NODA, NOBUAKI N92-11840
N92-11866
NOFFZ, GREGORY K. N92-11301
NOILHAN, JOEL N92-11503
NOLAN, M. P. N92-11690
NOLIN, ANNE W. N92-11482
NORDBERG, MAJ-LIZ N92-11526
NORMAN, J. M. N92-11550
NORMAN, M. R. N92-11916
NORMAND, M. N92-11454
N92-11456
NORTHAM, G. BURTON N92-11118
NOWICK, A. S. N92-11206
NUEHRENBERG, JURGEN N92-11806
NULLMEYER, ROBERT T. N92-11635

O

OBIKI, TOKUHIRO N92-11818
N92-11822
N92-11851
N92-11869
N92-11870
OBRIEN, J. C. N92-11781
ODA, T. N92-11852
OETTL, H. N92-11450
OGATA, H. N92-11839
OGATA, TAKASHI N92-11389
OGAWA, TOMOKO N92-11884
OGAWA, YUICHI N92-11833
OHKUBO, KUNIZO N92-11845
OHNISHI, MASASHI N92-11846
OHR, YOUNG GIE N92-11349
OHTAKE, I. N92-11842
OHYABU, NARUYOSHI N92-11817
N92-11866
OHYABU, NOBUYOSHI N92-11840
OKA, YOSHIHIDE N92-11870
OKADA, H. N92-11822
N92-11851
OKADA, HIROYUKI N92-11846
OKAMOTO, MASAO N92-11833
N92-11846
N92-11885
OKAMURA, SHOICHI N92-11857
N92-11858
N92-11861
OLINTO, A. V. N92-11945
OLIOSO, ALBERT N92-11543
OLIVA, JOSE R. N92-11272
ONEILL, NORMAN T. N92-11408
OOST, W. A. N92-11443
OPPENHEIMER, CLIVE N92-11498
ORAN, ELAINE S. N92-11304
ORKWIS, PAUL DAVID N92-11292
OSBORN, JIM N92-11234
N92-11244
OSBORN, T. N92-11602
OSTASHEVA, N. YE. N92-11619
OTSUKA, MICHIO N92-11840
OVERTON, ERIC N92-11252
OWEN, WILLIAM MANN, JR. N92-11938

P

PAAPE, JENS N92-11360
PADMANABHAN, S. N92-11573
PADOVAN, J. N92-11379
PADUA, D. N92-11689
PADULA, SHARON L. N92-11087
PAGANO, PETER J. N92-11070
PAINTER, S. L. N92-11802
PALOSCIA, SIMONETTA N92-11460
PAMPALONI, P. N92-11450
N92-11460
PAN, VICTOR N92-11723
PANTANI, LUCA N92-11533
N92-11544
PAPADOPOULOS, D. N92-11775
PAPROCKI, THOMAS H. N92-11028
N92-11029
PARIS, R. D. N92-11789
PARKER, GARETH J. N92-10995
PARKES, JAMES E. N92-11136
PARNELL, T. A. N92-11075
PARROT, J. F. N92-11523
PARTON, W. N92-11575
PARTRIDGE, HARRY N92-11770
PASHIN, S. S. N92-11619
PASTOR, M. S. N92-11387
PATER, RUTH H. N92-11199
PATTEN, K. O. N92-11772
PATTERSON, JAMES H., JR. N92-11762
PAUL, D. B. N92-11683
PAUL, D. M. N92-11906
PAUL, NANETTE L. N92-11565
PAUMUCCI, JEFF N92-11649
PAVLIS, E. C. N92-11584
PAVLIS, NIKOLAOS K. N92-11560
PAWU, KYAW THA N92-11467
N92-11506
PEARLSTEIN, D. L. N92-11888
PENA, CARMEN M. N92-11636
PENTTINEN, A. N92-10998
PEREZ-DAVILA, ALFREDO N92-11702
PEREZ-DAVIS, MARLA E. N92-11133
PEREZCUEVA, A. J. N92-11495
PERKINS, A. LOUISE N92-11728
N92-11729
N92-11735
PERKOVSKIY, A. V. N92-11620
PERRAS, SYLVAIN N92-11528
PERRY, BOYD, III N92-11010
PERRY, R. B. N92-11330
PESANT, ALAIN N92-11528
PETERS, JEFFREY L. N92-11003
PETERS, PALMER N. N92-11076
N92-11077
N92-11078
PETERS, T. J. N92-11233
N92-11242
PETERSON, B. J. N92-11826
PETERSON, MATTHEW C. N92-11586
PETERSON, S. N92-11132
PETIT, MICHEL N92-11455
PETROV, V. N. N92-11325
PETRZILKA, V. N92-11773
PHILIPPE, BERNARD N92-11744
PHILIPS, JOHN N92-11702
PHULPIN, THIERRY N92-11412
N92-11503
N92-11520
N92-11557
PIAN, THEODORE H. H. N92-11378
PIELKEL, R. A. N92-11575
PIERCE, AMY N92-11681
PILKINGTON, J. L. N92-11222
PINET, PATRICK N92-11438
PINTY, BERNARD N92-11469
PION, J. C. N92-11499
PIOTROWSKI, JACEK N92-11268
PIPPI, I. N92-11544
PLENCNER, ROBERT M. N92-11034
PLUMMER, S. E. N92-11483
PODAIRE, ALAIN N92-11474
N92-11494
N92-11513
N92-11518
N92-11525
N92-11529
POINTEL, J. G. N92-11505
PONNUSAMY, RAVI N92-11669
POPE, SHELLY KAY N92-11950
POPOV, N. F. N92-11618
PORYVKINA, L. V. N92-11537
POTOTZKY, ANTHONY S. N92-11010
POTTER, J. LEITH N92-11071
POTTER, SCOTT S. N92-11641
POWELL, EDWARD N92-11606
POWELL, T. N92-11602
POZDNYAKOV, D. V. N92-11534
PRABHAKARA, C. N92-11600
PRABHAKARAN, RAMAMURTHY N92-11374
PRATT, J. RICHARD N92-11200
PREINHAELTER, J. N92-11881
PREVOT, LAURENT N92-11454
N92-11456
N92-11506
PRICE, J. N92-11602
PRICE, JOHN C. N92-11419
PRIKHACH, A. S. N92-11396
N92-11417
PRINZ, GARY A. N92-11646
PRITTS, DOUGLAS P. N92-11004
PROBER, DANIEL E. N92-11275

PROST, M. T. N92-11524
PROVOST-GRELLIER, ANTOINE N92-11266
N92-11267
PUCHKOV, A. V. N92-11170
PULVERMACHER, M. K. N92-11057
PUTCHA, LAKSHMI N92-11628

Q

QI, J. N92-11477
N92-11552

R

RABITZ, HERSCHEL N92-11164
RADICATI, B. N92-11544
RAGSDALE, ROBERT N92-11108
RAIKAR, GANESH N. N92-11076
RAJAN, J. B. N92-11353
RAMANATHAN, M. N92-11163
RAMBO, P. W. N92-11227
RAMSTHALER, J. H. N92-11094
RAND, ROBERT S. N92-11562
N92-11563
RANTALA, TAPIO T. N92-11908
N92-11909
RASCHE, REINHARD N92-11647
RASH, JAMES L. N92-11044
N92-11062
RASMUSSEN, D. A. N92-11849
RASOOL, S. I. N92-11555
RAST, MICHAEL N92-11397
N92-11422
RASTELLO, M. L. N92-11184
RAZINKIN, S. M. N92-11618
RE, RICHARD J. N92-10975
READ, B. E. N92-11185
REDDY, RAKASI M. N92-11207
REDDY, SURENDER N92-11056
REDING, GREGORY J. N92-11598
REID, B. D. N92-11107
REINHOLD, C. O. N92-11904
REMY, D. N92-11515
RENARD, J. N92-11145
REUTOV, E. A. N92-11492
REVANKAR, S. T. N92-11322
RHODES, DAVID B. N92-11336
RIBE, F. L. N92-11827
RICE, EDWARD J. N92-11691
RICHTER, R. N92-11407
N92-11431
RIEDER, R. J. N92-11237
RINALDI, M. A. N92-11585
RINAT, A. S. N92-11892
RINDERLE, U. N92-11542
RINGLER, HEINZ N92-11820
ROACH, G. F. N92-11737
ROACH, ROBERT ALLEN N92-10985
ROBBINS, J. W. N92-11584
ROBERTS, L. A. N92-11703
ROBERTSON, D. C. N92-11566
ROBINSON, D. N. N92-11387
ROBINSON, R. M. N92-11585
ROCKAWAY, J. KENT N92-11071
ROCKWAY, MARTY R. N92-11635
RODRIGUE, GARRY N92-11730
ROGACKI, J. N92-11391
ROGER, JEAN-CLAUDE N92-11485
ROGERS, CRAIG A. N92-11036
ROGERS, DAVID N92-11590
N92-11743
ROGERS, F. J. N92-11939
ROGERS, MICHAEL M. N92-11303
ROHAL, R. N92-11115
ROLET, J. N92-11499
ROLFE, ROBERT N92-11681
ROLLIN, E. M. N92-11558
ROMANOSKI, G. R. N92-11205
ROME, J. A. N92-11802
RONDEAUX, GENEVIEVE N92-11484
ROSA, M. A. P. N92-11571
ROSARIO, JESUS A. N92-11245
ROSCH, GENE N92-11704
ROSEMA, ANDRIES N92-11545
ROSEN, M. D. N92-11874
ROSENBLUTH, M. N. N92-11890
ROSS, BRIAN H. N92-11634
ROSS, JUHAN N92-11465
ROTHERY, DAVID A. N92-11498
ROTHFUSS, HARALD N92-11431
ROTHSCHILD, B. N92-11602
ROUDOLFF, F. N92-11145
ROUGHGARDEN, J. N92-11602
ROUJEAN, JEAN-LOUIS N92-11480
ROULET, ESTEBAN N92-11774
N92-11956
ROYER, ALAIN N92-11408
N92-11493
ROZEHNAL, I. N92-11475
RUBIN, CLINTON T. N92-11626
RUDANT, JEAN-PAUL N92-11446
N92-11448
N92-11496
N92-11524
RUDDELL, S. A. N92-11794
RUDDUCK, R. N92-11065
RULE, W. K. N92-11079
RUSKIN, LESLIE N92-11702

S

SAAD, YOUCEF N92-11290
N92-11692
N92-11744
SADIER, S. N92-11256
SAEYNAETJOKI, M. N92-11326
SAINT, G. N92-11502
SAITO, KATSUNORI N92-11848
SAITO, R. N92-11839
N92-11841
SAIYED, NASEEM H. N92-11208
SALA, F. N92-11265
SALEEB, A. F. N92-11375
SALEM-SUGUI, S., JR. N92-11163
SALMONS, JAMES D. N92-11002
SALTZ, JOEL N92-11669
SANDBORN, V. A. N92-11318
SANG, YEMING N92-11960
SANO, FUMIMICHI N92-11822
N92-11850
N92-11853
N92-11856
N92-11869
N92-11870
SANTER, RICHARD N92-11406
N92-11409
N92-11416
N92-11485
SANTER, RICHARD P. N92-11413
SANUKI, H. N92-11796
N92-11797
N92-11878
SAPPER, JORG N92-11868
SASAKI, T. N92-11837
SATO, MASAHIRO N92-11127
SATO, MASAKAZU N92-11127
SATO, MOTOYASU N92-11818
N92-11822
N92-11845
N92-11851
N92-11856
N92-11869
SATO, RICHARD K. N92-11658
SATO, SOTOYASU N92-11853
SATOW, T. N92-11841
SAUCIER, GABRIELLE N92-11256
SAULE, ARTHUR V. N92-11691
SAUNDERS, BONITA V. N92-11727
SAUNDERS, J. D. N92-10976
SAVINA, V. P. N92-11619
SCHAICH, C. R. N92-11889
SCHAPERY, R. A. N92-11191
SCHAUB, WILLIAM R., JR. N92-11011
N92-11594
SCHINDLER, C. N92-11542
SCHLINGELHOF, MARIUS N92-10997
SCHMOCK, UWE N92-11750
SCHMUCK, GUIDO N92-11532
N92-11538
N92-11539
SCHMUGGE, THOMAS N92-11412
N92-11458
SCHNEIDER, T. N92-11437
N92-11805
SCHOESS, JEFF N. N92-11930
SCHOR, ANDREI L. N92-11704
SCHRAMM, DAVID N. N92-11946
SCHRECKENGHOST, DEBRA L. N92-11641
SCHREIBER, ROBERT N92-11656
N92-11693
N92-11696
N92-11723
SCHREIBER, WILLIAM F. N92-11225
SCHREIBER, WOLFGANG N92-11280
SCHROOTE, J. N92-11546
SCHULTZ, A. J. N92-11899
SCHULZE, NORMAN R. N92-11783
SCHWARTZ, R. W. N92-11901
SCHWENTEK, H. N92-11964
SCOTT, MICHAEL A. N92-11073
SCOTT, N. A. N92-11421
SCOTT, ROBERT C. N92-11010
SCROGGS, JEFFREY S. N92-11728
N92-11733
SCULLY, J. R. N92-11173
SEAGER, C. H. N92-11204
SEAGRAVES, SQUIRE B. N92-10987
SEDJO, R. A. N92-11580
SEGAL, H. M. N92-11578
SEGUIN, BERNARD N92-11494
N92-11513
N92-11521
SEKAR, R. R. N92-11353
SELLERS, P. J. N92-11554
SEMENOV, A. V. N92-11618
SEMERARO, DAVID N92-11290
SETNA, R. P. N92-11779
SEYHAN, E. N92-11428
SHA, W. T. N92-11321
SHAO-HU, WANG N92-11814
SHARIF, DAUD N92-11331
SHARMAN, MARTIN N92-11406
SHARP, L. E. N92-11804
SHARP, S. L. N92-11905
SHAW, LORETTA M. N92-11135
SHEBALIN, JOHN V. N92-11742
SHELTON, DUANE N92-11225
SHEN, Y. N92-11321
SHENHAR, JORAM N92-11338
SHEPHERD, KEVIN P. N92-11759
N92-11765
SHEPHERD, O. N92-11237
SHI, X.-H. N92-11804
SHIAO, MICHAEL C. N92-11373
SHIBUI, MASANAO N92-11837
N92-11838
SHIER, DOUGLAS R. N92-11748
SHIH, T.-H. N92-11302
SHIINA, SHOICHI N92-11848
SHIMIZU, JYUN-ICHIROU N92-11298
SHIMIZU, KATSUHIRO N92-11841
SHISHOV, A. A. N92-11618
SHOHET, JUDA L. N92-11821
N92-11825
N92-11826
SHOLOKHOV, A. A. N92-11325
SHROFF, GAUTAM N92-11653
SHUTKO, ANATOLI M. N92-11492
SICHEL, MARTIN N92-11304
SIGMUND, T. N92-11954
SIMHA, RAHUL N92-11672
SIMO, J. C. N92-11390
SIMON, FREDERICK F. N92-11299
SIMS, J. TERRY N92-11706
SIMSON, BERT G. N92-11226
SINCLAIR, M. N92-11204
SINGER, A. N92-11424
SIRAT, GABRIEL Y. N92-11337
SIROIS, E. N92-11178
SITZMANN, MICHAEL E. N92-11212
SKORIC, MILOS M. N92-11836
SLATER, P. N. N92-11395
SLOCUM, MICHAEL N92-11033
SMALL, D. L. N92-11925
SMITH, CLAYTON A. N92-11933
SMITH, D. E. N92-11584
SMITH, G. D. W. N92-11779
SMITH, H. H. N92-11180
SMOLINSKI, PATRICK J. N92-11671
SNEL, J. F. H. N92-11546
SNODGRASS, JOAN G. N92-11633
SNOEIJ, P. N92-11443
SNYDER, A. P. N92-11167
SOBRINO, JOSE A. N92-11410
N92-11507
SOFIA, SABATINO N92-11957
SOIZE, C. N92-11311
SOLIGNAC, J. L. N92-11308
SOLOMAN, RON N92-11006
N92-11007
SOLOMIN, G. I. N92-11619
SOMORJAI, G. A. N92-11160
SOVEY, JAMES S. N92-11136
SOWTER, ANDREW N92-11069
SPANJERS, G. N92-11827
SPARKS, D. O. N92-11249
SPARN, THOMAS P. N92-11052
SPARROW, JEANNE M. N92-11597
SPEAR, ROBERT J. N92-11209
SPEE, R. N92-11270
SPRINGFIELD, JAMES F. N92-11637
SRIVASTAVA, MAHESH P. N92-11847
ST.CLAIR, ANNE K. N92-11200
N92-11201
ST.ONGE, BENOIT N92-11530

STAENZ, KARL N92-11439
STALLCOP, J. R. N92-11770
STANLEY, JAMES H. N92-11363
N92-11365
STARCHVILLE, M. D. N92-11193
STEBBINS, ALBERT N92-11941
STEIER, W. H. N92-11274
STEPHENS, CRAIG A. N92-11299
STERNE, P. A. N92-11781
STEVEN, G. P. N92-11369
STEVEN, M. D. N92-11435
N92-11472
STEWART, ERIC C. N92-10994
STEWART, MARK E. M. N92-11328
STEWART, WILLIAM J. N92-11744
STOAKLEY, DIANE M. N92-11201
STOBER, FRED N92-11541
STOCK, K. D. N92-11184
STOECKEL, J. N92-11881
STOLL, M. P. N92-11462
STOLL, MAGALI N92-11412
N92-11503
STOLZE, DETLEF N92-10997
STONE, JAMES R. N92-11135
STORM, E. N92-11873
STRAHLER, ALAN H. N92-11486
STRAND, L. D. N92-11125
STRETTA, JEAN-MICHEL N92-11455
STUEBER, THOMAS J. N92-11139
STUTZMAN, WARREN L. N92-11036
N92-11559
SU, LOUISE T. N92-11922
SUDO, SHIGERU N92-11822
N92-11851
N92-11853
N92-11856
N92-11869
SUGAMA, HIDEO N92-11883
SUK, GO H. N92-11235
SULLIVAN, BRENDA M. N92-11759
N92-11765
SUMIYOSHI, F. N92-11867
SURDYK, SYLVIANE N92-11464
SUZUKI, KIYOMITSU N92-11848
SUZUKI, S. N92-11547
N92-11839
SWAIN, D. W. N92-11250
SWANSON, D. G. N92-11805
SWARZTRAUBER, PAUL N. N92-11224
N92-11658
N92-11659
N92-11700
SWIFT, BRIAN L. N92-11909
SWINDEMAN, R. W. N92-11181
SWINDLE, DAVID W. N92-11752
SZOEKE, A. N92-11786
SZTIPANOVITS, JANOS N92-11637

T

TACONET, O. N92-11454
N92-11456
N92-11511
TADANO, MAKOTO N92-11127
TADO, SHIGERU N92-11841
TAJIMA, T. N92-11872
TAKAHASHI, KUNIO N92-11547
TAKAHASHI, M. N92-11824
TAKAHASHI, R. K. N92-10981
TAKAHATA, K. N92-11842
N92-11867
TAKANO, H. N92-11837
N92-11838
TAKAYAMA, M. N92-11824
TAKEIRI, YASUHIKO N92-11857
N92-11861
N92-11870
TAKEO, M. N92-11839
N92-11842
TAKEUCHI, N. N92-11824
TAKITA, Y. N92-11862
TALMADGE, JOSEPH N. N92-11825
N92-11826
TAN, H. Q. N92-11375
TANNAS, LAWRENCE E., JR. N92-11225
TAYLOR, M. R. N92-11283
TAYLOR, R. L. N92-11390
TAYLOR, WILLIAM J. N92-11129
TEILLET, PHILIPPE M. N92-11395
N92-11413
N92-11414
N92-11530
THEOBALD, A. G. N92-11273
THIAGARAJAN, V. N92-11271
THIRY, MEDARD N92-11429
THOMAS, DONALD A. N92-11930
N92-11931
THOMAS, G. N92-11754
THOMAS, JOHN H. N92-11955
THOMPSON, HAYDN ASHLEY N92-11012
THOMPSON, JACK N92-10993
THOMPSON, R. L. N92-11475
THOMPSON, RICHARD A. N92-11285
N92-11300
TICHY, WALTER F. N92-11654
N92-11698
TIRRE, WILLIAM C. N92-11636
TISCHLER, SABINE N92-11407
TLAMICHA, A. N92-11953
N92-11954
TODOROKI, JIRO N92-11832
N92-11878
N92-11880
TOMITA, M. N92-11841
TOMLINS, P. E. N92-11185
TOMMASINI, DANIELE N92-11774
TONG, CHARLES N92-11700
TONG, G. MICHAEL N92-11063
TONI, MARIA PIA N92-11766
N92-11767
TONNER, PAUL D. N92-11365
TORRENCE, M. H. N92-11584
TORRES, R. N92-11065
TOU, T. Y. N92-11804
TOUZI, R. N92-11449
TOYODA, K. N92-11842
TOYOTA, K. N92-11841
TRANCHEFORT, J. N92-11505
TRIBALDOS, V. N92-11828
TRUDGILL, S. T. N92-11426
TSUDA, YOSHIYUKI N92-11842
TSUKAMOTO, TADANORI N92-11841
TSURUGA, SHIGENORI N92-11838
TUCK, LISA KAY N92-11572
TUMINARO, RAY S. N92-11701
TURKINA, T. I. N92-11617
TUTTLE, M. E. N92-11391
TUTTLE, MARIE H. N92-11030

U

UCHIDA, T. N92-11838
UDALOV, SERGEI N92-11084
N92-11085
UEDA, TETSUHIKO N92-10980
UENK, D. N92-11444
UENO, HIKARU N92-11848
USHAKOV, V. F. N92-11619
USTIN, SUSAN L. N92-11551

V

VALENTIN, C. N92-11515
VALETTE, J. C. N92-11520
VALOVIC, M. N92-11881
VANDAM, J. W. N92-11890
VANDENBOSCH, JEANNETTE MARIE N92-11415
VANHALA, JUKKA N92-11697
VANHALSEMA, D. N92-11443
VANLEERDAM, GERRIT CORNELIS N92-11913
VANOVERVELD, WILHELMINA MARIA CORNELIA J. N92-11684
VANRIJ, W. I. N92-11833
VANSCIVER, STEVEN W. N92-11294
N92-11295
N92-11296
VANVEEN, EELCO ANTHONIE N92-11919
VANZEIJTS, J. B. J. N92-11350
N92-11351
VARIAS, A. N92-11807
VASEK, THOMAS E. N92-11086
VELAZCO, RAOUL N92-11253
N92-11254
N92-11255
N92-11256
N92-11257
N92-11258
N92-11259
N92-11260
N92-11261
N92-11262
N92-11263
N92-11264
N92-11265
N92-11266
N92-11267
N92-11268
VERBER, CARL M. N92-11792
VERBRUGGHE, MICHEL N92-11401
N92-11403
N92-11409
VERDEBOUT, JEAN N92-11548
VERDON, JOSEPH M. N92-10979
VERHOEF, W. N92-11545
VERMOTE, ERIC N92-11402
N92-11406
N92-11409
N92-11416
VERSTRAETE, MICHEL M. N92-11469
VERWARDE, CHRISTIAN N92-11471
VETRONE, ROBERT H. N92-11136
VEUILLOT, J. P. N92-11310
VICKOS, J. B. N92-11529
VIDAL-MADJAR, DANIEL N92-11454
N92-11456
N92-11511
VIDAL, A. N92-11521
VIENS, MICHAEL J. N92-11187
VILA, J. P. N92-11715
N92-11719
VINEYARD, E. A. N92-11216
VIOVY, NICOLAS N92-11502
N92-11525
VISSERS, M. A. M. N92-11444
VITELLO, P. N92-11940
VODACEK, A. N92-11549
VOGELZANG, J. N92-11443
VOLAKIS, JOHN L. N92-11140
VOROBYEV, O. A. N92-11618
VORONKA, N. R. N92-11284
VUJKOVICCVIJIN, P. N92-11544

W

WACHI, Y. N92-11837
N92-11838
WADSWORTH, ALAIN N92-11448
N92-11455
WAKATANI, MASAHIRO N92-11851
N92-11883
WAKEHAM, STUART G. N92-11605
WALDMAN, JEFFREY N92-11177
WALDSPURGER, CARL A. N92-11649
WALLACE, A. K. N92-11270
WALLIS, RICHARD F. N92-11910
WALTER, ARTUR N92-11655
WALTERS, LAURIE C. N92-11630
WALTON, JAMES T. N92-11137
WANDERMAN, KEN N92-11920
WANG, H. H. N92-11899
WANG, J. R. N92-11458
WANG, P. S. N92-11375
WANG, Y. N92-11513
WARD, CHRISTINA C. N92-11082
WARMACK, R. J. N92-11905
WARREN, JOHN H. N92-11165
WARREN, P. J. N92-11779
WASSERMAN, MICHAEL B. N92-11167
WATANABE, HIROSIGE N92-11824
WATANABE, TSUGUHIRO N92-11834
WATARI, TETSUO N92-11845
N92-11846
WEBB, CHARLES D. N92-11019
WEBBON, BRUCE N92-11286
WEILAND, WILLIAM J. N92-11051
WEINSTEIN, STUART N92-11050
N92-11063
WEISGERBER, W. N92-11189
WEITZNER, H. N92-11891
WEIXELBAUM, L. N92-11881
WELDEN, TODD N92-11043
WELKER, JEAN E. N92-11583
WELP, U. N92-11899
WENDELL, L. L. N92-11601
WENZEL, U. N92-11881
WERLE, H. N92-11312
WERNTZ, DAVID G. N92-11047
WESSMAN, CAROL A. N92-11551
WEXLER, RUTH L. N92-11599
WHITBOURN, L. B. N92-11535
WHITEHEAD, V. C. N92-11485
WHITEMAN, J. R. N92-11674
WHITTAKER, WILLIAM L. N92-11358
WHITTREDGE, ROY N92-11706
WIERZIMOK, DIETMAR N92-11316
WIJNEN, M. M. N92-11428
WIKE, JEFFREY S. N92-11045
N92-11061
WILGEN, J. B. N92-11849
N92-11889
WILLEMIN, GUILLEMETTE N92-11519
WILLEY, JEFFERSON M. N92-11230
WILLEY, NORMAN F. N92-11354
WILLIAMS, DANIEL N92-11408
WILLIAMS, J. M. N92-11899

WILLIAMS, PETER M. N92-11604
WILLIAMSON, R. G. N92-11584
WILLIS, KIMBERLY J. N92-11561
WILLM, THIERRY N92-11528
WILLOUGHBY, JOHN K. N92-11042
WILSON, A. K. N92-11487
WILSON, DONALD L. N92-11958
WILSON, JOHN W. N92-11685
WINOWICH, NICHOLAS S. N92-11014
N92-11161
WIRINGA, R. B. N92-11778
WITKOP, D. L. N92-11388
WITTMEIER, HELGE N92-11437
WNEK, G. E. N92-11194
N92-11196
WNEK, GARY E. N92-11190
N92-11197
WOBIG, HORST N92-11811
WOLFE, HOWARD F. N92-11383
WON, DONG YEON N92-11917
WONCH, JEFFERY D. N92-11037
WONG, C. R. N92-11381
WONG, YEN F. N92-11044
N92-11062
WOOD, ERIC F. N92-11459
WOOD, R. H. N92-11169
WOOD, S. A. N92-11648
WOODARD, STANLEY E. N92-11087
WOODFORD, LYNN N92-11006
N92-11007
WOODRUM, LARRY C. N92-11004
WOODS, DAVID D. N92-11641
WRIGHT, JAY M. N92-11359
WRIGHT, STEVEN A. N92-11103

X

XIA, XINFU N92-11909

Y

YAGLE, ANDREW E. N92-11675
YAMADA, HIROSHI N92-11857
N92-11861
YAMAHIRA, TAKAYUKI N92-11282
YAMAMOTO, JUNYA N92-11839
N92-11842
N92-11864
N92-11867
YAMAMOTO, KEIICHI N92-11837
N92-11838
YAMASHINA, TOSHIRO N92-11813
YAMAZAKI, KOZO N92-11833
N92-11843
N92-11844
N92-11865
YAMAZAKI, Y. N92-11839
YAMZAKI, KOZO N92-11840
YANAGI, N. N92-11818
YANCEY, ROBERT N. N92-11363
YANG, C. N92-11065
YANG, C. Y. N92-11194
N92-11196
YANG, CHIA-YU N92-11190
YARKIN, A. N. N92-11324
YATSUI, KIYOSHI N92-11798
YAZERIAN, G. G. N92-11492
YESOU, HERVE N92-11499
YODH, G. B. N92-11961
YOO, J.-M. N92-11600
YOON, W. S. N92-11122
YOS, JERROLD M. N92-11285
YOSHIKAWA, SHOICHI N92-11816
YOUNG, L. A. N92-10983
YU, CHEN-KUO N92-11232
YU, L. H. N92-11350
N92-11351

Z

ZACEK, F. N92-11881
ZALLER, M. N92-11121
ZAMA, T. N92-11824
ZBINDEN, REGINA N92-11440
ZEEGERS, JOSEPHUS CATHARINA HENRICUS
N92-11314
ZEGE, E. P. N92-11396
N92-11417
ZEIN-SABATTOU, SALEH N92-11218
ZHANG, LIGANG G. N92-11764
ZHOU, D.-F. N92-11804
ZIADE, HAISSAM N92-11254
N92-11261
N92-11262
N92-11263
N92-11264
N92-11265
ZIMA, HANS N92-11670
ZININA, G. A. N92-11325
ZINOVYEV, V. M. N92-11619
ZOCH, DAVID R. N92-11050
N92-11058
N92-11063
ZODY, M. C. N92-11182
ZUBRIN, ROBERT N92-11098
N92-11214
ZUSHI, HIDEKI N92-11822
N92-11851
N92-11853
N92-11855
N92-11856
N92-11869

Typical Corporate Source Index Listing

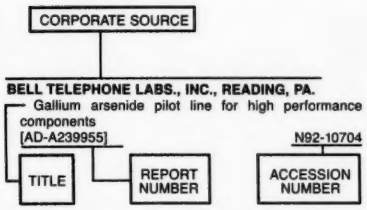

Listings in this index are arranged alphabetically by corporate source. The title of the document provides the user with a brief description of the subject matter. The report number helps to indicate the type of document cited (e.g., NASA report, translation, NASA contractor report). The accession number denotes the number by which the citation is identified. The titles are arranged under each corporate source in ascending accession number order.

A

ACADEMIA SINICA, HEFEI (CHINA).
The main fusion activities in Institute of Plasma Physics, Academia Sinica N92-11814

ACADEMY OF SCIENCES OF THE ESTONIAN SSR, TARTU.
Influence of the crop architecture parameters on crop BRDF: A Monte Carlo simulation N92-11465

ACADEMY OF SCIENCES (USSR), GORKY.
Nonlinear theory of synthetic aperture radar sea wave imaging N92-11451

ACADEMY OF SCIENCES (USSR), LENINGRAD.
Laser active remote sensing of phytoplankton in inland waters N92-11534

ACADEMY OF SCIENCES (USSR), MOSCOW.
Multiangular approach to solution of atmosphere optics reverse problems N92-11478
Airborne passive microwave remote sensing of land and water surface N92-11492

ADVANCED RESEARCH AND APPLICATIONS CORP., SUNNYVALE, CA.
A new radiographic corrosion inspection capability [AD-A231476] N92-11363
Supervoltage NDE techniques for large aerospace structures [AD-A240625] N92-11365

ADVISORY GROUP FOR AEROSPACE RESEARCH AND DEVELOPMENT, NEUILLY-SUR-SEINE (FRANCE).
Rotorcraft system identification [AGARD-AR-280] N92-11001

AERONAUTICAL RESEARCH LABS., MELBOURNE (AUSTRALIA).
Critical appraisal of the McDonnell Douglas closure model for predicting fatigue crack growth [ARL-STRUC-R-444] N92-11376

AEROSPACE CORP., EL SEGUNDO, CA.
A conjugate gradient based algorithm to minimize the sidelobe level of planar arrays with element failures [AD-A240667] N92-11242

AEROSPACE CORP., LOS ANGELES, CA.
A fast algorithm for plotting antenna and scattering patterns in three dimensions [AD-A240410] N92-11233

AEROSPATIALE, CANNES (FRANCE).
Land cover classification by multipolarized SAR imagery N92-11457

AGENCY FOR INTERNATIONAL DEVELOPMENT, WASHINGTON, DC.
Greenhouse gas emissions and the developing countries: Strategic options and the USAID response [PB91-209882] N92-11573

AGRICULTURAL RESEARCH SERVICE, BELTSVILLE, MD.
On the value of high spectral resolution measurements in the visible and near-infrared N92-11419

AIR FORCE ENVIRONMENTAL TECHNICAL APPLICATIONS CENTER, SCOTT AFB, IL.
C-29A aircraft altimeter errors [AD-A240486] N92-11011
Groves model accuracy study [AD-A240456] N92-11586
A method for estimating missing hourly temperatures using daily maximum and minimum temperatures [AD-A240394] N92-11594
March AFB forecasting rules of thumb evaluation [AD-A240458] N92-11595
Short-term hourly temperature interpolation [AD-A240489] N92-11596
Persian Gulf contrail altitude limits [AD-A240702] N92-11598
Conditional climatology of Ap: The relationship between various solar events (surges, prominences, filaments, radio bursts, x ray episodes) and geomagnetic storms [AD-A240457] N92-11958

AIR FORCE HUMAN RESOURCES LAB., BROOKS AFB, TX.
The development of Behaviorally Anchored Rating Scales (BARS) for evaluating USAF pilot training performance [AD-A239969] N92-11630
Cognitive factors involved in the first stage of programming skill acquisition [AD-A240566] N92-11636

AKADEMIYA NAUK BSSR, MINSK.
Modeling of visible and UV radiative transfer in the ocean-atmosphere system concepts, models, and programs N92-11396
Iterative procedures for atmospheric correction N92-11417

AKRON UNIV., OH.
On the symbolic manipulation and code generation for elasto-plastic material matrices [NASA-CR-187223] N92-11375
Engine dynamic analysis with general nonlinear finite element codes [NASA-CR-187222] N92-11379
Limit pressure of a circumferentially reinforced SiC/Ti ring [NASA-CR-187211] N92-11387

ALABAMA UNIV., HUNTSVILLE.
Analysis of surfaces from the LDEF A0114, phase 4 [NASA-CR-188990] N92-11074
The interactions of atmospheric cosmogenic radionuclides with spacecraft surfaces N92-11075
Effects on LDEF exposed copper film and bulk N92-11076
Measurements of erosion characteristics for metal and polymer surfaces using profilometry N92-11077
Pinhole cameras as sensors for atomic oxygen in orbit; application to attitude determination of the LDEF N92-11078
Navier-Stokes entropy controlled combustion instability analysis for liquid propellants N92-11122

ALABAMA UNIV., TUSCALOOSA.
MLITemp: A computer program to predict the thermal effects associated with hypervelocity impact damage to space station MLI [NASA-CR-184245] N92-11079

ALASKA UNIV., FAIRBANKS.
Photovoltaic energy system at an Alaskan site [PB91-201350] N92-11567

AMES LAB., IA.
Photoemission study of Ce/Ta(110) and Ce/W(110) interfaces and the catalytic oxidation effect [DE91-018167] N92-11903

ARGONNE NATIONAL LAB., IL.
Polarized x ray absorption spectroscopy for the study of superconductors and magnetic materials [DE91-017990] N92-11163
Direct-contact heat exchanger for swirling countercurrent flow of hot gas and finely divided solids: A parametric study [DE91-017229] N92-11291
Implementation of the flow-modulated skew-upward difference scheme in the momentum equation of the COMMIX-1C program: A first assessment [DE91-018013] N92-11321
Local interfacial area concentration measurement in bubbly flow [DE91-018702] N92-11322
Calorimetry measurements in less than 20 minutes [DE91-017318] N92-11330
Component cost analysis for compressed natural gas vehicles [DE91-017230] N92-11353
LAPACK: Linear algebra software for supercomputers [DE91-017316] N92-11660
Studying parallel program behavior with upshot [DE91-019072] N92-11710
Issues in parallel automatic differentiation [DE91-017311] N92-11726
Control of electron transfer rates by motions of atoms and molecules [DE91-018575] N92-11777
Variational Monte Carlo calculations of finite nuclei [DE91-018895] N92-11778
Meson-exchange calculation of the d(gamma,p)n in the GeV energy region [DE91-017994] N92-11785
ITER divertor sputtering erosion: Recent analysis for carbon, beryllium, tungsten, and niobium surfaces [DE91-017235] N92-11871
Current profile control for ITER with RF current drive [DE91-018597] N92-11888
Radiation induced growth of micro crystallites [DE91-016516] N92-11900
Vortex-lattice states of a two-dimensional electron system at strong magnetic fields [DE91-018551] N92-11916

ARIZONA STATE UNIV., TEMPE.
Design of a fast computer-based partial discharge diagnostic system [NASA-CR-189057] N92-11272
Computer aided surface representation [DE91-018872] N92-11688

ARIZONA UNIV., TUCSON.
Normalization of multidirectional red and NIR reflectances with the SAVI N92-11477
View-atmosphere-soil effects on vegetation indices derived from SPOT images N92-11552
Diffusion in the Io plasma torus and its relation to the torus spatial structure N92-11949
Laboratory measurements of the single-scattering properties of ammonia ice crystals N92-11950

ARMY AEROMEDICAL RESEARCH LAB., FORT RUCKER, AL.
Concept evaluation of the UH-60 externally mounted rescue hoist [AD-A240545] N92-11004
The hazard of exposure to impulse noise as a function of frequency, volume 2 [AD-A240530] N92-11762

ARMY ELECTRONIC PROVING GROUND, FORT HUACHUCA, AZ.
Methodology investigation. Phase 2: Software maturity model validation [AD-A231439] N92-11651

ARMY ENGINEER TOPOGRAPHIC LABS., FORT BELVOIR, VA.
Multispectral image maps from LANDSAT thematic mapper data [AD-A240453] N92-11562
A hybrid methodology for detecting cartographically significant features using LANDSAT TM imagery [AD-A240454] N92-11563
Thermal infrared spectra of natural and manmade materials: Implications for remote sensing [AD-A240455] N92-11564
Hourly and daily precipitation frequencies for the United States [AD-A240746] N92-11599

ARMY ENGINEER WATERWAYS EXPERIMENT STATION, VICKSBURG, MS.
KA-111, Phase C, M-1 propellant tests: Deflagration in partial confinement
[AD-A240185] N92-11211
Development of a reliability-based method for evaluating a pavement feature
[AD-A240747] N92-11366
ARMY LAB. COMMAND, WATERTOWN, MA.
Deformation of isodamp (A polyvinyl chloride-based elastomer) at various loading rates
[AD-A240393] N92-11189
ASSOCIATION AERONAUTIQUE ET ASTRONAUTIQUE DE FRANCE, PARIS.
Application of infrared thermography to thermal flux measurement in wind tunnels
[AAAF-NT-89-12] N92-11020
Preliminary studies for automizing thermal flux measurement examination by thermosensitive coloring
[AAAF-NT-89-28] N92-11288
ASSOCIAZIONE EURATOM-CNEN SULLA FUSIONE, FRASCATI (ITALY).
A possible modification of the FT Tokamak into a compact high field stellarator with separatrices N92-11863
ASTON UNIV., BIRMINGHAM (ENGLAND).
Drag coefficients with applications to satellite orbits N92-11069
ATMOSPHERIC AND ENVIRONMENTAL RESEARCH, INC., CAMBRIDGE, MA.
Mesoscale prediction and satellite cloud analysis for advanced meteorological processing systems
[AD-A240510] N92-11597
AUBURN UNIV., AL.
Design of the compact Auburn torsatron N92-11805
Electron temperature measurements on ATF using electron cyclotron emission N92-11849
AUSTRALIAN NATIONAL UNIV., CANBERRA.
The ANU Heliac Program N92-11804
AXIOMATIX, LOS ANGELES, CA.
Space station tracking requirements feasibility study, volume 2
[NASA-CR-185641-VOL-2] N92-11084
Space station tracking requirements feasibility study, volume 1
[NASA-CR-185641-VOL-1] N92-11085

B

BOEING AEROSPACE CO., SEATTLE, WA.
Quick trips to Mars N92-11111
BOSTON UNIV., MA.
Calculating the bidirectional reflectance of natural vegetation covers using Boolean models and geometric optics N92-11486
BRITISH NATIONAL SPACE CENTRE, HUNTINGDON (ENGLAND).
Assessment of the effect of specular reflectance on the relationships between vegetation indices and biomass N92-11483
ATLAS: An Auto-Tracking Land and Atmosphere Sensor for retrieval of atmospheric optical parameters and acquisition of bidirectional surface reflectance N92-11487
BROOKHAVEN NATIONAL LAB., UPTON, NY.
Particle bed reactor nuclear rocket concept N92-11095
Liquid annulus N92-11104
Reduction of FEL gain due to wiggler errors
[DE92-000482] N92-11350
The effect of wiggler errors on FEL gain
[DE92-000483] N92-11351
Photon stimulated desorption of neutral species from aluminum
[DE91-017004] N92-11784
BRUNEL UNIV., UXBRIDGE (ENGLAND).
Workshops on Efficient Use of Scientific Computing
[AD-A240175] N92-11674
BSA SERVICES, HOUSTON, TX.
Spectral fitting, shock layer modeling, and production of nitrogen oxides and excited nitrogen
[NASA-CR-185664] N92-11769
BUREAU DE RECHERCHES GEOLOGIQUES ET MINIERES, ORLEANS (FRANCE).
Contribution of NOAA-AVHRR satellite data in forest vegetation monitoring N92-11520

C

CALIFORNIA UNIV., BERKELEY.
Personal air transport: State of the art
[PB91-204768] N92-10991
Decomposition pathways of tetrahydrogen
[AD-A240623] N92-11166
CALIFORNIA UNIV., BERKELEY. LAWRENCE BERKELEY LAB.
Conversion of ethane and of propane to higher olefin hydrocarbons
[DE91-016896] N92-11160
Characterization of rare earth permanent magnets
[DE91-017010] N92-11754
Collisional energy transfer from excited nitrogen dioxide
[DE91-016989] N92-11772
CALIFORNIA UNIV., DAVIS.
Anisotropy of thermal infrared exitance above and within plant canopies N92-11467
CALIFORNIA UNIV., IRVINE.
Superionics
[AD-A240352] N92-11910
CALIFORNIA UNIV., LOS ANGELES.
Fatigue crack initiation
[AD-A240196] N92-11380
Domain-decomposed preconditionings for transport operators N92-11731
The TITAN reversed-field-pinch fusion reactor study, volume 4
[DE92-000138] N92-11895
The TITAN reversed-field-pinch fusion reactor study, volume 2
[DE92-000140] N92-11896
The TITAN reversed-field-pinch fusion reactor study, volume 1
[DE92-000141] N92-11897
Underlying generation mechanisms for the extragalactic gamma ray background and their implications for high-resolution gamma ray cosmology N92-11959
CALIFORNIA UNIV., SANTA BARBARA.
Nonlinear optical properties of semiconducting polymers
[AD-A240753] N92-11195
Electron acceleration by laser fields in a gas
[DE91-018477] N92-11345
Looking ahead to EOS: Update on NASA's Earth Observing Program N92-11556
CALSPAN-BUFFALO UNIV. RESEARCH CENTER, NY.
Studies of aerothermal loads generated in regions of shock/shock interaction in hypersonic flow
[NASA-CR-181893] N92-11319
CANADA CENTRE FOR REMOTE SENSING, OTTAWA (ONTARIO).
Altitude dependence in a semi-analytical atmospheric code N92-11413
Radiometric and atmospheric correction procedures for AVHRR preprocessing in the solar reflective channels N92-11414
Spectroscopic analysis of imaging spectrometer data for classification purposes N92-11439
CARNEGIE-MELLON UNIV., PITTSBURGH, PA.
Three dimensional migration and forward modelling of ground penetrating radar data
[AD-A240505] N92-11234
Ground penetrating radar data acquisition system
[AD-A240765] N92-11244
Leveling of the AMBLER walking machine: A comparison of methods
[NASA-CR-189015] N92-11358
Appearance simulator for computer vision research
[AD-A240506] N92-11679
Issues in real-time data management
[AD-A240712] N92-11926
CASE WESTERN RESERVE UNIV., CLEVELAND, OH.
Fracture toughness of carbon/carbon composites
[AD-A240200] N92-11143
CENTRE D'ETUDES AERODYNAMIQUES ET THERMIQUES, POITIERS (FRANCE).
Euromech 260: Advanced non-intrusive experimental techniques in fluid and plasma flows
[ETN-91-90104] N92-11313
CENTRE D'ETUDES DE METEOROLOGIE SPATIALE, LANNION (FRANCE).
Routine mapping of vegetation index with the AVHRR of NOAA11 N92-11405
CENTRE D'ETUDES ET DE RECHERCHES, TOULOUSE (FRANCE).
Numerical resolution of three dimensional Euler equations in totally unstructured mesh
[CERT-RF-1/3369-00/DERI-GAN] N92-10988
Secondary instability of the three dimensional laminar boundary layer in incompressible flow: Description of the calculation code
[CERT-RT-63/5618-54] N92-11306
Resolution of the Navier-Stokes equations applied to the computation of the laminar flow around a two dimensional wing profile
[CERT-RT-65/5604-35] N92-11307
Turbulent friction drag reduction: Boundary layer manipulators
[CERT-RSF-DERAT-62/5004-31] N92-11309
Characterization of African desert sites for the relative calibrating of wide field satellite optical sensors N92-11402
Database of SPOT histrograms N92-11517
Modeling of flexible polyarticulate chains: Bibliographic synthesis
[CERT-DERA-1/7735] N92-11927
CENTRE FOR AGROBIOLOGICAL RESEARCH, WAGENINGEN (NETHERLANDS).
Multifrequency radar measurements of potato, beet, and wheat during the AGRISCATT-88 campaign in the Netherlands N92-11444
The linking of crop growth models and multi-sensor remote sensing data N92-11512
CENTRE MACHINISME AGRICOLE GENIE RURAL EAUX FORETS, ANTONY (FRANCE).
Active microwave remote sensing and ground hydric state. Agriscatt '88 airborne campaign over the Orgeval basin (France) N92-11454
CENTRE MACHINISME AGRICOLE GENIE RURAL EAUX FORETS, MONTPELLIER (FRANCE).
Multidate analysis of NOAA-AVHRR data over France: Relationship with agroclimatic characteristics N92-11521
A simple model of canopy fluorescence N92-11543
CENTRE NATIONAL D'ETUDES DES TELECOMMUNICATIONS, ISSY-LES-MOULINEAUX (FRANCE).
Calibration and validation of a surface flux model in the framework of the HAPEX-MOBILHY experiment. Application to estimating the cover resistance N92-11511
CENTRE NATIONAL D'ETUDES SPATIALES, TOULOUSE (FRANCE).
Comparison between californium and cyclotron heavy ion tests N92-11266
CENTRE NATIONAL DE LA RECHERCHE SCIENTIFIQUE, GRENOBLE (FRANCE).
Large scale study of the microwave signature of the Antarctic ice sheet N92-11463
Comparison between the observed microwave spectral signatures over the Antarctic ice sheet and a snow emissivity model N92-11464
CENTRE NATIONAL DE LA RECHERCHE SCIENTIFIQUE, MEUDON-BELLEVUE (FRANCE).
Preliminary results of a spectro-imagery experiment (GER) over the Adriatic coastline of the Venice lagoon N92-11440
CENTRE NATIONAL DE RECHERCHES METEOROLOGIQUES, TOULOUSE (FRANCE).
TIMS calibration correction by comparison with PRT5 N92-11412
Some examples of satellite data utilization for atmospheric modeling at medium scale N92-11503
Remote sensing contribution to the APEX MOBILHY program N92-11557
CENTRO DE INVESTIGACIONES ENERGETICAS, MADRID (SPAIN).
Review of the TJ-II Flexible Heliac Project N92-11803
Second stability studies in a helical axis device: TJ-II N92-11807
Theory of electron cyclotron heating in the flexible heliac TJ-II N92-11828
STORM: A low aspect ratio torsatron for plasma stability N92-11829
CENTRO TECNICO AEROSPACIAL, SAN JOSE DOS CAMPOS (BRAZIL).
TEGEN: A one dimensional program to calculate a thermoelectric generator
[DE91-634444] N92-11571
CESKOSLOVENSKA AKADEMIE VED, PRAGUE.
Radiation forces to electrons in laser fields explained as scattering for ponderomotive momentum transfers
[IPPCZ-308] N92-11773
LHCD experiments on tokamak CASTOR
[IPPCZ-304] N92-11881
Spectral observations of solar radio bursts in the range of 2.0-4.5 GHz
[CAS-PUBL-76] N92-11953
Spectral observations of solar radio bursts at 2.0-4.5 GHz
[CAS-PUBL-77] N92-11954
CHEMICAL RESEARCH AND DEVELOPMENT CENTER, ABERDEEN PROVING GROUND, MD.
Time-resolved analytical pyrolysis mass spectrometry of biomaterials
[AD-A240624] N92-11167
CLEMSON UNIV., SC.
Development of high Tc (greater than 110K) Bi, Tl and Y-based materials as superconducting circuit elements
[NASA-CR-188999] N92-11902

COASTAL ENGINEERING RESEARCH CENTER, VICKSBURG, MS.
Index and bulk parameters for frequency-direction spectra measured at CERC field research facility
[AD-A240320] N92-11607
Use of theoretical wave height distributions in directional seas
[AD-A240411] N92-11608
COLLEGE OF WILLIAM AND MARY, WILLIAMSBURG, VA.
Algebraic aspects of network reliability problems
[AD-A240365] N92-11748
COLORADO STATE UNIV., FORT COLLINS.
Evaluation of high Reynolds number flow in a 180 degree turn-around-duct
[NASA-CR-184243] N92-11318
Grassland/atmosphere response to changing climate: Coupling regional and local scales
[DE91-016906] N92-11575
COLORADO UNIV., BOULDER.
TRUST: TDRSS Resource User Support Tool N92-11052
A computational procedure for the dynamics of flexible beams within multibody systems N92-11371
Retrievals of column atmospheric water vapor, vegetation liquid water, and cloud cover fraction from AVIRIS data N92-11427
Spectral identification (1.2-2.5 microns) and characterization of Paris (France) Basin kaolinite/smectite clays using a field spectrometer N92-11429
Integration of visible-through microwave-range multispectral image data sets for geologic mapping N92-11491
A conceptual framework for ecosystem modeling using remotely sensed inputs N92-11551
Application of modern mathematical concepts to plasma confinement
[DE92-000053] N92-11893
COLUMBIA UNIV., NEW YORK, NY.
On the nature of bulk electrical relaxation in silicate glasses
[DE92-000077] N92-11206
Development of a high resolution liquid xenon imaging chamber for gamma-ray astronomy
[NASA-CR-188994] N92-11332
COMPUTER SCIENCES CORP., BELTSVILLE, MD.
Ground Systems Development Environment (GSDE) interface requirements analysis
[NASA-CR-188822] N92-11702
COMPUTER SCIENCES CORP., FALLS CHURCH, VA.
Ground Systems Development Environment (GSDE) interface requirements analysis
[NASA-CR-188822] N92-11702
COMPUTER SCIENCES CORP., GREENBELT, MD.
Network Control Center User Planning System (NCC UPS) N92-11053
Polynomial optimization techniques for activity scheduling. Optimization based prototype scheduler N92-11056
COMPUTER TECHNOLOGY ASSOCIATES, INC., ROCKVILLE, MD.
What we were asked to do N92-11041
Human factors issues in the design of user interfaces for planning and scheduling N92-11049
CHIMES-2: A tool for automated HCI analysis N92-11051
CONNECTICUT UNIV., STORRS.
Convergence and performance of synchronous and asynchronous parallel and conventional iterative methods
[AD-A240286] N92-11707
CONSIGLIO NAZIONALE DELLE RICERCHE, FLORENCE (ITALY).
Passive microwave remote sensing of vegetation canopies: Experimental and modeling results N92-11460
Vegetation monitoring by means of spectral resolved fluorescence lidar N92-11533
Target signature by differential reflectance lidar, a feasibility study N92-11544
CONSIGLIO NAZIONALE DELLE RICHERCHE OLIVICOLTURA, PERUGIA (ITALY).
Simultaneous detection in blue and red bands of laser induced vegetation fluorescence N92-11539
COORDINATING RESEARCH COUNCIL, INC., ATLANTA, GA.
Effect of gasoline octane quality on vehicle acceleration performance
[AD-A240433] N92-11357
CORNELL UNIV., ITHACA, NY.
Synthesis of novel conducting solids
[AD-A240468] N92-11912
COUNCIL FOR NATIONAL ACADEMIC AWARDS (ENGLAND).
Infrared to millimetre observations of active galaxies N92-11932
CRANFIELD INST. OF TECH., BEDFORD (ENGLAND).
Radial inflow turbine study
[AD-A240169] N92-11015

D

DAVID TAYLOR RESEARCH CENTER, BETHESDA, MD.
Analysis of strain dependent damping in materials via modeling of material point hysteresis
[AD-A240298] N92-11381
DAYTON UNIV., OH.
A comparison of single cycle overload effect on Al-Li 2091-T81 plate and 2091-T83 sheet
[AD-A240627] N92-11179
Lessons learned in the development of the C-130 aircrew training system: A summary of Air Force on-site experience
[AD-A240554] N92-11635
DEFENSE SYSTEMS MANAGEMENT SCHOOL, FORT BELVOIR, VA.
Proceedings of the Acquisition Research Symposium: Imagination, Innovation, and Implementation, 1991, volume 1
[AD-A240260] N92-11676
Proceedings of the Acquisition Research Symposium: Acquisition for the Future, Imagination, Innovation, and Implementation, 1991, volume 2
[AD-A240261] N92-11677
DELAWARE UNIV., NEWARK.
Development of an experimental database and theories for prediction of thermodynamic properties of aqueous electrolytes and nonelectrolytes of geochemical significance at supercritical temperatures and pressures
[DE91-018493] N92-11169
DELHI UNIV. (INDIA).
Motion of charged particle in helical systems N92-11847
DEPARTMENT OF ENERGY, WASHINGTON, DC.
Office of Basic Energy Sciences
[DE91-019006] N92-11570
FEDIX: The on-line database retrieval service of Government information for colleges, universities, and other organizations
[DE91-018496] N92-11923
Integrated Risk Information System
[DE91-018503] N92-11924
DEPARTMENT OF THE ENVIRONMENT, LONDON (ENGLAND).
Scientific assessment of stratospheric ozone: 1989, volume 1
[NASA-TM-105116] N92-11576
Scientific assessment of stratospheric ozone: 1989. Volume 2: Appendix: AFEAS report
[NASA-TM-105117] N92-11577
DEPARTMENT OF THE NAVY, WASHINGTON, DC.
Centrifugal casting of composites
[AD-D014981] N92-11144
High density energetic materials
[AD-D014959] N92-11212
Impulse transmitter and quantum detection radar system
[AD-D014958] N92-11229
Programmable beam transform and beam steering control system for a phased array radar antenna
[AD-D014970] N92-11230
Communications interface and system for radiation recovery of a microprocessor portion thereof
[AD-D014977] N92-11245
Active radar stealth device
[AD-D014980] N92-11246
Enhanced clutter suppression apparatus for use with an infrared search and surveillance system
[AD-D014984] N92-11247
Microchannel electron source
[AD-D014956] N92-11276
Circuit probing system
[AD-D014966] N92-11277
Antiresonant nonlinear mirror for passive laser mode locking
[AD-D014951] N92-11343
Laser diode pumped, erbium-doped, solid state laser with high slope efficiency
[AD-D014968] N92-11347
In-line hydraulic dashpot
[AD-D014955] N92-11356
Geothermal energy conversion system
[AD-D014979] N92-11569
Thin film magnetic memory elements
[AD-D014971] N92-11646
Acoustic transponder receiver circuit
[AD-D014965] N92-11760
Micro photoreflectance semiconductor wafer analyzer
[AD-D014950] N92-11788
Compact optical RF spectrum analyzer
[AD-D014962] N92-11792
DEUTSCHE FORSCHUNGSANSTALT FUER LUFT- UND RAUMFAHRT, OBERPFAFFENHOFEN (GERMANY, F.R.).
The comparison of airborne imaging spectrometry and geochemical ground survey for the analysis of vegetation anomalies over waste deposits N92-11431
The spectral reflection behaviour of branches and branch components of healthy and damaged beech trees N92-11432
Evaluation of high spectral resolution laboratory reflectance data of healthy and damaged beech and spruce branches for the improvement of forest damage classification N92-11433
CO2 laser active remote sensing from 9 to 11 microns: Airborne and laboratory application N92-11535
Design and testing of a spectral-resolving fluorescence lidar system for remote sensing of vegetation N92-11540
DEUTSCHE FORSCHUNGSANSTALT FUER LUFT- UND RAUMFAHRT, WESSLING (GERMANY, F.R.).
Correction of atmospheric and topographic effects in LANDSAT TM images N92-11407
DEUTSCHE GEODAETISCHE KOMMISSION, MUNICH (GERMANY, F.R.).
The notion of artificial satellites in the anisotropic gravitational field of a uniformly rotating solid Earth model. A second order analytical solution
[SER-C-357] N92-11072
DRAPER (CHARLES STARK) LAB., INC., CAMBRIDGE, MA.
Advanced information processing system for advanced launch system: Avionics architecture synthesis
[NASA-CR-187554] N92-11704
Advanced information processing system for advanced launch system: Hardware technology survey and projections
[NASA-CR-187555] N92-11705
Advanced information processing system: Inter-computer communication services
[NASA-CR-187556] N92-11706

E

ECK RESEARCH CO., COLUMBIA, MO.
Energetics diagnosis of numerical simulation of atmospheric blocking
[NASA-CR-183503] N92-11581
ECOLE NATIONALE SUPERIEURE DES TELECOMMUNICATIONS, PARIS (FRANCE).
Basic concepts of low Earth orbit satellite systems for communications
[TELECOM-PARIS-91-D-001] N92-11248
Conoscopic holography. 1: Basic principles and physical basis. 2: Rigorous derivation
[TELECOM-PARIS-91-C-001] N92-11337
ECOLE POLYTECHNIQUE FEDERALE DE LAUSANNE (SWITZERLAND).
Texture indices sensitivity to spatial and spectral resolutions in semi-urban environments N92-11519
EDGERTON, GERMESHAUSEN AND GRIER, INC., IDAHO FALLS, ID.
Nuclear safety N92-11114
Strengthening of an AISI 1020 steel by aluminum-microalloying during liquid dynamic compaction
[DE91-018745] N92-11182
ELECTRONICS RESEARCH LAB., ADELAIDE (AUSTRALIA).
Using a discrete Fourier transform to estimate phase in interferometric direction finding
[AD-A231414] N92-10995
ENVIRONMENTAL ANALYSIS AND REMOTE SENSING, DELFT (NETHERLANDS).
Modeling of fluorescence light-canopy interaction N92-11545
EUROPEAN SPACE AGENCY, PARIS (FRANCE).
Physical Measurements and Signatures in Remote Sensing, volume 1
[ESA-SP-319-VOL-1] N92-11394
Physical Measurements and Signatures in Remote Sensing, volume 2
[ESA-SP-319-VOL-2] N92-11488
EUROPEAN SPACE AGENCY. EUROPEAN SPACE RESEARCH AND TECHNOLOGY CENTER, ESTEC, NOORDWIJK (NETHERLANDS).
The performance of the ESA Medium Resolution Imaging Spectrometer (MERIS) N92-11422

F

FEDERAL AVIATION ADMINISTRATION, ATLANTIC CITY, NJ.
Program plan: National aging aircraft research program
[DOT/FAA/CT-88/32-1] N92-10992
Evaluation of two high-speed runway exits
[DOT/FAA/CT-TN91/36] N92-11021
Prototype runway hold-short lighting system
[DOT/FAA/CT-TN91/43] N92-11028
Surface painted taxiway markings at Seattle-Tacoma International Airport
[DOT/FAA/CT-TN91/49] N92-11029

FEDERAL AVIATION ADMINISTRATION, WASHINGTON, DC.
EDMS: Microcomputer pollution model for civilian airports and Air Force bases, (user's guide)
[AD-A240528] N92-11578
Pilot's Automated Weather Support System (PAWSS) concepts demonstration project. Phase 1: Pilot's weather information requirements and implications for weather data systems design
[NASA-CR-188228] N92-11593

FERMI NATIONAL ACCELERATOR LAB., BATAVIA, IL.
Global analysis of fermion mixing with exotics
[NASA-CR-189006] N92-11774
Perturbations from strings don't look like strings!
[NASA-CR-189012] N92-11941
Superfluid-like turbulence in cosmology
[NASA-CR-189011] N92-11942
Cosmological constraints on pseudo-Nambu-Goldstone bosons
[NASA-CR-189010] N92-11943
Re-ionization and decaying dark matter
[NASA-CR-189009] N92-11944
Converting neutron stars into strange stars
[NASA-CR-189008] N92-11945
Cosmological structure formation
[NASA-CR-189007] N92-11946
Non scale-invariant density perturbations from chaotic extended inflation
[NASA-CR-189004] N92-11947
E sub 6 leptoquarks and the solar neutrino problem
[NASA-CR-189005] N92-11956

FLIGHT MECHANICS AND CONTROL, INC., HAMPTON, VA.
A methodology to assess the Best Estimate Trajectory (BET) results generated for the Kwajalein Missile Range
[AD-A240770] N92-11083

FLINDERS UNIV., BEDFORD PARK (AUSTRALIA).
Coupled-channel optical calculation of electron-hydrogen scattering: Elastic scattering from 0.5 to 30 eV
[DE91-634157] N92-11780

FLORIDA UNIV., GAINESVILLE.
Droplet Core Nuclear Rocket (DLNR) N92-11105
Vapor core propulsion reactors N92-11109
A theory of the earth's precession relative to the invariable plane of the solar system N92-11938

FORD AEROSPACE AND COMMUNICATIONS CORP., PALO ALTO, CA.
Multiple beam antenna/switch system study
[NASA-CR-183496] N92-11251

FORD AEROSPACE AND COMMUNICATIONS CORP., SEABROOK, MD.
Flexible Envelope Request Notation (FERN) N92-11050
Scheduling techniques in the Request Oriented Scheduling Engine (ROSE) N92-11058

G

GENERAL ATOMICS TECHNOLOGIES CORP., SAN DIEGO, CA.
The TITAN reversed-field-pinch fusion reactor study, volume 4
[DE92-000138] N92-11895
The TITAN reversed-field-pinch fusion reactor study, volume 2
[DE92-000140] N92-11896
The TITAN reversed-field-pinch fusion reactor study, volume 1
[DE92-000141] N92-11897

GENERAL ELECTRIC CO., CINCINNATI, OH.
Alloy modeling and experimental correlation for ductility enhancement in near stoichiometric single crystal nickel aluminide
[AD-A240151] N92-11175

GENERAL ELECTRIC CO., PHILADELPHIA, PA.
Hybrid propulsion systems for space exploration missions N92-11097

GENERAL ELECTRIC CO., SAN JOSE, CA.
A cermet fuel reactor for nuclear thermal propulsion N92-11096

GEORGIA INST. OF TECH., ATLANTA.
LV software support for supersonic flow analysis
[NASA-CR-188914] N92-10978
Measurement of frequency response in short thermocouple wires
[NASA-CR-187821] N92-11339
Illumination, optics, and retroreflectors for efficient landmark tracking N92-11790

GEORGIA UNIV., ATHENS.
Circular Statistical methods: Applications in spatial and temporal performance analysis
[AD-A240751] N92-11749

GOETTINGEN UNIV. (GERMANY, F.R.).
Monte Carlo model for transport equation in a plant canopy and its inversion N92-11481

GOSUDARSTVENNYI KOMITET PO ISPOLZOVANIYU ATOMNOI ENERGII, OBNINSK (USSR).
Bose-condensation in liquid helium under pressure
[DE91-634504] N92-11170
To the account of finite velocity of thermal diffusion in turbulent flows
[DE91-635593] N92-11323
Heat transfer in channels with uniformly swirled flow
[DE91-635594] N92-11324
Determination of nonstationary temperatures in high-stressed elements with pulsed heat sources
[DE91-635705] N92-11325

GRENOBLE-1 UNIV. (FRANCE).
Analysis of experimental results on functional testing and diagnosis of complex circuits N92-11254
Failure coverage of functional test methods: A comparative experimental evaluation N92-11255
Automatic generation of microprocessor test programs N92-11256
The GAPT system: A chain of test for microprocessors N92-11258
A microprocessor test approach allowing fault localisation N92-11261
Towards an automated system for the verification and diagnosis of intelligent VLSI circuits N92-11262
A method and tools for microprocessor validation: High safety function applications N92-11263
Top down IC failure analysis using an E-beam system coupled to a functional tester N92-11264
Automatic tools for microprocessor failure analysis N92-11265
Comparison between californium and cyclotron heavy ion tests N92-11266
Comparison between californium and cyclotron SEU tests N92-11267
An a priori approach to the evaluation of signature analysis efficiency N92-11268
Analysis of the surface state of two sub-polar glaciers using SPOT data and a numerical terrain model N92-11523
On the theory and numerical approximation of nonlinear hyperbolic problems
[ETN-91-99898] N92-11714
On a class of implicit and explicit schemes of Van-Leer type for scalar conservation laws N92-11715
Stable upwind schemes for hyperbolic conservation laws for with source terms N92-11716
An analysis of upwind schemes for inhomogeneous two dimensional conservation laws N92-11717
An analysis of some hyperbolic problems related to the shallow water model (chapter 6)
[IMAG-RR-579] N92-11718
Operator splitting, fractional steps, method and entropy condition for nonlinear hyperbolic systems N92-11719
Numerical analysis of the problem of long waves in shallow water N92-11720
On the solution for the problem of long waves in a perfect fluid N92-11721

GRENOBLE-1 UNIV., SAINT MARTIN D'HERES (FRANCE).
Hardware and software tools for microprocessor functional test N92-11257
Taking into account asynchronous signals in functional test of complex circuits N92-11259
Fault localization when testing complex circuits N92-11260

GROUPEMENT D'ETUDES ET DE RECHERCHES POUR LE DEVELOPPEMENT DE L'AGRONOMIE TROPICALE, PARIS (FRANCE).
Radiative transfer simulation on computer models of vegetation cover N92-11476

GROUPEMENT SCIENTIFIQUE DE TELEDETECTION DE STRASBOURG (FRANCE).
Experimental approach to emissivity problems and surface temperature in thermal infrared remote sensing N92-11462
Complementarity of temperature independent Thermal Infrared Spectral Indices (TISI) and NDVI: Compared properties and combined use for soil and vegetation discrimination N92-11490
Integration of Seasat and SPOT data, contribution to structural geology mapping in temperature environment N92-11499

GROUPEMENT SCIENTIFIQUE DE TELEDETECTION SPATIALE DE TOULOUSE (FRANCE).
Analysis of radar polarimetric data for the discrimination and monitoring of forest covers N92-11449

H

HARRIS CORP., MELBOURNE, FL.
OPUS: Optimal Projection for Uncertain Systems. Volume 1
[AD-A240372] N92-11080
OPUS: Optimal Projection for Uncertain Systems, volume 2
[AD-A240373] N92-11081
Tester Independent Support Software System (TISSS)
[AD-A240668] N92-11681

HARVARD UNIV., CAMBRIDGE, MA.
PET studies of components of high-level vision
[AD-A240202] N92-11624

HEBREW UNIV. OF JERUSALEM, REHOVOT (ISRAEL).
Simultaneous determination of six soil properties from the soil diffuse reflectance spectrum in the near infrared region (1-2.5 microns) N92-11424

HEIDELBERG UNIV. (GERMANY, F.R.).
Measurement of turbulent flow beneath the wind wave induced water surface, using picture repetition analysis
[ETN-91-90203] N92-11316

HELSINKI UNIV. OF TECHNOLOGY, ESPOO (FINLAND).
The role of fiber flocculation in chemical pulp refining
[ETN-91-90025] N92-11150
Fundamental aspects of the refining process N92-11151
A new hypothesis for the mechanics of refining N92-11152
Development of a fundamentally new refining method. Part 1: Basic design considerations N92-11153
Development of a fundamentally new refining method. Part 2: Operating conditions of the new refiner N92-11154
Effect of control variables and length of refining zone on the refining result with a new pilot refiner N92-11155
Comparison of a new refiner with a conventional refiner N92-11156
Homogeneity of refining action; effects on fiber and paper structure N92-11157
Control of the heterogeneity of the refining action N92-11158

HITACHI LTD. (JAPAN).
Pool-cooled superconducting magnet design of large helical device N92-11839
Behavior of vacuum vessel eddy current in large helical device N92-11840

HOKKAIDO UNIV., SAPPORO (JAPAN).
Graphites as plasma facing material of a large fusion device N92-11813

HONEYWELL, INC., MINNEAPOLIS, MN.
New methods in robust control
[AD-A240221] N92-11018

HUGHES ASSOCIATES, INC., WHEATON, MD.
Discharge system tests of Halon 1301 test gas simulants
[AD-A240679] N92-11193

I

IDAHO NATIONAL ENGINEERING LAB., IDAHO FALLS.
Low Pressure Nuclear Thermal Rocket (LPNTR) concept N92-11094

ILLINOIS UNIV., URBANA.
Effects of hydrogen and carbon on thermally activated deformation in nickel
[AD-A240496] N92-11178
Biochemical and biophysical studies of the E. coli respiratory chain
[DE91-016966] N92-11612
Reminding-based learning
[AD-A240370] N92-11634
Perceptual grouping and shape from texture
[AD-A240358] N92-11678
Cedar Project: Original goals and progress to date
[DE92-000032] N92-11689
Photoreflectance and H2O adsorption on GaAs(100)
[AD-A240391] N92-11911

IMPERIAL COLL. OF SCIENCE AND TECHNOLOGY, LONDON (ENGLAND).
Reciprocity theory of gas surface interactions
[IC-AERO-89-04] N92-11289
INDUSTRIAL QUALITY, INC., GAITHERSBURG, MD.
Development of data file standards for automated ultrasonic scanning systems. Exchange methods for digital ultrasonic inspection data
[AD-A240075] N92-11364
INSTITUT DE RECHERCHE EN AGRONOMIE TROPICALE, MONTPELLIER (FRANCE).
Estimation of the primary production in Sahelian region from radiometric data N92-11504
INSTITUT FRANCAIS DE RECHERCHE SCIENTIFIQUE POUR LE DEVELOPPEMENT EN COOPERATION, PARIS (FRANCE).
Multitemporal study of the Guyana coastline and estuaries using SPOT and LANDSAT imagery N92-11524
Spatial and spectral analysis of a degraded mangrove in south Senegal N92-11527
INSTITUT NATIONAL DE LA RECHERCHE AGRONOMIQUE, AVIGNON (FRANCE).
Estimation of the aerosol optical thickness from broadband turbidity measurements: Application to the atmospheric correction of SPOT images N92-11399
INSTITUT NATIONAL DE LA RECHERCHE AGRONOMIQUE, MONTFAVET (FRANCE).
Inter-calibrating of SPOT1-HRV, LANDSAT5-TM, and NOA11-AVHRR in the visible and near infrared field s N92-11401
Use of operation ART-SPOT to test the 5S model and the MTF of the SPOT N92-11403
On the nature of spectral shifts: Modeling and comparison to information contained in wide bands N92-11418
Estimation of the ground humidity under vegetation: Applications of semi-empirical models N92-11445
Validation of a ground spectral and directional reflectance model N92-11479
Joint use of remote sensing and agricultural production estimation models: Current trends N92-11501
Spectral estimates of PAR interception and biomass production of irrigated rice crops. 2: Model validation with SPOT data N92-11510
Temporal signatures using NOAA-AVHRR and land use mapping N92-11513
Study of the spatial variability of the hydrodynamic behavior of grounds at the Niger (Africa) using satellite images N92-11515
Spectral estimates of PAR interception and biomass production of irrigated rice crops. 1: Model elaboration with ground data N92-11522
Time-resolved spectroscopy of the blue fluorescence of spinach leaves N92-11538
INSTITUT NATIONAL DE LA RECHERCHE AGRONOMIQUE, RENNES (FRANCE).
Humidity measurement of naked ground by radar in conditions of excessive water N92-11453
INSTITUT NATIONAL DE LA RECHERCHE AGRONOMIQUE, THIVERVAL-GRIGNON (FRANCE).
Evaluation of vegetation cover characteristics using an airborne microwave scatterometer N92-11456
Construction of ground cover charts of a wheat canopy from reflectance measurements N92-11505
Using the radiative surface temperature in energy budget studies over plant canopies N92-11506
Simulation study of vegetation indices sensitivity using the middle infrared N92-11514
INSTITUT NATIONAL DE LA RECHERCHE AGRONOMIQUE, VILLENAVE D'ORNON (FRANCE).
Actual daily evapotranspiration monitoring using NOAA-AVHRR data from the HAPEX-MOBILHY campaigns N92-11509
INSTITUT NATIONAL DES SCIENCES APPLIQUEES DE ROUEN, MONT SAINT AIGNAN (FRANCE).
Theoretical study (Lagrangian modeling) of turbulent particulate dispersion
[ETN-91-99909] N92-11287
INSTITUT NATIONAL POLYTECHNIQUE, GRENOBLE (FRANCE).
Test and diagnosis of programmable integrated circuits
[ETN-91-99483] N92-11253
INSTITUT ZA NUKLEARNE NAUKE BORIS KIDRIC, BELGRADE (YUGOSLAVIA).
On strong RF plasma turbulence N92-11836
INSTITUTE FOR COMPUTER APPLICATIONS IN SCIENCE AND ENGINEERING, HAMPTON, VA.
Ignition and structure of a laminar diffusion flame in the field of a vortex
[NASA-CR-189042] N92-11162
Resonant frequency calculations using a hybrid perturbation-Galerkin technique
[NASA-CR-187632] N92-11640
Distributed memory compiler methods for irregular problems: Data copy reuse and runtime partitioning
[NASA-CR-187635] N92-11669
Vienna FORTRAN: A FORTRAN language extension for distributed memory multiprocessors
[NASA-CR-187634] N92-11670
Optimal processor assignment for pipeline computations
[NASA-CR-189047] N92-11672
Proceedings for the ICASE Workshop on Heterogeneous Boundary Conditions
[NASA-CR-187630] N92-11728
Multi-resolution analysis for ENO schemes
[NASA-CR-189043] N92-11736
INTERNATIONAL SPACE UNIV., INC., CAMBRIDGE, MA.
International program for Earth observations
[NASA-CR-188799] N92-11393

J

JAPAN ATOMIC ENERGY RESEARCH INST., NAKA.
Recent experiments in JT-60 N92-11812
JET PROPULSION LAB., CALIFORNIA INST. OF TECH., PASADENA.
Resource allocation planning helper (RALPH) N92-11047
User interface issues in supporting human-computer integrated scheduling N92-11048
Erosive augmentation of solid propellant burning rate: Motor size scaling effect N92-11125
Determination of the in-flight spectral and radiometric characteristics of the Airborne Visible/Infrared Imaging Spectrometer (AVIRIS) N92-11397
Comparison of two atmospheric correction models for a vegetated Airborne Visible/Infrared Imaging Spectrometer (AVIRIS) scene N92-11415
Use of high spectral resolution airborne visible/infrared imaging spectrometer data for geologic mapping: An overview N92-11420
Current status and future developments in radar remote sensing N92-11441
Airborne precursor missions in support of SIR-C/X-SAR N92-11450
On the use of passive microwaves at 37 GHz N92-11461
Spectral reflectance of thin snow N92-11482
Neotectonic studies of northern Baja California, Mexico, with LANDSAT thematic mapper and SPOT panchromatic imagery: Partitioning of dextral and extensional strain at the Pacific-North America plate boundary N92-11553
Dual frequency optical carrier technique for transmission of reference frequencies in dispersive media
[NASA-CASE-NPO-18007-1-CU] N92-11791
JOANNEUM RESEARCH CENTRE, GRAZ (AUSTRIA).
Phenological changes in the red edge shift of Norway spruce needles and their relationship to needle chlorophyll content N92-11423
JOHNS HOPKINS UNIV., COLUMBIA, MD.
The 27th JANNAF Combustion Subcommittee Meeting, Volume 3
[CPIA-PUBL-557-VOL-3] N92-11117
JOINT OCEANOGRAPHIC INST., INC., WASHINGTON, DC.
Theory and modeling in GLOBEC: A first step N92-11602
GLOBEC: Global Ocean Ecosystems Dynamics: A component of the US Global Change Research Program
[NASA-TM-105121] N92-11603
JOINT PUBLICATIONS RESEARCH SERVICE, ARLINGTON, VA.
JPRS report: Science and technology. USSR: Space. Feoktistov's Views on Future Directions for Space Program
[JPRS-USP-91-005] N92-11032
JPRS report: Science and technology. USSR: Life sciences
[JPRS-ULS-91-015] N92-11610
JPRS report: Science and technology. USSR: Life sciences
[JPRS-ULS-91-012] N92-11611
JPRS report: Science and technology. USSR: Life sciences
[JPRS-ULS-91-017] N92-11616
Effect of prolonged space flight on erythrocyte metabolism and membrane functional condition N92-11617
Efficacy of hyperbaric oxygenation in enhancing flight tolerance N92-11618
Toxicity assessment of combustion products in simulated space cabins N92-11619
Technical requirements of sick bays aboard space ships N92-11620
JOINT RESEARCH CENTRE OF THE EUROPEAN COMMUNITIES, ISPRA (ITALY).
The use of imaging spectrometry in Mediterranean land degradation and soil erosion hazard assessments N92-11430
Generalized formulation for semi-empirical radar models representing crop backscattering N92-11447
Dual polarization microwave backscatter signatures of bare and vegetated soils N92-11452
The use of a time-resolved lidar to study the water column N92-11548
Observation of DOM composition by synchronous fluorescence spectroscopy N92-11549

K

KAGOSHIMA UNIV. (JAPAN).
A study on the effects of Mt. Sakurajima's falling ash over crop and forest areas using image processing for LANDSAT-5, MOS-1, and Jafsa digital data N92-11497
KARLSRUHE UNIV. (GERMANY, F.R.).
Laser-induced blue fluorescence and red chlorophyll fluorescence signatures of differently pigmented leaves N92-11541
The laser-induced chlorophyll fluorescence ratio F690/F735 of spruce needles and beech leaves during the course of a year N92-11542
KATHOLIEKE UNIV. TE LEUVEN (BELGIUM).
An integrated modelling approach for the spectral identification of crops N92-11508
KENT STATE UNIV., OH.
Theoretical interpretation of high-energy nuclear collisions
[DE91-016965] N92-11782
KISARAZU NATIONAL COLL. OF TECHNOLOGY (JAPAN).
Laser induced fluorescence of growing camphor tree leaves: Influence of chlorophyll content on LIF spectral signature N92-11547
KOREA ADVANCED ENERGY RESEARCH INST., DAEDUK (REPUBLIC OF KOREA).
Studies on laser atomic spectroscopy
[DE91-628172] N92-11349
A study on the development of high T(sub c) superconducting materials
[DE91-629755] N92-11917
KYOTO UNIV. (JAPAN).
Review of Heliotron E experiment N92-11822
KYOTO UNIV., UJI (JAPAN).
Drift optimization of helical systems N92-11810
Analysis of scrape-off layer in toroidal helical systems N92-11815
Confinement studies of Heliotron E plasmas in magnetic surface variation experiments N92-11850
Profile measurements in magnetic surface variation experiments/multiple pellet injection experiments N92-11851
Impurity behavior in Heliotron E N92-11852
Edge plasma study in Heliotron E N92-11853
Recent diamagnetic measurements of toroidal coil experiments on Heliotron E N92-11854
Study of resistive interchange mode in Heliotron E N92-11855
Measurement of magnetic fluctuations in Heliotron E N92-11856
The 100 GHz half megawatt microwave transmission system development with whispering gallery mode N92-11869

L

LABORATOIRE DE METEOROLOGIE DYNAMIQUE, PARIS (FRANCE).
Space observation of the land-ocean-atmosphere system at high spectral resolution in the infrared: Perspectives and problems N92-11421
LASER PHOTONICS, INC., BEDFORD, MA.
Long wavelength semiconductor lasers development for infrared heterodyne applications
[NASA-CR-189243] N92-11341
LAWRENCE LIVERMORE NATIONAL LAB., CA.
Non-equilibrium microstructures produced during electron-beam and laser-beam surface modification of metallic alloys
[DE91-018466] N92-11174
Dispersion and stability of two electromagnetic solvers for triangular meshes
[DE91-016607] N92-11227
Trends in laser-plasma-instability experiments for laser fusion
[DE91-016923] N92-11344
Irradiance compensation control for high-energy laser propagation, part 2
[DE91-018489] N92-11348

Continuum x ray gauging of multiple-element materials
[DE91-017429] N92-11368
Geometrically exact shells models: Foundation and computational aspects with special reference to implicit large-scale calculations
[DE91-019014] N92-11390
A domain decomposition algorithm for solving large elliptic problems
[DE92-000096] N92-11690
Harnessing the killer micros: Applications from LLNL's massively parallel computing initiative
[DE91-018721] N92-11709
Critical properties of strongly interacting bosons on a lattice
[DE91-016926] N92-11771
Positron lifetimes in solids from first principles calculations
[DE92-000088] N92-11781
A realistic, gradual and economical approach to fusion power
[DE91-018464] N92-11786
Optical design of a high power fiber optic coupler
[DE91-016924] N92-11789
Stray light reduction in a WFOV star tracker lens
[DE91-018460] N92-11794
An IFE development strategy
[DE91-016918] N92-11873
Laser produced plasma soft x ray generation
[DE91-016925] N92-11874
Particle trajectories through MIRRORTRON configurations
[DE91-017084] N92-11876
OPAL opacities for astrophysical applications
[DE91-016922] N92-11939
Modeling UV and x ray oxygen emission in astrophysical plasmas
[DE91-016927] N92-11940

LAYTON (J. PRESTON), PRINCETON JUNCTION, NJ.
Comments on dual-mode nuclear space power and propulsion system concepts N92-11106

LEHMAN (HERBERT H.) COLL., BRONX, NY.
An improved Newton iteration for the generalized inverse of a matrix, with applications
[NASA-CR-186983] N92-11723

LILLE UNIV. (FRANCE).
Inflight calibration of channels 1 and 2 of AVHRR using desertic sites and clouds N92-11406
SPOT calibration on the test site La Crau (France) N92-11409
In flight calibration of large field of view sensors at short wavelength using the Rayleigh scattering N92-11416

LILLE-1 UNIV., VILLENEUVE-D'ASOQ (FRANCE).
Aircraft simulations of the POLDER experiment: First results N92-11471

LOCKHEED ENGINEERING AND SCIENCES CO., HAMPTON, VA.
Attitude identification for SCOLE using two infrared cameras
[NASA-CR-4397] N92-11338

LOCKHEED ENGINEERING AND SCIENCES CO., HOUSTON, TX.
Catalog of space shuttle earth observations handheld photography. Space transportation system 37 (STS-37) mission dates: April 5-11, 1991
[NASA-CR-189014] N92-11561

LOCKHEED MISSILES AND SPACE CO., PALO ALTO, CA.
Radiation belt dynamic and quasi-static modeling based on CRRES data
[AD-A240392] N92-11585

LOCUS, INC., ALEXANDRIA, VA.
The probability of multiple correct packet receptions in a multireceiver frequency-hopped spread-spectrum system
[AD-A240655] N92-11240

LOS ALAMOS NATIONAL LAB., NM.
Dumbo: A pachydermal rocket motor N92-11100
Calorimetry measurements in less than 20 minutes
[DE91-017318] N92-11330
Biological effects of minerals
[DE91-018183] N92-11615
Layer tracking, asymptotics, and domain decomposition N92-11732
The TITAN reversed-field-pinch fusion reactor study, volume 4
[DE92-000138] N92-11895
The TITAN reversed-field-pinch fusion reactor study, volume 2
[DE92-000140] N92-11896
The TITAN reversed-field-pinch fusion reactor study, volume 1
[DE92-000141] N92-11897
CYGNUS collaboration contributions to the twenty-second ICRC
[DE92-000258] N92-11961

LOUGHBOROUGH UNIV. OF TECHNOLOGY (ENGLAND).
An examination of the factors affecting the use of infra-red search and track systems in the air-to-air role
[ETN-91-99987] N92-11222

LOUISIANA STATE UNIV., BATON ROUGE.
Neutron star magnetic fields and implications for pulsars and gamma ray bursts N92-11960

LOYOLA COLL., BALTIMORE, MD.
High definition systems in Japan
[NASA-TM-105108] N92-11225

LUDWIG-MAXIMILIANS-UNIV., MUNICH (GERMANY, F.R.).
High resolution spectral measurements of vegetation and soil in field and laboratory N92-11437

M

MAINE UNIV., ORONO.
Numerical simulation of the reactive flow in advanced (HSR) combustors using KIVA-2
[NASA-CR-188996] N92-11014
Numerical prediction of turbulent flame stability in premixed/prevaporized (HSCT) combustors
[NASA-CR-188991] N92-11161

MARCONI CO. LTD., GREAT BADDOW (ENGLAND).
Modeling of radar backscattering from the sea surface using polarimetric-SAR observations N92-11442

MARTIN MARIETTA AEROSPACE, DENVER, CO.
Managing temporal relations in the MAESTRO scheduling system N92-11059
Nuclear rocket using indigenous Martian fuel NIMF N92-11098

MARTIN MARIETTA CORP., BETHESDA, MD.
Effect of locus of resource control on operational efficiency in distributed operations N92-11046

MARYLAND UNIV., COLLEGE PARK.
The probability of multiple correct packet receptions in a multireceiver frequency-hopped spread-spectrum system
[AD-A240655] N92-11240

MASSACHUSETTS INST. OF TECH., CAMBRIDGE.
Space engineering
[NASA-CR-187820] N92-11215
Advanced stress analysis methods applicable to turbine engine structures
[NASA-CR-187235] N92-11378
Experience with Acore: Implementing GHC with actors
[AD-A231409] N92-11649
The iterate manual
[AD-A231410] N92-11650
Model problem N92-11729
Nested ocean models: Work in progress N92-11735

MASSACHUSETTS INST. OF TECH., LEXINGTON.
An efficient A* stack decoder algorithm for continuous speech recognition with a stochastic language model
[AD-A240745] N92-11683

MASSACHUSETTS UNIV., AMHERST.
Direct imaging of deformation and disorder in extended-chain polymer fibers
[AD-A240651] N92-11192

MATERIALS RESEARCH LABS., MELBOURNE (AUSTRALIA).
An investigation of the material hazard of some insensitive high explosives
[MRL-TR-91-22] N92-11209
Approximate expressions for the magnetic field from an electric current source in a layered conducting medium
[MRL-TR-91-5] N92-11273

MAX-PLANCK-INST. FUER AERONOMIE, KATLENBURG-LINDAU (GERMANY, F.R.).
Activities report of the Max-Planck Institute for Aeronomy
[ETN-91-90233] N92-11964

MAX-PLANCK-INST. FUER PHYSIK UND ASTROPHYSIK, GARCHING (GERMANY, F.R.).
Limits of energy dissipation for x ray sensitive pn Charge Coupled Devices (CCDs)
[MPE-224] N92-11280
Diffusion and drift of charges in semiconductor detectors
[MBE-225] N92-11281

MAX-PLANCK-INST. FUER PLASMAPHYSIK, GARCHING (GERMANY, F.R.).
Status of the Wendelstein VII-X Project N92-11801
Optimization of Helias configurations N92-11806
Plasma transport in advanced stellarators N92-11811
Status of the WVII-AS Program N92-11820
Island studies for Helias Configurations N92-11835
Overview of engineering design of Wendelstein VII-X N92-11868

MCDONNELL-DOUGLAS ASTRONAUTICS CO., HUNTINGTON BEACH, CA.
Pellet bed reactor for nuclear propelled vehicles: Part 2: Missions and vehicle integration trades N92-11102

MCDONNELL-DOUGLAS CORP., SAINT LOUIS, MO.
New insulation constructions for aerospace wiring applications. Volume 1: Testing and evaluation
[AD-A240638] N92-11006
New insulation constructions for aerospace wiring applications. Volume 2: The 270 VDC arc tracking testing with power controllers
[AD-A240639] N92-11007

MCDONNELL-DOUGLAS SPACE SYSTEMS CO., HOUSTON, TX.
Resource representation in COMPASS N92-11060

MESSERSCHMITT-BOELKOW-BLOHM G.M.B.H., MUNICH (GERMANY, F.R.).
A systematic formulation, as an approach to air traffic
[MBB-Z-0371-91-PUB] N92-10996

MICHIGAN UNIV., ANN ARBOR.
A new technique for simulating composite material
[NASA-CR-188792] N92-11140
Advanced Langmuir Probe (LP)
[NASA-CR-180084] N92-11284
Non-invasive evaluation of the cardiac autonomic nervous system by PET
[DE91-018476] N92-11622
Fast algorithms for linear least-squares estimation of multi-dimensional random fields
[AD-A240249] N92-11675
Electron distributions and solar wind interaction with nonmagnetic planets N92-11952

MINNESOTA UNIV., MINNEAPOLIS.
Ultra high vacuum sputtering system
[AD-A240157] N92-11176

MISSOURI UNIV., ROLLA.
Mixed convection in two-dimensional laminar air flow with reverse flow regions N92-11293

MISSOURI UNIV., SAINT LOUIS.
Quantum 1/f noise in high technology applications including ultrasmall structures and devices
[AD-A240152] N92-11907

MITRE CORP., BEDFORD, MA.
Technology assessment of the Software Life Cycle Support Environment (SLCSE)
[AD-A240673] N92-11682

MITRE CORP., MCLEAN, VA.
Range Scheduling Aid (RSA) N92-11057

MITSUBISHI ELECTRIC CO., KOBE (JAPAN).
A compact helical device for a superconducting large helical coil N92-11842

MITSUBISHI FUSION CENTER, TOKYO (JAPAN).
Fundamental design on LHD with bath cooling method N92-11841

MOHAMMED V UNIV., RABAT (MOROCCO).
The considering of the slowing down effect in the formalism of probability tables. Application to the effective cross section calculation
[DE91-626722] N92-11751

MONTREAL UNIV. (QUEBEC).
Study of the spatial signature of forest covers by geometric-optic modeling N92-11530

MOTORBOOKS INTERNATIONAL PUBLISHERS AND WHOLESALERS, OSCEOLA, WI.
Space year 1991: The complete record of the year's space events
[ISBN-0-87938-482-4] N92-11031

MOUNT HOLYOKE COLL., SOUTH HADLEY, MA.
Nuclear transparency and double beta decay of molybdenum 100
[DE91-016963] N92-11172

MPB TECHNOLOGIES, INC., DORVAL (QUEBEC).
Laser-induced spectral signatures in investigations of sea upper layer N92-11537

MURCIA UNIV. (SPAIN).
The 4th International Workshop on Membrane Biotechnology and Membrane Diomaterials
[AD-A240481] N92-11614

MUSEE ROYAL DE L'AFRIQUE CENTRALE, TERVUREN (BELGIUM).
Suppression of aerosols on LANDSAT thematic mapper imagery N92-11411

N

NATIONAL ACADEMY OF SCIENCES - NATIONAL RESEARCH COUNCIL, WASHINGTON, DC.
Real-time earthquake monitoring: Early warning and rapid response
[NASA-CR-186701] N92-11582

NATIONAL AERONAUTICS AND SPACE ADMINISTRATION, WASHINGTON, DC.
Aeronautical engineering: A continuing bibliography with indexes (supplement 270)
[NASA-SP-7037(270)] N92-10973

Aeronautical engineering: A continuing bibliography with indexes (supplement 269)
[NASA-SP-7037(269)] N92-10974
Concepts, requirements, and design approaches for building successful planning and scheduling systems N92-11042
The great observatories for space astrophysics
[NASA-NP-128] N92-11066
Upper Atmosphere Research Satellite (UARS): A program to study global ozone change
[NASA-TM-105100] N92-11067
Nuclear thermal propulsion program overview N92-11089
Enabling the space exploration initiative: NASA's exploration technology program in space power
[NASA-TM-4325] N92-11131
A three dimensional radiative transfer method for optical remote sensing of vegetated land surfaces N92-11466
Optimum combinations of visible and near-infrared reflectances for estimating the fraction of photosynthetically available radiation absorbed by plants N92-11474
Use of multitemporal SPOT data in first ISLSCP field experiment N92-11554
Space observations for global change N92-11555
Scientific assessment of stratospheric ozone: 1989, volume 1
[NASA-TM-105116] N92-11576
Scientific assessment of stratospheric ozone: 1989. Volume 2: Appendix: AFEAS report
[NASA-TM-105117] N92-11577
GLOBEC: Global Ocean Ecosystems Dynamics: A component of the US Global Change Research Program
[NASA-TM-105121] N92-11603
Fusion energy for space missions in the 21st Century
[NASA-TM-4298] N92-11783
A bibliography of planetary geology and geophysics principal investigators and their associates, 1990-1991
[NASA-TM-4299] N92-11929

NATIONAL AERONAUTICS AND SPACE ADMINISTRATION. AMES RESEARCH CENTER, MOFFETT FIELD, CA.

NACA 0015 wing pressure and trailing vortex measurements
[NASA-TP-3151] N92-10981
Experimental study of an independently deflected wingtip mounted on a semispan wing
[NASA-TM-102842] N92-10983
Analysis of open loop higher harmonic control at high airspeeds on a modern four-bladed articulated rotor
[NASA-TM-103876] N92-11000
Cooling apparatus and couplings therefor
[NASA-CASE-ARC-11921-1] N92-11286
The three-dimensional evolution of a plane mixing layer. Part 1: The Kelvin-Helmholtz roll-up
[NASA-TM-103856] N92-11303
Perceptual style and air-to-air tracking performance
[NASA-TM-102868] N92-11629
Human Machine Interfaces for Teleoperators and Virtual Environments Conference
[NASA-CP-10071] N92-11638
Computer integrated documentation
[NASA-TM-103870] N92-11673
Tables of square-law signal detection statistics for Hann spectra with 50 percent overlap
[NASA-TM-103830] N92-11745

NATIONAL AERONAUTICS AND SPACE ADMINISTRATION. GODDARD SPACE FLIGHT CENTER, GREENBELT, MD.

Space Network Control Conference on Resource Allocation Concepts and Approaches
[NASA-CP-3124] N92-11039
Space Network Control (SNC) Conference on Resource Allocation Concepts and Approaches. Overview N92-11040
Proposed planning and scheduling services for the SNC in the CDOS era N92-11043
An RF interference mitigation methodology with potential applications in scheduling N92-11044
A method for interference mitigation in space communications scheduling N92-11062
A planning language for activity scheduling N92-11063
Mechanical properties of a porous mullite material
[NASA-TM-104547] N92-11187
Passive microwave remote sensing of soil moisture: Results from HAPEX, FIFE, and MONSOON 90 N92-11458
Synergistic use of multispectral satellite data for monitoring land surface change N92-11489
Urban heat island N92-11500
Wavelength shifts in fluorescence maxima of stressed and non-stressed Norway spruce needles over the growing season N92-11536
Analysis of altimetry over the Aral Sea
[NASA-TM-100759] N92-11583
LAGEOS geodetic analysis-SL7.1
[NASA-TM-104549] N92-11584
Optically thin cirrus clouds over oceans and possible impact on sea surface temperature of warm pool in western Pacific
[NASA-TM-104550] N92-11600
NSSDC data listing
[NASA-TM-105010] N92-11921

NATIONAL AERONAUTICS AND SPACE ADMINISTRATION. HUGH L. DRYDEN FLIGHT RESEARCH FACILITY, EDWARDS, CA.

Aerothermal test results from the first flight of the Pegasus air-launched space booster
[NASA-TM-4330] N92-11301

NATIONAL AERONAUTICS AND SPACE ADMINISTRATION. JOHN F. KENNEDY SPACE CENTER, COCOA BEACH, FL.

Debris/ice/TPS assessment and photographic analysis for Shuttle Mission STS-43
[NASA-TM-103823] N92-11038

NATIONAL AERONAUTICS AND SPACE ADMINISTRATION. LYNDON B. JOHNSON SPACE CENTER, HOUSTON, TX.

Quick application/release nut with engagement indicator
[NASA-CASE-MSC-21799-1] N92-11359
Observations of the Earth in polarized light from the US Space Shuttle N92-11485
Field trip guidebook on environmental impact of clays along the upper Texas coast
[NASA-TM-105097] N92-11572
Extra-corporeal blood access, sensing, and radiation methods and apparatuses
[NASA-CASE-MSC-21775-1] N92-11627
Intranasal scopolamine preparation and method
[NASA-CASE-MSC-21858-1] N92-11628
Lunar radiator shade
[NASA-CASE-MSC-21868-1] N92-11639
Making intelligent systems team players: Case studies and design issues. Volume 2: Fault management system cases
[NASA-TM-104738] N92-11641
The microgravity environment of the Space Shuttle Columbia middeck during STS-32
[NASA-TP-3140] N92-11930
The microgravity environment of the Space Shuttle Columbia payload bay during STS-32
[NASA-TP-3141] N92-11931

NATIONAL AERONAUTICS AND SPACE ADMINISTRATION. LANGLEY RESEARCH CENTER, HAMPTON, VA.

Static internal performance of ventral and rear nozzle concepts for short-takeoff and vertical-landing aircraft
[NASA-TP-3103] N92-10975
A comparison of airborne wake vortex detection measurements with values predicted from potential theory
[NASA-TP-3125] N92-10994
Maximized gust loads for a nonlinear airplane using matched filter theory and constrained optimization
[NASA-TM-104138] N92-11010
Model representation in the PANCOR wall interference assessment code
[NASA-TM-104152] N92-11022
Magnetic suspension and balance systems: A comprehensive, annotated bibliography
[NASA-TM-4318] N92-11030
User modeling techniques for enhanced usability of OPSMODEL operations simulation software
[NASA-TM-4306] N92-11035
Active vibration damping of the Space Shuttle remote manipulator system
[NASA-TM-104149] N92-11073
Multidisciplinary optimization of controlled space structures with global sensitivity equations
[NASA-TP-3130] N92-11087
A detailed investigation of staged normal injection into a Mach 2 flow N92-11118
Effects of elevated temperature on the viscoplastic modeling of graphite/polymeric composites
[NASA-TM-104160] N92-11149
Polyimides with improved compression moldability
[NASA-CASE-LAR-14457-1-CU] N92-11198
Low toxicity high temperature PMR polyimides
[NASA-CASE-LAR-14639-1] N92-11199
Diphenylmethane-containing dianhydride and polyimides prepared therefrom
[NASA-CASE-LAR-14487-1] N92-11200
A process for preparing an assembly of an article and a polyimide which resists dimensional change, delamination, and debonding when exposed to changes in temperature
[NASA-CASE-LAR-14538-1] N92-11201
Improved compression molding technology for continuous fiber reinforced composite laminates. Part 2: AS-4/Polyimidesulfone prepreg system
[NASA-TM-104133] N92-11207
Integral fill yarn insertion and beatup method
[NASA-CASE-LAR-14046-1] N92-11219
Woven angle ply fabric and apparatus and method for producing such fabrics
[NASA-CASE-LAR-14048-1] N92-11220
Calculations and curve fits of thermodynamic and transport properties for equilibrium air to 30000 K
[NASA-RP-1260] N92-11285
Computer codes for the evaluation of thermodynamic and transport properties for equilibrium air to 30000 K
[NASA-TM-104107] N92-11300
Schlieren system for visualizing the flow within a pipe of circular cross-section
[NASA-CASE-LAR-13944-1] N92-11336
Technique for calibrating angular measurement devices when calibration standards are unavailable
[NASA-TM-104148] N92-11340
Blind fastening apparatus
[NASA-CASE-LAR-14542-1] N92-11354
Conductive gage for crack length measurement
[NASA-CASE-LAR-14480-1-CU] N92-11374
Method of recertifying a loaded bearing member using a phase point
[NASA-CASE-LAR-14741-1] N92-11384
Sensitivity of Space Station alpha joint robust controller to structural modal parameter variations
[NASA-TM-104153] N92-11392
Rapidly quantifying the relative distention of a human bladder
[NASA-CASE-LAR-13901-2] N92-11621
User's manual for the Macintosh version of PASCO
[NASA-TM-104115] N92-11668
Cellular repair/misrepair track model
[NASA-TP-3124] N92-11685
A Fourier collocation time domain method for numerically solving Maxwell's equations
[NASA-TM-104162] N92-11742
Annoyance caused by advanced turboprop aircraft flyover noise: Comparison of different propeller configurations
[NASA-TP-3104] N92-11758
A new simulator for assessing subjective effects of sonic booms
[NASA-TM-104150] N92-11759
A loudness calculation procedure applied to shaped sonic booms
[NASA-TP-3134] N92-11765

NATIONAL AERONAUTICS AND SPACE ADMINISTRATION. LEWIS RESEARCH CENTER, CLEVELAND, OH.

Results from computational analysis of a mixed compression supersonic inlet
[NASA-TM-104475] N92-10976
Real-time fault diagnosis for propulsion systems
[NASA-TM-105303] N92-11017
Overview of the Beta II Two-Stage-To-Orbit vehicle design
[NASA-TM-105298] N92-11034
Development of a ninety string solar array simulator
[NASA-TM-105278] N92-11086
Nuclear Thermal Propulsion: A Joint NASA/DOE/DOD Workshop
[NASA-CP-10079] N92-11088
Nuclear thermal propulsion workshop overview N92-11090
Nuclear thermal rocket workshop reference system Rover/NERVA N92-11091
Safety issues N92-11115
Developments in REDES: The Rocket Engine Design Expert System N92-11120
JANNAF Liquid Rocket Combustion Instability Panel research recommendations N92-11124
Analytical study of nozzle performance for nuclear thermal rockets
[NASA-TM-105251] N92-11126
Linear quadratic servo control of a reusable rocket engine
[NASA-TM-105291] N92-11128
Improved thermodynamic modeling of the no-vent fill process and correlation with experimental data
[NASA-TM-104492] N92-11129
Technology readiness assessment of advanced space engine integrated controls and health monitoring
[NASA-TM-105255] N92-11130
Effect of particle size of Martian dust on the degradation of photovoltaic cell performance
[NASA-TM-105232] N92-11133
Plans for the development of cryogenic engines for space exploration
[NASA-TM-105250] N92-11135
Test facilities for high power electric propulsion
[NASA-TM-105247] N92-11136

An overview of tested and analyzed NTP concepts
[NASA-TM-105252] N92-11137
Effects of anisotropic conduction and heat pipe interaction on minimum mass space radiators
[NASA-TM-105297] N92-11138
Solid lubricants on pretreated surfaces
[NASA-CASE-LEW-14474-2] N92-11186
High-T sub c fluorine-doped YBa2Cu3O(y) films on ceramic substrates by screen printing
[NASA-TM-105296] N92-11188
Glass formation, properties, and structure of soda-yttria-silicate glasses
[NASA-TM-104488] N92-11202
Description of Liquid Nitrogen Experimental Test Facility
[NASA-TM-105215] N92-11208
Benefits of slush hydrogen for space missions
[NASA-TM-104503] N92-11214
Microgravity vibration isolation: An optimal control law for the one-dimensional case
[NASA-TM-105146] N92-11217
Thermal verification testing of commercial printed-circuit boards for spaceflight
[NASA-TM-105261] N92-11221
The 23 to 300 C demagnetization resistance of samarium-cobalt permanent magnets
[NASA-TP-3119] N92-11252
Modeling of the heat transfer in bypass transitional boundary-layer flows
[NASA-TP-3170] N92-11299
On the basic equations for the second-order modeling of compressible turbulence
[NASA-TM-105277] N92-11302
Turbulent fluid motion 3: Basic continuum equations
[NASA-TM-104386] N92-11317
An efficient and robust algorithm for two dimensional time dependent incompressible Navier-Stokes equations: High Reynolds number flows
[NASA-TM-104424] N92-11320
Euler solutions for an unbladed jet engine configuration
[NASA-TM-105332] N92-11328
First-passage problems: A probabilistic dynamic analysis for degraded structures
[NASA-TM-103755] N92-11373
Computers in aeronautics and space research at the Lewis Research Center
[NASA-TM-105096] N92-11642
Computer program for Bessel and Hankel functions
[NASA-TM-105154] N92-11691

NATIONAL AERONAUTICS AND SPACE ADMINISTRATION. MARSHALL SPACE FLIGHT CENTER, HUNTSVILLE, AL.

CFD code survey for thrust chamber application
N92-11119
An examination of the damage tolerance enhancement of carbon/epoxy using an outer lamina of spectra (R)
[NASA-TP-3160] N92-11142
A generalized method for multiple robotic manipulator programming applied to vertical-up welding
[NASA-TP-3163] N92-11218

NATIONAL AERONAUTICS AND SPACE ADMINISTRATION. PASADENA OFFICE, CA.

Dual frequency optical carrier technique for transmission of reference frequencies in dispersive media
[NASA-CASE-NPO-18007-1-CU] N92-11791

NATIONAL AEROSPACE LAB., TOKYO (JAPAN).

Unsteady aerodynamic calculations for general configurations by the double-point method
[NAL-TR-1101T] N92-10980
Calibration of turbine flowmeters for storable bipropellant engines
[NAL-TR-1091] N92-11127
Theoretical estimation of the viscous damping from liquid transient motion in tanks
[NAL-TR-1095] N92-11298

NATIONAL COUNCIL ON RADIATION PROTECTION AND MEASUREMENTS, BETHESDA, MD.

Development of recommendations in the area of ionizing radiations
[DE91-018527] N92-11623

NATIONAL INST. FOR FUSION SCIENCE, NAGOYA (JAPAN).

On radial electric field structure in CHS torsatron/heliotron
[NIFS-94] N92-11796
Influence of fast ion loss on radial electric field in Wendelstein 7-A stellarator
[NIFS-95] N92-11797
Symposium on Development and Applications of Intense Pulsed Particle Beams
[NIFS-PROC-8] N92-11798
Proceedings of the First International Toki Conference on Plasma Physics and Controlled Nuclear Fusion: Next Generation Experiments in Helical Systems
[NIFS-PROC-3] N92-11799
Present status of the Large Helical Device Project
N92-11800
The 3-D equilibria of helical systems: Magnetic islands and their control N92-11808
Confinement improvement by edge control
N92-11817
Effects of perturbing helical fields on confinement of Heliotron DR plasma N92-11818
Review of CHS experiment N92-11823
Destruction of magnetic surfaces in helical torus
N92-11832
Ripple diffusion and bootstrap current in LHD
N92-11833
Numerical analysis of temporal development of RF-heated plasma N92-11834
Optimization of design parameters for large helical device N92-11843
Effect of multi-layer operation of helical coil in large helical device N92-11844
ECH system in the large helical device N92-11845
ICRF heating program of the large helical device
N92-11846
Transport study of ECH and NBI plasmas in CHS
N92-11857
Effect of magnetic axis shift on CHS plasma characteristics N92-11858
A study of radiation collapse in CHS plasmas
N92-11859
Ion temperature and poloidal rotation profiles for NBI heated plasma in CHS N92-11860
Driven currents in neutral beam heated plasma
N92-11861
Power deposition during ECH in CHS N92-11862
Engineering design of large helical device
N92-11864
Operation scenario and structural design analysis of LHD (Large Helical Device) coils N92-11865
Engineering design of LHD vacuum vessel
N92-11866
Development of superconductor for large helical device N92-11867
NBI system with negative ion source in large helical device N92-11870
Experiments and applications of soliton physics
[NIFS-32] N92-11877
Effects of electric field on particle drift orbits in a l = 2 torsatron
[NIFS-31] N92-11878
Fokker-Planck equation in the presence of anomalous diffusion
[NIFS-29] N92-11879
Calculation of magnetic field of helical coils
[NIFS-18] N92-11880
ELMy-H mode as limit cycle and chaotic oscillations in tokamak plasmas
[NIFS-87] N92-11882
Nonlinear behavior of multiple-helicity resistive interchange modes near marginally stable states
[NIFS-89] N92-11883
Fluid description of ponderomotive force compatible with the kinetic one in a warm plasma
[NIFS-100] N92-11884
Rotations of bulk ions and impurities in non-axisymmetric toroidal systems
[NIFS-102] N92-11885

NATIONAL INST. OF STANDARDS AND TECHNOLOGY, GAITHERSBURG, MD.

Conformity Assessment Workshop on Electromagnetic Compatibility
[PB91-192989] N92-11226
Semiconductor measurement technology: NIST list of publications, 1962-1989 (revised March 1990)
[PB91-193961] N92-11269
Generation of smooth trajectories without planning
[NASA-CR-189013] N92-11712
Portable vectorized software for Bessel function evaluation
[PB91-216598] N92-11727

NATIONAL OCEANIC AND ATMOSPHERIC ADMINISTRATION, WASHINGTON, DC.

Scientific assessment of stratospheric ozone: 1989, volume 1
[NASA-TM-105116] N92-11576
Scientific assessment of stratospheric ozone: 1989. Volume 2: Appendix: AFEAS report
[NASA-TM-105117] N92-11577

NATIONAL OCEANOGRAPHIC DATA CENTER, WASHINGTON, DC.

Mariners Weather Log, Volume 35, Number 1, Winter 1991
[PB91-201129] N92-11591
Mariners Weather Log, Volume 35, Number 2, Spring 1991
[PB91-202572] N92-11592

NATIONAL PARK SERVICE, WASHINGTON, DC.

Study of alternatives: Dayton's Aviation heritage, Ohio
[PB91-202275] N92-10972

NATIONAL PHYSICAL LAB., TEDDINGTON (ENGLAND).

Contact angle and work of adhesion between Ni-based melts and non-metallic solids
[NPL-DMM(A)-23] N92-11171
Investigation of the stability of the spectral responsitivity of silicon photodiodes
[NPL-QU-87] N92-11184
Physical ageing and creep in PVC
[NPL-DMM(A)-21] N92-11185
Feasibility study on the Cold Hydrogen Maser (CHM)
[NPL-QU-89] N92-11342
Approximate large deflection analysis of circular plates loaded symmetrically
[NPL-DMM(A)-25] N92-11370
Intercomparison of the medium energy primary standards for x ray exposure of NPL and ENEA, Italy
[NPL-RSA(EXT)-18] N92-11766
Intercomparison of the low energy primary standards for x ray exposure of NPL and ENEA, Italy
[NPL-RSA(EXT)-19] N92-11767

NAVAL AIR DEVELOPMENT CENTER, WARMINSTER, PA.

Oxidation of titanium aluminide and its XD composite
[AD-A240401] N92-11177

NAVAL OBSERVATORY, WASHINGTON, DC.

Proceedings of the 127th Colloquium of the International Astronomical Union Reference Systems
[AD-A240207] N92-11933

NAVAL OCEAN SYSTEMS CENTER, SAN DIEGO, CA.

Shipboard antenna concepts: Structurally independent 2- to 6-MHz transmit antenna design
[AD-A240544] N92-11236
Conditional event algebras: Two new characterizations and their relations to Bayesian analysis
[AD-A240378] N92-11738
A re-examination of the relationship between fuzzy set theory and probability theory
[AD-A240243] N92-11746
Assignment of single values to probability intervals, evaluation of conditional events, and applications to combination of evidence
[AD-A240258] N92-11747
Database management system interface standard for Navy next generation computing resources
[AD-A240432] N92-11925

NAVAL OCEANOGRAPHIC AND ATMOSPHERIC RESEARCH LAB., BAY SAINT LOUIS, MS.

One-way nesting for a primitive equation ocean model
N92-11734

NAVAL POSTGRADUATE SCHOOL, MONTEREY, CA.

Developmental flight testing of a half scale unmanned air vehicle
[AD-A240347] N92-11002
Development of a 1/7th scale fighter UAV for flight research
[AD-A240703] N92-11008
Initial design study of existing flight control system of RPH and feasibility study of implementing HHC on the SH-60B
[AD-A240522] N92-11019
Parameter identification studies on the NASA/Ames Research Center Advanced Concepts Flight Simulator
[NASA-TM-105126] N92-11024
Calibration of the Naval Postgraduate School 3.5' x 5.0' academic wind tunnel
[AD-A240614] N92-11025
The Space Shuttle: An attempt at low-cost, routine access to space
[AD-A240589] N92-11037
Attitude control of flexible structures
[AD-A240520] N92-11082
Specification of difficult to test radar performance
[AD-A240398] N92-11232
The design of broadband radar absorbing surfaces
[AD-A240521] N92-11235
Discrete ARMA model for natural resonances in electromagnetic and acoustic scattering
[AD-A240656] N92-11241
VHDL simulation of the implementation of a costfunction circuit
[AD-A240430] N92-11278
Heat transfer, adiabatic effectiveness, and injectant distributions downstream of single and double rows of film-cooling holes with simple and compound angles
[AD-A240743] N92-11305
A calibration of the Naval Postgraduate School middle ultraviolet spectrograph and an analysis of the OII 2470 A and OI 2972 A emissions obtained from mid-latitude rocket observations
[AD-A240686] N92-11587

A diagnostic study of the velocity structure of a meandering jet using a primitive equation model with dynamic mode initialization
[AD-A240687] N92-11609

NAVAL RESEARCH LAB., WASHINGTON, DC.

High pressure turbine blade life extension
[AD-A240654] N92-11180

Discharge system tests of Halon 1301 test gas simulants
[AD-A240679] N92-11193

Pulse compression degradation due to open loop adaptive cancellation, part 1
[AD-A240552] N92-11238

Pulse compression degradation due to open loop adaptive cancellation, part 3
[AD-A240553] N92-11239

The probability of multiple correct packet receptions in a multireceiver frequency-hopped spread-spectrum system
[AD-A240655] N92-11240

Numerical simulations of detonation transmission
[AD-A240560] N92-11304

Linear theory of a quasioptical gyroklystron with nonuniform magnetic field
[AD-A240264] N92-11334

Tilted resonator experiments on a quasioptical gyrotron
[AD-A240680] N92-11335

A survey of scattering, attenuation, and size spectra studies of bubble layers and plumes beneath the air-sea interface
[AD-A240262] N92-11606

NAVAL SUBMARINE MEDICAL RESEARCH LAB., GROTON, CT.

The effect of blinking on subsequent dark adaptation
[AD-A240281] N92-11625

NAVAL WAR COLL., NEWPORT, RI.

The role of stealth in naval aviation and joint/combined operations
[AD-A240595] N92-11005

Insurance against catastrophe: SDI and the 3rd World nuclear proliferation problem
[AD-A240429] N92-11752

NETROLOGIC, INC., SAN DIEGO, CA.

Robotic non-destructive inspection of aircraft, phase 1
[AD-A240777] N92-11367

Fractal image compression
[AD-A240636] N92-11680

NEW MEXICO STATE UNIV., LAS CRUCES.

Engineering and instrumentation support of GL Research Balloon Program
[AD-A240616] N92-10987

NEW MEXICO UNIV., ALBUQUERQUE.

Pellet bed reactor for nuclear propelled vehicles: Part 1: Reactor technology N92-11101

NEW YORK UNIV., NEW YORK.

Perception and memory of pictures
[AD-A240364] N92-11633

Plasma properties
[DE91-018913] N92-11891

NIHON UNIV., TOKYO (JAPAN).

Equilibrium, stability, and transport in L = 1 compact helical axis configuration N92-11848

NORTH CAROLINA STATE UNIV., RALEIGH.

A Newton's method solver for the two-dimensional and axisymmetric Navier-Stokes equations N92-11292

Interface conditions for domain decomposition with radical grid refinement N92-11733

NOTRE DAME UNIV., IN.

Error control techniques for satellite and space communications
[NASA-CR-188997] N92-11228

NOTTINGHAM UNIV. (ENGLAND).

Candidate high spectral resolution derivative indices for the prediction of crop cover N92-11435

The effect of the distribution of chlorotic material on the reflectance of mixed canopies N92-11472

NSI TECHNOLOGY SERVICES CORP., DAYTON, OH.

Physicochemical properties and dissolution in simulated biological fluids of particles of beryllium-powered rocket motor exhaust and pure beryllium oxides calcined at low and high temperature
[AD-A240288] N92-11134

O

OAK RIDGE NATIONAL LAB., TN.

Nuclear fuels status N92-11113

Mixing effects in aqueous solutions at elevated temperatures
[DE91-017695] N92-11168

Creep response of a 9Cr-1Mo-V-Nb steel to varying stresses and temperatures
[DE91-017871] N92-11181

Moisture-induced environmental embrittlement of ordered intermetallic alloys at ambient temperatures
[DE91-018852] N92-11183

The effects of specimen geometry and size on the fracture toughness of nuclear graphites
[DE92-000056] N92-11205

Heat exchanger thermal performance for two nonazeotropic refrigerant mixtures
[DE91-017250] N92-11216

Results of folded waveguide tests on RFTF
[DE91-018930] N92-11249

Three-dimensional calculations of fields and loading for loop and folded waveguide ICRF antennas
[DE92-000065] N92-11250

Propagation behavior of small cracks in 304 stainless steel under biaxial low-cycle fatigue at elevated temperature
[DE91-018863] N92-11389

Gorter-Mellink pulsed-source problem in cylindrical and spherical geometry
[DE91-017249] N92-11725

New dimensions in atom probe analysis
[DE91-018926] N92-11779

Overview of the ATF-II studies N92-11802

Resistive MHD stability studies for ATF plasmas during operation in the second stability regime N92-11809

Overview of recent results from the Advanced Toroidal Facility N92-11819

Dissipative trapped electron modes in l = 2 torsatrons N92-11830

ECH experiments on ATF
[DE91-018845] N92-11889

Full-wave calculation of fast-wave current drive in tokamaks including k(parallel) variations
[DE92-000076] N92-11894

High l state population in O(7+) produced in ion-solid collisions
[DE91-018169] N92-11904

Progress in Photon Scanning-Tunneling Microscopy (PSTM)
[DE91-018174] N92-11905

Neutron diffraction from the flux line lattice
[DE91-018175] N92-11906

OBSERVATOIRE DE MIDI-PYRESNEES, TOULOUSE (FRANCE).

Near-infrared imaging spectroscopy: Learning from planetary geology N92-11438

OFFICE DE LA RECHERCHE SCIENTIFIQUE ET TECHNIQUE OUTRE-MER, MONTPELLIER (FRANCE).

Airborne SAR HAREM campaign: Results, targets features, ERS1 simulations, and operational satellite exploitation N92-11455

OFFICE DE LA RECHERCHE SCIENTIFIQUE ET TECHNIQUE OUTRE-MER, PARIS (FRANCE).

Influence of the viewing geometry on the spectral properties (high resolution visible and NIR) of selected soils from Arizona N92-11473

OFFICE NATIONAL D'ETUDES ET DE RECHERCHES AEROSPATIALES, PARIS (FRANCE).

Three dimensional numerical method for resolving small transonic perturbations in unstructured mesh
[ONERA-RT-56/3064-RY-006-R] N92-10989

Wing tip turbine: Analysis of the results of S2MA sounding of marginal vortex of the A320, technical summary
[ONERA-RTS-21/4365-AY-056A] N92-11009

Numerical simulation of the degradation of the folds of a laminated composite structure. Study of the importance of residual firing constraints
[ONERA-RT-8/7256-RY-094-R] N92-11145

Delamination propagation in a composite panel under compressive stress
[ONERA-RT-23/3542-RY-093-R] N92-11146

Hydrodynamic tunnel study of the marginal vortex breakdown in the pressure field of a wing profile
[ONERA-RSF-44/1147-AY-144A] N92-11308

Resolution of Navier-Stokes equations around profiles: Drag evolution
[ONERA-RTS-86/1685-AY-156A] N92-11310

Perfect compressible two dimensional boundary layer strong fluid coupling in the case of sharp leading edge profiles. Unsteady case of isolated profiles and steady case of blade grids
[ONERA-RT-43/1621-RY-006-R] N92-11311

Hydrodynamic flow visualization around an oscillating vane. Extension of study to the case of higher incidences and amplitudes and the starting off phase from permanent regime
[ONERA-RT-56/1369-AN] N92-11312

Acoustic propagation at low altitude: Effects of atmospheric turbulence (Villeau (France) test)
[ONERA-RT-15/3641-PY] N92-11588

Optimal control by wideband frequency. Application to acoustic control by piezoelectric technique
[ONERA-RT-6/3654-RY-006-R] N92-11713

Simulation of a nonlinear two degrees of freedom system. Study of the temporal response to a harmonic attraction
[ONERA-RT-17/1677-RY-091-R] N92-11755

Eighty years of aerospace technique through ATMA bulletins
[ETN-91-90097] N92-11963

OFFICE NATIONAL D'ETUDES ET DE RECHERCHES AEROSPATIALES, TOULOUSE (FRANCE).

Atmospheric correction in the thermal infrared: AVHRR case N92-11398

Modeling the behavior of a vegetation cover in the MIR, contribution of high spectral resolution N92-11434

Bidirectional reflectance and surface albedo: Physical modeling and inversion N92-11469

Normalization of bidirectional effects of surface reflectance on a series of multitemporal NOAA/AVHRRR data N92-11480

Combined use of Earth observation satellite and meteorological satellite for crop assessment in semiarid environments N92-11494

Integration of qualitative knowledge on operational models for following vegetation using temporal series of remote sensing images N92-11502

Modeling temporal evolution of the radiometric response measured by wideband sensors over temperate agricultural regions N92-11518

NOAA-AVHRR NDVI temporal profile classification and sensitivity to land use and climatic conditions in temperate region N92-11525

OFFICE OF NAVAL RESEARCH, ARLINGTON, VA.

A compact laser photocathode driven accelerator for the Plasma Wake Field Accelerator Program at UCLA
[AD-A240646] N92-11886

OHIO STATE UNIV., COLUMBUS.

Prediction of the pattern performance for the Aeroassist Flight Experiment (AFE) spacecraft
[NASA-CR-4409] N92-11065

Estimation of geopotential differences over intercontinental locations using satellite and terrestrial measurements
[NASA-CR-188992] N92-11560

OLD DOMINION UNIV., NORFOLK, VA.

Viscous computations of cold air/air flow around scramjet nozzle afterbody
[NASA-CR-4406] N92-10982

Further developments relating to the NASA Langley Research Center 13-inch magnetic suspension and balance system
[NASA-CR-188995] N92-11023

OPEN UNIV., MILTON (ENGLAND).

Monitoring volcanoes using short wavelength infrared images N92-11498

OREGON STATE UNIV., CORVALLIS.

High efficiency motor rewind study
[DE91-017162] N92-11270

Matter-wave interferometry with laser cooled atoms
[AD-A240531] N92-11776

P

PACIFIC NORTHWEST LAB., RICHLAND, WA.

Nuclear thermal/nuclear electric hybrids N92-11107

An assessment of the available windy land area and wind energy potential in the contiguous United States
[DE91-018887] N92-11601

Education in computational science: Role of the National Laboratories
[DE91-018823] N92-11687

PARIS VI UNIV. (FRANCE).

Moisture effects on spectral signatures and CIE-color of lateritic soils N92-11436

Radar image simulation to study the visual aptitude of observing slope and roughness effects N92-11446

Contribution of active microwaves to the structural analysis of epicontinental shelf-forms: Example of the English Channel N92-11448

Synergy of high resolution spatial microwave imagery and geomorphological optics N92-11496

PARIS XI UNIV., ORSAY (FRANCE).

Control of the physiological state of vegetation cover by remote sensing of fluorescent emission in the blue and red visible spectrum regions N92-11532

PENNSYLVANIA STATE UNIV., HERSHEY.

Serial averaging in the construction and validation of performance tests
[AD-A240313] N92-11632

PENNSYLVANIA STATE UNIV., UNIVERSITY PARK.

Prediction of forces and moments for hypersonic flight vehicle control effectors
[NASA-CR-188954] N92-11070

Explicit determination of the vapor fraction in flash calculations
[AD-A240376] N92-11165

PENNSYLVANIA UNIV., PHILADELPHIA.
Synthesis of novel polysiloxanes bearing polar groups
[AD-A240722] N92-11194
Synthesis and reactivity of silyl-ketene acetal-modified polysiloxanes preparation of polysiloxanes with high dielectric constraints
[AD-A240754] N92-11196
PHILIPS GLOEILAMPENFABRIEKEN N.V., EINDHOVEN (NETHERLANDS).
Spectroscopic studies of layered and bulk semiconductor materials
[ETN-91-90145] N92-11914
PHILLIPS LAB., EDWARDS AFB, CA.
Shielding requirements for particle bed propulsion systems
[AD-A240780] N92-11787
PHOTOMETRICS, INC., WOBURN, MA.
Design and operation of the GL/OPA mobile Doppler lidar
[AD-A240257] N92-11231
PHYSICS AND ELECTRONICS LAB. TNO, THE HAGUE (NETHERLANDS).
Dual-polarized scatterometer measurements of wind and mechanically generated waves in a very large wind/wave flume, the VIERS-1 project N92-11443
PITTSBURGH UNIV., PA.
Transient finite element computations on a variable transputer system
[NASA-CR-189060] N92-11671
POLISH ACADEMY OF SCIENCES, WARSAW.
From evapotranspiration to soil moisture investigation based on NOAA thermal infrared data, case study: Poland N92-11531
PRATT AND WHITNEY AIRCRAFT, WEST PALM BEACH, FL.
JANNAF Combustion Instability Panel Workshop report: Numerical methods in combustion instability N92-11123
Properties of aircraft fuels and related materials
[AD-A240650] N92-11213
PRINCETON UNIV., NJ.
A systematic approach to combustion model reduction and lumping
[AD-A240195] N92-11164
Comparison of passive microwave and model derived estimates for soil moisture fields N92-11459
Detached plasma and density limit of Tokamaks N92-11816
Kinematics and dynamics of barred galaxies N92-11937
PURDUE UNIV., WEST LAFAYETTE, IN.
Annual research summary, July 1, 1990 - June 30, 1991
[DE91-017408] N92-11962

R

RADIATION MONITORING DEVICES, INC., WATERTOWN, MA.
Solid state neutron dosimeter for space applications
[NASA-CR-185633] N92-11331
RANGE COMMANDERS COUNCIL, WHITE SANDS MISSILE RANGE, NM.
World Geodetic System 1984 (WGS-84) consolidated database for test ranges
[AD-A240621] N92-11026
A brief introduction to the universal documentation system. Universal documentation system handbook
[AD-A240622] N92-11027
RENSSELAER POLYTECHNIC INST., TROY, NY.
New polymer electrolyte hosts and their tetrabutylammonium chloride complexes. Relationships among concentration of polar groups, ESR spin probe response, and ionic conductivity
[AD-A240497] N92-11190
Study of silanization of silica and fiberglass using ESR spectroscopy and spin labelling
[AD-A240767] N92-11197
An improved Newton iteration for the generalized inverse of a matrix, with applications
[NASA-CR-186983] N92-11723
The TITAN reversed-field-pinch fusion reactor study, volume 4
[DE92-000138] N92-11895
The TITAN reversed-field-pinch fusion reactor study, volume 2
[DE92-000140] N92-11896
The TITAN reversed-field-pinch fusion reactor study, volume 1
[DE92-000141] N92-11897
RESEARCH INST. FOR ADVANCED COMPUTER SCIENCE, MOFFETT FIELD, CA.
A fast sorting algorithm for a hypersonic rarefied flow particle simulation on the connection machine
[NASA-CR-188903] N92-10977
Telescience workstation
[NASA-CR-188878] N92-11033
Television image compression and small animal remote monitoring
[NASA-CR-186614] N92-11223
Efficient detection of a CW signal with a linear frequency drift
[NASA-CR-188900] N92-11224
Application of Krylov exponential propagation to fluid dynamics equations
[NASA-CR-188887] N92-11290
Weather prediction using a genetic memory
[NASA-CR-185448] N92-11590
Sparse distributed memory
[NASA-CR-188841] N92-11643
A class of designs for a sparse distributed memory
[NASA-CR-188849] N92-11644
Threats and countermeasures for network security
[NASA-CR-188883] N92-11645
A parallel algorithm for the eigenvalues and eigenvectors for a general complex matrix
[NASA-CR-188854] N92-11653
Modula-2*: An extension of Modula-2 for highly parallel programs
[NASA-CR-188855] N92-11654
Fast secant methods for the iterative solution of large nonsymmetric linear systems
[NASA-CR-188867] N92-11655
Optimal parallel solution of sparse triangular systems
[NASA-CR-188872] N92-11656
Stopping computer crimes
[NASA-CR-188896] N92-11657
Solving the shallow water equations on the Cray X-MP/48 and the connection machine 2
[NASA-CR-188897] N92-11658
An O(log sup 2 N) parallel algorithm for computing the eigenvalues of a symmetric tridiagonal matrix
[NASA-CR-188898] N92-11659
Modelling default and likelihood reasoning as probabilistic reasoning
[NASA-CR-188936] N92-11661
Classification of posture maintenance data with fuzzy clustering algorithms
[NASA-CR-188949] N92-11662
ART/Ada design project, phase 1: Project plan
[NASA-CR-187313] N92-11663
Deploying expert systems in Ada
[NASA-CR-188938] N92-11664
ART/Ada design project, phase 1. Task 1 report: Overall design
[NASA-CR-188943] N92-11665
ART/Ada design project, phase 1. Task 2 report: Detailed design
[NASA-CR-188944] N92-11666
ART-Ada design project, phase 2
[NASA-CR-188940] N92-11667
Some fast elliptic solvers on parallel architectures and their complexities
[NASA-CR-188840] N92-11692
Efficient ICCG on a shared memory multiprocessor
[NASA-CR-188843] N92-11693
Policy issues in interconnecting networks
[NASA-CR-188844] N92-11694
The ARPANET after twenty years
[NASA-CR-188853] N92-11695
Optimal expression evaluation for data parallel architectures
[NASA-CR-187773] N92-11696
Neural networks and MIMD-multiprocessors
[NASA-CR-188481] N92-11697
Highly parallel computation
[NASA-CR-188871] N92-11698
Total recall in distributive associative memories
[NASA-CR-188884] N92-11699
Ordered fast fourier transforms on a massively parallel hypercube multiprocessor
[NASA-CR-188899] N92-11700
Analysis of a parallel multigrid algorithm
[NASA-CR-188906] N92-11701
Ground Systems Development Environment (GSDE) interface requirements analysis
[NASA-CR-188822] N92-11702
Learning to read aloud: A neural network approach using sparse distributed memory
[NASA-CR-188846] N92-11711
Optimal Chebyshev polynomials on ellipses in the complex plane
[NASA-CR-188836] N92-11722
An improved Newton iteration for the generalized inverse of a matrix, with applications
[NASA-CR-186983] N92-11723
New Bernstein type inequalities for polynomials on ellipses
[NASA-CR-186626] N92-11724
Statistical prediction with Kanerva's sparse distributed memory
[NASA-CR-187314] N92-11743
Numerical methods in Markov chain modeling
[NASA-CR-188908] N92-11744
About time
[NASA-CR-188870] N92-11753
Collision integrals and high temperature transport properties for N-N, O-O, and N-O
[NASA-CR-188907] N92-11770
An application for multi-person task synchronization
[NASA-CR-187712] N92-11918
Information technologies for astrophysics circa 2001
[NASA-CR-188868] N92-11936
RESOURCES FOR THE FUTURE, INC., BALTIMORE, MD.
Processes for identifying regional influences of and responses to increasing atmospheric CO2 and climate change: The MINK Project
[DE91-018604] N92-11580
RESOURCES FOR THE FUTURE, INC., WASHINGTON, DC.
Processes for identifying regional influences of and responses to increasing atmospheric CO2 and climate change: The MINK Project
[DE91-018601] N92-11579
RIJKSWATERSTAAT, DELFT (NETHERLANDS).
Comparison of in situ, aircraft- and satellite-derived surface reflectances in Flevoland (Netherlands) N92-11404
ROCHESTER UNIV., NY.
Sunspot dynamics
[NASA-CR-188978] N92-11955
LLE review
[DE91-018828] N92-11965
ROCKWELL INTERNATIONAL CORP., CANOGA PARK, CA.
NERVA upgrade: Non-nuclear components N92-11092
Wire core reactor for NTP N92-11099
Propulsion system needs N92-11112
Definition, technology readiness, and development cost of the orbit transfer vehicle engine integrated control and health monitoring system elements
[NASA-CR-187123] N92-11132
Hydrodynamic design of generic pump components
[NASA-CR-184252] N92-11361
ROME AIR DEVELOPMENT CENTER, GRIFFISS AFB, NY.
A thinned high frequency linear antenna array to study ionospheric structure
[AD-A240764] N92-11243
RUTGERS - THE STATE UNIV., NEW BRUNSWICK, NJ.
An investigation to find appropriate measures for evaluating interactive information retrieval N92-11922
RUTHERFORD APPLETON LAB., CHILTON (ENGLAND).
On the polarisation of tensor mesons in psi radiative decays and possible implications for the gluonic content of the theta(1720)
[RAL-90-091] N92-11768

S

SALFORD UNIV. (ENGLAND).
Multi-temporal monitoring of lake water quality N92-11426
Structural controls on the remotely sensed response of a coniferous forest plantation N92-11516
SANDIA NATIONAL LABS., ALBUQUERQUE, NM.
Fission fragment assisted reactor concept for space propulsion: Foil reactor N92-11103
A probabilistic model of intergranular stress corrosion cracking
[DE91-017986] N92-11173
Low volatile organic compound paints
[DE91-017984] N92-11203
Photothermal deflection spectroscopy of conjugated polymers
[DE91-018318] N92-11204
Nonaqueous secondary batteries
[DE91-017788] N92-11282
Case history: Failure analysis of a CMOS SRAM with an intermittent open contact
[DE91-018811] N92-11283
Melting efficiency in fusion welding
[DE91-017988] N92-11355
Overlooked fundamentals of resistance welding
[DE91-018814] N92-11362
Microstructural evolution during the thermomechanical fatigue of solder joints
[DE91-017309] N92-11372
Today's central receiver power plant
[DE91-017998] N92-11568

Process for controlling the thickness of an antireflection coating, and embodying apparatus
[DE91-017634] N92-11793
New high-T(sub c) benchmarks for organic and fullerene superconductors
[DE91-016406] N92-11899
Electrooptic effects and photosensitivities of PLZT thin films
[DE91-017067] N92-11901

SANTA BARBARA RESEARCH CENTER, GOLETA, CA.
Mapping photopolarimeter spectrometer instrument feasibility study for future planetary flight missions
[NASA-CR-189242] N92-11329

SCIENCE APPLICATIONS INTERNATIONAL CORP., LA JOLLA, CA.
Disposal methods N92-11116

SCIENCE APPLICATIONS INTERNATIONAL CORP., MCLEAN, VA.
Particle acceleration in space and radiation belt depletion
[AD-A240311] N92-11775

SCRIPPS INSTITUTION OF OCEANOGRAPHY, LA JOLLA, CA.
Bi-directional reflectance of finite and infinite clouds N92-11470
Studies of the physical and chemical stability of natural sea-surface films
[AD-A239818] N92-11604

SHERBROOKE UNIV. (QUEBEC).
Evaluation of atmospheric effects in high spectral resolution airborne images N92-11408
Evaluation of the quality of urban biotypes by remote sensing N92-11493
Evaluation of ground cover in agricultural environment by in situ measurements and multitemporal images for modeling hydric erosion N92-11528

SIMPSON WEATHER ASSOCIATES, INC., CHARLOTTESVILLE, VA.
Study and prototype of data system interactions for the Earth Observing System Data and Information System
[NASA-CR-183505] N92-11648

SKIDAWAY INST. OF OCEANOGRAPHY, SAVANNAH, GA.
Organic geochemistry of seawater particulate matter: Final data analysis interpretation
[AD-A240199] N92-11605

SOUTHAMPTON UNIV. (ENGLAND).
The UK Natural Environment Research Council Equipment Pool for Field Spectroscopy (NERC-EPFS) N92-11558

SOUTHWEST RESEARCH INST., SAN ANTONIO, TX.
Piston temperature measurement in a natural gas engine
[PB91-194357] N92-11352
Continuation of research into language concepts for the mission support environment
[NASA-CR-187818] N92-11652
A simulation study of interactions of Space-Shuttle generated electron beams with ambient plasma and neutral gas
[NASA-CR-189025] N92-11898

SPACE INDUSTRIES, INC., WEBSTER, TX.
Intelligent perturbation algorithms for space scheduling optimization N92-11055
Intelligent perturbation algorithms to space scheduling optimization N92-11064
Nonscanning climate sensor study
[NASA-CR-183506] N92-11589

SPACE TELESCOPE SCIENCE INST., BALTIMORE, MD.
SPIKE: AI scheduling techniques for Hubble Space Telescope N92-11054

SPARTA, INC., LEXINGTON, MA.
Development of a 3-D tree thermal response model for energy budget and scene simulation studies
[AD-A240693] N92-11565

SRI INTERNATIONAL CORP., MENLO PARK, CA.
Novel nonlinear laser diagnostic techniques
[AD-A240193] N92-11346

STANFORD UNIV., CA.
Computational study of the aerodynamics and control by blowing of asymmetric vortical flows over delta wings
[NASA-CR-187979] N92-10990
Precision pointing control of the spinning Gravity Probe B spacecraft N92-11068
Compression response of laminated composite panels containing multiple delaminations N92-11141

STATE UNIV. OF NEW YORK, ALBANY.
The modeling of complex continua: Fundamental obstacles and grand challenges
[DE91-018806] N92-11686

STATE UNIV. OF NEW YORK, BINGHAMTON.
Vegetation canopies and objects of arbitrary shapes: Computer generation and bidirectional reflectance calculations N92-11475
Biospheric models, measurements, and remote sensing of vegetation N92-11550

STATE UNIV. OF NEW YORK, STONY BROOK.
Training, muscle fatigue and stress fractures
[AD-A240386] N92-11626
Effects of the equation of state in neutron stars and in stellar collapse
[DE91-014534] N92-11935

STOCKHOLM UNIV. (SWEDEN).
Night-time LANDSAT thermal infrared imagery as a tool for climatological studies N92-11526

STRATEGIC AIR COMMAND, OFFUTT AFB, NE.
Strategic air command contrail formation study
[AD-A240467] N92-11003

STRATHCLYDE UNIV., GLASGOW (SCOTLAND).
Inverse problems and imaging (Pitman research notes in mathematics series Number 245)
[AD-A240333] N92-11737

STUTTGART UNIV. (GERMANY, F.R.).
Status of the WVII-AS Program N92-11820

SUPERCONDUCTING SUPER COLLIDER LAB., DALLAS, TX.
Coil shapes towards pure multipoles in circular regions: A numerical approach
[DE91-017239] N92-11271
BCD/CPS: An event-level GEANT3 parallelization via CPS
[DE91-017238] N92-11703

SURFACE OPTICS CORP., SAN DIEGO, CA.
Surface optical property measurements on bark and leaf samples
[AD-A240714] N92-11566

SVERDRUP TECHNOLOGY, INC., BROOK PARK, OH.
Mach 6.5 air induction system design for the Beta 2 two-stage-to-orbit booster vehicle
[NASA-CR-187233] N92-11013
Open cycle gas core nuclear rockets N92-11108
LOX/hydrogen coaxial injector atomization test program N92-11121
Evaluation of Kapton pyrolysis, arc tracking, and arc propagation on the Space Station Freedom (SSF) solar array Flexible Current Carrier (FCC)
[NASA-CR-189056] N92-11139
Lunar dust transport and potential interactions with power system components
[NASA-CR-4404] N92-11951

SVERDRUP TECHNOLOGY, INC., CLEVELAND, OH.
Computers in aeronautics and space research at the Lewis Research Center
[NASA-TM-105096] N92-11642

SYDNEY UNIV. (AUSTRALIA).
Studies in the form of finite element mass matrices for beams, plates and shells
[AERO-TN-9101] N92-11369

SYPHER-MUELLER INTERNATIONAL, INC., OTTAWA (ONTARIO).
Alternative fuels for heavy duty engines: Status of fleet trials
[DE91-018474] N92-11210

SYSTEMS CONTROL TECHNOLOGY, INC., ARLINGTON, VA.
Guidelines for integrating helicopter assets into emergency planning
[SCT-91RR-18] N92-10993

T

TAMPERE UNIV. OF TECHNOLOGY (FINLAND).
The phenomena of scalar mixing in turbulent gas-particle flows, measuring equipment, and measurements
[DE92-704034] N92-11327

TECHNICAL RESEARCH CENTRE OF FINLAND, ESPOO.
Navigation and positioning of mobile robots
[DE92-704014] N92-10998
Magnetic fluids and their applications
[DE92-704012] N92-11326

TECHNION RESEARCH AND DEVELOPMENT FOUNDATION LTD., HAIFA (ISRAEL).
Multi-disciplinary optimization of aeroservoelastic systems
[NASA-CR-188983] N92-11377

TECHNISCHE HOCHSCHULE, DARMSTADT (GERMANY, F.R.).
Oriented matroids and projective invariant theory
[ETN-91-90181] N92-11740

TECHNISCHE UNIV., BERLIN (GERMANY, F.R.).
The electronic aeronautical chart for general aeronautics: A system specification
[ILR-MITT-263(1991)] N92-10997
Buckling values and optimization of carbon fiber reinforced compression chord plates with rectangular stringers
[ILR-MITT-259(1991)] N92-11148
Insulated Gate Bipolar Transistors (IGBT) modelization for circuit simulation and utilization in pulse modulated inverters
[ETN-91-90149] N92-11279
Development of a personal computer program for milling the shapes of wind turbine blades. Theory and application
[ILR-MITT-243(1990)] N92-11360
Experimental determination of the material parameter of two viscoelastic synthetic materials, using creep tests
[ILR-MITT-244(1990)] N92-11385
Calculation of general shells of revolution, using a semi analytical process
[ILR-MITT-262(1991)] N92-11386
The ULM: A RISC for LISP. System architecture
[ETN-91-90162] N92-11647
A synchronization and charge distribution process for the parallel multilevel logic simulation
[ETN-91-90152] N92-11708
Extended algebraic graph transformation
[ETN-91-90151] N92-11739
Representation of phi meromorphic functions, when phi and a linear differential polynomial in phi have maximum finite zeros
[ETN-91-90202] N92-11741
On the maximum entropy principle for Markov chains and processes
[ETN-91-90150] N92-11750
The strong coupling limit for polaron models
[ETN-91-90163] N92-11757
The recombination behavior of a laser induced electron hole plasma in pin diodes and silicon base material
[ETN-91-90153] N92-11887
Thermal annealing studies of Fe and Ti implanted in GaAs and InP
[ETN-91-90148] N92-11915
Open document processing and the ISOTEXT system
[ETN-91-90160] N92-11928

TECHNISCHE UNIV., EINDHOVEN (NETHERLANDS).
The behaviour of fire-exposed composite steel/concrete slabs
[ISBN-90-386-0031-3] N92-11147
Critical velocities and mutual friction in He-3-He-4 II mixtures at temperatures below 100 mK
[ETN-91-90132] N92-11314
Deformation and breakup of drops in simple shear flows
[ETN-91-90143] N92-11315
On the capacity region for deterministic two-way channels and write-unidirectional memories
[ETN-91-90147] N92-11684
Light scattering experiments on Brownian motion in shear flow and in colloidal crystals
[ETN-91-90134] N92-11756
Surface analysis of catalysts by low-energy ion scattering
[ETN-91-90133] N92-11913
Spectroscopic studies of layered and bulk semiconductor materials
[ETN-91-90145] N92-11914
Modelling product structures by generic bills-of-material
[ETN-91-90146] N92-11919

TEXAS A&M UNIV., COLLEGE STATION.
Damage evolution in filled elastomers
[AD-A240532] N92-11191

TEXAS UNIV., AUSTIN.
Power-law energy spectrum and orbital stochasticity
[DE91-017387] N92-11872
Continuum damping of high mode number toroidal Alfven waves
[DE91-018891] N92-11890

TEXAS UNIV., HOUSTON.
Discussion summary: Fictitious domain methods N92-11730

TEXTRON BELL AEROSPACE CO., BUFFALO, NY.
Slave finite element for non-linear analysis of engine structures. Volume 2: Programmer's manual and user's manual
[NASA-CR-187225] N92-11388

TEXTRON BELL HELICOPTER, FORT WORTH, TX.
Technology needs for high speed rotorcraft (3)
[NASA-CR-186433] N92-10999

TOHOKU UNIV., SENDAI (JAPAN).
Experimental studies of a helical axis stellarator (TU-Heliac) N92-11824

TOSHIBA CORP., YOKOHAMA (JAPAN).
Structural design of large helical device N92-11837
Research and development of forced flow superconducting coils for large helical device N92-11838

TOULOUSE UNIV. (FRANCE).
Detection and characterization of active fires in west Africa with LANDSAT thematic mapper and NOAA N92-11529

TRI-UNIV. MESON FACILITY, VANCOUVER (BRITISH COLUMBIA).
Comparative study of final state interaction contributions to the dynamic response of quantum fluids
[DE91-631020] N92-11892
On the evolution of a superconducting cosmic string network
[DE91-630995] N92-11948
TRW, INC., REDONDO BEACH, CA.
Automating the conflict resolution process N92-11061
TRW SPACE TECHNOLOGY LABS., REDONDO BEACH, CA.
ISEE/ICE plasma wave data analysis
[NASA-CR-189244] N92-11795
TRW SYSTEMS GROUP, REDONDO BEACH, CA.
Automated conflict resolution issues N92-11045
TULANE UNIV., NEW ORLEANS, LA.
A grid-free method for high Reynolds number flow around an immersed elastic structure
[AD-A240048] N92-10984

U

UNITED NATIONS ENVIRONMENT PROGRAMME, NAIROBI (KENYA).
Scientific assessment of stratospheric ozone: 1989, volume 1
[NASA-TM-105116] N92-11576
Scientific assessment of stratospheric ozone: 1989. Volume 2: Appendix: AFEAS report
[NASA-TM-105117] N92-11577
UNITED TECHNOLOGIES CORP., EAST HARTFORD, CT.
Structural tailoring of advanced turboprops (STAT): User's manual
[NASA-CR-187101] N92-11016
UNITED TECHNOLOGIES RESEARCH CENTER, EAST HARTFORD, CT.
Development of unsteady aerodynamic analyses for turbomachinery aeroelastic and aeroacoustic applications
[NASA-CR-4405] N92-10979
Nuclear light bulb N92-11110
The effects of Reynolds number, rotor incidence angle and surface roughness on the heat transfer distribution in a large-scale turbine rotor passage
[NASA-CR-187693] N92-11297
UNIVERSIDAD COMPLUTENSE, MADRID (SPAIN).
Low-n stability calculations for three dimensional stellarator configurations N92-11831
UNIVERSITE DES SCIENCES ET TECHNIQUES DE LILLE (FRANCE).
Specular and diffuse components of plant canopy reflectance at the wavelengths of 550 and 630 nm N92-11484
UNIVERSITIES SPACE RESEARCH ASSOCIATION, COLUMBIA, MD.
Modelling default and likelihood reasoning as probabilistic reasoning
[NASA-CR-188936] N92-11661
UNIVERSITY COLL., LONDON (ENGLAND).
Measurement, simulation, and analysis of the directional reflectance properties of Earth surface materials N92-11468
UNIVERSITY COLL. OF NORTH WALES, BANGOR.
Parallel processing applications for gas turbine engine control N92-11012
UNIVERSITY OF SOUTHERN CALIFORNIA, LOS ANGELES.
Joint services electronics program research in electronics
[AD-A240155] N92-11274

V

VALENCIA UNIV., BURJASSOT (SPAIN).
Maximum evapotranspiration monitoring over La Mancha, Spain, using NOAA-AVHRR data N92-11507
VALENCIA UNIV. (SPAIN).
A split-window method for obtaining crop temperatures N92-11410
NOAA-AVHRR contribution to the analysis or urban heat islands N92-11495
VANDERBILT UNIV., NASHVILLE, TN.
Aerodynamic calculations related to tethered sub-satellite experiments
[NASA-CR-188964] N92-11071
Laser Raman diagnostics in subsonic and supersonic turbulent jet diffusion flames N92-11159
Robot graphic simulation testbed
[NASA-CR-188998] N92-11637
VIRGINIA POLYTECHNIC INST. AND STATE UNIV., BLACKSBURG.
Large deployable antenna program. Phase 1: Technology assessment and mission architecture
[NASA-CR-4410] N92-11036
The science benefits of and the antenna requirements for microwave remote sensing from geostationary orbit
[NASA-CR-4408] N92-11559
VIRGINIA UNIV., CHARLOTTESVILLE.
Distributed sensor system decision analysis using team strategies
[AD-A240250] N92-11333
Large deformation induced failures in nonlinear solids
[AD-A240369] N92-11382
VISIDYNE, INC., BURLINGTON, MA.
Aircraft lidar sensitivity study for measuring water vapor
[AD-A240549] N92-11237
VRIJE UNIV., AMSTERDAM (NETHERLANDS).
Atmospheric correction of satellite borne imagery investigated by means of a sensitivity analysis of the entire remote sensing process N92-11400
A multi-sensor approach to spectral signature analysis of inland waters N92-11428

W

WAGENINGEN AGRICULTURAL UNIV. (NETHERLANDS).
Feasibility of the red edge index for the detection of nitrogen deficiency N92-11425
(L)EAF: A remote sensing fluoresensor N92-11546
WANDERMAN (KEN) AND ASSOCIATES, INC., STATEN ISLAND, NY.
A generalized strategy for building resident database interfaces
[NASA-CR-189246] N92-11920
WASHINGTON STATE UNIV., PULLMAN.
Quantitative ray methods for scattering of sound by spherical shells
[AD-A240255] N92-11761
Wavefields near transverse cusp caustics produced by reflecting ultrasonic transients and tone bursts from curved surfaces
[AD-A240641] N92-11763
Scattering of tone bursts from spherical shells: Computations based on Fourier transform method
[AD-A240642] N92-11764
Chemical reactivity and electronic structure of silicon microclusters
[AD-A240276] N92-11908
Structure of the Si45 cluster
[AD-A240278] N92-11909
WASHINGTON UNIV., SEATTLE.
Thermoviscoplastic response of Ti-15-3 under various loading conditions
[NASA-CR-187621] N92-11391
Numerical and experimental studies of simulated toroidicity effects in a linear high-beta heliac N92-11827
Coaxial slow source
[DE91-016947] N92-11875
Report on carbon and nitrogen abundance studies
[NASA-CR-188803] N92-11934
WATER CONSERVATION LAB., PHOENIX, AZ.
Comparison of atmospheric correction procedures for visible and near-IR satellite sensor output N92-11395
WEST VIRGINIA UNIV., MORGANTOWN.
Experimental investigation of the effects of blowing on bursting of strake vortices
[AD-A240256] N92-10985
WESTINGHOUSE ELECTRIC CORP., MADISON, PA.
Upgraded NERVA systems: Enabler nuclear system N92-11093
WISCONSIN UNIV., MADISON.
Superfluid helium dynamics
[NASA-CR-188814] N92-11294
Characterizing He II flow through porous materials using counterflow data
[CD-4] N92-11295
Thermal behavior of the SHOOT gallery arm
[CD-21] N92-11296
Pictures and anaphora
[AD-A240153] N92-11631
Status of the Torsatron/Stellarator Program N92-11821
Diverted particle-flux studies in the IMS and Proto-Cleo stellarators N92-11825
Pressure and potential measurements in IMS during electron cyclotron heating N92-11826
WORLD METEOROLOGICAL ORGANIZATION, GENEVA (SWITZERLAND).
Scientific assessment of stratospheric ozone: 1989, volume 1
[NASA-TM-105116] N92-11576
Scientific assessment of stratospheric ozone: 1989. Volume 2: Appendix: AFEAS report
[NASA-TM-105117] N92-11577
WRIGHT LAB., WRIGHT-PATTERSON AFB, OH.
Subsonic wind tunnel testing handbook
[AD-A240263] N92-10986
Nonlinear aspects of aerospace structures at high excitation levels flat aluminum beams and plates studied
[AD-A240600] N92-11383

Y

YALE UNIV., NEW HAVEN, CT.
Physics of ultrasmall superconducting circuits
[AD-A240156] N92-11275
Long term synaptic plasticity and learning in neuronal networks
[AD-A240366] N92-11613
Development of a system for accurate forecasting of solar activity
[AD-A240359] N92-11957
YELLOWSTONE NATIONAL PARK, WY.
Winter use plan: Environmental assessment
[PB91-194027] N92-11574

Typical Contract Number Index Listing

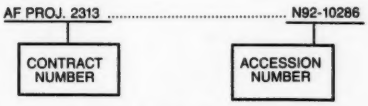

Listings in this index are arranged alphanumerically by contract number. Under each contract number the accession numbers denoting documents that have been produced as a result of research done under that contract are arranged in ascending order. The accession number denotes the number by which the citation is identified.

AF PROJ. 2304 ..... N92-11675
N92-11678
N92-11748
AF PROJ. 2305 ..... N92-11275
N92-11907
AF PROJ. 2308 ..... N92-11164
AF PROJ. 2311 ..... N92-11957
AF PROJ. 2312 ..... N92-11613
AF PROJ. 2313 ..... N92-11631
N92-11633
N92-11634
AF PROJ. 2404 ..... N92-10986
AF PROJ. 3484 ..... N92-11176
AF PROJ. 4600 ..... N92-11243
AF PROJ. 6177 ..... N92-10984
AF PROJ. 6302 ..... N92-11134
AF PROJ. 7601 ..... N92-11585
AF-AFOSR-0017-89 ..... N92-11675
AF-AFOSR-0047-88 ..... N92-11707
AF-AFOSR-0047-89 ..... N92-11613
AF-AFOSR-0054-88 ..... N92-11957
AF-AFOSR-0061-90 ..... N92-11678
AF-AFOSR-0070-89 ..... N92-11164
AF-AFOSR-0071-89 ..... N92-11748
AF-AFOSR-0138-89 ..... N92-11176
AF-AFOSR-0139-88 ..... N92-10977
AF-AFOSR-0270-88 ..... N92-11275
AF-AFOSR-0275-85 ..... N92-11192
AF-AFOSR-0295-89 ..... N92-10984
AF-AFOSR-0367-89 ..... N92-11631
AF-AFOSR-0416-89 ..... N92-11907
AF-AFOSR-0442-89 ..... N92-11633
AF-AFOSR-0447-89 ..... N92-11634
AF-AFOSR-0470-89 ..... N92-11382
AFRC-PG42/328 ..... N92-11435
ATP-87/CNES/1254 ..... N92-11463
N92-11464
ATP-88/50/N/5111 ..... N92-11505
BMFT-0339290A N92-11540
CICYT-ESP-89-0436 ..... N92-11410
CNES-833/CNES/885527 ..... N92-11485
CNES-833/87/4891/02 ..... N92-11403
CNES-833/89/5935/00 ..... N92-11409
CRSNG-GP-8643 ..... N92-11493
CS-76-90 ..... N92-11474
DA PROJ. 3E1-62777-A-878 ..... N92-11762
DA PROJ. 3M1-61102-BS-15 ..... N92-11626
N92-11762
DA PROJ. 3M4-63807-D-836 ..... N92-11004
DA PROJ. 4A1-61102-B-52-C N92-11564
DAAH01-87-D-0021 ..... N92-11122
DAAL03-86-D-0001 ..... N92-11749
DAAL03-86-K-0112 ..... N92-11723
DAAL03-88-K-0085 ..... N92-11701
N92-11731
DAJA45-89-C-0006 ..... N92-11015
DAJA45-89-M-0086 ..... N92-11737
DAJA45-90-M-0034 ..... N92-11614
DAJA45-90-M-0298 ..... N92-11674
DAMD17-90-Z-0054 ..... N92-11585
N92-11626
DARPA ORDER 4976 ..... N92-11679
DARPA ORDER 9526 ..... N92-11910
DASG60-91-C-0024 ..... N92-11083
DE-AC02-76CH-00016 ..... N92-11350
N92-11351
N92-11784
DE-AC03-76SF-00098 ..... N92-11160
N92-11754
N92-11772
DE-AC03-84ER-53158 ..... N92-11895
N92-11896
N92-11897
DE-AC04-76DP-00789 ..... N92-11173
N92-11203
N92-11204
N92-11282
N92-11283
N92-11355
N92-11362
N92-11372
N92-11568
N92-11793
N92-11899
N92-11901
DE-AC05-84OR-21400 ..... N92-11168
N92-11181
N92-11183
N92-11205
N92-11216
N92-11249
N92-11250
N92-11389
N92-11725
N92-11779
N92-11802
N92-11809
N92-11819
N92-11849
N92-11857
N92-11889
N92-11894
N92-11904
N92-11905
N92-11906
DE-AC05-86OR-21400 ..... N92-11830
DE-AC06-76RL-01830 ..... N92-11579
N92-11580
N92-11601
N92-11687
DE-AC35-89ER-40486 ..... N92-11271
N92-11703
DE-AS05-76ER-04936 ..... N92-11768
DE-BI79-90BP-06048 ..... N92-11270
DE-FC03-85DP-40200 ..... N92-11965
DE-FG02-84ER-40158 ..... N92-11944
DE-FG02-85ER-25001 ..... N92-11689
DE-FG02-85ER-52118 ..... N92-11895
N92-11896
N92-11897
DE-FG02-85ER-53207 ..... N92-11805
N92-11893
DE-FG02-86ER-40251 ..... N92-11782
DE-FG02-86ER-45247 ..... N92-11916
DE-FG02-86ER-53216 ..... N92-11821
N92-11826
DE-FG02-86ER-53223 ..... N92-11891
DE-FG02-87ER-13716 ..... N92-11612
DE-FG02-87ER-25041 ..... N92-11688
DE-FG02-87ER-40317 ..... N92-11935
DE-FG02-88ER-45341 ..... N92-11206
DE-FG02-89ER-14080 ..... N92-11169
DE-FG02-90ER-25084 ..... N92-11686
DE-FG02-90ER-40553 ..... N92-11172
DE-FG02-90ER-40606 ..... N92-11945
DE-FG02-90ER-60932 ..... N92-11575
DE-FG02-90ER-61091 ..... N92-11622
DE-FG02-91ER-40606 ..... N92-11946
DE-FG03-86ER-52126 ..... N92-11895
N92-11896
N92-11897
DE-FG03-87ER-25037 ..... N92-11701
N92-11731
DE-FG03-88ER-53275 ..... N92-11890
DE-FG03-90ER-40545 ..... N92-11345
DE-FG05-80ET-53088 ..... N92-11872
N92-11890
DE-FG05-86ER-45259 ..... N92-11899
DE-FG05-90ER-60951 ..... N92-11623
DE-FG06-87ER-53243 ..... N92-11875
DE-FG07-89ID-12855 ..... N92-11182
DE-FG85-85ER-53192 ..... N92-11805
DE-GI01-87CE-50182 ..... N92-11210
DRET-88-218 ..... N92-11287
DRET-89-34-01 ..... N92-11311
DRET-89-34-001 ..... N92-10989
N92-11145
N92-11308
N92-11310
N92-11713
DRET-89-001-118 ..... N92-11588
DRET-89-002-29 ..... N92-10988
DRET-90-1430/A000 ..... N92-11313
DTFA01-87-C-00014 ..... N92-10993
DTFA01-90-4-01019 ..... N92-11593
ECSC-7210-SA/509 ..... N92-11147
EEC-3444-88-08 ..... N92-11513
EEC-3444-88-08-ES-IPF N92-11525
EEC-3447-88-08-ES-ISPF N92-11518
F04611-87-K-0030 ..... N92-11166
F04701-88-C-0089 ..... N92-11233
N92-11242
F19628-86-C-0102 ..... N92-11231
F19628-87-C-0085 ..... N92-11775
F19628-88-C-0009 ..... N92-10987
F19628-88-C-0013 ..... N92-11237
F19628-88-C-0038 ..... N92-11565
F19628-88-C-0086 ..... N92-11597
F19628-89-C-0001 ..... N92-11682
F19628-89-C-0128 ..... N92-11566
F19628-90-C-0002 ..... N92-11683
F19628-90-C-0003 ..... N92-11926
F30602-81-C-0169 ..... N92-11333
F30602-84-C-0168 ..... N92-11681
F33615-85-C-2508 ..... N92-11213
F33615-85-C-5151 ..... N92-11363
F33615-87-C-1499 ..... N92-11679
F33615-88-C-5511 ..... N92-11365
F33615-89-C-3001 ..... N92-10985
F33615-89-C-5605 ..... N92-11006
N92-11007
F33615-90-C-0005 ..... N92-11635
F33615-90-C-5915 ..... N92-11179
F49620-88-C-0052 ..... N92-11175
F49620-88-C-0067 ..... N92-11274
F49620-88-C-0077 ..... N92-11018
F49620-89-C-0011 ..... N92-11080
N92-11081
F49620-89-C-0073 ..... N92-11192
F49620-90-C-0044 ..... N92-11346
GRI-5089-293-1848 ..... N92-11352
JPL-958456 ..... N92-11491
MIPR-FY1455-89-N0670 ..... N92-11305
NAGW-21 ..... N92-11215
NAGW-812 ..... N92-11076
N92-11077
N92-11078
NAGW-965 ..... N92-10977
NAGW-1143 ..... N92-11491
NAGW-1175 ..... N92-11358
NAGW-1321 ..... N92-11946
NAGW-1340 ..... N92-11774
N92-11941
N92-11942
N92-11943
N92-11944
N92-11945
N92-11946
N92-11947
N92-11956
NAGW-1370 ..... N92-11332
NAGW-1474 ..... N92-11486
NAGW-1601 ..... N92-11491
NAGW-1708 ..... N92-11377
NAGW-1936 ..... N92-11898
NAGW-1968 ..... N92-11474
NAGW-2123 ..... N92-11955

NAG1-569 ..... N92-11207
NAG1-811 ..... N92-10982
NAG1-849 ..... N92-11070
NAG1-878 ..... N92-11071
NAG1-889 ..... N92-11470
NAG1-974 ..... N92-11391
NAG1-1108 ..... N92-11902
NAG1-1142 ..... N92-11023
NAG1-1228 ..... N92-11074
NAG2-541 ..... N92-11140
NAG3-33 ..... N92-11378
NAG3-298 ..... N92-11375
NAG3-307 ..... N92-11375
NAG3-379 ..... N92-11387
NAG3-1033 ..... N92-11161
NAG3-1115 ..... N92-11014
NAG3-1139 ..... N92-11272
NAG3-1152 ..... N92-11671
NAG3-1215 ..... N92-10978
NAG5-419 ..... N92-11284
NAG5-557 ..... N92-11228
NAG5-900 ..... N92-11474
NAG5-1031 ..... N92-11294
NAG5-1255 ..... N92-11934
NAG5-1329 ..... N92-11560
NAG5-1469 ..... N92-11393
NAG8-690 ..... N92-11637
NAG9-435 ..... N92-11652
NASA ORDER C-99066-G N92-11302
N92-11328
NASA ORDER S-28187-D N92-11712
NAS1-17450 ..... N92-11065
NAS1-17721 ..... N92-11319
NAS1-18471 ..... N92-11036
N92-11559
NAS1-18565 ..... N92-11704
N92-11705
N92-11706
NAS1-18585 ..... N92-11593
NAS1-18605 ..... N92-11162
N92-11640
N92-11669
N92-11670
N92-11672
N92-11728
N92-11731
N92-11733
N92-11736
NAS1-19000 ..... N92-11207
N92-11338
NAS2-13072 ..... N92-10999
NAS2-13210 ..... N92-11673
NAS3-23279 ..... N92-11388
NAS3-23773 ..... N92-11132
NAS3-23941 ..... N92-11016
NAS3-25266 ..... N92-11013
N92-11121
N92-11139
N92-11951
NAS3-25425 ..... N92-10979
NAS5-28703 ..... N92-11795
NAS5-30090 ..... N92-11589
NAS5-30128 ..... N92-11581
NAS5-30297 ..... N92-11251
NAS5-30304 ..... N92-11920
NAS5-30445 ..... N92-11341
NAS5-30531 ..... N92-11329
NAS5-31180 ..... N92-11648
NAS7-918 ..... N92-11791
NAS8-36645 ..... N92-11076
N92-11077
N92-11078
NAS8-36955 ..... N92-11122
NAS8-38186 ..... N92-11318
NAS8-38555 ..... N92-11079
NAS8-38863 ..... N92-11361
NAS8-38870 ..... N92-11297
NAS9-17414 ..... N92-11084
N92-11085
NAS9-17900 ..... N92-11561
NAS9-18328 ..... N92-11331
NAS9-18493 ..... N92-11769
NCA2-233 ..... N92-11701
NCC2-378 ..... N92-11743
NCC2-387 ..... N92-10977
N92-11223
N92-11224
N92-11290
N92-11590
N92-11643
N92-11644
N92-11645
N92-11653
N92-11654
N92-11655
N92-11656
N92-11657
N92-11658
N92-11659
N92-11661
N92-11692
N92-11693
N92-11694
N92-11695
N92-11696
N92-11697
N92-11698
N92-11699
N92-11700
N92-11701
N92-11711
N92-11722
N92-11723
N92-11724
N92-11744
N92-11753
N92-11770
N92-11918
N92-11936
NCC2-408 ..... N92-11590
N92-11644
N92-11699
N92-11711
N92-11743
NCC3-135 ..... N92-11339
NCC9-16 ..... N92-11662
N92-11663
N92-11664
N92-11665
N92-11666
N92-11667
N92-11702
NERC-GR3/6373 ..... N92-11435
NERC-GR3/7020 ..... N92-11468
NERC-GR3/7901 ..... N92-11468
NERC-GR9/14 ..... N92-11498
NERC-GT4/88/GS/87 ..... N92-11498
NR PROJ. S15-65 ..... N92-11193
NRL PROJ. RR0-1109 ..... N92-11304
NSF ASC-88-19374 ..... N92-11669
NSF ASC-90-03002 ..... N92-11731
NSF AST-88-22595 ..... N92-11946
NSF AST-22595 ..... N92-11945
NSF CCR-87-17942 ..... N92-11692
NSF CCR-88-05782 ..... N92-11723
NSF DCR-85-09970 ..... N92-11692
NSF DMS-87-1461[illegible] N92-11701
NSF DMS-88-11863 ..... N92-11736
NSF ECS-88-22654 ..... N92-11656
NSF ECS-89-02528 ..... N92-11225
NSF ECS-89-07391 ..... N92-11656
NSF ECS-89-57475 ..... N92-11731
NSF INT-86-13332 ..... N92-11744
NSF MIP-84-10110 ..... N92-11692
NSF PHY-84-51275 ..... N92-11805
NSG-3283 ..... N92-11379
NSG-7562 ..... N92-11955
N00014-85-C-0141 ..... N92-11761
N92-11763
N00014-85-K-0124 ..... N92-11649
N92-11650
N00014-86-K-0153 ..... N92-11380
N00014-86-K-0514 ..... N92-11195
N00014-86-K-0610 ..... N92-11653
N92-11723
N00014-86-K-0691 ..... N92-11736
N00014-87-K-0144 ..... N92-11604
N00014-88-K-0139 ..... N92-11912
N00014-88-K-0392 ..... N92-11910
N00014-88-K-0460 ..... N92-11649
N00014-88-K-0732 ..... N92-11190
N92-11194
N92-11196
N92-11197
N00014-89-J-1421 ..... N92-11143
N00014-89-J-3012 ..... N92-11191
N00014-89-J-3088 ..... N92-11764
N00014-90-J-1193 ..... N92-11908
N92-11909
N00014-90-J-1769 ..... N92-11178
N00014-90-J-1785 ..... N92-11605
N00014-90-J-1952 ..... N92-11886
N00014-90-J-1994 ..... N92-11632
N00014-91-C-0001 ..... N92-11117
N00014-91-C-0095 ..... N92-11367
N00014-91-C-0117 ..... N92-11680
N00014-91-J-1198 ..... N92-11776
N00014-91-J-1243 ..... N92-11624
N00014-91-J-1269 ..... N92-11912
N00019-89-C-0275 ..... N92-11364
ORNL ORDER 19X-3591-C N92-11821
PNTS-AI/0693/1769 ..... N92-11401
PROJ. 90-17 ..... N92-11142
PROJ. 723194 ..... N92-11560
RICIS PROJ. AI-19 ..... N92-11662
RICIS PROJ. SE-19 ..... N92-11663
N92-11664
N92-11665
N92-11666
N92-11667
RICIS PROJ. SE-34 ..... N92-11702
STPA-BT-85-95-004 ..... N92-11755
STPA-85-95-009 ..... N92-11009
STPA-85-95-009-51 ..... N92-11309
SWRI PROJ. 05-3531 ..... N92-11652
SWRI PROJ. 15-3399 ..... N92-11898
W-31-109-ENG-38 ..... N92-11163
N92-11291
N92-11321
N92-11322
N92-11330
N92-11353
N92-11660
N92-11710
N92-11726
N92-11731
N92-11777
N92-11778
N92-11785
N92-11871
N92-11888
N92-11899
N92-11900
N92-11916
W-7405-ENG-36 ..... N92-11330
N92-11615
N92-11895
N92-11896
N92-11897
N92-11961
W-7405-ENG-48 ..... N92-11174
N92-11227
N92-11344
N92-11348
N92-11368
N92-11390
N92-11690
N92-11709
N92-11771
N92-11781
N92-11786
N92-11789
N92-11794
N92-11873
N92-11874
N92-11876
N92-11939
N92-11940
W-7405-ENG-82 ..... N92-11903
108-41-60 ..... N92-11745
199-04-16-11 ..... N92-11685
307-51-00 ..... N92-11188
474-46-10 ..... N92-11139
474-74-10 ..... N92-11086
505-59-30-01 ..... N92-10982
505-59-36 ..... N92-11000
505-59-40 ..... N92-11301
505-59-54-01 ..... N92-11022
505-59-85-01 ..... N92-11030
505-61-51 ..... N92-10981
N92-10983
N92-11629
505-62-00 ..... N92-11202
505-62-21 ..... N92-11302
N92-11320
N92-11328
N92-11691
505-62-30-01 ..... N92-10975
505-62-40 ..... N92-11013
505-62-52 ..... N92-11299
505-63-5B N92-10979
N92-11375
N92-11378
N92-11379
N92-11388
505-63-50-04 ..... N92-11149
N92-11391
505-63-50-15 ..... N92-11010
505-63-51-09 ..... N92-11758
505-64-70-01 ..... N92-11742
505-68-10-01 ..... N92-10994
505-69-40 ..... N92-11034
505-90-01 ..... N92-11317
505-90-52-01 ..... N92-11162
N92-11640
N92-11669
N92-11670
N92-11672

	N92-11728
	N92-11736
506-40-21-01	N92-11319
506-40-91-01	N92-11285
	N92-11300
506-41-41	N92-11133
	N92-11951
506-42-31	N92-11136
506-42-72	N92-11126
506-43-41-01	N92-11087
506-43-71-05	N92-11668
506-46-21-56	N92-11704
	N92-11705
	N92-11706
506-48-00	N92-11129
506-49-3101	N92-11035
506-59-61-01	N92-11338
510-01-50	N92-11387
510-02-11	N92-11207
537-02-23	N92-10976
537-03-21-03	N92-11759
	N92-11765
553-13-00	N92-11373
582-01-11	N92-11017
	N92-11128
590-12-12	N92-11673
590-13-11	N92-11252
590-13-21	N92-11138
590-14-31-02	N92-11392
590-14-41-02	N92-11073
590-21-31	N92-10979
590-41-14-03	N92-11036
	N92-11559
591-23-00	N92-11208
591-41-41	N92-11135
592-01-11-12	N92-11065
593-12-11	N92-11130
593-71-00	N92-11088
593-71-11	N92-11137
694-03-OH	N92-11221
694-03-0C	N92-11217
763-01-21	N92-11214
992-35-12-18	N92-11340

Typical Report Number Index Listing

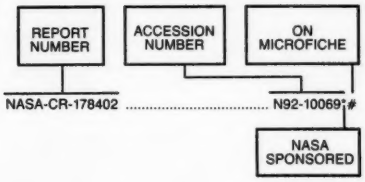

Listings in this index are arranged alphanumerically by report number. The accession number denotes the number by which the citation is identified. An asterisk (*) indicates that the item is a NASA report. A pound sign (#) indicates that the item is available on microfiche.

A-90210 ..... N92-10983* #
A-91032 ..... N92-11629* #
A-91037 ..... N92-11745* #
A-91056 ..... N92-10981* #
A-91115-PT-1 ..... N92-11303* #
A-91167 ..... N92-11673* #
A-91190 ..... N92-11000* #

AAAF-NT-89-12 ..... N92-11020 #
AAAF-NT-89-28 ..... N92-11288 #

AAMRL-TR-90-062 ..... N92-11134 #

AD-A231409 ..... N92-11649 #
AD-A231410 ..... N92-11650 #
AD-A231414 ..... N92-10995 #
AD-A231439 ..... N92-11651 #
AD-A231476 ..... N92-11363 #
AD-A239818 ..... N92-11604 #
AD-A239969 ..... N92-11630 #
AD-A240048 ..... N92-10984 #
AD-A240075 ..... N92-11364 #
AD-A240151 ..... N92-11175 #
AD-A240152 ..... N92-11907 #
AD-A240153 ..... N92-11631 #
AD-A240155 ..... N92-11274 #
AD-A240156 ..... N92-11275 #
AD-A240157 ..... N92-11176 #
AD-A240169 ..... N92-11015 #
AD-A240175 ..... N92-11674 #
AD-A240185 ..... N92-11211 #
AD-A240193 ..... N92-11346 #
AD-A240195 ..... N92-11164 #
AD-A240196 ..... N92-11380 #
AD-A240199 ..... N92-11605 #
AD-A240200 ..... N92-11143 #
AD-A240202 ..... N92-11624 #
AD-A240207 ..... N92-11933 #
AD-A240221 ..... N92-11018 #
AD-A240243 ..... N92-11746 #
AD-A240249 ..... N92-11675 #
AD-A240250 ..... N92-11333 #
AD-A240255 ..... N92-11761 #
AD-A240256 ..... N92-10985 #
AD-A240257 ..... N92-11231 #
AD-A240258 ..... N92-11747 #
AD-A240260 ..... N92-11676 #
AD-A240261 ..... N92-11677 #
AD-A240262 ..... N92-11606 #
AD-A240263 ..... N92-10986 #
AD-A240264 ..... N92-11334 #
AD-A240276 ..... N92-11908 #
AD-A240278 ..... N92-11909 #
AD-A240281 ..... N92-11625 #
AD-A240286 ..... N92-11707 #
AD-A240288 ..... N92-11134 #
AD-A240298 ..... N92-11381 #
AD-A240311 ..... N92-11775 #
AD-A240313 ..... N92-11632 #
AD-A240314 ..... N92-11561* #
AD-A240320 ..... N92-11607 #
AD-A240333 ..... N92-11737 #
AD-A240347 ..... N92-11002 #
AD-A240352 ..... N92-11910 #
AD-A240358 ..... N92-11678 #
AD-A240359 ..... N92-11957 #
AD-A240364 ..... N92-11633 #
AD-A240365 ..... N92-11748 #
AD-A240366 ..... N92-11613 #
AD-A240369 ..... N92-11382 #
AD-A240370 ..... N92-11634 #
AD-A240372 ..... N92-11080 #
AD-A240373 ..... N92-11081 #
AD-A240376 ..... N92-11165 #
AD-A240378 ..... N92-11738 #
AD-A240386 ..... N92-11626 #
AD-A240391 ..... N92-11911 #
AD-A240392 ..... N92-11585 #
AD-A240393 ..... N92-11189 #
AD-A240394 ..... N92-11594 #
AD-A240398 ..... N92-11232 #
AD-A240401 ..... N92-11177 #
AD-A240410 ..... N92-11233 #
AD-A240411 ..... N92-11608 #
AD-A240429 ..... N92-11752 #
AD-A240430 ..... N92-11278 #
AD-A240432 ..... N92-11925 #
AD-A240433 ..... N92-11357 #
AD-A240453 ..... N92-11562 #
AD-A240454 ..... N92-11563 #
AD-A240455 ..... N92-11564 #
AD-A240456 ..... N92-11586 #
AD-A240457 ..... N92-11958 #
AD-A240458 ..... N92-11595 #
AD-A240467 ..... N92-11003 #
AD-A240468 ..... N92-11912 #
AD-A240481 ..... N92-11614 #
AD-A240486 ..... N92-11011 #
AD-A240489 ..... N92-11596 #
AD-A240496 ..... N92-11178 #
AD-A240497 ..... N92-11190 #
AD-A240505 ..... N92-11234 #
AD-A240506 ..... N92-11679 #
AD-A240510 ..... N92-11597 #
AD-A240520 ..... N92-11082 #
AD-A240521 ..... N92-11235 #
AD-A240522 ..... N92-11019 #
AD-A240528 ..... N92-11578 #
AD-A240530 ..... N92-11762 #
AD-A240531 ..... N92-11776 #
AD-A240532 ..... N92-11191 #
AD-A240544 ..... N92-11236 #
AD-A240545 ..... N92-11004 #
AD-A240549 ..... N92-11237 #
AD-A240552 ..... N92-11238 #
AD-A240553 ..... N92-11239 #
AD-A240554 ..... N92-11635 #
AD-A240560 ..... N92-11304 #
AD-A240566 ..... N92-11636 #
AD-A240587 ..... N92-11024* #
AD-A240589 ..... N92-11037 #
AD-A240595 ..... N92-11005 #
AD-A240600 ..... N92-11383 #
AD-A240614 ..... N92-11025 #
AD-A240616 ..... N92-10987 #
AD-A240621 ..... N92-11026 #
AD-A240622 ..... N92-11027 #
AD-A240623 ..... N92-11166 #
AD-A240624 ..... N92-11167 #
AD-A240625 ..... N92-11365 #
AD-A240627 ..... N92-11179 #
AD-A240636 ..... N92-11680 #
AD-A240638 ..... N92-11006 #
AD-A240639 ..... N92-11007 #
AD-A240641 ..... N92-11763 #
AD-A240642 ..... N92-11764 #
AD-A240646 ..... N92-11886 #
AD-A240650 ..... N92-11213 #
AD-A240651 ..... N92-11192 #
AD-A240654 ..... N92-11180 #
AD-A240655 ..... N92-11240 #
AD-A240656 ..... N92-11241 #
AD-A240667 ..... N92-11242 #
AD-A240668 ..... N92-11681 #
AD-A240673 ..... N92-11682 #
AD-A240679 ..... N92-11193 #
AD-A240680 ..... N92-11335 #
AD-A240686 ..... N92-11587 #
AD-A240687 ..... N92-11609 #
AD-A240693 ..... N92-11565 #
AD-A240702 ..... N92-11598 #
AD-A240703 ..... N92-11008 #
AD-A240712 ..... N92-11926 #
AD-A240714 ..... N92-11566 #
AD-A240716 ..... N92-11638* #
AD-A240722 ..... N92-11194 #
AD-A240743 ..... N92-11305 #
AD-A240745 ..... N92-11683 #
AD-A240746 ..... N92-11599 #
AD-A240747 ..... N92-11366 #
AD-A240751 ..... N92-11749 #
AD-A240753 ..... N92-11195 #
AD-A240754 ..... N92-11196 #
AD-A240764 ..... N92-11243 #
AD-A240765 ..... N92-11244 #
AD-A240766 ..... N92-11358* #
AD-A240767 ..... N92-11197 #
AD-A240770 ..... N92-11083 #
AD-A240777 ..... N92-11367 #
AD-A240780 ..... N92-11787 #

AD-D014950 ..... N92-11788 #
AD-D014951 ..... N92-11343 #
AD-D014955 ..... N92-11356 #
AD-D014956 ..... N92-11276 #
AD-D014958 ..... N92-11229 #
AD-D014959 ..... N92-11212 #
AD-D014962 ..... N92-11792
AD-D014965 ..... N92-11760 #
AD-D014966 ..... N92-11277
AD-D014968 ..... N92-11347
AD-D014970 ..... N92-11230
AD-D014971 ..... N92-11646
AD-D014977 ..... N92-11245
AD-D014979 ..... N92-11569
AD-D014980 ..... N92-11246
AD-D014981 ..... N92-11144
AD-D014984 ..... N92-11247

AERO-TN-9101 ..... N92-11369 #

AFOSR-91-0706TR ..... N92-11346 #
AFOSR-91-0707TR ..... N92-11631 #
AFOSR-91-0714TR ..... N92-11164 #
AFOSR-91-0717TR ..... N92-11748 #
AFOSR-91-0721TR ..... N92-11678 #
AFOSR-91-0727TR ..... N92-11613 #
AFOSR-91-0728TR ..... N92-11957 #
AFOSR-91-0730TR ..... N92-10984 #
AFOSR-91-0739TR ..... N92-11633 #
AFOSR-91-0740TR ..... N92-11018 #
AFOSR-91-0741 ..... N92-11675 #
AFOSR-91-0742TR ..... N92-11907 #
AFOSR-91-0743TR ..... N92-11175 #
AFOSR-91-0745TR ..... N92-11176 #
AFOSR-91-0746TR ..... N92-11275 #
AFOSR-91-0748TR ..... N92-11274 #
AFOSR-91-0750TR ..... N92-11707 #
AFOSR-91-0751TR ..... N92-11382 #
AFOSR-91-0754TR ..... N92-11080 #
AFOSR-91-0755TR ..... N92-11081 #
AFOSR-91-0758TR ..... N92-11634 #

AFWAL-TR-88-4234 ..... N92-11363 #

AGARD-AR-280 ..... N92-11001 #

AI-M-1106 ..... N92-11649 #
AI-M-1236 ..... N92-11650 #

AIAA-91-1379 ..... N92-11129* #
AIAA-91-1999 ..... N92-11126* #
AIAA-91-2581 ..... N92-10976* #
AIAA-91-3175 ..... N92-11034* #
AIAA-91-3196 ..... N92-11013* #
AIAA-91-3438 ..... N92-11135* #
AIAA-91-3499 ..... N92-11136* #

AIAA-91-3503 ..... N92-11137* #
AIAA-91-3578 ..... N92-11126* #
AIAA-91-3601 ..... N92-11130* #

AID-PN-ABG-833 ..... N92-11573 #

AK-RD-91-05 ..... N92-11567 #

AL-TP-1991-0018 ..... N92-11636 #
AL-TP-1991-0022 ..... N92-11630 #
AL-TP-1991-0032 ..... N92-11635 #

ALS/TR-91-007 ..... N92-11282 #
ALS/TR-91-015 ..... N92-11793 #

ANL-90/51 ..... N92-11322 #
ANL-91/15 ..... N92-11710 #

ANL/CP-71984 ..... N92-11330 #
ANL/CP-72218 ..... N92-11900 #
ANL/CP-72758 ..... N92-11163 #
ANL/CP-73037 ..... N92-11777 #
ANL/CP-73548 ..... N92-11888 #
ANL/CP-73796 ..... N92-11660 #
ANL/CP-73798 ..... N92-11726 #
ANL/CP-74020 ..... N92-11916 #
ANL/CP-74237 ..... N92-11778 #

ANL/ESD/TM-16 ..... N92-11291 #
ANL/ESD/TM-18 ..... N92-11353 #

ANL/FPP/TM-255 ..... N92-11871 #

ANL/MFRI-8 ..... N92-11321 #

ANL/PP-64910 ..... N92-11785 #

AR-006-351 ..... N92-11273 #
AR-006-375 ..... N92-11209 #
AR-006-626 ..... N92-11376 #

ARACOR-FR-743-91 ..... N92-11365 #

ARACOR-FR469-88 ..... N92-11363 #

ARI-SR-16 ..... N92-11749 #

ARL-STRUC-R-444 ..... N92-11376 #

AVSCOM-TR-91-A-003 ..... N92-10981* #

BHTI-699-099-329 ..... N92-10999* #

BNL-46474 ..... N92-11784 #
BNL-46582 ..... N92-11350 #
BNL-46608 ..... N92-11351 #

CA/TL-91-03 ..... N92-10991 #

CAL-1922 ..... N92-11332* #

CAS-PUBL-76 ..... N92-11953 #
CAS-PUBL-77 ..... N92-11954 #

CD-4 ..... N92-11295* #
CD-21 ..... N92-11296* #

CERC-MP-91-7 ..... N92-11607 #

CERC-TR-91-6 ..... N92-11608 #

CERT-DERA-1/7735 ..... N92-11927 #

CERT-RF-1/3369-00/DERI-GAN ..... N92-10988 #

CERT-RSF-DERAT-62/5004-31 ..... N92-11309 #

CERT-RT-63/5618-54 ..... N92-11306 #
CERT-RT-65/5604-35 ..... N92-11307 #

CIT-REF-06/769E(5) ..... N92-11015 #

CMOTT-91-08 ..... N92-11302* #

CMU-RI-TR-91-11 ..... N92-11244 #
CMU-RI-TR-91-12 ..... N92-11234 #
CMU-RI-TR-91-13 ..... N92-11358* #
CMU-RI-TR-91-16 ..... N92-11679 #

CMU/SEI-91-TR-17 ..... N92-11926 #

CONF-901059-1 ..... N92-11754 #
CONF-910189-2 ..... N92-11726 #
CONF-910247-3 ..... N92-11344 #
CONF-910298-2 ..... N92-11771 #
CONF-910399-3-REV-1 ..... N92-11368 #
CONF-910430-19 ..... N92-11901 #
CONF-910505-396 ..... N92-11784 #
CONF-910505-399 ..... N92-11876 #
CONF-910626-12 ..... N92-11786 #
CONF-910711-7 ..... N92-11940 #
CONF-910736-7 ..... N92-11899 #
CONF-910736-17 ..... N92-11906 #
CONF-910774-76 ..... N92-11330 #
CONF-910799-1 ..... N92-11709 #
CONF-910802-2 ..... N92-11568 #
CONF-910803-3 ..... N92-11216 #
CONF-910869-5 ..... N92-11888 #
CONF-910869-7 ..... N92-11249 #
CONF-910869-10 ..... N92-11889 #
CONF-910869-11 ..... N92-11250 #
CONF-910874-2 ..... N92-11206 #
CONF-911003-8 ..... N92-11372 #
CONF-911003-9 ..... N92-11355 #
CONF-911003-13 ..... N92-11174 #
CONF-911003-15 ..... N92-11362 #
CONF-911048-1 ..... N92-11389 #
CONF-911115-2 ..... N92-11283 #
CONF-911179-1 ..... N92-11173 #
CONF-9009320-2 ..... N92-11935 #
CONF-9009427-1 ..... N92-11777 #
CONF-9010298-12 ..... N92-11939 #
CONF-9104203-5 ..... N92-11874 #
CONF-9104210-7 ..... N92-11873 #
CONF-9104258-2 ..... N92-11687 #
CONF-9104290-1 ..... N92-11660 #
CONF-9105254-1 ..... N92-11181 #
CONF-9106275-1 ..... N92-11183 #
CONF-9106277-1 ..... N92-11182 #
CONF-9107115-26 ..... N92-11789 #
CONF-9107115-42 ..... N92-11163 #
CONF-9107115-46 ..... N92-11794 #
CONF-9107136-6 ..... N92-11900 #
CONF-9107155-2 ..... N92-11904 #
CONF-9107170-1 ..... N92-11916 #
CONF-9108114-2 ..... N92-11168 #
CONF-9108118-7 ..... N92-11350 #
CONF-9108118-8 ..... N92-11351 #
CONF-9108132-1 ..... N92-11725 #
CONF-9108141-2-EXC ..... N92-11961 #
CONF-9108142-2 ..... N92-11778 #
CONF-9108150-2 ..... N92-11781 #
CONF-9108153-1 ..... N92-11905 #
CONF-9108156-1 ..... N92-11204 #
CONF-9108160-1 ..... N92-11779 #
CONF-9109108-7 ..... N92-11227 #
CONF-9109200-1 ..... N92-11894 #
CONF-9109266-1 ..... N92-11205 #
CONF-9109274-1 ..... N92-11203 #

CPIA-PUBL-557-VOL-3 ..... N92-11117 #

CRC-574 ..... N92-11357 #

CRDEC-TR-290 ..... N92-11167 #

CSC/TM-91/6102 ..... N92-11702* #

CTA-IEAV-NT-006/90 ..... N92-11571 #

DE91-014534 ..... N92-11935 #
DE91-016406 ..... N92-11899 #
DE91-016516 ..... N92-11900 #
DE91-016607 ..... N92-11227 #
DE91-016896 ..... N92-11160 #
DE91-016906 ..... N92-11575 #
DE91-016918 ..... N92-11873 #
DE91-016922 ..... N92-11939 #
DE91-016923 ..... N92-11344 #
DE91-016924 ..... N92-11789 #
DE91-016925 ..... N92-11874 #
DE91-016926 ..... N92-11771 #
DE91-016927 ..... N92-11940 #
DE91-016947 ..... N92-11875 #
DE91-016963 ..... N92-11172 #
DE91-016965 ..... N92-11782 #
DE91-016966 ..... N92-11612 #
DE91-016989 ..... N92-11772 #
DE91-017004 ..... N92-11784 #
DE91-017010 ..... N92-11754 #
DE91-017067 ..... N92-11901 #
DE91-017084 ..... N92-11876 #
DE91-017162 ..... N92-11270 #
DE91-017229 ..... N92-11291 #
DE91-017230 ..... N92-11353 #
DE91-017235 ..... N92-11871 #
DE91-017238 ..... N92-11703 #
DE91-017239 ..... N92-11271 #
DE91-017249 ..... N92-11725 #
DE91-017250 ..... N92-11216 #
DE91-017309 ..... N92-11372 #
DE91-017311 ..... N92-11726 #
DE91-017316 ..... N92-11660 #
DE91-017318 ..... N92-11330 #
DE91-017387 ..... N92-11872 #
DE91-017408 ..... N92-11962 #
DE91-017429 ..... N92-11368 #
DE91-017634 ..... N92-11793 #
DE91-017695 ..... N92-11168 #
DE91-017788 ..... N92-11282 #
DE91-017871 ..... N92-11181 #
DE91-017984 ..... N92-11203 #
DE91-017986 ..... N92-11173 #
DE91-017988 ..... N92-11355 #
DE91-017990 ..... N92-11163 #
DE91-017994 ..... N92-11785 #
DE91-017998 ..... N92-11568 #
DE91-018013 ..... N92-11321 #
DE91-018167 ..... N92-11903 #
DE91-018169 ..... N92-11904 #
DE91-018174 ..... N92-11905 #
DE91-018175 ..... N92-11906 #
DE91-018183 ..... N92-11615 #
DE91-018318 ..... N92-11204 #
DE91-018460 ..... N92-11794 #
DE91-018464 ..... N92-11786 #
DE91-018466 ..... N92-11174 #
DE91-018474 ..... N92-11210 #
DE91-018476 ..... N92-11622 #
DE91-018477 ..... N92-11345 #
DE91-018489 ..... N92-11348 #
DE91-018493 ..... N92-11169 #
DE91-018496 ..... N92-11923 #
DE91-018503 ..... N92-11924 #
DE91-018527 ..... N92-11623 #
DE91-018551 ..... N92-11916 #
DE91-018575 ..... N92-11777 #
DE91-018597 ..... N92-11888 #
DE91-018601 ..... N92-11579 #
DE91-018604 ..... N92-11580 #
DE91-018702 ..... N92-11322 #
DE91-018721 ..... N92-11709 #
DE91-018745 ..... N92-11182 #
DE91-018806 ..... N92-11686 #
DE91-018811 ..... N92-11283 #
DE91-018814 ..... N92-11362 #
DE91-018823 ..... N92-11687 #
DE91-018828 ..... N92-11965 #
DE91-018845 ..... N92-11889 #
DE91-018852 ..... N92-11183 #
DE91-018863 ..... N92-11389 #
DE91-018872 ..... N92-11688 #
DE91-018887 ..... N92-11601 #
DE91-018891 ..... N92-11890 #
DE91-018895 ..... N92-11778 #
DE91-018913 ..... N92-11891 #
DE91-018926 ..... N92-11779 #
DE91-018930 ..... N92-11249 #
DE91-019006 ..... N92-11570 #
DE91-019014 ..... N92-11390 #
DE91-019072 ..... N92-11710 #
DE91-626722 ..... N92-11751 #
DE91-628172 ..... N92-11349 #
DE91-629755 ..... N92-11917 #
DE91-630995 ..... N92-11948 #
DE91-631020 ..... N92-11892 #
DE91-634157 ..... N92-11780 #
DE91-634444 ..... N92-11571 #
DE91-634504 ..... N92-11170 #
DE91-635593 ..... N92-11323 #
DE91-635594 ..... N92-11324 #
DE91-635705 ..... N92-11325 #
DE92-000032 ..... N92-11689 #
DE92-000053 ..... N92-11893 #
DE92-000056 ..... N92-11205 #
DE92-000065 ..... N92-11250 #
DE92-000076 ..... N92-11894 #
DE92-000077 ..... N92-11206 #
DE92-000088 ..... N92-11781 #
DE92-000096 ..... N92-11690 #
DE92-000138 ..... N92-11895 #
DE92-000140 ..... N92-11896 #
DE92-000141 ..... N92-11897 #
DE92-000258 ..... N92-11961 #
DE92-000482 ..... N92-11350 #
DE92-000483 ..... N92-11351 #
DE92-704012 ..... N92-11326 #
DE92-704014 ..... N92-10998 #
DE92-704034 ..... N92-11327 #

DODA-006-443 ..... N92-10995 #

DOE/BP-06048/1 ..... N92-11270 #

DOE/CE-50182/T3 ..... N92-11210 #

DOE/DP-40200/166 ..... N92-11965 #

DOE/EH-0194 N92-11924 #

DOE/ER-0500 N92-11923 #
DOE/ER-0507P N92-11570 #
DOE/ER-13716/2 N92-11612 #
DOE/ER-14080/2 N92-11169 #
DOE/ER-25001/T6 N92-11689 #
DOE/ER-25041/4 N92-11688 #
DOE/ER-25084/2 N92-11686 #
DOE/ER-40251/6 N92-11782 #
DOE/ER-40317/7 N92-11935 #
DOE/ER-40545/T1 N92-11345 #
DOE/ER-40553/2 N92-11172 #
DOE/ER-53207/6 N92-11893 #
DOE/ER-53223/169 N92-11891 #
DOE/ER-53243/4 N92-11875 #
DOE/ER-60932/T1 N92-11575 #
DOE/ER-60951/2 N92-11623 #
DOE/ER-61091/1 N92-11622 #

DOE/ET-53088/503 N92-11872 #
DOE/ET-53088/518 N92-11890 #

DOE/RL-01830T-H6 N92-11579 #
DOE/RL-01830T-H9 N92-11580 #

DOT/FAA/CT-TN91/36 N92-11021 #
DOT/FAA/CT-TN91/43 N92-11028 #
DOT/FAA/CT-TN91/49 N92-11029 #

DOT/FAA/CT-88/32-1 N92-10992 #

DOT/FAA/EE-88-6 N92-11578 #
DOT/FAA/EE-91-3 N92-11578 #

DOT/FAA/RD-90/11 N92-10993 #
DOT/FAA/RD-91/9 N92-11593* #

DTRC/SME-91/34 N92-11381 #

E-6011 N92-11373* #
E-6046 N92-11299* #
E-6123 N92-11252* #
E-6145 N92-11951* #
E-6196 N92-11317* #
E-6257 N92-11320* #
E-6322 N92-10976* #
E-6336 N92-11202* #
E-6350 N92-11129* #
E-6364 N92-11214* #
E-6422 N92-11217* #
E-6439 N92-11691* #
E-6456 N92-11088* #
E-6528 N92-10979* #
E-6530 N92-11208* #
E-6556 N92-11133* #
E-6576 N92-11136* #
E-6579 N92-11135* #
E-6580 N92-11126* #
E-6581 N92-11137* #
E-6584 N92-11130* #
E-6593 N92-11221* #
E-6600 N92-11302* #
E-6601 N92-11086* #
E-6602 N92-11013* #
E-6628 N92-11128* #
E-6635 N92-11188* #
E-6636 N92-11138* #
E-6641 N92-11034* #
E-6650 N92-11017* #
E-6655 N92-11139* #
E-6695 N92-11328* #

EE-SATCOM-91-1 N92-11559* #

EGG-M-91290 N92-11182 #

ERL-0530-RN N92-10995 #

ESA-SP-319-VOL-1 N92-11394 #
ESA-SP-319-VOL-2 N92-11488 #

ESD-TR-91-111 N92-11683 #

ESD-91-TR-17 N92-11926 #

ESL-TR-91-31 N92-11578 #

ESM-28 N92-11780 #

ETL-0498 N92-11599 #
ETL-0587 N92-11564 #
ETL-0589 N92-11563 #
ETL-0590 N92-11562 #

ETN-91-90012 N92-11072

ETN-91-90025 N92-11150 #
ETN-91-90063 N92-11394 #
ETN-91-90064 N92-11488 #
ETN-91-90075 N92-10988 #
ETN-91-90079 N92-11306 #
ETN-91-90080 N92-11307 #
ETN-91-90081 N92-11927 #
ETN-91-90082 N92-11009 #
ETN-91-90084 N92-11308 #
ETN-91-90085 N92-11309 #
ETN-91-90086 N92-11310 #
ETN-91-90089 N92-11713 #
ETN-91-90090 N92-11145 #
ETN-91-90091 N92-11588 #
ETN-91-90092 N92-11755 #
ETN-91-90093 N92-11146 #
ETN-91-90094 N92-11311 #
ETN-91-90095 N92-11312 #
ETN-91-90096 N92-10989 #
ETN-91-90097 N92-11963 #
ETN-91-90104 N92-11313 #
ETN-91-90114 N92-11248 #
ETN-91-90115 N92-11337 #
ETN-91-90131 N92-11147 #
ETN-91-90132 N92-11314 #
ETN-91-90133 N92-11913 #
ETN-91-90134 N92-11756 #
ETN-91-90143 N92-11315 #
ETN-91-90145 N92-11914 #
ETN-91-90146 N92-11919 #
ETN-91-90147 N92-11684 #
ETN-91-90148 N92-11915 #
ETN-91-90149 N92-11279 #
ETN-91-90150 N92-11750 #
ETN-91-90151 N92-11739 #
ETN-91-90152 N92-11708 #
ETN-91-90153 N92-11887 #
ETN-91-90160 N92-11928 #
ETN-91-90162 N92-11647 #
ETN-91-90163 N92-11757 #
ETN-91-90181 N92-11740 #
ETN-91-90199 N92-10996 #
ETN-91-90200 N92-11280 #
ETN-91-90201 N92-11281 #
ETN-91-90202 N92-11741 #
ETN-91-90203 N92-11316 #
ETN-91-90204 N92-11360 #
ETN-91-90205 N92-11385 #
ETN-91-90206 N92-11148 #
ETN-91-90208 N92-11386 #
ETN-91-90209 N92-10997 #
ETN-91-90233 N92-11964 #
ETN-91-99483 N92-11253 #
ETN-91-99864 N92-11184
ETN-91-99865 N92-11342
ETN-91-99871 N92-11766
ETN-91-99872 N92-11767
ETN-91-99876 N92-11185
ETN-91-99877 N92-11171
ETN-91-99878 N92-11370
ETN-91-99880 N92-11289 #
ETN-91-99882 N92-11768 #
ETN-91-99898 N92-11714 #
ETN-91-99909 N92-11287 #
ETN-91-99953 N92-11020 #
ETN-91-99969 N92-11288 #
ETN-91-99987 N92-11222 #

FEI-1974 N92-11170 #
FEI-1981 N92-11323 #
FEI-2017 N92-11324 #
FEI-2047 N92-11325 #

FERMILAB-CONF-91/202-A N92-11945* #
FERMILAB-CONF-91/214-A N92-11941* #
FERMILAB-CONF-91/239-A N92-11942* #
FERMILAB-CONF-91/266-A N92-11946* #

FERMILAB-PUB-91/203-A N92-11947* #
FERMILAB-PUB-91/206-A N92-11956* #
FERMILAB-PUB-91/207-A N92-11774* #
FERMILAB-PUB-91/240-A N92-11943* #
FERMILAB-PUB-91/260-A N92-11944* #

GETA-91-02 N92-11352 #

GL-TR-90-0340 N92-10987 #

GORMP-20 N92-11576* #
GORMP-20 N92-11577* #

GRI-91/0070 N92-11352 #

H-1672 N92-11301* #

HSRC-C910684 N92-11018 #

IC-AERO-89-04 N92-11289 #

ICASE-IR-19 N92-11728* #

ICASE-91-68 N92-11640* #
ICASE-91-69 N92-11162* #
ICASE-91-72 N92-11670* #
ICASE-91-73 N92-11669* #
ICASE-91-77 N92-11736* #
ICASE-91-79 N92-11672* #

ICOMP-91-19 N92-11302* #
ICOMP-91-23 N92-11328* #

IFSR-503 N92-11872 #
IFSR-518 N92-11890 #

ILR-MITT-243(1990) N92-11360 #
ILR-MITT-244(1990) N92-11385 #
ILR-MITT-259(1991) N92-11148 #
ILR-MITT-262(1991) N92-11386 #
ILR-MITT-263(1991) N92-10997 #

IMAG-RR-579 N92-11718 #

INIS-MF-12808 N92-11751 #

INT-PATENT-CLASS-A61B-8/00 N92-11621*

IPPCZ-304 N92-11881 #
IPPCZ-308 N92-11773 #

IQI-F-91-0726 N92-11364 #

IS-T-1494 N92-11903 #

ISBN-0-87938-482-4 N92-11031
ISBN-2-7170-0945-0 N92-11020 #
ISBN-2-7170-0961-2 N92-11288 #
ISBN-3-7696-9405-8 N92-11072
ISBN-90-386-0031-3 N92-11147 #
ISBN-92-807-1255-1 N92-11576* #
ISBN-92-835-0632-4 N92-11001 #
ISBN-92-9092-118-8 N92-11394 #
ISBN-92-9092-118-8 N92-11488 #

ISSN-0065-5325 N92-11072
ISSN-0143-7313 N92-11171
ISSN-0178-0719 N92-11280 #
ISSN-0178-0719 N92-11281 #
ISSN-0243-0177 N92-11020 #
ISSN-0243-0177 N92-11288 #
ISSN-0308-7247 N92-11289 #
ISSN-0309-3050 N92-11184
ISSN-0309-3050 N92-11342
ISSN-0379-6566 N92-11394 #
ISSN-0379-6566 N92-11488 #
ISSN-0389-4010 N92-10980 #
ISSN-0389-4010 N92-11127 #
ISSN-0389-4010 N92-11298 #
ISSN-0751-1337 N92-11337 #
ISSN-0751-1345 N92-11248 #
ISSN-0915-633X N92-11796 #
ISSN-0915-633X N92-11797 #
ISSN-0915-633X N92-11877 #
ISSN-0915-633X N92-11878 #
ISSN-0915-633X N92-11879 #
ISSN-0915-633X N92-11880 #
ISSN-0915-633X N92-11882 #
ISSN-0915-633X N92-11883 #
ISSN-0915-633X N92-11884 #
ISSN-0915-633X N92-11885 #
ISSN-0915-6348 N92-11798 #
ISSN-0915-6348 N92-11799 #
ISSN-0955-9655 N92-11766
ISSN-0955-9655 N92-11767
ISSN-0959-2423 N92-11185
ISSN-0959-2423 N92-11370

JIAA-TR-104 N92-10990* #

JPRS-ULS-91-012 N92-11611 #
JPRS-ULS-91-015 N92-11610 #
JPRS-ULS-91-017 N92-11616 #

JPRS-USP-91-005 N92-11032 #

KAERI/RR-830/89 N92-11349 #
KAERI/RR-837/89 N92-11917 #

L-16850 N92-11758* #
L-16899 N92-10994* #
L-16902 N92-10975* #
L-16907 N92-11285* #
L-16913 N92-11765* #
L-16915 N92-11035* #

L-16949 ..... N92-11685* #
L-16974 ..... N92-11030* #

LA-UR-91-2911 ..... N92-11961 #

LA-12184-MS ..... N92-11615 #

LBL-29553 ..... N92-11754 #
LBL-30599 ..... N92-11772 #
LBL-30784 ..... N92-11160 #

LESC-29483 ..... N92-11561* #

M-671 ..... N92-11142* #
M-672 ..... N92-11218* #

MBB-Z-0371-91-PUB ..... N92-10996 #

MBE-225 ..... N92-11281 #

MM-27010-91-1 ..... N92-11191 #

MPE-224 ..... N92-11280 #

MRL-TR-91-5 ..... N92-11273 #
MRL-TR-91-22 ..... N92-11209 #

MTL-TR-91-16 ..... N92-11189 #

NADC-90122-60 ..... N92-11177 #

NAL-TR-1091 ..... N92-11127 #
NAL-TR-1095 ..... N92-11298 #
NAL-TR-1101T ..... N92-10980 #

NAS 1.15:4298 ..... N92-11783* #
NAS 1.15:4299 ..... N92-11929* #
NAS 1.15:4306 ..... N92-11035* #
NAS 1.15:4318 ..... N92-11030* #
NAS 1.15:4325 ..... N92-11131* #
NAS 1.15:4330 ..... N92-11301* #
NAS 1.15:100759 ..... N92-11583* #
NAS 1.15:102842 ..... N92-10983* #
NAS 1.15:102868 ..... N92-11629* #
NAS 1.15:103755 ..... N92-11373* #
NAS 1.15:103823 ..... N92-11038* #
NAS 1.15:103830 ..... N92-11745* #
NAS 1.15:103856 ..... N92-11303* #
NAS 1.15:103870 ..... N92-11673* #
NAS 1.15:103876 ..... N92-11000* #
NAS 1.15:104107 ..... N92-11300* #
NAS 1.15:104115 ..... N92-11668* #
NAS 1.15:104133 ..... N92-11207* #
NAS 1.15:104138 ..... N92-11010* #
NAS 1.15:104148 ..... N92-11340* #
NAS 1.15:104149 ..... N92-11073* #
NAS 1.15:104150 ..... N92-11759* #
NAS 1.15:104152 ..... N92-11022* #
NAS 1.15:104153 ..... N92-11392* #
NAS 1.15:104160 ..... N92-11149* #
NAS 1.15:104162 ..... N92-11742* #
NAS 1.15:104386 ..... N92-11317* #
NAS 1.15:104424 ..... N92-11320* #
NAS 1.15:104475 ..... N92-10976* #
NAS 1.15:104488 ..... N92-11202* #
NAS 1.15:104492 ..... N92-11129* #
NAS 1.15:104503 ..... N92-11214* #
NAS 1.15:104547 ..... N92-11187* #
NAS 1.15:104549 ..... N92-11584* #
NAS 1.15:104550 ..... N92-11600* #
NAS 1.15:104738 ..... N92-11641* #
NAS 1.15:105010 ..... N92-11921* #
NAS 1.15:105096 ..... N92-11642* #
NAS 1.15:105097 ..... N92-11572* #
NAS 1.15:105100 ..... N92-11067* #
NAS 1.15:105108 ..... N92-11225* #
NAS 1.15:105116 ..... N92-11576* #
NAS 1.15:105117 ..... N92-11577* #
NAS 1.15:105121 ..... N92-11603* #
NAS 1.15:105126 ..... N92-11024* #
NAS 1.15:105146 ..... N92-11217* #
NAS 1.15:105154 ..... N92-11691* #
NAS 1.15:105215 ..... N92-11208* #
NAS 1.15:105232 ..... N92-11133* #
NAS 1.15:105247 ..... N92-11136* #
NAS 1.15:105250 ..... N92-11135* #
NAS 1.15:105251 ..... N92-11126* #
NAS 1.15:105252 ..... N92-11137* #
NAS 1.15:105255 ..... N92-11130* #
NAS 1.15:105261 ..... N92-11221* #
NAS 1.15:105277 ..... N92-11302* #
NAS 1.15:105278 ..... N92-11086* #
NAS 1.15:105291 ..... N92-11128* #
NAS 1.15:105296 ..... N92-11188* #
NAS 1.15:105297 ..... N92-11138* #
NAS 1.15:105298 ..... N92-11034* #

NAS 1.15:105303 ..... N92-11017* #
NAS 1.15:105332 ..... N92-11328* #
NAS 1.21:7037(269) N92-10974*
NAS 1.21:7037(270) N92-10973*
NAS 1.26:4397 ..... N92-11338* #
NAS 1.26:4404 ..... N92-11951* #
NAS 1.26:4405 ..... N92-10979* #
NAS 1.26:4406 ..... N92-10982* #
NAS 1.26:4408 ..... N92-11559* #
NAS 1.26:4409 ..... N92-11065* #
NAS 1.26:4410 ..... N92-11036* #
NAS 1.26:180084 ..... N92-11284* #
NAS 1.26:181893 ..... N92-11319* #
NAS 1.26:183496 ..... N92-11251* #
NAS 1.26:183503 ..... N92-11581* #
NAS 1.26:183505 ..... N92-11648* #
NAS 1.26:183506 ..... N92-11589* #
NAS 1.26:184243 ..... N92-11318* #
NAS 1.26:184245 ..... N92-11079* #
NAS 1.26:184252 ..... N92-11361* #
NAS 1.26:185448 ..... N92-11590* #
NAS 1.26:185633 ..... N92-11331* #
NAS 1.26:185641-VOL-1 ..... N92-11085* #
NAS 1.26:185641-VOL-2 ..... N92-11084* #
NAS 1.26:185664 ..... N92-11769* #
NAS 1.26:186433 ..... N92-10999* #
NAS 1.26:186614 ..... N92-11223* #
NAS 1.26:186626 ..... N92-11724* #
NAS 1.26:186701 ..... N92-11582* #
NAS 1.26:186983 ..... N92-11723* #
NAS 1.26:187101 ..... N92-11016* #
NAS 1.26:187123 ..... N92-11132* #
NAS 1.26:187211 ..... N92-11387* #
NAS 1.26:187222 ..... N92-11379* #
NAS 1.26:187223 ..... N92-11375* #
NAS 1.26:187225 ..... N92-11388* #
NAS 1.26:187233 ..... N92-11013* #
NAS 1.26:187235 ..... N92-11378* #
NAS 1.26:187313 ..... N92-11663* #
NAS 1.26:187314 ..... N92-11743* #
NAS 1.26:187554 ..... N92-11704* #
NAS 1.26:187555 ..... N92-11705* #
NAS 1.26:187556 ..... N92-11706* #
NAS 1.26:187621 ..... N92-11391* #
NAS 1.26:187630 ..... N92-11728* #
NAS 1.26:187632 ..... N92-11640* #
NAS 1.26:187634 ..... N92-11670* #
NAS 1.26:187635 ..... N92-11669* #
NAS 1.26:187693 ..... N92-11297* #
NAS 1.26:187712 ..... N92-11918* #
NAS 1.26:187773 ..... N92-11696* #
NAS 1.26:187818 ..... N92-11652* #
NAS 1.26:187820 ..... N92-11215* #
NAS 1.26:187821 ..... N92-11339* #
NAS 1.26:187979 ..... N92-10990* #
NAS 1.26:188228 ..... N92-11593* #
NAS 1.26:188481 ..... N92-11697* #
NAS 1.26:188792 ..... N92-11140* #
NAS 1.26:188799 ..... N92-11393* #
NAS 1.26:188803 ..... N92-11934* #
NAS 1.26:188814 ..... N92-11294* #
NAS 1.26:188822 ..... N92-11702* #
NAS 1.26:188836 ..... N92-11722* #
NAS 1.26:188840 ..... N92-11692* #
NAS 1.26:188841 ..... N92-11643* #
NAS 1.26:188843 ..... N92-11693* #
NAS 1.26:188844 ..... N92-11694* #
NAS 1.26:188846 ..... N92-11711* #
NAS 1.26:188849 ..... N92-11644* #
NAS 1.26:188853 ..... N92-11695* #
NAS 1.26:188854 ..... N92-11653* #
NAS 1.26:188855 ..... N92-11654* #
NAS 1.26:188867 ..... N92-11655* #
NAS 1.26:188868 ..... N92-11936* #
NAS 1.26:188870 ..... N92-11753* #
NAS 1.26:188871 ..... N92-11698* #
NAS 1.26:188872 ..... N92-11656* #
NAS 1.26:188878 ..... N92-11033* #
NAS 1.26:188883 ..... N92-11645* #
NAS 1.26:188884 ..... N92-11699* #
NAS 1.26:188887 ..... N92-11290* #
NAS 1.26:188896 ..... N92-11657* #
NAS 1.26:188897 ..... N92-11658* #
NAS 1.26:188898 ..... N92-11659* #
NAS 1.26:188899 ..... N92-11700* #
NAS 1.26:188900 ..... N92-11224* #
NAS 1.26:188903 ..... N92-10977* #
NAS 1.26:188906 ..... N92-11701* #
NAS 1.26:188907 ..... N92-11770* #
NAS 1.26:188908 ..... N92-11744* #
NAS 1.26:188914 ..... N92-10978* #
NAS 1.26:188936 ..... N92-11661* #
NAS 1.26:188938 ..... N92-11664* #
NAS 1.26:188940 ..... N92-11667* #
NAS 1.26:188943 ..... N92-11665* #
NAS 1.26:188944 ..... N92-11666* #

NAS 1.26:188949 ..... N92-11662* #
NAS 1.26:188954 ..... N92-11070* #
NAS 1.26:188964 ..... N92-11071* #
NAS 1.26:188978 ..... N92-11955* #
NAS 1.26:188983 ..... N92-11377* #
NAS 1.26:188990 ..... N92-11074* #
NAS 1.26:188991 ..... N92-11161* #
NAS 1.26:188992 ..... N92-11560* #
NAS 1.26:188994 ..... N92-11332* #
NAS 1.26:188995 ..... N92-11023* #
NAS 1.26:188996 ..... N92-11014* #
NAS 1.26:188997 ..... N92-11228* #
NAS 1.26:188998 ..... N92-11637* #
NAS 1.26:188999 ..... N92-11902* #
NAS 1.26:189004 ..... N92-11947* #
NAS 1.26:189005 ..... N92-11956* #
NAS 1.26:189006 ..... N92-11774* #
NAS 1.26:189007 ..... N92-11946* #
NAS 1.26:189008 ..... N92-11945* #
NAS 1.26:189009 ..... N92-11944* #
NAS 1.26:189010 ..... N92-11943* #
NAS 1.26:189011 ..... N92-11942* #
NAS 1.26:189012 ..... N92-11941* #
NAS 1.26:189013 ..... N92-11712* #
NAS 1.26:189014 ..... N92-11561* #
NAS 1.26:189015 ..... N92-11358* #
NAS 1.26:189025 ..... N92-11898* #
NAS 1.26:189042 ..... N92-11162* #
NAS 1.26:189043 ..... N92-11736* #
NAS 1.26:189047 ..... N92-11672* #
NAS 1.26:189056 ..... N92-11139* #
NAS 1.26:189057 ..... N92-11272* #
NAS 1.26:189060 ..... N92-11671* #
NAS 1.26:189242 ..... N92-11329* #
NAS 1.26:189243 ..... N92-11341* #
NAS 1.26:189244 ..... N92-11795* #
NAS 1.26:189246 ..... N92-11920* #
NAS 1.55:3124 ..... N92-11039* #
NAS 1.55:10071 ..... N92-11638* #
NAS 1.55:10079 ..... N92-11088* #
NAS 1.60:3103 ..... N92-10975* #
NAS 1.60:3104 ..... N92-11758* #
NAS 1.60:3119 ..... N92-11252* #
NAS 1.60:3124 ..... N92-11685* #
NAS 1.60:3125 ..... N92-10994* #
NAS 1.60:3130 ..... N92-11087* #
NAS 1.60:3134 ..... N92-11765* #
NAS 1.60:3140 ..... N92-11930* #
NAS 1.60:3141 ..... N92-11931* #
NAS 1.60:3151 ..... N92-10981* #
NAS 1.60:3160 ..... N92-11142* #
NAS 1.60:3163 ..... N92-11218* #
NAS 1.60:3170 ..... N92-11299* #
NAS 1.61:1260 ..... N92-11285* #
NAS 1.71:ARC-11921-1 ..... N92-11286* #
NAS 1.71:LAR-13944-1 ..... N92-11336* #
NAS 1.71:LAR-14046-1 ..... N92-11219* #
NAS 1.71:LAR-14048-1 ..... N92-11220* #
NAS 1.71:LAR-14457-1-CU ..... N92-11198* #
NAS 1.71:LAR-14480-1-CU ..... N92-11374* #
NAS 1.71:LAR-14487-1 ..... N92-11200* #
NAS 1.71:LAR-14538-1 ..... N92-11201* #
NAS 1.71:LAR-14542-1 ..... N92-11354* #
NAS 1.71:LAR-14639-1 ..... N92-11199* #
NAS 1.71:LAR-14741-1 ..... N92-11384* #
NAS 1.71:LEW-14474-2 ..... N92-11186* #
NAS 1.71:MSC-21775-1 ..... N92-11627* #
NAS 1.71:MSC-21799-1 ..... N92-11359* #
NAS 1.71:MSC-21858-1 ..... N92-11628* #
NAS 1.71:MSC-21868-1 ..... N92-11639* #
NAS 1.71:NPO-18007-1-CU ..... N92-11791* #
NAS 1.83:128 ..... N92-11066* #

NASA-CASE-ARC-11921-1 ..... N92-11286* #

NASA-CASE-LAR-13901-2 ..... N92-11621*
NASA-CASE-LAR-13944-1 ..... N92-11336* #
NASA-CASE-LAR-14046-1 ..... N92-11219* #
NASA-CASE-LAR-14048-1 ..... N92-11220* #
NASA-CASE-LAR-14457-1-CU ..... N92-11198* #
NASA-CASE-LAR-14480-1-CU ..... N92-11374* #
NASA-CASE-LAR-14487-1 ..... N92-11200* #
NASA-CASE-LAR-14538-1 ..... N92-11201* #
NASA-CASE-LAR-14542-1 ..... N92-11354* #
NASA-CASE-LAR-14639-1 ..... N92-11199* #
NASA-CASE-LAR-14741-1 ..... N92-11384* #

NASA-CASE-LEW-14474-2 ..... N92-11186* #

NASA-CASE-MSC-21775-1 ..... N92-11627* #
NASA-CASE-MSC-21799-1 ..... N92-11359* #
NASA-CASE-MSC-21858-1 ..... N92-11628* #
NASA-CASE-MSC-21868-1 ..... N92-11639* #

NASA-CASE-NPO-18007-1-CU ..... N92-11791* #

NASA-CP-3124 N92-11039* #
NASA-CP-10071 N92-11638* #
NASA-CP-10079 N92-11088* #

NASA-CR-4397 N92-11338* #
NASA-CR-4404 N92-11951* #
NASA-CR-4405 N92-10979* #
NASA-CR-4406 N92-10982* #
NASA-CR-4408 N92-11559* #
NASA-CR-4409 N92-11065* #
NASA-CR-4410 N92-11036* #
NASA-CR-180084 N92-11284* #
NASA-CR-181893 N92-11319* #
NASA-CR-183496 N92-11251* #
NASA-CR-183503 N92-11581* #
NASA-CR-183505 N92-11648* #
NASA-CR-183506 N92-11589* #
NASA-CR-184243 N92-11318* #
NASA-CR-184245 N92-11079* #
NASA-CR-184252 N92-11361* #
NASA-CR-185448 N92-11590* #
NASA-CR-185633 N92-11331* #
NASA-CR-185641-VOL-1 N92-11085* #
NASA-CR-185641-VOL-2 N92-11084* #
NASA-CR-185664 N92-11769* #
NASA-CR-186433 N92-10999* #
NASA-CR-186614 N92-11223* #
NASA-CR-186626 N92-11724* #
NASA-CR-186701 N92-11582* #
NASA-CR-186983 N92-11723* #
NASA-CR-187101 N92-11016* #
NASA-CR-187123 N92-11132* #
NASA-CR-187211 N92-11387* #
NASA-CR-187222 N92-11379* #
NASA-CR-187223 N92-11375* #
NASA-CR-187225 N92-11388* #
NASA-CR-187233 N92-11013* #
NASA-CR-187235 N92-11378* #
NASA-CR-187313 N92-11663* #
NASA-CR-187314 N92-11743* #
NASA-CR-187554 N92-11704* #
NASA-CR-187555 N92-11705* #
NASA-CR-187556 N92-11706* #
NASA-CR-187621 N92-11391* #
NASA-CR-187630 N92-11728* #
NASA-CR-187632 N92-11640* #
NASA-CR-187634 N92-11670* #
NASA-CR-187635 N92-11669* #
NASA-CR-187693 N92-11297* #
NASA-CR-187712 N92-11918* #
NASA-CR-187773 N92-11696* #
NASA-CR-187818 N92-11652* #
NASA-CR-187820 N92-11215* #
NASA-CR-187821 N92-11339* #
NASA-CR-187979 N92-10990* #
NASA-CR-188228 N92-11593* #
NASA-CR-188481 N92-11697* #
NASA-CR-188792 N92-11140* #
NASA-CR-188799 N92-11393* #
NASA-CR-188803 N92-11934* #
NASA-CR-188814 N92-11294* #
NASA-CR-188822 N92-11702* #
NASA-CR-188836 N92-11722* #
NASA-CR-188840 N92-11692* #
NASA-CR-188841 N92-11643* #
NASA-CR-188843 N92-11693* #
NASA-CR-188844 N92-11694* #
NASA-CR-188846 N92-11711* #
NASA-CR-188849 N92-11644* #
NASA-CR-188853 N92-11695* #
NASA-CR-188854 N92-11653* #
NASA-CR-188855 N92-11654* #
NASA-CR-188867 N92-11655* #
NASA-CR-188868 N92-11936* #
NASA-CR-188870 N92-11753* #
NASA-CR-188871 N92-11698* #
NASA-CR-188872 N92-11656* #
NASA-CR-188878 N92-11033* #
NASA-CR-188883 N92-11645* #
NASA-CR-188884 N92-11699* #
NASA-CR-188887 N92-11290* #
NASA-CR-188896 N92-11657* #
NASA-CR-188897 N92-11658* #
NASA-CR-188898 N92-11659* #
NASA-CR-188899 N92-11700* #
NASA-CR-188900 N92-11224* #
NASA-CR-188903 N92-10977* #
NASA-CR-188906 N92-11701* #
NASA-CR-188907 N92-11770* #
NASA-CR-188908 N92-11744* #
NASA-CR-188914 N92-10978* #
NASA-CR-188936 N92-11661* #
NASA-CR-188938 N92-11664* #
NASA-CR-188940 N92-11667* #
NASA-CR-188943 N92-11665* #
NASA-CR-188944 N92-11666* #
NASA-CR-188949 N92-11662* #
NASA-CR-188954 N92-11070* #
NASA-CR-188964 N92-11071* #
NASA-CR-188978 N92-11955* #
NASA-CR-188983 N92-11377* #
NASA-CR-188990 N92-11074* #
NASA-CR-188991 N92-11161* #
NASA-CR-188992 N92-11560* #
NASA-CR-188994 N92-11332* #
NASA-CR-188995 N92-11023* #
NASA-CR-188996 N92-11014* #
NASA-CR-188997 N92-11228* #
NASA-CR-188998 N92-11637* #
NASA-CR-188999 N92-11902* #
NASA-CR-189004 N92-11947* #
NASA-CR-189005 N92-11956* #
NASA-CR-189006 N92-11774* #
NASA-CR-189007 N92-11946* #
NASA-CR-189008 N92-11945* #
NASA-CR-189009 N92-11944* #
NASA-CR-189010 N92-11943* #
NASA-CR-189011 N92-11942* #
NASA-CR-189012 N92-11941* #
NASA-CR-189013 N92-11712* #
NASA-CR-189014 N92-11561* #
NASA-CR-189015 N92-11358* #
NASA-CR-189025 N92-11898* #
NASA-CR-189042 N92-11162* #
NASA-CR-189043 N92-11736* #
NASA-CR-189047 N92-11672* #
NASA-CR-189056 N92-11139* #
NASA-CR-189057 N92-11272* #
NASA-CR-189060 N92-11671* #
NASA-CR-189242 N92-11329* #
NASA-CR-189243 N92-11341* #
NASA-CR-189244 N92-11795* #
NASA-CR-189246 N92-11920* #

NASA-NP-128 N92-11066* #

NASA-RP-1260 N92-11285* #

NASA-SP-7037(269) N92-10974*
NASA-SP-7037(270) N92-10973*

NASA-TM-4298 N92-11783* #
NASA-TM-4299 N92-11929* #
NASA-TM-4306 N92-11035* #
NASA-TM-4318 N92-11030* #
NASA-TM-4325 N92-11131* #
NASA-TM-4330 N92-11301* #
NASA-TM-80225 N92-11030* #
NASA-TM-84661 N92-11030* #
NASA-TM-100759 N92-11583* #
NASA-TM-102842 N92-10983* #
NASA-TM-102868 N92-11629* #
NASA-TM-103755 N92-11373* #
NASA-TM-103823 N92-11038* #
NASA-TM-103830 N92-11745* #
NASA-TM-103856 N92-11303* #
NASA-TM-103870 N92-11673* #
NASA-TM-103876 N92-11000* #
NASA-TM-104107 N92-11300* #
NASA-TM-104115 N92-11668* #
NASA-TM-104133 N92-11207* #
NASA-TM-104138 N92-11010* #
NASA-TM-104148 N92-11340* #
NASA-TM-104149 N92-11073* #
NASA-TM-104150 N92-11759* #
NASA-TM-104152 N92-11022* #
NASA-TM-104153 N92-11392* #
NASA-TM-104160 N92-11149* #
NASA-TM-104162 N92-11742* #
NASA-TM-104386 N92-11317* #
NASA-TM-104424 N92-11320* #
NASA-TM-104475 N92-10976* #
NASA-TM-104488 N92-11202* #
NASA-TM-104492 N92-11129* #
NASA-TM-104503 N92-11214* #
NASA-TM-104547 N92-11187* #
NASA-TM-104549 N92-11584* #
NASA-TM-104550 N92-11600* #
NASA-TM-104738 N92-11641* #
NASA-TM-105010 N92-11921* #
NASA-TM-105096 N92-11642* #
NASA-TM-105097 N92-11572* #
NASA-TM-105100 N92-11067* #
NASA-TM-105108 N92-11225* #
NASA-TM-105116 N92-11576* #
NASA-TM-105117 N92-11577* #
NASA-TM-105121 N92-11603* #
NASA-TM-105126 N92-11024* #
NASA-TM-105146 N92-11217* #
NASA-TM-105154 N92-11691* #
NASA-TM-105215 N92-11208* #
NASA-TM-105232 N92-11133* #
NASA-TM-105247 N92-11136* #
NASA-TM-105250 N92-11135* #
NASA-TM-105251 N92-11126* #
NASA-TM-105252 N92-11137* #
NASA-TM-105255 N92-11130* #
NASA-TM-105261 N92-11221* #
NASA-TM-105277 N92-11302* #
NASA-TM-105278 N92-11086* #
NASA-TM-105291 N92-11128* #
NASA-TM-105296 N92-11188* #
NASA-TM-105297 N92-11138* #
NASA-TM-105298 N92-11034* #
NASA-TM-105303 N92-11017* #
NASA-TM-105332 N92-11328* #

NASA-TP-3103 N92-10975* #
NASA-TP-3104 N92-11758* #
NASA-TP-3119 N92-11252* #
NASA-TP-3124 N92-11685* #
NASA-TP-3125 N92-10994* #
NASA-TP-3130 N92-11087* #
NASA-TP-3134 N92-11765* #
NASA-TP-3140 N92-11930* #
NASA-TP-3141 N92-11931* #
NASA-TP-3151 N92-10981* #
NASA-TP-3160 N92-11142* #
NASA-TP-3163 N92-11218* #
NASA-TP-3170 N92-11299* #

NAVY-CASE-72700 N92-11229 #
NAVY-CASE-72996 N92-11356 #
NAVY-CASE-73010 N92-11276 #
NAVY-CASE-73298 N92-11212 #

NIFS-PROC-3 N92-11799 #
NIFS-PROC-8 N92-11798 #

NIFS-18 N92-11880 #
NIFS-29 N92-11879 #
NIFS-31 N92-11878 #
NIFS-32 N92-11877 #
NIFS-87 N92-11882 #
NIFS-89 N92-11883 #
NIFS-94 N92-11796 #
NIFS-95 N92-11797 #
NIFS-100 N92-11884 #
NIFS-102 N92-11885 #

NIST/SP-400/72 N92-11269 #

NISTIR-4611 N92-11226 #
NISTIR-4615 N92-11727 #
NISTIR-4622 N92-11712* #

NOSC-TD-2127 N92-11236 #

NPL-DMM(A)-21 N92-11185
NPL-DMM(A)-23 N92-11171
NPL-DMM(A)-25 N92-11370

NPL-QU-87 N92-11184
NPL-QU-89 N92-11342

NPL-RSA(EXT)-18 N92-11766
NPL-RSA(EXT)-19 N92-11767

NRL-MR-6823 N92-11606 #
NRL-MR-6861 N92-11180 #
NRL-MR-6881 N92-11334 #
NRL-MR-6882 N92-11240 #
NRL-MR-6884 N92-11304 #
NRL-MR-6887 N92-11335 #
NRL-MR-6898 N92-11193 #

NRL-9107-PT-1 N92-11238 #
NRL-9310-PT-3 N92-11239 #

NSMRL-1170 N92-11625 #

NSSDC/WDC-A-R/S-91-19 N92-11921* #

ONERA-RSF-44/1147-AY-144A N92-11308 #

ONERA-RT-6/3654-RY-006-R N92-11713 #
ONERA-RT-8/7256-RY-094-R N92-11145 #
ONERA-RT-15/3641-PY N92-11588 #
ONERA-RT-17/1677-RY-091-R N92-11755 #
ONERA-RT-23/3542-RY-093-R N92-11146 #
ONERA-RT-43/1621-RY-006-R N92-11311 #
ONERA-RT-56/1369-AN N92-11312 #
ONERA-RT-56/3064-RY-006-R N92-10989 #

ONERA-RTS-21/4365-AY-056A N92-11009 #
ONERA-RTS-86/1685-AY-156A N92-11310 #

OSU-409 N92-11560* #

OSU-715559-7 ..... N92-11065* #

OTN-033124 ..... N92-10996 #

PB91-100032 ..... N92-11225* #
PB91-192989 ..... N92-11226 #
PB91-193961 ..... N92-11269 #
PB91-194027 ..... N92-11574 #
PB91-194357 ..... N92-11352 #
PB91-201129 ..... N92-11591 #
PB91-201350 ..... N92-11567 #
PB91-202275 ..... N92-10972 #
PB91-202572 ..... N92-11592 #
PB91-204768 ..... N92-10991 #
PB91-209882 ..... N92-11573 #
PB91-216598 ..... N92-11727 #
PB91-217414 ..... N92-11712* #

PL-TR-91-2008 ..... N92-11597 #
PL-TR-91-2009 ..... N92-11566 #
PL-TR-91-2057 ..... N92-11231 #
PL-TR-91-2074 ..... N92-11237 #
PL-TR-91-2104 ..... N92-11775 #
PL-TR-91-2108 ..... N92-11565 #
PL-TR-91-2159 ..... N92-11585 #
PL-TR-91-3018 ..... N92-11787 #
PL-TR-91-3059 ..... N92-11166 #

PNL-SA-19923 ..... N92-11687 #

PNL-7789 ..... N92-11601 #

PUR-91017408 ..... N92-11962 #

PWA-FR-21509 ..... N92-11213 #

PWA-5967-43 ..... N92-11016* #

R/D-5824-AN-01 ..... N92-11015 #
R/D-6105-MA-02 ..... N92-11737 #
R/D-6490-MA-93 ..... N92-11674 #
R/D-6606-BC-02 ..... N92-11614 #

RADC-TR-90-186 ..... N92-11243 #

RAL-90-091 ..... N92-11768 #

RCC-750-91 ..... N92-11026 #

RCC/DG-501-90 ..... N92-11027 #

REPT-86.59 ..... N92-11567 #
REPT-89B00108 ..... N92-11583* #
REPT-91B00130 ..... N92-11039* #
REPT-91B00143 ..... N92-11187* #
REPT-91B00153 ..... N92-11584* #
REPT-91RC11706 ..... N92-11361* #
REPT-92B00006 ..... N92-11600* #
REPT-160-573 ..... N92-11377* #

RI-RD-91-193 ..... N92-11361* #

RI/RD91-150 ..... N92-11132* #

RIACS-TR-89-1 ..... N92-11033* #
RIACS-TR-89-5 ..... N92-11722* #
RIACS-TR-89-02 ..... N92-11743* #
RIACS-TR-89-16 ..... N92-11692* #
RIACS-TR-89-22 ..... N92-11643* #
RIACS-TR-89-24 ..... N92-11693* #
RIACS-TR-89-25 ..... N92-11694* #
RIACS-TR-89-27 ..... N92-11711* #
RIACS-TR-89-30 ..... N92-11644* #
RIACS-TR-89-34 ..... N92-11654* #
RIACS-TR-89-35 ..... N92-11653* #
RIACS-TR-89-38 ..... N92-11695* #
RIACS-TR-89-39 ..... N92-11744* #
RIACS-TR-89-41 ..... N92-11701* #
RIACS-TR-89-43 ..... N92-11770* #
RIACS-TR-89-44 ..... N92-10977* #
RIACS-TR-89-47 ..... N92-11657* #
RIACS-TR-89-48 ..... N92-11658* #
RIACS-TR-89-49 ..... N92-11659* #
RIACS-TR-89-50 ..... N92-11700* #
RIACS-TR-89-51 ..... N92-11224* #
RIACS-TR-90-6 ..... N92-11590* #
RIACS-TR-90-9 ..... N92-11697* #
RIACS-TR-90-12 ..... N92-11724* #
RIACS-TR-90-15 ..... N92-11696* #
RIACS-TR-90-16 ..... N92-11723* #
RIACS-TR-90-19 ..... N92-11223* #
RIACS-TR-90-24 ..... N92-11918* #
RIACS-TR-90-31 ..... N92-11655* #
RIACS-TR-90-33 ..... N92-11936* #
RIACS-TR-90-34 ..... N92-11753* #
RIACS-TR-90-35 ..... N92-11698* #
RIACS-TR-90-36 ..... N92-11656* #
RIACS-TR-90-50 ..... N92-11661* #
RIACS-TR-91-2 ..... N92-11645* #
RIACS-TR-91-03 ..... N92-11699* #
RIACS-TR-91-06 ..... N92-11290* #

RL-TR-91-116 ..... N92-11333 #
RL-TR-91-163 ..... N92-11681 #
RL-TR-91-166 ..... N92-11682 #

R91-957907-3 ..... N92-10979* #
R8807-3-VOL-1 ..... N92-11085* #
R8807-3-VOL-2 ..... N92-11084* #

S-640 ..... N92-11930* #
S-641 ..... N92-11931* #
S-652 ..... N92-11641* #

SAC/DOW/CP-91/001 ..... N92-11003 #

SAND-90-2530C ..... N92-11173 #
SAND-91-0741C ..... N92-11283 #
SAND-91-1326C ..... N92-11355 #
SAND-91-1461C ..... N92-11372 #
SAND-91-1506C ..... N92-11901 #
SAND-91-1728C ..... N92-11899 #
SAND-91-1756C ..... N92-11362 #
SAND-91-1883C ..... N92-11204 #
SAND-91-1890C ..... N92-11568 #
SAND-91-1894C ..... N92-11203 #

SBRC-90-1045 ..... N92-11329* #

SCT-91RR-18 ..... N92-10993 #

SER-C-357 ..... N92-11072

SISSA-104/91/EP ..... N92-11774* #

SI89-R07JWH001 ..... N92-11589* #

SR-1 ..... N92-11237 #
SR-1 ..... N92-11585 #
SR-2 ..... N92-11566 #
SR-8 ..... N92-11565 #

SRI-MP-91-160 ..... N92-11346 #

SSCL-399-REV-1 ..... N92-11271 #
SSCL-413 ..... N92-11703 #

SSD-TR-91-27 ..... N92-11242 #
SSD-TR-91-28 ..... N92-11233 #

SSD-TR00608 ..... N92-11251* #

SWRI-3178-1.6.1 ..... N92-11352 #

TELECOM-PARIS-91-C-001 ..... N92-11337 #
TELECOM-PARIS-91-D-001 ..... N92-11248 #

TR-1 ..... N92-11764 #
TR-11 ..... N92-11763 #
TR-43 ..... N92-11194 #
TR-44 ..... N92-11196 #
TR-90-01 ..... N92-11632 #
TR-009(6925-05)-6 ..... N92-11233 #
TR-930 ..... N92-11683 #
TR-0091(6925-05)-3 ..... N92-11242 #

TRI-PP-89-6 ..... N92-11892 #
TRI-PP-89-7 ..... N92-11948 #

TRW-46179-6041-UT-00 ..... N92-11795* #

TTKK-LT-69 ..... N92-11327 #

UCLA/PPG-1200-VOL-1 ..... N92-11897 #
UCLA/PPG-1200-VOL-2 ..... N92-11896 #
UCLA/PPG-1200-VOL-4 ..... N92-11895 #

UCRL-CR-107856 ..... N92-11390 #

UCRL-ID-107112-PT-2 ..... N92-11348 #

UCRL-JC-104111-REV-1 ..... N92-11368 #
UCRL-JC-105833 ..... N92-11873 #
UCRL-JC-105909 ..... N92-11344 #
UCRL-JC-106273 ..... N92-11876 #
UCRL-JC-106331 ..... N92-11771 #
UCRL-JC-106443 ..... N92-11786 #
UCRL-JC-106888 ..... N92-11794 #
UCRL-JC-106988 ..... N92-11781 #
UCRL-JC-107117 ..... N92-11940 #
UCRL-JC-107382 ..... N92-11874 #
UCRL-JC-107495 ..... N92-11939 #
UCRL-JC-107591 ..... N92-11789 #
UCRL-JC-107685 ..... N92-11227 #
UCRL-JC-107698 ..... N92-11174 #
UCRL-JC-108197 ..... N92-11709 #

UCRL-LR-108186 ..... N92-11690 #

UDR-TR-91-16 ..... N92-11179 #

UMICH-025921-23-T ..... N92-11140* #

US-PATENT-APPL-SN-118993 ..... N92-11621*
US-PATENT-APPL-SN-187804 ..... N92-11230
US-PATENT-APPL-SN-281139 ..... N92-11760 #
US-PATENT-APPL-SN-358213 ..... N92-11621*
US-PATENT-APPL-SN-360173 ..... N92-11646
US-PATENT-APPL-SN-382977 ..... N92-11245
US-PATENT-APPL-SN-395223 ..... N92-11247
US-PATENT-APPL-SN-429426 ..... N92-11347
US-PATENT-APPL-SN-436847 ..... N92-11144
US-PATENT-APPL-SN-463063 ..... N92-11792
US-PATENT-APPL-SN-520472 ..... N92-11198* #
US-PATENT-APPL-SN-532416 ..... N92-11277
US-PATENT-APPL-SN-539942 ..... N92-11569
US-PATENT-APPL-SN-583624 ..... N92-11246
US-PATENT-APPL-SN-635016 ..... N92-11343 #
US-PATENT-APPL-SN-635215 ..... N92-11788 #
US-PATENT-APPL-SN-651062 ..... N92-11199* #
US-PATENT-APPL-SN-652821 ..... N92-11276 #
US-PATENT-APPL-SN-674638 ..... N92-11356 #
US-PATENT-APPL-SN-687602 ..... N92-11229 #
US-PATENT-APPL-SN-695144 ..... N92-11212 #
US-PATENT-APPL-SN-703238 ..... N92-11791* #
US-PATENT-APPL-SN-703649 ..... N92-11286* #
US-PATENT-APPL-SN-705474 ..... N92-11374* #
US-PATENT-APPL-SN-720153 ..... N92-11384* #
US-PATENT-APPL-SN-736880 ..... N92-11201* #
US-PATENT-APPL-SN-743489 ..... N92-11354* #
US-PATENT-APPL-SN-747152 ..... N92-11336* #
US-PATENT-APPL-SN-750158 ..... N92-11200* #
US-PATENT-APPL-SN-759367 ..... N92-11359* #
US-PATENT-APPL-SN-760633 ..... N92-11627* #
US-PATENT-APPL-SN-760670 ..... N92-11186* #
US-PATENT-APPL-SN-765273 ..... N92-11639* #
US-PATENT-APPL-SN-765615 ..... N92-11628* #
US-PATENT-APPL-SN-766597 ..... N92-11219* #
US-PATENT-APPL-SN-766609 ..... N92-11220* #
US-PATENT-APPL-SN-929869 ..... N92-11621*

US-PATENT-CLASS-GU-527 ..... N92-11569

US-PATENT-CLASS-3T1-12 ..... N92-11245
US-PATENT-CLASS-128-661.03 ..... N92-11621*
US-PATENT-CLASS-250-203.3 ..... N92-11247
US-PATENT-CLASS-324-77K N92-11792
US-PATENT-CLASS-324-158P N92-11277
US-PATENT-CLASS-342-6 ..... N92-11246
US-PATENT-CLASS-365-170 ..... N92-11646
US-PATENT-CLASS-367-2 ..... N92-11760 #

US-PATENT-5,003,779 ..... N92-11569
US-PATENT-5,008,680 ..... N92-11230
US-PATENT-5,008,859 ..... N92-11760 #
US-PATENT-5,014,279 ..... N92-11347
US-PATENT-5,022,027 ..... N92-11245
US-PATENT-5,023,545 ..... N92-11277
US-PATENT-5,025,143 ..... N92-11247
US-PATENT-5,025,416 ..... N92-11646
US-PATENT-5,025,849 ..... N92-11144
US-PATENT-5,027,055 ..... N92-11792
US-PATENT-5,036,323 ..... N92-11246
US-PATENT-5,058,591 ..... N92-11621*

USAARL-91-18-VOL-2 ..... N92-11762 #

USAAVSCOM-TR-90-A-004 ..... N92-11629* #

USAFETAC/PR-90/006 ..... N92-11596 #
USAFETAC/PR-91/009 ..... N92-11598 #
USAFETAC/PR-91/011 ..... N92-11011 #
USAFETAC/PR-91/012 ..... N92-11586 #
USAFETAC/PR-91/013 ..... N92-11595 #
USAFETAC/PR-91/017 ..... N92-11594 #

USAFETAC/TN-91/006 ..... N92-11958 #

UTK-90-14 ..... N92-11768 #

UTRC/R91-970057-3 ..... N92-11297* #

UWAERP-33 ..... N92-11875 #

VTT-TIED-1207 ..... N92-11326 #
VTT-TIED-1210 ..... N92-10998 #

WES/TR/GL-91-14 ..... N92-11366 #

WES/TR/SL-91-11 ..... N92-11211 #

WL-TM-91-311-FIBG ..... N92-11383 #

WL-TR-91-2036 ..... N92-11213 #
WL-TR-91-3065 ..... N92-10985 #
WL-TR-91-3073 ..... N92-10986 #
WL-TR-91-4011 ..... N92-11192 #
WL-TR-91-4038 ..... N92-11365 #
WL-TR-91-4050 ..... N92-11179 #
WL-TR-91-4066-VOL-1 ..... N92-11006 #
WL-TR-91-4066-VOL-2 ..... N92-11007 #

WSU-DC/91/TR-61 ..... N92-11909 #

WSU/DC/91/TR-62 ..... N92-11908 #

Appendix

NASA SCIENTIFIC AND TECHNICAL INFORMATION PROGRAM PRODUCTS AND SERVICES

The NASA Scientific and Technical Information (STI) Program provides for the collection and announcement of aerospace-related reports and literature obtained worldwide through agreements and exchanges. The result of the collection is the comprehensive NASA STI Database that covers aeronautics, space, and supporting disciplines.

The STI Database, documents generated or obtained by NASA, and products and services derived from or supporting the database are made available to the NASA research community and to the public. Descriptions and sources of these items are presented in the following pages.

Scientific and Technical Aerospace Reports (*STAR*) is an abstract journal, listing citations with abstracts for aerospace-related reports obtained from worldwide sources. *STAR* is issued on the 8th and 23rd of each month and announces current documents that have been entered into the NASA STI Database during the previous two weeks. The reports are of the following types:

- NASA, NASA contractor, and NASA grantee reports;
- Reports issued by other U.S. Government agencies, domestic and foreign institutions, universities, and private firms;
- Translations in report form;
- NASA-owned patents and patent applications;
- Other U.S. Government agency and foreign patents and patent applications;
- Domestic and foreign dissertations and theses.

Journal, book, and conference literature, journal translations, and certain foreign dissertations having the same subject scope as *STAR* are announced in a companion journal, *International Aerospace Abstracts* (*IAA*). *IAA* is issued on the 1st and 15th of each month and is available from the American Institute of Aeronautics and Astronautics, Technical Information Service, 555 West 57th Street, 12th Floor, New York, NY 10019.

ELIGIBILITY AND REGISTRATION FOR NASA STI PRODUCTS AND SERVICES

Organizations of the type listed below that have registered with NASA can receive products and services.

- NASA offices and installations, contractors, subcontractors, grantees, and consultants;
- Other U.S. Government agencies and their contractors;
- Libraries in the United States that have arrangements with NASA to maintain collections of NASA documents for public reference;
- Other organizations in the United States having a need for NASA documents in work related to aeronautics and space research;
- Organizations abroad that have established reciprocal documents exchange arrangements with NASA.

Only the central service points or central points of document acquisition and control within qualified organizations are eligible to register for NASA STI products and services. Domestic organizations that may be eligible to receive various classes of NASA publications and services should address their requests for registration or further information to:

NASA Center for AeroSpace Information
ATTN: Registration Services
P.O. Box 8757
Baltimore, MD 21240-0757
301-621-0153

Organizations abroad should direct requests to:

National Aeronautics and Space Administration
Director, Scientific and Technical Information Program
Code JTT
Washington, DC 20546
USA
703-271-5640

SUBJECT SCOPE

The subject scope of *STAR* and *IAA* includes all aspects of aeronautics and space research and development, supporting basic and applied research, and applications. Aerospace aspects of Earth resources, energy development, conservation, oceanography, environmental protection, urban transportation, and other topics of high national priority are also covered.

HOW TO USE *STAR* SUBJECT CATEGORIES

Abstracts in *STAR* are categorized by 10 major subject divisions that are divided further into 76 specific subject categories. The subject divisions and categories are listed in the Table of Contents together with a note for each that defines its scope and provides any cross-references. For example:

16 SPACE TRANSPORTATION
Includes passenger and cargo space transportation, e.g., shuttle operations; and space rescue techniques. For related information see also *03 Air Transportation and Safety* and *18 Spacecraft Design, Testing and Performance.* For space suits see *54 Man/System Technology and Life Support.*

CROSS-REFERENCES

Individual *STAR* abstracts are not ordinarily cross-referenced, except for certain conference reports or book translations that have had separate abstracts written for their component papers or chapters. Citations and abstracts of the components follow immediately after those of the parent document. When the subject content of a component differs sufficiently from the general content of the parent, a cross-reference citation also is printed at the end of the category to which it normally would have been assigned if it were independent.

DOCUMENTS ON MICROFICHE

Documents available on microfiche are designated by a pound sign (#) following the accession number.

LIMITED REPRODUCIBILITY

A note of limited reproducibility appears in the citation, if there are factors affecting the reproducibility of more than 20% of the document. These factors include faint or broken type, color photographs, black and white photographs, foldouts, dot matrix print, or some other factor that limits the reproducibility of the document. This notation also appears on the microfiche header with the specific factor checked off on a list visible in the second frame.

COLOR COPIES

An increasing number of NASA scientific and technical reports are being produced with color graphs, charts, illustrations, and photographs. An indication that a document has color pages follows the source and pricing (SAP) information in the *STAR* citation.

Registered users of the NASA Scientific and Technical Information Program will receive ordered documents with color at no additional cost, as long as stock copies of the document are available. Otherwise, an additional fee of $2.00 per color page will be charged. The NASA Center for AeroSpace Information staff will contact registered users to determine individual user's needs.

NASA PATENTS AND PATENT APPLICATIONS

Patents and patent applications owned by NASA are announced in *STAR* under appropriate subject categories and are referenced in the *STAR* indexes. In the Report/Accession Number Index, patents are indexed by the NASA Case Number, and the U.S. Patent Class. Patent applications are indexed by the NASA Case Number and the U.S. Patent Application Serial Number.

Printed copies of patents (which are not microfiched) are available for purchase from the U.S. Patent and Trademark Office.

NASA patent application specifications are sold in both paper copy and microfiche by the National Technical Information Service (NTIS). The US-Patent-Appl-SN-number should be used in ordering either paper copy or microfiche from NTIS.

When ordering patents, the U.S. Patent Number should be used, and payment must be remitted in advance, by money order or check payable to the Commissioner of Patents and Trademarks. Prepaid purchase coupons for ordering are also available from the U.S. Patent and Trademark Office.

The patents and patent applications announced in *STAR* are owned by NASA and are available for royalty-free licensing. Requests for licensing terms and further information should be addressed to:

National Aeronautics and Space Administration
Associate General Counsel for Intellectual Property
Code GP
Washington, DC 20546

SOURCES FOR DOCUMENTS

One or more sources from which a document announced in *STAR* is available to the public is given in each citation. The most commonly indicated sources and their acronyms or abbreviations are listed on page A-6. If the publication is available from a source other than those listed, the publisher and address will be displayed on the availability line or in combination with the corporate source line.

Avail: NTIS. Sold by the National Technical Information Service. Prices for hard copy (HC) and microfiche (MF) are indicated by a price code following the letters HC or MF in the *STAR* citation. Current values for the price codes are given in the tables on page A-7.

Initially distributed microfiche under the NTIS SRIM (Selected Research in Microfiche) is available at greatly reduced unit prices. For this service and for information concerning subscription to NASA printed reports, consult the NTIS Subscription Section, Springfield, VA 22161.

NOTE ON ORDERING DOCUMENTS: When ordering NASA publications (those followed by the * symbol), use the N accession number. NASA patent applications (only the specifications are offered) should be ordered by the US-Patent-Appl-SN number. Non-NASA publications (no asterisk) should be ordered by the AD, PB, or other *report number* shown on the last line of the citation, not by the N accession number. It is also advisable to cite the title and other bibliographic identification.

Avail: SOD (or GPO). Sold by the Superintendent of Documents, U.S. Government Printing Office, in hard copy. The current price and order number are given following the availability line. (NTIS will fill microfiche requests, as indicated above, for those documents identified by a # symbol.)

Avail: BLL (formerly NLL): British Library Lending Division, Boston Spa, Wetherby, Yorkshire, England. Photocopies available from this organization at the price shown. (If none is given, address inquiry to the BLL.)

Avail: DOE Depository Libraries. Organizations in U.S. cities and abroad that maintain collections of Department of Energy reports, usually in microfiche form, are listed in *Energy Research Abstracts.* Services available from the DOE and its depositories are described in a booklet, *DOE Technical Information Center - Its Functions and Services* (TID-4660), which may be obtained without charge from the DOE Technical Information Center.

Avail: ESDU. Pricing information on specific data, computer programs, and details on Engineering Sciences Data Unit (ESDU) topic categories can be obtained from ESDU International Ltd. Requesters in North America should use the Virginia address while all other requesters should use the London address, both of which are on page A-6.

Avail: Fachinformationszentrum, Karlsruhe. Sold by the Fachinformationszentrum Energie, Physik, Mathematik GMBH, Eggenstein Leopoldshafen, Federal Republic of Germany, at the price shown in deutschmarks (DM).

Avail: HMSO. Publications of Her Majesty's Stationery Office are sold in the U.S. by Pendragon House, Inc. (PHI), Redwood City, CA. The U.S. price (including a service and mailing charge) is given, or a conversion table may be obtained from PHI.

Avail: NASA Public Document Rooms. Documents so indicated may be examined at or purchased from the National Aeronautics and Space Administration, Public Documents Room (Room 126), 600 Independence Ave., S.W., Washington, DC 20546, or public document rooms located at NASA installations, and the NASA Pasadena Office at the Jet Propulsion Laboratory.

Avail: Univ. Microfilms. Documents so indicated are dissertations selected from *Dissertation Abstracts* and are sold by University Microfilms as xerographic copy (HC) and microfilm. All requests should cite the author and the Order Number as they appear in the citation.

Avail: US Patent and Trademark Office. Sold by Commissioner of Patents and Trademarks, U.S. Patent and Trademark Office, at the standard price of $1.50 each, postage free. (See discussion of NASA patents and patent applications below.)

Avail: (US Sales Only). These foreign documents are available to users within the United States from the National Technical Information Service (NTIS). They are available to users outside the United States through the International Nuclear Information Service (INIS) representative in their country, or by applying directly to the issuing organization.

Avail: USGS. Originals of many reports from the U.S. Geological Survey, which may contain color illustrations, or otherwise may not have the quality of illustrations preserved in the microfiche or facsimile reproduction, may be examined by the public at the libraries of the USGS field offices whose addresses are listed on page A-6. The libraries may be queried concerning the availability of specific documents and the possible utilization of local copying services, such as color reproduction.

Avail: Issuing Activity, or Corporate Author, or no indication of availability. Inquiries as to the availability of these documents should be addressed to the organization shown in the citation as the corporate author of the document.

FEDERAL DEPOSITORY LIBRARIES: To provide the general public with greater access to U.S. Government publications, Congress established the Federal Depository Library Program under the Government Printing Office (GPO), with 52 regional depositories responsible for permanent retention of material, inter-library loan, and reference services. (These libraries are not sales outlets.) At least one copy of nearly every NASA and NASA-sponsored publication, either in printed or microfiche format, is received and retained by the 52 regional depositories. A list of the regional GPO libraries, appears on page A-8. A local library can contact a regional depository library to help locate specific reports, or direct contact may be made by an individual.

PUBLIC COLLECTION OF NASA DOCUMENTS

An extensive collection of NASA and NASA-sponsored publications is maintianed by the British Library Lending Divison, Boston Spa, Wetherby, Yorkshire, England, for public access. The British Library Lending Division also has available many of the non-NASA publications cited in *STAR*.

European requesters may purchase facsimile copy or microfiche of NASA and NASA-sponsored documents, those identified by both the symbols # and * from ESA—Information Retrieval Service, European Space Agency, 8-10 rue Mario-Nikis, 75738 Paris CEDEX 15, France.

SUBMITTING DOCUMENTS

All users of this abstract service are urged to forward reports to be considered for announcement in *STAR*. This will aid NASA in its efforts to provide the fullest possible coverage of all scientific and technical publications that might support aeronautics and space research and development. If you have prepared relevant reports (other than those you will transmit to NASA, DOD, or DOE through the usual contract- or grant-reporting channels), please send them for consideration to the NASA Center for AeroSpace Information, P.O. Box 8757, Baltimore, MD 21240-0757.

Reprints of journal articles, book chapters, and conference papers are also welcome. These will be considered for announcement in *STAR*'s companion journal, *IAA*.

You may specify a particular source to be included in a report announcement if you wish; otherwise the report will be placed on a public sale at the National Technical Information Service. Copyrighted publications will be announced but not distributed or sold.

PURCHASE OF *STAR*

STAR is publicly available on annual subscription from the Superintendent of Documents, U.S. Government Printing Office, Washington, DC 20402.

STAR is available to registered users on annual subscription from the NASA Center for AeroSpace Information, ATTN: Registration Services, P.O. Box 8757, Baltimore, MD 21240-0757.

Microfiche of the abstract sections of *STAR* are available, on annual subscription only, from NTIS as PB92-911300, Attn: Subscriptions, 5285 Port Royal Road, Springfield, VA 22161. Annual subscription rates are $100.00 North America; $200.00 foreign. Abstract sections for previous years retroactive to 1964 are available at the current rates.

ADDRESSES OF ORGANIZATIONS

American Institute of Aeronautics and Astronautics
Technical Information Service
555 West 57th Street, 12th Floor
New York, New York 10019

British Library Lending Division,
Boston Spa, Wetherby, Yorkshire,
England

Commissioner of Patents and Trademarks
U.S. Patent and Trademark Office
Washington, DC 20231

Department of Energy
Technical Information Center
P.O. Box 62
Oak Ridge, Tennessee 37830

European Space Agency-Information Retrieval Service
ESRIN
Via Galileo Galilei
00044 Frascati (Rome) Italy

Engineering Sciences Data Unit International
P.O. Box 1633
Manassas, Virginia 22110

Engineering Sciences Data Unit International, Ltd.
251-259 Regent Street
London, W1R 7AD, England

Fachinformationszentrum Energie, Physik, Mathematik
GMBH
7514 Eggenstein Leopoldshafen
Federal Republic of Germany

Her Majesty's Stationery Office
P.O. Box 569, S.E. 1
London, England

NASA Center for AeroSpace Information
P.O. Box 8757
Baltimore, Maryland 21240-0757

National Aeronautics and Space Administration
Scientific and Technical Information Program (JTT)
Washington, DC 20546

National Technical Information Service
5285 Port Royal Road
Springfield, Virginia 22161

Pendragon House, Inc.
899 Broadway Avenue
Redwood City, California 94063

Superintendent of Documents
U.S. Government Printing Office
Washington, DC 20402

University Microfilms
A Xerox Company
300 North Zeeb Road
Ann Arbor, Michigan 48106

University Microfilms, Ltd.
Tylers Green
London, England

U.S. Geological Survey Library National Center
MS 950
12201 Sunrise Valley Drive
Reston, Virginia 22092

U.S. Geological Survey Library
2255 North Gemini Drive
Flagstaff, Arizona 86001

U.S. Geological Survey
345 Middlefield Road
Menlo Park, California 94025

U.S. Geological Survey Library
Box 25046
Denver Federal Center, MS914
Denver, Colorado 80225

NTIS PRICE SCHEDULES

(Effective October 1, 1991)

Schedule A
STANDARD PRICE DOCUMENTS AND MICROFICHE**

PRICE CODE	NORTH AMERICAN PRICE	FOREIGN PRICE
A01	$ 9.00	$ 18.00
A02	12.50	25.00
A03	17.00	34.00
A04-A05	19.00	38.00
A06-A09	26.00	52.00
A10-A13	35.00	70.00
A14-A17	43.00	86.00
A18-A21	50.00	100.00
A22-A25	59.00	118.00
A99	*	*
N01	60.00	120.00
N02	59.00	118.00
N03	20.00	40.00

Schedule E
EXCEPTION PRICE DOCUMENTS AND MICROFICHE**

PRICE CODE	NORTH AMERICAN PRICE	FOREIGN PRICE
E01	$11.00	$ 22.00
E02	14.00	28.00
E03	16.00	32.00
E04	19.00	38.00
E05	21.00	42.00
E06	24.00	48.00
E07	27.00	54.00
E08	30.00	60.00
E09	33.00	66.00
E10	36.00	72.00
E11	39.00	78.00
E12	43.00	86.00
E13	46.00	92.00
E14	50.00	100.00
E15	54.00	108.00
E16	59.00	118.00
E17	64.00	128.00
E18	69.00	138.00
E19	76.00	152.00
E20	88.00	176.00
E99	*	*

* Contact NTIS for price quote.

** Effective January 1, 1991, the microfiche copy of any new document entering the NTIS collection will be priced the same as the paper copy of the document.

IMPORTANT NOTICE

NTIS Shipping and Handling Charges

U.S., Canada, Mexico — ADD $3.00 per TOTAL ORDER

All Other Countries — ADD $4.00 per TOTAL ORDER

Exceptions — Does NOT apply to:

ORDERS REQUESTING NTIS RUSH HANDLING
ORDERS FOR SUBSCRIPTION OR STANDING ORDER PRODUCTS *ONLY*

NOTE: Each additional delivery address on an order requires a separate shipping and handling charge.

FEDERAL REGIONAL DEPOSITORY LIBRARIES

ALABAMA

AUBURN UNIV. AT MONTGOMERY LIBRARY
Documents Dept.
7300 University Drive
Montgomery, AL 36117-3596
(205) 244-3650 FAX: (205) 244-0678

UNIV. OF ALABAMA
Amelia Gayle Gorgas Library
Govt. Documents
Box 870266
Tuscaloosa, AL 35487-0266
(205) 348-6046 FAX: (205) 348-8833

ARIZONA

DEPT. OF LIBRARY, ARCHIVES, AND PUBLIC RECORDS
Federal Documents
Third Floor State Capitol
1700 West Washington
Phoenix, AZ 85007
(602) 542-4121 FAX: (602) 542-4400; 542-4500

ARKANSAS

ARKANSAS STATE LIBRARY
State Library Services
One Capitol Mall
Little Rock, AR 72201
(501) 682-2869

CALIFORNIA

CALIFORNIA STATE LIBRARY
Govt. Publications Section
914 Capitol Mall - P.O. Box 942837
Sacramento, CA 94237-0001
(916) 322-4572 FAX: (916) 324-8120

COLORADO

UNIV. OF COLORADO - BOULDER
Norlin Library
Govt. Publications
Campus Box 184
Boulder, CO 80309-0184
(303) 492-8834 FAX: (303) 492-2185

DENVER PUBLIC LIBRARY
Govt. Publications Dept. BS/GPD
1357 Broadway
Denver, CO 80203
(303) 571-2135

CONNECTICUT

CONNECTICUT STATE LIBRARY
231 Capitol Avenue
Hartford, CT 06106
(203) 566-4971 FAX: (203) 566-3322

FLORIDA

UNIV. OF FLORIDA LIBRARIES
Documents Dept.
Library West
Gainesville, FL 32611-2048
(904) 392-0366 FAX: (904) 392-7251

GEORGIA

UNIV. OF GEORGIA LIBRARIES
Govt. Documents Dept.
Jackson Street
Athens, GA 30602
(404) 542-8949 FAX: (404) 542-6522

HAWAII

UNIV. OF HAWAII
Hamilton Library
Govt. Documents Collection
2550 The Mall
Honolulu, HI 96822
(808) 948-8230 FAX: (808) 956-5968

IDAHO

UNIV. OF IDAHO LIBRARY
Documents Section
Moscow, ID 83843
(208) 885-6344 FAX: (208) 885-6817

ILLINOIS

ILLINOIS STATE LIBRARY
Reference Dept.
300 South Second
Springfield, IL 62701-1796
(217) 782-7596 FAX: (217) 524-0041

INDIANA

INDIANA STATE LIBRARY
Serials/Documents Section
140 North Senate Avenue
Indianapolis, IN 46204
(317) 232-3678 FAX: (317) 232-3728

IOWA

UNIV. OF IOWA LIBRARIES
Govt. Publications Dept.
Washington & Madison Streets
Iowa City, IA 52242
(319) 335-5926 FAX: (319) 335-5830

KANSAS

UNIV. OF KANSAS
Govt. Documents & Map Library
6001 Malatt Hall
Lawrence, KS 66045-2800
(913) 864-4660 FAX: (913) 864-5380

KENTUCKY

UNIV. OF KENTUCKY LIBRARIES
Govt. Publications/Maps Dept.
Lexington, KY 40506-0039
(606) 257-3139 FAX: (606) 257-1563; 257-8379

LOUISIANA

LOUISIANA STATE UNIV.
Middleton Library
Govt. Documents Dept.
Baton Rouge, LA 70803
(504) 388-2570 FAX: (504) 388-6992

LOUISIANA TECHNICAL UNIV.
Prescott Memorial Library
Govt. Documents Dept.
305 Wisteria Street
Ruston, LA 71270-9985
(318) 257-4962 FAX: (318) 257-2447

MAINE

TRI-STATE DOCUMENTS DEPOSITORY
Raymond H. Fogler Library
Govt. Documents & Microforms Dept.
Univ. of Maine
Orono, ME 04469
(207) 581-1680

MARYLAND

UNIV. OF MARYLAND
Hornbake Library
Govt. Documents/Maps Unit
College Park, MD 20742
(301) 454-3034 FAX: (301) 454-4985

MASSACHUSETTS

BOSTON PUBLIC LIBRARY
Govt. Documents Dept.
666 Boylston Street
Boston, MA 02117
(617) 536-5400 ext. 226
FAX: (617) 267-8273; 267-8248

MICHIGAN

DETROIT PUBLIC LIBRARY
5201 Woodward Avenue
Detroit, MI 48202-4093
(313) 833-1440; 833-1409
FAX: (313) 833-5039

LIBRARY OF MICHIGAN
Govt. Documents Unit
P.O. Box 30007
Lansing, MI 48909
(517) 373-0640 FAX: (517) 373-3381

MINNESOTA

UNIV. OF MINNESOTA
Wilson Library
Govt. Publications Library
309 19th Avenue South
Minneapolis, MN 55455
(612) 624-5073 FAX: (612) 626-9353

MISSISSIPPI

UNIV. OF MISSISSIPPI
J.D. Williams Library
Federal Documents Dept.
106 Old Gym Bldg.
University, MS 38677
(601) 232-5857 FAX: (601) 232-5453

MISSOURI

UNIV. OF MISSOURI - COLUMBIA
Ellis Library
Govt. Documents
Columbia, MO 65201
(314) 882-6733 FAX: (314) 882-8044

MONTANA

UNIV. OF MONTANA
Maureen & Mike Mansfield Library
Documents Div.
Missoula, MT 59812-1195
(406) 243-6700 FAX: (406) 243-2060

NEBRASKA

UNIV. OF NEBRASKA - LINCOLN
D.L. Love Memorial Library
Documents Dept.
Lincoln, NE 68588
(402) 472-2562

NEVADA

UNIV. OF NEVADA
Reno Library
Govt. Publications Dept.
Reno, NV 89557
(702) 784-6579 FAX: (702) 784-1751

NEW JERSEY

NEWARK PUBLIC LIBRARY
U.S. Documents Div.
5 Washington Street - P.O. Box 630
Newark, NJ 07101-0630
(201) 733-7812 FAX: (201) 733-5648

NEW MEXICO

UNIV. OF NEW MEXICO
General Library
Govt. Publications Dept.
Albuquerque, NM 87131-1466
(505) 277-5441 FAX: (505) 277-6019

NEW MEXICO STATE LIBRARY
325 Don Gaspar Avenue
Santa Fe, NM 87503
(505) 827-3826 FAX: (505) 827-3820

NEW YORK

NEW YORK STATE LIBRARY
Documents/Gift & Exchange Section
Federal Depository Program
Cultural Education Center
Albany, NY 12230
(518) 474-5563 FAX: (518) 474-5786

NORTH CAROLINA

UNIV. OF NORTH CAROLINA - CHAPEL HILL
CB#3912, Davis Library
BA/SS Dept.—Documents
Chapel Hill, NC 27599
(919) 962-1151 FAX: (919) 962-0484

NORTH DAKOTA

NORTH DAKOTA STATE UNIV. LIBRARY
Documents Office
Fargo, ND 58105
(701) 237-8886 FAX: (701) 237-7138
In cooperation with Univ. of North Dakota, Chester Fritz Library
Grand Forks

OHIO

STATE LIBRARY OF OHIO
Documents Dept.
65 South Front Street
Columbus, OH 43266
(614) 644-7051 FAX: (614) 752-9178

OKLAHOMA

OKLAHOMA DEPT. OF LIBRARIES
U.S. Govt. Information Div.
200 NE 18th Street
Oklahoma City, OK 73105-3298
(405) 521-2502, ext. 252, 253
FAX: (405) 525-7804

OKLAHOMA STATE UNIV.
Edmon Low Library
Documents Dept.
Stillwater, OK 74078
(405) 744-6546 FAX: (405) 744-5183

OREGON

PORTLAND STATE UNIV.
Millar Library
934 SW Harrison - P.O. Box 1151
Portland, OR 97207
(503) 725-3673 FAX: (503) 725-4527

PENNSYLVANIA

STATE LIBRARY OF PENN.
Govt. Publications Section
Walnut St. & Commonwealth Ave. - P.O. Box 1601
Harrisburg, PA 17105
(717) 787-3752

SOUTH CAROLINA

CLEMSON UNIV.
Cooper Library
Public Documents Unit
Clemson, SC 29634-3001
(803) 656-5174 FAX: (803) 656-3025
In cooperation with Univ. of South Carolina, Thomas Cooper Library, Columbia

TENNESSEE

MEMPHIS STATE UNIV. LIBRARIES
Govt. Documents
Memphis, TN 38152
(901) 678-2586 FAX: (901) 678-2511

TEXAS

TEXAS STATE LIBRARY
United States Documents
P.O. Box 12927 - 1201 Brazos
Austin, TX 78711
(512) 463-5455 FAX: (512) 463-5436

TEXAS TECH. UNIV. LIBRARY
Documents Dept.
Lubbock, TX 79409
(806) 742-2268 FAX: (806) 742-1920

UTAH

UTAH STATE UNIV.
Merrill Library & Learning Resources Center, UMC-3000
Documents Dept.
Logan, UT 84322-3000
(801) 750-2684 FAX: (801) 750-2677

VIRGINIA

UNIV. OF VIRGINIA
Alderman Library
Govt. Documents
Charlottesville, VA 22903-2498
(804) 924-3133 FAX: (804) 924-4337

WASHINGTON

WASHINGTON STATE LIBRARY
Document Section
MS AJ-11
Olympia, WA 98504-0111
(206) 753-4027 FAX: (206) 753-3546

WEST VIRGINIA

WEST VIRGINIA UNIV. LIBRARY
Govt. Documents Section
P.O. Box 6069
Morgantown, WV 26506
(304) 293-3640

WISCONSIN

ST. HIST. SOC. OF WISCONSIN LIBRARY
Govt. Publications Section
816 State Street
Madison, WI 53706
(608) 262-2781 FAX: (608) 262-4711
In cooperation with Univ. of Wisconsin-Madison, Memorial Library

MILWAUKEE PUBLIC LIBRARY
Documents Div.
814 West Wisconsin Avenue
Milwaukee, WI 53233
(414) 278-2167 FAX: (414) 278-2137

WYOMING

WYOMING STATE LIBRARY
Supreme Court & Library Bldg.
Govt. Publications
Cheyenne, WY 82002
(307) 777-5920 FAX: (307) 777-6289

*U.S. G.P.O.-1992:313-125:60002

National Aeronautics and
Space Administration
Code JTT
Washington, D.C.
20546-0001

Official Business
Penalty for Private Use, $300

SPECIAL FOURTH-CLASS RATE
POSTAGE & FEES PAID
NASA
PERMIT No. G27

POSTMASTER: If Undeliverable (Section 158
Postal Manual) Do Not Return